Organic Peroxides in Radical Chemistry

and

Stereochemical Study of the Intramolecular Schmidt Reaction

Inaugural dissertation

of the Faculty of Science,

University of Bern

presented by

Lars Gnägi

from Bellmund / BE

Supervisor of the doctoral thesis:

Prof. Dr. Philippe Renaud

Department of Chemistry, Biochemistry, and Pharmaceutical Sciences

University of Bern

Organic Peroxides in Radical Chemistry

and

Stereochemical Study of the Intramolecular Schmidt Reaction

Inaugural dissertation

of the Faculty of Science,

University of Bern

presented by

Lars Gnägi

from Bellmund / BE

Supervisor of the doctoral thesis:

Prof. Dr. Philippe Renaud

Department of Chemistry, Biochemistry, and Pharmaceutical Sciences

University of Bern

Accepted by the Faculty of Science.

Bern, 04.03.2021

The Dean:

Prof. Dr. Z. Balogh

I consider one of the most important duties of any scientist the teaching of science to students and to the general public.

– Isaac Asimov –

Acknowledgements

I would like to thank Philippe Renaud for giving me the opportunity to work on several different projects in his group and thus to get in touch with many aspects of organic chemistry. I am grateful for his support as well as for the freedom he gave me to develop and follow my own ideas. I would like to express my gratitude for entrusting me with the supervision of a bachelor student, of two master students, and of Robin during his entire laboratory apprenticeship. I appreciated the time to organize, teach and lead this small team very much.

I would like to thank David Procter and Martin Lochner for taking their time to evaluate my thesis and being part of the examination committee.

Thomas Wirth is acknowledged for hosting me at Cardiff University and giving me a valuable insight to flow synthesis. Thank you, Jakob Seitz, Tobias Hokamp, Micol Santi, Matthew Tailby, Marina Raynbird, and the rest of the group for making these months such a pleasant experience!

A big THANKS goes to Robin Schärer for his priceless work during the two and a half years of his apprenticeship. With his curiosity, practical skills, and independent way of working in the lab he contributed significantly to the successful outcome of the projects. I could not imagine a better person to supervise!

I also want to thank the rest of my small team, David Ohde, Michael Hofstetter and Remo Arnold for being excellent students and giving me the opportunity to become a better teacher.

I would like to thank all the members of the infamous *Dütschschwizerlabor* S375, Manuel Gnägi-Lux, Daniel Meyer, Robin Schärer, Alexander Wittwer, Fabian Walther, Michael Hofstetter, Severin Martz, Nadja Niggli, Remo Arnold and Elena Pruteanu for sharing your good vibes, enthusiastic support of YB, all the pranks, excellent taste of music, and for your heartfelt friendship.
It was a pleasure to spend time inside and – equally important – outside the lab with friends like you. We were truly only lucky…

Of course, I want also to thank the other current and former characters I met during my overall seven (!) years in the Renaud group for the great time in the lab, at the coffee table, and during apéros: Könu, Beni, Camilo, Jane, Andrey, Julien, Nico M, Nico V, Valentin, Cédric, Jojo, Chrigu, Gong, Sankar, Vlada, Dace, Agathe, Anja, Eloïse, Émy, Fabrice, Joy, Qi, Lise, Melinda, Phipu, Gaetano, Kleni, Gulsana, Willi, Sam and Pedro.

The teams of the *Werkstatt* (Thomas, Hansjürg, Adrian, René), *Hausdienst* (Christof, Heiner, Sämu) and *Materialausgabe* (Simon, Michel, Dani, Marco) are acknowledged for their help, the many open discussions, and the all the gossip we exchanged.

I would like to thank Sandra Zbinden, Beatrice Thönen and Franziska Bornhauser for their invaluable administrative support in any situation and at any time.

The royal society of chemistry and the swiss national science foundation are acknowledged for funding the stay in Cardiff and the projects in Bern, respectively.

Many thanks to *gli italiani* and other friends from the department for spending our time together and motivating me to learn a new language: Francesco, Rebecca, Fabio, Georgia, Stefano, Piero, Arianna, Giuseppe, Fulvio, Giovanni, Matteo, Alessandro, René, Valentine, Pavel, Jürg, Michał, and Tomasz.

An dieser Stelle möchte ich auch meiner Familie und meinen Freunden (im speziellen Thomas, Melanie und Lorenz) danken. Danke, dass ihr mich ohne zu zögern unterstützt, aufgemuntert und immer wieder von neuem motiviert habt – ein solch tolles soziales Umfeld ist nicht selbstverständlich.
Merci Michelle, dass du immer für mich da bist.

Abstract

Organic peroxides and organic azides are highly energetic functional groups and have been utilized in many synthetic applications for over a hundred years. The first part of this thesis focuses on organic peroxides as a source of radicals. After a general introduction to organic peroxides in radical chemistry in chapter 1, peroxyoxalates and diacyl peroxides move into the focus of this thesis (chapters 2-5). Di-*tert*-butyl peroxyoxalates (DTBPO) was found to be an ideal radical initiator in the key step of our short enantioselective synthesis of the natural product (+)-brefeldin C described in chapter 2.

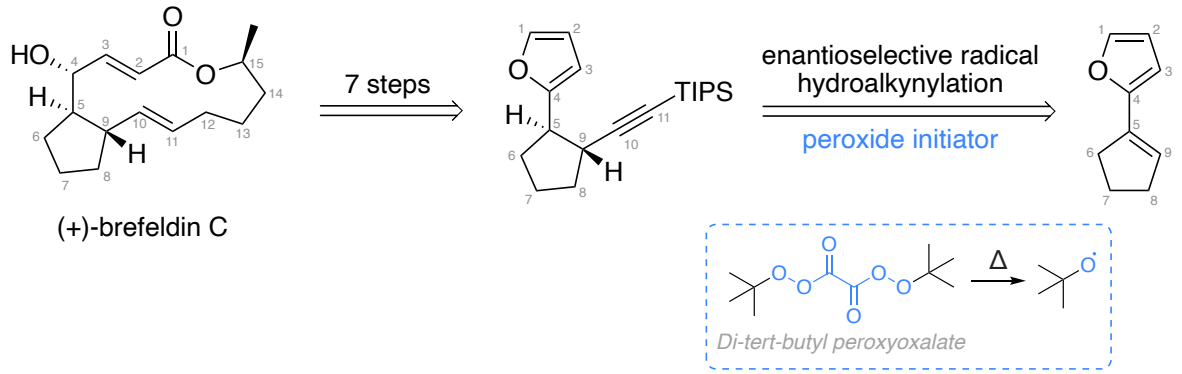

(+)-brefeldin C

Inspired by the thermal decomposition of DTBPO, peroxyoxalates were studied as a source of tertiary alkoxy radicals. An operationally simple method to access these radicals from tertiary alkyl hydroperoxides was developed using oxalyl chloride and is presented in chapter 3. The alkoxy radicals have been used in particular for the synthesis of various 4' functionalized alcohols *via* 1,5-hydrogen atom transfer and subsequent trapping of the relocated radical with a suitable radical trap.

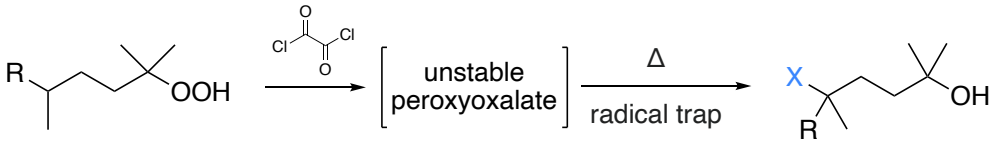

tertiary alkyl hydroperoxide *1,4-functionalized alcohol*

The one-pot procedure is fast, does not require workup after the reaction, and yields the functionalized alcohols in moderate to excellent yields. Unpublished results from work using this method and investigations on an analogous mechanism based on borinate radicals are compiled in chapter 4.

Due to the unstable nature of organic peroxides and the hazards associated with their handling, a safer approach to their synthesis and direct use in continuous flow was investigated in chapter 5. It has been found that clean dilauroyl peroxide can be formed in excellent yield and can be used directly as an initiator in a subsequent reaction that is connected in series.

In the second part of this thesis, the stereochemical challenges of the intramolecular Schmidt reaction and the strategies to address them are introduced in chapter 6.

Our investigations to control the stereochemistry of the triflate-mediated intramolecular Schmidt reaction are summarized in two draft manuscripts in chapters 7 and 8. Our group has developed a protocol to run the reaction under nonacidic conditions using azidotriflates: After an initial intramolecular S_N2 reaction between the azide and the triflate moiety, an intermediate aminodiazonoium salt is formed, which undergoes a stereoselective 1,2-shift with concomitant N_2 elimination. The substitution has been found to proceed highly stereospecifically. The formed iminium triflate is reduced diastereoslectively in a second step to the bicyclic amine. Remarkably, the chiral alcohol center controls the entire process and thus only one of the four possible diastereomers is obtained in a highly selective manner. The method has been used for the concise synthesis of a lehmizidine- and an indolizidine alkaloid that represent components of *myrmicaria melanogaster* ant venom.

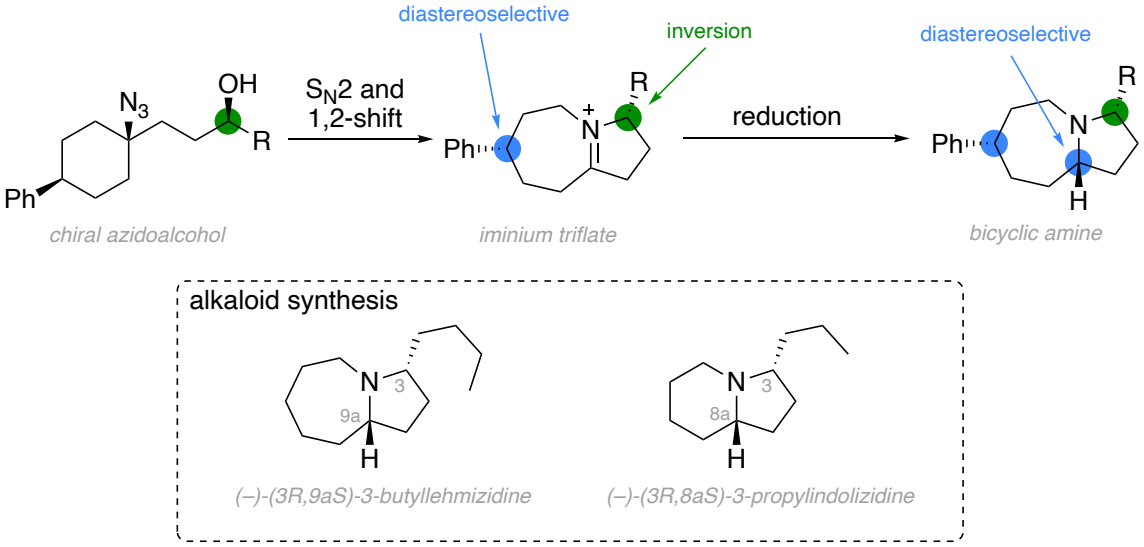

It was further investigated whether the method is applicable to access bridgehead-functionalized azabicycles from the corresponding prefunctionalized azidoalcohols. The results of this study complement previous finding that have been conducted in two precedent PhD theses and are presented in the last chapter of this thesis.

List of abbreviations & symbols

$(COCl)_2$	Oxalyl chloride
9-BBN	9-Borabicyclo(3.3.1)nonane
Ac	Acetyl
AIBN	Azobisisobutyronitrile
Alox	Aluminium oxide (e.g., for chromatography)
APEX	Acetone peroxide
aq.	Aqueous
ATRA	Atom transfer radical addition
BDE	Bond dissociation energy
Bn	Benzyl
BPR	Back-pressure regulator
Bz	Benzoyl
c	Concentration
CAD	Computer-aided design
catBH	Catecholborane
Cp	Cyclopentadienyl anion
d	Doublet
δ	Chemical shift
DBNE	Di-*n*-butylnorephedrine
DBP	Dibenzoyl peroxide
DCC	*N,N'*-Dicyclohexylcarbodiimide
DDQ	2,3-Dichloro-5,6-dicyano-1,4-benzoquinone
Δ	Heating
DFT	Density functional theory
DIBAL(H)	Diisobutylaluminium hydride
DIH	1,3-Diiodo-5,5-dimethylhydantoin
DLP	Dilauroyl peroxide
DMAP	4-(Dimethylamino)pyridine
DMDO	Dimethyldioxirane
DMF	*N,N*-Dimethylformamide
DMNE	Dimethylnorephedrine
DMSO	Dimethylsulfoxide
DoE	Design of experiments
dppf	1,1'-Bis(diphenylphosphino)ferrocene
dr	Diastereomeric ratio
DTBHN	Di-*tert*-butyl hyponitrite

DTBPO	Di-*tert*-butyl peroxyoxalate
EI	Electron impact ionization
EPR	Electron paramagnetric resonance
equiv	Equivalent
er	Enantiomeric ratio
ESI	Electron spray ionization
ETFE	Ethylene tetrafluoroethylene
EtIOAc	Ethyl iodoacetate
FEP	Fluorinated ethylene propylene
FTIR	Fourier-transform infrared (spectroscopy)
HAT	Hydrogen atom transfer
hex	*n*-hexyl
HPLC	High-pressure liquid chromatography
HTP	High-test peroxide
Ipc_2BH	Diisopinocampheyl borane
$IpcBH_2$	Monoisopinocampheylborane
IPP	Diisopropyl peroxide
IR	Infrared spectroscopy
ISR	Intramolecular Schmidt reaction
J	Coupling constant
LA	Lewis acid
LG	Leaving group
LMCT	Ligand-to-metal charge transfer
M	Molarity (mol/L)
m	Multiplet
m/z	Mass-to-charge ratio
*m*CPBA	*meta*-chloroperbenzoic acid
Me	Methyl
mL	Milliliter
mmol	Millimole
mp	Melting point
MPLC	Medium-pressure liquid chromatography
MS	Mass spectroscopy
MsCl	Mesyl chloride
n-Bu-CBS	*n*-butyl Corey-Bakshi-Shibata catalyst
	(*S*)-1-Butyl-3,3-diphenylhexahydropyrrolo [1,2-c][1,3,2]oxazaborole
n.d.	Not determined
NBS	*N*-Bromosuccinimide
NFASs	*N*-fluoro-*N*-arylsulfonamides

NMR	Nuclear magnetic resonance
Nu	Nucleophile
o.n.	Overnight
$^1O_2$	Singlet oxygen
$^3O_2$	Triplet oxygen
OMs	Mesylate
PAN	Peroxyacetly nitrates
PCET	Proton-coupled electron transfer
PCTFE	Polychlorotrifluoroethylene
PEEK	Polyether ether ketone
Ph	Phenyl
PIDA	Phenyliodine(III) diacetate
Pin	Pinacol
PMB	*para*-methoxybenzene
PPE	Personal protective equipment
ppm	Parts per million
PPTS	Pyridinium para-toluenesulfonate
*p*TsOH	*para*-toluenesulfonic acid
Q	Volumetric flow rate
q	Quadruplet
quint	Quintet
R	Rest (or substituent)
r	Radius
RAFT	Reversible-addition-fragmentation chain-transfer
Re	Reynolds number
ρ	Density
ROS	Reactive oxygen species
rt	Room temperature (ca. 25 °C)
s	Singlet
SADT	Self-accelerating decomposition temperature
SET	Single electron transfer
S_N2	Nucleophilic substitution, 2nd order
T	Temperature
t	time *or* triplet (NMR)
TBAF	Tetrabutylammonium fluoride
TBME	*tert*-Butyl methyl ether
TBS	*tert*-Butyldimethylsilyl
TBSCl	*tert*-Butyldimethylsilyl chloride
*t*Bu	*tert*-Butyl

TEMPO	2,2,6,6-Tetramethylpiperidinyloxyl radical
Tf	Triflyl
TIPS	Triisopropyl silyl
TLC	Thin layer chromatography
TMS	Tetramethylsilane
t_{res}	Residence time
Ts	Toluene sulfonyl
TS	Transition state
UHP	Urea hydrogen peroxide complex
UV	ultra violett
v	Flow speed
V	Volume
VOC	Volatile organic compounds
wt%	weight percentage

Table of contents

Part one

Organic Peroxides in Radical Chemistry

The first part of this thesis contains five chapters on organic peroxides and how they are used in radical reactions.

Chapter 1 provides a general introduction to organic peroxides such as synthetic aspects, chemical reactivities, and associated concepts. In chapter 2, the enantioselective total synthesis of the natural product (+)-brefeldin C is presented, which involves an organic peroxide as a radical initiator. A new synthetic method to generate alkoxy radicals from hydroperoxides and used for remote functionalisation is the topic of chapter 3. Unpublished results of this study as well as preliminary investigations on a method relying on borinate radicals are compiled in chapter 4. The final chapter focuses on a more technological aspect and continuous flow synthesis is presented as a method to enhance process safety and reduce reaction time: The development of the synthesis and direct use of diacyl peroxides as radical initiators of an atom transfer radical addition reaction in continuous flow are presented in chapter 5.

Chapter 1

General Aspects of Organic Peroxides in Radical Chemistry

1. General Aspects of Organic Peroxides in Radical Chemistry

1.1 Introduction

Peroxides are much more than just an ingredient of bleaching agents. Their story started more than 200 years ago, when Alexander von Humboldt first described barium peroxide in 1799. As eloquently reported by Gilbert in his German article published in *Annalen der Physik*, it was Louis Jacques Thénard, along with Joseph Louis Gay-Lussac, who first described the formation of hydrogen peroxide from sodium peroxide and discovered the bleaching activity of the new compound.[1] However, due to the lack of an efficient production method, these substances had little applications until the early 21st century. Initially, hydrogen peroxide was first manufactured by electrolysis of sulfuric acid, but the breakthrough came with the two step anthraquinone process (Figure 1.1), which was patented by the *IG Farben Industrie* in Germany in the 1940s. This process is responsible for almost the entire production of hydrogen peroxide today and it supplies this reagent for the paper-, electronics-, detergents-, textile-, and chemical industries as well as for wastewater treatment on a scale of several million tons a year.[2,3]

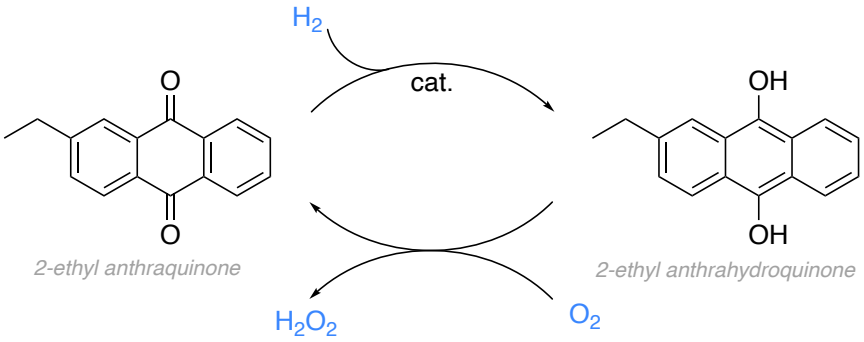

Figure 1.1. Simplified general reaction scheme of the anthraquinone process

The reverse reaction is used in nature by *Brachininae* beetles for self-defense: A concentrated solution (almost 30%) is injected in an abdominal "explosion chamber" together with hydroquinone and decomposed catalytically from where the boiling water and hot gas that are produced in this violent reaction are sprayed towards predators.[4]

But as mentioned earlier – the story does not end with hydrogen peroxide. Organic peroxides are literally illuminative substances as nature demonstrates in *Lampyridae* fireflies. Luminescent beetles manage to produce light by the luciferase catalyzed decomposition of a variety of peroxide-containing compounds. The excited-state products reach their energetic ground state by emission of a photon (Figure 1.2).[5,6]

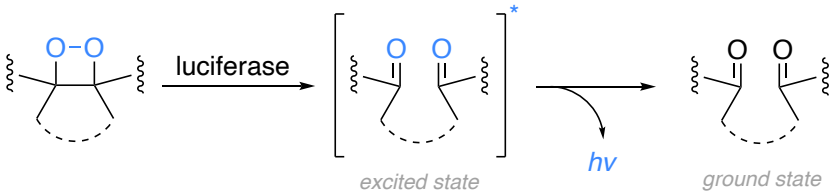

Figure 1.2. Basic principle of chemiluminescence exemplarly illustrated with a dioxetane

Not only animals but also plants make use of peroxides: In 1912/13, Wallach and Nelson reported the structure of Ascaridol, the first organic peroxide discovered in nature and isolated from *dysphania ambrosioides*.[7] Due to the high reactivity of the peroxide bond, this moiety is not very commonly found in natural products, which makes the list of natural organic peroxides rather short. Some of these compounds have attracted great interest either due to their peculiar chemical structure (e.g., Rhodophytin[8]), while others are investigated due to their antiviral properties (e.g., Artemisinin[9,10]), or because they have been identified as important intermediates in oxidative metabolic pathways such as members of the prostaglandin family[11,12] (Figure 1.3).

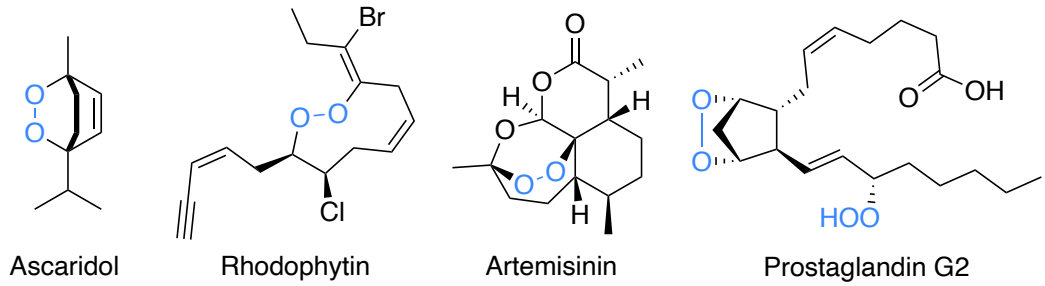

Ascaridol Rhodophytin Artemisinin Prostaglandin G2

Figure 1.3. Structures of naturally occurring organic peroxides

Due to the relatively labile nature of the peroxide bond, organic peroxides can easily undergo homolytic cleavage, which leads to the formation of two radicals. Industry has taken advantage of this feature and utilizes them as initiators, mostly for radical polymerization processes.[13]

The lability of the oxygen-oxygen bond, however, has also its drawbacks. Peroxides are often associated with danger because they, especially in larger quantities, pose a certain risk of explosion. Their sensitivity to shock, sparks, friction, heat, electrostatic discharge, light or contact with metals, and oxidizing / reducing materials makes them quite difficult to handle. Even compounds with low decomposition rates are problematic because they are sometimes self-reacting and therefore accelerate their own decomposition, which can lead to unpredictable explosions.[14] Commercially available organic peroxides are often phlegmatized and must be kept within the recommended storage

temperature. However, too much cooling can be disadvantageous as well, since crystallization can sometimes lead to explosive precipitates.[15,16] It is therefore of central importance to always take all possible safety measures (cutting proof gloves, safety shields, tongs, etc.) when handling organic peroxides in the laboratory. As a noteworthy example, the unconscious mixing of acetone and hydrogen peroxide has to be mentioned since it easily forms highly unstable peroxides (APEX, acetone peroxides), which have caused severe accidents in the past.[17,18] The same mixture has been misused for bomb manufacturing by criminals due to the uncontrolled accessibility of the required (household) chemicals.

In summary, peroxides are widespread compounds that contain the oxygen-oxygen bond as common structural motif and have attracted great attention both in academia and industry and have versatile applications ranging from small scale to millions of tons per year.

1.2 Overview of organic peroxides and their synthesis

Organic peroxides are a structurally diverse class of compounds and share the common oxygen-oxygen bond as a common moiety. However, the properties, synthesis, and the reactivity of these compounds can differ significantly from each other. The aim of chapter 1 is to provide the context and background information for the first part of this thesis. This subchapter (1.2) introduces the synthesis and general use of the most common sub-classes of organic peroxides as they appear throughout the first part of this thesis. Among the many different synthetic methods available, only the most general principles are described.[16,19–21] Their reactivity and aspects on how to form carbon- or oxygen-centered radicals from organic peroxides are described in the next subchapter (1.3). Synthetic applications and name reactions involving organic peroxides in radical chemistry are presented in the last subchapter (1.4).

1.2.1 Hydrogen peroxide and related species

Both organic and inorganic peroxides are, in the most general representation, structurally related to molecular oxygen and thus share the common word stem “ox”. Following the IUPAC nomenclature, the prefix *peroxo* is used for inorganic peroxides, whereas *peroxy* is used for organic peroxides.[19,22] Numerous important species that are related to molecular oxygen are presented below (Figure 1.4).

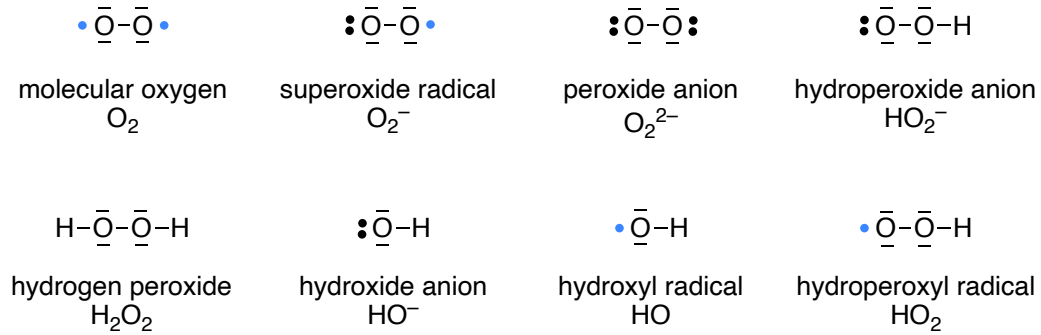

Figure 1.4. Selection of compounds derived from oxygen and their generalized structures; unpaired electrons are depicted as blue dots; two black dots and black lines stand for a lone pair

Almost all of them are biologically highly significant as they are endogenous species formed during intracellular oxidative processes. Due to their highly reactive nature, they are called *reactive oxygen species* (ROS), and act as potent cell damaging agents such as the superoxide anion, hydroperoxide anion, the hydroperoxyl radical, hydrogen peroxide, and the hydroxyl radical. Therefore, cells evolved an efficient machinery to scavenge ROS either enzymatically (most notably by the enzyme superoxide dismutase) or with antioxidants such as vitamin C.[23]

Hydrogen peroxide, discovered in 1818 by Louis Jacques Thénard, is by far the most important peroxide in industry today. Due to the advantages in stability and handling, the solid peroxides (e.g., Na_2O_2) were of greater practical use than hydrogen peroxide solutions for quite a long time. Sodium peroxide therefore gained industrial importance and was first produced on a commercial scale by the Castner process in 1899. It lost its importance when hydrogen peroxide could be more cost-effectively

manufactured by the anthraquinone process; today on a scale of millions of tons per year.[24] Most of it is used in the paper industries for cellulose bleaching and as a disinfectant in wastewater treatment. Hydrogen peroxide is commercially available as an aqueous solution (generally 30 wt%). Solution of higher concentrations (e.g., accessed through fractional distillation) are increasingly oxidizing and possess risk of explosion when in contact with a variety of materials.[25] Extremely high purity (98%) hydrogen peroxide termed high-test peroxide (HTP) has many applications in the aerospace industry and is used as a potent green rocket propellant. Curiously in this case, lowering the amount of water increases the stability of HTP.[26] Anhydrous solutions of hydrogen peroxide are not commercially available. Methods to concentrate hydrogen peroxide by distillation, thaw-freezing, or extraction with diethyl ether[24,27–30] or dichloromethane are reported but, due to the extreme hazard, not of practical significance.[31] Sources of anhydrous hydrogen peroxide safe to handle are urea hydrogen peroxide complex (UHP) or various metal peroxides.[22] As a chemical reagent, it is mostly used as a nucleophile and in epoxidation of electron-poor alkenes.

As a side note, polyoxides (H_2O_n) have long been considered as not being stable and thus inexistent.[32] Since the 1960s, several studies demonstrated the existence of neutral hydrogen polyoxides H_2O_3, H_2O_4 and H_2O_5 at low temperature. Although extremely short-lived in the presence of water, they show relatively stable forms in anhydrous environments. Detailed theoretical studies suggest that longer polyoxide chains, especially if the two hydrogen atoms are not substituted, are not stable under experimental conditions.[33–36]

1.2.2 Organic peroxides

Organic peroxides share the structural motif of two oxygen atoms connected directly "R–O–O–R", where one or both hydrogen atoms are substituted. They are thus all derivatives of H_2O_2 (Figure 1.5).

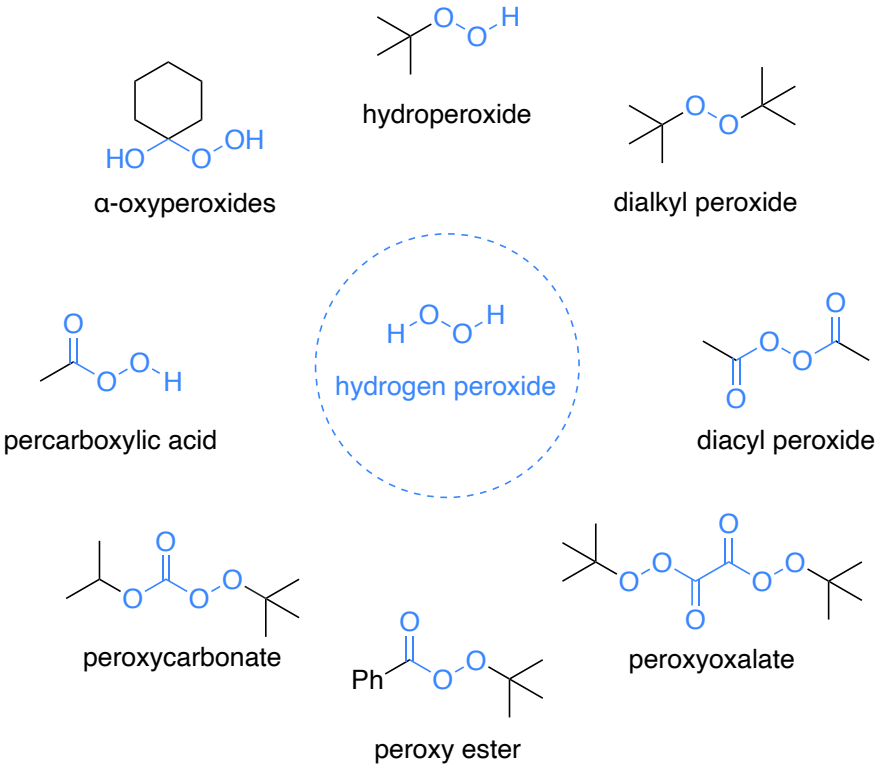

Figure 1.5. Overview of organic compounds bearing the peroxide structure

1.2.2.1 Hydroperoxides

Although hydroperoxides are widespread in nature, their synthetic accessibility is strongly limited on scale due to the hazardous chemicals and/or processes involved. Hydroperoxides are relatively stable compounds which can be concentrated and purified, even by distillation, as long as the temperature is kept reasonably low. The thermal stability is mainly defined by the dissociation energy of the O–O bond.[19] Due to the inductive effect of the two oxygen atoms, the hydroperoxide proton is less tightly bound which results in a rather acidic behavior (pK_a between 10 - 13).[37] Curiously, also their peculiar (strong) smell is similar to carboxylic acids. Some of the more general synthetic methods available to produce hydroperoxides are depicted below (Figure 1.6) and subsequently explained in more detail.

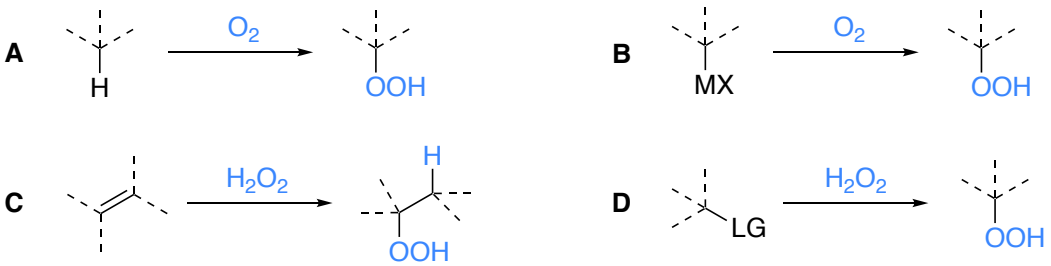

Figure 1.6. Synthetic access to alkyl hydroperoxides (LG stands for any suitable leaving group)

Autoxidation of hydrocarbons (Figure 1.6, **A**)

Hydrocarbons react with atmospheric oxygen by autoxidation which naturally occurs during aging and decomposition of organic matter. Generally, autoxidation is rather slow, requires elevated temperatures, and is not chemoselective. Therefore, tedious separation and purification of the obtained mixture of products is often necessary if a synthetic method relies on autoxidation.

However, autoxidation is industrially used for the production of simple tertiary hydroperoxides such as *tert*-butyl hydroperoxide and cumene hydroperoxide. *tert*-Butyl hydroperoxide is an important reagent for manufacturing propylene oxide (Halcon process)[38] and cumene hydroperoxide serves as the reactive intermediate in the production of phenol and acetone (Cumene process, Hock reaction).[39,40] The large-scale production of hydrogen peroxide also relies on autoxidation: the oxidation step of the anthraquinone process mentioned earlier also follows this general pathway (Figure 1.7).

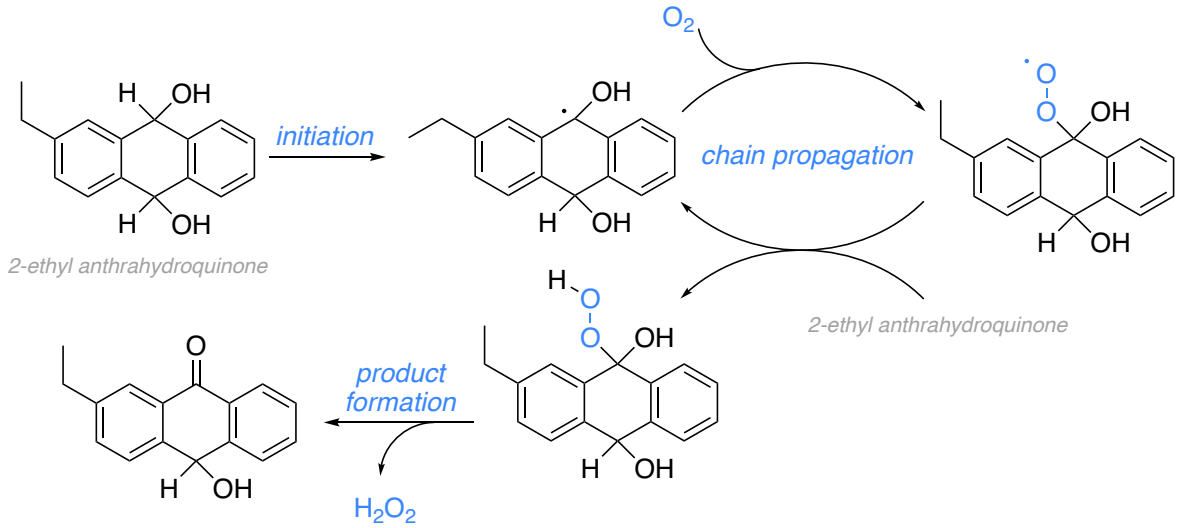

Figure 1.7. Autoxidation of anthrahydroquinone involving hydroperoxide formation (only one of two oxidation cycles is shown)

An external radical initiator is often not necessary because it is assumed that impurities (e.g., molecular oxygen) serve as initiators and abstract the benzylic hydrogen atom of anthraquinone. Once initiated, oxygen gas, which is bubbled through the anthrahydroquinone solution, reacts with the anthraquinone radical and forms a peroxy radical intermediate. This sustains the chain by abstraction of another hydrogen atom and the resulting peroxyketal eliminates the desired hydrogen peroxide.

Autoxidation of organometallic reagents (Figure 1.6, **B**)

Grignard reagents, formed from the corresponding alkyl halides, are transferred to a solvent saturated with oxygen which results in the desired hydroperoxide product. Tertiary hydroperoxides are obtained in high yields whereas secondary and primary hydroperoxides are formed in moderate or low yields, respectively.[41] However, the use of pure oxygen in ethereal solvents under very reactive conditions is not recommended due to the risk of explosion. Alternatively, organozinc halides are transformed to hydroperoxides in perfluorinated solvents.[42]

Addition of hydrogen peroxide to olefins (Figure 1.6, **C**)

Hydrogen peroxide can be added to olefins under strongly acidic conditions (cf. chapter 4).[43,44] In presence of a halogen, β-halo hydroperoxides are obtained in good yields.[45,46] The products are very sensitive to basic conditions and regioselectivity can be an issue.

Alkylation of hydrogen peroxide (Figure 1.6, **D**)

Hydrogen peroxide can be alkylated under basic or acidic conditions using a variety of electrophiles (alkyl halides, -sulfonates, -sulfates, etc.) affording the target hydroperoxides.[19,47,48] The reaction of alkaline hydrogen peroxide with epoxides affords β-hydroxy hydroperoxides. If the reactions proceed under acidic conditions, the hydroperoxide products stand in an equilibrium with carbenium ions that can be trapped with suitable nucleophiles.[49] The reaction of hydrogen peroxides with dialkylsulfates is known since a long time and yields some simple hydroperoxides but, due to tremendous danger associated with dialkylsulfates, the method has its clear limitations. Moreover, side reactions based on the generation of sulfuric- and peroxysulfuric acid involved are disadvantageous.[50,51]

A recent work by Liu takes advantage of well working alkylation methods to obtain primary, secondary and tertiary hydroperoxides in good to excellent yields (Figure 1.8).[52]

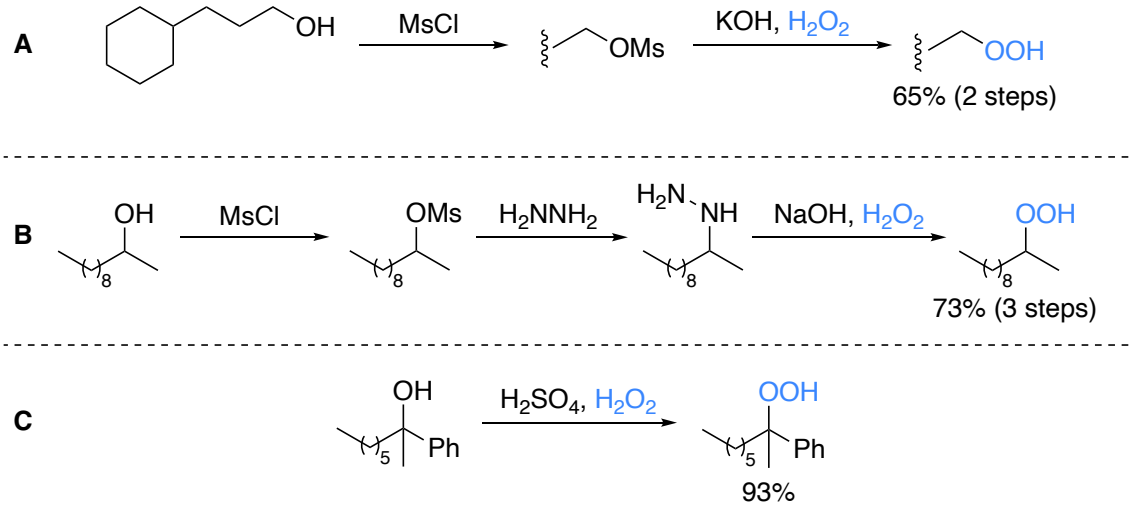

Figure 1.8. Representative example of hydroperoxide synthesis by Liu

Primary hydroperoxides are obtained in high yields from the corresponding alcohols. The two-step procedure consists of the high yielding conversion of the alcohol into the corresponding leaving group such as mesylate or tosylate. Advantageously, all intermediates can be used as a crude. In the second step, the nucleophilic substitution with hydrogen peroxide under basic condition leads to the desired hydroperoxide (Figure 1.8, **A**).[52,53] This method has been applied in the studies presented in chapter 4 for the synthesis of primary and secondary hydroperoxides. Under these S_N2 conditions, secondary hydroperoxides are obtained in lower yields and need extended reaction time which makes this method less efficient.[47] The sterically hindered back-side attack slows down the rate of substitution and gives rise to two major side reactions: E2 elimination to the olefin and hydrolysis to the original alcohol.[47]

An alternative method was reported by Casteel[54] (and later used by Liu and Ball) with which the secondary alkyl hydroperoxides are obtained in a three-step Wolff-Kishner type process starting from the corresponding alcohol (Figure 1.8, **B**).[52,54–57] After mesylation, the intermediate was converted to an alkyl hydrazine, which was then reacted with hydrogen peroxide under basic conditions in a sealed flask at elevated temperature. Obviously, the laboratory use of hydrazine in excess poses an enormous health risk, which renders this method without special equipment challenging. In a similar process, unsaturated secondary alkyl hydroperoxides are obtained from *N*-alkenyl-*N'*-*p*-tosylhydrazines as described by Bloodworth.[58] Especially allyl hydroperoxides are also obtained from the reaction of the corresponding halide with silver(I) salts and subsequent trapping of the carbocationic species with hydrogen peroxide.[59] Benzylic hydroperoxides are obtained, although in low yields, upon reaction of an arylalkane with *tert*-butyl hydroperoxide catalyzed by calcinated $ZnCrCO_3$-HTlc (hydrotalcite-like compound).[60]

Tertiary hydroperoxides cannot be accessed using the hydroperoxide anion as a nucleophile but rely on acidic, and thus S_N1, conditions. Tertiary alcohols are added slowly as a solution in an aprotic high-boiling point solvent, usually dioxane, to a concentrated solution of Caro's acid (also known as "piranha acid", H_2SO_5, peroxymonosulfuric acid) with subsequent heating (Figure 1.8, **C**).[52] The use of Caro's acid has its safety limitation, but the method is generally reliable and hydroperoxides are usually obtained in good to very good yields. However, the method is limited to substrates, which tolerate these extremely oxidative and acidic conditions. Interestingly, enantiopure tertiary hydroperoxides can be obtained after kinetic resolution of racemic tertiary hydroperoxides using enantiopure phosphines which proceeds *via* reduction of the undesired enantiomer to the corresponding alcohol.[61]

Use of 2-methoxyprop-2-yl hydroperoxide as a masked form of hydrogen peroxide

To circumvent some of the problems encountered in the above section, especially the presence of water and the unwanted formation of dialkylperoxides, 2-methoxyprop-2-yl hydroperoxide may be an interesting alternative reagent to access the desired products (Figure 1.9).

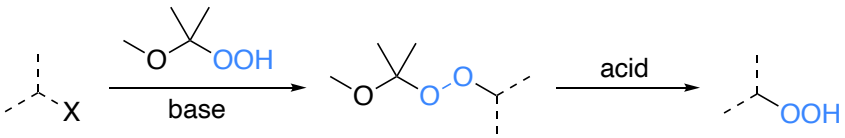

Figure 1.9. Formation of primary and secondary hydroperoxides using 2-methoxyprop-2-yl hydroperoxide

This perhemiketal, that is obtained from the ozonolysis of 2,3-dimethylbutene (cf. section 1.2.2.2), is alkylated to form an intermediate dialkylperoxide, which is further hydrolyzed to the desired hydroperoxide under acidic conditions.[62] However, the basic conditions face the same troubles of low yield and formation of side products as discussed above.

Hydroperoxymercuration

Particularly for the formation of secondary hydroperoxides, a method of Bloodworth describes their synthesis in a four step procedure and moderate to good yields (Figure 1.10).[63–65]

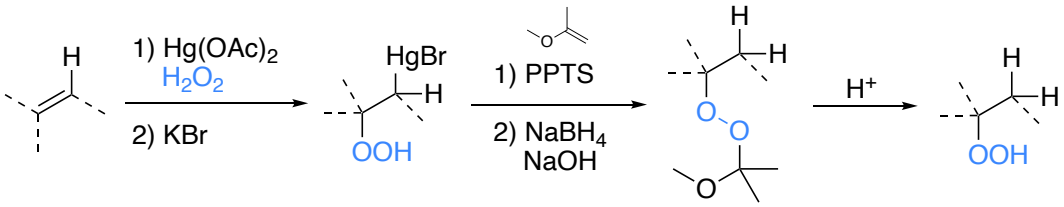

Figure 1.10. Bloodworths four-step hydroperoxymercuration method, PPTS = pyridinium p-toluenesulfonate

The obtained hydroperoxymercurials cannot be demercurated directly because the hydroperoxide group is reduced under these conditions. The hydroperoxide is therefore protected with 2-methoxypropene for the reductive demercuration step and subsequently deprotected under acidic conditions. Despite the good regioselectivity for the hydroxymercuration step, the use of organomercury compounds is a clear drawback of this method.

Addition of singlet oxygen to olefins

Singlet oxygen, generated from triplet oxygen by photosensitizers or UV light, reacts with olefins most probably *via* an 1,3-addition[66] (ene reaction, Figure 1.11) and concomitant allyl shift.

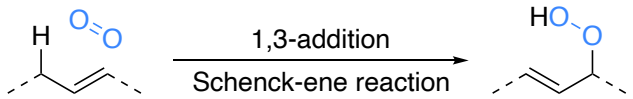

Figure 1.11. Formation of allylic hydroperoxides with singlet oxygen via the ene reaction

Since the first synthesis of Ascaridol in 1944 by Schenck and Ziegler[67], the method was regularly used for the synthesis of natural products (e.g., Plakorin[68]). Reactions via a diradical-, dipolar-, or two step mechanism have also been proposed (see section 1.2.2.3). The mechanism and stereocontrol of this reaction have been studied in detail (Figure 1.12).[69]

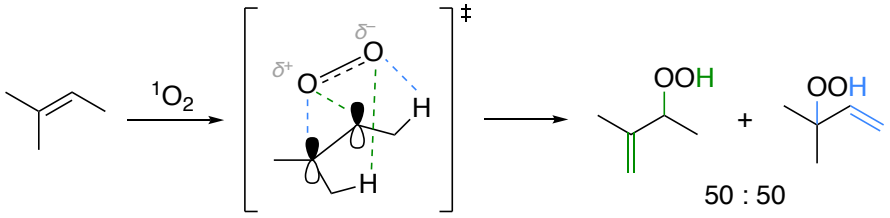

Figure 1.12. Transition state model for the hydroperoxidation of a trisubstituted olefin

A sterically controlled initial formation of an exciplex structure is proposed. In this transition state, an allylic proton is then abstracted, preferentially from the more substituted side of the double bond (*cis* effect). The transition state including the most allylic hydrogen atoms will lead to the major product. If one of the allylic position is more substituted than the other, the proton abstraction will take place there.[20] A mixture of hydroperoxides is obtained with diene systems as shown in the study of

linolenates by Chan[70]. Remarkably high stereo- and regioselectivity is observed for hydroperoxidation within zeolithes[71–73] or using soy bean lipoxygenase-1[74].

Addition of triplet oxygen to olefins (autoxidation)

Peroxygenation of alkenes with triplet oxygen is a radical chain reaction and proceeds *via* a mechanism very close to the one depicted in the athrahydroquinone autoxidation (Figure 1.7) and involves allyl radicals as intermediates. This reaction has been extensively studied – especially on polyunsaturated fatty acids (linolic acid, oleic acid, arachidonic acid, etc.) and the prostaglandin family, as they participate in a variety of metabolic processes.[12,19,75–77] Upon initial abstraction of a hydrogen atom, the generated radical can undergo reaction with oxygen and the peroxyl radical sustains the chain. The initiation step can be facilitated by azobisisobutyronitrile (AIBN)[78] or by a transition metal catalyst; e.g., cobalt(II) was extensively studied to catalyze hydroperoxidation (and triethylsilylperoxidation) of activated olefins and dienes.[79–83]

1.2.2.2 α-oxyperoxides

The group of α-oxyperoxides (also peracetals and perketals) encompasses several structural subclasses (Figure 1.13).[19] The analogous classes of α-aminoperoxides are not further discussed in this chapter as they exhibit similar properties to α-oxyperoxides and are not of significance in this thesis.[19]

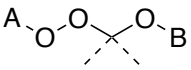

A	B	Name
H	H	α-hydroxyhydroperoxide
H	R	α-alkoxyhydroperoxide
H	OH	geminal bishydroperoxide
H	OR	α-hydroperoxyperoxide
R	H	α-hydroxyperoxide
R	R	α-alkoxyperoxide
R	OR	geminal diperoxide, peroxyketal

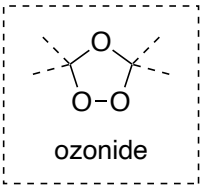

ozonide

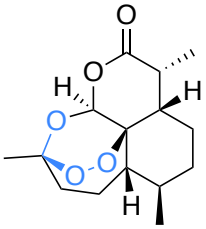

Artemisinin

Figure 1.13. Overview and examples of α-oxyperoxides

The best-known examples of α-oxyperoxides are probably the cyclic polymeric compounds that are formed from α-alkoxyhydroperoxides in acidic environment such as triacetone peroxide and the cyclic alkoxyperoxides (ozonides) which are formed during the ozonolysis process. These are generally very unstable, cannot be isolated easily and only few stable compounds are known.[19] α-Oxyperoxides are used for vulcanianzation, polymerization and hardening of polyester resins such as methyl ethyl ketone

peroxide.[19,21,84] Natural products bearing an α-oxyperoxide, particularly the 1,2,4-tetraoxane system as seen in Artemisinin[10], have attracted great interest due to their antimalarial properties.

Autoxidation

The activated α-position is prone to undergo autoxidation which follows the same pathway as already described for the formation of hydroperoxides (section 1.2.2.1). Autoxidation is the easiest for acetals, followed by ethers and lastly, alcohols. However, autoxidation processes are generally not of practical use because formation of product mixtures is possible. Ethereal solvents (diethyl ether, THF, dioxane, etc.) are prone to undergo autoxidation after prolonged exposure to UV-light resulting in the formation of α-oxyperoxides. They should therefore be stored in amber flasks or in the dark to minimize the risk of explosion upon concentration.[85,86]

Ozonolysis

After the formation of ozonides during ozonolysis, α-oxyperoxides can be formed as fragmentation products in the presence of alcohols. However, the process is not very selective and is thus not often of practical use.[21,87,88] Ozonolysis of 2,3-dimethyl-2-butene affords 2-methoxy-2-propyl hydroperoxide, which is used as a reagent for the synthesis of hydroperoxides (cf. 1.2.2.1).[62]

Addition of peroxides to carbonyl groups

Carbonyl electrophiles form a multitude of peroxides relatively easily, which is exemplified for ketones below (Figure 1.14).[19]

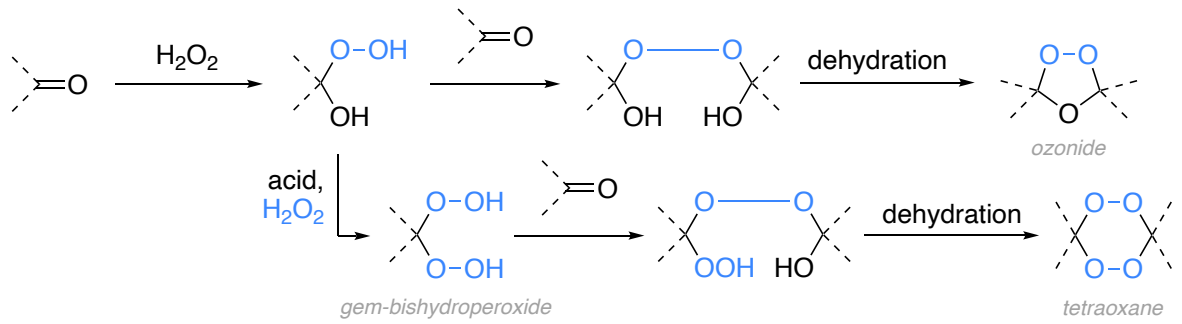

Figure 1.14. Selected examples of peroxide additions to ketones

The relatively stable *gem*-bishydroperoxides have been used as reagents for oxidation and epoxidation and are able to liberate singlet oxygen. They are accessible in high yields under (strongly) acidic conditions, or under mild conditions using Re_2O_7 as a catalyst[89]. They can react further to tetra- and hexaoxanes, which are of biological relevance since their antimalarial and antitumor activities have been shown to be equal to or higher than the activity of Artemisinin.[90–93]

1.2.2.3 Dialkyl peroxides

Depending on the size of the alkyl substituents, dialkyl peroxides are relatively stable and have variable decomposition temperatures, which makes them attractive as radical initiators for industrial

polymerization processes. Highly strained dialkyl peroxides such as dioxetanes are involved in bio- and chemiluminescence processes (cf. 1.2.2.6).

An important subclass of dialkyl peroxides (and of α-oxyperoxides) are endoperoxides, which are found in a variety of natural compounds and often show potent biological activity such as Cardamom Peroxide (antimalarial), Yingzhasou A (antimalarial), prostaglandins (hormones), Chondrillin (antitumor), Plakorin (antifungal & antibacterial).[20] Their formation is described later (cf. 1.4.2).

Alkylation of hydrogen peroxide or hydroperoxides

With (an excess of) alkylating agents, primary or secondary dialkyl peroxides are accessible from hydrogen peroxide or hydroperoxides. Tertiary dialkyl peroxides are obtained under acidic conditions from the corresponding olefins. Alternatively, upon treatment of β-halo hydroperoxides[46] with a base, the peroxide anion is able to substitute the halogen and form a 1,2-dioxetane (Figure 1.15).[94]

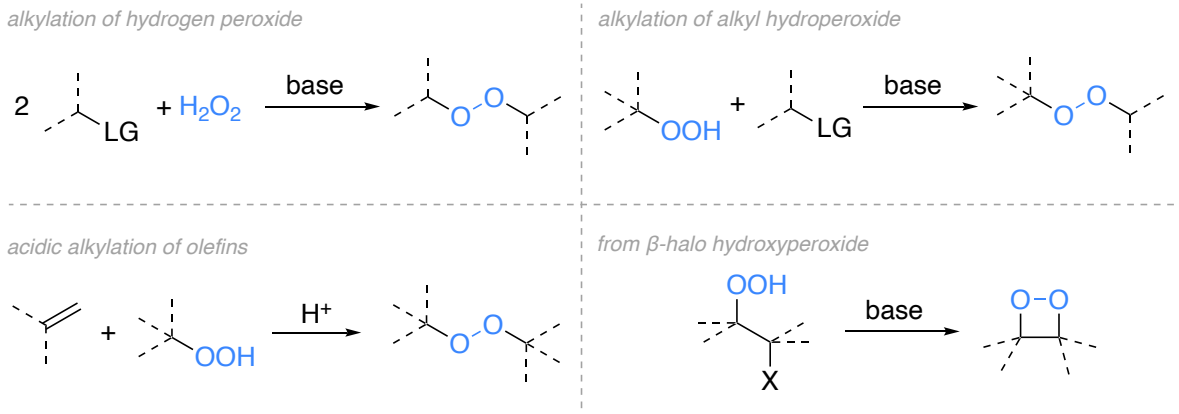

Figure 1.15. Formation of dialkyl peroxides from hydrogen peroxide or alkyl hydroperoxides; LG = suitable leaving group; X = halogen atom

Autoxidation

For the formation of dialkyl peroxides, autoxidation is only effective in a limited number of cases. The involved radicals have to be stabilized (e.g., *bis*-triphenylmethyl peroxide). With activated alkenes (styrene, vinyl chloride, etc.), autoxidation will lead to polymerization.[19]

Cycloadditions: 1,2-addition and 1,4-addition

The [2+2] cycloaddition of singlet oxygen (produced by UV-light or a photosensitizer) to electron rich olefins affords dioxetanes stereospecifically.[95] The ene reaction leading to allylic hydroperoxides is a known side reaction, especially for electron-poor alkenes.

The formation of endoperoxides *via* Diels-Alder type [4+2] cycloaddition of singlet oxygen was already used by Schenck in his first synthesis of Ascaridol (Figure 1.16, **left**).[67] However, all reactions involving singlet oxygen compete with each other, which is illustrated for the diene below and has been theoretically investigated in detail (Figure 1.16, **right**).[96,97]

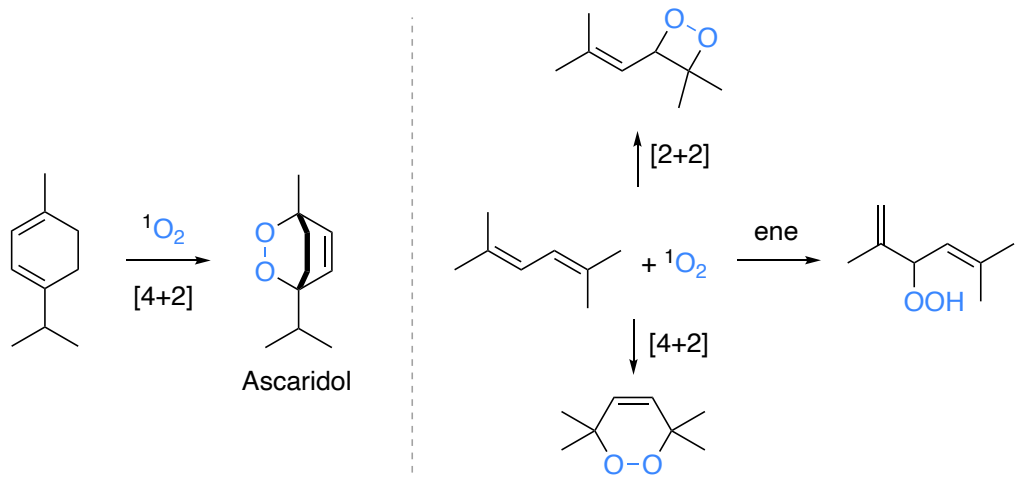

Figure 1.16. Formation of Ascaridol by Schenck (left) and possible products of the reaction of a diene with singlet oxygen (right)

The relative rate constants for the three possible reaction modes strongly depend on the substrate and the reaction conditions. For example, cyclohexadiene reacts exclusively to the endoperoxide whereas for substituted cyclohexadienes, a mixture of the endoperoxide and the hydroperoxide is observed. The competition between the ene reaction and the [2+2] addition on the same substrate can be illustrated on a simple example, for which several intermediates have been proposed (Figure 1.17).

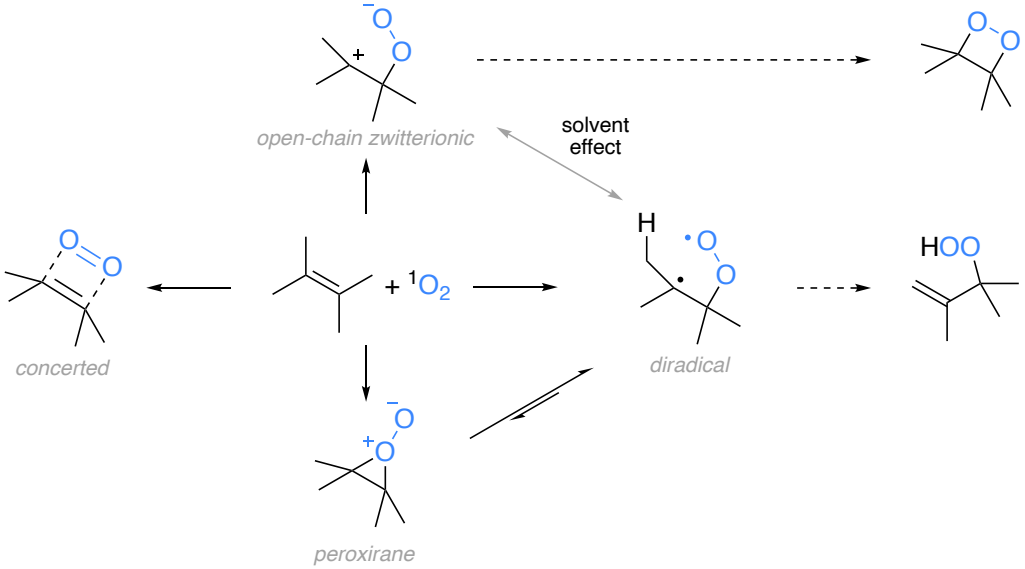

Figure 1.17. Proposed reactive intermediates for the formation of dioxetane and hydroperoxide upon singlet oxygen addition to an olefin

Questions about a concerted or a nonconcerted reaction mode have been raised for all pericyclic reactions.[98] The debate about the exact mode still continues but the diradical species has been identified in computational calculations as part of the lowest-energy pathways. The peroxirane represents a theoretically possible intermediate but since the formation of a 1,2-dioxirane product would require the passing over high energy barrier, reactions do not proceed *via* this pathway. The diradical species exhibits a rather large high dipole moment due to its zwitterionic character[99] which makes it possible that the solvent finally determines which pathway is followed: increasing solvent polarity could

enhance the zwitterionic character, which will ultimately lead to the dioxetane, whereas otherwise the formation of a hydroperoxide will occur by abstraction of an allylic proton. The experimental observation that the [2+2] addition is quite dependent on the solvent supports this theory.[96,97,100]

Other than from photoactivation, singlet oxygen can also be obtained from the molybdate catalyzed disproportionation of hydrogen peroxide. This “dark” singlet oxygen has been efficiently used in a well-controlled continuous flow process by Wirth.[101]

From inorganic peroxides

Strong inorganic oxidation agents are able to form peroxides from the corresponding ketones. For example, the selective oxidation reagent dimethyldioxirane (DMDO) is obtained from acetone reacted with Oxone® (potassium monoperoxosulfate) in a buffered aqueous solution. Advantageously, DMDO can be codistilled with acetone, resulting in a pure and exactly titratable solution, which is relatively stable over time. DMDO forms acetone as the only byproduct which is superior to many other oxidating or epoxidating reagents.[102]

Peroxymercuration

Mercury acetate promotes the formation of dialkyl peroxides in the presence of hydroperoxides in a two-step procedure.[21,103] The mercury-containing intermediates can be reductively demercurized as mentioned in before (chapter 1.2.2.1).

1.2.2.4 Peracids

Percarboxylic acids are generally less acidic than the corresponding carboxylic acid due to the absence of resonance stabilization of the carboxylate, and substitution effects on the pK_a are weak. Percarboxylic acids exhibit high oxidation potentials and are thus mainly used for oxidation and epoxidation reactions (e.g., using *m*-chloroperbenzoic acid, *m*CPBA). These compounds show explosive behavior if they are pure or highly concentrated, especially if the alkyl substituent is a short chain. Commercial percarboxylic acids are usually available in a stable phlegmatized form and purified (if necessary) only prior to use, e.g., by acid/base extraction. They enjoy increasing attention as bleaching and disinfectant agents due to their ecological safety. Several general methods exist to prepare percarboxylic acids.[19,21]

Acid catalyzed equilibration

Carboxylic acids react with hydrogen peroxide under acidic conditions and stand in an equilibrium with their corresponding peroxy form. The equilibrium is dependent on the proportion and concentration of hydrogen peroxide. However, the purification of the peracids may be tedious (continuous extraction, azeotropic distillation, selective precipitation of the product, etc.).

Autoxidation of aldehydes

Aldehydes react with oxygen to peracids in a radical autoxidation reaction. The drawback of this process is, that the excess of aldehyde can lead to a disproportionation to the carboxylic acid, which requires a careful control of the reaction conditions.

Perhydrolysis of acyl chlorides or esters

Under basic conditions, esters (and anhydrides), and acyl chlorides are reacted with hydrogen peroxide resulting in the desired peracids and one equivalent of chloride or alcohol, respectively. Likewise, the reaction also can be carried out with peroxydicarbonates or diacyl peroxides.

Under acidic conditions, peroxyketals that were described in chapter 1.2.2.1 are hydrolyzed to the peracid in good yields.[62]

1.2.2.5 Diacyl peroxides & percarbonates

Symmetrical diacyl peroxides like dibenzoyl peroxide (DBP) and a variety of percarbonates (e.g., diisopropyl peroxydicarbonate) are used mainly as hardeners or radical initiators for polymerization due to the low dissociation energy of the oxygen-oxygen bond. Depending on the substituent, these compounds are effective at variable temperatures (Figure 1.18).[19,104–106]

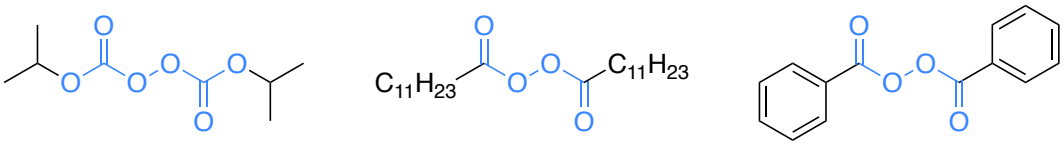

diisopropyl peroxydicarbonate
55 °C

dilauroyl peroxide
80 °C

dibenzoyl peroxide
95 °C

Figure 1.18. Examples of diacyl peroxydes and peroxydicarbonates; a half-life time of 1 hour is observed at the indicated temperature

If the substituent is not an aryl group, further dissociation of the carboxyl radical will lead to alkyl radicals after elimination of CO_2. Due to their explosive tendency, these compounds are commercially available only as phlegmatized mixtures.

Acylation

The main access to diacyl peroxides is the acylation of hydrogen peroxide or sodium peroxide with carboxylic acid chlorides or anhydrides. Moreover, they can also be obtained by the relatively easy acylation of percarboxylic acids under basic conditions. The same reaction with alkyl chloroformates yields percarbonates.

1.2.2.6 Peresters & peroxyoxalates

Percarboxylic acid esters are mostly used as precursor compounds of alkyl radicals after liberation of CO_2 – especially the *tert*-butyl esters are preferred due to their facile homolytic cleavage.[19,107] Unsymmetric esters afford a carboxyl radical (or alkyl radical) and an alkoxy radical after scission of the

peroxide bond. Especially copper(I) ions efficiently induce the decomposition of peresters.[19] Peresters are prone to undergo facile hydrolysis and if the *OO*-substituent is a primary or secondary alkyl group, a rapid decomposition to aldehydes or ketones and a carboxylic acid takes place upon increased temperature (Figure 1.19).[108,109]

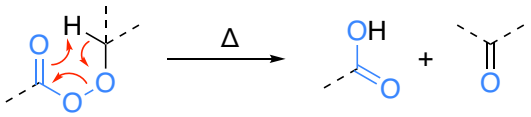

Figure 1.19. Thermal decomposition of primary or secondary peresters

A special class of peresters is formed under photochemical conditions in the atmosphere as part of smog. Volatile organic compounds (VOC) react with atmospheric nitrogen and oxygen to peroxyacyl nitrates (PAN) which are relatively stable and act as strong lachrymatory and irritating agents. Due to their high solubility in water, they are well absorbed on skin and thus suspected of causing skin cancer.[110–112]

Esterification

As percarboxylates are not particularly nucleophilic, the esterification of a percarboxylic acid and a suitable alkylating agent is not effective. Therefore, ester formation is usually performed by acylation (using acyl chlorides or anhydrides) of alkyl hydroperoxides under basic conditions or by esterification of hydroperoxides and carboxylic acids under acidic conditions.[19]

Cyclodehydration

An alternative pathway to form perester is the cyclodehydration of α-hydroperoxycarboxylic acids, e.g., by using dicyclohexylcarbodiimide (DCC) as a coupling reagent leading to 1,2-dioxetanes (Figure 1.20, **top left**).[113] Fireflies are able to form and decompose such 1,2-dioxetan-3-ones enzymatically for bioluminescence.

From oxalic acid derivatives

Oxalyl chloride reacts with hydroperoxides under basic conditions and form disubstituted peroxyoxalates (Figure 1.20, **top right**). These compounds are known as potent low-temperature radical initiators such as di-*tert*-butyl peroxyoxalate.[114,115] In a more special case, oxalic acid diesters react with hydrogen peroxide to 1,2-dioxetane-3,4-dione. The later spontaneously decays into two molecules of CO_2, out of which, one is in an excited state. This excited CO_2 molecule is able to activate a fluorophore, which emits a photon upon relaxation to the ground state (Figure 1.20, **bottom**). This process is utilized in chemiluminescent assays in biochemistry and immunology.[113]

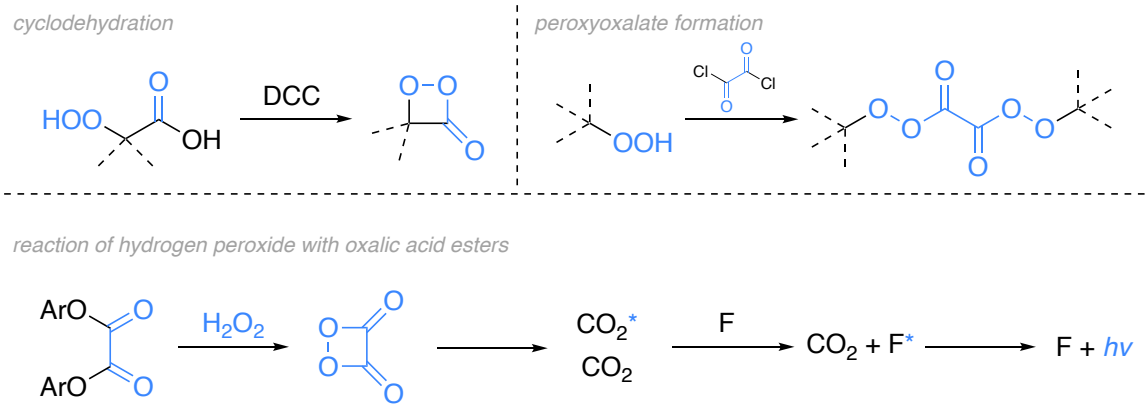

Figure 1.20. Formation and decay of 1,2-dioxetane-3,4-dione; F = fluorophore

1.3 Organic peroxides as a source of radicals

1.3.1 General considerations

Handling and storage

On small scale, the adequate use of personal protective equipment (PPE) and standard safety precautions is sufficient for safe handling of organic peroxides. On larger scales (e.g., several grams, several millimoles), increased protection with a blast shield and cutting proof gloves or the use of tongs is recommended. In all cases, unintentional exposure to heat, shock, and contamination (dust, traces of metals, ash) must be avoided. The chemical compatibility of the employed compounds should always be checked in advance using standard reference literature.[16,19] If the compound is not described, the risk should be estimated on related compounds.

Hydrogen peroxide and organic peroxides should be destroyed prior to disposal by prolonged reductive treatment (sodium thiosulfate or iron(II) sulfate) or under acidic conditions using iodide mixtures.[116] Spills can be cleaned up with large amount of water or adequate organic solvent with subsequent treatment of the used material with one of the above solutions.

Explosive potential, self-accelerating decomposition temperature (SADT)

Pure liquid hydrogen peroxide is especially insensitive to mechanic stress whereas highly concentrated aqueous solutions pose an extreme explosive potential.[117] Organic peroxides are not professionally employed as explosives but they generally represent compounds that are particularly unstable and may thus explode unintentionally.[118] Depending on the structure and the kind of peroxide involved, the sensitivity towards external influences may differ significantly. In general, the sensitivity is increased if:

- a highly polarized and thus weak peroxide bond is present (e.g., dialkyl peroxide vs. diacyl peroxide)
- compounds have a high oxygen content (e.g., diacetyl peroxide vs. dilauroyl peroxide).
- compounds are pure or highly concentrated (e.g., crystalline vs. solubilized form)

To estimate the explosive potential of peroxides, tests of detonation and deflagration ability, energy release, and sensitivity towards stress, friction and heat are evaluated.[19] Organic peroxides should always be stored cold and well below their indicated self-accelerating decomposition temperature (SADT).[119,120]

Toxicity

Apart from their effect as local skin irritants causing dermatitis, their ability to generate free radicals has been discussed to cause indirect carcinogenicity. However, due to the relatively high reactivity of the peroxides, they are quickly metabolized to lesser toxic metabolites such as carboxylic acids or alcohols. Volatile compounds like *tert*-butyl hydroperoxide pose a higher risk because of possible inhalation and damage of internal organs.[121,122]

Active oxygen

One of the two oxygen atoms in a peroxide bond is termed *active* and thus the term refers to the relative concentration of peroxide-bound oxygen in a given compound. Generally, the energy content and therefore the physical hazard associated with the peroxide correlates with the amount of active oxygen. For any given compound it is defined as follows:

$$active\ oxygen\ content\ (\%) = \frac{number\ of\ peroxide\ groups}{molecular\ mass\ [g/mol]} \times 16\ [g/mol] \times purity\ (\%)$$

Very high numbers are reached in small molecules like methyl hydroperoxide (33.3%) or methyl ethyl ketone peroxide (22.8%).

1.3.2 Fragmentation and decarboxylation reactions

The oxygen-oxygen single bond stands out as a labile structural feature of all organic peroxides. Several different types of radical can be formed from organic peroxides such as alkyl, alkoxy, peroxyl, and acyloxy radicals (Figure 1.21).

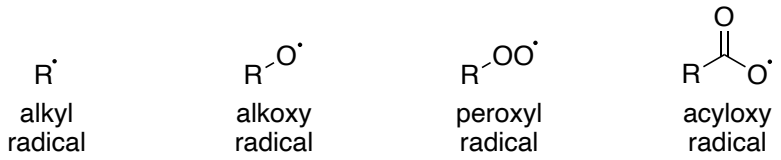

Figure 1.21. Types of radicals accessible from organic peroxides

Compared to the mean bond dissociation energy (BDE) of a carbon-carbon bond (ca. 85 kcal/mol), the BDE of a peroxide bond is half as much or even less, as the following figure shows for some selected examples[123,124] (Figure 1.22).

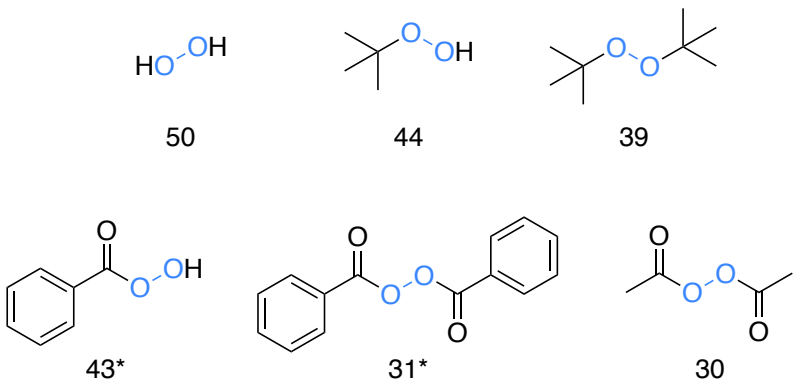

*Figure 1.22. BDE values for selected organic peroxides [kcal/mol]; *calculated values[124]*

Together with azo initiators (e.g., AIBN), peroxides are most widely used thermal radical initiators. The detailed decomposition mechanism, however, has been discussed controversially since the seminal studies by Kharash in the late 1940s.

1.3.2.1 Mechanism of decomposition

Multiple decomposition pathways have been proposed and investigated, particularly in the case of diacetyl peroxide (Figure 1.23).[125–128] Szwarc has shown that diacetyl peroxide irreversibly decomposes in a first-order reaction.[129,130] Besides CO_2, methane, ethane, and methyl acetate have been identified as the major products.

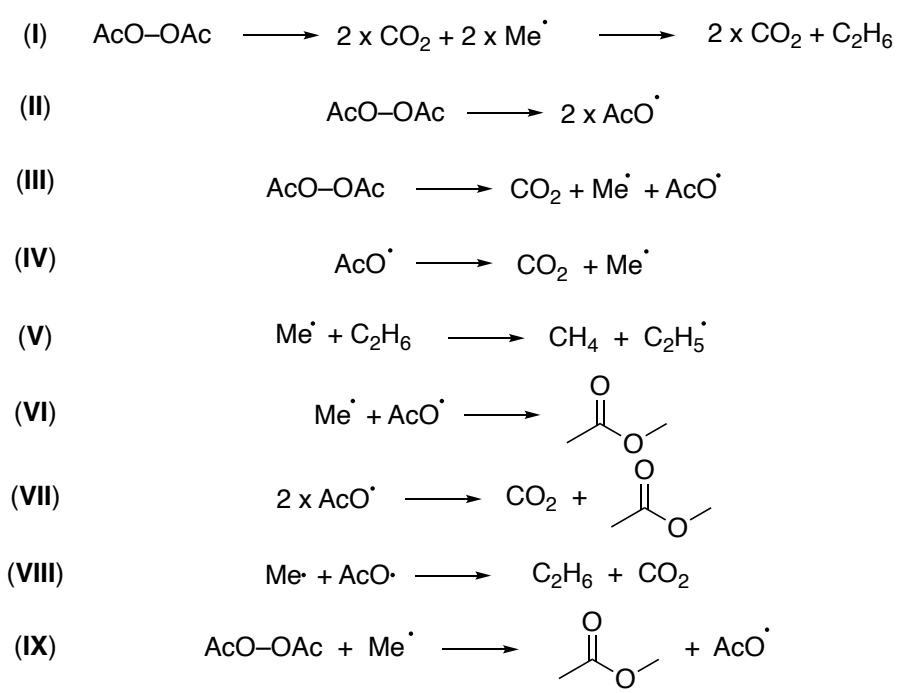

Figure 1.23. Proposed reactions in diacetyl peroxide decomposition

The simultaneous breaking of all three bonds (**I**) resulting in CO_2 and ethane alone is very unlikely. The initial cleavage of only one bond, the peroxide bond (**II**), resulting in two acetoxy radicals or a two-bond cleavage (**III**) are much more likely[131] and in good accordance to experimental observations by Kharash.[132] The decomposition of diacetyl peroxide was shown to be viscosity-dependent. This is explained by an in-cage recombination of the two acetoxy radicals, which has approximately the same rate constant as the decarboxylation reaction.[133]

Other than recombining to diacetyl peroxide, the acetoxy radicals can further decompose *via* the mentioned decarboxylation process to give carbon dioxide and the corresponding alkyl radical (**IV**) – a process which is fast because the extrusion of carbon dioxide is thermodynamically favored.[134] The life-time of an acetoxy radical (4.3×10^{-10} seconds at 60 °C) is about an order of magnitude longer than the life-time of a pair of methyl radicals until they recombine in-cage to ethane (in the order of 10^{-11} seconds[133]). Thus, the formation of ethane gas through recombination of two methyl radicals occurs only after a certain time frame during which the radicals are able to diffuse out of the solvent cage.[133] This is supported by the observation that higher amounts of ethane are observed in more viscous solvents that hinder the radicals in diffusing far away from each other.

In any case, only a small amount of ethane gas is observed, which points out that only a fraction of the methyl radicals undergoes dimerization.[135] Szwarc also observed variable quantities of methane, which can originate from the reaction of the free methyl radicals with ethane (**V**). This could be the reason for the decreased formation of ethane at higher temperatures.[130] However, the reactive methyl radicals can not only abstract hydrogen atoms from ethane but also from the solvent or other scavengers such as quinone which keeps the amount of ethane low.[135]

Moreover, it is important to understand the formation of methyl acetate. On the one hand, its formation can be explained by a direct recombination of an acyl radical with a methyl radical in a solvent cage (**VI**)[136]. However, if this is true, the activation energy for such a process has to be very low.[133] The disproportionation of two acyl radicals (**VII**) forming carbon dioxide and methyl acetate as well as the formation of ethane and carbon dioxide from a methyl radial and an acetoxy radical (**VIII**) have been described not to be of major importance.[137]

More interestingly, methyl acetate is efficiently formed by the induced decomposition of diacetyl peroxide by a methyl radical (**IX**). The formed acetoxy radical will quickly decompose to form a new methyl radical, which can induce the next decomposition, and thus sustains the chain.[132,138,139] Such a mechanism is particularly important for thermally more stable compounds as it allows an efficient decomposition at temperatures below their thermal decomposition temperature.

A computational study by Balbuena showed that the initial one-bond or two-bond cleavage strongly depends on the kind of substituent. The presence of electron donating groups (e.g., in diacetyl peroxide or also in dimethyl peroxocarbonate) results in a stronger peroxide bond and thus, preferentially a one-bond cleavage with subsequent decarboxylation. The more polarized the peroxide bond gets under the influence of electron withdrawing substituents, the more likely the two-bond cleavage gets as shown for trifluoroacetyl peroxide.[140] Interestingly, the BDE of the ROO–H bond in hydroperoxides is independent on the alkyl group and its α-substitution since this seems to influence only the R–OOH or the RO–OH bond BDE.[141]

1.3.2.2 Kinetics of decarboxylation and fragmentation reactions

Alkyl radicals can not only be formed by decarboxylation but also by fragmentation of (tertiary) alkoxy radicals e.g., originating from dialkyl peroxides. The rate of decarboxylation and fragmentation correlates with the stability of the generated radical (tertiary > secondary > primary > methyl > phenyl) and is generally very fast (Table 1.1).[142]

Table 1.1. Decarboxylation- and fragmentation rates of acyloxy- and alkoxy radicals

Reaction scheme	Solvent, T	k [s^{-1}]
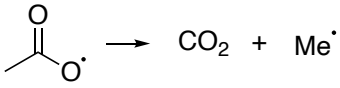	*n*-hexanes, 60 °C	1.6×10^9 [133]
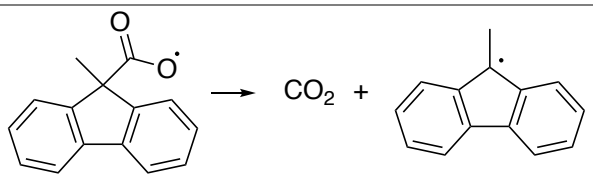	CH_3CN, rt	1.8×10^{10} [143]
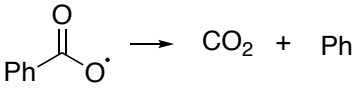	CCl_4, rt	$\sim 10^6$ [143]
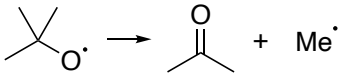	CCl_4, rt	1.0×10^4 [144]
	PhH, rt	1.4×10^4 [144]
	t-BuOH, rt	1.9×10^5 [144]
	acetic acid, rt	3.4×10^5 [144]
	H_2O, rt	1.4×10^6 [145]
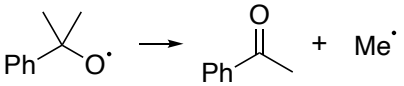	PhH, rt	3.7×10^5 [146]
	t-BuOH, rt	5.8×10^5 [146]
	CH_3CN, rt	6.3×10^5 [146]

The formation of alkyl radicals *via* a decarboxylation is generally a very fast process with little difference if the formed radical is stabilized or not (methyl vs. fluorene). An exception is the formation of aryl (and vinyl[147]) radicals since the dissociation energy for the fragmentation of the C–C bond connecting the aryl and the carbonyl moiety is higher, which results in a much lower rate constant. In fact, the decarboxylation rates are so slow that hydrogen atom transfer reactions ($k \approx 10^7$ s^{-1}) start to compete and thus, the corresponding aryl carboxylic acid are often formed.[148]

The fragmentation rates of alkoxy radicals are several orders of magnitudes slower than the decarboxylation rates of acyloxy radicals and are also relatively solvent dependent.

1.3.2.3 Solvent and concentration effects

In the gaseous phase, the energy to break the peroxide bond equals the total amount of energy needed to decompose the peroxide compound. In a solvent, the same amount of energy is needed to break the peroxide bond, but the energy needed to decompose the compound is higher. As the decomposition takes place in a solvent cage, the fragments have to leave this cage prior to recombination in order to decompose further. This makes the overall energy needed to decompose the compound higher than in the gaseous phase. It has been experimentally shown that the rates of recombination indeed increase

at lower temperatures at which the radicals are moving less. This is also the case for peroxides other than diacetyl peroxides (e.g., di-*tert*-butyl peroxide, benzoyl peroxide, and *tert*-butyl perbenzoate).[129]

The variation of the concentration in highly diluted systems (below 0.1 mol/L) causes a change in the reaction rate of only a few percentages, and in solutions below 0.01 mol/L, the reaction rates almost perfectly fit first-order kinetics. A tenfold increase in concentration in solutions above 0.1 mol/L results in an increased rate of about 10%, for which an induced decomposition is suggested (1.3.2.1, **IX**). Interestingly, the kinetic behavior seems to be independent of the nature of the solvent (e.g., aromatic, aliphatic, polar, acids).[129]

If one compares different classes of peroxides, their behavior may be significantly different than the one described for diacetyl peroxide. Especially compounds susceptible to induced decomposition and polar effects may exhibit a dramatically different behavior in different solvents. For example, diisopropyl peroxydicarbonate (IPP) shows a significantly altered 10 h half-life depending on the solvent: 18 °C in methanol, 35 °C in benzene, 45 °C in aliphatic hydrocarbons, 50 °C in trichloroethylene.[149]

1.3.3 Organic peroxides as radical initiators

1.3.3.1 Thermal initiation

Organic peroxides play an important role in the plastics industry where they are used as initiators for radical polymerizations.[150] Mostly, these peroxides are decomposed thermally and some have been studied by calorimetry in great detail.[151–153] As discussed in the previous chapter, the strength of the peroxide bond and thus the stability of the peroxide is largely dependent on the structure of the adjacent functional groups. This allows to choose the right peroxide-based initiator according to the desired decomposition temperature. The following figure shows typical temperature ranges for the 10-hour half-life of different classes of organic peroxides (Figure 1.24).

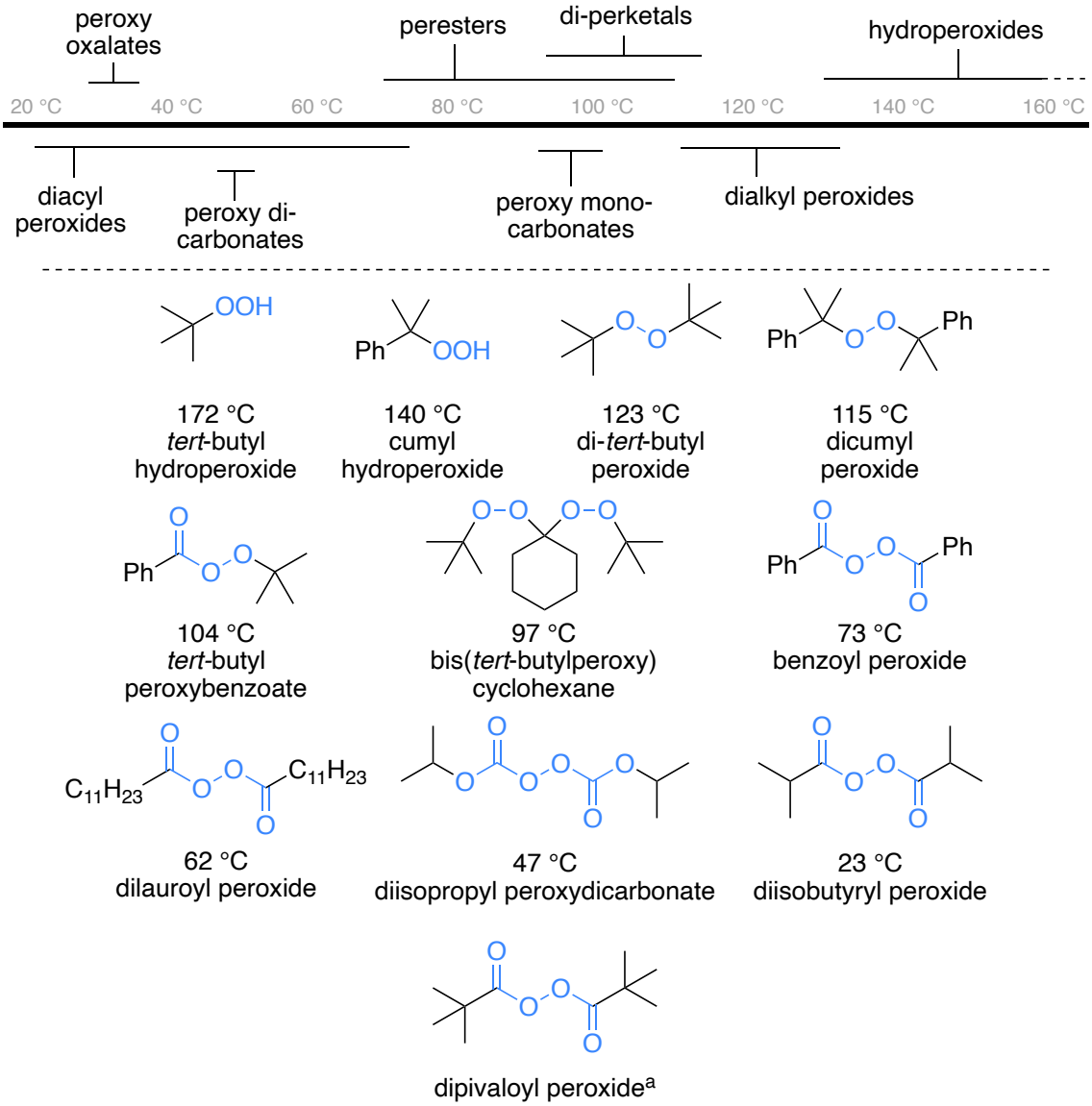

Figure 1.24. 10-hour half-life temperature for different peroxide classes; [a] exact temperature not available

In the case of diacyl peroxides, one can increase the reactivity by increasing the relative stability of the radical formed after homolytic cleavage (e.g., diacetyl vs. diisobutyryl peroxide). However, one has to

be careful what to aim for. If the generated radical is too stable or if the rate of decomposition is increased too much, the process may be less effective to initiate further reactions and might also pose a considerable risk during handling.[154] For example, dipivaloyl peroxide is even less stable than isobutyryl peroxide.[155]

It is apparent that some classes show a much greater variability of the half-life temperature than others. This is generally the case, if the substituents have a large effect on the stability of the compound. In turn, if this effect is small, the half-life temperatures remain almost unchanged in the entire class.[149,156,157] Detailed reviews exist for many peroxide-based initiators.[104,114,158]

1.3.3.2 Induced initiation

Alkoxy radicals

Faster decomposition rates have been observed for diacyl peroxides, if they face presence of alkoxy radicals. They are able to react with the peroxide bond or an aryl moiety and thus induce the decomposition. The change in decomposition rate is depending on the solvent.[159–161]

Acidic conditions

Alkyl hydroperoxides and *gem*-bisperoxides are usually not used as thermal initiators, partly due to their high half-life temperature but also because they can be much more conveniently used at low temperatures by induced initiation under various conditions. Under acidic conditions, vinyl peroxides are formed relatively easily from ketones with hydroperoxides or by hydrolysis of *gem*-bisperoxides.[162] These decompose to the desired alkoxy radical and an α-carbonyl radical at room temperature or even below 0 °C, which is much lower than their thermal decomposition temperature (Figure 1.25).[163]

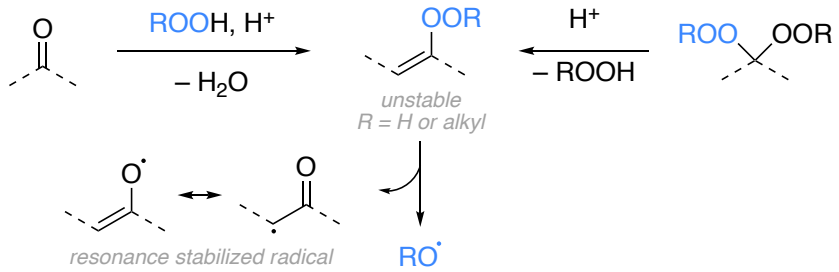

Figure 1.25. Acid catalyzed formation of unstable vinyl peroxides

The use of hydrogen peroxide or *gem*-dihydroperoxyketals under the same reaction conditions affords hydroxy radicals.[162]

Transition metal catalysis

Since many peroxides are sensitive to the presence of transition metals (e.g., iron, cobalt)[149,164] or non-metals such as iodine/iodide, redox chemistry is another attractive method to activate these initiators, namely by Fenton-type chemistry as exemplified for hydroperoxides[163] (Figure 1.26).

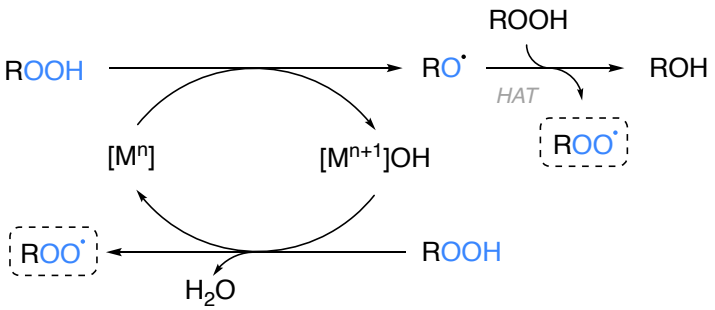

Figure 1.26. Fenton-type generation of radicals from hydroperoxides; HAT = hydrogen atom transfer

The reaction of a hydroperoxide and a transition metal proceeds *via* single electron transfer (SET) and leads to an alkoxy radical and a metal hydroxide. This radical is able to abstract a hydrogen atom from another hydroperoxide due to its low BDE and polar effects, leading to an alcohol and a peroxyl radical. The metal hydroxide itself will react further as well. A second SET and abstraction of a hydrogen atom from a hydroperoxide will lead to water and another peroxyl radical. Overall, Fenton-type chemistry results in the formation of peroxyl radicals, water and alcohols when starting from alkyl hydroperoxides. An analogous reaction was discovered by Kharasch in which peresters are cleaved homolytically to afford alkoxy radicals using copper species.[165,166] Copper and iron salts have been used to decompose dialkyl peroxides.[167,168] Advantageously, multiple oxidation states of the metals are able to induce the decomposition of the peroxide in a catalytic manner as seen in the above figure. Reductive processes generate the desired alkoxy radical by peroxide bond cleavage whereas oxidative processes generate peroxyl radicals. Apart from the widely used promotors in the polymer industry such as cobalt naphthenate, also a transition metal contamination is able to induce such peroxide decomposition. This poses a significant safety risk, if the metals are mixed with the peroxide unintendedly. Obviously, if the peroxide decomposes to multiple radicals from one molecule (e.g., peroxalates), and is susceptible to induced decomposition, the process can become autocatalytic and lead to explosions, if gaseous products are formed. In order to design an efficient radical reaction, be it for preparative or for polymerization purposes, it is often important to reduce and optimize the amount of metal ion promotors. If the concentration of transition metal is too high in a given solution, the reaction of a radical with the metal ion can trap the radical and generate ions, which stops the chain process since these species are not able to sustain or initiate the desired processes anymore.[163]

Photoactivation

Diacyl peroxides absorb radiation below 300 nm[169] but the use of photosensitizers is usually preferred over direct irradiation.[170,171] The photolysis of acetyl peresters was used for example by Watt for selective generation of alkoxy radicals in steroid analogues.[172] Interestingly, the decomposition mechanism is slightly different from the thermal one, which proceeds *via* a one-bond cleavage resulting in two benzoyloxyl radicals. Photolysis, however, triggers a two-bond cleavage similar to what was discussed above (cf. 1.3.2). In case of benzoyl peroxide, the photoactivated moiety fragments twice, leading to a phenyl radical and carbon dioxide whereas the other moiety ends up as a benzoyloxyl

radical. This radical does not behave differently to the thermally generated ones and is thus not in an excited state.[173] About 20% of the radicals in this process recombine to phenyl benzoate.[104,174,175]

1.3.3.3 Type of generated radicals

The following types of radicals can be formed from peroxide-based radical initiators (Figure 1.27). Acyloxy radicals usually decompose so rapidly that they are not used for preparative applications.

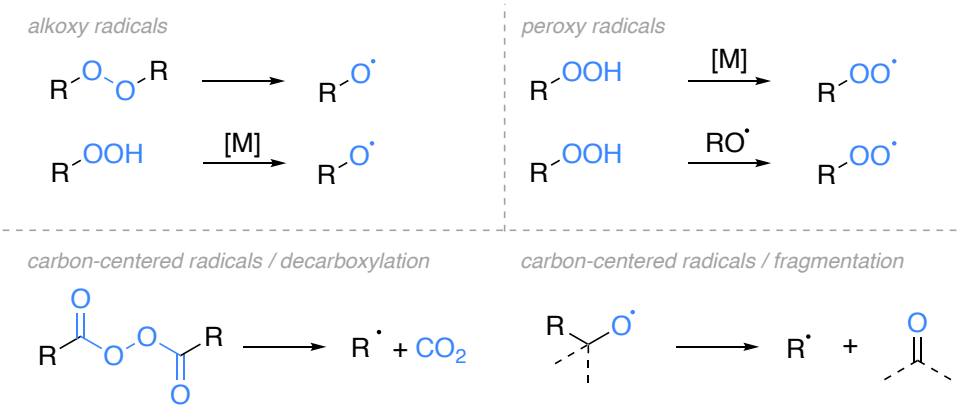

Figure 1.27. Types of radicals generated from peroxide-based radical initiators

Alkoxy radicals:

Under thermal conditions, homolytic cleavage of dialkyl peroxides leads directly to alkoxy radicals whereas decomposition of peroxyoxalates and peroxydicarbonates is accompanied by the elimination of carbon dioxide. Unsymmetrical peresters generate at least one alkoxy radical. Alkoxy radicals can also be generated from hydroperoxides by induced decomposition under acidic condition or using a variety of salts or complexes of transition metals, namely from cobalt[149], iron[52,176] and copper.[56,57]

Peroxy radicals:

Initiation of peroxides in combination with metals (or iodine species) leads to peroxy radicals either directly by hydrogen atom abstraction or indirectly by hydrogen atom abstraction of intermediate alkoxy radicals.[163] The proton can also be abstracted by alkoxy radicals.

Carbon-centered radicals / decarboxylation:

Decomposition of diacyl peroxides leads to acyloxy radicals, which can react directly (which is rare due to their high rate of decarboxylation) or decarboxylate further to give the corresponding aryl (e.g., from dibenzoyl peroxide) or alkyl radicals (e.g., dilauroyl peroxide). The reactivity (and life-time) of the acyloxy radical (decarboxylation vs. hydrogen abstraction leading to carboxylic acids) seems to be influenced by its formation.[177]

Carbon-centered radicals / fragmentation:

Alkoxy radicals, especially tertiary ones, are well known to undergo β-scission to a ketone and a carbon-centered radical. The fragmentation rate is greatly depending on the stability of the generated radical

and thus increased in the case of highly stabilized carbon-centered radical.[178] However, the fragmentation pathway is an attractive option to generate non-stabilized methyl radicals by "deacetonation" from *tert*-butoxy radicals.[179–182]

1.4 Concepts and name reactions

The following chapter gives an overview about general concepts and name reactions of radical reactions starting from or involving organic peroxides.

1.4.1 Wieland rearrangement

The first free-radical rearrangement was described more than a hundred years ago by Heinrich Otto Wieland in 1911 when heating *bis*(triphenylmethyl)peroxide (Figure 1.28).[183]

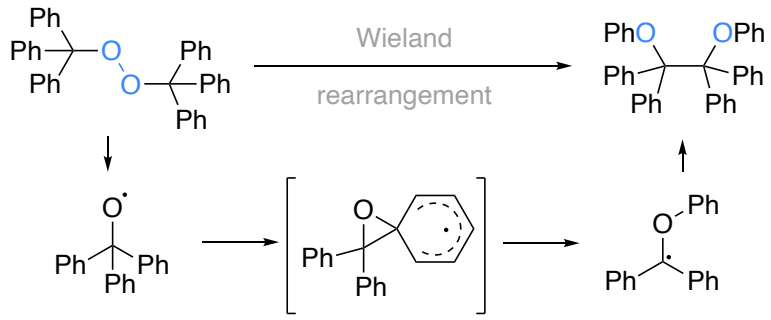

Figure 1.28. Mechanism of the Wieland rearrangement

The dialkyl peroxide decomposes thermally into two alkoxy radicals which undergo phenyl migration and the two rearranged radicals then dimerize to the final product. The epoxy radical intermediate has been computationally confirmed almost hundred years after the original publication. The rate of the rearrangement decreases with increasing solvent polarity.[184]

1.4.2 Endoperoxide formation

Peroxy radicals are formed upon fast trapping of molecular oxygen by alkyl radicals (cf. 1.2.2.1) or by abstraction of the hydroperoxide's hydrogen atom.[185] This task can be accomplished by oxygen as observed in the Schenck and Smith rearrangement, by alkoxy or other peroxy radicals[186], or using metal catalysts.[12,163,187] Since the BDE of the hydroperoxide H–O bond is ca. 15-20 kcal/mol weaker than the corresponding alcohol H–O bond, alkoxy radicals are suitable to initiate radical reactions of peroxyl radicals. Using low-temperature initiators, these reactions can take place under mild conditions.[20]

Since the peroxyl radical reacts efficiently with internal olefins, endoperoxides become accessible. In the presence of two olefins at different positions, the 5-*exo* cyclisation takes place selectively.[188] The spirocyclisation of akene hydroperoxides was studied for the formation of Cardamom peroxide

analogues and has shown that the process is effective for 5-*exo* and 6-*exo* cyclisations but failed for 7-*exo* cyclisations.[189] The 6-*exo* cyclisation has been beautifully used for the consecutive formation of endoperoxides by Porter (Figure 1.29). [190,191]

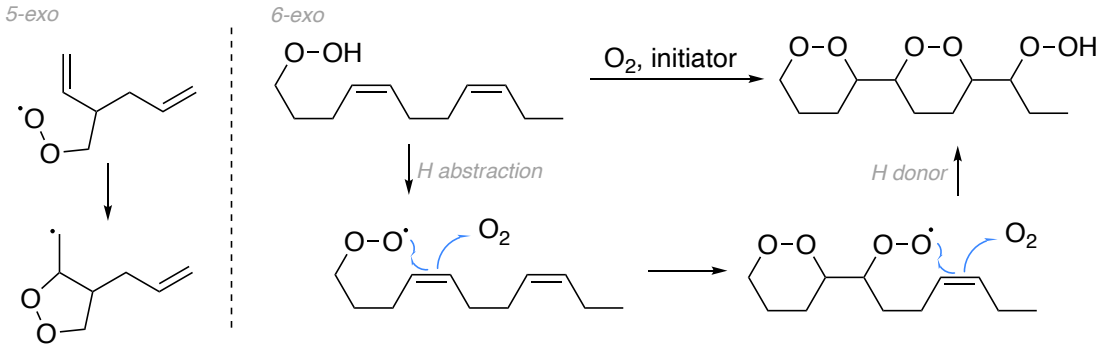

Figure 1.29 5-exo and 6-exo cyclisation cascade for endoperoxide formation

Polyenes have been studied in particular detail to form endoperoxides because they occur naturally in many lipids (e.g., arachidonic acid) and derivatives thereof. The autoxidation of such polyenes results in a complex mixture of hydroperoxides and has been thoroughly investigated by Porter.[185,192,193] Along with Porter, also Corey was working on lipid hydroperoxides and has used a hydroperoxide derivative of arachidonic acid for his synthesis of prostaglandin PGG_2. In this work, he introduced a new method to access peroxyl radicals using samarium diiodide and oxygen.[12] Proposedly, the mixture contains a samarium peroxide intermediate ($I_2Sm–OO–SmI_2$) which fragments to a samarium oxide radical that acts as active species to abstract a hydrogen atom. This method was used effectively in the synthesis of Yingzhaosu C by Boukouvalas.[187]

1.4.3 Rearrangements of allyl hydroperoxides

In 1958, Schenck discovered a rearrangement of cholesterol-derived hydroperoxides in chloroform.[194] The mechanism of this allylic rearrangement (with retention of stereochemistry) has been investigated in detail only several decades later but was basically already correctly proposed by Schenck early on.[195] One and a half decades later, Smith discovered a second rearrangement on the same substrate that lead to the epimerization of the hydroperoxide group (Figure 1.30).[196]

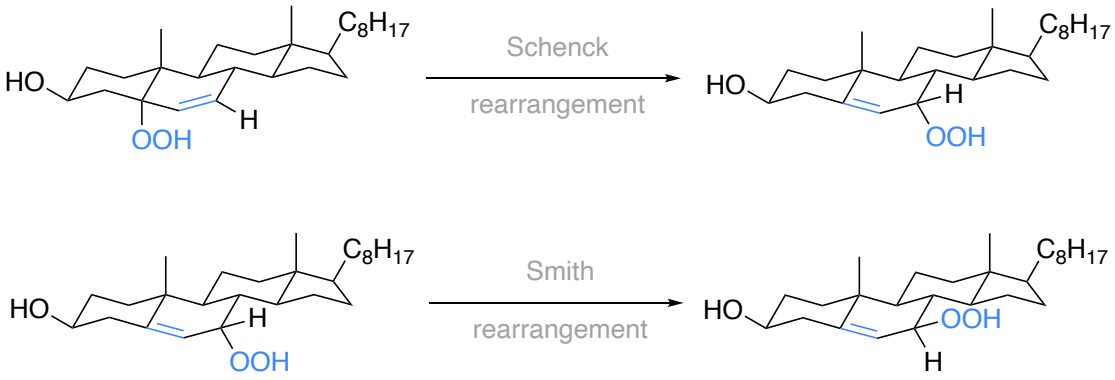

Figure 1.30. Original discoveries of the Schenck and Smith rearrangements

Schenck rearrangement

The mechanism of the slow Schenck rearrangement has been investigated in detail.[99,197–199] The early finding, that the process can be accelerated using radical initiators or transition metal salts pointed out, that the basis has to be a radical mechanism, which was later confirmed by EPR spectroscopy.[200]

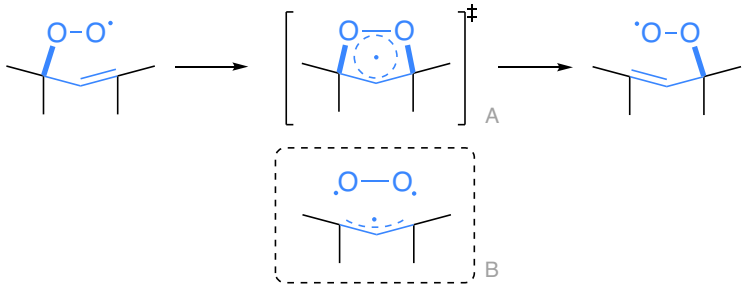

Figure 1.31. Mechanism of the Schenck rearrangement via a cyclic transition state (A) or caged radicals (B)

The reaction is initiated by abstraction of the hydroperoxide and final position of the equilibrium follows the stability of the involved olefin (disubstituted vs. trisubstituted olefin) and is greatly influenced by steric effects.[197] Porter proposed that the transformation proceeds *via* a 5-membered transition state (Figure 1.31, **A**), which explains the stereoselectivity already noticed in the original discovery and was confirmed in experiments with acyclic systems.[201] However, the stereochemical "memory" could also be explained by a strongly caged[199] and, at least to some degree, dissociated intermediate of an allyl radical and triplet oxygen (**B**). Beckwith and later also Porter suggest this based on the fact that at increased temperatures and depending on the solvent viscosity, the incorporation (or loss) of ^{18}O-labelled triplet oxygen is observed.[200,202–204] The competition between hydrogen abstraction and the Schenck rearrangement pathway has been used in radical clock experiments to measure rate constants.[205] In addition to these mechanistic studies, the stereospecific Schenck rearrangement has been successfully applied as a key step in the total synthesis of Plakorin and *enantio*-Chondrillin by Dussault.[68]

Smith rearrangement

Mechanistically, the Smith rearrangement is very close to the Schenck rearrangement. It is believed, that in this case, the degree of dissociation of the allyl radical and the oxygen is higher, which allows the oxygen to move relatively freely to the other side of the allyl radical. Moreover, an increased exchange with external oxygen is expected in this case.[185] (Figure 1.32).

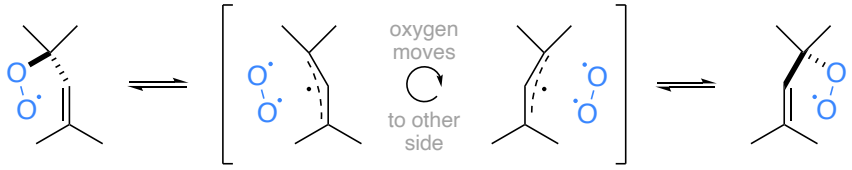

Figure 1.32 Proposed mechanism of the Smith rearrangement

Only few examples have been reported of this very slow and reversible epimerization process and only partial conversion was achieved. [200,206,207]

1.4.4 Story reaction

Thermal (mostly above 150 °C) or photolytic decomposition of cyclic di- and triperoxides is a general method to form macrocyclic compounds and was discovered by Story in the late 1960s. However, a mixture of a cycloalkane, a lactone and a ketone is obtained in variable proportions depending on the mode of decomposition (Figure 1.33).[208–212]

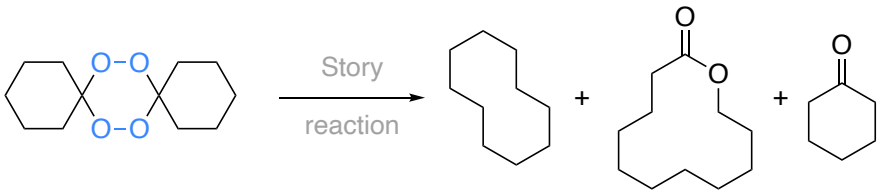

initiation	cycloalkane (%)	lactone (%)	ketone(%)
thermal	44	23	21
photolytic	14	10	20

Figure 1.33. Story's original discovery of the reaction

Mechanistically, what happens first is the initial homolytic cleavage of a peroxide bond. If, after the formation of the initial diradical, the loss of molecular oxygen takes place and leads to the formation of the observed ketone. If this oxygen extrusion does not take place, an intermediate cyclic diacyl peroxide is formed, which decomposes very quickly at these high temperatures. If both of the acyloxy radicals undergo decarboxylation, the cyclic diradical can recombine and form a cycloalkane. If only one of the two decarboxylations takes place, a lactone is formed; probably *via* in-cage recombination of the acyloxy radical and the alkyl radical. Since the mixture of products obtained in this reaction suffer from poor selectivity, the reaction is mostly applied to unsaturated endoperoxides for the formation of diepoxides and epoxyketones (Figure 1.34).[213]

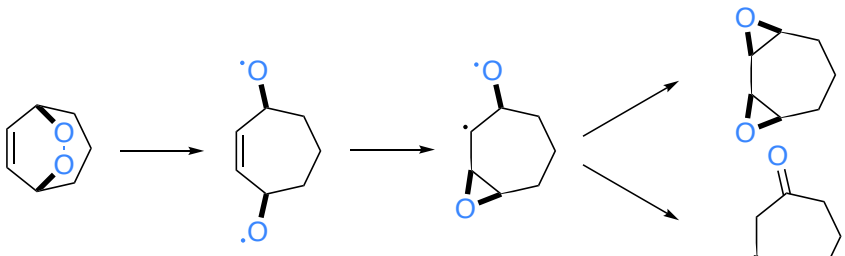

initiation	diepoxide (%)	keto epoxide (%)
thermal	90	10
photolytic	33	67

Figure 1.34. Mechanism and obtained products of the Story reaction of unsaturated endoperoxides

Here, the diradical reacts swiftly with the olefin forming a first epoxide and a carbon centered radical. At this stage, a hydrogen atom shift and collapse of the alkoxy radical will produce a ketone. Alternatively, a recombination of both radicals will lead to the formation of a second epoxide.

Interestingly, under photolytic conditions, the keto epoxide is obtained as the major product – opposite to what is obtained for the same reaction under thermal conditions. This is explained by the formation of a triplet biradical (which is more probable under photolytic conditions) and thus, a longer life-time of the radical which delays the formation of the diepoxide and ultimately leads to the formation of the ketone.[214] However, also conformational effects largely influence the observed product proportions.[215] Under much milder conditions, the reaction can be initiated using transition metals (particularly iron), which mostly suppresses the formation of ketones.[216]

1.4.5 Alkoxy radicals and hydrogen atom transfer

1.4.5.1 Generation of alkoxy radicals

Despite the versatile utility of alkoxy radicals, their synthetic access remains a challenge and many methods have been invented to address the problems that these methods still have. Limitations are caused by chemical incompatibility, toxicity, poor atom economy, and, not rarely, high costs. Hartung has reviewed many current strategies to access alkoxy radicals from the corresponding alcohols.[217] The most straightforward access to alkoxy radicals is, obviously, by homolytic cleavage of an alcohol O–H bond. However, due to the high BDE of this bond, this is not a facile approach.[218] Direct oxidation of an alcohol can be achieved using a strong oxidant (e.g., $Pb(OAc)_4$, I_2/PhIO, I_2/HgO),[217,218] Suarez cleavage[219], proton-coupled electron transfer (PCET)[220–223], or ligand-to-metal electron transfer (LMCT).[224,225]

Another approach is the formation of a weak O–X bond in order to facilitate a homolytic cleavage of this bond. Be it, by conversion of alcohols into labile heteroatom-ethers (e.g., O–N, O–S, O–Cl) or by substitution of the alcohol with a moiety that already contains a weak O–X bond (e.g., *N*-alkoxy compounds or peroxides).[217] Most interestingly, peroxides have some advantageous features that other precursors do not have. For example, the atom economy can be better, one can choose the "mode" of initiation (which is depending on the peroxide), introduction of (hydro-)peroxides is relatively easily and cheap, and (at least some peroxide classes) are rather stable. After Barton's pioneering nitrite (RO–NO) homolysis[226], Smith[227] and Walling[228–230] introduced hypochlorite (RO–Cl) homolysis to access alkoxy radicals (Figure 1.35).

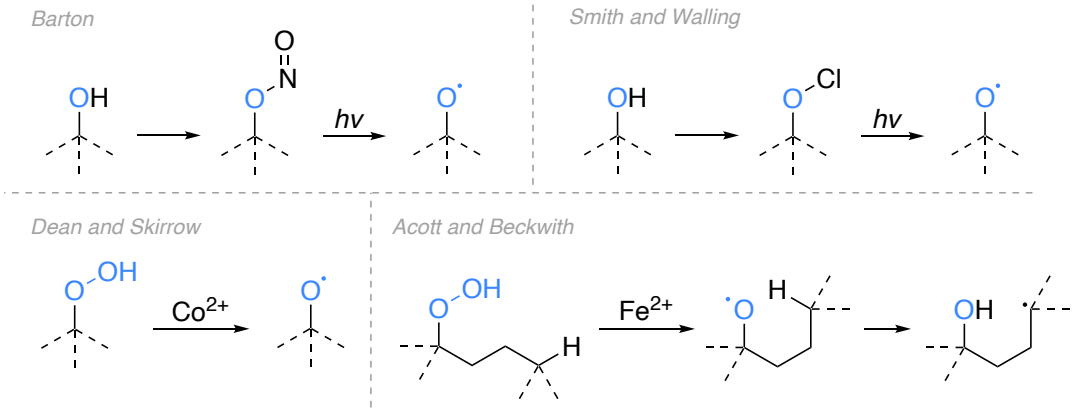

Figure 1.35. Concepts of Barton, Smith and Walling to access alkoxy radicals

In parallel to the studies on those type-**I** precursors, Dean and Skirrow found that hydroperoxides are decomposed to alkoxy and peroxyl radicals by cobalt(II) and cobalt(III) species, respectively.[231] At the same time, Kochi reported that diacyl and dialkyl peroxides as well as peresters and hydroperoxids are readily decomposed to alkoxy radicals using catalytic amounts of copper(I) salts and other reducing agents leading to unsaturated alcohols.[232] The formed copper(II) species is reduced back to copper(I) by a carbon centered radical ultimately leading to olefins *via* oxidative elimination.[233,234] Acott and Beckwith made use of this reaction too and described the iron(II) mediated δ-hydroxylation (in the presence of water), δ-chlorination (in the presence of copper(II) chloride) and the formation of δ,ε-unsaturated alcohols, however, with little selectivity.[235]

1.4.5.2 Reactions of alkoxy radicals

A wide range of reactions involve alkoxy radicals and their reactivity is subdivided in five general groups as depicted in pathways a-e below (Figure 1.36).[217]

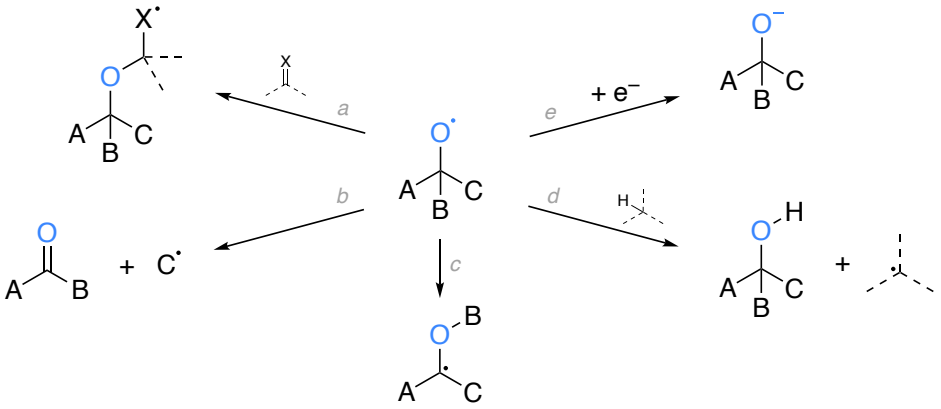

Figure 1.36. Basic reaction (a-e) of alkoxy radicals with substituents A, B, C not further specified

a. Addition to multiple bonds resulting in (cyclic) ethers.
b. Homolytic cleavage (β-scission) leading to a carbonyl and an alkyl radical. In cyclic molecules, this process results in a ring opening.
c. Rearrangements as described previously (e.g., Wieland rearrangement, chapter 1.4.1)
d. Homolytic substitution with relocation of the radical. If this process takes place intramolecularly, the hydrogen atom transfer relocates the radical to a remote position.
e. Single electron transfer (SET) reactions. Since alkoxy radicals are highly oxidizing species, only reductions are of synthetic significance. In the presence of reducing metal ions, the ratio between fragmentation and reduction is largely depending on the structure of the alkoxy radicals.[232]

Hydrogen atom transfers involving alkoxy radicals

Since the time when Hofmann (later also Löffler and Freytag) discovered hydrogen atom transfer reactions involving *N*-centered radicals, almost 150 years have passed and much research has been conducted.[236,237] A breakthrough was the research of Barton who, in analogy to the Hoffman-Löffler-Freytag reaction, developed the first alkoxy radical based C-H functionalization in 1961.[226] Since then,

also hydroperoxides have repetitively been used as alkoxy radical precursors to obtain remotely functionalized alcohols in a selective fashion.[238] For primary *n*-alkyl alkoxy radicals, the 1,5- and 1,6-HAT are entropically and thermodynamically favored over other "1,*n*-HAT" reactions. (Figure 1.37).[235,239–242]

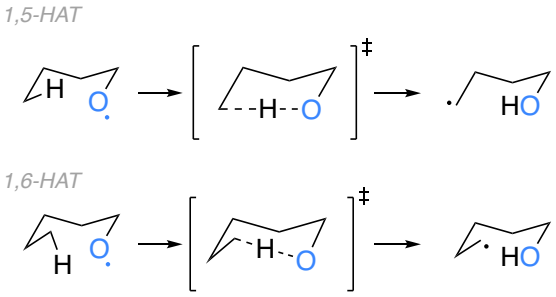

Figure 1.37 Transition states for 1,5- and 1,6-HAT reactions

Interestingly, a perfect 6-membered chair-like structure in the transition state is not favorable for a 1,5-HAT since the most favored transition state structure for an efficient reaction features an almost linear C–H–O arrangement. This leads to a pseudo 5-membered *envelope*-conformation but with one long side.[240] Similarly, the 7-membered transition state of a 1,6-HAT resembles more closely a chair conformation of a 6-membered ring, again, with one long bond. Therefore, a 7-membered transition state is, counterintuitively, thermodynamically slightly favored by 0.8 kcal/mol.[241] However, if entropic factors are also considered, then the 1,5-HAT is overall favored by about 1.8 kcal/mol free energy which makes the 1,5-HAT (2.7 x 10^7 s^{-1} at 20 °C[243]) about 10 times faster than the 1,6-HAT.[238,239] Exception to this are cases in which no hydrogen atom is present at the 5' position, other C–H bonds are significantly more activated (e.g., benzylic, tertiary, etc.), or when the geometry does not support a HAT to take place.[238,244]

1.4.5.3 Selective δ-functionalization starting from hydroperoxides

Čeković, a student of Walling, investigated the synthetic use of the relocated radical in more detail based on the preceding studies (Figure 1.38).[245]

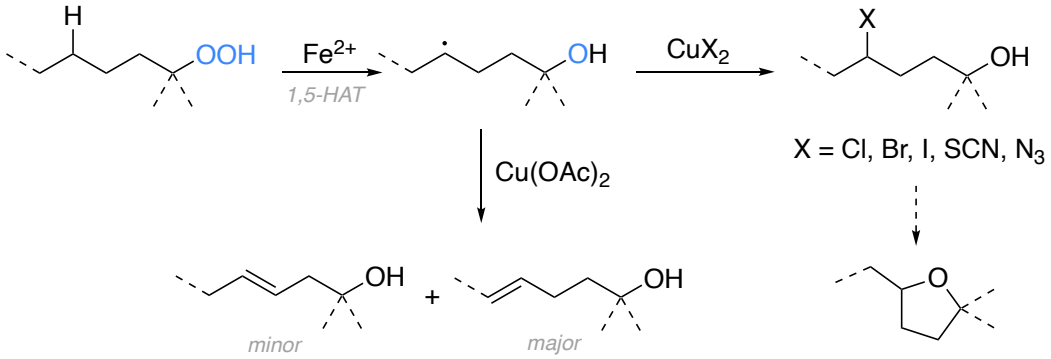

Figure 1.38. Čeković's use of the relocated radical

After reduction of the hydroperoxide to the corresponding alkoxy radical and subsequent 1,5-HAT, it was found that the relocated radical undergoes oxidative elimination to the unsaturated alcohol in the

presence of copper(II) acetate.[246,247] The major formation of the γ-δ olefin can be explained by the more favorable arrangement in the transition state in which the copper atom is complexed between the carbocation on one side and the oxygen atom on the other side.[235] If copper(II) salts other than acetate are used, the δ-position is selectively functionalized with halides, isocyanates or azides. If the installed (secondary) functional group is a good leaving group too, intramolecular nucleophilic substitution will lead to the formation of tetrahydrofuran derivatives.[247,248]

In a relatively recent report of Ball, this methodology was extended to a copper catalyzed process that uses an ammonium chloride salt as the chloride source for remote C–H chlorination. Copper(I) serves as reducing agent to form the alkoxy radical required for HAT. The formed copper(II) chloride species then serves as the effective chlorinating agent of the relocated radical like in the work of Čeković. Choice of the right amine catalyst, presence of water and acidic conditions appear to be of central importance to effect the desired transformation with only little formation of the corresponding ketone or non-functionalized alcohol. Advantageously, alkoxy radicals can be formed under these conditions from primary, secondary, and tertiary hydroperoxides (Figure 1.39, left).[56]

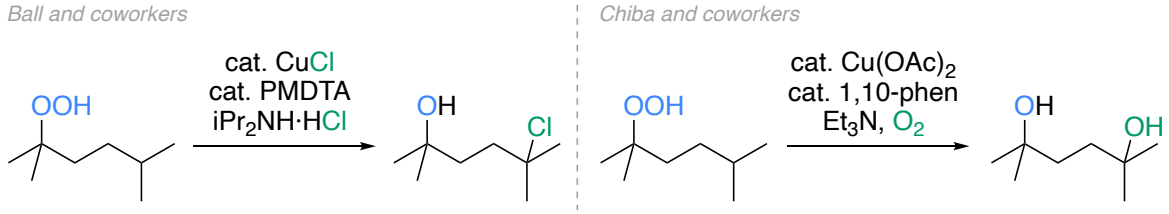

Figure 1.39. Copper catalyzed methods for 1,5-chlorination and -hydroxylation reported by Ball and Chiba (PMDTA = N,N,N′,N′′,N′′-pentamethyldiethylenetriamine; 1,10-phen = 1,10-phenanthroline)

A method related to the one reported by Ball was published by Chiba for the formation of 1,4-diols from hydroperoxides (Figure 1.39, right). Single-electron reduction of copper(II) to copper(I) by triethylamine affords the active copper species that effects the reductive cleavage of the hydroperoxide. After 1,5-HAT, the resulting radical is trapped by molecular oxygen forming an intermediate copper(II)-peroxide species which will lead to the desired 1,4-diol. However, if the relocated radical is a secondary radical, an oxidation to the ketone may represent a competing reaction.[57]

A different approach to access 1,4 diols, inspired by the oxidative metabolism of heme iron complexes, was reported by Taniguchi, who combined the autoxidation of alkenes and iron catalyzed alkoxy radical formation (Figure 1.40).[249]

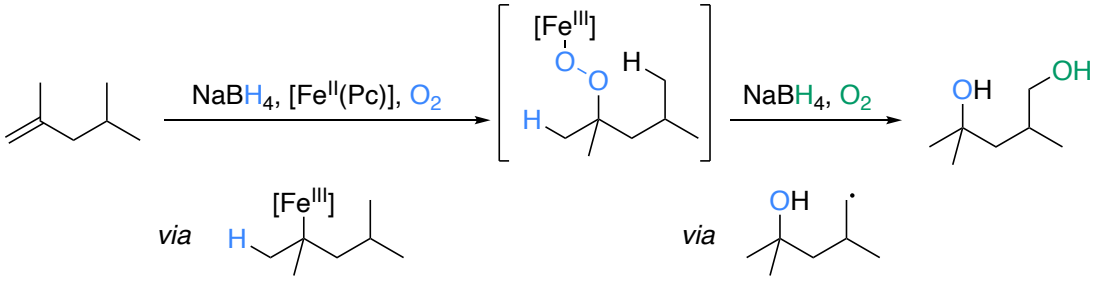

Figure 1.40. Taniguchis 1,4-diol synthesis from alkenes; Pc = phtalocyanine

In the presence of an iron(II) phtalocyanine complex and sodium borohydride, the alkene is reduced and an intermediate organo-iron(III) complex. Oxygen insertion into the iron-carbon bond results in an iron-peroxide intermediate. Reductive cleavage of this iron peroxide species (in analogy to the process presented above for hydroperoxides) will lead to the desired alkoxy radical which undergoes 1,5-HAT. Under the present reaction conditions, the relocated radical will be trapped by molecular oxygen and reduced by sodium borohydride, resulting in the final 1,4-diol similar to the work of Chiba.[249]

1.5 Summary

Organic peroxides are derivatives of hydrogen peroxide and contain at least one weak oxygen-oxygen bond as a common structural feature. The physical instability of these compounds makes their synthesis not only challenging from a synthetic point of view but is also technically demanding. Many synthetic methods have been developed to access organic peroxides; all of them use either molecular oxygen, hydrogen peroxide, or another organic peroxide as reactants.

Organic peroxides take part in a multitude of radical reactions due to the easy homolytic cleavage of the peroxide bond. On industrial scale, organic peroxides are mainly used as radical initiators under thermal or metal catalyzed conditions. Moreover, the synthesis of organic peroxides is of great importance for preparative chemistry since many naturally occurring compounds that contain a peroxide are biologically active, which makes these compounds a worthwhile target for pharmaceutical research.

1.6 References

[1] Thenard, Gilbert, *Annalen der Physik* **1820**, *64*, 1–30.

[2] H. Offermanns, G. Dittrich, N. Steiner, *Chemie in unserer Zeit* **2000**, 10.

[3] J. M. Campos-Martin, G. Blanco-Brieva, J. L. G. Fierro, *Angewandte Chemie International Edition* **2006**, *45*, 6962–6984.

[4] H. Schildknecht, K. Holoubek, *Angewandte Chemie* **1961**, *73*, 1–7.

[5] E. H. White, E. Rapaport, H. H. Seliger, T. A. Hopkins, *Bioorganic Chemistry* **1971**, *1*, 92–122.

[6] F. McCapra, in *Methods in Enzymology*, Elsevier, **2000**, pp. 3–47.

[7] E. K. Nelson, *J. Am. Chem. Soc.* **1913**, *35*, 84–90.

[8] W. Fenical, *J. Am. Chem. Soc.* **1974**, *96*, 5580–5581.

[9] Coordinating Group for Research on the Structure of Qing Hau Sau, *Kexue Tongbao (Chinese Edition)* **1977**, *22*, 142.

[10] Qinghaosu Antimalaria Coordinating Research Group, *Chinese Medical Journal* **1979**, *92*, 811.

[11] M. Hamberg, J. Svensson, B. Samuelsson, *PNAS* **1974**, *71*, 3824–3828.

[12] E. J. Corey, Z. Wang, *Tetrahedron Letters* **1994**, *35*, 539–542.

[13] P. Nesvadba, in *Encyclopedia of Radicals in Chemistry, Biology and Materials*, American Cancer Society, **2012**.

[14] *Prudent Practices in the Laboratory: Handling and Management of Chemical Hazards, Updated Version*, National Academies Press, Washington, D.C., **2011**.

[15] In *A Comprehensive Guide to the Hazardous Properties of Chemical Substances*, John Wiley & Sons, Ltd, **2006**, pp. 719–740.

[16] R. Pohanish, S. Greene, *Wiley Guide to Chemical Incompatibilities*, **2009**.

[17] F. Schoofs, *Journal de Pharmacie de Belgique* **n.d.**, *11*, 1929.

[18] E. J. Schwoegler, *Chemical & Engineering News* **1985**, *63*, 6.

[19] H. Klenk, P. H. Götz, R. Siegmeier, W. Mayr, in *Ullmann's Encyclopedia of Industrial Chemicals*, Wiley-VCH, **2011**.

[20] Z. Rappoport, *The Chemistry of Peroxides*, **2006**.

[21] J. Sanchez, T. N. Myers, in *Kirk-Othmer Encyclopedia of Chemical Technology*, American Cancer Society, **2000**.

[22] H. Jakob, S. Leininger, T. Lehmann, S. Jacobi, S. Gutewort, in *Ullmann's Encyclopedia of Industrial Chemicals*, Wiley-VCH, **2011**.

[23] K. Krumova, G. Cosa, **2016**, 1–21.

[24] W. C. Schumb, C. N. Satterfield, R. L. Wentworth, *Hydrogen Peroxide*, Massachusetts Institute Of Technology, **1953**.

[25] A. S. Rao, H. R. Mohan, J. Iskra, in *Encyclopedia of Reagents for Organic Synthesis*, American Cancer Society, **2013**.

[26] D. D. Davis, **2005**, 300.

[27] *J. Chem. Technol. Biotechnol.* **1900**, *19*, 766–808.

[28] L.-C. Maillard, *Bull. Soc. chim* **1900**, 559–563.

[29] J. H. Walton, H. A. Lewis, *J. Am. Chem. Soc.* **1916**, *38*, 633–638.

[30] F. R. Paulsen, *Chemistry and Industry* **1956**, 1274.

[31] P. Dussault, *Safe Use of Hydrogen Peroxide in the Organic Lab*, **2018**.

[32] S. W. Benson, *J. Chem. Phys.* **1960**, *33*, 306–307.

[33] Bozo. Plesnicar, Stane. Kaiser, Andrej. Azman, *J. Am. Chem. Soc.* **1973**, *95*, 5476–5477.

[34] D. J. Mckay, J. S. Wright, *J. Am. Chem. Soc.* **1998**, *120*, 1003–1013.

[35] P. S. Nangia, S. W. Benson, *J. Phys. Chem.* **1979**, *83*, 1138–1142.

[36] X. Xu, W. A. Goddard, *PNAS* **2002**, *99*, 15308–15312.

[37] D. Barnard, K. R. Hargrave, G. M. C. Higgins, *J. Chem. Soc.* **1956**, 2845.

[38] T. A. Nijhuis, M. Makkee, J. A. Moulijn, B. M. Weckhuysen, *Ind. Eng. Chem. Res.* **2006**, *45*, 3447–3459.

[39] N. Oku, J. Tsuji, *Process for Producing Propylene Oxide*, **2004**, US20040133018A1.

[40] H. Hock, S. Lang, *Berichte der deutschen chemischen Gesellschaft (A and B Series)* **1944**, *77*, 257–264.

[41] C. Walling, S. A. Buckler, *J. Am. Chem. Soc.* **1955**, *77*, 6032–6038.

[42] I. Klement, P. Knochel, *Synlett* **1995**, *1995*, 1113–1114.

[43] Yu. N. Ogibin, A. O. Terent"ev, V. P. Ananikov, G. I. Nikishin, *Russian Chemical Bulletin* **2001**, *50*, 2149–2155.

[44] Y. N. Ogibin, A. O. Terent'ev, A. V. Kutkin, G. I. Nikishin, *Tetrahedron Letters* **2002**, *43*, 1321–1324.

[45] M. Schulz, A. Rieche, K. Kirschke, *Chem. Ber.* **1967**, *100*, 370–374.

[46] K. R. Kopecky, J. H. van de Sande, C. Mumford, *Can. J. Chem.* **1968**, *46*, 25–34.

[47] H. R. Williams, H. S. Mosher, *J. Am. Chem. Soc.* **1954**, *76*, 2987–2990.

[48] H. R. Williams, H. S. Mosher, *J. Am. Chem. Soc.* **1954**, *76*, 2984–2987.

[49] A. G. Davies, R. V. Foster, R. Nery, *J. Chem. Soc.* **1954**, *0*, 2204–2209.

[50] S. S. Medwedew, E. N. Alexejewa, *Ber. dtsch. Chem. Ges. A/B* **1932**, *65*, 137–142.

[51] R. Criegee, G. Müller, *Chemische Berichte* **1956**, *89*, 238–240.

[52] H. Guan, S. Sun, Y. Mao, L. Chen, R. Lu, J. Huang, L. Liu, *Angewandte Chemie International Edition* **2018**, 11413–11417.

[53] Y. L. Tnay, G. Y. Ang, S. Chiba, *Beilstein Journal of Organic Chemistry* **2015**, *11*, 1933–1943.

[54] D. A. Casteel, K.-E. Jung, *J. Chem. Soc. Perkin Trans. 1* **1991**, 2597–2598.

[55] C. Chatgilialoglu, M. Ballestri, D. Vecchi, D. P. Curran, *Tetrahedron Letters* **1996**, *37*, 6383–6386.

[56] R. Kundu, Z. T. Ball, *Org. Lett.* **2010**, *12*, 2460–2463.

[57] P. C. Too, Y. L. Tnay, S. Chiba, *Beilstein J. Org. Chem.* **2013**, *9*, 1217–1225.

[58] A. J. Bloodworth, J. L. Courtneidge, R. J. Curtis, M. D. Spencer, *J. Chem. Soc., Perkin Trans. 1* **1990**, 2951–2955.

[59] A. A. Frimer, *J. Org. Chem.* **1977**, *42*, 3194–3196.

[60] B. M. Choudary, N. Narender, V. Bhuma, *Synlett* **1994**, *1994*, 641–642.

[61] T. G. Driver, J. R. Harris, K. A. Woerpel, *J. Am. Chem. Soc.* **2007**, *129*, 3836–3837.

[62] P. Dussault, A. Sahli, *J. Org. Chem.* **1992**, *57*, 1009–1012.

[63] A. J. Bloodworth, M. D. Spencer, *Journal of Organometallic Chemistry* **1990**, *386*, 299–304.

[64] A. J. Bloodworth, C. J. Cooksey, D. Korkodilos, *Journal of the Chemical Society, Chemical Communications* **1992**, *0*, 926–927.

[65] A. J. Bloodworth, R. J. Curtis, M. D. Spencer, N. A. Tallant, *Tetrahedron* **1993**, *49*, 2729–2750.

[66] A. A. Frimer, *Chem. Rev.* **1979**, *79*, 359–387.

[67] Günther, O. Schenck, K. Ziegler, *Naturwissenschaften* **1944**, *32*, 157–157.

[68] P. H. Dussault, K. R. Woller, *J. Am. Chem. Soc.* **1997**, *119*, 3824–3825.

[69] L. M. Stephenson, M. J. Grdina, M. Orfanopoulos, *Acc. Chem. Res.* **1980**, *13*, 419–425.

[70] H. W.-S. Chan, *J Amer Oil Chem Soc* **1977**, *54*, 100–104.

[71] R. J. Robbins, V. Ramamurthy, *Chem. Commun.* **1997**, 1071–1072.

[72] X. Li, V. Ramamurthy, *J. Am. Chem. Soc.* **1996**, *118*, 10666–10667.

[73] E. L. Clennan, J. P. Sram, A. Pace, K. Vincer, S. White, *J. Org. Chem.* **2002**, *67*, 3975–3978.

[74] G. Iacazio, G. Langrand, J. Baratti, G. Buono, C. Triantaphylides, *J. Org. Chem.* **1990**, *55*, 1690–1691.

[75] H. W. Gardner, *Free Radical Biology and Medicine* **1989**, *7*, 65–86.

[76] P. E. Correa, G. Hardy, D. P. Riley, *J. Org. Chem.* **1988**, *53*, 1695–1702.

[77] C. Schneider, N. A. Porter, A. R. Brash, *Chem. Res. Toxicol.* **2004**, *17*, 937–941.

[78] A. S. K. Hashmi, M. C. Blanco Jaimes, A. M. Schuster, F. Rominger, *J. Org. Chem.* **2012**, *77*, 6394–6408.

[79] Y. Matsushita, K. Sugamoto, T. Matsui, *Chemistry Letters* **2006**, 1381–1384.

[80] K. Sugamoto, Y. Matsushita, T. Matsui, *J. Chem. Soc., Perkin Trans. 1* **1998**, 3989–3998.

[81] Y. Matsusita, K. Sugamoto, T. Matsui, *Chem. Lett.* **1993**, *22*, 925–928.

[82] T. Tokuyasu, S. Kunikawa, K. J. McCullough, A. Masuyama, M. Nojima, *J. Org. Chem.* **2005**, *70*, 251–260.

[83] T. Tokuyasu, S. Kunikawa, A. Masuyama, M. Nojima, *Org. Lett.* **2002**, *4*, 3595–3598.

[84] N. A. Milas, A. Golubović, *J. Am. Chem. Soc.* **1959**, *81*, 5824–5826.

[85] A. Rieche, R. Meister, *Angewandte Chemie* **1936**, *49*, 101–103.

[86] H. Rein, *Angew. Chem.* **1950**, *62*, 120–120.

[87] R. Criegee, G. Wenner, *Justus Liebigs Annalen der Chemie* **1949**, *564*, 9–15.

[88] K. Griesbaum, M. Meister, *Chemische Berichte* **1987**, *120*, 1573–1580.

[89] P. Ghorai, P. H. Dussault, *Org. Lett.* **2008**, *10*, 4577–4579.

[90] J. H. van Tonder, *Synlett* **2014**, *25*, 1629–1630.

[91] R. Amewu, A. V. Stachulski, S. A. Ward, N. G. Berry, P. G. Bray, J. Davies, G. Labat, L. Vivas, P. M. O'Neill, *Organic & Biomolecular Chemistry* **2006**, *4*, 4431–4436.

[92] A. O. Terent'ev, M. M. Platonov, I. B. Krylov, V. V. Chernyshev, G. I. Nikishin, *Organic & Biomolecular Chemistry* **2008**, *6*, 4435–4441.

[93] Y. Dong, Y. Tang, J. Chollet, H. Matile, S. Wittlin, S. A. Charman, W. N. Charman, J. S. Tomas, C. Scheurer, C. Snyder, B. Scorneaux, S. Bajpai, S. A. Alexander, X. Wang, M. Padmanilayam, S. R. Cheruku, R. Brun, J. L. Vennerstrom, *Bioorganic & Medicinal Chemistry* **2006**, *14*, 6368–6382.

[94] W. Adam, W. J. Baader, *Angewandte Chemie International Edition in English* **1984**, *23*, 166–167.

[95] P. D. Bartlett, A. P. Schaap, **n.d.**, 3.

[96] F. Sevin, M. L. McKee, *J. Am. Chem. Soc.* **2001**, *123*, 4591–4600.

[97] A. Maranzana, G. Ghigo, G. Tonachini, *J. Am. Chem. Soc.* **2000**, *122*, 1414–1423.

[98] M. Prein, W. Adam, *Angewandte Chemie International Edition in English* **1996**, *35*, 477–494.

[99] S. L. Boyd, R. J. Boyd, L. R. C. Barclay, *J. Am. Chem. Soc.* **1990**, *112*, 5724–5730.

[100] C. W. Jefford, *Chemical Society Reviews* **1993**, *22*, 59–66.

[101] M. Elsherbini, R. K. Allemann, T. Wirth, *Chemistry – A European Journal* **2019**, *25*, 12486–12490.

[102] J. K. Crandall, R. Curci, L. D'Accolti, C. Fusco, in *Encyclopedia of Reagents for Organic Synthesis*, American Cancer Society, **2005**.

[103] A. J. Bloodworth, R. J. Bunce, *Journal of the Chemical Society, Perkin Transactions 1* **1972**, *0*, 2787–2792.

[104] T. V. RajanBabu, F. Gagosz, in *Encyclopedia of Reagents for Organic Synthesis*, American Cancer Society, **2005**.

[105] W. A. Strong, *Ind. Eng. Chem.* **1964**, *56*, 33–38.

[106] E. F. J. Duynstee, M. L. Esser, R. Schellekens, *European Polymer Journal* **1980**, *16*, 1127–1134.

[107] D. Meyer, H. Jangra, F. Walther, H. Zipse, P. Renaud, *Nat Commun* **2018**, *9*, 1–10.

[108] B. G. Dixon, G. B. Schuster, *J. Am. Chem. Soc.* **1981**, *103*, 3068–3077.

[109] B. G. Dixon, G. B. Schuster, *Journal of the American Chemical Society* **1979**, 3.

[110] A. S. Rao, H. R. Mohan, in *Encyclopedia of Reagents for Organic Synthesis*, American Cancer Society, **2001**.

[111] T. E. Kleindienst, *Res. Chem. Intermed.* **1994**, *20*, 335–384.

[112] A. Vyskocil, C. Viau, S. Lamy, *Human & Experimental Toxicology* **1998**, 212–220.

[113] V. Ji Ram, A. Sethi, M. Nath, R. Pratap, in *The Chemistry of Heterocycles* (Eds.: V. Ji Ram, A. Sethi, M. Nath, R. Pratap), Elsevier, **2019**, pp. 93–147.

[114] J. Boukouvalas, J. M. Tanko, *Encyclopedia of Reagents for Organic Synthesis* **2007**.

[115] P. D. Bartlett, E. P. Benzing, R. E. Pincock, *J. Am. Chem. Soc.* **1960**, *82*, 1762–1768.

[116] K. Hughes, **n.d.**, 17.

[117] *Sauerstoff*, Springer Berlin Heidelberg, **1966**.

[118] R. Meyer, J. Köhler, A. Homburg, *Explosives*, Wiley-VCH, Weinheim, **2007**.

[119] *Safety and Handling of Organic Peroxides*, Organic Peroxide Producers Safety Division Of The Society Of The Plastics Industry, **2012**.

[120] "Organische Peroxide - BG RCI," can be found under https://www.bgrci.de/exinfode/ex-schutz-wissen/antworten-auf-haeufig-gestellte-fragen/organische-peroxide, **n.d.**

[121] E. P. Floyd, H. E. Stokenger, *American Industrial Hygiene Association Journal* **1958**, *19*, 205–212.

[122] In *The MAK-Collection for Occupational Health and Safety*, American Cancer Society, **2012**, pp. 250–260.

[123] Ph. D. James Speight, *Lange's Handbook of Chemistry, Sixteenth Edition*, McGraw-Hill Education, New York, **2005**.

[124] R. D. Bach, H. B. Schlegel, *J. Phys. Chem. A* **2020**, *124*, 4742–4751.

[125] S. Gambarjan, *Berichte der deutschen chemischen Gesellschaft* **1909**, *42*, 4003–4013.

[126] E. S. Shanley, *J. Am. Chem. Soc.* **1950**, *72*, 1419–1419.

[127] L. P. KUHN, *Chem. Eng. News Archive* **1948**, *26*, 3197.

[128] J. Slagle, H. Shine, *J. Org. Chem.* **1959**, *24*, 107–107.

[129] M. Levy, M. Steinberg, M. Szwarc, *J. Am. Chem. Soc.* **1954**, *76*, 5978–5981.

[130] A. Rembaum, M. Szwarc, *J. Am. Chem. Soc.* **1954**, *76*, 5975–5978.

[131] M. J. Goldstein, *Tetrahedron Letters* **1964**, *5*, 1601–1607.

[132] M. S. Kharasch, E. V. Jensen, W. H. Urry, *The Journal of Organic Chemistry* **1945**, *10*, 386–393.

[133] W. Braun, L. Rajbenbach, F. R. Eirich, *J. Phys. Chem.* **1962**, *66*, 1591–1595.

[134] A. J. Paine, J. Warkentin, *Canadian Journal of Chemistry* **2011**, 491.

[135] M. Levy, M. Szwarc, *J. Am. Chem. Soc.* **1954**, *76*, 5981–5985.

[136] T. Kashiwagi, S. Kozuka, S. Oae, *Tetrahedron* **1970**, *26*, 3619–3629.

[137] R. Kaptein, J. Brokken-Zijp, F. J. J. De Kanter, *J. Am. Chem. Soc.* **1972**, *94*, 6280–6287.

[138] M. S. Kharasch, H. C. McBay, W. H. Urry, *The Journal of Organic Chemistry* **1945**, *10*, 394–400.

[139] M. S. Kharasch, H. C. McBay, W. H. Urry, *The Journal of Organic Chemistry* **1945**, *10*, 401–405.

[140] Z. Gu, Y. Wang, P. B. Balbuena, *J. Phys. Chem. A* **2006**, *110*, 2448–2454.

[141] J. M. Simmie, G. Black, H. J. Curran, J. P. Hinde, *J. Phys. Chem. A* **2008**, *112*, 5010–5016.

[142] R. A. Sheldon, J. K. Kochi, *J. Am. Chem. Soc.* **1970**, *92*, 4395–4404.

[143] J. W. Hilborn, J. A. Pincock, *J. Am. Chem. Soc.* **1991**, *113*, 2683–2686.

[144] Y. P. Tsentalovich, L. V. Kulik, N. P. Gritsan, A. V. Yurkovskaya, *J. Phys. Chem. A* **1998**, *102*, 7975–7980.

[145] Michael. Erben-Russ, Christa. Michel, Wolf. Bors, Manfred. Saran, *J. Phys. Chem.* **1987**, *91*, 2362–2365.

[146] D. V. Avila, C. E. Brown, K. U. Ingold, J. Lusztyk, *J. Am. Chem. Soc.* **1993**, *115*, 466–470.

[147] M. Newcomb, in *Encyclopedia of Radicals in Chemistry, Biology and Materials*, American Cancer Society, **2012**.

[148] X.-Q. Hu, Z.-K. Liu, Y.-X. Hou, Y. Gao, *iScience* **2020**, *23*, 101266.

[149] C. S. Sheppard, V. R. Kamath, *Polymer Engineering & Science* **1979**, *19*, 597–606.

[150] *Ullmann's Encyclopedia of Industrial Chemicals*, **2005**.

[151] Y.-S. Duh, C.-S. Kao, W.-L. W. Lee, *J Therm Anal Calorim* **2017**, *127*, 1071–1087.

[152] Y.-S. Duh, C.-S. Kao, W.-L. W. Lee, *J Therm Anal Calorim* **2017**, *127*, 1089–1098.

[153] R. Ball, *Ind. Eng. Chem. Res.* **2013**, *52*, 922–933.

[154] J. E. Guillet, T. R. Walker, M. F. Meyer, J. P. Hawk, E. B. Towne, *I&EC Product Research and Development* **1964**, *3*, 257–261.

[155] J. E. Leffler, A. A. More, *J. Am. Chem. Soc.* **1972**, *94*, 2483–2487.

[156] "Half-Life of Initiators," can be found under http://polymerdatabase.com/polymer%20chemistry/t-half2.html, **n.d.**

[157] O. J. Walker, *J. Chem. Soc.* **1928**, 2040–2045.

[158] N. Charrier, in *Encyclopedia of Reagents for Organic Synthesis*, American Cancer Society, **2007**.

[159] P. D. Bartlett, K. Nozaki, *J. Am. Chem. Soc.* **1947**, *69*, 2299–2306.

[160] W. E. Cass, *J. Am. Chem. Soc.* **1947**, *69*, 500–503.

[161] Cheves. Walling, Zivorad. Čeković, *J. Am. Chem. Soc.* **1967**, *89*, 6681–6684.

[162] M. Klussmann, *Chemistry – A European Journal* **2018**, *24*, 4480–4496.

[163] A. Székely, M. Klussmann, *Chemistry – An Asian Journal* **2019**, *14*, 105–115.

[164] E. Giménez-Arnau, L. Haberkorn, L. Grossi, J.-P. Lepoittevin, *Tetrahedron* **2008**, *64*, 5680–5691.

[165] M. S. Kharasch, G. Sosnovsky, *J. Am. Chem. Soc.* **1958**, *80*, 756–756.

[166] M. S. Kharasch, G. Sosnovsky, N. C. Yang, *J. Am. Chem. Soc.* **1959**, *81*, 5819–5824.

[167] A. S. Olson, A. J. Jameson, S. K. Kyasa, B. W. Evans, P. H. Dussault, *ACS Omega* **2018**, *3*, 14054–14063.

[168] R. T. Gephart, C. L. McMullin, N. G. Sapiezynski, E. S. Jang, M. J. B. Aguila, T. R. Cundari, T. H. Warren, *J. Am. Chem. Soc.* **2012**, *134*, 17350–17353.

[169] C. Walling, *Radiation Research Supplement* **1963**, *3*, 3–16.

[170] C. Walling, M. J. Gibian, *J. Am. Chem. Soc.* **1965**, *87*, 3413–3417.

[171] C. Luner, M. Szwarc, *J. Chem. Phys.* **1955**, *23*, 1978–1979.

[172] R. W. Freerksen, W. E. Pabst, M. L. Raggio, S. A. Sherman, R. R. Wroble, D. S. Watt, *Journal of the American Chemical Society* **1977**, 7.

[173] J. C. Bevington, T. D. Lewis, *Trans. Faraday Soc.* **1958**, *54*, 1340–1344.

[174] C. Reichardt, J. Schroeder, P. Vöhringer, D. Schwarzer, *Phys. Chem. Chem. Phys.* **2008**, *10*, 1662–1668.

[175] J. C. Scaiano, L. C. Stewart, *J. Am. Chem. Soc.* **1983**, *105*, 3609–3614.

[176] Ž. Čeković, M. M. Green, *J. Am. Chem. Soc.* **1974**, *96*, 3000–3002.

[177] P. S. Skell, D. D. May, **n.d.**, 2.

[178] M. Buback, M. Kling, S. Schmatz, *Zeitschrift für Physikalische Chemie* **2005**, *219*, 1205–1222.

[179] H. Kiefer, T. G. Traylor, *Tetrahedron Letters* **1966**, *7*, 6163–6168.

[180] Y. P. Tsentalovich, L. V. Kulik, N. P. Gritsan, A. V. Yurkovskaya, *J. Phys. Chem. A* **1998**, *102*, 7975–7980.

[181] T. Nakamura, W. K. Busfield, I. D. Jenkins, E. Rizzardo, S. H. Thang, S. Suyama, *J. Org. Chem.* **2000**, *65*, 16–23.

[182] N. D. C. Tappin, P. Renaud, *Advanced Synthesis & Catalysis* **2021**, *363*, 275–282.

[183] H. Wieland, *Berichte der deutschen chemischen Gesellschaft* **1911**, *44*, 2550–2556.

[184] G. A. DiLabio, K. U. Ingold, S. Lin, G. Litwinienko, O. Mozenson, P. Mulder, T. T. Tidwell, *Angewandte Chemie International Edition* **2010**, *49*, 5982–5985.

[185] N. A. Porter, S. E. Caldwell, K. A. Mills, *Lipids* **1995**, *30*, 277–290.

[186] E. Praske, R. V. Otkjær, J. D. Crounse, J. C. Hethcox, B. M. Stoltz, H. G. Kjaergaard, P. O. Wennberg, *J. Phys. Chem. A* **2019**, *123*, 590–600.

[187] J. Boukouvalas, R. Pouliot, Y. Fréchette, *Tetrahedron Letters* **1995**, *36*, 4167–4170.

[188] A. J. Bloodworth, R. J. Curtis, N. Mistry, *J. Chem. Soc., Chem. Commun.* **1989**, 954–955.

[189] L. Cointeaux, J.-F. Berrien, J. Mayrargue, *Tetrahedron Letters* **2002**, *43*, 6275–6277.

[190] N. A. Porter, A. N. Roe, A. T. McPhail, *J. Am. Chem. Soc.* **1980**, *102*, 7574–7576.

[191] A. N. Roe, A. T. McPhail, N. A. Porter, *J. Am. Chem. Soc.* **1983**, *105*, 1199–1203.

[192] Ned. A. Porter, M. O. Funk, D. Gilmore, R. Isaac, J. Nixon, *J. Am. Chem. Soc.* **1976**, *98*, 6000–6005.

[193] N. A. Porter, B. A. Weber, H. Weenen, J. A. Khan, *J. Am. Chem. Soc.* **1980**, *102*, 5597–5601.

[194] G. O. Schenck, O.-A. Neumüller, W. Eisfeld, *Angewandte Chemie* **1958**, *70*, 595–595.

[195] G. O. Schenck, O.-A. Neumüller, W. Eisfeld, *Justus Liebigs Annalen der Chemie* **1958**, *618*, 202–210.

[196] J. I. Teng, M. J. Kulig, L. L. Smith, G. Kan, J. E. Van Lier, *J. Org. Chem.* **1973**, *38*, 119–123.

[197] W. F. Brill, *J. Chem. Soc., Perkin Trans. 2* **1984**, 621–627.

[198] S. Olivella, A. Solé, *J. Am. Chem. Soc.* **2003**, *125*, 10641–10650.

[199] S. L. Boyd, R. J. Boyd, Z. Shi, L. R. C. Barclay, N. A. Porter, *J. Am. Chem. Soc.* **1993**, *115*, 687–693.

[200] A. L. J. Beckwith, A. G. Davies, I. G. E. Davison, A. Maccoll, M. H. Mruzek, *J. Chem. Soc., Perkin Trans. 2* **1989**, 815–824.

[201] N. A. Porter, J. K. Kaplan, P. H. Dussault, *J. Am. Chem. Soc.* **1990**, *112*, 1266–1267.

[202] N. A. Porter, K. A. Mills, S. E. Caldwell, G. R. Dubay, *J. Am. Chem. Soc.* **1994**, *116*, 6697–6705.

[203] K. A. Mills, S. E. Caldwell, G. R. Dubay, N. A. Porter, *J. Am. Chem. Soc.* **1992**, *114*, 9689–9691.

[204] J. R. Lowe, Ned. A. Porter, *J. Am. Chem. Soc.* **1997**, *119*, 11534–11535.

[205] D. A. Pratt, K. A. Tallman, N. A. Porter, *Acc. Chem. Res.* **2011**, *44*, 458–467.

[206] H.-S. Dang, A. G. Davies, C. H. Schiesser, *Journal of the Chemical Society, Perkin Transactions 1* **1990**, *0*, 789–794.

[207] A. G. Davies, *Journal of Chemical Research* **2009**, *2009*, 533–544.

[208] P. R. Story, D. D. Denson, C. E. Bishop, B. C. Clark, J.-C. Farine, *J. Am. Chem. Soc.* **1968**, *90*, 817–818.

[209] P. R. Story, Bunge. Lee, C. E. Bishop, D. D. Denson, Peter. Busch, *J. Org. Chem.* **1970**, *35*, 3059–3062.

[210] J. R. Sanderson, P. R. Story, *J. Org. Chem.* **1974**, *39*, 3463–3469.

[211] J. R. Sanderson, P. R. Story, K. Paul, *J. Org. Chem.* **1975**, *40*, 691–695.

[212] K. Paul, P. R. Story, P. Busch, J. R. Sanderson, *J. Org. Chem.* **1976**, *41*, 1283–1285.

[213] H. A. J. Carless, R. Atkins, G. K. Fekarurhobo, *Tetrahedron Letters* **1985**, *26*, 803–806.

[214] K. K. Maheshwari, P. de Mayo, D. Wiegand, *Canadian Journal of Chemistry* **1970**, *48*, 3265.

[215] H. A. J. Carless, R. J. Batten, *J. Chem. Soc., Perkin Trans. 1* **1987**, 1999–2007.

[216] I. A. Yaremenko, V. A. Vil', D. V. Demchuk, A. O. Terent'ev, *Beilstein J. Org. Chem.* **2016**, *12*, 1647–1748.

[217] J. Hartung, T. Gottwald, K. Špehar, *Synthesis* **2002**, *2002*, 1469–1498.

[218] Y.-R. Luo, *Handbook of Bond Dissociation Energies in Organic Compounds*, **2003**.

[219] In *Comprehensive Organic Name Reactions and Reagents*, American Cancer Society, **2010**, pp. 2718–2721.

[220] K. Zhao, K. Yamashita, J. E. Carpenter, T. C. Sherwood, W. R. Ewing, P. T. W. Cheng, R. R. Knowles, *J. Am. Chem. Soc.* **2019**, *141*, 8752–8757.

[221] C. M. Morton, Q. Zhu, H. Ripberger, L. Troian-Gautier, Z. S. D. Toa, R. R. Knowles, E. J. Alexanian, *J. Am. Chem. Soc.* **2019**, *141*, 13253–13260.

[222] E. Tsui, A. J. Metrano, Y. Tsuchiya, R. R. Knowles, *Angewandte Chemie International Edition* **2020**, *59*, 11845–11849.

[223] E. Tsui, H. Wang, R. R. Knowles, *Chem. Sci.* **2020**, *11*, 11124–11141.

[224] A. Hu, J.-J. Guo, H. Pan, Z. Zuo, *Science* **2018**, *361*, 668–672.

[225] A. Hu, J.-J. Guo, H. Pan, H. Tang, Z. Gao, Z. Zuo, *J. Am. Chem. Soc.* **2018**, *140*, 1612–1616.

[226] D. H. R. Barton, J. M. Beaton, L. E. Geller, M. M. Pechet, *J. Am. Chem. Soc.* **1961**, *83*, 4076–4083.

[227] F. D. Greene, M. L. Savitz, H. H. Lau, F. D. Osterholtz, W. N. Smith, *J. Am. Chem. Soc.* **1961**, *83*, 2196–2198.

[228] C. Walling, R. T. Clark, *J. Am. Chem. Soc.* **1974**, *96*, 4530–4534.

[229] C. Walling, A. Padwa, *J. Am. Chem. Soc.* **1961**, *83*, 2207–2208.

[230] Cheves. Walling, Albert. Padwa, *J. Am. Chem. Soc.* **1963**, *85*, 1597–1601.

[231] M. H. Dean, G. Skirrow, *Trans. Faraday Soc.* **1958**, *54*, 849–862.

[232] J. K. Kochi, *J. Am. Chem. Soc.* **1962**, *84*, 1193–1197.

[233] J. K. Kochi, *J. Am. Chem. Soc.* **1963**, *85*, 1958–1968.

[234] J. K. Kochi, A. Bemis, C. L. Jenkins, *J. Am. Chem. Soc.* **1968**, *90*, 4616–4625.
[235] B. Acott, A. Beckwith, *Australian Journal of Chemistry* **1964**, *17*, 1342.
[236] A. W. Hofmann, *Berichte der deutschen chemischen Gesellschaft* **1881**, *14*, 2725–2736.
[237] K. Löffler, C. Freytag, *Berichte der deutschen chemischen Gesellschaft* **1909**, *42*, 3427–3431.
[238] L. M. Stateman, K. M. Nakafuku, D. A. Nagib, *Synthesis* **2018**, *50*, 1569–1586.
[239] Y. Zou, X.-S. Xue, Y. Deng, A. B. Smith, K. N. Houk, *Org. Lett.* **2019**, *21*, 5894–5897.
[240] A. E. Dorigo, K. N. Houk, *J. Am. Chem. Soc.* **1987**, *109*, 2195–2197.
[241] A. E. Dorigo, K. N. Houk, *J. Org. Chem.* **1988**, *53*, 1650–1664.
[242] A. C. Davis, J. S. Francisco, *J. Am. Chem. Soc.* **2011**, *133*, 18208–18219.
[243] J. H. Horner, S.-Y. Choi, M. Newcomb, *Org. Lett.* **2000**, *2*, 3369–3372.
[244] M. Nechab, S. Mondal, M. Bertrand, *Chemistry - A European Journal* **2014**, *20*, 16034–16059.
[245] Ž. Čeković, *Tetrahedron* **2003**, *59*, 8073–8090.
[246] Z. Cekovic, M. M. Green, *J. Am. Chem. Soc.* **1974**, *96*, 3000–3002.
[247] Ž. Čeković, Lj. Dimttruević, G. Djokić, T. Srnić, *Tetrahedron* **1979**, *35*, 2021–2026.
[248] Z. Čeković, M. Cvetković, *Tetrahedron Letters* **1982**, *23*, 3791–3794.
[249] T. Hashimoto, D. Hirose, T. Taniguchi, *Angewandte Chemie International Edition* **2014**, *53*, 2730–2734.

Chapter 2

A Short Synthesis of (+)-Brefeldin C through Enantioselective Radical Hydroalkynylation

Lars Gnägi, Severin Vital Martz, Daniel Meyer, Robin Marc Schärer, and Philippe Renaud,

Chem. Eur. J. **2019**, *25*, 11646 – 11649

Author contributions
LG conducted the majority of the experimental work, SVM and DM conducted preliminary experiments, and RMS supported experimental work. LG and PR were responsible for writing of the article.

2. A Short Synthesis of (+)-Brefeldin C through Enantioselective Radical Hydroalkynylation

2.1 Abstract

A very concise total synthesis of (+)-brefeldin C starting from 2-furanylcyclopentene is described. This approach is based on an unprecedented enantioselective radical hydroalkynylation process to introduce the two cyclopentane stereocenters in a single step. The use of a furan substituent allows a high trans diastereoselectivity to be achieved during the radical process and it contains the four carbon atoms C1–C4 of the natural product in an oxidation state closely related to the one of the target molecule. The eight-step synthesis requires six product purifications and it provides (+)-brefeldin C in 18% overall yield.

2.2 Introduction

In 1958, the group of Singleton isolated a new compound called decumbin from *Penicillium decumbens,* which showed toxicity properties against rats and goldfish.[1] Four years later, Betina et al. isolated a compound called cyanein from *Penicillium cyaneum*, which displayed antibiotic properties against pathogenic and non-pathogenic fungi and demonstrated significant inhibition of HeLa cell multiplication.[2,3] Later, Härri isolated and characterized two new compounds from *Penicillium brefeldianum*, named brefeldin A and brefeldin C.[4] Sigg later confirmed the equivalence of decumbin, cyanein and brefeldin A (Figure 2.1).[5]

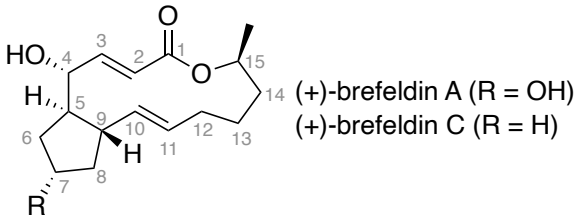

Figure 2.1. Structures of (+)-brefeldin A and C

Few compounds have triggered so much the interest of the scientific community. Indeed, brefeldin A has been investigated as a lead molecule for drug development due to its promising biological activities in the antitumor,[6] antifungal,[4] and antiviral[7] fields. Its ability to disrupt the Golgi apparatus acted as a magnet for biochemists and chemical biologists interested in intracellular protein trafficking.[8,9] However, these promises have not yet led to clinical applications. The unique biological profile of brefeldin A, C, and analogues[10] has attracted a lot of interest in the synthetic organic chemistry community. The first synthesis of the racemic brefeldin A was reported by Corey and Wollenberg[11] in 1976 followed by around 40 total and formal syntheses.[11–51] Brefeldin C was prepared for the first time

by total synthesis in 1988 by Schreiber and Meyers[52] followed by Takano,[25] Guingant (along with aspects of the biological properties of BFA)[48,53] and Tsunoda.[54] Following the pioneer work of Corey and Wollenberg,[11] the majority of the syntheses of brefeldin A and C accessed the 13-membered ring lactone in high yields by macrolactonization.[55] On the other hand, the preparation of the polysubstituted 5-membered ring has been achieved using very diverse strategies. Among them, the one reported by Kobayashi which used a furan moiety to introduce the C(1)–C(4) carbon atoms retained all our attention due to its conciseness.[35]

Recently, our group reported a method for enantioselective hydroazidation of trisubstituted nonactivated alkenes.[56] This reaction was extended to other enantioselective hydrofunctionalization processes such as hydrobromination,[56] hydrofluroination,[57] hydrosulfurization[56], and hydroallylation.[56] Brown et al. have pioneered the enantioselective hydroalkynylation of alkenes.[58] However, their multistep approach was lengthy and required severe reaction conditions to convert alkylboronates to thexyl(alkyl)boranes before treatment with lithium acetylide and iodine under Zweifel type conditions.[59–62] Due to its obvious synthetic interest, the enantioselective hydroalkynylation of unactivated alkenes has been recently reinvestigated[63] but its scope remains so far limited to electron rich[64,65] and electron poor alkenes.[66,66] The only unactivated alkenes that were enantioselectively hydroalkynylated were strained system such as cyclopropene[67] and norbornene derivatives[68–70] and aryl substituted conjugated dienes.[71] The simple enantio-random hydroalkynylation of non-activated alkenes with Markovnikov regioselectivity has been described in 2017 by Cui and co-workers using iron catalysis.[72] Before that, we had developed the enantio-random hydroalkynylation of unactivated alkenes using a hydroboration radical alkynylation process.[73]

2.3 Results and discussion

Herein, we report a concise synthesis of (+)-brefeldin C based on an unprecedented enantioselective version of our radical mediated hydroalkynylation. The conciseness of the reaction could be achieved by using a furan ring to introduce the first four carbon of the macrolactone with the desired oxidation state in a particularly straightforward manner. The retrosynthetic analysis of the synthesis is depicted in Scheme 2.1. Brefeldin C will be prepared from the corresponding seco acid **I** *via* Yamaguchi macrolactonization and stereoselective reduction of the resulting α-β unsaturated ketone according to the seminal work of Corey and Wollenberg.[11] In analogy to the work of Kobayashi in his syntheses of brefeldin A[35] and of macrosphelides A and B,[74,75] the 3-carboxyacryloyl chain (carbon C1–C4) will be prepared *via* oxidative opening of the furan ring of **II**. The pentan-4-ol-1-yl side chain (carbon C12–C16) will be inserted via a Suzuki-Miyaura cross-coupling process starting from iodide **III** in analogy to the work of Guingant.[48,53] The (*E*)-iodide **III** will be obtained from the alkyne **IV** via a hydrozirconation-iodination process.[76] The planned key reaction of our approach is the enantioselective and diastereoselective hydroalkynylation of 1-furanylcyclopentene **V** that has to be designed based on our previous work.[73,56]

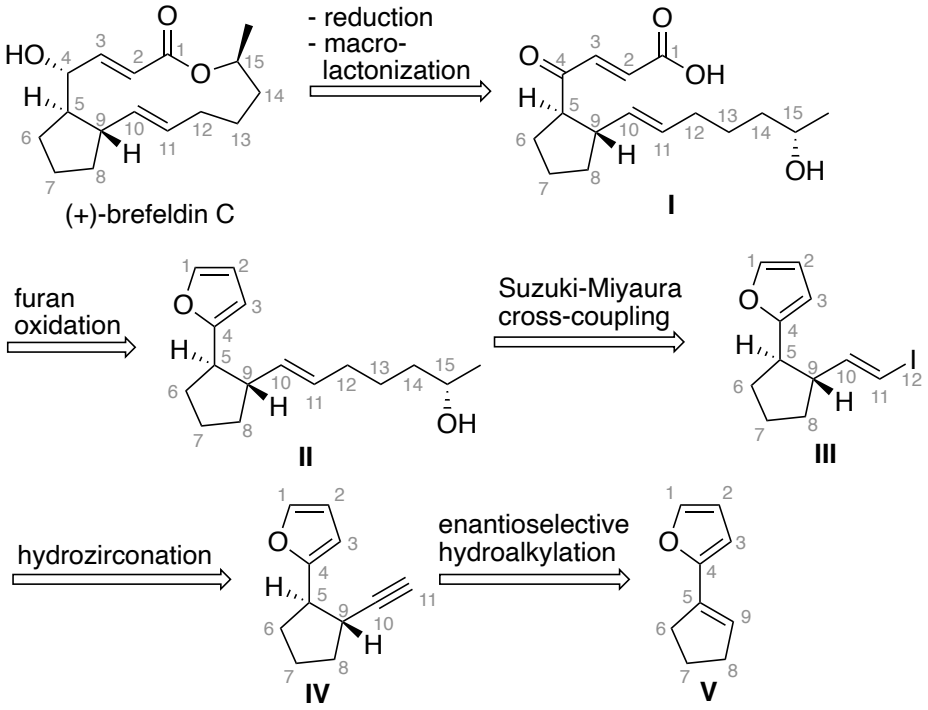

Scheme 2.1. Retrosynthesis of (+)-befeldin C

The enantioselective hydroalkynylation of 1-furanylcyclopentene **1** was investigated first since this substrate was already used in our hydroazidation study[56] and we knew that it can be hydroborated using (+)-monoisopinocampheylbroane in high enantiomeric excess according to Brown's procedure.[77,78] Hydroboration of **1** with (+)-monoisocampheylborane was directly followed by conversion to the *B*-catecholborane upon successive treatment with acetaldehyde and catechol according to the procedure developed for the enantioselective hydroazidation reaction.[56] The *in situ* generated *B*-alkylcatecholborane was treated with trimethylsilylethynyl phenyl sulfone in the presence of di-*tert*-butyl hyponitrite as a radical precursor (Scheme 2.2). Satisfyingly, the desired hydroethynylated product **2a** was obtained as a single diastereomer (*trans/cis* ≥98:2) in 10–40% yield depending on the run. The resulting TMS-protected alkyne **2a** was immediately desilylated to give the terminal alkyne **3** in nearly quantitative yield. However, compounds **2a** and **3** were found to be unstable when heated. The irreproducibility of the yield of the hydroalkynylation was attributed to partial decomposition of **2a** during the radical process in refluxing dichloromethane (about 60 °C). Therefore, we decided to use the triisopropylsilyl (TIPS) protected ethynyl sulfone as radical trap to introduce the ethynyl moiety. Gratifyingly and in contrast to the TMS-protected sulfone, the preparation of the triisopropylethynyl phenyl sulfone was achieved in 98% yield from TIPS-acetylene and the corresponding product **2b** is bench stable. Running the hydroalkynylation reaction with this reagent afforded the TIPS-protected alkyne *trans*-**2b** in 43% yield when run with di-*tert*butyl hyponitrite[79] (DTBHN) as an initiator. By initiating the reaction with to di-*tert*-butyl peroxyoxalate[80,81] (DTBPO), the reaction time could be decreased from 1 day (DTBHN) down to 40 min which resulted in an increased yield of 70% (up to 85% on small scale). An enantiomeric purity of 95:5 was determined after desilylation to **3** by HPLC. This enantiomeric purity is identical within experimental error to the one measured for 2-

furanylcyclopentanol obtained upon oxidation of the organoborane intermediate with $NaOH/H_2O_2$ (see supporting information) demonstrating that the radical process is taking place without epimerization.

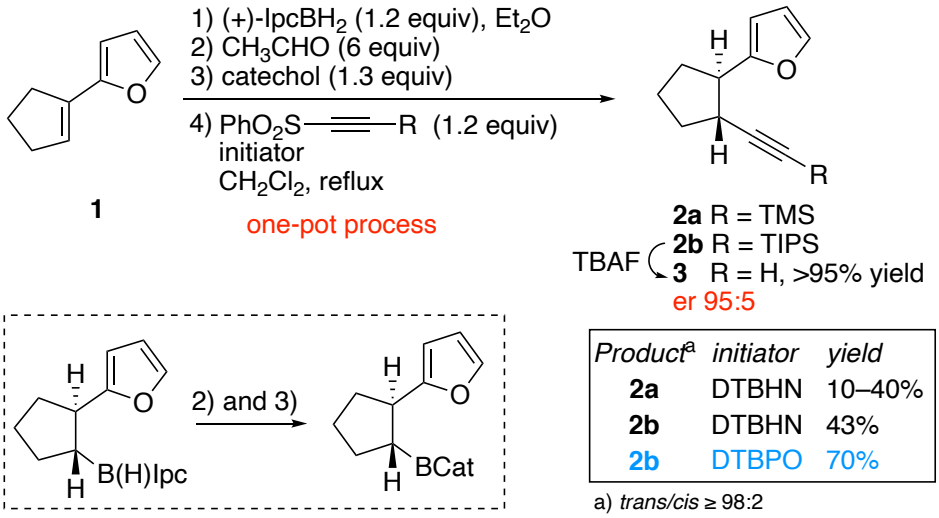

*Scheme 2.2. Enantioselective hydroalkynylation of **1***

With the TIPS-protected alkyne **2b** in hand, we next focussed on the introduction of C12-C16 chain via Suzuki-Miyaura coupling in analogy to work of Guingant (**Error! Reference source not found.**).[48] The *p*-methoxybenzyl (PMB) protected alkenol **4** was conveniently accessible in two steps from (*S*)-propylene epoxide[48,82] and it was converted to **5** by hydroboration with 9-BBN. Due to its volatility and instability, the deprotected alkyne **3** obtained by treatment of **2b** with TBAF was immediately converted into the vinyl iodide **6** *via* hydrozirconation using the Schwartz reagent followed by treatment with iodine.[76,83] The Suzuki-Miyaura cross-coupling process delivered **7** in good 53% yield over 3 steps. At this stage, compound **7** contains all the C-atoms present in (+)-brefeldin C and the remaining steps are dealing with functional group interconversion. Oxidation of the furan to the access the *trans*-4-oxo-2-alkenoic acid was attempted next. The oxidation method reported by Salomon was tried first since it should deliver directly the desired acid upon simple treatment with sodium chlorite under acidic conditions. The reaction conditions were optimized on 2-cyclopentylfuran (see supporting material) to give the desired acid in 74% yield. However, all attempts to oxidize **7** failed to give the desired product. Moreover, it was observed that Salomon's conditions were partly deprotecting PMB ethers. Therefore, it was decided to deprotect first the PMB ether. This deprotection turned out to more difficult than expected since most standard conditions (DDQ, trifluoroacetic acid, triflic acid, cerium ammonium nitrate, etc.) were either degrading **7** or led to the desired free alcohol **8** contaminated with impurities difficult to remove by chromatographic purification. Gratifyingly, treatment of **7** in methanol with 4 M aqueous HCl afforded the clean deprotected alcohol **8** in 89% yield. After another extensive screening of furan oxidation conditions, we used a two-step one-pot procedure inspired by the work of Jørgensen[84], Kobayashi[35,75] and Blair.[85] Furan **8** was first treated with NBS in H_2O/acetone in the presence of $NaHCO_3$ followed by treatment with pyridine to obtain the ring opened 4-oxo-2-alken1-al intermediate **9** that was rapidly filtered through a pad of silica gel. Pinnick oxidation of the aldehyde **9**

afforded the acid **10** in 85% yield overall yield from furan **8**. Yamaguchi type lactonization provided **11** that was stereoselectively reduced to (+)-brefeldin C upon treatment with $NaBH_4$ in analogy to the work of Corey and Wollenberg.[11] The structure of (+)-Brefeldin C was confirmed by X-ray crystallography (Scheme 2.3).

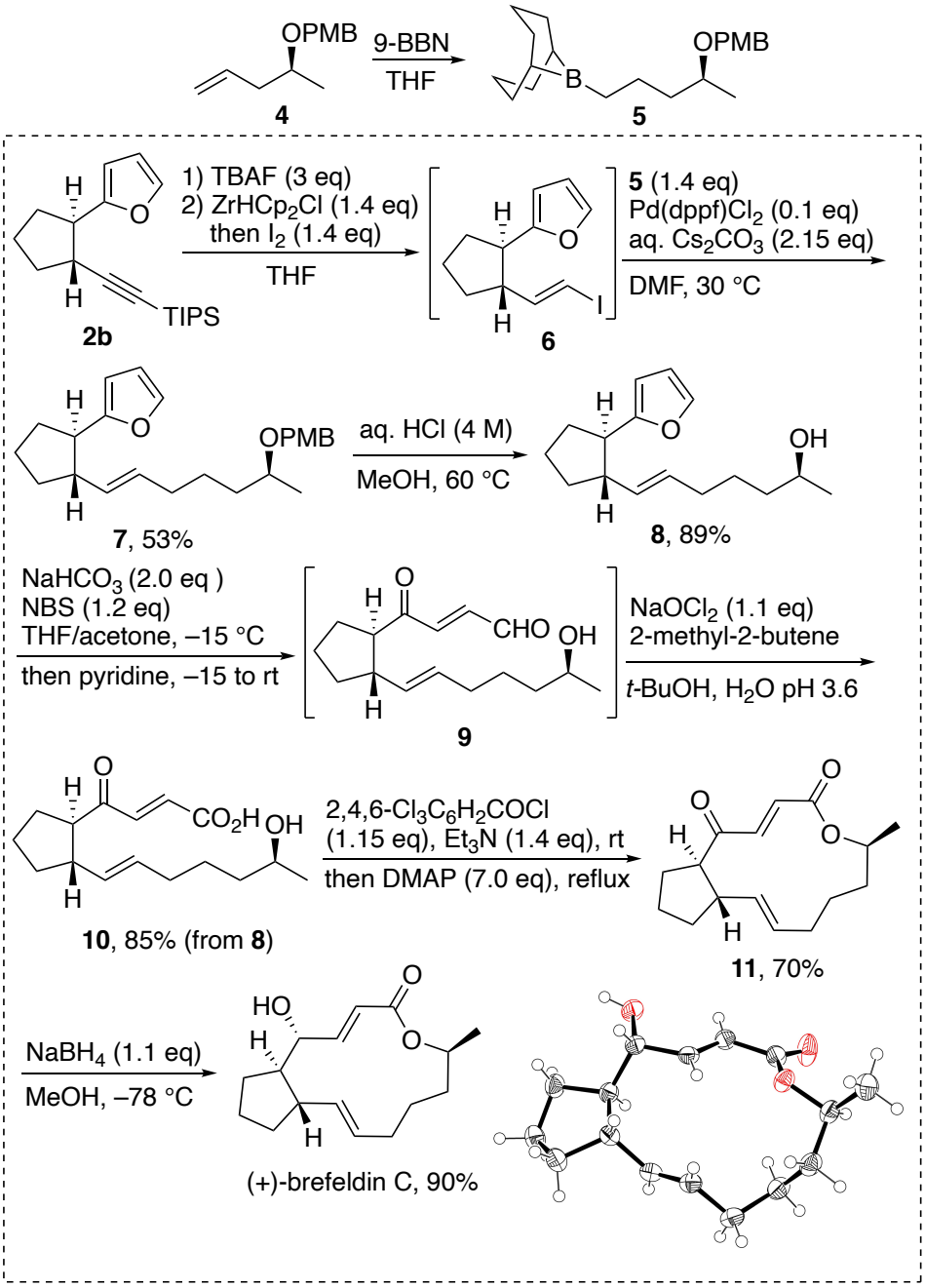

Scheme 2.3. Conversion of alkyne 2b into (+)-brefeldin C. X-ray single crystal structure of (+)-brefeldin C (50% probability ellipsoids).

2.4 Conclusion

In conclusion, we have reported a very concise total synthesis of (+)-brefeldin C starting from 2-furanylcyclopentene using an unprecedented enantioselective radical hydroalkynylation process to

introduce the two cyclopentane stereocenters in a single step. To achieve efficiently this key transformation, a TIPS protected alkynyl sulfone was used together with radical initiation with DTPBO at 40 °C. The use of the furan substituent was crucial for the success of this synthesis. Indeed, it allows to achieve a high *trans* diastereoselectivity during the radical process and it contains the four carbon atoms C1–C4 of the natural product in an oxidation state closely related to the one of the target molecule. The longest linear sequence of the synthesis involves eight steps, six product purifications and it provides (+)-brefeldin C in 18% overall yield.

2.5 Acknowledgements

The Swiss National Science Foundation (Project 200020_172621) and the University of Bern are gratefully acknowledged for financial support.

Keywords: hydroalkynylation • asymmetric synthesis • enantioselective reaction • radical reaction • alkynylsulfone • natural product.

2.6 References

[1] V. L. Singleton, N. Bohonos, A. Ja. Ullstrup, *Nature* **1958**, *181*, 1072–1073.

[2] V. Betina, K. Horáková, Z. Baráth, *Naturwissenschaften* **1962**, *49*, 241–241.

[3] V. Betina, P. Nemec, J. Dobias, Z. Baráth, *Folia Microbiol.* **1962**, *7*, 353–357.

[4] E. Härri, W. Loeffler, H. P. Sigg, H. Stähelin, C. Tamm, *Helv. Chim. Acta* **1963**, *46*, 1235–1243.

[5] H. P. Sigg, *Helv. Chim. Acta* **1964**, *47*, 1401–1415.

[6] V. Betina, *Neoplasma* **1969**, *16*, 23–32.

[7] G. Tamura, K. Ando, S. Suzuki, A. Takatsuki, K. Arima, *J. Antibiot.* **1968**, *21*, 160–161.

[8] J. Lippincott-Schwartz, L. C. Yuan, J. S. Bonifacino, R. D. Klausner, *Cell* **1989**, *56*, 801–813.

[9] A. Dinter, E. G. Berger, *Histochemistry* **1998**, *109*, 571–590.

[10] S.-M. Paek, *Marine Drugs* **2018**, *16*, 133.

[11] E. J. Corey, R. H. Wollenberg, *Tetrahedron Lett.* **1976**, *17*, 4705–4708.

[12] E. J. Corey, R. H. Wollenberg, D. R. Williams, *Tetrahedron Lett.* **1977**, *18*, 2243–2246.

[13] P. A. Bartlett, F. R. Green, *J. Am. Chem. Soc.* **1978**, *100*, 4858–4865.

[14] A. E. Greene, C. Le Drian, P. Crabbe, *J. Am. Chem. Soc.* **1980**, *102*, 7583–7584.

[15] Y. Köksal, P. Raddatz, E. Winterfeldt, *Angew. Chem. Int. Ed. Engl.* **1980**, *19*, 472–473.

[16] H. Ohrui, H. Kuzuhara, *Agric. Biol. Chem.* **1980**, *44*, 907–912.

[17] M. Honda, K. Hirata, H. Sueoka, T. Katsuki, M. Yamaguchi, *Tetrahedron Lett.* **1981**, *22*, 2679–2682.

[18] P. Raddatz, E. Winterfeldt, *Angew. Chem. Int. Ed. Engl.* **1981**, *20*, 286–287.

[19] C. Le Drian, A. E. Greene, *J. Am. Chem. Soc.* **1982**, *104*, 5473–5483.

[20] H.-J. Gais, K. L. Lukas, *Angew. Chem. Int. Ed. Engl.* **1984**, *23*, 142–143.

[21] T. Kitahara, K. Mori, *Tetrahedron* **1984**, *40*, 2935–2944.

[22] K. Nakatani, S. Isoe, *Tetrahedron Lett.* **1985**, *26*, 2209–2212.

[23] K. Ueno, H. Suemune, S. Saeki, K. Sakai, *Chem. Pharm. Bull.* **1985**, *33*, 4021–4025.

[24] B. M. Trost, Joseph. Lynch, Patrice. Renaut, D. H. Steinman, *J. Am. Chem. Soc.* **1986**, *108*, 284–291.

[25] S. Hatakeyama, K. Osanai, H. Numata, S. Takano, *Tetrahedron Lett.* **1989**, *30*, 4845–4848.

[26] E. J. Corey, P. Carpino, *Tetrahedron Lett.* **1990**, *31*, 7555–7558.

[27] S. Hatakeyama, K. Sugawara, M. Kawamura, S. Takano, *Synlett* **1990**, *1990*, 691–693.

[28] J. Nokami, M. Ohkura, Y. Dan-Oh, Y. Sakamoto, *Tetrahedron Lett.* **1991**, *32*, 2409–2412.

[29] D. F. Taber, L. J. Silverberg, E. D. Robinson, *J. Am. Chem. Soc.* **1991**, *113*, 6639–6645.

[30] G. Solladie, O. Lohse, *J. Org. Chem.* **1993**, *58*, 4555–4563.

[31] A. J. Carnell, G. Casy, G. Gorins, A. Kompany-Saeid, R. McCague, H. F. Olivo, S. M. Roberts, A. J. Willetts, *J. Chem. Soc., Perkin Trans. 1* **1994**, *0*, 3431–3439.

[32] H. Miyaoka, M. Kajiwara, *J. Chem. Soc., Chem. Commun.* **1994**, *0*, 483–484.

[33] V. Bernardes, N. Kann, A. Riera, A. Moyano, M. A. Pericas, A. E. Greene, *J. Org. Chem.* **1995**, *60*, 6670–6671.

[34] K. Tomooka, K. Ishikawa, T. Nakai, *Synlett* **1995**, *1995*, 901–902.

[35] Y. Kobayashi, K. Watatani, Y. Kikori, R. Mizojiri, *Tetrahedron Letters* **1996**, *37*, 6125–6128.

[36] R. K. Haynes, W. W.-L. Lam, L.-L. Yeung, I. D. Williams, A. C. Ridley, S. M. Starling, S. C. Vonwiller, T. W. Hambley, P. Lelandais, *J. Org. Chem.* **1997**, *62*, 4552–4553.

[37] P. Ducray, B. Rousseau, C. Mioskowski, *J. Org. Chem.* **1999**, *64*, 3800–3801.

[38] D. Kim, J. Lee, P. J. Shim, J. I. Lim, H. Jo, S. Kim, *J. Org. Chem.* **2002**, *67*, 764–771.

[39] D. Kim, J. Lee, P. J. Shim, J. I. Lim, T. Doi, S. Kim, *J. Org. Chem.* **2002**, *67*, 772–781.

[40] Y.-G. Suh, J.-K. Jung, S.-Y. Seo, K.-H. Min, D.-Y. Shin, Y.-S. Lee, S.-H. Kim, H.-J. Park, *J. Org. Chem.* **2002**, *67*, 4127–4137.

[41] B. M. Trost, M. L. Crawley, *J. Am. Chem. Soc.* **2002**, *124*, 9328–9329.

[42] Y. Wang, D. Romo, *Org. Lett.* **2002**, *4*, 3231–3234.

[43] T. Hübscher, G. Helmchen, *Synlett* **2006**, *2006*, 1323–1326.

[44] S.-Y. Seo, J.-K. Jung, S.-M. Paek, Y.-S. Lee, S.-H. Kim, Y.-G. Suh, *Tetrahedron Letters* **2006**, *47*, 6527–6530.

[45] W. Lin, C. K. Zercher, *J. Org. Chem.* **2007**, *72*, 4390–4395.

[46] Y. Wu, J. Gao, *Org. Lett.* **2008**, *10*, 1533–1536.

[47] M.-Y. Kim, H. Kim, J. Tae, *Synlett* **2009**, *2009*, 1303–1306.

[48] S. Archambaud, F. Legrand, K. Aphecetche-Julienne, S. Collet, A. Guingant, M. Evain, *Eur. J. Org. Chem.* **2010**, *2010*, 1364–1380.

[49] M. Fuchs, A. Fürstner, *Angew. Chem. Int. Ed.* **2015**, *54*, 3978–3982.

[50] S. Raghavan, M. K. R. Yelleni, *J. Org. Chem.* **2016**, *81*, 10912–10921.

[51] Z. Xiong, K. J. Hale, *Org. Lett.* **2016**, *18*, 4254–4257.

[52] S. L. Schreiber, H. V. Meyers, *J. Am. Chem. Soc.* **1988**, *110*, 5198–5200.

[53] S. Archambaud, K. Aphecetche-Julienne, A. Guingant, *Synlett* **2005**, 139–143.

[54] M. Inai, T. Nishii, S. Mukoujima, T. Esumi, H. Kaku, K. Tominaga, H. Abe, M. Horikawa, T. Tsunoda, *Synlett* **2011**, 1459–1461.

[55] Y. Kobayashi, K. Watatani, *J. Synth. Org. Chem. Jpn.* **1997**, *55*, 110–120.

[56] D. Meyer, P. Renaud, *Angew. Chem. Int. Ed.* **2017**, *56*, 10858–10861.

[57] D. Meyer, H. Jangra, F. Walther, H. Zipse, P. Renaud, *Nat. Commun.* **2018**, *9*, 4888.

[58] H. C. Brown, V. K. Mahindroo, N. G. Bhat, B. Singaram, *J. Org. Chem.* **1991**, *56*, 1500–1505.

[59] Akira. Suzuki, Norio. Miyaura, Shigeo. Abiko, Mitsuomi. Itoh, H. C. Brown, J. A. Sinclair, M. Mark. Midland, *J. Am. Chem. Soc.* **1973**, *95*, 3080–3081.

[60] A. Suzuki, N. Miyaura, S. Abiko, M. Itoh, M. M. Midland, J. A. Sinclair, H. C. Brown, *J. Org. Chem.* **1986**, *51*, 4507–4511.

[61] D. P. Canterbury, G. C. Micalizio, *J. Am. Chem. Soc.* **2010**, *132*, 7602–7604.

[62] R. Armstrong, V. Aggarwal, *Synthesis* **2017**, *49*, 3323–3336.

[63] Z.-X. Wang, X.-Y. Bai, B.-Jie. Li, *Synlett* **2017**, *28*, 509–514.

[64] X.-Y. Bai, W.-W. Zhang, Q. Li, B.-Jie. Li, *J. Am. Chem. Soc.* **2018**, *140*, 506–514.

[65] X.-Y. Bai, Z.-X. Wang, B.-Jie. Li, *Angew. Chem., Int. Ed.* **2016**, *55*, 9007–9011.

[66] Z.-X. Wang, X.-Y. Bai, H.-C. Yao, B.-Jie. Li, *J. Am. Chem. Soc.* **2016**, *138*, 14872–14875.

[67] H.-L. Teng, Y. Ma, G. Zhan, M. Nishiura, Z. Hou, *ACS Catal.* **2018**, *8*, 4705–4709.

[68] B. Fan, J. Xu, Q. Yang, S. Li, H. Chen, S. Liu, L. Yu, Y. Zhou, Lin. Wang, *Org. Lett.* **2013**, *15*, 5956–5959.

[69] J. Hu, Q. Yang, J. Xu, C. Huang, B. Fan, J. Wang, C. Lin, Z. Bian, A. S. C. Chan, *Org. Biomol. Chem.* **2013**, *11*, 814–820.

[70] Q. Yang, P. Y. Choy, B. Fan, F. Yee. Kwong, *Adv. Synth. Catal.* **2015**, *357*, 2345–2350.

[71] M. Shirakura, Michinori. Suginome, *Angew. Chem., Int. Ed.* **2010**, *49*, 3827–3829, S3827/1-S3827/64.

[72] Y. Shen, B. Huang, J. Zheng, C. Lin, Y. Liu, S. Cui, *Org. Lett.* **2017**, *19*, 1744–1747.

[73] Schaffner, Arnaud-Pierre, Darmency, Vincent, Renaud Philippe, *Angew. Chem. Int. Ed.* **2006**, *45*, 5847–5849.

[74] Y. Kobayashi, B. G. Kumar, T. Kurachi, *Tetrahedron Lett.* **2000**, 1559–1563.

[75] Y. Kobayashi, G. B. Kumar, T. Kurachi, H. P. Acharya, T. Yamazaki, T. Kitazume, *J. Org. Chem.* **2001**, *66*, 2011–2018.

[76] D. W. Hart, T. F. Blackburn, J. Schwartz, *J. Am. Chem. Soc.* **1975**, *97*, 679–680.

[77] H. C. Brown, N. M. Yoon, *J. Am. Chem. Soc.* **1977**, *99*, 5514–5516.

[78] H. C. Brown, J. R. Schwier, B. Singaram, *J. Org. Chem.* **1978**, *43*, 4395–4397.

[79] J. Boukouvalas, S. Cren, P. Renaud, *Encyclopedia of Reagents for Organic Synthesis* **2007**, DOI 10.1002/047084289X.rd062.pub2.

[80] P. D. Bartlett, E. P. Benzing, R. E. Pincock, *J. Am. Chem. Soc.* **1960**, *82*, 1762–1768.

[81] J. Boukouvalas, J. M. Tanko, *Encyclopedia of Reagents for Organic Synthesis* **2007**.

[82] P. Kumar, P. Gupta, S. Vasudeva Naidu, *Chem. Eur. J.* **2006**, *12*, 1397–1402.

[83] Y. Zhao, V. Snieckus, *Org. Lett.* **2014**, *16*, 390–393.

[84] B. M. Paz, L. Klier, L. Næsborg, V. H. Lauridsen, F. Jensen, K. A. Jørgensen, *Chem. Eur. J.* **2016**, *22*, 16810–16818.

[85] J. S. Arora, T. Oe, I. A. Blair, *J. Labelled Comp. Radiopharm.* **2011**, *54*, 247–251.

2.7 Experimental section

General information

Techniques

All reactions requiring anhydrous conditions were performed in heat-gun, oven or flame dried glassware under an argon atmosphere. An ice bath was used to obtain a temperature of 0 °C. To obtain a temperature of –78 °C, a bath of acetone was cooled with dry ice. To obtain temperatures of –40 °C and –15 °C, a bath of isopropanol or acetonitrile was cooled to the desired temperature using dry ice. Silica gel 60 Å (40–63 µm) from Silicycle was used for flash column chromatography. Thin layer chromatography (TLC) was performed on Silicycle silica gel 60 F254 plates, visualization under UV light (254 nm) and/or by dipping in a solution of (NH4)2MoO4 (15.0 g), Ce(SO4)2 (0.5 g), H2O (90 mL), conc. H2SO4 (10 mL); or KMnO4 (3 g), K2CO3 (20 g) and NaOH 5% (3 mL) in H2O (300 mL) and subsequent heating. Anhydrous sodium sulfate was used as drying reagent.

Materials

Commercial reagents were used without further purification unless otherwise stated. Dry solvents for reactions were filtered over columns of dried alumina under a positive pressure of argon. Solvents for extractions (Et_2O, *n*-pentane, CH_2Cl_2, EtOAc) and flash column chromatography were of technical grade and distilled prior to use. Commercial dry DMF was used without further purification.

Instrumentation

^1H and ^{13}C NMR spectra were recorded on a Bruker Avance IIIHD-300 spectrometer operating at 300 MHz for ^1H and 75 MHz for ^{13}C at rt (24-25°C) unless otherwise stated. Some ^1H and ^{13}C NMR spectra were recorded on a Bruker Avance IIIHD-400 or a Bruker Avance II-400 spectrometer (^1H: 400 MHz; ^{13}C: 75 MHz). Chemical shifts (δ) are reported in parts per million (ppm) using the residual solvent or $Si(CH_3)_4$ (δ = 0.00 for ^1H NMR spectra) as an internal standard. Multiplicities are given as s (singlet), d (doublet), t (triplet), q (quadruplet), m (multiplet), and br (broad). Coupling constant (*J*) is reported in Hz. In ^{13}C-NMR spectra, the peak positions are reported on one decimal unless the difference in chemical shift between two signals is small and required two decimals.Infrared spectra were recorded on a Jasco FT-IR-460 plus spectrometer equipped with a Specac MKII Golden Gate Single Reflection Diamond ATR system and are reported in wave numbers (cm^{-1}). At maximum, the ten most prominent peaks are reported.

Low resolution mass spectra were recorded on a Waters Micromass Autospec Q mass spectrometer in EI mode at 70 eV or were taken from GC-MS analyses performed on a Finnigan Trace GC-MS (quadrupole mass analyzer using EI mode at 70 eV) fitted with a Macherey-Nagel Optima delta-3-0.25 µm capillary column (20 m, 0.25 mm); gas carrier: He 1.4 mL/min; injector: 220 °C split mode.

HRMS analyses and accurate mass determinations were performed on a Thermo Scientific LTQ Orbitrap XL mass spectrometer using ESI mode (positive ion mode). Melting points were measured on a Büchi B-545 apparatus and are corrected. Syringe filters with polytetrafluoroethylene membrane were used with a pore size of 0.45µm from Machery-Nagel (CHROMAFIL®Xtra PTFE 0.45).

Synthesis

Preparation of reagents

(+)-Isopinocampheylborane-TMEDA complex

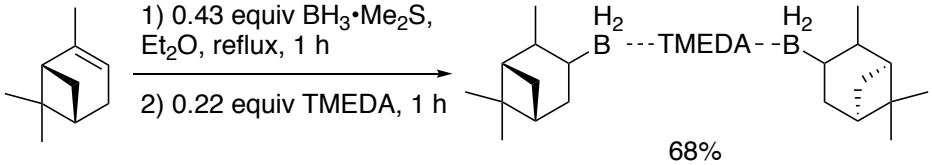

68%

Borane-dimethylsulfide (15.0 mL, 150 mmol) was dissolved in dry Et_2O (85 mL) and (+)-α-pinene (54.8 mL, 345 mmol) was added dropwise in such a rate that the reaction mixture refluxed gently. The mixture was refluxed for 1 h. TMEDA (11.3 mL, 75 mmol) was added to the reaction mixture and the mixture was refluxed for 1 h. Seedlings of TMEDA·2BH_2Ipc were added, so that the product started to crystallize. A thick white suspension was formed which was then stored in the freezer overnight. The suspension was filtered and washed with pentane. The crude product was dried under high vacuum which afforded the title compound (21.2 g, 68%).

Colorless crystals; $[\alpha]_D^{23}$ = +67.6 (c = 9.3, THF) (lit.[1] $[\alpha]_D^{23}$ = +69.03 (c = 9.33, THF)); ^{1}H-NMR (300 MHz, $CDCl_3$): δ 3.31 – 3.06 (m, 4H), 2.63 (s, 6H), 2.59 (s, 6H), 2.20 (ddt, J = 8.2, 6.1, 3.1 Hz, 2H), 2.12 – 2.04 (m, 2H), 1.85 (td, J = 5.9, 3.4 Hz, 4H), 1.73 (td, J = 5.8, 2.0 Hz, 2H), 1.61 – 1.53 (m, 2H), 1.16 (s, 6H), 1.09 (s, 6H), 1.00 (d, J = 7.0 Hz, 6H), 0.78 (d, J = 8.9 Hz, 2H), 0.66 (s, 2H); ^{13}C-NMR (75 MHz, $CDCl_3$): δ 57.4, 51.1, 51.0, 48.8, 43.1, 42.4, 39.1, 38.2, 34.3, 28.6, 25.8, 23.0, 22.8; ^{11}B-NMR (96 MHz, $CDCl_3$): δ 1.2 (s). Physical and spectral data are in accordance with literature data.[1,2]

(+)-Monoisopinocampheylborane

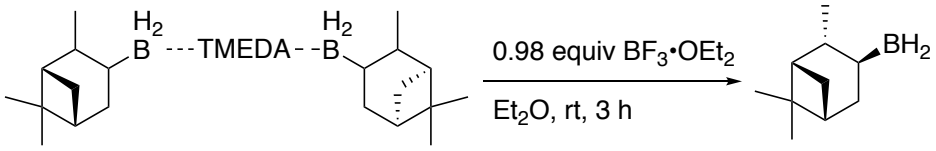

98%

To a suspension of TMEDA·2BH_2Ipc (10.41 g, 25 mmol) in dry Et_2O (34 mL) was dropwise added BF_3·Et_2O (6.2 mL, 49.0 mmol). The mixture was stirred at rt for 3 h. By using a thick needle, the suspension was then transferred to a filter chamber under Argon atmosphere. The solid TMEDA·2BF_3 complex was washed with dry Et_2O until a total volume of 62 mL of the filtrate containing (+)-IpcBH_2 (49 mmol, 98%) was obtained.

Colorless transparent solution; $[\alpha]_D^{23}$ = +52.9 (c=11.6, Et_2O) (lit.[3] $[\alpha]_D^{23}$ = +39.93 (c=11.6, Et_2O)); ^{11}B-NMR (96 MHz, $CDCl_3$): δ 22.6 (s). Physical and spectral data are in accordance with literature data.[3,2] The concentration of the solution was determined by hydrolysis of (+)-IpcBH$_2$ in a 1:1:1 mixture of water/THF/ethylene glycol (30 mL) and subsequent gas-volumetric analysis using the setup depicted below:

Note: To generate stable values of H_2, it is recommended to perform a blank injection of Et_2O (1.8 mL) prior to injecting (+)-IpcBH$_2$ solution.

Volume of (+)-IpcBH$_2$ solution in Et_2O, V_{IpcBH_2}:	1.8 mL
V_{H_2}; measurement 1:	75.8 mL
V_{H_2}; measurement 2:	75.8 mL
V_{H_2}; measurement 3:	75.8 mL
Average volume H_2 formed:	75.8 mL
Standard atmospheric pressure, p:	1013 mbar
Ambient pressure, p_a:	955 mbar
Vapor pressure of water at 296 K, p_v:	28 mbar
Temperature, $t_{0°C}$:	273 K
Temperature, $t_{24°C}$:	297 K

$$n(H_2) = \frac{(p_a - p_v) \times t_{0°C} \times (V_{H_2} - V_{IpcBH_2})}{p \times t_{24°C} \times 22.4 \times V_{IpcBH_2}}$$

$$n(H_2) = \frac{(955\ mbar - 28\ mbar) \times 273\ K \times (75.8\ ml - 1.8\ ml)}{1013\ mbar \times 297\ K \times 22.4\ \frac{L}{mol} \times 1.8\ ml} = 1.540\ mol$$

$$n\big((+)IpcBH_2\big) = 0.770\ \frac{mol}{L}$$

Di-*tert*-butylhyponitrite (DTBHN)

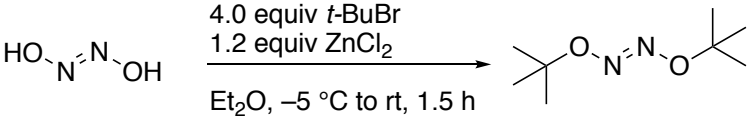

52%

Under high vacuum, sodium *trans*-hyponitrite hydrate was dried for 3 days to a constant weight. The dry sodium *trans*-hyponitrite (5.37 g, 50.7 mmol) was added to *tert*-butyl bromide (45.5 mL, 405 mmol) followed by the addition of dry Et_2O (25 mL). The mixture was cooled to –5 °C. A suspension of $ZnCl_2$ (2 M in Et_2O, 30.4 mL, 60.8 mmol) was cannulated to the reaction mixture at 0 °C. The suspension was allowed to stir at rt for 1.5 h and was then filtered. The filtrate was extracted with water (100 mL) and the aqueous layer was extracted with Et_2O (50 mL). The combined organic layers

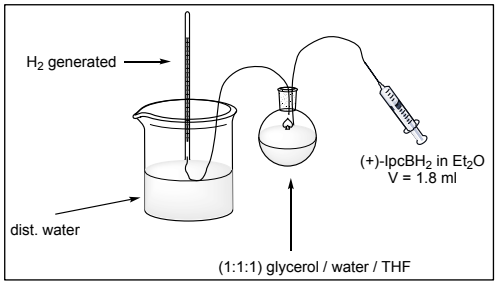

were washed with brine (50 mL), dried over Na_2SO_4, and concentrated at rt. Recrystallisation from pentane afforded di-*tert*-butylhyponitrite (4.56 g, 52%).
Colorless crystals; ^{1}H-NMR (300 MHz, $CDCl_3$): δ 1.39 (s, 9H); ^{13}C-NMR (75 MHz, $CDCl_3$): δ 81.2, 27.8. Physical and spectral data are in accordance with literature data.[4,5]

Di-*tert*-butyl peroxyoxalate (DTBPO)

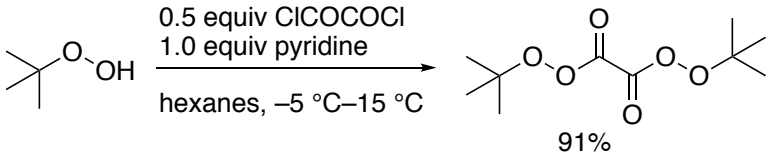

DTBPO is sensitive to heat and shock and therefore a potent explosive. This compound should only be handled with extreme care and appropriate safety precautions (small scale, avoid scratching, use of a blast shield and cut protection gloves).

A solution of freshly opened oxalyl chloride (0.86 mL, 10.0 mmol) in dry hexane (10 mL) was added to a stirred solution of pyridine (1.61 mL, 20.0 mmol) and *tert*-butyl hydroperoxide (3.64 mL, 5.5 mol/L in decane, 20.0 mmol) in dry hexane (20 mL) at –5 °C. The mixture was allowed to warm up to 15 °C, filtered and washed with pentane. The filtrate was cooled to –78 °C and the liquid was removed with a syringe. The solid residue was diluted with pentane (20 mL), cooled to –78 °C, and decantated. This process was repeated twice. The residue was crystallized from pentane at –25 °C overnight. The liquid was removed with a needle and the crystals were dried under high vacuum at 0 °C which afforded di-*tert*-butyl peroxyoxalate (2.14 g, 91%).
Colorless crystals; ^{1}H-NMR (300 MHz, $CDCl_3$): δ 1.38 (s, 18H); ^{13}C-NMR (75 MHz, $CDCl_3$): δ 154.3 (very weak signal), 85.9, 26.1. Physical and spectral data are in accordance with literature data.[6]

Trimethyl(2-phenylsulfanylethynyl)silane

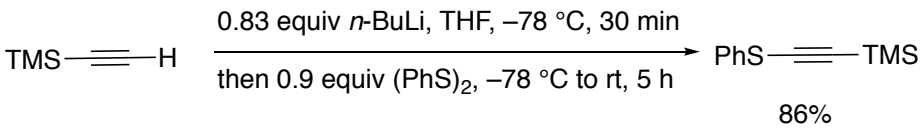

Ethynyl(trimethyl)silane (12.2 mL, 88.0 mmol) in dry THF (80 mL) was cooled to –78 °C. *n*-BuLi (2.5 M in hexane, 29.0 mL, 72.5 mmol) was added dropwise. The mixture was stirred at –78 °C for 30 min. Diphenyldisulfide (17.5 g, 80.2 mmol) in dry THF (40 mL) was added at –78 °C. After being stirred at –78 °C for 30 min, the reaction mixture was allowed to warm up to rt and stirred for 5 h. The reaction mixture was cooled to 0 °C and dist. water (40 mL) and Et_2O (80 mL) were added. The mixture was washed with a solution of NaOH (0.1 M in H_2O, 3x 40 mL) and dist. water (3 x 10 mL). The organic phase was dried over Na_2SO_4 and concentrated. FC (heptanes) afforded trimethyl(2-phenylsulfanylethynyl)silane (14.3 g, 86%).

Yellowish liquid; R_f 0.58 (heptanes); ^{1}H-NMR (300 MHz, $CDCl_3$): δ 7.45 – 7.37 (m, 2H), 7.33 (ddd, *J* = 7.9, 5.8, 1.9 Hz, 2H), 7.25 – 7.18 (m, 1H), 0.25 (s, 9H); ^{13}C-NMR (75 MHz, $CDCl_3$): δ 132.4, 129.3, 126.6, 126.2, 106.4, 90.2, 0.0. Physical and spectral data are in accordance with literature data.[7,8]

Trimethyl((phenylsulfonyl)ethynyl)silane

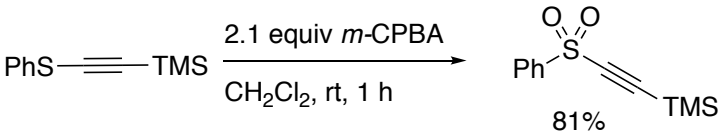

To a stirred solution of trimethyl(2-phenylsulfanylethynyl)silane (14.3 mL, 69.3 mmol) in CH_2Cl_2 (80 mL) was added dropwise a solution of *m*-CPBA (77.0%, 32.6 g, 145 mmol) in CH_2Cl_2 (400 mL). After being stirred at rt for 1 h, the reaction mixture was cooled to 0 °C and a sat. $NaHCO_3$ solution (300 mL) was added. The reaction mixture was stirred at rt for 15 min and was extracted with CH_2Cl_2 (50 mL), once more washed with a cold sat. aq. $NaHCO_3$ solution (100 mL), and washed with dist. water (2 x 100 mL). The organic phase was dried over Na_2SO_4 and concentrated. The product was repeatedly precipitated from Et_2O at –25 °C, filtered off and dried under high vacuum affording trimethyl((phenylsulfonyl)ethynyl)silane (13.5 g, 81%).

White solid; R_f 0.70 (heptanes); ^{1}H-NMR (300 MHz, $CDCl_3$) δ 8.06 – 7.95 (m, 2H), 7.67 (d, *J* = 7.4 Hz, 1H), 7.63 – 7.53 (m, 2H), 0.22 (s, 9H); ^{13}C-NMR (75 MHz, $CDCl_3$): δ 141.9, 134.8, 129.9, 128.0, 102.7, 98.6, -0.6. Physical and spectral data are in accordance with literature data.[7]

Trimethyl(2-phenylsulfanylethynyl)silane

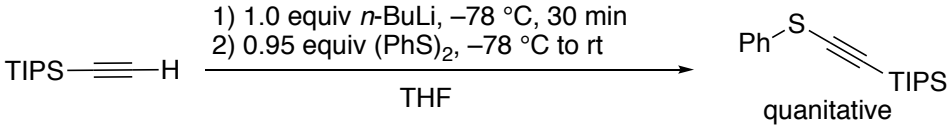

(Triisopropylsilyl)acetylene (30 mL, 134 mmol) was dissolved in dry THF (100 mL) and the solution was cooled to –78 °C. *n*-BuLi (2.5 M in hexane, 50.6 mL, 126 mmol) was added dropwise and the mixture was stirred for 30 min at this temperature. Diphenyldisulfide (27.6 g, 126 mmol) in dry THF (44 mL) was slowly added at –78 °C. After being stirred at –78 °C for 30 min, the reaction mixture was allowed to warm up to rt and stirred overnight. The reaction mixture was cooled to 0 °C, stirred for further 10 min and subsequently treated with dist. water (60 mL). The reaction mixture was diluted with Et2O (50 mL). The phases were separated and the aqueous phase was extracted twice with Et_2O (50 mL). The combined organic phase was washed with aq. NaOH (0.1 M, 2 x 100 mL), dist. water (3 x 50 mL) and brine (50 mL). The organic phase was dried over Na_2SO_4, concentrated and the obtained oil was dried under high vacuum. Trimethyl(2-phenylsulfanylethynyl)silane was obtained after FC (heptanes) (36 g, quantitative).

Yellowish oil; R_f 0.75 (heptanes); ^{1}H-NMR (300 MHz, $CDCl_3$): δ 7.45 – 7.37 (m, 2H), 7.33 (ddd, *J* = 7.9, 5.8, 1.9 Hz, 2H), 7.25 – 7.18 (m, 1H), 0.25 (s, 9H); ^{13}C-NMR (75 MHz, $CDCl_3$): δ 132.4, 129.3, 126.6, 126.2, 106.4, 90.2, 0.0. Physical and spectral data are in accordance with literature data.[9,8,10]

Triisopropyl((phenylsulfonyl)ethynyl)silane

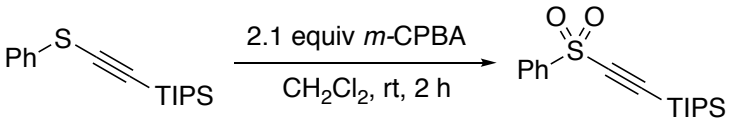

98%

To a stirred solution of the crude trimethyl(2-phenylsulfanylethynyl)silane in dry CH_2Cl_2 was added drop wise a solution of *m*-CPBA (77%, 60 g, 265 mmol) in dry CH_2Cl_2 at rt over 2 h using a dropping funnel. The white suspension was stirred for 2 h until complete consumption of the thioether. The reaction was cooled to 0 °C and transferred into a beaker flask. Sat. $NaHCO_3$ (250 ml) was added and the mixture was stirred vigorously for 20 min at rt to give a white suspension. The organic phase was separated and the aqueous phase was extracted twice with CH_2Cl_2. The combined organic phases were washed with sat. $NaHCO_3$, water and brine, dried over Na_2SO_4 and concentrated. FC (Et_2O/pentane 1:9) afforded triisopropyl((phenylsulfonyl)ethynyl)silane (39.8 g, 98%).

Colorless, viscous oil; R_f 0.63 (Et_2O/pentane 1:9); ^{1}H-NMR (300 MHz, $CDCl_3$): δ 8.06 – 7.95 (m, 2H), 7.67 (d, *J* = 7.4 Hz, 1H), 7.63 – 7.53 (m, 2H), 0.22 (s, 9H); ^{13}C-NMR (75 MHz, $CDCl_3$): δ 141.9, 134.8, 129.9, 128.0, 102.7, 98.6, -0.6. Physical and spectral data are in accordance with literature data.[10]

Enantioselective hydroboration

2-(Cyclopent-1-en-1-yl)furan (1)

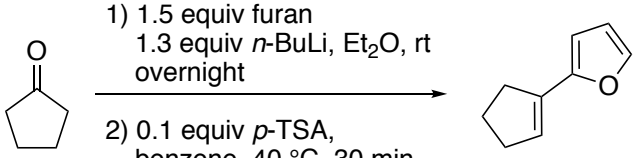

1 67%

To a solution of freshly distilled furan (25.0 mL, 344 mmol) in dry Et_2O (250 mL) was added dropwise *n*-BuLi (2.5 M in hexane, 120 mL, 300 mmol) at 0 °C. After being stirred at 0 °C for 1 h, a white suspension was observed to which freshly distilled cyclopentanone (20.0 mL, 225 mmol) in dry Et_2O (100 mL) was added at 0 °C. The mixture was stirred at this temperature for 1 h, then allowed to warm to rt and stirred overnight. The mixture was treated with dist. water (30 mL) and was then filtered over Celite®, dried over Na_2SO_4, and concentrated. The crude 1-(furan-2-yl)cyclopentane-1-ol[11] was dissolved in dry benzene (400 mL) and *p*-toluenesulfonic acid (4.3 g, 22.5 mmol) was added at rt. The mixture was stirred at 40 °C for 30 min. The mixture was diluted with water (100 mL) and the organic layer was separated. The benzene layer was concentrated and the residue was re-dissolved in EtOAc. The above aqueous layer was extracted with EtOAc (3 x 100ml). All combined organic layers were washed twice with sat. aq. $NaHCO_3$, dried over Na_2SO_4 and concentrated in vacuo. The residue was filtered through a pad of silica which was then thoroughly washed with pentane. The filtrate was concentrated in vacuo. Distillation (50 °C, 2 mbar) afforded **1** (20.3 g, 67%).

Colorless liquid; R_f 0.61 (pentane); ^{1}H-NMR (300 MHz, $CDCl_3$): *δ* 7.36 (d, *J* = 1.5 Hz, 1H), 6.37 (dd, *J* = 3.3, 1.8 Hz, 1H), 6.17 (d, *J* = 3.3 Hz, 1H), 6.11 – 6.07 (m, 1H), 2.67 – 2.48 (m, 4H), 2.05 – 1.94 (m,

2H); ^{13}C-NMR (75 MHz, $CDCl_3$): δ 152.7, 141.6, 133.0, 125.0, 111.1, 106.0, 33.3, 32.6, 23.4. Physical and spectral data are in accordance with literature data.[2]

(±)-*trans*-2-(2-Furanyl)cyclopentanol

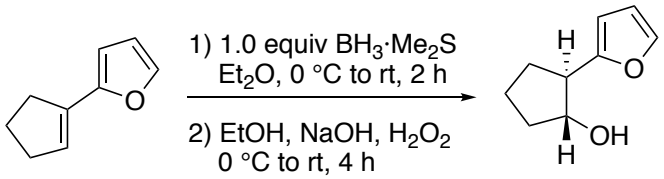

63%

To a solution of 2-(cyclopent-1-en-1-yl)furan (134 mg, 1.0 mmol) in dry Et_2O (2 mL) was added dropwise BH_3·DMS (0.10 mL, 1.0 mmol) at 0 °C. The reaction was allowed to warm to rt and stirred for 2 h. The reaction mixture was cooled to 0 °C and treated with EtOH (2 mL), a solution of aq. NaOH (3 M, 2 mL), and a solution of H_2O_2 (30% in H_2O, 2 mL). The reaction mixture was allowed to stir at rt for 4 h. The mixture was diluted with dist. water (20 mL) and extracted with Et_2O (20 and 10 mL). The organic layers were washed with dist. water (2 x 10 mL), dried over Na_2SO_4, and concentrated. FC (pentane/Et_2O 6:4) afforded *trans*-2-(2-furanyl)cyclopentanol (96 mg, 63%).

Colorless liquid; R_f 0.30 (pentane/Et_2O 6:4); ^{1}H-NMR (300 MHz, $CDCl_3$): δ 7.33 (d, J = 1.2 Hz, 1H), 6.29 (dd, J = 3.1, 1.9 Hz, 1H), 6.05 (d, J = 3.2 Hz, 1H), 4.24 (q, J = 6.5 Hz, 1H), 2.99 (q, J = 7.9 Hz, 1H), 2.22 – 1.97 (m, 3H), 1.92 – 1.58 (m, 4H); ^{13}C NMR (75 MHz, $CDCl_3$): δ 157.2, 141.3, 110.1, 104.5, 78.1, 47.5, 33.8, 28.8, 21.7. Physical and spectral data are in accordance with literature data.[2]

(1*R*,2*R*)-2-(Furan-2-yl)cyclopentan-1-ol

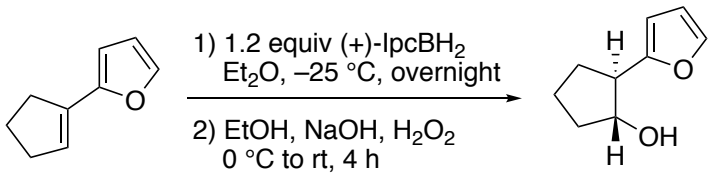

92%

To a solution of (+)-$IpcBH_2$ (0.77 M Et_2O, 1.2 mmol) was added the 2-(cyclopent-1-en-1-yl)furan (134 mg, 1.0 mmol) at –78 °C. The mixture was stored in the freezer at –25 °C overnight. The reaction was treated with EtOH (2 mL) at –25 °C and allowed to warm up to 0 °C. Then, aq. NaOH (3 M, 2 mL) and H_2O_2 (30% in H_2O, 2 mL) were added. The mixture was stirred at rt for 4 h, diluted with water (20 mL), and extracted with Et_2O (20/10 mL). The organic layers were washed with water (2 x 10 mL), dried over Na_2SO_4, and concentrated. FC (CH_2Cl_2/Et_2O 92:8) afforded the title compound (140 mg, 92%).

Colorless liquid; R_f 0.55 (CH_2Cl_2/Et_2O 92:8); ^{1}H-NMR (300 MHz, $CDCl_3$): δ 7.40–7.28 (m, 1H), 6.29 (dd, J = 3.2, 1.9 Hz, 1H), 6.05 (d, J = 3.2 Hz, 1H), 4.24 (q, J = 6.5 Hz, 1H), 2.99 (dd, J = 14.9, 7.9 Hz, 1H), 2.21–1.97 (m, 2H), 2.04 (s, 1H), 1.90–1.58 (m, 4H); ^{13}C NMR (75 MHz, $CDCl_3$): δ 157.2, 141,3, 110.1, 104.5, 78.1, 47.5, 33.8, 28.8, 21.7 Er 94:6. Physical and spectral data are in accordance with literature data.[2,12]

HPLC trace of (±)-*trans*-2-(2-furyl)cyclopentanol (CHIRALPAK IC-3; hexane/iPrOH 98:2; 1 mL min^{-1}, λ = 210 nm)

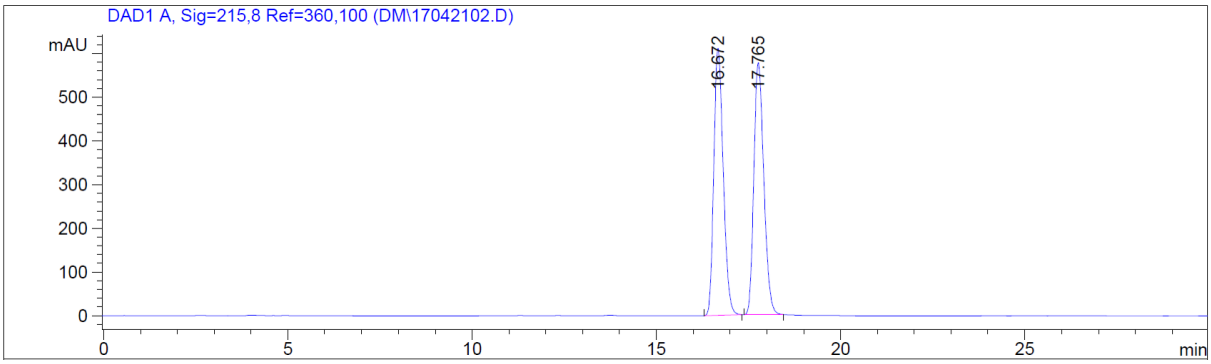


```
Signal 1: DAD1 A, Sig=215,8 Ref=360,100

Peak RetTime Type  Width     Area      Height     Area
  #   [min]       [min]   [mAU*s]     [mAU]       %
----|-------|----|-------|----------|----------|--------|
   1  16.672 BB    0.2775 1.08664e4   611.00970  50.0635
   2  17.765 BB    0.2932 1.08388e4   576.80896  49.9365
```

HPLC trace of (1*R*,2*R*)-2-(furan-2-yl)cyclopentan-1-ol (CHIRALPAK IC-3; hexane/iPrOH 98:2; 1 mL min^{-1}, λ = 210 nm)

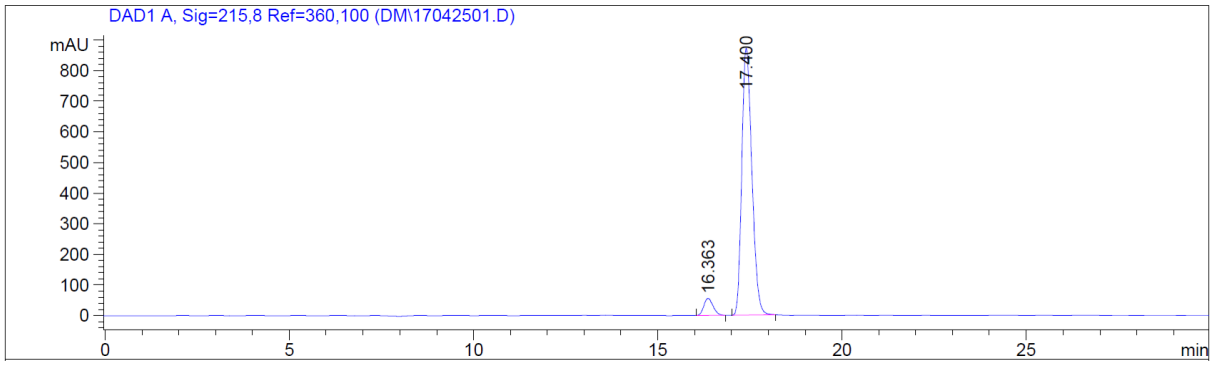


```
Signal 1: DAD1 A, Sig=215,8 Ref=360,100

Peak RetTime Type  Width     Area      Height     Area
  #   [min]       [min]   [mAU*s]     [mAU]       %
----|-------|----|-------|----------|----------|--------|
   1  16.363 BB    0.2705  966.49951   55.69291   5.5057
   2  17.400 BB    0.2963 1.65881e4   870.70294  94.4943

Totals :                 1.75546e4   926.39585
```

Enantioselective hydroalkynylation

(±)-*trans*-2-(2-Ethynylcyclopentyl)furan (3)[13]

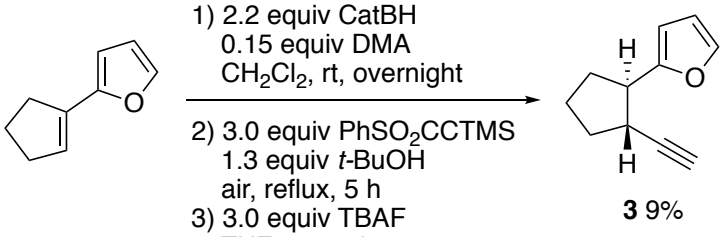

3 9%

To a solution of 2-(cyclopenten-1-yl)furan (134 mg, 1.00 mmol) and dry N,N-dimethylacetamide (DMA) (14 μL, 0.15 mmol) in dry CH_2Cl_2 (1 mL) was added dropwise catecholborane (235 μL, 2.2 mmol) at 0

°C. The reaction mixture was allowed to stir at rt for 16 h. The reaction mixture was treated with *t*BuOH (0.124 mL, 1.3 mmol) at 0 °C and stirred at rt for 15 min. Then, 2-(benzenesulfonyl)ethynyl-trimethylsilane (713 mg, 3.0 mmol) was added portionwise. The solution was heated to reflux and DTBHN (8 mg, 0.46 mmol) was added every hour. After being stirred for a total of 3 h (three additions of initiator) t pentane (20 mL) was added and the mixture was washed with water (3 x 10 mL). The organic phases were dried over Na_2SO_4 and concentrated. FC (pentane) afforded the unstable TMS-protected alkyne (*unstable*; 30 mg, 13%) which was rapidly dissolved in dry THF (2 mL) and treated with TBAF (1M in THF, 0.4 mL, 1.38 mmol). After stirring for 1.5 h, the reaction mixture was diluted with pentane (30 mL) and washed with water (3 x 20 mL). The solution was dried by passing through a pad of Na_2SO_4 and concentrated. FC (pentane) afforded (±)-**3** (15 mg, 9%) as a single diastereomer.
Colorless liquid; R_f 0.52 (pentane); ^{1}H-NMR (300 MHz, $CDCl_3$): δ 7.33 (dd, J = 1.7, 0.7 Hz, 1H), 6.29 (dd, J = 3.1, 1.9 Hz, 1H), 6.11 (d, J = 3.2 Hz, 1H), 3.15 (d, J = 8.2 Hz, 1H), 2.78 (s, 1H), 2.20 – 2.05 (m, 3H), 1.79 (tt, J = 6.0, 3.4 Hz, 4H); ^{13}C-NMR (75 MHz, $CDCl_3$): δ 156.9, 141.2, 110.0, 104.6, 87.2, 68.8, 46.1, 36.0, 33.4, 31.2, 24.0; IR (cm^{-1}): 3312, 2942, 2865, 1463, 1260, 1010, 883, 798, 728, 676. Physical and spectral data are in accordance with literature data.[13]

(((1*R*,2*R*)-2-(Furan-2-yl)cyclopentyl)ethynyl)triisopropylsilane (2b)

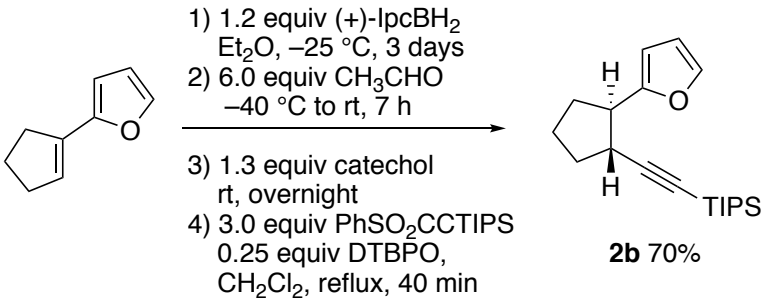

2b 70%

To a stirred solution of (+)-IpcBH$_2$ (0.77 M in Et_2O, 6.0 mmol) at –78 °C was added 2-(cyclopenten-1-yl)furan (671mg, 5.0 mmol). After 30 min, the mixture was stored in the freezer at –25°C for 3 nights. The mixture was cooled to –40 °C and acetaldehyde (1.7 mL, 30.0 mmol) was added dropwise. The cooling bath was exchanged with an ice bath after 20 min and the reaction mixture was stirred at this temperature for 30 min and then allowed to warm up to rt. After stirring at rt for 8 h, the reaction mixture was cooled to 0 °C before catechol (720 mg, 6.5 mmol) was added and the solution was stirred at rt overnight. The volatiles were carefully removed under vacuum and to the residues were quickly added dry CH_2Cl_2 (19 mL), triisopropyl((phenylsulfonyl)ethynyl)silane (4.8 g, 15.0 mmol) and a solution of DTBPO (290 mg, 1.25 mmol) in dry CH_2Cl_2 (3 mL). The reaction mixture was immediately put in a preheated oil bath at 60 °C for 40 min. After cooling, the reaction mixture was diluted with pentane (20 mL) and dist. water (20 mL). The mixture was extracted with pentane (3 x 20 mL) and the combined organic phases were dried over Na_2SO_4, filtered and concentrated. FC (pentane) afforded **2b** (1.11 g, 70%) as a single *trans* diastereomer.
Note: Enantioselective hydroboration can be performed equally well in one night. The radical reaction however appears to be scale-dependent. 10 mmol scale: 38%; 5 mmol: 70%; 0.7 mmol: 85%

Colorless liquid; R_f 0.74 (heptanes/EtOAc 5:5); $[\alpha]_D^{23}$ = –127.5 (c = 1, $CHCl_3$); ^{1}H-NMR (300 MHz, $CDCl_3$): δ 7.30 (dd, *J* = 1.8, 0.8 Hz, 1H), 6.27 (dd, *J* = 3.1, 1.9 Hz, 1H), 6.08 (d, *J* = 3.2 Hz, 1H), 3.13 (s, 1H), 2.80 (s, 1H), 2.16 – 2.05 (m, 2H), 1.80 (dd, *J* = 3.9, 2.3 Hz, 4H), 1.03 (s, 21H); ^{13}C-NMR (75 MHz, $CDCl_3$): δ 157.2, 141.0, 111.8, 109.9, 104.6, 80.5, 46.7, 37.5, 33.6, 30.9, 23.9, 18.6, 18.5, 11.3; IR (cm^{-1}): 2941, 2891, 2864, 2166, 1506, 1463, 1383, 1236, 1150, 1071, 1010, 918, 882, 796, 727, 673; HRMS calc. for $C_{20}H_{33}O_3Si$ $[M+H]^+$: 317.2301, found: 317.2300; Er determined after conversion to **3** (see below)

2-((1*R*,2*R*)-2-Ethynylcyclopentyl)furan (3)

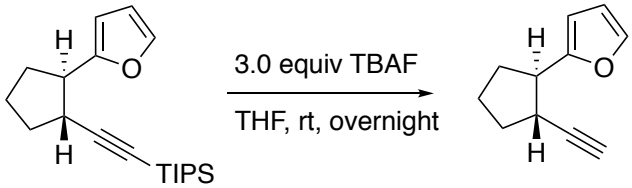

2b **3** quant.

To a solution of (1*R*,2*R*)-**2b** (316 mg, 1.0 mmol) in dry THF (2.5 mL) was added TBAF (1M in THF, 3 mL) and the mixture was stirred at rt overnight. Water (10 mL) was added and the mixture was extracted with pentane (3 x 10 mL). The organic phase was washed with dist. water (3 x 30 mL), dried over Na_2SO_4, and concentrated. FC (pentane) afforded (1*R*,2*R*)-**3** (160 mg, quantitative).

Colorless liquid; R_f 0.28 (heptanes); er 95:5; $[\alpha]_D^{23}$ = –11.3 (c = 1, THF); ^{1}H-NMR (300 MHz, $CDCl_3$): δ 7.33 (dd, *J* = 1.7, 0.7 Hz, 1H), 6.29 (dd, *J* = 3.1, 1.9 Hz, 1H), 6.11 (d, *J* = 3.2 Hz, 1H), 3.15 (d, *J* = 8.2 Hz, 1H), 2.78 (s, 1H), 2.20 – 2.05 (m, 3H), 1.79 (tt, *J* = 6.0, 3.4 Hz, 4H); ^{13}C-NMR (75 MHz, $CDCl_3$): δ 156.9, 141.2, 110.0, 104.6, 87.2, 68.8, 46.1, 36.0, 33.4, 31.2, 24.0.

HPLC trace of *trans*-(±)-3 (CHIRALPAK IC-3; hexane; 1 mL min^{-1}, λ = 210 nm).

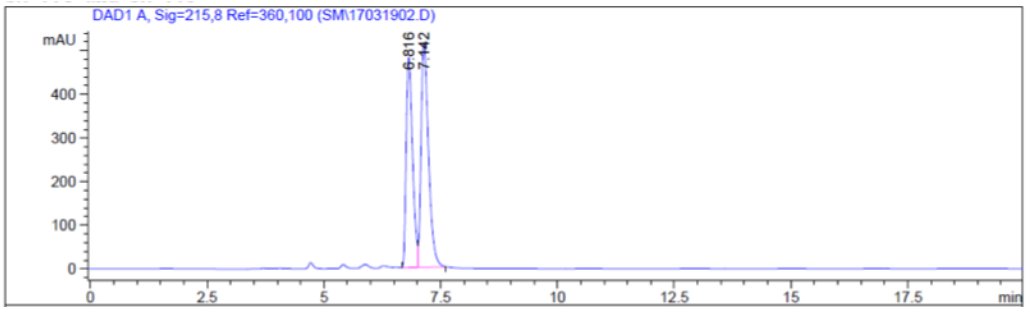

Signal 1: DAD1 A, Sig=215,8 Ref=360,100

Peak #	RetTime [min]	Type	Width [min]	Area [mAU*s]	Height [mAU]	Area %
1	6.816	BV	0.1467	4582.18115	482.85602	44.5268
2	7.142	VB	0.1693	5708.65186	515.14417	55.4732
Totals :				1.02908e4	998.00018	

HPLC trace of enantiomerically enriched (1*R*,2*R*)-**3** (CHIRALPAK IC-3; hexane; 1 mL min^{-1}, λ = 210 nm)

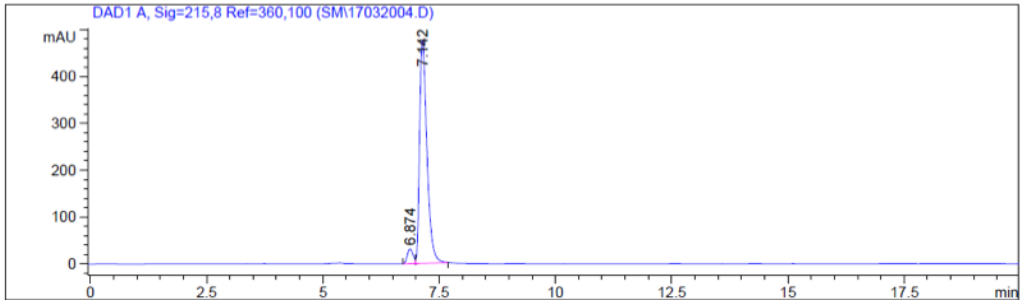

Signal 1: DAD1 A, Sig=215,8 Ref=360,100

Peak #	RetTime [min]	Type	Width [min]	Area [mAU*s]	Height [mAU]	Area %
1	6.874	BV	0.1349	268.07962	30.98556	4.8955
2	7.142	VB	0.1655	5208.01270	476.55481	95.1045
Totals :				5476.09232	507.54037	

Model study for the oxidative furan opening

2-Cyclopentylfuran

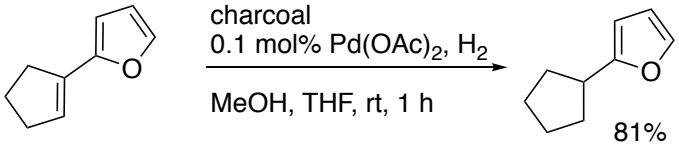

81%

The procedure was adapted from literature.[14]

To a stirred suspension of active charcoal (25.6 mg) and 2-(cyclopent-1-en-1-yl)furan (1.5 g, 11.2 mmol) in dry MeOH was added a $Pd(OAc)_2$ solution (1 mL, 0.011 mmol) prepared in advance by dissolving $Pd(OAc)_2$ (25.6 mg, 0.112 mmol) in dry THF (10 mL) under inert atmosphere. The suspension was stirred for 10 min and then a balloon of H_2 was mounted. Via a small needle, H_2 was continuously bubbled through the mixture for 1 h. The mixture was filtered through a pad of Celite®, washed with pentane and concentrated. FC (pentane) afforded 2-cyclopentylfuran (1.23 g, 81%).

Colorless liquid; R_f 0.78 (pentane); ^{1}H-NMR (300 MHz, $CDCl_3$): δ 7.32 – 7.27 (m, 1H), 6.26 (dd, J = 3.0, 1.9 Hz, 1H), 5.97 (d, J = 3.1 Hz, 1H), 3.07 (s, 1H), 2.00 (dd, J = 7.3, 4.7 Hz, 2H), 1.78 – 1.58 (m, 6H); ^{13}C-NMR (75 MHz, $CDCl_3$): δ 160.1, 140.6, 109.9, 103.1, 38.7, 31.8, 25.2. Physical and spectral data are in accordance with literature data.[15]

(*E*)-4-Cyclopentyl-4-oxobut-2-enal

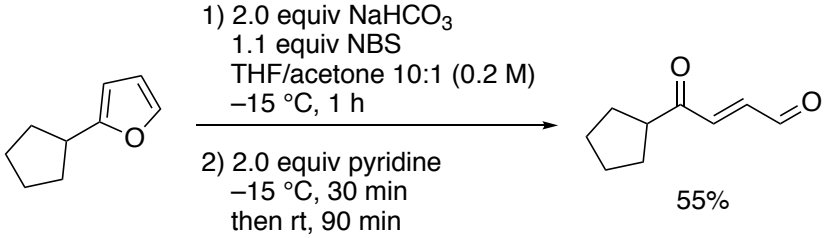

55%

The procedure was adapted from literature.[16]

To a suspension of 2-cyclopentylfuran (100 mg, 0.73 mmol) and $NaHCO_3$ (123 mg, 1.47 mmol) in 3.8 mL of solvent (acetone/water 10:1) was added NBS (144 mg, 0.81 mmol) at –15 °C. The yellow suspension was stirred for 1 h before addition of pyridine (0.12 mL, 1.54 mmol). The mixture was stirred for 30 min, warmed up to rt and then stirred for 1.5 h. The mixture was then directly loaded on column without workup or concentration. FC (heptanes/EtOAc 7:3) afforded (*E*)-4-cyclopentyl-4-oxobut-2-enal (0.4 mmol, 55%).

Note: The compound is sensitive to acid and thermally labile (partial decomposition occurs already during ^{13}C-NMR measurement). The nature (acidity) of the used silica gel is important.

Yellow oil; R_f 0.74 (heptanes/EtOAc 5:5); ^{1}H-NMR (300 MHz, $CDCl_3$): δ 9.78 (d, J = 7.2 Hz, 1H), 6.84 (d, J = 16.2 Hz, 1H), 6.86 (d, J = 7.2 Hz, 1H), 3.27 – 3.14 (m, 1H), 1.94 – 1.77 (m, 4H), 1.75 – 1.60 (m, 4H); ^{13}C-NMR (75 MHz, $CDCl_3$): δ 202.0, 193.4, 144.9, 137.6, 50.0, 29.0, 26.2; IR (cm^{-1}): 2956, 2923, 2870, 2853, 1694, 1452, 1118, 981, 908, 730; HRMS calc. for $C_9H_{13}O_2$ $[M+H]^+$: 153.0910, found: 153.0908.

(*E*)-4-Cyclopentyl-4-oxobut-2-enoic acid

Procedure 1

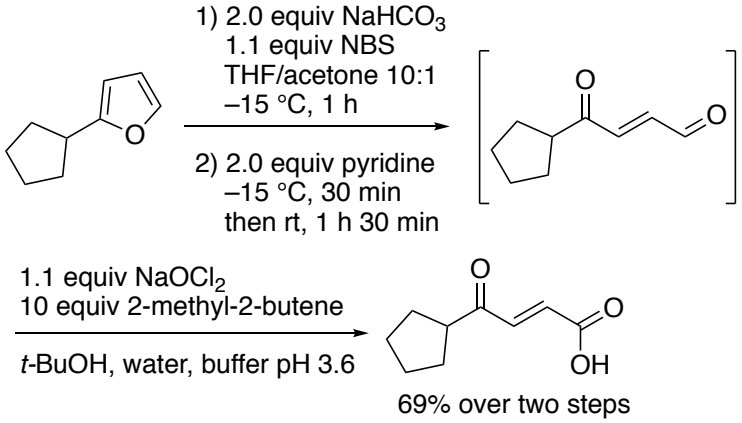

69% over two steps

The procedure was adapted from literature.[16]

To a mixture of crude (*E*)-4-cyclopentyl-4-oxobut-2-enal (65 mg, 0.43 mmol), 2-methyl-2-butene (0.45 mL, 4.27 mmol), *t*BuOH (0.96 mL) and a pH 3.6 phosphate buffer (0.48 mL) [prepared in advance of by dissolving $Na_2HPO_4 \cdot H_2O$ (1.73 g) and citric acid monohydrate in H_2O (Milli-Q water, 98.6 g)] was added a solution of $NaClO_2$ (53.1 mg, 0.47 mmol) in H_2O (Milli-Q water, 0.14 mL). The mixture was stirred at rt for 2 h. The liquids were removed under high vacuum and the residue was dissolved in EtOAc and brine was added. The clear phases were separated and the aqueous phase was acidified to pH 4 with a few drops of aq. HCl. The now turbid suspension was extracted 3 x with EtOAc. The combined organic phases were dried over Na_2SO_4, filtered and concentrated. FC (heptanes/EtOAc/formic acid 60:40:1) afforded (*E*)-4-cyclopentyl-4-oxobut-2-enoic acid (50 mg, 69% over two steps).

White solid; R_f 0.42 (heptanes/EtOAc/formic acid 60:40:1); m.p. 104-107 °C; ^{1}H-NMR (300 MHz, $CDCl_3$): δ 7.22 (d, J = 15.9 Hz, 1H), 6.71 (d, J = 15.9 Hz, 1H), 3.14 (ddd, J = 15.7, 8.4, 7.2 Hz, 1H), 1.92 – 1.76 (m, 4H), 1.72 – 1.60 (m, 4H); ^{13}C-NMR (75 MHz, $CDCl_3$): δ 201.4, 170.3, 140.9, 129.6,

50.4, 28.7, 26.1; IR (cm^{-1}): 3064, 2963, 2869, 1683, 1661, 1429, 1278, 1195, 1009, 642; HRMS: calc. for $C_9H_{13}O_3$ $[M+H]^+$: 169.0865; found 169.0856.

Procedure 2

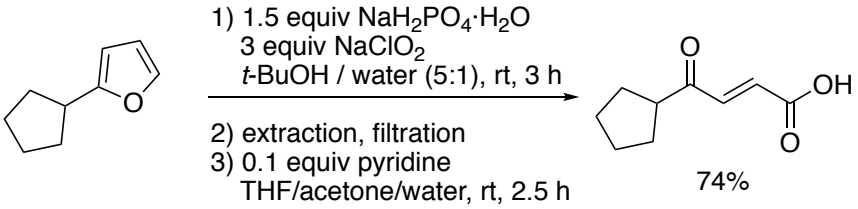

The procedure was adapted from literature.[17]

To a stirred solution of 2-cyclopentylfuran (140 mg, 1.03 mmol) in a solution of *t*BuOH/H_2O (5:1, 5 mL) was added $NaH_2PO_4 \cdot H_2O$ (207 mg, 1.50 mmol) and $NaClO_2$ (80%, 340 mg, 3.09 mmol) at rt. The reaction mixture was stirred for 3 h and the reaction mixture was extracted with Et_2O (3 x 10 mL), washed with brine (2 x 15 mL), dried over Na_2SO_4 and concentrated. The crude product was dissolved in THF/acetone/H_2O (5:4:1, 4 mL) and dry pyridine (10 µl, 0.12 mmol) was added at rt. The reaction mixture was stirred for 2.5 h and the reaction mixture was extracted with Et_2O (3 x 10 mL), washed with aq. $NaHSO_4$ (5%, 20 mL) and water (20 mL). The organic layers were dried over Na_2SO_4 and concentrated. MPLC (pentane/Et_2O 6:3 to 0:10) afforded (*E*)-4-cyclopentyl-4-oxobut-2-enoic acid (129 mg, 74%).

Synthesis of (+)-brefeldin C

(*S*)-Pent-4-en-2-ol

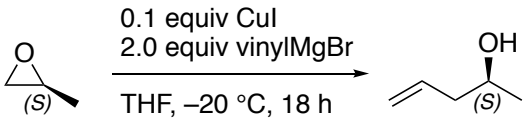

CuI (5.34 g, 28 mmol) was added to a round bottomed flask and dried by heating under vacuum. Dry THF (108 mL) was added and the solution was cooled to –20 °C using a cryostat under constant stirring. Vinylmagnesium bromide (1 M in THF, 542 mL, 542 mmol) was added *via* cannula over 1 h. *S*-(–)-propylene oxide (19 mL, 271 mmol) dissolved in dry THF (10 mL) was added in portions of 1 mL over 3 h. *Note: delayed exothermic behavior*. The reaction mixture was stirred at –20 °C for 18 h, allowed to warm up to rt and was transferred to a sat. aq. NH_4Cl solution (250 mL) *via* cannula. The phases were separated and the blue aqueous phase was extracted 3 x with Et_2O. The combined organic phases were washed with brine, dried over Na_2SO_4, and concentrated. Distillation (70 °C, 150 mbar) afforded (*S*)-pent-4-en-2-ol (12.5 g, 55%).

Colorless crystals; R_f 0.28 (Et_2O/pentane 2:8); $[\alpha]_D^{23}$ = +4.0 (c = 1, $CHCl_3$) (lit.[18] $[\alpha]_D^{23}$ = +10.86 (c = 3.2, Et_2O)); ^{1}H-NMR (300 MHz, $CDCl_3$): δ 5.89 – 5.73 (m, 1H), 5.14 (dhept, *J* = 4.2, 1.0 Hz, 1H), 5.09 (dt, *J* = 2.1, 1.1 Hz, 1H), 3.90 – 3.77 (m, 1H), 2.30 – 2.10 (m, 2H), 1.78 (d, *J* = 6.9 Hz, 1H), 1.19 (dd, *J*

= 6.2, 0.8 Hz, 3H); ^{13}C-NMR (75 MHz, $CDCl_3$): δ 36.2, 119.4, 68.3, 45.1, 24.1. Physical and spectral data are in accordance with literature data.[18]

(*S*)-1-Methoxy-4-((pent-4-en-2-yloxy)methyl)benzene (4)

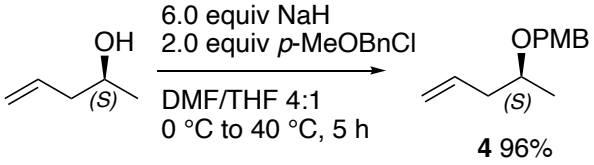

4 96%

To a stirred suspension of NaH (60 % in mineral oil, 4.75 g, 124 mmol) in dry DMF (100 mL) was added dropwise a solution of (*S*)-pent-4-en-2-ol (1.78 g, 20.7 mmol) and *p*-methoxybenzyl chloride (5.8 mL, 41.3 mmol) in dry THF (20 mL) at 0 °C. The suspension was stirred at 40 °C for 5 h. The reaction mixture was cooled to 0 °C and sat. aq. NH_4Cl (30 mL) was slowly added. The mixture extracted with Et_2O (3 x 100 mL) and the combined organic phases were washed with brine (2 x 30 mL), dried over Na_2SO_4 and concentrated. FC (heptanes/EtOAc 95:5) afforded **4** (4.07 g, 96%).

Colorless liquid; R_f 0.21 (heptanes/EtOAc 95:5); $[\alpha]_D^{23}$ = +8.7 (c = 1, $CHCl_3$) (lit.[19] $[\alpha]_D^{20}$ = +10.1 (c = 1, MeOH)); ^{1}H-NMR (300 MHz, $CDCl_3$): δ 7.27 (d, *J* = 8.3 Hz, 2H), 6.90 – 6.82 (m, 2H), 5.83 (d, *J* = 7.1 Hz, 1H), 5.12 – 5.01 (m, 2H), 4.46 (q, *J* = 11.4 Hz, 2H), 3.80 (s, 3H), 3.56 (dd, *J* = 12.2, 6.1 Hz, 1H), 2.43 – 2.15 (m, 2H), 1.18 (d, *J* = 6.2 Hz, 3H); ^{13}C-NMR (75 MHz, $CDCl_3$): δ 159.1, 135.1, 131.1, 129.1, 116.8, 113.8, 74.1, 70.0, 55.3, 40.9, 19.5. Physical and spectral data are in accordance with literature data.[19]

2-((1*R*,2*S*)-2-((*S*,*E*)-6-((4-methoxybenzyl)oxy)hept-1-en-1-yl)cyclopentyl)furan (7)

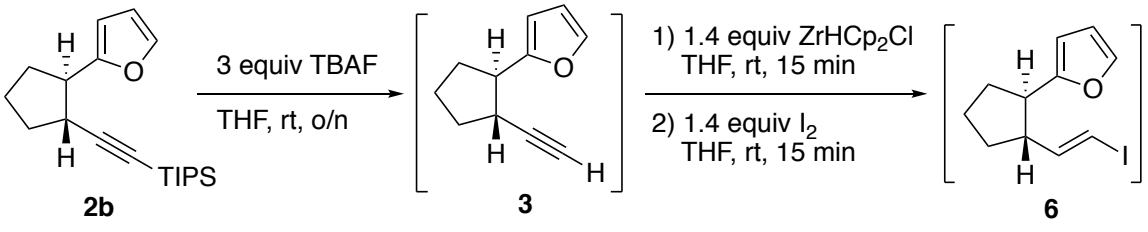

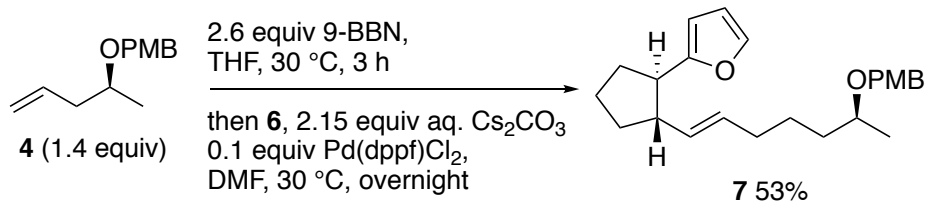

7 53%

Preparation of **3**

To a solution of **2b** (636 mg, 2.0 mmol) in dry THF (5 mL) was added TBAF (1M in THF, 5 mL, 6 mmol) and the mixture was stirred at rt overnight. Water (10 mL) was added and the mixture was extracted with pentane (3 x 10 mL). The organic phase was washed with dist. water (3 x 30 mL), dried over Na_2SO_4, and concentrated to afford the crude terminal alkyne **3**.

Preparation of **6**

The crude **3** was dissolved in dry THF (20 mL) and added to a solution of Schwartz' reagent (1.14 g, 4.4 mmol) in dry THF (12 mL). After stirring for 15 min at rt, a solution of I_2 (1.12 g, 4.4 mmol) in dry THF (5.9 mL) was added to the bright yellow mixture, which results in a sharp change of colour to black. After 15 min of stirring at rt, the reaction was treated with water (10 mL). The reaction mixture was extracted with Et_2O (3 x 50 mL), washed several times with 10% aq. $Na_2S_2O_3$ until the solution became colorless. The organic phase was dried over Na_2SO_4 and quickly concentrated. The crude iodide **6** was only rapidly purified by FC (pentane; R_f 0.43) and then dissolved in dry DMF (24 mL) for the next step.

Preparation of 5

A stirred solution of (*S*)-**4** (920 mg, 4.2 mmol) in dry THF (22 mL) was treated with a solution of 9-BBN (0.5 M in THF, 16.4 mL, 8.2 mmol) and kept at 30 °C for 3 h. This crude solution of **5** was used as it stands for the next step.

Preparation of **7**

A degassed 3 M solution of Cs_2CO_3 (2.2 g, 6.8 mmol) in water (2.2 mL) was added to the solution of **5** (see above) followed by the crude vinyl iodide **6** solution (see above) and $Pd(dppf)Cl_2 \cdot CH_2Cl_2$ (260 mg, 0.32 mmol). The dark solution was stirred overnight at 30 °C and treated with a sat. aq. NH_4Cl (20 mL). The mixture was extracted with Et_2O (3 x 10 mL) and the combined organic phases were dried over Na_2SO_4, filtered and concentrated. FC (pentane/Et_2O 95:5) afforded **7** (623 mg, 53%).

Colorless oil; R_f 0.35 (pentane / Et_2O 95:5); $[\alpha]_D^{23}$ = –8.2 (c = 0.4, $CHCl_3$); ^{1}H-NMR (300 MHz, $CDCl_3$): δ 7.22 – 7.16 (m, 3H), 6.83 – 6.74 (m, 2H), 6.18 (dd, J = 3.1, 1.9 Hz, 1H), 5.90 (d, J = 3.1 Hz, 1H), 5.36 – 5.18 (m, 2H), 4.34 (d, J = 20.6 Hz, 2H), 3.72 (s, 3H), 3.44 – 3.33 (m, 1H), 2.68 (q, J = 8.8 Hz, 1H), 2.53 – 2.38 (m, 1H), 2.05 – 1.93 (m, 1H), 1.92 – 1.79 (m, 3H), 1.78 – 1.59 (m, 3H), 1.51 – 1.17 (m, 5H), 1.08 (d, J = 6.1 Hz, 3H); ^{13}C-NMR (75 MHz, $CDCl_3$): δ 159.1, 140.8, 133.3, 131.4, 130.1, 129.3, 113.8, 110.0, 104.1, 74.5, 70.0, 55.4, 48.9, 45.5, 36.0, 33.1, 32.6, 31.9, 25.5, 23.9, 19.8; IR (cm^{-1}): 2934, 2862, 1612, 1587, 1512, 1454, 1372, 1337, 1301, 1245, 1172, 1133, 1110, 1070, 1036, 1009, 965, 909, 884, 821, 728, 648; HRMS calc. for $C_{24}H_{33}O_3$ $[M+H]^+$: 369.2424, found: 369.2427.

(*S*,*E*)-7-((1*S*,2*R*)-2-(Furan-2-yl)cyclopentyl)hept-6-en-2-ol (8)

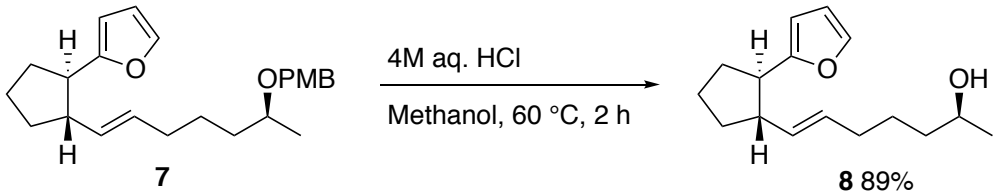

7 **8** 89%

To a solution of **7** (100 mg, 0.27 mmol) in MeOH (7 mL) was added aq. HCl (4 M, 5 mL) at rt. The white suspension was stirred at 60 °C for 2 h (the reaction mixture turned dark) and sat. aq. $NaHCO_3$ was added until the pH was neutral. The mixture was extracted with CH_2Cl_2 and the organic phase was dried over Na_2SO_4, filtered and concentrated. FC (heptanes/EtOAc 8:2) afforded **8** (60 mg, 89%).

Note: Yield is generally lower on larger scale. It is recommended to split a larger batch up for parallel deprotection.

Colorless oil; R_f 0.22 (heptanes/EtOAc 8:2); $[\alpha]_D^{23}$ = –67.4 (c = 1, $CHCl_3$); ^{1}H-NMR (300 MHz, $CDCl_3$): δ 7.29 (dd, J = 1.9, 0.8 Hz, 1H), 6.26 (dd, J = 3.2, 1.9 Hz, 1H), 5.98 (dt, J = 3.2, 0.8 Hz, 1H), 5.45 – 5.27 (m, 2H), 3.76 (q, J = 5.8 Hz, 1H), 2.76 (q, J = 8.8 Hz, 1H), 2.53 (tt, J = 9.7, 6.9 Hz, 1H), 2.11 – 1.88 (m, 4H), 1.75 (dddd, J = 16.3, 10.3, 8.0, 3.9 Hz, 3H), 1.53 – 1.21 (m, 6H), 1.16 (d, J = 6.2 Hz, 3H); ^{13}C-NMR (75 MHz, $CDCl_3$): δ 158.7, 140.8, 133.6, 129.9, 110.0, 104.1, 68.2, 49.0, 45.6, 38.8, 38.8, 33.1, 32.5, 32.0, 25.7, 25.7, 23.9, 23.6, 23.6 IR (cm^{-1}): 3341, 2929, 2871, 1595, 1506, 1452, 1373, 1009, 964, 726; HRMS calc. for $C_{16}H_{25}O_2$ $[M+H]^+$: 249.1849, found: 249.1844

(*E*)-4-((1*R*,2*S*)-2-((*S*,*E*)-6-Hydroxyhept-1-en-1-yl)cyclopentyl)-4-oxobut-2-enoic acid (10)

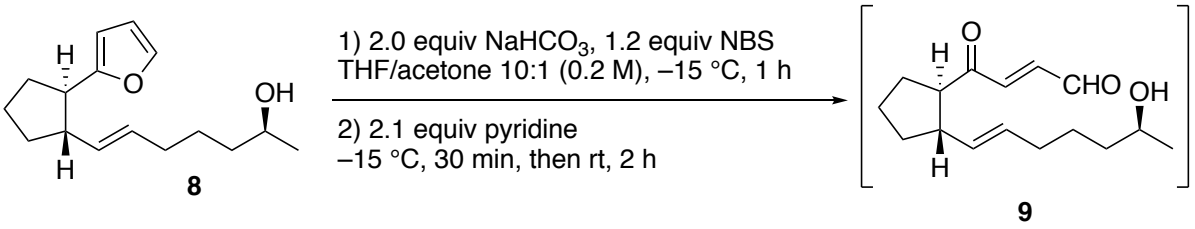

8 **9**

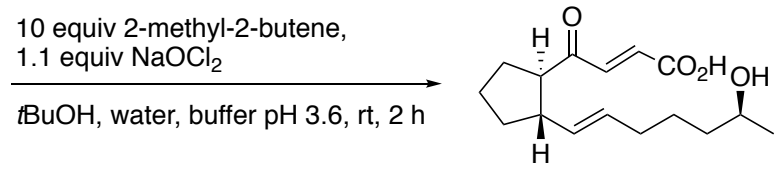

10 85% over two steps

To a stirred solution of $NaHCO_3$ (20 mg, 0.24 mmol) and **8** (30 mg, 0.12 mmol) in acetone/water (10:1, 0.63 mL) at –15 °C was added NBS (26 mg, 0.15 mmol). The yellow solution was stirred at this temperature for 1 h. Then, pyridine (21 μL, 0.25 mmol) was added, the mixture was stirred for 30 min and allowed to warm up to rt and the orange solution was stirred for 2 h. The reaction mixture was directly loaded on a silica gel column without workup nor concentration. Rapid purification by FC (heptanes/EtOAc 5:5) afforded the intermediate enal **9** as yellowish oil which was used without further purification in the next step.

Note: The compound is very sensitive to acid.[20] Partial decomposition was observed in presence of silica gel.

To a mixture of crude **9** (33 mg), 2-methyl-2-butene (0.13 mL, 1.25 mmol), *t*BuOH (0.28 mL) and the phosphate buffer (0.14 mL) was added a solution of $NaClO_2$ (15.5 mg, 0.14 mmol) in Milli-Q water (40 μL). The mixture was stirred at rt for 2 h. The liquids were removed under high vacuum and the residue was dissolved in EtOAc and brine. The clear phases were separated and the aq. phase was acidified to pH 4 with a few drops of aq. HCl. The turbid suspension was extracted 3 x with EtOAc. The combined organic phase was dried over Na_2SO_4, filtered and concentrated. FC (heptanes/EtOAc/formic acid 50:50:1) afforded **10** (29 mg, 85% over two steps).

Note: It is recommended to use the crude acid directly for the lactonization step without purification by column.

Yellow sticky residue; R_f 0.36 (heptanes/EtOAc/formic acid 50:50:1); $[\alpha]_D^{23}$ = –20.7 (c = 1 $CHCl_3$); ^{1}H-NMR (300 MHz, $CDCl_3$): δ 7.19 (d, J = 15.8 Hz, 1H), 6.66 (d, J = 15.8 Hz, 1H), 5.49 – 5.34 (m, 2H),

3.90 – 3.75 (m, 1H), 2.89 (td, *J* = 8.8, 7.2 Hz, 1H), 2.55 (p, *J* = 8.9 Hz, 1H), 2.03 (ddt, *J* = 11.4, 7.8, 4.5 Hz, 3H), 1.91 (tdd, *J* = 13.5, 8.6, 5.2 Hz, 2H), 1.86 – 1.55 (m, 4H), 1.54 – 1.31 (m, 6H), 1.18 (d, *J* = 6.2 Hz, 3H); ^{13}C-NMR (75 MHz, $CDCl_3$): *δ* 201.32, 168.51, 141.12, 133.46, 131.29, 129.85, 77.48, 77.16, 76.84, 68.71, 57.07, 48.31, 38.49, 34.86, 32.41, 28.19, 25.77, 25.27, 23.02; IR (cm^{-1}): 3429, 2922, 2856, 1679, 1406, 1288, 1212, 1091, 996, 968; HRMS calc. for $C_{16}H_{23}O_4$ $[M–H^+]^–$: 279.1602, found: 279.1610

4-Dehydro-brefeldin C (11)

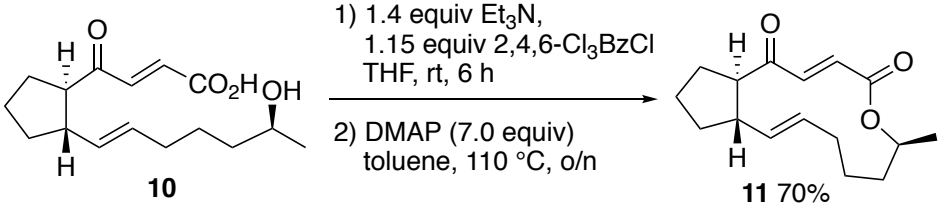

To a solution of **10** (62mg, 0.22 mmol) in dry THF (12.8 mL) were added dropwise Et_3N (43 *μ*L, 0.31 mmol) and 2,4,6-trichlorobenzoyl chloride (40 *μ*L, 0.26 mmol). After 8 h of stirring at rt, the reaction mixture was diluted with dry toluene (28.5 mL). This solution was transferred slowly via cannula to a refluxing solution of DMAP (190 mg, 1.55 mmol) in dry toluene (28.5 mL). The cannula was rinsed with dry toluene (5 mL). The mixture was heated under reflux overnight. The reaction mixture was cooled down to rt and filtered through 1 cm of Celite®. The Celite® cake was thoroughly washed with dry toluene. The clear orange filtrate was concentrated affording a brown slurry. FC (pentane/Et_2O 9:1) afforded **11** (40.5 mg, 70%).

Colorless residue; R_f 0.34 (pentane/Et_2O 9:1); $[\alpha]_D^{23}$ = +3.0 (c = 0.22 $CHCl_3$); ^{1}H-NMR (300 MHz, $CDCl_3$): *δ* 7.81 (d, *J* = 15.9 Hz, 1H), 6.41 (d, *J* = 15.9 Hz, 1H), 5.90 (ddd, *J* = 15.0, 10.8, 4.1 Hz, 1H), 5.46 (ddd, *J* = 15.0, 9.4, 1.5 Hz, 1H), 4.67 (dqd, *J* = 10.3, 6.1, 2.5 Hz, 1H), 2.66 – 2.45 (m, 2H), 2.27 – 2.09 (m, 2H), 2.06 – 1.39 (m, 12H), 1.33 (d, *J* = 6.2 Hz, 3H), 1.29 – 1.11 (m, 2H); ^{13}C-NMR (75 MHz, $CDCl_3$): *δ* 201.3, 166.4, 140.7, 135.9, 132.9, 128.14, 73.7, 58.3, 48.7, 35.3, 34.4, 32.5, 25.9, 25.3, 20.5; IR (cm^{-1}): 2956, 2925, 2855, 1720, 1455, 1378, 1267, 1119, 1073, 1039; HRMS calc. for $C_{16}H_{23}O_3$ $[M+H]^+$: 263.1642, found: 263.1649. Physical and spectral data are in accordance with literature data.[21]

(+)-Brefeldin C

The procedure was adapted from literature.[22]

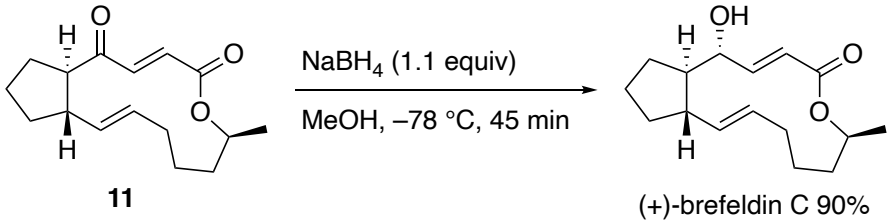

To a solution of **11** (15 mg, 0.06 mmol) in MeOH (2 mL) at –78 °C was added $NaBH_4$ (3 mg, 0.06 mmol). The mixture was stirred at –78 °C for 45 min. After warming up to rt, a sat. aq. $NaHCO_3$ solution (4 mL) was added. The white suspension was extracted with CH_2Cl_2 (3 x 10 mL) and the organic phases were

dried over Na_2SO_4, filtered and concentrated. FC (heptanes/EtOAc 7:3) afforded (+)-brefeldin C (13 mg, 90%).

White solid; R_f 0.38 (heptanes/EtOAc 7:3); m.p. 155–162 °C (lit.[23] m.p. 160–161 °C); $[\alpha]_D^{23}$ = +23.9 (c = 0.42 $CHCl_3$) (lit. $[\alpha]_D^{23}$ = +121 (c = 0.07, MeOH)[19] and $[\alpha]_D^{23}$ = +119.8 (c = 1, $CHCl_3$)[24]); ^{1}H-NMR (300 MHz, $CDCl_3$): δ 7.37 (dd, J = 15.7, 3.1 Hz, 1H), 5.90 (dd, J = 15.7, 2.0 Hz, 1H), 5.72 (ddd, J = 15.0, 10.2, 4.7 Hz, 1H), 5.19 (dd, J = 15.2, 9.5 Hz, 1H), 4.86 (dqd, J = 11.0, 6.3, 1.8 Hz, 1H), 4.09 (dt, J = 9.6, 2.5 Hz, 1H), 2.25 (p, J = 8.7 Hz, 1H), 2.01 (tdd, J = 13.0, 6.1, 3.3 Hz, 2H), 1.91 – 1.78 (m, 2H), 1.78 – 1.32 (m, 9H), 1.26 (d, J = 6.2 Hz, 3H), 1.00 – 0.89 (m, 1H); ^{13}C-NMR (75 MHz, $CDCl_3$): δ 166.4, 152.0, 136.5, 130.5, 117.5, 76.2, 71.8, 54.2, 47.1, 35.3, 34.3, 32.1, 32.0, 26.9, 25.4, 21.0; IR (cm^{-1}): 3435, 2954, 2922, 2848, 1686, 1641, 1447, 1266, 1118, 978; HRMS calc. for $C_{16}H_{24}O_3$ $[M+H]^+$: 265.1798, found: 265.1806. Physical and spectral data are in accordance with literature data, except for the amplitude of the optical rotation. The structure of (+)-brefeldin C synthesized by us was confirmed by single crystal X-ray crystallography. Suitable crystals were obtained upon evaporation of a solution of (+)-brefeldin C in heptanes/EtOAc under vacuum.

X-Ray crystal structure report of (+)-brefeldin C[25]

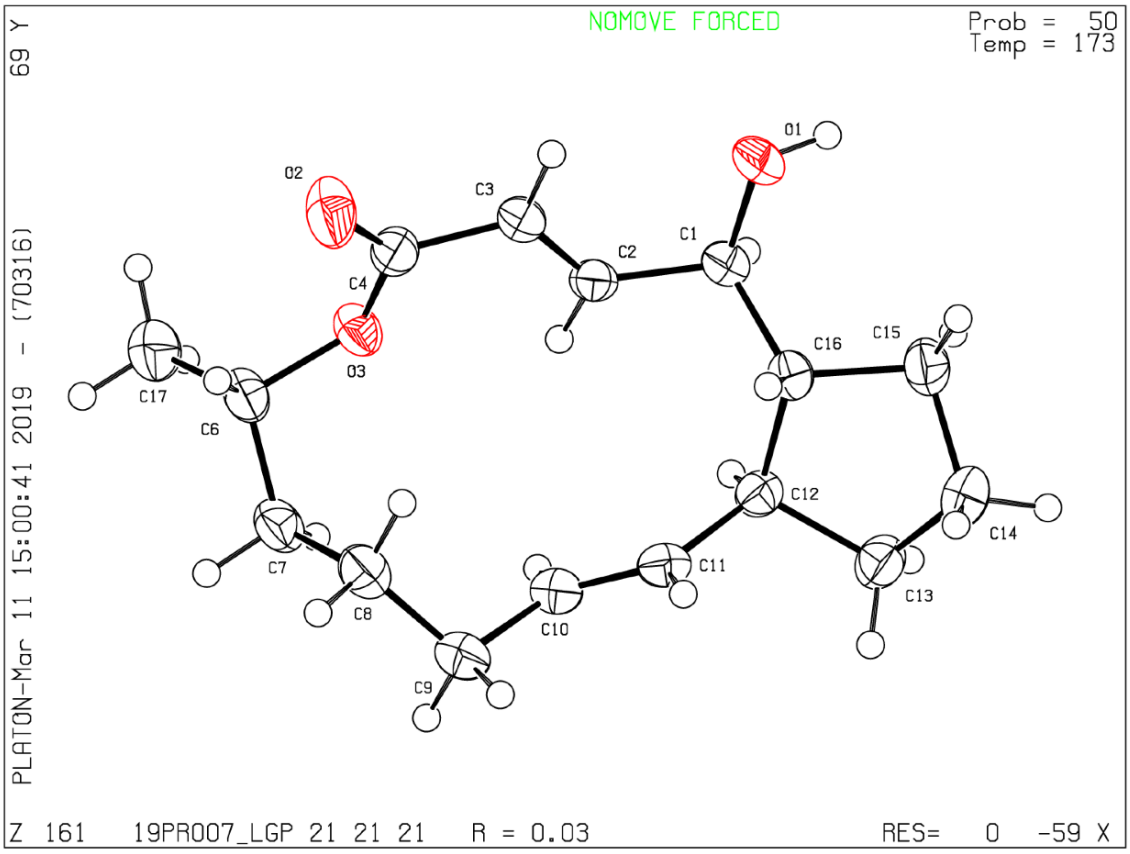

Crystal-Structure Determination. A crystal of $C_{16}H_{24}O_3$ was mounted in air at ambient conditions. All measurements were made on a *RIGAKU Synergy S* area-detector diffractometer[26] using mirror optics monochromated Cu *K*α radiation (λ = 1.54184 Å).[27] The unit cell constants and an orientation matrix for data collection were obtained from a least-squares refinement of the setting angles of reflections in the range 9.988° < 2θ < 144.482°. A total of 562 frames were collected using ω scans, with 0.05 seconds exposure time, a rotation angle of 0.5° per frame, a crystal-detector distance of 31.0 mm, at T = 173(2) K.

Data reduction was performed using the *CrysAlisPro* program.[26] The intensities were corrected for Lorentz and polarization effects, and an absorption correction based on the multi-scan method using SCALE3 ABSPACK in *CrysAlisPro* was applied.[26] Data collection and refinement parameters are given in *Table 1.*

The structure was solved by direct methods using *SHELXT*,[28] which revealed the positions of all non-hydrogen atoms of the title compound. All non-hydrogen atoms were refined anisotropically. H-atoms were assigned in geometrically calculated positions and refined using a riding model where each H-atom was assigned a fixed isotropic displacement parameter with a value equal to 1.2Ueq of its parent atom (1.5Ueq for methyl groups).

Refinement of the structure was carried out on F^2 using full-matrix least-squares procedures, which minimized the function $\Sigma w(F_o^2 - F_c^2)^2$. The weighting scheme was based on counting statistics and included a factor to downweight the intense reflections. All calculations were performed using the *SHELXL-2014/7*[28] program in OLEX2.[29]

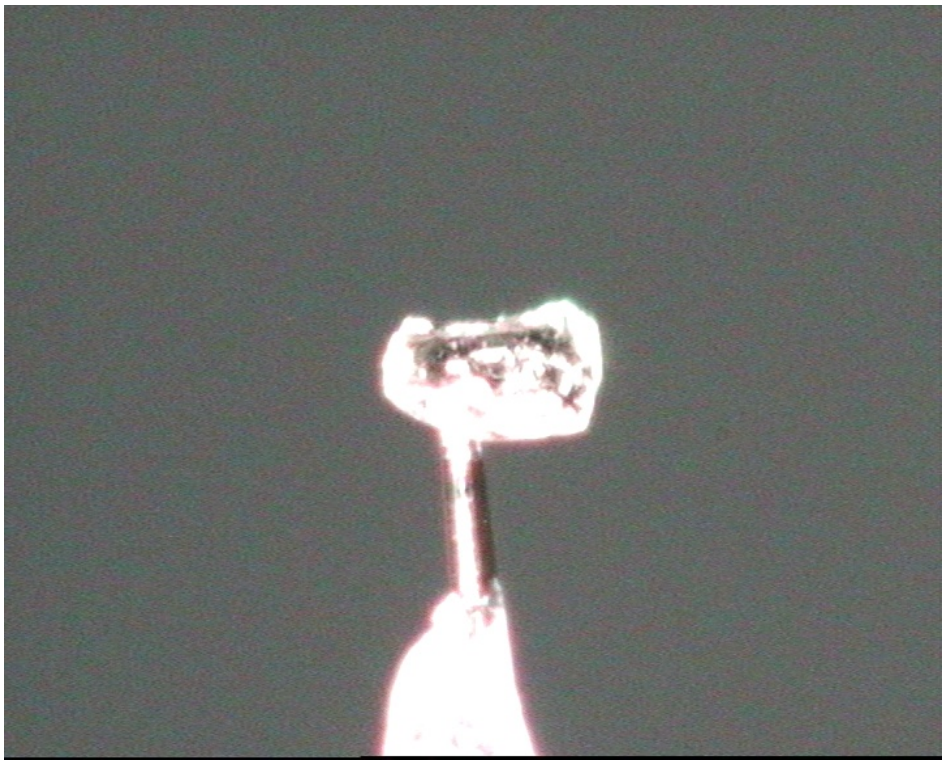

A single crystal of the compound mounted on a glass fiber.

References

[1] H. C. Brown, A. K. Mandal, N. M. Yoon, B. Singaram, J. R. Schwier, P. K. Jadhav, *J. Org. Chem.* **1982**, *47*, 5069–5074.

[2] D. Meyer, P. Renaud, *Angew. Chem. Int. Ed.* **2017**, *56*, 10858–10861.

[3] H. C. Brown, B. Singaram, *J. Am. Chem. Soc.* **1984**, *106*, 1797–1800.

[4] G. David Mendenhall, *Tetrahedron Lett.* **1983**, *24*, 451–452.

[5] J. Boukouvalas, S. Cren, P. Renaud, in *Encyclopedia of Reagents for Organic Synthesis*, Wiley, Hoboken, **2007**, DOI: 10.1002/047084289X.rd062.pub2.

[6] P. D. Bartlett, E. P. Benzing, R. E. Pincock, *J. Am. Chem. Soc.* **1960**, *82*, 1762–1768.

[7] J. L. García Ruano, J. Alemán, C. G. Paredes, *Org. Lett.* **2006**, *8*, 2683–2686.

[8] S. Racine, B. Hegedüs, R. Scopelliti, J. Waser, *Chem. Eur. J.* **2016**, *22*, 11997–12001.

[9] R. Frei, J. Waser, *J. Am. Chem. Soc.* **2013**, *135*, 9620–9623.

[10] W. Song, N. Zheng, M. Li, K. Dong, J. Li, K. Ullah, Y. Zheng, *Org. Lett.* **2018**, *20*, 6705–6709.

[11] F. D. Ferrari, A. J. Ledgard, R. Marquez, *Tetrahedron* **2011**, *67*, 4988–4994.

[12] H. C. Brown, A. K. Gupta, J. V. N. V. Prasad, *Bull. Chem. Soc. Jpn.* **1988**, *61*, 93–100.

[13] Schaffner, Arnaud-Pierre, Darmency, Vincent, Renaud Philippe, *Angew. Chem. Int. Ed.* **2006**, *45*, 5847–5849.

[14] F.-X. Felpin, E. Fouquet, *Chem. Eur. J.* **2010**, *16*, 12440–12445.

[15] J. Haner, K. Jack, M. L. Menard, J. Howell, J. Nagireddy, M. A. Raheem, W. Tam, *Synthesis* **2012**, *44*, 2713–2722.

[16] Y. Kobayashi, G. B. Kumar, T. Kurachi, H. P. Acharya, T. Yamazaki, T. Kitazume, *J. Org. Chem.* **2001**, *66*, 2011–2018.

[17] S. P. Annangudi, M. Sun, R. G. Salomon, *Synlett* **2005**, 1468–1470.

[18] P. Kumar, P. Gupta, S. Vasudeva Naidu, *Chem. Eur. J.* **2006**, *12*, 1397–1402.

[19] S. Archambaud, F. Legrand, K. Aphecetche-Julienne, S. Collet, A. Guingant, M. Evain, *Eur. J. Org. Chem.* **2010**, *2010*, 1364–1380.

[20] B. M. Paz, L. Klier, L. Næsborg, V. H. Lauridsen, F. Jensen, K. A. Jørgensen, *Chem. Eur. J.* **2016**, *22*, 16810–16818.

[21] S. L. Schreiber, H. V. Meyers, *J. Am. Chem. Soc.* **1988**, *110*, 5198–5200.

[22] E. J. Corey, R. H. Wollenberg, *Tetrahedron Lett.* **1976**, *17*, 4705–4708.

[23] S. Nozoe, M. Sunagawa, T. Ohta, *Heterocycles* **1979**, *13*, 267–270.

[24] M. Inai, T. Nishii, S. Mukoujima, T. Esumi, H. Kaku, K. Tominaga, H. Abe, M. Horikawa, T. Tsunoda, *Synlett* **2011**, 1459–1461.

[25] CCDC 1937167 Contain the Supplementary Crystallographic Data for This Paper. These Data Are Provided Free of Charge by The Cambridge Crystallographic Data Centre.

[26] *CrysAlisPro (Version 1.171.40.37a)*, Oxford Diffraction Ltd., Yarnton, Oxfordshire, UK, **2018**.

[27] P. Macchi, H.-B. Bürgi, A. S. Chimpri, J. Hauser, Z. Gál, *J. Appl. Cryst.* **2011**, *44*, 763–771.

[28] G. M. Sheldrick, *Acta Cryst A* **2015**, *71*, 3–8.

[29] O. V. Dolomanov, L. J. Bourhis, R. J. Gildea, J. a. K. Howard, H. Puschmann, *J. Appl. Cryst.* **2009**, *42*, 339–341.

Chapter 3

Generation of Tertiary Alkoxy Radicals from Tertiary Hydroperoxides: Remote Functionalization of Unactivated C–H Bonds

Lars Gnägi, Robin Marc Schärer, and Philippe Renaud

draft manuscript

Author contributions
LG conducted the majority of the experimental work with support of RMS. LG and PR were responsible for writing of the article.

3 Generation of Tertiary Alkoxy Radicals from Tertiary Alkyl Hydroperoxides: Remote Functionalization of Unactivated C–H bonds

3.1 Abstract

A general method to form tertiary alkoxyl radicals under mild conditions is presented. Tertiary hydroperoxides are transformed to their corresponding peroxyoxalates and decomposed under thermal conditions liberating a pair of alkoxy radicals. After translocation of the radical (1,5 hydrogen atom transfer) the remote carbon-centered radical is functionalized by using a variety of arylsulfonyl radical traps. Furthermore, intramolecular alkoxy radical addition to olefins and ring-opening *via* β-fragmentation are demonstrated.

3.2 Introduction

The selective functionalization of unactivated aliphatic sp^3 C–H bonds still remains one of the most challenging topics in synthetic organic chemistry.[1] Numerous methods with high regio- and stereoselectivity are available today which involve transition metal catalysis.[2,3]
In addition to these methods, the radical 1,5-hydrogen atom transfer (HAT) of alkoxy radicals was recognized early as an important directing effect, too.[4] It offers an efficient and selective option to perform radical functionalization of alcohols at position 4.[5] Moreover, using alkoxy radicals, also β-fragmentation and intramolecular cyclization to alkenes can also be performed.

Due to the ubiquity of aliphatic alcohols, the generation of alkoxy radicals from the hydroxy group is very attractive. In addition, alkoxy radicals are electrophilic species and therefore exhibit complementary reactivity to nucleophilic alcohols.[6] However, the direct access to alkoxy radicals *via* hydrogen abstraction is difficult due to the high bond dissociation energy and its polarization towards the oxygen atom. Since Barton's original discovery of oxygen-centered radicals *via* nitrite homolysis[7], several different approaches to access alkoxy radicals have emerged (Figure 3.1).[8]

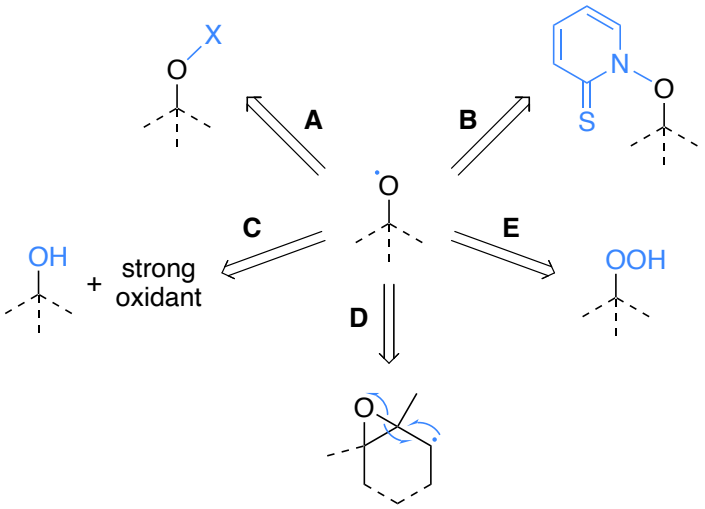

Figure 3.1. General approaches to access alkoxy radicals

Weak oxygen-heteroatom bonds facilitate homolytic cleavage of the O–X bond such as in hypohalides or nitrites (Figure 3.1, **A**), *N*-alkoxy compounds, or Barton esters (Figure 3.1, **B**). Oxidation of alcohols delivers alkoxy radicals, too. This can be achieved by the Suárez cleavage[9], by cerium-mediated ligand-to-metal charge transfer (LMCT)[10,11] or using strong oxidants such as $Pb(OAc)_4$. Recently, Knowles achieved this task *via* proton-coupled electron transfer (PCET) (Figure 3.1, **C**).[12–15]. Radicals adjacent to highly strained epoxides can lead to alkoxy radicals *via* β-fragmentation (Figure 3.1, **D**).[8,16] After the pioneering work of Smith[17] and Walling[18,19] using hypochlorites to perform δ-C-H halogenations, the hydroperoxyl group moved quickly into the focus in the nieteen seventies. Homolysis of the weak oxygen-oxygen bond in (hydro-)peroxides has the advantage that these radical precursors are more stable than hypohalides, do not require to be formed *in situ*, and are accessible using standard procedures (Figure 3.1, **E**).[20] Since then, hydroperoxides have attracted great attention in the community to access alkoxy radicals and many methods have been reported for the formation of selectively functionalized alcohols via 1,5-HAT (Figure 3.2).

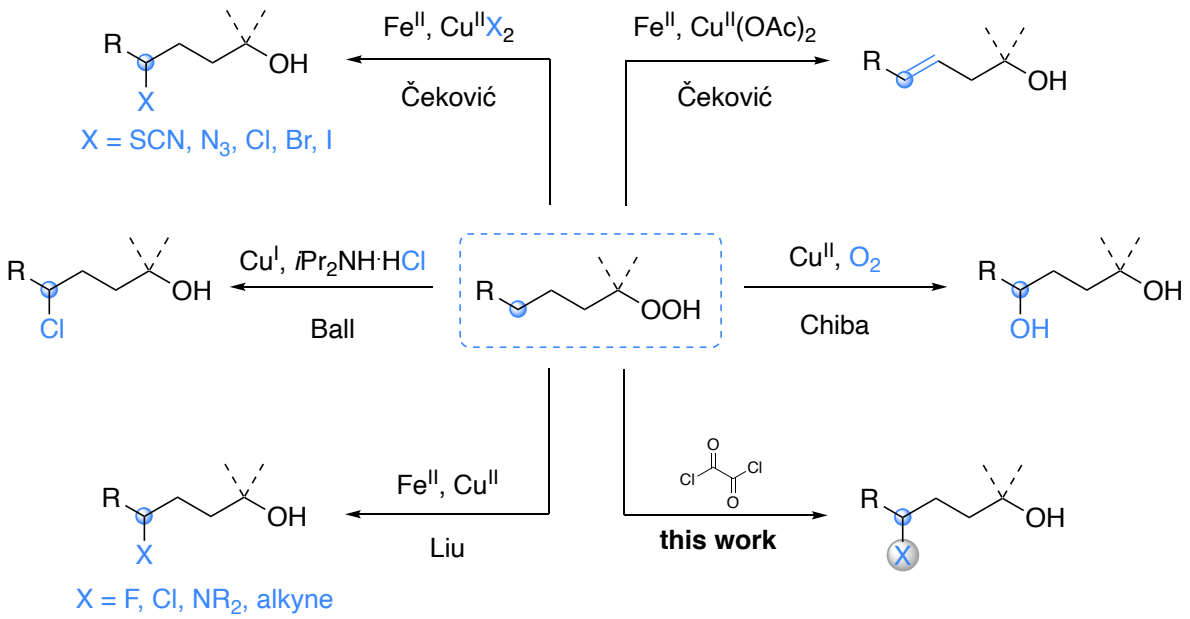

Figure 3.2. Radical remote functionalization of alkyl hydroperoxides based on 1,5-HAT chemistry

Initially, Čeković developed a procedure based on iron(II) and copper(II) dual catalysis to introduce a variety of functional groups. Iron(II) induces the homolytic cleavage of the O–O bond and, after 1,5-HAT, the C-centered radical is trapped by Cu(II) salts[21]; the use of $Cu(OAc)_2$ furnishes the corresponding *trans*-olefins after SET oxidation[21,22]. The Fe(II)/Cu(II) system has also been successfully applied to achieve regioselective radical cyclisations[23,24]. In recent years, Ball[25] reported a novel procedure for δ-C-H chlorination. Oxidation of Cu(I) forms the alkoxy radical which undergoes 1,5-HAT and the generated $CuCl_2$ acts as chlorinating reagent, which sustains the chain by the release of Cu(I) and the formation of the chlorinated product. An important extension to access 1,4-diols was accomplished by Taniguchi[26], who starts from alkenes and involves a transient iron-peroxo complex. Furthermore, Chiba[27] used triethylamine to reduce Cu(II) to Cu(I), which forms the alkoxy radical as similarly described in the work of Ball. After a 1,5-HAT, the radical is trapped by oxygen leading to the desired hydroxy group. Lately, Liu and co-workers published a porphyrine-mediated protocol and extended the method to introduce fluorine and to form C-C bonds by the introduction of alkyne groups[20].

Based on our experience in working with di-*tert*-butyl peroxyoxalate as radical initiator[28], we aimed to design a metal- and additive-free method to generate alkoxy radicals under thermal conditions. The generation of *tert*-butoxy radicals by thermal decomposition of di-*tert*-butyl peroxyoxalate (DTBPO) was first reported by Bartlett in 1960[29]. Due to its low decomposition temperature ($t_{1/2}$ 60 °C = 6.8 min), DTBPO is a particularly attractive initiator for thermally sensitive radical reactions and has been applied in free radical chemistry[30]. Despite the potential safety issues that such peroxyoxalates pose due to their explosive nature, our group has used DTBPO successfully for the generation of alkyl radicals from alkyl catecholboranes, e.g. in our synthesis of (+)-brefeldin C[28].

We assumed the clean and quantitative formation of tertiary alkoxy radicals can be achieved from the decomposition of dialkyl peroxyoxalates, which are easily accessible from the corresponding alkyl hydroperoxides. Upon reaction with oxalyl chloride, alkyl hydroperoxides form dialkyl peroxyoxalates, which are expected to be roughly as stable as DTBPO and can therefore be decomposed under similar thermal conditions.

3.3 Results and discussion

3.3.1 1,5-hydrogen atom transfer

As a starting point to investigate the desired reaction sequence, we chose the synthesis of DTBPO to study the formation of peroxyoxalates. By doing so we realized that the quantification of peroxyoxalate formation is not trivial. Reaction monitoring by GC was not possible due to the instability of the compound. Also, monitoring by NMR turned out unsuccessful because the signals of the substrate and the product are indistinguishable. Isolation of DTBPO requires several recystallisation steps and should anyway be avoided due to the instability of the compound. Standard iodometric titration as well as more specialized methods[31] proved to be not reproducible, supposedly since the peroxyoxalate as well as unreacted hydroperoxide both cause a color indication and because thermal decomposition of the peroxyoxalate is taking place during the measurement. Moreover, the sensitivity of the titration was quite low – a problem that has recently been discussed for peroxide-containing compounds in the industry using dip sticks[32]. To circumvent the problem of direct quantification of the intermediate peroxyoxalates, we monitored only the consumption of hydroperoxide **1** by TLC. To study the basic reactivity of the system, we chose the remote one-pot phenylthiolation leading to **2** as our model system (Table 3.1).

Table 3.1. Optimization of model system on 1 mmol scale; indicated yields are isolated yields

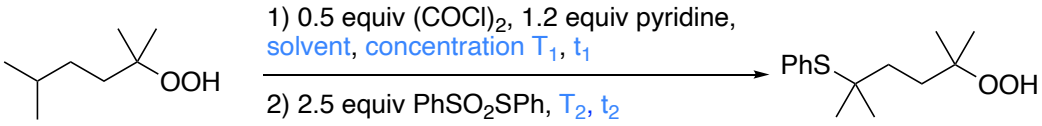

1 **2**

Entry	Solvent	c [mol/L]	T_1 [°C]	t_1 [min]	T_2 [°C]	t_2 [min]	yield [%]
1	MeCN	0.2	10	5	70	15	42
2	MeCN	0.2	10	5	70	45	13
3	CH_2Cl_2	0.2	10	5	reflux	15	8
4	PhH	0.2	10	5	70	15	63
5	hexanes	0.2	10	5	reflux	45	63
6	TBME	0.2	10	5	reflux	15	71
7	TBME	0.2	–20	10	reflux	15	44
8	TBME	0.1	10	5	reflux	15	49

9	TBME	0.5	10	5	reflux	15	63
10	TBME	0.2	10	5	reflux	45	86
11	TBME	0.2	10	5	reflux	45	85 [a]
12	TBME	0.2	10	5	reflux	45	54 [b]
13	TBME	0.2	10	5	reflux	45	74 [c]
14	TBME	0.2	10	5	reflux	45	55 [d]
15	TBME	0.2	10	5	reflux	45	85 [e]

[a] 1.05 equiv pyridine, [b] filtration after first step, [c] based on oxalyl chloride as limiting reagent (0.45 equiv), [d] all reagents added at once, [e] open to air, solvents an apparatus not dried

Our screening showed that in polar solvents all resulting salts were dissolved and the desired product **2** was formed rapidly. Unfortunately, the product also gradually decomposed over prolonged reaction time (entries 1-3). In benzene (entry 4), which only partially dissolved the pyridinium hydrochloride, an increase in yield was observed but the resulting sticky mass was difficult to purify. Therefore, we tested hexanes and TBME to precipitate the salts and thus simplify product purification (entries 5-10). Gratifyingly, longer reaction time in unipolar solvents did not lead to decomposition of the product anymore. Prolonged time for peroxyoxalate formation at lower temperature (to avoid their decomposition) as well as different concentrations were not beneficial to the reaction (entries 7-9). Following the reaction by GC showed that product formation ceased after 35 min. The best result was thus obtained when the perester formation (which we assume is almost instantaneous) is performed quickly and the time for the radical step is set to 45 min. Furthermore, we found that a minimal excess of 1.05 equivalent of pyridine is enough to reach the same yield. Filtration to remove precipitates after the first step, the use of oxalyl chloride as limiting reagent, as well as other types of bases (K_2CO_3, DMAP, triethylamine) resulted in a decreased yield. The apparatus and solvents do not necessarily need to be dried (HPLC quality TBME was used). With our optimized reaction conditions in hand, we investigated the introduction of different residues using phenylsulfonyl radical traps (Figure 3.3).

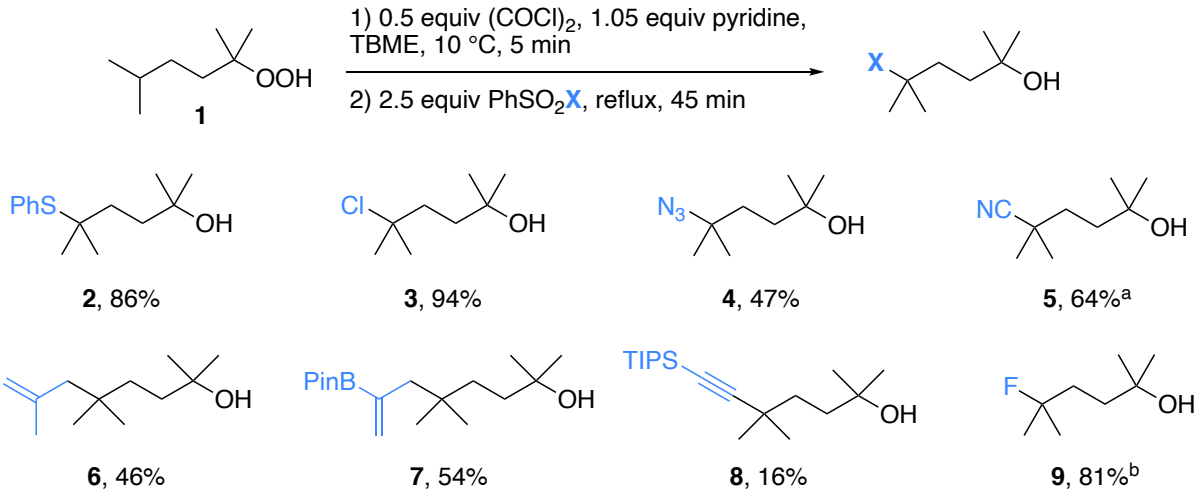

Figure 3.3. Scope of 1,4-functionalise products; [a] decantation after step 1, [b] NFASS as fluorinating reagent[33]

Similar to the phenylthiolation to **2**, the chlorination to **3** also worked excellently. The azidation still afforded **4** in good yields. Interestingly, when we tried to introduce the nitrile group using *p*TsCN as radical trap, the chlorinated product was obtained instead. We found, that *p*TsCN reacts rapidly with the pyridinium chloride precipitate forming *p*TsCl. Decantation of the reaction mixture before addition of *p*TsCN suppressed the formation of *p*TsCl completely, resulting in a clean formation of the desired nitrile **5** in good yield. We were delighted to achieve carbon-carbon bond formation in allylated- and allylborylated products **6** and **7** in 46% and 54% yield, respectively. The introduction of the TIPS protected alkynyl group in **8** proceeded in 16% yield. The low yield is best explained by the high steric bulk of both the tertiary radical and the arylsulfonyl radical trap. Fluorination using our recently developed *N*-fluoro-*N*-arylsulfonylamides (NFASS[33]) afforded **9** in high yield. The method works well also for the remote functionalization of secondary centers (Figure 3.4).

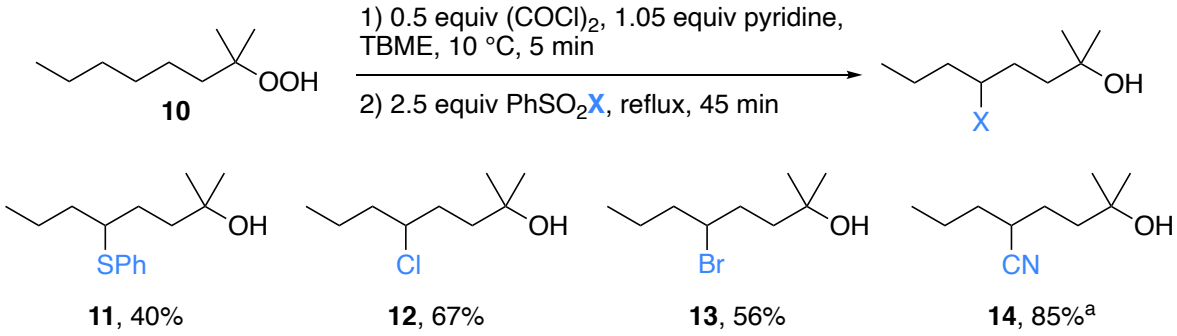

Figure 3.4. CH_2 functionalisation via 1,5-HAT; [a] decantation after step 1

The CH_2-functionalization of hydroperoxide **10** affords phenylthiolated (**11**), halogenated (**12** and **13**), and cyanated (**14**) products in moderate to very good yields.

The proposed mechanism of this non-chain process is explained as follows. In the first step, hydroperoxide **15** is converted to the corresponding thermally unstable peroxyoxalate **16** upon reaction with oxalyl chloride and pyridine (Figure 3.5).

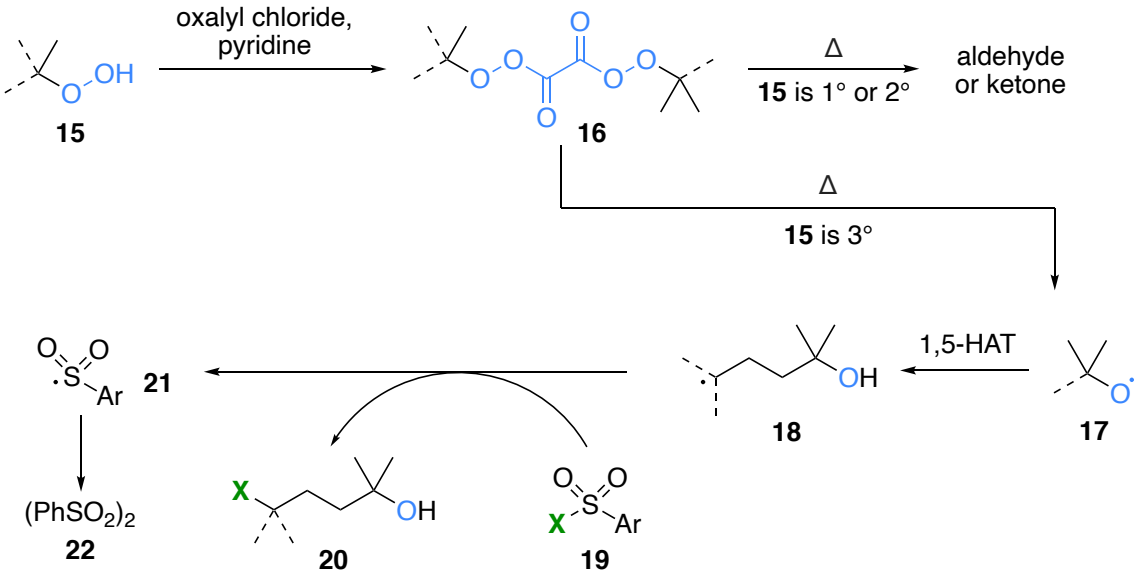

Figure 3.5. Proposed mechanism

If **15** is a primary or secondary hydroperoxide, the non-radical oxidation product (aldehyde or ketone) will be obtained as demonstrated by Dixon and Schuster.[34,35] In the case of tertiary hydroperoxides, the peroxyoxalate decomposes to the alkoxy radical **17** with concomitant release of CO_2. The alkoxy radical undergoes subsequent 1,5-HAT and affords the relocated carbon-centered radical **18**. This radical is trapped with arylsulfonyl **19**, leading to the desired 1,4-functionalized alcohol **20**. The remaining arylsulfonyl radical **21** ultimately dimerizes to **22**.

3.3.2 Fragmentation & cyclisation

In a next step, our method was applied for radical transformations other than the 1,5-HAT process (Figure 3.6).

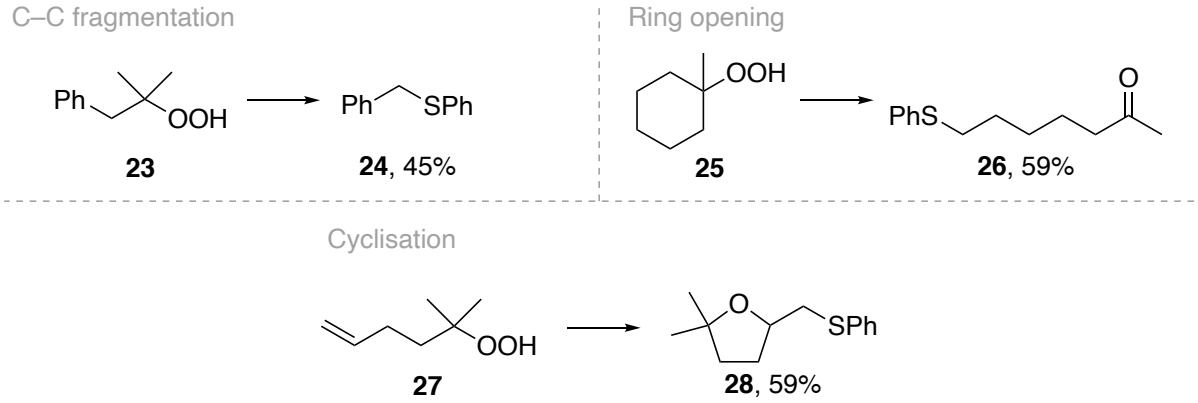

Figure 3.6. Fragmentation and cyclization reactions involving tertiary alkoxy radicals using the optimized conditions

Fragmentation of the tertiary alkoxy radical from **23** results in the formation of a benzylic radical which leads to **24** in reasonable yield. The generation of a methyl radical is energetically unfavorable and is therefore improbable to be considered as a significant competing side reaction[36,37] as the scission at β-position forming a primary radical is expected to be faster by orders of magnitude[37]. The same fragmentation of the cyclic system in **25** affords a primary alkyl radical and thus, the ring-opened product **26**. Cyclic ether **28** is obtained in good yield upon 5-exo-trig cyclisation from **27**.

3.4 Conclusion

We have developed a reliable metal- and additive free method to generate alkoxy radicals from hydroperoxides in quantitative manner. These alkoxy radicals have been utilized for the synthesis of a variety of 1,4-functionalized alcohols *via* 1,5-hydrogen atom transfer and for fragmentation as well as radical cyclisation. The two step one-pot procedure is operationally simple, fast, and does not require workup after the reaction.

3.5 Acknowledgements

Manuel Gnägi-Lux is acknowledged for the generous gift of alkyl tosylate reagents.

Keywords: peroxyoxalates • alkoxy radicals • hydrogen atom transfer • radical reaction • remote functionalisation • organic peroxides

3.6 References

[1] T. Newhouse, P. S. Baran, *Angewandte Chemie International Edition* **2011**, *50*, 3362–3374.

[2] M. C. White, *Science* **2012**, *335*, 807–809.

[3] T. W. Lyons, M. S. Sanford, *Chem. Rev.* **2010**, *110*, 1147–1169.

[4] B. Acott, A. Beckwith, *Australian Journal of Chemistry* **1964**, *17*, 1342.

[5] L. M. Stateman, K. M. Nakafuku, D. A. Nagib, *Synthesis* **2018**, *50*, 1569–1586.

[6] J. Hartung, I. Kempter, T. Gottwald, M. Schwarz, R. Kneuer, *Tetrahedron: Asymmetry* **2009**, *20*, 2097–2104.

[7] D. H. R. Barton, J. M. Beaton, L. E. Geller, M. M. Pechet, *J. Am. Chem. Soc.* **1961**, *83*, 4076–4083.

[8] J. Hartung, T. Gottwald, K. Špehar, *Synthesis* **2002**, *2002*, 1469–1498.

[9] In *Comprehensive Organic Name Reactions and Reagents*, American Cancer Society, **2010**, pp. 2718–2721.

[10] A. Hu, J.-J. Guo, H. Pan, H. Tang, Z. Gao, Z. Zuo, *J. Am. Chem. Soc.* **2018**, *140*, 1612–1616.

[11] A. Hu, J.-J. Guo, H. Pan, Z. Zuo, *Science* **2018**, *361*, 668–672.

[12] C. M. Morton, Q. Zhu, H. Ripberger, L. Troian-Gautier, Z. S. D. Toa, R. R. Knowles, E. J. Alexanian, *J. Am. Chem. Soc.* **2019**, *141*, 13253–13260.

[13] E. Tsui, A. J. Metrano, Y. Tsuchiya, R. R. Knowles, *Angewandte Chemie International Edition* **2020**, *59*, 11845–11849.

[14] E. Tsui, H. Wang, R. R. Knowles, *Chem. Sci.* **2020**, *11*, 11124–11141.

[15] K. Zhao, K. Yamashita, J. E. Carpenter, T. C. Sherwood, W. R. Ewing, P. T. W. Cheng, R. R. Knowles, *J. Am. Chem. Soc.* **2019**, *141*, 8752–8757.

[16] P. Renaud, M. P. Sibi, *Radicals in Organic Synthesis*, **2001**.

[17] F. D. Greene, M. L. Savitz, H. H. Lau, F. D. Osterholtz, W. N. Smith, *J. Am. Chem. Soc.* **1961**, *83*, 2196–2198.

[18] C. Walling, A. Padwa, *J. Am. Chem. Soc.* **1961**, *83*, 2207–2208.

[19] Cheves. Walling, Albert. Padwa, *J. Am. Chem. Soc.* **1963**, *85*, 1597–1601.

[20] H. Guan, S. Sun, Y. Mao, L. Chen, R. Lu, J. Huang, L. Liu, *Angewandte Chemie International Edition* **2018**, 11413–11417.

[21] Ž. Čeković, Lj. Dimttruević, G. Djokić, T. Srnić, *Tetrahedron* **1979**, *35*, 2021–2026.

[22] Ž. Čeković, M. M. Green, *J. Am. Chem. Soc.* **1974**, *96*, 3000–3002.

[23] Y. Nonami, J. Baran, J. Sosnicki, H. Mayr, A. Masuyama, M. Nojima, *J. Org. Chem.* **1999**, *64*, 4060–4063.

[24] A. Masuyama, T. Sugawara, M. Nojima, K. J. McCullough, *Tetrahedron* **2003**, *59*, 353–366.

[25] R. Kundu, Z. T. Ball, *Org. Lett.* **2010**, *12*, 2460–2463.

[26] T. Hashimoto, D. Hirose, T. Taniguchi, *Angewandte Chemie International Edition* **2014**, *53*, 2730–2734.

[27] P. C. Too, Y. L. Tnay, S. Chiba, *Beilstein J. Org. Chem.* **2013**, *9*, 1217–1225.

[28] L. Gnägi, S. V. Martz, D. Meyer, R. M. Schärer, P. Renaud, *Chemistry – A European Journal* **2019**, *25*, 11646–11649.

[29] P. D. Bartlett, E. P. Benzing, R. E. Pincock, *J. Am. Chem. Soc.* **1960**, *82*, 1762–1768.

[30] J. Boukouvalas, J. M. Tanko, *Encyclopedia of Reagents for Organic Synthesis* **2007**.

[31] V. R. Kokatnur, M. Jelling, *J. Am. Chem. Soc.* **1941**, *63*, 1432–1433.

[32] Y. Jiang, X. Song, N. Hou, C. Pan, *Org. Process Res. Dev.* **2019**, *23*, 2538–2542.

[33] D. Meyer, H. Jangra, F. Walther, H. Zipse, P. Renaud, *Nat Commun* **2018**, *9*, 1–10.

[34] B. G. Dixon, G. B. Schuster, *J. Am. Chem. Soc.* **1981**, *103*, 3068–3077.

[35] B. G. Dixon, G. B. Schuster, *Journal of the American Chemical Society* **1979**, 3.

[36] J. K. Kochi, *J. Am. Chem. Soc.* **1962**, *84*, 1193–1197.

[37] M. Buback, M. Kling, S. Schmatz, *Zeitschrift für Physikalische Chemie* **2005**, *219*, 1205–1222.

3.7 Experimental section

General information

Techniques

All reactions requiring anhydrous conditions were performed in heat-gun, oven, or flame dried glassware under an argon atmosphere. An ice bath was used to obtain a temperature of 0 °C. To obtain a temperature of –78 °C, a bath of acetone was cooled with dry ice. To obtain temperatures of –40 °C and –15 °C, a bath of isopropanol or acetonitrile was cooled to the desired temperature using dry ice. Silica gel 60 Å (40–63 µm) from Silicycle was used for flash column chromatography. Thin layer chromatography (TLC) was performed on Silicycle silica gel 60 F_{254} plates, visualization under UV light (254 nm) and/or by dipping in a solution of $(NH_4)_2MoO_4$ (15.0 g), $Ce(SO_4)_2$ (0.5 g), H_2O (90 mL), conc. H_2SO_4 (10 mL); or $KMnO_4$ (3 g), K_2CO_3 (20 g) and NaOH 5% (3 mL) in H_2O (300 mL) and subsequent heating. Anhydrous sodium sulfate was used as drying reagent.

Deactivated silica gel for the purification of boron-containing compounds:
$B(OH)_3$ (25 g) was dissolved in EtOH (technical grade, 500 mL) and stirred overnight. Silica gel (300 mL, approx. 150 g) was suspended in the boric acid solution and stirred for 1 h. The suspension was filtered through a frit and washed with EtOH (technical grade, 500 mL). The silica was then dried under reduced pressure (100mbar, 2 h) and stored in a glass container.

Materials

Commercial reagents were used without further purification unless otherwise stated. Dry solvents for reactions were filtered over columns of dried alumina under a positive pressure of argon. Solvents for extractions (Et_2O, *n*-pentane, CH_2Cl_2, EtOAc, heptanes) and flash column chromatography were of technical grade and distilled prior to use. Commercial dry pyridine was used without further purification.

Instrumentation

^1H and ^{13}C NMR spectra were recorded on a Bruker Avance IIIHD-300 spectrometer operating at 300 MHz for ^1H and 75 MHz for ^{13}C at room temperature (24-25°C) unless otherwise stated. Some ^1H and ^{13}C NMR spectra were recorded on a Bruker Avance IIIHD-400 or a Bruker Avance II-400 spectrometer (^1H: 400 MHz; ^{13}C: 75 MHz). Chemical shifts (δ) are reported in parts per million (ppm) using the residual solvent or $Si(CH_3)_4$ (δ = 0.00 for ^1H NMR spectra) as an internal standard. Multiplicities are given as s (singlet), d (doublet), t (triplet), q (quadruplet), m (multiplet), and br (broad). Coupling constant (*J*) is reported in Hz. In ^{13}C-NMR spectra, the peak positions are reported on one decimal unless the difference in chemical shift between two signals is small and requires two decimals. Infrared spectra were recorded on a Jasco FT-IR-460 plus spectrometer equipped with a Specac MKII Golden Gate Single Reflection Diamond ATR system and are reported in wave numbers (cm^{-1}). At maximum, the ten most prominent peaks are reported. Low resolution mass spectra were recorded on a Waters

Micromass Autospec Q mass spectrometer in EI mode at 70 eV or were taken from GC-MS analyses performed on a Finnigan Trace GC-MS (quadrupole mass analyzer using EI mode at 70 eV) fitted with a Macherey-Nagel Optima delta-3-0.25 µm capillary column (20 m, 0.25 mm); gas carrier: He 1.4 mL/min; injector: 220 °C split mode. HRMS analyses and accurate mass determinations were performed on a Thermo Scientific LTQ Orbitrap XL mass spectrometer using ESI mode. Melting points were measured on a Büchi B-545 apparatus and are corrected. Syringe filters with polytetrafluoroethylene membrane were used with a pore size of 0.45 µm (or 5 µm) from Machery-Nagel (e.g. CHROMAFIL®Xtra PTFE 0.45). Medium pressure liquid chromatography (MPLC) was performed with a CombiFlash® Rf+ system from Teledyne Isco using RediSep® single-use normal phase columns.

Synthesis

Synthesis of hydroperoxides

2,5-dimethylhexan-2-ol

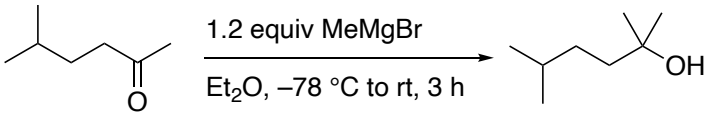

87%

To a mechanically stirred solution of 5-methylhexan-2-one (35 mL, 250 mmol) in dry Et_2O (290 mL) was slowly added MeMgBr (3 M in ether, 100ml, 300 mmol, 1.2 equiv) via cannula at –78 °C. After complete addition, the dry ice was removed from the bath and the mixture was allowed to slowly warm up to rt over a period of 3h. The reaction mixture was treated with sat. aq. NH_4Cl (100 mL), water (200 mL) and the phases were separated. The aqueous phase was extracted twice with ether and the combined organic phase was dried over Na_2SO_4, filtered and concentrated. Distillation (10 mbar, 65°C) afforded 2,5-dimethylhexan-2-ol (28.3 g, 87%).

Colorless liquid; $\mathbf{R_f}$ 0.19 (1:9 EtOAc:heptanes); **^{1}H-NMR** (300 MHz, $CDCl_3$) δ 1.58 – 1.42 (m, 3H), 1.32 – 1.27 (m, 1H), 1.26 – 1.20 (m, 2H), 1.20 (s, 6H), 0.89 (d, J = 6.6 Hz, 6H); **^{13}C-NMR** (75 MHz, $CDCl_3$) δ13C NMR (75 MHz, CDCl3) δ 71.2, 41.9, 33.5, 29.4, 28.7, 22.8; physical and spectral data are in accordance with literature data.[1]

2-hydroperoxy-2,5-dimethylhexane (1)

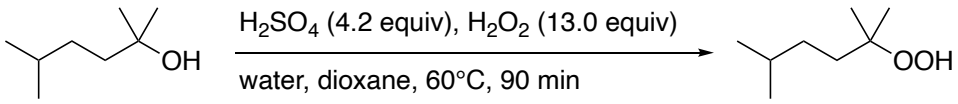

75%

A solution of sulfuric acid (3.6 mL, 64.7 mmol, 4.2 equiv) in water (2.6 mL) was cooled to –10 °C and hydrogen peroxide (20.5 mL, 200 mmol, 13 equiv) was added cautiously. To this mixture, a solution of 2,5-dimethylhexan-2-ol (2.0 g, 15.4 mmol) in dioxane (15.5 mL) was added dropwise without the ice bath. Then, the reaction was stirred at 60 °C. After 90 min, the mixture cooled down to rt and was diluted

with water. The mixture was extracted 3x with EtOAc and the combined organic phase was dried over Na_2SO_4, filtered and concentrated. FC (9:1 heptanes:EtOAc) afforded 2-hydroperoxy-2,5-dimethylhexane (1.7 g, 75%).

Colorless oil, **R_f** 0.26 (9:1 heptanes:EtOAc); **^{1}H-NMR** (300 MHz, $CDCl_3$) δ 7.20 – 7.11 (m, 1H), 1.60 – 1.42 (m, 3H), 1.26 – 1.15 (m, 2H), 1.21 (s, 6H), 0.89 (d, J = 6.6 Hz, 6H); **^{13}C-NMR** (75 MHz, $CDCl_3$) δ 83.2, 36.4, 33.1, 28.6, 24.0 22.8; physical and spectral data are in accordance with literature data.[2]

2-methyloctan-2-ol

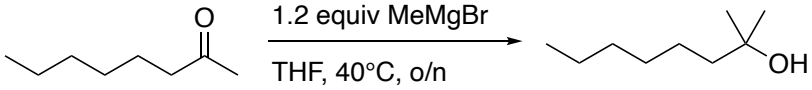

45%

To a solution of MeMgBr (3.0 M in Et_2O, 40 mL, 120 mmol, 1.2 equiv) in dry THF (20 mL) was added dropwise 2-ocatanone (15.7 mL, 100 mmol) at rt. The mixture was stirred at 40 °C for 5 h. Water (20 mL) and brine (80 mL) were added and the resulting suspension was extracted with ether. The organic phase was dried over Na_2SO_4, filtered and concentrated. Distillation (5 mbar, 70 °C head-temperature) afforded 2-methyloctan-2-ol (8.2 g, 45%).

Colorless liquid, **R_f** 0.17 (9:1 heptanes:EtOAc); **^{1}H-NMR** (300 MHz, $CDCl_3$) δ 1.52 – 1.23 (m, 11H), 1.20 (s, 6H), 0.94 – 0.83 (m, 3H); **^{13}C-NMR** (75 MHz, $CDCl_3$) δ 71.2, 44.2, 32.0, 30.0, 29.4, 24.5, 22.8, 14.2; physical and spectral data are in accordance with literature data.[3]

2-hydroperoxy-2-methyloctane (10)

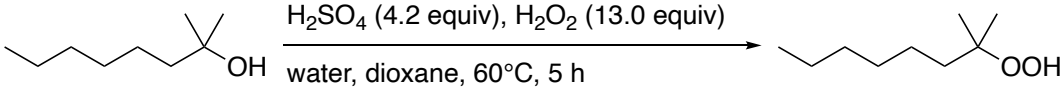

72%

A solution of sulfuric acid (1.2 mL, 21.0 mmol, 4.2 equiv) in water (0.83 mL) was cooled to –10 °C and hydrogen peroxide (6.7 mL, 65.3 mmol, 13.0 equiv) was added cautiously. To this mixture, a solution of 2-methyloctan-2-ol (721 mg, 5.0 mmol) in dioxane (5.0 mL) was added dropwise without the ice bath. Then, the reaction was stirred at 60 °C. After 5 h, the mixture cooled down to rt and was diluted with water. The mixture was extracted 3x with EtOAc and the combined organic phase was dried over Na_2SO_4, filtered and concentrated. FC (9:1 heptanes:EtOAc) afforded 2-hydroperoxy-2-methyloctane (580 mg, 72%).

Colorless liquid, **R_f** 0.22 (9:1 heptanes:EtOAc); **^{1}H-NMR** (300 MHz, $CDCl_3$) δ 7.14 (d, J = 6.7 Hz, 1H), 1.53 (dd, J = 9.8, 5.7 Hz, 2H), 1.36 – 1.25 (m, 8H), 1.21 (s, 6H), 0.93 – 0.82 (m, 3H); **^{13}C-NMR** (75 MHz, $CDCl_3$) δ 83.1, 38.7, 32.0, 30.0, 24.1, 24.0, 22.8, 14.2; **HRMS** calc. for $C_9H_{19}O$ $[M+H]^+$: 143.1430, found: 143.1435; **IR** (cm^{-1}): 3375, 2928, 2858, 1467, 1364, 1246, 1207, 1149, 843, 724

2-methyl-1-phenylpropan-2-ol

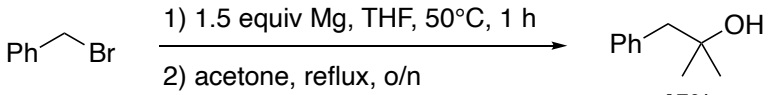

45%

Benzyl bromide (17.8 mL, 150 mmol) was slowly added to a stirred solution of Mg turnings (5.47 g, 225 mmol, 1.5 equiv) and one crystal of iodine in dry THF (84 mL) at 50 °C. Upon complete addition, the mixture was stirred for 1 h and acetone (13.3 mL) was added slowly. The mixture was stirred at reflux overnight. After cooling to rt, aq. HCl (10%, 150 mL) was added and the mixture was extracted twice with CH_2Cl_2. The organic phase was dried over Na_2SO_4, filtered and concentrated. Distillation (1 mbar, 80° head-temperature) afforded 2-methyl-1-phenylpropan-2-ol (10.0 g, 45%).

Colorless liquid, $\mathbf{R_f}$ 0.36 (8:2 heptanes:EtOAc); **^{1}H-NMR** (300 MHz, $CDCl_3$) δ 7.38 – 7.22 (m, 5H), 2.80 (s, 2H), 1.26 (s, 6H); **^{13}C-NMR** (75 MHz, $CDCl_3$) δ 137.9, 130.6, 128.3, 126.6, 70.9, 49.9, 29.3; physical and spectral data are in accordance with literature data.[4]

(2-hydroperoxy-2-methylpropyl)benzene (23)

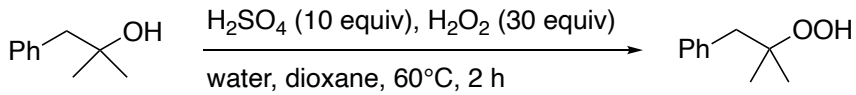

55%

A solution of sulfuric acid (5.6 mL, 100 mmol, 10.0 equiv) in water (2.0 mL) was cooled to –10 °C and hydrogen peroxide (30.6 mL, 300 mmol, 30.0 equiv) was added cautiously. To this mixture, a solution of 2-methyl-1-phenylpropan-2-ol (1.5 g, 10.0 mmol) in dioxane (10.0 mL) was added dropwise without the ice bath. Then, the reaction was stirred at 60 °C. After 2 h, the reaction was poured it into sat. aq. $NaHCO_3$ (50 mL) and the solution was extracted 3x with EtOAc. The organic phase was dried over Na_2SO_4, filtered and concentrated. FC (8:2 pentane:Et_2O) afforded (2-hydroperoxy-2-methylpropyl)benzene (914 mg, 55%).

Colorless liquid, $\mathbf{R_f}$ 0.66 (8:2 pentane:Et_2O); **^{1}H-NMR** (300 MHz, $CDCl_3$) δ 7.42 – 7.21 (m, 5H), 2.92 (s, 2H), 1.24 (s, 6H); **^{13}C-NMR** (75 MHz, $CDCl_3$) δ 137.8, 130.6, 128.2, 126.5, 83.2, 44.6, 24.1; physical and spectral data are in accordance with literature data.[5]

1-methylcyclohexan-1-ol

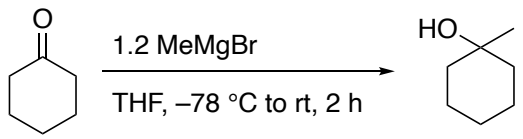

42%

To a mechanically stirred solution of cyclohexanone (8.0 mL, 77.2 mmol) in dry Et_2O (140 mL) was slowly added MeMgBr (3.0 M in Et_2O, 30.9 mL, 92.6 mmol, 1.2 equiv) at –78 °C. The mixture was slowly warmed up to rt and stirred for 2 h. The mixture was carefully poured into sat. aq. NH_4Cl and the mixture was extracted with ether. The organic phase was washed with brine, dried over Na_2SO_4, filtered and

concentrated. Distillation (20 mbar, 61 °C head-temperature) afforded 1-methylcyclohexan-1-ol (3.75 g, 42%).

Colorless liquid, **R_f** 0.21 (8:2 heptanes:EtOAc); **^{1}H-NMR** (300 MHz, $CDCl_3$) δ 1.67 – 1.38 (m, 9H), 1.36 – 1.24 (m, 2H), 1.20 (s, 3H); **^{13}C-NMR** (75 MHz, $CDCl_3$) δ 70.1, 39.6, 29.7, 25.8, 22.8; physical and spectral data are in accordance with literature data.[6]

1-hydroperoxy-1-methylcyclohexane (25)

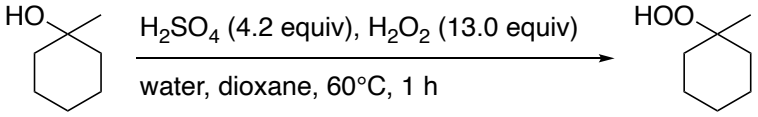

15%

A solution of sulfuric acid (3.5 mL, 63.0 mmol, 4.2 equiv) in water (2.5 mL) was cooled to –10 °C and hydrogen peroxide (20.0 mL, 196 mmol, 13.0 equiv) was added cautiously. To this mixture, a solution of 1-methylcyclohexan-1-ol (1.7 g, 15.0 mmol) in dioxane (15.0 mL) was added dropwise without the ice bath. Then, the reaction was stirred at 60 °C. After 1 h, the mixture cooled down to rt and was diluted with water. The mixture was extracted 3x with EtOAc and the combined organic phase was dried over Na_2SO_4, filtered and concentrated. FC (8:2 heptanes:EtOAc) afforded 1-hydroperoxy-1-methylcyclohexane (300 mg, 15%).

Colorless liquid, **R_f** 0.47 (8:2 heptanes:EtOAc); **^{1}H-NMR** (300 MHz, $CDCl_3$) δ 1.82 – 1.25 (m, 9H), 1.24 (s, 3H), 0.92 – 0.80 (m, 1H); **^{13}C-NMR** (75 MHz, $CDCl_3$) δ 81.9, 34.6, 25.8, 24.0, 22.4; physical and spectral data are in accordance with literature data.[5]

2-methylhex-5-en-2-ol

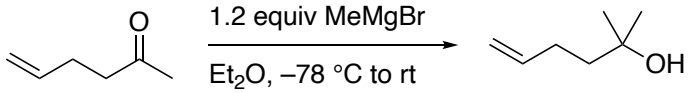

81%

To a mechanically stirred solution of hex-5-en-2-one (8.7 mL, 75 mmol) in dry Et_2O (88 mL) was slowly added MeMgBr (3.0 M in Et_2O, 30 mL, 90 mmol, 1.2 equiv) at –78 °C. The mixture was slowly warmed up to rt and stirred for 1 h. The mixture was poured into sat. aq. NH_4Cl and the mixture was extracted with Et_2O. The organic phase was washed with brine, dried over Na_2SO_4, filtered and concentrated. Distillation (10 mbar, 46 °C head-temperature) afforded 2-methylhex-5-en-2-ol (6.9 g, 81%).

Colorless liquid, **R_f** 0.28 (8:2 heptanes:EtOAc); **^{1}H-NMR** (300 MHz, $CDCl_3$) δ 5.86 (ddt, J = 16.8, 10.1, 6.5 Hz, 1H), 5.11 – 4.90 (m, 2H), 2.22 – 2.08 (m, 2H), 1.63 – 1.52 (m, 2H), 1.28 – 1.25 (m, 1H), 1.24 (s, 6H); **^{13}C-NMR** (75 MHz, $CDCl_3$) δ 139.2, 114.6, 71.1, 42.9, 29.4, 28.9; physical and spectral data are in accordance with literature data.[7]

5-hydroperoxy-5-methylhex-1-ene (27)

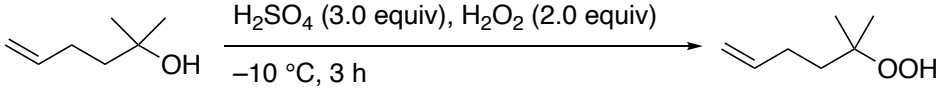

22%

To a stirred emulsion of 2-methylhex-5-en-2-ol (1.7 g, 15 mmol) and hydrogen peroxide (3.8 mL, 37.5 mmol, 2.5 equiv) was added sulfuric acid (2.5 mL, 45 mmol, 3.0 equiv) dropwise at –10 °C. The temperature was carefully monitored during the addition and kept at –10 °C for further 2 h. As side product formation was observed by TLC, the mixture was diluted with water (10 mL) and treated with sat. aq. $NaHCO_3$ (10 mL). The mixture was extracted three times with EtOAc and the organic phase was dried over Na_2SO_4, filtered and concentrated. FC (8:2 heptanes:EtOAc) afforded 5-hydroperoxy-5-methylhex-1-ene (400 mg, 22%).

Slightly yellow liquid, $\mathbf{R_f}$ 0.46 (8:2 heptanes:EtOAc); **^{1}H-NMR** (300 MHz, $CDCl_3$) δ 7.20 (s, 1H), 5.86 (ddt, J = 16.8, 10.2, 6.6 Hz, 1H), 5.05 (dq, J = 17.1, 1.7 Hz, 1H), 4.96 (ddt, J = 10.1, 2.3, 1.3 Hz, 1H), 2.18 – 2.01 (m, 2H), 1.72 – 1.61 (m, 2H), 1.23 (s, 6H); **^{13}C-NMR** (75 MHz, $CDCl_3$) δ 139.1, 114.6, 82.7, 37.6, 28.4, 24.1; physical and spectral data are in accordance with literature data.[7]

Synthesis of radical traps

S-phenyl benzenesulfonothioate

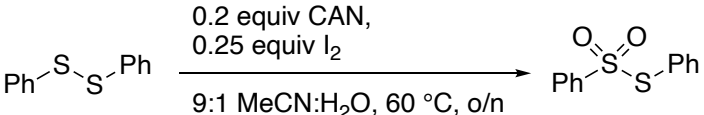

72%

To a mechanically stirred solution of cerium ammonium sulfate (21.9 g, 40 mmol, 0.2 equiv) in solvent (9:1 MeCN:water, 800 mL) was added diphenyl disulfide (43.7 g, 43.7 g, 200 mmol) and heated up to 60 °C. When all solids have dissolved, iodine (12.7 g, 12.7 g, 0.25 equiv) is added at once and the mixture was stirred overnight while air was constantly bubbled through the mixture.

Note: The exhaust was washed with a diluted solution of thiosulfate as there is a significant amount of iodine vapor flushed out of the reaction!

The mixture was transferred into a separatory funnel and diluted with EtOAc (250 mL). Then, aq. sodium thiosulfate (5%, 450 mL) was added and the iodine was fully reduced. The phases were quickly separated, the aqueous phase was extracted 2x EtOAc (500 mL) and the combined organic phase was washed with 50% brine, dried over Na2SO4, filtered and concentrated. Polar side products and traces of iodine were removed by FC (9:0.25:0.75 pentane:CH_2Cl_2:Et_2O. The crude product was dissolved in roughly the same volume of methanol and then precipitated at –80 °C (35.9 g, 72%).

White solid, $\mathbf{R_f}$ 0.40 (8:2 heptanes:EtOAc); **^{1}H-NMR** (300 MHz, CD_2Cl_2) δ 7.63 – 7.38 (m, 12H), 7.38 – 7.30 (m, 8H); **^{13}C-NMR** (75 MHz, CD_2Cl_2) δ 143.3, 136.9, 134.2, 131.9, 129.8, 129.3, 128.2, 127.8

This compound is also commercially available.

Trimethyl(2-phenylsulfanylethynyl)silane

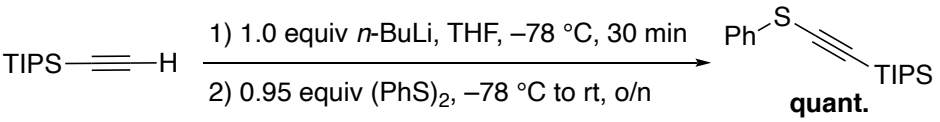

quant.

(Triisopropylsilyl)acetylene (30 mL, 134 mmol) was dissolved in dry THF (100 mL) and the solution was cooled to –78 °C. *n*-BuLi (2.5 M in hexane, 50.6 mL, 126 mmol) was added dropwise and the mixture was stirred for 30 min at this temperature. Diphenyldisulfide (27.6 g, 126 mmol) in dry THF (44 mL) was slowly added at –78 °C. After being stirred at –78 °C for 30 min, the reaction mixture was allowed to warm up to rt and stirred overnight. The reaction mixture was cooled to 0 °C, stirred for further 10 min and subsequently treated with dist. water (60 mL). The reaction mixture was diluted with Et2O (50 mL). The phases were separated and the aqueous phase was extracted twice with Et_2O (50 mL). The combined organic phase was washed with aq. NaOH (0.1 M, 2 x 100 mL), dist. water (3 x 50 mL) and brine (50 mL). The organic phase was dried over Na_2SO_4, concentrated and the obtained oil was dried under high vacuum. Trimethyl(2-phenylsulfanylethynyl)silane was obtained after FC (heptanes) (36 g, quantitative) and used directly for the next step.

Yellowish oil; $\mathbf{R_f}$ 0.75 (heptanes); **^{1}H-NMR** (300 MHz, $CDCl_3$): δ 7.49 – 7.40 (m, 2H), 7.37 – 7.29 (m, 2H), 7.25 – 7.18 (m, 1H), 1.13 (d, J = 1.7 Hz, 21H); **^{13}C-NMR** (75 MHz, $CDCl_3$): δ 133.0, 129.3, 126.5, 126.1, 103.4, 91.2, 18.8, 11.5; physical and spectral data are in accordance with literature data.[8]

Triisopropyl((phenylsulfonyl)ethynyl)silane

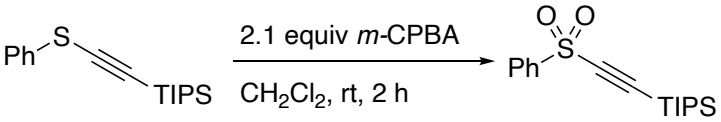

98%

To a stirred solution of the crude trimethyl(2-phenylsulfanylethynyl)silane in dry CH_2Cl_2 was added drop wise a solution of *m*-CPBA (77%, 60 g, 265 mmol) in dry CH_2Cl_2 at rt over 2 h using a dropping funnel. The white suspension was stirred for 2 h until complete consumption of the thioether. The reaction was cooled to 0 °C and transferred into a beaker flask. Sat. $NaHCO_3$ (250 ml) was added and the mixture was stirred vigorously for 20 min at rt to give a white suspension. The organic phase was separated and the aqueous phase was extracted twice with CH_2Cl_2. The combined organic phases were washed with sat. $NaHCO_3$, water and brine, dried over Na_2SO_4 and concentrated. FC (Et_2O/pentane 1:9) afforded triisopropyl((phenylsulfonyl)ethynyl)silane (39.8 g, 98%).

Colorless, viscous oil; $\mathbf{R_f}$ 0.63 (Et_2O/pentane 1:9); **^{1}H-NMR** (300 MHz, $CDCl_3$): δ 8.06 – 7.98 (m, 2H), 7.70 – 7.62 (m, 1H), 7.61 – 7.53 (m, 2H), 1.26 – 0.96 (m, 21H); **^{13}C-NMR** (75 MHz, $CDCl_3$): δ 142.2, 134.2, 129.4, 127.3, 101.0, 100.8, 18.4, 11.0; physical and spectral data are in accordance with literature data.[8]

Benzenesulfonyl azide

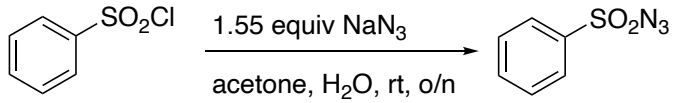

92%

A solution of sodium aziede (30.2 g, 465 mmol, 1.55 equiv) in water (193 mL) was added dropwise to a solution of benzenesulfonyl chloride (38.3 mL, 300 mmol) in acetone (645 mL) at 0 °C. The resulting biphasic mixture was vigorously stirred at room temperature overnight. Acetone was removed under reduced pressure and the residue was extracted three times with Et_2O (200 mL). The combined organic phase was washed with aq. $NaHCO_3$ (200 mL), brine (200 mL), dried over Na_2SO_4, filtered and concentrated. Recrystallisation from Et_2O (50 mL) at –78 °C afforded benzenesulfonyl azide (50.3 g, 92%) after drying on high vacuum overnight.

Colorless liquid; **R_f** 0.45 (1:9 EtOAc:heptanes); **^{1}H-NMR** (300 MHz, CD_2Cl_2): δ 8.00 – 7.90 (m, 2H), 7.79 – 7.69 (m, 1H), 7.68 – 7.57 (m, 2H); **^{13}C-NMR** (75 MHz, CD_2Cl_2): δ 138.8, 135.3, 130.2, 127.8; physical and spectral data are in accordance with literature data.[9]

((2-methylallyl)sulfonyl)benzene

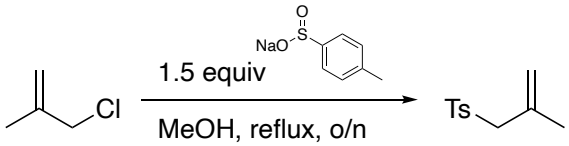

74%

Adapted from a patent of Hoffmann-La Roche Inc.[10]

3-chloro-2-methyl-prop-1-ene (2.7 g, 30 mmol) and toluenesulfinic acid sodium salt (8.0 g, 45 mmol, 1.5 equiv) were dissolved in dry methanol (60 mL) under argon and refluxed overnight. The mixture was cooled down to rt and concentrated. Water and ether were added and the mixture was extracted with ether. The combined organic phase was washed with sat. aq. NH_4Cl, dried over Na_2SO_4, filtered and concentrated. The white solid was dissolved in a minimal amount of ether and the product was precipitated by addition of heptanes. The solid was filtered off and dried under vaccum (4.7 g, 74%).

Off-white solid; **mp** 70-71 °C; **R_f** 0.36 (8:2 heptanes:EtOAc); **^{1}H-NMR** (300 MHz, $CDCl_3$): δ 7.74 (d, J = 8.3 Hz, 1H), 7.32 (d, J = 8.0 Hz, 1H), 5.20 – 4.85 (m, 1H), 4.68 (s, 1H), 3.74 (s, 1H), 2.43 (s, 2H), 1.85 (s, 2H); **^{13}C-NMR** (75 MHz, $CDCl_3$): δ 144.7, 135.6, 133.6, 129.7, 128.6, 120.8, 64.6, 22.8, 21.7; physical and spectral data are in accordance with literature data.[11]

4-methylbenzenesulfonyl iodide

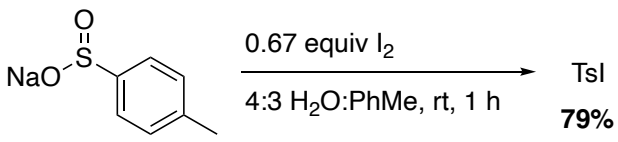

79%

To a solution of sodium toluenesulfinate (8.9 g, 50 mmol) in water (100 mL) was added a solution of iodine (8.5 g, 0.67 equiv) in toluene (150 mL). The reaction mixture was protected against light and

stirred for 1 h at rt. The phases were separated and the organic phase was washed with water (ca. 50mL), dried over Na_2SO_4 and filtered. Heptanes (150 mL) was added and the product was crystallized in at 5 °C overnight. The supernatant was decanted, the product was washed with heptanes and dried on HV (7.47 g, 79%).

Yellow crystals; **mp** 86-88 °C; **^{1}H-NMR** (300 MHz, $CDCl_3$): δ 7.78 – 7.72 (m, 2H), 7.38 – 7.30 (m, 2H), 2.47 (s, 3H); **^{13}C-NMR** (75 MHz, $CDCl_3$): δ 147.7, 146.4, 129.8, 125.6, 22.0; physical and spectral data are in accordance with literature data.[12]

4,4,5,5-tetramethyl-2-(3-tosylprop-1-en-2-yl)-1,3,2-dioxaborolane

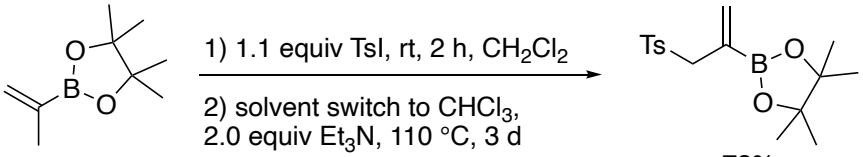

73%

2-isopropenyl-4,4,5,5-tetramethyl-1,3,2-dioxaborolane (1.68 g, 10 mmol) was dissolved in dry CH_2Cl_2 and 4-methylbenzenesulfonyl iodide (3.1 g, 11 mmol, 1.1 equiv) was added. The mixture was stirred at rt for 2 h and subsequently concentrated. The residue was dissolved in $CHCl_3$ (stabilized with EtOH, 13 mL) and transferred into a sealed tube. Et_3N (2.8 mL, 20 mmol, 2.0 equiv) was added and the mixture was stirred at 110 °C for 3 days. The mixture was cooled down to rt, treated with water and the phases were separated. The aqueous phase was extracted with Et_2O, and the combined organic phases were washed once with 5% aq. $Na_2S_2O_3$, twice with 1M aq. HCl, then dried over Na_2SO_4, filtered and concentrated. The residue was dissolved in heptanes and heated to 75°C which resulted in a brown liquid. Upon cooling down to rt, a brown solid precipitated and the supernatant yellow solution was transferred in another flask, where 4,4,5,5-tetramethyl-2-(3-tosylprop-1-en-2-yl)-1,3,2-dioxaborolane crystallized immediately (2.36 g, 73%).

Yellow solid; **R_f** 0.29 (8:2 heptanes:EtOAc); **^{1}H-NMR** (300 MHz, $CDCl_3$): δ 7.69 – 7.59 (m, 2H), 7.26 – 7.20 (m, 2H), 6.01 (d, J = 2.6 Hz, 1H), 5.71 (d, J = 2.5 Hz, 1H), 3.83 (d, J = 1.0 Hz, 2H), 2.35 (s, 3H), 1.08 (s, 12H); **^{13}C-NMR** (75 MHz, $CDCl_3$): δ 144.4, 138.5, 136.0, 129.6, 129.2, 84.2, 60.9, 24.7, 21.7; **^{11}B-NMR** (96 MHz, $CDCl_3$): δ 29.3 (s); physical and spectral data are in accordance with literature data.[13]

4-methylbenzenesulfonyl bromide

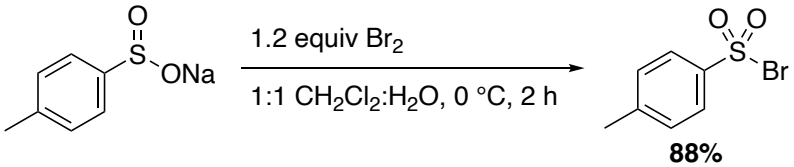

88%

To a solution of sodium 4-methylbenzenesulfinate (8.9 g, 50 mmol) in CH_2Cl_2/H_2O (1:1, 150 mL) was added stepwise a solution of bromine (3.12 mL, 60 mmol, 1.2 equiv) in CH_2Cl_2 (75 mL) at 0°C. After complete addition, the mixture was stirred for 2 h at 0 °C, protected from light. TBME was added and the organic phase was separated. The aqueous phase was extracted with TBME once. The organic

phases were washed with water and then with 5% aq. $Na_2S_2O_3$, until the organic phase was colorless. The combined organic phase was dried, filtrated and evaporated to yield the product as a white solid (10.3 g, 88%).

White solid; **R_f** 0.63 (9:1 pentane:Et_2O); **mp** 90.6–91.2 °C; **^{1}H-NMR** (300 MHz, $CDCl_3$): δ 7.89 (d, J = 8.5 Hz, 2H), 7.39 (d, J = 8.1 Hz, 2H), 2.49 (s, 3H); **^{13}C-NMR** (75 MHz, $CDCl_3$): δ 146.9, 144.8, 130.3, 126.7, 22.0; physical and spectral data are in accordance with literature data.[14]

N-fluoro-2,4,6-trimethyl-N-(4-(trifluoromethyl)phenyl)benzenesulfonamide

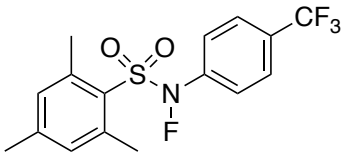

This compound was prepared as we have reported previously.[15]

Radical reactions

General procedure

A dry flask was charged with TBME (5 mL), hydroperoxide (1 mmol), pyridine (1.05 equiv) and cooled to 10 °C. Oxalyl chloride (0.5 equiv) was added drop wise and the mixture was stirred for 5 min. The radical trapping reagent (2.5 equiv) was added and the mixture was refluxed in a preheated oil bath for 45 min. The mixture was concentrated and loaded directly on a silica column for purification.

2,5-dimethyl-5-(phenylthio)hexan-2-ol (2)

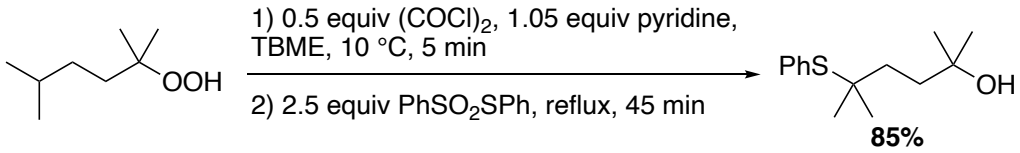

85%

Prepared according to the general procedure from 2-hydroperoxy-2,5-dimethylhexane (146 mg, 1 mmol), pyridine (85 μL, 1.05 mmol, 1.05 equiv) oxalyl chloride (43 μL, 0.5 mmol, 0.5 equiv) and S-phenyl benzenesulfonothioate (626 mg, 2.5 mmol, 2.5 equiv). FC (8:1.5:0.5 CH_2Cl_2:pentane:Et_2O) afforded 2,5-dimethyl-5-(phenylthio)hexan-2-ol (202 mg, 85%).

Colorless oil; **R_f** 0.40 (8:1.5:0.5 CH_2Cl_2:pentane:Et_2O); **^{1}H-NMR** (300 MHz, $CDCl_3$) δ 7.48 – 7.42 (m, 2H), 7.31 – 7.20 (m, 3H), 1.65 – 1.44 (m, 4H), 1.27 (s, 1H), 1.16 (s, 6H), 1.15 (s, 6H); **^{13}C-NMR** (75 MHz, $CDCl_3$) δ 137.6, 132.4, 128.8, 128.6, 71.0, 49.1, 38.7, 36.7, 29.5, 29.1; **HRMS** calc. for $C_{14}H_{22}OSNa$ $[M+Na]^+$: 261.1284, found: 261.1294; **IR** (cm^{-1}): 3380, 2964, 2925, 1472, 1363, 1088, 1025, 907, 748, 694

5-chloro-2,5-dimethylhexan-2-ol (3)

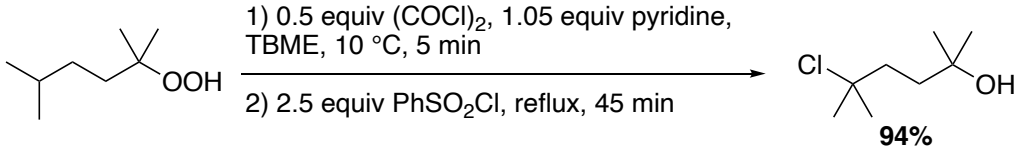

Prepared according to the general procedure from 2-hydroperoxy-2,5-dimethylhexane (146 mg, 1 mmol), pyridine (85 μL, 1.05 mmol, 1.05 equiv) oxalyl chloride (43 μL, 0.5 mmol, 0.5 equiv) and benzenesulfonyl chloride (0.32 mL, 2.5 mmol, 2.5 equiv). FC (8:1.5:0.5 CH_2Cl_2:pentane:Et_2O) afforded 5-chloro-2,5-dimethylhexan-2-ol (155 mg, 94%).

Colorless oil; $\mathbf{R_f}$ 0.20 (8:1.5:0.5 CH_2Cl_2:pentane:Et_2O); **^{1}H-NMR** (300 MHz, $CDCl_3$) δ 1.87 – 1.63 (m, 4H), 1.58 (s, 6H), 1.26 (s, 1H), 1.24 (s, 6H); **^{13}C-NMR** (75 MHz, $CDCl_3$) δ 71.1, 70.7, 40.5, 39.0, 32.6, 29.5; **HRMS** calc. for $C_8H_{17}OClNa$ $[M+Na]^+$: 187.0860, found: 187.0861; **IR** (cm^{-1}): 3381, 2969, 2930, 1469, 1452, 1370, 1217, 1094, 908, 575

5-azido-2,5-dimethylhexan-2-ol (4)

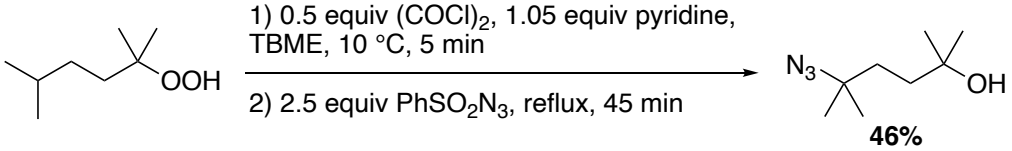

Prepared according to the general procedure from 2-hydroperoxy-2,5-dimethylhexane (146 mg, 1 mmol), pyridine (85 μL, 1.05 mmol, 1.05 equiv) oxalyl chloride (43 μL, 0.5 mmol, 0.5 equiv) and benzenesulfonyl azide (460 mg, 2.5 mmol, 2.5 equiv). FC (8:1.5:0.5 CH_2Cl_2:pentane:Et_2O) afforded 2,5-dimethyl-5-(phenylthio)hexan-2-ol (78 mg, 46%).

Colorless oil; $\mathbf{R_f}$ 0.20 (8:1.5:0.5 CH_2Cl_2:pentane:Et_2O); **^{1}H-NMR** (300 MHz, $CDCl_3$) δ 1.65 – 1.46 (m, 4H), 1.27 (s, 6H), 1.23 (s, 6H); **^{13}C-NMR** (75 MHz, $CDCl_3$) δ 70.7, 61.6, 38.1, 36.0, 26.2; **HRMS** calc. for $C_8H_{17}N_3ONa$ $[M+Na]^+$: 194.1264, found: 194.1263; **IR** (cm^{-1}): 3391, 2970, 2875, 2091, 1745, 1467, 1369, 1255, 1101, 908

5-hydroxy-2,2,5-trimethylhexanenitrile (5)

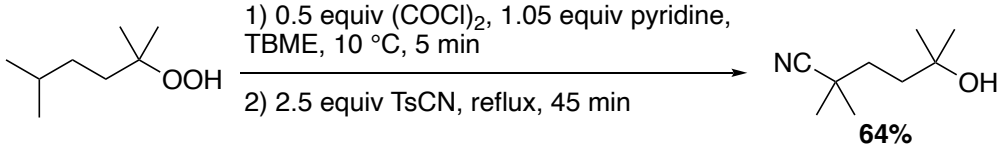

Prepared according to the general procedure from 2-hydroperoxy-2,5-dimethylhexane (146 mg, 1 mmol), pyridine (85 μL, 1.05 mmol, 1.05 equiv), and oxalyl chloride (43 μL, 0.5 mmol, 0.5 equiv). The mixture was taken up with a syringe and passed through a syringe filter (5 μm) to remove the pyridinium chloride precipitate. To the clear solution, tosyl cyanide (475 mg, 2.5 mmol, 2.5 equiv). FC (8:1.5:0.5 CH_2Cl_2:pentane:Et_2O) afforded 5-hydroxy-2,2,5-trimethylhexanenitrile (64%).

Colorless oil; $\mathbf{R_f}$ 0.36 (8:1.5:0.5 CH_2Cl_2:pentane:Et_2O); **^{1}H-NMR** (300 MHz, CD_2Cl_2) δ 1.85 – 1.58 (m, 4H), 1.56 (s, 6H), 1.19 (s, 6H); **^{13}C-NMR** (75 MHz, CD_2Cl_2) δ 71.8, 70.6, 40.8, 39.2, 32.7, 29.6; **HRMS**

calc. for $C_9H_{18}NO$ $[M+H]^+$: 156.1383, found: 156.1378; **IR** (cm^{-1}): 3384, 2970, 2930, 2160, 1468, 1370, 1137, 1094, 909, 575

2,5,5,7-tetramethyloct-7-en-2-ol (6)

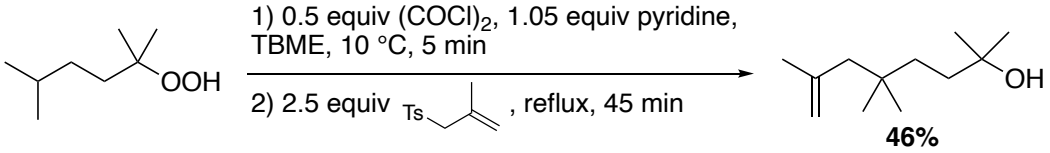

46%

Prepared according to the general procedure from 2-hydroperoxy-2,5-dimethylhexane (146 mg, 1 mmol), pyridine (85 μL, 1.05 mmol, 1.05 equiv) oxalyl chloride (43 μL, 0.5 mmol, 0.5 equiv) and ((2-methylallyl)sulfonyl)benzene (440 mg, 2.5 mmol, 2.5 equiv). FC (8:1.5:0.5 CH_2Cl_2:pentane:Et_2O) afforded 2,5,5,7-tetramethyloct-7-en-2-ol (46%).

Colorless oil; $\mathbf{R_f}$ 0.35 (8:1.5:0.5 CH_2Cl_2:pentane:Et_2O); **^{1}H-NMR** (300 MHz, CD_2Cl_2) δ 4.84 (dq, J = 2.9, 1.5 Hz, 1H), 4.64 (dq, J = 2.6, 0.9 Hz, 1H), 1.95 (d, J = 0.8 Hz, 2H), 1.78 (dd, J = 1.5, 0.8 Hz, 3H), 1.50 – 1.42 (m, 2H), 1.37 (s, 1H), 1.32 – 1.24 (m, 2H), 1.21 (s, 6H), 0.89 (s, 6H); **^{13}C-NMR** (75 MHz, CD_2Cl_2) δ 143.8, 114.1, 71.1, 49.6, 38.1, 36.8, 33.4, 29.6, 27.5, 25.5; **HRMS** calc. for $C_{12}H_{25}O$ $[M+H]^+$: 185.1900, found: 185.1899; **IR** (cm^{-1}): 3367, 2964, 1640, 1469, 1365, 1288, 1148, 907, 889, 733

2,5,5-trimethyl-7-(4,4,5,5-tetramethyl-1,3,2-dioxaborolan-2-yl)oct-7-en-2-ol (7)

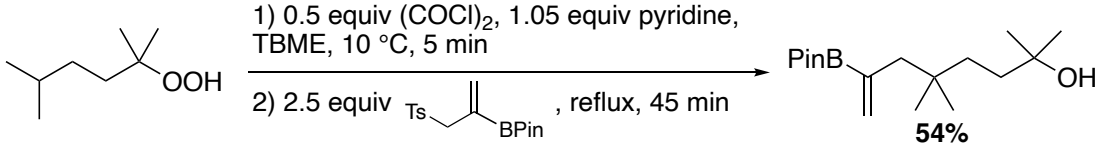

54%

Prepared according to the general procedure from 2-hydroperoxy-2,5-dimethylhexane (146 mg, 1 mmol), pyridine (85 μL, 1.05 mmol, 1.05 equiv) oxalyl chloride (43 μL, 0.5 mmol, 0.5 equiv) and 4,4,5,5-tetramethyl-2-(3-tosylprop-1-en-2-yl)-1,3,2-dioxaborolane (806 mg, 2.5 mmol, 2.5 equiv). FC with boronic acid deactivated silica gel (8:1.5:0.5 CH_2Cl_2:pentane:Et_2O) afforded 5-hydroxy-2,2,5-trimethylhexanenitrile (160 mg, 54%).

Yellow oil; $\mathbf{R_f}$ 0.31 (8:1.5:0.5 CH_2Cl_2:pentane:Et_2O); **^{1}H-NMR** (300 MHz, CD_2Cl_2) δz 5.88 (d, J = 3.8 Hz, 1H), 5.55 (d, J = 3.8 Hz, 1H), 2.08 (d, J = 1.0 Hz, 2H), 1.52 – 1.40 (m, 2H), 1.40 (s, 1H), 1.28 – 1.21 (m, 2H), 1.26 (s, 12H), 1.20 (s, 6H), 0.82 (s, 6H); **^{13}C-NMR** (75 MHz, CD_2Cl_2) δ 132.4, 83.6, 71.3, 47.1, 38.2, 36.6, 33.7, 29.4, 26.7, 24.9; *Note: the signal of the tertiary carbon α to boron is not visible in ^{13}C-NMR;* ; **^{11}B-NMR** (96 MHz, $CDCl_3$): δ 30.3 (s); **HRMS** calc. for $C_{17}H_{33}BO_3Na$ $[M+Na]^+$: 319.2415, found: 319.2421; **IR** (cm^{-1}): 3370, 2963, 2933, 2867, 1422, 1364, 1302, 1141, 863, 732

2,5,5-trimethyl-7-(triisopropylsilyl)hept-6-yn-2-ol (8)

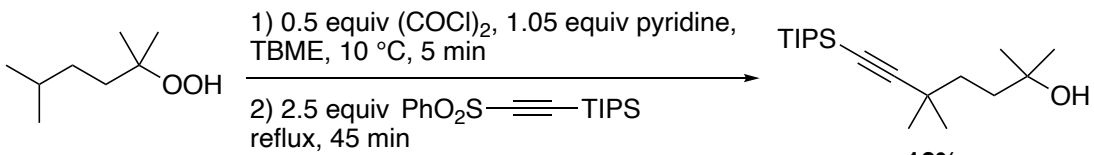

16%

Prepared according to the general procedure from 2-hydroperoxy-2,5-dimethylhexane (146 mg, 1 mmol), pyridine (85 μL, 1.05 mmol, 1.05 equiv) oxalyl chloride (43 μL, 0.5 mmol, 0.5 equiv) and Triisopropyl((phenylsulfonyl)ethynyl)silane (806 mg, 2.5 mmol, 2.5 equiv). FC (8:1.5:0.5 CH_2Cl_2:pentane:Et_2O) afforded 2,5-dimethyl-5-(phenylthio)hexan-2-ol (50 mg, 16%).

Colorless oil; **R_f** 0.60 (8:1.5:0.5 CH_2Cl_2:pentane:Et_2O); **^{1}H-NMR** (300 MHz, CD_2Cl_2) δ 1.69 – 1.39 (m, 4H), 1.25 (q, J = 3.1 Hz, 1H), 1.19 (s, 6H), 1.16 (s, 6H), 1.10 – 0.81 (m, 21H); **^{13}C-NMR** (75 MHz, CD_2Cl_2) δ 117.1, 79.5, 70.9, 40.0, 38.1, 32.3, 29.6, 29.5, 18.9, 11.7; **HRMS** calc. for $C_{19}H_{39}OSi$ $[M+H]^+$: 311.2765, found: 311.2758; **IR** (cm^{-1}): 3376, 2941, 2865, 2157, 1464, 1382, 1363, 882, 674, 658

5-fluoro-2,5-dimethylhexan-2-ol (9)

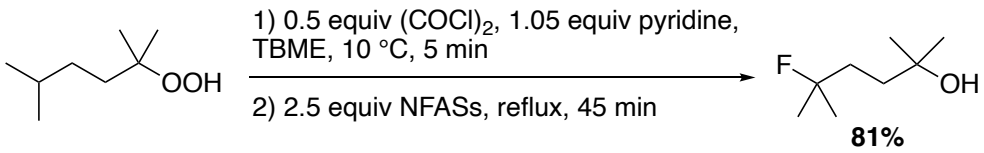

81%

Prepared according to the general procedure from 2-hydroperoxy-2,5-dimethylhexane (146 mg, 1 mmol), pyridine (85 μL, 1.05 mmol, 1.05 equiv) oxalyl chloride (43 μL, 0.5 mmol, 0.5 equiv) and N-fluoro-2,4,6-trimethyl-N-[4-(trifluoromethyl)phenyl]benzenesulfonamide[15] (903 mg, 2.5 mmol, 2.5 equiv). FC (8:1.5:0.5 CH_2Cl_2:pentane:Et_2O) afforded 5-fluoro-2,5-dimethyl-hexan-2-ol (120 mg, 81%).

Yellow oil; R_f 0.40 (8:1.5:0.5 CH_2Cl_2:pentane:Et_2O); ^{1}H-NMR (300 MHz, $CDCl_3$) δ 1.77 – 1.51 (m, 4H), 1.39 (s, 3H), 1.31 (s, 3H), 1.23 (s, 6H); ^{13}C-NMR (75 MHz, $CDCl_3$) δ 96.8, 94.6, 70.7, 37.8, 37.7, 36.1, 35.8, 29.4, 27.0, 26.7; ^{19}F-NMR (282 MHz, $CDCl_3$) δ 96.8; HRMS calc. for $C_8H_{17}OFNa$ $[M+Na]^+$: 171.1156, found: 171.1155; IR (cm^{-1}): 3394, 2977, 2872, 1471, 1373, 1132, 1102, 876, 781, 751

2-methyl-5-(phenylthio)octan-2-ol (11)

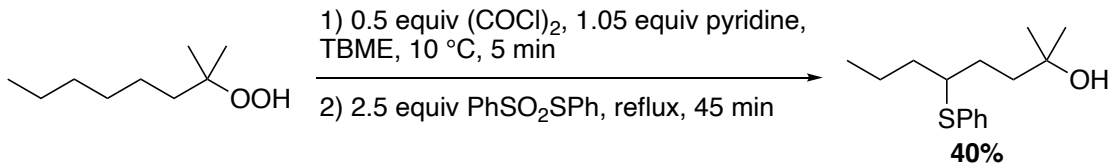

40%

Prepared according to the general procedure from 2-hydroperoxy-2-methyloctane (160 mg, 1 mmol), pyridine (85 μL, 1.05 mmol, 1.05 equiv) oxalyl chloride (43 μL, 0.5 mmol, 0.5 equiv) and S-phenyl benzenesulfonothioate (626 mg, 2.5 mmol, 2.5 equiv). FC (8:1.5:0.5 CH_2Cl_2:pentane:Et_2O) afforded 2-methyl-5-(phenylthio)octan-2-ol (100 mg, 40%).

Colorless oil; **R_f** 0.35 (8:1.5:0.5 CH_2Cl_2:pentane:Et_2O); **^{1}H-NMR** (300 MHz, CD_2Cl_2) δ 7.42 – 7.36 (m, 2H), 7.33 – 7.17 (m, 3H), 3.18 – 3.01 (m, 1H), 1.72 – 1.43 (m, 8H), 1.16 (s, 6H), 0.90 (t, J = 7.1 Hz, 3H); **^{13}C-NMR** (75 MHz, CD_2Cl_2) δ 136.3, 132.1, 129.2, 126.9, 70.9, 49.6, 40.9, 37.2, 29.5, 29.4, 29.4, 20.4, 14.2; **HRMS** calc. for $C_{15}H_{24}OSNa$ $[M+Na]^+$: 275.1440, found: 275.1439; **IR** (cm^{-1}): 3386, 2960, 2930, 2871, 1376, 1265, 954, 737, 711, 692

5-chloro-2-methyloctan-2-ol (12)

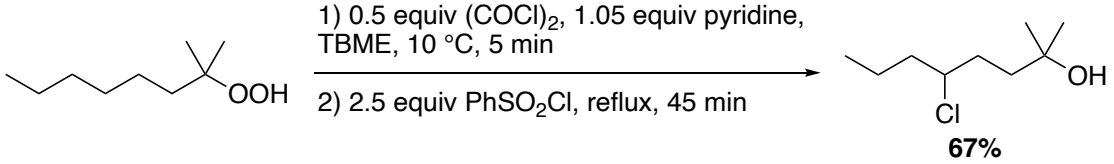

67%

Prepared according to the general procedure from 2-hydroperoxy-2-methyloctane (160 mg, 1 mmol), pyridine (85 μL, 1.05 mmol, 1.05 equiv) oxalyl chloride (43 μL, 0.5 mmol, 0.5 equiv) and phenylsulfonyl chloride (442 mg, 2.5 mmol, 2.5 equiv). FC (8:1.5:0.5 CH_2Cl_2:pentane:Et_2O) afforded 5-chloro-2-methyloctan-2-ol (120 mg, 67%).

Colorless oil; R_f 0.35 (8:1.5:0.5 CH_2Cl_2:pentane:Et_2O); ^{1}H-NMR (300 MHz, $CDCl_3$) δ 3.97 – 3.85 (m, 1H), 1.95 – 1.32 (m, 10H), 1.23 (d, J = 3.2 Hz, 6H), 0.93 (t, J = 7.3 Hz, 3H); ^{13}C-NMR (75 MHz, $CDCl_3$) δ 70.8, 64.5, 40.8, 40.6, 33.4, 29.8, 29.3, 19.9, 13.7; HRMS calc. for $C_9H_{19}ONaCl$ $[M+Na]^+$: 201.1017, found: 201.1017; IR (cm^{-1}): 3380, 2961, 2929, 2874, 1466, 1378, 1140, 931, 908, 763

5-bromo-2-methyloctan-2-ol (13)

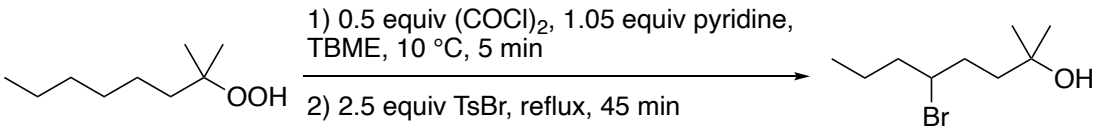

85%

Prepared according to the general procedure from 2-hydroperoxy-2-methyloctane (160 mg, 1 mmol), pyridine (85 μL, 1.05 mmol, 1.05 equiv), oxalyl chloride (43 μL, 0.5 mmol, 0.5 equiv), and tosyl bromide (588 mg, 2.5 mmol, 2.5 equiv). FC (8:1.5:0.5 CH_2Cl_2:pentane:Et_2O) afforded 5-bromo-2-methyloctan-2-ol (189 mg, 85%).

Colorless oil; R_f 0.30 (8:1.5:0.5 CH_2Cl_2:pentane:Et_2O); ^{1}H-NMR (300 MHz, $CDCl_3$) δ 4.04 (tt, J = 8.2, 4.8 Hz, 1H), 2.04 – 1.68 (m, 5H), 1.67 – 1.35 (m, 4H), 1.24 (d, J = 3.4 Hz, 6H), 0.93 (t, J = 7.3 Hz, 3H); ^{13}C-NMR (75 MHz, $CDCl_3$) δ 70.8, 59.0, 41.6, 41.4, 34.0, 29.9, 29.3, 21.0, 13.6; HRMS calc. for $C_9H_{19}ONaBr$ $[M+Na]^+$: 245.0511, found: 245.0509; IR (cm^{-1}): 3365, 2960, 2932, 2873, 1465, 1378, 1259, 1133, 924, 907

5-hydroxy-5-methyl-2-propylhexanenitrile (14)

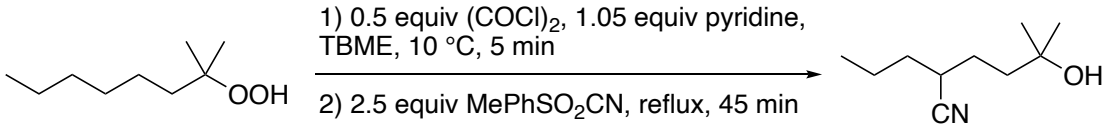

56%

Prepared according to the general procedure from 2-hydroperoxy-2-methyloctane (160 mg, 1 mmol), pyridine (85 μL, 1.05 mmol, 1.05 equiv), and oxalyl chloride (43 μL, 0.5 mmol, 0.5 equiv). The mixture was taken up with a syringe and passed through a syringe filter (5 μm) to remove the pyridinium chloride precipitate. To the clear solution, tosyl cyanide (453 mg, 2.5 mmol, 2.5 equiv). FC (8:1.5:0.5 CH_2Cl_2:pentane:Et_2O) afforded 5-hydroxy-5-methyl-2-propylhexanenitrile (95 mg, 56%).

Colorless oil; R_f 0.23 (8:1.5:0.5 CH_2Cl_2:pentane:Et_2O); ^{1}H-NMR (300 MHz, $CDCl_3$) δ 2.61 – 2.46 (m, 1H), 1.80 – 1.32 (m, 9H), 1.24 (d, J = 3.2 Hz, 6H), 1.01 – 0.87 (m, 3H); ^{13}C-NMR (75 MHz, $CDCl_3$) δ 122.4, 70.6, 41.0, 34.5, 31.9, 29.9, 29.2, 27.2, 20.6, 13.7; HRMS calc. for $C_{10}H_{19}NONa$ $[M+Na]^+$: 192.1359, found: 192.1359; IR (cm^{-1}): 2448, 2964, 2937, 2873, 2241, 1467, 1378, 1209, 1145, 941

Benzyl(phenyl)sulfane (24)

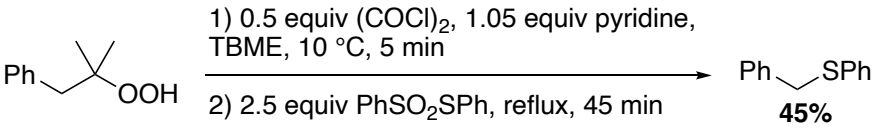

Prepared according to the general procedure from (2-hydroperoxy-2-methylpropyl)benzene (166 mg, 1 mmol), pyridine (85 μL, 1.05 mmol, 1.05 equiv) oxalyl chloride (43 μL, 0.5 mmol, 0.5 equiv) and S-phenyl benzenesulfonothioate (626 mg, 2.5 mmol, 2.5 equiv). FC (98:2 pentane:Et_2O) afforded benzyl(phenyl)sulfane (90 mg, 45%).

Colorless solid; **R_f** 0.63 (98:2 pentane:Et_2O); **^{1}H-NMR** (300 MHz, CD_2Cl_2) δ 7.43 – 7.15 (m, 10H), 4.18 (s, 2H); **^{13}C-NMR** (75 MHz, CD_2Cl_2) δ 138.0, 136.9, 129.9, 129.2, 129.2, 128.8, 127.5, 126.6, 39.1

8-(phenylthio)octan-2-one (26)

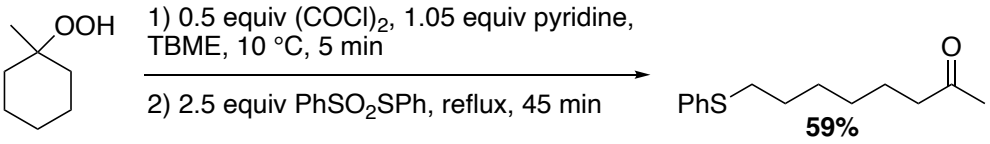

Prepared according to the general procedure from 1-hydroperoxy-1-methylcyclohexane (240 mg, 1.8 mmol), pyridine (156 μL, 1.94 mmol, 1.05 equiv) oxalyl chloride (78 μL, 0.92 mmol, 0.5 equiv) and S-phenyl benzenesulfonothioate (1.15 g, 4.61 mmol, 2.5 equiv). FC (58:40:2 pentane:CH_2Cl_2:Et_2O) afforded 8-(phenylthio)octan-2-one (240 mg, 59%).

Colorless oil; **R_f** 0.37 (8:2 pentane:Et_2O); **^{1}H-NMR** (300 MHz, CD_2Cl_2) δ 7.34 – 7.24 (m, 4H), 7.20 – 7.12 (m, 1H), 2.92 (dd, J = 7.8, 6.8 Hz, 2H), 2.40 (t, J = 7.2 Hz, 2H), 2.08 (s, 3H), 1.70 – 1.49 (m, 4H), 1.48 – 1.35 (m, 2H), 1.48 – 1.34 (m, 2H); **^{13}C-NMR** (75 MHz, CD_2Cl_2) δ 208.8, 137.4, 129.2, 129.1, 126.0, 43.7, 33.6, 30.0, 29.3, 28.6, 23.7; **HRMS** calc. for $C_{14}H_{21}OS$ $[M+H]^+$: 237.1308, found: 237.1310; **IR** (cm^{-1}): 2930, 2857, 1712, 1583, 1480, 1438, 1357, 1161, 737, 689

2,2-dimethyl-5-((phenylthio)methyl)tetrahydrofuran (28)

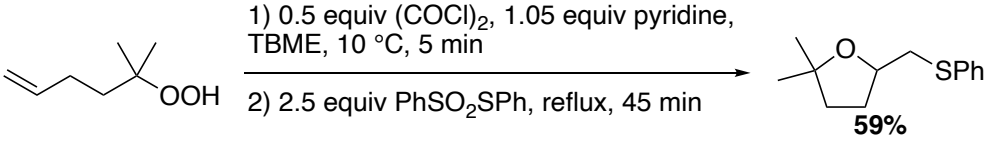

Prepared according to the general procedure from 5-hydroperoxy-5-methylhex-1-ene (130 mg, 1 mmol), pyridine (85 μL, 1.05 mmol, 1.05 equiv) oxalyl chloride (43 μL, 0.5 mmol, 0.5 equiv) and S-phenyl benzenesulfonothioate (626 mg, 2.5 mmol, 2.5 equiv). FC (8:1.5:0.5 CH2Cl2:pentane:Et2O) afforded 2,2-dimethyl-5-((phenylthio)methyl)tetrahydrofuran (130 mg, 59%).

Yellow oil; **R_f** 0.40 (8:1.5:0.5 CH_2Cl_2:pentane:Et_2O); **^{1}H-NMR** (300 MHz, CD_2Cl_2) δ 7.38 – 7.33 (m, 2H), 7.28 (ddd, J = 7.8, 6.7, 1.3 Hz, 2H), 7.21 – 7.13 (m, 1H), 4.20 – 4.06 (m, 1H), 3.18 – 2.89 (m, 2H), 2.22 – 1.99 (m, 1H), 1.86 – 1.65 (m, 3H), 1.24 (s, 3H), 1.19 (s, 3H); **^{13}C-NMR** (75 MHz, CD_2Cl_2) δ 137.4, 129.21, 129.20, 126.1, 81.7, 77.5, 39.9, 38.6, 31.8, 29.3, 28.1; **HRMS** calc. for $C_{13}H_{18}ONaS$ $[M+Na]^+$: 245.0971, found: 245.0976; **IR** (cm^{-1}): 2967, 2925, 2869, 1583, 1364, 1138, 1037, 1025, 736, 689

References

[1] W. C. Agosta, A. M. Foster, *J. Org. Chem.* **1972**, *37*, 61–63.

[2] B. Acott, A. Beckwith, *Australian Journal of Chemistry* **1964**, *17*, 1342.

[3] K.-P. Shing, Y. Liu, B. Cao, X.-Y. Chang, T. You, C.-M. Che, *Angewandte Chemie International Edition* **2018**, *57*, 11947–11951.

[4] D. K. Ahn, Y. W. Kang, S. K. Woo, *J. Org. Chem.* **2019**, *84*, 3612–3623.

[5] S. Kyasa, R. N. Meier, R. A. Pardini, T. K. Truttmann, K. T. Kuwata, P. H. Dussault, *J. Org. Chem.* **2015**, *80*, 12100–12114.

[6] Y. Ishii, T. Iwahama, S. Sakaguchi, K. Nakayama, Y. Nishiyama, *J. Org. Chem.* **1996**, *61*, 4520–4526.

[7] A. J. Bloodworth, A. G. Davies, R. S. Hay-Motherwell, *J. Chem. Soc., Perkin Trans. 2* **1988**, 575–582.

[8] L. Gnägi, S. V. Martz, D. Meyer, R. M. Schärer, P. Renaud, *Chem. Eur. J.* **2019**, *25*, 11646–11649.

[9] D. Meyer, P. Renaud, *Angew. Chem. Int. Ed.* **2017**, *56*, 10858–10861.

[10] *Carbocyclic HIV Protease Inhibitors*, **n.d.**, US6632826, 2003, B1.

[11] C. M. M. da S. Corrêa, M. A. B. C. S. Oliveira, *J. Chem. Soc., Perkin Trans. 2* **1987**, 811–814.

[12] Y. Jiang, Q.-Q. Wang, S. Liang, L.-M. Hu, R. D. Little, C.-C. Zeng, *J. Org. Chem.* **2016**, *81*, 4713–4719.

[13] N. Guennouni, C. Rasset-Deloge, B. Carboni, M. Vaultier, *Synlett* **1992**, *1992*, 581–584.

[14] L. Fu, X. Bao, S. Li, L. Wang, Z. Liu, W. Chen, Q. Xia, G. Liang, *Tetrahedron* **2017**, *73*, 2504–2511.

[15] D. Meyer, H. Jangra, F. Walther, H. Zipse, P. Renaud, *Nat Commun* **2018**, *9*, 1–10.

Chapter 4

Unpublished Results

4 Unpublished Results

Following the proof-of-concept described in the previous chapter 3, the scope of the method for more complex synthetic applications was investigated next. The mild and metal free method to generate alkoxy radicals from tertiary hydroperoxides has been studied with the goal to selectively modify complex molecules such as steroids, to form cyclic ethers found in the skeleton of many natural products, and to open bicyclic peroxides to access macrocycles. However, the synthesis of these substrates proved to be challenging.

At the end of this chapter, a new approach to generate alkoxy radicals from hydroperoxides is presented: An alkyl boron peroxide obtained from an alkyl hydroperoxide and a dialkylborane has been demonstrated to fragment to a persistent borinate radical and the desired alkoxy radical.

4.1 Attempted functionalization of steroid derivatives

4.1.1 Studies on estrone

Estrone's structure is particularly interesting when studying the hydrogen atom transfer reaction since the relocation of the radical is not trivial and several possible HAT products are theoretically possible (Figure 4.1).

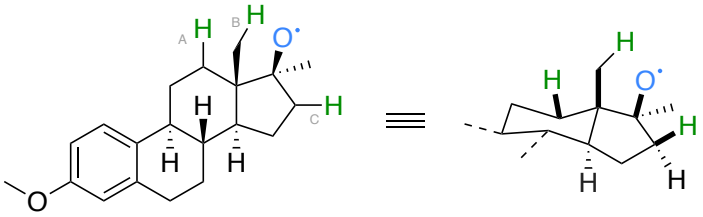

Figure 4.1 Potential hydrogen atoms (A, B, C) highlighted in green of an estrone derivative participating in a HAT reaction

Due to structural constraints, a 1,5-HAT is not possible since all hydrogen atoms at the 5' position are spatially inaccessible. The target hydrogen atoms within distance are found at:

A. the cyclohexane moiety requiring a 1,4-HAT over a relatively long distance and at an unfavorable angle of the C–H–O axis.
B. the methyl group *syn* to the alkoxy radical, also requiring a 1,4-HAT over a shorter distance but still at an unfavorable angle of the C–H–O axis.
C. the cyclopentane ring, requiring a 1,3-HAT.

If one of these unusual hydrogen atom transfers[1] would be successful, this would represent a novel selective functionalization method of these natural products. However, due to the unfavorable (non-linear) arrangement of the C-H–O axis, all of these processes are very challenging. The required alkyl hydroperoxide was attempted to be synthesized from estrone (Figure 4.2).

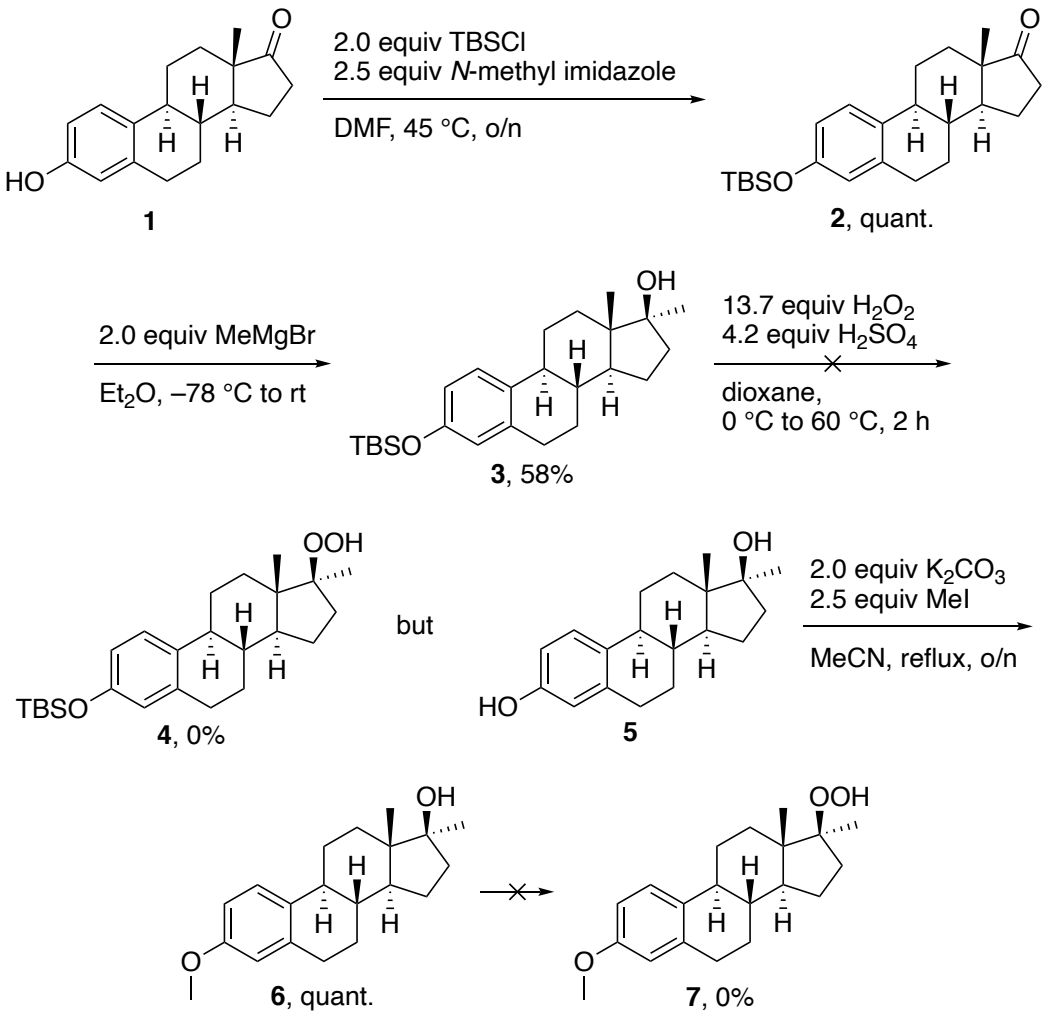

Figure 4.2. Attempted synthesis of estrone hydroperoxides

In a first step, the free alcohol of estrone **1** was protected with a TBS group for the subsequent Grignard reaction. Stereoselective methylation of ketone **2** afforded alcohol **3** in 58% yield.[2] Hydroperoxidation of this tertiary alcohol affording **4** using our standard conditions was not successful. Instead of **4**, the only product isolated of this reaction was the deprotected methyl estrone derivative **5** since the TBS-group was not stable under the strongly acidic conditions applied.

Therefore, the phenol moiety was reprotected with a methyl group affording **6** in quantitative yield and the hydroperoxidation was tested again. However, even after extensive screening of conditions, the alcohol could not be converted to the desired product **7**. The tertiary alcohol was decomposed in this reaction and none of the decomposition products could be characterized.

Since the hydroperoxide formation failed, the formation of the alkoxy radical and the investigation on the HAT process could not be performed and no further attempts were made on this substrate.

It is not surprising, that the hydroperoxide formation is challenging since this observation was already made for another cyclic alcohol, 1-hydroperoxy-1-methylcyclohexane **9**, for which the yield was rather low (15%, cf. chapter 3). Furthermore, it was found that the formation of a hydroperoxide also fails for other tertiary alcohols (Figure 4.3).

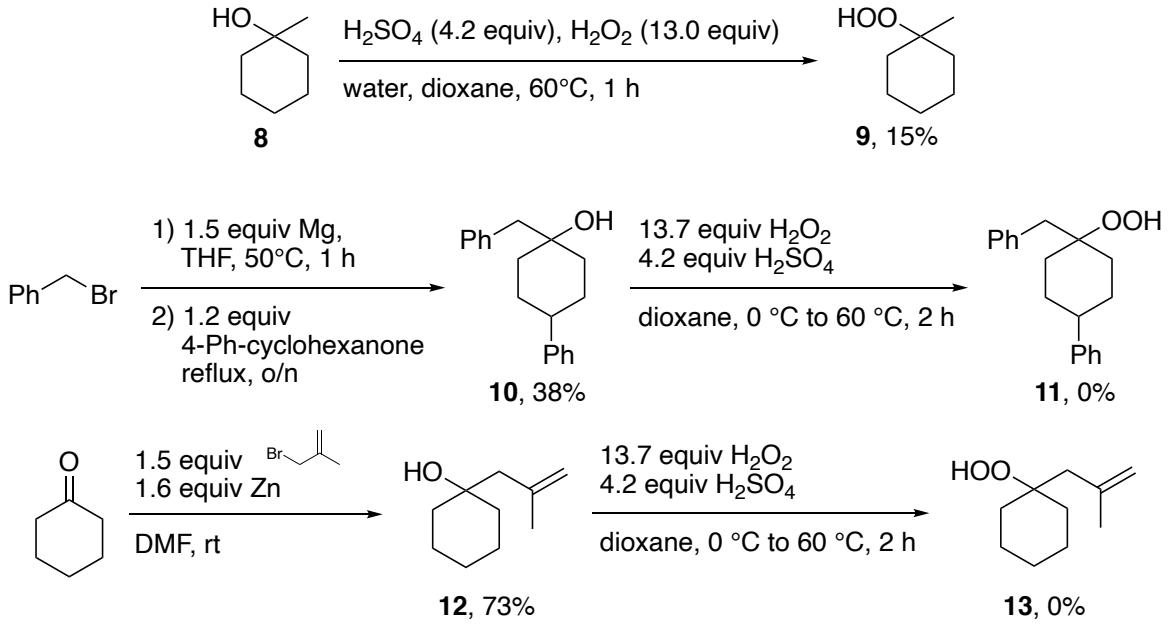

Figure 4.3 Unsuccessful formation of tertiary hydroperoxides

The formation is unsuccessful, if the tertiary center is adjacent to a well stabilized position (e.g., benzylic) such as in alcohol **10** which is obtained upon addition of a benzyl Grignard reagent to 4-phenyl cyclohexanone. Under the applied hydroperoxidation conditions, the alcohol is decomposed. In the case of alcohol **12**, it was observed that the presence of olefins is further complicating the reaction. Even though the hydroperoxide is expected to be formed from the alcohol, no hydroperoxide formation was observed. This can be rationalized by the decomposed of the olefin under the employed harsh reaction conditions. A similar finding was already made in the synthesis of 5-hydroperoxy-5-methylhex-1-ene (22%, cf. chapter 3). Consequently, both hydroperoxides **11** and **13** could not be obtained.

It can be concluded that the formation of cyclic tertiary hydroperoxides is very difficult in general and seem to be impossible for cyclopentane systems. The process is further complicated in the presence of olefins.

4.1.2 Studies on pregnenolone

Since the formation of the targeted estrone hydroperoxide failed, pregnenolone hydroperoxide was chosen as a new substrate since the tertiary alcohol is not cyclic which should be favorable for the formation of the hydroperoxide. The target compound was prepared similarly to the described estrone derivative (Figure 4.4).

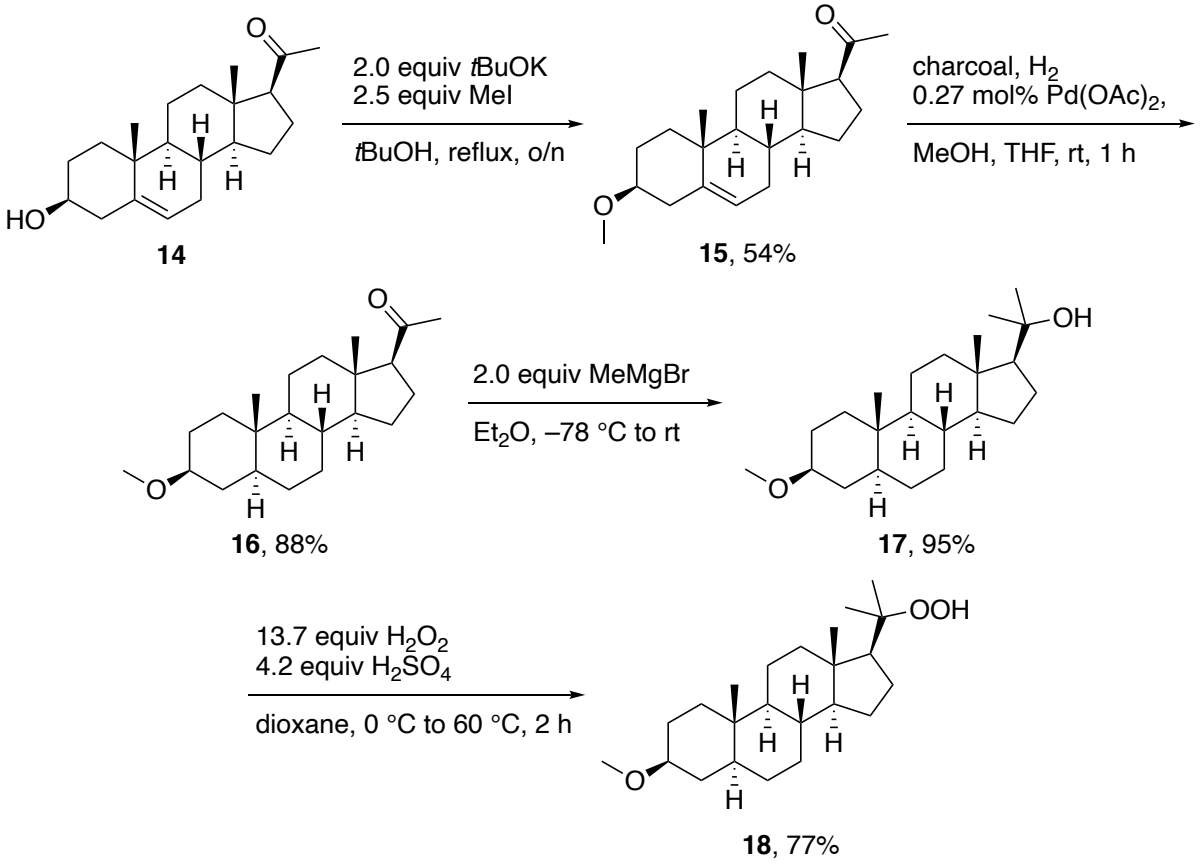

Figure 4.4. Synthesis of pregnenolone hydroperoxide

Pregnenolone **14** was first protected with a methyl group affording methylether **15** in moderate yield. The olefin moiety in **15** was then reduced since it could cause problems under the strongly acidic conditions in the last hydroperoxidation step as seen before. Addition of a methyl Grignard reagent to **16** afforded the tertiary alcohol **17** in excellent yield which was transformed to the corresponding hydroperoxide **18** without any problems. With this hydroperoxide in hand, the alkoxy radical can be formed using the previously established method. Again, three hydrogen atoms are within range for a HAT reaction (Figure 4.5).

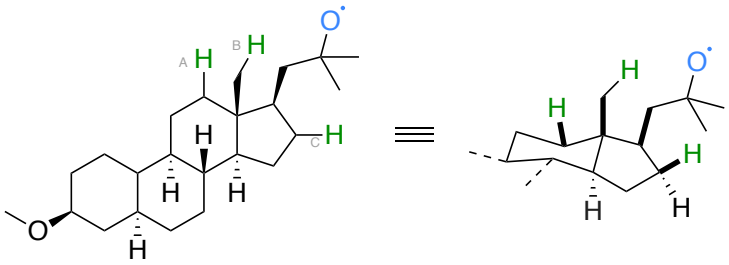

Figure 4.5 Potential hydrogen atoms (A, B, C) highlighted in green of a pregnenolone derivative participating in a HAT reaction

In the pregnenolone case, the distance of the HAT is extended by one carbon atom which makes the 1,5-HAT on the methyl group (position B) much more favorable than on the two other positions:

A. This hydrogen atom at the cyclohexane ring could undergo a 1,5-HAT too but is not well aligned since the rigid structure of the skeleton points the alkoxy radical and the hydrogen atom away from each other.

C. This hydrogen atom is spatially close to the alkoxy radical, but a linear arrangement required for an efficient HAT is not given.

Based on this information, the HAT reaction from the hydroperoxide **X** should result in the selective functionalization of the methyl group (Figure 4.6).

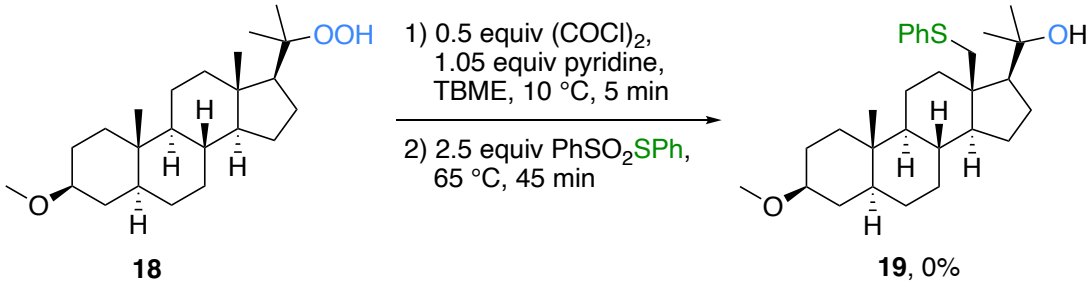

18 **19**, 0%

Figure 4.6 Attempted 1,5-HAT and subsequent functionalization of the methyl group

Interestingly, thioether **19** was not obtained from this reaction. Instead, only alcohol **17** was isolated as the only product. A closer investigation of the proceeding of the reaction revealed that the formation of the peroxyoxalate is complete and thus, full conversion of the hydroperoxide was achieved. It is assumed that the thermal decomposition of the peroxyoxalate will therefore deliver the key alkoxy radical intermediate.

Two pathways are plausible which lead to the formation of the alcohol product 17 (Figure 4.7).

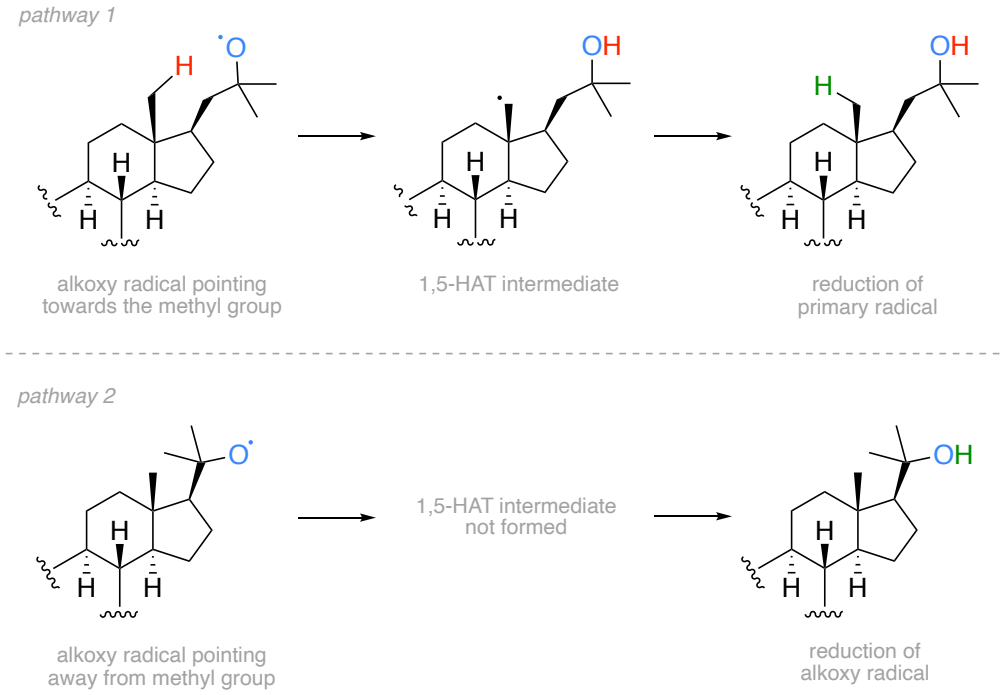

Figure 4.7. Pathways that lead to the formation of alcohol 17; external hydrogen atoms indicated in green

If, as expected, the 1,5-HAT takes place, the hydrogen atom would be abstracted from the methyl group which leads to the formation of a primary radical (Figure 4.7, pathway 1). But if the subsequent trapping of this reactive radical is slow, e.g., due to steric hindrance, the primary radical will react with an external hydrogen atom which can outcompete the formation of the desired product. Benzenesulfonyl bromide was also tested as radical trap since it gave superior results to S-phenyl benzenesulfonothioate in the previous study (chapter 3). However, also in this experiment, the methyl-functionalized product was not formed. Consequently, it cannot be ruled out, that the HAT is not taking place at all (Figure 4.7, pathway B). One possible reason could be that the alkoxy radical is pointing away from the methyl group and therefore be directly reduced by an external hydrogen atom.

Further investigation on estrone and pregnenolone hydroperoxides have not been conducted. However, with a more extended screening of radical traps, the reason of the formation of the non-functionalized alcohol could be studied in more detail. In any case, the functionalization of the methyl group of pregnenolone seems to be much more challenging than initially expected and requires more adaptations to the previously established procedure.

4.2 Attempted synthesis of benzopyranes and benzofuranes

Dihydrobenzopyranes (= chromanes) and dihydrobenzofuranes are bicyclic structures which have a 5- or 6-membered heterocyclic ring annulated to a phenyl moiety and are found often as core structures of natural compounds such as in vitamin E (α-Tocopherol) or as secondary metabolites that are abundant in plants and thus in food like in tea, cocoa, and berries (e.g. flavonoid family, catechins).[3,4] These substance classes express a very diverse biological activity (e.g. Stachybotrylactam) which makes them interesting target structures for organic synthesis (Figure 4.8).

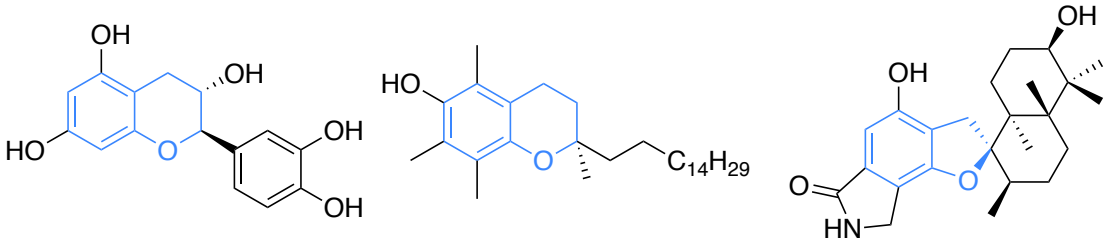

(+)-catechin
strong anti-oxidant potential

α-Tocopherol
(Vitamin E)

Stachybotrylactam
HIV-1 protease inhibitor

Figure 4.8 Examples of naturally occurring dihydrobenzopyranes and dihydrobenzofuranes

Although there is a plethora of literature on homolytic aromatic substitution involving alkyl radicals, only very few annulation strategies are reported using alkoxy radicals for the intramolecular formation of oxygen containing bicycles.[5–10] The general steps one has to control in such a process are depicted below (Figure 4.9).

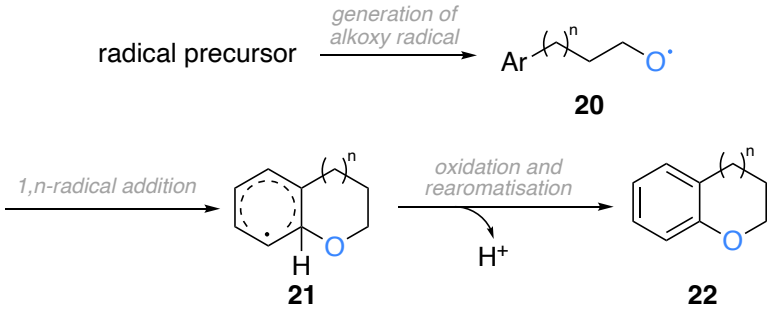

Figure 4.9 General steps in radical annulation via homolytic aromatic substitution

Previous studies have mostly engaged alcohols as radical precursors which were first converted to a hypoiodite (e.g. using DIH) or hypervalent iodine species (e.g. using PIDA) which underwent homolytic cleavage when irradiated with a tungsten lamp.[5,10,11] The alkoxy radical **20** then adds to the aryl moiety forming a bicyclic radical intermediate **21** which has to be further oxidized to the corresponding carbocation. Loss of a proton during rearomatization gives the final annulated product **22**.

Since the required alkoxy radicals can be formed from the corresponding hydroperoxide as described in the previous chapter, we assumed the annulated products will become accessible too using our developed method. In order to test this hypothesis, radical precursors with various chain lengths were synthesized (Figure 4.10).

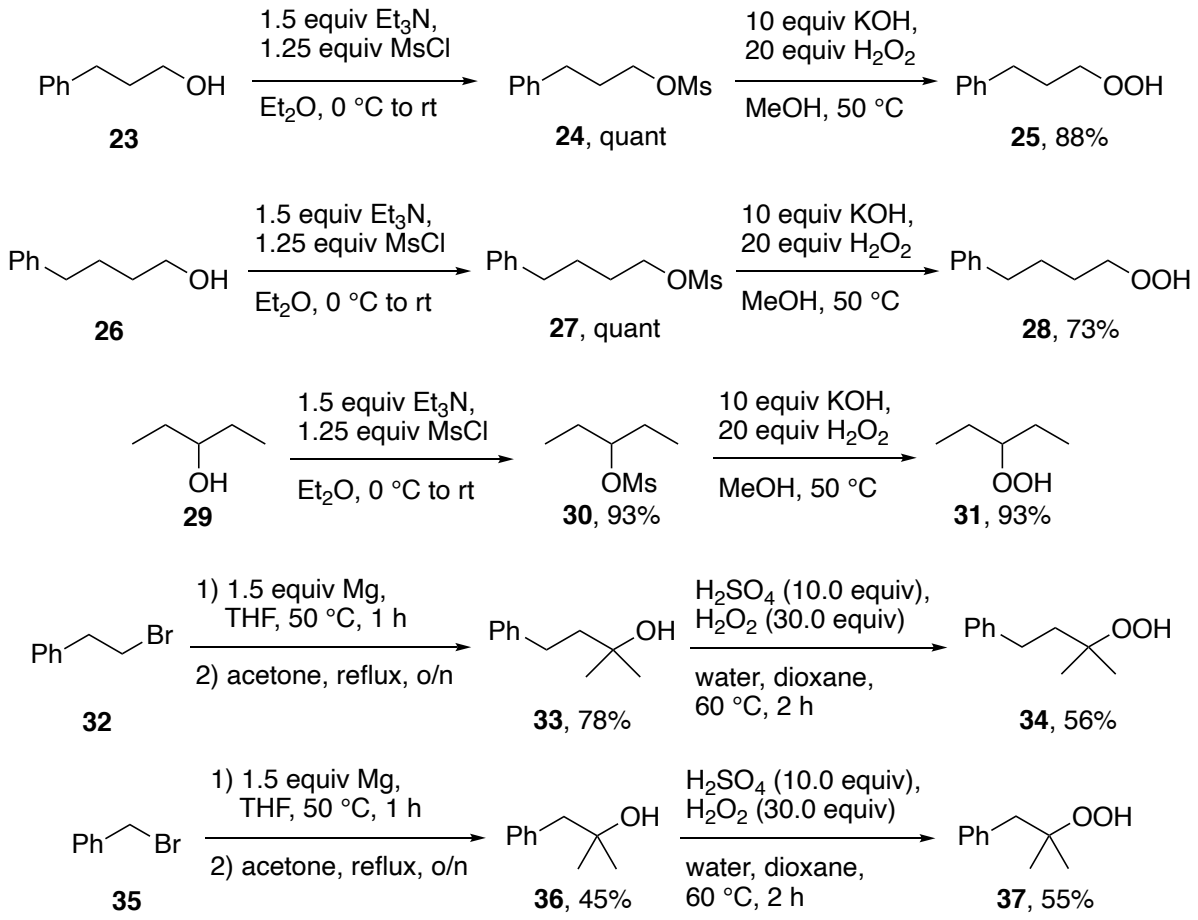

Figure 4.10 Synthesis of hydroperoxides as radical precursors

Two primary hydroperoxides **25** and **28** with a chain length of 3 and 4 carbons were obtained from the corresponding alcohols **23** and **26** *via* mesylation (**24** and **27**) and nucleophilic displacement with hydrogen peroxide in 88% and 77% yield, respectively. Using the same conditions, a secondary hydroperoxide **31** was obtained in even higher yield from 3-pentanol **29** which is somewhat surprising since Mosher described rather low yields with this method.[12] However, hydrogen peroxide and potassium hydroxides were not used in such a large excess and at lower temperatures, too. The tertiary hydroperoxides **34** and **37** were obtained from (2-bromoethyl)benzene **32** and benzyl bromide **35** after transformation to the corresponding Grignard reagents and addition to acetone which yielded the tertiary alcohols **33** and **36** in 78% and 45% yield, respectively. Hydroperoxidation under acidic condition afforded the hydroperoxides in moderate yield.

With these hydroperoxides in hand, the peroxyoxalate formation and subsequent thermal decomposition was investigated next. As expected from literature precedent, the primary hydroperoxide **28** did not afford any product of radical processes. Even in the presence of *S*-phenyl benzenesulfonothioate, which would lead to functionalization at the benzylic position, only yielded the corresponding aldehyde **38** as a result of oxidation (Figure 4.11).[13,14]

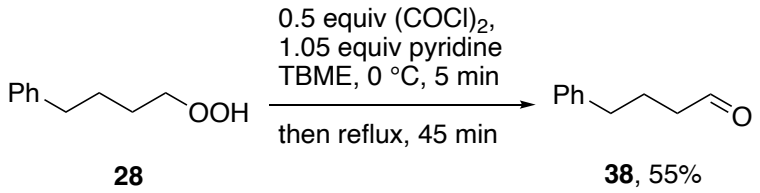

Figure 4.11 Oxidation to aldehyde X instead of alkoxy radical formation

Therefore, further experiments with primary and secondary hydroperoxides **25**, **28**, and **31** were not performed. Under the developed reaction conditions, the tertiary hydroperoxides can potentially form four different products, depending on the prevailing pathway (Figure 4.12).

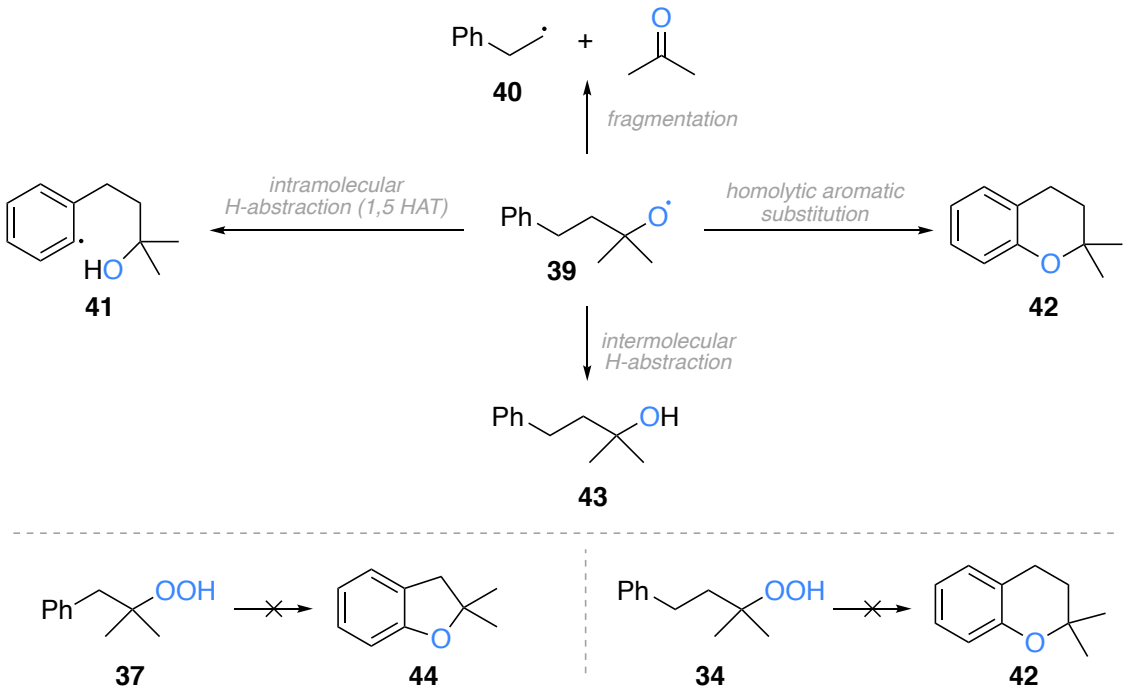

Figure 4.12 Possible reactivities of tertiary alkoxy radical X;
unsuccessful attempts to form heterobicycles via electrophilic aromatic substitution

For example, fragmentation of radical **39** (obtained from hydroperoxide **34**) as analogously described in chapter 3 for hydroperoxide **37**, will lead to the primary radical **40** and acetone. An intramolecular H-abstraction *via* 1,5-HAT is improbable since the BDE of the aromatic hydrogen atom (ca. 112 kcal/mol) is higher than the BDE of the formed O–H bond (ca. 102 kcal/mol) and thus, formation of an aryl radical **41** is not expected.[15] A homolytic aromatic substitution of the alkoxy radical will give the desired dimethyl chromane **42**. Lastly, an intermolecular H-abstraction will give back alcohol **43** that was used as substrate to obtain the hydroperoxide.

Unfortunately, under none of the employed reaction conditions, the annulated 2,2-dimethyl-2,3-dihydrobenzofuran **44** and 2,2-dimethylchromane **42** products were obtained. In most of the cases, alcohols were isolated as the only product. Since the conversion of the hydroperoxide was complete and thus the intermediate peroxyoxalate is assumed to be formed quantitatively, it is believed that the

alkoxy radical was formed as expected upon thermal decomposition of the peroxyoxalate. Based on the fact that only the alcohol could be clearly identified as a product in the reaction mixture, it is most probable that an issue during the addition and/or rearomatisation step has occurred.

Very recently, Wallentin's group reported a photocatalytic method involving hypervalent iodine reagents to form alkoxy radicals similar to the (photo-)chemistry of hypoiodides.[16] In this publication, similar tertiary *gem*-dimethyl and even more bulky *gem*-diphenyl alkoxy radicals afforded the chromane products. (Figure 4.13).[17]

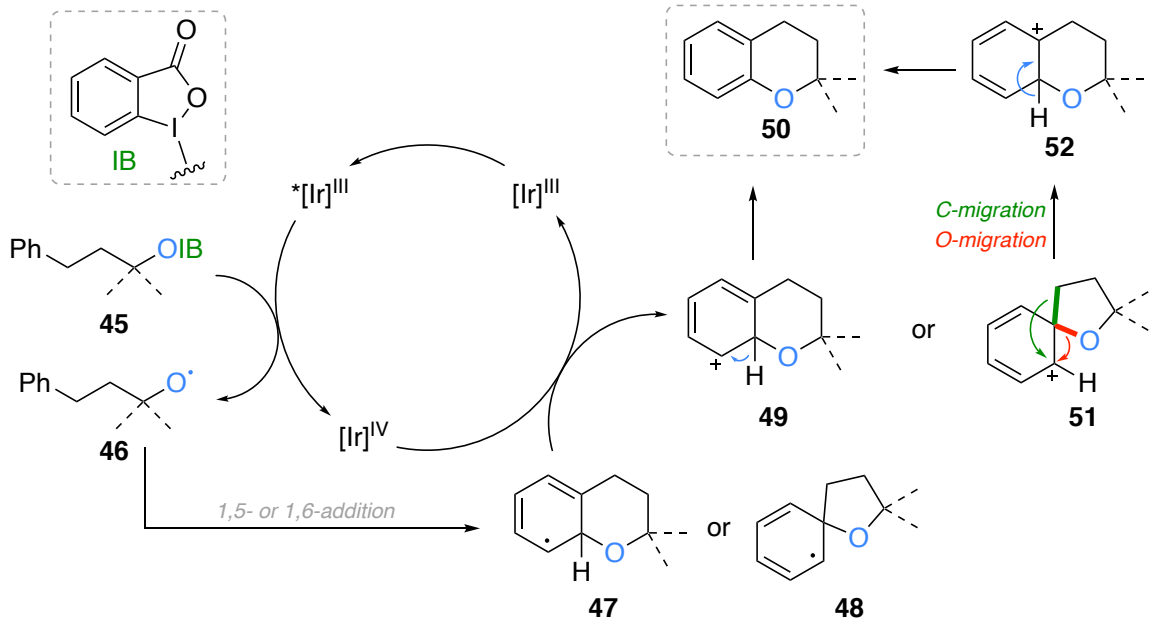

Figure 4.13 Proposed mechanism of Wallentin's chromane synthesis; [Ir] = fac-Ir(ppy)$_3$

Single-electron reduction of the benziodoxolone **45** by the photoactivated Ir^{III} photocatalyst furnishes the alkoxy radical **46** which adds to the aromatic moiety. Both 1,5-addition (*ipso* addition) and 1,6-addition (*ortho* addition) are assumed to take place in parallel. The simultaneously formed Ir^{IV} species functions as an oxidant of the carbon centered radicals **47** or **48**, leading to the corresponding carbocationic intermediates (**49** and **51**). Loss of a proton and rearomatisation of carbocation **49** leads directly to the final chromane product **50**. The spirocyclic carbocationic intermediate **51** undergoes rearrangement by 1,2-migration of either the carbon- or the oxygen substituent, resulting in a tertiary carbocationic intermediate **52** that subsequently also undergoes rearomatisation to the final chroman product. The reason for Wallentin's group to assume a spirocyclic intermediate from a 1,5-addition is, that in case the aryl moiety is non-symmetrically substituted, a 1,2-carbon migration from the spirocyclic intermediate explains the formation of the observed minor regioisomers. In case of a 1,2-oxygen migration, the product is indistinguishable from the product of 1,6-addition pathway.

The only major difference to their reaction conditions is the temperature (35 °C lower) that could slow down the undesired fragmentation side reaction. Apart from this, the 1,n-addition should take place as

expected. The use of electron rich aryl groups could enhance the addition step since alkoxy radicals exhibit electrophilic properties in addition to olefins.[18] However, electron-poor arenes have been reported to work well[8] and it can therefore be concluded, that the nature of the arene does not represent a dominant factor for the success of the transformation.

Since the addition of the alkoxy radical to the aryl moiety (at the *ipso* or *ortho* position) is an intramolecular reaction, the addition is also not expected to be greatly affected by the initiation conditions. However, the Ir^{IV} species used by Walling might additionally act as a very efficient oxidant and oxidize the cyclic species as soon as it is formed. This does not seem to be the case in our system. It is possible, that such a spirocyclic radical is isomerized to a primary radical, whose oxidation to the primary carbocation would be slow (Figure 4.14).

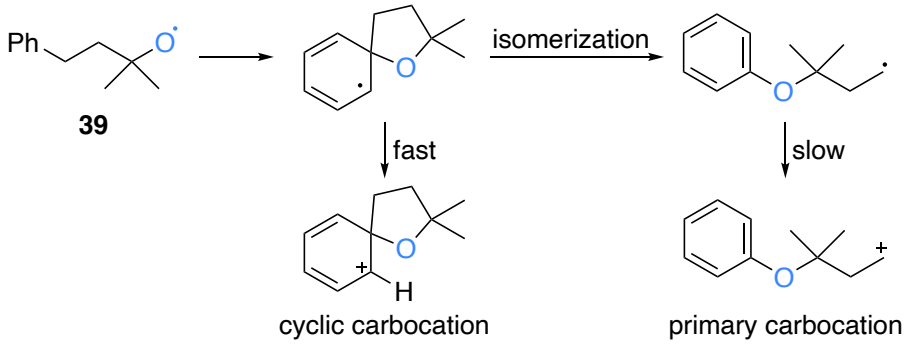

*Figure 4.14. Oxidation of radicals derived from alkoxy radical **39**.*

However, no products were observed that would arise from any of these pathways. Most probably, the oxidation is therefore the problematic step. Zard has demonstrated that slow oxidations are effectively accelerated by addition of dibenzoyl peroxide as a co-oxidant.[19] Furthermore, iron(III) salts have been used by Baciocchi to effect oxidation of intermediate radicals.[20] However, the use of transition metal salts must not interfere with the peroxyoxalate compound before its decomposition not to hamper the formation of the required alkoxy radical.

A more detailed study of the oxidation conditions will therefore be necessary in order to obtain the annulated chromane and 2,3-dihydrobenzofuran compounds.

4.3 Towards the synthesis of macrocycles from peracetals

The fragmentation of alkoxy radicals has been studied for the construction of macrocycles by Schreiber and Ogibin.[21–23] If the alkoxy radical is positioned at a bridgehead position of an (unsymmetric) bicycle, fragmentation of the bridging C–C bond will afford a secondary carbon centered radical on an expanded ring. In strained bicyclic systems, the cleavage of the bridging C–C bond is expected to be even more favored because of strain release. This method is particularly attractive since it allows the formation of olefins or the introduction of other functional groups upon trapping of the radical. Schreiber has reported the synthesis of (±)-Recifeiolide using Walling's iron(II)/copper(II) acetate conditions (Figure 4.15).[22]

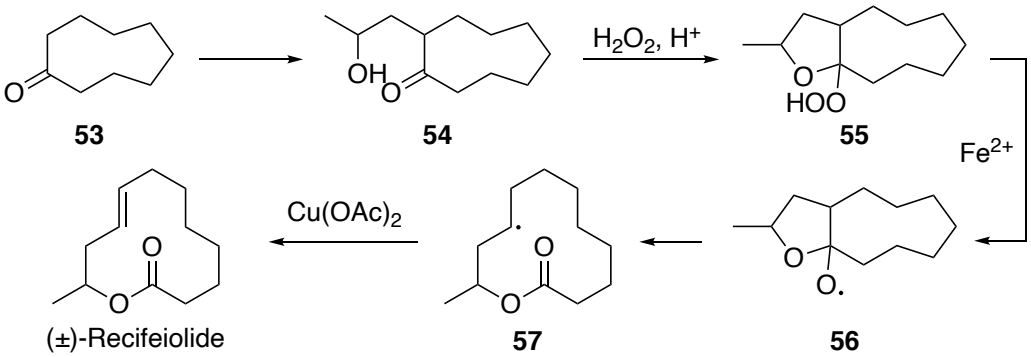

Figure 4.15 Schreiber's synthesis of (±)-Recifeiolide

Alkylation of cyclononanone **53** afforded alcohol **54** which is converted to the tertiary hydroperoxide **55**. Iron-catalyzed decomposition leads to the alkoxy radical **56** which readily fragments to the ring expanded lactone radical **57**. Copper mediated oxidation-elimination furnishes racemic Recifeiolide.[22] The group of Ogibin has used copper salts for both the fragmentation and oxidative elimination in their syntheses of macrolactones.[21,24,25]

Such a transformation would fit well in the project scope, as the required tertiary hydroperoxide precursors are easily available under acidic conditions from the corresponding alcohols (cf. chapter 1). More challenging is the synthesis of such bicyclic systems possessing an alcohol function at the bridgehead position (e.g., decalol **59**). Most of these compounds are available from the rather unselective autoxidation processes and thus have to be tediously separated from other isomeric products. The regioselective hydroxylation of symmetric and unsymmetric hydrocarbons (*e.g.* decalin **59**) is achieved by various aryl-substituted perbenzoic acids[26] and by ozonization.[27–30] Alternatively, radical cyclisation of primary ketoiodides **60** yields bicyclic tertiary alcohols **61** (Figure 4.16).[31]

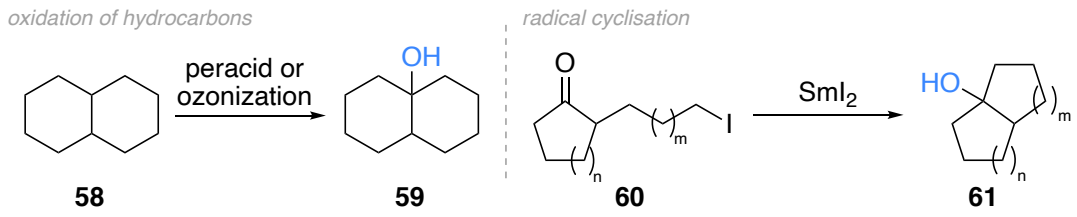

Figure 4.16 Synthesis of bicyclic hydrocarbons with a tertiary alcohol at the bridgehead position

The latter method is synthetically preferred since the size of the annulated second ring can be controlled by the length of the alkyl chain which itself can be easily introduced by C-alkylation of a ketone. The hydroperoxide is then introduced *via* hydroperoxidation of the tertiary alcohol. Another strategy is the direct hydroperoxidation of olefins or enolethers. For these, the hydroperoxidation proceeds regioselectively due to the stabilization of the carbocation by the oxygen atom.

Our goal was to test our method for the synthesis of macrolactones on the substrate reported by Ogibin and the required bicyclic peracetal was synthesized from cyclododecanone (Figure 4.17).[21]

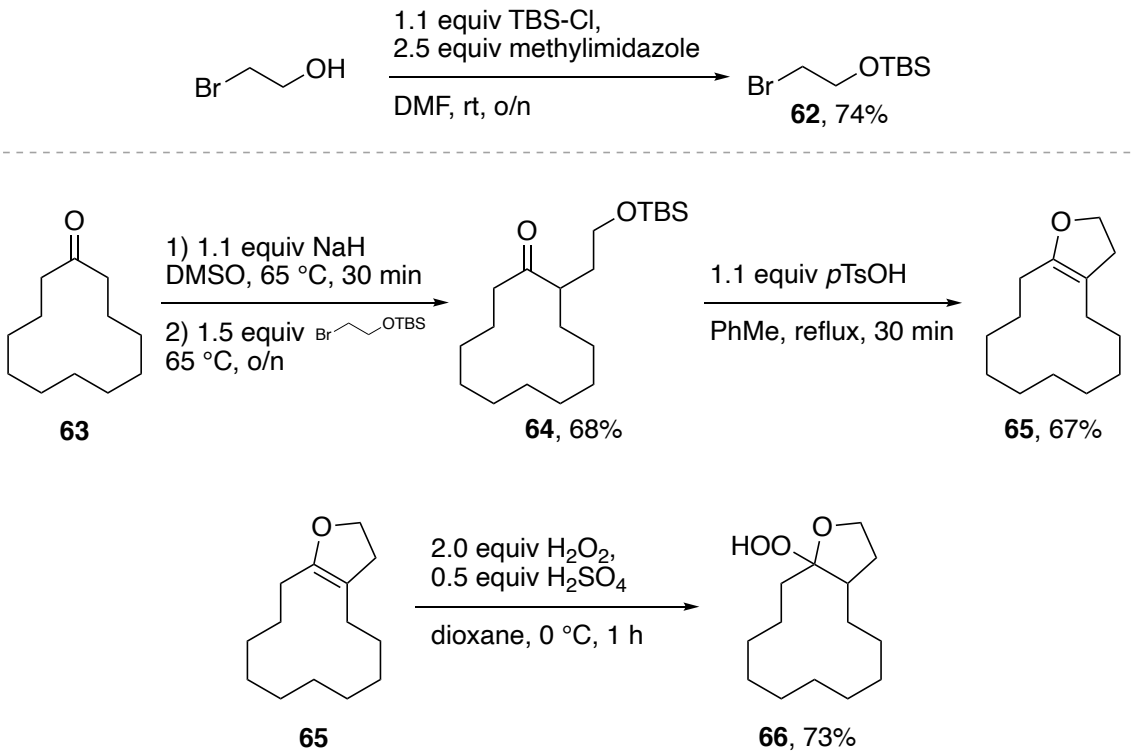

Figure 4.17 Synthesis of peracetal radical precursor

C-alkylation of cyclododecanone **63** with TBS-protected 2-bromo ethanol **62** afforded the α-alkylated ketone **64**. Screening of several reaction conditions revealed that the alkylation takes place most selectively if the sodium enolate is formed first using NaH. Under these conditions, exclusively the C-alkylated product is obtained, albeit in moderate yield. Simultaneous deprotection of the TBS-group, cyclisation to the acetal and elimination to the bicyclic enolether **65** was obtained in satisfying yield using a stoichiometric amount of *p*-TsOH. The acid can also be used catalytically which, however, results in decreased amount and purity of product and requiring longer reaction time. Cautious treatment of the bicyclic enolether **65** with acidic hydrogen peroxide cleanly affords the desired peracetal **66** as a stable solid and with complete regioselectivity.

When applying the established reaction conditions to form the peroxyoxalate and its decomposition, no ring opened product **67** was obtained (Figure 4.18).

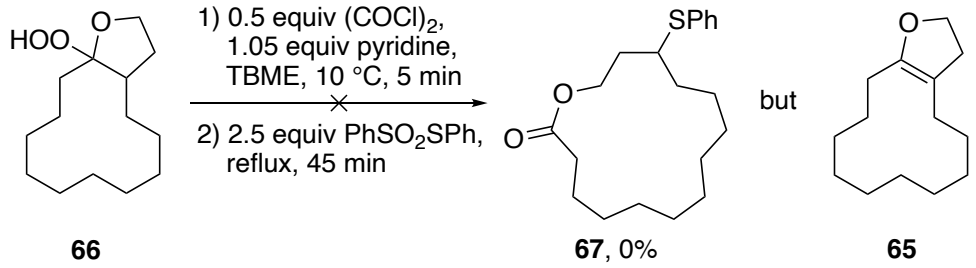

66 **67**, 0% **65**

Figure 4.18 Unsuccessful radical macrolactonization

Interestingly, only enolether **65** was formed. Detailed monitoring of the reaction revealed that the conversion of the peracetal **66** is complete and the peroxyoxalate is formed. However, after a few minutes, the enolether starts to be formed spontaneously while still at low temperature, and thus before the second step. It can be concluded that the peroxyoxalate acts as a leaving group here and the presence of pyridine is probably further enhancing the elimination.

It is yet to be investigated, if the same process takes place from tertiary alkyl substituted hydroperoxides which stabilize the carbocation less efficiently. So far, the investigation on this substrate has been discontinued.

4.4 Generation of alkoxy radicals from hydroperoxides using organoboranes

The motivation to form peroxyoxalates from hydroperoxides was to form an intermediate which has a lower bond strength of the oxygen-oxygen bond and is thus labile enough to decompose homolytically at relatively low temperatures. However, the formation of peroxyoxalates from hydroperoxides is not the only way to achieve such a destabilization of the peroxide bond. Research in polymer science demonstrated, that oxygen-oxygen bonds are also homolytically cleaved in organoboron peroxides at ambient temperature. We assumed, that such unstable intermediates are accessible from hydroperoxides and successfully applied this strategy on the same compound with which we conducted the optimization of our previously described method (cf. chapter 3).

4.4.1 Use of borinate radicals for radical polymerizations

For many years, the organoboron/oxygen system has mainly been used in the polymer industry and in academic research for controlled polymerization processes or generation of alkyl radicals. Alkyl boronic compounds react in many ways with molecular oxygen forming oxygen- and carbon- centered radical species that are able to initiate radical reactions.[32,33] The formation of such metalorganic peroxides is of particular interest and can be formed as follows and as comprehensively explained in an early paper by Davies (Figure 4.19).[32]

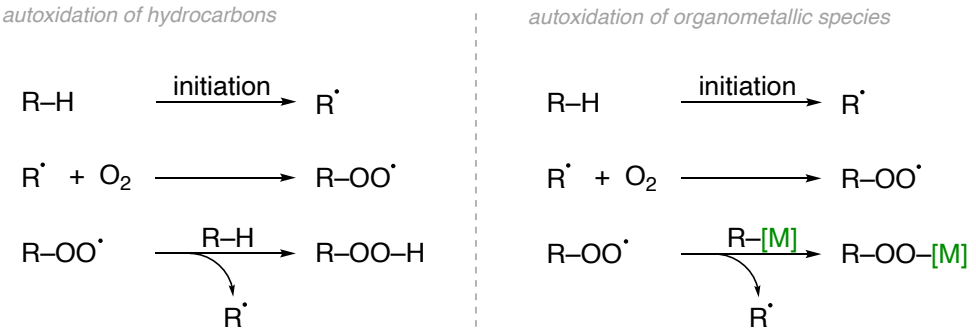

Figure 4.19 Autoxidation of hydrocarbons and organometallic species

Similar to the autoxidation of hydrocarbons, initial formation of an alkoxyl radical is leading to a peroxy radical upon reaction with molecular oxygen. For hydrocarbons, this peroxy radical abstracts another hydrogen atom resulting in the formation of a hydroperoxide and a new alkyl radical that sustains the chain (Figure 4.19, left). In the presence of an organometallic species like a trialkyl borane, the peroxy radical is able to react with it, thereby forming an organometallic peroxide. The ejected alkyl radical again sustains the radical chain (Figure 4.19, right).

In the case of trialkyl boranes, the autoxidation results in the formation of dialkyl(alkylperoxy)boranes which represent another form of a destabilized peroxide bond susceptible for homolytic cleavage as previously seen in peroxyoxalates (Figure 4.20).[34]

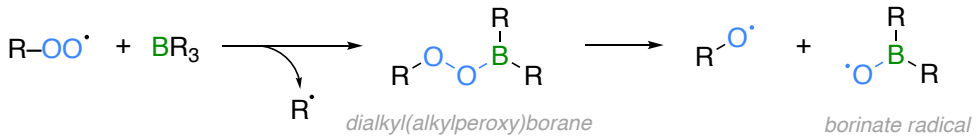

Figure 4.20 Autoxidation of trialkyl borane and homolytic fragmentation

The rate constants of the homolysis of dialkyl(alkylperoxy)boranes to an alkyl radical and a borinate radical have been determined for boranes with an *n*-butyl (1.1×10^5 s^{-1}) and an *s*-butyl (3.8×10^4 s^{-1}) alkyl substituents which is comparable to DTBPO (7.0×10^5) at 35 °C.[32,35]

Even though such systems could work technically in an analogous manner to the peroxyoxalate methods, the use of the corresponding trialkyl boranes and their autoxidation is not of preparative significance due to the pyrophoric nature of trialkyl boranes and the difficulties associated to their controlled preparation. Research in polymer science has shown a way to circumvent these difficulties by using a special type of trialkyl boranes: non-symmetric alkyl-9-borabicyclononane (alkyl-9-BBN) compounds are obtained in a straightforward manner from the corresponding olefins by hydroboration with 9-borabicyclononane (9-BBN). These compounds exhibit greater stability than other trialkyl borates, but still form alkoxy radicals which initiate the polymerization process and have effectively been used for the synthesis of ultra-high-molecular-weight polystyrene.[36] This method has a big advantage since the bulky borinate radicals are persistent species and are thus able to recombine to and re-dissociate easily from the end of the growing polymer chain – a process which is known as reversible-addition-fragmentation chain-transfer polymerization (RAFT polymerization).[37] The borane-mediated living radical polymerization has been reviewed and a general mechanism is depicted below (Figure 4.21).[38–43]

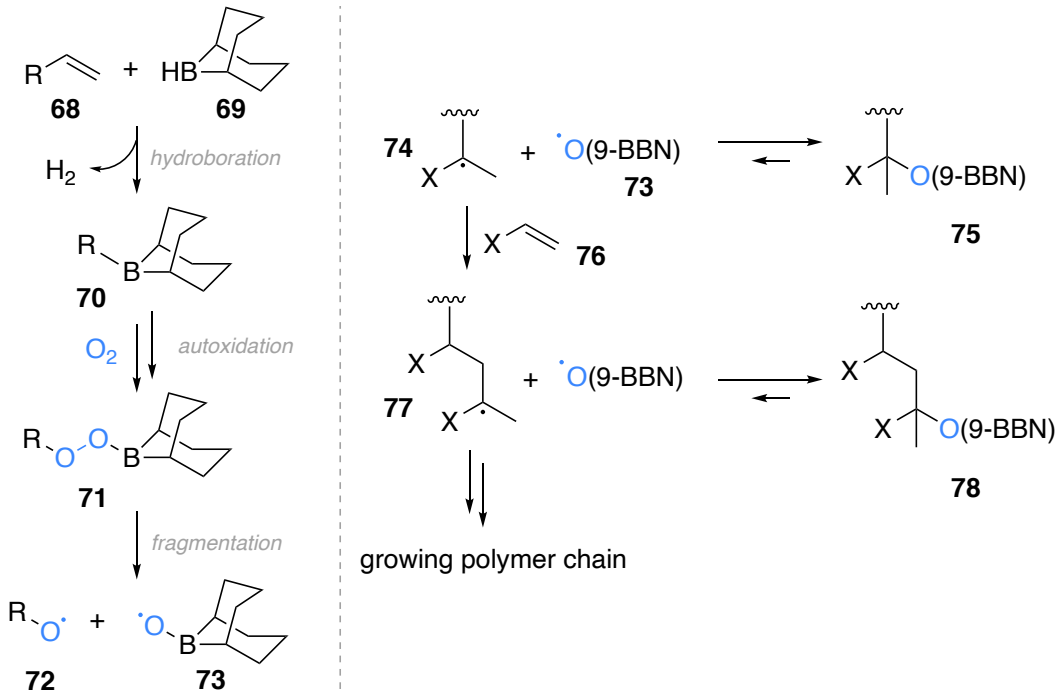

*Figure 4.21 Formation of 9-BBN borinate radical **73** and two steps of RAFT polymerization of a vinyl monomer*

Hydroboration of olefin **68** with 9-BBN **69** affords the starting alkyl-9-BBN species **70** which is transformed to the boron peroxide autoxidation product **71**. It is important that the oxygen is added very slowly to avoid overoxidation. The selectivity of insertion of the oxygen is high (70-90%) and in favor of the non-cyclic alkyl substituent due to unfavorable ring strain of an insertion into the 9-BBN moiety.[38] The peroxide then undergoes homolytic cleavage to an alkoxy radical **72** that initiates the polymerization reaction and the borinate radical **73** which is used in the polymerization process but does not react with the monomers. Interestingly, the stabilization of the borinate radical is due to back donation of electron density from the oxygen atom to the empty p-orbital of the boron atom which is analogous but opposite to the nitroxide radicals (*e.g.,* TEMPO) where the electron density of the occupied nitrogen lone pair acts as donator to the oxygen centered radical.[38]

During the polymerization, the propagating end of a polymer chain (**74**) reacts with the persistent borinate radical affording a rather stable radical adduct **75** (termed "dormant stage" of propagating site). Dissociation of the borinate radical liberates again the active radical polymer chain (**74**) that reacts with a new monomer **76** and elongates the chain by one unit (**77**). The borinate radical is now again able to react with this free end of the chain (**78**). Repetition of this process takes place until the polymerization process has come to an end due to the complete consumption of monomers. Such polymerizations take place at room temperature and usually require several hours to several days to complete. It has been shown that polar and coordinating solvents (e.g. THF, DMSO) give higher yields than non-coordinating solvents (e.g. benzene)[42] which is presumably based on the enhanced reactivity of complexed peroxyboranes.[44,45]

However, this improved process still suffers from the rather delicate conditions leading to the desired borinate radical. Chung and coworkers have elegantly solved this problem using a combination of an alcohol and 9-BBN (Figure 4.22).

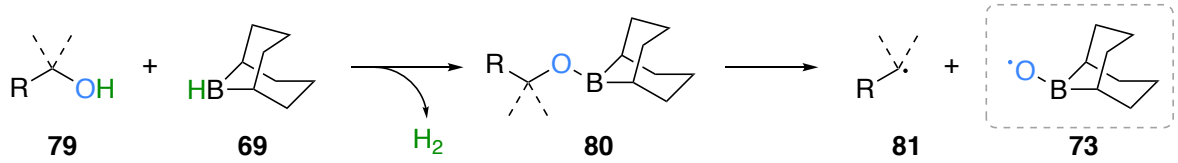

79 **69** **80** **81** **73**

Figure 4.22 Borinate formation from alcohols and 9-BBN

Reaction of 9-BBN **69** with a free alcohol **79** forms a trialkyl borinate **80** which very closely resembles the dormant stage of the polymers' propagating site.[42] Dissociation of the borinate radical **73** liberates an alkyl radical **81**, which, like alkoxy radical **72** in the above-described process, will react with a monomer and thus start the polymerization process.

Advantageously, the structure of alcohol **79** can be designed in such a way that the corresponding radical **81** closely resembles the structure of the monomer (and thus the polymers' propagating site) which enhances the compatibility of the initiating system with the polymerization process.

4.4.2 Aim of the project

Motivated by these preceding studies, we aimed to develop a method to generate alkoxy radicals from hydroperoxides based on the described concepts without the detour of forming peroxyoxalates and thus avoiding the use of corrosive oxalyl chloride and the formation of salts. Such a process will allow a wider range of solvents since no salt precipitation has to be enforced. Taking advantage of the persistent nature of the 9-BBN borinate radical, a synthesis of 1,4-diols is a conceivable option *via* recombination of the relocated radical with the borinate radical and subsequent oxidation (Figure 4.23).

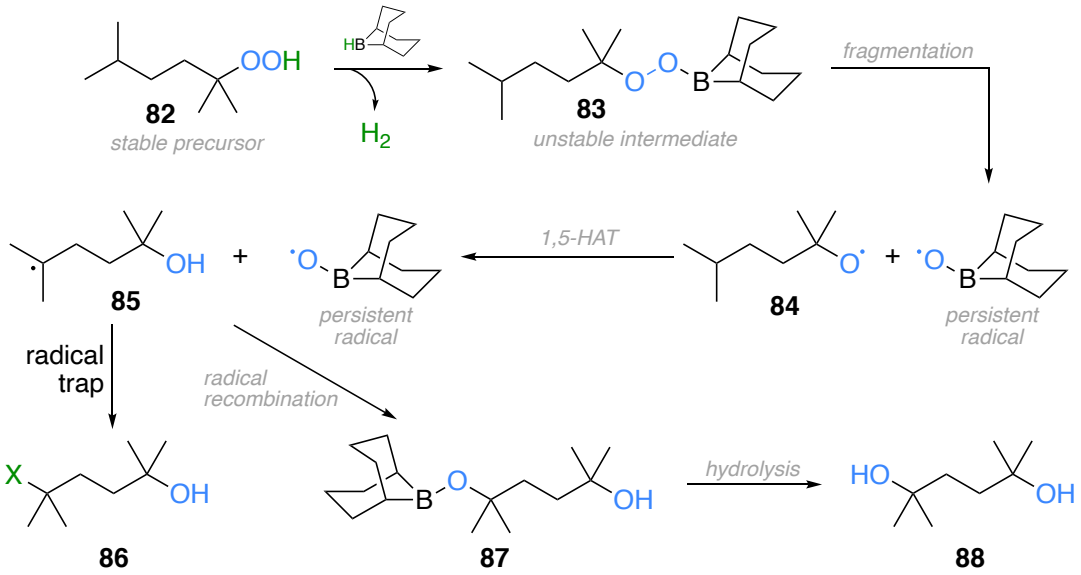

Figure 4.23 Synthetic plan for the synthesis of functionalized alcohols from hydroperoxides using 9-BBN

The tertiary hydroperoxide **82** used in chapter 3 is expected to react with 9-BBN similar to the alcohol in the work of Chung, which will result in an unstable peroxide intermediate **83**. Hydrogen gas is produced as the only side product and will not interfere in the next steps of the reaction as it leaves the reaction mixture. Oxygen is not expected to be problematic since 9-BBN is stable under ambient conditions. Fragmentation of intermediate **83** will lead to the same tertiary alkoxy radical **84** as obtained after thermal decomposition of the previously described peroxyoxalates and will undergo a subsequent 1,5-HAT leading to the relocated alkyl radical **85**. The persistent borinate radical is not expected to react at this stage. In the presence of a radical trap, the alkyl radical is functionalized which results in the alcohol **86**. If no radical trap is present, the alkyl radical can recombine with the persistent radical, as it is the case in RAFT polymerization, leading to the borinate intermediate **87** which, upon oxidative workup, can be transformed to the corresponding 1,4-diol **88**.

4.4.3 Fragmentation of hydroperoxides using 9BBN

In a first proof-of-concept reaction, all parameters of the reaction were set according to the general procedure described in chapter three except for the switch from the oxalyl chloride / pyridine combination to a solution of 9-BBN (Figure 4.24).

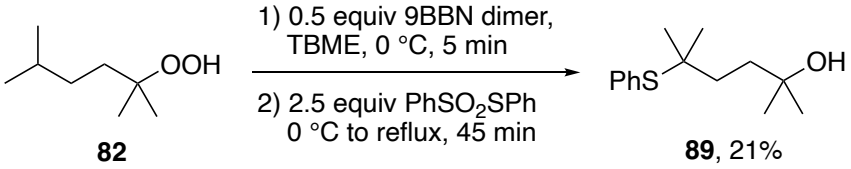

Figure 4.24 Proof-of-concept chalkogenation of the model hydroperoxide

Immediately after the addition of 9BBN to hydroperoxide **82**, the evolution of hydrogen gas was observed as expected and the functionalized alcohol **89** was obtained in a promising yield of 21%. Reduced alcohol was observed as a side product but was not quantified.

Next, it was attempted to obtain the 1,4-diol **88** when the radical trap was not added to the reaction mixture (Figure 4.25).

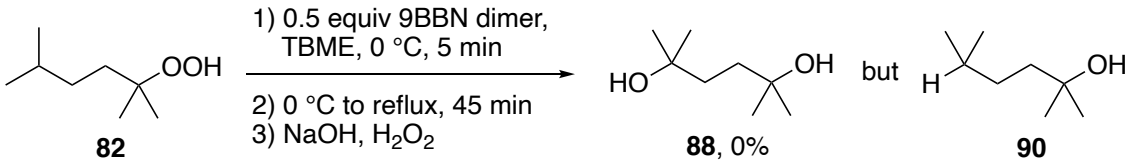

*Figure 4.25 Attempted synthesis of 1,4-diol **88***

Unfortunately, the 1,4-diol **88** was not obtained in the first attempt, but the reaction yielded cleanly the reduced alcohol **90** as the only product (which was not quantified). This can be explained by hydrogen atom abstraction from the solvent before the recombination with the borinate radical can occur.

From these two experiments, it is concluded that in the presence of an excess of the radical trap, the functionalized product is obtained. However, the recombination with the (equimolar amount of) borinate radical is slow and thus outcompeted by a hydrogen abstraction process.

These observations show the feasibility of the attempted processes and during a future optimization of the reaction conditions, the following points will have to be addressed:

- **Temperature**: An increase in the reaction temperature does not only accelerate the fragmentation of the peroxide bond but also increases the chance of hydrogen abstraction which results in the formation of the reduced alcohol. On the other hand, elevated temperatures might be required to enable an efficient trapping of the alkyl radical for functionalization.
- **Solvent**: Hydrogen abstraction leading to the alcohol product is not only enhanced at higher temperatures but also strongly depends on the solvent. Although TBME is not a particularly

good hydrogen donor, it might not be the best choice for this transformation. A compromise has to be found between solvent polarity which enhances the reactivity of the borinate intermediate, and solvent proticity which probably increases the rate of undesired side-reactions. The effect of water being present in the reaction is worth investigating since it is polar (which is beneficial for radical reactions involving organoboranes[45]) but does not act as a hydrogen atom donor.

- **Substrates**: Possibly, also non-tertiary hydroperoxides can be used as radical precursors since the oxidation to the aldehyde[13,14] might not take place. Also, peracetal **66** (cf. previous subchapter) represents an interesting substrate to be tested since the elimination to the enolether might not occur.

In summary, the use of a stoichiometric amount of 9-BBN to promote alkoxy radical formation from alkyl hydroperoxides has been demonstrated in a proof-of-concept example which set the basis for further investigation of this method. Advantageously, the absence of acids, bases, salts and potentially explosive intermediates allows a wider range of reaction conditions to be tested and will enable the introduction of alcohols at the position of the relocated radical – a task that cannot be achieved otherwise since radical traps that deliver oxygen substituents directly do not exist.

4.5 References

[1] M. Nechab, S. Mondal, M. Bertrand, *Chemistry - A European Journal* **2014**, *20*, 16034–16059.

[2] C. Djerassi, L. Miramontes, G. Rosenkranz, F. Sondheimer, *J. Am. Chem. Soc.* **1954**, *76*, 4092–4094.

[3] J. Bae, N. Kim, Y. Shin, S.-Y. Kim, Y.-J. Kim, *Biomedical Dermatology* **2020**, *4*, 8.

[4] M. Isemura, *Molecules* **2019**, *24*, 528.

[5] S. Furuyama, H. Togo, *Synlett* **2010**, *2010*, 2325–2329.

[6] T. Muraki, H. Togo, M. Yokoyama, *Tetrahedron Letters* **1996**, *37*, 2441–2444.

[7] K. Ohkubo, T. Kobayashi, S. Fukuzumi, *Opt. Express, OE* **2012**, *20*, A360–A365.

[8] Y.-W. Zheng, P. Ye, B. Chen, Q.-Y. Meng, K. Feng, W. Wang, L.-Z. Wu, C.-H. Tung, *Org. Lett.* **2017**, *19*, 2206–2209.

[9] J. D. Hepworth, B. M. Heron, in *Progress in Heterocyclic Chemistry* (Eds.: G.W. Gribble, T.L. Gilchrist), Elsevier, **1998**, pp. 292–319.

[10] A. Pelter, A. Hussain, G. Smith, R. S. Ward, *Tetrahedron* **1997**, *53*, 3879–3916.

[11] H. Togo, T. Muraki, Y. Hoshina, K. Yamaguchi, M. Yokoyama, *Journal of the Chemical Society, Perkin Transactions 1* **1997**, *0*, 787–794.

[12] H. R. Williams, H. S. Mosher, *J. Am. Chem. Soc.* **1954**, *76*, 2987–2990.

[13] B. G. Dixon, G. B. Schuster, *J. Am. Chem. Soc.* **1981**, *103*, 3068–3077.

[14] B. G. Dixon, G. B. Schuster, *Journal of the American Chemical Society* **1979**, 3.

[15] Y.-R. Luo, *Handbook of Bond Dissociation Energies in Organic Compounds*, **2003**.

[16] J. Lee, J. Oh, S. Jin, J.-R. Choi, J. L. Atwood, J. K. Cha, *J. Org. Chem.* **1994**, *59*, 6955–6964.

[17] A. R. Rivero, P. Fodran, A. Ondrejková, C.-J. Wallentin, *Org. Lett.* **2020**, *22*, 8436–8440.

[18] J. Hartung, I. Kempter, T. Gottwald, M. Schwarz, R. Kneuer, *Tetrahedron: Asymmetry* **2009**, *20*, 2097–2104.

[19] L. Petit, I. Botez, A. Tizot, S. Z. Zard, *Tetrahedron Letters* **2012**, *53*, 3220–3224.

[20] E. Baciocchi, E. Muraglia, *Tetrahedron Letters* **1993**, *34*, 5015–5018.

[21] Yu. N. Ogibin, A. O. Terent"ev, V. P. Ananikov, G. I. Nikishin, *Russian Chemical Bulletin* **2001**, *50*, 2149–2155.

[22] S. L. Schreiber, *J. Am. Chem. Soc.* **1980**, *102*, 6163–6165.

[23] S. L. Schreiber, B. Hulin, W. Liew, *Tetrahedron* **1986**, *42*, 2945–2950.

[24] Y. N. Ogibin, A. O. Terent'ev, A. V. Kutkin, G. I. Nikishin, *Tetrahedron Letters* **2002**, *43*, 1321–1324.

[25] Y. N. Ogibin, A. O. Terent'ev, A. V. Kutkin, G. I. Nikishin, *Tetrahedron Letters* **2002**, 4.

[26] W. Müller, H.-J. Schneider, *Angewandte Chemie International Edition in English* **1979**, *18*, 407–408.

[27] Louis. Long, *Chem. Rev.* **1940**, *27*, 437–493.

[28] Z. Cohen, E. Keinan, Y. Mazur, T. H. Varkony, *J. Org. Chem.* **1975**, *40*, 2141–2142.

[29] H. Varkony, S. Pass, Y. Mazur, *Journal of the Chemical Society, Chemical Communications* **1974**, *0*, 437–438.

[30] R. A. Berglund, in *Encyclopedia of Reagents for Organic Synthesis*, American Cancer Society, **2001**.

[31] G. A. Molander, J. B. Etter, *Tetrahedron Letters* **1984**, *25*, 3281–3284.

[32] A. G. Davies, K. U. Ingold, B. P. Roberts, R. Tudor, *J. Chem. Soc. B* **1971**, 698–712.

[33] C. Ollivier, P. Renaud, *Chem. Rev.* **2001**, *101*, 3415–3434.

[34] J. Furukawa, T. Tsuruta, *Journal of Polymer Science* **1959**, *36*, 275–286.

[35] P. D. Bartlett, E. P. Benzing, R. E. Pincock, *J. Am. Chem. Soc.* **1960**, *82*, 1762–1768.

[36] C. Zhao, R. Sugimoto, Y. Naruoka, *Chin J Polym Sci* **2018**, *36*, 592–597.

[37] C. Lv, Y. Du, X. Pan, *Journal of Polymer Science* **2020**, *58*, 14–19.

[38] T. C. Chung, W. Janvikul, H. L. Lu, *J. Am. Chem. Soc.* **1996**, *118*, 705–706.

[39] T. C. Chung, H. Hong, in *Advances in Controlled/Living Radical Polymerization*, American Chemical Society, **2003**, pp. 481–495.

[40] Z.-C. Zhang, T. C. M. Chung, in *Controlled/Living Radical Polymerization: Progress in RAFT, DT, NMP & OMRP*, American Chemical Society, **2009**, pp. 331–344.

[41] D. E. Bergbreiter, G. F. Xu, *Macromolecules* **1995**, *28*, 4756–4758.

[42] M. Ohkura, T. C. M. Chung, *Journal of Polymer Science Part A: Polymer Chemistry* **2014**, *52*, 2889–2893.

[43] M. Yu. Zaremski, E. S. Garina, M. E. Gurskii, Yu. N. Bubnov, *Polym. Sci. Ser. B* **2013**, *55*, 304–326.

[44] K. Kojima, M. Nishina, M. Yoshikuni, *Nippon Kagaku Kaishi* **1973**, *1973*, 2405–2409.

[45] H. Yorimitsu, H. Shinokubo, S. Matsubara, K. Oshima, K. Omoto, H. Fujimoto, *J. Org. Chem.* **2001**, *66*, 7776–7785.

4.6 Experimental section

General information

Techniques

All reactions requiring anhydrous conditions were performed in heat-gun, oven, or flame dried glassware under an argon atmosphere. An ice bath was used to obtain a temperature of 0 °C. To obtain a temperature of –78 °C, a bath of acetone was cooled with dry ice. To obtain temperatures of –40 °C and –15 °C, a bath of isopropanol or acetonitrile was cooled to the desired temperature using dry ice. Silica gel 60 Å (40–63 µm) from Silicycle was used for flash column chromatography. Thin layer chromatography (TLC) was performed on Silicycle silica gel 60 F_{254} plates, visualization under UV light (254 nm) and/or by dipping in a solution of $(NH_4)_2MoO_4$ (15.0 g), $Ce(SO_4)_2$ (0.5 g), H_2O (90 mL), conc. H_2SO_4 (10 mL); or $KMnO_4$ (3 g), K_2CO_3 (20 g) and NaOH 5% (3 mL) in H_2O (300 mL) and subsequent heating. Anhydrous sodium sulfate was used as drying reagent.

Materials

Commercial reagents were used without further purification unless otherwise stated. Dry solvents for reactions were filtered over columns of dried alumina under a positive pressure of argon. Solvents for extractions (Et_2O, *n*-pentane, CH_2Cl_2, EtOAc, heptanes) and flash column chromatography were of technical grade and distilled prior to use. Commercial dry pyridine was used without further purification.

Instrumentation

^1H and ^{13}C NMR spectra were recorded on a Bruker Avance IIIHD-300 spectrometer operating at 300 MHz for ^1H and 75 MHz for ^{13}C at room temperature (24-25°C) unless otherwise stated. Some ^1H and ^{13}C NMR spectra were recorded on a Bruker Avance IIIHD-400 or a Bruker Avance II-400 spectrometer (^1H: 400 MHz; ^{13}C: 75 MHz). Chemical shifts (δ) are reported in parts per million (ppm) using the residual solvent or $Si(CH_3)_4$ (δ = 0.00 for ^1H NMR spectra) as an internal standard. Multiplicities are given as s (singlet), d (doublet), t (triplet), q (quadruplet), m (multiplet), and br (broad). Coupling constant (*J*) is reported in Hz. In ^{13}C-NMR spectra, the peak positions are reported on one decimal unless the difference in chemical shift between two signals is small and requires two decimals. Infrared spectra were recorded on a Jasco FT-IR-460 plus spectrometer equipped with a Specac MKII Golden Gate Single Reflection Diamond ATR system and are reported in wave numbers (cm^{-1}). At maximum, the ten most prominent peaks are reported. Low resolution mass spectra were recorded on a Waters Micromass Autospec Q mass spectrometer in EI mode at 70 eV or were taken from GC-MS analyses performed on a Finnigan Trace GC-MS (quadrupole mass analyzer using EI mode at 70 eV) fitted with a Macherey-Nagel Optima delta-3-0.25 µm capillary column (20 m, 0.25 mm); gas carrier: He 1.4 mL/min; injector: 220 °C split mode. HRMS analyses and accurate mass determinations were performed on a Thermo Scientific LTQ Orbitrap XL mass spectrometer using ESI mode. Melting points were measured on a Büchi B-545 apparatus and are corrected. Syringe filters with

polytetrafluoroethylene membrane were used with a pore size of 0.45 µm (or 5 µm) from Machery-Nagel (e.g. CHROMAFIL®Xtra PTFE 0.45). Medium pressure liquid chromatography (MPLC) was performed with a CombiFlash® Rf+ system from Teledyne Isco using RediSep® single-use normal phase columns.

Syntheses

(8*R*,9*S*,13*S*,14*S*)-3-((tert-butyldimethylsilyl)oxy)-13-methyl-6,7,8,9,11,12,13,14,15,16-decahydro-17H-cyclopenta[a]phenanthren-17-one (2)

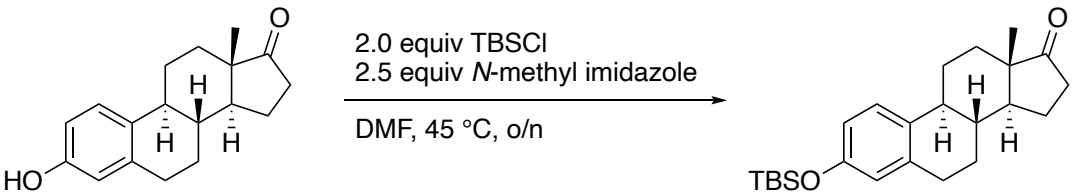

quant.

To a mixture of estrone **1** (5.4 g, 20.0 mmol) and TBS-Cl (6.0 g, 40 mmol, 2.0 equiv) in dry DMF (80 mL) was added methylimidazole (4.0 mL, 50 mmol, 2.5 equiv). The mixture was stirred overnight at 45 °C, poured in sat. aq. NH_4Cl (50 mL) and extracted with Et_2O. The combined organic phase was dried over Na_2SO_4, filtered and concentrated. FC (8:2 pentane:Et2O) afforded **2** (7.6 g, quant.).

White solid; **R_f** 0.33 (9:1 pentane:Et_2O); **^{1}H-NMR** (300 MHz, $CDCl_3$) δ = 7.12 (dd, J = 8.5, 1.1 Hz, 1H), 6.63 (dd, J = 8.4, 2.7 Hz, 1H), 6.58 (s, 1H), 2.92 – 2.78 (m, 2H), 2.58 – 1.88 (m, 7H), 1.67 – 1.35 (m, 6H), 0.98 (s, 9H), 0.91 (s, 3H), 0.19 (s, 6H); **^{13}C-NMR** (75 MHz, $CDCl_3$) δ = 115.1, 68.2, 40.1, 30.6, 27.5, 26.2, 26.1, 25.1, 24.3, 22.4, 22.2, 22.1, 21.8, 19.6; physical and spectral data are in accordance with literature data.[1]

(8R,9S,13S,14S,17S)-3-((tert-butyldimethylsilyl)oxy)-13,17-dimethyl-7,8,9,11,12,13,14,15,16,17-decahydro-6H-cyclopenta[a]phenanthren-17-ol (3)

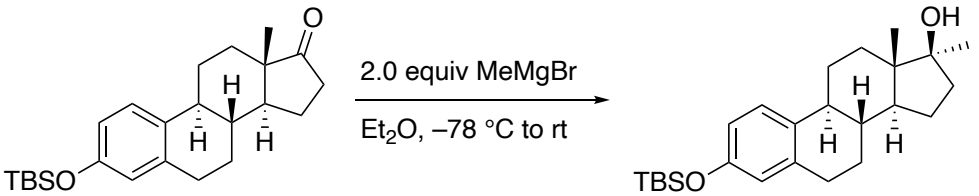

58%

To a solution of MeMgBr (6.7 mL, 3.0 M in Et_2O, 20 mmol, 2.0 equiv) in dry THF (23.3 mL) was added a solution of **2** (3.85 g, 10 mmol) in dry THF (20 mL) at –78 °C. After 30 min, the dry ice was removed and a slightly yellow solution was formed, which was stirred at rt for 2 h. Then, To drive the reaction to completion, another portion of MeMgBr (2 mL, 3.0 M in Et_2O, 6.0 mmol, 0.6 equiv) was added and the mixture was stirred at 45 °C for 1 h. The mixture was poured in sat. aq. NH_4Cl (50 mL) and extracted with Et_2O. The combined organic phase was dried over Na_2SO_4, filtered and concentrated. FC (8:2 pentane:Et_2O) afforded **3** (2.32 g, 58%).

White solid; **R_f** 0.20 (7:3 pentane:Et_2O); **mp** 52-58 °C; **^{1}H-NMR** (300 MHz, $CDCl_3$) δ = 7.12 (dd, J = 8.5, 1.0 Hz, 1H), 6.61 (dd, J = 8.4, 2.7 Hz, 1H), 6.55 (d, J = 2.6 Hz, 1H), 2.87 – 2.76 (m, 2H), 2.31 (ddd, J =

9.4, 4.6, 3.0 Hz, 1H), 2.16 (q, J = 5.3 Hz, 1H), 1.94 – 1.74 (m, 3H), 1.73 – 1.30 (m, 9H), 1.28 (s, 3H), 0.98 (s, 9H), 0.90 (s, 3H), 0.19 (s, 6H); **^{13}C-NMR** (75 MHz, $CDCl_3$) δ = 153.5, 138.0, 126.2, 120.1, 117.3, 81.9, 49.9, 46.0, 44.1, 39.8, 39.2, 31.9, 29.8, 27.6, 26.4, 26.0, 23.1, 18.3, 14.0, 1.1, -4.2; **HRMS** calc. for $C_{25}H_{41}O_2Si$ $[M+H]^+$: 401.2870, found: 401.2858; **IR** (cm^{-1}):34.11, 2928, 2856, 1607, 1495, 1286, 1251, 945, 836, 778; **$[\alpha]_D^{25}$** = +41.4° (c = 1.0, $CHCl_3$)

(8*R*,9*S*,13*S*,14*S*,17*S*)-13,17-dimethyl-7,8,9,11,12,13,14,15,16,17-decahydro-6H-cyclopenta[a]phenanthrene-3,17-diol (5)

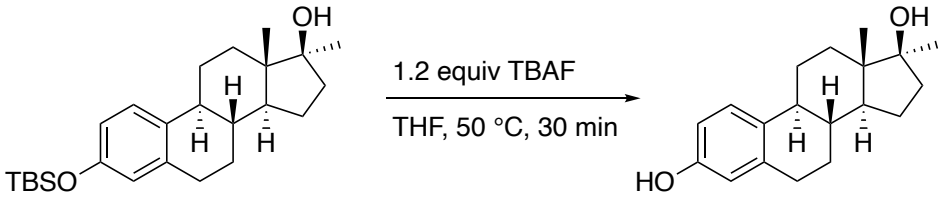

97%

To a solution of **3** (2.24 g, 5.6 mmol) in dry THF (15 mL) was added TBAF (1.0 M in THF, 6.7 mL, 6.7 mmol, 1.2 equiv) at rt. The mixture was stirred at 50 °C for 30 min, treated with water (50 mL) and extracted with Et_2O. The organic phase was dried over Na_2SO_4, filtered and concentrated. FC (6:4 heptanes:EtOAc) afforded **5** (1.56 g, 97%).

White solid; **R_f** 0.37 (6:4 pentane:Et_2O); **^{1}H-NMR** (300 MHz, $CDCl_3$) δ = 7.19 – 7.12 (m, 1H), 6.63 (dd, J = 8.4, 2.8 Hz, 1H), 6.57 (d, J = 2.7 Hz, 1H), 2.88 – 2.77 (m, 2H), 2.40 – 2.23 (m, 1H), 2.15 (dq, J = 9.9, 4.8 Hz, 1H), 1.95 – 1.58 (m, 5H), 1.55 – 1.31 (m, 7H), 1.29 (s, 3H), 0.90 (s, 3H); **^{13}C-NMR** (75 MHz, $CDCl_3$) δ = 153.6, 138.4, 132.7, 126.6, 115.4, 112.8, 82.2, 49.8, 45.9, 44.0, 39.8, 39.1, 31.8, 29.8, 27.5, 26.4, 25.9, 23.1, 14.0; physical and spectral data are in accordance with literature data.[2]

(8*R*,9*S*,13*S*,14*S*,17*S*)-3-methoxy-13,17-dimethyl-7,8,9,11,12,13,14,15,16,17-decahydro-6H-cyclopenta[a]phenanthren-17-ol (6)

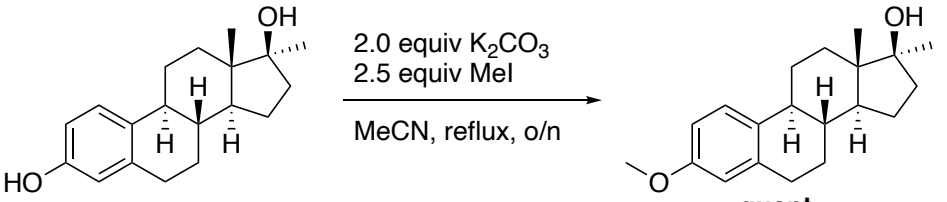

quant.

To a suspension of K_2CO_3 (1.51 g, 10.9 mmol, 2.0 equiv) and **5** (1.56 g, 5.5 mmol) in MeCN (35 mL) was added MeI (0.85 mL, 13.6 mmol, 2.5 equiv) at rt. The mixture was refluxed overnight (95 °C), cooled down to rt, treated with water (50 mL), brine (50 mL) and extracted with EtOAc (3 x 50 mL). The combined organic phase was washed with brine, dried over Na_2SO_4, filtered and concentrated. FC (8:2 heptanes:EtOAc) afforded **6** (1.63 g, quant).

Sticky mass; **R_f** 0.27 (8:2 heptanes:EtOAc); **^{1}H-NMR** (300 MHz, $CDCl_3$) δ = 7.21 (dd, J = 8.6, 1.1 Hz, 1H), 6.72 (dd, J = 8.6, 2.8 Hz, 1H), 6.64 (d, J = 2.8 Hz, 1H), 3.78 (s, 3H), 2.87 (ddd, J = 10.0, 5.1, 2.5 Hz, 2H), 2.42 – 2.22 (m, 1H), 2.23 – 2.12 (m, 1H), 1.94 – 1.76 (m, 3H), 1.76 – 1.30 (m, 9H), 1.30 (s, 3H), 0.90 (s, 3H); **^{13}C-NMR** (75 MHz, $CDCl_3$) δ = 157.6, 138.1, 132.8, 126.4, 113.9, 111.6, 81.9, 55.3,

49.8, 45.9, 44.0, 39.8, 39.2, 31.8, 30.0, 27.6, 26.5, 26.0, 23.1, 14.0; physical and spectral data are in accordance with literature data.[3]

1-Benzyl-4-phenylcyclohexan-1-ol (10)

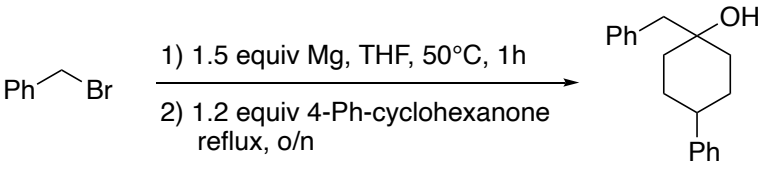

38%

Benzyl bromide (17.8 mL, 150 mmol) was slowly added to a suspension of magnesium turnings (5.5 g, 225 mmol, 1.5 equiv) and one crystal of iodine in dry THF (83 mL) at 75 °C. Upon complete addition, the mixture was refluxed for 3 h and then, 4-phenyl cyclohexanone (31.4 g, 180 mmol, 1.2 equiv) in dry THF (35 mL) was slowly added. The mixture was refluxed at 80 °C overnight. The mixture cooled down to rt, poured into aq. HCl (0.5 M, 300 mL) and stirred for 15 min. The mixture was extracted 3 x with CH_2Cl_2. The organic phase was dried over Na_2SO_4, filtered and concentrated. FC (85:15 heptanes:EtOAc) afforded two separate diastereomers of 1-benzyl-4-phenylcyclohexan-1-ol (10.3 g, 26% and 4.7 g, 12 %).

Major diastereomer:

White solid; **R_f** 0.35 (8:2 heptanes:EtOAc); **mp** 80 °C; **^{1}H-NMR** (300 MHz, CD_2Cl_2) δ 7.39 – 7.09 (m, 10H), 2.77 (s, 2H), 2.46 (tt, J = 12.0, 3.5 Hz, 1H), 1.88 – 1.55 (m, 7H); **^{13}C-NMR** (75 MHz, CD_2Cl_2) δ 147.9, 137.7, 131.1, 128.6, 128.4, 127.2, 126.8, 126.2, 70.5, 50.7, 44.4, 37.7, 29.7; **HRMS** calc. for $C_{19}H_{22}ONa$ $[M+Na]^+$: 289.1563, found: 289.1563; **IR** (cm^{-1}): 3408, 3025, 2922, 2856, 1711, 1600, 1493, 1450, 758, 696; physical and spectral data are in accordance with literature data.[4]

Minor diastereomer:

Colorless oil; **R_f** 0.26 (8:2 heptanes:EtOAc); **^{1}H-NMR** (300 MHz, CD_2Cl_2) δ 7.39 – 7.18 (m, 10H), 2.97 (s, 2H), 2.66 (tt, J = 11.3, 4.0 Hz, 1H), 1.98 – 1.48 (m, 10H); **^{13}C-NMR** (75 MHz, CD_2Cl_2) δ 147.1, 138.0, 131.1, 128.8, 128.6, 127.3, 126.8, 126.4, 71.8, 43.9, 43.3, 38.5, 31.6; **HRMS** calc. for $C_{19}H_{22}ONa$ $[M+Na]^+$: 289.1563, found: 289.1562; **IR** (cm^{-1}): 3429, 3025, 2926, 2857, 1601, 1493, 1449, 1080, 755, 696: physical and spectral data are in accordance with literature data.[4]

1-(2-Methylallyl)cyclohexan-1-ol (12)

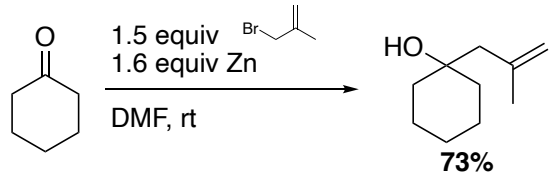

73%

To a solution of cyclohexanone (2.6 mL, 25 mmol) and 3-bromo-2-methylprop-1-ene (3.8 mL, 37.7 mmol, 1.5 equiv) in dry DMF (25 mL) were added small pieces of Zn metal (2.6 g, 40.2 mmol, 1.6 equiv) at rt. The temperature was carefully monitored with an internal thermometer and if the temperature exceeded 40 °C, it was cooled below 30 °C using an ice bath. After 30 min, the mixture was poured into sat. aq. NH_4Cl (100 mL). The mixture was extracted with Et_2O and the organic phase was washed

with brine, dried over Na_2SO_4, filtered and concentrated. After removal of all residual solvent (10 mbar, T_{bath} = 50 °C), distillation (10 mbar, T_{head} = 80 °C) afforded 1-(2-methylallyl)cyclohexan-1-ol (2.83 g, 73 %).

Colorless liquid; **R_f** 0.60 (8:2 heptanes:EtOAc); **^{1}H-NMR** (300 MHz, $CDCl_3$) δ 4.92 (dq, J = 2.9, 1.5 Hz, 1H), 4.74 (dq, J = 2.6, 0.9 Hz, 1H), 2.18 (d, J = 0.9 Hz, 2H), 1.83 (t, J = 1.2 Hz, 3H), 1.68 – 1.17 (m, 10H); **^{13}C-NMR** (75 MHz, $CDCl_3$) δ 142.8, 114.8, 71.2, 50.0, 38.0, 25.9, 25.5, 22.5; physical and spectral data are in accordance with literature data.[5]

1-((3*S*,8*S*,9*S*,10*R*,13*S*,14*S*,17*S*)-3-methoxy-10,13-dimethyl-2,3,4,7,8,9,10,11,12,13,14,15,16,17-tetradecahydro-1H-cyclopenta[a]phenanthren-17-yl)ethan-1-one (15)

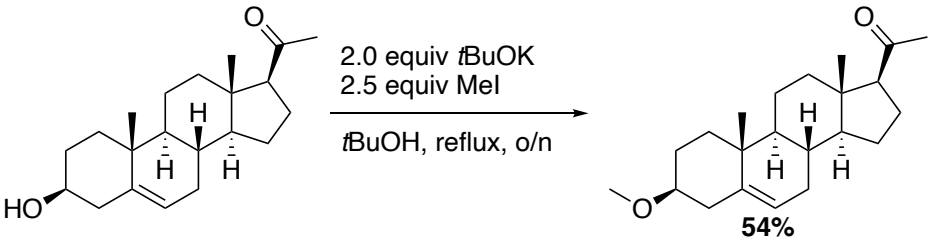

54%

To a sonicated solution of tBuOK (3.55 g, 31.6 mmol, 2.0 equiv) in *t*BuOH (55 mL) was added pregnenolone **14** (5 g, 15.8 mmol) and MeI (2.5 mL, 39.5 mmol, 2.5 equiv) at rt. The mixture was refluxed at 100 °C and after 1, 2, and 5 h, an additional portion of MeI (2.5 mL, 39.5 mmol, 2.5 equiv) was added. Then, the mixture was refluxed overnight, cooled down to rt, treated with water (50 mL), brine (50 mL) and extracted with CH_2Cl_2 (3 x 50 mL). The combined organic phase was washed with brine, dried over Na_2SO_4, filtered and concentrated. FC (8:2 heptanes:EtOAc) afforded **15** (2.8 g, 54%) in about 90% purity and contaminated only with unreacted pregnenolone.

White solid; **R_f** 0.47 (8:2 heptanes:EtOAc); **^{1}H-NMR** (300 MHz, $CDCl_3$) δ = 5.35 (ddt, J = 6.2, 4.0, 1.8 Hz, 1H), 3.35 (d, J = 2.3 Hz, 3H), 3.06 (tt, J = 11.3, 4.5 Hz, 1H), 2.53 (t, J = 8.8 Hz, 1H), 2.45 – 2.33 (m, 1H), 2.24 – 2.14 (m, 1H), 2.13 (d, J = 1.4 Hz, 3H), 2.09 – 1.04 (m, 16H), 1.00 (d, J = 4.4 Hz, 3H), 0.63 (s, 2H); **^{13}C-NMR** (75 MHz, $CDCl_3$) δ = 209.6, 141.0, 121.4, 80.3, 63.8, 57.0, 55.7, 50.2, 44.1, 39.0, 38.8, 37.3, 37.0, 32.0, 31.9, 31.6, 28.1, 24.6, 22.9, 21.2, 19.5, 13.3; physical and spectral data are in accordance with literature data.[6]

1-((3*S*,5S,8R,9S,10*S*,13*S*,14*S*,17*S*)-3-methoxy-10,13-dimethylhexadecahydro-1H-cyclopenta[a]phenanthren-17-yl)ethan-1-one (16)

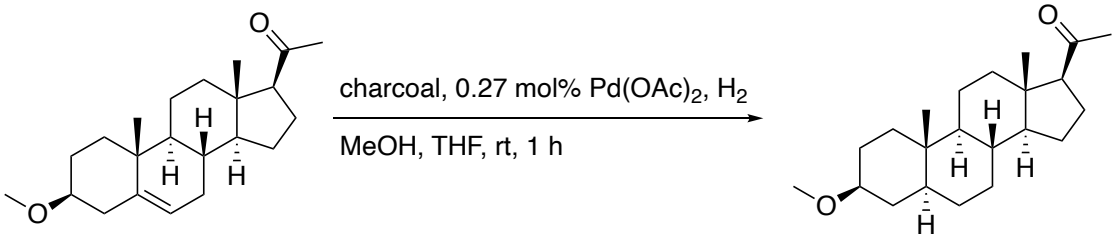

88%

To a solution of **15** (2.83 g, 8.56 mmol) in EtOH (100 mL) and hexanes (20 mL) was added Pd/C (5%, 0.5 g, 0.27 mol%) and stirred vigorously at rt. The flask was evacuated and back-filled with H_2 from a

balloon three times. With a mounted balloon of H_2, the mixture was stirred at rt for 1 h. The crude was filtered over celite, washed with ethanol and concentrated under reduced pressure. No further purification was needed to obtain the clean product **16** (2.5 g, 88%).

White solid; $\mathbf{R_f}$ 0.51 (85:15 heptanes:EtOAc); **^{1}H-NMR** (300 MHz, $CDCl_3$) δ = 3.31 (s, 3H), 3.10 (tt, J = 10.9, 4.7 Hz, 1H), 2.49 (t, J = 8.9 Hz, 1H), 2.21 – 2.08 (m, 1H), 2.08 (s, 3H), 2.04 – 1.92 (m, 1H), 1.92 – 1.80 (m, 1H), 1.77 – 1.50 (m, 6H), 1.44 – 0.81 (m, 13H), 0.77 (s, 3H), 0.71 – 0.59 (m, 1H), 0.59 (s, 3H); **^{13}C-NMR** (75 MHz, $CDCl_3$) δ = 209.7, 79.9, 63.9, 56.8, 55.6, 54.4, 44.9, 44.3, 39.2, 37.0, 35.9, 35.6, 34.4, 32.2, 31.6, 28.8, 28.0, 24.5, 22.9, 21.3, 13.6, 12.4; physical and spectral data are in accordance with literature data.[7]

2-((3*S*,5*S*,8*R*,9*S*,10*S*,13*S*,14*S*,17*S*)-3-methoxy-10,13-dimethylhexadecahydro-1H-cyclopenta[*a*]phenanthren-17-yl)propan-2-ol (17)

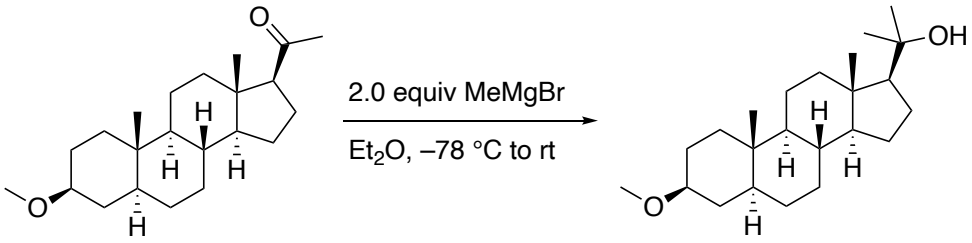

95%

To a solution of MeMgBr (3.0 M in Et_2O, 5 mL, 15 mmol, 2.0 equiv) in dry THF (35 mL) was added a solution of **16** (2.5 g, 7.5 mmol) in dry THF (10 mL) at –78 °C. The mixture was allowed to warm up to rt overnight, treated with water (20 mL) and sat. aq. NH_4Cl (20 mL) and Et_2O (20 mL). The mixture was extracted with Et_2O (3 x 50 mL), and the organic phase was washed with brine, dried over Na_2SO_4, filtered and concentrated. FC (85:15 heptanes:EtOAc) afforded **17** (2.5 g, 95%).

White solid; $\mathbf{R_f}$ 0.27 (85:15 heptanes:EtOAc); **mp** 149-151 °C; **^{1}H-NMR** (300 MHz, $CDCl_3$) δ = 3.33 (s, 3H), 3.11 (tt, J = 11.1, 4.7 Hz, 1H), 2.04 (dt, J = 12.3, 3.2 Hz, 1H), 1.94 – 1.79 (m, 1H), 1.67 (dddt, J = 20.3, 10.3, 8.2, 4.8 Hz, 6H), 1.54 – 0.84 (m, 22H), 0.80 (d, J = 5.7 Hz, 6H), 0.61 (ddd, J = 12.1, 10.5, 4.3 Hz, 1H); **^{13}C-NMR** (75 MHz, $CDCl_3$) δ = 79.9, 77.0, 73.5, 60.3, 56.6, 55.5, 54.4, 44.8, 43.0, 40.4, 36.9, 35.8, 34.9, 34.3, 32.0, 31.0, 30.0, 28.9, 27.9, 23.8, 23.1, 21.1, 13.7, 12.3; **elemental analysis** calc. for $C_{23}H_{40}O_2$: 79.25% C, 11.57% H, found: 79.00% C, 11.52% H; **IR** (cm^{-1}): 3481, 2926, 2845, 1445, 1376, 1361, 1172, 1089, 944, 930; **$[\alpha]_D^{25}$** = –3.4° (c = 1.0, $CHCl_3$)

(3*S*,5*S*,8*R*,9*S*,10*S*,13*S*,14*S*,17*S*)-17-(2-hydroperoxypropan-2-yl)-3-methoxy-10,13-dimethylhexadecahydro-1H-cyclopenta[*a*]phenanthrene (18)

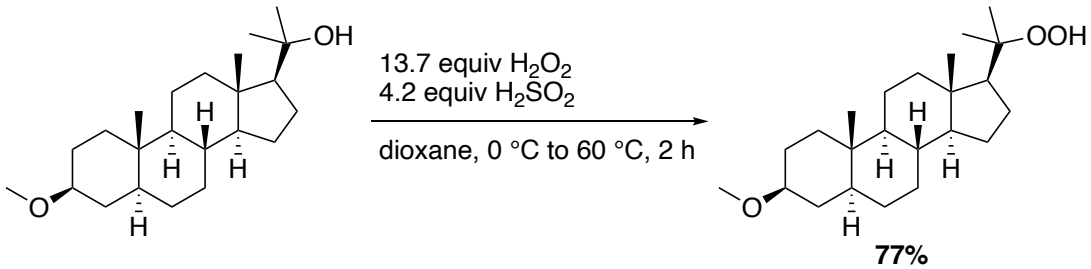

77%

A solution of sulfuric acid (0.47 mL, 8.4 mmol, 4.2 mmol) in water (0.33 mL) at 0 °C was added hydrogen peroxide (20%, 4.0 mL, 27.4 mmol, 13.7 equiv) was added cautiously. After complete addition, the ice bath was removed and a solution of **17** (700 mg, 2.0 mmol) in dioxane (5 mL) and THF (1 mL) was added dropwise. Then, the reaction was stirred at 60 ºC for 2 h, cooled down to rt and treated with water (10 mL). The mixture was extracted with EtOAc (3 x 20 mL), dried over Na_2SO_4, filtered and concentrated. FC (9:1 pentane:Et_2O) afforded **18** (560 mg, 77%).

White solid; **R_f** 0.34 (85:15 heptanes:EtOAc); **mp** 155-158 °C; **^{1}H-NMR** (300 MHz, $CDCl_3$) δ = 7.20 (s, 1H), 3.33 (s, 3H), 3.12 (tt, J = 11.0, 4.7 Hz, 1H), 2.02 (dt, J = 12.1, 2.9 Hz, 1H), 1.93 – 1.80 (m, 1H), 1.77 – 1.43 (m, 8H), 1.43 – 0.82 (m, 18H), 0.77 (d, J = 9.8 Hz, 6H), 0.60 (ddt, J = 11.8, 9.8, 4.7 Hz, 1H); **^{13}C-NMR** (75 MHz, $CDCl_3$) δ = 86.0, 80.1, 57.8, 56.6, 55.7, 54.5, 44.9, 43.0, 40.2, 37.1, 35.9, 35.2, 34.5, 32.1, 29.0, 28.0, 24.6, 24.2, 23.9, 23.4, 21.2, 14.4, 12.4; **elemental analysis** calc. for $C_{23}H_{40}O_3$: 75.78% C, 11.06% H, found: 77.23% C, 11.28% H; **IR** (cm^{-1}):3429, 3341, 2928, 2847, 1445, 1379, 1361, 1086, 929, 597; **$[\alpha]_D$** = –1.8° (c = 1.0, $CHCl_3$)

3-Phenylpropyl methanesulfonate (24)

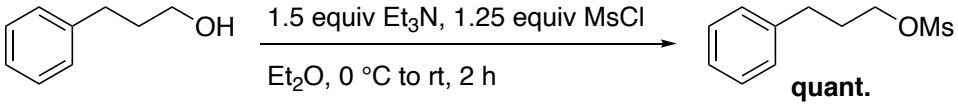

quant.

A solution of 3-phenylpropan-1-ol (13.6 mL, 100 mmol) and triethylamine (20.9 mL, 150 mmol, 1.5 equiv) in dry Et_2O (200 mL) was cooled to 0 °C and MsCl (9.7 mL, 125 mmol, 1.25 equiv) was added drop wise. After 10 min, the mixture was warmed up to rt and stirred for 2 h. Then, sat. aq. NH_4Cl and water were added and the phases were separated. The aqueous phase was extracted 3 x with Et_2O and the combined organic phase was dried over Na_2SO_4, filtered, and concentrated. No further purification was needed to yield clean 3-phenylpropyl methanesulfonate (21.4 g, quant.).

Yellow oil; **R_f** 0.18 (7:3 pentane:Et_2O); **^{1}H-NMR** (300 MHz, $CDCl_3$) δ 7.29 – 7.06 (m, 5H), 4.15 (t, J = 6.3 Hz, 2H), 2.91 (s, 3H), 2.68 (dd, J = 8.3, 6.8 Hz, 2H), 2.08 – 1.93 (m, 2H); **^{13}C-NMR** (75 MHz, $CDCl_3$) δ 140.4, 128.7, 128.6, 126.4, 69.3, 37.4, 31.6, 30.7; physical and spectral data are in accordance with literature data.[8]

(3-Hydroperoxypropyl)benzene (25)

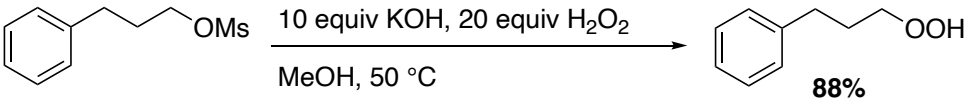

88%

To a stirred solution of aq. H_2O_2 (30%, 10.2 mL, 100 mmol, 20 equiv) was added aq. KOH (50 w%, 5.6 g, 50 mmol, 10 equiv) at 0 °C. After 5 min, a solution of 3-phenylpropyl methanesulfonate (1.07 g, 10 mmol) in MeOH (14 mL) was added and the mixture was stirred for 1 h at 50 °C. The mixture was stirred at 50°C for 1h, cooled down to rt, poured into brine, and extracted with Et_2O. The combined organic phase was dried over Na_2SO_4, filtered, and concentrated. MPLC (gradient from 95:5 to 75:25 pentane:Et_2O) afforded (3-hydroperoxypropyl)benzene (666 mg, 88%).

Colorless oil; **R_f** 0.45 (8:2 pentane:Et_2O); **^{1}H-NMR** (300 MHz, $CDCl_3$) δ 7.89 (s, 1H), 7.40 – 7.17 (m, 5H), 4.08 (t, J = 6.4 Hz, 2H), 2.74 (dd, J = 8.6, 6.8 Hz, 2H), 2.11 – 1.94 (m, 2H); **^{13}C-NMR** (75 MHz,

$CDCl_3$) δ 141.6, 129.0, 128.6, 126.1, 76.4, 32.2, 29.3; **HRMS** calc. for $C_9H_{12}O_2$ $[M]^+$: 152.08318, found: 152.08335; **IR** (cm^{-1}): 3369, 3026, 2945, 1603, 1496, 1454, 1367, 1029, 745, 698

4-Phenylbutyl methanesulfonate (27)

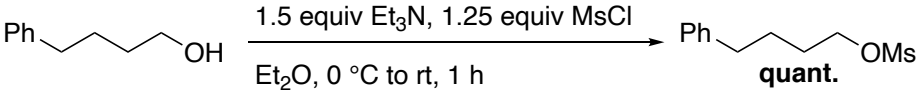

To a solution of 4-phenyl-1-butanol (3 mL, 20 mmol) and triethylamine (4.2 mL, 30 mmol, 1.5 equiv) in dry Et_2O (40 mL) was added MsCl (1.95 mL, 25 mmol, 1.25 equiv) drop wise at 0 °C. After 10 min, the mixture was warmed up to rt and stirred for 1 h. The mixture was treated with sat. aq. NH_4Cl, water, and the phases were separated. The aqueous phase was extracted with ether and the combined organic phase was dried over Na_2SO_4, filtered, and concentrated. No further purification was performed to obtain clean 4-phenylbutyl methanesulfonate (4.56 g, quant.).

Colorless oil; $\mathbf{R_f}$ 0.38 (6:4 pentane:Et_2O); **^{1}H-NMR** (300 MHz, $CDCl_3$) δ = 7.30 (ddt, J = 7.3, 6.3, 1.1 Hz, 2H), 7.26 – 7.13 (m, 3H), 4.29 – 4.18 (m, 2H), 2.98 (s, 3H), 2.67 (t, J = 7.0 Hz, 2H), 1.88 – 1.67 (m, 4H); **^{13}C-NMR** (75 MHz, $CDCl_3$) δ = 141.6, 128.5, 128.5, 126.0, 70.0, 37.3, 35.2, 28.7, 27.2; physical and spectral data are in accordance with literature data.[9]

(4-Hydroperoxybutyl)benzene (28)

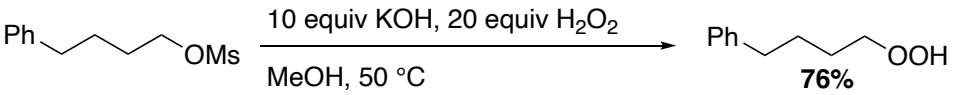

To a stirred solution of aq. H_2O_2 (30%, 28.6 mL, 280 mmol, 20 equiv) was added aq. KOH (50 w%, 15.7 g, 140 mmol, 10.0 equiv) at 0 °C. After 5 min, a solution of 3-phenylpropyl methanesulfonate (3.2 g, 14.0 mmol) in MeOH (40 mL) was added and the mixture was stirred for 1 h at 50 °C. The mixture was stirred at 50°C for 1h, cooled down to rt, poured into brine, and extracted with Et_2O. The combined organic phase was dried over Na_2SO_4, filtered, and concentrated. FC (9:1 pentane:Et_2O) afforded (4-hydroperoxybutyl)benzene (1.78 g, 73%).

Colorless oil; $\mathbf{R_f}$ 0.39 (9:1 pentane:Et_2O); **^{1}H-NMR** (300 MHz, $CDCl_3$) δ 7.81 (d, J = 1.7 Hz, 1H), 7.34 – 7.26 (m, 2H), 7.19 (ddt, J = 7.3, 3.2, 1.9 Hz, 3H), 4.10 – 3.99 (m, 2H), 2.66 (td, J = 7.4, 3.7 Hz, 2H), 1.70 (ddt, J = 6.1, 4.9, 2.9 Hz, 4H); **^{13}C-NMR** (75 MHz, $CDCl_3$) δ 142.2, 128.6, 128.5, 126.0, 77.1, 35.7, 27.8, 27.3; physical and spectral data are in accordance with literature data.[10]

Pentan-3-yl methanesulfonate (30)

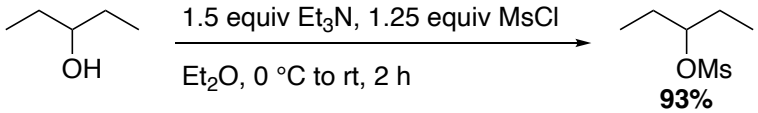

To a solution of pentan-3-ol (10.8 mL, 100 mmol) and triethylamine (20.1 mL, 150 mmol, 1.5 equiv) in dry Et_2O (200 mL) was added MsCl (9.7 mL, 125 mmol, 1.25 equiv) drop wise at 0 °C. After 10 min, the mixture was warmed up to rt and stirred for 2 h. The mixture was treated with sat. aq. NH_4Cl, water, and the phases were separated. The aqueous phase was extracted with ether and the combined

organic phase was dried over Na_2SO_4, filtered, and concentrated. No further purification was performed to obtain clean pentan-3-yl methanesulfonate (15.4 g, 93%).

Yellow oil; **R_f** 0.29 (9:1 pentane:Et_2O); **^{1}H-NMR** (300 MHz, $CDCl_3$) δ = 4.58 (p, J = 6.0 Hz, 1H), 2.98 (s, 3H), 1.75 – 1.66 (m, 4H), 0.96 (t, J = 7.5 Hz, 6H); **^{13}C-NMR** (75 MHz, $CDCl_3$) δ = 86.5, 38.7, 27.0, 9.4; physical and spectral data are in accordance with literature data.[11]

3-Hydroperoxypentane (31)

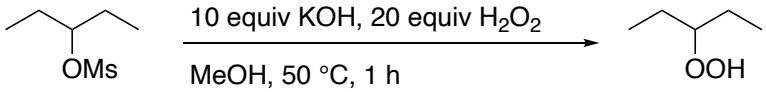

94%

To a stirred solution of aq. H_2O_2 (30%, 10.2 mL, 100 mmol, 20 equiv) was added aq. KOH (50 w%, 5.6 g, 50 mmol, 10.0 equiv) at 0 °C. After 5 min, a solution of pentan-3-yl methanesulfonate (830 mg, 5.0 mmol) in MeOH (14 mL) was added and the mixture was stirred for 1 h at 50 °C. The mixture was stirred at 50°C for 1 h, cooled down to rt, poured into brine, and extracted with Et_2O. The combined organic phase was dried over Na_2SO_4, filtered, and concentrated. FC (95:5 pentane:Et_2O) afforded 3-hydroperoxypentane (490 mg, 94%).

Colorless liquid; **R_f** 0.28 (95:5 pentane:Et_2O); **^{1}H-NMR** (300 MHz, $CDCl_3$) δ 7.62 (d, J = 10.0 Hz, 1H), 3.79 (p, J = 5.9 Hz, 1H), 1.73 – 1.45 (m, 5H), 0.93 (t, J = 7.5 Hz, 6H); **^{13}C-NMR** (75 MHz, $CDCl_3$) δ = 88.1, 24.3, 9.7; **HRMS** calc. for $C_5H_{12}O_2$ $[M]^+$: 104.08318, found: 104.08327; **IR** (cm^{-1}): 3371, 2966, 2938, 2880, 1462, 1382, 1348, 1132, 944, 863

2-Methyl-4-phenylbutan-2-ol (33)

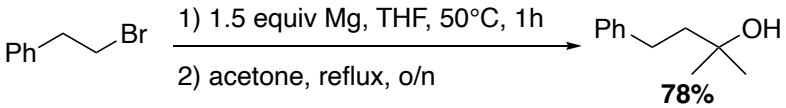

78%

2-phenyl ethylbromide (27.9 mL, 150 mmol) was slowly added to a suspension of Mg turnings (5.5 g, 225 mmol, 1.5 equiv) and one crystal of iodine in dry THF (85 mL) at 50 °C. Upon complete addition, the mixture was stirred for 1 h at 50 °C and then, anhydrous acetone (13.3 mL, 180 mmol, 1.2 equiv) was slowly added. The mixture was refluxed overnight, cooled down to rt, poured into sat. aq. $NaHCO_3$ (200 mL) and extracted with Et_2O. The organic phase was dried over Na_2SO_4, filtered and concentrated. Distillation (1 mbar, T_{head} = 95 °C) afforded 2-methyl-4-phenylbutan-2-ol (19.1 g, 78%).

Colorless oil; **R_f** 0.25 (8:2 heptanes:EtOAc); **^{1}H-NMR** (300 MHz, $CDCl_3$) δ = 7.45 – 7.23 (m, 5H), 2.87 – 2.76 (m, 2H), 1.96 – 1.84 (m, 2H), 1.40 (s, 6H); **^{13}C-NMR** (75 MHz, $CDCl_3$) δ = 142.7, 128.5, 128.4, 125.9, 71.0, 45.9, 30.9, 29.4; physical and spectral data are in accordance with literature data.[12]

(3-hydroperoxy-3-methylbutyl)benzene (34)

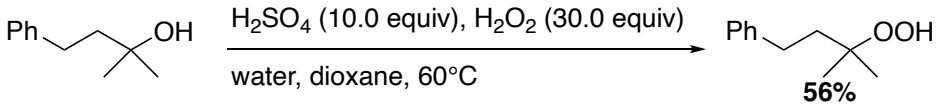

56%

A solution of sulfuric acid (2.3 mL, 42 mmol, 4.2 equiv) in water (2 mL) was cooled to –10 ºC, and of H_2O_2 (13.3 mL, 130 mmol, 13 equiv) was added cautiously. At rt, a solution of 2-methyl-4-phenyl-butan-

2-ol (1.67 g, 10 mmol) in dioxane (10 mL) was added dropwise to the mixture. Then, the reaction was stirred at 60 ºC for 1 h, cooled down and poured into sat. aq. $NaHCO_3$ (50 mL). The solution was extracted EtOAc, dried over Na_2SO_4, filtered and concentrated. FC (8:2 heptanes:EtOAc) afforded (3-hydroperoxy-3-methylbutyl)benzene (1.0 g, 56 %).

Colorless liquid; $\mathbf{R_f}$ 0.44 (8:2 heptanes:EtOAc); **^{1}H-NMR** (300 MHz, $CDCl_3$) δ = 7.50 – 7.44 (m, 1H), 7.37 – 7.19 (m, 5H), 2.81 – 2.66 (m, 2H), 2.00 – 1.88 (m, 2H), 1.34 (s, 6H); **^{13}C-NMR** (75 MHz, $CDCl_3$) δ = 142.6, 128.5, 128.4, 125.9, 82.7, 40.4, 30.4, 24.1; physical and spectral data are in accordance with literature data.[13]

The synthesis of compounds 36 and 37 has been described in the previous chapter (3).

4-Phenylbutanal (38)

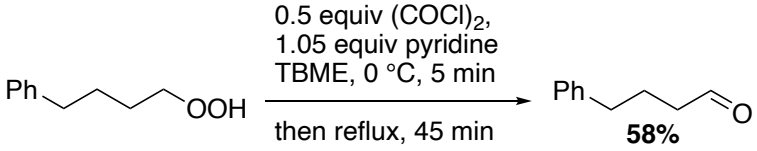

A dry flask was charged with TBME (5 mL), pyridine (85 µL), and (4-hydroperoxybutyl)benzene (152 mg). To the solution was added oxalyl chloride (42 µL) at 10 °C. After 5 min, the mixture was put in a preheated oil bath at 65 °C (reflux). After 45 min, the mixture was concentrated and loaded directly on column. FC (5.25 : 4 : 0.75 pentane:CH_2Cl_2:Et_2O) afforded 4-phenylbutanal (86 mg, 58%).

Colorless oil; $\mathbf{R_f}$ 0.68 (5.25 : 4 : 0.75 pentane:CH_2Cl_2:Et_2O); **^{1}H-NMR** (300 MHz, $CDCl_3$) δ 9.76 (t, J = 1.6 Hz, 1H), 7.26 (s, 2H), 7.24 – 7.14 (m, 3H), 2.66 (dd, J = 8.3, 6.8 Hz, 2H), 2.46 (td, J = 7.3, 1.6 Hz, 2H), 1.98 (dp, J = 8.8, 7.5 Hz, 2H); **^{13}C-NMR** (75 MHz, $CDCl_3$) δ 202.4, 141.4, 128.6, 128.5, 126.3, 43.3, 35.2, 23.8

This compound is also commercially available.

(2-Bromoethoxy)(tert-butyl)dimethylsilane (62)

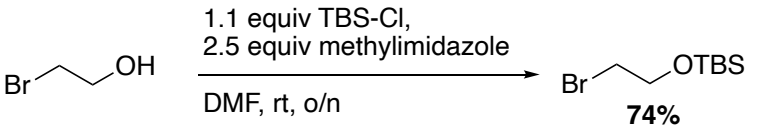

To a solution of TBS-Cl (8.3 g, 55 mmol, 1.1 equiv) and 2-bromoethanol (3.6 mL, 50 mmol) in dry DMF (50 mL) was added 1-methyl imidazole (10 mL, 125 mmol, 2.5 equiv) underneath surface. The mixture was stirred at rt overnight, treated with sat. aq. NH_4Cl and pentane. The phases were separated and the aqueous phase was extracted twice with pentane. The combined organic phase was washed twice with brine, dried over Na_2SO_4, filtered and concentrated. FC (95:5 pentane:Et2O) afforded (2-bromoethoxy)(tert-butyl)dimethylsilane (8.8 g, 74%).

Colorless oil; $\mathbf{R_f}$ 0.95 (8:2 pentane:Et_2O); **^{1}H-NMR** (300 MHz, $CDCl_3$) δ = 3.86 – 3.71 (m, 2H), 3.45 (t, J = 6.2 Hz, 1H), 3.31 (t, J = 6.5 Hz, 1H), 0.82 (s, 9H), 0.00 (s, 6H); **^{13}C-NMR** (75 MHz, $CDCl_3$) δ = 63.8, 63.7, 45.3, 33.4, 26.0, 18.5, -5.1, -5.2; physical and spectral data are in accordance with literature data.[14]

2-(2-((tert-butyldimethylsilyl)oxy)ethyl)cyclododecan-1-one (64)

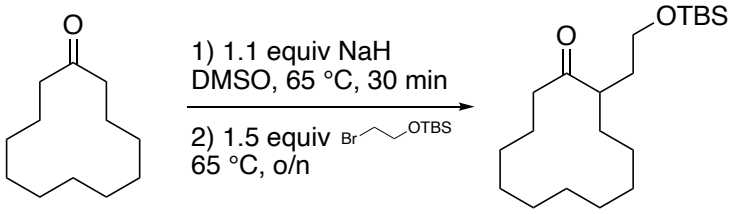

68%

To a suspension of NaH (90%, 280 mg, 1.1 equiv) in dry DMSO (20 mL) was added cyclododecanone **63** (1.8 g, 10.0 mmol) and stirred at rt for 30 min. Then, 2-bromoethoxy-tert-butyl-dimethyl-silane (3.6 g, 15 mmol, 1.5 equiv) was added and the mixture was stirred at 65 °C overnight. Then, water and pentane were added, the aqueous phase was extracted with pentane, and the combined organic phase was dried over Na_2SO_4, filtered, and concentrated.

FC (98:2 heptanes:EtOAc in heptanes) afforded 2-(2-((tert-butyldimethylsilyl)oxy)ethyl)cyclododecan-1-one (2.3 g, 68%).

Colorless oil; $\mathbf{R_f}$ 0.66 (95:5 pentane:Et_2O); **^{1}H-NMR** (300 MHz, $CDCl_3$) δ = 3.65 – 3.48 (m, 2H), 2.72 (dddt, J = 27.0, 16.8, 8.2, 3.9 Hz, 2H), 2.35 (ddd, J = 16.7, 8.3, 3.9 Hz, 1H), 1.98 – 1.81 (m, 1H), 1.66 (ttd, J = 17.6, 7.8, 6.9, 2.8 Hz, 4H), 1.56 (d, J = 5.7 Hz, 1H), 1.38 – 1.11 (m, 16H), 0.87 (s, 11H), 0.02 (s, 6H); **^{13}C-NMR** (75 MHz, $CDCl_3$) δ = 214.6, 61.3, 48.3, 37.6, 34.2, 29.8, 26.2, 26.1, 25.8, 24.2, 24.0, 23.7, 22.6, 22.4, 22.1, -5.3; **HRMS** calc. for $C_{20}H_{41}O_2Si$ $[M+H]^+$: 341.2870, found: 341.2860; **IR** (cm^{-1}): 2927, 2856, 1706, 1470, 1361, 1251, 1094, 833, 773, 728

2,3,4,5,6,7,8,9,10,11,12,13-dodecahydrocyclododeca[*b*]furan (65)

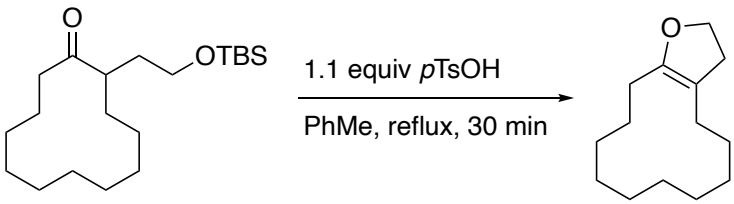

67%

To a solution of 2-(2-((tert-butyldimethylsilyl)oxy)ethyl)cyclododecan-1-one (3.41 g, 10 mmol) in dry toluene (100 mL) was added *p*TsOH monohydrate (2.0 g, 10.5 mmol, 1.05 equiv) and the mixture was heated to reflux for 30 min. Then, the mixture was cooled down to rt, treated with $NaHCO_3$ and extracted with heptanes. The organic phase was dried over Na_2SO_4 filtered and concentrated. FC (98:2 heptanes:EtOAc) afforded 2,3,4,5,6,7,8,9,10,11,12,13-dodecahydrocyclododeca[*b*]furan (1.4 g, 67%).

White solid; $\mathbf{R_f}$ 0.72 (95:5 pentane:Et_2O); **^{1}H-NMR** (300 MHz, $CDCl_3$) δ = 4.15 (t, J = 9.3 Hz, 2H), 2.49 (tt, J = 9.2, 1.3 Hz, 2H), 2.20 – 2.06 (m, 4H), 1.60 – 1.41 (m, 4H), 1.40 – 1.12 (m, 15H); **^{13}C-NMR** (75 MHz, $CDCl_3$) δ = 151.2, 107.7, 68.0, 33.1, 25.8, 25.1, 25.0, 25.0, 24.7, 24.5, 23.4, 22.8, 22.5, 22.4; **HRMS** calc. for $C_{14}H_{25}O$ $[M+H]^+$: 209.1900, found: 209.1894; **IR** (cm^{-1}): 2926, 2851, 1706, 1690, 1467, 1443, 1206, 999, 835, 737

13a-hydroperoxytetradecahydrocyclododeca[*b*]furan (66)

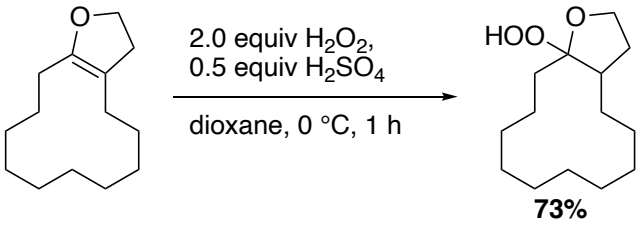

73%

A stock solution on a 10 mmol scale was prepared first:
To H_2O_2 (21%, 3.1 mL, 20 mmol, 2.0 equiv) was added sulfuric acid (510 mg, 5 mmol, 0.5 equiv) and dioxane (3.0 mL) which afforded 6.4 mL of stock solution.

To the stock solution (0.83 mL) was added a solution of 2,3,4,5,6,7,8,9,10,11,12,13-dodeca hydrocyclododeca[*b*]furan (300 mg, 1.3 mmol) in dioxane (6.5 mL) at 0 °C. After 1 h, the mixture was treated with sat. aq. $NaHCO_3$. The solution was extracted with Et_2O, and the organic phase was dried over Na_2SO_4, filtered and concentrated. MPLC (gradient from 1:9 to 3:7 Et_2O:pentane) afforded 13a-hydroperoxytetradecahydrocyclododeca[*b*]furan (230 mg, 73%).
White solid; **R_f** 0.72 (95:5 pentane:Et_2O); **mp** 100-103 °C; **^{1}H-NMR** (300 MHz, $CDCl_3$) δ = 8.46 – 7.41 (m, 1H), 4.11 (td, J = 8.8, 2.4 Hz, 1H), 3.94 – 3.80 (m, 1H), 2.30 (qd, J = 13.5, 12.5, 9.6 Hz, 1H), 2.16 – 1.99 (m, 2H), 1.91 – 1.58 (m, 3H), 1.36 (tdt, J = 20.7, 10.8, 4.1 Hz, 19H); **^{13}C-NMR** (75 MHz, $CDCl_3$) δ = 115.1, 68.2, 40.1, 30.6, 27.5, 26.2, 26.1, 25.1, 24.3, 22.4, 22.2, 22.1, 21.8, 19.6; **HRMS** calc. for $C_{14}H_{25}O_3$ $[M–H]^+$: 241.1809, found: 241.1808; **elemental analysis** calc. for $C_{14}H_{26}O_3$: 69.38% C, 10.81% H, found: 69.54% C, 10.89% H; **IR** (cm^{-1}): 3280, 2922, 2901, 2846, 1471, 1444, 1120, 1013, 962, 652

References

[1] Y. Matsuya, S. Masuda, N. Ohsawa, S. Adam, T. Tschamber, J. Eustache, K. Kamoshita, Y. Sukenaga, H. Nemoto, *European Journal of Organic Chemistry* **2005**, *2005*, 803–808.

[2] A. B. Edsall, A. K. Mohanakrishnan, D. Yang, P. E. Fanwick, E. Hamel, A. D. Hanson, G. E. Agoston, M. Cushman, *J. Med. Chem.* **2004**, *47*, 5126–5139.

[3] G. L. Lackner, K. W. Quasdorf, L. E. Overman, *J. Am. Chem. Soc.* **2013**, *135*, 15342–15345.

[4] C.-C. Li, X.-J. Dai, H. Wang, D. Zhu, J. Gao, C.-J. Li, *Org. Lett.* **2018**, *20*, 3801–3805.

[5] T. Shono, M. Ishifune, S. Kashimura, *Chem. Lett.* **1990**, *19*, 449–452.

[6] W. Xie, H. Peng, D.-I. Kim, M. Kunkel, G. Powis, L. H. Zalkow, *Bioorganic & Medicinal Chemistry* **2001**, *9*, 1073–1083.

[7] J. Hora, *Collect. Czech. Chem. Commun.* **1966**, *31*, 2737–2744.

[8] S. Albrecht, A. Defoin, C. Tarnus, *Synthesis* **2006**, *2006*, 1635–1638.

[9] L. A. S. Romeiro, M. da Silva Ferreira, L. L. da Silva, H. C. Castro, A. L. P. Miranda, C. L. M. Silva, F. Noël, J. B. Nascimento, C. V. Araújo, E. Tibiriçá, E. J. Barreiro, C. A. M. Fraga, *European Journal of Medicinal Chemistry* **2011**, *46*, 3000–3012.

[10] R. Kundu, Z. T. Ball, *Org. Lett.* **2010**, *12*, 2460–2463.

[11] U. Zutter, H. Iding, P. Spurr, B. Wirz, *J. Org. Chem.* **2008**, *73*, 4895–4902.

[12] T. Iwasaki, K. Agura, Y. Maegawa, Y. Hayashi, T. Ohshima, K. Mashima, *Chemistry – A European Journal* **2010**, *16*, 11567–11571.

[13] H. Kropf, H. V. Wallis, *Synthesis* **1981**, *1981*, 237–240.

[14] B. A. Messerle, K. Q. Vuong, *Organometallics* **2007**, *26*, 3031–3040.

Chapter 5

Continuous Flow Synthesis of Diacyl Peroxides

5 Continuous Flow Synthesis of Diacyl Peroxides

Enabling technologies have changed the chemical science in the last decades and will have a great impact to chemistry in the future. The ever-increasing performance of computers has opened the doors for many tasks to be taken over by machines and optimized computationally:

- **Computer-assisted retrosynthesis**: The rational design of synthetic pathways to obtain the target molecule is one of the central skills of organic chemists which is gained during year-long training and experience in the laboratory. Prof. E. J. Corey formalized the concept of retrosynthetic analysis and was awarded the Nobel prize in 1990.[1] In the last decade, particularly Bartosz Grzybowski and co-workers have revolutionized this field with their retrosynthesis software *Chematica*, which was later purchased by Merck and made commercially available as *Synthia TM*. Within minutes, the software is able to predict synthetic plans that are able to outperform the reported routes by experienced chemists.[2–4]
- **Combinatorial and parallel synthesis**: Automated purification and rapid product analysis is now a fundamental technology to generate and evaluate massive databases, *e.g.* in the pharmaceutical industry, which would never be possible to this extent when manually performed by chemists.[5]
- **Online reaction monitoring:** New devices that allow close and real time monitoring the proceeding of a chemical reaction (e.g., by IR, NMR, UV, VIS, Raman, refraction index, etc.) and the evolution of reaction products (and intermediates). They have helped greatly to understand chemical reactions in detail and are of outmost importance to the industry, especially on large scale, to ensure a safe and reliable production of large quantities of material.
- **Machine learning**: Artificial intelligence, especially the ability of algorithms to recognize patterns in large amount of data, is a powerful method to optimize synthetic protocols.[6] Automated experimentation, online reaction monitoring, and statistical analysis such as design of experiments (DoE) are indispensable today in industrial processes for the optimization of reaction conditions to ensure a maximum of purity and quantity of the target products.

In addition to classical batch chemistry, another enabling technology provides access to exotic reaction conditions, short reaction times and safe scalability:

- **Continuous flow synthesis**. The reagents are mixed continuously in a system of tubes, which means that only a small amount of chemicals react at a time. Due to the small size, the reaction takes place at the point of mixing, and external reaction conditions can be controlled very closely. As the apparatus is built from standardized parts, the setup is easily modified and customized. Advantageously, this flow synthesis is highly automatable and can be combined with the above technologies.

In an extreme case, an almost unsupervised and fully automated optimization of synthetic methods becomes possible when all technologies are combined together.[7]

5.1 An introduction to synthesis in continuous flow

Our group has purchased an apparatus to perform continuous flow synthesis only recently and therefore, commissioning of the apparatus, customization of the machine's setup, and acquiring of the specific knowledge about continuous flow synthesis had to be done prior to run chemical reactions. This subchapter provides a general introduction to the used setup before the principles of flow chemistry are explained briefly based on recently published comprehensive reviews.[8–11]

5.1.1 Microreactor technology

Microreactor technology provides unique control over reaction conditions and has attracted increasing attention, particularly in the new millennium. In flow chemistry, chemical reactions are run not batchwise in flasks with stirring for a certain time. They are performed using an apparatus in which the reaction solution is pumped under pressure through one or multiple external reactors with collection of the final solution at the end of the process. A schematic overview (Figure 5.1) and the apparatus from VAPOURTEC® (Figure 5.2) that has been used in this study are given below.

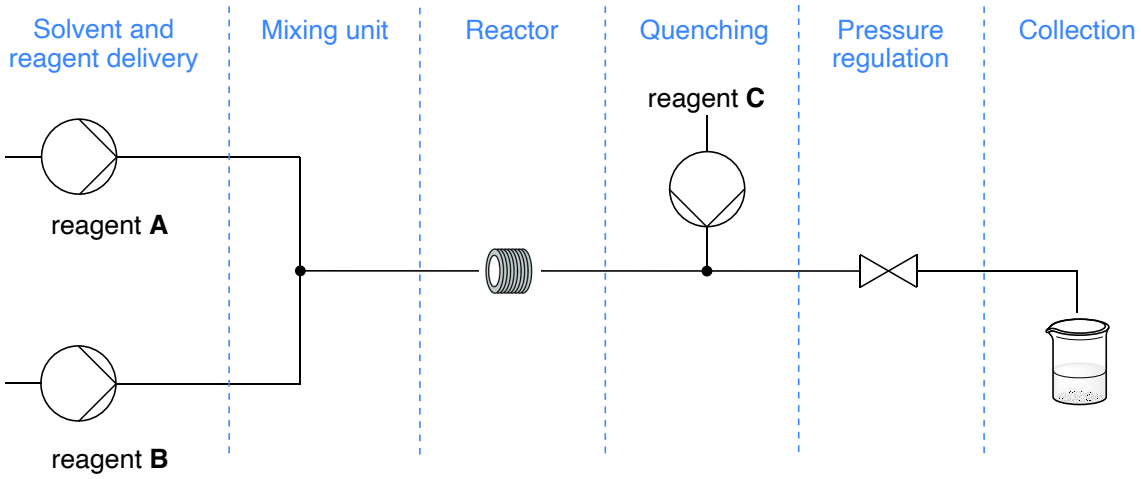

Figure 5.1. Schematic example of a two-feed continuous flow setup with a quenching feed

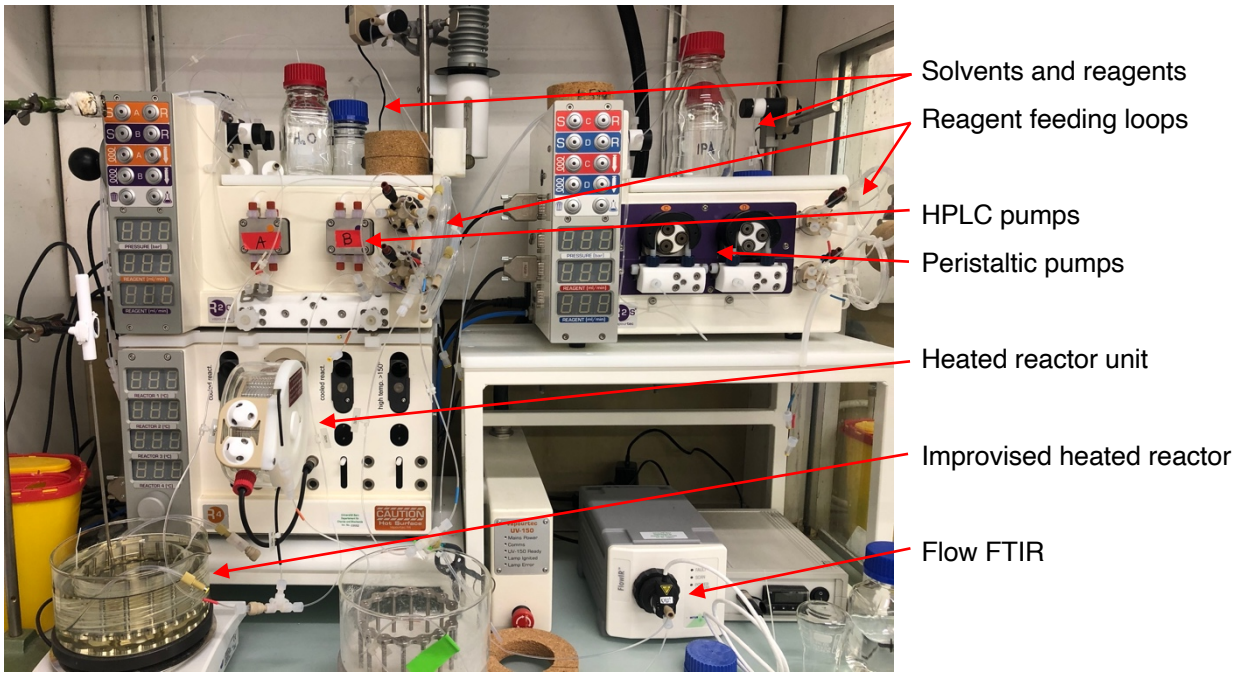

Figure 5.2. Representative setting of the used VAPOURTEC flow chemistry apparatus

5.1.1.1 Tubing

Due to the reactivity of certain chemicals, the tubing has to be made out of inert material. Polyfluorinated polymers such as FEP (fluorinated ethylene propylene) are preferred materials for tubing since classical Teflon® (polytetrafluorethylene) is difficult to manufacture. Nuts are usually made out of ETFE (ethylene-tetrafluoroethylene-copolymer) as it shows excellent mechanical and chemical stability. The fittings do not come to contact with the chemicals and therefore, highly resistant materials such as PCTFE (polychlorotrifluoroethylene) are only used when contamination during setup or disassembling is a problem. Usually, PEEK (polyether ether ketone) fittings are used (Figure 5.3).

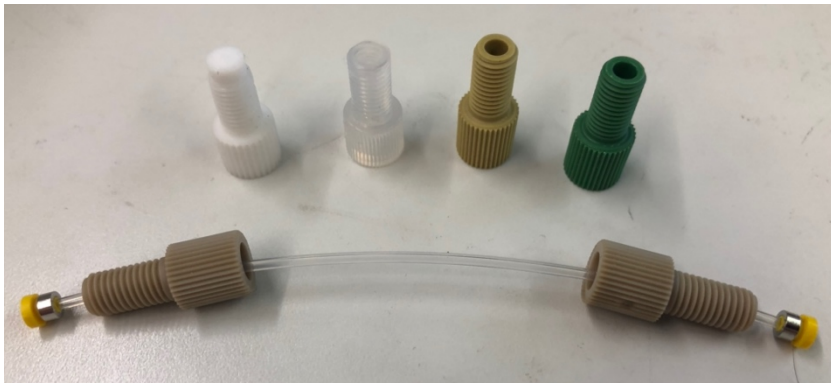

Figure 5.3. Back: Teflon® stopper (white), PCTFE (transparent) and PEEK (brown, green) fittings; front: assembly of FEP tubing with flangeless ETFE nuts (yellow) and PEEK fitting (beige)

5.1.1.2 Solvent and reagent delivery

In the VAPOURTEC® system, the separated reagent solutions are pumped to the point of mixing using either HPLC pumps or peristaltic pumps. HPLC pumps have the advantage of higher pressures (up to 20 bars) but are susceptible to pressure fluctuations and the presence of gases which leads to an automatic safety shutdown of the pumps. They are able to accurately deliver liquids from rather small to large amounts per time (0.25 – 5.0 ml/min). Highly corrosive chemicals are not compatible with HPLC pumps as they would interact with the metal alloy of the pump head.

Peristaltic pumps operate at slightly lower pressures (up to 10 bars) and can pump suspensions as well as gas bubbles at pump rates of 0.25-10 ml/min. However, the peristaltic pumps do induce a higher pressure fluctuation compared to HPLC pumps. In the most basic setup, syringe pumps can also be considered as pumping modules but lack the possibility to switch from solvent to reagent during conditioning and flushing of the reactor, *i.e.*, the dead volume is not negligible for small scale reactions. Additionally, syringe pumps are limited by the size of the syringe and literally cannot operate continuously.

Solvent and reagent solutions are usually connected to the same pump and a manifold to enable switching between two containers from where the liquid is sucked in. During conditioning of the apparatus and after complete injection of the reagent solution, solvent is constantly pumped through the apparatus. For medium to large volumes (> 10 mL), the reagent is placed in a bottle connected to a T-shape manifold that is connected to the pump. For smaller quantities (< 10 mL in our case) and sensitive reagents, the solution can be loaded to a reagent loop that is connected to a 6-port manifold which is installed after the pump. The reagent is then pushed out of the loop by the pumped solvent. Advantageously, the reagent does never come to contact with the pumping module.

Figure 5.4. ***Left****: bottled reagent and solvent connected to a T-shaped manifold;* ***middle****: 6-port manifold with 2 mL feeding loop;* ***right****: 6-port manifold with adjustable 10 mL feeding loop*

5.1.1.3 Mixing units[9]

Once the reagents are pumped to the reactor, the two liquids have to be rapidly and efficiently mixed so that a chemical reaction of the reagents can occur.

Passive mixing relies exclusively on diffusion or chaotic advection – the T-piece represents probably the simplest mixing unit. Since laminar flow is predominant in microfluidic devices a relatively long distance is passed until diffusion-controlled mixing would be complete. Sophisticated geometries of the mixing unit effect an increase in turbulent behavior or chaotic advection and thus shorten the distance until mixing is complete.

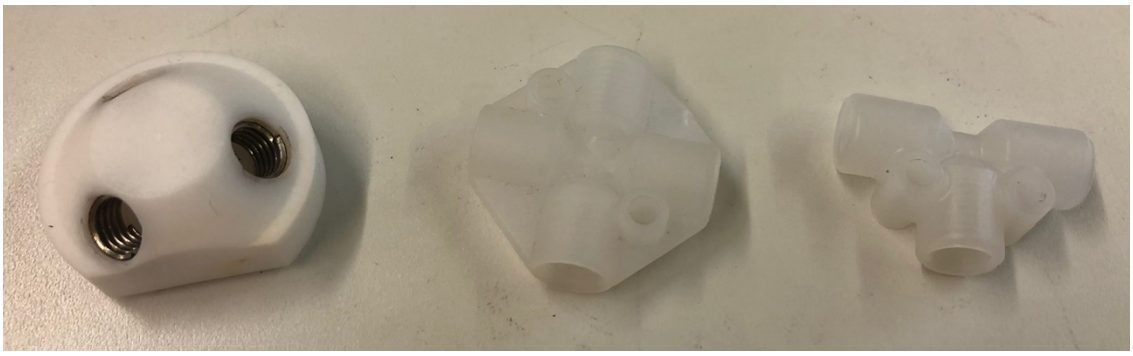

Figure 5.5. From left to right: Y-, cross- and T-shaped mixing units.

Active mixers require external energy and disturb the liquid inside the reactor. This can be achieved through serial segmentation, alternating pressure (*e.g.*, pulsing), application of magnetic or electric fields, vibration (e.g., ultrasound), or integrated microstirrers. A special case of mixing unit is represented by the gas-liquid reactor in which pressurized gas diffuses through a semipermeable membrane into the solution inside the reactor unit.

5.1.1.4 Reactors

The reaction takes place in a reactor in which the external conditions are set. Heating and cooling (–70 °C to 250 °C in our case) can be very well controlled since the heat transfer takes place almost immediately. Irradiation as well as electrochemical processes using an external electrical field can also be performed. Solid reagents can be used in packed-, fluidized-, and mixed-bed reactors where the solubilized reagents are pumped through a column containing a solid reagent. In all the cases, the high volume to surface ratio is key for a rapid transfer of heat and light. Once the optimal conditions are found, scale-up is relatively easy by increasing the amount of substrate pumped through the apparatus over a longer time using the same settings.

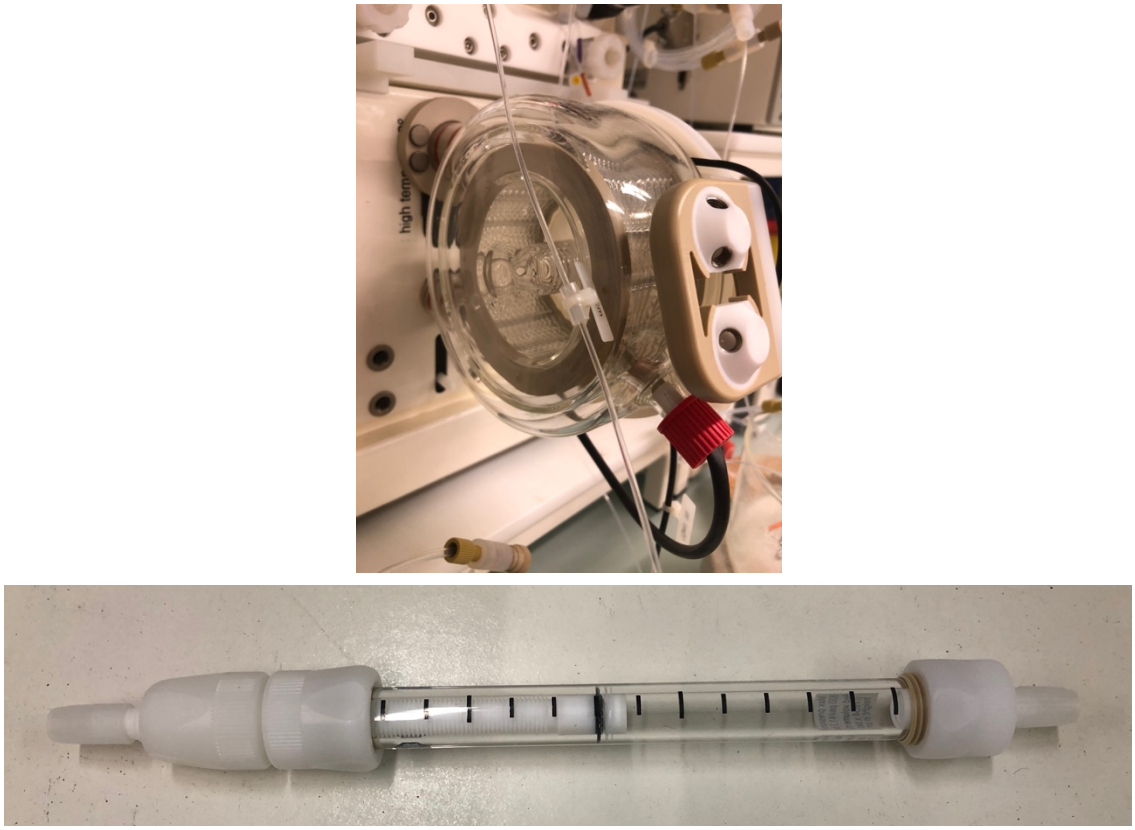

Figure 5.6. VAPOURTEC® tubular heated reactor unit with a 10 mL volume (top) and OMNIFIT® fixed-bed reactor unit (bottom)

5.1.1.5 Pressure and flow regulation

Back pressure regulators (BPR)

BPRs are special valves that can be passed by the liquid in only one direction. They exercise a constant pressure against the direction of the flow and the valve is only opened above a certain pressure limit. Therefore, the section between the pumping module and the BPR remains under constant pressure. Serial installation of BPRs leads to an overall increase of the pressure according to classical mechanics. For example, the pressure of the system is at 10 bar, if two BPR of 5 bar are consecutively installed. BPR are available as preset cartridges with a fixed-pressure or as manually adjustable units.

Check valves

In the presence of pressure fluctuations caused by the pumping modules or differences in pumped volumes, a reversion in flow-direction can occur. Check-valves ensure a unidirectional flow of the liquids at a minimum of back pressure (the cracking pressure is usually below 0.2 bar). They can be inserted at any position in the apparatus.

Figure 5.7. Top: adjustable back pressure regulator (left) and in-line check valves; Bottom: BPR assembly with preset back pressure cartridge

5.1.1.6 Quenching, collection, and additional equipment

Quenching

If required, a quench solution can be fed to the flow path after a previous reactor unit. If necessary, a subsequent reactor unit to facilitate the quench can be installed. It is recommended, that the quench is fed into the pressurized part of the apparatus to control flow, pressure and temperature of the quenching. Quenching in the non-pressurized part of the apparatus can lead to uncontrolled evolution of gas or boiling of the solvent which makes control of flow speed and temperature very difficult.

Phase separator

The most common technique of in-line purification is liquid-liquid separation. A semipermeable membrane can be used to separate aqueous from organic phase letting either the organic or the aqueous phase pass through the membrane. For example, such a device can separate an aqueous quenching solution from the solvent containing the desired product before collection which simplifies workup and purification. Careful control of the back pressure over the membranes as well as the right choice of the properties of the membranes are key for a successful separation of the two phases.

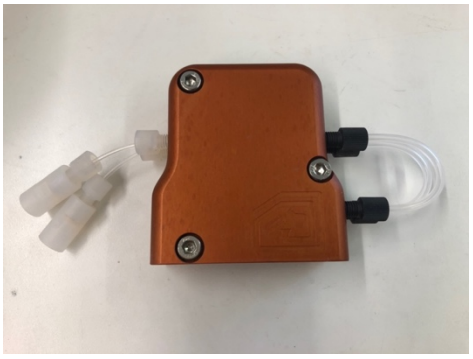

Figure 5.8. SEP-10 phase separator from ZAIPUT Flow Technologies®

In-line reaction monitoring

Analysis of the collected solution after it passed the entire setup is one option to monitor the proceeding of the process but has the disadvantage that there is always a delay between the collection of the sample and the result of the analysis. Moreover, reactive intermediates are not easily monitored offline. Using flow-through analysis cells for FTIR, NMR, etc., the reaction can be analyzed live and without the need of sample preparation which is beneficial for extensive optimization of reaction conditions.

Collection

Standard collection equipment consists of a manifold which is able to switch between a waste and a collection line either programmed to proceed automatically or operated manually. The time of operation is accurately calculated by the flow chemistry software. Alternatively, a fraction collector similar to a preparative HPLC or MPLC can be used when multiple runs of the same reaction but with various conditions is performed.

Additive manufacturing

In the last ten years, 3D printing has enabled relatively easy and quick access to custom-designed reactors and other laboratory hardware. With respect to the limitations given by the availability of substrate material, chemical compatibility, and resolution of the printer, a multitude of predesigned equipment is openly available online that can be further adapted according to the specific need (reactors, fittings, channels, chips, mixers, etc.) with relatively intuitive CAD (computer assisted design) software.[12]

5.1.2 Parameters of a flow process

Due to the many factors influencing a chemical process in continuous flow, optimization of reaction conditions quickly becomes complex. Statistical multi-parameter optimization using DoE (using programs like MODDE® by Sartorius) is key when a reaction needs to be screened and optimized in great detail involving a combination of quantitative (solvent, reactor geometry, catalyst, reagent, mixing technique, etc.) and qualitative (residence time, pressure, flow speed, concentration, temperature, etc.) parameters.[13] Monitoring of a defined output parameter (e.g. isolated yield, GC-yield, peak area in in-line analysis, etc.) at high precision and consistency is of central importance since DoE requires a large amount of experiments to be performed which makes it almost impossible to perform uniform product purification for every single entry. The automated processes in flow are ideal for DoE optimization since the system reproducibility and reliability is primarily dependent on the machine and less on the operator.

5.1.2.1 Residence time

Since a chemical reaction is started continuously at the point of mixing or upon initiation of the reaction inside a reactor, the concentration of the reagents does not decrease over the time of the entire process but over the time a certain segment of the liquid passes through a given distance of the tubing.

Therefore, time indications are not given for the entire process as it is the case for batch processes but are indicated as residence time, i.e., the time the reagents spend inside a specific section of the tubing. The residence time is defined as:

$$t_{res} = \frac{V}{v}$$

t_{res} = residence time; V = volume of the section of interest; v = flow speed

This means, the time for a chemical reaction to take place can be influenced by changing the volume of the reactor or by changing the speed, with which reagents are pumped through the reactor unit.

5.1.2.2 Flow profile

In an ideal case, a sample would enter and exit the tube at sharply defined times and thus, the sample can be pictured as a plug that is flowing through the tube. However, friction on the wall induces convection and leads to a parabolic velocity profile of the plug (Figure 5.9, top). Diffusion contributes as well to broadening of the sample. Consequently, the plugs get dispersed which leads to the sample exiting the tube as a (gaussian) distributed peak with a period of increasing concentration at the beginning (fronting) and decreasing concentration at the end of the sample (tailing).

If the sample is not a small droplet, the front an end part of the sample remains distributed, but the main fraction of the sample behaves like a large plug and therefore has a constant concentration, which is called the steady-state (Figure 5.9, bottom).

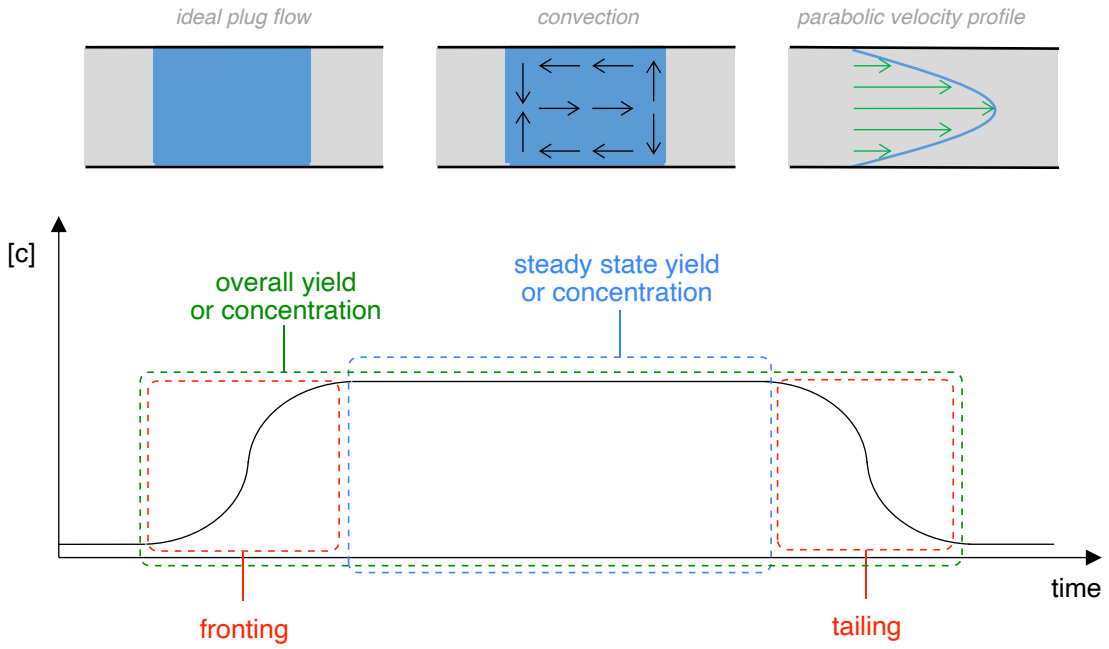

Figure 5.9. Schematic representation of plug flow, a parabolic laminar flow profile, and development of product concentration over the course of a reaction

If one changes only the size of the sample, the area of fronting and tailing remains constant and thus, only the steady-state area is increased or decreased. The area, and thus the amount of product, in the fronting and tailing is constant for a given reactor setup (Figure 5.10, red square). Consequently, the percentage of fronting and tailing decreases with increasing scale and on large scale, the overall yield (or concentration) is approximately the same as the steady state values.

Figure 5.10. Comparison of product distribution of a small- (top) and a large-scale reaction (bottom) using the same settings of the apparatus. The red square indicates the same area of fronting.

For very small-scale reactions, it is difficult to obtain a steady-state concentration of the product since all the material may be present in the fronting and tailing part of the plug. However, in a large-scale chemical reaction, the percentage of fronting and tailing is relatively small.
Consequently, one has to be precise when indicating the yield or concentration of a sample:

Yield:
If the *entire* product is collected from the earliest to the latest moment it is exiting the apparatus and isolated, the yield is termed as the overall yield of a reaction. If only the area is collected where the product is present in steady state, the yield will be *lower* than the overall yield since product in the fronting and tailing are is discarded.

Concentration:
If one determines the *concentration* of the product in the overall collected liquid, it is diluted by the excess solvent in the fronting and tailing area and thus results in a *lower* concentration than in the steady state area.

It is therefore important to decide prior to optimizing a reaction, if it will be optimized based on the yield (or product concentration) in the steady state or based on the overall yield or concentration of the product collected after every run. It is mostly more convenient to determine the values in the steady state of a process, since one does not have to wait for the run to be completed.

5.1.2.3 Viscosity and the Reynolds number

The viscosity of a liquid measures its resistance to deformation at a given rate at a given temperature. “Mobile” liquids (e.g., pentane, hot water, ethanol, etc.) have low viscosity values whereas “thick” liquids (e.g., oil, syrup, honey, ethylene glycol, paraffin oil etc,) are highly viscous.

The dimensionless Reynolds number is a useful value in fluid dynamics, describes the behavior, and is used to predict the flow pattern of a fluid.[14] For fluids passing through a cylindrical tube, it is defined as

$$Re = \frac{2 * r * v * \rho}{\eta}$$

Re = Reynolds number; r = radius of the tube; v = average flow speed;
ρ = density of fluid; η = viscosity

Reynolds numbers above ca. 2000-2300 indicate turbulent flow which would be beneficial for efficient mixing. However, for most microfluid applications, only low Reynolds numbers are achieved and thus, laminar flow is predominant. For example, the Reynolds numbers of water (ρ = 1000 g/cm³; η = 1.0 mPa*s) that is pumped at constant speed (Q = 1 mL/min) through a straight section of a tube (1 mm diameter) at 20 °C is calculated as follows:

$$v = \frac{Q}{q} = \frac{1 * 10^{-6}\, {m^3}/{min}}{(0.0005\ m)^2 * \pi} = 1.27\, {m}/{min} \quad ; q = cross\ section\ of\ the\ tube$$

$$Re_{H_2O} = \frac{2 * 0.0005\ m * 1000\, {kg}/{m^3} * 1{,}27\, {m}/{s}}{1 * 10^{-3}\ Pa * s} = 1270$$

Consequently, efficient mixing is not expected to take place in the tube at low Reynolds numbers and if one relies entirely on mixing by diffusion, the length of the tube to achieve mixing has to be sufficiently long. If mixing by diffusion is not sufficient, mixing units are built in the flow path which consist of complex geometries (obstacles on the wall or in the channel, zig-zag shapes, twisted channels, Tesla structures, etc.) in order to force the fluid to change its direction rapidly and often, which results in turbulent flow inside the mixing unit.[9,15]

For less viscous liquids, the Reynolds number may be significantly different. If diethyl ether (ρ = 0.713 g/cm³; η = 0.224 mPa*s) is pumped using the same machine settings, the Reynolds number is:

$$Re_{diethyl\ ether} = \frac{2 * 0.0005\ m * 713\, {kg}/{m^3} * 1{,}27\, {m}/{s}}{2.24 * 10^{-4}\ Pa * s} = 4042$$

and therefore, turbulent flow is expected to be present inside the tube, resulting in efficient mixing without special mixing units. A rough estimation of the Reynolds number gives a good indication, how

well mixing may take place in the chosen setup. In special cases (e.g., biphasic mixtures), it may still be beneficial to put an active mixing unit to ensure proper mixing of the reagents to shorten the length of tubing for the mixing process.

5.1.3 Characteristics of flow synthesis

Mass and heat transfer

The fundamental difference between batch and flow processes are found in the transfer of heat and mixing. Flow technology is often advantageous for processes that rely on heat or mass transport because mixing (if the right mixing technique is used) and heat transport is almost instantaneous due to the immense surface/volume ratio. Since reaction times can be decreased by orders of magnitudes due to fast heat and mass transport, the overall time of the process is reduced as well which consequently reduces the cost which is an important parameter for both academia and industry.[16] Automated systems also offer precise control of reaction conditions and are relatively easy to scale up because the physical effects present in small reactors can be well transferred to larger systems which is not always the case for batch reactions.[17]

"Exotic" reaction conditions

The reason for such efficient reactions is not only the fast transfer of heat and mass but also because in the pressurized system, exotic reaction conditions can be reached that are otherwise impossible in batch. Batch reactions are usually limited to the boiling point of the solvent (or reagents) but in flow, extreme conditions can be used with little effort. For example, dichloromethane can be heated up to 150 °C, acetone to 240 °C, and THF to 190 °C in the VAPOURTEC® system (up to 20 bars of pressure). Sequential reactors allow to change the external factors (temperature, irradiation, etc.) within seconds from one to the other reactor.

Scalability

Scalability is relatively easy in two ways: prolonged run times with bigger input feeding and/or numbering up of the size of the apparatus. Flow technology allow to scale up processes, that are impossible or very difficult on scale in batch such as microwave conditions or photochemical reactions, which has been demonstrated on kilogram scale in a number of cases.[18–21] Cooling is another problem in batch due to slower mass and heat transport but also due to the cost associated with this task. In flow, cold to very cold temperatures of –100 °C are used on large scale and make it possible to perform reactions such as boric acid synthesis and Matteson homologation.[22,23]

Solid reagents

The use of solids in continuous flow still remains a challenge and shows the limitation of the technology. Fixed-bed reactors can be used but are significantly larger than the tubing which complicates for

example the heat transfer and the dispersion. In addition, the scalability is limited to the size (and thus loading) of the reactor.[24,25]

Hazardous reactions[26,27]

In light of the principles of green chemistry, flow synthesis is attractive since produced waste and consumed energy can be reduced while at the same time, the safety of a process can be increased. In batch, highly reactive chemicals and harsh conditions are often avoided if the safety of a process cannot be guaranteed although, from a purely chemical point of view, highly reactive low molecular weight compounds are often ideal reagents as they promise good atom economy at lower cost. Process safety in flow is achieved by miniaturization because per time, only small amounts of reactive material is present in the reactor. In case of a problem, the apparatus can be shut down quickly leaving only minimal amounts of material inside the reactor since unreacted material is not yet fed into the apparatus and products have already exited the machine. This particular point makes flow chemistry especially attractive for reactions that are highly exothermic, have the tendency of runaway behavior, or involve explosive, poisonous, or unstable intermediates.

5.2 Aim of the project

Iodine-atom transfer reactions have been studied in our group for more than twenty years and are an attractive method for C-C bond formation. The reaction can be achieved using toxic tin reagents or dilauroyl peroxide (DLP).[28] One drawback is that the side-products derived from DLP are often difficult to separate from the desired products. This problem can be solved using diacetyl peroxide since all side-products are volatile due to their low molecular weight. As diacetyl peroxide and DLP have comparable 1-hour half-life temperatures (80 °C for DLP, 87 °C for diacetyl peroxide[29]), the reaction is expected to work equally well with both initiators. Advantageously, diacetyl peroxide decomposes to two methyl radicals and is thus expected to be more efficient in the iodine abstraction step as the methyl radical is even less stabilized than the primary lauroyl radical. However, diacetyl peroxide should not be used in batch since it is highly explosive in pure form (cf. chapter 1).

Motivated by the following prerequisites, we aimed at the safe synthesis, handling, and use of diacetyl peroxide in flow:

- Per time, only small amounts of peroxide are present in the apparatus.
- The pressurized system can be heated to temperatures, at which the peroxides decompose within seconds and are thus not present anymore in the obtained product solutions.
- Radical initiators that decompose to gaseous products are well tolerated as Ryu has demonstrated using azo-initiators that liberate nitrogen gas.[30]

Advantageously, the iodine atom transfer radical addition (ATRA) sequence developed in our group is an ideal model system to study and optimize the two steps separately (Figure 5.11).

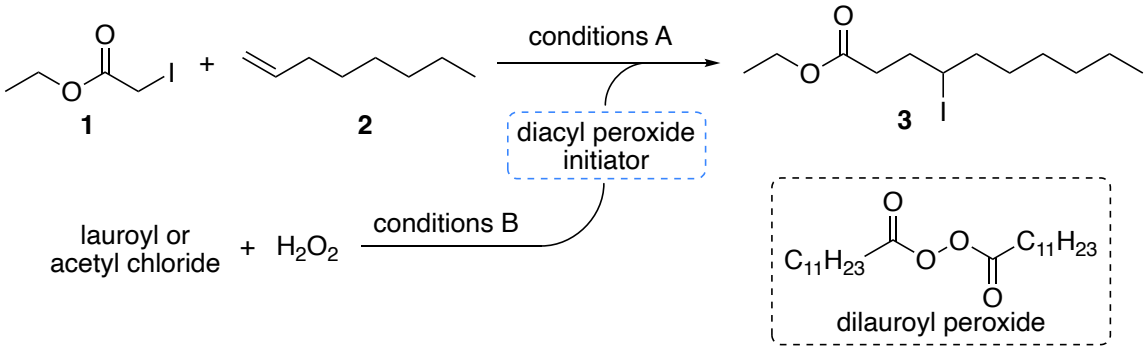

Figure 5.11. Iodine ATRA model reaction

In this model case, the reaction between (lacrimatory[31]) ethyl 2-iodoacetate **1**, 1-octene **2**, and the initiator DLP affords the ATRA product **3** (conditions A). The synthesis of (isolable) DLP from lauroyl chloride and hydrogen peroxide (conditions B) can be studied independently from the ATRA reaction.

Acetyl chloride will be used instead of lauroyl chloride for the synthesis of diacetyl peroxide and we assumed that the optimized conditions for the synthesis of DLP can be adapted without changes.

5.3 Results and discussion

Several challenges have to be addressed when the ATRA reaction is performed in flow:

- In the original protocol, the reaction is reinitiated several times which indicates that the radical chain is not 100% efficient.[28] Reinitiation is however not possible in flow.
- If the initiator is present in high amounts, iodine abstraction from the product is not impossible at elevated temperatures.
- The synthesis of diacyl peroxides by acylation of aqueous hydrogen peroxides is not trivial and the influence of aqueous hydrogen chloride in the subsequent reaction is not clear.

Therefore, the task was divided in subproblems that will be discussed next. First, the ATRA reaction is optimized independently (5.3.1) from the synthesis of DLP in flow (5.3.2) before the two processes are coupled together (5.3.3). The further use of the obtained product is discussed at the end (5.3.4).

5.3.1 Development of iodine ATRA reaction in flow

At first, several test reactions were performed in batch following the literature protocol to later compare the proceeding in batch and flow (Table 5.1).

Table 5.1 ATRA test reactions in batch

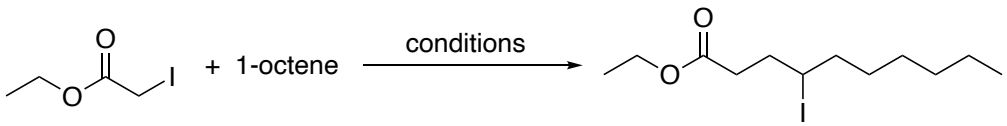

1.0 equiv 2.0 equiv **3**

Entry	Conditions	Isolated yield
1	4 x 2 mol% DLP, every 2 h, benzene (0.27 M), reflux, 8 h	89%
2	4 x 2 mol% DLP, every 2 h, MeCN (0.27 M), 85 °C, 8 h	14%
3	8 mol% DLP via syringe pump over 6 h, benzene (0.27 M), 85 °C, 8 h	42%
4	constant concentration of 5 mol% DLP (syringe pump), benzene (0.27 M), 85 °C, 8 h	84%

Using the original protocol, the product is obtained in equally high yield (entry 1, 89% vs. 93%[28]) The reaction takes several hours to complete and requires portion wise addition of initiator. Acetonitrile was tested as solvent because it is expected to be an ideal solvent for the synthesis of DLP (polar, miscible with water) but the reaction almost failed (entry 2). If the initiator is added by syringe pump, the yield is significantly reduced because it takes quite a long time, until sufficient amount of initiator is present in the reaction (entry 3). Portion wise addition of DLP, results in an oscillating amount of initiator present in the reaction mixture. To flatten this oscillation, the reaction was performed with an initial amount of 5

mol% of DLP and subsequent addition of DLP by syringe pump (entry 4) at the rate of its consumption assuring a constant level of DLP (and thus production of radicals) in the reaction which results in a similar yield to entry 1. It therefore seems to be important that initiator has to be present until the reaction is complete. Since portion wise addition is technically not possible in a flow process, the reaction has to be performed at higher temperatures in order to assure complete decomposition and thus quantitative formation of radicals in the reactor. Consequently, higher amount of initiator may be required at the risk of over-initiation and thus uncontrolled side-reactions.

The ATRA reaction was then studied in flow using a single feeding line of a solution containing all the reagents. The results of the screening are summarized on the next page (Table 5.2). Gratifyingly, the composition of the reagent solution very similar to the one used in batch resulted in almost the same high yield as in batch (entry 1). Due to health concerns using benzene, no more experiments were performed with this solvent. Similar to what has been observed for acetonitrile, solvents that can act as hydrogen atom donors result in lower yields (entry 2). Variation of the residence time and reaction temperature with *n*-hexanes did not affect the yield significantly (entries 3-9). Moreover, it was noticed that dilution as well as an increase in initiator results in poorer yields due to hydrogen abstraction from the solvent or side reactions. *t*-Butanol as well as dichloromethane gave high yields similar to benzene with little or no response to a change in concentration (entries 10-14). The yield is not increased in the presence of a large excess of olefin (entry 15).

From a technical point of view, high concentrations (0.25 M) and long residence times (40 min) as in entry 12 represent the lower performance limit of the pumps as they cannot pump accurately at such low rates. Therefore, the residence time was shortened and the concentrations lowered (entry 13) to increase pump rates. However, with these settings, the maximum capacity of the reactor was reached (10 mL) and a bigger reactor had to be built in order to reach the desired long residence times. With the help of the mechanical workshop of the department, a stainless-steel variant of the holder was manufactured onto which the tubing was coiled and immersed in an oil bath (entry 14, Figure 5.12).

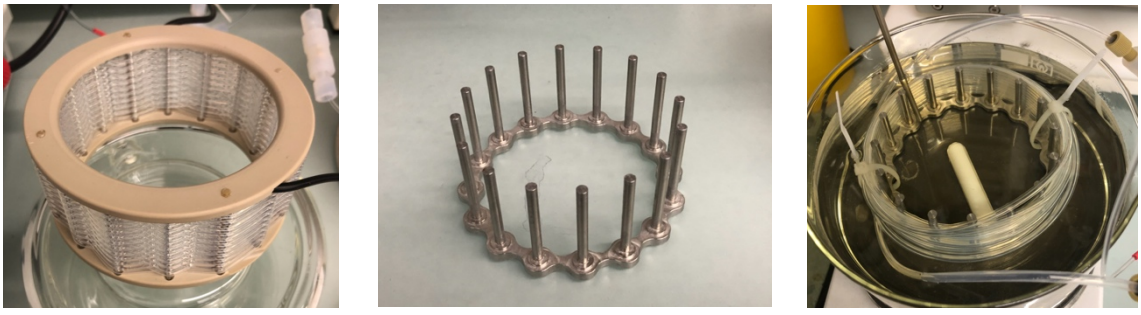

Figure 5.12. Left: commercial 10 mL reactor; middle: self-made stainless-steel holder; right: self-made 20 mL reactor immersed in oil bath

With these results in hand, the synthesis of the diacyl peroxide was investigated next (Table 5.2).

Table 5.2. Screening of conditions of ATRA reaction in flow

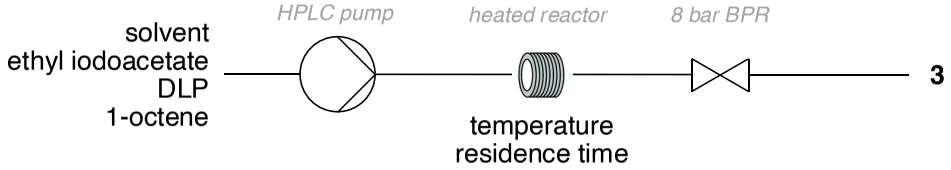

Entry	EtIOAc [equiv]	1-octene [equiv]	DLP [equiv]	Solvent	concentration [mol/L]	residence time [min]	Temperature [° C]	Yield	Comment
1	1	2	0.2	benzene	0.25	40	100	81%	Lower limit of pump capacity reached
2	1	2	0.2	TBME	0.25	25	100	51%	Orange color
3	1	2	0.2	*n*-Hexane	0.25	25	100	64%	colorless, DLP not fully consumed
4	1	2	0.2	*n*-Hexane	0.25	25	120	60%	colorless, DLP not fully consumed
5	1	2	0.2	*n*-Hexane	0.25	10	130	60%	colorless, DLP not fully consumed
6	1	2	0.2	*n*-Hexane	0.25	5	140	60%	-
7	1	2	0.2	*n*-Hexane	0.05	5	140	43%	EtIOAc not fully consumed
8	1	2	0.5	*n*-Hexane	0.25	5	140	44%	More DLP does not consume more EtIOAc
9	1	2	0.15	*n*-Hexane	0.25	40	100	66%	Lower limit of pump capacity reached
10	1	2	0.15	*t*-Butanol	0.25	40	100	78%	Lower limit of pump capacity reached
11	1	2	0.15	*t*-Butanol	0.15	40	100	76%	Lower limit of pump capacity reached
12	1	2	0.15	CH_2Cl_2	0.25	40	100	78%	Lower limit of pump capacity reached
13	1	2	0.15	CH_2Cl_2	0.125	30	110	78%	-
14	1	2	0.15	CH_2Cl_2	0.125	30	110	77%	Self-made reactor: 20 mL tubing in oil bath (110 °C)
15	1	5	0.15	CH_2Cl_2	0.125	30	110	76%	No increase in yield with more olefin

EtIOAc = ethyl 2-iodoacetate; TBME = *tert*-butyl methyl ether

5.3.2 Synthesis of DLP in flow

The synthesis of diacetyl peroxide **5** is performed by acylation of hydrogen peroxide with acetyl chloride **4** under alkaline conditions (Figure 5.1).[32–34]

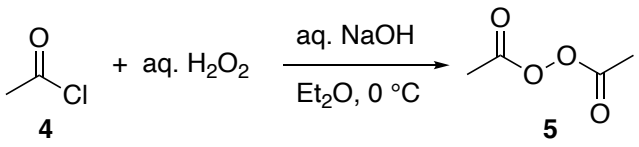

Figure 5.13. Synthesis of diacetyl peroxide

This synthesis is, however, not practicable in continuous flow since is biphasic and, more importantly, diacetyl peroxide is reported to precipitate, which would lead to blockage of the flow reactor. This situation would be dangerous as it represents kind of a self-made detonating cord. In order to reduce the operational hazard of working with diacetyl peroxide, optimization was performed with its harmless analogue, dilauroyl peroxide (DLP). The goal is that at a later stage, the optimized DLP conditions can be adapted for the synthesis of diacetyl peroxide in flow.

An alternative to the biphasic Schotten-Baumann method would be to use anhydrous hydrogen peroxide and perform the synthesis in an organic solvent. However, alkali metal peroxides (Na_2O_2, Li_2O_2) are insoluble in organic solvents. Urea hydrogen peroxide complex (UHP) is soluble in polar organic solvents such as acetonitrile. Unfortunately, the use of acetonitrile would cause issues in the ATRA reaction as described above. Solubility tests showed that only about 10 mg of UHP can be dissolved per milliliter of acetonitrile at 25 °C and the amount is further decreased upon addition of unpolar solvents. Furthermore, solubility tests revealed that DLP is insoluble in acetonitrile. After extensive screening of conditions, the cleanest (batch) result was achieved with a mixture of solvents and DLP was quantitatively formed (Figure 5.14).

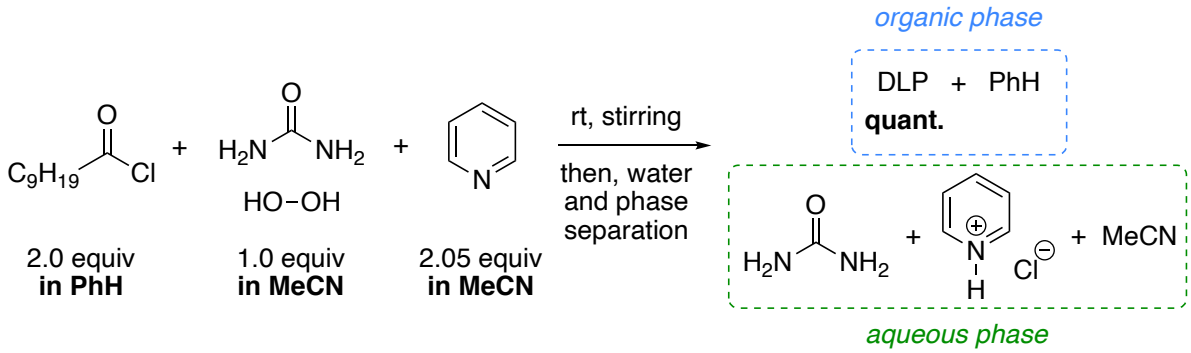

Figure 5.14. Synthesis of dilauroyl peroxide

Though this protocol looks similar to the Schotten-Baumann method, it has the advantage of not involving a biphasic mixture for the reaction. Moreover, the sodium hydroxide solution would have to be relatively concentrated, which is not well compatible with the phase separator. Addition of water only for washing is feasible in flow using a phase separator. Initial tests have shown that in flow the mixing of the reagents proceeds well, and the reaction is fast but the formation of an emulsion during the

washing step does not take place. Instead, immiscible droplets of water and organic solvents passed sequentially through the tube, leaving salts and acetonitrile back in the organic phase. To solve this issue, an active mixing unit had to be built that is capable of processing large volumes per time while having only a small internal volume to not further complicate the calculation of the residence times. After a fruitful discussion with Prof. John Blacker, a self-made mixing unit was designed and manufactured in collaboration with the mechanical workshop of the department (Figure 5.15).[35]

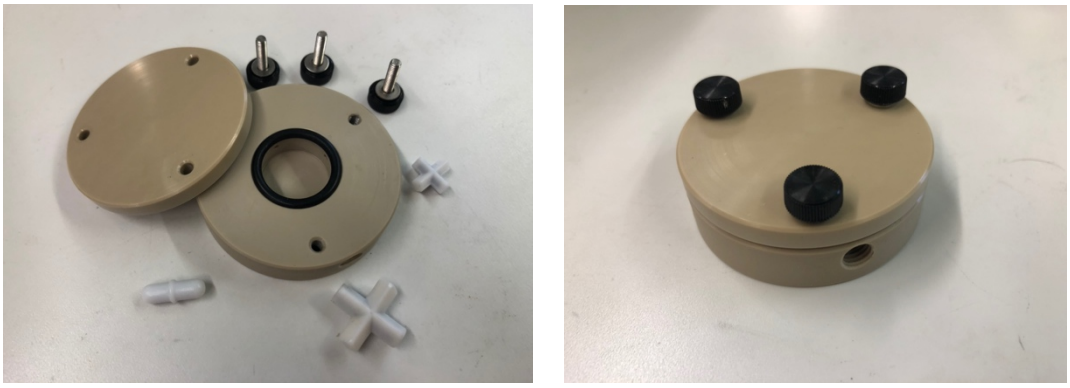

Figure 5.15. Self-made active mixing unit in open and closed form

The mixing unit is made out of PEEK polymer material, sealed with a chemically resistant O-ring, and can be operated at pressures below 5 bar. The cap can is held in place and tightened with three screws. Liquids can enter (or exit) at four positions and are mixed inside by a stirring bar. Dependent on the size of the stirring bar, the internal volume ranges between 1.2 mL and 2 mL. For technical reasons, this prototype reactor was built with PEEK but chemically more resistant material can be used in the future if necessary due to chemical incompatibilities.

With this device and a phase separator equipped with a hydrophobic membrane, test runs were conducted for the flow synthesis of DLP (Figure 5.16).

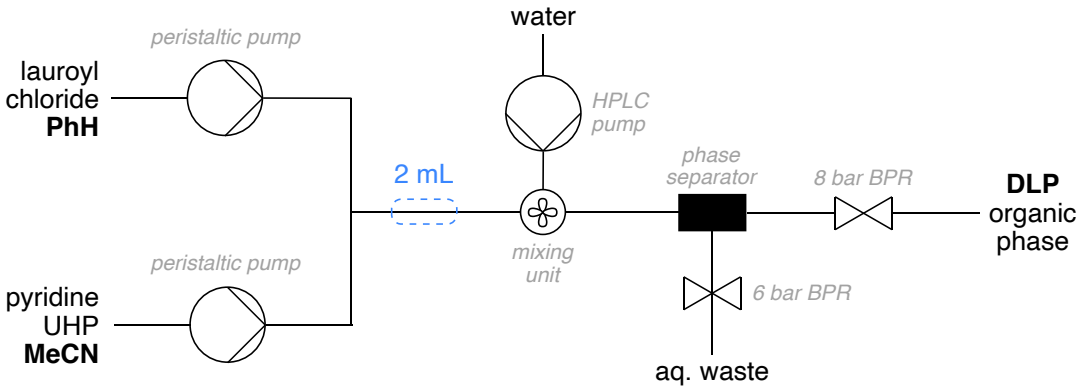

Figure 5.16. Setup for flow synthesis of DLP including a washing step

The formation of DLP successfully took place within the 2 mL of tube before the mixing unit, in which water was added and an emulsion was formed. This emulsion proved to be stable until it reached the phase separator, but the two phases could not be cleanly separated.

Even after extensive experimentation, the following technical issues could not be fully resolved:

- Acetonitrile could not be fully removed from the organic phase even if a large excess of water was used for washing. Moreover, as acetonitrile is miscible with both water and benzene, the products were found in both of the phases. Therefore, a reproducible concentration of DLP in the organic phase was not achieved.
- Pyridinium chloride caused membrane clogging after several runs.
- The above problems persisted independently of the nature of the membrane (hydrophilic, hydrophobic).

In addition to the abovementioned issues, the concentration of DLP was very low (0.03 mmol/mL) because rather large amounts of organic solvents had to be used due to the poor solubility of UHP in acetonitrile/benzene mixtures.

Due to the issues that were faced in connection with the separation of the phases, a process had to be developed that does not require aqueous washing. Therefore, anhydrous hydrogen peroxide was used that is obtained by extraction of aqueous hydrogen peroxide.[36,37] It was found that reproducible concentrations of H_2O_2 (of 1.4 mol/L) are obtained when 21% aqueous hydrogen peroxide was extracted with half the volume of TBME. This solution of hydrogen peroxide was then reacted with lauroyl chloride according to the method developed in chapter 3. Full conversion is achieved quickly affording DLP and pyridinium chloride. However, the pyridinium chloride is not soluble and what has been an advantage in the batch method, turned out to be a clear drawback in flow. In a first attempt, it was tried to filter the precipitate in a cartridge containing sand and sodium sulfate (Figure 5.17).

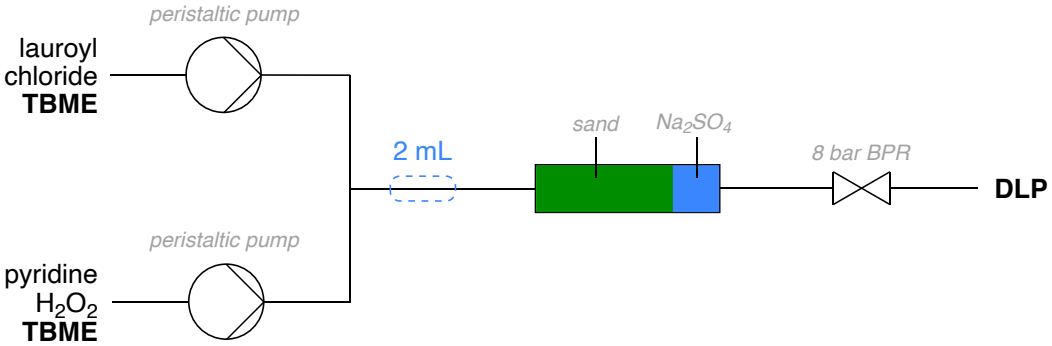

Figure 5.17. Attempted removal of precipitate by filtration

Even though the suspension that was immediately formed upon mixing of the reagents was transported to the column filled with sand (to filter the precipitate) and sodium sulfate (to filter finer particles and polar side products) the system got blocked sooner or later and no run could be completed as planned. Fortunately, the obtained DLP solution was visually and also chemically clean. In order to avoid the formation of insoluble side products, several tests were conducted with an immobilized base next. The small bed of sodium sulfate at the end of the column was kept for all tests (Table 5.3).

Table 5.3. Screening of solid supported bases

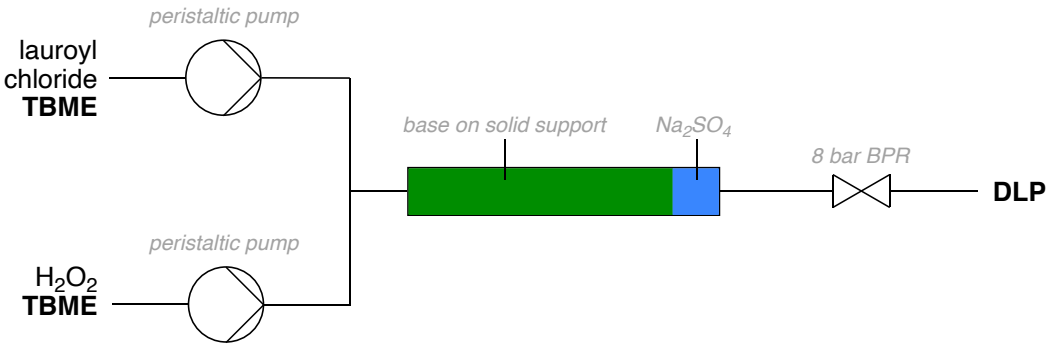

Entry	Type of resin	Isolated yield of DLP	Comment
1	Amberlyst A21, Na_2SO_4 spacer, basic alox	35%	Unidentified side product
2	Pyridine on silica, Na_2SO_4 spacer, basic alox	93%	Unidentified side product, HCl gas formation, H_2O_2 in product solution
3	Pyridine on silica, Na_2SO_4 spacer, increased amount of basic alox	92%	Unidentified side product, HCl gas formation, H_2O_2 in product solution
4	Pyridine on silica, Na_2SO_4 spacer, anhydrous K_3PO_4	n.d.	Unidentified side product, HCl gas formation
5	Pyridine on silica, Na_2SO_4 spacer, K_3PO_4, basic alox	82%	Unidentified side product, very little HCl gas formation

The strongly basic ion exchange Amberlyst A21 resin containing a tertiary amine yielded only little product together with an unidentified side product. Basic alox was added to the column in order to trap liberated HCl gas (entry 1). Next, silica gel functionalized with pyridine afforded a high yield of DLP but unfortunately, the side product was still present in the product, HCl gas was formed, and hydrogen peroxide was detected in the product solution (entry 2). Because an increased amount of basic alox was ineffective to remove the HCl gas (entry 3), it was replaced by anhydrous potassium phosphate. Interestingly, the evolution of HCl gas persisted but the hydrogen peroxide was now removed completely (entry 4). A combination of potassium phosphate and basic alox resulted in a reduced amount of HCl gas and effective removal of unreacted hydrogen peroxide (entry 5). In all the cases, the unidentified side product was present which, by ^{13}C-NMR analysis, seems to be a derivative of lauroyl chloride. However, it could not be isolated and characterized, nor be assigned to lauric acid (by hydrolysis of lauroyl chloride) nor lauric peracid (by perhydrolysis of lauroyl chloride).

Pyridine proved to be highly efficient to activate the acyl chloride and its use resulted in high yields of DLP. It was assumed that it is unimportant whether pyridine is used as free reagent or as functionalized silica gel, and therefore one has to find a method to only remove it efficiently from the solution. In chapter 3, it was found that dichloromethane can fully solubilize the pyridinium hydrochloride salt which would also enable the DLP formation in the tube without the risk of precipitate formation and thus blocking of the apparatus. Salts and other highly polar products can be very easily removed by silica gel which is applied daily for flash column chromatography. Therefore, it should also be possible to use the silica as an efficient filter for the salt and since dichloromethane is a polar solvent, DLP should pass the silica without noticeable chromatographic effect (Figure 5.18).

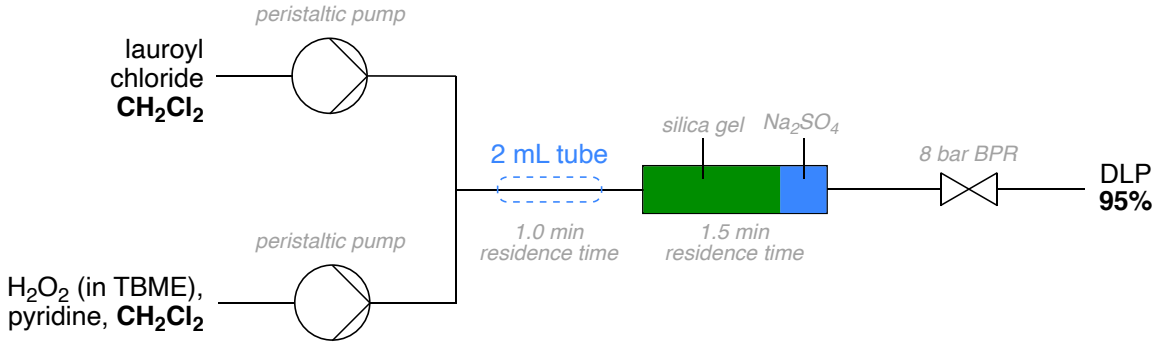

Figure 5.18. Synthesis of DLP in flow in dichloromethane as solvent

The setup was very similar to what has been tested before (Figure 5.17). DLP was efficiently formed after mixing of the reagents and the pyridinium hydrochloride did stay fully solubilized. As expected, the silica gel completely removed the pyridinium hydrochloride salt and no clogging was observed. DLP passed the silica gel without additional delay or dispersion and was obtained as a single product in 95% after evaporation of the solvent.

This technically simple setup proved to be the most efficient for the synthesis of DLP and is also ideal for the subsequent ATRA reaction: Steady state concentration of DLP is reached quickly with little fronting and tailing due to the rather small size of the silica column.

5.3.3 Coupling of the two processes

In order to achieve an efficient process, the course of the DLP concentration has to overlay with the course of the concentration of ethyl 2-iodoacetate and 1-ocetene in a way that the ratio of the three reagents is 1:2:0.15 (EtIOAc:1-octene:DLP) according to the above findings (Table 5.2). For technical reasons, a residence time of 15 min at 120 °C was set for the ATRA reaction as this allows for a pump speed of 1 mL/min for each pump (Figure 5.19).

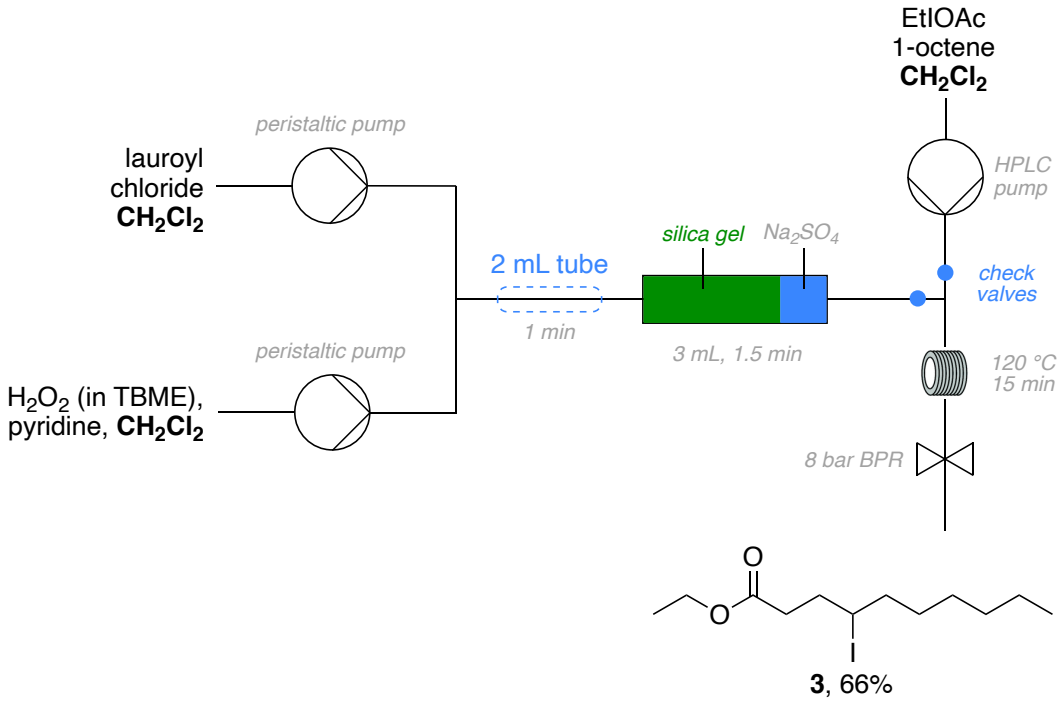

Figure 5.19. Setup for ATRA reaction coupled to precedent in-line synthesis of DLP

Gratifyingly, the first test to couple the two reactions worked well and the iodoester **3** was obtained in 66% yield. One factor that could be responsible for the slightly lower yield compared to the ATRA reaction alone, is the presence of TBME since this has been used to extract the hydrogen peroxide from the aqueous solution. Now that the proof-of-concept reaction worked well, an extraction of hydrogen peroxide with dichloromethane can be performed which requires again a precise determination of the peroxide concentration.

A detailed optimization of the technical (flow rates, ratios of DLP and reagent solutions, overlap/overlay of the steady-state areas, etc.) and chemical parameters (individual reagent concentrations, residence time, amount of silica in the filtration column, etc.) will be conducted to further increase the yield. A more detailed optimization using design of experiment software is planned now that the technical prerequisites are fulfilled.

5.3.4 Further use of the products

The products obtained from the ATRA reaction are not particularly stable due to the presence of a secondary iodide which results in gradual decomposition over several days. Apart from liberated iodine, none of the decomposition products could be identified. It may become important to use the ATRA product as a substrate in another in-line reaction step. In the light of our investigations in the Schmidt reaction (cf. part two of this thesis), the iodoesters can serve as intermediates for the synthesis of functionalized pyrrolidines (Figure 5.20).

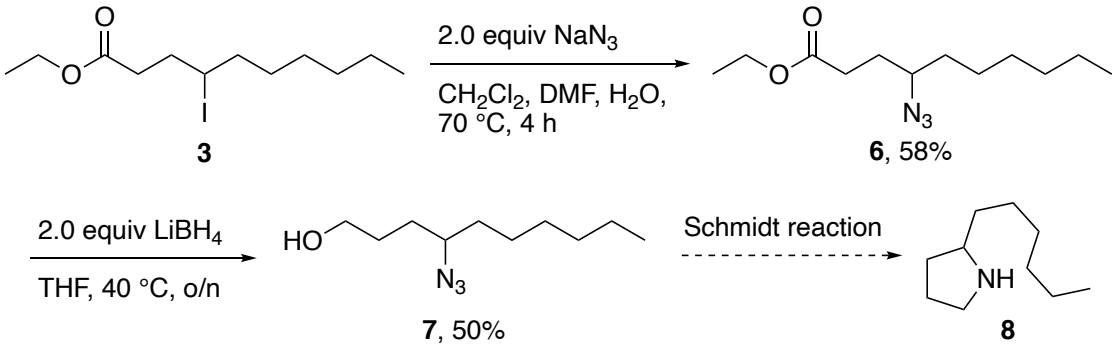

Figure 5.20. Further use of iodine ATRA products

The synthesis of the reference compounds has been performed in batch. A solution of **3** in CH_2Cl_2, similar to the one obtained from the flow process, was treated with a solution of sodium azide to substitute the iodide with an azide group. Azidoester **6** was obtained in moderate yield. The combination of DMF and water was chosen because it prevents the formation of an emulsion or a precipitation, which is important to ensure a good mixing of the reagents. The ester was reduced with lithium borohydride to the corresponding azidoalcohol **7**, leaving the azide function untouched. The intramolecular Schmidt reaction leading to pyrrolidine **8** has not been studied to date.

5.4 Conclusion and outlook

Enabling technologies such as automated synthesis, online reaction monitoring, statistical optimization of the reaction conditions and flow synthesis expand the scope of chemical reactions and allow for a closer monitoring. Using a commercial flow chemistry apparatus from VAPOURTEC®, the iodine atom transfer radical addition to an olefin was successfully transferred from a time-consuming batch process to a much faster continuous process providing the product in high yield.

The reaction relies on the diacyl peroxide initiator DLP which, however, can be an issue since the side products from the thermal decomposition of DLP are sometimes difficult to remove from apolar products due to their low volatility and low polarity. The use of low molecular weight diacyl peroxide initiators such as diacetyl peroxide will potentially solve these challenges but pose a much higher risk due to the explosive nature of the compound. It has been demonstrated that the diacyl peroxide can be synthesized in continuous flow in high yield and purity by acylation of hydrogen peroxide, using pyridine as a base, with a subsequent in-line removal of the pyridinium chloride salt.

As a proof-of-concept, the synthesis of dilauroyl peroxide was successfully coupled to the iodine ATRA reaction that is initiated by the DLP produced in the previous step. The high yielding method to synthesize dilauroyl peroxide in flow will be adapted for the synthesis and in-line use of diacetyl peroxide in the future.

The iodoesters can be used for the synthesis of functionalized pyrrolidines but apart from the synthesis of the reference compounds, no investigations have been conducted yet. Once the flow processes are fully optimized, a third reaction sequence can be implemented, for example to substitute the iodide with more stable functional groups.

5.5 Experimental section

General information

Techniques

Silica gel 60 Å (40–63 µm) from Silicycle was used for flash column chromatography. Thin layer chromatography (TLC) was performed on Silicycle silica gel 60 F_{254} plates, visualization under UV light (254 nm) and/or by dipping in a solution of $(NH_4)_2MoO_4$ (15.0 g), $Ce(SO_4)_2$ (0.5 g), H_2O (90 mL), conc. H_2SO_4 (10 mL); or $KMnO_4$ (3 g), K_2CO_3 (20 g) and NaOH 5% (3 mL) in H_2O (300 mL) and subsequent heating. Anhydrous sodium sulfate was used as drying reagent.

Materials

Commercial reagents were used without further purification unless otherwise stated. Solvents for extractions, reactions and flash column chromatography were of technical grade and distilled prior to use with the exception of reagent grade *t*-BuOH.

Instrumentation

^1H and ^{13}C NMR spectra were recorded on a Bruker Avance IIIHD-300 spectrometer operating at 300 MHz for ^1H and 75 MHz for ^{13}C at room temperature (24-25°C) unless otherwise stated. Some ^1H and ^{13}C NMR spectra were recorded on a Bruker Avance IIIHD-400 or a Bruker Avance II-400 spectrometer (^1H: 400 MHz; ^{13}C: 75 MHz). Chemical shifts (δ) are reported in parts per million (ppm) using the residual solvent or $Si(CH_3)_4$ (δ = 0.00 for ^1H NMR spectra) as an internal standard. Multiplicities are given as s (singlet), d (doublet), t (triplet), q (quadruplet), m (multiplet), and br (broad). Coupling constant (J) is reported in Hz. In ^{13}C-NMR spectra, the peak positions are reported on one decimal unless the difference in chemical shift between two signals is small and requires two decimals.

Flow synthesis

Reactions in continuous flow were performed with a VAPOURTEC® flow reactor consisting of an R2S module (peristaltic pumps), an R2C+ module (HPLC pumps), and an R4 module (reactor heater unit). The apparatus was operated and the flow models were predicted with the flow commander software (version V1.11 and V1.12). A standard 10 mL VAPOURTEC® heated reactor was used up to temperatures of 140 °C. For bigger volumes, a self-made reactor unit consisting of a 20 mL coiled tube was immersed in an oil bath that was heated to the desired temperature. A benchtop Mettler-Toledo flowIR® (operated by Mettler-Toledo IC-IR® software) was used for online reaction monitoring and was operated at ambient temperature and pressure.

Syntheses

Synthesis ethyl 2-iodoacetate (1)

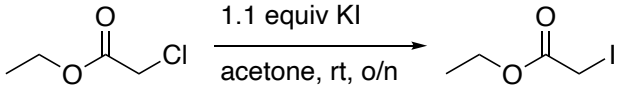

The synthesis was performed in a well-ventilated fume hood and personal protection with a gas mask is recommended during the workup due to the lacrimatory properties of the product.[31]

To a stirred suspension of potassium iodide (54.8 g, 330 mmol, 1.1 mmol) in acetone (500 mL) was added ethyl 2-chloroacetate (32 mL, 36.8 g, 300 mmol) at rt. The suspension covered with Al foil, stirred overnight, and then concentrated under reduced pressure. The residue was diluted with water (150 mL) and extracted with pentane (300 / 150 mL). The organic layers were washed with aq. sodium thiosulfate solution (5%, 150 mL) and water (150 mL). The organic layers were dried over Na_2SO_4, filtrated, and concentrated to yield ethyl 2-iodoacetate (51 g, 79%).

yellow liquid; **^{1}H NMR** (400 MHz, $CDCl_3$) δ = 4.24 – 4.14 (m, 2H), 3.67 (q, J = 0.6 Hz, 2H), 1.31 – 1.22 (m, 3H); **^{13}C NMR** (101 MHz, $CDCl_3$) δ = 168.8, 62.2, 13.9, –5.2; Spectral and analytical data are in accordance to what we have reported previously.[38]

Hydrogen peroxide extraction

In a 50 mL separatory funnel was placed a titrated solution of aq. H_2O_2 (21%, 10 mL) to which HPLC grade TBME (5 mL) was added. The mixture was vigorously shaken for 30 seconds and the phases were allowed to separate. The lower aqueous phase was removed and then, the organic phase collected in a separate flask without further washing or drying. Standard iodometric titration[39] indicated a concentration of 1.4 mol/L. The solution was stored ice-cooled and used within one day.

Synthesis of DLP in continuous flow

Solution A

Pyridine (0.33 mL, 4.1 mmol, 2.05 equiv) and H_2O_2 (1.4 M in TBME, 1.42 mL, 2 mmol) were dissolved in CH_2Cl_2 (2.25 mL).

Solution B

Lauroyl chloride (0.93 mL, 4.2 mmol, 2.1 equiv) was dissolved in CH_2Cl_2 (3.1 mL).

Each solution was pumped by a peristaltic pump at a speed of 1.0 mL/min and mixed in a T-piece. The reagents were allowed to react inside a wide-diameter section of tubing (2.1 mm ID, 2 mL total volume) and were pumped to an adjustable fixed-bed Omnifit® column filled with silica gel (2.0 g) and a thin layer of Na_2SO_4 (resulting in a capacity of 3.0 mL of liquid). The solution containing the product was automatically collected after passing an 8 bar BPR at the times predicted by the flow commander software.

DLP (755 mg, 95%) was obtained upon evaporation of the solvent, drying on high vacuum, and was indistinguishable from commercially available DLP both by TLC and NMR.

Ethyl 4-iododecanoate (3)

Single ATRA experiment

A solution of ethyl 2-iodoacetate (642 mg, 3.0 mmol), 1-octene (0.96 mL, 6.0 mmol, 2.0 equiv), and DLP (180 mg, 0.3 mmol, 0.15 equiv) in CH_2Cl_2 (22 mL) was pumped at a rate of 1.5 mL/min to the reactor unig using the HPLC pump module. The self-made reactor unit consisted of coiled tubing (2.1 mm internal diameter) that was submerged in an oil bath at 110 °C, resulting in a residence time of 30 min. The slightly pink solution was collected at the times predicted by the flow commander software, concentrated under reduced pressure and loaded directly on column. FC (98:2 pentane:Et_2O) afforded ethyl 4-iododecanoate (754 mg, 77%).

yellow liquid; **rf** 0.35 (98:2 pentane:Et_2O); **^{1}H NMR** (400 MHz, $CDCl_3$) δ = 4.25 – 4.07 (m, 3H), 2.64 – 2.38 (m, 2H), 2.07 (tdd, J = 7.8, 5.6, 2.3 Hz, 2H), 1.94 – 1.83 (m, 1H), 1.78 – 1.64 (m, 1H), 1.50 (ddd, J = 14.6, 8.7, 4.0 Hz, 1H), 1.45 – 1.36 (m, 1H), 1.35 – 1.23 (m, 9H), 0.91 – 0.84 (m, 3H); **^{13}C NMR** (101 MHz, $CDCl_3$) δ = 172.9, 60.7, 40.9, 38.6, 35.6, 34.6, 31.8, 29.6, 28.6, 22.7, 14.4, 14.2; Spectral and analytical data are in accordance to what we have reported previously.[28]

Coupling of DLP synthesis and ATRA reaction

Solution A (10 mL)

Pyridine (0.17 mL, 2.05 mmol, 2.05 equiv) and H_2O_2 (1.4 M in TBME, 0.7 mmol, 1.0 mmol) were dissolved in CH_2Cl_2 (9.1 mL).

Solution B (10 mL)

Lauroyl chloride (0.47 mL, 2.1 mmol, 2.1 equiv) was dissolved in CH_2Cl_2 (9.5 mL).

Solution C (20 mL)

Ethyl 2-iodoacetate (1.07 g, 5.0 mmol) and 1-octene (1.6 mL, 10.0 mmol, 2.0 equiv) were dissolved in CH_2Cl_2 (18 mL).

The setup for the synthesis of DLP was used as previously described. The tube after the Onmifit® column was connected to the setup of the ATRA reaction (also used as previously described) using a T-piece. The solutions were pumped at a speed of 1 mL/min each fully automated by the flow commander software. The collected product was purified as described in the above section.

Ethyl 4-azidodecanoate (6)

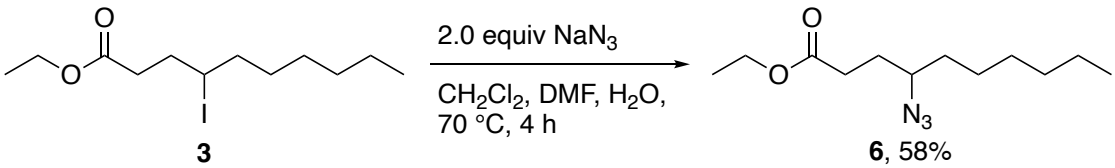

3 **6**, 58%

To a solution of 4-iododecanoate (740 mg, 2.27 mmol) in CH_2Cl_2 (22 mL) was added a solution of sodium azide (300 mg, 4.55 mmol, 2.0 equiv) in DMF/water (3:1, 12 mL) and the mixture was stirred at 70 °C for 4 h, then cooled down to rt, treated with water, and extracted with CH_2Cl_2. The organic phase

was washed with brine, dried over Na_2SO_4 and concentrated. FC (98:2 pentane:Et_2O) afforded ethyl 4-azidodecanoate (315 mg, 58%).

Colorless oil; **rf** 0.24 (98:2 pentane:Et_2O); **^{1}H NMR** (400 MHz, $CDCl_3$) δ = 4.13 (q, J = 7.1 Hz, 2H), 3.30 (tdd, J = 9.1, 5.7, 4.2 Hz, 1H), 2.53 – 2.30 (m, 2H), 1.88 (dddd, J = 14.2, 8.3, 7.2, 4.2 Hz, 1H), 1.71 (dddd, J = 14.2, 9.1, 7.8, 6.5 Hz, 1H), 1.54 (dtd, J = 11.7, 6.3, 5.6, 3.9 Hz, 2H), 1.47 – 1.37 (m, 1H), 1.37 – 1.21 (m, 10H), 0.93 – 0.83 (m, 3H); **^{13}C NMR** (101 MHz, $CDCl_3$) δ = 173.1, 62.4, 60.6, 34.5, 31.8, 31.0, 29.7, 29.2, 26.1, 22.7, 14.3, 14.2; **HRMS** calc. for $[M+H]^+$: 242.1863, found: 242.1865; **IR** (cm^{-1}): 2929, 2858, 2094, 1733, 1457, 1375, 1251, 1164, 1031, 857

4-azidodecan-1-ol (7)

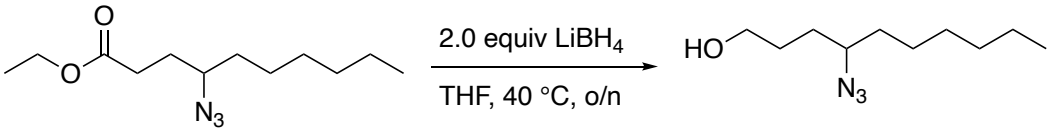

6 **7**, 50%

To a stirred solution of ethyl 4-azidodecanoate (241 mg, 1.0 mmol) in dry THF (9 mL) was added a solution of $LiBH_4$ (2.0 M in THF, 1.0 mL, 2.0 mmol, 2.0 equiv) at 0 °C. The mixture was stirred at 40 °C overnight, diluted with Et_2O and carefully treated with aq. sat. NH_4Cl. The mixture was extracted with Et_2O and the combined organic phase was washed with brine, dried over Na_2SO_4, and concentrated. FC (98:2 pentane:Et_2O) afforded ethyl 4-azidodecan-1-ol (100 mg, 50%).

Colorless oil; **rf** 0.41 (6:4 pentane:Et_2O); **^{1}H NMR** (400 MHz, $CDCl_3$) δ = 3.68 (t, J = 6.0 Hz, 2H), 3.35 – 3.22 (m, 1H), 1.81 – 1.17 (m, 16H), 0.94 – 0.82 (m, 3H); **^{13}C NMR** (101 MHz, $CDCl_3$) δ = 117.6, 63.1, 62.7, 34.6, 31.8, 30.9, 29.4, 29.2, 26.2, 22.7, 14.2; spectral data are in accordance literature values.[40]

5.6 References

[1] "The Nobel Prize in Chemistry 1990," can be found under https://www.nobelprize.org/prizes/chemistry/1990/corey/facts/, **n.d.**

[2] S. G. Davey, *Nature Reviews Chemistry* **2018**, *2*, 1–1.

[3] C. W. Coley, L. Rogers, W. H. Green, K. F. Jensen, *ACS Cent. Sci.* **2017**, *3*, 1237–1245.

[4] T. Klucznik, B. Mikulak-Klucznik, M. P. McCormack, H. Lima, S. Szymkuć, M. Bhowmick, K. Molga, Y. Zhou, L. Rickershauser, E. P. Gajewska, A. Toutchkine, P. Dittwald, M. P. Startek, G. J. Kirkovits, R. Roszak, A. Adamski, B. Sieredzińska, M. Mrksich, S. L. J. Trice, B. A. Grzybowski, *Chem* **2018**, *4*, 522–532.

[5] C. Musonda, K. Chibale, *CMC* **2004**, *11*, 2518–2533.

[6] F. Strieth-Kalthoff, F. Sandfort, M. H. S. Segler, F. Glorius, *Chem. Soc. Rev.* **2020**, *49*, 6154–6168.

[7] C. W. Coley, D. A. Thomas, J. A. M. Lummiss, J. N. Jaworski, C. P. Breen, V. Schultz, T. Hart, J. S. Fishman, L. Rogers, H. Gao, R. W. Hicklin, P. P. Plehiers, J. Byington, J. S. Piotti, W. H. Green, A. J. Hart, T. F. Jamison, K. F. Jensen, *Science* **2019**, *365*, DOI 10.1126/science.aax1566.

[8] M. B. Plutschack, B. Pieber, K. Gilmore, P. H. Seeberger, *Chemical Reviews* **2017**, *117*, 11796–11893.

[9] G. Cai, L. Xue, H. Zhang, J. Lin, *Micromachines* **2017**, *8*, 274.

[10] D. E. Fitzpatrick, C. Battilocchio, S. V. Ley, *ACS Cent. Sci.* **2016**, *2*, 131–138.

[11] F. E. Valera, M. Quaranta, A. Moran, J. Blacker, A. Armstrong, J. T. Cabral, D. G. Blackmond, *Angewandte Chemie - International Edition* **2010**, *49*, 2478–2485.

[12] A. J. Capel, R. P. Rimington, M. P. Lewis, S. D. R. Christie, *Nature Reviews Chemistry* **2018**, *2*, 422.

[13] P. M. Murray, F. Bellany, L. Benhamou, D.-K. Bučar, A. B. Tabor, T. D. Sheppard, *Org. Biomol. Chem.* **2016**, *14*, 2373–2384.

[14] P. A. Tipler, G. Mosca, *Physik: für Studierende der Naturwissenschaften und Technik*, Springer Berlin Heidelberg, Berlin, Heidelberg, **2019**.

[15] C.-C. Hong, J.-W. Choi, C. H. Ahn, *Lab Chip* **2004**, *4*, 109.

[16] V. Hessel, I. V. Gürsel, Q. Wang, T. Noël, J. Lang, *Chemical Engineering & Technology* **2012**, *35*, 1184–1204.

[17] R. L. Hartman, J. P. McMullen, K. F. Jensen, *Angewandte Chemie International Edition* **2011**, *50*, 7502–7519.

[18] T. H. Rehm, *ChemPhotoChem* **2020**, *4*, 235–254.

[19] C. Sambiagio, T. Noël, *Trends in Chemistry* **2020**, *2*, 92–106.

[20] L. D. Elliott, M. Berry, B. Harji, D. Klauber, J. Leonard, K. I. Booker-Milburn, *Org. Process Res. Dev.* **2016**, *20*, 1806–1811.

[21] B. D. A. Hook, W. Dohle, P. R. Hirst, M. Pickworth, M. B. Berry, K. I. Booker-Milburn, *J. Org. Chem.* **2005**, *70*, 7558–7564.

[22] H. Usutani, D. G. Cork, *Org. Process Res. Dev.* **2018**, *22*, 741–746.

[23] C. Stueckler, P. Hermsen, B. Ritzen, M. Vasiloiu, P. Poechlauer, S. Steinhofer, A. Pelz, C. Zinganell, U. Felfer, S. Boyer, M. Goldbach, A. de Vries, T. Pabst, G. Winkler, V. LaVopa, S. Hecker, C. Schuster, *Org. Process Res. Dev.* **2019**, *23*, 1069–1077.

[24] R. L. Hartman, *Org. Process Res. Dev.* **2012**, *16*, 870–887.

[25] A. Baker, M. Graz, R. Saunders, G. J. S. Evans, I. Pitotti, T. Wirth, *Journal of Flow Chemistry* **2015**, *5*, 65–68.

[26] M. Movsisyan, E. I. P. Delbeke, J. K. E. T. Berton, C. Battilocchio, S. V. Ley, C. V. Stevens, *Chem. Soc. Rev.* **2016**, *45*, 4892–4928.

[27] B. Gutmann, C. O. Kappe, *Journal of Flow Chemistry* **2017**, *7*, 65–71.

[28] C. Ollivier, T. Bark, P. Renaud, *Synthesis* **2000**, 1598–1602.

[29] *Ullmann's Encyclopedia of Industrial Chemicals*, **2005**.

[30] T. Fukuyama, I. Ryu, *Encyclopedia of Radicals in Chemistry, Biology and Materials* **2012**, DOI 10.1002/9781119953678.rad035.

[31] J. Patočka, K. Kuča, *Military Medical Science Letters* **2015**, *84*, 128–139.

[32] S. Gambarjan, *Berichte der deutschen chemischen Gesellschaft* **1909**, *42*, 4003–4013.

[33] C. Qian, D. Lin, Y. Deng, X.-Q. Zhang, H. Jiang, G. Miao, X. Tang, W. Zeng, *Org. Biomol. Chem.* **2014**, *12*, 5866–5875.

[34] L. S. Silbert, D. Swern, *J. Am. Chem. Soc.* **1959**, *81*, 2364–2367.

[35] M. R. Chapman, M. H. T. Kwan, G. King, K. E. Jolley, M. Hussain, S. Hussain, I. E. Salama, C. González Niño, L. A. Thompson, M. E. Bayana, A. D. Clayton, B. N. Nguyen, N. J. Turner, N. Kapur, A. J. Blacker, *Org. Process Res. Dev.* **2017**, *21*, 1294–1301.

[36] J. H. Walton, H. A. Lewis, *J. Am. Chem. Soc.* **1916**, *38*, 633–638.

[37] F. R. Paulsen, *Chemistry and Industry* **1956**, 1274.

[38] D. Meyer, P. Renaud, *Angewandte Chemie - International Edition* **2017**, *56*, 10858–10861.

[39] V. R. Kokatnur, M. Jelling, *J. Am. Chem. Soc.* **1941**, *63*, 1432–1433.

[40] X. Bao, Q. Wang, J. Zhu, *Angewandte Chemie International Edition* **2019**, *58*, 2139–2143.

Part two

Stereochemical Study of the Intramolecular Schmidt Reaction

In parallel to the work on organic peroxides, studies on the triflate-based intramolecular Schmidt reaction were conducted.

The second part of this thesis briefly discusses the stereochemistry of this reaction to build alkaloid skeletons in chapter 6. Our findings are summarized in two draft manuscripts in the following chapters. Chapter 7 contains a comprehensive stereochemical study of the reaction. With support of X-ray crystallographic data and computational studies of our collaborators, the stereoselectivity for the diastereoselective synthesis of alkaloid skeletons was elucidated. The selectivity of the method was demonstrated by the enantioselective synthesis of two alkaloids occurring in ant venom. Taking advantage of the diastereoselective process, the synthesis of bridgehead-functionalized bicyclic amines is presented in chapter 8.

Chapter 6

Diastereoselective Intramolecular Schmidt Reaction

6 Diastereoselective Intramolecular Schmidt Reaction

The intramolecular Schmidt reaction was independently discovered by Pearson and Aubé in the early 1990s and emerged as a useful tool to construct azabicyclic alkaloid skeletons.[1–3] This rearrangement process has been part of several master- PhD- and postdoc projects in our group in which the reaction has been run under basic, instead of acidic conditions which has some advantages in regard to functional group tolerance.[4–14] This chapter provides a brief overview of the strategies that have been developed to control the diastereoselectivity of the intramolecular Schmidt reaction. The results of the work conducted during this thesis are compiled in the two draft manuscripts found in the following chapters 7 and 8.

6.1 The underlying challenge

The intramolecular Schmidt reaction involves an intramolecular nucleophilic attack of an azide on a cationic species with subsequent rearrangement. Cationic species in an alkyl azide such as shown in **1**, are accessible from a variety of precursors under Lewis- or Brønstedt acid conditions. The nucleophilic azide attacks the cation, leading to an aminodiazonium ion **2**, which rearranges with concomitant loss of dinitrogen. It is proposed that the 1,2-migration is a concerted process, in which the bond antiperiplanar to the departing nitrogen moiety is shifted.[15] The rearranged compound further reacts to the final product **4**, usually *via* hydrolysis or reduction of iminium ion **3** (Figure 6.1).[9,16]

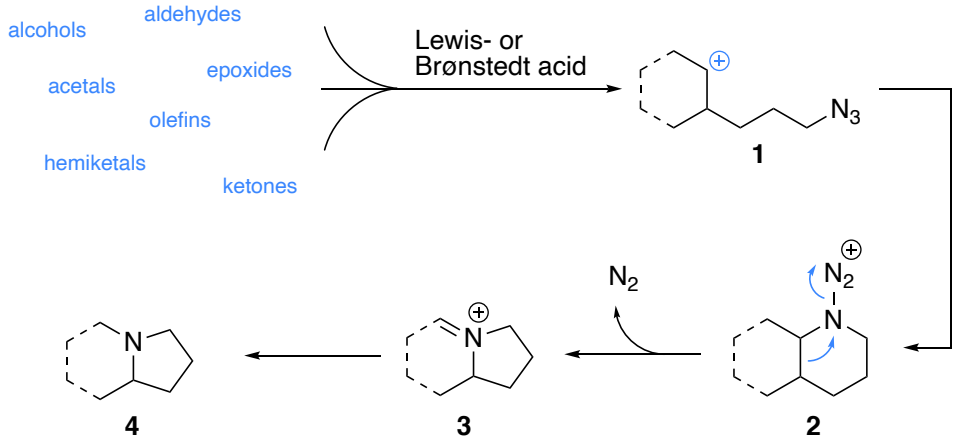

Figure 6.1. General mechanism of the intramolecular Schmidt reaction

Two inherent problems arise from this mechanism:[15,17]

- Cations can rearrange before being attacked by the azide which can lead to a mixture of aminodiazonium ions.
- If the substituents are similar to each other, the 1,2-migration can be unselective, which leads to a mixture of isomeric products.

These issues have been investigated in detail by Pearson and the resulting products of the different pathway are illustrated below (Figure 6.2).[17]

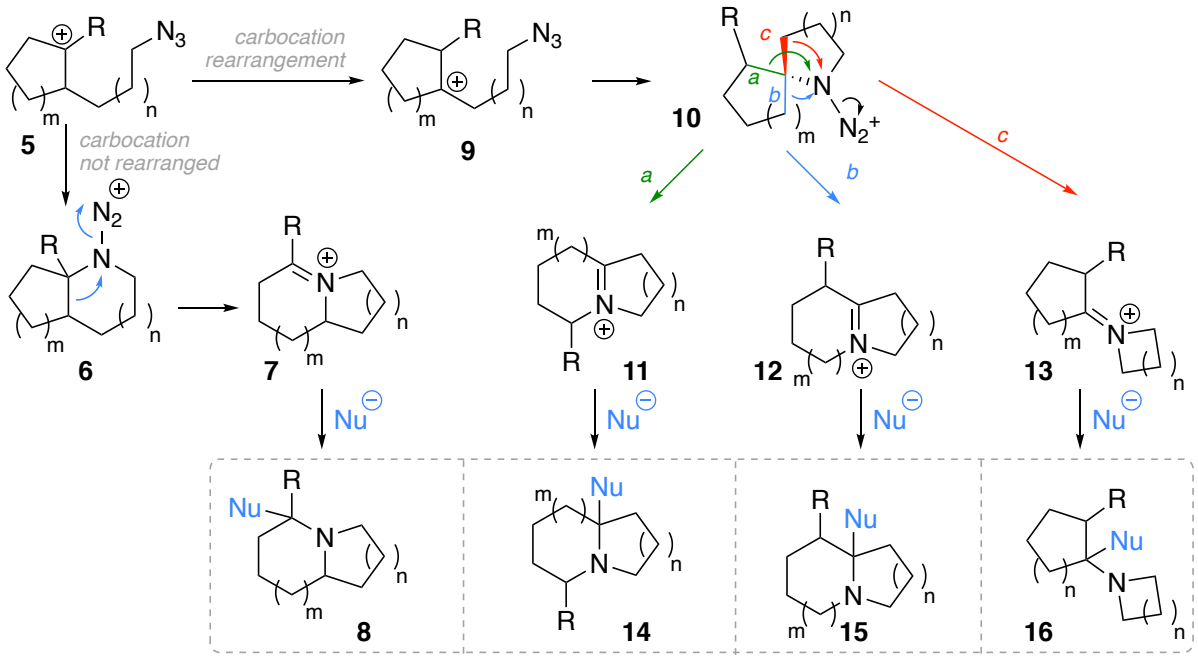

Figure 6.2. Mechanistic rationale for the formation of product mixtures as exemplified by Pearson[17]

An initially generated carbocation **5** (e.g., from a tertiary alcohol under acidic conditions) can be directly attacked by the azide, leading to aminodiazonium **6**, which rearranges to iminium **7**. The 1,2-migration of the bridging bond in this system is favored due to the formation of a stabilized iminium ion. In the case of a carbocation rearrangement such as **9**, the nucleophilic attack of the azide moiety will generate a spirocyclic aminodiazonium ion **10**. Now, three bonds have the possibility to migrate, which results in two regioisomeric bicyclic iminium ions (**11**, **12**) and, in the case of the migration of the C–C bond that tethered the azide group, an exocyclic iminium **13** is formed.

Upon reaction with a suitable nucleophile, the corresponding amines (**8**, **14**, **15**, **16**) are formed. In case the nucleophilic addition is not fully stereoselective, additional isomers will be formed. The relative rates of the carbocation rearrangement and of the 1,2-migration is strongly dependent on the substituent on the carbocation formed in the first step, on the tether length, and on the size of the rings.[17,18]

Several strategies have been investigated to address the regioselectivity issues and are highlighted in the following subchapter.

6.2 Strategies to control the regioselectivity

6.2.1 Prevention of carbocation rearrangement

The simplest way to avoid the formation of multiple products, is to prevent the carbocation from rearrangement since in this case, only one product is formed as one bond migration is clearly preferred. Pearson has demonstrated this in deuteration experiments of phenyl- and *n*-hexyl substituted azidoalcohols (**17**, **20**). The stabilized benzylic cation **19** formed from **17** was not rearranged and thus, indolizidine **18** was obtained as single product. The intramolecular Schmidt reaction of hexyl-substituted azidoalcohol **20**, on the other hand, afforded indolizidines **21** and **22**, which arise from a rearranged carbocation **23** (Figure 6.3).[15,17]

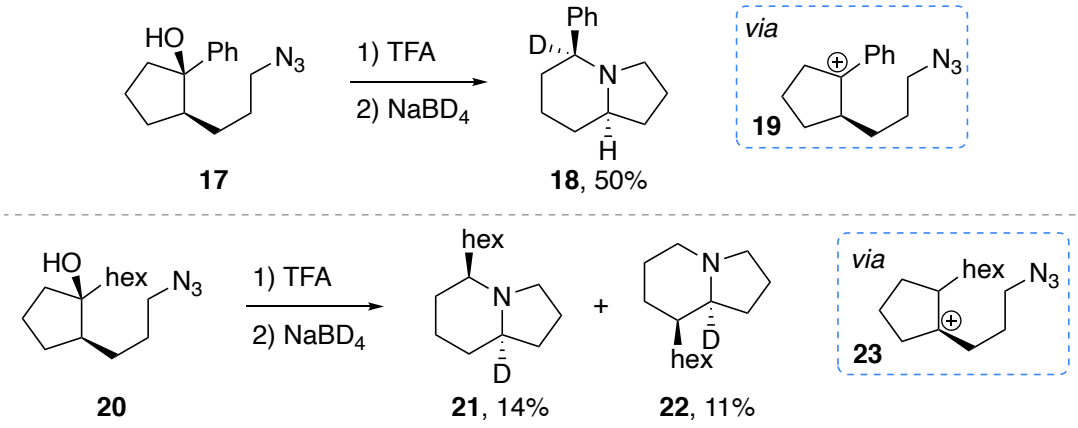

Figure 6.3. Substituent effect on carbocation rearrangement; hex = n-hexyl group; TFA = trifluoroacetic acid

The stabilizing effect of naphthalene and other aryl substituents has been successfully applied to control the regiochemical outcome of the reaction.[1,19] In addition to these findings, also the tether length is of central importance since longer tether lengths result in slower nucleophilic addition, which allows the carbocation to rearrange.[17,18]

6.2.2 Steric and electronic control of the 1,2-migration

Based on their previous studies on ring expansion / lactam formation[20–22], Aubé and coworkers developed a regioselective ring expansion of cyclic ketones with hydroxy azides.[23,24] The use of aldehydes furnishes oxazolines.[25] Depending on the substituent, the position of the diazonium substituent in the spirocyclic intermediate can be influenced and allows control over which bond is going to migrate (Figure 6.4).

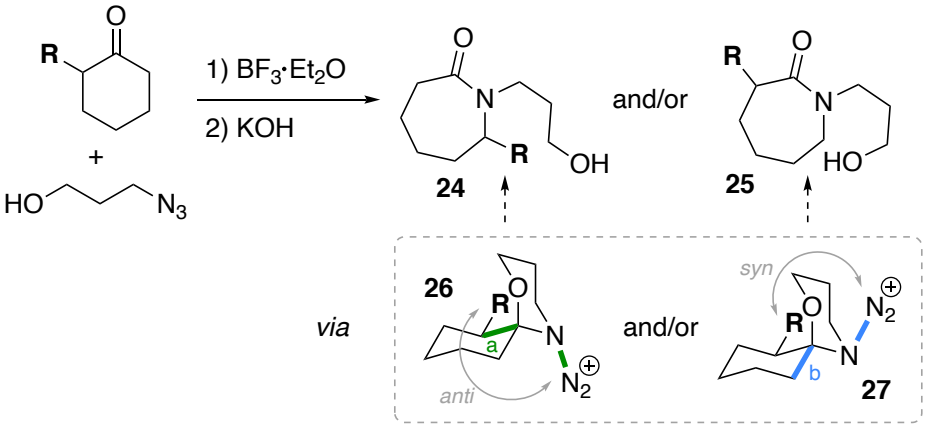

Figure 6.4. Influence of substituents on diazonium position

Even though the diazonium moiety is small and cylindrical, increased steric bulk (e.g., isopropyl, *tert*-butyl) of the ring substituent orients the diazonium *anti* to the substituent (conformation **26**), which leads to the migration of bond **a**, and formation of **24** after hydrolysis. Electron withdrawing substituents (e.g., bromide, phenyl, methoxy) result in the formation of the other regioisomer **25**. This result was assumed to be a kinetic effect as these substituents may slow down the migration of bond **a**, and thus, migration of bond **b** *via* conformation **27** becomes more likely.[23]

The stereochemical outcome of the 1,2-migration was further investigated by Aubé.[26] Installation of a chiral center next to the alcohol, such as in azidoalcohol **28**, results in the formation of an aminodiazonium intermediate that can be present in two conformations (**29**, **30**), from which the one with the phenyl substituent in the more stable equatorial position (**29**) is preferred. In this conformation, the bond migration *anti* to the phenyl group encounters no steric hindrance and the 1,2-migration leads to iminium ether **31** as the major product. In conformation **30**, the phenyl group is found in the disfavored axial position and hinders the migration of the indicated bond. Thus, iminium ether **32** is obtained only as a minor product. Hydrolysis of the iminium ether affords lactam **33** in excellent diastereomeric ratio (Figure 6.5, top).

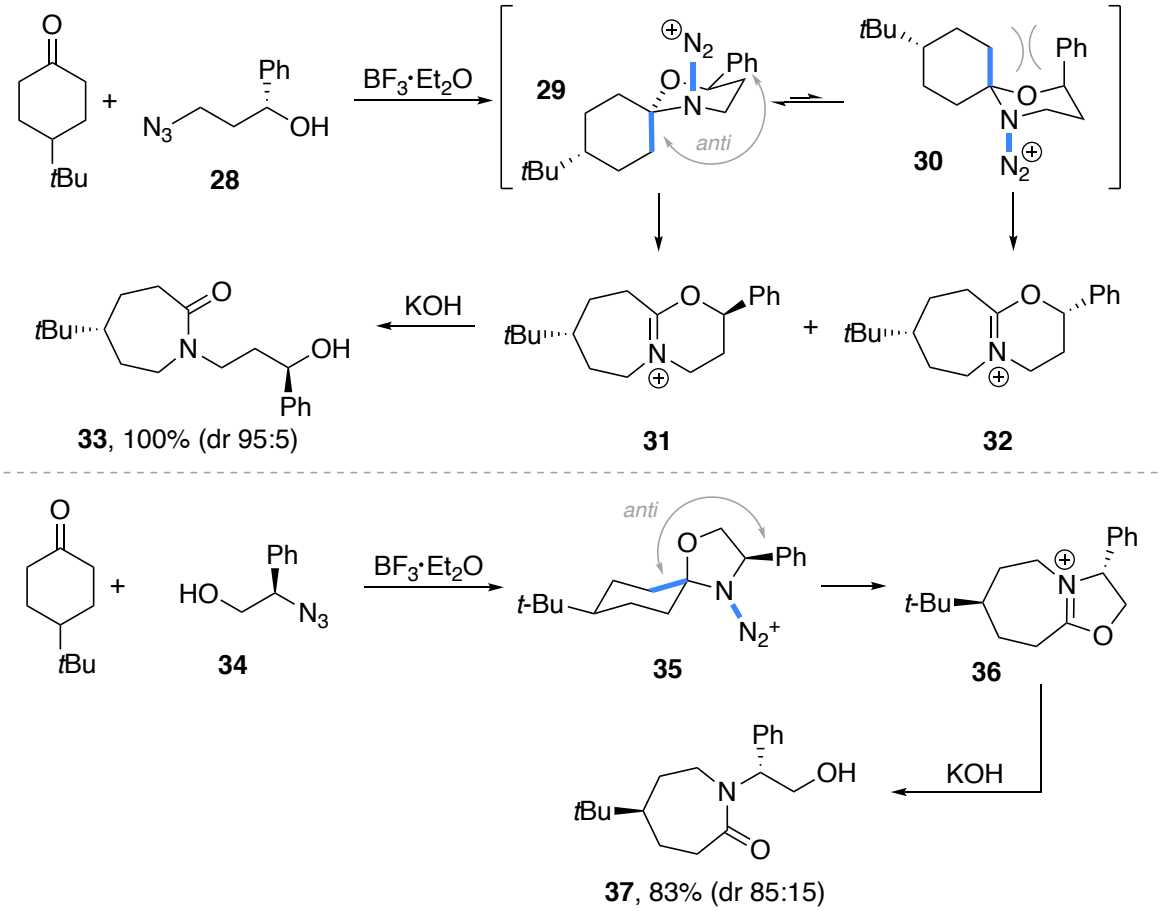

Figure 6.5. Regioselective 1,2-migration controlled by steric effects of on-tether substituents

A similar observation was made when the phenyl substituent was placed next to the azide group such as in azidoalcohol **34** (Figure 6.5, bottom). Again, the migration of the bond *anti* to the phenyl group, indicated in the aminodiazonium **35**, is observed. Upon hydrolysis of the intermediate iminium ether **36**, lactam **37** was obtained still in good diastereomeric ratio. The effect of the substituent on the ketone moiety was found to have very little, if any, effect on the outcome of the reaction.[26]

Interestingly, if the phenyl substituent was placed in the 2' position between the azide and the alcohol, a peculiar outcome of the reaction was observed. The reaction of 4-*tert*-butyl cyclohexanone with azidoalcohol **37** afforded lactam **40** in excellent yield and as a single diastereomer. This result is rationalized by a cation-π interaction (**38**) between the phenyl and the diazonium moiety which, in this case, gets stabilized in the axial position and thus facilitates the axial C-C bond migration to iminium ether **39** (Figure 6.6).[27]

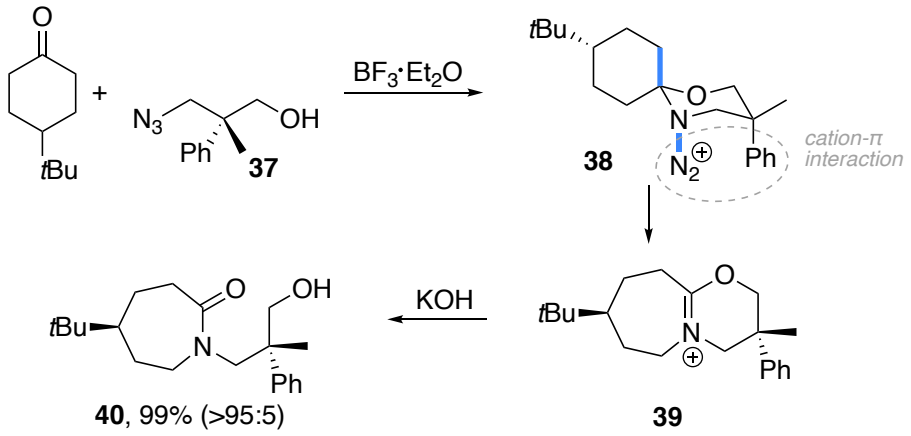

Figure 6.6. Effect of cation-π interaction of the on-tether phenyl substituent

This assumption was confirmed in a subsequent report by Aubé:[28] In the case of azidoketone **41**, the phenyl substituent is found in an axial position in the reactive conformation (**42**) which leads to the exclusive formation of lactam **44** after migration of the bridging bond **a** of aminodiazonium **43** as indicated. However, if the azidoketone is found in the conformation in which the aryl substituent is equatorial (e.g., assisted by an additional equatorial *tert*-butyl group,) such as in **45**, the position of the diazonium moiety is now found to be *syn* to the aryl group (**46**), which facilitates the migration of the **b** bond. This leads to the formation of lactam **47** (Figure 6.7).

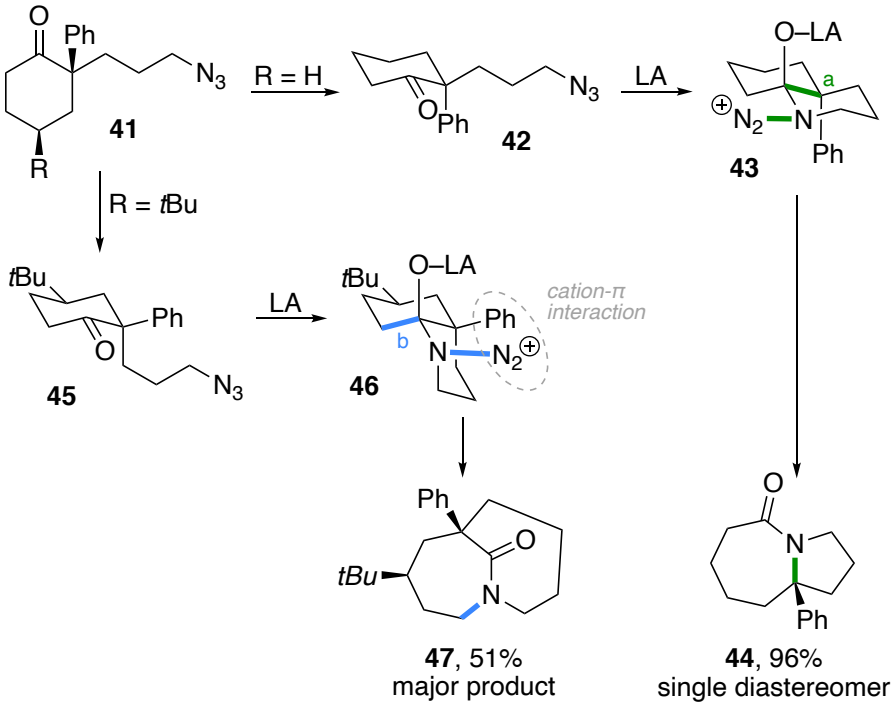

*Figure 6.7. Proposed cation-π interaction resulting in the formation of **47***

6.2.3 Avoiding carbocation formation

The most straightforward way to prevent a carbocation rearrangement is obviously if the process does not proceed *via* a carbocation. Such a strategy was investigated by Pearson, in which the Schmidt reaction is not promoted by a proton but by mercury salts. In this case, olefin **48** is converted to a mercuronium ion **49** which is regioselectively opened to aminodiazonium **50** by the azide. Reduction and reductive demercuration of iminium **51** furnishes exclusively azabicylce **52** (Figure 6.8).[29]

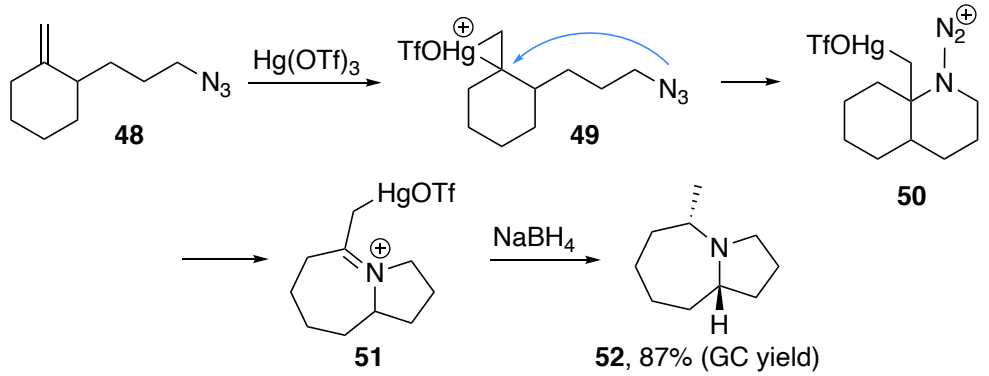

Figure 6.8. Regioselective rationale for the mercury-promoted Schmidt reaction

Moreover, the presence of the mercurio group inhibits the migration of the alkyl group which gives one a possibility to control the regioselectivity of the 1,2-migration. Reddy and Baskaran have developed a similar stereoselective protocol based on the opening of epoxides which has later been used for regioselective arene amination.[26,30,31]

Another way to prevent the formation of a carbocation was developed in our group about ten years ago. This method allows the use of primary electrophilic carbon centers as demonstrated on the enantioselective synthesis of (–)-indolizidine 167B (**56**).[32] In this complementary protocol of the Schmidt reaction, the azidoalcohol **53** is transformed to the corresponding triflate which is readily substituted by the azide moiety. The diazonium intermediate **54** then undergoes a 1,2-migration to iminium **55** as explained before. Stereoselective reduction of the iminium furnished the desired indolizidine alkaloid.

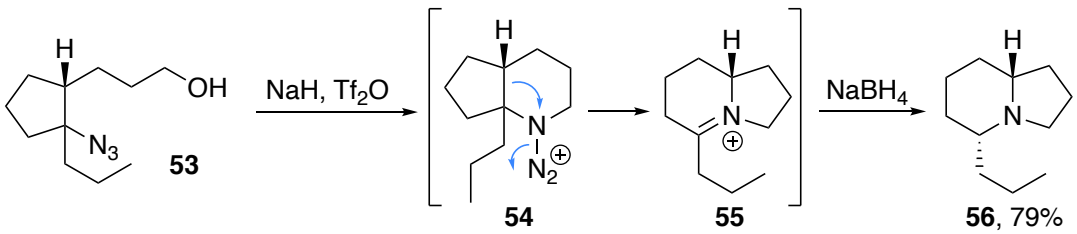

Figure 6.9. Enantioselective synthesis of indolizidine 167B under nonacidic conditions

Moreover, compared to the harsh conditions employed previously (triflic acid, trifluoroacetic acid, or boron trifluoride) the mild conditions of this method are advantageous for acid-labile groups (e.g., acetals) and thus, a broader range of functional groups can be used.

However, the method exhibits the same lack of regioselectivity as the transformation reported by Pearson.[32] This is not surprising since both processes involve the same aminodiazonium intermediate as illustrated below (Figure 6.10).

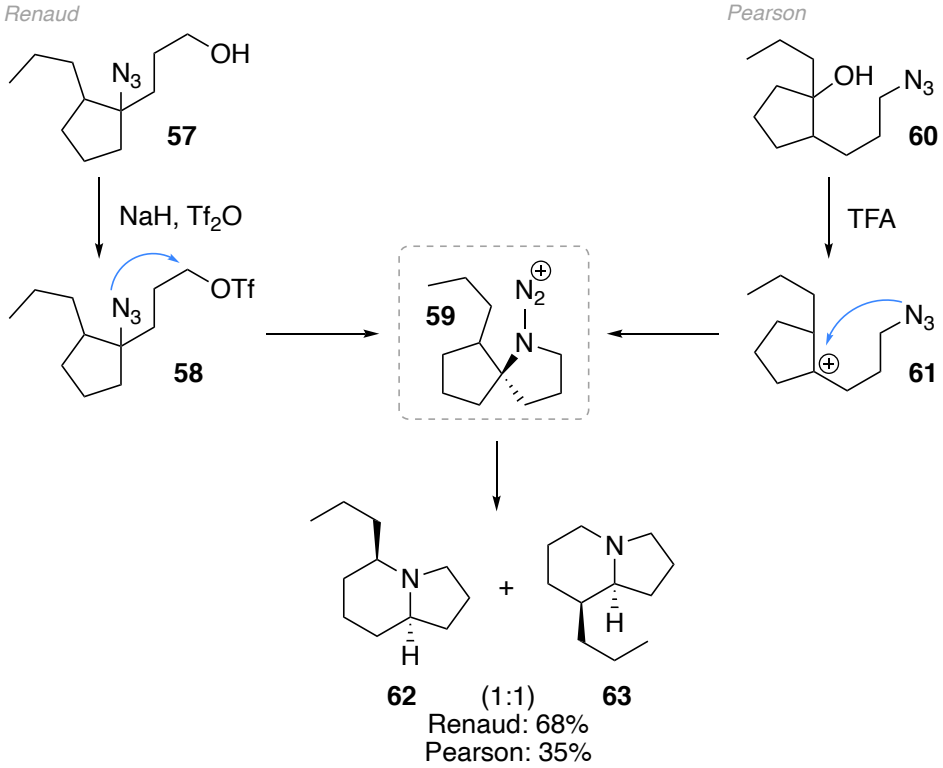

Figure 6.10. Common aminodiazonium intermediate in the methods of Renaud and Pearson

Conversion of azidoalcohol **57** to the corresponding triflate **58** affords the spirocyclic intermediate **59**, The very same intermediate is also obtained by trapping of the rearranged carbocation **61** that is generated from treatment of **60** with a strong acid. Therefore, both protocols afford a mixture of indolizidine products **62** and **63**.

In his PhD thesis, Ajoy Kapat developed a highly diastereoselective approach to reduce or functionalize the iminium ion **64** derived from azidoalcohol **63**. The obtained pyrroloazepines **65** are obtained as single diastereomers and in good to excellent yields (Figure 6.11).

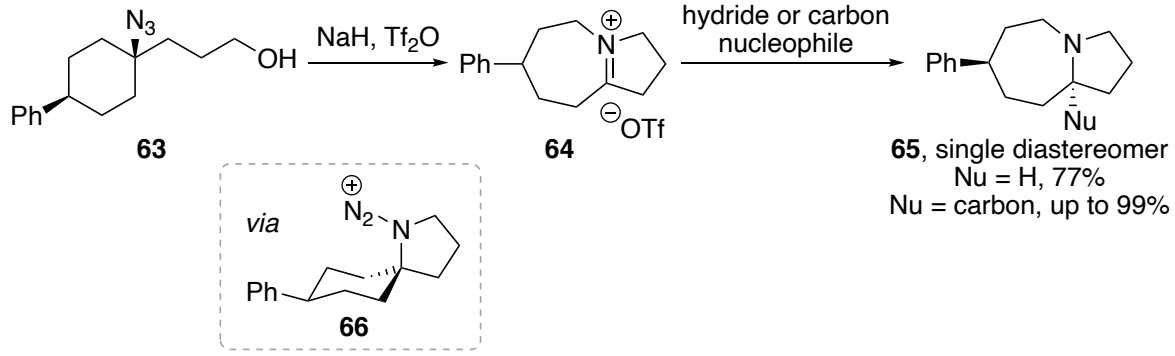

Figure 6.11. Diastereoselective formation of 65

It was assumed that the selectivity is governed by the phenyl substituent on the 7-membered ring of the iminium triflate, which effectively shields one face of the molecule and thus, makes it inaccessible for the nucleophile. However, since the involved aminodiazonium intermediate **66** is mirror-symmetric, no differentiation of the two C-C bonds takes place and thus, the migration is non-regioselective.

6.3 Conclusions and outlook

The intramolecular Schmidt reaction is a powerful tool to construct azabicyclic alkaloid skeletons and lactams from a variety of alkylazides.[3,16,32,33] The stereochemical control of the transformation is challenging since rearrangement of the involved carbocation and/or unselective alkyl migration can lead to mixtures of products. Several strategies have been developed to overcome the difficulties encountered over the last thirty years.

Our group has contributed to this research by developing a complementary method to promote the Schmidt reaction based on azidotriflates. However, the stereochemistry and detailed mechanism of the triflate-based Schmidt reaction have not been studied in detail yet. Moreover, the origin of the high selectivity for the reduction step is not fully understood. Furthermore, it needs to be investigated, if a regioselective migration can be achieved using the directive effect of substituents similar to what was observed for the lactam formation under acidic conditions by Aubé.

At this point, we set out to investigate the stereoselectivity of the triflate-mediated Schmidt reaction. Our work to overcome the lack of regioselectivity and the findings we made, are compiled in two draft manuscripts, which are presented in the next two chapters of this thesis.

6.4 References

[1] W. H. Pearson, J. M. Schkeryantz, *Tetrahedron Letters* **1992**, *33*, 5291–5294.

[2] J. Aubé, G. L. Milligan, *Journal of the American Chemical Society* **1991**, *113*, 8965–8966.

[3] E. Nyfeler, P. Renaud, *Chimia* **2006**, *60*, 276–284.

[4] D. Ohde, Studies on the Intramolecular Schmidt Reaction, Bachelor thesis, University of Bern, **2017**.

[5] G. Tekleab, Rearrangement of Secondary Hydroxylamines, Master thesis, University of Bern, **2017**.

[6] A. Kapat, Recent Progress in Intramolecular Schmidt Reaction and Radical Azidation, PhD thesis, University of Bern, **2011**.

[7] A. Kapat, *Intramolecular Schmidt Rearrangement Involving Secondary δ-Azido Alcohols*, University Of Bern, **2012**.

[8] F. Giornal, *Intramolecular Schmidt Rearrangement Involving Secondary δ-Azido Alcohols*, University Of Bern, **2013**.

[9] E. Nyffeler, From Radical Azidation to Schmidt Rearrangement, PhD thesis, University of Bern, **2005**.

[10] L. Gnägi, Studies on the Diastereoselective Intramolecular Schmidt Reaction for the Construction of Octahydro-1H-Pyrrolo [1,2-a]Azepine Skeletons, Master thesis, University of Bern, **2016**.

[11] N. E. Niggli, Towards the Total Synthesis of (±) -Lasubine I via Intramolecular Schmidt Reaction, Master thesis, University of Bern, **2017**.

[12] J. Cinqualbre, Exploiting Enamine / Iminium Chemistry to Decorate Nitrogen-Containing Rings via Aminonitriles Joséphine Cinqualbre, PhD thesis, University of Bern, **2017**.

[13] P. S. Locher, Towards the Synthesis of (±)-Lehmizidine 275A via Hydroazidation and Intramolecular Schmidt Rearrangement, Master thesis, University of Bern, **2013**.

[14] R. Arnold, Towards the Total Synthesis of Lehmizidine 275A, Master thesis, University of Bern, **2020**.

[15] W. H. Pearson, R. Walavalkar, J. M. Schkeryantz, W. K. Fang, J. D. Blickensdorf, *Journal of the American Chemical Society* **1993**, *115*, 10183–10194.

[16] S. Grecian, J. Aubé, in *Organic Azides*, John Wiley & Sons, Ltd, **2010**, pp. 191–237.

[17] W. H. Pearson, R. Walavalkar, *Tetrahedron* **2001**, *57*, 5081–5089.

[18] G. L. Milligan, C. J. Mossman, J. Aubé, *J. Am. Chem. Soc.* **1995**, *117*, 10449–10459.

[19] W. H. Pearson, B. M. Gallagher, *Tetrahedron* **1996**, *52*, 12039–12048.

[20] C. J. Mossman, J. Aubé, *Tetrahedron* **1996**, *52*, 3403–3408.

[21] P. Desai, K. Schildknegt, K. A. Agrios, C. Mossman, G. L. Milligan, J. Aubé, *J. Am. Chem. Soc.* **2000**, *122*, 7226–7232.

[22] V. Gracias, G. L. Milligan, J. Aube, *J. Am. Chem. Soc.* **1995**, *117*, 8047–8048.

[23] B. T. Smith, V. Gracias, J. Aubé, *J. Org. Chem.* **2000**, *65*, 3771–3774.

[24] V. Gracias, K. E. Frank, G. L. Milligan, J. Aubé, *Tetrahedron* **1997**, *53*, 16241–16252.

[25] J. G. Badiang, J. Aubé, *J. Org. Chem.* **1996**, *61*, 2484–2487.

[26] K. Sahasrabudhe, V. Gracias, K. Furness, B. T. Smith, C. E. Katz, D. S. Reddy, J. Aubé, *J. Am. Chem. Soc.* **2003**, *125*, 7914–7922.

[27] C. E. Katz, J. Aubé, *J. Am. Chem. Soc.* **2003**, *125*, 13948–13949.

[28] M. Szostak, L. Yao, J. Aubé, *Organic Letters* **2009**, *11*, 4386–4389.

[29] W. H. Pearson, D. A. Hutta, W. Fang, *J. Org. Chem.* **2000**, *65*, 8326–8332.

[30] P. G. Reddy, S. Baskaran, *The Journal of organic chemistry* **2004**, *69*, 3093–101.

[31] S. Lang, A. R. Kennedy, J. A. Murphy, A. H. Payne, *Organic Letters* **2003**, *5*, 3655–3658.

[32] A. Kapat, E. Nyfeler, G. T. Giuffredi, P. Renaud, *Journal of the American Chemical Society* **2009**, *131*, 17746–7.

[33] A. Kapat, P. S. Kumar, S. Baskaran, *Beilstein J. Org. Chem.* **2007**, *3*, 49.

Chapter 7

Stereoselective and Stereospecific Triflate Mediated Intramolecular Schmidt Reaction: Easy Access to Alkaloid Skeletons

Lars Gnägi, Remo Arnold, Florence Giornal, Harish Jangra, Ajoy Kapat, Erich Nyfeler, Robin Marc Schärer, Hendrik Zipse, and Philippe Renaud

Angewandte Chemie International Edition, ***2021****, ASAP*

The supporting information can be found in the appendix.

Author contributions

LG conducted the majority of the experimental work with assistance of RMS. FG, AK, and EN conducted preliminary experiments. HJ and HZ performed theoretical calculations. LG, HZ and PR were responsible for writing of the article.

7 Stereoselective and Stereospecific Triflate Mediated Intramolecular Schmidt Reaction: Easy Access to Alkaloid Skeletons

7.1 Abstract

The stereoselectivity and stereospecificity of the triflate mediated intramolecular Schmidt reaction of substituted 3-(1-azidocyclohexyl)propanol derivatives leading to octahydro-1*H*-pyrrolo[1,2-a]azepine, the structural skeleton of several important families of alkaloids such as the *Stemona* alkaloids, has been examined. The reaction involves an initial intramolecular S_N2 reaction between the azide moiety and the triflate affording an intermediate spirocyclic aminodiazonoium salt that undergoes the expected 1,2-shift/N_2-elimination followed by hydride mediated iminium salt reduction. Remarkably, chiral alcohols are converted to the azabicylic derivative with no or limited racemization. The initial asymmetric alcohol center controls the diastereoselectivity of the whole process leading to the formation of one out of the four possible diastereoisomers of disubstituted octahydro-1*H*-pyrrolo[1,2-a]azepine. The origin of the stereoselectivity is rationalized based on theoretical calculations. The concise synthesis of (–)-(*cis*)-3-propylindolizidine and (–)-(*cis*)-3-butyllehmizidine, two alkaloids found in the venom of workers of the ant *Myrmicaria melanogaster*, is reported.

7.2 Introduction

In the early 1990s, Aubé[1–5] and Pearson[6] independently reported an intramolecular Schmidt reaction involving the reaction of alkyl azides with cationic species obtained by diverse procedures including treatment of ketones, aldehydes, hemiketals, ketals, alkenes, alcohols and epoxides with Lewis or Brønstedt acids.[7,8] This reaction was applied for the synthesis of a variety of nitrogen containing heterocycles and naturally occurring alkaloids.[9,10] The regioselectivity of the carbon-to-nitrogen 1,2-shift was rationalized by assuming a concerted migration mechanism over a nitrenium formation. In the concerted process, migration of a bond that is approximately antiperiplanar[1,11] to the departing nitrogen in the aminodiazonium ion being preferred (Scheme 7.1, **A**).[6] No regioselectivity was observed for the reaction leading to indolizidine from tertiary alcohols (Scheme 7.1, **B**), this was rationalized by a non-regioselective 1,2-shift of the intermediate spirocyclic aminodiazonium salt resulting from the rearrangement of the initially formed cation followed by reaction with the azide. In such a system, the aminodiazonium salt is believed to exist as a rapidly equilibrating mixture of epimers at the nitrogen atom.[6] This assumption is in accordance with calculations by Glaser, who reported that the activation barrier on the pyramidal nitrogen is low.[7] The stereochemical outcome of the intramolecular Schmidt reaction has also been examined by Aubé, who discussed the preferential migration of the on-tether

substituent and reported that the stereochemistry at the migrating carbon was preserved similarly to what is observed for other sextet rearrangement processes.[8] More interestingly, by using chiral 1,2- and 1,3-azidoalcohols, good to excellent control of the stereochemistry could be obtained for the desymmetrization of 4-substituted cyclohexanone (Scheme 7.1, **C**).[9,10,12] This process requires formation of an aminodiazonium cation bearing a chiral center next to the azido group followed by a stereoselective 1,2-shift. The C–C bond *anti* to the phenyl group at the chiral center of the azidoalcohol is migrating. Assuming antiperiplanar migration suggests that the migration involves a conformation where the diazonium substituent is lying *cis* to the phenyl ring.

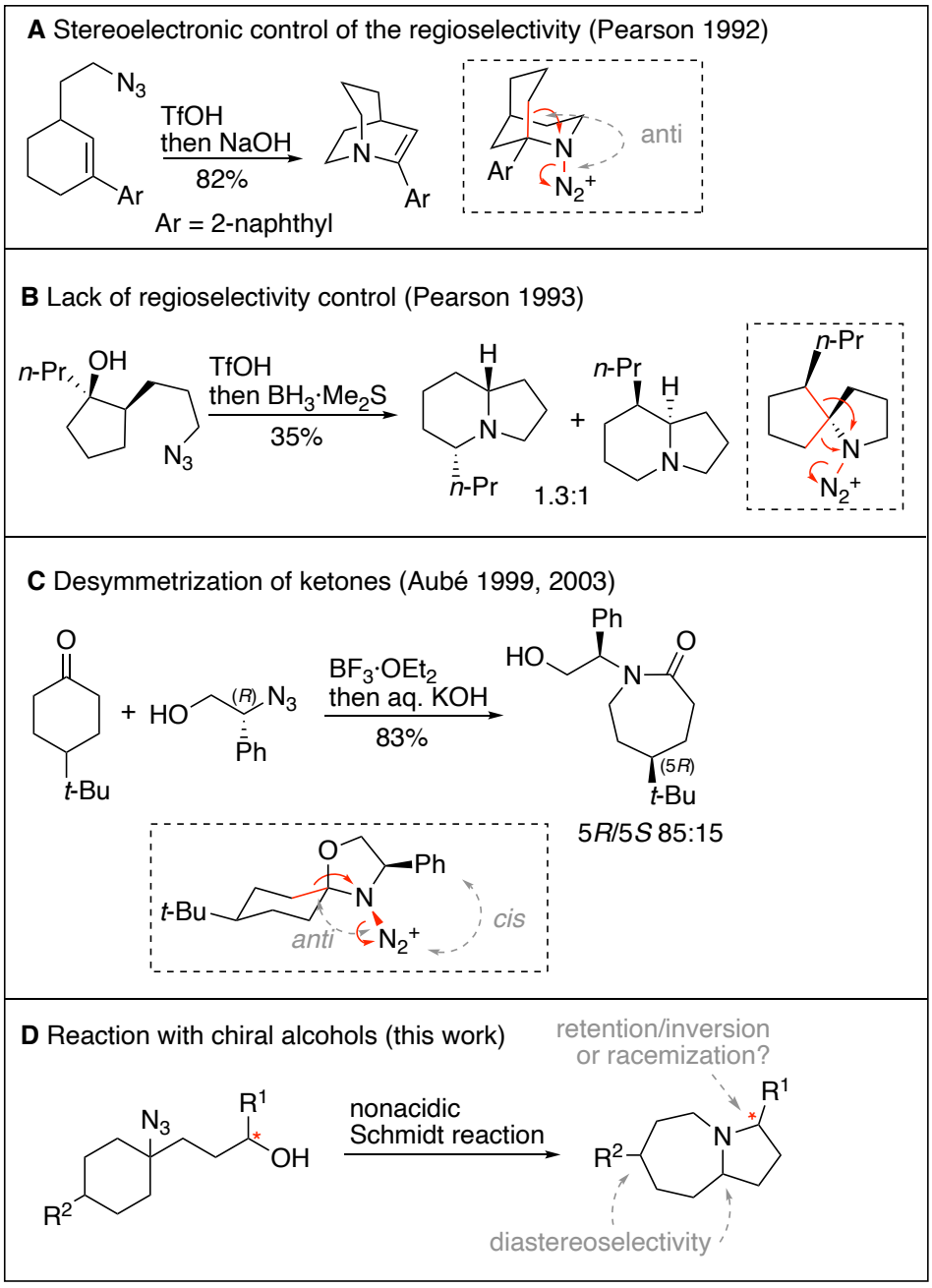

Scheme 7.1. Regio- and stereoselectivity of the intramolecular Schmidt reaction

In a recent paper, we reported a modified protocol in which the Schmidt reaction is run under nonacidic conditions by converting azidoalcohols into azidotriflates that rearrange spontaneously. This approach allows to avoid rearrangement of the intermediate carbocations (see Scheme 7.1, **B**) and was used for a concise synthesis of indolizidine 167B.[11] Interestingly, racemization caused by the formation of carbocation intermediates is expected to be suppressed opening new opportunities for asymmetric Schmidt reactions involving chiral azidoalcohols. For instance, the preparation of enantiomercially enriched substituted octahydro-1*H*-pyrrolo[1,2-a]azepine,[12] a skeleton found in many alkaloid natural products such as *Stemona* alkaloids[13] and dendrobatid frog alkaloids,[14,15] is expected to be possible starting from easily available azidoalcohols such as 1-substituted 3-(1-azidocyclohexyl)propan-1-ols (Scheme 7.1, **D**). We report here that such reactions involving a chiral alcohol as unique element of asymmetry are highly diastereoselective and take place with no or very limited racemization.

7.3 Results and discussion

7.3.1 Reactivity of the system and 1,2-stereocontrol of the iminium reduction by an adjacent silyloxy group

The reaction conditions were optimized with the dioxolanyl acetal **1**. Under our optimized conditions,[11] the octahydropyrroloazepine **2** was obtained in good yield using DIBAL as a reducing agent (Scheme 7.2).

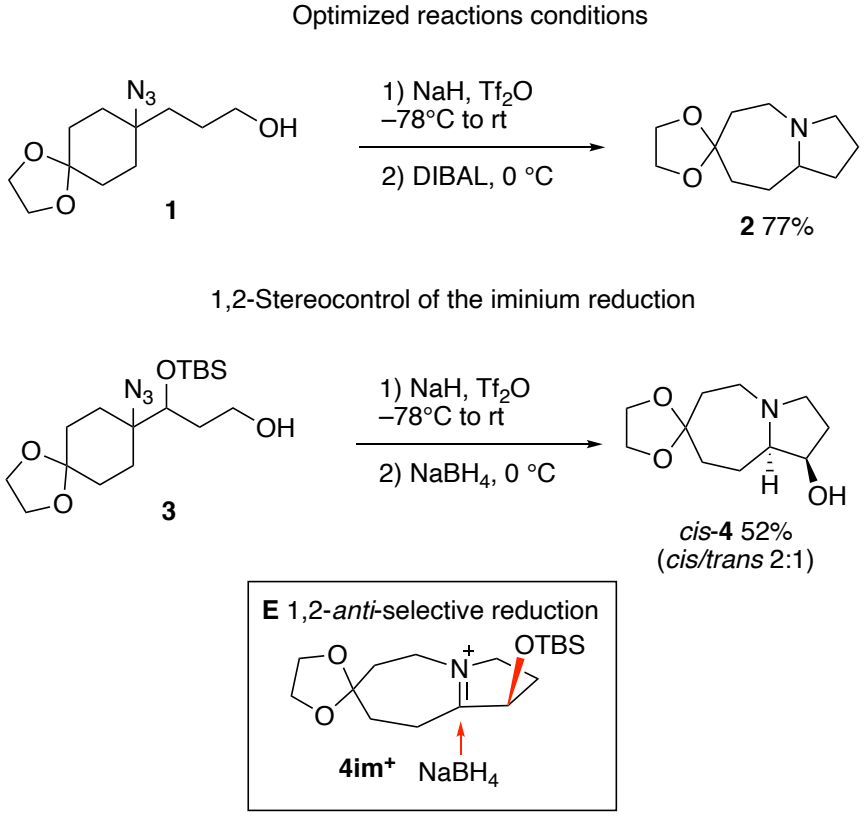

*Scheme 7.2. Formation of pyrrolo[1,2-a]azepine **2** and **4** and stereoselectivity of the reduction of the iminium salt **4im**⁺*

Starting from the azidoalcohol **3** containing an asymmetric center adjacent to the azido group, a moderate stereocontrol for the hydride addition to iminium ion **4im**$^+$ using $NaBH_4$ leading to *cis*-**4** (after desilylation) was observed. As expected, the hydride delivery is taking place *anti* to the bulky silyloxy group (Scheme 7.2, **E**). Increasing the control of the diastereoselectivity using DIBAL was not attempted.

7.3.2 1,4-Stereocontrol of the iminium reductions and stereoselective 1,2-shift

When the acetal is replaced by a phenyl group, the starting material **5** remains achiral but the iminium ion intermediate **6im**$^+$ is chiral. Therefore, the stereochemical outcome of the reduction of the iminium ion **6im**$^+$ is controlled via a 1,4-induction process. Product **6** was formed with a moderate stereocontrol when reacted with $NaBH_4$, $NaBH_3CN$ and $LiAlH_4$. An excellent *cis* stereocontrol was obtained with DIBAL (Table 7.1).

*Table 7.1. 1,4-Stereocontrol during the Schmidt reaction converting azidoalcohol **5** to pyrrolo[1,2-a]azepine **6***

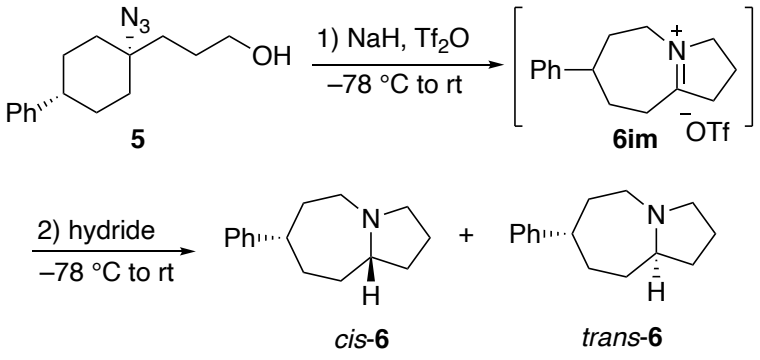

Entry	Reagent	Yield[a]	*cis*/*trans*[b]
1	$NaBH_4$	n.d.	67:33
2	$NaBH_3(CN)$	n.d	64:36
3	$LiAlH_4$	60%	84:16
4	DIBAL	98%	>95:5

[a]) Isolated yields. [b]) Determined by 1-H-NMR analysis of the crude products.

The very high *cis* diastereoselectivity observed for the reduction of the iminium ion **6im**$^+$ (1,4-induction) is puzzling. Two hypothesis were considered to explain the favoured *anti* addition (relative to the phenyl group) of the hydride: 1) strong cation-π interactions between the phenyl group and the iminium ion favour a conformation where one face of the iminium ion is shielded; 2) an extended conformation presenting a more reactive convex face. To clarify this point, a detailed analysis of the conformational space of cation **6im**$^+$ was performed (see supporting information for full details). All the QM results are reported at the PCM(CH_2Cl_2,ua0)/DLPNO-CCSD(T)/cc-pVTZ//B3LYP-D3/6-31G(d) level of theory. The best cation-π interaction-induced folded conformation is 12.5 kJ/mol and 18.3 kJ/mol higher in terms of enthalpy (ΔH_{sol}) and free energy (ΔG_{sol}) with respect to the global minimum extended conformation

(Figure 7.1). Thus, preference for a folded conformation of iminium cation (**6im**$^+$) due to cation-π interactions as initially hypothesized is not supported by these results. Restricted conformational analysis of iminium salt **6im** indicates that triflate anion prefers to coordinate to the concave face of the iminium ion intermediate, however the energy difference between the concave/convex coordination of the triflate anion is low (1.0 kJ mol^{-1}). This conformation was also found to be prevalent in the solid-state structure of **6im** determined by single crystal X-ray analysis (Figure 7.1).[16] In the lowest energy conformer of iminium salt **6im**, the face *syn* to the phenyl group is blocked by triflate anion, thus favouring the formation of the *cis* product through *anti* addition of the hydride (Model **F**).

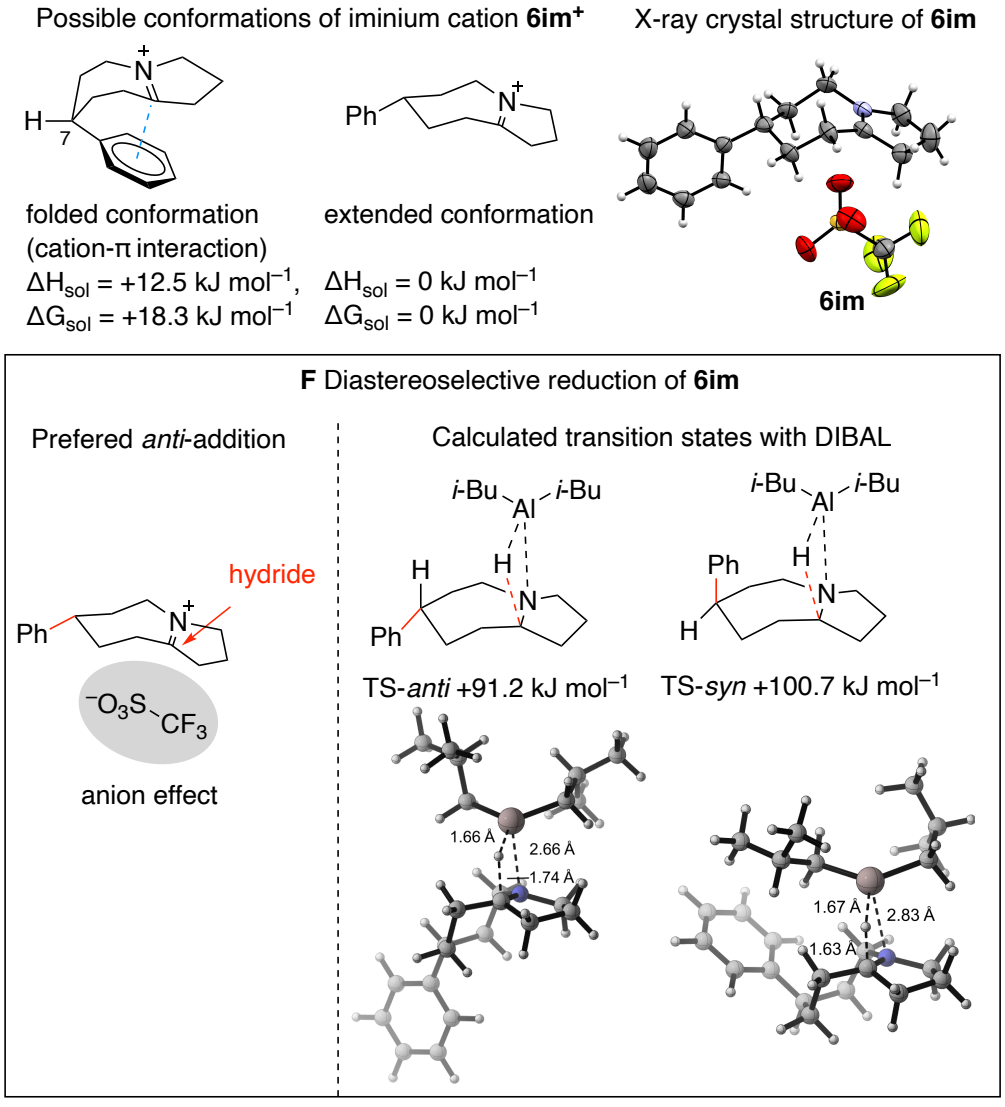

*Figure 7.1. Conformational energetics of iminium cation **6im**$^+$. X-ray structure analysis of **6im** (ellipsoids drawn at 50% probability) and proposed model for 1,4-induction during hydride addition to **6im** as well as calculated anti and syn transition state barriers (based on best conformer) for the reaction of **6im**$^+$ with DIBAL. Calculations have been performed at the PCM(CH_2Cl_2,ua0)/DLPNO-CCSD(T)/cc-pVTZ//B3LYP-D3/6-31G(d) level of theory.*

Calculation of transition state energies were performed to get a better understanding of the factors governing the stereochemistry of the reduction of **6im**$^+$ with DIBAL. Reaction barriers calculated for the reduction of cation **6im**$^+$ with DIBAL predict a 9.5 kJ mol^{-1} preference for the formation of *cis*-**6** (TS-*anti*)

relative to *trans*-**6** (TS-*syn*) (Figure 7.1). Both transition states involve hydride addition from the convex face of the iminium ion and destabilization of TS-*syn* over TS-*trans* may be attributed to steric interaction with the phenyl substituent on the convex (*exo*) face. These results imply that the experimentally observed stereoselectivity is a kinetic phenomenon, *cis*-**6**·Al(*i*-Bu)$_2^+$ being less stable than *trans*-**6**·Al(*i*-Bu)$_2^+$ by 10.9 kJ mol^{-1} in CH_2Cl_2 (see supporting information).

The Schmidt reaction with the OTBS substituted alcohol **7** containing a single asymmetric center at C(1) (product numbering) was investigated. The configuration of the starting material **7** was assigned by single crystal X-ray analysis of the 3,5-dinitrobenzoate ester **7dnb**.[16]

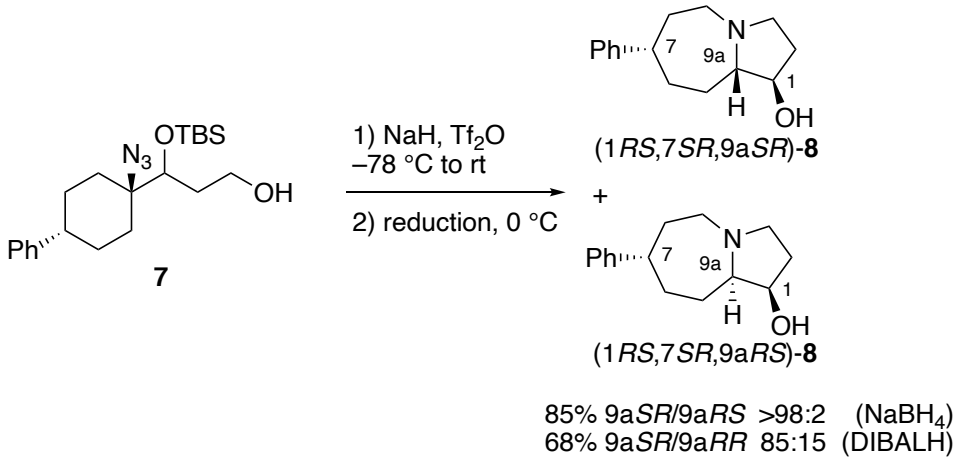

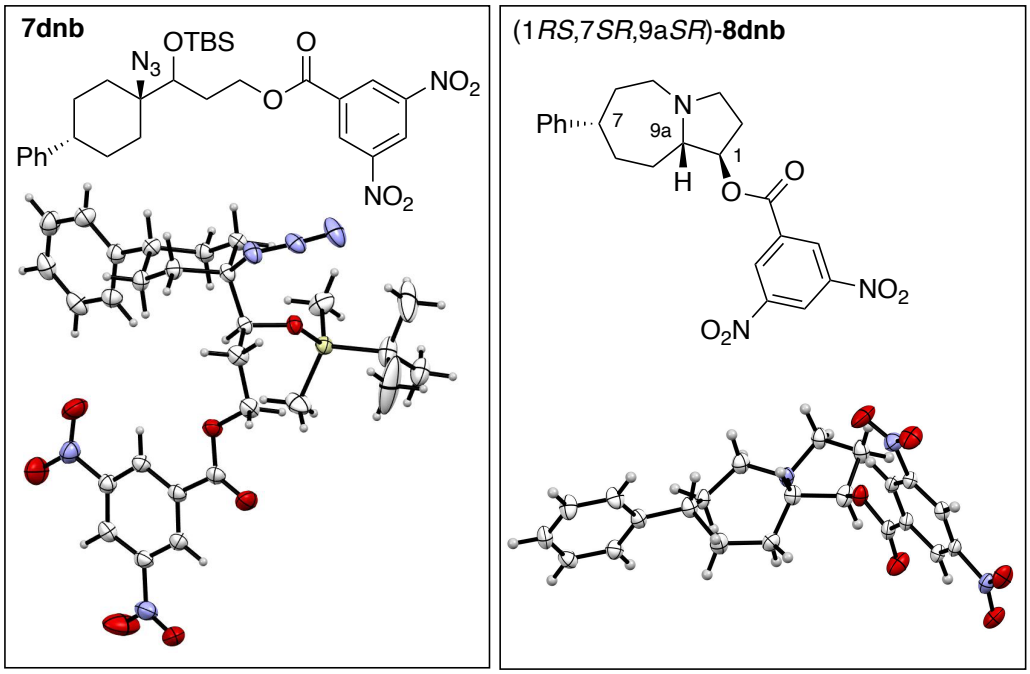

*Scheme 7.3. Stereochemical outcome of the intramolecular Schmidt reaction with **7**. X-ray structure analysis of **7dnb** and **8dnb** (major diastereomer) (ellipsoids drawn at 50% probability)*

During the Schmidt reaction, a second chiral center at C(7) is created during the 1,2-migration process and a third one at C(9a) is introduced during the final hydride addition step. Desilylation during workup eventually leads to aminoalcohol **8**. When the reaction was run with DIBAL, a mixture of 2 diastereomers (out of the four possible) in a 85:15 ratio was observed. By running the final iminium reduction step with

$NaBH_4$, a single diastereomer was obtained (Scheme 7.3). The 3,5-dinitrobenzoate ester **8dnb** was prepared from the major isomer of **8** by acylation with 3,5-dinitrobenzoyl chloride. Its relative (1*RS*,7*SR*,9a*SR*) configuration could be determined unambiguously by single crystal X-ray analysis (Scheme 7.3).[16] Based on the relative configuration of the starting azide **7** (azido group *trans* to the phenyl substituent, see X-ray structure of **7dnb** in Scheme 7.3) and the relative configuration of the final product **8** (see X-ray structure of **8dnb** in Scheme 7.3), one can conclude that the C–C bond *anti* to the OTBS group is migrating (Figure 7.2, **G**) and that the final hydride addition to the iminium ion **7im**$^+$ is taking place *anti* to the phenyl group (1,4-induction) and *syn* to the adjacent OTBS group.

The remarkable diastereoselectivity of the 1,2-migration process is supported by reaction path calculations. Migration of the *anti* C–C bond in the aminodiazonium ion **7ad**$^+$ enjoys a barrier advantage of at least 15 kJ mol^{-1} (see Figure 7.2, **G**). This barrier difference is largely similar in the gas phase or in solution and may thus derive predominantly from differences in the alignment of the reacting C–C and C–N bonds with the surrounding substrate scaffold. The ring nitrogen atom is significantly more pyramidal in the TS as compared to the aminodiazonium precursor, and then becomes almost planar in the product iminium ion (see SI for more details).[17] It should be added that the energetic benefit of the *anti* over the *syn* transition state is completely lost upon formation of the respective iminium ions *cis*-**8im**$^+$/*trans*-**8im**$^+$ (which are found to be isoenergetic). The final hydride addition to the iminium ion *trans*-**8im**$^+$ is taking place *anti* to the phenyl group (1,4-induction) and *syn* to the adjacent OTBS group. This process was examined through theoretical calculations in CH_2Cl_2 solution.[18] The ten energetically most favourable conformations of this cation are of the extended type, which precludes control of the reduction step through a folded transition state (see supporting information).
Conformational analysis of the full ion pair *trans*-**8im**, however, indicates that the silyloxy substituent present in this system directs the triflate anion exclusively to the *anti* (relative to OTBS or bottom) face of the iminium ion. The energetically best conformer with the triflate anion in top location is located 19.5 kJ mol^{-1} higher in energy, which is in full support of the model presented in Figure 7.2 **H**. The use of a smaller reducing agent ($NaBH_4$) instead of DIBAL favours the top face approach by minimizing destabilizing interactions with the OTBS group.

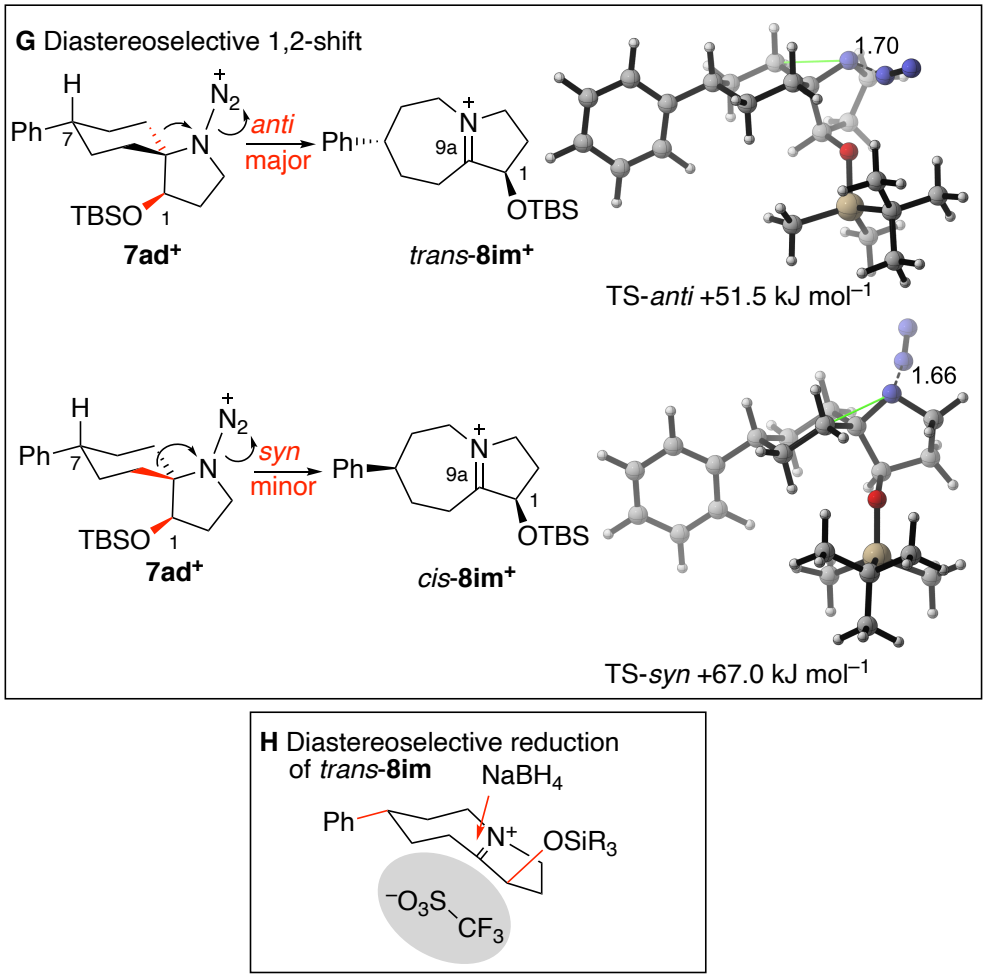

*Figure 7.2. Rationalization of the stereochemical outcome of the conversion of **7** to **8** and transition state barriers (ΔG_{sol} , in kJ mol^{-1}) for concerted C to N bond migration (anti and syn relative to OTBS group) calculated at the PCM(CH_2Cl_2,ua0)/DLPNO-CCSD(T)/cc-pVTZ//B3LYP-D3/6-31G(d) level of theory.*

7.3.3 Stereospecificity of the Schmidt reaction involving chiral alcohols

In Pearson's version of the intramolecular Schmidt reaction, the alcohol center is converted to a cation, therefore this center cannot be used to control the absolute configuration of the final product.[6] The triflate mediated version of the Schmidt reaction offers a possibility to use a chiral alcohol to control the absolute configuration of the products since the reaction most probably does not involve the formation of a cationic intermediate (at least for primary and secondary alcohols). To test this hypothesis, four different chiral alcohols **10**–**13** bearing a single chiral center at the alcohol position were prepared (Scheme 7.4). Alcohols (*S*)-**10** and **11** were prepared by a (–)-*N,N*-dibutyl-*D*-norephedrine ((–)-DBNE) and (+)-*N*-methyl ephedrine catalyzed enantioselective addition[19–22] of Et_2Zn ((*S*)-**10**) and phenylacetylene ((*R*)-**11**) to the aldehyde **9** prepared by oxidation of the primary alcohol **5**. Brown asymmetric allylboration[23] of **9** afforded the homoallylic alcohol (*R*)-**12**. Finally, the benzylic alcohol (*R*)-**13** was prepared from ketone **14** via CBS-mediated enantioselective reduction.[24] The absolute configurations of **10**–**13** were attributed based on reported stereochemical outcome of similar reactions.

For compound **10**, single crystal X-ray analysis of the 4-bromo-3-nitrobenzoate ester **10bnb**[16] confirmed its (*S*)-absolute configuration in accordance with expectations.[25]

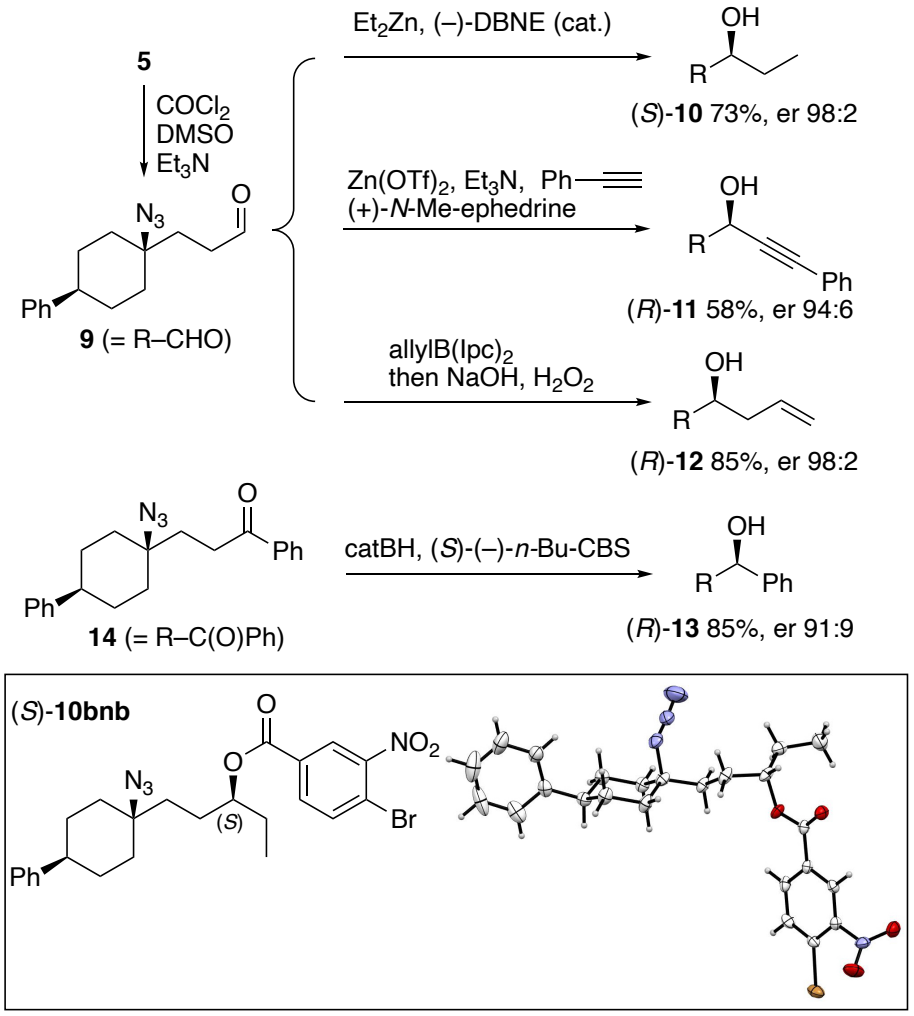

*Scheme 7.4. Preparation of chiral alcohols **10–13**. X-ray structure analysis of (S)-**10bnb** (ellipsoids drawn at 50% probability).*

The intramolecular Schmidt reaction involving **10–13** was investigated next (Table 7.2). Under the standard reaction conditions, all four alcohols gave the desired bicyclic amides **15–18** in 32–85% yield as a single diastereomer. Interestingly, the enantiomeric ratio of the starting material was fully preserved for **15** and **16** and only slight loss of optical purity was observed for **17** and even more remarkably for **18** derived from the benzylic alcohol **13**. The absolute configuration of **15** could be established using single crystal X-ray analysis of its (*R*)-mandelic acid salt (Figure 7.3).[16]

*Table 7.2. Intramolecular Schmidt reaction involving enantioenriched chiral alcohols **10–13***

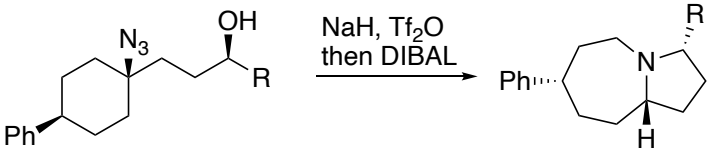

10–13 **15–18**

Entry	Alcohol	R	er[b]	Product	Yield[a]	er[c]
1	(*S*)-**10**	Et	98:2	**15**	85%	93:7
2	(*R*)-**11**	PhC≡C	94:6	**16**	32%	95:5
3	(*R*)-**12**	CH_2=$CHCH_2$	98:2	**17**	79%	92:8
4	(*R*)-**13**	Ph	91:9	**18**	71%	78:22

a) Isolated yields. b) Determined by HPLC analysis. c) Determined by GC analysis.

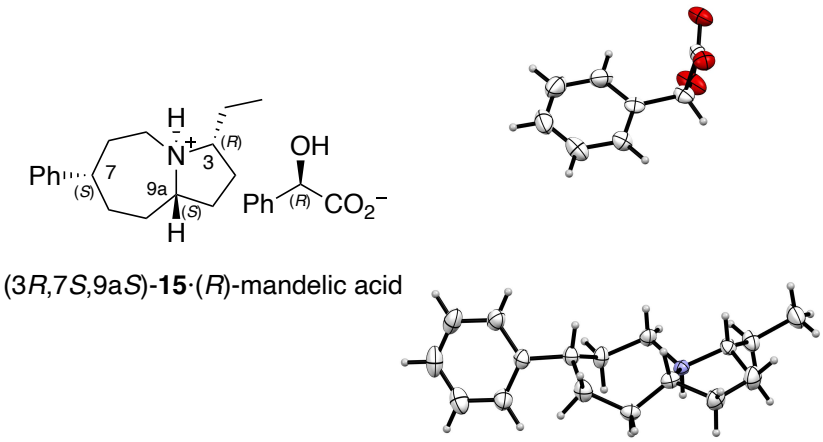

(3*R*,7*S*,9a*S*)-**15**·(*R*)-mandelic acid

*Figure 7.3. Determination of the absolute configuration of (3R,7S,9aS)-**15** by X-ray structure analysis of its (R)-mandelic salt (ellipsoids drawn at 50% probability).*

The absolute configurations (*S*)-**10** and (3*R*)-**15** demonstrate that the intramolecular Schmidt reaction proceeds with inversion of configuration at the alcohol stereocenter. This indicates that an S_N2-type mechanism is involved in the formation of the intermediate spirocyclic aminodiazonium salt **10ad**$^+$ (Figure 7.4, **I**). Even the benzylic alcohol **13** reacts mainly via an S_N2 pathway since only limited racemization is observed. The diastereoselectivity of 1,2-shift is then controlled by the C(3) chiral center according to Figure 7.4 (**J**). Selective migration of the C–C bond *anti* to the substituent at position 3 is observed. Since migration is expected to occur *anti* to the N–N_2^+ bond, it suggests that the C(3) substituent and the diazonium residue are *cis* to each other in the reactive conformation of the aminodiazonium intermediate **10ad**$^+$. This result is in accordance with Aubé's results discussed in Scheme 7.1 (**C**),[10] and also fully supported by theoretical calculations of the reaction energy profiles (see supporting information).[18] The *anti*-migration pathway is found to be 8.5 kJ mol^{-1} more favourable than the respective *syn*-migration pathway (Figure 7.4, **J**). Finally, the reduction leading to the formation of the third asymmetric center at C(9a) is fully controlled by cooperative 1,4- and 1,3-induction processes from C(3) and C(7) (Figure 7.4, **K**).

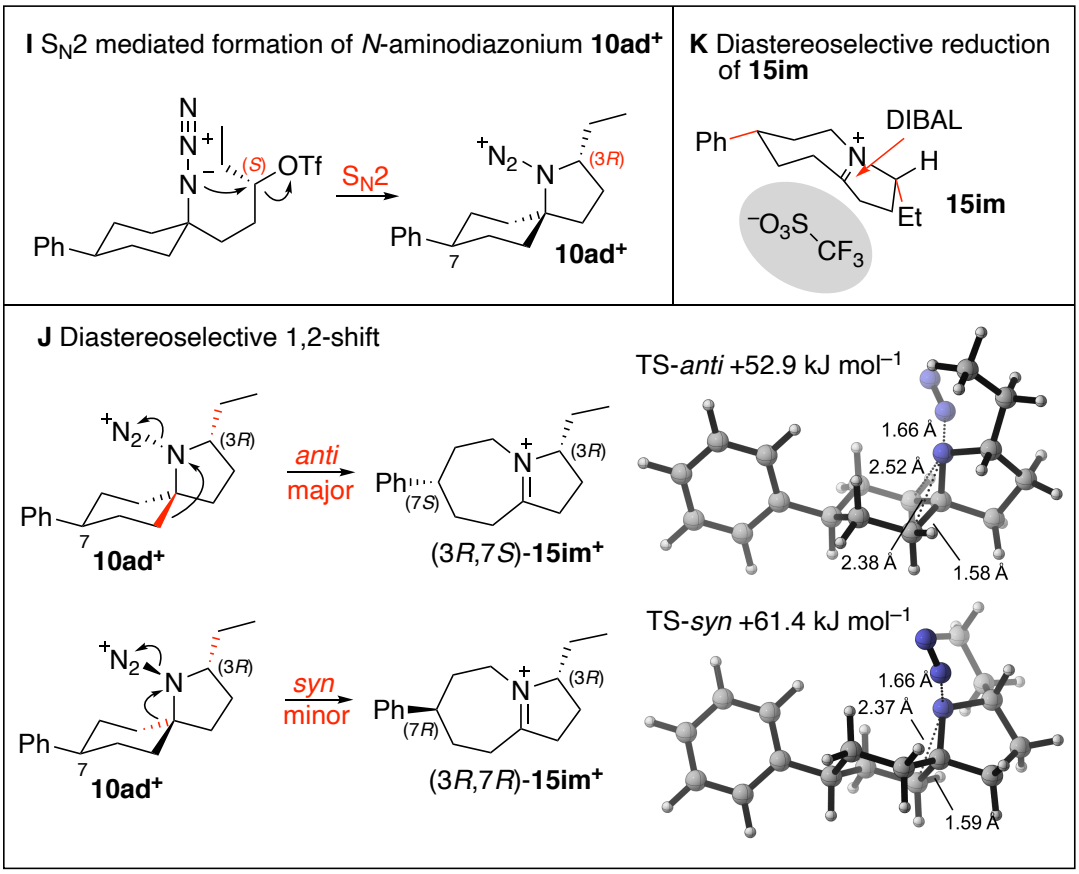

*Figure 7.4. Stereochemical outcome of the reactions with chiral alcohol **10**. Transition state barriers (ΔG_{sol}, in kJ mol^{-1}) calculated at the PCM(CH_2Cl_2,ua0)/DLPNO-CCSD(T)/cc-pVTZ//B3LYP-D3/6-31G(d) level of theory.*

7.3.4 Concise synthesis of indolizidine and lehmizidine alkaloids

To demonstrate the potential of our stereospecific and stereoselective intramolecular Schmidt reaction, the synthesis of two alkaloids, 3-propylindolizidine (*cis*)-**19** and *epi*-3-butyllehmizidine (*cis*)-**20** was attempted. These two alkaloids were discovered in the venom of workers of the ant *Myrmicaria melanogaster* from Brunei.[26] The relative configuration of the naturally occurring (*cis*)-**19** and (*trans*)-**20** was attributed based on a non-stereoselective synthesis of racemic (*trans/cis*)-**19** and (*trans/cis*)-**20** and their absolute configuration remains unknown to date.[26] (–)-(3*R*,8a*S*)-**19** was prepared from methylenecyclopentane (Scheme 7.5, **K**). The aldehyde **21** was prepared in 53% overall yield via radical mediated azidoalkylation, reduction with $LiBH_4$ and Swern oxidation. Brown asymmetric allylboration[23] with (–)-$(Ipc)_2BCl$/(allyl)MgBr afforded the key enantiorenriched azidoalcohol (*R*)-**22** in 58% yield (er 94:6). Treatment of (*R*)-**22** with NaH and Tf_2O followed by DIBAL reduction of the iminium ion intermediate gave the 3-allylindolizidine (3*R*,8a*S*)-**23** as a single diastereomer and highly preserved enantiomeric ratio (er 91:9). Finally, hydrogenation of the allyl group afforded the naturally occurring (–)-(3*R*,8a*S*)-**19** (or its enantiomer) that was fully characterized. The same strategy starting from methylenecyclohexane was used for the synthesis of (3a*R*,9a*S*)-3-butyllehmizidine (3a*R*,9a*S*)-**20**, the (C3) (or C(8a)) epimer of the naturally occurring (*trans*)-**20** (Scheme 7.5, **L**). In this case, the alcohol (*R*)-**25** (er 93:7) was obtained by enantioselective butylation of aldehyde **24** with a preformed dibutylzinc

solution in the presence of (–)-DBNE. To the best of our knowledge, this is the first time such an enantioselective alkylation has been run directly with a crude non-distilled dialkylzinc solution generated from the corresponding primary alkyllithium.[27,28] Conversion of (*R*)-**25** to the *epi*-3-butyllehmizidine (–)-(3*R*,9a*S*)-**20** was performed according to our standard reaction conditions (NaH/Tf_2O) using DIBAL in the final reduction step. As anticipated, the reaction is completely diastereoselective and the product enantiomeric purity (er 91:9) matches closely the one of the starting alcohol (*R*)-**25**.

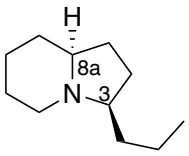

(*cis*)-3-propylindolizidine (*Z*)-**19**

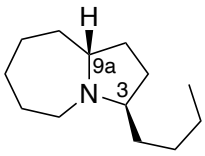

(*trans*)-3-butyllehmizidine (*E*)-**20**

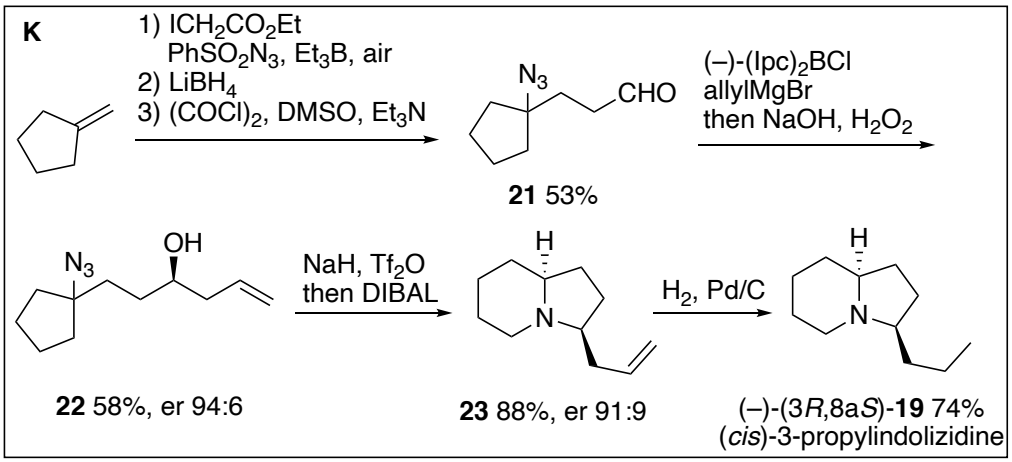

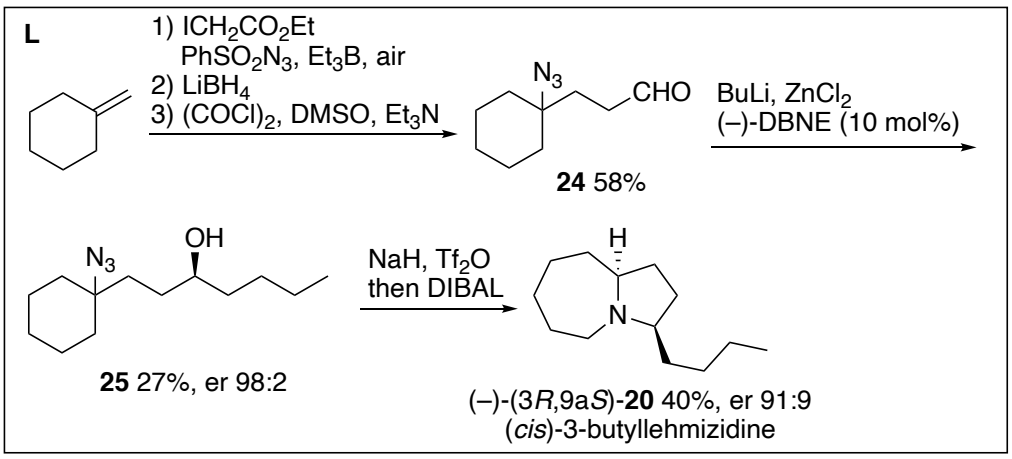

*Scheme 7.5. Synthesis of enantioenriched 3-alkylated indolizidine-(Z)-**19** and lehmizidine (Z)-**20** alkaloids*

7.4 Conclusion

We have demonstrated that the triflate mediated intramolecular Schmidt reaction can be highly diastereoselective when a chiral center is present in the carbon chain linking the azide and the alcohol. Interestingly, when the chirality is at the alcohol center, the process involves an initial intramolecular S_N2 reaction between the azide moiety and the triflate. Starting from easily available enantiopure chiral secondary alcohols, azacycles are obtained with inversion of the stereocenter with no or limited

racemization. With suitable substrates, highly diastereoselective 1,2-alkyl shifts are observed. Finally, the stereochemistry of the final reduction step using a hydride source is also fully diastereoselective, allowing to prepare selectively in a single step one out of the four possible diastereoisomers of disubstituted octahydro-1*H*-pyrrolo[1,2-a]azepine in a highly enantioenriched form. The stereospecific intramolecular Schmidt reaction has been applied for the first diastereo- and enantioselective syntheses of the naturally occurring alkaloid (*Z*)-3-propylindolizidine and for (*Z*)-3-butyllehmizidine, the epimer of the isolated natural compound.

7.5 Acknowledgements

The Swiss National Science Foundation (Project 200020_172621) is gratefully acknowledged for financial support. Konrad Uhlmann is acknowledged for performing GC and HPLC analyses. We thank the group of Chemical Crystallography of the University of Bern (Prof. Dr. P. Macchi) for the X-ray structure solution as well as PD Dr. Simon Grabowsky, Dr. Michal Andrzejewski and Dr. Michelle Ernst for their help in solving X-ray crystal structures. We thank Prof. Eva Hevia and Leonie Bole for helpful discussions about organozinc reagents. We would also like to thank the Leibniz Supercomputing Centre (www.lrz.de) for generous allocation of computational resources.

Keywords: azide • Schmidt reaction • stereochemistry • 1,2-migration • azabicyclic compounds • alkaloids

7.6 References

[1] J. Aubé, G. L. Milligan, *J. Am. Chem. Soc.* **1991**, *113*, 8965–8966.

[2] W. H. Pearson, J. M. Schkeryantz, *Tetrahedron Lett.* **1992**, *33*, 5291–5294.

[3] S. Grecian, J. Aubé, in *Org. Azides*, John Wiley & Sons, Ltd, **2010**, pp. 191–237.

[4] E. Nyfeler, P. Renaud, *CHIMIA* **2006**, *60*, 276–284.

[5] R. V. Hoffman, A. Kumar, *J. Org. Chem.* **1985**, *50*, 1859–1863.

[6] W. H. Pearson, R. Walavalkar, J. M. Schkeryantz, W. K. Fang, J. D. Blickensdorf, *J. Am. Chem. Soc.* **1993**, *115*, 10183–10194.

[7] R. Glaser, G. S. C. Choy, *J. Phys. Chem.* **1991**, *95*, 7682–7693.

[8] G. L. Milligan, C. J. Mossman, J. Aubé, *J. Am. Chem. Soc.* **1995**, *117*, 10449–10459.

[9] K. Furness, J. Aubé, *Org. Lett.* **1999**, *1*, 495–498.

[10] K. Sahasrabudhe, V. Gracias, K. Furness, B. T. Smith, C. E. Katz, D. S. Reddy, J. Aubé, *J. Am. Chem. Soc.* **2003**, *125*, 7914–7922.

[11] A. Kapat, E. Nyfeler, G. T. Giuffredi, P. Renaud, *J. Am. Chem. Soc.* **2009**, *131*, 17746–17747.

[12] R. Liu, O. Gutierrez, D. J. Tantillo, J. Aubé, *J. Am. Chem. Soc.* **2012**, *134*, 6528–6531.

[13] R. A. Pilli, G. B. Rosso, M. D. C. F. De Oliveira, in *Alkaloids Chem. Biol.* (Ed.: G.A. Cordell), Academic Press, **2005**, pp. 77–173.

[14] T. H. Jones, H. L. Voegtle, H. M. Miras, R. G. Weatherford, T. F. Spande, H. M. Garraffo, J. W. Daly, D. W. Davidson, R. R. Snelling, *J. Nat. Prod.* **2007**, *70*, 160–168.

[15] H. M. Garraffo, P. Jain, T. F. Spande, J. W. Daly, Tappey. H. Jones, L. J. Smith, V. E. Zottig, *J. Nat. Prod.* **2001**, *64*, 421–427.

[16] **N.d.**, CCDC 2011652, 2011804, 2011803, 2011282, and 2011286 contain the supplementary crystallographic data for compound 6im, 7dnb, 8dnb, 10bnb, and 15·(R)-mandelic acid. These data can be obtained free of charge from The Cambridge Crystallographic Data Centre via http://www.ccdc.cam.ac.uk/data_request/cif.

[17] O. Gutierrez, J. Aubé, D. J. Tantillo, *J. Org. Chem.* **2012**, *77*, 640–647.

[18] **N.d.**, All geometry optimizations and calculations of thermochemical corrections to 298.15 K have been performed at the B3LYP-D3/6-31G(d) level of theory. Refined energy calculations base on these geomnetries have then been performed with the DLPNO-CCSD(T)/cc-pVTZ method. Calculations of solvation free energies for dichloromethane (DCM, CH2Cl2) solution employ the gas phase geometries and the IEFPCM continuum solvation model with UA0 radii. Combination of the solvation free energies with the gas phase free energies calculated at DLPNO-CCSD(T)/cc-pVTZ level yields the free energies in solution (G298) mentioned in the text (see SI file for further details).

[19] R. Noyori, *Asymmetric Catalysis in Organic Synthesis*, Wiley, New York, **1994**.

[20] K. Soai, Y. Kawase, A. Oshio, *J. Chem. Soc. Perkin 1* **1991**, 1613–1615.

[21] K. Soai, S. Niwa, *Chem. Rev.* **1992**, *92*, 833–856.

[22] K. Soai, T. Hayase, K. Takai, T. Sugiyama, *J. Org. Chem.* **1994**, *59*, 7908–7909.

[23] H. C. Brown, P. K. Jadhav, *J. Am. Chem. Soc.* **1983**, *105*, 2092–2093.

[24] E. J. Corey, C. J. Helal, *Angew. Chem. Int. Ed.* **1998**, *37*, 1986–2012.

[25] K. Soai, T. Shibata, *J. Synth. Org. Chem. Jpn.* **1997**, *55*, 994–1005.

[26] T. H. Jones, H. L. Voegtle, H. M. Miras, R. G. Weatherford, T. F. Spande, H. M. Garraffo, J. W. Daly, D. W. Davidson, R. R. Snelling, *J. Nat. Prod.* **2007**, *70*, 160–168.

[27] E. Negishi, D. R. Swanson, C. J. Rousset, *J. Org. Chem.* **1990**, *55*, 5406–5409.

[28] G. Valot, D. Mailhol, C. S. Regens, D. P. O'Malley, E. Godineau, H. Takikawa, P. Philipps, A. Fürstner, *Chem. – Eur. J.* **2015**, *21*, 2398–2408.

7.7 Experimental section

Supplementary information about the computational methods can be found in the appendix.

7.8 Experimental section

Supplementary information about the computational methods can be found in the appendix.

General information

Techniques

All reactions requiring anhydrous conditions were performed in heat-gun, oven or flame dried glassware under an argon atmosphere. An ice bath was used to obtain a temperature of 0 °C. To obtain a temperature of –78 °C, a bath of acetone was cooled with dry ice. To obtain temperatures of –40 °C and –15 °C, a bath of isopropanol or acetonitrile was cooled to the desired temperature using dry ice. Silica gel 60 Å (40–63 µm) from Silicycle was used for flash column chromatography. Deactivated silica gel: The abovementioned silica gel was suspended in in Et_2O and 20w% of HMDS, then filtered, washed with Et_2O and dried on HV overnight. Deactivated TLC plates: silica plates are dipped in 7M NH_3 in MeOH and then dried. Thin layer chromatography (TLC) was performed on Silicycle silica gel 60 F254 plates, visualization under UV light (254 nm) and/or by dipping in a solution of $(NH_4)_2MoO_4$ (15.0 g), $Ce(SO_4)_2$ (0.5 g), H_2O (90 mL), conc. H_2SO_4 (10 mL); or $KMnO_4$ (3 g), K_2CO_3 (20 g) and NaOH 5% (3 mL) in H_2O (300 mL) and subsequent heating. Anhydrous sodium sulfate was used as drying reagent.

Materials

Commercial reagents were used without further purification unless otherwise stated. Dry solvents for reactions were filtered over columns of dried alumina under a positive pressure of argon. Solvents for extractions (Et_2O, *n*-pentane, CH_2Cl_2, EtOAc) and flash column chromatography were of technical grade and distilled prior to use. Commercial dry DMF was used without further purification.

Instrumentation

^1H and ^{13}C NMR spectra were recorded on a Bruker Avance IIIHD-300 spectrometer operating at 300 MHz for ^1H and 75 MHz for ^{13}C at room temperature (24-25°C) unless otherwise stated. Some ^1H and ^{13}C NMR spectra were recorded on a Bruker Avance IIIHD-400 or a Bruker Avance II-400 spectrometer (^1H: 400 MHz; ^{13}C: 75 MHz). Chemical shifts (δ) are reported in parts per million (ppm) using the residual solvent or $Si(CH_3)_4$ (δ = 0.00 for ^1H NMR spectra) as an internal standard. Multiplicities are given as s (singlet), d (doublet), t (triplet), q (quadruplet), m (multiplet), and br (broad). Coupling constant (*J*) is reported in Hz. In ^{13}C-NMR spectra, the peak positions are reported on one decimal unless the difference in chemical shift between two signals is small and required two decimals. Infrared spectra were recorded on a Jasco FT-IR-460 plus spectrometer equipped with a Specac MKII Golden Gate

Single Reflection Diamond ATR system and are reported in wave numbers (cm^{-1}). At maximum, the ten most prominent peaks are reported. Low resolution mass spectra were recorded on a Waters Micromass Autospec Q mass spectrometer in EI mode at 70 eV or were taken from GC-MS analyses performed on a Finnigan Trace GC-MS (quadrupole mass analyzer using EI mode at 70 eV) fitted with a Macherey-Nagel Optima delta-3-0.25 µm capillary column (20 m, 0.25 mm); gas carrier: He 1.4 mL/min; injector: 220 °C split mode. GC analyses were performed on a ThermoFisher Trace GC ultra, fitted with a chiral Restek Rt®-bDEXm capillary column (20 m, 0.25 mm ID, 0.25 µm), helium as carrier gas (1.2 mL/min), and FID (290 °C base temperature, 35 mL/min H_2, 350 mL/min air); temperature gradients are indicated for each compound. HRMS analyses and accurate mass determinations were mode). Melting points were measured on a Büchi B-545 apparatus and are corrected. Syringe filters with polytetrafluoroethylene membrane were used with a pore size of 0.45µm from Machery-Nagel (CHROMAFIL®Xtra PTFE 0.45). Medium pressure liquid chromatography (MPLC) was performed with a CombiFlash® Rf+ system from Teledyne Isco using RediSep® single-use normal phase columns.

Syntheses

Azidoalcohols **1** and **5**, di-*tert*-butyl hyponitrite (DTBHN), and 3-pyridine sulfonyl azide ($PySO_2N_3$) were prepared as we have reported previously.[1]

Preparation of 3

2-(Phenylsulfonyl)-1,7,10-trioxadispiro[2.2.46.23]dodecane (S1)

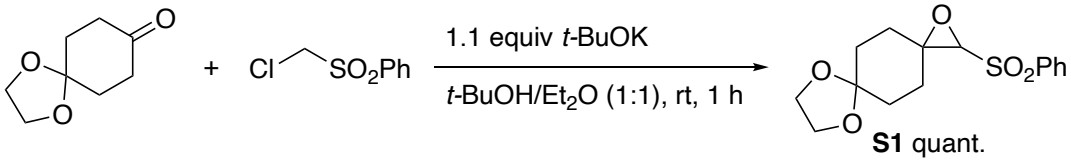

S1 quant.

1,4-dioxaspiro[4.5]decan-8-one (4 g, 25.6 mmol) and chlormethylsulfonyl-benzene (4.9 g, 25.7 mmol, 1.0 equiv) were dissolved in *t*BuOH (25 mL) and Et_2O (75 mL) under Ar at 0 °C. A sonicated solution of *t*BuOK (3.1 g, 27.6 mmol, 1.1 equiv) in *t*BuOH (50 mL) was added slowly to the above solution. After complete addition, the mixture was stirred at rt for 1 h. Water (100 mL) was added and the suspension was extracted 3 × with EtOAc. The organic phase was dried over Na_2SO_4, filtered and concentrated. **S1** was obtained without further purification (7.9 g, quant.).

White solid; Rf 0.33 (4:6 EtOAc/heptanes); mp 124–125°C; ^{1}H-NMR (300 MHz, $CDCl_3$) δ 8.00–7.91 (m, 2H), 7.75–7.65 (m, 1H), 7.65–7.55 (m, 2H), 4.04–3.91 (m, 4H), 3.85 (s, 1H), 2.52–2.30 (m, 2H), 2.03–1.72 (m, 5H), 1.62–1.47 (m, 1H); ^{13}C-NMR (75 MHz, $CDCl_3$) δ 139.0, 134.4, 129.6 (2C), 128.4 (2C), 107.5, 74.5, 68.0, 64.7, 64.6, 33.03, 32.97, 32.4, 25.2; HRMS calc. for $C_{15}H_{19}O_5S$ $[M+H]^+$: 311.0948, found: 311.0939; IR (cm^{-1}): 2965, 2942, 2888, 1444, 1419, 1319, 1305, 1136, 1082, 931.

8-Azido-1,4-dioxaspiro[4.5]decane-8-carbaldehyde (S2)

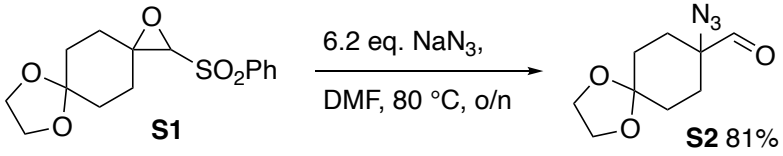

S1 **S2** 81%

A solution of **S1** (1 g, 3.2 mmol) and sodium azide (1.3 g, 20 mmol, 6.2 equiv) in dry DMF (20 mL) was stirred at 80 °C overnight. The mixture was treated with water (10 mL) and extracted 3x with EtOAc. The organic phase was washed 3x with brine, dried over Na_2SO_4, filtered and concentrated. MPLC (gradient from 4:6 to 6:4 EtOAc/heptanes) afforded **S2** (553 mg, 81%).

Colorless oil; Rf 0.27 (3:7 EtOAc/heptanes); ^{1}H-NMR (300 MHz, $CDCl_3$) δ 9.48 (s, 1H), 4.11–3.80 (m, 4H), 2.11–1.50 (m, 8H); ^{13}C-NMR (75 MHz, $CDCl_3$) δ 198.4, 107.3, 68.4, 64.7, 64.6, 30.1 (2C), 27.1 (2C); HRMS calc. for $C_9H_{13}O_3N_3Na$ $[M+Na]^+$: 234.0849, found: 234.0844; IR (cm^{-1}): 2954, 2886, 2111, 1727, 1442, 1262, 1099, 1031, 945, 926.

1-(8-Azido-1,4-dioxaspiro[4.5]decan-8-yl)propane-1,3-diol (S3)

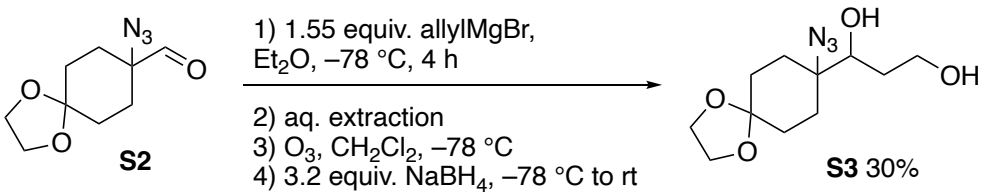

To a solution of **S2** (3.0 g, 14.2 mmol) in dry Et_2O (75 mL) at –78 °C was added a solution of allylmagnesium bromide (1 M in Et_2O, 22 mL, 22 mmol, 1.55 equiv). After stirring for 4 h, the suspension was allowed to warm up to rt and was treated with an aqueous solution (1:1:1 water/brine/sat. $NaHCO_3$). The organic layer was separated, washed with brine, dried over Na_2SO_4 and filtered. The aqueous phase was extracted 3x with CH_2Cl_2, washed with brine, dried over Na_2SO_4 and filtered. The combined organic phase was immediately cooled to –78 °C and ozonolysis was performed at a flow rate of 2.0 g O_3/h until the solution turned deep blue (ca. 1 h). The mixture was flushed with oxygen for 45 min at the same flow rate. $NaBH_4$ (1.7 g, 45 mmol, 3.2 equiv) was added at –78 °C. After 10 min, the flask was equipped with a balloon of Ar and the suspension was allowed to warm up to rt overnight. The mixture was treated with water (200 mL), sat. $NaHCO_3$ (50 mL) and extracted 3x with CH_2Cl_2. The organic phase was dried over Na_2SO_4, filtered and concentrated. FC (8:2 EtOAc/heptanes) afforded **S3** (1.1 g, 30%).

Colorless oil; Rf 0.22 (8:2 EtOAc/heptanes); ^{1}H-NMR (300 MHz, $CDCl_3$) δ 4.03–3.73 (m, 7H), 1.91–1.56 (m, 8H); ^{13}C-NMR (75 MHz, $CDCl_3$) δ 108.1, 78.3, 65.7, 64.6, 64.4, 61.9, 32.7, 30.68, 30.66, 28.4, 28.3; HRMS calc. for $C_{11}H_{19}O_4N_3Na$ $[M+Na]^+$: 280.1268, found: 280.1264; IR (cm^{-1}): 3381, 2953, 2932, 2883, 2095, 1438, 1258, 1091, 1035, 930.

5-(8-Azido-1,4-dioxaspiro[4.5]decan-8-yl)-2,2,3,3,9,9,10,10-octamethyl-4,8-dioxa-3,9-disilaundecane (S4)

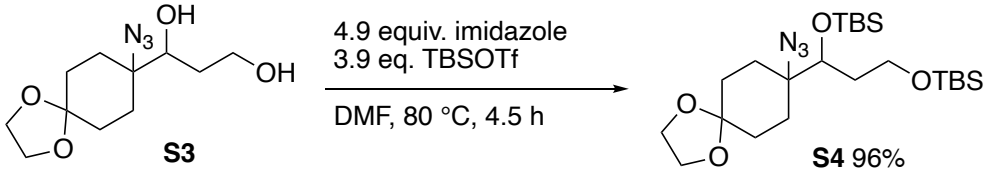

To a stirred solution of **S3** (1.85 g, 7.2 mmol) in dry DMF (50 mL) was added imidazole (2.4 g, 35.2 mmol, 4.9 equiv) and, underneath surface, TBS triflate (6.5 mL, 28.2 mmol, 3.9 equiv) at rt. The solution was stirred at 80 °C for 4.5 h, cooled down to rt and treated with water. The mixture was extracted 3x with pentane and the organic phase was washed with brine, dried over Na_2SO_4, filtered and concentrated under reduced pressure. FC (1:9 EtOAc/heptanes) afforded **S4** (3.4 g, 96%).

Colorless oil; Rf 0.35 (1:9 EtOAc/heptanes); ^{1}H-NMR (300 MHz, $CDCl_3$) δ 4.01–3.88 (m, 4H), 3.82–3.63 (m, 3H), 2.14–2.02 (m, 1H), 1.98–1.50 (m, 10H), 0.92 (s, 9H), 0.89 (s, 9H), 0.11 (d, J = 2.8 Hz, 6H), 0.05 (s, 6H); ^{13}C-NMR (75 MHz, $CDCl_3$) δ 117.6, 108.3, 66.1, 64.6, 64.4, 59.8, 36.8, 30.8, 30.7, 29.5, 29.3, 26.1 (3C), 18.42, 18.39, -4.0, -4.2, -5.07, -5.12; HRMS calc. for $[M+H]^+$: 486.3178, found: 486.3165; IR (cm^{-1}): 2952, 2930, 2883, 2857, 2103, 1254, 1093, 1037, 833, 772.

3-(8-Azido-1,4-dioxaspiro[4.5]decan-8-yl)-3-((*tert*-butyldimethylsilyl)oxy)propan-1-ol (3)

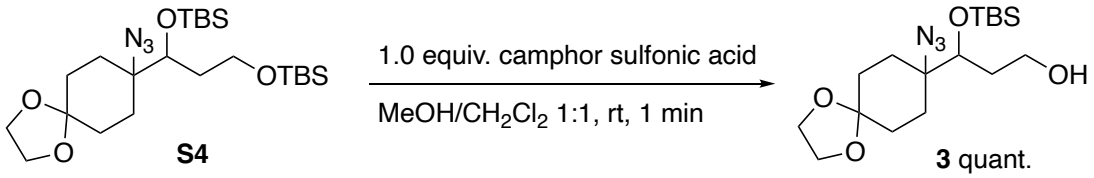

To a stirred solution of **S4** (220 mg, 0.45 mmol) in a mixture of MeOH (2 mL) and CH_2Cl_2 (2 mL) was added camphor sulfonic acid (100 mg, 0.43 mmol, 0.95 equiv) at rt open to air. After 1 min, the reaction was treated with sat. aq. $NaHCO_3$ and the mixture was extracted 3x with EtOAc. The organic phase was washed with brine, dried over Na_2SO_4 and concentrated. FC (3:7 EtOAc/heptanes) afforded **3** (170 mg, quant.).

Colorless oil; Rf 0.20 (3:7 EtOAc/heptanes); ^{1}H-NMR (300 MHz, C_6D_6) δ 3.67–3.39 (m, 7H), 2.21–1.51 (m, 10H), 1.00 (s, 10H), 0.04 (d, J = 1.8 Hz, 6H); ^{13}C-NMR (75 MHz, C_6D_6) δ 108.1, 77.4, 65.5, 64.5, 64.3, 58.5, 35.8, 30.7, 30.5, 29.6 (2C), 25.9 (3C), 18.2, -4.1, -4.5; HRMS calc. for $C_{17}H_{33}O_4N_3NaSi$ $[M+Na]^+$: 394.2133, found: 394.2121; IR (cm^{-1}): 3433, 2954, 2930, 2884, 2857, 2103, 1256, 1092, 835, 730.

Preparation of 7

6-Phenyl-2-(phenylsulfonyl)-1-oxaspiro[2.5]octane (S5)

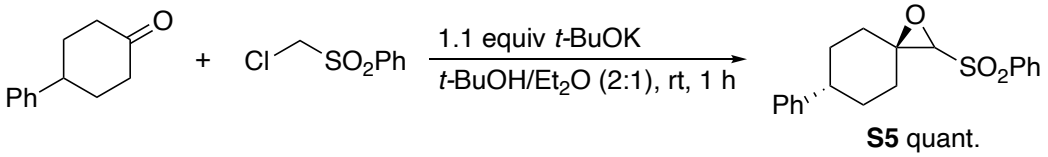

To a stirred solution of 4-phenyl cyclohexanone (8.71 g, 50 mmol) and chlormethylsulfonyl-benzene (9.13 g, 50 mmol, 1.0 equiv) in solvent (2:1 *t*BuOH/Et_2O, 300 mL) was slowly added a sonicated solution of *t*BuOK (6 g, 53.5 mmol, 1.1 equiv) in *t*BuOH (70 mL) under Ar at 0 °C. After complete addition, the mixture was stirred at rt for 1 h. Water (100 mL) was added and the suspension was extracted 3x with EtOAc. The organic phase was dried over Na_2SO_4, filtered and concentrated. **S5** was obtained without further purification (16.42 g, quant.).

White solid; Rf 0.38 (7:3 pentane/Et_2O); mp 119-121°C; ^{1}H-NMR (300 MHz, $CDCl_3$) δ 8.09–7.90 (m, 2H), 7.77–7.55 (m, 3H), 7.38–7.14 (m, 5H), 3.87 (s, 1H), 2.79–2.58 (m, 2H), 2.27–2.00 (m, 3H), 1.99–1.74 (m, 3H), 1.35–1.23 (m, 1H); ^{13}C-NMR (75 MHz, $CDCl_3$) δ 146.0, 139.1, 134.4, 129.6 (2C), 128.7 (2C), 128.4 (2C), 126.9 (2C), 126.5 (2C), 75.0, 68.3, 43.2, 34.9, 31.6, 31.5, 28.0; HRMS calc. for $C_{19}H_{20}O_3NaS$ $[M+Na]^+$: 351.1025, found: 351.1038; IR (cm^{-1}): 2936, 1490, 1445, 1318, 1245, 1179, 1151, 1088, 1071, 930.

1-Azido-4-phenylcyclohexane-1-carbaldehyde (S6)

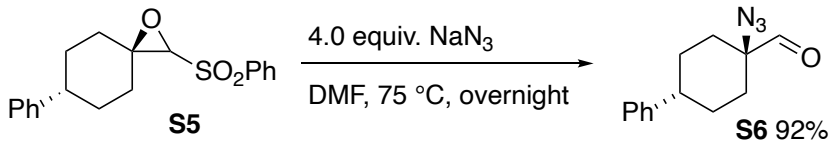

To a stirred solution of sodium azide (6.5 g, 100 mmol, 4.0 equiv) in anhydrous DMF (75 mL) was added a solution of **S5** (8.21g, 25mmol) in anhydrous DMF (85 mL) at rt. The mixture was stirred at 75 °C overnight. The mixture was cooled down to rt, diluted with water (250 mL), and extracted 3x with Et_2O. The combined organic phase was washed with water, brine, dried over Na_2SO_4, filtered and concentrated. FC (8:2 pentane/Et_2O) afforded **S6** (5.27 g, 92%).

Yellowish oil; Rf 0.83-0.55 (smirred; 8:2 pentane/Et_2O); ^{1}H-NMR (300 MHz, $CDCl_3$) δ 9.55 (s, 1H), 7.48–7.09 (m, 10H), 2.64 (tt, J = 11.3, 3.6 Hz, 2H), 2.49–2.19 (m, 4H), 2.11–1.91 (m, 3H), 1.90–1.55 (m, 7H); ^{13}C-NMR (75 MHz, $CDCl_3$) δ 197.7, 145.3, 128.6 (2C), 126.8 (2C), 126.5, 66.9, 42.6, 30.4 (2C), 30.1 (2C); HRMS calc. for $C_{13}H_{16}ON$ $[M+H]^+$: 202.1226, found: 202.1232; IR (cm^{-1}): 2934, 2082, 1728, 1601, 1494, 1450, 1228, 1058, 755, 698.

1-(1-Azido-4-phenylcyclohexyl)but-3-en-1-ol (S7)

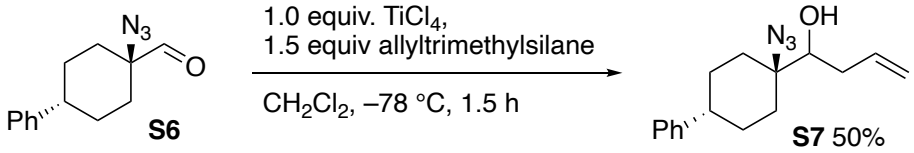

To a stirred solution of **S6** (460 mg, 2 mmol) in dry CH_2Cl_2 (4 mL) under Ar at –78 °C was added $TiCl_4$ (0.22 mL, 2 mmol, 1.0 equiv) underneath surface before a solution of allyltrimethylsilane (0.49 mL, 3 mmol, 1.5 equiv) in dry CH_2Cl_2 (2 mL) was added slowly underneath surface. After 1.5 h of stirring at –78 °C, the reaction was treated with aq. HCl (1 M, 10 mL) and water (10 mL). After 15 min of stirring at rt, the mixture was extracted 3x with Et_2O. The combined organic phase was washed with water, brine, dried over Na_2SO_4, filtered and concentrated. MPLC (gradient 99:1 to 90:10 pentane/Et_2O) afforded **S7** (271 mg, 50%).

Note: **S7** is unstable and decomposes within a few hours when stored at 5 °C.

Colorless oil; Rf 0.21 (9:1 pentane/Et_2O); ^{1}H-NMR (300 MHz, $CDCl_3$) δ 7.31–7.23 (m, 2H), 7.22–7.12 (m, 3H), 6.00–5.79 (m, 1H), 5.24–5.11 (m, 2H), 3.94 (ddd, J = 9.7, 6.7, 3.1 Hz, 1H), 2.75–2.56 (m, 1H), 2.50–2.32 (m, 2H), 2.25 (dt, J = 14.5, 8.8 Hz, 1H), 2.14 (d, J = 7.2 Hz, 1H), 1.98–1.46 (m, 7H); ^{13}C-NMR (75 MHz, $CDCl_3$, crude spectrum) δ 145.5, 135.1, 128.6 (2C), 126.9 (2C), 126.4, 118.8, 70.9, 66.0, 42.6, 36.0, 32.3, 31.2, 29.7, 29.4; HRMS calc. for $C_{16}H_{22}ON$ $[M(-N_2)+H]^+$: 244.1696, found: 244.1705; IR (cm^{-1}): 2928, 2098, 1601, 1494, 1450, 1268, 1040, 944, 759, 699.

1-(1-Azido-4-phenylcyclohexyl)propane-1,3-diol (S8)

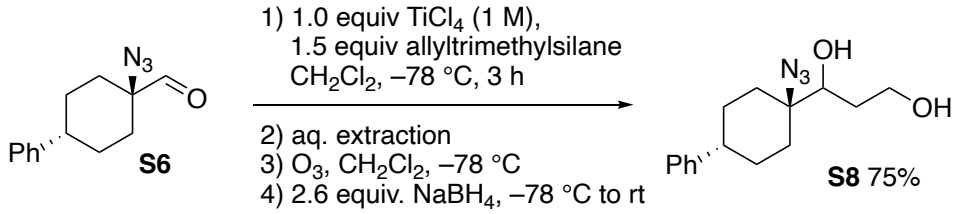

To a stirred solution of **S6** (2.29 g, 10 mmol) in dry CH_2Cl_2 (40 mL) was added a solution of $TiCl_4$ (1.23 mL, 10 mmol, 1.0 equiv) in dry CH_2Cl_2 (12 mL) under Ar at –78 °C underneath surface. A solution of allyltrimethylsilane (2.43 mL, 15 mmol, 1.5 equiv) in dry CH_2Cl_2 (20 mL) was added slowly underneath surface. The mixture was stirred for 4 h at –78 °C and was then allowed to warm up to rt. After addition of sat. K_2CO_3 solution (50 mL), the suspension was stirred for 5 min. A sat. solution of Rochelle's salt (50 mL) was added, the mixture was stirred for 5 min and extracted twice with water. The aqueous phase was reextracted with CH_2Cl_2 (3x 10ml). The combined organic phase was washed with brine, dried over Na_2SO_4, and filtered through a POR_4 frit glas. The resulting pink solution was immediately cooled to –78 °C and ozonolysis was performed at a flow rate of 1.5g O_3/h until the solution turned deep blue (ca. 30 min). The mixture was then flushed with oxygen for 45 min at the same flow rate. $NaBH_4$ (1 g, 26.4 mmol, 2.6 equiv) was added at –78 °C, a balloon of Ar was mounted and the mixture was stirred for 1 h. It was then subsequently allowed to warm up to rt overnight. The mixture was treated with water (100 mL) and extracted 3x with CH_2Cl_2. The combined organic phase was washed with water, brine, dried over Na_2SO_4, filtered and concentrated. FC (9:1 pentane/Et_2O) afforded **S8** (2.07 g, 75%).

Colorless oil; Rf 0.21 (9:1 pentane/Et_2O); ^{1}H-NMR (300 MHz, $CDCl_3$) δ 7.34–7.25 (m, 2H), 7.25–7.15 (m, 3H), 4.19 (dd, J = 8.4, 4.5 Hz, 1H), 4.02–3.79 (m, 2H), 3.01 (s, 2H), 2.67 (tt, J = 10.9, 4.0 Hz, 1H), 2.50–2.36 (m, 1H), 2.02–1.47 (m, 9H); ^{13}C-NMR (75 MHz, CDCl3) δ 145.5, 128.6 (2C), 126.9, 126.3, 71.4, 66.3, 61.3, 42.5, 32.4, 32.1, 30.8, 29.5, 29.4; HRMS calc. for $C_{15}H_{22}O_2N$ $[M(-N_2)+H]^+$: 248.1645, found: 248.1643; IR (cm^{-1}): 3351, 2935, 2096, 1494, 1450, 1262, 1057, 1011, 924, 756, 698.

1-(1-Azido-4-phenylcyclohexyl)-3-((tert-butyldimethylsilyl)oxy)propan-1-ol (S9)

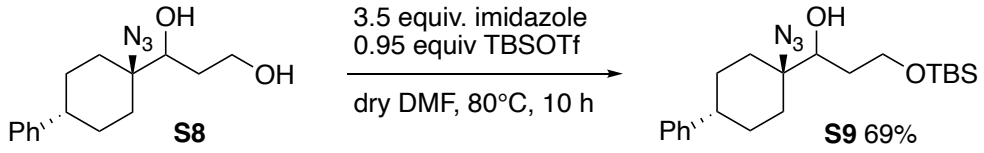

To a stirred solution of **S8** (6.78 g, 24.6 mmol) in dry DMF (100 mL) was added imidazole (5.87 g, 86.2 mmol, 3.5 equiv) and TBSOTf (5.3 mL, 23.2 mmol, 0.95 eq) under Ar at rt. After 10 h, the mixture was treated with water (100 mL) and extracted 3x with Et_2O. The combined organic phase was washed with water, brine, dried over Na_2SO_4, filtered and concentrated. FC (95:5 pentane/Et_2O) afforded **S9** (6.5 g, 69%).

White solid; mp 103-107 °C; Rf 0.58 (9:1 pentane/Et_2O); ^{1}H-NMR (300 MHz, $CDCl_3$) δ 7.34–7.26 (m, 2H), 7.25–7.16 (m, 3H), 4.30–4.19 (m, 1H), 4.05–3.93 (m, 1H), 3.92–3.79 (m, 1H), 3.28 (d, J = 3.8 Hz,

1H), 2.78–2.61 (m, 1H), 2.59–2.44 (m, 1H), 2.03–1.49 (m, 10H), 0.92 (s, 9H), 0.11 (s, 3H), 0.10 (s, 3H); ^{13}C-NMR (75 MHz, $CDCl_3$) δ 145.8, 128.6 (2C), 127.0 (2C), 126.3, 72.1, 65.9, 62.4, 42.7, 32.7, 32.5, 30.8, 29.7, 29.5, 26.0 (3C), 18.3, –5.3 (2C); HRMS calc. for $C_{21}H_{36}O_2N_3Si$ $[M+H]^+$: 390.2571, found: 390.2584; IR (cm^{-1}): 3460, 2930, 2099, 1494, 1452, 1254, 1079, 943, 835, 761.

5-(1-Azido-4-phenylcyclohexyl)-2,2,3,3,9,9,10,10-octamethyl-4,8-dioxa-3,9-disilaundecane (S10)

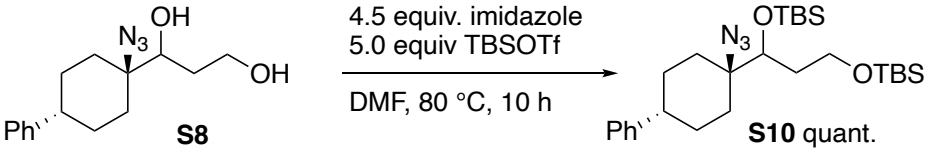

To a stirred solution of **S8** (1.2 g, 3.1 mmol) in dry DMF (14.4 mL) was added imidazole (0.86 g, 11.0 mmol, 4.5 equiv) and TBS-OTf (4.14 mL, 15.7 mmol, 5 equiv) under Ar at rt. After solubilization of all solids, the mixture was heated to 80 °C for 10 h. The mixture was cooled down to rt, treated with water (100 mL), and extracted 3x with Et_2O. The combined organic phase was washed with water, brine, dried over Na_2SO_4, filtered and concentrated. FC (96:4 pentane/Et_2O) afforded **S10** (1.56 g, quant.).

Colorless oil; Rf 0.78 (96:4 pentane/Et_2O); ^{1}H-NMR (300 MHz, $CDCl_3$) δ 7.36–7.26 (m, 2H), 7.24–7.17 (m, 3H), 4.30 (dd, J = 5.9, 3.5 Hz, 1H), 3.77 (dd, J = 7.3, 5.6 Hz, 2H), 2.68 (td, J = 9.9, 4.0 Hz, 1H), 2.50–2.34 (m, 1H), 2.07–1.41 (m, 10H), 0.91 (s, 9H), 0.90 (s, 9H), 0.16 (s, 3H), 0.10 (s, 3H), 0.06 (s, 6H), 0.05 (s, 3H); ^{13}C-NMR (75 MHz, $CDCl_3$) δ 145.6, 128.4 (2C), 126.8 (2C), 126.2, 71.2, 66.2, 59.7, 42.2, 36.3, 33.0, 30.9, 29.7, 28.9, 25.97 (3C), 25.95 (3C), 18.34, 18.26, –4.1, –4.2, –5.26, –5.29; HRMS calc. for $C_{27}H_{49}O_2N_3NaSi$ $[M+Na]^+$: 526.3256, found: 526.3274; IR (cm^{-1}): 2929, 2858, 2100, 1470, 1361, 1257, 1090, 833, 777, 700.

3-(1-Azido-4-phenylcyclohexyl)-3-((tert-butyldimethylsilyl)oxy)propan-1-ol (7)

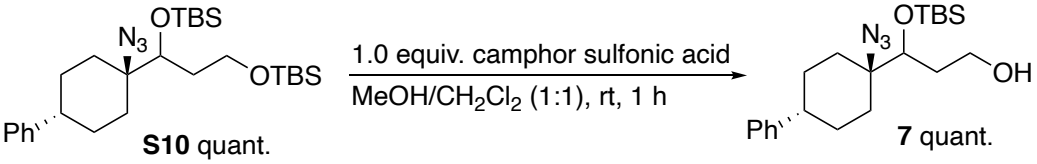

To a stirred solution of **S10** (3.9 g, 10 mmol) in a mixture of MeOH and CH_2Cl_2 (1:1, 100 mL) was added camphor sulfonic acid (2.32 g, 10mmol, 1.0 equiv) and the mixture was stirred for 1 h at rt. The reaction was treated with sat. $NaHCO_3$ (50 mL) and extracted 3x with Et_2O. The combined organic phase was washed with water, brine, dried over Na_2SO_4, filtered and concentrated. FC (7:3 pentane/Et_2O) afforded **7** (1.52 g, quant.).

Colorless oil; Rf 0.40 (7:3 Pentane/Et_2O); ^{1}H-NMR (300 MHz, $CDCl_3$) δ 7.27–7.18 (m, 2H), 7.17–7.08 (m, 3H), 4.16 (t, J = 4.3 Hz, 1H), 3.85 (dt, J = 11.1, 6.1 Hz, 1H), 3.65 (dt, J = 11.1, 6.1 Hz, 1H), 2.83–2.50 (m, 2H), 2.38–2.15 (m, 1H), 1.96–1.34 (m, 9H), 0.85 (s, 9H), 0.06 (s, 3H), 0.03 (s, 3H); ^{13}C-NMR (75 MHz, $CDCl_3$) δ 145.2, 128.5 (2C), 126.8 (2C), 126.2, 72.1, 65.5, 58.3, 41.7, 35.3, 32.9, 30.7, 29.3, 28.8, 25.9 (3C), 18.2, –4.0, –4.4; HRMS calc. for $C_{21}H_{35}O_2N_3NaSi$ $[M+Na]^+$: 412.2391, found: 412.2386; IR (cm^{-1}): 2929, 2857, 2101, 1471, 1254, 1089, 1007, 834, 773, 698.

Synthesis of azidoalcohols 10-13

3-(c*is*-1-Azido-4-phenylcyclohexyl)propanal (9)

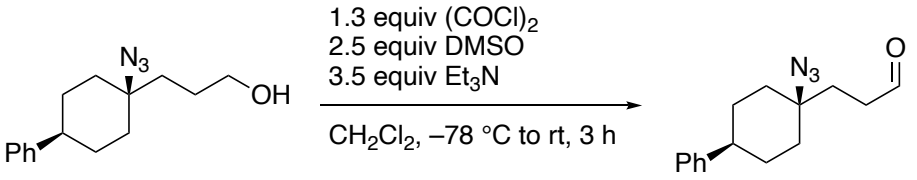

5 **9** 83%

To a stirred solution of oxalylchloride (1.7 g, 13.5 mmol, 1.1 mL, 1.3 equiv) in CH_2Cl_2 (5 mL) at –78 °C was added DMSO (2.0 g, 26 mmol, 1.8 mL, 2.5 equiv) and stirred for 30 min. Then, **5**[1] (2.7 g, 10.4 mmol) in CH_2Cl_2 (25 mL) was added at –78 °C and stirred for 30 minutes. The reaction mixture was treated with Et_3N (3.6 g, 36.9 mmol, 5 mL, 3.5 equiv) and stirred for 5 min at –78 °C. The mixture was warmed up to rt and stirred for 2 h. The reaction mixture was poured into a mixture of brine and saturated $NaHCO_3$ (20 ml) and extracted with Et_2O (3 × 20 mL). The combined organic layers were dried over anhydrous Na_2SO_4 and concentrated. FC (25:75 Et_2O/pentane) afforded **9** (2.2 g, 83%).

White solid; Rf 0.68 (4:6 Et_2O/pentane); mp 49-50 °C; ^{1}H-NMR (300 MHz, CD_2Cl_2) δ = 9.81 (t, J = 1.3 Hz, 1H), 7.37–7.11 (m, 5H), 2.61 (ddd, J = 7.9, 7.0, 1.4 Hz, 2H), 2.57–2.44 (m, 1H), 1.98–1.83 (m, 4H), 1.82–1.65 (m, 4H), 1.57–1.42 (m, 2H); ^{13}C-NMR (75 MHz, CD_2Cl_2) δ = 201.6, 147.1, 128.8, 127.2, 126.5, 63.1, 43.8, 38.7, 35.1, 33.4, 29.9; HRMS calc. for $C_{15}H_{19}N_3ONa$ $[M+Na]^+$: 280.1420, found: 280.1414; IR (cm^{-1}): 2939, 2831, 2732, 2089, 1717, 1493, 1452, 1266, 760, 701.

1-(c*is*-1-Azido-4-phenylcyclohexyl)pentan-3-ol ((±)-10)

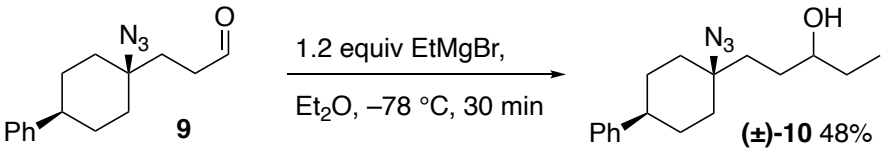

9 **(±)-10** 48%

To a stirred solution of **9** (0.04 g, 0.16 mmol) in Et_2O (1.5 mL) at –78 °C was added dropwise EtMgBr (1.0M in Et_2O, 0.19 mL, 1.2 equiv) and stirred for 30 min. The solution was treated with sat. NH_4Cl (1.5 mL) and diluted with Et_2O (5 mL) and water (5 mL). The organic layer was separated, dried over anhydrous Na_2SO_4 and concentrated. FC (pentane/Et_2O 8:2 to 6:4) afforded (±)-**10** (20 mg, 48%).

Colorless oil; Rf 0.38 (4:6 Et_2O/pentane); ^{1}H-NMR (300 MHz, CD_2Cl_2) δ = 7.36–7.11 (m, 5H), 3.52 (dq, J = 7.5, 3.8 Hz, 1H), 2.59–2.41 (m, 1H), 1.95–1.37 (m, 14H), 0.96 (t, J = 7.4 Hz, 3H); ^{13}C-NMR (75 MHz, CD_2Cl_2) δ = 147.3, 128.7, 127.2, 126.4, 73.6, 63.8, 53.8, 44.0, 37.7, 35.3, 35.1, 31.0, 30.7, 30.1, 10.1 HRMS calc. for $C_{17}H_{25}N_3ONa$ $[M+Na]^+$: 310.1890, found: 310.1888; IR (cm^{-1}): 2926, 2857, 2091, 1726, 1449, 1256, 1112, 927, 755, 698

HPLC analysis: Daicel CHIRALPAK OJ; hexane/TBME 50:50; 1 mL min^{-1}, λ= 254 nm

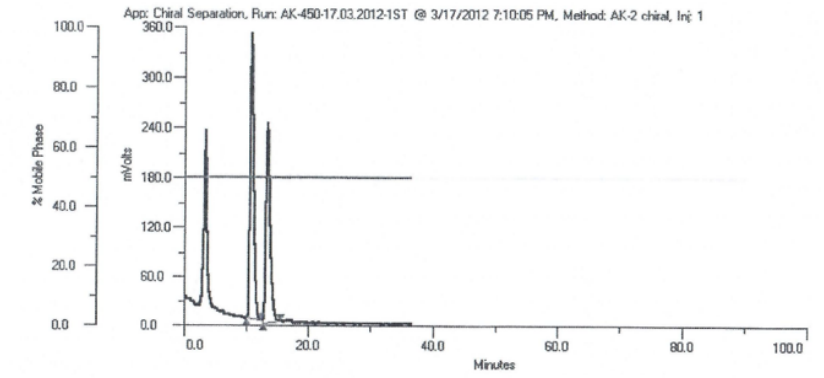

Sample Table

Retention Time (min)	Area (uVmin/100)	Area %	Height (mV)	Height %
10.7958	23402872.4641	53.9509	345.5607	58.6619
13.4542	19975247.1292	46.0491	243.5111	41.3381

(*S*)-1-(*cis*-1-Azido-4-phenylcyclohexyl)pentan-3-ol ((*S*)-10)

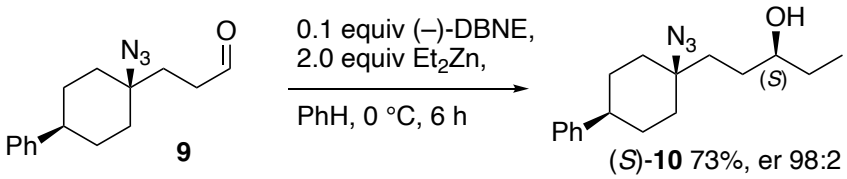

(*S*)-**10** 73%, er 98:2

A solution of **9** (0.50 g, 1.94 mmol, 1.0 equiv) in toluene (1.0 mL) was added to a solution of (–)-*N,N*-dibutyl-*D*-norephedrine ((–)-DBNE)[2–4] (0.053 g, 0.2 mmol, 0.1 eq.) in toluene (2.0 mL) at rt and stirred for 30 minutes. At 0 °C, diethylzinc (1 M in toluene, 3.9 mL, 3.9 mmol, 2.0 equiv) was added dropwise and the reaction mixture was stirred for 6 h. The reaction mixture was treated with sat. aq. NH_4Cl solution (5 mL) and the aqueous layer was extracted with Et_2O (3 × 10 mL). The combined organic layer was dried over Na_2SO_4 and concentrated. FC (pentane/Et_2O 8:2 to 6:4) afforded (*S*)-**10** (0.404 g, 73%).

Analytical data are consistent with the racemic compound. $[\alpha]_D^{25}$ = +8 (c = 1.5, CH_2Cl_2).

The enantiomeric ratio (er 98:2) was determined by HPLC: Daicel CHIRALPAK OJ; hexane/TBME 50:50; 1 mL min^{-1}, λ= 254 nm.

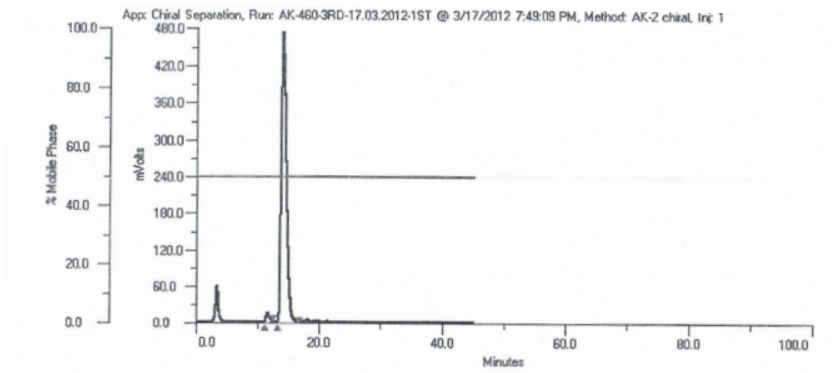

5-(*cis*-1-Azido-4-phenylcyclohexyl)-1-phenylpent-1-yn-3-ol ((±)-11)

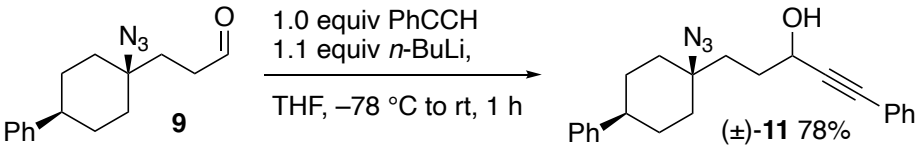

n-BuLi (2.4M in hexanes, 0.54 mL, 1.29 mmol, 1.1 equiv) was added dropwise to a solution of phenylacetylene (0.12 g, 1.17 mmol, 1.0 equiv) in dry THF (3.5 mL) at –78 °C. The solution was stirred for 15 min. A solution of **9** (0.30 g, 1.17 mmol) in dry THF (2.0 mL) was added dropwise, and the reaction mixture as allowed to reach room temperature. The reaction was quenched with NH_4Cl (15 mL) and the aqueous layer was extracted with EtOAc (3 × 15 mL). Et_2O (2 × 30 mL). The combined organic layers were washed with brine (30 mL), dried over Na_2SO_4 and concentrated under reduced pressure. FC (pentane/Et_2O 8:2 to 7:3) afforded (±)-**11** (330 mg, 78%).

Colorless oil; Rf 0.27 (7:3 pentane/Et_2O); ^{1}H-NMR (300 MHz, CD_2Cl_2) δ = 7.55–7.10 (m, 10H), 4.65 (q, J = 5.7 Hz, 1H), 2.51 (ddd, J = 15.8, 9.4, 7.3 Hz, 1H), 2.15 (d, J = 5.3 Hz, 1H), 2.03–1.70 (m, 9H), 1.60–1.26 (m, 3H); ^{13}C-NMR (75 MHz, CD_2Cl_2) δ = 147.3, 132.0, 129.2, 128.9, 128.8, 128.7, 127.2, 126.5, 123.0, 90.2, 85.3, 63.5, 63.1, 44.0, 37.0, 35.2, 32.4, 30.0; HRMS calc. for $C_{23}H_{26}N_3O$ $[M+H]^+$: 360.2070, found: 360.2067 IR (cm^{-1}): 3339, 2927, 2858, 2091, 1599, 1489, 1442, 1255, 754, 690.

HPLC analysis: Daicel CHIRALPAK ID-3, hexane/TBME 80:20; 1 mL min^{-1}, λ= 254 nm.

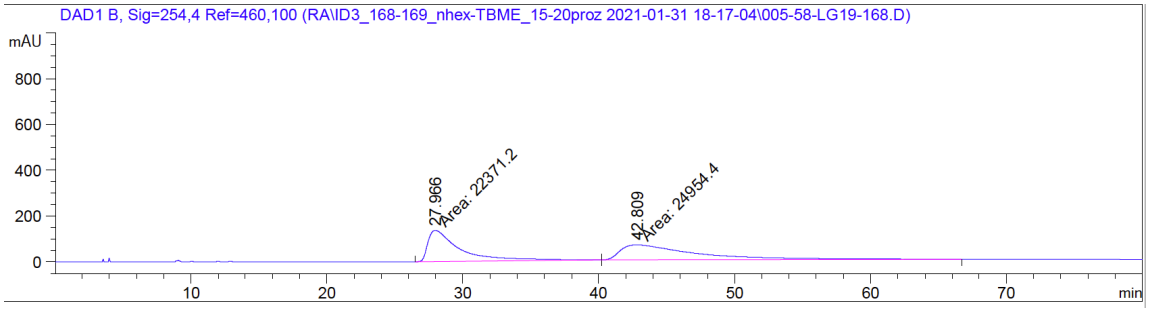

Signal 2: DAD1 B, Sig=254,4 Ref=460,100

Peak #	RetTime [min]	Type	Width [min]	Area [mAU*s]	Height [mAU]	Area %
1	27.966	MM	2.7460	2.23712e4	135.78154	47.2707
2	42.809	MM	6.3538	2.49544e4	65.45805	52.7293
Totals :				4.73256e4	201.23959	

(*R*)-5-(*cis*-1-Azido-4-phenylcyclohexyl)-1-phenylpent-1-yn-3-ol ((*R*)-11)

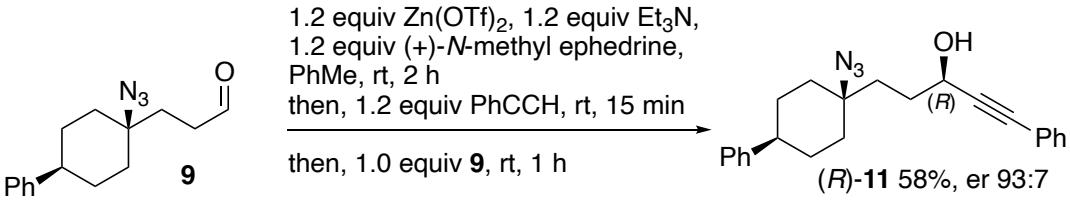

A solution of zinc triflate (0.85 g, 2.33 mmol, 1.2 eq.), (+)-*N*-methyl ephedrine[5,6] (0.42 g, 2.33 mmol, 1.2 eq.) and Et_3N (0.24 g, 2.33 mmol, 1.2 eq.) in dry toluene (6.0 mL) was stirred for 2 h under an argon at rt. Phenylacetylene (0.24 g, 2.33 mmol, 1.2 eq.) was added in one portion and the reaction mixture was stirred for 15 minutes. A solution of **9** (0.50 g, 1.94 mmol, 1.0 eq.) in dry toluene (5.0 mL) was added and the reaction mixture was stirred for 1 h until completion. The reaction was quenched by addition of a sat. NH_4Cl (15 mL). The reaction mixture was poured into Et_2O (30 mL), the layers were separated and the aqueous layer was extracted with Et_2O (3 × 30 mL). The combined organic layers were dried over Na_2SO_4 and concentrated under reduced pressure. FC (pentane/Et_2O 8:2) afforded (*R*)-**11** (410 mg, 58%).

Analytical data are consistent with the racemic compound; $[\alpha]_D^{25}$ = –3.0 (c = 0.9, $CDCl_3$).

The enantiomeric ratio (er 94:6) was determined by HPLC: Daicel CHIRALPAK ID-3, hexane/TBME 80:20; 1 mL min^{-1}, λ= 254 nm.

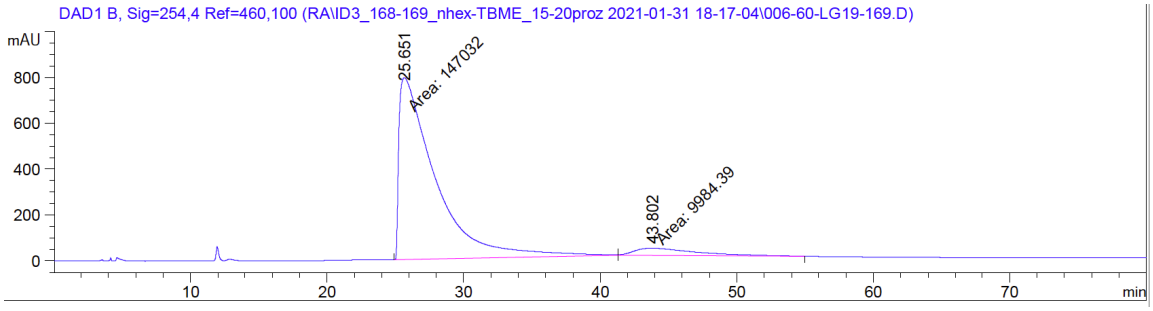

Signal 2: DAD1 B, Sig=254,4 Ref=460,100

Peak #	RetTime [min]	Type	Width [min]	Area [mAU*s]	Height [mAU]	Area %
1	25.651	MM	3.0907	1.47032e5	792.87891	93.6412
2	43.802	MM	5.3409	9984.39063	31.15726	6.3588
Totals :				1.57016e5	824.03617	

1-(*cis*-1-Azido-4-phenylcyclohexyl)hex-5-en-3-ol ((±)-12)

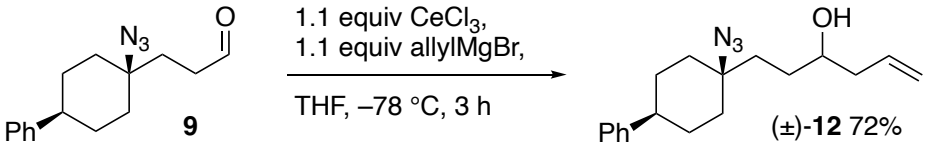

Dry cerium trichloride (0.106 g, 0.43 mmol, 1.1 equiv) in dry THF (1.2 mL) was sonicated at rt for 30 min until the mixture turned yellow. Allyl magnesium bromide was added dropwise at 0 °C (1M in THF, 0.43 mL, 0.43 mmol, 1.1 equiv) and the solution was stirred at this temperature for 1.5 h. At –78 °C, a solution of **9** (0.100 g, 0.39 mmol, 1.0 equiv) in THF (1.2 mL) was added, and the mixture was stirred for 3 h. The reaction was treated by addition of sat. NH_4Cl (5 mL) and the reaction mixture was allowed to warm up to rt. The mixture was extracted with Et_2O (3 × 10 mL), the combined organic phase was dried over Na_2SO_4 and concentrated. FC (gradient 8:2 to 6:4 pentane/Et_2O) afforded (±)-1**2** (84 mg, 72%).

Colorless oil; Rf 0.34 (6:4 pentane/Et_2O) ^{1}H-NMR (300 MHz, CD_2Cl_2) δ 7.36–7.12 (m, 5H), 5.96–5.76 (m, 1H), 5.20–5.10 (m, 2H), 3.64 (dh, J = 8.4, 4.2 Hz, 1H), 2.50 (ddd, J = 15.7, 9.4, 7.2 Hz, 1H), 2.34 (dddt, J = 13.8, 5.8, 4.4, 1.4 Hz, 1H), 2.25–2.11 (m, 1H), 1.95–1.41 (m, 13H); ^{13}C-NMR (75 MHz, CD_2Cl_2): δ 147.3, 135.3, 128.7, 127.2, 126.4, 118.3, 71.1, 63.8, 53.8, 44.0, 42.5, 37.7, 35.3, 35.1, 31.0, 30.0; HRMS calc. for $C_{18}H_{26}N_3O$ $[M+H]^+$: 300.2065, found: 300.2065; IR (cm^{-1}): 3331, 2925, 2858, 2090, 1450, 1256, 994, 915, 756, 698.

HPLC analysis: Daicel CHIRALPAK IA-3, hexane/TBME 70:30; 1 mL min^{-1}, λ= 210 nm.

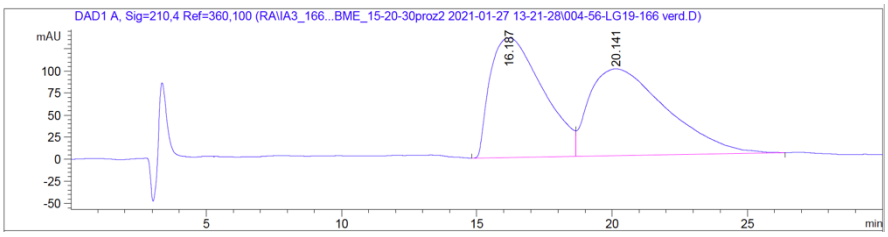

Signal 1: DAD1 A, Sig=210,4 Ref=360,100

Peak #	RetTime [min]	Type	Width [min]	Area [mAU*s]	Height [mAU]	Area %
1	16.187	BV	1.6179	1.83188e4	135.44289	48.3713
2	20.141	VB	2.3421	1.95524e4	98.31781	51.6287
Totals :				3.78712e4	233.76070	

(*R*)-1-(*cis*-1-Azido-4-phenylcyclohexyl)hex-5-en-3-ol ((*R*)-12)

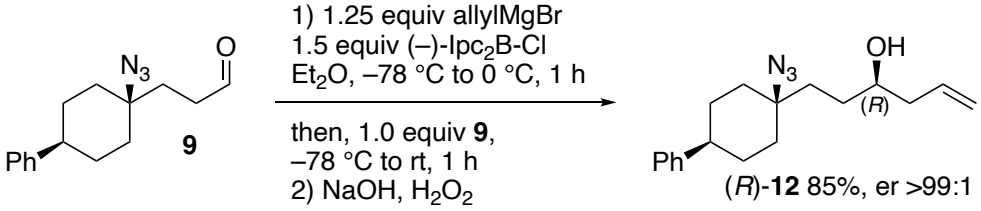

Allylmagnesium bromide (1.0M in Et_2O, 2.43 mL, 2.43 mmol, 1.25 equiv) was added at –78 °C to a solution of (–)-B-Chlorodiisopinocampheylborane ((–)-DIP chloride)[7] (1.7M in hexanes, 1.73 mL, 2.92

mmol, 1.5 equiv) in dry Et_2O (12 mL). The solution was stirred at 0 °C for 1 h and then allowed to warm up to rt. The contents of this flask were transferred *via* a cannula equipped with a filter into another flask to remove all salts. A solution of **9** (0.50 g, 1.94 mmol, 1.0 equiv) in Et_2O (6.0 mL) was added dropwise at –78 °C and the reaction mixture was stirred at this temperature for 1 h. It was warmed up to rt before NaOH (3 M, 2.15 mL) and 30% aq. H_2O_2 (0.9 mL) were added and the mixture was heated up to 45 °C for 1 h. The mixture was extracted with Et_2O (2 × 30 mL), the combined organic phase was washed with brine (30 mL), dried over Na_2SO_4 and concentrated. FC (pentane/Et_2O 8:2 to 7:3) afforded (*R*)-**12** (494 mg, 85%).

Analytical data are consistent with the racemic compound; $[\alpha]_D^{25}$ = +10 (c = 0.4, $CDCl_3$).

The enantiomeric ratio (er 98:2) was determined by HPLC: Daicel CHIRALPAK IA-3, hexane/TBME 70:30; 1 mL min^{-1}, λ= 210 nm.

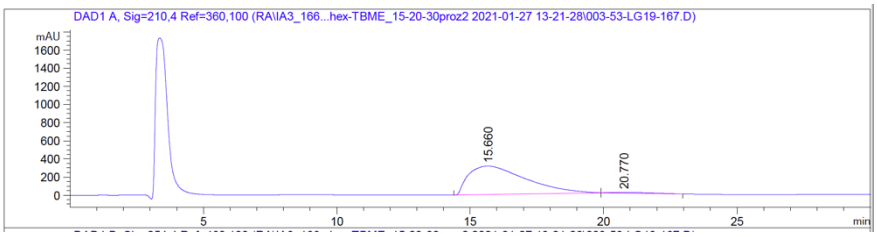

Peak #	RetTime [min]	Type	Width [min]	Area [mAU*s]	Height [mAU]	Area %
1	15.660	BB	2.1326	4.66776e4	313.22586	98.1616
2	20.770	BB	1.3724	874.20911	7.53011	1.8384
Totals :				4.75518e4	320.75597	

3-(*cis*-1-Azido-4-phenylcyclohexyl)-1-phenylpropan-1-one (14)

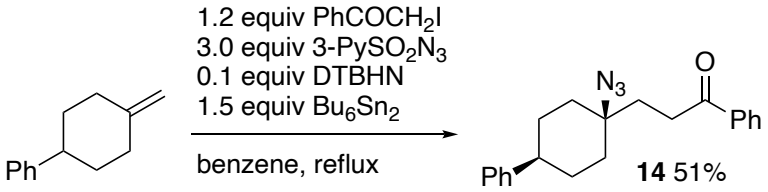

DTBHN[1] (10 mg, 0.06 mmol, 0.03 equiv) was added to a solution of 4-phenyl-1-methylenecyclohexane (345 mg, 2 mmol, 1 equiv), 2-iodo-1-phenyl-ethanone[8,9] (590 mg, 2.4 mmol, 1.2 equiv), Bu_6Sn_2 (1.5 mL, 3 mmol, 1.5 equiv.) and 3-$PySO_2N_3$[1] (1.1 g, 6 mmol, 3 equiv) in dry benzene. The mixture was stirred at reflux for 1 h. Upon completion, the reaction mixture was cooled down to rt and the solvent was removed under reduced pressure. FC (9:1 pentane/Et_2O) afforded **14** as a mixture of diastereomers (425mg, 1.3 mmol, 64%). A second purification step afforded the major isomer (51%).

White solid; mp 81–82 °C; Rf 0.17 (1:9 Et_2O/pentane); ^{1}H-NMR (300 MHz, CD_2Cl_2) δ = 8.07–7.96 (m, 2H), 7.67–7.58 (m, 1H), 7.54 (t, J = 7.7 Hz, 3H), 7.38–7.18 (m, 5H), 3.26–3.14 (m, 2H), 2.66–2.51 (m, 1H), 2.16–2.05 (m, 2H), 2.00 (dq, J = 14.1, 2.9 Hz, 2H), 1.88–1.72 (m, 4H), 1.70–1.51 (m, 3H); ^{13}C-NMR (101 MHz, CD_2Cl_2) δ = 199.5, 147.2, 137.4, 133.5, 129.0, 128.9, 128.8, 128.6, 128.3, 127.2,

126.5, 63.5, 43.9, 35.5, 35.3, 33.1, 30.0; HRMS calc. for $C_{21}H_{24}N_3O$ $[M+H]^+$: 224.1914, found: 334.1919; IR (cm^{-1}): 2915, 2853, 2097, 1684, 1491, 1448, 758, 739, 699, 688.

3-(*cis*-1-Azido-4-phenylcyclohexyl)-1-phenylpropan-1-ol ((±)-13)

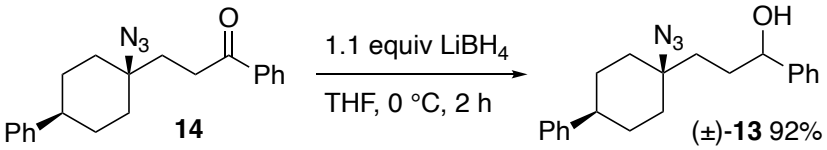

$LiBH_4$ (37.0 mg, 1.7 mmol, 1.1 equiv) was added at 0 °C to a solution of **14** (0.5 g, 1.5 mmol, 1.0 equiv) in dry THF (16 mL) under a flux of argon. The reaction mixture was stirred at this temperature for 2 h. The reaction mixture was diluted with EtOAc (15 mL) and treated with sat. aq. NH_4Cl (10 mL). The organic layer was washed with sat. aq. NH_4Cl (2 × 10 mL), brine (10 mL), dried over Na_2SO_4 and concentrated. FC (pentane/Et_2O 10:0 to 8:2) afforded (±)-**13** (0.47 g, 92%).

Colorless oil; Rf 0.22 (8:2 pentane/Et_2O); ^{1}H-NMR (300 MHz, CD_2Cl_2) δ = 7.46–7.11 (m, 10H), 4.69 (ddd, J = 7.1, 5.2, 3.4 Hz, 1H), 2.48 (ddd, J = 15.7, 9.4, 7.2 Hz, 1H), 2.11–1.35 (m, 14H) ^{13}C-NMR (75 MHz, CD_2Cl_2) δ = 147.3, 145.1, 128.9, 128.7, 128.0, 127.2, 126.4, 126.3, 74.8, 63.7, 43.9, 37.8, 35.2, 35.1, 33.3, 30.0; HRMS calc. for $C_{21}H_{25}N_3ONa$ $[M+Na]^+$: 358.1890, found: 358.1884; IR (cm^{-1}): 3341, 2927, 2857, 2092, 1493, 1450, 1258, 1055, 755, 697.

HPLC analysis: Daicel CHIRALPAK IA-3, hexane/TBME 70:30; 1 mL min^{-1}, λ= 220 nm.

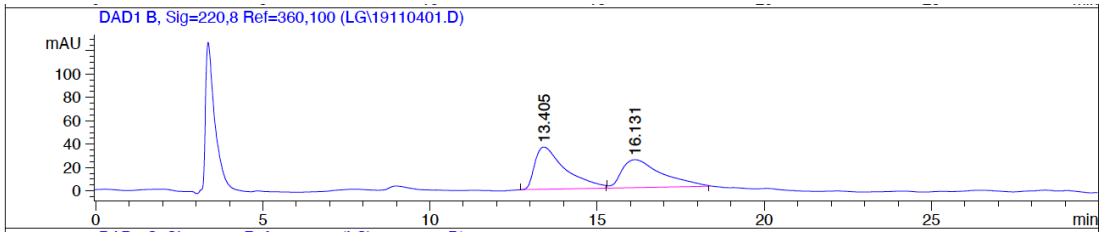


```
Signal 2: DAD1 B, Sig=220,8 Ref=360,100

Peak RetTime Type  Width     Area      Height     Area
  #   [min]      [min]   [mAU*s]     [mAU]       %
----|-------|----|-------|----------|----------|--------|
   1  13.405 BB    0.8997 2296.99146   36.22612  53.5314
   2  16.131 BB    1.2026 1993.93579   23.86783  46.4686
```

(*R*)-3-(*cis*-1-Azido-4-phenylcyclohexyl)-1-phenylpropan-1-ol ((*R*)-13)

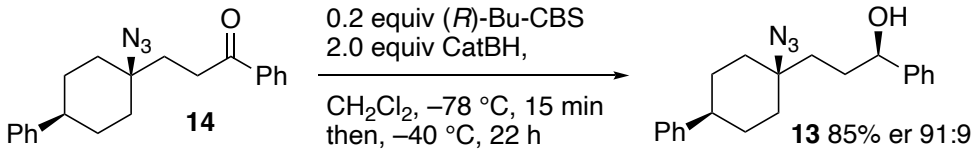

A flask under inert atmosphere was charged with commercial (*S*)-butyl CBS[10] reagent (1 M in toluene, 0.15 mL, 0.15 mmol, 0.2 equiv). The solvent was removed by applying vacuum, and the CBS reagent was dissolved in dry CH_2Cl_2 (7.5 mL). Catecholborane (0.16 mL, 180 mg, 1.5 mmol, 2.0 eq.) was added and the reaction mixture was cooled to –78 °C. Ketone **14** (0.250 g, 0.75 mmol, 1.0 equiv) was added

and the reaction mixture was stirred for 15 min at –78 °C. the mixture was allowed to warm up to –40 °C and stirred at this temperature overnight (thermostat) and at 0 °C in the fridge. The reaction was treated by addition of MeOH (0.5 mL) and warmed up to room temperature. The reaction mixture was diluted with Et_2O (30 mL) and the organic phase was washed with a 2:1 solution of 1 M NaOH and sat $NaHCO_3$. The aqueous phase was extracted with Et_2O (3 × 10 mL) and the combined organic phase was dried over Na_2SO_4 and concentrated. FC (pentane/Et_2O 9:1 to 7:3) afforded (*R*)-**13** (241 mg, 85%). Analytical data are consistent with the racemic compound; $[\alpha]_D^{25}$ = –16 (c = 1.0, $CDCl_3$).

The enantiomeric ratio (er 91:1) was determined by HPLC: Daicel CHIRALPAK IA-3, hexane/TBME 70:30; 1 mL min^{-1}, λ= 220 nm.

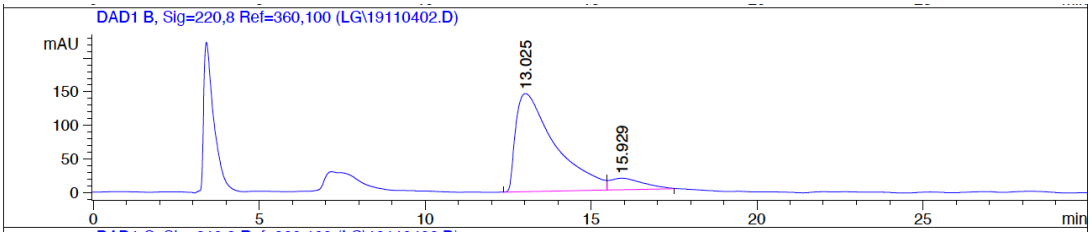


```
Signal 2: DAD1 B, Sig=220,8 Ref=360,100

Peak RetTime Type  Width     Area      Height     Area
  #   [min]       [min]   [mAU*s]     [mAU]       %
----|-------|----|-------|----------|----------|--------|
   1  13.025 BB    1.1830 1.20347e4   146.09892  90.9398
   2  15.929 BB    0.9343 1198.99756   17.22016   9.0602
```

Intramolecular Schmidt reaction

General procedure

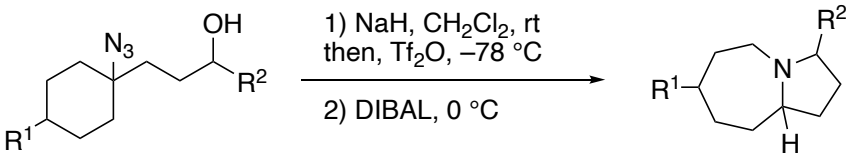

A solution of azidoalcohol in CH_2Cl_2 was slowly added to a slurry of sodium hydride in CH_2Cl_2 at rt, and the suspension (c = 0.15 M) stirred for 1 h. The reaction mixture was cooled to –78 °C with dry ice, triflic anhydride was added dropwise, and it was stirred at this temperature for 1 h. The dry ice bath was removed and the mixture was allowed to warm up to rt and extrusion of nitrogen (bubbles formation) was observed. DIBAL was added dropwise at 0 °C, and the resulting solution was stirred for 1 h at 0 °C. The reaction mixture was diluted twice with CH_2Cl_2 and treated carefully with aq. NaOH (1 M). The organic layer was washed with NaOH (1 M), the aqueous phase was extracted with CH_2Cl_2 (3 ×), the combined organic phase was dried over Na_2SO_4 and concentrated. FC (basic alumina or deactivated silica gel with pentane/Et_2O) afforded the pyrroloazepine.

Octahydrospiro[pyrrolo[1,2-a]azepine-7,2'-[1,3]dioxolane] (2)

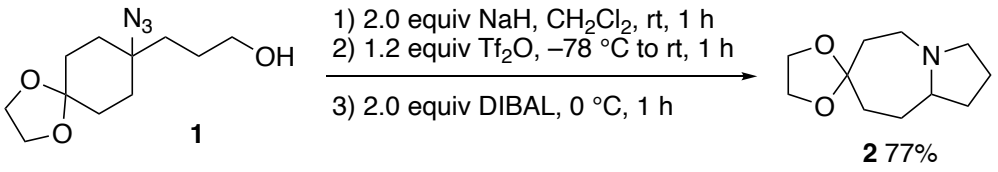

The preparation of **2** from **1** was described previously.[1]

cis-Octahydrospiro[pyrrolo[1,2-*a*]azepine-7,2'-[1,3]dioxolan]-1-ol (*cis*-4)

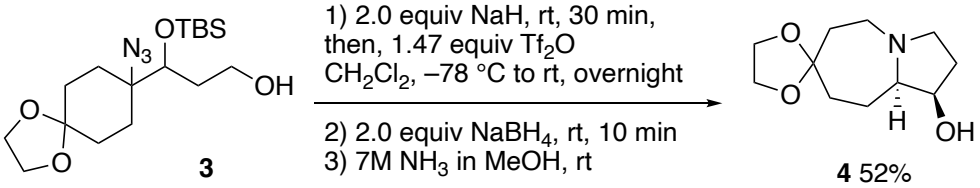

To a stirred solution of **3** (150 mg, 0.4 mmol) in dry CH_2Cl_2 (4 mL) was added sodium hydride (20 mg, 0.8 mmol, 2.0 equiv) at rt. After 30 min, the mixture was cooled to –78 °C and triflic anhydride (0.1 mL, 0.6 mmol, 1.47 equiv) was added drop wise. The dry ice bath was fully loaded with dry ice, covered with aluminium foil and allowed to warm up slowly to rt overnight. After addition of sodium borohydride (31 mg, 0.81 mmol, 2.0 equiv), the mixture was stirred at rt for 5min before ammonia in MeOH (7 M, 0.1 mL) was added drop wise. The resulting solution was stirred for 5min at rt and directly loaded on column. FC (HMDS deactivated silica gel, 95:5 CH_2Cl_2/7 M solution of NH_3 in MeOH) afforded *cis*-**4** as an inseparable mixture of diastereomers (45 mg, dr 1:2, 52%).

Colorless oil; Rf 0.20 in CH_2Cl_2 + 6% of ammonia (7 M solution in MeOH), HMDS-deactivated silica plates; ^{1}H-NMR (400 MHz, C_6D_6) δ 3.77 and 3.66 (ddd, J = 6.2, 3.9, 1.7 Hz and ddd, J = 8.4, 6.5, 4.9 Hz, total 1H), 3.58–3.38 (m, 4H), 3.09 and 3.02 (s and d, J = 1.5 Hz, total 1H), 2.82–2.61 (m, 2H), 2.54–2.40 (m, 2H), 2.35–1.37 (m, 12H); ^{13}C-NMR major (101 MHz, C_6D_6) δ 112.4, 77.7, 74.2, 64.2, 64.0, 53.7, 49.4, 39.4, 37.0, 33.1, 26.6; ^{13}C-NMR minor (101 MHz, C_6D_6) δ 112.5, 75.0, 72.5, 64.1, 63.97 (in shoulder of major peak), 53.8, 49.2, 39.3, 36.9, 34.1, 23.5; HRMS calc. for $C_{11}H_{20}NO_3$ $[M+H]^+$: 214.1438, found: 214.1438; IR (cm^{-1}): 3340, 2935, 2827, 1648, 1442, 1340, 1222, 1091, 1020, 930.

cis-7-Phenyloctahydro-1H-pyrrolo[1,2-a]azepine (*cis*-6)

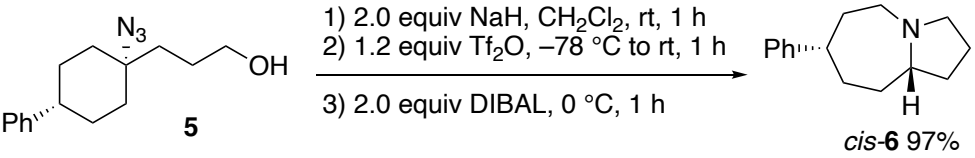

Cis-**6** was prepared according to the general procedure from azidoalcohol **5** (130 mg, 0.5 mmol), sodium hydride (90% in mineral oil, 26 mg, 1.0 mmol, 2.0 equiv), triflic anhydride (0.1 mL, 0.6 mmol, 1.2 equiv) and DIBAL (1 M in cyclohexane, 1.0 mL, 1.0 mmol, 1.0 equiv). FC (deactivated silica gel, 9:1 Et_2O/pentane) afforded *cis*-**6**[1] in 97% (105 mg, 0.49 mmol).

Yellow oil; Rf 0.39 (deactivated silica plates; 1% NH_3 (7M in MeOH) in Et_2O); ^{1}H-NMR (300 MHz, CD_2Cl_2) δ = 7.34–7.05 (m, 5H), 3.19–3.00 (m, 2H), 2.82 (dddd, J = 11.1, 8.3, 5.7, 2.6 Hz, 1H), 2.48 (qd,

J = 8.2, 2.8 Hz, 1H), 2.37–2.18 (m, 2H), 2.07–1.55 (m, 9H), 1.46 (dddd, J = 12.9, 10.2, 8.0, 5.3 Hz, 1H); ^{13}C-NMR (75 MHz, CD_2Cl_2) δ = 150.3, 128.7, 127.0, 126.0, 64.5, 57.9, 56.8, 45.0, 37.8, 34.3, 34.2, 33.3, 22.9.

7-Phenyloctahydro-1*H*-pyrrolo[1,2-*a*]azepin-1-ol (8)

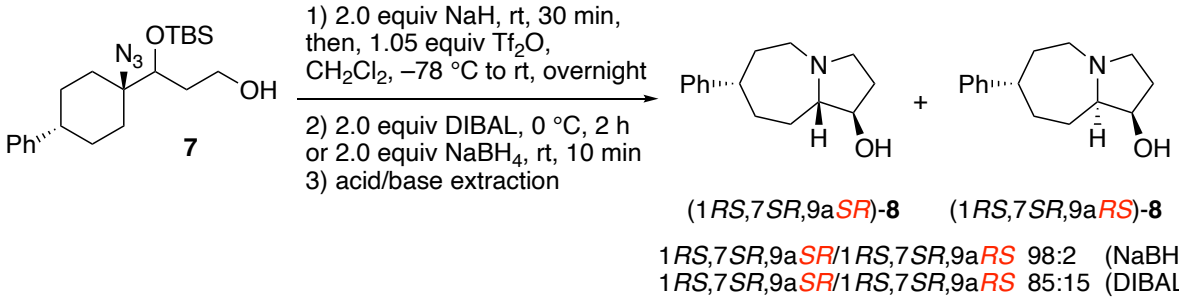

(1*RS*,7*SR*,9a*SR*)-**8** (1*RS*,7*SR*,9a*RS*)-**8**

1*RS*,7*SR*,9a*SR*/1*RS*,7*SR*,9a*RS* 98:2 ($NaBH_4$)
1*RS*,7*SR*,9a*SR*/1*RS*,7*SR*,9a*RS* 85:15 (DIBAL)

To a stirred suspension of NaH (95% solution in mineral oil, 253 mg, 10 mmol, 2.0 equiv) in dry CH_2Cl_2 (25 mL) at –78 °C was added dropwise a solution of **7** (1.95 g, 5 mmol) in dry CH_2Cl_2 (25 mL). After stirring for 30 min, Tf_2O (0.88 mL, 5.2 mmol, 1.05 eq.) was added drop wise. The mixture was stirred for 4 h at –78 °C before it was allowed to warm up to rt and stirred for 14 h. The mixture was cooled to 0 °C and a solution of DIBAL (1 M in hexanes, 11 mL, 11 mmol, 2.1 equiv) was added over 10 min and stirred for 2 h. The reaction was diluted with CH_2Cl_2 (20 mL) and treated with aq. NaOH (0.5 M, 20 mL) and brine (50 mL). The aqueous layer was extracted twice with CH_2Cl_2. The combined organic phase was acidified with aq. HCl (1 M, 50 mL), stirred for 10 min and separated. The organic layer was extracted twice with aq. HCl (1 M, 50 mL). The aqueous phase was then basified with aq. NaOH (6 M) to reach a basic pH. The mixture was stirred for 5 min and extracted 3 × with CH_2Cl_2. The combined organic phase was washed with aq. NaOH (0.5 M), dried over Na_2SO_4 and concentrated. Without further purification, **8** was obtained as a mixture of diastereoisomers (900 mg, 85%, dr 85:15). The two diastereomers were separated by FC (CH_2Cl_2 with 5% 8M NH_3 in MeOH). Yields of the separated diastereomers were not determined due to repeated purification steps.

Performing the reduction with $NaBH_4$ (3.8 g, 10 mmol, 2 equiv) instead of DIBAL afforded (1*RS*,7*SR*,9a*SR*)-**8** as a single diastereomer (900 mg, 85%, dr >98:2).

(1*RS*,7*SR*,9a*SR*)-**8** (major)

Yellowish oil; Rf 0.17 in CH_2Cl_2 with 5% 7M NH_3 in MeOH; ^{1}H-NMR (300 MHz, C_6D_6) δ 7.23–7.16 (m, 2H), 7.13–7.04 (m, 3H), 3.68 (ddd, *J* = 7.7, 5.2, 3.8 Hz, 1H), 2.94–2.82 (m, 2H), 2.73–2.61 (m, 1H), 2.47 (td, *J* = 9.3, 8.0 Hz, 1H), 2.36–2.26 (m, 1H), 2.19 (td, *J* = 11.9, 2.2 Hz, 1H), 2.04–1.64 (m, 7H), 1.43 (dddd, *J* = 12.9, 7.9, 3.8, 2.3 Hz, 1H), 1.32 (s, 1H); ^{13}C-NMR (75 MHz, C_6D_6) δ 149.8, 128.8 (2C), 127.0 (2C), 126.0, 78.8, 72.9, 56.2, 54.5, 45.4, 37.9, 33.7, 33.4, 30.9; HRMS calc. for $C_{15}H_{22}ON$ $[M+H]^+$: 232.1696, found: 232.1693; IR (cm^{-1}): not obtained, compound is rapidly decomposed in air.

(1*RS*,7*SR*,9a*RS*)-**8** (minor)

Colorless oil; Rf 0.28 in DCM with 5% 7M NH_3 in MeOH; ^{1}H-NMR (300 MHz, C_6D_6) δ 7.23–7.16 (m, 2H), 7.13–7.04 (m, 3H), 3.02 (ddd, J = 14.2, 9.5, 6.0 Hz, 2H), 2.72–2.58 (m, 1H), 2.32 (s, 1H), 2.24–1.53 (m, 10H), 1.51–1.27 (m, 2H); ^{13}C-NMR (75 MHz, C_6D_6) δ 150.0, 128.8 (2C), 127.1 (2C), 126.0, 64.3, 57.7, 56.4, 45.3, 37.9, 34.2, 34.1, 33.3, 23.0; HRMS calc. for $C_{15}H_{22}ON$ $[M+Na]^+$: 232.1696, found: 232.1691; IR (cm^{-1}): not obtained, compound is rapidly decomposed in air.

(3*RS*,7*SR*,9a*SR*)-3-Ethyl-7-phenyloctahydro-1*H*-pyrrolo[1,2-*a*]azepine ((±)-15)

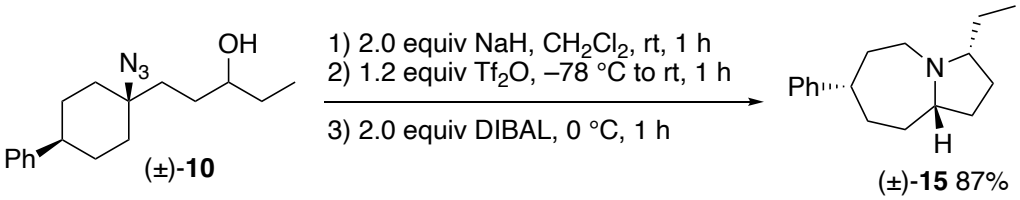

Prepared according to the general procedure. Starting from racemic (±)-**10** (190 mg, 0.66 mmol), NaH (90% in mineral oil, 34 mg, 1.32 mmol, 2.0 equiv), triflic anhydride (133 µL, 0.79 mmol, 1.2 equiv), and DIBAL (1 M in cyclohexane, 1.32 mL, 1.32 mmol, 2.0 equiv). FC (deactivated silica, 95:5 pentane/Et_2O) afforded (±)-**15** (140 mg, 87%) as a single diastereomer (racemic).

Colorless oil; Rf 0.28 (deactivated silica plates, 9:1 pentane/Et_2O); ^{1}H-NMR (300 MHz, $CDCl_3$) δ 7.23-7.18 (m, 2H), 7.13-7.05 (m, 3H), 3.15 (ddd, J = 11.7, 4.5, 2.7 Hz, 1H), 2.81-2.72 (m, 1H), 2.57-2.48 (m, 1H), 2.20-2.11 (m, 1H), 2.03 (ddd, J = 11.1, 2.1 Hz, 1H), 1.93-1.58 (m, 9H), 1.42- 1.12 (m, 3H), 0.81 (t, J = 7.21 Hz, 3H); ^{13}C-NMR (75 MHz, $CDCl_3$) δ 149.7, 128.4, 126.7, 125.6, 69.0, 65.9, 55.0, 45.0, 37.5, 33.8, 33.0, 31.5, 28.7, 27.3, 10.8; HRMS calc. for $C_{17}H_{26}N$ $[M+H]^+$: 244.2060, found: 244.2056; IR (cm^{-1}): 2927, 2873, 2792, 1602, 1492, 1451, 1356, 1177, 755, 697.

GC analysis of the mixture of enantiomers was performed using standard settings (cf. general information) and isothermal conditions (110 °C).

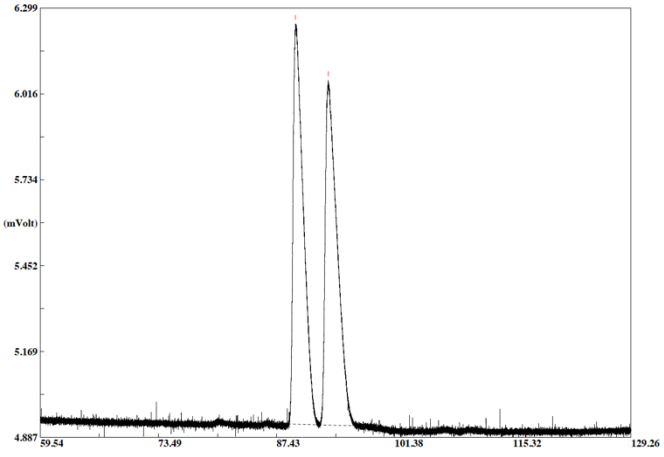

Peak Number #	Area %	Ret.Time	Area	BC
1	50.0133	89.67	1093247	mi
2	49.9867	93.50	1092667	mi
Totals	100.0000		2185914	

(3*R*,7*S*,9a*S*)-3-Ethyl-7-phenyloctahydro-1*H*-pyrrolo[1,2-*a*]azepine ((3*R*,7*S*,9a*S*)-15)

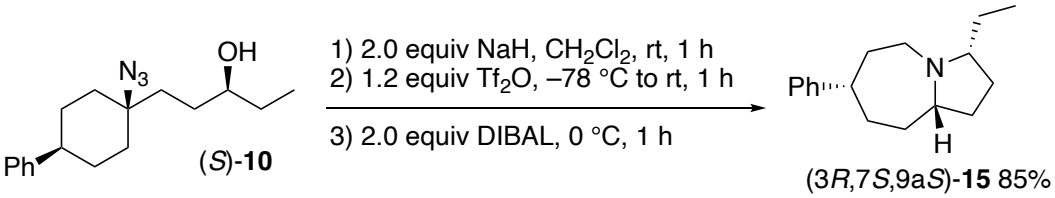

Prepared according to the general procedure. Starting from (*S*)-**10** (90 mg, 0.31 mmol, er 96:4), NaH (90% in mineral oil, 16 mg, 0.62 mmol, triflic anhydride (63 μL, 0.38 mmol, 1.2 mmol), and DIBAL (1M in cyclohexane, 0.62 mL, 0.62 mmol). FC (deactivated silica, 95:5 pentane/Et_2O) afforded **15** (65 mg, 85%).

Analytical data are consistent with the racemic compound; $[\alpha]_D^{25} = -48$ (c = 1, CH_2Cl_2).

The enantiomeric ratio (er 93:7) was determined by GC analysis using the conditions described for the racemic compound.

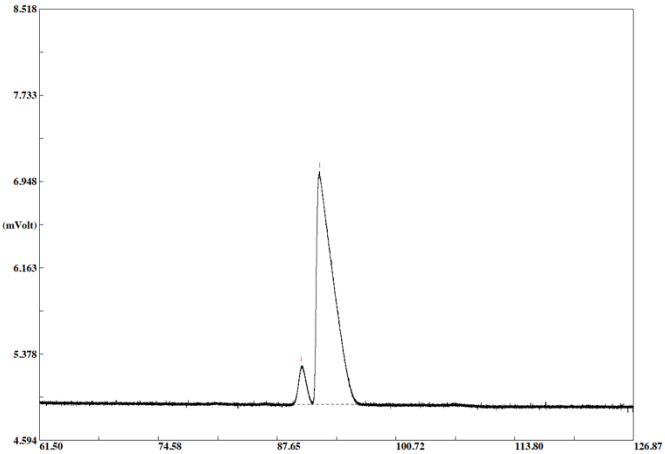

Peak Number #	Area %	Ret.Time	Area	BC
1	7.1247	90.31	202771	mi
2	92.8753	92.32	2643248	mi
Totals	100.0000		2846019	

(3*SR*,7*SR*,9a*SR*)-7-Phenyl-3-(phenylethynyl)octahydro-1*H*-pyrrolo[1,2-*a*]azepine ((±)-16)

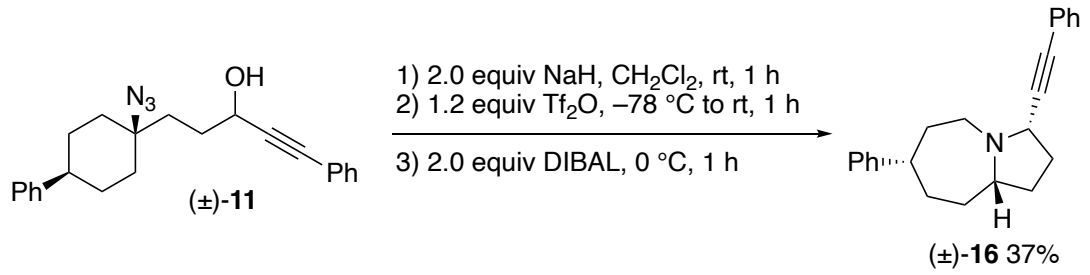

Prepared according to general procedure, starting from racemic (±)-**11** (115 mg, 0.32 mmol), NaH (90% in mineral oil, 16 mg, 0.64 mmol, 2.0 eq.), triflic anhydride (65 µL, 0.38 mmol, 1.2 eq.) and DIBAL (1M in cyclohexanes, 0.64 mL, 0.64 mmol, 2.0 eq.). FC (deactivated silica gel, 5% Et_2O in pentane) afforded racemic (±)-**16** (37 mg, 37%).

Appearance yellow oil Rf 0.16 (deactivated silica plates, 5% Et_2O in pentane) ^{1}H-NMR (300 MHz, CD_2Cl_2) δ = 7.47–7.39 (m, 2H), 7.34–7.11 (m, 8H), 3.54 (ddd, J = 12.1, 4.6, 3.1 Hz, 1H), 3.31 (dd, J = 9.3, 7.0 Hz, 1H), 2.91–2.79 (m, 1H), 2.69–2.58 (m, 1H), 2.23 (td, J = 11.9, 2.3 Hz, 1H), 2.14–1.74 (m, 10H); ^{13}C-NMR (75 MHz, CD_2Cl_2) δ = 150.2, 132.0, 128.8, 128.7, 128.4, 127.0, 126.0, 123.8, 91.0, 83.1, 64.8, 59.1, 55.4, 45.1, 37.8, 34.2, 33.4, 32.2, 31.0; HRMS calc. for $C_{23}H_{26}N$ $[M+H]^+$: 316.2060, found: 316.2052 IR (cm^{-1}): 3024, 2927, 2794, 1598, 1489, 1354, 1171, 754, 690, 533.

GC analysis was performed using standard settings (cf. general information) and the following temperature gradient: 40 °C (1 min), 4 °C/min, 240 °C (10 min)

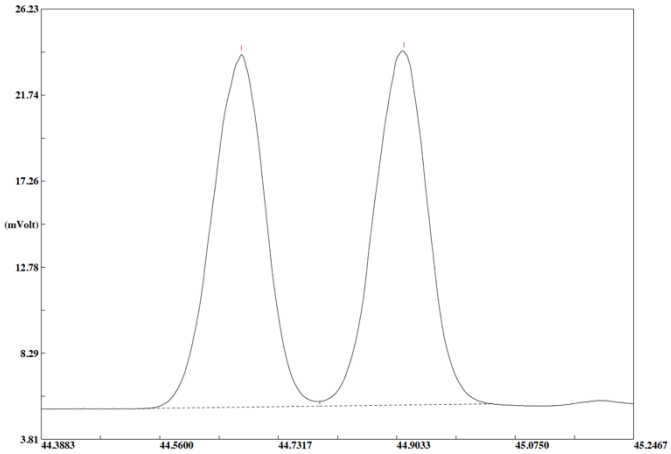

Peak Number #	Area %	Ret.Time	Area	BC
1	49.8563	44.68	983271	mi
2	50.1437	44.91	988939	mi
Totals	100.0000		1972210	

(3*S*,7*S*,9a*S*)-7-Phenyl-3-(phenylethynyl)octahydro-1*H*-pyrrolo[1,2-*a*]azepine ((3*S*,7*S*,9a*S*)-16)

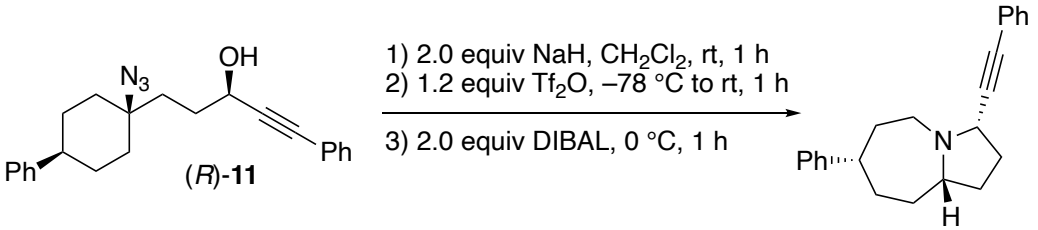

(3*S*,7*S*,9a*S*)-**16** 32%

Prepared according to general procedure, starting from (*R*)-**11** (0.36 g, 1.0 mmol, er 93:7), NaH (60% in mineral oil, 80 mg, 2.0 mmol, 2.0 eq.), triflic anhydride (0.34 g, 1.2 mmol, 1.2 eq.) and DIBAL (1M in hexanes, 2.0 mL, 2.0 mmol, 2.0 eq.). FC (pentane/Et_2O 10:0 to 70:3) afforded (3*S*,7*S*,9a*S*)-**16** in 32% yield (101 mg, 0.32 mmol).

Analytical data are consistent with the racemic compound; $[\alpha]_D^{25}$ = –67 (c = 1.0, CH_2Cl_2).

The enantiomeric ratio (er 95:5) was determined by GC analysis using the same settings as for the racemic compound.

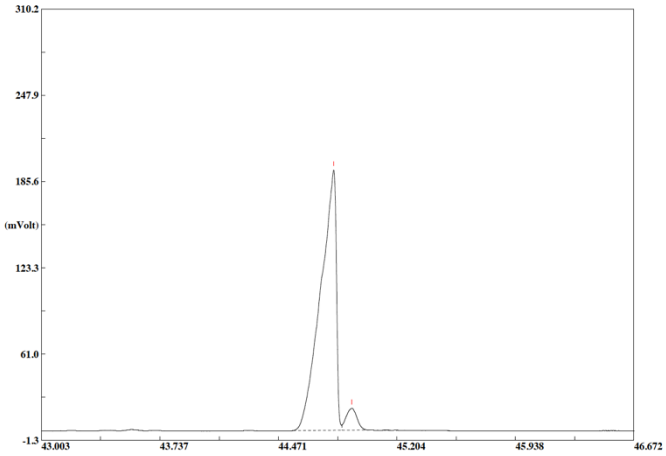

Peak Number #	Area %	Ret.Time	Area	BC
1	94.5417	44.81	12706840	mi
2	5.4583	44.93	733626	mi
Totals	100.0000		13440470	

(3*SR*,7*SR*,9a*SR*)-3-Allyl-7-phenyloctahydro-1*H*-pyrrolo[1,2-*a*]azepine ((±)-17)

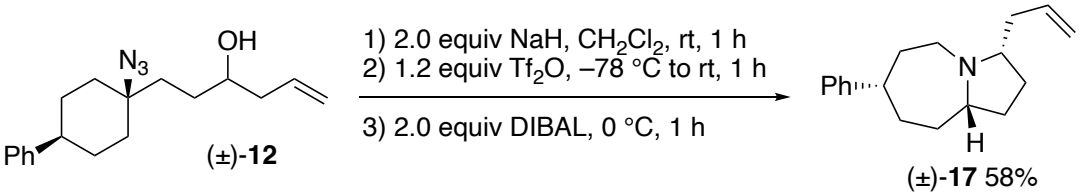

Prepared according to the general procedure, starting from racemic (±)-**12** (85 mg, 0.28 mmol), NaH (90% in mineral oil, 15 mg, 0.57 mmol, 2.0 equiv), triflic anhydride (57 µL, 0.34 mmol, 1.2 equiv) and DIBAL (1M in cyclohexanes, 0.57 mL, 0.57 mmol, 2.0 equiv). FC (deactivated silica gel, 4% Et_2O in pentane) afforded racemic (±)-**17** (40 mg, 58%).

Colorless oil; Rf 0.28 (deactivated silica plates, 9:1 pentane/Et_2O); ^{1}H-NMR (300 MHz, CD_2Cl_2) δ = 7.39–7.08 (m, 5H), 5.85 (ddt, J = 17.1, 10.2, 7.0 Hz, 1H), 5.14–4.89 (m, 2H), 3.17 (dt, J = 12.3, 3.9 Hz, 1H), 2.89–2.75 (m, 1H), 2.75–2.58 (m, 1H), 2.51–2.29 (m, 2H), 2.19 (ddd, J = 12.2, 10.7, 3.1 Hz, 1H), 2.12–1.98 (m, 1H), 1.96–1.61 (m, 8H), 1.55–1.23 (m, 4H), 1.02–0.75 (m, 1H); ^{13}C-NMR (75 MHz, CD_2Cl_2) δ = 150.4, 137.0, 128.7, 127.1, 125.9, 116.0, 66.7, 66.0, 54.9, 45.3, 39.7, 38.5, 34.1, 33.7, 32.0, 29.2; HRMS calc. for $C_{18}H_{26}N$ $[M+H]^+$: 316.2060, found: 316.2055; IR (cm^{-1}): 2926, 2792, 1738, 1493, 1451, 1272, 1122, 908, 755, 698.

GC analysis was performed using standard settings (cf. general information) and the following temperature gradient: 125 °C (80 min), 2 °C/min, 240 °C (10 min)

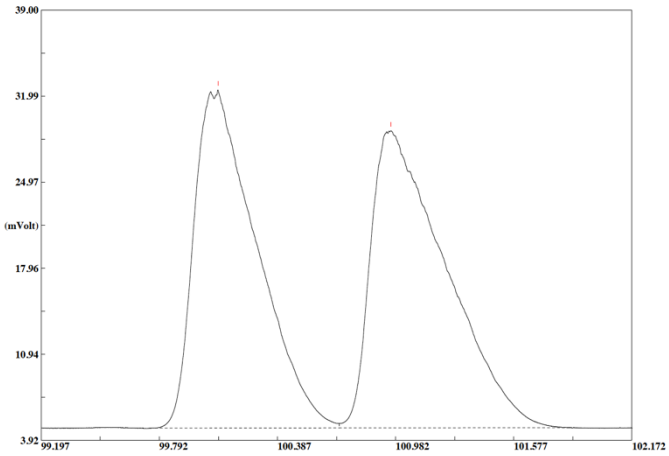

Peak Number #	Area %	Ret.Time	Area	BC
1	48.8026	100.09	6049100	mi
2	51.1974	100.96	6345948	mi
Totals	100.0000		12395050	

(3*S*,7*S*,9a*S*)-3-Allyl-7-phenyloctahydro-1*H*-pyrrolo[1,2-*a*]azepine ((3*S*,7*S*,9a*S*)-17)

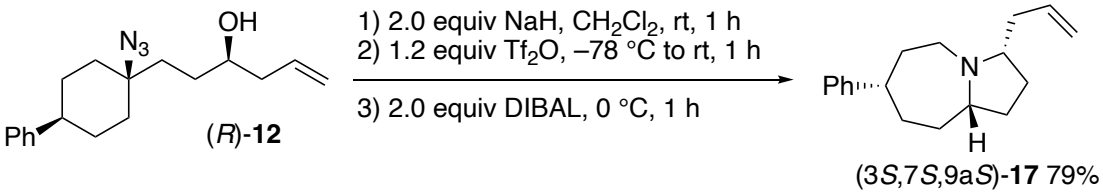

Prepared according to the general procedure, starting from (*R*)-**12** (0.40 g, 1.34 mmol), NaH (60% in mineral oil, 0.11 g, 2.68 mmol, 2.0 eq.), triflic anhydride (0.46 g, 1.61 mmol, 1.2 eq.) and DIBAL (1M in hexanes, 2.7 mL, 2.7 mmol, 2.0 eq.). FC (pentane/EtO 10:0 to 70:3) afforded (3*S*,7*S*,9a*S*)-**17** (273 mg, 79%).

Analytical data are consistent with the racemic compound; $[\alpha]_D^{25}$ = –37 (c = 1.0, CH_2Cl_2)

The enantiomeric ratio (er 92:8) was determined by GC analysis using the same settings as for the racemic compound.

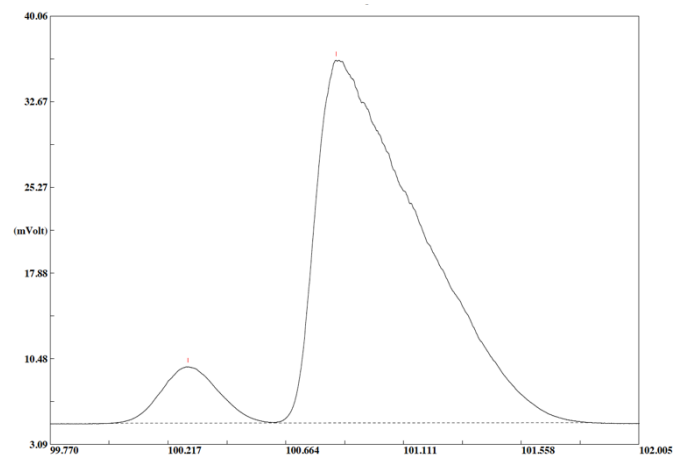

Peak Number #	Area %	Ret.Time	Area	BC
1	7.9107	100.29	741270	mi
2	92.0894	100.86	8629260	mi
Totals	100.0000		9370530	

(3*SR*,7*SR*,9a*SR*)-3,7-Diphenyloctahydro-1*H*-pyrrolo[1,2-*a*]azepine ((±)-18)

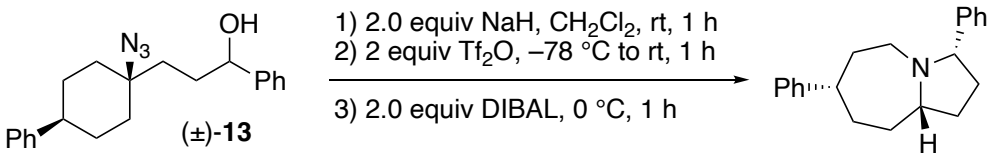

(±)-**18** 53%

Prepared according to the general procedure, starting from (±)-**13** (0.18 g, 0.54 mmol, 1.0 eq.), NaH (90% in mineral oil, 27 mg, 1.07 mmol, 2.0 eq.), triflic anhydride (108 µL, 0.64 mmol, 1.2 eq.) and DIBAL (1M in cyclohexanes, 1.07 mL, 1.07 mmol, 2.0 eq.). FC (deactivated silica gel, 1% Et_2O in pentane) afforded (±)-**18** (83 mg, 53%).

Colorless oil; Rf 0.50 (deactivated silica plates, 5% Et_2O in pentane); mp 68-70 °C; ^{1}H-NMR (300 MHz, CD_2Cl_2) δ = 7.40 (tt, J = 7.0, 1.3 Hz, 2H), 7.36–7.10 (m, 8H), 3.50–3.40 (m, 1H), 2.93–2.77 (m, 2H), 2.28–2.14 (m, 1H), 2.12–1.95 (m, 3H), 1.95–1.75 (m, 4H), 1.75–1.65 (m, 1H), 1.66–1.54 (m, 2H); ^{13}C-NMR (75 MHz, CD_2Cl_2) δ= 150.4, 145.5, 128.7, 128.6, 127.7, 127.1, 127.0, 125.9, 72.4, 65.3, 54.6, 45.0, 38.8, 34.6, 34.2, 32.5; HRMS calc. for $C_{21}H_{26}N$ [M+H]$^+$: 292.2060, found: 292.2071; IR (cm^{-1}): 3024, 2917, 1601, 1492, 1449, 1067, 917, 754, 695, 548.

GC analysis was performed using standard settings (cf. general information) and the following temperature gradient: 120 °C (60 min), 4 °C/min, 240 °C (10 min)

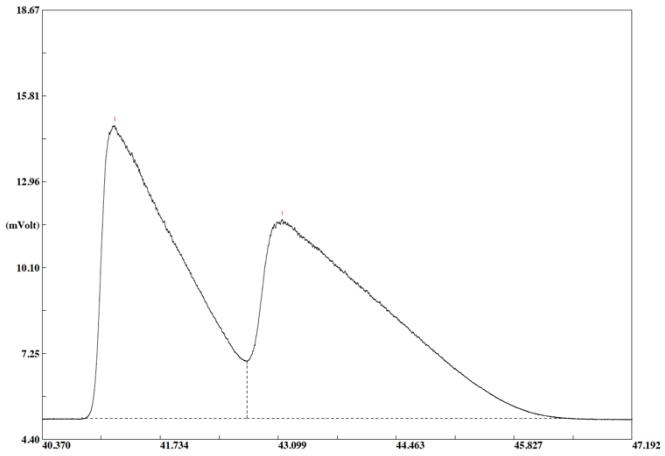

Peak Number #	Area %	Ret.Time	Area	BC
1	48.1020	41.21	6013646	mi
2	51.8980	43.15	6488224	mi
Totals	100.0000		12501870	

(3*S*,7*S*,9a*S*)-3,7-Diphenyloctahydro-1*H*-pyrrolo[1,2-*a*]azepine ((3*S*,7*S*,9a*S*)-18)

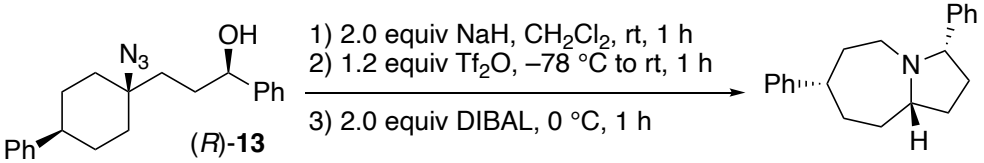

(3*S*,7*S*,9a*S*)-**18** 71%

Prepared according to the general procedure, starting from (*R*)-**13** (220 mg, 0.66 mmol, er 87:13), NaH (90% in mineral oil, 34 mg, 1.31 mmol, 2.0 equiv), triflic anhydride (130 µL, 0.79 mmol, 1.2 equiv) and

DIBAL (1M in cyclohexanes, 1.3 mL, 1.3 mmol, 2.0 equiv). FC (pentane to pentane/EtO 7:3) afforded (3*S*,7*S*,9a*S*)-**18** (110 mg, 71%).

Analytical data are consistent with the racemic compound; $[\alpha]_D^{25}$ = –50 (c = 1.0, CH_2Cl_2).

The enantiomeric ratio (er 78:22) was determined by GC analysis using the same settings as for the racemic compound.

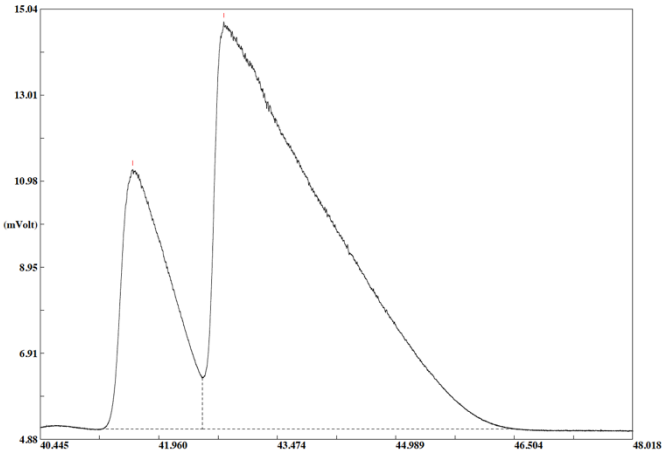

Peak Number #	Area %	Ret.Time	Area	BC
1	21.6585	41.63	2601921	mi
2	78.3415	42.79	9411495	mi
Totals	100.0000		12013420	

Derivatizations for X-ray crystallographic analysis

7-Phenyl-1,2,3,5,6,7,8,9-octahydropyrrolo[1,2-*a*]azepin-4-ium trifluoromethanesulfonate (6im)

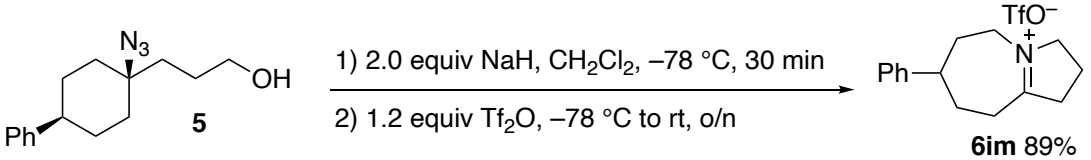

6im 89%

A solution of **5** (518 mg, 2 mmol) was added slowly to the slurry of NaH (60% in mineral oil, 96 mg, 4.0 mmol, 2.0 equiv) in dry CH_2Cl_2 (16 mL) at –78 °C. After stirring for 30 minutes, Tf_2O (405 µL, 2.39 mmol, 1.2 equiv) was added drop wise and stirred for 8 h at –78 °C. The cooling bath was removed, the reaction mixture was allowed to warm up to rt and stirred for 18 h. The reaction mixture was treated with H_2O and aqueous layer was extracted with CH_2Cl_2. The combined organic layers were dried over anhydrous Na_2SO_4, concentrated under reduced pressure to give the crude product. Purification by recrystallisation from CH_2Cl_2/Et_2O afforded **6im** as light yellow crystalline solid (651 mg, 89%) suitable for single crystal X-ray crystallographic analysis.

Mp 124.0-124.3 °C. ^{1}H-NMR (300 MHz, $CDCl_3$) δ = 7.25-7.10 (m, 5H), 4.46-4.27(m, 2H), 4.15-4.04(m, 1H), 3.83 (ddd, J = 15, 3, 2.7 Hz, 1H), 3.41-3.26 (m, 2H), 3.05-2.82 (m, 3H), 2.28 (q, J = 8.1 Hz, 2H), 2.03-1.88 (m, 3H), 1.79 (dtd, J = 11.7, 11.7, 2.7 Hz, 1H). ^{13}C-NMR (75 MHz, $CDCl_3$) δ = 195.8, 145.0, 128.8, 127.0, 126.6, 63.7, 51.5, 47.4, 41.6, 31.1, 30.1, 28.3, 18.6; IR (cm^{-1}): 1690, 1493, 1451, 1397, 1258, 1221, 1149, 1029, 751 HRMS calc. for $C_{15}H_{20}N$ $[M+H]^+$: 214.1590; found 214.1592

3-((*cis*)-1-Azido-4-phenylcyclohexyl)-3-((*tert*-butyldimethylsilyl)oxy)propyl 3,5-dinitrobenzoate (7dnb)

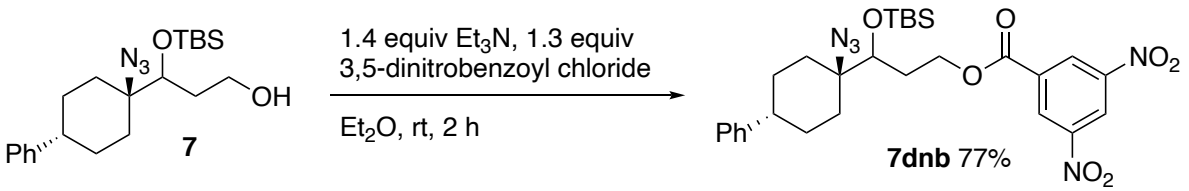

To a stirred solution of **7** (230 mg 1 mmol) in dry Et_2O (2.5 mL) was added Et_3N (0.2 mL, 1.4 mmol, 1.4 eq.) and 3,5-dinitrobenzoyl chloride (300mg, 1.3mmol, 1.3 eq.). The mixture was stirred at rt for 2 h. The reaction was treated with sat. NH_3 (25% in water, 1.5 mL) and water (10 mL). The mixture was extracted 3x with Et_2O. The organic layers were washed with a solution of $NaHSO_4$ (10% aq.) and twice with water. The combined organic layers were dried over Na_2SO_4 and concentrated under reduced pressure. The crude product was dissolved in CH_2Cl_2 and filtered through a short column of silica (lower part) and Na_2SO_4 (upper part). Evaporation of the solvent afforded **7dnb** (450 mg, 77%).

Crystallisation: The product was dissolved in Et_2O, filtered through three in-line syringe filters (POR 0.45) in a round bottom flask to allow a slow evaporation of the solvent which afforded crystals of **7dnb** suitable for single crystal X-ray crystallographic analysis.

Yellowish crystals; Rf 0.83 in 7:3 pentane/Et_2O; mp 115-116 °C; ^{1}H-NMR (300 MHz, $CDCl_3$) δ 9.22 (t, J = 2.2 Hz, 1H), 9.15 (d, J = 2.1 Hz, 2H), 7.35–7.27 (m, 2H), 7.24–7.17 (m, 3H), 4.84 (ddd, J = 11.0, 8.4, 6.2 Hz, 1H), 4.63 (ddd, J = 11.0, 8.4, 6.6 Hz, 1H), 4.25 (t, J = 4.4 Hz, 1H), 2.76 (dd, J = 10.0, 6.3 Hz, 1H), 2.32 (d, J = 10.8 Hz, 1H), 2.26–2.11 (m, 2H), 2.06–1.96 (m, 1H), 1.96–1.87 (m, 1H), 1.87–1.70 (m, 3H), 1.65–1.51 (m, 2H), 0.96 (s, 9H), 0.19 (s, 3H), 0.14 (s, 3H); ^{13}C-NMR (75 MHz, $CDCl_3$) δ 162.5, 148.7, 144.9, 134.0, 129.7 (2C), 128.5 (2C), 126.7 (2C), 126.3, 122.4, 71.9, 65.4, 63.7, 41.2, 32.7, 31.8, 30.3, 29.0, 28.8, 25.8 (3C), 18.2, –4.1, –4.3; HRMS calc. for $C_{28}H_{37}O_7N_5NaSi$ $[M+Na]^+$: 606.2354, found: 606.2355; IR (cm^{-1}): 3091, 2928, 2857, 2107, 1722, 1543, 1343, 1281, 1171, 1091

(1*RS*,7*SR*,9a*SR*)-7-Phenyloctahydro-1*H*-pyrrolo[1,2-*a*]azepin-1-yl 3,5-dinitrobenzoate (8dnb)

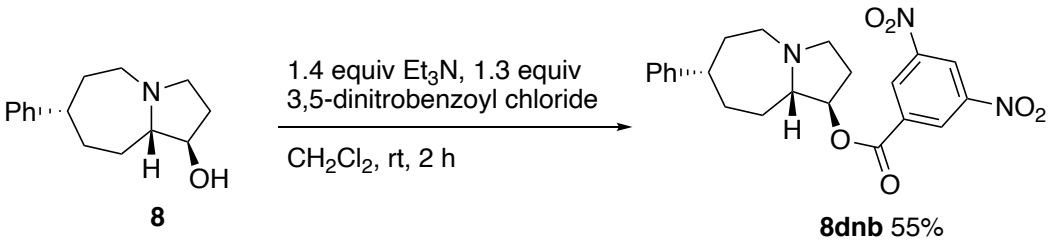

To a stirred solution of (1*RS*,7*SR*,9a*SR*)-**8** (600 mg, 2.6mmol, major diastereomer) in dry CH_2Cl_2 (6.5 mL) was added Et_3N (0.52 mL, 3.6mmol, 1.4 eq.) and 3,5-dinitrobenzoyl chloride (780 mg, 3.4mmol, 1.3 eq.). The mixture was stirred at rt for 2 h before addition of NH_3 (25% in water, 5 mL) and water (10 mL). The mixture was extracted 3 × with Et_2O. The organic layers were filtered through a cylinder of Na_2SO_4 (upper part) and silica (lower part, previously deactivated using Et_3N in CH_2Cl_2) and concentrated under reduced pressure. FC (CH_2Cl_2 with 5% 8M NH_3 in MeOH) afforded **8dnb** (608 mg, 55%).

Crystallisation: The product was dissolved in Et_2O, filtered through three in-line syringe filters (POR 0.45) in a round bottom flask to allow a slow evaporation of the solvent which afforded crystals of **8dnb** suitable for single crystal X-ray crystallographic analysis.

Brown solid; Rf 0.56 in 1:9 MeOH/CH_2Cl_2; mp 113-115°C; ^{1}H-NMR (300 MHz, CD_2Cl_2) δ 9.22 (t, J = 2.1 Hz, 1H), 9.15 (d, J = 2.2 Hz, 2H), 7.32–7.23 (m, 2H), 7.23–7.12 (m, 3H), 5.13 (ddd, J = 7.0, 4.2, 2.4 Hz, 1H), 3.25–3.07 (m, 2H), 2.91–2.65 (m, 3H), 2.46 (td, J = 12.0, 2.8 Hz, 1H), 2.41–2.24 (m, 1H), 2.21–2.07 (m, 1H), 2.06–1.77 (m, 6H); ^{13}C-NMR (101 MHz, $CDCl_3$) δ 162.5, 148.7, 144.9, 134.0, 129.4 (2C), 128.5 (2C), 126.7 (2C), 126.3, 122.4, 71.9, 65.4, 63.7, 41.2, 32.7, 31.8, 30.3, 29.0, 28.8, 25.8 (3C), 18.2, –4.1, –4.3; HRMS calc. for $C_{22}H_{24}N_3O_6$ $[M+H]^+$: 426.1660, found: 426.1643; IR (cm^{-1}): 3096, 2928, 2809, 1722, 1543, 1343, 1280, 1172, 1073, 922.

(*S*)-1-((*cis*)-1-azido-4-phenylcyclohexyl)pentan-3-yl 4-bromo-3-nitrobenzoate ((*S*)-10dnb)

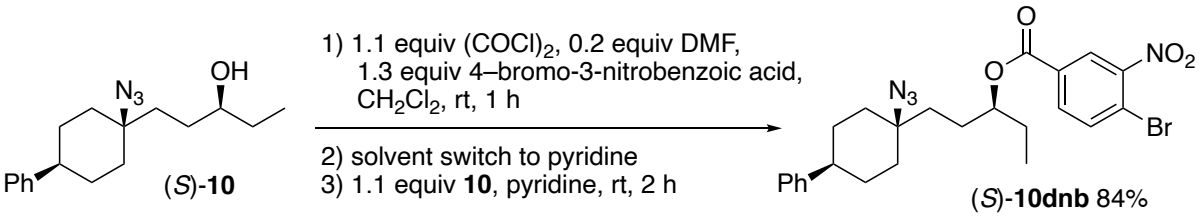

Oxalyl chloride (0.19 mL, 2.2 mmol, 1.1 eq.) followed by dry DMF (15 µL, 0.19mmol, 0.2 eq.) were added to a solution of 4-bromo-3-nitrobenzoic acid (352 mg, 1.43 mmol, 1.3 eq.) in dry CH_2Cl_2 (2.5 mL) at rt and stirred for 1 h. The mixture was evaporated to dryness, and the yellowish resulting solid taken up in dry pyridine (0.6 mL). This solution was added to a solution of (*S*)-**10** (312 mg, 1.1 mmol, 1.0 eq.) in dry pyridine (2.0 mL) at rt and stirred for 2 h. The reaction mixture was diluted with a solution of aq. HCl (1M, 10 mL) and the aqueous mixture was extracted with CH_2Cl_2 (3 × 10 mL). The combined organic phase was washed with brine (15 mL), dried over $MgSO_4$ and concentrated under reduced pressure. Recrystallization (hexane/Et_2O mixture 2:1) afforded crystals of (*S*)-**10dnb** (481 mg, 84%) suitable for single crystal X-ray crystallographic analysis.

Colorless crystals; Rf 0.37 (1:9 Et_2O/pentane); mp 93–94 °C; ^{1}H-NMR (300 MHz, CD_2Cl_2) δ = 8.46 (d, J = 2.0 Hz, 1H), 8.10 (dd, J = 8.4, 2.0 Hz, 1H), 7.88 (d, J = 8.4 Hz, 1H), 7.35–7.12 (m, 5H), 5.11 (p, J = 6.2 Hz, 1H), 2.57–2.38 (m, 1H), 1.95–1.58 (m, 12H), 1.52–1.34 (m, 2H), 0.97 (t, J = 7.4 Hz, 3H); ^{13}C-NMR (75 MHz, $CDCl_3$) δ 163.7, 150.0, 146.5, 135.5, 133.6, 131.2, 128.5, 126.5, 126.3, 119.6, 77.7, 63.1, 43.6, 36.8, 35.00, 34.95, 29.5, 27.6, 27.1, 9.73; HRMS calc. for $C_{24}H_{28}N_4O_3Br$ $[M+H]^+$: 515.1288, found: 515.1289; IR (cm^{-1}): 2930, 2869, 2091, 1709, 1535, 1287, 1245, 902, 756, 703; $[\alpha]_D$ = +20 (c = 1.0, CH_2Cl_2).

(3*R*,7*S*,9a*S*)-3-ethyl-7-phenyldecahydropyrrolo[1,2-*a*]azepin-4-ium (*R*)-2-hydroxy-2-phenylacetate ((*3R,7S,9aS*)-15·(*R*)-mandelic acid)

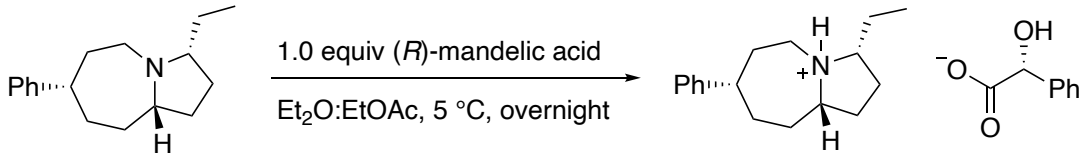

15 (*3R,7S,9aS*)-**15**·(*R*)-mandelic acid

To a stirred solution of (3*R*,7*S*,9a*S*)-**15** (149 mg, 0.61 mmol) in dry Et_2O (1 mL) was added a solution of (*R*)-mandelic acid (93 mg, 0.61 mmol, 1.0 equiv) in dry Et_2O (1 mL) and stirred overnight. Upon concentration, a white solid was obtained. Recrystalization in the fridge from Et_2O and a minimal amount of EtOAc afforded the salt as colorless crystals suitable for s single crystal X-ray crystallographic analysis. No yield was determined.

Colorless crystals; mp 85–93 °C (decomposition); ^{1}H-NMR (300 MHz, $CDCl_3$) δ 7.43–7.35 (m, 3H), 7.24–7.07 (m, 7H), 6.98–6.90 (m, 2H), 3.65–3.50 (m, 1H), 3.21–3.05 (m, 1H), 2.79–2.58 (m, 2H), 2.32 (t, J = 12.1 Hz, 1H), 2.11 (dq, J = 19.7, 10.6, 9.1 Hz, 2H), 1.83–1.36 (m, 9H), 1.33–0.94 (m, 12H), 0.89–0.66 (m, 7H); ^{13}C-NMR (75 MHz, C_6D_6) δ 177.6, 148.2, 142.8, 129.0, 128.3, 127.3, 127.2, 127.0, 126.6, 74.4, 71.5, 67.5, 43.5, 32.8, 32.5, 30.2, 29.6, 27.6, 27.0, 23.5, 11.0; IR (cm^{-1}): 3384, 2933, 1705, 1600, 1494, 1452, 1185, 1056, 728, 697; $[\alpha]_D^{25}$ = –69 (c = 1.0, CH_2Cl_2)

Synthesis of (3*R*,8a*S*)-3-propylindolizidine ((3*R*,8a*S*)-19)

3-(1-Azidocyclopentyl)propanal (21)

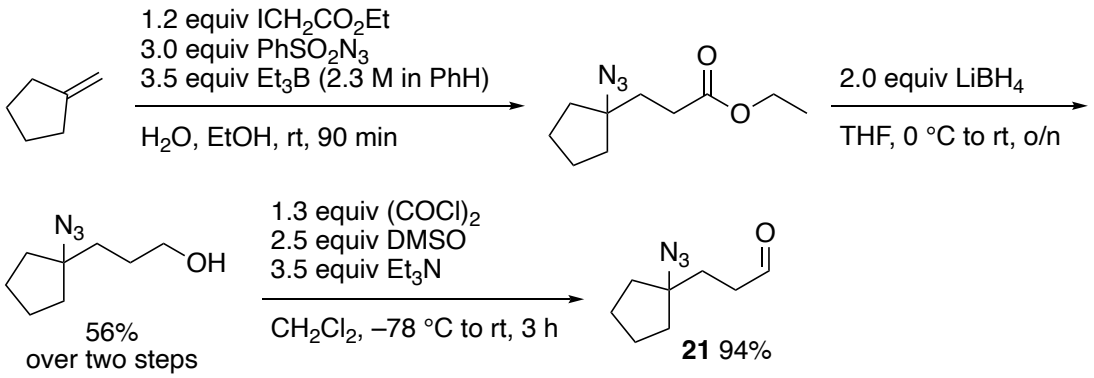

Carboazidation

To a stirred solution of methylenecyclopentane (411 mg, 5.0 mmol), ethyl iodoacetate (1.28 g, 6.0 mmol, 1.2 equiv), and phenylsulfonyl azide (2.75 g, 15.0 mmol, 3.0 equiv) in ethanol (11.3 mL) and water (1.25 mL) was added a solution of triethylborane (2.2 M in hexanes, 8 mL, 17.5 mmol, 3.5 equiv) *via* syringe pump during 90 min open to air at rt. After complete addition, pentane (20 mL) was added, the layers were separated and the aqueous layer was extracted with Et_2O (2 × 20 mL). The combined organic phase was washed with brine, dried over Na_2SO_4, filtered and concentrated.

To remove the excess $PhSO_2N_3$, the crude mixture was dissolved in dry THF (20 mL), cooled to 0 °C and treated with $LiBH_4$ (2 M in THF, 5 mL, 10 mmol, 2.0 equiv) until TLC showed complete consumption of $PhSO_2N_3$ (typically 20-30 min). The mixture was poured into 50% aq. NH_4Cl (20 mL) and extracted

with Et_2O. The combined organic phase was washed with brine, dried over Na_2SO_4, filtered and concentrated. FC (8:2 pentane/CH_2Cl_2) removed the major part of the reduced $PhSO_2N_3$. Analytical data of the crude ester are consistent with the literature data.[11]

Ester reduction

To a stirred solution of crude ester (ca. 0.5 g) in dry THF (10 mL), was added with $LiBH_4$ (2.0 M in THF, 5 mL, 10 mmol, 2.0 equiv) at 0 °C and then stirred overnight at 40 °C. The mixture was poured in sat. aq. NH_4Cl (20 mL) and extracted with Et_2O (2 × 20 mL). The combined organic phase was washed with brine, dried over Na_2SO_4, filtered and concentrated. FC (5:5 pentane/Et_2O) afforded **19** (450 mg, 56% over 2 steps).

Colorless liquid; Rf 0.29 (5:5 pentane:Et_2O); ^{1}H-NMR (300 MHz, $CDCl_3$) δ 3.75–3.58 (m, 2H), 1.92–1.47 (m, 16H); ^{13}C-NMR (75 MHz, $CDCl_3$) δ = 73.5, 63.1, 37.1, 35.5, 28.6, 23.9; Analytical data are consistent with literature data.[12]

Swern oxidation

To a stirred solution of oxalyl chloride (0.56 mL, 6.5 mmol, 1.3 equiv) in dry CH_2Cl_2 (20 mL) at –78 °C was added dropwise DMSO (0.89 mL, 12.5 mmol, 2.5 equiv) in dry CH_2Cl_2 (4 mL) and stirred for 30 min. Then, a solution of **19** (848 mg, 5.0 mmol) in dry CH_2Cl_2 (21 mL) was added at –78 °C and stirred for 30 min. The reaction mixture was treated with Et_3N (2.4 mL, 17.5 mmol, 3.5 equiv) at –78 °C and stirred at this temperature for 5 min. The mixture was allowed to warm up to rt and stirred for 1 h. The mixture was poured in a mixture of brine and sat $NaHCO_3$ (1:1, 100 mL) and was extracted with Et_2O (3 × 100 mL). The organic layers were dried over Na_2SO_4 and concentrated. FC (8:2 pentane/Et_2O) afforded **21** (800 mg, 94%).

Yellow liquid; Rf 0.56 (8:2 pentane:Et_2O); ^{1}H-NMR (300 MHz, $CDCl_3$) δ 9.81 (t, J = 1.4 Hz, 1H), 2.59 (ddd, J = 7.8, 6.9, 1.4 Hz, 2H), 1.95 (dd, J = 8.3, 6.9 Hz, 2H), 1.90–1.65 (m, 6H), 1.57 (dddd, J = 13.6, 11.8, 5.4, 3.7 Hz, 2H); ^{13}C-NMR (75 MHz, $CDCl_3$) δ = 201.50, 72.7, 40.2, 37.1, 31.3, 23.9; HRMS calc. for $C_8H_{14}NO$ $[(M-N_2)+H]^+$: 140.1070, found: 140.1071; IR (cm^{-1}): 2960, 2874, 2826, 2724, 2093, 1721, 1450, 1253, 956, 567.

(*R*)-1-(1-Azidocyclopentyl)hex-5-en-3-ol ((*R*)-22)

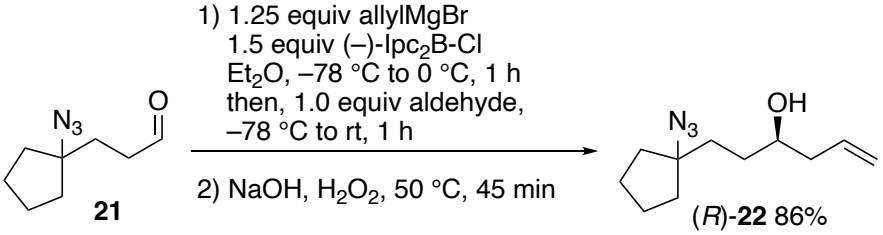

To a solution of (–)-*B*-chlorodiisopinocamphylborane ((–)-DIP chloride[7]) (50% in hexanes, 1.04 mL, 1.5 mmol, 1.5 equiv) in dry Et_2O (4.8 mL) was added allylmagnesium bromide (1.0 M in Et_2O, 1.25 mL, 1.25 mmol, 1.25 equiv) at –78 °C. The solution was warmed up to rt and stirred for 1 h. The suspension was taken up in a syringe and passed through a 0.2 µm filter into another flask to remove all precipitates. To this solution was added a solution of **21** (167 mg) in Et_2O (3 mL) at –78 °C and stirred for 1.5 h. The

mixture was then allowed to warm up to rt and treated with NaOH (2.0 M, 1.25 mL) and H_2O_2 (20%, 0.5 mL). This mixture was stirred at 45 °C for 1 h, cooled down to rt and extracted with Et_2O (3 × 25 mL). The organic phase was dried over Na_2SO_4, filtered and concentrated. Two consecutive FC (8:2 CH_2Cl_2/toluene) afforded (*R*)-**22** (180 mg, 86%).

Colorless liquid; Rf 0.22 (8:2 pentane/Et_2O); ^{1}H-NMR (300 MHz, $CDCl_3$) δ 5.92–5.72 (m, 1H), 5.20–5.10 (m, 2H), 3.64 (tt, J = 7.9, 4.4 Hz, 1H), 2.40–2.24 (m, 1H), 2.16 (dt, J = 13.9, 7.9 Hz, 1H), 2.01–1.43 (m, 14H); ^{13}C-NMR (75 MHz, $CDCl_3$) δ = 134.6, 118.6, 73.6, 70.8, 42.2, 37.3, 36.9, 35.2, 32.4, 23.9, 23.9; HRMS calc. for $C_{11}H_{20}N_3O$ $[M+H]^+$: 210.1601, found: 210.1602; IR (cm^{-1}): 3346, 2946, 2872, 2092, 1641, 1451, 1254, 993, 958, 914; $[\alpha]_D^{25}$ = +4.75 (c = 1.0, $CHCl_3$);

The enantiomeric ratio (er 94:6) was determined by HPLC analysis: Daicel CHIRALPAK IA-3, hexane/TBME 85:15; 1 mL min^{-1}, λ= 220 nm.

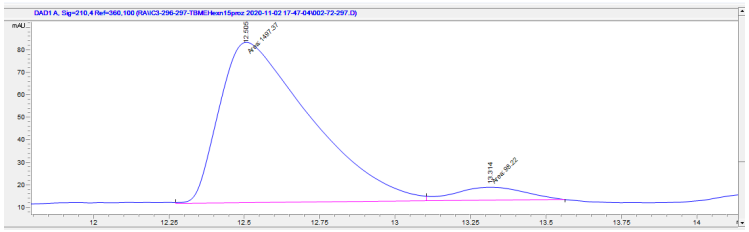

Signal 1: DAD1 A, Sig=210,4 Ref=360,100

Peak #	RetTime [min]	Type	Width [min]	Area [mAU*s]	Height [mAU]	Area %
1	12.505	MF	0.3500	1497.36804	71.30020	93.8443
2	13.314	FM	0.2755	98.22005	5.94297	6.1557
Totals :				1595.58809	77.24317	

(±)-1-(1-Azidocyclopentyl)hexan-3-ol ((±)-22)

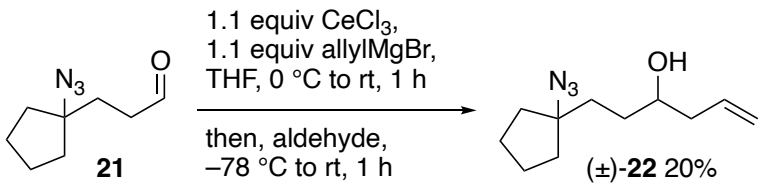

To dry and stirred $CeCl_3$ powder (325 mg, 1.3 mmol, 1.1 equiv) was slowly added dry THF (4.2 mL) at 0 °C, resulting in a white milky suspension which was stirred for 90 min at rt. The mixture was cooled down to 0 °C, allylmagnesium bromide (1.0 M in Et_2O, 4.1 mL, 4.1 mmol, 3.4 equiv) was added slowly until the yellow/orange color persisted. The suspension was stirred at rt for 90 min, resulting in a yellow solution containing a white precipitate. It was cooled down to –78 °C and a solution of **21** (200 mg, 1.2 mmol) in dry THF (3 mL) was added dropwise. The mixture was allowed to slowly warm up to rt overnight. The mixture was carefully treated with sat. aq. NH_4Cl and extracted with Et_2O. The organic phase was dried over Na_2SO_4, filtered and concentrated. FC (8:2 pentane/Et_2O) afforded (±)-**22** (50 mg, 20%).

Analytical data are consistent with the enantiopure compound.

HPLC analysis: Daicel CHIRALPAK IA-3, hexane/TBME 85:15; 1 mL min^{-1}, λ= 220 nm.

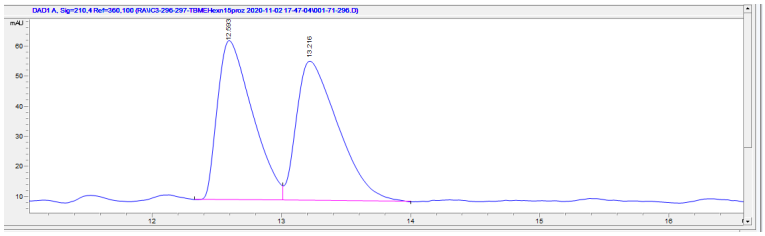

Signal 1: DAD1 A, Sig=210,4 Ref=360,100

Peak #	RetTime [min]	Type	Width [min]	Area [mAU*s]	Height [mAU]	Area %
1	12.593	BV	0.2813	993.97021	52.87953	48.8762
2	13.216	VB	0.3398	1039.67676	46.33947	51.1238
Totals :				2033.64697	99.21900	

(3*S*,8a*S*)-3-allyloctahydroindolizine ((3*S*,8a*S*)-23)

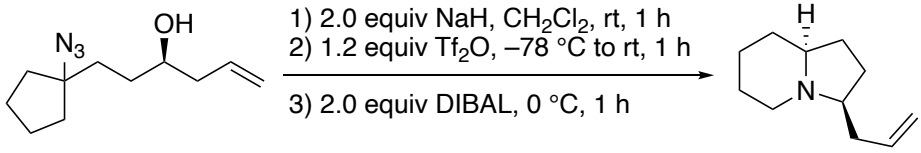

(*R*)-**22** (3*S*,8a*S*)-**23** 88%

To a suspension of NaH (22 mg, 0.84 mmol, 2.0 equiv) in dry CH_2Cl_2 (2 mL) was added a solution of (*R*)-**22** (88 mg, 0.42 mmol) in CH_2Cl_2 (1.5 mL). The mixture was stirred at rt for 30 min. Then, the mixture was cooled down to –78 °C and Tf_2O (0.085 mL, 0.5 mmol, 1.2 equiv) was added dropwise. The mixture was stirred at this temperature for 1 h, and then allowed to warm up slowly to 0 °C. The mixture was first stirred at 0 °C for 30 min and then at rt for another 30 min. To the mixture was added DIBAL (1 M in hexanes, 0.84 mL, 0.84 mmol, 2.0 equiv) at 0 °C and the mixture was then stirred at 0 °C for 1 h. The mixture was diluted with CH_2Cl_2 (3.5 mL), slowly treated with aq. NaOH (1 M, 2.5 mL), and extracted with CH_2Cl_2. The organic phase was washed with aq. NaOH (1 M), brine, dried over Na_2SO_4, filtered and concentrated. No further purification was required to obtain clean (3*S*,8a*S*)-**23** (61 mg, 88%).

Yellow oil; Rf 0.60 (deactivated TLC plates, 1% NH_3/MeOH in Et_2O);

^{1}H-NMR (300 MHz, C_6D_6) δ = 5.98–5.73 (m, 1H), 5.15–4.96 (m, 2H), 3.09–2.99 (m, 1H), 2.42–2.32 (m, 1H), 2.22–2.04 (m, 2H), 1.93–1.04 (m, 17H), 1.01–0.73 (m, 1H); ^{13}C-NMR (75 MHz, C_6D_6) δ 136.5, 116.1, 65.6, 64.3, 51.5, 38.4, 31.9, 29.8, 28.2, 26.2, 25.01; HRMS calc. for $C_{11}H_{20}N$ $[M+H]^+$: 166.1590, found: 166.1592; IR (cm^{-1}): 3076, 2929, 2856, 2786, 2751, 2708, 1640, 1441, 1119, 908; $[\alpha]_D^{25}$ = –34.6 (c = 1.0, CH_2Cl_2)

The enantiomeric ratio (er 91:9) was determined by GC analysis using the same settings as for the racemic compound.

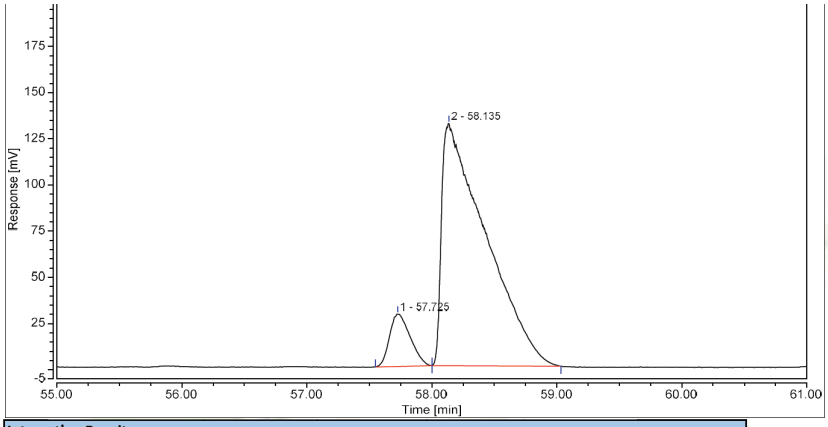

Integration Results						
No.	Peak Name	Retention Time min	Area mV*min	Height mV	Relative Area %	Relative Height %
1		57.725	5.433	28.359	9.21	17.78
2		58.135	53.533	131.154	90.79	82.22
Total:			**58.966**	**159.513**	**100.00**	**100.00**

(±)-(*cis*)-3-Allyloctahydroindolizine ((±)-(*cis*)-23)

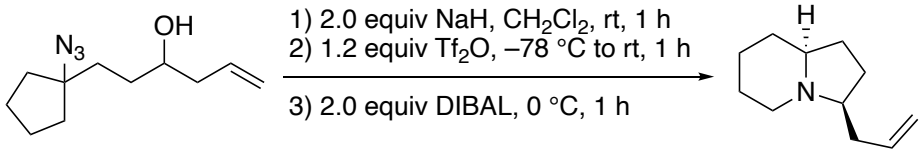

(±)-**22**

(±)-(*cis*)-**23** 84%

To a suspension of NaH (15 mg, 0.56 mmol, 2.0 equiv) in dry CH_2Cl_2 (1.5 mL) was added a solution of (±)-**22** (30 mg, 0.14 mmol) in CH_2Cl_2 (1.0 mL). The mixture was stirred at rt for 30 min. Then, the mixture was cooled down to –78 °C and Tf_2O (0.030 mL, 0.17 mmol, 1.2 equiv) was added dropwise. The mixture was stirred at this temperature for 1 h, and then allowed to warm up slowly to 0 °C. The mixture was first stirred at 0 °C for 30 min and then at rt for another 30 min. To the mixture was added DIBAL (1 M in hexanes, 0.30 mL, 0.30 mmol, 2.0 equiv) at 0 °C and the mixture was then stirred at 0 °C for 1 h. The mixture was diluted with CH_2Cl_2 (2.5 mL), slowly treated with aq. NaOH (1 M, 3.0 mL), and extracted with CH_2Cl_2. The organic phase was washed with aq. NaOH (1 M), brine, dried over Na_2SO_4, filtered and concentrated. No further purification was required to obtain clean (±)-(*cis*)-**23** (20 mg, 84%). Analytical data are consistent with the enantiopure compound.

GC analysis was performed using standard settings (cf. general information) and the following temperature gradient: 50 °C (1 min), 0.5 °C/min, 220 °C (10 min)

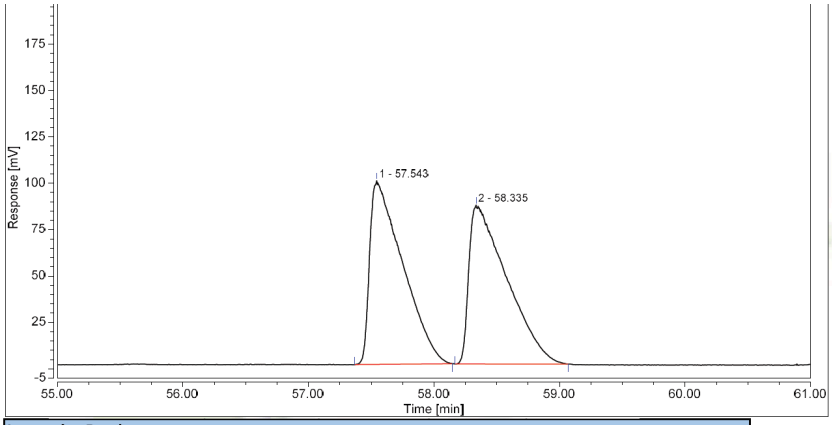

Integration Results						
No.	Peak Name	Retention Time min	Area mV*min	Height mV	Relative Area %	Relative Height %
1		57.543	30.010	98.993	50.15	53.60
2		58.335	29.830	85.703	49.85	46.40
Total:			**59.840**	**184.697**	**100.00**	**100.00**

(3*R*,8a*S*)-3-Propylindolizidine ((3*R*,8a*S*)-19)

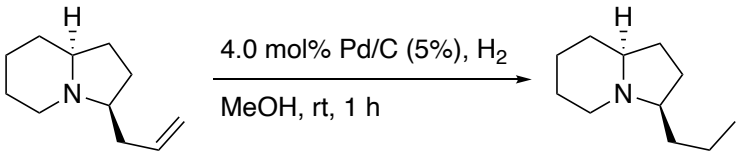

(3*S*,8a*S*)-**23** (3*R*,8a*S*)-**19** 76%

To solution of (3*S*,8a*S*)-**23** (47 mg, 0.28 mmol) in MeOH (5 mL) was added Pd/C (5%, 24 mg, 0.01 mmol, 4 mol%) and stirred vigorously at rt. The flask was evacuated and back-filled with H_2 from a balloon (three times). With a mounted balloon of H_2, the mixture was stirred at rt for 1 h. The mixture was filtered over Celite®, washed with MeOH, and concentrated. The residue was dissolved in CH_2Cl_2 (10 mL) and aq. NaOH (1.0 M, 10 mL). The phases were separated, the aqueous phase was extracted with CH_2Cl_2 (2 × 20 mL), and the combined organic phase was dried over Na_2SO_4, filtered, and concentrated. FC (9:1 pentane/Et2O + 1% 7M NH_3 in MeOH) afforded (3*R*,8a*S*)-**19** (36 mg, 76%).
Yellow oil; Rf 0.3 (deactivated TLC plates, 9:1 pentane/Et_2O + 1% 7M NH_3 in MeOH); ^{1}H-NMR (300 MHz, C_6D_6) δ 3.09 (dt, J = 9.4, 2.6 Hz, 1H), 2.07 (dtd, J = 10.6, 7.5, 4.3 Hz, 1H), 1.90–1.05 (m, 16H), 0.91 (t, J = 7.0 Hz, 3H); ^{13}C-NMR (75 MHz, C_6D_6) δ 65.7, 65.1, 51.6, 36.3, 32.0, 29.8, 28.7, 26.2, 25.2, 19.7, 14.9; HRMS calc. for $C_{11}H_{22}N$ [M+H]$^+$: 168.1747, found: 168.1751; IR (cm^{-1}):2927, 2856, 2756, 2714, 1743, 1457, 1193, 1119, 909; $[\alpha]_D^{25}$ = –42 (c = 1.0, CH_2Cl_2).

Literature IR spectra:[13]

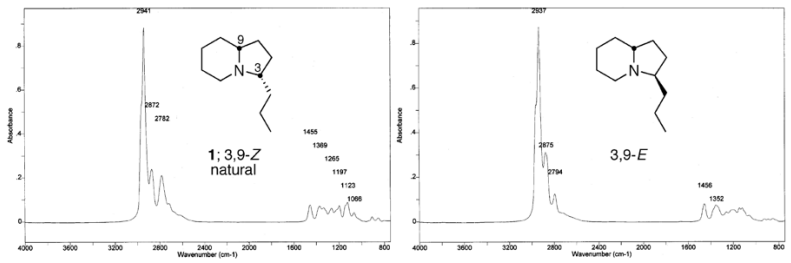

Measured IR spectrum:

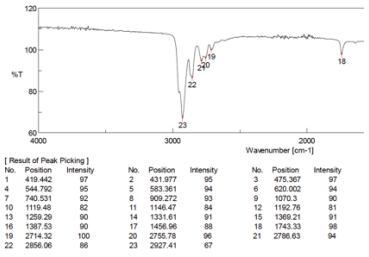

The peaks are each shifted by 12 cm^{-1} compared to the literature precedent.

Synthesis of (3*R*,8a*S*)-3-butyllehmizidine (3*R*,8a*S*)-20

3-(1-Azidocyclohexyl)propanal (24)

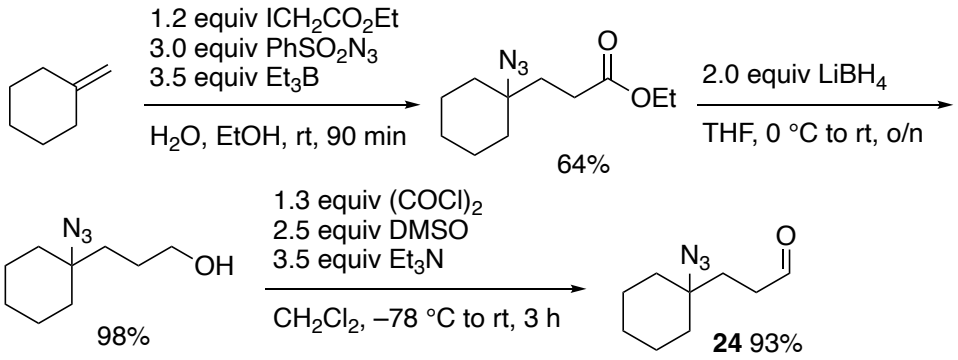

Carboazidation

To a mixture of water (1.25 mL) and EtOH (11.3 mL) were added methylenecyclohexane (510 mg, 5.0 mmol), iodoethyl acetate (1.28 g, 6.0 mmol, 1.2 equiv) and benzenesulfonyl azide (2.75 g, 15 mmol, 3.0 equiv). A solution of Et_3B (2.3 M in benzene, 7.6 mL) was added via syringe pump over 90 min. The mixture was treated with pentane and the phases were separated. The aqueous phase was extracted with ether and the combined organic phase was washed with brine, dried over Na_2SO_4, filtered and concentrated. To remove the remaining $PhSO_2N_3$, the crude mixture was dissolved in dry THF (20ml), cooled to 0 °C and treated with $LiBH_4$ (2 M in THF, 5 mL, 10 mmol, 2. equiv) until TLC showed complete consumption of $PhSO_2N_3$ (typically 20-30 min). Advantageously, the ester was not reduced in this step since this reaction is slow and required higher temperatures (see next step).

The mixture was poured into 50% aq NH_4Cl and extracted with Et_2O. The combined organic phase was washed with brine, dried over Na_2SO_4, filtered and concentrated. FC (9:1 pentane/Et_2O) afforded ethyl 3-(1-azidocyclohexyl)propanoate (715 mg, 64%).

Colorless liquid; Rf 0.44 (9:1 pentane:Et_2O); ^{1}H-NMR (300 MHz, $CDCl_3$) δ 4.14 (q, J = 7.1 Hz, 2H), 2.45–2.34 (m, 2H), 1.94–1.82 (m, 2H), 1.73–1.62 (m, 2H), 1.61–1.46 (m, 5H), 1.43–1.21 (m, 3H), 1.26 (t, 7.2 Hz, 3H); ^{13}C-NMR (75 MHz, $CDCl_3$) δ 173.5, 63.4, 60.7, 34.9, 34.5, 28.8, 25.5, 22.2, 14.3; HRMS calc. for $C_{11}H_{20}N_3O_2$ $[M+H]^+$: 226.1550, found:226.1543; IR (cm^{-1}): 3203, 2933, 2859, 2096, 1733, 1449, 1254, 1167, 1022, 597.

Reduction

To a stirred solution of ethyl 3-(1-azidocyclohexyl)propanoate (2.3 g, 10 mmol) in dry THF (20 mL) was added $LiBH_4$ (2 M in THF, 10 mL, 2.0 mmol, 2.0 equiv) at 0 °C. The mixture was stirred at 40 °C overnight. The mixture was diluted with Et_2O and carefully added to a sat. aq. NH_4Cl. The mixture was extracted with Et_2O and the organic layer was washed with water and brine, dried over Na_2SO_4 and concentrated. FC (5:5 pentane/Et_2O) afforded 3-(1-azidocyclohexyl)propan-1-ol (1.8 g, 98%).

Colorless liquid; Rf 0.33 (5:5 pentane/Et_2O); ^{1}H-NMR (300 MHz, $CDCl_3$) δ 3.67 (t, J = 5.8 Hz, 2H), 1.75–1.16 (m, 15H); ^{13}C-NMR (75 MHz, $CDCl_3$) δ 64.0, 63.2, 34.7, 26.7, 25.6, 22.3; HRMS calc. for $C_9H_{18}NO$ $[(M-N_2)+H]^+$: 156.1383, found: 156.1376; IR (cm^{-1}): 3329, 2931, 2857, 2094, 1449, 1254, 1143, 1056, 912, 592.

Swern oxidation

To a stirred solution of oxalyl chloride (0.56 mL, 6.5 mmol, 1.3 equiv) in dry CH_2Cl_2 (18 mL) at –78 °C was added dropwise DMSO (0.88 mL, 12.5 mmol, 2.5 equiv) in dry CH_2Cl_2 (4 mL) and stirred for 30 min. Then, a solution of 3-(1-azidocyclohexyl)propan-1-ol (968 mg, 5.0 mmol) in dry CH_2Cl_2 (23 mL) was added at –78 °C and stirred for 30 min. The reaction mixture was treated with Et_3N (2.4 mL, 17.5 mmol, 3.5 equiv) at –78 °C and stirred for 5 min. The mixture was allowed to warm up to rt and stirred for 1 h. Then, it was poured in a mixture of brine and sat $NaHCO_3$ (1:1, 100 mL) and was extracted with Et_2O (3 × 100 mL). The organic layers were dried over Na_2SO_4 and concentrated. FC (5:5 pentane/Et_2O) afforded **24** (842 mg, 93%).

Yellow oil; Rf 0.72 (5:5 pentane/Et_2O); ^{1}H-NMR (300 MHz, $CDCl_3$) δ 9.82 (d, J = 1.4 Hz, 1H), 2.56 (td, J = 7.7, 1.4 Hz, 2H), 1.87 (dd, J = 8.3, 7.0 Hz, 2H), 1.74–1.11 (m, 11H); ^{13}C-NMR (75 MHz, $CDCl_3$) δ 201.5, 63.3, 38.4, 34.7, 31.8, 25.4, 22.2; HRMS calc. for $C_9H_{16}NO$ $[(M\text{-}N_2)+H]^+$: 154.1226, found: 154.1221; IR (cm^{-1}): 2932, 2857, 2723, 2095, 1722, 1448, 1253, 1141, 911, 592.

(±)-1-(1-Azidocyclohexyl)heptan-3-ol ((±)-25)

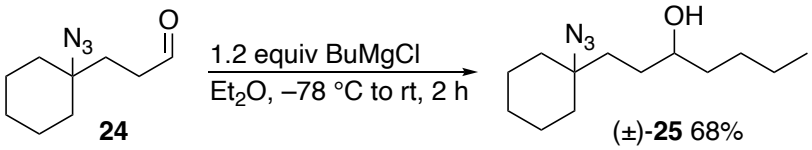

24 (±)-**25** 68%

To a solution of BuMgCl (2 M in Et_2O, 0.6 mL, 1.2 mmol, 1.2 equiv) in dry Et_2O (2.5 mL) was added dropwise a solution of **24** (197 mg, 1.0 mmol) in dry Et_2O (0.5 mL) at –78 °C. After 10 min, cooling bath was removed and the reaction mixture was stirred at rt for 2 h. The mixture was treated with sat. aq. NH_4Cl (25 mL) and extracted with Et_2O (3 × 25 mL). The combined organic layer was washed with brine (70 mL), dried over Na_2SO_4 and concentrated. FC (8:2 pentane/Et_2O) afforded (±)-**25** (163 mg, 68%).

Colorless liquid; Rf 0.31 (8:2 pentane:Et_2O); ^{1}H-NMR (300 MHz, $CDCl_3$) δ 3.58 (tt, J = 8.3, 4.2 Hz, 1H), 1.82–1.12 (m, 22H), 0.91 (t, J = 6.9 Hz, 3H); ^{13}C-NMR (75 MHz, $CDCl_3$) δ 72.3, 64.1, 37.5, 36.1, 34.9, 34.6, 31.1, 28.0, 25.6, 22.9, 22.3, 22.23 14.2; HRMS calc. for $C_{13}H_{26}NO$ $[(M\text{-}N_2)+H]^+$: 212.2009, found: 212.2005; IR (cm^{-1}): 3344, 2929, 2857, 2095, 1450, 1254, 1034, 956, 902, 592.

(*S*)-1-(1-Azidocyclohexyl)heptan-3-ol ((*S*)-25)

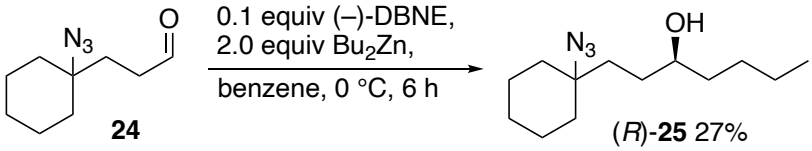

24 (*R*)-**25** 27%

Preparation of a dibutylzinc solution

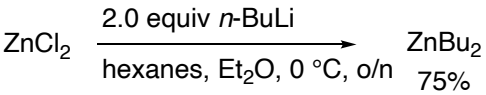

In a flame dried 2-neck flask was placed dry hexane (2 mL) and *n*-BuLi (2.5 M in hexanes, 8 mL, 20 mmol, 2.0 equiv). Under stirring at 0 °C was added dry Et_2O (10 mL) and immediately afterwards, solid

$ZnCl_2$ (1.36 g, 10 mmol). After the addition, the flask was wrapped in aluminum foil and stirred over night at rt. The white suspension was transferred into flame dried microwave vial and centrifuged for 5 min at 1 G. The clear supernatant was then transferred into flame dried graduated tube and stored in the freezer (–25 °C).

Addition of solid $ZnCl_2$

Suspension after overnight reaction

Solution after centrifugation

The obtained dibutylzinc solution (17 mL) was titrated against iodine[14] (c = 0.42 M, 75%): in a dry 25 mL flask, I_2 was dissolved in a solution of LiCl (5 mL, 0.5 M in THF). Dibutylzinc solution was added dropwise until the color of the iodine disappeared (see pictures below).

Starting solution

During titration

Titration end point

Entry	I_2	Volume Bu_2Zn	[Bu_2Zn]
1	135 mg	0.60 mL	0.44 M
2	139 mg	0.59 mL	0.46 M
3	136 mg	0.62 mL	0.43 M
Average			0.44 M

Calculation for entry 1: $0.5 * \frac{135\ mg}{254.8\ {}^{g}/_{mol}} = 0.264\ mmol$

$$\frac{0.264\ mmol}{0.60\ mL} = 0.44\ {}^{mol}/_{L}$$

Asymmetric butylation

To a solution of (–)-DBNE (53 mg, 0.2 mmol, 0.1 equiv) in dry toluene (1 mL) was added **24** (362 mg, 2.0 mmol) and the mixture was stirred for 20 min. Then, $ZnBu_2$ (0.44 M, 9.1mL, 4.0 mmol, 2.0 equiv) was added dropwise at 0 °C. The mixture was then allowed to warm up to rt and stirred overnight. The mixture was treated with sat. aq. NH_4Cl (50 mL), extracted with Et_2O (3 × 30 mL), washed with brine (50 mL), dried over Na_2SO_4, and concentrated. FC (7:3 pentane/Et_2O) afforded (*R*)-**26** (130 mg, 27%).

Analytical data are consistent with the racemic compound; $[\alpha]_D^{25}$ = +1.2 (c = 1.0, CH_2Cl_2).

The enantiomeric ratio was determined by HPLC analysis on a chiral column of its *para*-methoxybenzyl ether (PMB) derivative (see below).

(±)-1-(((1-(1-Azidocyclohexyl)heptan-3-yl)oxy)methyl)-4-methoxybenzene

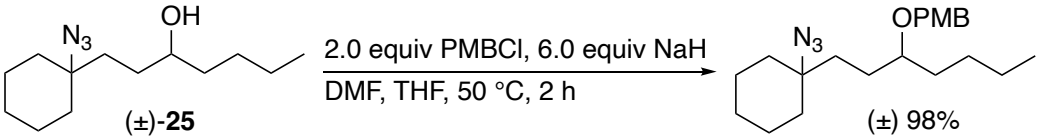

To a suspension of NaH (90% in mineral oil, 100 mg, 3.75 mmol, 6.0 equiv) in dry DMF (2.5 mL) was added a solution of (±)-**25** (150 mg, 0.63 mmol) and *para*-methoxybenzyl chloride (PMBCl) (0.175 mL, 1.25 mmol, 2.0 equiv) in dry THF (0.63 mL) at 0 °C. Then mixture was then stirred at 50 °C for 2 h, cooled to rt, treated with sat. aq. NH_4OH, stirred for 30 min, and extracted with CH_2Cl_2. The combined organic phase was washed with brine, dried over Na_2SO_4, and concentrated. FC (9:1 heptanes/EtOAc) afforded the PMB-ether derivative (220 mg, 98%).

Colorless liquid; Rf 0.50 (9:1 heptanes:EtOAc); ^{1}H-NMR (300 MHz, $CDCl_3$) δ 7.30–7.24 (m, 2H), 6.92–6.83 (m, 2H), 4.44 (s, 2H), 3.80 (s, 3H), 3.37 (p, J = 5.2 Hz, 1H), 1.73–1.18 (m, 21H), 0.96–0.87 (m, 3H); ^{13}C-NMR (75 MHz, $CDCl_3$) δ 159.3, 131.2, 129.5, 113.9, 78.7, 70.6, 64.3, 55.4, 35.4, 34.9, 34.6, 33.7, 27.8, 27.2, 25.6, 23.0, 22.3, 22.3, 14.3; HRMS calc. for $C_{21}H_{33}N_3O_2Na$ $[M+Na]^+$: 382.2465, found: 382.2462; IR (cm^{-1}): 2930, 2857, 2096, 1512, 1454, 1245, 1172, 1065, 1036, 819.

HPLC analysis: Daicel CHIRALPAK IA-3, hexane/*i*PrOH 99:1; 1 mL min^{-1}, λ= 254 nm.

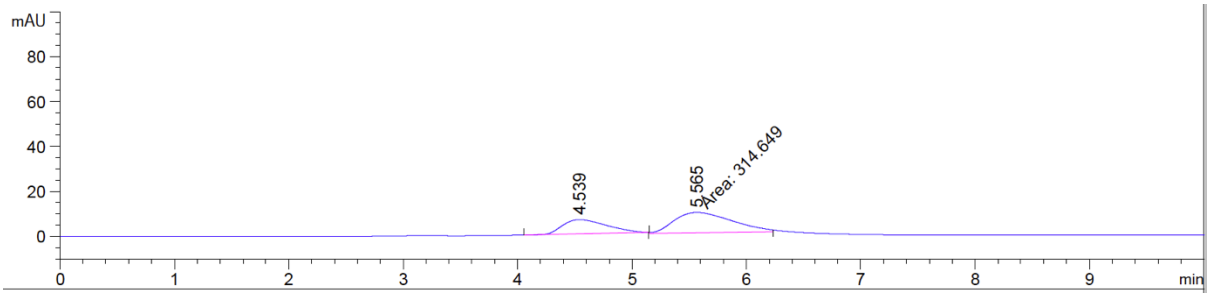

Signal 1: DAD1 A, Sig=254,4 Ref=360,100

Peak #	RetTime [min]	Type	Width [min]	Area [mAU*s]	Height [mAU]	Area %
1	4.539	BB	0.3869	169.37386	6.31619	34.9930
2	5.565	MM	0.5850	314.64874	8.96493	65.0070
Totals :				484.02260	15.28112	

(*S*)-1-(((1-(1-Azidocyclohexyl)heptan-3-yl)oxy)methyl)-4-methoxybenzene

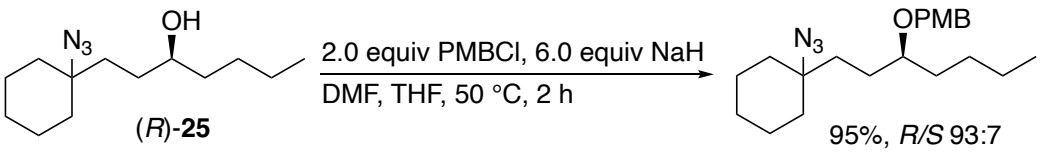

To a suspension of NaH (90% in mineral oil, 64 mg, 2.5 mmol, 6.0 equiv) in dry DMF (1.7 mL) was added a solution of (*R*)-**25** (100 mg, 0.42 mmol) and PMBCl (0.12 mL, 0.84 mmol, 2.0 equiv) in dry THF (0.42 mL) at 0 °C. Then mixture was then stirred at 50 °C for 5 h, cooled to rt, treated with sat. aq. NH_4OH, stirred for 30 min, and extracted with CH_2Cl_2. The combined organic phase was washed with brine, dried over Na_2SO_4, and concentrated. FC (9:1 heptanes/EtOAc) afforded the PMB-ether derivative (142 mg, 95%).

Analytical data are consistent with the racemic compound; $[\alpha]_D^{25}$ = +0.7 (c = 1.0, $CHCl_3$).

The enantiomeric ratio (er 91:9) was determined by HPLC analysis: Daicel CHIRALPAK IA-3, hexane/*i*PrOH 99:1; 1 mL min^{-1}, λ= 254 nm)

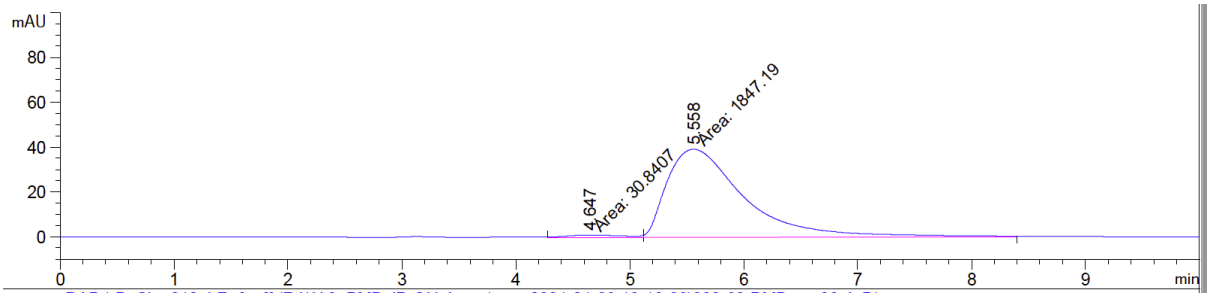

Signal 1: DAD1 A, Sig=254,4 Ref=360,100

Peak #	RetTime [min]	Type	Width [min]	Area [mAU*s]	Height [mAU]	Area %
1	4.647	MF	0.5618	30.84072	9.14891e-1	1.6422
2	5.558	FM	0.7850	1847.19348	39.22004	98.3578
Totals :				1878.03421	40.13493	

(±)-(*cis*)-3-butyloctahydro-1H-pyrrolo[1,2-a]azepine or (±)-(*cis*)-3-butyllehmizidine ((±)-20)

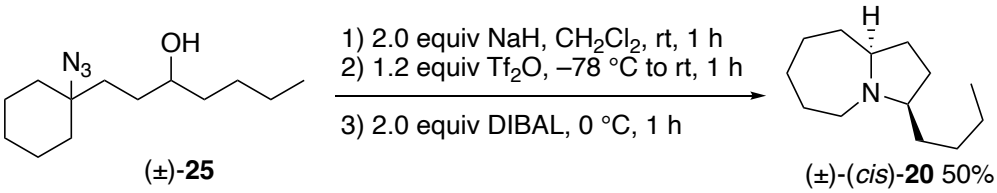

(±)-**25** (±)-(*cis*)-**20** 50%

To a suspension of NaH (30 mg, 1.15 mmol, 2.0 equiv) in dry CH_2Cl_2 (2 mL) was added a solution of (±)-**25** (137 mg, 0.57 mmol) in CH_2Cl_2 (2 mL). The mixture was stirred at rt for 30 min. Then, the mixture was cooled down to –78 °C and Tf_2O (0.115 mL, 0.69 mmol, 1.2 equiv) was added dropwise. The mixture was stirred at this temperature for 1 h, and then allowed to warm up slowly to 0°C. The mixture was first stirred at 0 °C for 30 min and then at rt for another 30 min. To the mixture was added DIBAL (1 M in hexanes, 1.14 mL, 1.14 mmol, 2.0 equiv) at 0 °C and the mixture was then stirred at 0 °C for 1 h. The mixture was diluted with CH_2Cl_2 (3.5 mL), slowly treated with aq. NaOH (1 M, 3 mL), extracted with CH_2Cl_2. The organic phase was washed with aq. NaOH (1 M), dried over Na_2SO_4, filtered and concentrated. FC (deactivated silica gel, 1% NH_3/MeOH in Et_2O) afforded (±)-(*cis*)-**20** (53 mg, 50%) as a single diastereomer.

Colorless liquid; Rf 0.37–0.19 (deactivated TLC plates, 1% NH_3/MeOH in Et_2O); ^{1}H-NMR (300 MHz, $CDCl_3$) δ 3.08 (dt, J = 12.4, 4.8 Hz, 1H), 2.39 (qt, J = 7.7, 2.5 Hz, 1H), 2.23 (dq, J = 8.5, 5.2, 3.2 Hz,

1H), 2.06 (ddd, J = 12.5, 8.9, 4.1 Hz, 1H), 1.87–1.09 (m, 19H), 0.88 (t, J = 7.0 Hz, 3H); ^{13}C-NMR (75 MHz, C_6D_6) δ 67.6, 66.6, 53.7, 36.8, 35.1, 32.0, 30.1, 29.5, 28.9, 26.7, 26.4, 23.6, 14.5; HRMS calc. for $C_{13}H_{26}N$ $[M+H]^+$: 196.2060, found: 196.2054; IR (cm^{-1}): 2924, 2857, 2791, 1454, 1377, 1353, 1180, 1150, 1123, 728.

GC analysis was performed using standard settings (cf. general information) and the following temperature gradient: 50 °C (1 min), 0.5 °C/min, 220 °C (10 min)

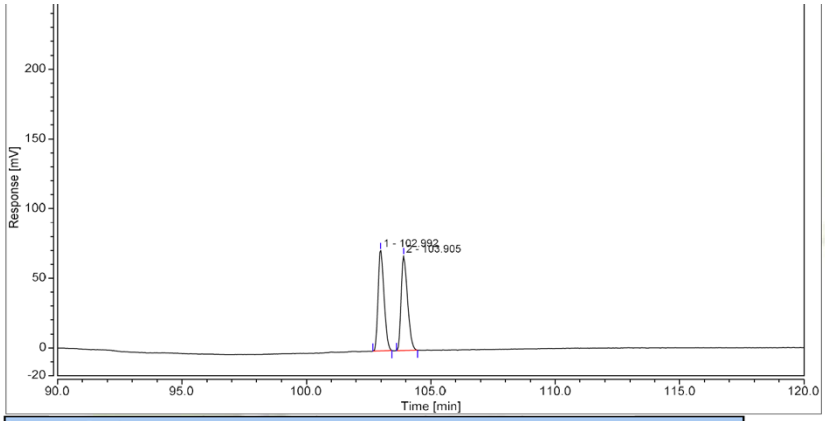

Integration Results						
No.	Peak Name	Retention Time min	Area mV*min	Height mV	Relative Area %	Relative Height %
1		102.992	19.920	72.026	49.76	51.44
2		103.905	20.110	67.993	50.24	48.56
Total:			**40.030**	**140.019**	**100.00**	**100.00**

(3*R*,9a*S*)-3-butyloctahydro-1H-pyrrolo[1,2-a]azepine or (3*R*,9a*S*)-3-butyllehmizidine ((3*R*,9a*S*)-20)

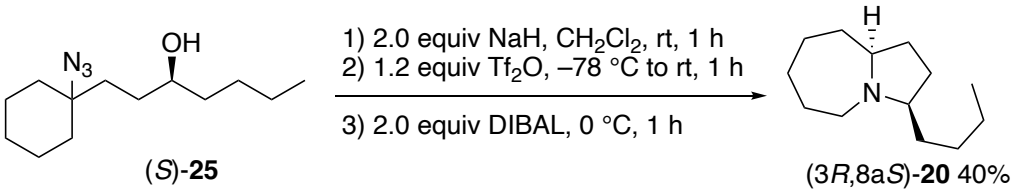

(*S*)-**25** (3*R*,8a*S*)-**20** 40%

To a suspension of NaH (26 mg, 1.0 mmol, 2.0 equiv) in dry CH_2Cl_2 (2 mL) was added a solution of (*S*)-**25** (er 93:7, 120 mg, 0.5 mmol) in CH_2Cl_2 (1.5 mL). The mixture was stirred at rt for 30 min then, cooled down to –78 °C and Tf_2O (0.1 mL, 0.6 mmol, 1.2 equiv) was added dropwise. The mixture was stirred at this temperature for 1 h, and then allowed to warm up slowly to 0°C. The mixture was first stirred at 0 °C for 30 min and then at rt for another 30 min. DIBAL (1 M in hexanes, 1 mL, 1.0 mmol, 2.0 equiv) was added at 0 °C and the mixture was then stirred at 0 °C for 1 h, diluted with CH_2Cl_2 (3.5 mL), slowly treated with aq. NaOH (1 M, 3 mL), and extracted with CH_2Cl_2. The organic phase was washed with aq. NaOH (1 M), dried over Na_2SO_4, filtered and concentrated. FC (deactivated silica gel, 1% NH_3/MeOH in Et_2O) afforded (3*R*,9a*S*)-**20** (36 mg, 40%).

Analytical data are consistent with the racemic compound; $[\alpha]_D^{25}$ = –49.6 (c = 1.0, $CHCl_3$)

The enantiomeric ratio (er 91:9) was determined by GC analysis using the same settings as for the racemic compound.

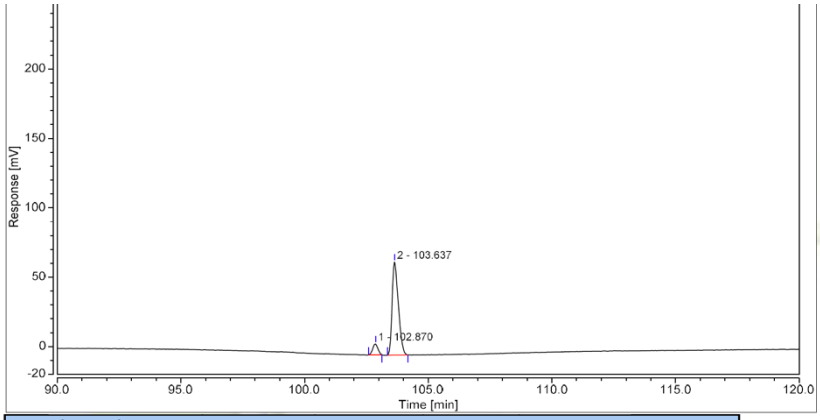

Integration Results

No.	Peak Name	Retention Time min	Area mV*min	Height mV	Relative Area %	Relative Height %
1		102.870	1.876	7.927	8.77	10.57
2		103.637	19.513	67.040	91.23	89.43
Total:			**21.388**	**74.967**	**100.00**	**100.00**

Literature IR sprectra:[13]

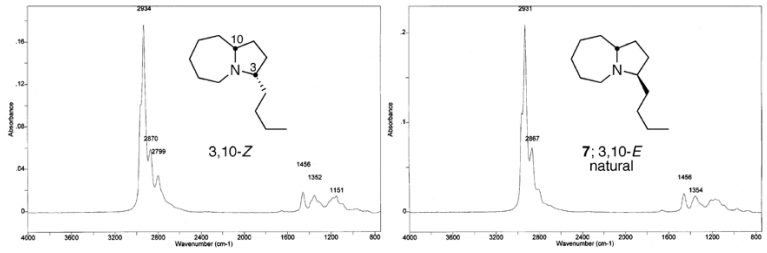

Measured IR spectrum:

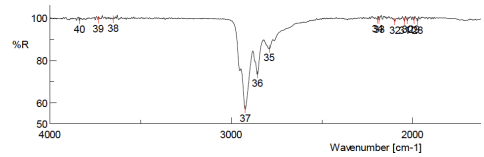

[Result of Peak Picking]

No.	Position	Intensity	No.	Position	Intensity	No.	Position	Intensity
1	408.835	93.4177	2	416.549	99.6485	3	425.227	90.1867
4	434.869	92.4003	5	455.118	89.2647	6	476.813	93.2671
7	488.866	93.0988	8	508.151	97.3057	9	526.954	97.0019
10	563.112	97.2688	11	602.646	95.7668	12	638.323	95.83
13	666.767	96.8338	14	727.996	92.6703	15	865.4	94.0937
16	896.255	93.5086	17	925.182	93.2171	18	955.555	91.7144
19	987.375	91.8859	20	1017.27	92.4433	21	1123.33	86.9961
22	1149.85	81.7088	23	1179.74	82.8539	24	1315.7	91.0793
25	1353.3	87.2564	26	1376.93	88.6308	27	1453.58	79.9373
28	1973.79	98.3704	29	1993.55	98.9082	30	2029.23	98.7778
31	2045.62	98.5287	32	2098.65	98.3351	33	2185.44	98.7863
34	2194.6	99.1684	35	2791.46	85.4204	36	2856.54	73.2938
37	2923.56	56.8361	38	3652.03	99.453	39	3734.96	99.2168
40	3837.65	98.7778						

The peaks are shifted by 10 cm^{-1} compared to the literature precedent.

X-ray crystal structure reports

Structure report of 6im

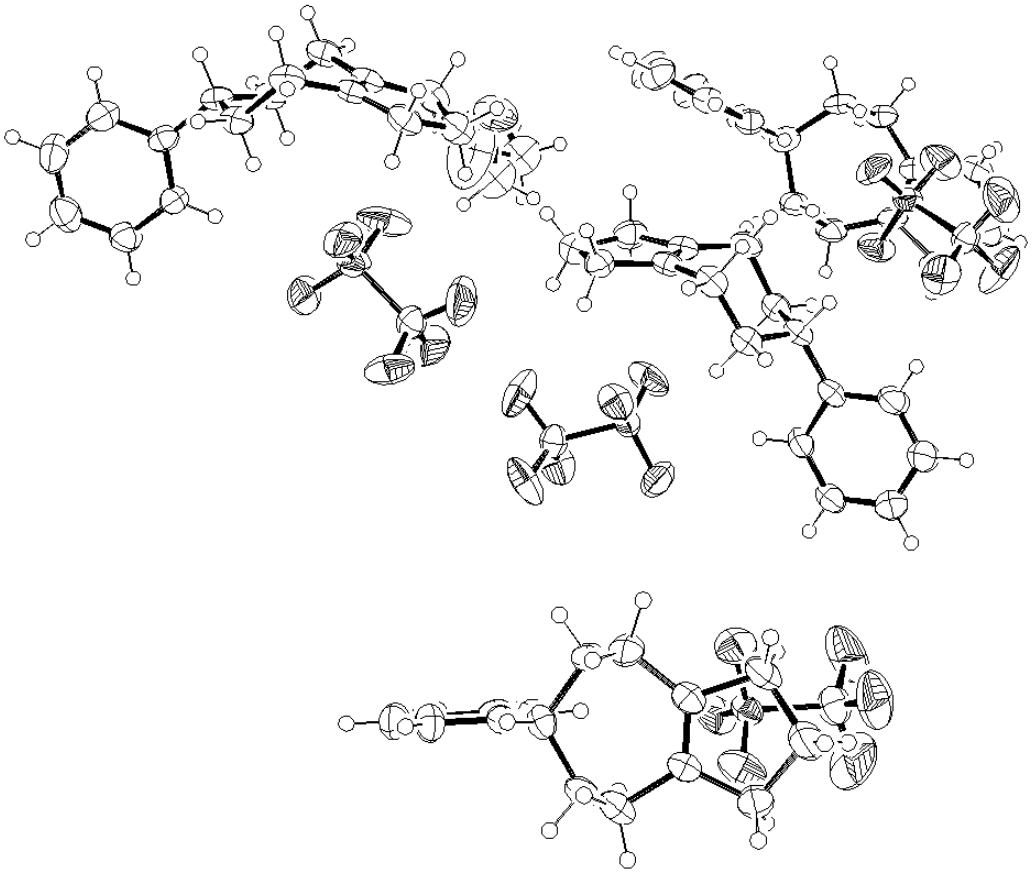

Crystal-Structure Determination–A colorless transparent crystal of $C_{65}H_{82}N_4F_{12}O_{12}S_4Cl_2$ was mounted in air and used for X-ray structure determination at ambient conditions. All measurements were made on an *Oxford Diffraction SuperNova* area-detector diffractometer[15] using mirror optics monochromated Mo *K*α radiation (λ = 0.71073 Å) and Al filtered.[16] The unit cell constants and an orientation matrix for data collection were obtained from a least-squares refinement of the setting angles of reflections in the range 1.5° < θ < 27.2°. A total of 543 frames were collected using ω scans, with 50+50 seconds exposure time, a rotation angle of 1.0° per frame, a crystal-detector distance of 65.1 mm, at T = 173(2) K.

Data reduction was performed using the CrysAlisPro[15] program. The intensities were corrected for Lorentz and polarization effects, and an absorption correction based on the multi-scan method using SCALE3 ABSPACK in CrysAlisPro[15] was applied.

The structure was solved by direct methods using SHELXS-97[17], which revealed the positions of all non-hydrogen atoms of the title compound. The non-hydrogen atoms were refined anisotropically. All H-atoms were placed in geometrically calculated positions and refined using a riding model where each H-atom was assigned a fixed isotropic displacement parameter with a value equal to 1.2Ueq of its parent atom.

The structure contains four ionic pairs of $[C_{15}H_{20}N]^+$ $[CF_3SO_3]^-$ in the asymmetric unit, a feature which is quite unusual but caused by only one molecule of CH_2Cl_2 being present in the asymmetric unit (with disordered conformation). Careful check did not suggest any alternative metrics, nor higher symmetry and the best solution is in *triclinic* P-1.

Due to the molecular pseudo-symmetry, the iminium nitrogen in all the four independent molecules is actually disordered over the two possible sites, which means that the two enantiomeric forms are superimposed, differing only in the position of the iminium N/C atoms. No attempts were made to refine a model with the two distinct forms, and N/C positions were forced to coincide, to avoid divergence in the refinement. The site occupation was freely refined to values very close to 50%:50% per each cationic site (note that of course the centrosymmetric nature of the species also implies a perfect racemic mixture).

Refinement of the structure was carried out on F^2 using full-matrix least-squares procedures, which minimized the function $\Sigma w(F_o^2-F_c^2)^2$. The weighting scheme was based on counting statistics and included a factor to downweight the intense reflections. All calculations were performed using the *SHELXL-97*[17] program.

Structure report of 7dnb

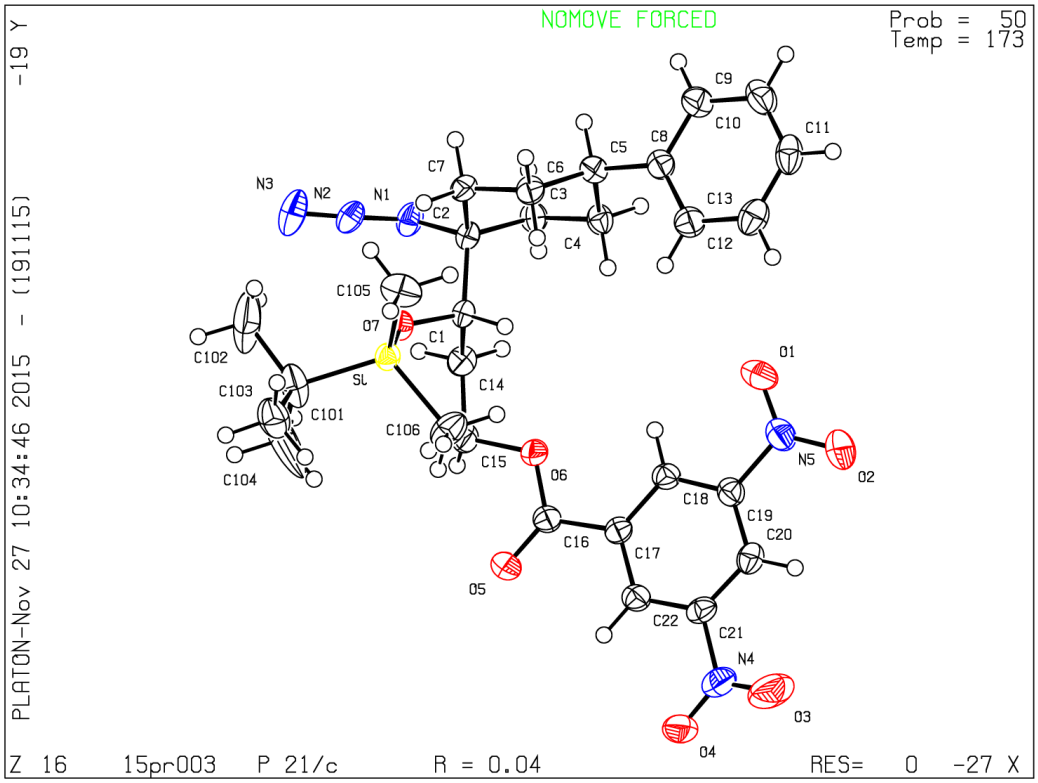

Crystal-Structure Determination–A colorless transparent crystal of [$C_{28}H_{37}N_5O_7Si$] was mounted in air and used for X-ray structure determination at ambient conditions. All measurements were made on an *Oxford Diffraction SuperNova* area-detector diffractometer[15] using mirror optics monochromated Mo *K*α radiation (λ = 0.71073 Å) and Al filtered.[16] The unit cell constants and an orientation matrix for data collection were obtained from a least-squares refinement of the setting angles of reflections in the range 1.5° < θ < 27.4°. A total of 1093 frames were collected using ω scans, with 2.5+2.5 seconds exposure time, a rotation angle of 1° per frame, a crystal-detector distance of 65.1 mm, at T = 173(2) K.

Data reduction was performed using the CrysAlisPro[15] program. The intensities were corrected for Lorentz and polarization effects, and an absorption correction based on the multi-scan method using SCALE3 ABSPACK in CrysAlisPro[15] was applied.

The structure was solved by direct methods using SHELXS-97[17], which revealed the positions of all non-hydrogen atoms of the title compound. The non-hydrogen atoms were refined anisotropically. All H-atoms were placed in geometrically calculated positions and refined using a riding model where each H-atom was assigned a fixed isotropic displacement parameter with a value equal to 1.2Ueq of its parent atom.

Refinement of the structure was carried out on F^2 using full-matrix least-squares procedures, which minimized the function $\Sigma w(F_o^2-F_c^2)^2$. The weighting scheme was based on counting statistics and included a factor to downweight the intense reflections. All calculations were performed using the *SHELXL-97*[17] program.

Structure report of (1*RS*,7*SR*,9a*SR*)-8dnb

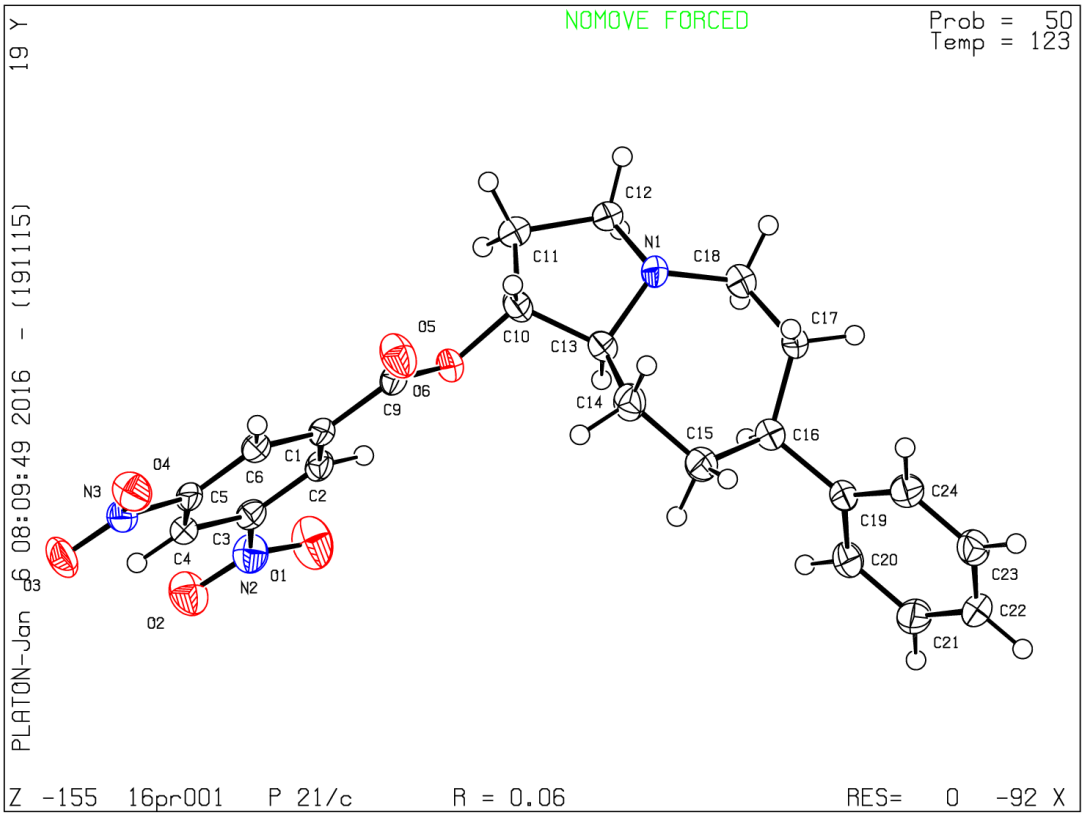

Crystal-Structure Determination–A colorless transparent crystal of [$C_{22}H_{23}N_3O_6$] was mounted in air and used for X-ray structure determination at ambient conditions. All measurements were made on an *Oxford Diffraction SuperNova* area-detector diffractometer[15] using mirror optics monochromated Mo *K*α radiation (λ = 0.71073 Å) and Al filtered.[16] The unit cell constants and an orientation matrix for data collection were obtained from a least-squares refinement of the setting angles of reflections in the range 2.1° < θ < 27.2°. A total of 1206 frames were collected using ω scans, with 60+60 seconds exposure time, a rotation angle of 1° per frame, a crystal-detector distance of 65.1 mm, at T = 123(2) K.

Data reduction was performed using the CrysAlisPro[15] program. The intensities were corrected for Lorentz and polarization effects, and an absorption correction based on the multi-scan method using SCALE3 ABSPACK in CrysAlisPro[15] was applied.

The structure was solved by direct methods using SHELXS-97[17], which revealed the positions of all non-hydrogen atoms of the title compound. The non-hydrogen atoms were refined anisotropically. All H-atoms were placed in geometrically calculated positions and refined using a riding model where each H-atom was assigned a fixed isotropic displacement parameter with a value equal to 1.2Ueq of its parent atom.

Refinement of the structure was carried out on F^2 using full-matrix least-squares procedures, which minimized the function $\Sigma w(F_o^2-F_c^2)^2$. The weighting scheme was based on counting statistics and

included a factor to downweight the intense reflections. All calculations were performed using the *SHELXL-97*[17] program.

Structure report of (S)-10dnb

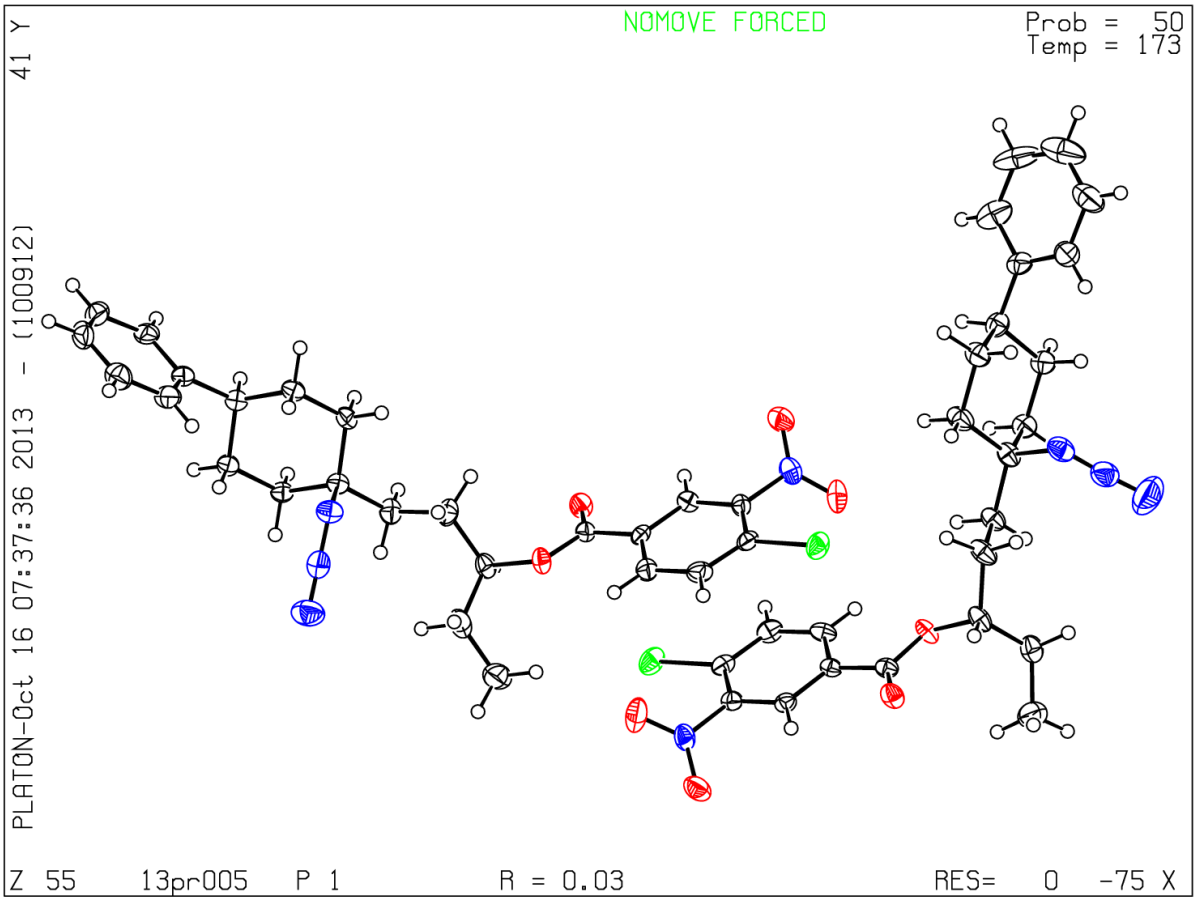

Crystal-Structure Determination–A colorless transparent crystal of [$C_{24}H_{27}BrN_4O_4$] was mounted in air and used for X-ray structure determination at ambient conditions. All measurements were made on an *Oxford Diffraction SuperNova* area-detector diffractometer[15] using mirror optics monochromated Mo *K*α radiation (λ = 0.71073 Å) and Al filtered.[16] The unit cell constants and an orientation matrix for data collection were obtained from a least-squares refinement of the setting angles of reflections in the range 1.8° < θ < 27.3°. A total of 989 frames were collected using ω scans, with 7.5+7.5 seconds exposure time, a rotation angle of 1.0° per frame, a crystal-detector distance of 65.1 mm, at T = 173(2) K.
Data reduction was performed using the CrysAlisPro[15] program. The intensities were corrected for Lorentz and polarization effects, and an absorption correction based on the multi-scan method using SCALE3 ABSPACK in CrysAlisPro[15] was applied.

The structure was solved by direct methods using SHELXS-97[17], which revealed the positions of all non-hydrogen atoms of the title compound. The non-hydrogen atoms were refined anisotropically. All

H-atoms were placed in geometrically calculated positions and refined using a riding model where each H-atom was assigned a fixed isotropic displacement parameter with a value equal to 1.2Ueq of its parent atom. Only H1 was freely refined.

Refinement of the structure was carried out on F^2 using full-matrix least-squares procedures, which minimized the function $\Sigma w(F_o^2-F_c^2)^2$. The weighting scheme was based on counting statistics and included a factor to downweight the intense reflections. All calculations were performed using the *SHELXL-97*[17] program.

The unit cell contains two independent molecules of the same chirality. The absolute configuration is quite well ascertained because of the presence of Br atoms. In fact the Flack parameter is -0.009(3) indicating the correctness of the configuration, known with high precision.

Structure report of (3*R*,7*S*,9a*S*)-15·(*R*)-mandelic acid

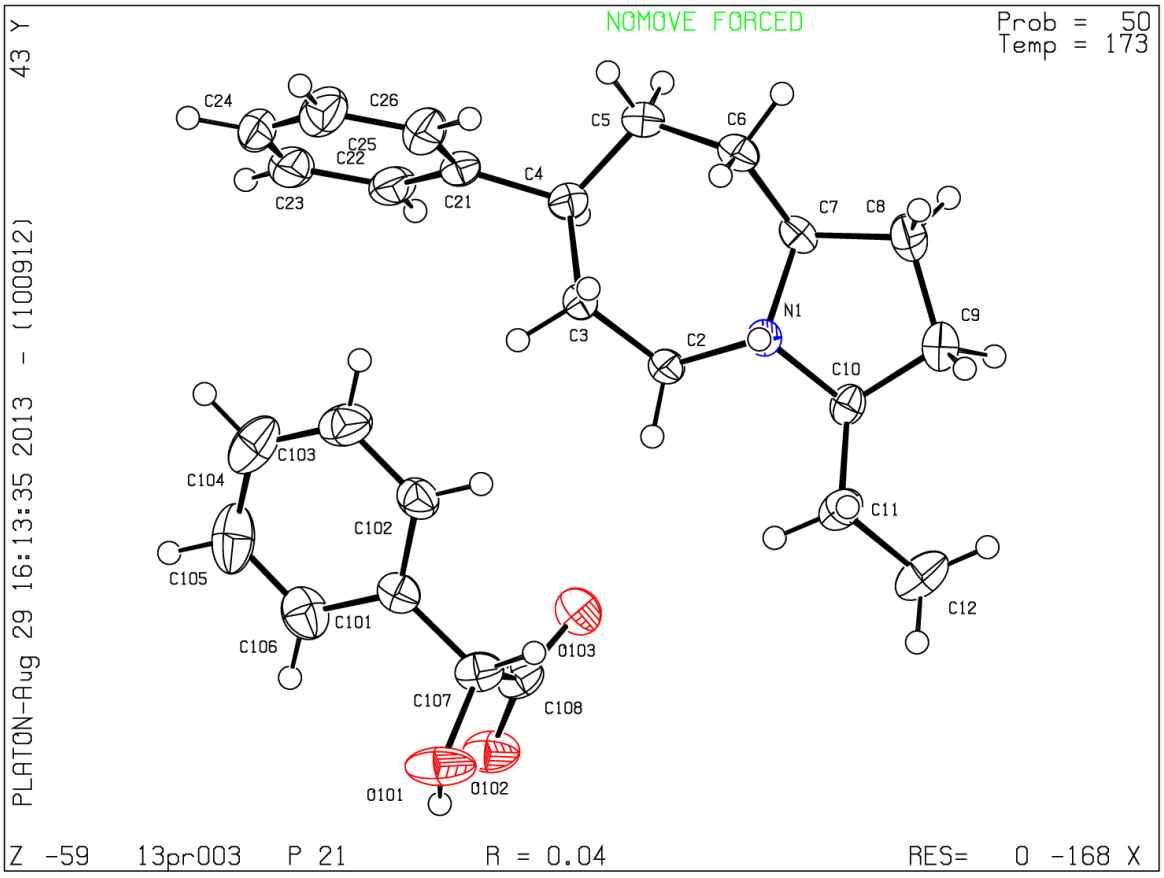

Crystal-Structure Determination–A colorless transparent crystal of $[C_{17}H_{26}N]$ $[C_8H_7O_3]$ was mounted in air and used for X-ray structure determination at ambient conditions. All measurements were made on an *Oxford Diffraction SuperNova* area-detector diffractometer[15] using mirror optics monochromated Mo *K*α radiation (λ = 0.71073 Å) and Al filtered.[16] The unit cell constants and an orientation matrix for data collection were obtained from a least-squares refinement of the setting angles of reflections in the

range $2° < \theta < 28.°$. A total of 1121 frames were collected using ω scans, with 10+10 seconds exposure time, a rotation angle of 1.0° per frame, a crystal-detector distance of 65.1 mm, at T = 173(2) K.

Data reduction was performed using the CrysAlisPro[15] program. The intensities were corrected for Lorentz and polarization effects, and an absorption correction based on the multi-scan method using SCALE3 ABSPACK in CrysAlisPro[15] was applied.

The structure was solved by direct methods using SHELXS-97[17], which revealed the positions of all non-hydrogen atoms of the title compound. The non-hydrogen atoms were refined anisotropically. All H-atoms were placed in geometrically calculated positions and refined using a riding model where each H-atom was assigned a fixed isotropic displacement parameter with a value equal to 1.2Ueq of its parent atom. Only H1 was freely refined.

Refinement of the structure was carried out on F^2 using full-matrix least-squares procedures, which minimized the function $\Sigma w(F_o^2 - F_c^2)^2$. The weighting scheme was based on counting statistics and included a factor to downweight the intense reflections. All calculations were performed using the *SHELXL-97*[17] program.

References

[1] A. Kapat, E. Nyfeler, G. T. Giuffredi, P. Renaud, *Journal of the American Chemical Society* **2009**, *131*, 17746–7.

[2] K. Soai, T. Shibata, *J. Syn. Org. Chem., Jpn.* **1997**, *55*, 994–1005.

[3] K. Soai, T. Hayase, K. Takai, T. Sugiyama, *J. Org. Chem.* **1994**, *59*, 7908–7909.

[4] K. Soai, S. Niwa, *Chem. Rev.* **1992**, *92*, 833–856.

[5] D. E. Frantz, R. Fässler, C. S. Tomooka, E. M. Carreira, *Acc. Chem. Res.* **2000**, *33*, 373–381.

[6] D. E. Frantz, R. Fässler, E. M. Carreira, *J. Am. Chem. Soc.* **2000**, *122*, 1806–1807.

[7] H. C. Brown, P. K. Jadhav, *J. Am. Chem. Soc.* **1983**, *105*, 2092–2093.

[8] P. Klahn, H. Erhardt, A. Kotthaus, S. F. Kirsch, *Angew. Chem. Int. Ed.* **2014**, *53*, 7913–7917.

[9] G. Yin, M. Gao, N. She, S. Hu, A. Wu, Y. Pan, *Synthesis* **2007**, *2007*, 3113–3116.

[10] E. J. Corey, C. J. Helal, *Angew. Chem. Int. Ed.* **1998**, *37*, 1986–2012.

[11] P. Panchaud, C. Ollivier, P. Renaud, S. Zigmantas, *J. Org. Chem.* **2004**, *69*, 2755–2759.

[12] X. Bao, Q. Wang, J. Zhu, *Angewandte Chemie International Edition* **2019**, *58*, 2139–2143.

[13] T. H. Jones, H. L. Voegtle, H. M. Miras, R. G. Weatherford, T. F. Spande, H. M. Garraffo, J. W. Daly, D. W. Davidson, R. R. Snelling, *J. Nat. Prod.* **2007**, *70*, 160–168.

[14] A. Krasovskiy, P. Knochel, *Synthesis* **2006**, 890–891.

[15] *Oxford Diffraction, CrysAlisPro (Version 1.171.34.44)*, Oxford Diffraction Ltd., Yarnton, Oxfordshire, UK, **2010**.

[16] P. Macchi, H.-B. Bürgi, A. S. Chimpri, J. Hauser, Z. Gál, *Journal of Applied Crystallography* **2011**, *44*, 763–771.

[17] G. M. Sheldrick, *Acta crystallographica. Section A, Foundations of crystallography* **2008**, *64*, 112–22.

Chapter 8

Diastereoselective Synthesis of Bridgehead-Functionalized Bicyclic Amines

Ajoy Kapat, Joséphine Cinqualbre, Lars Gnägi, and Philippe Renaud

draft manuscript prepared by Lars Gnägi

Author contributions
LG conducted the studies on primary azides, AK performed the functionalization of iminium triflates, and JC investigated aminonitrile chemistry.

8 Diastereoselective Synthesis of Bridgehead-Functionalized Bicyclic Amines

8.1 Abstract

The highly diastereoselective synthesis of α-amino quaternary functionalized bicyclic amines is described. This new method relies on the formation of iminium triflates in an intramolecular Schmidt rearrangement and subsequent trapping with carbon nucleophiles in a one-pot reaction. Iminium triflates are transformed into their corresponding quaternary alkyl-, alkenyl-, alkynyl- and arylamines. Furthermore, we report the formation of versatile α-aminonitriles with the same method and further derivatisation thereof affording aminoketones and aminoacids. The synthesis of bridgehead-functionalized azabicycles from prefunctionalized azidoalcohols was attempted, but unsuccessful.

8.2 Introduction

Polycyclic amines with an azaquaternary center represent a broad class of natural alkaloids, most of them consisting of an indolizidine- (e.g. Cyclindricine family, Lepadiformine, Daphnane, Calyciphylline L, Serratine, Erythrinane), a pyrroloazepine- (e.g. Cephalotaxine, Stemonamine), or a quinolizidine- (e.g. Fasicularin, Marcfortine A, (-)-Lycopodine) core structure (Figure 8.1).

This class of alkaloids contains an unusual azaspiro system fused to an azepine ring and is particularly interesting due to its potent and variable biological effects and has therefore been known in Asian folk medicine for the treatment of respiratory diseases and as antihelmetics[1,2]. A representative example is Cephalotaxine, a harringtonine alkaloid isolated from *Cephalotaxus harringtonia*[3]. In the 1970s it was shown that Cephalotaxine and its derivatives show significant activity against experimental leukemia[4,5] and inhibit HeLa cell protein biosynthesis[6]. In the 1990s, Cephalotaxine was investigated as treatment against chloroquine-resistant malaria[7], and recently, studies report activity against Hepatitis B[8] and varicella zoster[9]. Because of their potent pharmacological activity and unique structure, a tremendous amount of research has been carried out in this field[5,10–30]. Furthermore, many formal[31–44], racemic[45–60], and enantioselective[31,61–73] syntheses of Cephalotaxine have been published to date; some of the work was reviewed in the past[74–77]. Among the numerous syntheses proposed in literature, diverse strategies such as iminium[65] and *N*-Acyliminium ion chemistry[30,32], transannular rearrangement[57] and cyclisation[54], Pd-catalyzed annulation[62,64], regioselective dipolar cycloaddition[67], SET-promoted photocyclization[55], and amidyl radical cyclizations (for Deoxyserratine)[78] proved promising to access the desired polycyclic skeleton.

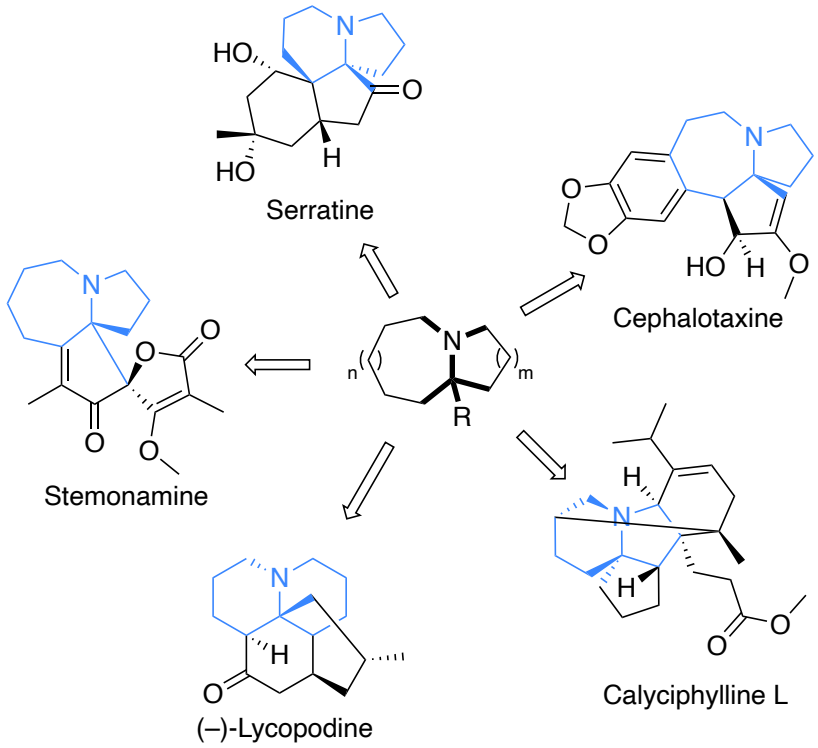

Figure 8.1. Structure of representative alkaloids containing azaquaternary centers

An elegant method to obtain the quaternary substituted bicyclic core structure is the intramolecular Schmidt reaction (ISR), which has been extensively studied by Aubé and Pearson[79–85] and which was applied for the synthesis of various natural products.[86,87] The reaction between an azide and a cationic species generated using Lewis- or Brønstedt acids affords an aminodiazonium intermediate, from which an antiperiplanar bond migration takes place, forming the final bicyclic amine (Figure 8.2).

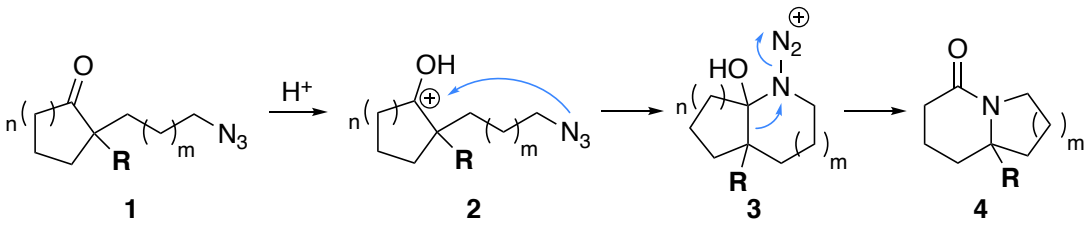

Figure 8.2. Synthesis of bicyclic amides with a substituted bridgehead position by Aubé

In order to form azabicylces with a substituted bridgehead position, the substituent is installed prior to the closure of the cycle as reported by Aubé.

8.2.1 Stereochemistry of the Schmidt reaction

The stereochemical control in this reaction is a challenge either due to carbocation rearrangements or by lack or regioselectivity of the migration as reported by Pearson. The lack of regioselectivity of the 1,2-migration is assumed to be caused by a rapid epimerization of the diazonium substituent in the spirocyclic aminodiazonium intermediate **5**. It is proposed that the bond antiperiplanar to the departing dinitrogen is migrating, and due to the epimerization of it, both bonds become similarly likely to migrate.

Upon reduction of the iminium ions after the rearrangement, two regioisomers **6** and **7** are obtained in almost equivalent quantities (Figure 8.3).[82,85]

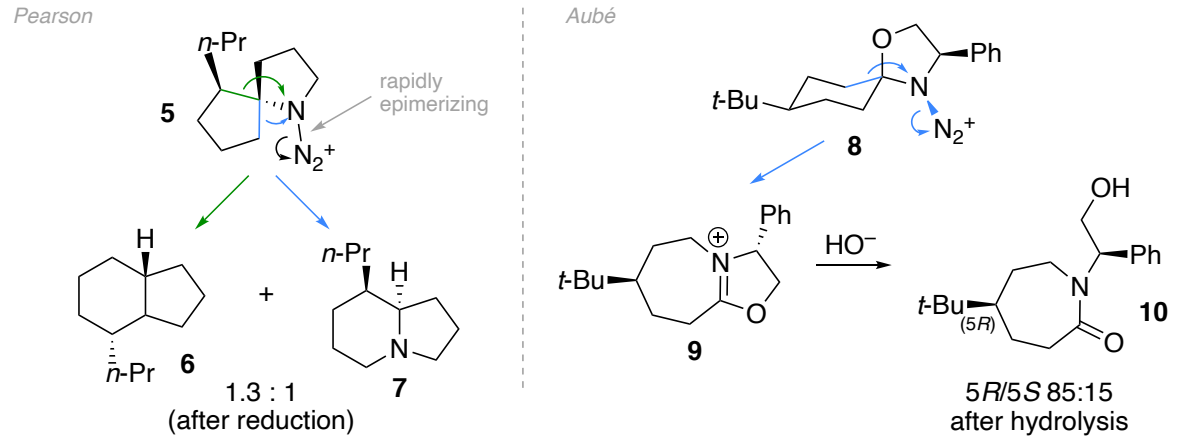

Figure 8.3. Lack (left) and control (right) of regioselectivity of the 1,2-migration

A diastereoselective migration has been achieved by Aubé, who introduced a chiral center next to the azide by desymmetrization of achiral ketones. In this case, the phenyl substituent in aminodiazonium **8** is controls the position of the diazonium substituent and thus, enables a selective 1,2-migration. Hydrolysis of the 9 affords lactam 5*R*-10 as a major diastereomer.[88]

About 10 years ago, our group developed a nonacidic variation of the ISR. Instead of starting from an azidoketone, an azidoaldehyde **11** is transformed to the triflate in a first step. The azidotriflate rearranges spontaneously to an iminium ion **12**, which is reduced to the bicyclic amine **13** in a second step. These mild reaction conditions are complementary to the initial work and were applied successfully in the enantioselective synthesis of indolizidine 167B.[89] Recently, we investigated the stereocontrol of the triflate-mediated ISR in detail and achieved excellent selectivity both for the 1,2-migration as well as for the reduction of the iminium intermediate (Figure 8.4).[90]

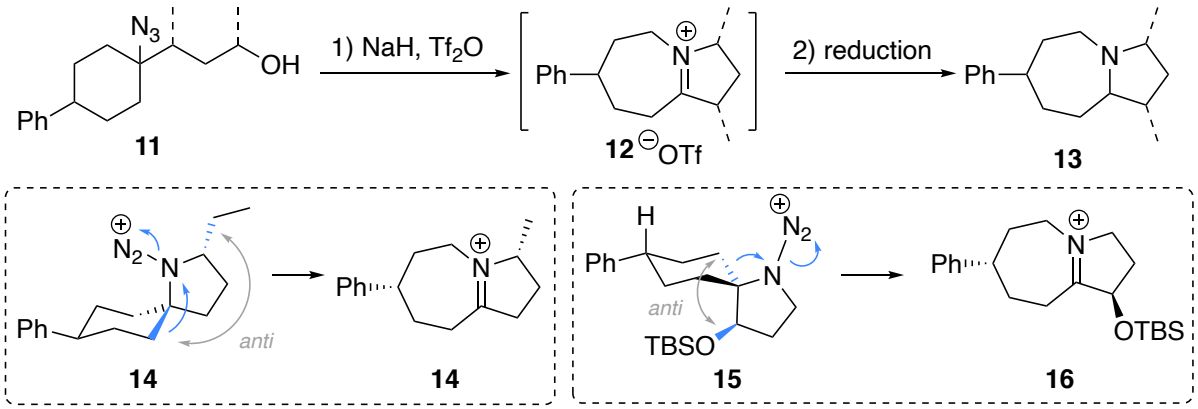

Figure 8.4. Stereocontrol of the 1,2-migration by substituents on the 5-membered ring

We found that the nucleophilic attack of the azide proceeds with high stereospecificity, and thus, the chiral substituent next to the azide in aminodiazonium ion **14** is accessible from chiral secondary azidoalcohols. Analogous to the work of Aubé, the diazonium ion is *cis* to the substituent, resulting in

iminium **14** after migration of the bond which is *anti* to the substituent. Interestingly, the migration can also be controlled by a substituent on the other side of the ring such as silylether **15**. In this case too, the migration takes place *anti* to the substituent affording iminium **16** as a single diastereomer. In addition to the selectivity observed for the migration, also the reduction of the iminium ion takes place with high selectivity *anti* to the phenyl group present at the 7-membered ring. However, these bicyclic amines do not contain the tertiary carbon center which is present in many natural products.

Motivated by the high stereocontrol achieved in the reduction of the iminium ion, we aimed at the introduction of carbon substituents to construct tertiary carbon centers. To achieve this goal, two strategies were envisaged: We reasoned that the reducing agent can be simply replaced by a suitable nucleophile and thus, iminium **17** will be functionalized at the bridgehead position affording **18** in a diastereoselective manner, directed by other substituents, e.g., the phenyl group of **17** (Figure 8.5).

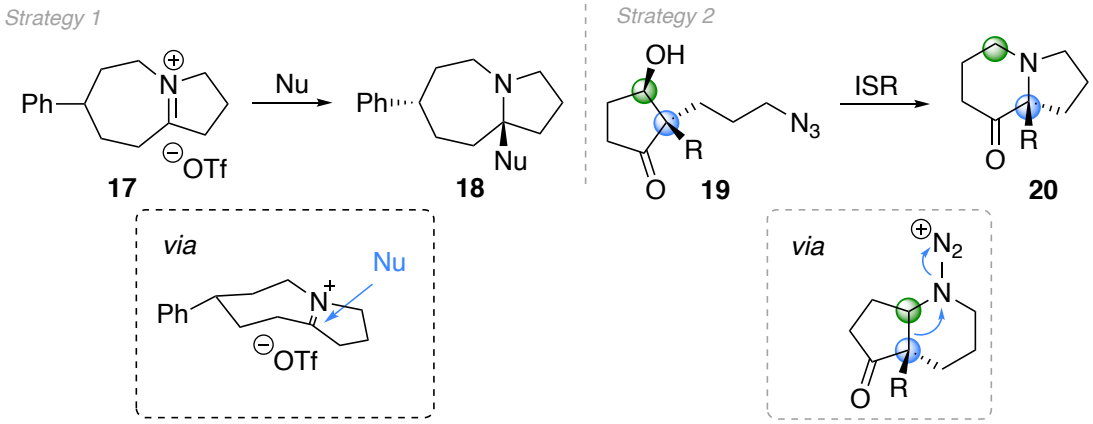

Figure 8.5. Strategies for the formation of bridgehead-substituted bicyclic amines

Ten years ago, Zhang reported a construction of azaquaternary pyrroloazepine skeletons *via* ISR of desymmetrized 1,3-diketones using chiral Brønsted acids, albeit in moderate enantioselectivity.[91] A more robust reductive desymmetrization of azidoketones will furnish azidoalcohols such as **19**, which will be transformed to the substituted indolizidine **20**.[92–96] Unlike in the previous strategy, this approach does not rely on any directive effect by other substituents since the chiral center is installed prior to the rearrangement as we have shown for a trisubstituted carbon center in our previous enantioselective synthesis of (–)-Indolizdine 167B.[89]

8.3 Results and discussion

8.3.1 Functionalization of iminium triflates

We started our investigation using azidoalcohol **21** as a model substrate. Reacting the iminium triflate **22** with allylmagnesium bromide and afforded alkylated product **23** already in acceptable yield (34%, entry 1). The reaction conditions were further optimized (Table 8.1).

Table 8.1. Optimization of Grignard reagent addition to quaternary iminium ion 2

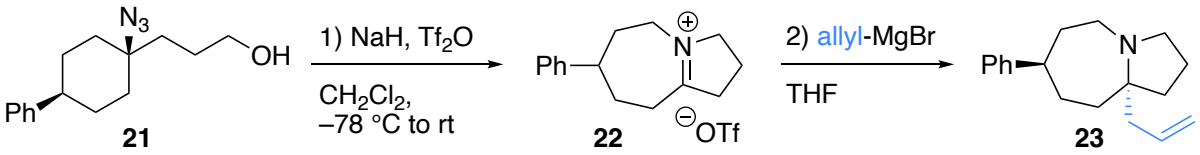

Entry	equiv (BrMgX)	temp	Yield (%)
1	1.0	–34 °C	34
2	1.0	–78 °C	90
3	2.0	–78 °C	96
4	3.0	–78 °C	80

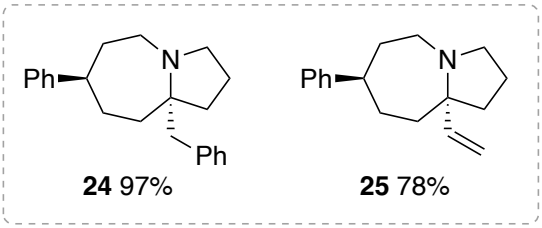

Addition of Grignard reagent to **22** in CH_2Cl_2 at low temperature almost tripled the yield (90%, entry 2). Increasing the amount of nucleophile to 2 equivalents, resulted in an excellent yield of 95% (entry 3). A further increase of Grignard reagent resulted in a slightly decreased yield (entry 4). As expected, the products are obtained as single diastereomers. This can be rationalized by the steric bulk of the engaged carbon nucleophiles, which is comparable to DIBALH. We also attempted to introduce the allyl group to the iminium ion under a metal free condition using allyltrimethylsilane as a nucleophile. But this reaction did not provide the desired product, which could be due to the lower nucleophilicity of allyltrimethylsilane. Addition of benzyl- and vinyl Grignards to **22** successfully afforded **24a** and **6c** in 97% and 78% yield respectively.

Advantageously, **22** can be prepared and isolated as a stable salt according to our previously reported procedure.[90] Therefore, the functionalization can be performed directly starting from the salt and thus, the first step can be skipped. Next, we tested the sensitivity of the iminium ion towards to strong bases. Not surprisingly, the iminium ion is deprotonated leading to the formation of enamine **26** (Figure 8.6).

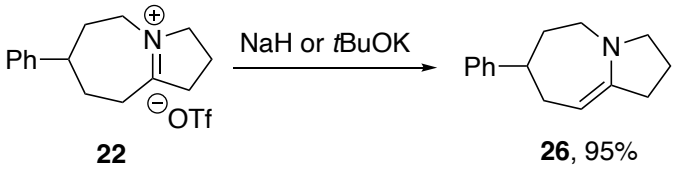

22 **26**, 95%

Figure 8.6. Deprotonation of iminium triflate X leads to the efficient formation of enamine 26

Therefore, exact control over the reaction conditions is important to obtain the desired products avoiding the formation of enamine side products. Aryl groups appear often in biologically active natural alkaloids such as Lasubine[97,98], nupharamine[99], or dopamine analogues. In our first attempts to introduce aryl moieties, arylmagnesium as well as arylcerium reagents failed to deliver the desired arylsubstituted tertiary amines in good yields, mainly due to the formation of the homocoupling product in significant quantities. Magnesium as well as cerium have higher oxidation potentials, hence arylmagnesium and arylcerium reagents are prone to undergo homocoupling. Since lithium has a lower oxidation potential, aryl lithium reagents might avoid homocoupling formation. However, the addition of organolithium species to dichloromethane leads to the formation of carbenes[100] and, therefore the one-pot reaction could not be performed and we used the isolated iminium triflate salt as reactant (Figure 8.7).

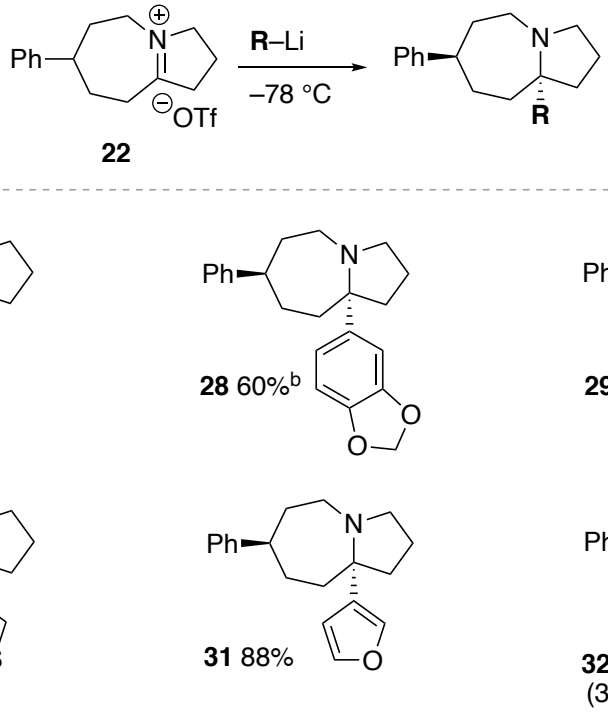

*Figure 8.7. nucleophilic diastereoselective addition of organolithium reagnts to iminium ion **22**. a) homocoupling formation observed; b) NMR yield; c) by addition as organocerium reagent*

At first, additions of aryllithium reagents were performed in THF and significant amounts of the phenyl addition product were formed. After realizing that the major side reaction was the opening of THF, we switched the solvent from THF to Et_2O, which resulted in the formation of **27** in 64% yield. Although the formation of the homocoupled product could not be avoided completely, significant improvement in terms of yield of the desired product was achieved. The addition of 2-lithio-3,4-(methylenedioxa) benzene provided the desired product **28** in 60% (NMR yield). The homocoupled product has similar

polarity to **27**, therefore the isolation was unsuccessful. The addition of 4-lithioflurorobenzene furnished amine **29** in good yield. An increased amount of organolithium reagents was used (3.0 equiv) due to the low conversion originating from the lower nucleophilicity of 4-lithioflurorobenzene. Next, addition of 2-lithiothiofuran and 3-lithiofuran furnished the desired products **30** and **31** in 77% and 88% yield, respectively. No homocoupling products were observed during the formation of **30** and **31**. Since the sp hybridized carbanion is much less basic compared to the aryl reagents, deprotonation of the iminium triflate is not expected to be an issue. Reaction with 3-lithiotrimethylsilyl acetylide afforded the desired product **32** in 56% yield. In fact, addition of the nucleophilic alkyne as an organolithium reagent turned out to be more efficient than when added as a supposedly more nucleophilic organocerium reagent (39% yield) (Figure 8.8).

The wide distribution of alkyl side chains adjacent to the tertiary amine[101] is an important motif we wanted to access with our method. To avoid beforementioned enamine formation, organocerium reagents proved to be the method of choice because they are more nucleophilic and less basic[102]. The addition of organocerium reagents to chiral imines has been used in the synthesis of several alkaloids[103,104], was previously used in our group in thioiminium chemistry[105], and effectively formed the desired alkylation products (Figure 8.8).

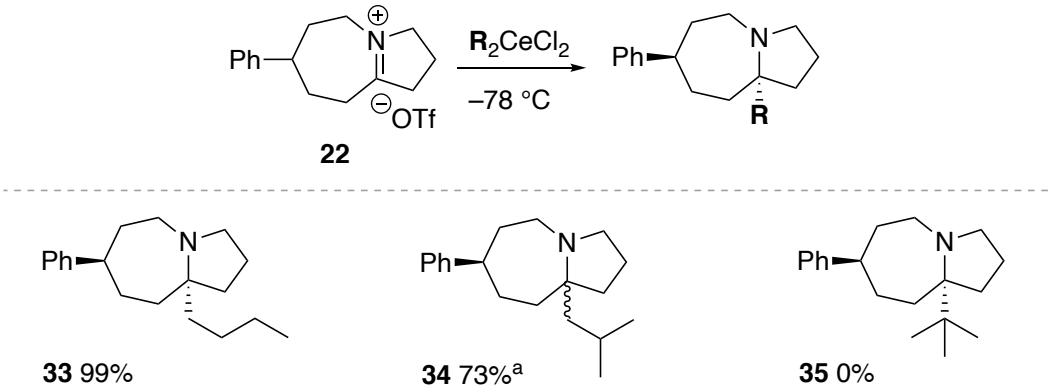

*Figure 8.8. Scope of nucleophilic diastereoselective addition of organocerium reagents to iminium ion **22**.*
[a] 2:1 mixture of diastereomers

With organocerium reagents, we were able to introduce the *n*-butyl and *s*-butyl side chains in **33** and **34** in good yields. The addition of the *t*-butyl substituent for the formation of **35** failed which is assumed to be caused by deprotonation of the iminium ion or due to steric reasons. However, no clean enamine formation was observed.

Except for **34**, the bicyclic amine was formed as a single diastereomer which was expected based on our previous reported diastereoselective addition of hydride to iminium **22**.[90] Structural analysis of **24** by 2D-NMR, where correlation peaks due to the spatial proximity of H7, H5 and H11 were observed, supports the *trans* geometry of the products (Figure 8.9).

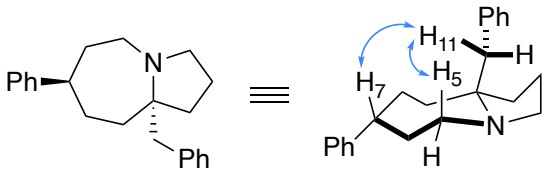

*Figure 8.9. ROESY 2D-NMR correlation signals of **24***

Having introduced different nonfunctionalized carbon nucleophiles (sp^3, sp^2, sp hybridized) we turned our attention to the formation of α-aminonitriles as versatile intermediates for the preparation of functionalized amino substituted quaternary centres. α-Aminonitriles are formed upon cyanation of iminium ions and can readily be converted to a variety of synthetic building blocks[106,107]. The treatment of the iminium triflate intermediate with an aqueous solution of NaCN furnished aminonitrile **36** as a 1:1 mixture of diastereomers in 87% yield. Attempts to separate the two diastereomers over silica gel, or aluminium oxide chromatography column, or using preparative HPLC were unsuccessful. Preparation of non-racemic α-aminonitrile was already achieved by Aitken[108]. Based on our previous findings, we anticipated to obtain a diastereoselective formation of α-aminonitrile by using Nagata's[109] reagent (Et_2AlCN); unfortunately without success. The transformation of α-aminonitrile **36** into a variety of derivatives was therefore investigated starting from a mixture of **36** (Figure 8.10).

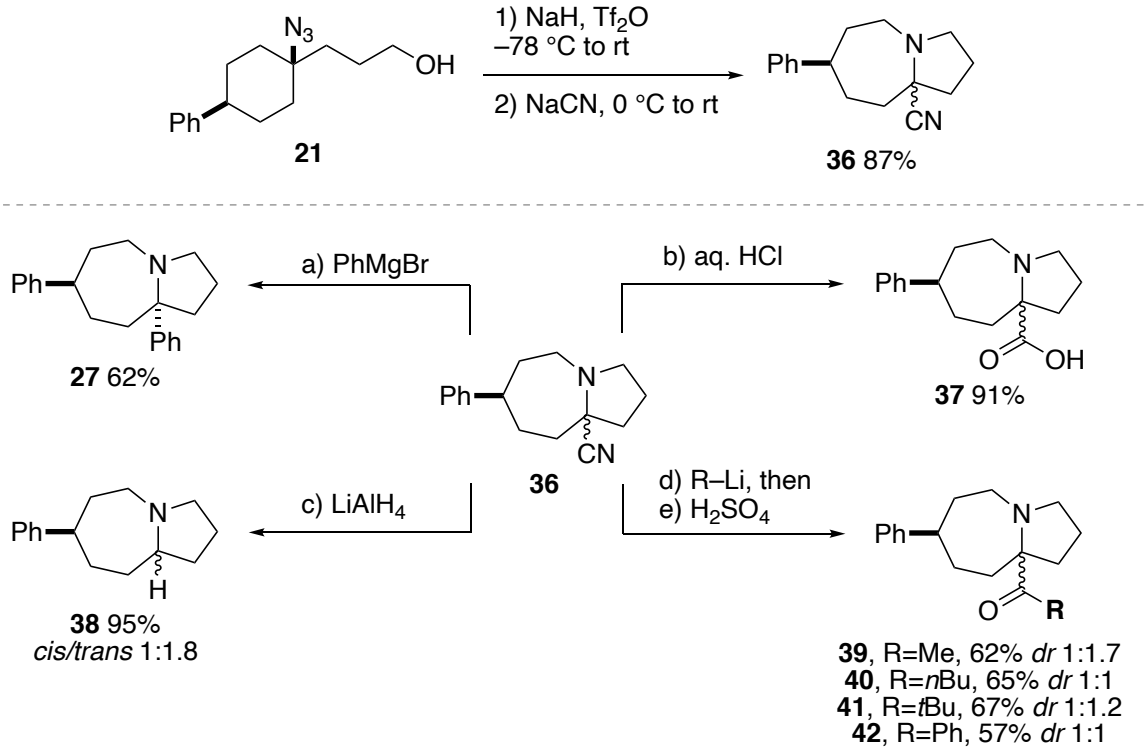

*Figure 8.10. Formation and derivatization of α-aminonitrile **8** formed upon treatment of iminium **2** with NaCN. Conditions: a) 2.2 equiv PhMgBr, THF, rt; b) aq. HCl, reflux; c) 2.0 equiv $LiAlH_4$, THF, –78 °C to rt; d) 1.5 equiv R-Li, THF, –60 °C to 0 °C; e) H_2SO_4 / H_2O, 0 °C*

As for the direct reaction of iminium with Grignard reagents (vide supra), **27** is obtained in the Bruylants reaction as a single diastereomer (Figure 8.10). This result is supported by the work of Aitken who proposed an iminium intermediate in the reaction of α-aminonitriles with two equivalents of Grignard

reagent: the first equivalent is used to complex the cyanide moiety of **36** and forms back the iminium intermediate **22**, with which the second equivalent reacts as nucleophile. Simple acidic treatment as firstly described by Strecker, leads to excellent conversion towards α-amino acid **37**. The reduction of α-aminonitriles derived from pyrrolizidine to give the corresponding diamine is known[110], however, no example on quinolizidine, indolizidine, or pyrrolo[1,2- *a*]azepine is described. Our attempts to convert **36** to the corresponding diamine were unsuccessful upon treatment with $LiAlH_4$. The only product observed was amine **38**, arising from the reduction of iminium **22**. For direct installation of a carbonyl on the iminium, an umpolung of polarity (such as the acyl anion in the benzoin condensation or the dithiane in the Corey-Seebach reaction) would be required. An interesting alternative is the addition of organolithium reagents directly onto α-aminonitriles, which results in the formation of ketones. Methyllithium and *n*-butyl lithium afforded aminoketones **39** and **40** in good yields. Gratifyingly, also large *t*-butyl (**41**) and aromatic phenyl (**42**) substituents were installed in comparable yields. In this transformation, all products were obtained as a mixture of diastereomers.

8.3.2 ISR of prefunctionalized azidoalcohols

In order to study the second strategy to construct the bridgehead-functionalized amines *via* ISR, the substituent is installed prior to the rearrangement. As a proof of concept, a simple azidoalcohol without substituent was employed to test the method (Figure 8.11).

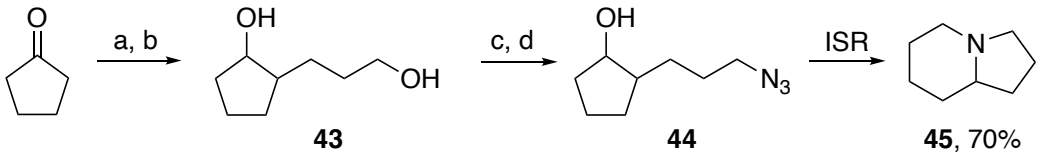

Figure 8.11. Formation of 45. Conditions: a) pyrrolidine, methyl methacrylate, 59%; b) $LiAlH_4$, 89%; c) TsCl, Et_3N, 64%; d) NaN_3, 59%

Alkylation of cyclopentanone with methyl methacrylate and subsequent reduction afforded the to the diol **43**, which was subsequently transformed to the azidoalcohol **44**. ISR using our standard conditions yielded, as expected, indolizidine **45** in good yield, indifferent on the diastereomer of **44** used. Next, the quaternary methyl substituent was installed. *Trans*-azidodiol **46** was obtained from 2-methylcyclopentane-1,3-dione in five steps (Figure 8.12). A desymmetrization of the diketone by selective reduction of only one ketone group was not attempted.

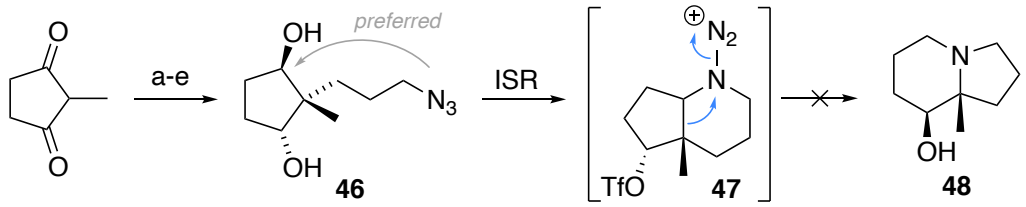

Figure 8.12. Attempted synthesis of 48. Conditions: a) acrolein, 90%, b) $NaBH(OAc)_3$, 55%; c) MsCl, pyridine, 76%; d) NaN_3, 93%; e) $NaBH_4$, 28% (trans)

We expected that one of the triflated alcohols will be substituted preferentially and thus provide one major diastereomer. Rearrangement of aminodiazonium **47** was expected to afford aminoalcohol **48**

after hydrolysis of the remaining triflate. However, **48** was not obtained and in fact, **46** was decomposed under the reaction conditions. None of the products formed could be characterized. It was assumed that the formation of two triflates was complicating the reaction. Therefore, we examined a simplified case in which only one alcohol is present. Starting from methyl cyclopentanone, azidoalcohol **49** was obtained in four steps (Figure 8.13).

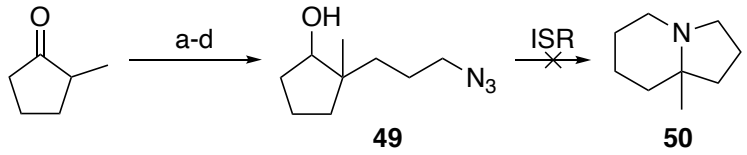

Figure 8.13. Attempted synthesis of 50. Conditions: a) R-(+)-1-phenylethylamine, methyl methacrylate, 88%; b) $LiAlH_4$, 84%; c) TsCl, Et_3N, 48%; d) NaN_3, 97%

Unfortunately, also in this case, no methyl indolizidine **50** was formed. Again, the azidoalcohol was decomposed and no product of the reaction could be identified. Since the only difference to the well working substrate **44** is the presence of the tertiary center, we decided to change the substrate to a slightly larger 6-membered ring and started, again, without the substituent at the bridgehead position. The synthesis of the required azidoalcohol turned out to be more challenging than initially expected (Figure 8.14).

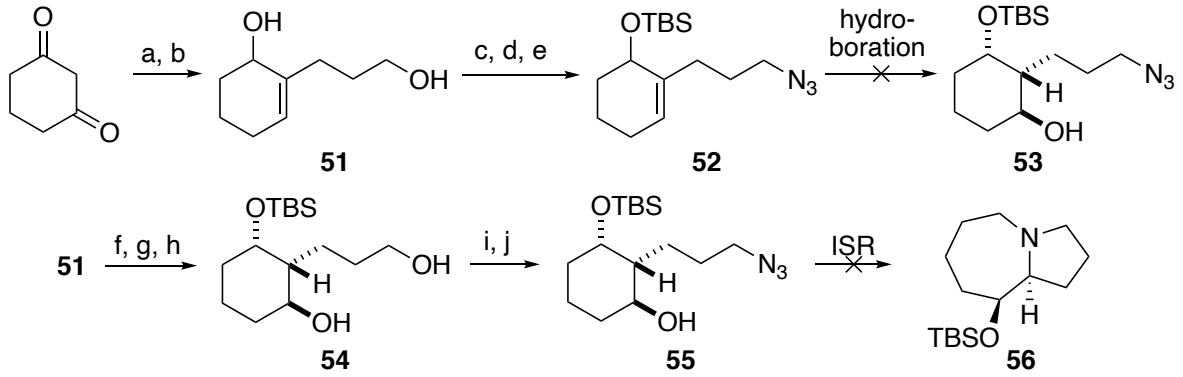

Figure 8.14. Attempted synthesis of 50. Conditions: a) NaH, methyl acrylate; b) $LiAlH_4$; c) TsCl, Et_3N, 20% over 3 steps; d) NaN_3, 20%; e) TBSCl, imidazole, 75%; f) TBSCl, imidazole, 36% over 3 steps; g) 9-BBN, then NaOH, H_2O_2, 78%; h) D-(+)-10-camphorsulfonic acid, 50%; i) TsCl, Et_3N; d) NaN_3, 29% over 2 steps

Diol **51** was formed from 1,3-cyclopentadione over two steps from which the TBS-protected azidoalcohol **52** is accessible in a straightforward manner. However, installation of the alcohol *via* hydroboration was not successful, most probably because the azide group is not tolerated. Therefore, the alcohol was installed earlier in the synthesis. Introduction of the azide in **55** starting from diol **54** was successful. Unfortunately, also here, the ISR did not provide the rearranged product **56** and instead, decomposition of the starting material was observed again.

To rationalize these findings, we suggest that if the carbon next to the tertiary nitrogen atom is stabilized (e.g., tertiary center), the iminium intermediate can decompose right after the rearrangement. The fragmentation to a cationic imine species will result in a multitude of further products, which is in accordance with our experimental observation (Figure 8.15).

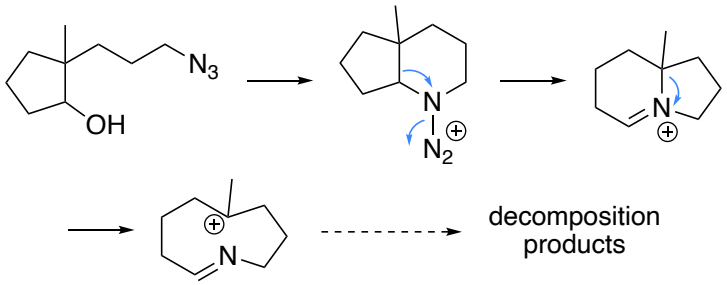

Figure 8.15. Proposed decomposition of iminium intermediates

Although analyses by NMR and GC-MS suggest that aldehydes (e.g., from hydrolysis of an imine) are formed, we were not able to isolate any clean products. Further controlled decomposition to the ring opened imine or aldehyde after hydrolysis was not attempted.

8.4 Conclusion

In conclusion we have developed a versatile strategy to construct bicylic amines having quaternary centres α-to the tertiary amines via intramolecular Schmidt rearrangement involving γ-azidoalcohol followed by C-C bond formation through nucleophilic addition, in a one-pot procedure. A wide range of nucleophiles has been introduced and bicyclic amines were isolated in good to excellent yields with excellent levels of diastereoselectivity. Furthermore, we showed that the formation of α-aminonitriles offers an attractive synthetic pathway to access a variety of α-amino functionalized pyrroloazepines. The intramolecular Schmidt reaction of prefunctionalized azidoalcohols that would afford a bridgehead-substituted amine were not successful, which can be rationalized by a cationic decomposition.

8.5 References

[1] R. A. Pilli, M. da C. F. de Oliveira, Nat. Prod. Rep. 2000, 17, 117–127.

[2] R. A. Pilli, G. B. Rosso, M. da C. F. de Oliveira, Natural Product Reports 2010, 27, 1908–1908.

[3] W. W. Paudler, G. I. Kerley, J. McKay, J. Org. Chem. 1963, 28, 2194–2197.

[4] H. M. Kantarjian, M. Talpaz, V. Santini, A. Murgo, B. Cheson, S. M. O'Brien, Cancer 2001, 92, 1591–1605.

[5] K. L. Mikolajczak, C. R. Smith, D. Weisleder, J. Med. Chem. 1977, 20, 328–332.

[6] M.-T. Hang, Molecular Pharmacology 1975, 11, 511–519.

[7] J. M. Whaun, N. D. Brown, Annals of Tropical Medicine & Parasitology 1990, 84, 229–237.

[8] M. R. Romero, M. A. Serrano, T. Efferth, M. Alvarez, J. J. G. Marin, Planta Med 2007, 73, 552–558.

[9] J.-E. Kim, Y.-J. Song, J Microbiol. 2019, 57, 74–79.

[10] S. Raucher, D. S. Jones, R. E. Stenkamp, J. Org. Chem. 1985, 50, 4523–4526.

[11] C. Gauvin-Hussenet, D. Séraphin, D. Cartier, J.-Y. Laronze, J. Lévy, Tetrahedron Letters 1993, 34, 465–468.

[12] M. Ikeda, M. Ikeda, K. Matsubayashi, T. Imoto, K. Kitao, H. Ishibashi, T. Sato, HETEROCYCLES 1994, 38, 1237.

[13] Z. Jin, F. L. Puchs, Tetrahedron Letters 1996, 37, 5253–5256.

[14] E. R. de Oliveira, F. Dumas, J. d'Angelo, Tetrahedron Letters 1997, 38, 3723–3726.

[15] G. A. Molander, M. Hiersemann, Tetrahedron Letters 1997, 38, 4347–4350.

[16] D. Schinzer, U. Abel, P. G. Jones, Synlett 1997, 1997, 632–634.

[17] L. S. Beall, A. Padwa, Tetrahedron Letters 1998, 39, 4159–4162.

[18] K. I. Booker-Milburn, L. F. Dudin, C. E. Anson, S. D. Guile, Org. Lett. 2001, 3, 3005–3008.

[19] S.-H. Kim, J. K. Cha, Synthesis 2000, 2000, 2113–2116.

[20] L. Planas, J. Pérard-Viret, J. Royer, M. Selkti, A. Thomas, Synlett 2002, 2002, 1629–1632.

[21] S. M. Worden, R. Mapitse, C. J. Hayes, Tetrahedron Letters 2002, 43, 6011–6014.

[22] W.-D. Z. Li, H. Yang, Tetrahedron 2005, 61, 5037–5042.

[23] T. Taniguchi, A. Ishita, M. Uchiyama, O. Tamura, O. Muraoka, G. Tanabe, H. Ishibashi, J. Org. Chem. 2005, 70, 1922–1925.

[24] L. F. Tietze, T. Kinzel, Pure and Applied Chemistry 2007, 79, 629–650.

[25] A. K. Lawrence, K. Gademann, Synthesis 2008, 2008, 331–351.

[26] M. R. Sun, H. T. Lu, H. Yang, Journal of Chemical Research 2009, 2009, 255–257.

[27] F. Berhal, J. Pérard-Viret, J. Royer, Tetrahedron: Asymmetry 2010, 21, 325–332.

[28] M. Marguerit, G. Little, Y. Wang, L. He, S. Allwein, J. Reif, J. Rossi, R. Roemmele, R. Bakale, European Journal of Organic Chemistry 2015, 2015, 8003–8010.

[29] J. Ouyang, X. Mi, Y. Wang, R. Hong, Synlett 2017, 28, 762–772.

[30] Q. Wang, A. Padwa, Org. Lett. 2006, 8, 601–604.

[31] Q. Liu, E. M. Ferreira, B. M. Stoltz, J. Org. Chem. 2007, 72, 7352–7358.
[32] Y. Koseki, H. Sato, Y. Watanabe, T. Nagasaka, Org. Lett. 2002, 4, 885–888.
[33] M. Ikeda, S. A. A. E. Bialy, K. Hirose, M. Kotake, T. Sato, S. M. M. Bayomi, I. A. Shehata, A. M. Abdelal, L. M. Gad, T. Yakura, Chemical & Pharmaceutical Bulletin 1999, 47, 983–987.
[34] W. R. Esmieu, S. M. Worden, D. Catterick, C. Wilson, C. J. Hayes, Org. Lett. 2008, 10, 3045–3048.
[35] W.-D. Z. Li, B.-C. Ma, J. Org. Chem. 2005, 70, 3277–3280.
[36] M. G. Gonçalves-Martin, S. Zigmantas, P. Renaud, Helvetica Chimica Acta 2012, 95, 2502–2514.
[37] K.-J. Xiao, J.-M. Luo, X.-E. Xia, Y. Wang, P.-Q. Huang, Chemistry – A European Journal 2013, 19, 13075–13086.
[38] Q.-W. Zhang, K. Xiang, Y.-Q. Tu, S.-Y. Zhang, X.-M. Zhang, Y.-M. Zhao, T.-C. Zhang, Chemistry – An Asian Journal 2012, 7, 894–898.
[39] P. Gouthami, R. Chegondi, S. Chandrasekhar, Org. Lett. 2016, 18, 2044–2046.
[40] J. H. Siitonen, L. Yu, J. Danielsson, G. Di Gregorio, P. Somfai, J. Org. Chem. 2018, 83, 11318–11322.
[41] Z.-W. Zhang, C.-C. Wang, H. Xue, Y. Dong, J.-H. Yang, S. Liu, W.-Q. Liu, W.-D. Z. Li, Org. Lett. 2018, 20, 1050–1053.
[42] H. Jeon, Y. Chung, S. Kim, J. Org. Chem. 2019, 84, 8080–8089.
[43] M. Sun, H. Lu, Y. Wang, H. Yang, H. Liu, J. Org. Chem. 2009, 74, 2213–2216.
[44] S. El Bialy, M. Ismail, L. Gad, A. Abdelal, Medicinal Chemistry Research 2002, 11.
[45] J. Auerbach, S. M. Weinreb, J. Am. Chem. Soc. 1972, 94, 7172–7173.
[46] M. F. Semmelhack, B. P. Chong, L. D. Jones, J. Am. Chem. Soc. 1972, 94, 8629–8630.
[47] M. F. Semmelhack, B. P. Chong, R. D. Stauffer, T. D. Rogerson, A. Chong, L. D. Jones, J. Am. Chem. Soc. 1975, 97, 2507–2516.
[48] S. M. Weinreb, J. Auerbach, J. Am. Chem. Soc. 1975, 97, 2503–2506.
[49] T. P. Burkholder, P. L. Fuchs, J. Am. Chem. Soc. 1988, 110, 2341–2342.
[50] T. P. Burkholder, P. L. Fuchs, J. Am. Chem. Soc. 1990, 112, 9601–9613.
[51] M. E. Kuehne, W. G. Bornmann, W. H. Parsons, T. D. Spitzer, J. F. Blount, J. Zubieta, J. Org. Chem. 1988, 53, 3439–3450.
[52] H. Ishibashi, M. Okano, H. Tamaki, K. Maruyama, T. Yakura, M. Ikeda, J. Chem. Soc., Chem. Commun. 1990, 1436–1437.
[53] M. Ikeda, M. Okano, K. Kosaka, M. Kido, H. Ishibashi, Chemical & Pharmaceutical Bulletin 1993, 41, 276–281.
[54] X. Lin, R. W. Kavash, P. S. Mariano, J. Am. Chem. Soc. 1994, 116, 9791–9792.
[55] X. Lin, R. W. Kavash, P. S. Mariano, J. Org. Chem. 1996, 61, 7335–7347.
[56] L. F. Tietze, H. Schirok, Angewandte Chemie International Edition in English 1997, 36, 1124–1125.
[57] W.-D. Z. Li, Y.-Q. Wang, Org. Lett. 2003, 5, 2931–2934.

[58] B.-C. Ma, Y.-Q. Wang, W.-D. Z. Li, J. Org. Chem. 2005, 70, 4528–4530.
[59] W.-D. Z. Li, W.-G. Duo, C.-H. Zhuang, Org. Lett. 2011, 13, 3538–3541.
[60] X.-Y. Ma, X.-T. An, X.-H. Zhao, J.-Y. Du, Y.-H. Deng, X.-Z. Zhang, C.-A. Fan, Org. Lett. 2017, 19, 2965–2968.
[61] N. Isono, M. Mori, J. Org. Chem. 1995, 60, 115–119.
[62] L. F. Tietze, H. Schirok, J. Am. Chem. Soc. 1999, 121, 10264–10269.
[63] L. F. Tietze, H. Schirok, M. Wöhrmann, K. Schrader, European Journal of Organic Chemistry 2000, 2000, 2433–2444.
[64] L. F. Tietze, H. Schirok, M. Wöhrmann, Chemistry – A European Journal 2000, 6, 510–518.
[65] L. Planas, J. Pérard-Viret, J. Royer, J. Org. Chem. 2004, 69, 3087–3092.
[66] I. Baussanne, B. Dudot, J. Pérard-viret, L. Planas, J. Royer, Arkivoc 2005, 2006, 57.
[67] J. D. Eckelbarger, J. T. Wilmot, D. Y. Gin, J. Am. Chem. Soc. 2006, 128, 10370–10371.
[68] Z. Zhao, P. S. Mariano, Tetrahedron 2006, 62, 7266–7273.
[69] T. Nagasaka, H. Sato, S. Saeki, Tetrahedron: Asymmetry 1997, 8, 191–194.
[70] A. Hameed, A. J. Blake, C. J. Hayes, J. Org. Chem. 2008, 73, 8045–8048.
[71] T. Taniguchi, H. Ishibashi, Org. Lett. 2008, 10, 4129–4131.
[72] T. Taniguchi, S. Yokoyama, H. Ishibashi, J. Org. Chem. 2009, 74, 7592–7594.
[73] X. Ju, C. M. Beaudry, Angewandte Chemie International Edition 2019, 58, 6752–6755.
[74] L. F. Tietze, A. Modi, Medicinal Research Reviews 2000, 20, 304–322.
[75] S. M. Weinreb, Chem. Rev. 2006, 106, 2531–2549.
[76] L. F. Tietze, A. Düfert, Pure and Applied Chemistry 2010, 82, 1375–1392.
[77] H. Abdelkafi, B. Nay, Nat. Prod. Rep. 2012, 29, 845–869.
[78] J. Cassayre, F. Gagosz, S. Z. Zard, Angewandte Chemie International Edition 2002, 41, 1783–1785.
[79] J. Aubé, G. L. Milligan, Journal of the American Chemical Society 1991, 113, 8965–8966.
[80] G. L. Milligan, C. J. Mossman, J. Aubé, J. Am. Chem. SOC 1995, 117, 10449–10459.
[81] W. H. Pearson, J. M. Schkeryantz, Tetrahedron Letters 1992, 33, 5291–5294.
[82] W. H. Pearson, R. Walavalkar, J. M. Schkeryantz, W. K. Fang, J. D. Blickensdorf, Journal of the American Chemical Society 1993, 115, 10183–10194.
[83] K. J. Frankowski, R. Liu, G. L. Milligan, K. D. Moeller, J. Aubé, Angewandte Chemie - International Edition 2015, 54, 10555–10558.
[84] W. H. Pearson, B. M. Gallagher, Tetrahedron 1996, 52, 12039–12048.
[85] W. H. Pearson, R. Walavalkar, Tetrahedron 2001, 57, 5081–5089.
[86] E. Nyfeler, P. Renaud, Chimia 2006, 60, 276–284.
[87] S. Grecian, J. Aubé, in Organic Azides, John Wiley & Sons, Ltd, 2010, pp. 191–237.
[88] K. Sahasrabudhe, V. Gracias, K. Furness, B. T. Smith, C. E. Katz, D. S. Reddy, J. Aubé, J. Am. Chem. Soc. 2003, 125, 7914–7922.
[89] A. Kapat, E. Nyfeler, G. T. Giuffredi, P. Renaud, Journal of the American Chemical Society 2009, 131, 17746–7.

[90] L. Gnägi, R. Arnold, F. Giornal, H. Jangra, A. Kapat, E. Nyfeler, H. Zipse, R. M. Schärer, P. Renaud, 2020, DOI 10.26434/chemrxiv.12594962.v2.
[91] M. Yang, Y. M. Zhao, S. Y. Zhang, Y. Q. Tu, F. M. Zhang, Chemistry - An Asian Journal 2011, 6, 1344–1347.
[92] B. List, Tetrahedron 2002, 58, 5573–5590.
[93] S. Breitler, E. M. Carreira, Angewandte Chemie International Edition 2013, 52, 11168–11171.
[94] J. M. Carr, T. S. Snowden, Tetrahedron 2008, 64, 2897–2905.
[95] J. Deschamp, O. Riant, Organic Letters 2009, 11, 1217–1220.
[96] P. Bovicelli, P. Lupattelli, A. Sanetti, E. Mincione, Tetrahedron Letters 1995, 36, 3031–3034.
[97] T. G. Back, M. D. Hamilton, Org. Lett. 2002, 4, 1779–1781.
[98] M. N. V. G., R. Dyapa, S. V. Pansare, Org. Lett. 2015, 17, 5312–5315.
[99] A. Stoye, G. Quandt, B. Brunnhöfer, E. Kapatsina, J. Baron, A. Fischer, M. Weymann, H. Kunz, Angewandte Chemie International Edition 2009, 48, 2228–2230.
[100] G. L. Closs, J. Am. Chem. Soc. 1962, 84, 809–813.
[101] J. W. Daly, J. Med. Chem. 2003, 46, 445–452.
[102] H.-J. Liu, K.-S. Shia, X. Shang, B.-Y. Zhu, Tetrahedron 1999, 55, 3803–3830.
[103] W. Oppolzer, C. G. Bochet, Tetrahedron Letters 1995, 36, 2959–2962.
[104] W. Oppolzer, C. G. Bochet, E. Merifield, Tetrahedron Letters 1994, 35, 7015–7018.
[105] A. Agosti, S. Britto, P. Renaud, Organic Letters 2008, 10, 1417–1420.
[106] T. Opatz, Synthesis 2009, 2009, 1941–1959.
[107] D. Enders, J. P. Shilvock, Chemical Society Reviews 2000, 29, 359–373.
[108] V. Beaufort-Droal, E. Pereira, V. Théry, D. J. Aitken, Tetrahedron 2006, 62, 11948–11954.
[109] W. Nagata, M. Yoshioka, S. Hirai, Tetrahedron Letters 1962, 3, 461–466.
[110] L. Bréthous, N. Garcia-Delgado, J. Schwartz, S. Bertrand, D. Bertrand, J.-L. Reymond, J. Med. Chem. 2012, 55, 4605–4618.

8.6 Experimental section

*Note: The syntheses and compound characterizations described in the PhD theses of Ajoy Kapat and of Joséphine Cinqualbre (**21** - **42**, see author contribution) are included here for the sake of completeness of the draft manuscript. The NMR spectra, however, are not reported again and are thus also not included in the appendix of this thesis.*

General information

Techniques

All reactions requiring anhydrous conditions were performed in heat-gun, oven or flame dried glassware under an argon atmosphere. An ice bath was used to obtain a temperature of 0 °C. To obtain a temperature of –78 °C, a bath of acetone was cooled with dry ice. To obtain temperatures of –40 °C and –15 °C, a bath of isopropanol or acetonitrile was cooled to the desired temperature using dry ice. Silica gel 60 Å (40–63 µm) from Silicycle was used for flash column chromatography. Deactivated silica gel: The abovementioned silica gel was suspended in in Et_2O and 20w% of HMDS, then filtered, washed with Et_2O and dried on HV overnight. Deactivated TLC plates: silica plates are dipped in 7M NH_3 in MeOH and then dried. Thin layer chromatography (TLC) was performed on Silicycle silica gel 60 F_{254} plates, visualization under UV light (254 nm) and/or by dipping in a solution of $(NH_4)_2MoO_4$ (15.0 g), $Ce(SO_4)_2$ (0.5 g), H_2O (90 mL), conc. H_2SO_4 (10 mL); or $KMnO_4$ (3 g), K_2CO_3 (20 g) and NaOH 5% (3 mL) in H_2O (300 mL) and subsequent heating. Anhydrous sodium sulfate was used as drying reagent.

Materials

Commercial reagents were used without further purification unless otherwise stated. Dry solvents for reactions were filtered over columns of dried alumina under a positive pressure of argon. Solvents for extractions (Et_2O, *n*-pentane, CH_2Cl_2, EtOAc) and flash column chromatography were of technical grade and distilled prior to use. Commercial dry DMF was used without further purification.

Instrumentation

^1H and ^{13}C NMR spectra were recorded on a Bruker Avance IIIHD-300 spectrometer operating at 300 MHz for ^1H and 75 MHz for ^{13}C at room temperature (24-25°C) unless otherwise stated. Some ^1H and ^{13}C NMR spectra were recorded on a Bruker Avance IIIHD-400 or a Bruker Avance II-400 spectrometer (^1H: 400 MHz; ^{13}C: 75 MHz). Chemical shifts (δ) are reported in parts per million (ppm) using the residual solvent or $Si(CH_3)_4$ (δ = 0.00 for ^1H NMR spectra) as an internal standard. Multiplicities are given as s (singlet), d (doublet), t (triplet), q (quadruplet), m (multiplet), and br (broad). Coupling constant (*J*) is reported in Hz. In ^{13}C-NMR spectra, the peak positions are reported on one decimal unless the difference in chemical shift between two signals is small and required two decimals. Infrared spectra were recorded on a Jasco FT-IR-460 plus spectrometer equipped with a Specac MKII Golden Gate Single Reflection Diamond ATR system and are reported in wave numbers (cm^{-1}). At maximum, the

ten most prominent peaks are reported. Low resolution mass spectra were recorded on a Waters Micromass Autospec Q mass spectrometer in EI mode at 70 eV or were taken from GC-MS analyses performed on a Finnigan Trace GC-MS (quadrupole mass analyzer using EI mode at 70 eV) fitted with a Macherey-Nagel Optima delta-3-0.25 □m capillary column (20 m, 0.25 mm); gas carrier: He 1.4 mL/min; injector: 220 °C split mode. HRMS analyses and accurate mass determinations were mode). Melting points were measured on a Büchi B-545 apparatus and are corrected. Syringe filters with polytetrafluoroethylene membrane were used with a pore size of 0.45µm from Machery-Nagel (CHROMAFIL®Xtra PTFE 0.45). Medium pressure liquid chromatography (MPLC) was performed with a CombiFlash® Rf+ system from Teledyne Isco using RediSep® single-use normal phase columns.

Syntheses

Synthesis pyrroloazepines by nucleophilic addition

Azidoalcohol **21**[9] and iminium triflate **22**[10] were prepared as we have reported previously.

General procedure A – addition of Grignard reagents

A solution of azidoalcohol **21** (1.0 equiv) in dry CH_2Cl_2 was added slowly to a suspension of NaH (2.0 equiv) in dry CH_2Cl_2 (0.15 M) at –78 °C. After stirring for 30 minutes, Tf_2O (1.2 equiv) was added dropwise and the mixture was stirred for 8 h at –78 °C. The mixture was allowed to warm up to room temperature overnight. THF was added in a 2:1 ratio (CH_2Cl_2:THF) and the mixture was cooled down to –78 °C. The Grignard reagent (2.0 equiv) was added, the mixture was stirred for 2 h, treated with sat. aq. NH_4Cl, and warmed up to rt. The two layers were separated and the aqueous was extracted with Et_2O. The combined organic phase was dried over Na_2SO_4, filtered, and concentrated. The products were obtained without further purification.

General procedure B – addition of organolithium reagents

To a stirred solution of aryl lithium reagent in dry Et_2O was added solid iminium triflte salt at –78 °C. The mixture was stirred for 2 h, diluted with Et_2O, treated with water, and stirred for a few minutes. The two phases were separated, and the aqueous layer was extracted with CH_2Cl_2. The combined organic phase was dried over Na_2SO_4, filtered, and concentrated. The products were obtained without further purification.

General procedure C – addition of organocerium reagents

A suspension of $CeCl_3$ (2.0 equiv) in THF was sonicated at rt for 30 min. The alkyl lithium reagent (2.0 equiv) was added drop wise to the above suspension at –78 °C. The yellow organocerium solution was stirred for 30 min before solid iminium triflte salt (1.0 equiv) was added to the solution at –78 °C and stirred for 2 h. The colorless mixture was diluted with Et_2O, treated with water, and stirred for a few minutes. The two phases were separated, and the aqueous layer was extracted with CH_2Cl_2. The combined organic phase was dried over Na_2SO_4, filtered, and concentrated. The products were obtained without further purification.

(7*S*,9a*S*)-9a-allyl-7-phenyloctahydro-1*H*-pyrrolo[1,2-*a*]azepine (23)

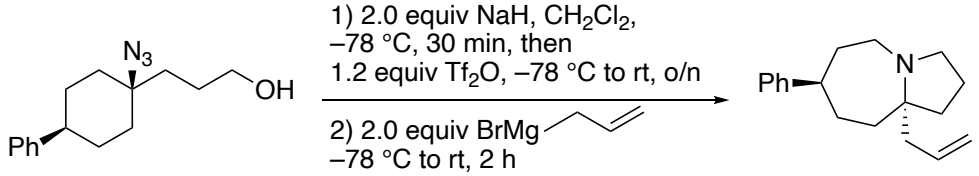

Preparation according to the general procedure **A** from azidoalcohol **21** (114 mg, 0.44 mmol), dry CH_2Cl_2 (3.0 mL), NaH (21 mg, 0.88 mmol, 2.0 equiv), Tf_2O (148 mg, 0.53 mmol, 89 µL, 1.2 equiv), dry

THF (1.5 mL), and allylmagnesium bromide (1 M in Et_2O, 0.88 mL, 0.88 mmol, 2.0 equiv) afforded **23** (99%, 113mg).

Colorless oil; **^{1}H-NMR** (300 MHz, $CDCl_3$) δ = 7.22-7.05 (m, 5H), 5.77 (ddd, J = 19.5, 9.9, 2.4 Hz, 1H), 4.99-4.93 (dd, J = 9.9, 9.9 Hz, 2H), 3.25-3.18 (m, 1H), 3.06-2.84 (m, 2H), 2.78-2.71 (m, 1H), 2.49 (tt, J = 11.4, 3.6 Hz, 1H), 2.11-1.97 (m, 3H), 1.82-1.35 (m, 9H); **^{13}C-NMR** (75 MHz, $CDCl_3$) δ = 148.7, 136.6, 126.4, 126.7, 125.8, 116.6, 64.2, 51.7, 49.3, 47.0, 45.9, 40.0, 36.3, 33.2, 30.7, 23.5; **HRMS** calc. for $[M+H]^+$: 256.2060, found: 256.2063; **IR** (cm^{-1}): 2921, 1636, 1601, 1491, 1448, 1360, 1168, 906, 754, 697

(7*S*,9a*S*)-9a-benzyl-7-phenyloctahydro-1*H*-pyrrolo[1,2-*a*]azepine (24)

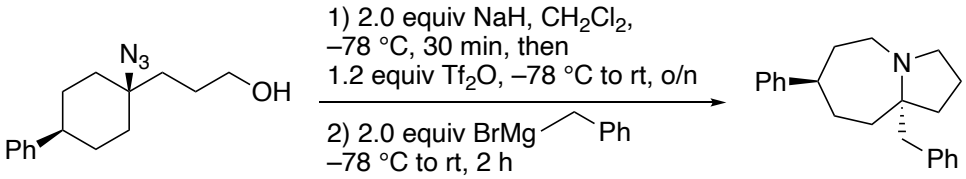

Preparation according to the general procedure **A** from azidoalcohol **21** (104 mg, 0.40 mmol), dry CH_2Cl_2 (3.0 mL), NaH (19 mg, 0.80 mmol, 2.0 equiv), Tf_2O (135 mg, 0.48 mmol, 81 µL, 1.2 equiv), dry THF (1.5 mL), and benzylmagnesium bromide (2 M in Et_2O, 0.4 mL, 0.80 mmol, 2.0 equiv) afforded **24** (97%, 119 mg).

Colorless oil; **^{1}H-NMR** (300 MHz, $CDCl_3$) δ = 7.19-7.05 (m, 10H), 3.21 (ddd, J = 11.1, 7.2, 5.4 Hz, 1H), 3.00 (dt, J = 11.4, 2.1 Hz, 1H), 2.82 (dd, J = 11.4, 9 Hz, 1H), 2.68 (t, J = 5.4 Hz, 1H), 2.56 (d, J = 9.3 Hz, 1H), 2.46 (d, J = 9.3 Hz, 1H), 2.41 (m, 1H), 2.01 (ddd, J = 19.8, 9.3, 1.5 Hz, 1H), 1.76-1.37 (m, 7H), 1.41-1.37 (m, 1H), 1.26-1.14 (m, 1H); **^{13}C-NMR** (75 MHz, $CDCl_3$) δ = 148.7, 139.8, 130.8, 128.3, 127.4, 126.7, 125.6, 65.0, 51.5, 49.5, 47.8, 45.5, 40.8, 36.4, 33.2, 30.7, 26.9, 23.3; **HRMS** calc. for $[M+H]^+$: 306.2216, found: 306.2218; **IR** (cm^{-1}): 3024, 2922, 1600, 1491, 1449, 1361, 1166, 754, 696

(7*S*,9a*S*)-7-phenyl-9a-vinyloctahydro-1*H*-pyrrolo[1,2-*a*]azepine (25)

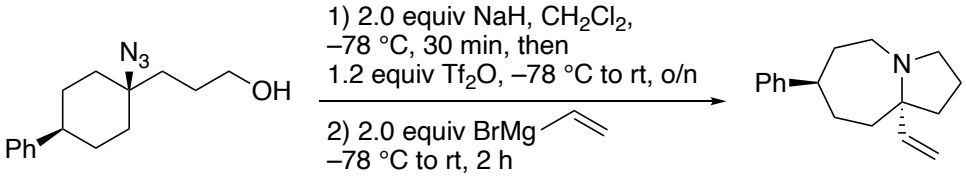

Preparation according to the general procedure **A** from azidoalcohol **21** (100 mg, 0.38 mmol), dry CH_2Cl_2 (3.0 mL), NaH (18 mg, 0.77 mmol, 2.0 equiv), Tf_2O (130 mg, 0.46 mmol, 78 µL, 1.2 equiv), dry THF (1.5 mL), and vinylmagnesium bromide (0.25 M in Et_2O, 3.0 mL, 0.77 mmol, 2.0 equiv) afforded **25** (78%, 78 mg).

Yellow crystalline solid; **^{1}H-NMR** (300 MHz, $CDCl_3$) δ = 7.23-7.07 (m, 5H), 5.8 dd, J = 17.1, 10.2 Hz, 1H), 5.06 (dd, J = 17.1, 2.1 Hz, 1H), 4.89 (dd, J = 10.2, 2.1 Hz, 1H), 3.25 (dd, J = 15, 7.8 Hz, 1H), 3.04 (ddd, J = 15, 4.7, 2.7 Hz, 1H), 2.89 (dd, J = 11.7, 1.5 Hz, 1H), 2.86–2.77 (m, 1H), 2.52 (tt, J = 11.7, 3.9 Hz, 1H), 2.02 (dtd, J = 11.7, 12.0, 2.7 Hz, 1H), 1.90- 1.59 (m, 8H), 1.48 (dtt, J = 14.1, 4.2, 2.4 Hz, 1H);

^{13}C-NMR (75 MHz, $CDCl_3$) δ = 148.7, 145.4, 128.3, 126.7, 125.8, 110.1, 65.9, 51.8, 48.7, 46.1, 38.7, 38.1, 37.8, 30.7, 22.8; **HRMS** calc. for $[M+H]^+$: 242.1909, found: 242.1905; **IR** (cm^{-1}): 3080, 2922, 2849, 2782, 1636, 1491, 1449, 1359, 911, 758

(*S*)-7-phenyl-2,3,5,6,7,8-hexahydro-1*H*-pyrrolo[1,2-*a*]azepine (26)

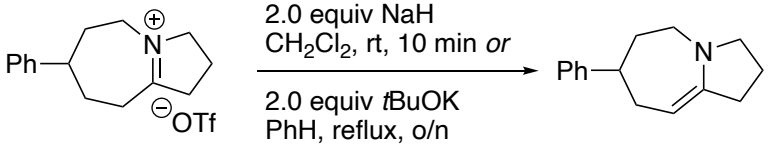

Method 1

To a solution of iminium triflate **22** (150 mg, 0.41 mmol) in dry CH_2Cl_2 (4 mL), was added NaH (66 mg, 0.82 mmol, 2 equiv) and the mixture was stirred at rt for 10 min. The mixture was filtered and evaporated to afford **26** (127 mg, 95%).

Method 2

To a solution of aminonitrile **36** (50 mg, 0.2 mmol) in dry PhH (2 mL) was added *t*BuOK (46.7 mg, 0.403 mmol, 2 equiv) and the resulting solution was refluxed overnight. The obtained suspension was filtered and evaporated to afford **26** (41 mg, 93%).

Yellow oil; **^{1}H-NMR** (300 MHz, $CDCl_3$) δ = 7.31 – 7.15 (m, 5H), 4.70 – 4.67 (m, 1H), 3.13 – 3.06 (m, 2H), 2.85 (ddd, J = 9.7, 8.6, 6.0 Hz, 1H), 2.81 – 2.39 (m, 6H), 2.02 – 1.94 (m, 2H), 1.80 – 1.64 (m, 1H), 1.61 – 1.51 (m, 1H); **^{13}C-NMR** (75 MHz, $CDCl_3$) δ = 149.6, 149.1, 128.7, 127.2, 126.1, 93.0, 57.4, 52.1, 46.9, 38.6, 37.5, 34.0, 23.5; **HRMS** calc. for $[M+H]^+$: 214.1590, found: 214.1590; **IR** (cm^{-1}): 2360, 2279, 1617, 1452, 1329, 1161, 1337, 811

(7*S*,9a*S*)-7,9a-diphenyloctahydro-1*H*-pyrrolo[1,2-*a*]azepine (27)

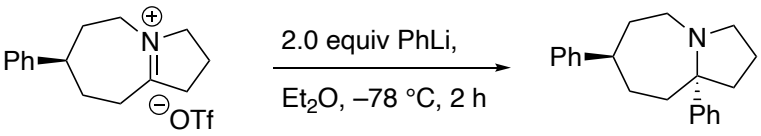

Preparation according to general procedure **B** from phenyl lithium (1.56 M in hexanes, 0.30 mmol, 0.19 mL, 2.0 equiv), dry Et_2O (1.6 mL), and iminium triflate **22** (57 mg, 0.15 mmol, 1.0 equiv) afforded **27** (64%, 33 mg).

Sticky oil; **^{1}H-NMR** (300 MHz, $CDCl_3$) δ = 7.48-7.20 (m, 10H), 3.55 (ddd, J = 10.5, 6.9, 6 Hz, 1H), 3.36 (ddd, J = 15, 3.6, 3.0 Hz, 1H), 3.11 (dd, J = 7.2, 6.9 Hz, 1H), 3.087-3.041 (m, 1H), 2.59 (tt, J = 12, 3.6 Hz, 2H), 2.2 (dd, J = 12, 3.6 Hz, 2H), 2.06-1.68 (m, 6H), 1.63-1.58 (m, 1H); **^{13}C-NMR** (75 MHz, $CDCl_3$) δ = 152.2, 148.6, 128.3, 127.8, 126.7, 126.0, 125.8, 125.4, 77.2, 67.9, 51.7, 49.1, 46.3, 41.6, 33.8, 31.2, 23.3; **HRMS** calc. for $[M+H]^+$: 292.2060, found: 292.2062; **IR** (cm^{-1}): 3022, 2921, 2785, 1489, 1443, 1200, 1028, 754, 697

(7*S*,9a*S*)-9a-(benzo[*d*][1,3]dioxol-5-yl)-7-phenyloctahydro-1*H*-pyrrolo[1,2-*a*]azepine (28)

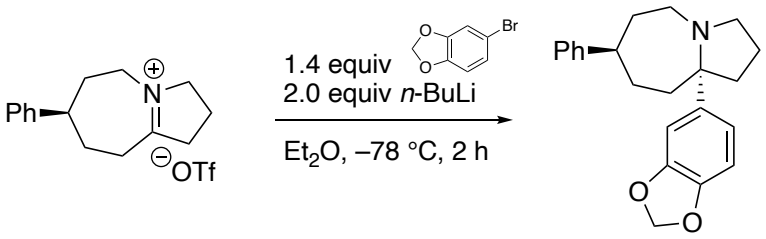

Preparation according to general procedure **B** from 5-bromobenzo[d][1,3]dioxole (41 mg, 0.2 mmol, 1.4 equiv), *n*-butyl lithium (2.4M, 0.28 mmol, 0.11 mL, 2.0 equiv), dry Et_2O (2.0 mL), and iminium triflate **22** (50 mg, 0.14 mmol, 1.0 equiv) afforded **28** (60% NMR yield) in mixture with its homocoupling product (34 mg total mass) after filtration over deactivated silica using pentane as an eluent.

Note: An isolated yield was not determined.

^{1}H-NMR (300 MHz, $CDCl_3$) δ = 7.24-7.07 (m, 6H), 6.79(dd, J = 8.1, 1.8 Hz, 1H), 6.68 (d, J = 8.1 Hz, 1H), 5.85 (s, 2H), 3.39 (ddd, J = 10.5, 8.7, 6.3 Hz, 1H), 3.19 (ddd, J = 15.0, 3.6, 2.7 Hz, 1H), 2.95 (dd, J = 6.6, 6.3 Hz, 1H), 2.91 (ddd, J = 15.0, 12, 1 Hz, 1H), 2.45 (tt, J = 12, 3.6 Hz, 1H), 2.39 (dd, J = 15, 8.1 Hz, 1H), 2.04 (dd, J = 12, 3.6 Hz, 2H), 1.86-1.56 (m, 6H), 1.5-1.43 (m, 1H); **^{13}C-NMR** (75 MHz, $CDCl_3$) δ = 148.5, 147.2, 146.8, 145.2, 128.3, 126.7, 125.8, 118.8, 113.0, 107.5, 107.0, 100.7, 69.9, 51.6, 49.1, 46.1, 41.7, 33.7, 31.2, 23.3

(7*S*,9a*S*)-9a-(4-fluorophenyl)-7-phenyloctahydro-1*H*-pyrrolo[1,2-*a*]azepine (29)

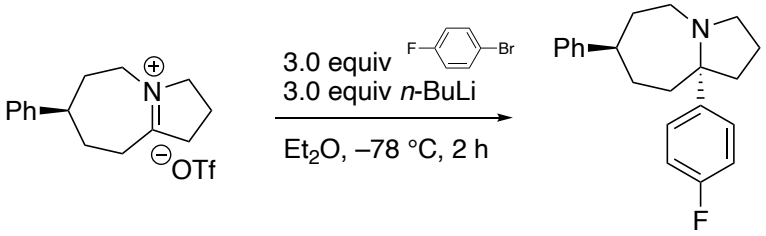

Preparation according to general procedure **B** from bromo-4-fluorobenzene (72 mg, 0.42 mmol, 3.0 equiv), *n*-butyl lithium (2.5 M in hexanes, 0.42 mmol, 0.17 mL, 3.0 equiv), dry Et_2O (2.0 mL), and iminium triflate **22** (50 mg, 0.14 mmol, 1.0 equiv) afforded **29** (75%, 32 mg).

Colorless oil; **^{1}H-NMR** (300 MHz, $CDCl_3$) δ = 7.31-7.08 (m, 7H), 6.89 (t, J = 8.7 Hz, 2H), 3.40 (ddd, J = 12.3, 4.5, 7.5 Hz, 1H), 3.22 (ddd, J = 15.3, 3.6, 2.7 Hz, 1H), 2.99-2.88 (m, 2H), 2.51-2.39 (m, 2H), 2.06 (dq, J = 12, 2.4 Hz, 1H), 2.12-2.03 (m, 1H), 1.87-1.45 (m, 7H); **^{13}C-NMR** (75 MHz, $CDCl_3$) δ = 148.4, 147.8, 128.4, 127.5, 127.3, 126.7, 125.8, 114.4, 67.6, 53.4, 51.7, 49.1, 46.2, 41.7, 33.7, 31.1, 23.3; **HRMS** calc. for $[M+H]^+$: 310.1966; found: 310.1970; **IR** (cm^{-1}): 3022, 2926, 2860, 1601, 1501, 1218, 1154, 908, 832, 727, 699

(7*S*,9a*S*)-7-phenyl-9a-(thiophen-3-yl)octahydro-1*H*-pyrrolo[1,2-*a*]azepine (30)

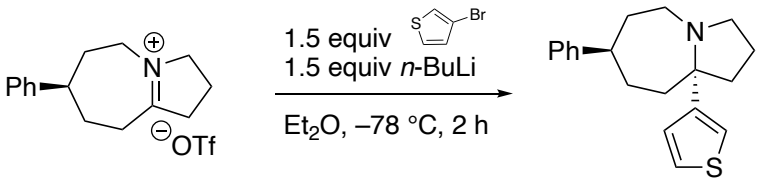

Preparation according to general procedure **B** from 2-bromothiofuran (31 mg, 0.24 mmol, 23 µL, 1.5 equiv), *n*-butyl lithium (2.4 M in hexanes, 0.24 mmol, 0.10 mL, 3.0 equiv), dry Et_2O (2.0 mL), and iminium triflate **22** (57 mg, 0.16 mmol, 1.0 equiv) afforded **30** (76%, 36 mg).

Colorless oil; **^{1}H-NMR** (300 MHz, $CDCl_3$) δ = 7.24-7.07 (m, 5H), 6.99 (d, J = 5.1 Hz, 1H), 6.90 (dd, J = 5.1, 3.9 Hz, 1H), 6.65 (d, J = 3.9 Hz, 1H), 3.35-3.27 (m, 1H), 3.18-3.03 (m, 1H), 2.92 (t, J = 7.5 Hz, 1H), 2.50 (tt, J = 12, 4.2 Hz, 1H), 2.45-2.37 (m, 1H), 2.18-1.67 (m, 9H), 1.48 (d, J = 13.2 Hz, 1H); **^{13}C-NMR** (75 MHz, $CDCl_3$) δ = 148.3, 128.4, 127.6, 126.7, 125.9, 122.6, 120.4, 66.4, 51.5, 49.1, 46.1, 42.4, 41.7, 33.3, 31.6, 23.6; **HRMS** calc. for $[M+H]^+$: 298.1467, found: 298.1616; **IR** (cm^{-1}): 3023, 2921, 1600, 1490, 1448, 754, 695

(7*S*,9a*S*)-9a-(furan-3-yl)-7-phenyloctahydro-1*H*-pyrrolo[1,2-*a*]azepine (31)

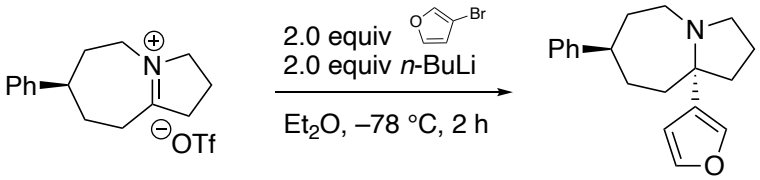

Preparation according to general procedure **B** from 2-bromothiofuran (44 mg, 0.29 mmol, 26 µL, 2.0 equiv), *n*-butyl lithium (2.5 M in hexanes, 0.29 mmol, 0.12 mL, 2.0 equiv), dry Et_2O (2.0 mL), and iminium triflate **22** (50 mg, 0.14 mmol, 1.0 equiv) afforded **31** (76%, 36 mg).

Colorless oil; **^{1}H-NMR** (300 MHz, $CDCl_3$) δ = 7.27 (t, J = 1.8 Hz, 1H), 7.24-7.19 (m, 3H), 7.15-7.07 (m, 3H), 6.19 (dd, J = 1.8, 0.9 Hz, 1H), 3.29 (q, J = 7.8 Hz, 1H), 3.12-2.95 (m, 2H), 2.87-2.82 (m, 1H), 2.57-2.47 (m, 1H), 2.22-1.62 (m, 10H), 1.53-1.44 (m, 1H); **^{13}C-NMR** (75 MHz, $CDCl_3$) δ = 148.4, 142.9, 138.7, 135.8, 128.4, 126.7, 125.8, 109.3, 63.0, 51.5, 48.8, 46.1, 40.3, 33.6, 29.3, 30.9, 23.4; **HRMS** calc. for $[M+H]^+$: 282.1852, found: 282.1838; **IR** (cm^{-1}): 3024, 2922, 2788, 1491, 1449, 1157, 1021, 698

(7*S*,9a*S*)-7-phenyl-9a-((trimethylsilyl)ethynyl)octahydro-1*H*-pyrrolo[1,2-*a*]azepine (32)

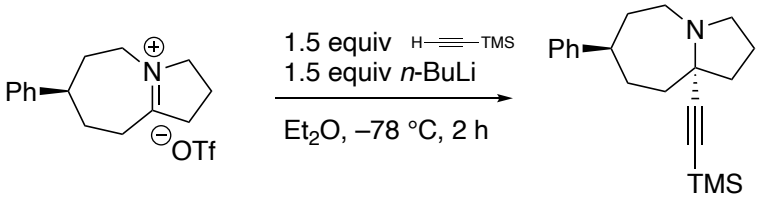

Preparation according to general procedure **B** from 3-trimethylsilylacetelene (59 mg, 0.6 mmol, 82 µL, 1.5 equiv), *n*-butyl lithium (2.5 M in hexanes, 0.6 mmol, 0.24 mL, 1.5 equiv), dry Et_2O (3.4 mL), and iminium triflate **22** (103 mg, 0.4 mmol, 1.0 equiv). FC (deactivated silicagel, 19:1 pentane:Et_2O saturated with NH_3) afforded **32** (54%, 67 mg).

Colorless oil; **^{1}H-NMR** (300 MHz, $CDCl_3$) δ = 7.37-7.17 (m, 5H), 3.25 (dq, J = 9.6, 1.5 Hz, 1H), 3.09-2.97 (m, 2H), 2.64 (t, J = 12.6 Hz, 2H), 2.3-2.19 (m, 1H), 2.17-1.96 (m, 4H), 1.95-1.67 (m, 5H), 0.28 (s, 9H); **^{13}C-NMR** (75 MHz, $CDCl_3$) δ = 149.8, 128.4, 126.7, 125.6, 105.9, 91.4, 63.2, 53.7, 51.4, 44.5, 41.5, 36.7, 34.6, 32.7, 20.5, 0.4; **HRMS** calc. for $[M+H]^+$: 312.2142, found: 312.2146; **IR** (cm^{-1}): 2926, 2808, 2149, 1601, 1492, 1451, 1248, 857, 837, 756, 732, 698

(7*S*,9a*S*)-9a-butyl-7-phenyloctahydro-1*H*-pyrrolo[1,2-*a*]azepine (33)

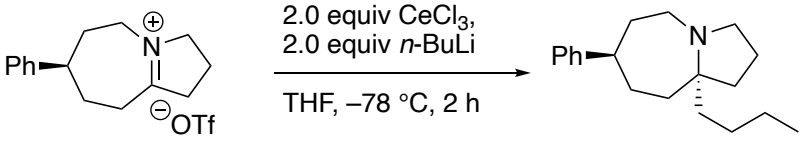

Preparation according to general procedure **C** from $CeCl_3$ (140 mg, 0.56 mmol, 2.0 equiv), dry THF (1.6 mL), *n*-butyl lithium (2.47 M in hexane, 0.56 mmol, 0.22 mL 2.0 equiv), and iminium triflate **22** (103 mg, 0.28 mmol) afforded **33** (99%, 77 mg).

Colorless oil; **^{1}H-NMR** (300 MHz, $CDCl_3$) δ = 7.23-7.06 (m, 5H), 3.24 (dd, J = 15.6, 9 Hz, 1H), 3.1 (ddd, J = 15.6, 3.9, 3.9 Hz, 1H), 3.01 (ddd, J = 15.0, 13.8, 1.5 Hz, 1H), 2.93-2.79 (m, 1H), 2.56 (tt, J = 11.7, 3.9 Hz, 1H), 2.08 (ddd, J = 11.7, 3.9, 3.0 Hz, 1H), 1.83-1.12 (m, 15H), 0.84 (t, J = 7.2 Hz, 3H); **^{13}C-NMR** (75 MHz, $CDCl_3$) δ = 147.9, 128.3, 126.6, 125.9, 66.0, 51.8, 48.5, 46.3, 41.3, 38.5, 36.1, 32.4, 30.4, 27.4, 23.4, 23.3, 14.1; **HRMS** calc. for $[M+H]^+$: 272.2373, found: 272.2375; **IR** (cm^{-1}): 3025, 2953, 2924, 1601, 1491, 1449, 1170, 754, 697

(7*S*)-9a-isobutyl-7-phenyloctahydro-1*H*-pyrrolo[1,2-*a*]azepine (34)

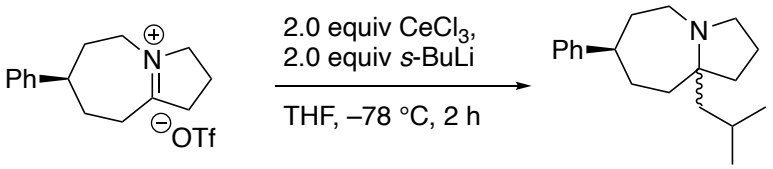

Preparation according to general procedure **C** from $CeCl_3$ (135 mg, 0.55 mmol, 2.0 equiv), dry THF (1.6 mL), *s*-butyl lithium (1.4 M in hexane, 0.56 mmol, 0.4 mL 2.0 equiv), and iminium triflate **22** (100 mg, 0.27 mmol) afforded **34** (74%, 55 mg) as a mixture of diastereomers (dr 2:1).

Colorless oil; **HRMS** calc. for $[M+H]^+$: 272.2373, found: 272.2378 **IR** (cm^{-1}): 2958, 2924, 2871, 2786, 1491, 1449, 754, 697

For mixture of two diastereomer **^{1}H-NMR** (300 MHz, $CDCl_3$) δ = 7.22-7.06 (m, 5H), 3.35-3.25 (m,1H), 3.1-2.73 (m, 2H) 2.47-2.73 (tt, J = 11.4, 3.6 Hz, 1H), 2.06 (dq, J = 12.3, 2.4 Hz, 1H), 1.88-1.37 (m, 11H), 1.29-1.07 (m, 2H), 1.01-0.72 (m,7H)

For major diastereomer **^{13}C-NMR** (75 MHz, $CDCl_3$) δ = 148.8, 128.3, 126.7, 125.7, 67.9, 51.6, 49.5, 46.6, 45.8, 37.9, 34.3, 32.8, 30.8, 26.9, 24.3, 24.2, 14.8, 13.2

For minor diastereomer **^{13}C-NMR** (75 MHz, $CDCl_3$) δ = 148.8, 128.4, 126.7, 125.8, 67.5, 51.7, 49.6, 46.3, 46.2, 38.4, 33.8, 32.7, 30.7, 29.7, 25.0, 24.0, 14.1, 13.3

Derivatization of α-aminonitriles

General procedure D – addition of organolithium reagents to α-aminonitriles

Adaption of a literature procedure[11]. To a solution of aminonitrile **36** in dry THF or dry Et_2O was added the organolithium reagent dropwise over a period of 15 min at –78 °C, warmed up to rt and stirred for 1 h. The mixture was treated with aq. HCl or aq. H_2SO_4 (1 M) at 0 °C and stirred at rt overnight, then neutralized with sat. aq. $NaHCO_3$ and basified with aq. NaOH (1 M). The aqueous phase was separated and extracted three times with CH_2Cl_2. The combined organic layers were dried over Na_2SO_4, filtered and concentrated.

(7*S*)-7-phenylhexahydro-1*H*-pyrrolo[1,2-*a*]azepine-9a(5*H*)-carbonitrile (36)

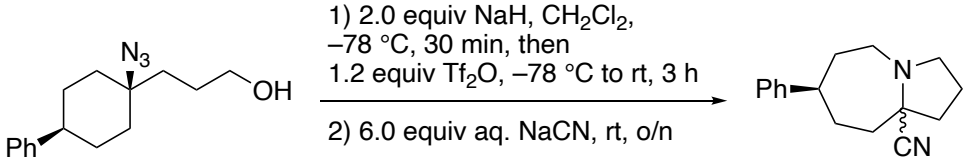

To a solution of azido alcohol **21** (777 mg, 3 mmol) in CH_2Cl_2 (24 mL) was slowly added NaH (144 mg, 6 mmol, 2.0 equiv.) at –78 °C. After stirring for 30 min, Tf_2O (0.61 mL, 3.6 mmol, 1.2 equiv.) was added dropwise and the reaction mixture was allowed to reach rt over 3 h. NaCN (882 mg, 1 M in water, 6.0 equiv.) was added, the mixture was stirred at rt overnight, treated with sat. aq. Na_2CO_3 (20 mL), and extracted with CH_2Cl_2 (3 x 40 mL). The combined organic phase was dried over Na_2SO_4, filtered, and concentrated which afforded an inseparable mixture of diastereomers of **36** (633 mg, 88%).

Yellow oil; **^{1}H-NMR** (300 MHz, $CDCl_3$) δ = 7.37 – 7.21 (m, 10H), 3.29 – 3.22 (m, 1H), 3.19 – 2.92 (m, 6H), 2.88 – 2.71 (m, 3H), 2.71 – 2.45 (m, 1H), 2.33 – 1.77 (m, 19H); **^{13}C-NMR** (75 MHz, $CDCl_3$) δ = 148.7, 148.5, 128.6, 128.6, 126.8, 126.6, 126.1, 120.8, 120.2, 65.4, 65.2, 56.1, 53.7, 50.7, 49.5, 45.2, 44.0, 41.0, 39.7, 39.4, 35.6, 35.4, 35.3, 33.5, 31.3, 22.0 20.6; **HRMS** calc. for $[M+H]^+$: 241.1699, found: 241.1701; **IR** (cm^{-1}): 2929, 1600, 1492, 1451, 1337, 758, 699

(7*S*,9a*S*)-7,9a-diphenyloctahydro-1*H*-pyrrolo[1,2-*a*]azepine (27)

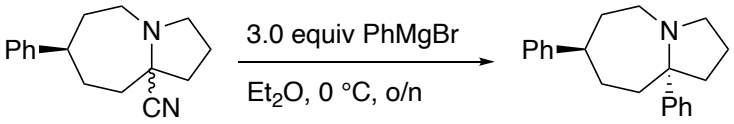

To a solution of aminonitrile **36** (100 mg, 0.40 mmol) in dry Et_2O (2 mL), was added PhMgCl (3.6 mL, 2 M in THF, 3.0 equiv.) at 0 °C and the mixture was stirred at rt overnight. The mixture was diluted with Et_2O (10 mL), cooled down to 0 °C, treated with aq. sat. NH_4Cl (10 mL), and the phases were separated. The organic phase was washed twice with aq. sat. $NaHCO_3$, dried over Na_2SO_4, filtered and concentrated to afford **27** (180 mg, 62%).

Note: Analytical data are described above for this compound.

7-phenylhexahydro-1*H*-pyrrolo[1,2-*a*]azepine-9a(5*H*)-carboxylic acid (37)

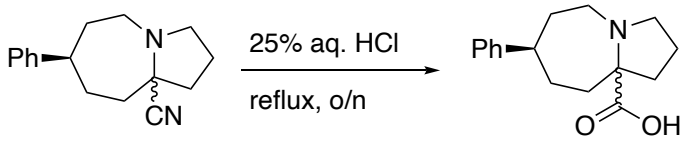

A solution of aminonitrile **36** (50 mg, 0.2 mmol) in aq. HCl (25%, 2 mL) was refluxed overnight. The mixture was neutralized with sat. aq. $NaHCO_3$, then basified with aq. NaOH (1 M), and extracted three times with EtOAc. The combined organic phase was dried over Na_2SO_4, filtered and concentrated which afforded **37** (48 mg, 92%).

White solid; **^{1}H-NMR** (300 MHz, $CDCl_3$) δ = 7.36 – 7.23 (m, 5H), 4.57 – 4.44 (m, 2H), 4.04 – 3.97 (m, 1H), 3.58 – 3.42 (m, 2H), 3.42 – 3.33 (m, 1H), 3.20 – 3.05 (m, 2H), 2.48 – 2.37 (m, 2H), 2.16 – 1.93 (m, 5H); **^{13}C-NMR** (75 MHz, $CDCl_3$) δ = 196.1, 145.2, 129.0, 127.1, 126.8, 64.1, 52.2, 47.3, 42.3, 31.5, 31.0, 28.8, 19.3

7-phenyloctahydro-1*H*-pyrrolo[1,2-*a*]azepine (38)

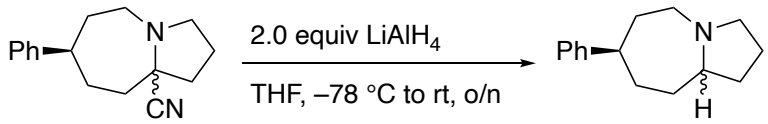

To a solution of aminonitrile **36** (50 mg, 0.20 mmol) in dry THF (2 mL) was added $LiAlH_4$ (0.4 mL, 1 M in THF, 2.0 equiv.) at –78 °C. The mixture was then stirred at rt overnight. The mixture was diluted with Et_2O (20 mL) and cooled down to 0 °C. Water (15 mL) was slowly added, followed by aq. NaOH (1 M, 15 mL). This mixture was allowed to warm up to rt and was stirred for 15 min. The aqueous phase was separated and extracted three times with Et_2O, (20 mL). The combined organic phase was dried over Na_2SO_4, filtered and concentrated which afforded **38** as a mixture of diastereoisomers (41 mg, 95%, *cis/trans*, 1:2). The diastereomers were not separated.

Colorless oil; **^{1}H-NMR** (300 MHz, $CDCl_3$) δ = 7.40 – 7.24 (m, 15H), 3.35 – 3.21 (m, 3H), 3.18 – 3.01 (m, 3H), 2.97 – 2.88 (m, 2H), 2.81 – 2.70 (m, 2H), 2.66 – 2.56 (m, 3H), 2.48 – 2.34 (m, 4H), 2.28 – 2.08 (m, 6H), 2.05 – 1.76 (m, 21H), 1.68 – 1.54 (m, 4H); **^{13}C-NMR** (75 MHz, $CDCl_3$) δ = 149.7, 149.6, 128.5, 128.5, 126.8, 126.7, 125.8, 125.8, 66.1, 64.4, 57.8, 56.9, 53.0, 44.9, 44.7, 37.3, 36.5, 36.1, 35.7, 34.0, 33.9, 33.7, 33.0, 29.8, 23.3, 22.5; physical and spectral data are in accordance with literature data[9].

1-((7*S*)-7-phenylhexahydro-1*H*-pyrrolo[1,2-*a*]azepin-9a(5*H*)-yl)ethan-1-one (39)

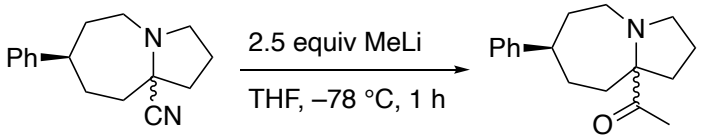

Preparation according to general procedure **D** from aminonitrile **36** (240 mg, 1 mmol), dry THF (3 mL), MeLi (1.6 mL, 1.6 M in Et_2O, 2.5 equiv.), and aq. HCl (1M, 3 mL). FC (neutral alox, pentane:EtOAc, 9:1) afforded **39** (total 180 mg, 70%) as two separate diastereomers (dr 1.7:1).

Colorless oil; **HRMS** calc. for $[M+H]^+$: 258.1846, found: 258.1852; **IR** (cm^{-1}): 2924, 1698, 1450, 1345, 1153, 907, 732, 699

Major diastereoisomer **^{1}H-NMR** (300 MHz, $CDCl_3$) δ = 7.36 – 7.20 (m, 5H), 3.47 – 3.39 (m, 1H), 3.29 – 3.23 (m, 1H), 3.14 – 3.10 (m, 1H), 2.90 (t, J = 7.4 Hz, 1H), 2.68 – 2.59 (m, 1H), 2.29 (s, 3H), 2.25 – 2.10 (m, 2H), 2.01 – 1.77 (m, 7H), 1.64 – 1.60 (m, 1H); **^{13}C-NMR** (75 MHz, $CDCl_3$) δ = 215.8, 148.1, 128.6, 126.8, 126.1, 74.2, 51.6, 49.1, 47.2, 36.3, 35.3, 33.6, 31.0, 25.9, 24.4

Minor diastereoisomer **^{1}H-NMR** (300 MHz, $CDCl_3$) δ = 7.31 – 7.14 (m, 5H), 3.26 – 3.21 (m, 2H), 2.99 – 2.86 (m, 2H), 2.67 (t, J = 11.3 Hz, 1H), 2.36 – 2.29 (m, 1H), 2.34 (s, 3H), 2.21 – 2.10 (m, 1H), 2.05 – 1.97 (m, 1H), 1.89 – 1.65 (m, 6H), 1.56 – 1.43 (m, 1H); **^{13}C-NMR** (75 MHz, $CDCl_3$) δ = 217.2, 147.9, 128.5, 126.8, 126.1, 56.9, 51.8, 47.5, 41.1, 35.7, 34.4, 34.2, 29.8, 28.1, 24.2

1-((7*S*)-7-phenylhexahydro-1*H*-pyrrolo[1,2-*a*]azepin-9a(5*H*)-yl)ethan-1-one (40)

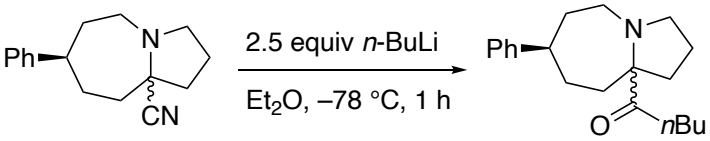

Preparation according to general procedure **D** from aminonitrile **36** (240 mg, 1 mmol), dry Et_2O (6 mL), *n*-BuLi (0.5 mL, 2.5 M in hexanes, 1.2 equiv), and aq. H_2SO_4 (1 M, 3 mL). FC (neutral alox, pentane:EtOAc, 8:2) afforded **40** (total 195 mg, 65%) as two separate diastereomers (dr 1:1).

Colourless oil; **HRMS** calc. for $[M+H]^+$: 300.2136, found: 300.2142; **IR** (cm^{-1}): 2923, 1699, 1492, 1451, 1173, 907, 756, 699

Isomer 1 **^{1}H-NMR** (300 MHz, $CDCl_3$) δ = 7.35 – 7.18 (m, 5H), 3.46 – 3.38 (m, 1H), 3.24 (ddd, J = 15.2, 4.1, 2.4 Hz, 1H), 3.12 – 3.09 (m, 1H), 3.04 – 2.97 (m, 1H), 2.76 – 2.56 (m, 3H), 2.25 – 2.12 (m, 2H), 2.11 – 1.97 (m, 1H), 1.96 – 1.72 (m, 6H), 1.62 – 1.55 (m, 3H), 1.38 – 1.31 (m, 2H), 0.95 (t, J = 7.3 Hz, 3H); **^{13}C-NMR** (75 MHz, $CDCl_3$) δ = 218.0, 148.2, 128.5, 126.8, 126.1, 74.4, 51.7, 49.1, 47.4, 37.3, 36.4, 35.5, 33.7, 31.1, 26.5, 24.4, 22.7, 14.1

Isomer 2 **^{1}H-NMR** (300 MHz, $CDCl_3$) δ = 7.31 – 7.13 (m, 5H), 3.26 – 3.22 (m, 2H), 3.01 – 2.97 (m, 2H), 2.93 – 2.87 (m, 1H), 2.76 – 2.72 (m, 2H), 2.36 (dd, J = 14.4, 6.2 Hz, 1H), 2.19 – 2.11 (m, 1H), 2.05 – 1.98 (m, 1H), 1.86 – 1.57 (m, 8H), 1.50 – 1.34 (m, 3H), 0.97 (t, J = 7.3 Hz, 3H); **^{13}C-NMR** (75 MHz, $CDCl_3$) δ = 210.3, 148.0, 128.5, 126.8, 126.1, 57.1, 51.9, 47.5, 41.3, 39.7, 35.9, 34.6, 34.2, 30.5, 29.9, 26.3, 22.7, 14.2

2,2-dimethyl-1-((7*S*)-7-phenylhexahydro-1*H*-pyrrolo[1,2-*a*]azepin-9a(5*H*)-yl)propan-1-one (41)

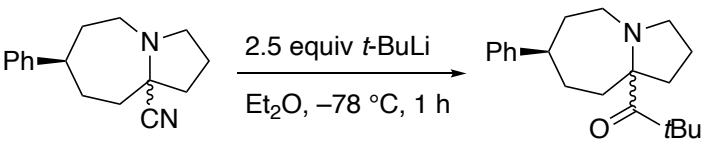

Preparation according to general procedure **D** from aminonitrile **36** (50 mg, 0.2 mmol), dry Et_2O (0.5 mL), *t*-BuLi (0.2 mL, 2.5 M in hexanes, 2.5 equiv), and aq. H_2SO_4 (1 M, 3 mL) afforded **41** (total 195 mg, 65%) as a mixture of diastereomers (dr 1:2).

Colorless oil; **HRMS** calc. for $[M+H]^+$: 300.2136, found: 300.2142; **IR** (cm^{-1}): 2923, 1699, 1492, 1451, 1173, 907, 756, 699

For the mixture of diastereoisomers **^{1}H-NMR** (300 MHz, $CDCl_3$) δ = 7.37 – 7.14 (m, 10H), 3.42 – 3.30 (m, 2H), 3.28 – 3.16 (m, 2H), 3.05 – 2.79 (m, 3H), 2.69 – 2.54 (m, 3H), 2.51 – 2.34 (m, 2H), 2.20 – 2.06 (m, 3H), 1.96 – 1.74 (m, 10H), 1.70 – 1.53 (m, 5H), 1.38 (s, 18H); **^{13}C-NMR** (75 MHz, $CDCl_3$) δ = 190.9, 189.9, 147.9, 147.3, 128.5, 128.5, 126.9, 126.8, 126.1, 126.1, 76.3, 74.7, 56.4, 51.8, 51.0, 48.8, 46.0, 39.1, 38.9, 38.9, 37.4, 35.8, 35.3, 34.1, 32.9, 32.6, 32.1, 30.3, 29.8, 23.8, 23.4

phenyl((7*S*)-7-phenylhexahydro-1*H*-pyrrolo[1,2-*a*]azepin-9a(5*H*)-yl)methanone (42)

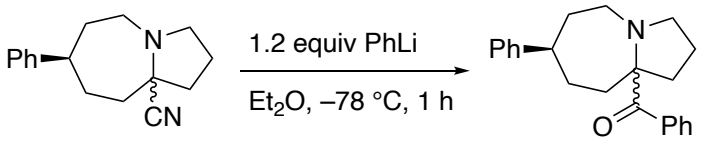

Preparation according to general procedure **D** from aminonitrile **36** (240 mg, 1 mmol), dry Et_2O (6 mL), PhLi (1.7 M in Et2O, 0.7 mL, 1.2 equiv), and aq. H_2SO_4 (1 M, 3 mL). FC (neutral alox, pentane:EtOAc, 8:2) afforded **42** (total 182 mg, 57%) as two separate diastereomers (dr 1:1).

Colourless oil; **HRMS** calc. for $[M+H]^+$: 320.1999, found: 320.2009; **IR** (cm^{-1}): 2922, 1669, 1445, 1345, 1176, 969, 758, 698

Isomer 1 **^{1}H-NMR** (300 MHz, $CDCl_3$) δ = 7.92 – 7.89 (m, 2H), 7.43 – 7.31 (m, 3H), 7.18 – 7.01 (m, 3H), 6.95 – 6.93 (m, 2H), 3.20 – 3.11 (m, 2H), 2.94 – 2.85 (m, 2H), 2.59 (tt, J = 11.6, 3.3 Hz, 1H), 2.50 – 2.39 (m, 2H), 1.94 – 1.64 (m, 6H), 1.61 – 1.48 (m, 1H), 1.46 – 1.32 (m, 1H); **^{13}C-NMR** (75 MHz, $CDCl_3$) δ = 208.5, 148.2, 139.5, 130.9, 128.9, 128.5, 128.0, 126.8, 126.1, 74.8, 51.4, 48.6, 47.2, 37.3, 36.8, 33.7, 31.1, 23.8

Isomer 2 **^{1}H-NMR** (300 MHz, $CDCl_3$) δ = 7.84 – 7.81 (m, 2H), 7.54 – 7.40 (m, 3H), 7.34 – 7.29 (m, 2H), 7.23 – 7.18 (m, 3H), 3.51 (dd, J = 15.8, 8.5 Hz, 1H), 3.21 – 2.96 (m, 3H), 2.56 – 2.46 (m, 1H), 2.42 (dd, J = 13.0, 7.4 Hz, 1H), 2.30 (ddd, J = 14.9, 7.5, 2.5 Hz, 1H), 2.20 – 2.01 (m, 3H), 1.99 – 1.69 (m, 4H), 1.60 – 1.58 (m, 1H); **^{13}C-NMR** (75 MHz, $CDCl_3$) δ = 208.8, 148.3, 139.1, 131.6, 129.4, 128.5, 128.1, 126.7, 126.0, 76.5, 55.8, 51.0, 47.1, 41.7, 36.6, 34.9, 34.1, 24.0

Schmidt reaction of prefunctionalized azidoalcohols

General procedure E – reduction with $LiAlH_4$

To a suspension of $LiAlH_4$ in dry Et_2O at 0 °C was added dropwise a solution of substrate in a small volume of dry Et_2O. The temperature was kept below 5 °C during the time of addition. After complete addition, the mixture was stirred for 1 h at 0 °C. Under vigorous stirring and careful control of the temperature, Glauber's salt (Na_2SO_4 decahydrate) was added in small portions over a period of 1 h at 0 °C. Then, anhydrous Na_2SO_4 was added, the resulting suspension was filtered through a POR4 fritte and concentrated.

General procedure F – tosylation

To a solution of substrate in dry CH_2Cl_2 was added tosyl chloride and triethylamine. The mixture was stirred at 0 °C for 6 h, treated with water, and extracted 3x with CH_2Cl_2. The combined organic phase was dried over Na_2SO_4, filtered, and concentrated.

General procedure G – azide formation

A stirred solution of substrate and sodium azide in dry DMF was heated up to 100 °C. After 3 h, the mixture was cooled down to rt, treated with water, and extracted 3x with EtOAc. The organic phase was dried over Na_2SO_4, filtered, and concentrated.

Preparation and ISR of 44

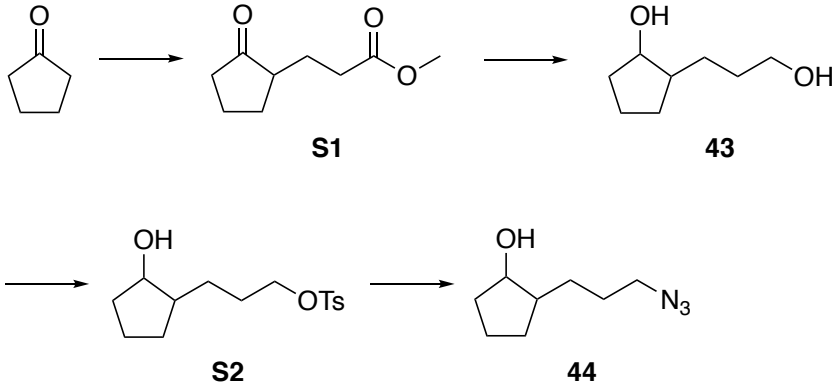

Methyl 3-(2-oxocyclopentyl)propanoate (S1)

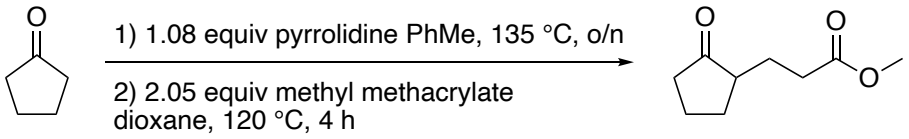

A stirred solution of cyclopentanone (10 mL, 113 mmol) and pyrrolidine (10 mL, 122 mmol, 1.08 equiv) in toluene (100 mL) was heated to reflux at 135 °C overnight using a Dean-Stark apparatus. The mixture was concentrated under reduced pressure and the residue was dissolved in dioxane (100 mL). After addition of methyl acrylate (21 mL, 232 mmol, 2.05 equiv), the mixture was heated to reflux for 4 h at 120 °C. Water (10 mL) was added and the mixture was heated to reflux for 1 h at 120 °C. The mixture was then concentrated slowly under reduced pressure. The dark red smelly residue was dissolved in EtOAc and a few spatulas of amberlite® acidic residue was added. The mixture was stirred, filtered over a pad of silica and the resulting solution was concentrated. MPLC (gradient from 0:10 to 3:7 EtOAc:heptanes) afforded **S1** (59%, 11.3 g).

Colorless oil; **Rf** 0.33 (3:7 EtOAc:heptanes); **^{1}H-NMR** (300 MHz, $CDCl_3$) δ 3.65 (s, 3H), 2.47 – 2.36 (m, 2H), 2.36 – 1.92 (m, 6H), 1.87 – 1.40 (m, 3H); **^{13}C-NMR** (75 MHz, $CDCl_3$) δ 220.5, 173.8, 51.7, 48.4, 38.1, 32.0, 29.6, 25.0, 20.7; physical and spectral data are in accordance with literature data.[1]

2-(3-hydroxypropyl)cyclopentan-1-ol (43)

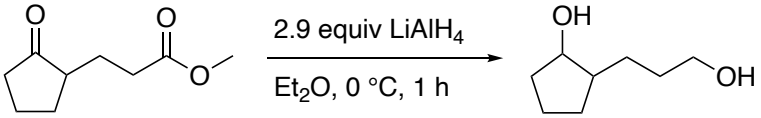

Prepared according to the general procedure **E** from $LiAlH_4$ (6.5 g, 170 mmol, 2.9 equiv), Et_2O (500 mL), methyl 3-(2-oxocyclopentyl) propanoate **S1** (10 g, 58.8 mmol) in dry Et_2O (15 mL), and Glauber's salt (50 g, 155 mmol, 2.6 equiv) which afforded **43** as a mixture of diastereomers (89%, 7.56 g). A separation was not attempted.

Colorless oil; **Rf** 0.17 in 8:2 EtOAc:heptanes; **^{1}H-NMR** (300 MHz, $CDCl_3$) δ 4.16 (ddd, J = 5.3, 3.8, 1.6 Hz, 0.2H), 3.80 (q, 0.7H), 3.71 – 3.58 (m, 1.9H), 2.35 (s, 2H), 2.00 – 1.05 (m, 11H); **^{13}C-NMR** (75 MHz, $CDCl_3$) δ 79.2, 74.5, 63.0, 62.9, 47.8, 50.0, 34.9, 34.8, 31.6, 31.2, 30.4, 30.1, 29.3, 25.3, 21.9; **HRMS** calc. for $C_8H_{16}O_2Na$ $[M+Na]^+$: 167.1043, found: 167.1038; **IR** (cm^{-1}): 3308, 2933, 2867, 2361, 1450, 1341, 1053, 1020, 936, 915

3-(2-hydroxycyclopentyl)propyl 4-methylbenzenesulfonate (S2)

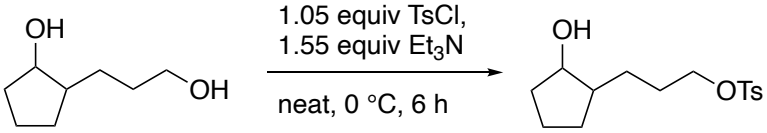

Prepared according to the general procedure **F** from 2-(3-hydroxypropyl)cyclopentan-1-ol **43** (7.44 g, 51.4 mmol), dry CH_2Cl_2 (120 mL), tosyl chloride (10.0 g, 52.5 mmol, 1.05 equiv), and triethylamine (11 mL, 78.9 mmol, 1.55 equiv). MPLC (gradient from 2:8 to 5:5 Et_2O:pentane) afforded two diastereomers of **S2** (64%, 9.8 g).

Note: Trace impurities of the major diastereomers could not be fully removed in the minor fractions. The compounds were not dried to complete dryness as they are not stable over time and were used immediately for the next step.

Minor (2.0 g, 13%)

Colorless oil; **Rf** 0.24 in 5:5 Et_2O:pentane; **^{1}H-NMR** (300 MHz, $CDCl_3$) δ 7.79 (d, J = 8.3 Hz, 2H), 7.37 – 7.31 (m, 2H), 4.10 (td, J = 4.1, 1.5 Hz, 1H), 4.04 (t, J = 6.4 Hz, 2H), 2.79 (s, 1H), 2.45 (s, 3H), 1.87 – 1.26 (m, 12H); **^{13}C-NMR** (75 MHz, $CDCl_3$) δ 144.8, 133.3, 130.0 (2C), 128.0 (2C), 74.9, 70.9, 45.2, 35.0, 28.7, 28.1, 25.1, 21.8, 21.8; **HRMS** calc. for $C_{15}H_{22}O_4NaS$ $[M+Na]^+$: 321.1119, found: 321.1131; **IR** (cm^{-1}): 2940, 2871, 1601, 1351, 1172, 1096, 957, 915, 813, 661

Major (7.8 g, 51%)

Colorless oil; **Rf** 0.19 in 5:5 Et_2O:pentane; **^{1}H-NMR** (300 MHz, $CDCl_3$) δ 7.82 – 7.75 (m, 2H), 7.37 – 7.31 (m, 2H), 4.04 (t, J = 6.4 Hz, 2H), 3.76 (q, J = 5.6 Hz, 1H), 2.45 (s, 3H), 1.96 – 1.43 (m, 10H), 1.28 – 1.03 (m, 2H); **^{13}C-NMR** (75 MHz, $CDCl_3$) δ 144.8, 133.3, 130.0 (2C), 128.0 (2C), 79.2, 70.9, 47.7, 34.9, 30.0, 29.7, 27.8, 21.9, 21.8; **HRMS** calc. for $C_{15}H_{22}O_4NaS$ $[M+Na]^+$: 321.1119, found: 321.1131; **IR** (cm^{-1}): 2942, 2867, 1596, 1452, 1353, 1172, 1095, 930, 814, 661

2-(3-azidopropyl)cyclopentan-1-ol (44)

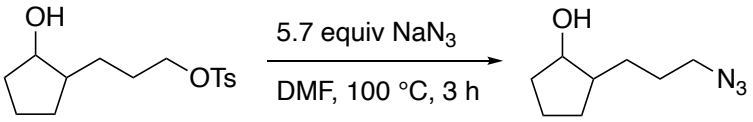

From minor S2

Prepared according to the general procedure **G** from 3-(2-hydroxycyclopentyl)propyl 4-methylbenzene sulfonate **S2** (1.2 g, 4 mmol), sodium azide (1.5 g, 23.1 mmol, 5.7 equiv) and dry DMF (25 mL). MPLC (gradient from 2:8 to 5:5 Et2O:pentane) afforded **44** (59%, 400 mg).

Colorless oil; **Rf** 0.56 in 5:5 Et_2O:pentane; **^{1}H-NMR** (300 MHz, $CDCl_3$) δ 4.15 (td, J = 4.1, 1.7 Hz, 1H), 3.30 (t, J = 6.6 Hz, 2H), 1.93 – 1.30 (m, 11H), 1.25 (s, 1H); **^{13}C-NMR** (75 MHz, $CDCl_3$) δ 74.7, 51.9, 45.5, 35.2, 28.9, 28.1, 26.5, 21.9; **HRMS** calc. for $C_8H_{16}ON$ $[M+H]^+$: 142.1226, found: 142.1223; **IR** (cm^{-1}): 3384, 2936, 2866, 2087, 1449, 1349, 1248, 1027, 988, 862

From major S2

Prepared according to the general procedure C from 3-(2-hydroxycyclopentyl)propyl 4-methylbenzene sulfonate **S2** (6.5 g, 21.8 mmol), sodium azide (8.0 g, 123 mmol, 5.7 equiv) and dry DMF (60 mL). MPLC (gradient from 2:8 to 5:5 Et2O:pentane) afforded **44** (94%, 3.5 g).

Colorless oil; **Rf** 0.47 in Et_2O:pentane; **1H-NMR** (300 MHz, $CDCl_3$) δ 3.82 (q, J = 5.6 Hz, 1H), 3.28 (t, J = 6.6 Hz, 2H), 2.02 – 1.81 (m, 2H), 1.81 – 1.46 (m, 7H), 1.45 (s, 1H), 1.36 – 1.07 (m, 2H); **^{13}C-NMR** (75 MHz, $CDCl_3$) δ 79.3, 51.8, 48.0, 35.0, 31.1, 30.2, 27.8, 21.9; **HRMS** calc. for $C_8H_{16}ON$ $[M+H]^+$: 142.1226, found: 142.1222; **IR** (cm^{-1}): 3333, 2936, 2871, 2087, 1449, 1346, 1253, 1067, 1023, 971

Octahydroindolizine (45)

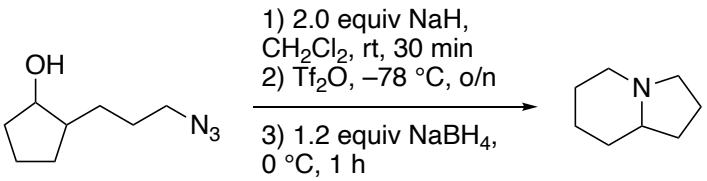

To a solution of 2-(3-azidopropyl)cyclopentan-1-ol **44** (130 mg, 0.77 mmol) in dry CH_2Cl_2 (5 mL) was added sodium hydride (90% in mineral oil, 36 mg, 1.57 mmol, 2 eq.) and stirred at rt. After 30 min, the mixture was cooled to –78 °C, triflic anhydride (0.2 mL, 1.2 mmol, 1.55 eq.) was added drop wise, and the mixture was allowed to warm up slowly to rt overnight. The mixture was cooled to 0 °C, sodium borohydride (36 mg, 0.9 mmol, 1.2 equiv) was added, and the mixture was stirred for 1 h. The resulting suspension was then carefully treated with aq. NaOH (0.5 M, 10 mL), ammonia (7 M solution in MeOH, 2 mL) and extracted 3x with CH_2Cl_2. The combined organic phase was washed with a 1:1 mixture of brine and aq. NaOH (0.5 M), dried over Na_2SO_4 and concentrated. FC (CH_2Cl_2 + 3% of ammonia, 7 M solution in MeOH) afforded **50** (70%, 70 mg).

*Note: There is no difference in the outcome of the reaction starting from the cis or the trans azidoalcohol **44**.*

Slightly yellow liquid; **Rf** 0.47 in CH_2Cl_2 + 3% of ammonia, 7 M solution in MeOH; **^{1}H-NMR** (400 MHz, C_6D_6) δ 3.05 – 2.92 (m, 2H), 1.95 (q, J = 8.7 Hz, 1H), 1.87 (ddd, J = 11.7, 10.7, 2.9 Hz, 1H), 1.73 – 1.54 (m, 6H), 1.53 – 1.32 (m, 3H), 1.30 – 1.06 (m, 2H); **^{13}C-NMR** (101 MHz, C_6D_6) δ 64.5, 54.7, 53.4, 31.7, 31.2, 26.2, 25.2, 21.4; physical and spectral data are in accordance with literature data.[2]

Preparation of 46

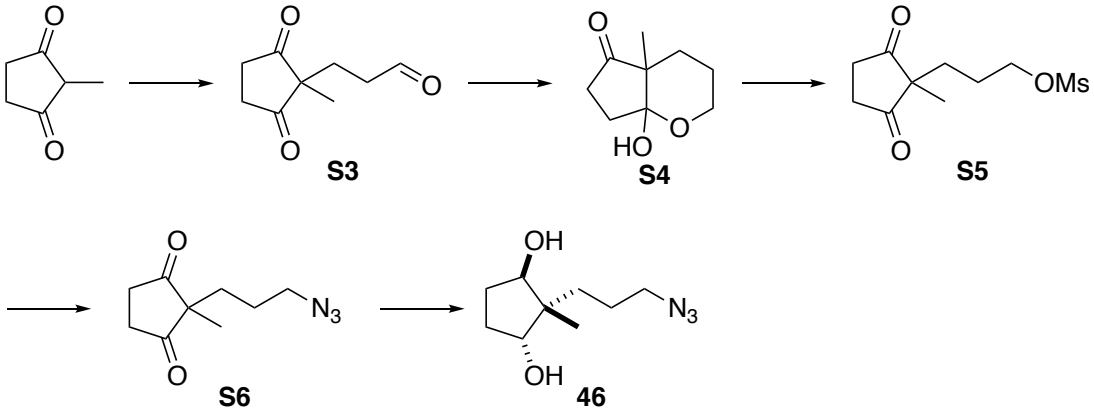

3-(1-methyl-2,5-dioxocyclopentyl)propanal (S3)

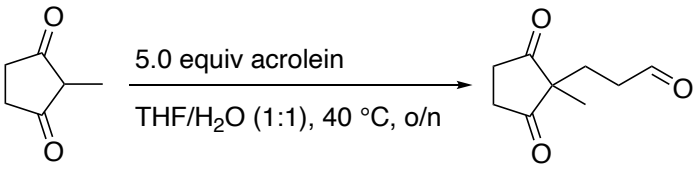

To a stirred solution of 2-methyl-1,3-cyclopentanedione (10.0 g, 84.7 mmol) in solvent (1:1 THF:water, 100 mL) was added acrolein (30 mL, 435 mmol, 5.0 equiv) at rt. The mixture was stirred at 40 °C overnight. The mixture was concentrated and purified by FC (4:6 EtOAc:heptanes) which afforded **S3** (90%, 13.3 g).

Colorless oil; **Rf** 0.20 in 4:6 EtOAc:heptanes; **^{1}H-NMR** (300 MHz, $CDCl_3$) δ 9.65 (t, *J* = 1.1 Hz, 1H), 2.78 (s, 4H), 2.46 (ddd, *J* = 7.6, 7.0, 1.1 Hz, 2H), 1.91 (dd, *J* = 7.8, 7.0 Hz, 2H), 1.11 (s, 3H); **^{13}C-NMR** (75 MHz, $CDCl_3$) δ 215.7, 200.9 (2C), 55.2, 38.4, 34.9 (2C), 26.1, 19.4; **HRMS** calc. for $C_9H_{12}O_3Na$ $[M+Na]^+$: 191.0679, found: 191.0673; **IR** (cm^{-1}): 2942, 2730, 2360, 2342, 1718, 1317, 1133, 1026, 1013, 6684

7a-hydroxy-4a-methylhexahydrocyclopenta[b]pyran-5(2H)-one (S4)

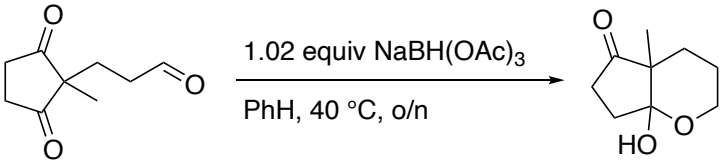

To a stirred solution of 3-(1-methyl-2,5-dioxo-cyclopentyl)propanal **S3** (5.0 g, 29.7 mmol) in dry benzene (100 mL) was added sodium triacetoxyborohydride (6.6 g, 30.3 mmol, 1.02 equiv). The mixture was stirred at 40 °C overnight, treated with water (100ml), and extracted 3x with EtOAc. The combined

organic phase was washed with brine, dried over Na_2SO_4, filtered, and concentrated. FC (EtOAc:heptanes 4:6) afforded **S4** (55%, 2.8 g).

White solid; **Rf** 0.31 in 4:6 EtOAc:heptanes; **mp** 70-71 °C; **^{1}H-NMR** (300 MHz, $CDCl_3$) δ 3.89 – 3.74 (m, 1H), 3.65 – 3.53 (m, 1H), 2.55 – 2.29 (m, 3H), 2.22 – 1.94 (m, 4H), 1.58 – 1.32 (m, 3H), 1.00 (s, 3H); **^{13}C-NMR** (75 MHz, $CDCl_3$) δ 218.1, 117.62, 103.0, 60.9, 51.2, 35.6, 33.2, 26.8, 23.0, 21.0; **HRMS** calc. for $C_9H_{14}O_3Na$ $[M+Na]^+$: 193.0835, found: 193.0839; **IR** (cm^{-1}): 3347, 2950, 1746, 1312, 1259, 1197, 1103, 1061, 1011, 952

3-(1-methyl-2,5-dioxocyclopentyl)propyl methanesulfonate (S5)

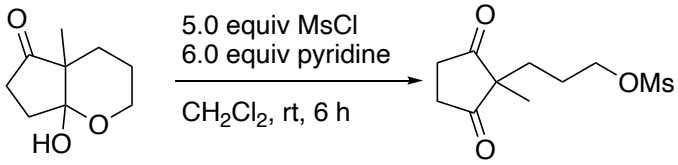

To a stirred solution of 7a-hydroxy-4a-methylhexahydrocyclopenta[b]pyran-5(2H)-one **S4** (2.5 g, 14.7 mmol) in dry CH_2Cl_2 (10 mL) were added mesyl chloride (5.7 mL, 73.4 mmol, 5.0 equiv) and pyridine (7.3 mL, 88.1 mmol, 6.0 equiv). The mixture was stirred at rt for 6 h, diluted with water and extracted 3x with CH_2Cl_2. The combined organic phase was washed twice with aq. $CuSO_4$ (0.5 M), water, brine, dried over Na_2SO_4, filtered and concentrated. FC (6:4 EtOAc:heptanes) afforded **S5** (76%, 2.8 g).

Slightly yellowish oil; **Rf** 0.35 in 6:4 EtOAc:heptanes; **^{1}H-NMR** (300 MHz, $CDCl_3$) δ 4.14 (t, J = 5.9 Hz, 2H), 3.00 (s, 3H), 2.94 – 2.65 (m, 4H), 1.82 – 1.57 (m, 4H), 1.15 (s, 3H); **^{13}C-NMR** (75 MHz, $CDCl_3$) δ 215.9, 69.5, 56.0, 37.4, 35.0 (2C), 30.3, 24.3, 19.8; **HRMS** calc. for $C_{10}H_{16}O_5NaS$ $[M+Na]^+$: 271.0616, found: 271.0618; **IR** (cm^{-1}): 2923, 2359, 1716, 1456, 1419, 1347, 1170, 958, 917, 799

2-(3-azidopropyl)-2-methylcyclopentane-1,3-dione (S6)

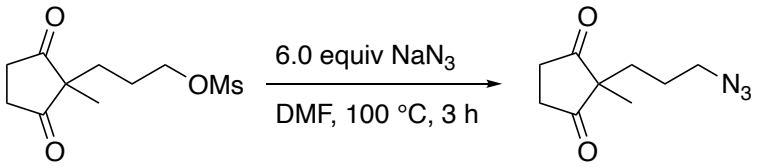

Prepared according to the general procedure C from 3-(1-methyl-2,5-dioxocyclopentyl)propyl methanesulfonate **S5** (10.2 g, 41.1 mmol), sodium azide (16.0 g, 246 mmol, 6.0 equiv) and dry DMF (100 mL). FC (6:4 EtOAc:heptanes) afforded **S6** (93%, 7.44 g).

Colorless oil; **Rf** 0.52 in 4:6 EtOAc:heptanes; **^{1}H-NMR** (75 MHz, $CDCl_3$) δ 3.23 (t, J = 6.6 Hz, 2H), 2.92 – 2.64 (m, 4H), 1.76 – 1.62 (m, 2H), 1.53 – 1.38 (m, 2H), 1.14 (s, 3H); **^{13}C-NMR** (300 MHz, $CDCl_3$) δ 216.0, 56.3, 51.4, 35.2 (2C), 31.8, 24.2, 19.9; physical and spectral data are in accordance with literature data.[6]

2-(3-azidopropyl)-2-methylcyclopentane-1,3-diol (47)

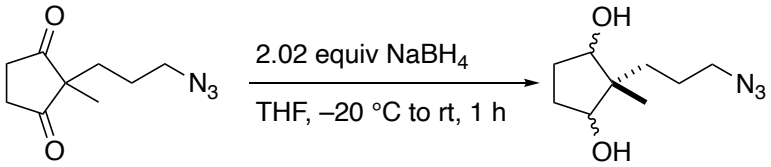

To a solution of 2-(3-azidopropyl)-2-methylcyclopentane-1,3-dione **S6** (2.0 g, 10.2 mmol) in dry THF at –20 °C was added sodium borohydride (800 mg, 20.7 mmol, 2.02 equiv). The mixture was allowed to slowly warm up to rt while the color turned from slight orange to dark red. After 1 h, the reaction was treated with water (50 mL) resulting in a bright red solution which was extracted 3x with EtOAc (50 mL). The combined organic phase was washed with brine, dried over Na_2SO_4, filtered, and concentrated. FC (CH_2Cl_2 + 3% MeOH) afforded three diastereomers:

Trans (238 mg, 28%)

Colorless oil; **Rf** 0.15 in CH_2Cl_2 + 3% MeOH; **^{1}H-NMR** (400 MHz, $CDCl_3$) δ 4.12 – 3.99 (m, 1H), 3.95 – 3.84 (m, 1H), 3.32 (t, J = 6.7 Hz, 2H), 2.29 – 2.08 (m, 2H), 1.79 – 1.22 (m, 9H), 0.86 (s, 3H); **^{13}C-NMR** (101 MHz, $CDCl_3$) δ 78.9, 78.8, 52.5, 48.3, 31.0, 30.3, 30.2, 24.3, 16.2; **HRMS** calc. for $C_9H_{18}N_3O_2$ $[M+H]^+$: 200.1394, found: 200.1397; **IR** (cm^{-1}): 3376, 2940, 2875, 2989, 1723, 1463, 1255, 1148, 1022, 970

***Cis*-major** (750 mg, 56%)

Colorless oil; **Rf** 0.29 in CH_2Cl_2 + 3% MeOH; **^{1}H-NMR** (300 MHz, $CDCl_3$) δ 3.84 – 3.76 (m, 2H), 3.41 – 3.29 (m, 2H), 2.35 (d, J = 6.8 Hz, 2H), 2.22 – 2.04 (m, 2H), 1.95 – 1.80 (m, 2H), 1.77 – 1.64 (m, 4H), 0.77 (s, 3H); **^{13}C-NMR** (101 MHz, $CDCl_3$) δ 80.5 (2C), 52.5, 50.2, 32.2 (2C), 27.9, 24.4, 21.1; **HRMS** calc. for $C_9H_{18}N_3O_2$ $[M+H]^+$: 200.1394, found: 200.1397; **IR** (cm^{-1}): 3387, 2940, 2871, 2089, 1731, 1457, 1248, 1150, 1038, 989

***Cis*-Minor** (225 mg, 17%)

Colorless oil; **Rf** 0.21 in CH_2Cl_2 + 3% MeOH; **^{1}H-NMR** (300 MHz, $CDCl_3$) δ 3.78 (s, 2H), 3.26 (t, J = 6.7 Hz, 2H), 2.17 – 2.01 (m, 2H), 1.97 (s, 2H), 1.86 – 1.70 (m, 2H), 1.70 – 1.52 (m, 2H), 1.30 – 1.16 (m, 2H), 1.07 (s, 3H); **^{13}C-NMR** (101 MHz, $CDCl_3$) δ 79.3 (2C), 52.2, 49.1, 35.0, 31.2 (2C), 24.0, 13.0; **HRMS** calc. for $C_9H_{18}N_3O_2$ $[M+H]^+$: 200.1394, found: 200.1394; **IR** (cm^{-1}): 3366, 2942, 2869, 2089, 1723, 1451, 1254, 1146, 1020, 985

The relative configuration of the two *cis*-isomers has not been assigned.

Preparation of 49

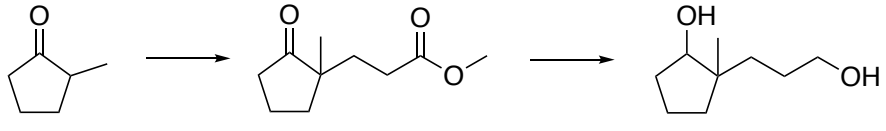

S7 **S8**

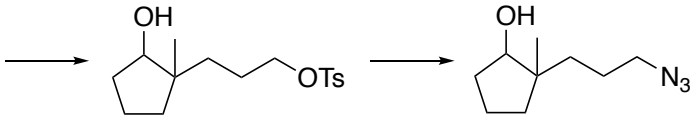

S9 **49**

Methyl 3-(1-methyl-2-oxocyclopentyl)propanoate (S7)

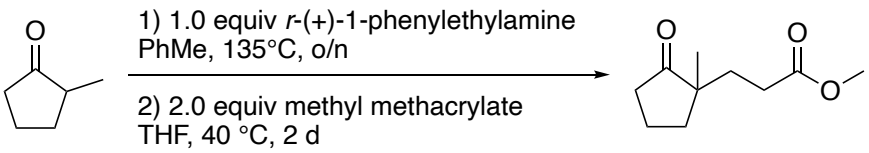

To a solution of 2-methylcyclopentanone (22.0 mL, 206 mmol) in dry toluene (150 mL) under argon was added r(+)-1-phenylethylamine (26.8 mL, 206 mmol, 1.0 equiv). The mixture was refluxed overnight at 135 °C using a Dean-Stark apparatus. The mixture was concentrated and the residue was dissolved in dry THF (150 mL) under argon. Methyl acrylate (38 mL, 419 mmol, 2.0 equiv) was added and the mixture was stirred for 2 days at 40 °C. The reaction was treated with 20% aq. acetic acid and extracted 3x with EtOAc. The combined organic phase was washed with aq. NaOH (2 M), with brine, dried over Na_2SO_4 and concentrated. MPLC (gradient from 0:10 to 2:8 EtOAc:heptanes) afforded **S7** (88%, 33.3 g).

Pale yellow oil; **Rf** 0.38 in 2:8 EtOAc:heptanes; **^{1}H-NMR** (300 MHz, $CDCl_3$) δ 3.65 (s, 3H), 2.45 – 2.10 (m, 4H), 1.99 – 1.61 (m, 6H), 1.00 (s, 3H); **^{13}C-NMR** (75 MHz, $CDCl_3$) δ 222.6, 174.0, 51.8, 47.6, 37.6, 36.1, 31.5, 29.4, 21.5, 18.7; physical and spectral data are in accordance with literature data.[3,4]

2-(3-hydroxypropyl)-2-methylcyclopentan-1-ol (S8)

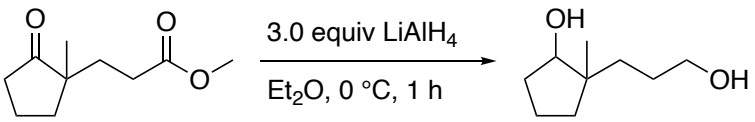

Prepared according to the general procedure **E** from $LiAlH_4$ (4.1 g, 94.4 mmol, 3.0 equiv), Et_2O (200 mL), methyl 3-(2-oxocyclopentyl) propanoate **S7** (5.8 g, 31.5 mmol) in dry Et_2O (20 mL), and Glauber's salt (32 g, 100 mmol, 3.0 equiv). MPLC (gradient from 5:5 to 8:2 EtOAc:heptanes) afforded **S8** as a mixture of diastereomers (84%, 4.2 g). A separation was not attempted.

Highly viscous oil; **Rf** 0.28 in 8:2 EtOAc:heptanes; **^{1}H-NMR** (300 MHz, $CDCl_3$) δ 3.81 – 3.57 and (m, 3H), 2.16 – 1.91 (m, 1H), 1.87 – 1.16 (m, 12H), 0.92 and 0.86 (two s, total 3H); **^{13}C-NMR** (75 MHz, $CDCl_3$) major diastereomer: δ 80.2, 63.6, 44.2, 36.4, 36.0, 32.4, 28.1, 19.3, 18.4; minor diastereomer: δ 80.0, 63.2, 46.2, 36.4, 33.0, 31.3, 27.9, 23.1, 20.4; physical and spectral data are in accordance with literature data.[5]

3-(2-hydroxy-1-methylcyclopentyl)propyl 4-methylbenzenesulfonate (S9)

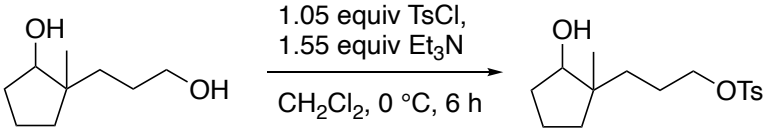

Prepared according to the general procedure **F** from **S8** (1.7 g, 10.7 mmol), dry CH_2Cl_2 (25 mL), tosyl chloride (2.2 g, 11.5 mmol, 1.05 equiv), and triethylamine (2.4 mL, 17.2 mmol, 1.55 equiv). MPLC (gradient from 5:5 to 2:8 EtOA:heptanes) afforded **S9** as two separate diastereomers.

Note: prolonged reaction time leads to bis-tosylation.

A Minor (490 mg, 13%)

Note: trace impurities of the major diastereomers could not be fully removed

Colorless oil; **Rf** 0.35 in 4:6 EtOA:heptanes; **^{1}H-NMR** (400 MHz, $CDCl_3$) δ 7.81 – 7.77 (m, 2H), 7.37 – 7.32 (m, 2H), 4.04 (t, J = 6.6 Hz, 2H), 3.70 (dd, J = 5.6, 2.8 Hz, 1H), 2.45 (s, 3H), 2.09 – 1.97 (m, 1H), 1.79 – 1.24 (m, 10H), 0.80 (s, 3H); **^{13}C-NMR** (101 MHz, $CDCl_3$) δ 144.8, 133.4, 130.0 (2), 128.0 (2C), 80.6, 71.6, 45.7, 35.6, 33.2, 31.0, 25.0, 23.2, 21.8, 20.3; **HRMS** calc. for $C_{16}H_{25}O_4S$ $[M+H]^+$: 313.1468, found: 313.1463; **IR** (cm^{-1}): 3551, 3421, 2956, 2873, 1598, 1352, 1172, 916, 812, 661

B Major (1.3 g, 35%)

Colorless oil; **Rf** 0.28 in 4:6 EtOA:heptanes; **^{1}H-NMR** (300 MHz, $CDCl_3$) δ 7.75 – 7.69 (m, 2H), 7.33 – 7.26 (m, 2H), 3.95 (t, J = 6.5 Hz, 2H), 3.59 (t, J = 6.9 Hz, 1H), 2.39 (s, 3H), 1.99 – 1.82 (m, 2H), 1.72 – 1.05 (m, 9H), 0.79 (s, 3H); **^{13}C-NMR** (75 MHz, $CDCl_3$) δ 144.7, 133.0, 129.8 (2C), 127.8 (2C), 80.0, 71.5, 43.9, 35.8, 35.7, 32.3, 24.5, 21.6, 19.2, 18.0; **HRMS** calc. for $C_{16}H_{25}O_4S$ $[M+H]^+$: 313.1468, found: 313.1460; **IR** (cm^{-1}): 3551, 3428, 2955, 2872, 1598, 1353, 1173, 918, 812, 661

2-(3-azidopropyl)-2-methylcyclopentan-1-ol (49)

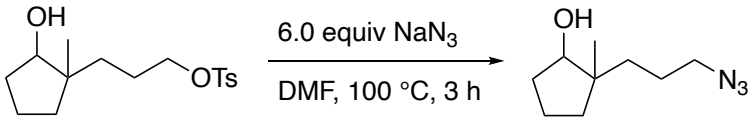

From minor

Prepared according to the general procedure **G** from 3-(2-hydroxy-1-methylcyclopentyl)propyl 4-methylbenzenesulfonate **S9** (210 mg, 0.67 mmol), sodium azide (260 mg, 4.0 mmol, 6.0 equiv) and dry DMF (10 mL). MPLC (gradient to 2:8 EtOAc:heptanes) afforded **49** (97%, 120 mg).

Colorless oil; **Rf** 0.37 in 2:8 EtOAc:heptanes; **^{1}H-NMR** (300 MHz, $CDCl_3$) δ 3.73 (t, J = 6.9 Hz, 1H), 3.26 (t, J = 6.8 Hz, 2H), 2.10 – 1.92 (m, 1H), 1.81 – 1.18 (m, 10H), 0.92 (s, 3H); **^{13}C-NMR** (75 MHz, $CDCl_3$) δ 80.5, 52.5, 45.9, 35.8, 33.4, 32.4, 24.8, 23.3, 20.4; **HRMS** calc. for $C_9H_{18}NO$ $[(M-N_2)+H]^+$: 156.1383, found: 156.1381; **IR** (cm^{-1}): 2951, 2869, 2089, 1456, 1347, 1247, 1072, 986, 903, 553

From major

Prepared according to the general procedure **G** from 3-(2-hydroxy-1-methylcyclopentyl)propyl 4-methylbenzenesulfonate **S9** (2.4 g, 7.6 mmol), sodium azide (3 g, 46.1 mmol, 6.0 equiv) and dry DMF (40 mL). MPLC (gradient to 2:8 EtOAc:heptanes) afforded **49** (86%, 1.2 g).

Colorless oil; **Rf** 0.32 in 2:8 EtOAc:heptanes; **^{1}H-NMR** (300 MHz, $CDCl_3$) δ 3.73 (t, J = 6.9 Hz, 1H), 3.26 (t, J = 6.8 Hz, 2H), 2.10 – 1.94 (m, 1H), 1.80 – 1.16 (m, 10H), 0.92 (s, 3H); **^{13}C-NMR** (75 MHz, $CDCl_3$) δ 80.5, 52.4, 44.4, 37.5, 36.0, 32.7, 24.6, 19.4, 18.2; **HRMS** calc. for $C_9H_{18}N_3O$ $[M+H]^+$: 184.1444, found: 184.1442; **IR** (cm^{-1}): 2954, 2871, 2089, 1724, 1453, 1347, 1257, 1077, 1034, 555

Preparation of 52

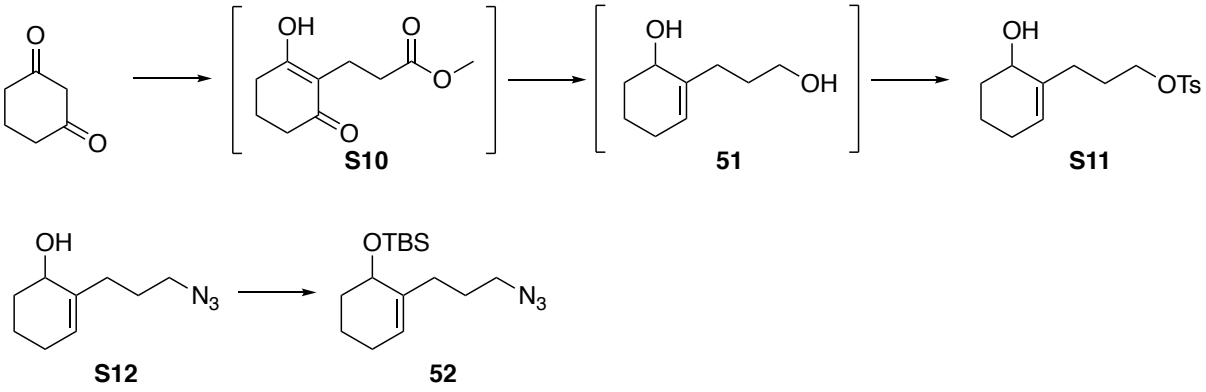

methyl 3-(2,6-dioxocyclohexyl)propanoate (S10)

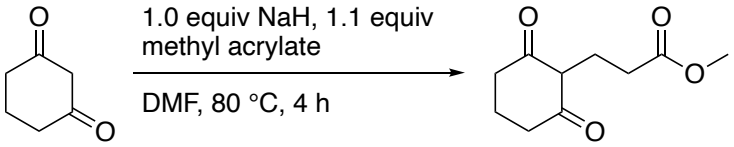

To a stirred solution of cyclohexane-1,3-dione (5 g, 45 mmol) in dry DMF (50 mL) was added portion wise sodium hydride (1.2 g, 45 mmol, 1.0 equiv) and methyl acrylate (4.5 mL, 55 mmol, 1.1 equiv). The orange solution was stirred at 80 °C for 4 h, then cautiously acidified to pH 1 in an ice bath by addition of aq. HCl (4 M) and subsequently concentrated under reduced pressure at 60 °C which afforded the corresponding crude ester **S10** (**Rf** 0.4 in 4:6 EtOAc:heptanes) as a brown solid (10 g). No further purification was performed as crude spectral data are in accordance with literature data[7].

2-(3-hydroxypropyl)cyclohex-2-en-1-ol (51)

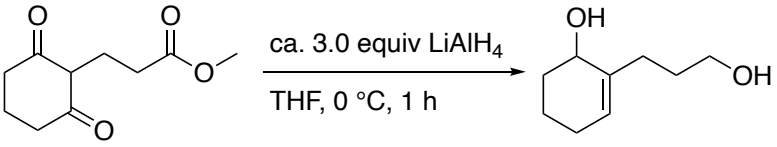

Prepared according to the general procedure **E** from $LiAlH_4$ (5.5 g, 145 mmol), THF (100 mL), methyl 3-(2,6-dioxocyclohexyl)propanoate **S10** (10 g) in dry THF (20 mL), and Glauber's salt (50 g, 145 mmol). Unpolar side products were removed by FC (pure EtOAc) which afforded the crude diol **51** (**Rf** 0.27 in

EtOAc) as a slightly yellowish oil (3.4 g). No further purification was performed as crude spectral data are in accordance with literature data.[8]

3-(6-hydroxycyclohex-1-en-1-yl)propyl 4-methylbenzenesulfonate (S11)

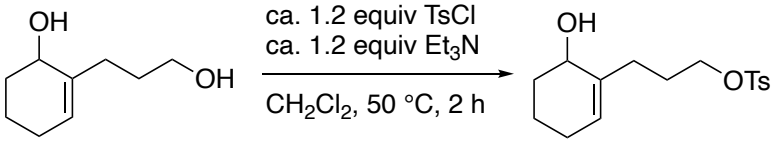

To a solution of crude 2-(3-hydroxypropyl)cyclohex-2-en-1-ol **51** in dry CH_2Cl_2 (120 mL) was added triethylamine (4.9 mL, 68 mmol) and tosyl chloride (12.9 g, 68 mmol). The mixture was refluxed at 50 °C for 2 h, cooled down to rt, and treated with water (100 mL). The organic layer was separated, washed two times with aq. sat. $NaHCO_3$, dried over Na_2SO_4, filtered, and concentrated. FC (4:6 EtOAc:heptanes) afforded **S11** (20% over 3 steps, 2.9 g).

Note: This compound is only stable up to 24 h when stored at 5 °C.

Colorless oil; **Rf** 0.26 in 4:6 EtOAc:heptanes; **^{1}H-NMR** (300 MHz, $CDCl_3$) δ 7.77 (d, *J* = 8.3 Hz, 2H), 7.33 (d, *J* = 8.0 Hz, 2H), 5.49 – 5.38 (m, 1H), 4.02 (t, *J* = 6.3 Hz, 2H), 3.98 – 3.91 (m, 1H), 2.43 (s, 3H), 2.24 – 1.42 (m, 10H); **^{13}C-NMR** (75 MHz, $CDCl_3$) δ 144.8, 137.5, 133.2, 129.9, 128.0, 126.3, 70.3, 66.8, 32.4, 29.9, 27.3, 25.4, 21.7, 18.1; **HRMS** calc. for $C_{16}H_{22}O_4NaS$ $[M+Na]^+$: 333.1131, found: 333.1129; **IR** (cm^{-1}): 2928, 2860, 2361, 1599, 1444, 1354, 1174, 1097, 928, 812

2-(3-azidopropyl)cyclohex-2-en-1-ol (S12)

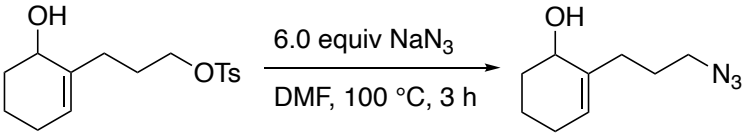

Prepared according to the general procedure **G** from 3-(6-hydroxycyclohex-1-en-1-yl)propyl 4-methylbenzenesulfonate **S11** (2.5 g, 8.1 mmol), sodium azide (3.2 g, 49.2 mmol, 6.0 equiv) and dry DMF (30 mL). FC (3:7 EtOAc:heptanes) afforded **S12** (38%, 560 mg).

Slightly yellow oil; **Rf** 0.35 in 3:7 EtOAc:heptanes; **^{1}H-NMR** (300 MHz, $CDCl_3$) δ 5.62 – 5.52 (m, 1H), 4.12 – 3.98 (m, 1H), 3.27 (t, *J* = 6.8 Hz, 2H), 2.34 – 1.46 (m, 10H); **^{13}C-NMR** (75 MHz, $CDCl_3$) δ 138.0, 126.1, 66.9, 51.3, 32.5, 31.3, 27.4, 25.5, 18.2; **HRMS** calc. for $C_9H_{16}ON$ $[(M-N_2)+H]^+$: 154.1226, found: 154.1223; **IR** (cm^{-1}): 3347, 2926, 2863, 2087, 1444, 1348, 1254, 1043, 980, 913

((2-(3-azidopropyl)cyclohex-2-en-1-yl)oxy)(tert-butyl)dimethylsilane (52)

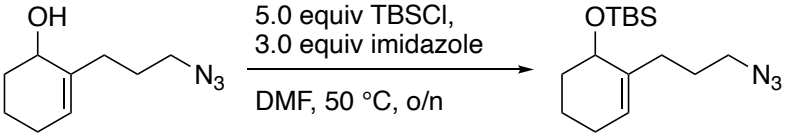

To a stirred solution of 2-(3-azidopropyl)cyclohex-2-en-1-ol **S12** (130 mg, 0.7 mmol) in dry DMF (10 mL) was added TBDMS-Cl (540 mg, 3.6 mmol, 5.0 equiv) and imidazole (440 mg, 4.3 mmol, 3 equiv) at rt. The mixture was stirred at 50 °C overnight, treated with water (20 mL), and extracted 3x with

Et_2O. The combined organic phase was washed 3x with brine (50 mL), dried over Na_2SO_4, filtered, and concentrated. FC (1:9 EtOAc:heptanes) afforded **52** (75%, 160 mg).

Colorless oil; **Rf** 0.77 in 1:9 EtOAc:heptanes; **^{1}H-NMR** (300 MHz, $CDCl_3$) δ 5.60 – 5.44 (m, 1H), 4.16 – 4.04 (m, 1H), 3.26 (td, *J* = 7.0, 2.0 Hz, 2H), 2.28 – 1.17 (m, 10H), 0.90 (s, 9H), 0.09 (s, 6H); **^{13}C-NMR** (75 MHz, $CDCl_3$) δ 138.8, 125.0, 68.1, 51.4, 33.1, 30.9, 29.9, 27.4, 26.1, 25.6, 19.1, 18.3, -3.9, -4.6; **HRMS** calc. for $C_{15}H_{29}N_3ONaSi$ $[M+Na]^+$: 318.1972, found: 318.1967; **IR** (cm^{-1}): 2926, 2854, 2091, 1461, 1252, 1073, 1015, 898, 833, 771

Preparation of 55

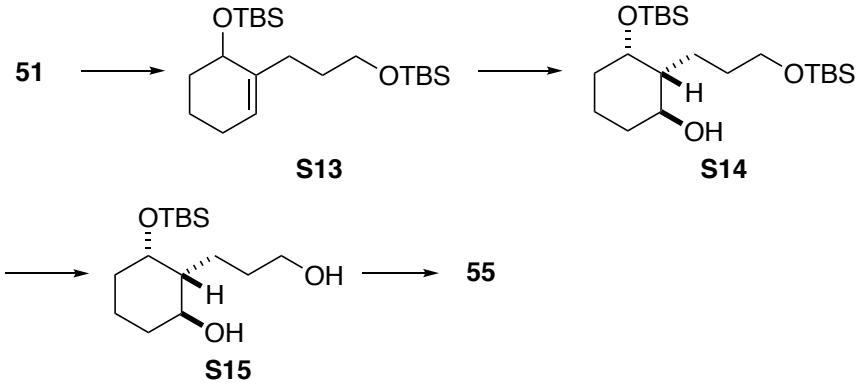

tert-butyl(3-(6-((tert-butyldimethylsilyl)oxy)cyclohex-1-en-1-yl)propoxy)dimethylsilane (S13)

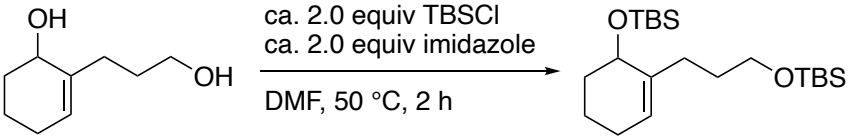

To a stirred solution of crude 2-(3-hydroxypropyl)cyclohex-2-en-1-ol **51** in dry DMF (100 mL) were added TBSCl (16 g, 100 mmol) and imidazole (7 g, 100 mmol). The mixture was stirred at 50 °C for 2 h, cooled down to rt, treated with water (100 mL), and extracted 3x with pentane. The combined organic phases were dried over Na_2SO_4, filtered and concentrated. FC (1% Et_2O in pentane) afforded **S13** (37% over 3 steps, 6.4 g).

Colorless liquid; **Rf** 0.26 in 1% Et_2O in pentane; **^{1}H-NMR** (300 MHz, $CDCl_3$) δ 5.53 – 5.44 (m, 1H), 4.13 – 4.05 (m, 1H), 3.60 (td, *J* = 6.6, 1.4 Hz, 2H), 2.18 – 1.37 (m, 10H), 0.90 (d, *J* = 1.3 Hz, 18H), 0.09 (s, 5H), 0.04 (s, 7H); **^{13}C-NMR** (75 MHz, $CDCl_3$) δ 139.8, 124.0, 68.1, 63.3, 33.2, 31.3, 30.1, 26.2, 26.1, 19.0, 18.5, 18.3, -4.0, -4.5, -5.1; **HRMS** calc. for $C_{21}H_{44}O_2NaSi_2$ $[M+Na]^+$: 407.2772, found: 407.2766; **IR** (cm^{-1}): 2931, 2856, 1472, 1251, 1083, 1018, 962, 829, 769, 664

(1S,2R,3S)-3-((tert-butyldimethylsilyl)oxy)-2-(3-((tert-butyldimethylsilyl)oxy)propyl) cyclohexan-1-ol (S14)

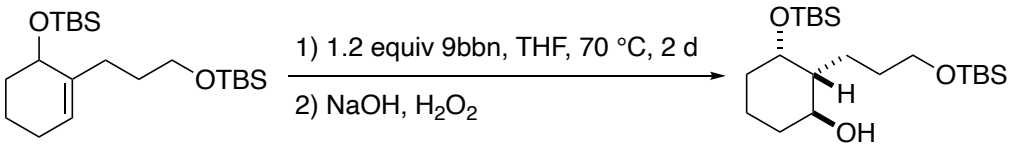

To neat tert-butyl(3-(6-((tert-butyldimethylsilyl)oxy)cyclohex-1-en-1-yl)propoxy)dimethylsilane **S13** (2.65 g, 6.9 mmol) was added a solution of 9-BBN (0.5 M in THF, 16 mL, 8.3 mmol, 1.2 equiv) under argon. The mixture was stirred at 70 °C for two days, cooled down to 0 °C and treated with aq. NaOH (2 M, 13 mL) and aq. H_2O_2 (30%, 13 mL). After 15 min, the mixture was extracted 3x with Et_2O and the combined organic phase was dried over Na_2SO_4, filtered, and concentrated. FC (15:85 EtOAc:heptanes) afforded **S14** (78%, 2.17 g).

Colorless oil; **Rf** 0.40 in 15:85 EtOAc:heptanes; **^{1}H-NMR** (400 MHz, $CDCl_3$) δ 3.86 (s, 1H), 3.80 – 3.71 (m, 1H), 3.61 (td, *J* = 6.3, 1.6 Hz, 3H), 1.99 – 1.85 (m, 1H), 1.76 – 1.18 (m, 12H), 0.90 (d, *J* = 3.5 Hz, 18H), 0.15 – -0.01 (m, 12H); **^{13}C-NMR** (101 MHz, $CDCl_3$) δ 72.9, 71.3, 63.3, 47.6, 30.8, 30.5, 30.3, 26.2, 26.1, 26.1, 26.0, 26.0, 25.7, 18.5, 18.1, 16.1, -4.5, -4.9, -5.1, -5.1; **HRMS** calc. for $C_{21}H_{47}O_3Si_2$ $[M+H]^+$: 403.3058, found: 403.3052; **IR** (cm^{-1}): 3356, 2931, 2856, 1461, 1361, 1253, 1097, 1023, 832, 770

(1S,2R,3S)-3-((tert-butyldimethylsilyl)oxy)-2-(3-hydroxypropyl)cyclohexan-1-ol (S15)

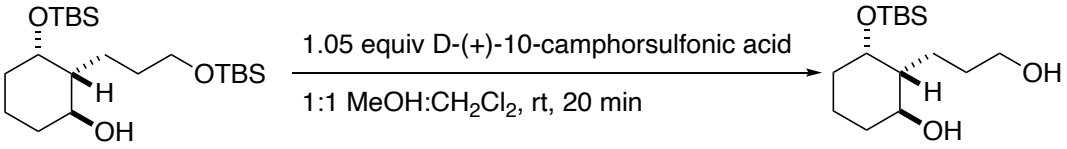

To a stirred solution of (1S,2R,3S)-3-((tert-butyldimethylsilyl)oxy)-2-(3-((tert-butyldimethylsilyl)oxy) propyl)cyclohexan-1-ol **S14** (1.5 g, 3.7 mmol) in solvent (1:1 MeOH:CH_2Cl_2, 40 mL) was added D-(+)-10-camphorsulfonic acid (900 mg, 3.9 mmol, 1.05 equiv). The mixture was stirred at rt for 20 min, treated with sat. aq. $NaHCO_3$ and extracted 3x with Et_2O. The combined organic phase was dried over Na_2SO_4, filtered, and concentrated. FC (8:2 EtOAc:heptanes) afforded **S15** (50%, 534 mg).

White solid; **mp** 82.5 – 84 °C; **Rf** 0.2 in 8:2 EtOAc:heptanes; **^{1}H-NMR** (300 MHz, $CDCl_3$) δ 4.10 – 3.98 (m, 1H), 3.74 – 3.58 (m, 3H), 2.02 – 1.87 (m, 1H), 1.81 – 1.62 (m, 4H), 1.59 – 1.41 (m, 6H), 1.41 – 1.15 (m, 4H), 0.89 (s, 9H), 0.04 (d, *J* = 0.8 Hz, 6H); **^{13}C-NMR** (75 MHz, $CDCl_3$) δ 70.9, 69.2, 63.3, 49.8, 33.4, 30.6, 26.0, 23.5, 19.0, 18.3, -4.0, -4.9; **HRMS** calc. for $C_{15}H_{33}O_3Si$ $[M+H]^+$: 289.2193, found: 289.2192; **IR** (cm^{-1}): 3253, 2927, 2855, 1461, 1251, 1053, 1020, 1000, 831, 770

(1S,2R,3S)-2-(3-azidopropyl)-3-((tert-butyldimethylsilyl)oxy)cyclohexan-1-ol (55)

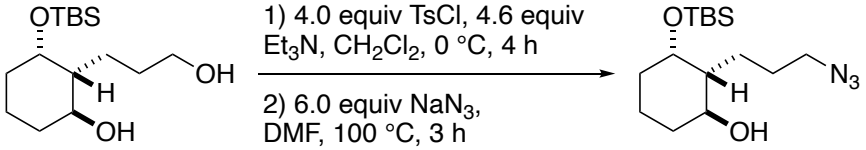

To a stirred solution of (1S,2R,3S)-3-((tert-butyldimethylsilyl)oxy)-2-(3-hydroxypropyl) cyclohexan-1-ol **S15** (1.08 g, 3.74 mmol) in dry CH_2Cl_2 (25 mL) at 0 °C were added tosyl chloride (2.9 g, 15.2 mmol, 4.0 equiv) and triethylamine (2.4 mL, 17.2 mmol, 4.6 equiv). After stirring for 4 h at 0 °C, the mixture was concentrated. The residue was treated according to the general procedure C with sodium azide (1.4 g, 22 mmol, 6.0 equiv) and dry DMF (50 mL). FC (3:7 EtOAc:heptanes) afforded **55** (29%, 341 mg). Colorless oil; **Rf** 0.54 in 3:7 EtOAc:heptanes; **^{1}H-NMR** (300 MHz, $CDCl_3$) δ 4.07 – 4.00 (m, 1H), 3.65 (tt, J = 9.6, 4.2 Hz, 1H), 3.26 (t, J = 4.7 Hz, 2H), 1.94 (dtd, J = 12.1, 4.1, 1.5 Hz, 1H), 1.81 – 1.14 (m, 13H), 0.89 (s, 9H), 0.05 (s, 6H); **^{13}C-NMR** (75 MHz, $CDCl_3$) δ 70.7, 69.0, 52.1, 49.9, 35.6, 33.3, 27.0, 26.0, 24.7, 19.0, 18.3, -4.0, -5.0; **HRMS** calc. for $C_{15}H_{32}N_3O_2Si$ $[M+H]^+$: 314.2258 , found: 314.2258; **IR** (cm^{-1}): 3339, 2931, 2856, 2091, 1461, 1252, 1057, 1020, 831, 771

References

[1] G. Stork, A. Brizzola, H. Landesman, J. Szmuszkovicz, R. Terrell, *J Am Chem Soc* **1963**, *85*, 207.

[2] S. Veeraswamy, A. Anjaiah, Y. Satyanarayana, A. Jayashree, *Asian J. Chem.* **2015**, *27*, 1667–1670.

[3] R. Horinouchi, K. Kamei, R. Watanabe, N. Hieda, N. Tatsumi, K. Nakano, Y. Ichikawa, H. Kotsuki, *Eur. J. Org. Chem.* **2015**, *2015*, 4457–4463.

[4] J. Y. Kang, R. G. Carter, *Org. Lett.* **2012**, *14*, 3178–3181.

[5] H. Imase, K. Tanaka, *Chem. Lett.* **2009**, *38*, 1152–1153.

[6] K. J. Frankowski, R. Liu, G. L. Milligan, K. D. Moeller, J. Aubé, *Angew. Chem. - Int. Ed.* **2015**, *54*, 10555–10558.

[7] M. Konno, T. Nakae, S. Shigeru, I. Katushiro, N. Hisao, H. Nobuyuki, *Synlett* **n.d.**

[8] J. A. M. Peters, T. A. P. Posthumus, N. P. Van Vliet, F. J. Zeelen, W. S. Johnson, *J. Org. Chem.* **1980**, *45*, 2208–2214.

[9] A. Kapat, E. Nyfeler, G. T. Giuffredi, P. Renaud, *J. Am. Chem. Soc.* **2009**, *131*, 17746–7.

[10] L. Gnägi, R. Arnold, F. Giornal, H. Jangra, A. Kapat, E. Nyfeler, H. Zipse, R. M. Schärer, P. Renaud, **2020**, DOI 10.26434/chemrxiv.12594962.v2.

[11] O. G. Mancheño, R. Gómez Arrayás, J. Adrio, J. C. Carretero, *J. Org. Chem.* **2007**, *72*, 10294–10297.

Appendix

Appendix

NMR Spectra of Chapter 2

^{1}H NMR (300 MHz, $CDCl_3$)
(+)IpcBH$_2$ TMEDA complex

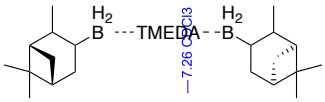

^{13}C NMR (75 MHz, $CDCl_3$)
(+)IpcBH$_2$ TMEDA complex

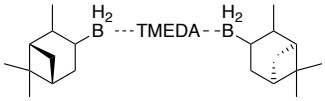

^{11}B NMR (96 MHz, $CDCl_3$)
(+)IpcBH$_2$ TMEDA complex

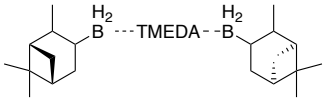

^{11}B NMR (96 MHz, $CDCl_3$)
(+)IpcBH$_2$

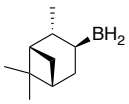

^{1}H NMR (300 MHz, $CDCl_3$)
Di-*tert*-butylhyponitrite (DTBHN)

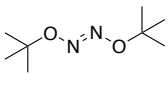

^{13}C NMR (75 MHz, $CDCl_3$)
Di-*tert*-butylhyponitrite (DTBHN)

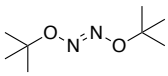

^{1}H NMR (300 MHz, $CDCl_3$)
Di-*tert*-butyl peroxyoxalate (DTBPO)

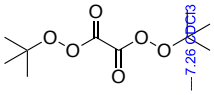

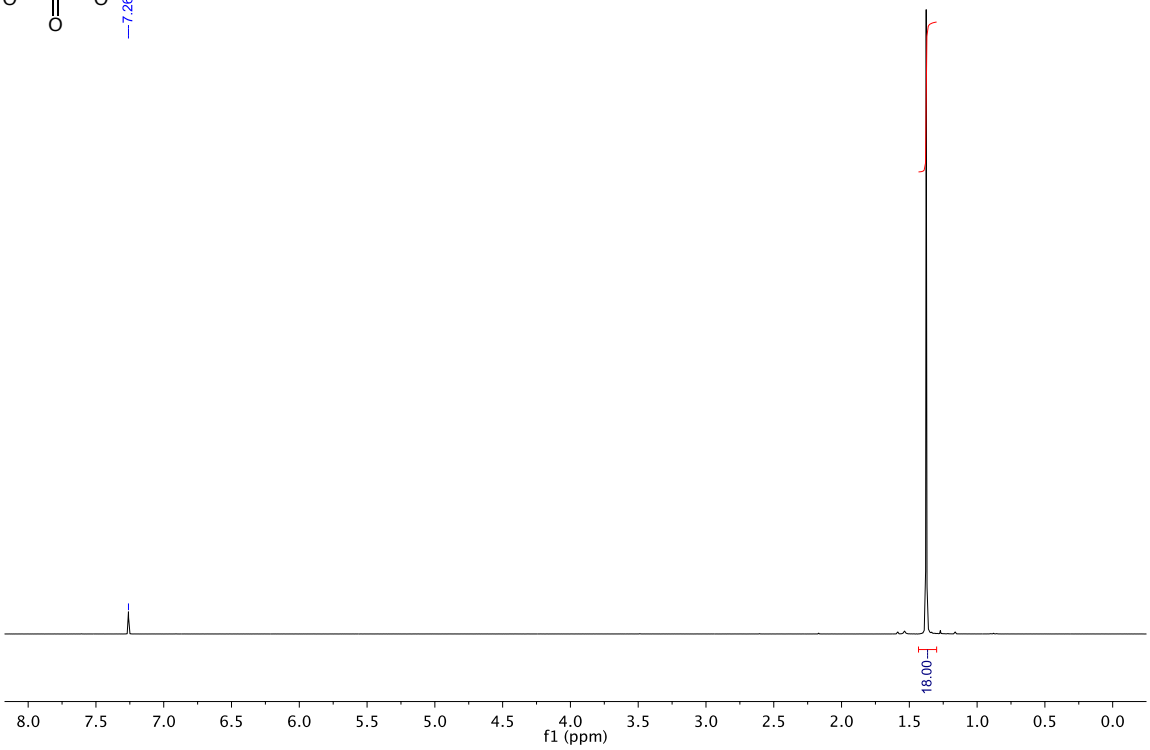

^{13}C NMR (75 MHz, $CDCl_3$)
Di-*tert*-butyl peroxyoxalate (DTBPO)

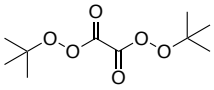

^{1}H NMR (300 MHz, $CDCl_3$)
Trimethyl(2-phenylsulfanylethynyl)silane

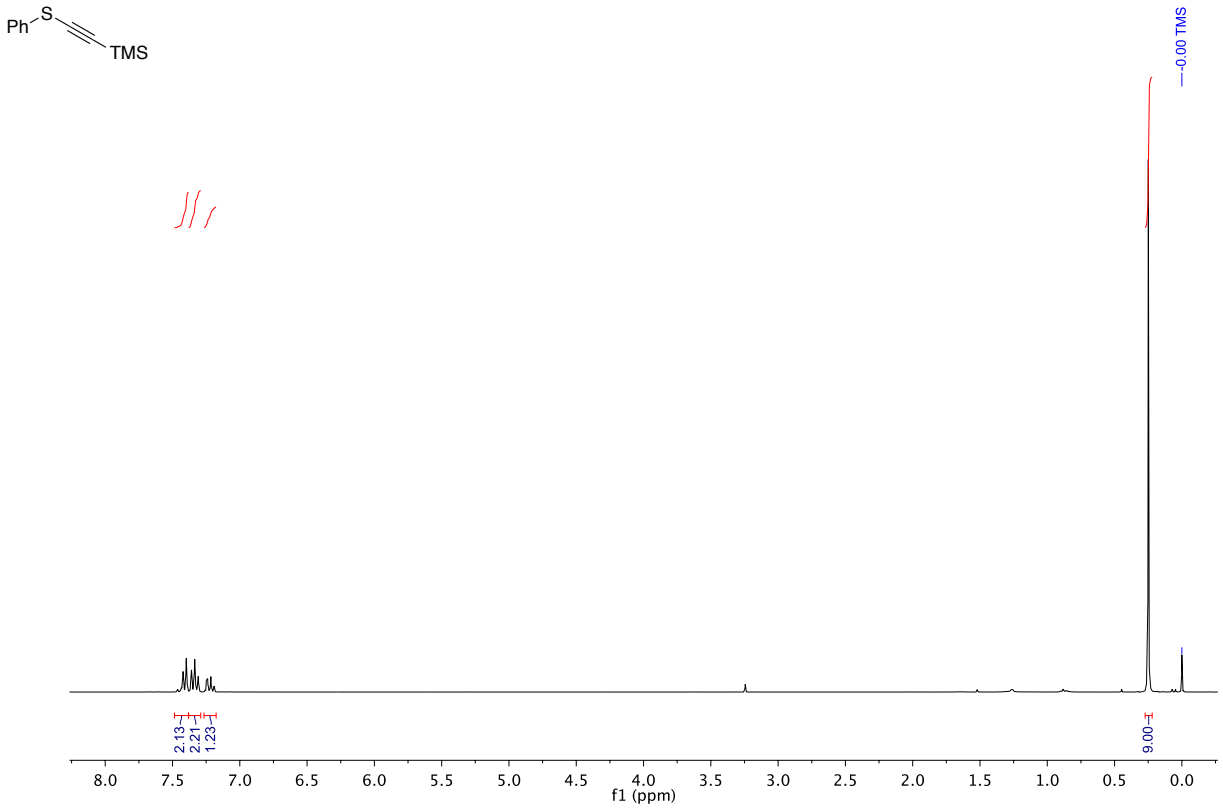

^{13}C NMR (75 MHz, $CDCl_3$)
Trimethyl(2-phenylsulfanylethynyl)silane

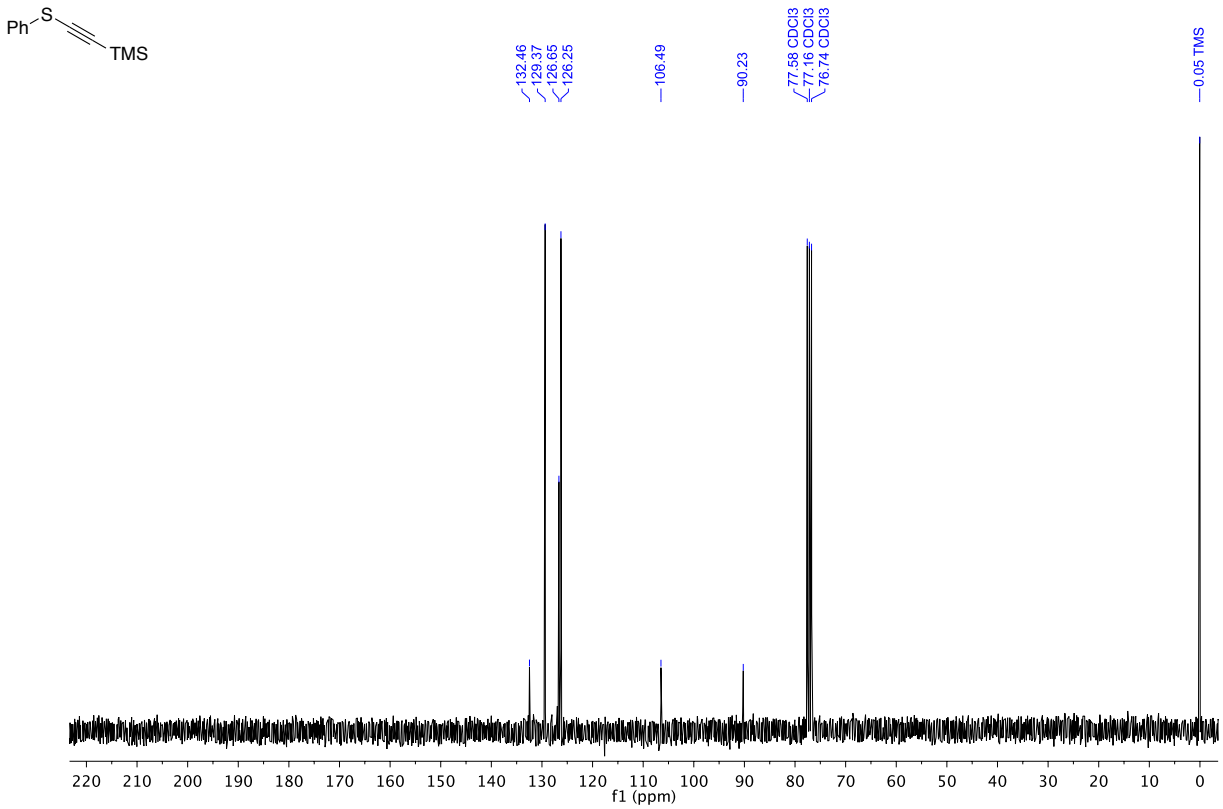

^{1}H NMR (300 MHz, $CDCl_3$)
Trimethyl((phenylsulfonyl)ethynyl)silane

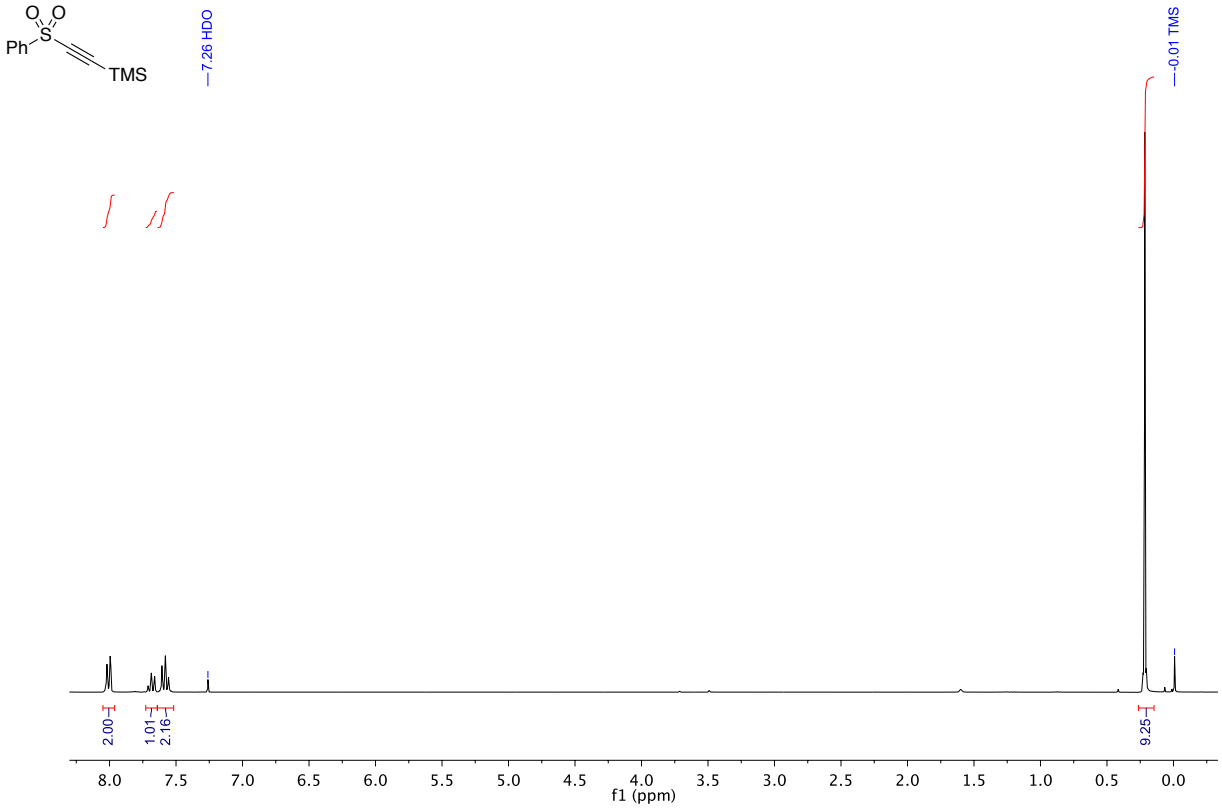

^{13}C NMR (75 MHz, $CDCl_3$)
Trimethyl((phenylsulfonyl)ethynyl)silane

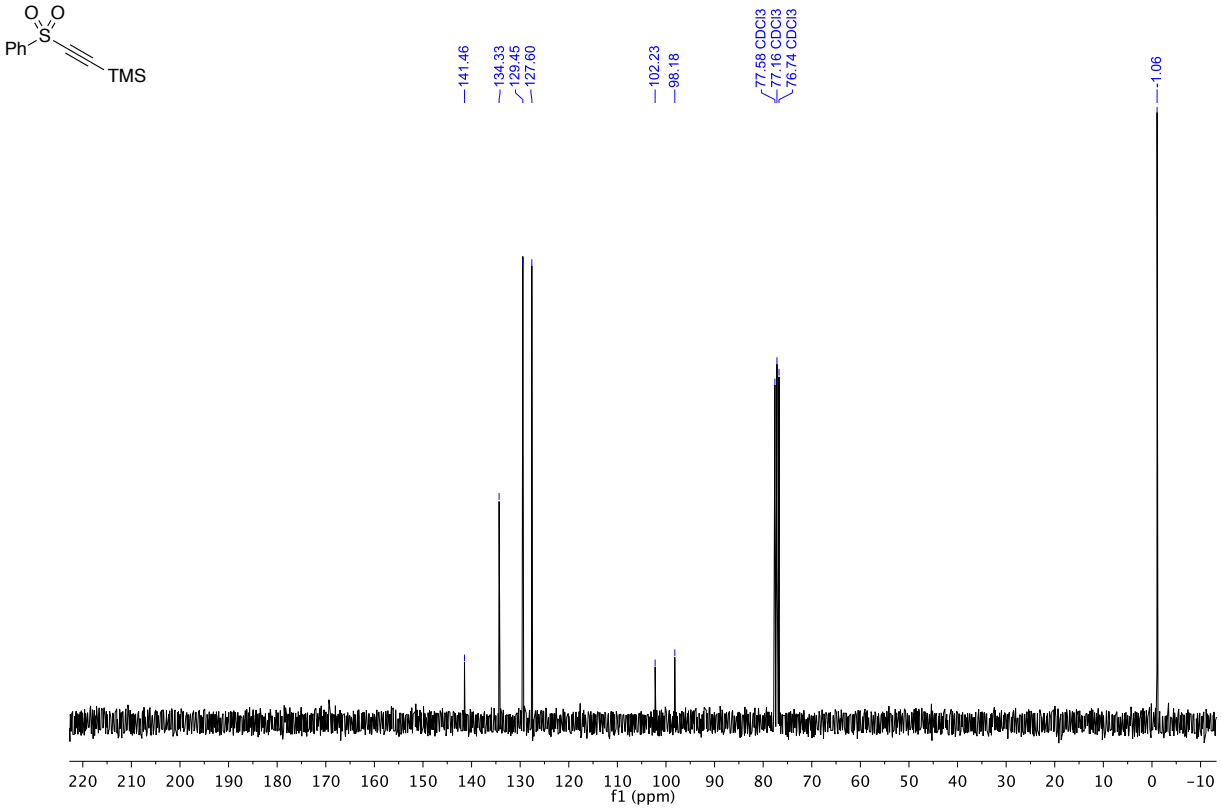

^{1}H NMR (300 MHz, $CDCl_3$)
Triisopropyl((phenylsulfonyl)ethynyl)silane

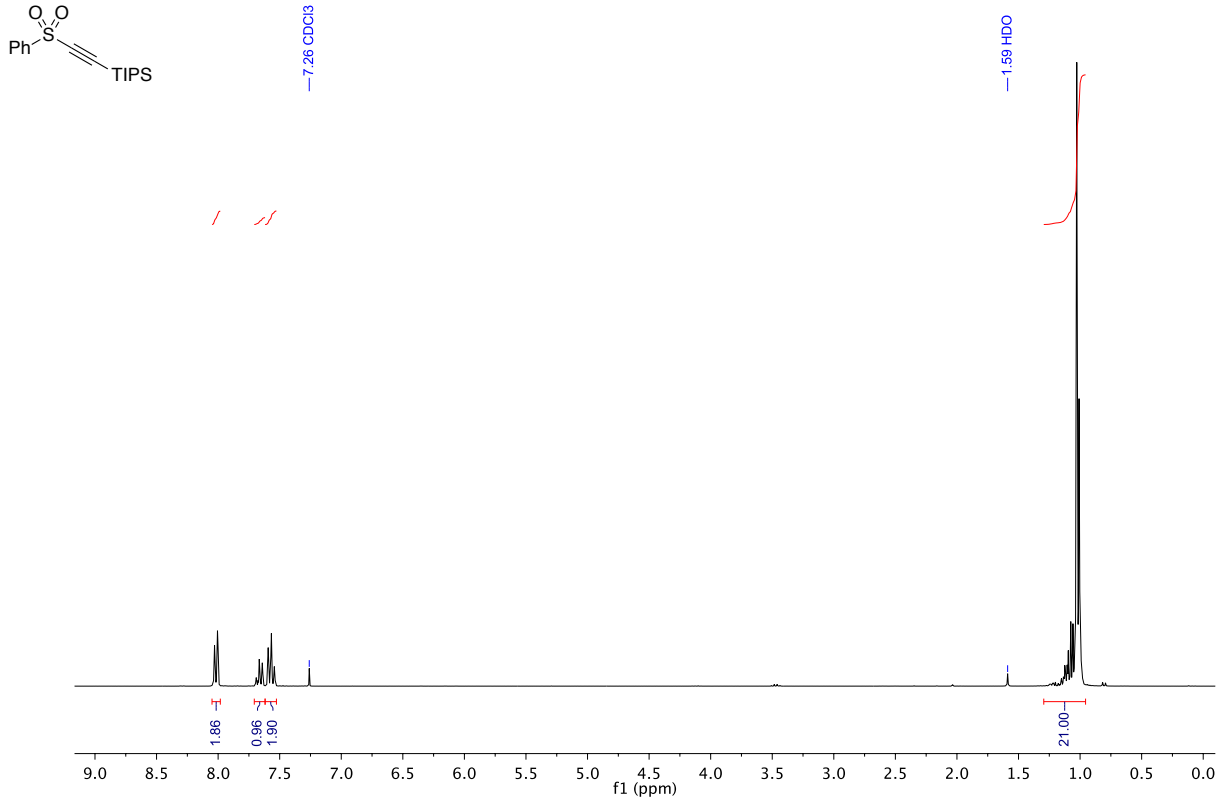

^{13}C NMR (75 MHz, $CDCl_3$)
Triisopropyl((phenylsulfonyl)ethynyl)silane

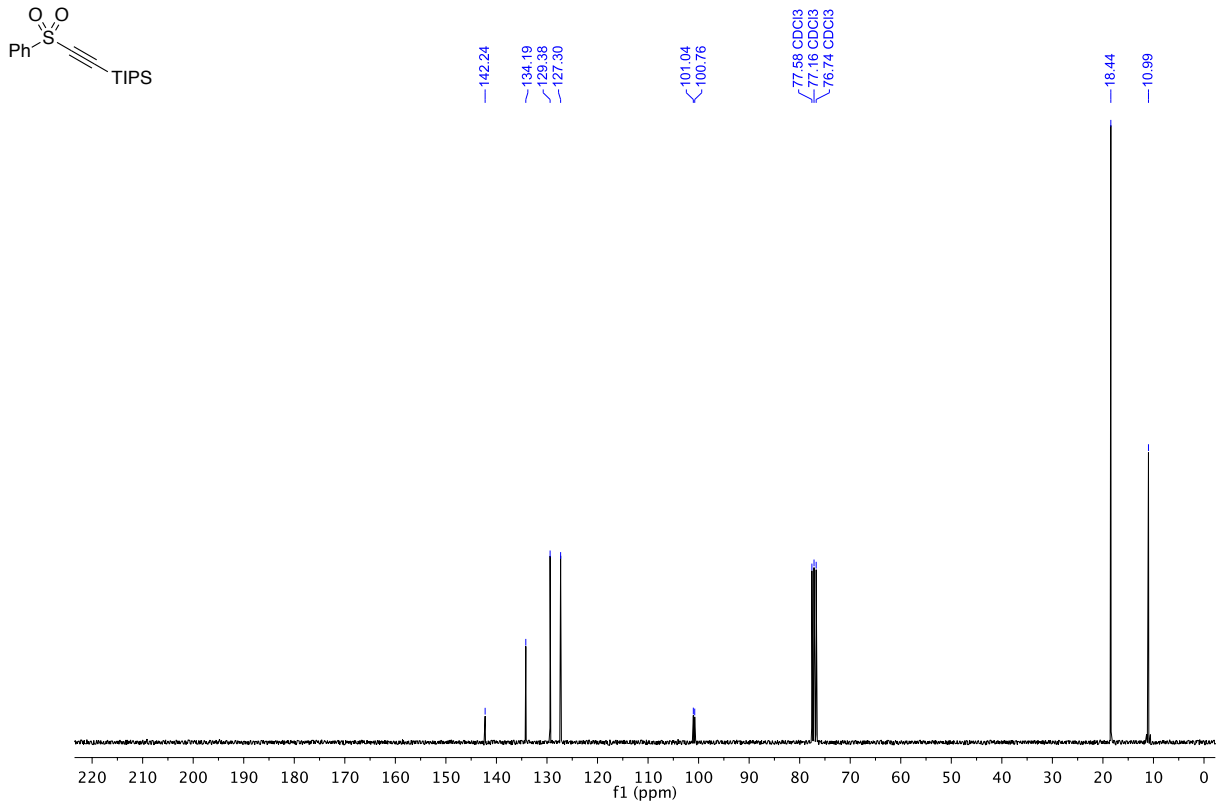

^{1}H NMR (300 MHz, $CDCl_3$)
2-(Cyclopent-1-en-1-yl)furan (**1**)

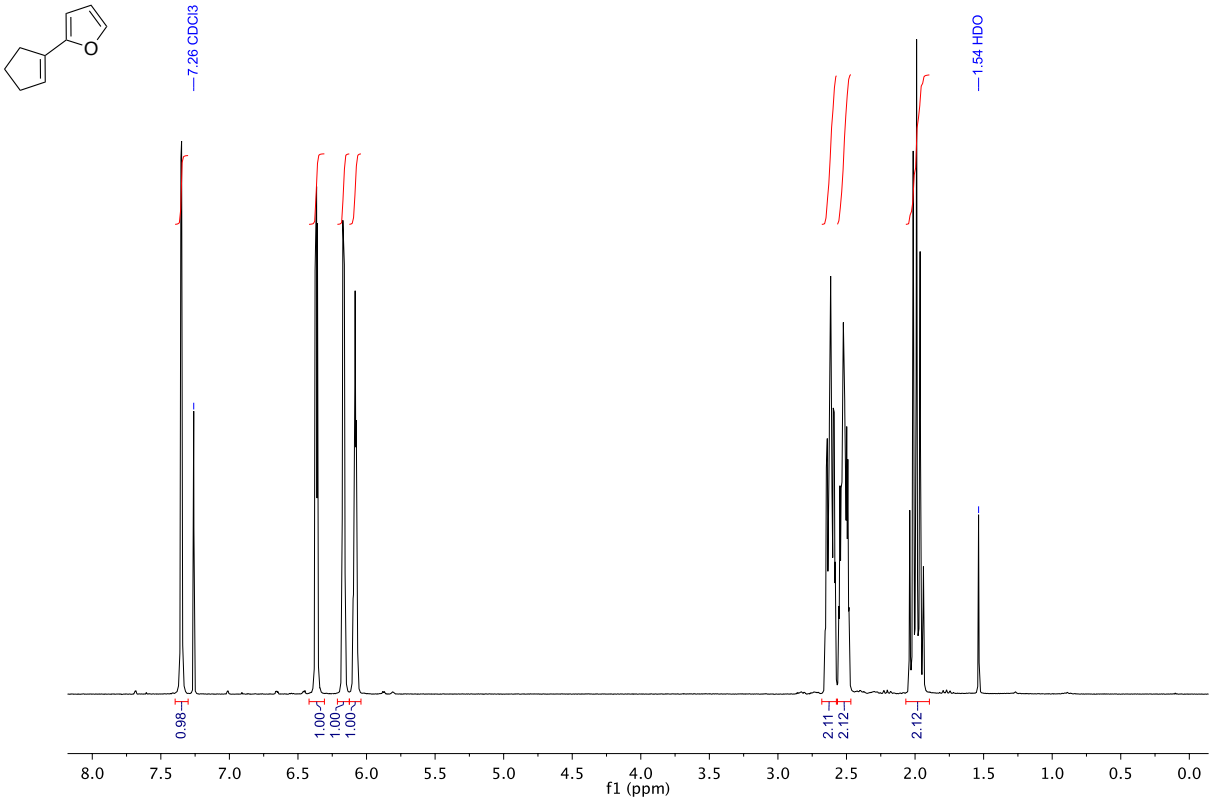

^{13}C NMR (75 MHz, $CDCl_3$)
2-(Cyclopent-1-en-1-yl)furan (**1**)

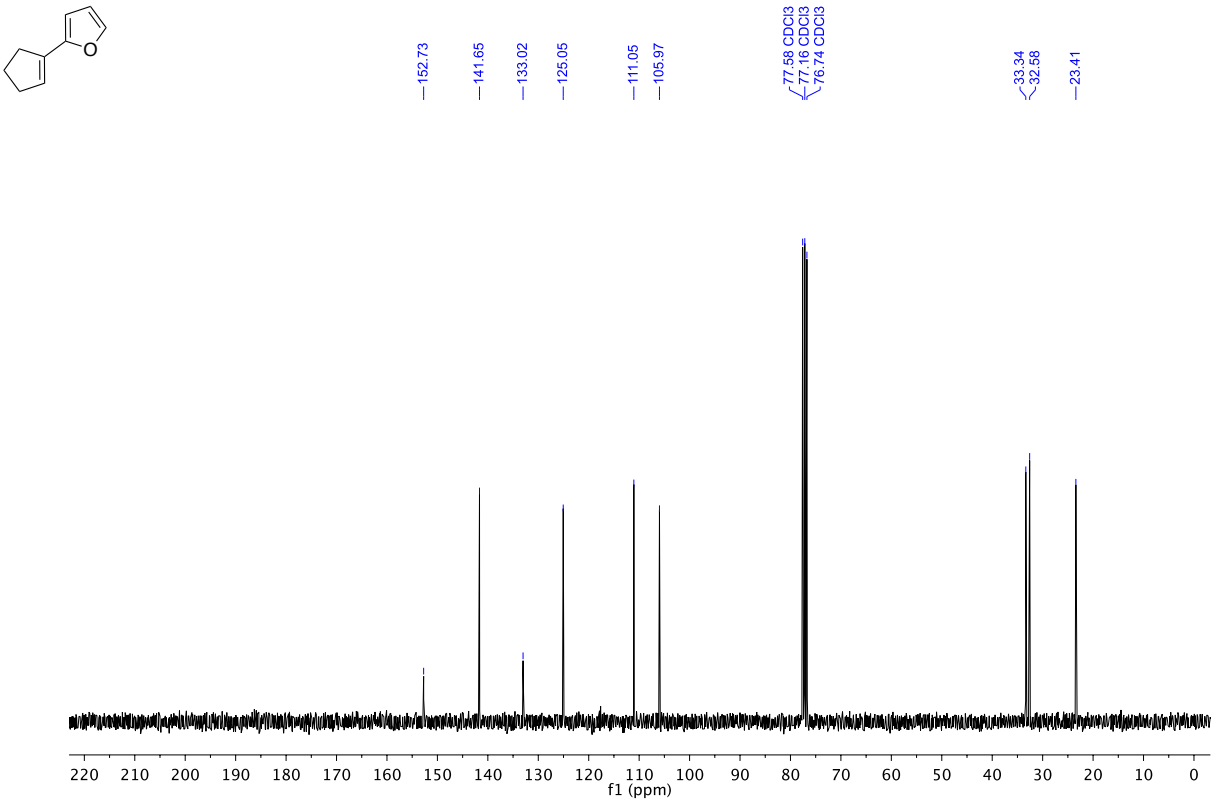

^{1}H NMR (300 MHz, $CDCl_3$)
trans-2-(2-furyl)cyclopentanol / (1*R*,2*R*)-2-(Furan-2-yl)cyclopentan-1-ol

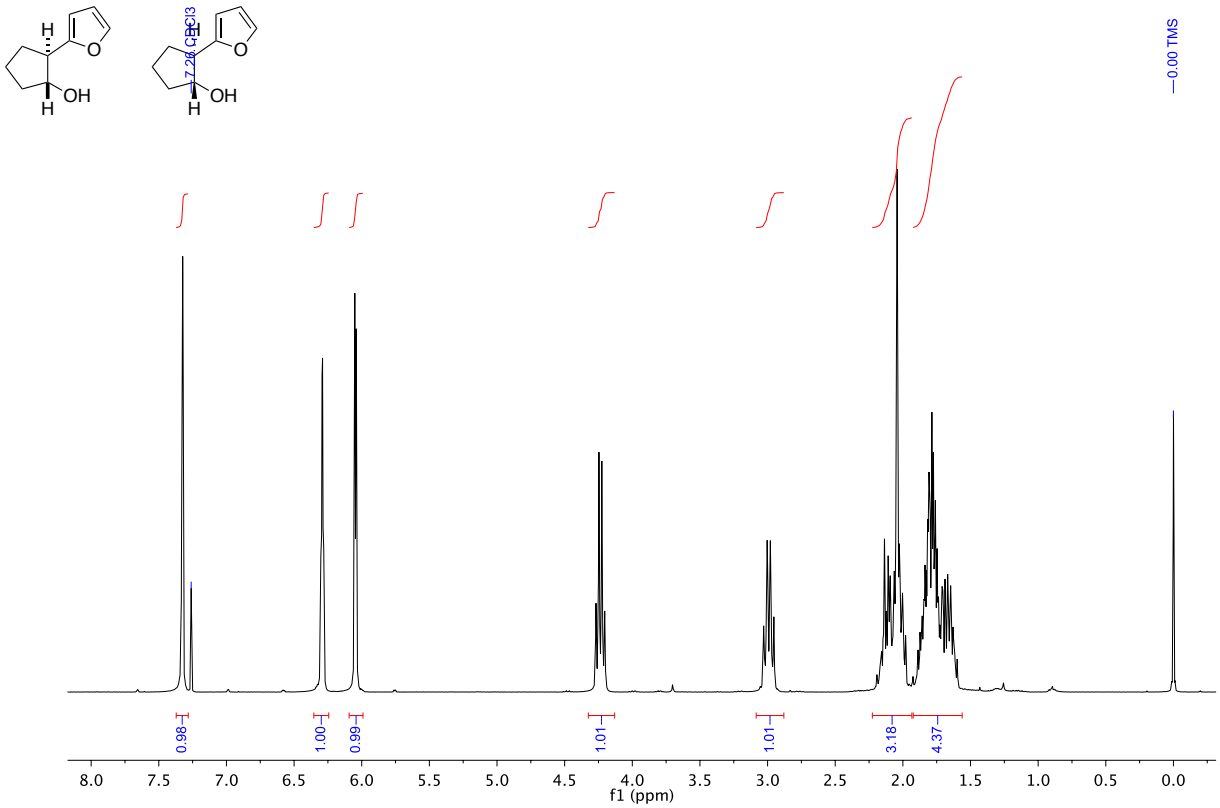

^{13}C NMR (75 MHz, $CDCl_3$)
trans-2-(2-furyl)cyclopentanol / (1*R*,2*R*)-2-(Furan-2-yl)cyclopentan-1-ol

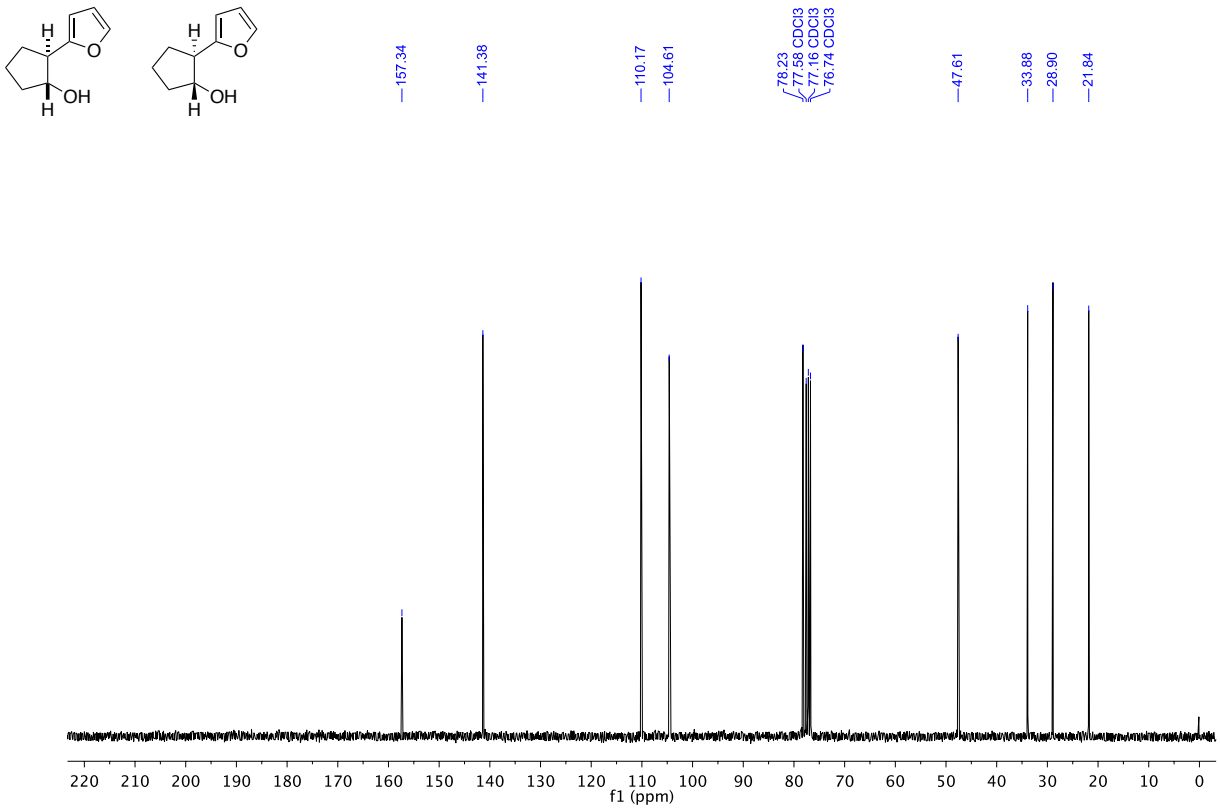

^{1}H NMR (300 MHz, $CDCl_3$)
trans-2-(2-ethynylcyclopentyl)furan / 2-((1*R*,2*R*)-2-ethynylcyclopentyl)furan (**3**)

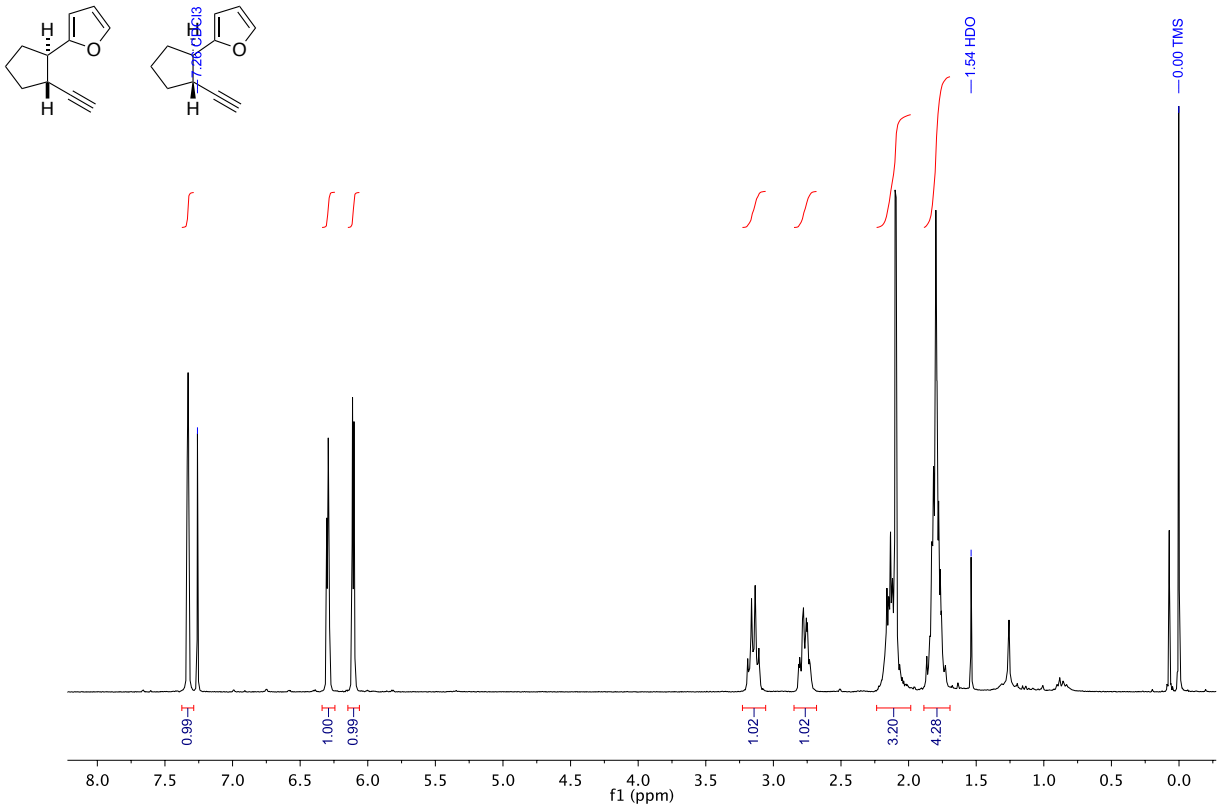

^{13}C NMR (75 MHz, $CDCl_3$)
trans-2-(2-ethynylcyclopentyl)furan / 2-((1*R*,2*R*)-2-ethynylcyclopentyl)furan (**3**)

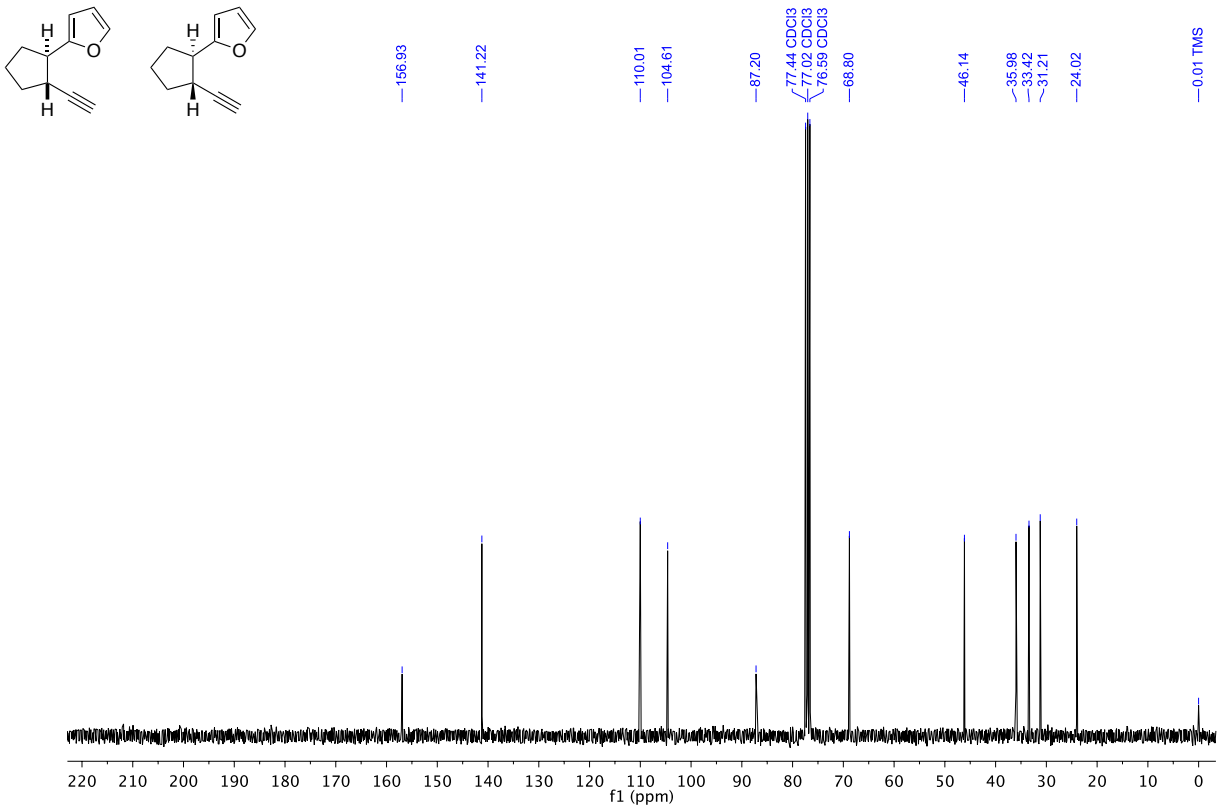

^{1}H NMR (300 MHz, $CDCl_3$)
(((1*R*,2*R*)-2-(furan-2-yl)cyclopentyl)ethynyl)triisopropylsilane (**2b**)

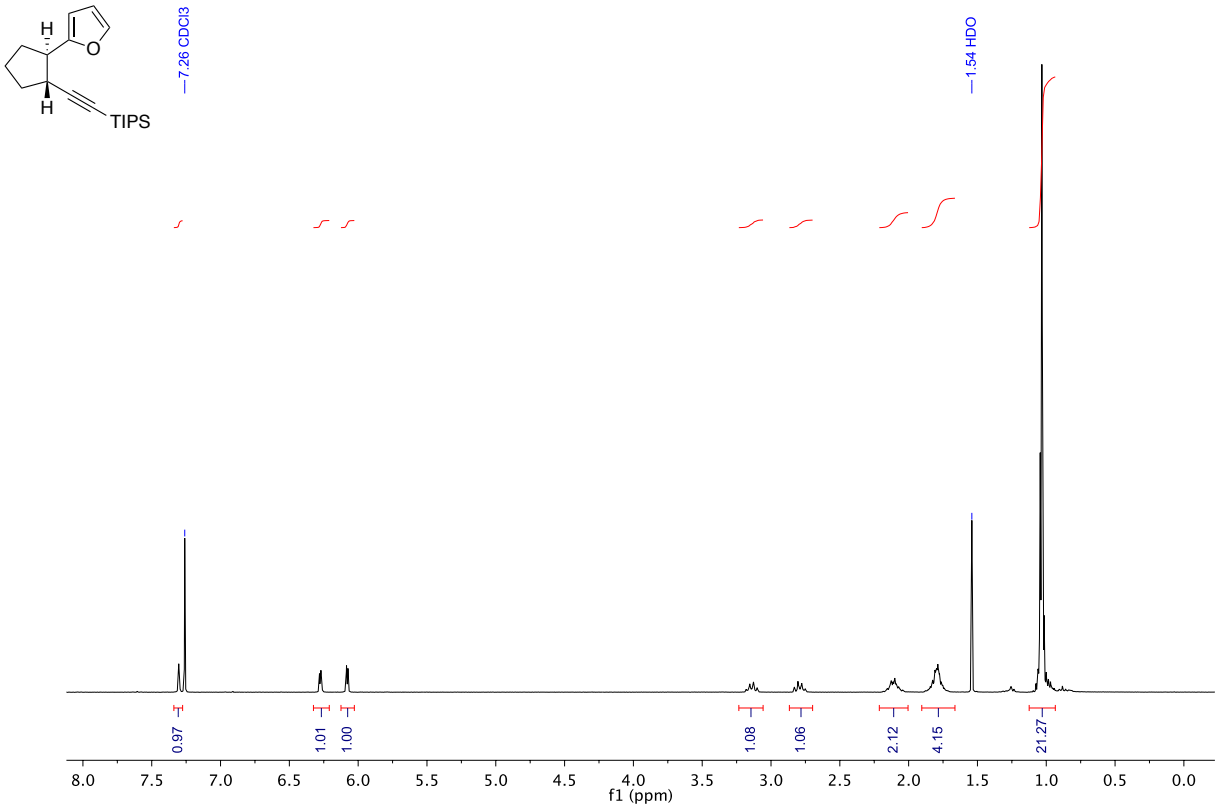

^{13}C NMR (75 MHz, $CDCl_3$)
(((1*R*,2*R*)-2-(furan-2-yl)cyclopentyl)ethynyl)triisopropylsilane (**2b**)

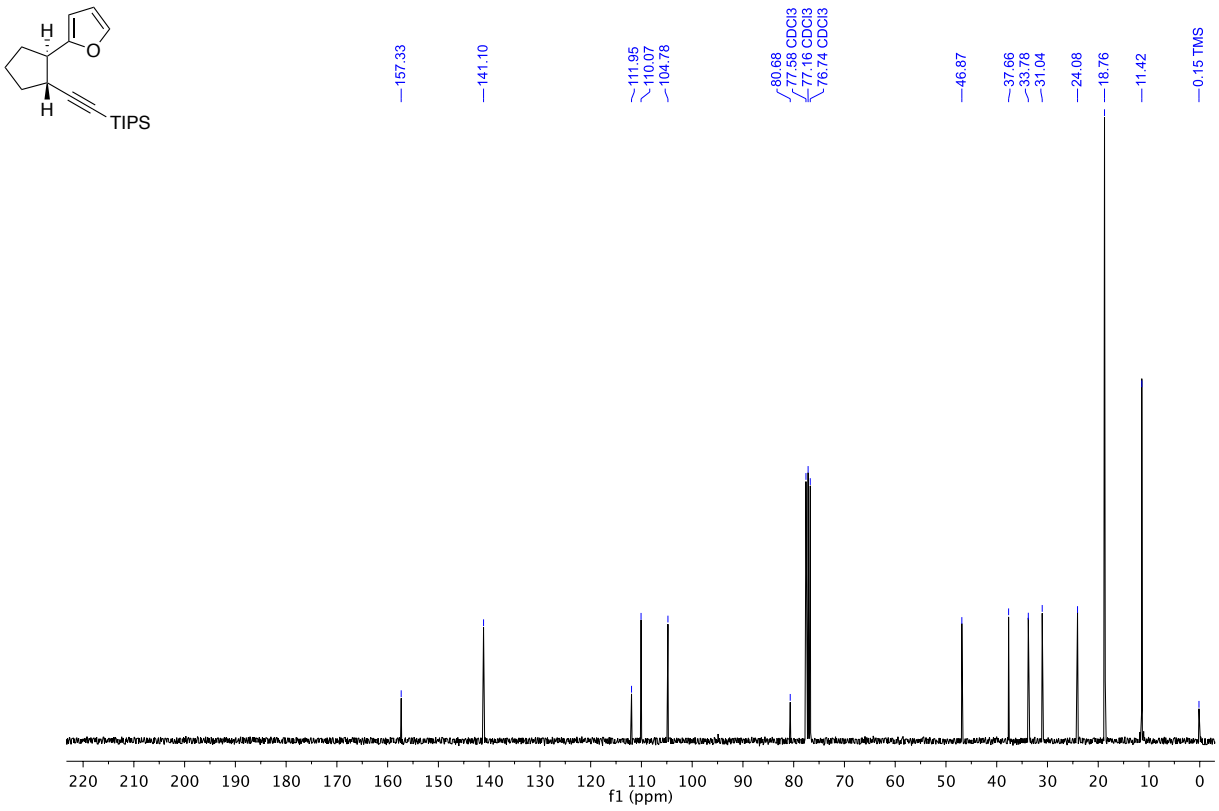

^{1}H NMR (300 MHz, $CDCl_3$)
2-cyclopentylfuran

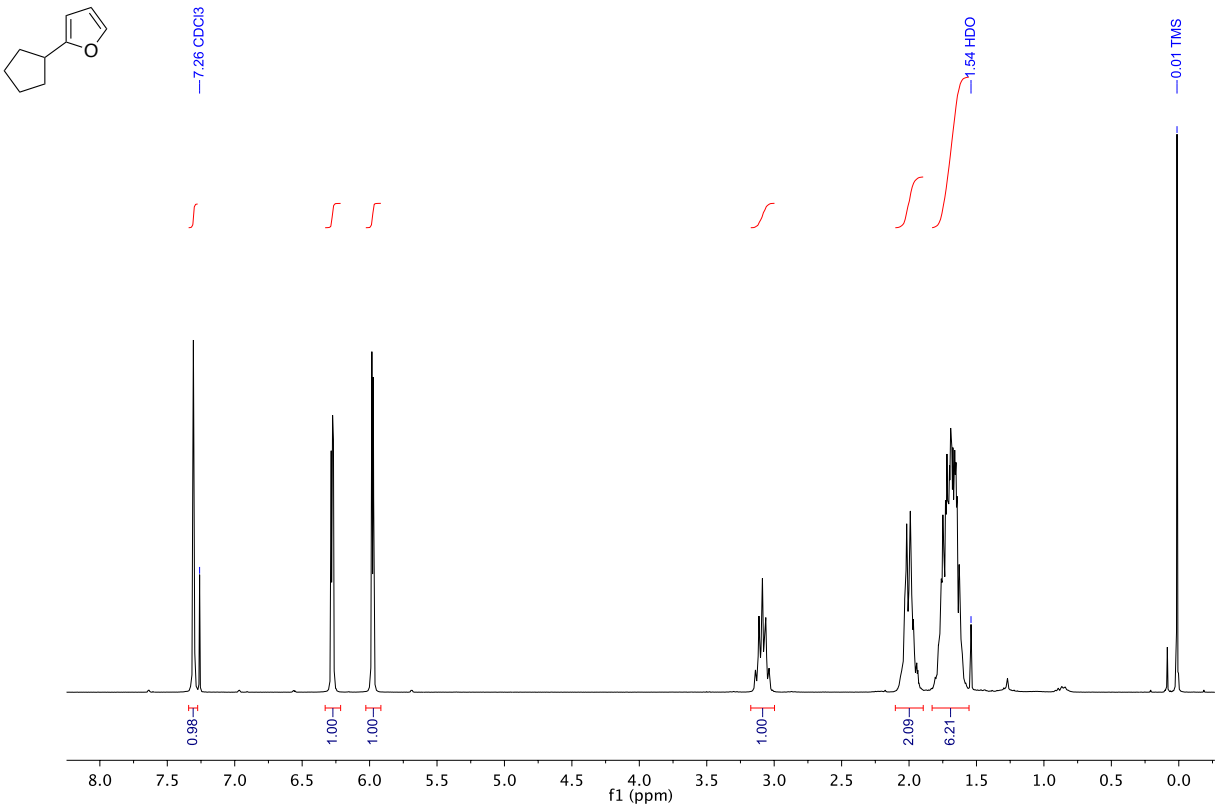

^{13}C NMR (75 MHz, $CDCl_3$)
2-cyclopentylfuran

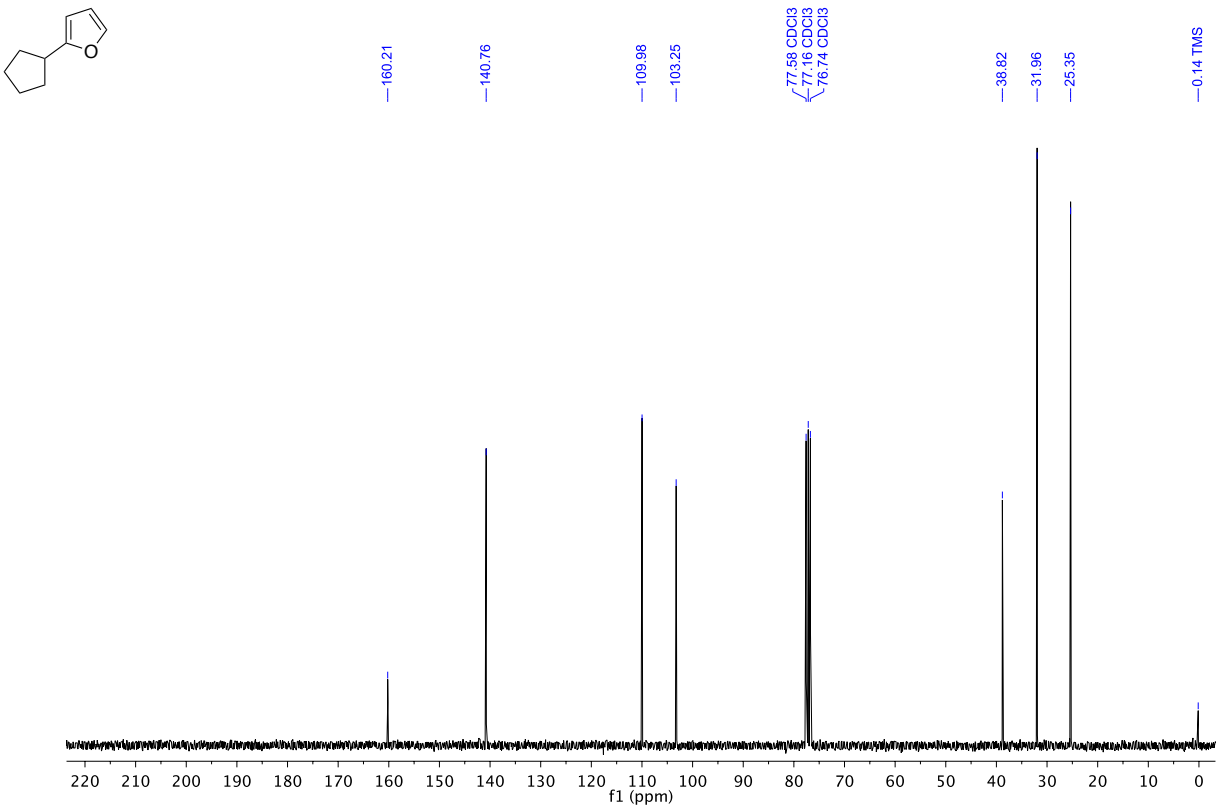

^{1}H NMR (300 MHz, $CDCl_3$)
(*E*)-4-cyclopentyl-4-oxobut-2-enal

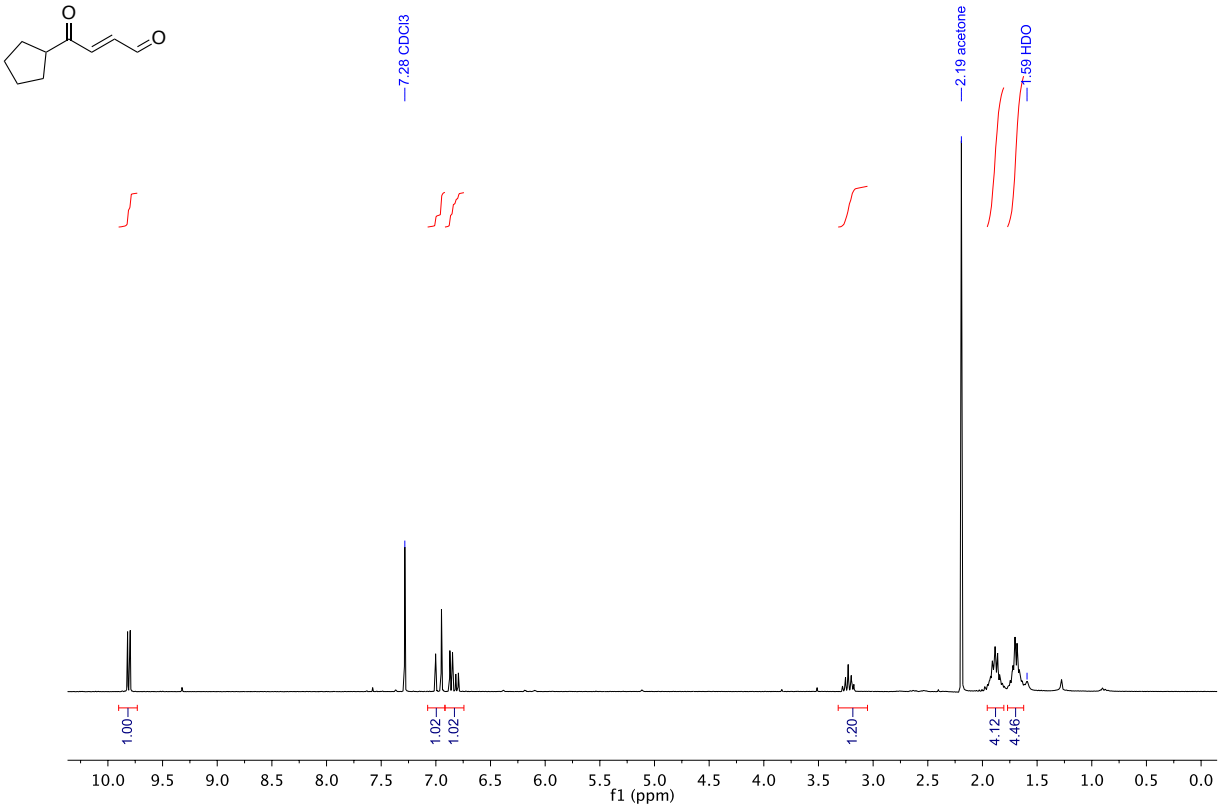

^{13}C NMR (75 MHz, $CDCl_3$)
(*E*)-4-cyclopentyl-4-oxobut-2-enal (*partial decomposition during time of measurement)*

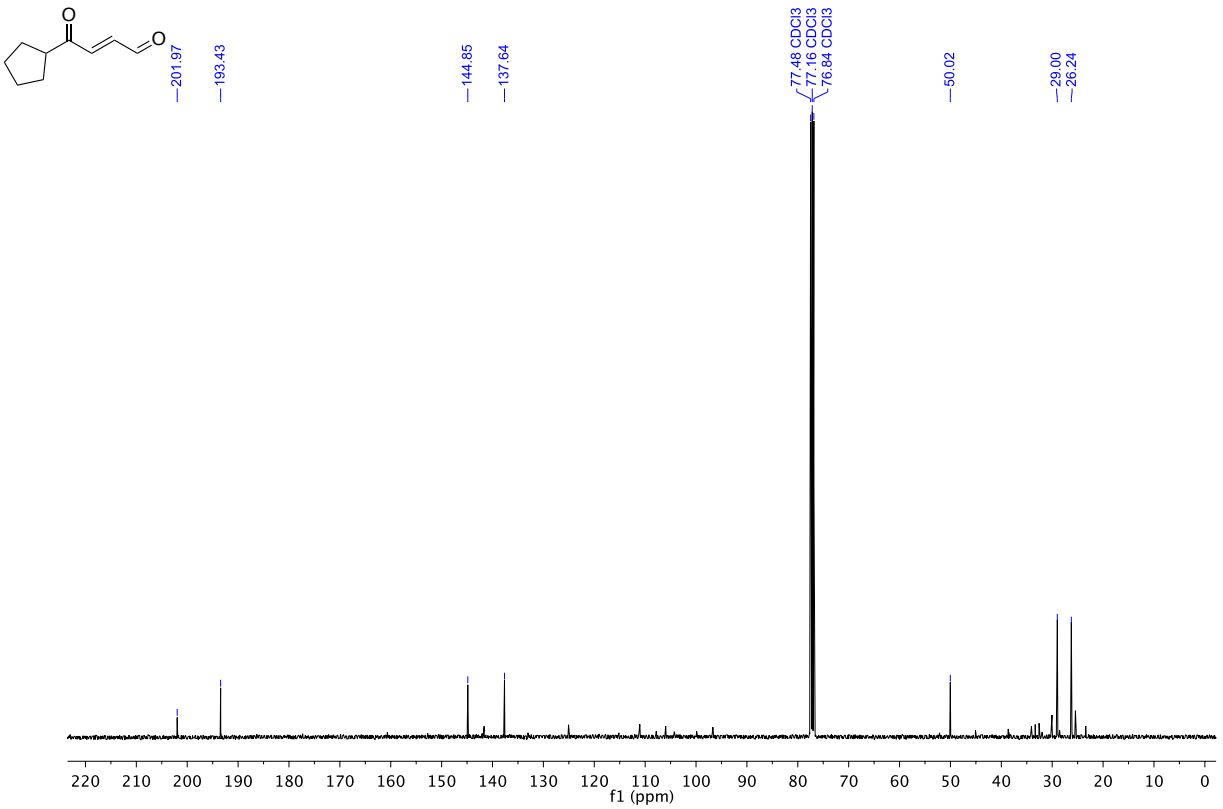

^{1}H NMR (300 MHz, $CDCl_3$)
(*E*)-4-cyclopentyl-4-oxobut-2-enoic acid

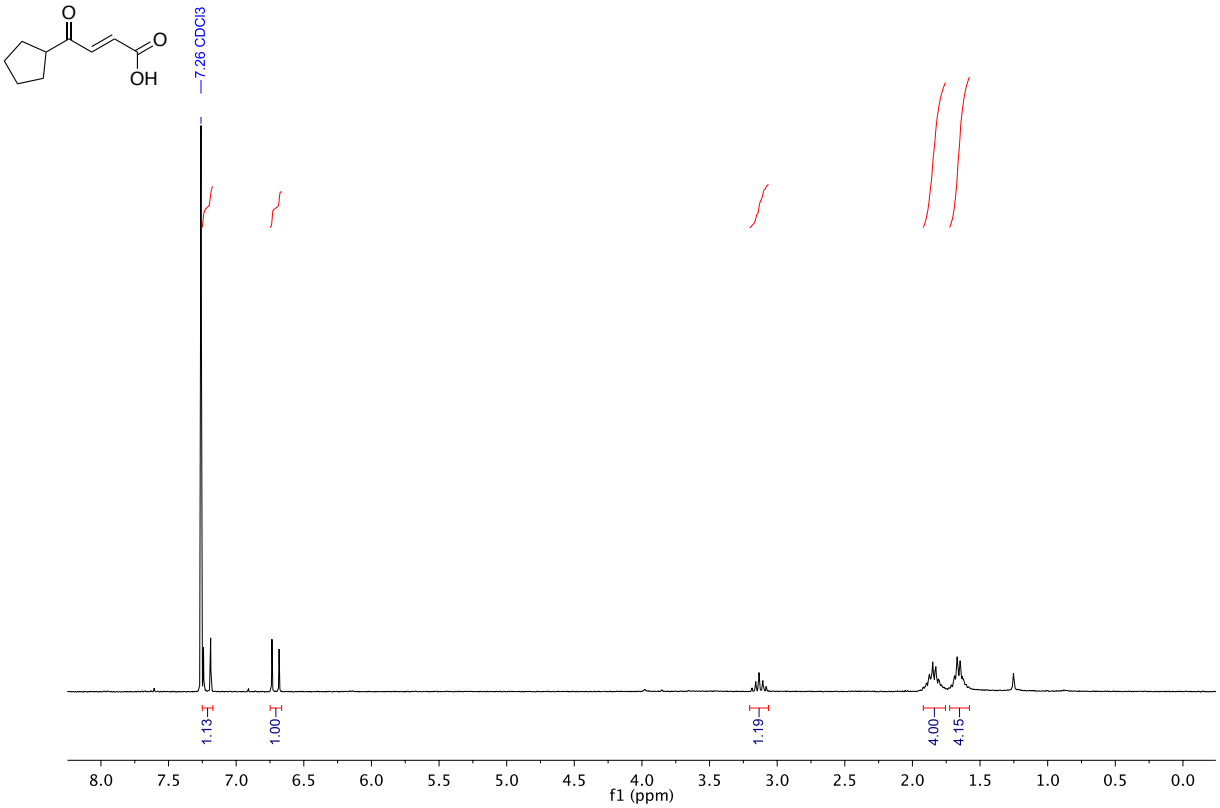

^{13}C NMR (75 MHz, $CDCl_3$)
(*E*)-4-cyclopentyl-4-oxobut-2-enoic acid

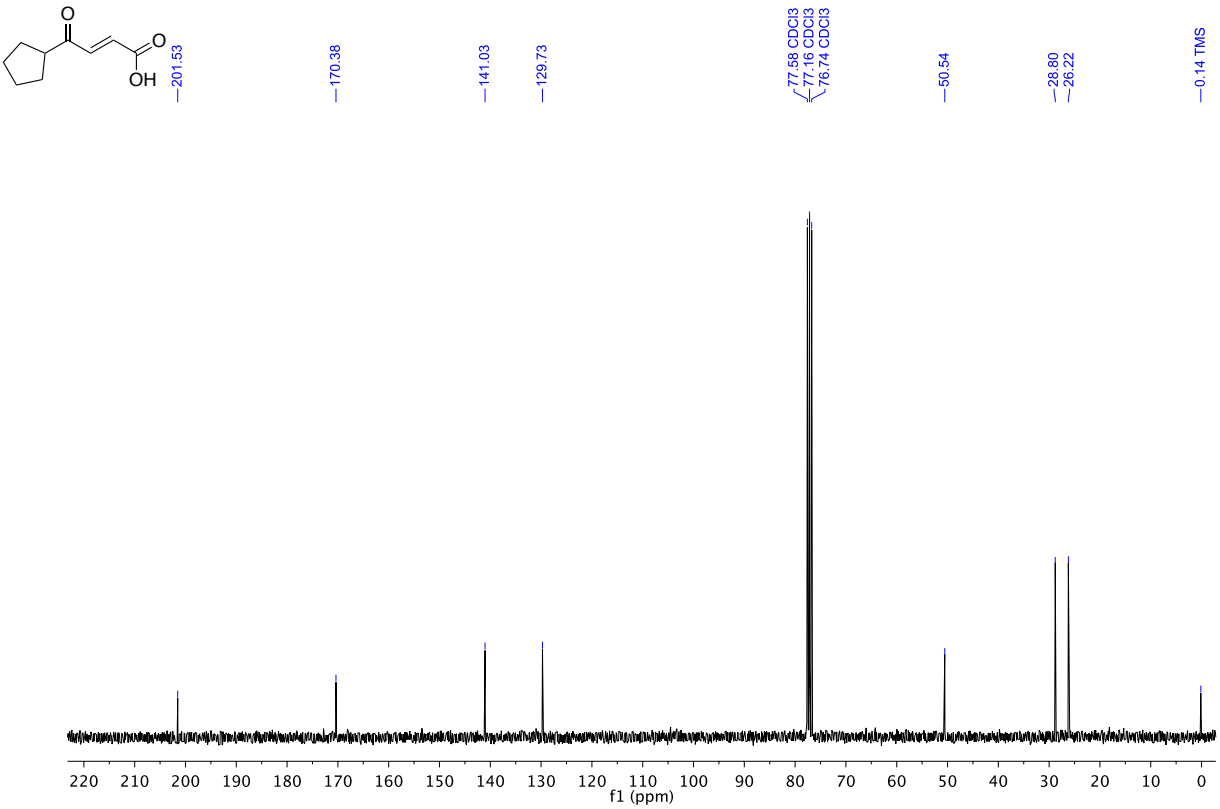

^{1}H NMR (300 MHz, $CDCl_3$)
(*S*)-pent-4-en-2-ol

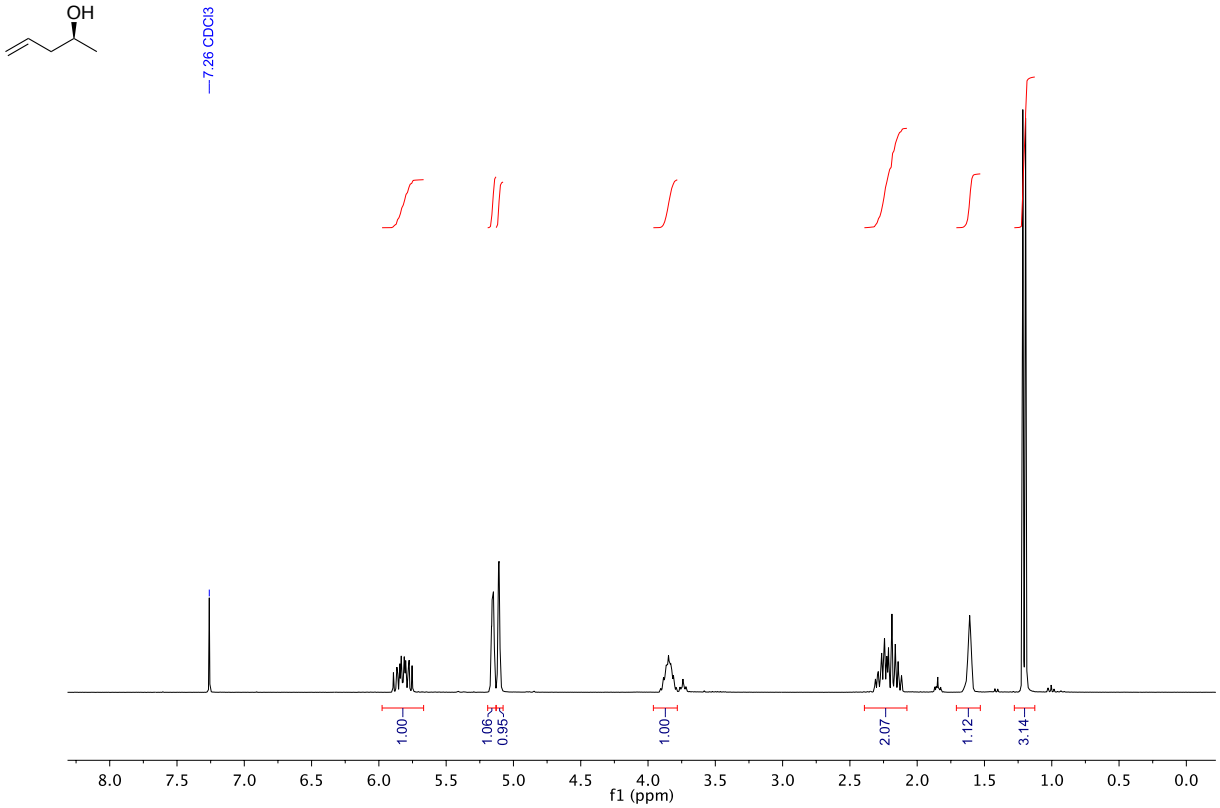

^{13}C NMR (75 MHz, $CDCl_3$)
(*S*)-pent-4-en-2-ol

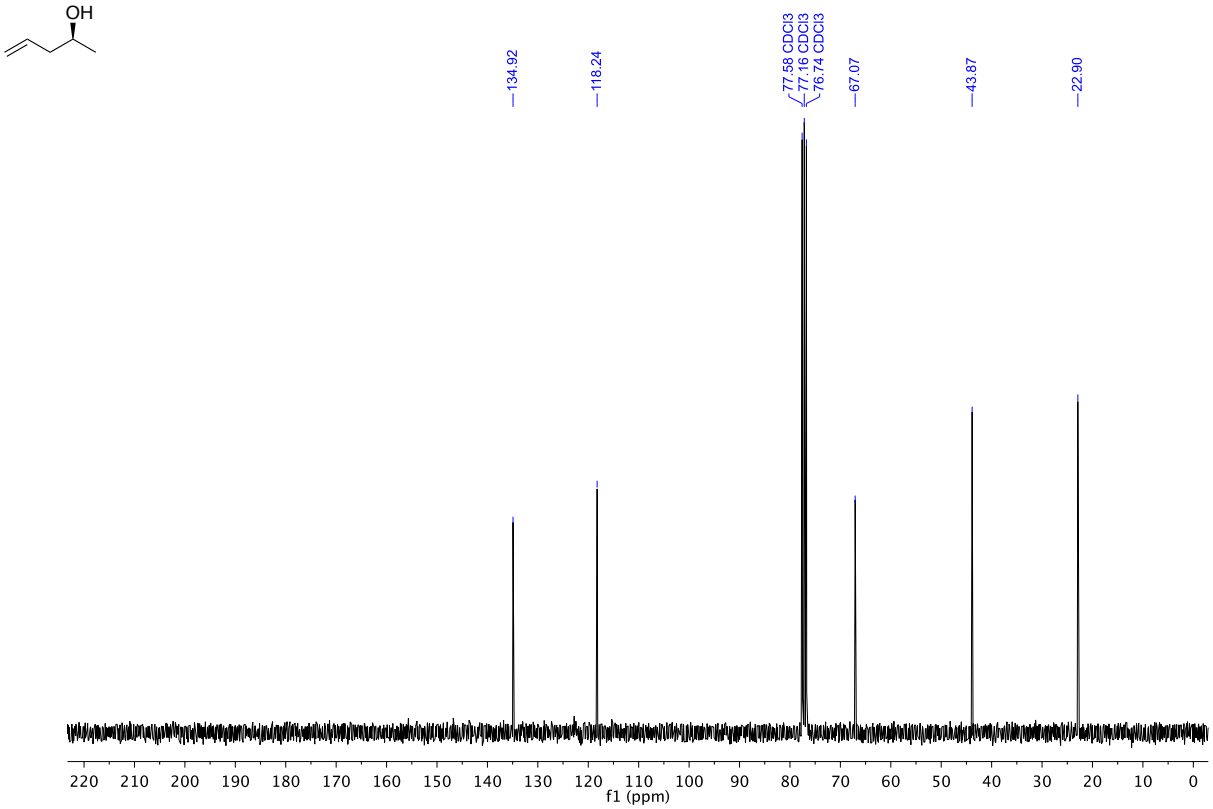

^{1}H NMR (300 MHz, $CDCl_3$)
(*S*)-1-methoxy-4-((pent-4-en-2-yloxy)methyl)benzene (**4**)

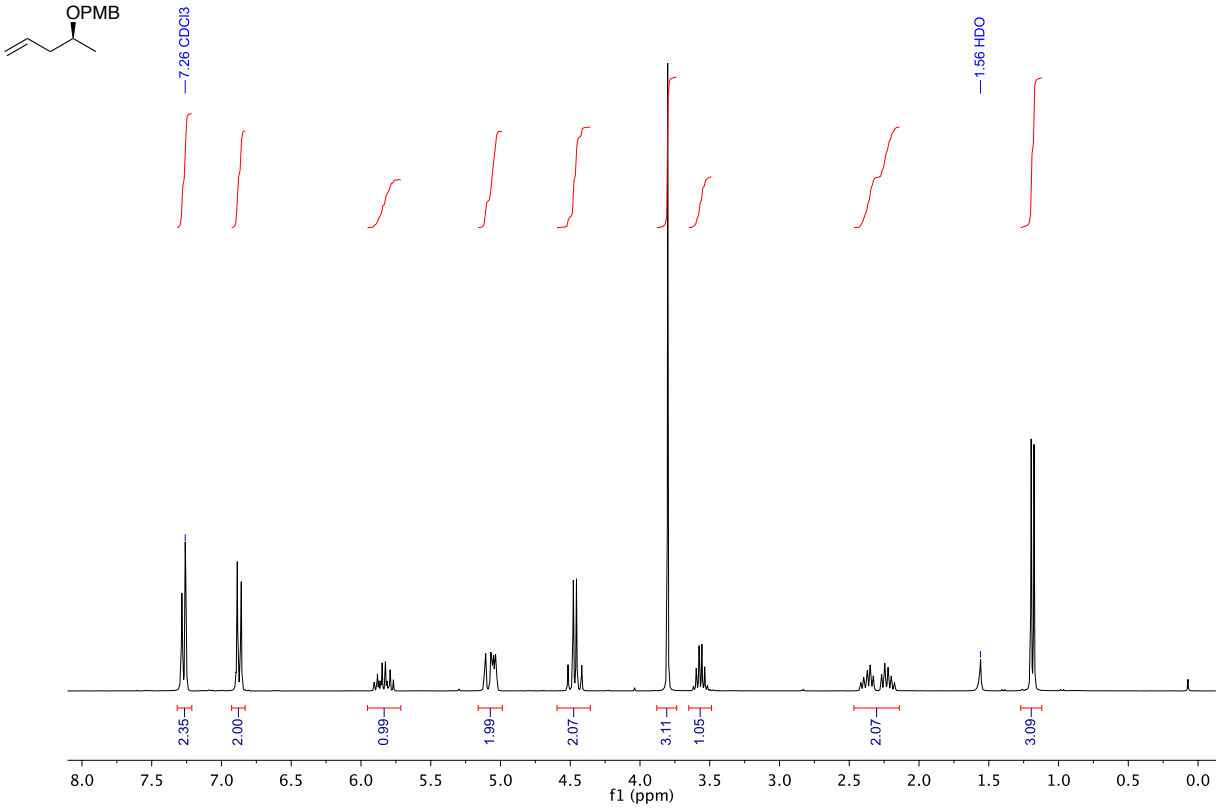

^{13}C NMR (75 MHz, $CDCl_3$)
(*S*)-1-methoxy-4-((pent-4-en-2-yloxy)methyl)benzene (**4**)

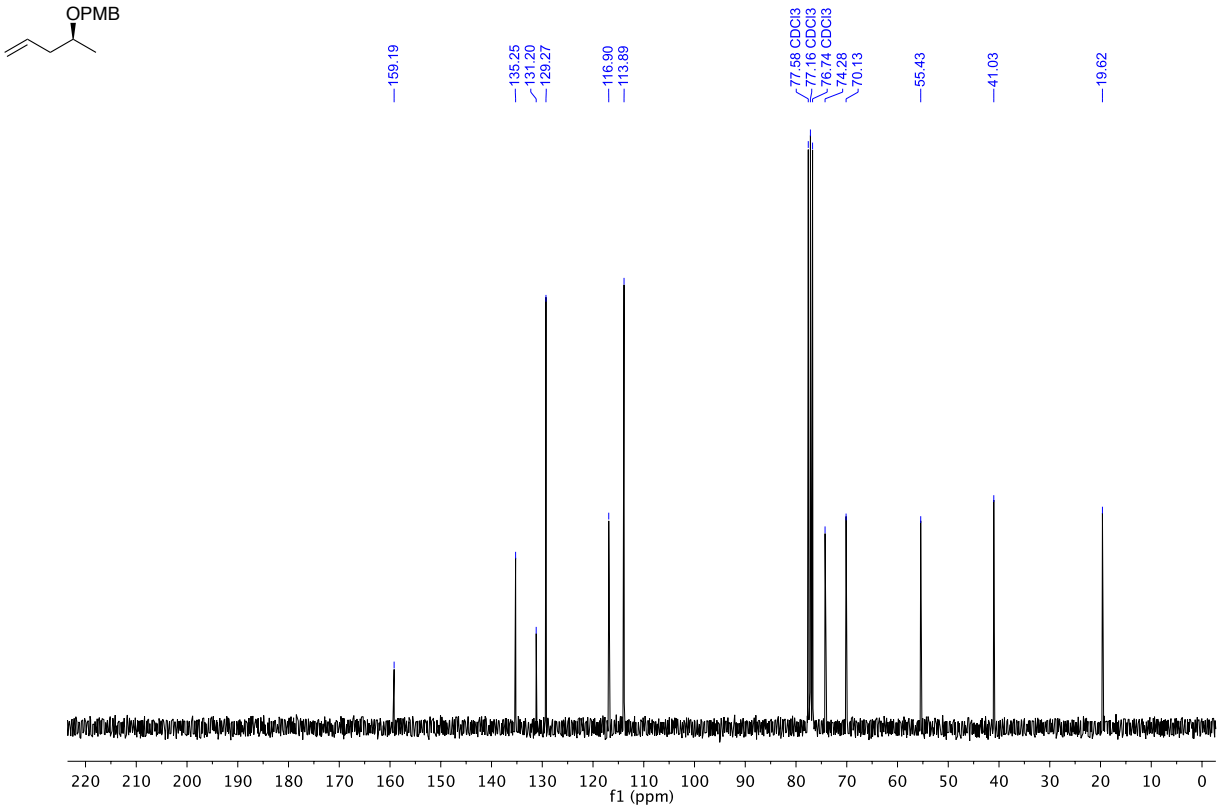

^{1}H NMR (300 MHz, $CDCl_3$)
2-((1*R*,2*S*)-2-((*S*,*E*)-6-((4-methoxybenzyl)oxy)hept-1-en-1-yl)cyclopentyl)furan (**7**)

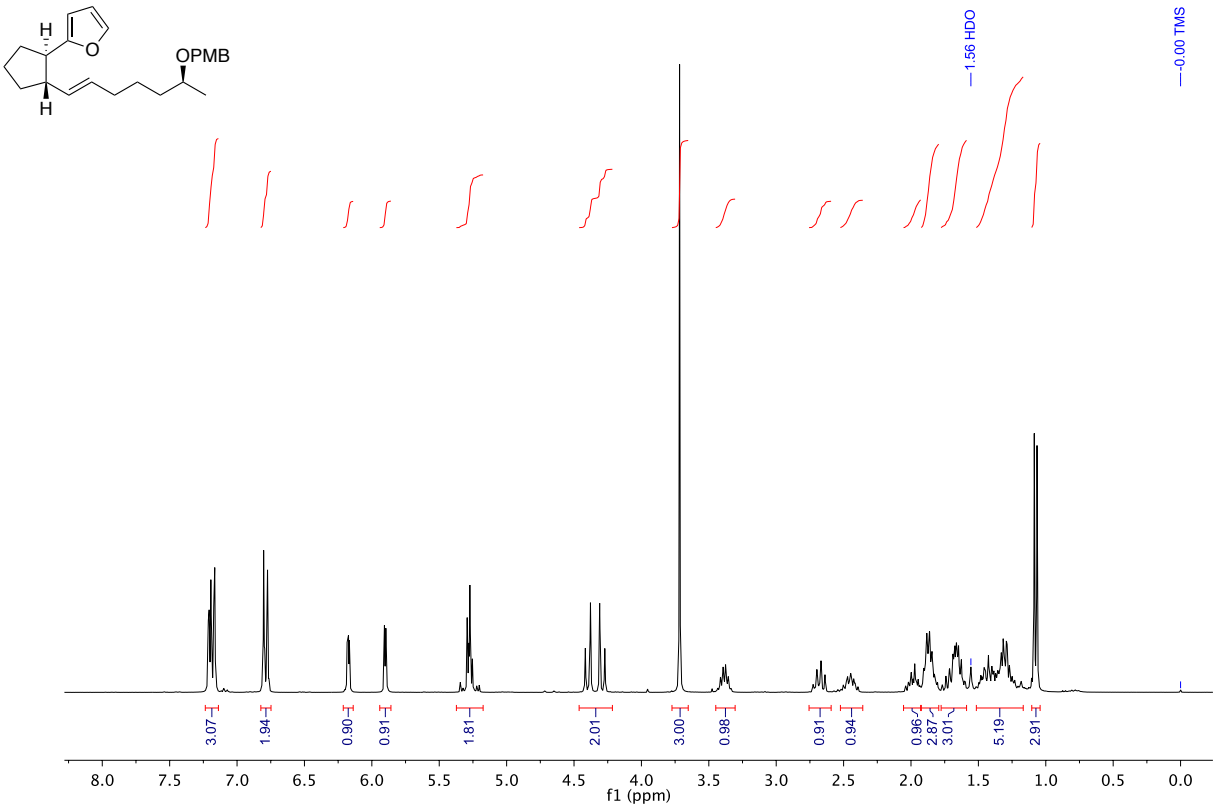

^{13}C NMR (75 MHz, $CDCl_3$)
2-((1*R*,2*S*)-2-((*S*,*E*)-6-((4-methoxybenzyl)oxy)hept-1-en-1-yl)cyclopentyl)furan (**7**)

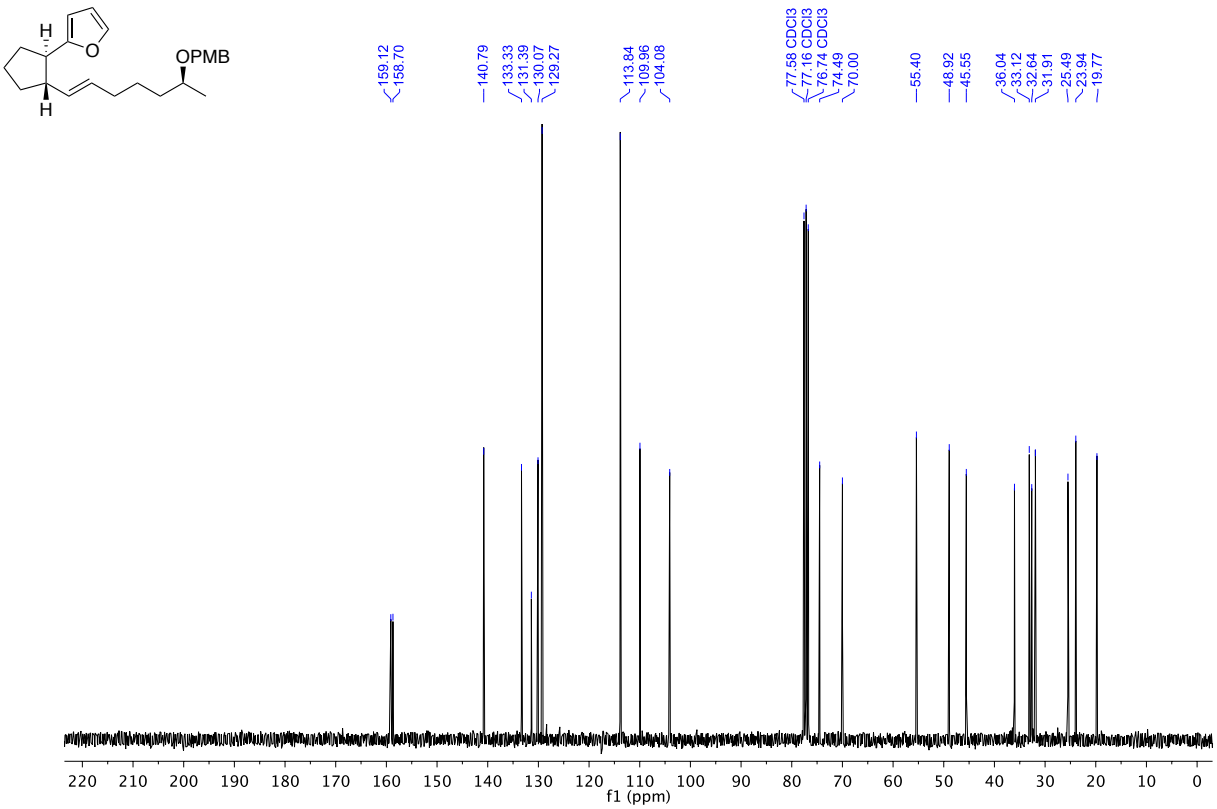

^{1}H NMR (300 MHz, $CDCl_3$)
(*S*,*E*)-7-((1*S*,2*R*)-2-(furan-2-yl)cyclopentyl)hept-6-en-2-ol (**8**)

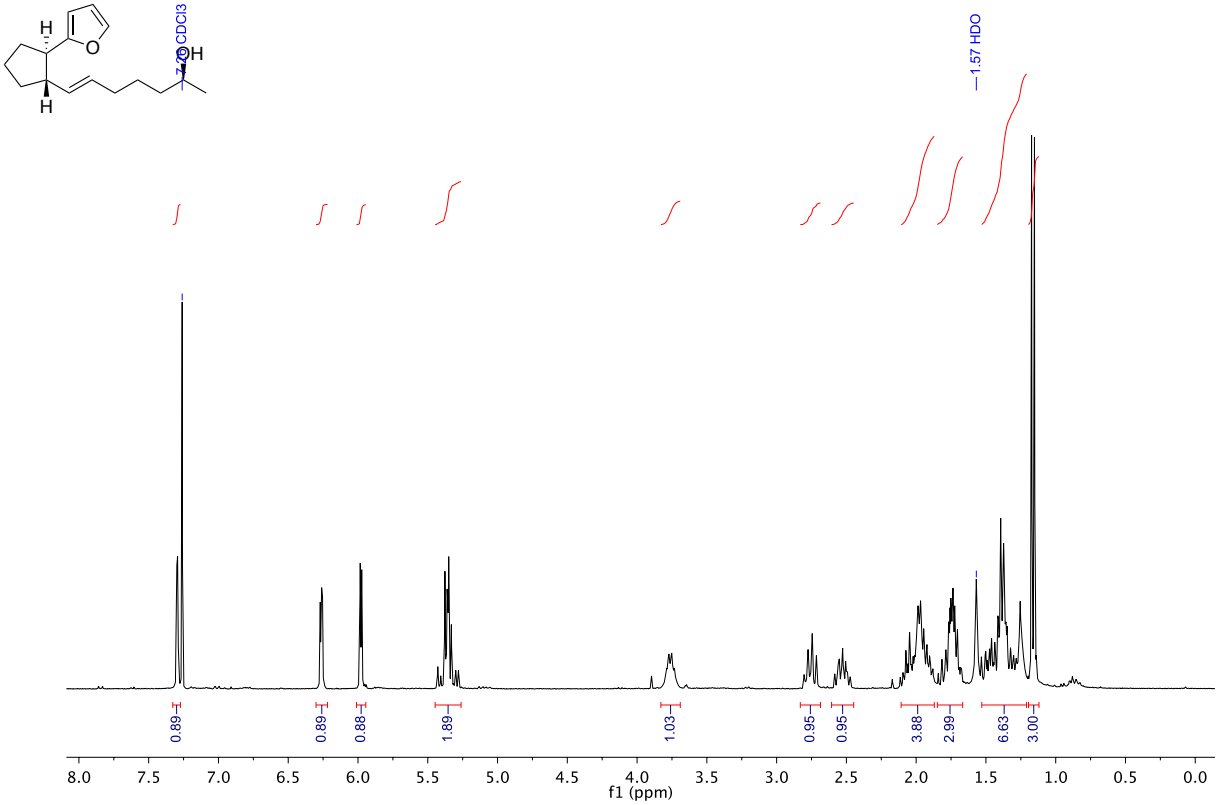

^{13}C NMR (75 MHz, $CDCl_3$)
(*S*,*E*)-7-((1*S*,2*R*)-2-(furan-2-yl)cyclopentyl)hept-6-en-2-ol (**8**)

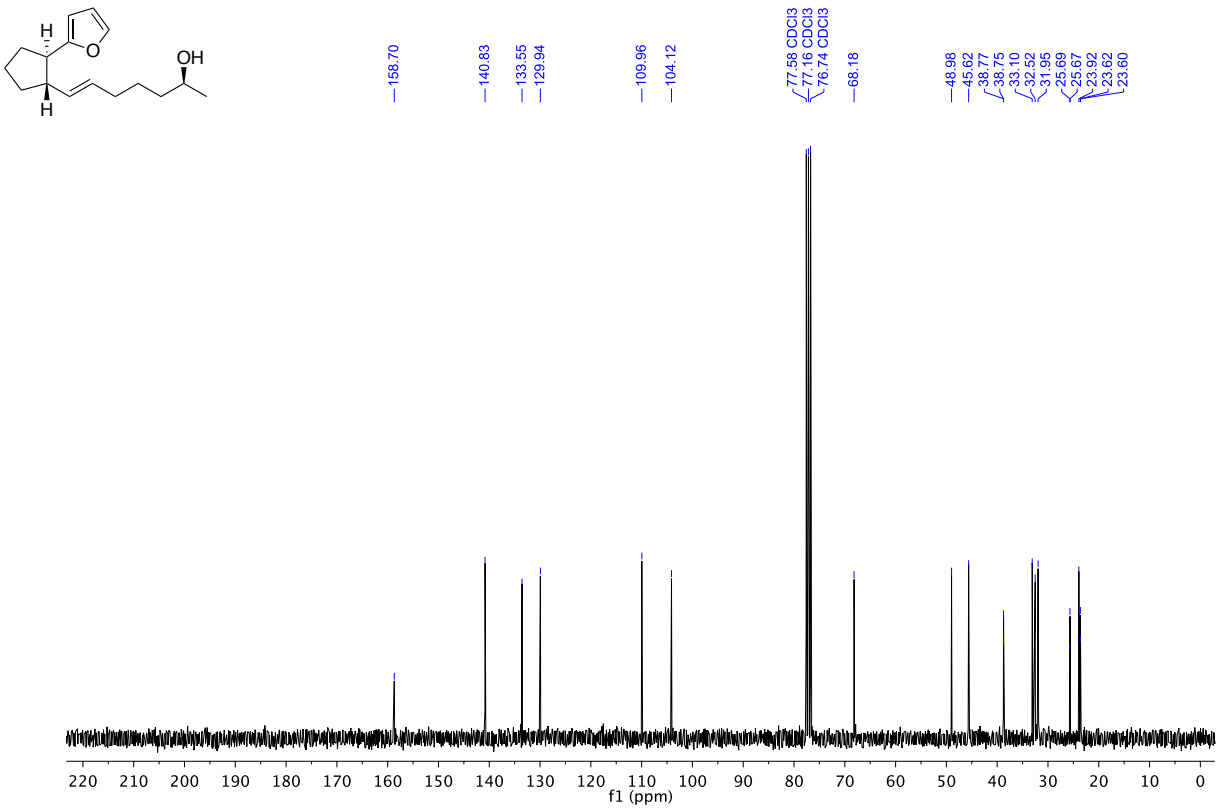

^{1}H NMR (300 MHz, $CDCl_3$)
(*E*)-4-((1*R*,2*S*)-2-((*S*,*E*)-6-hydroxyhept-1-en-1-yl)cyclopentyl)-4-oxobut-2-enoic acid (**10**)

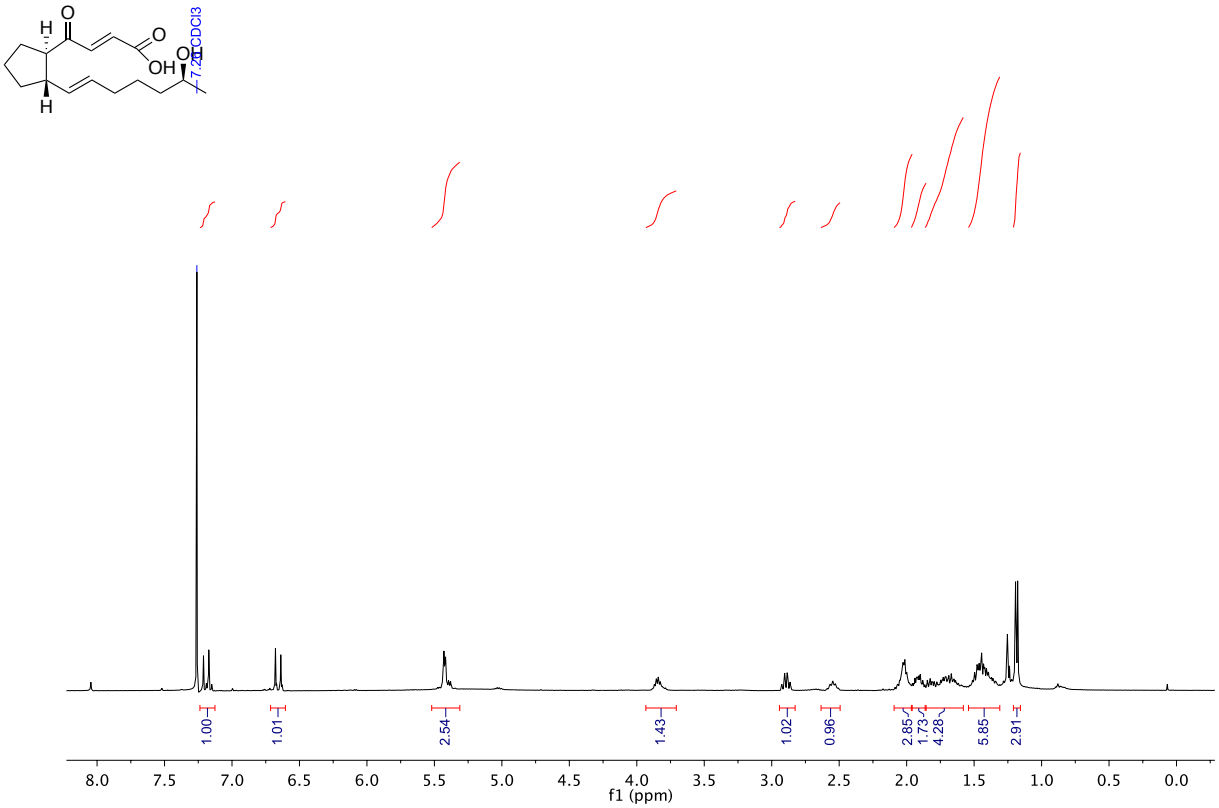

^{13}C NMR (75 MHz, $CDCl_3$)
(*E*)-4-((1*R*,2*S*)-2-((*S*,*E*)-6-hydroxyhept-1-en-1-yl)cyclopentyl)-4-oxobut-2-enoic acid (**10**)

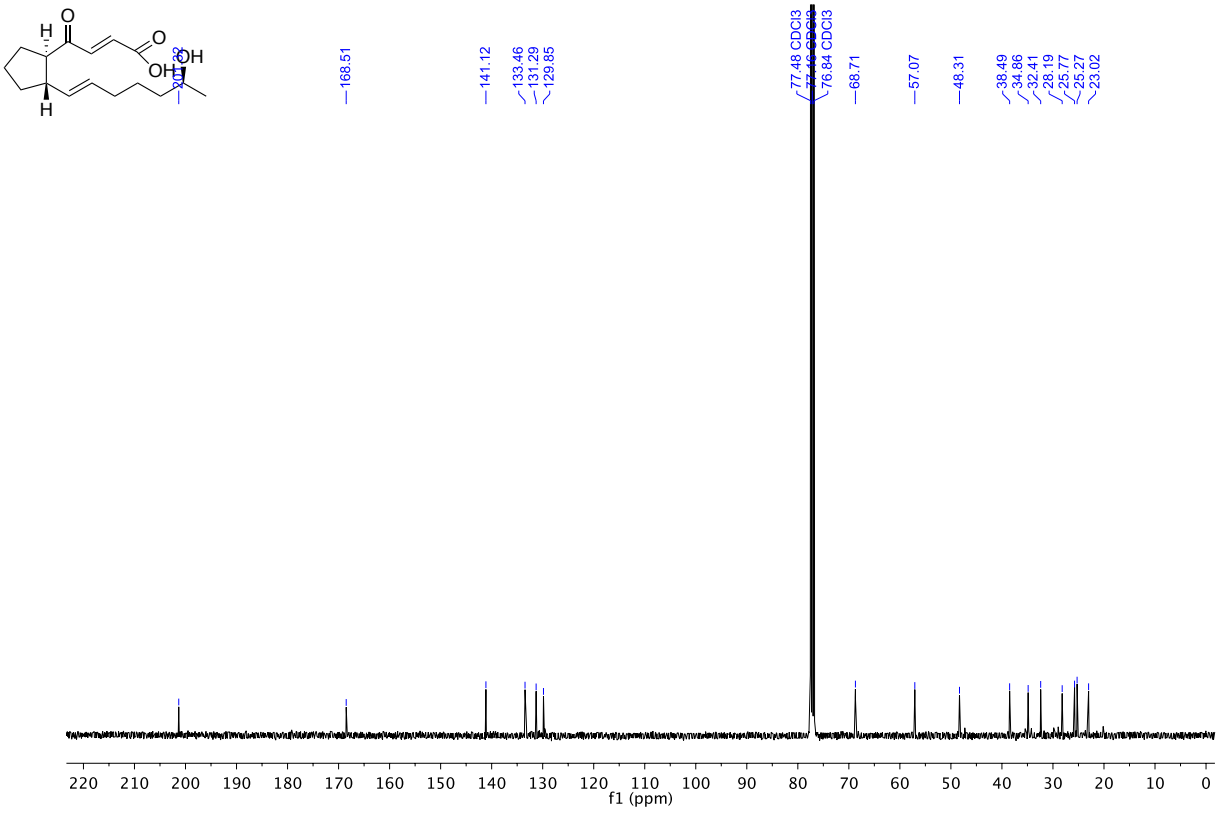

^{1}H NMR (300 MHz, $CDCl_3$)
4-dehydro-brefeldin C (**11**)

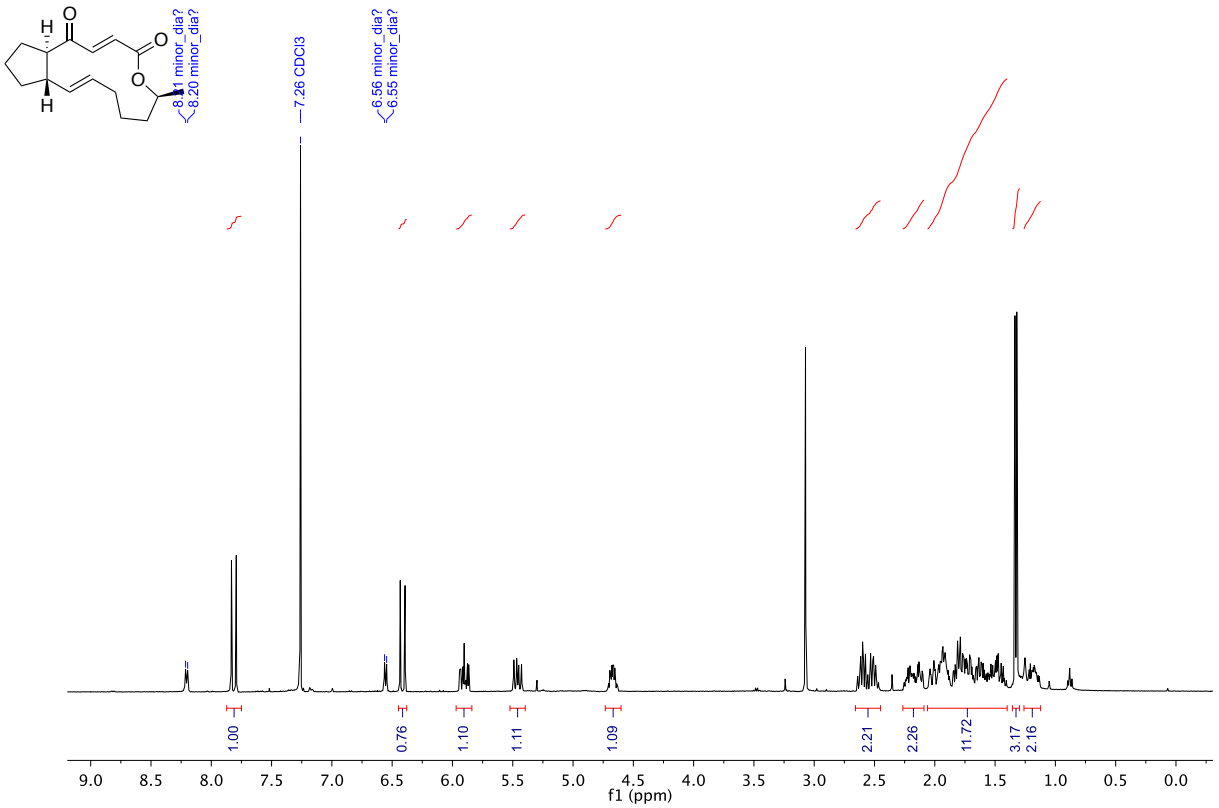

^{13}C NMR (75 MHz, $CDCl_3$)
4-dehydro-Brefeldin C (**11**)

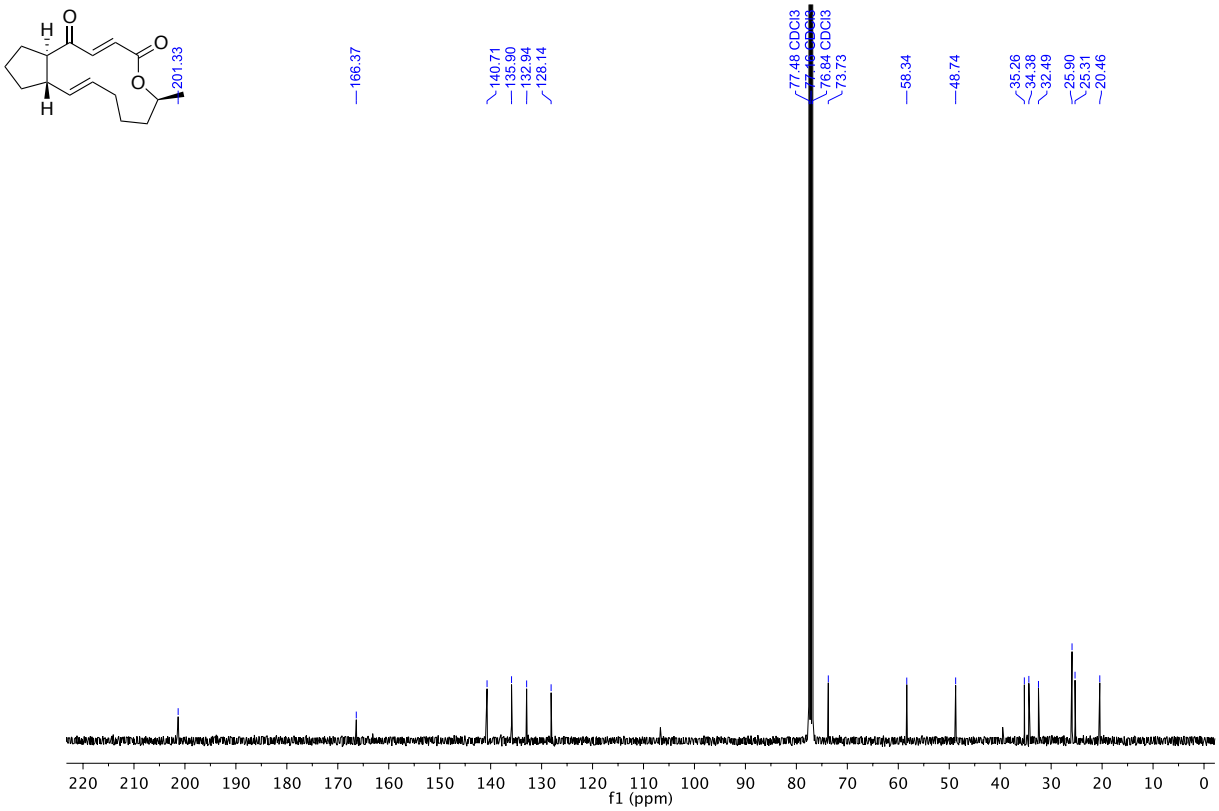

^{1}H NMR (300 MHz, $CDCl_3$)
(+)-brefeldin C

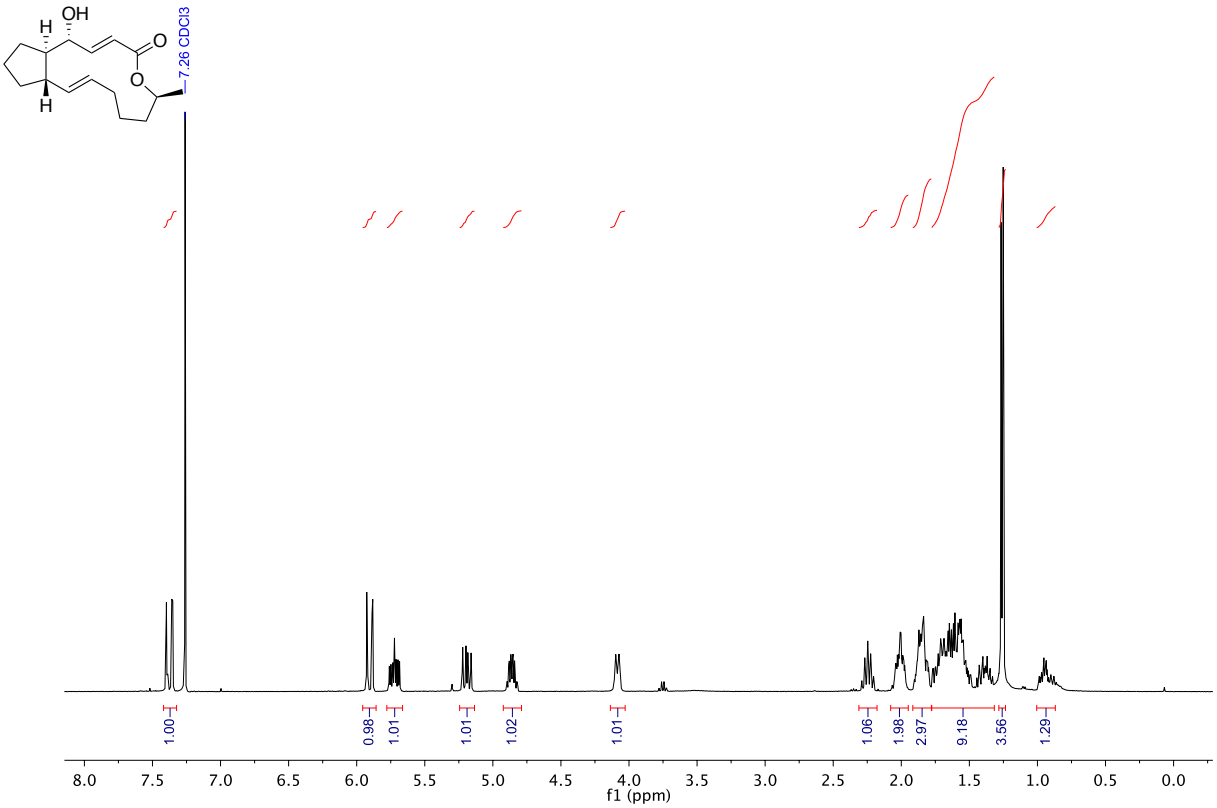

^{13}C NMR (75 MHz, $CDCl_3$)
(+)-brefeldin C

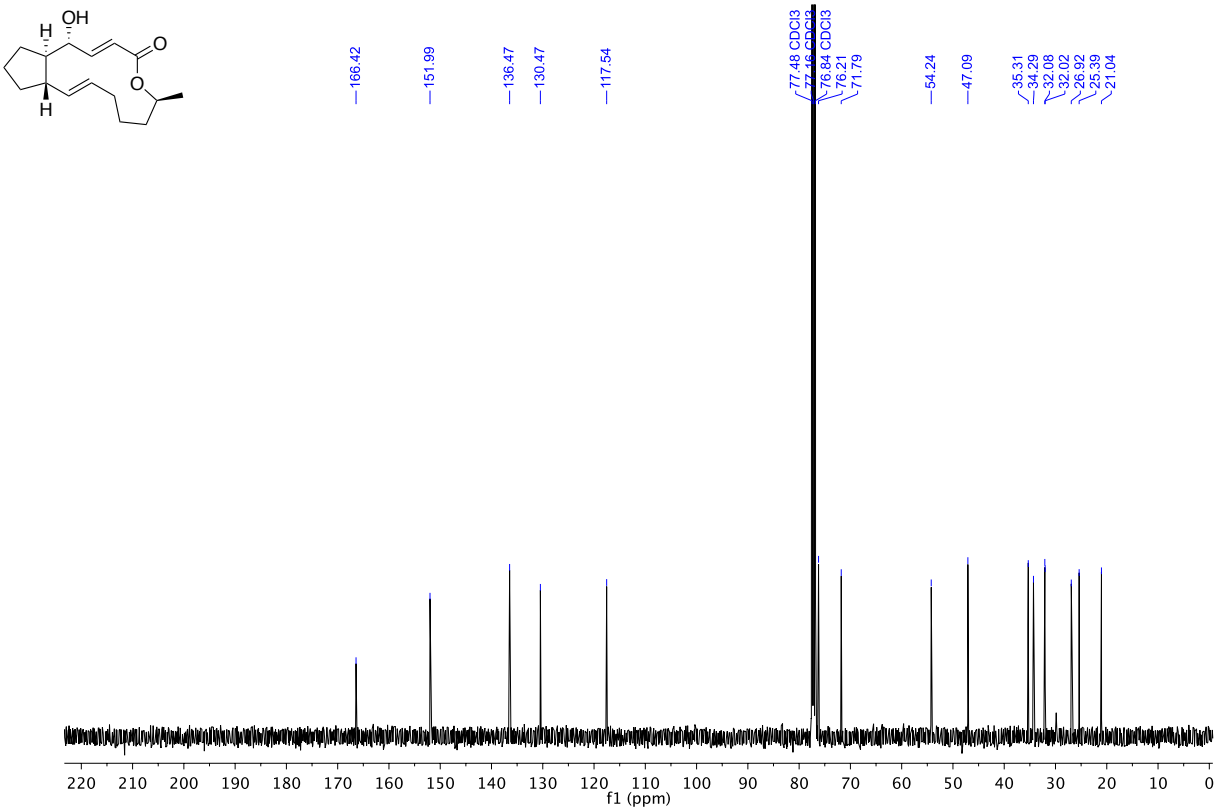

Appendix

NMR Spectra of Chapter 3

^{1}H NMR (300 MHz, $CDCl_3$)
2,5-dimethylhexan-2-ol

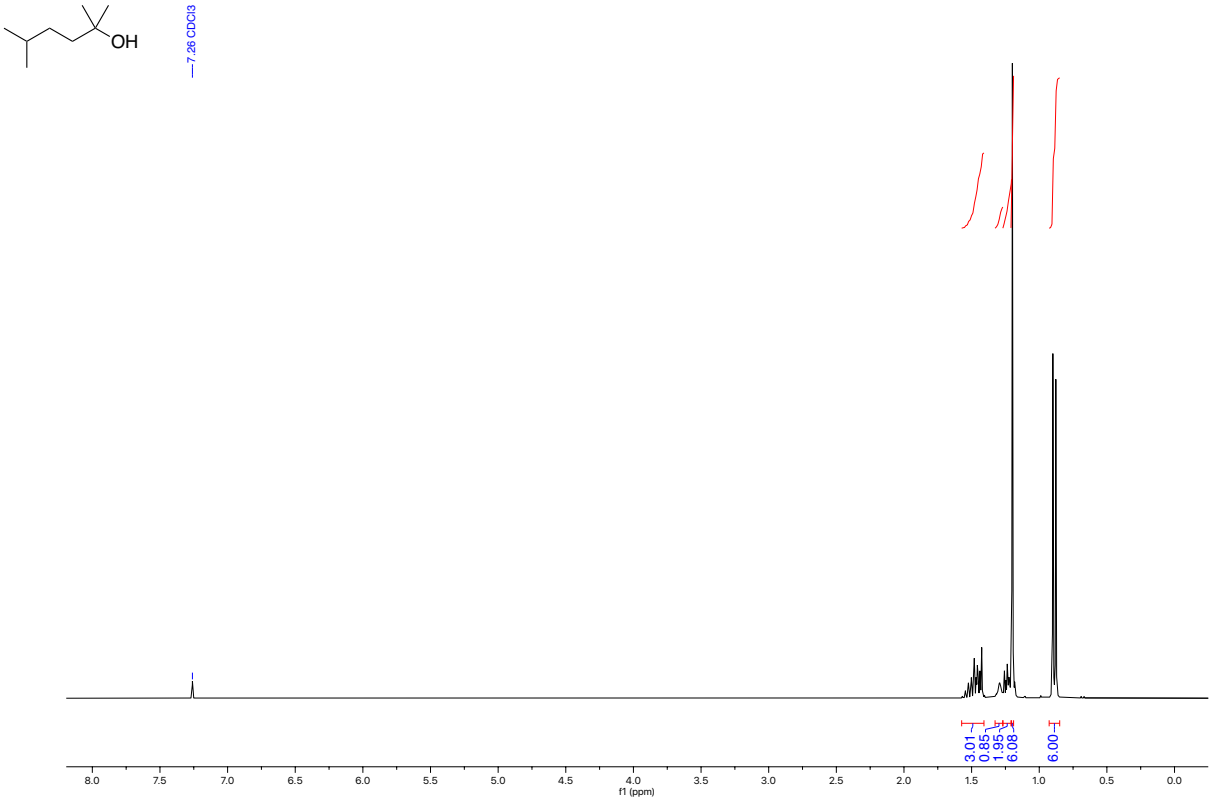

^{13}C NMR (75 MHz, $CDCl_3$)
2,5-dimethylhexan-2-ol

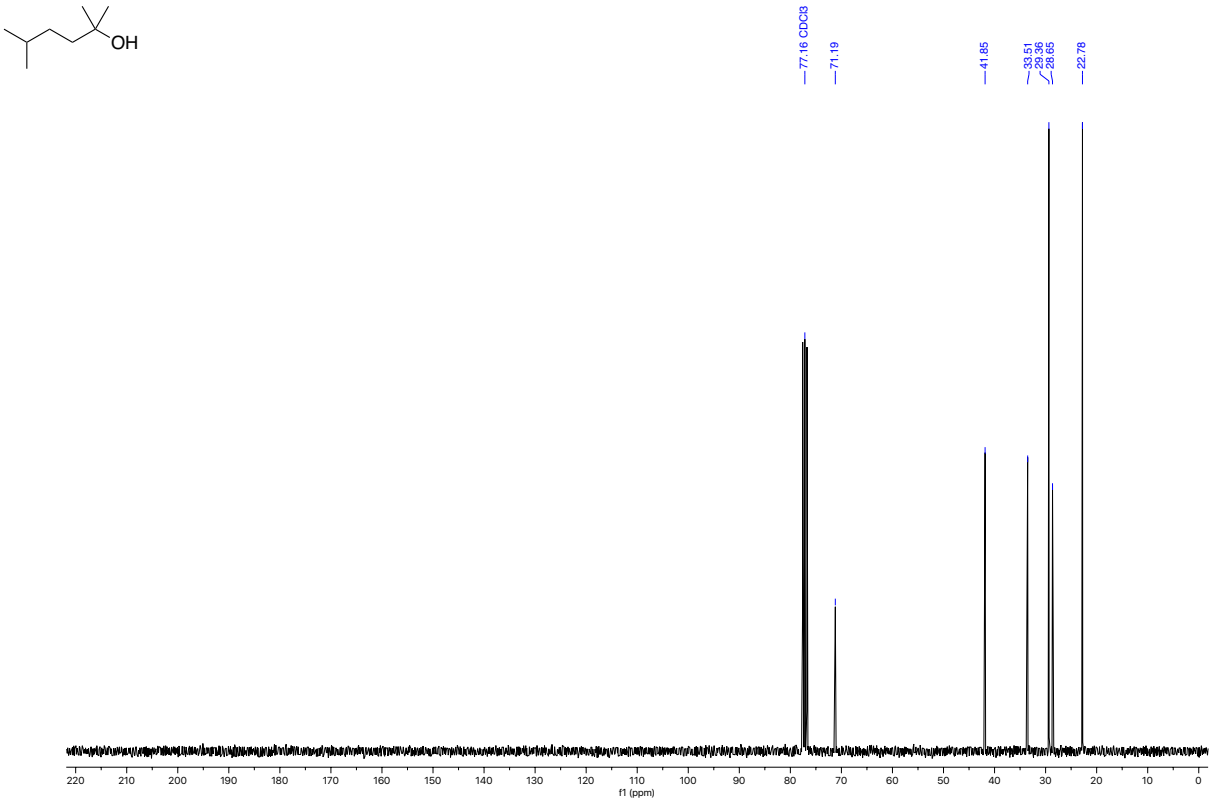

^{1}H NMR (300 MHz, $CDCl_3$)
2-hydroperoxy-2,5-dimethylhexane

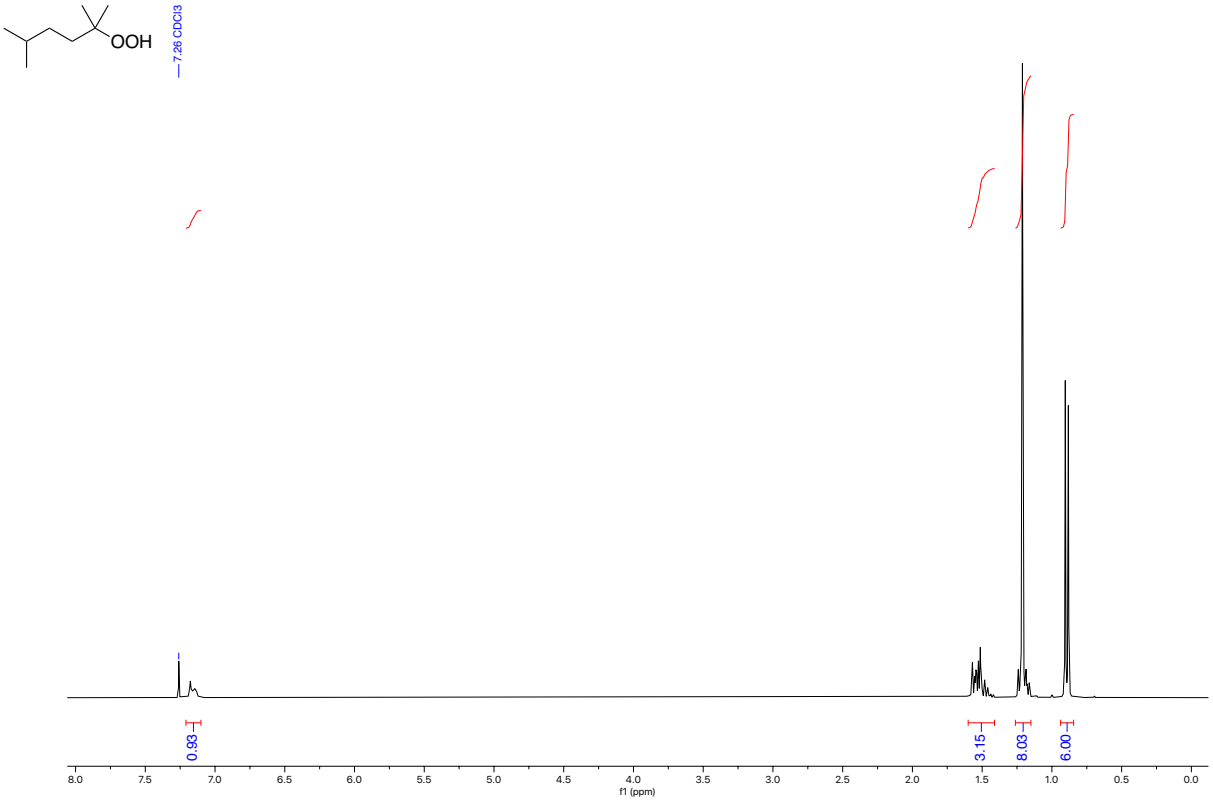

^{13}C NMR (75 MHz, $CDCl_3$)
2-hydroperoxy-2,5-dimethylhexane

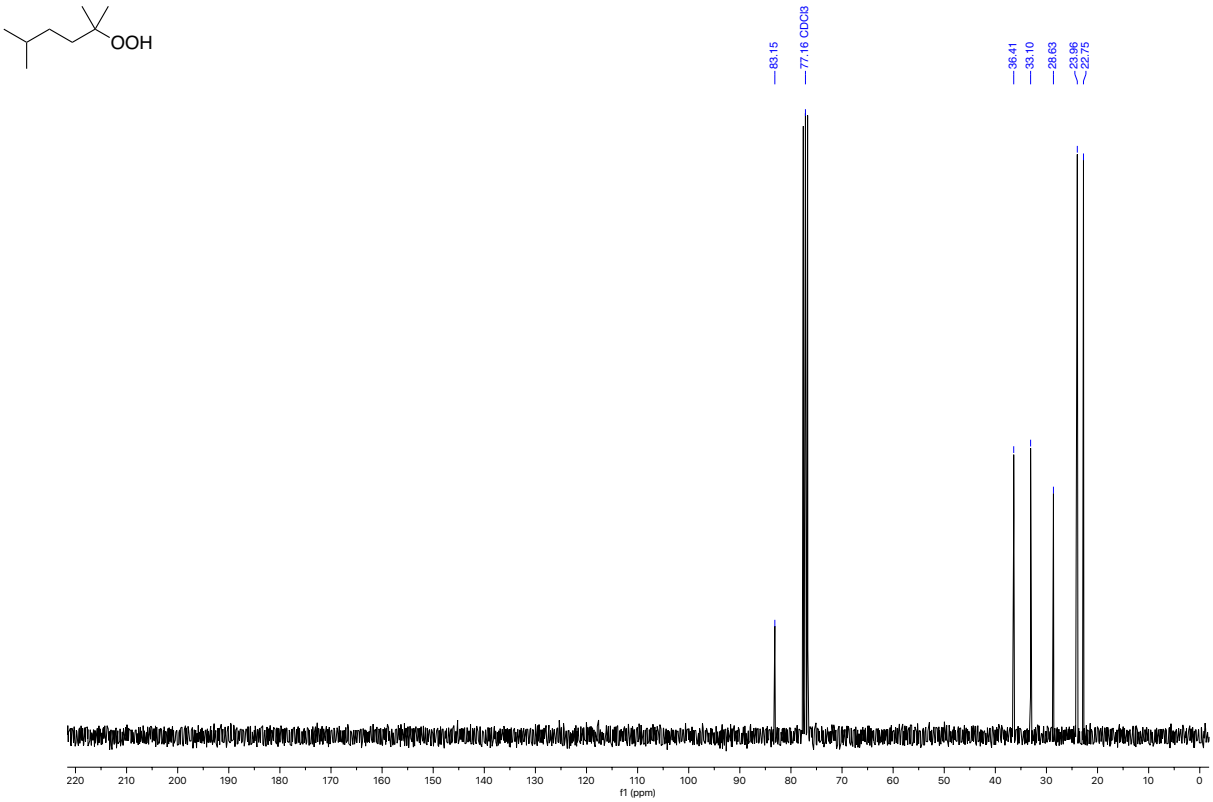

^{1}H NMR (300 MHz, $CDCl_3$)
2-methyloctan-2-ol

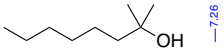

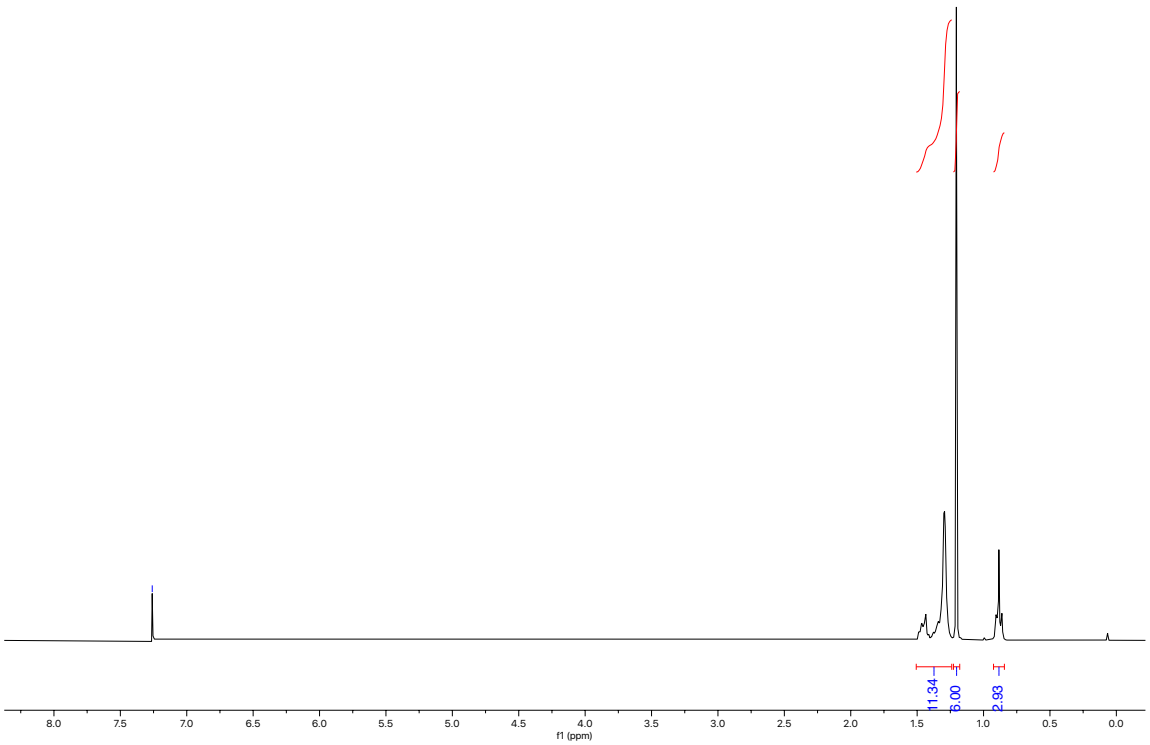

^{13}C NMR (75 MHz, $CDCl_3$)
2-methyloctan-2-ol

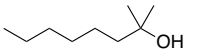

^{1}H NMR (300 MHz, $CDCl_3$)
2-hydroperoxy-2-methyloctane

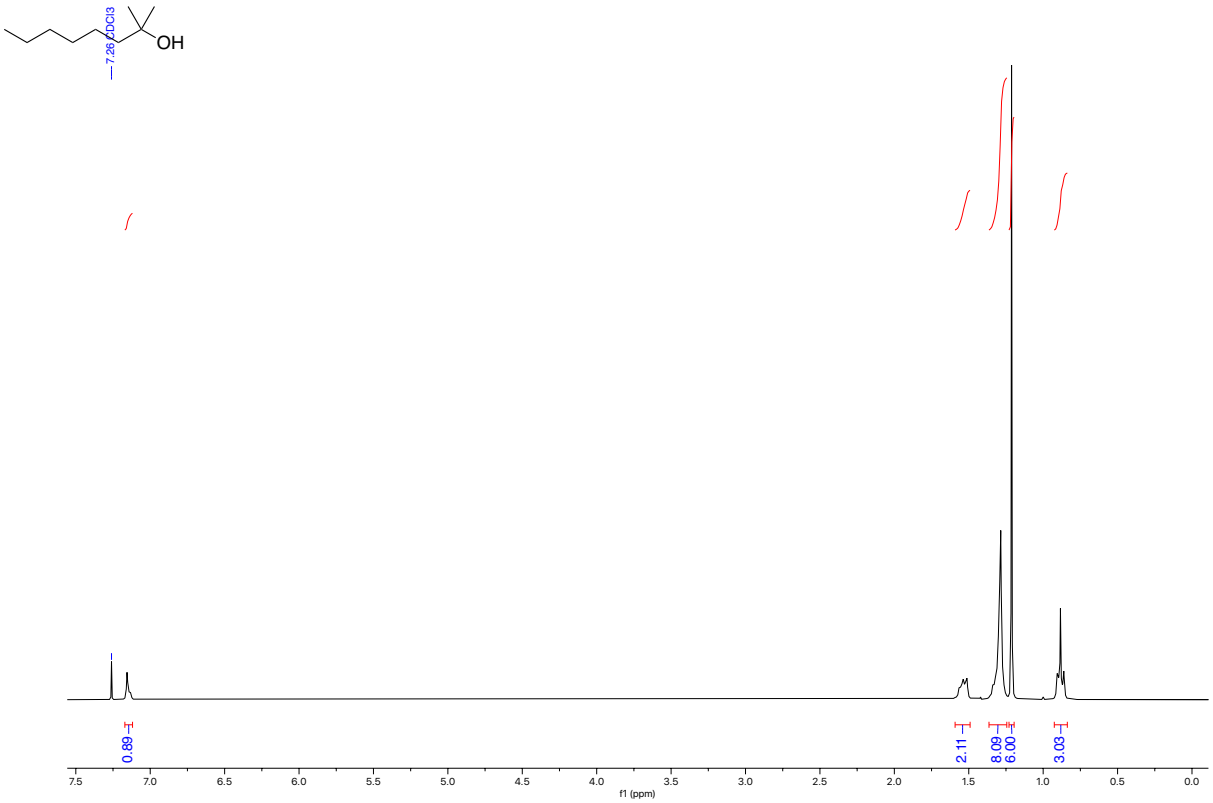

^{13}C NMR (75 MHz, $CDCl_3$)
2-hydroperoxy-2-methyloctane

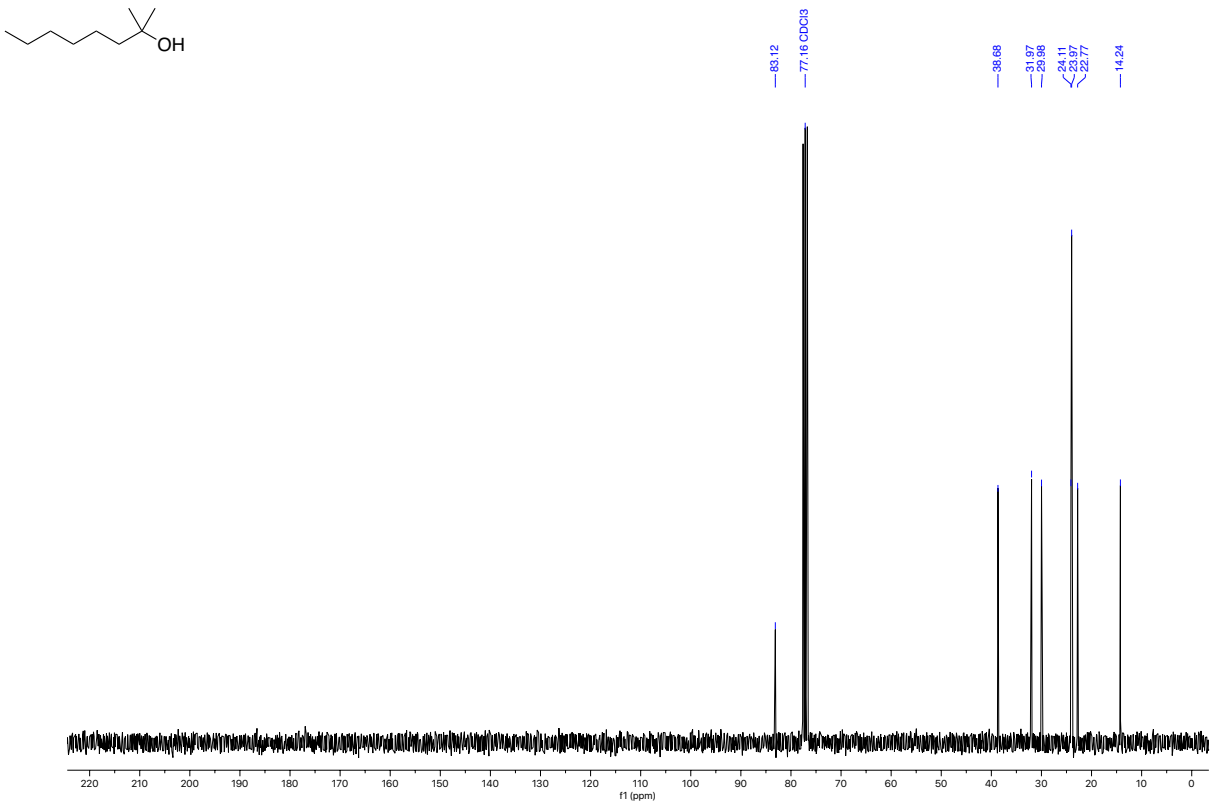

^{1}H NMR (300 MHz, $CDCl_3$)
1-methylcyclohexan-1-ol

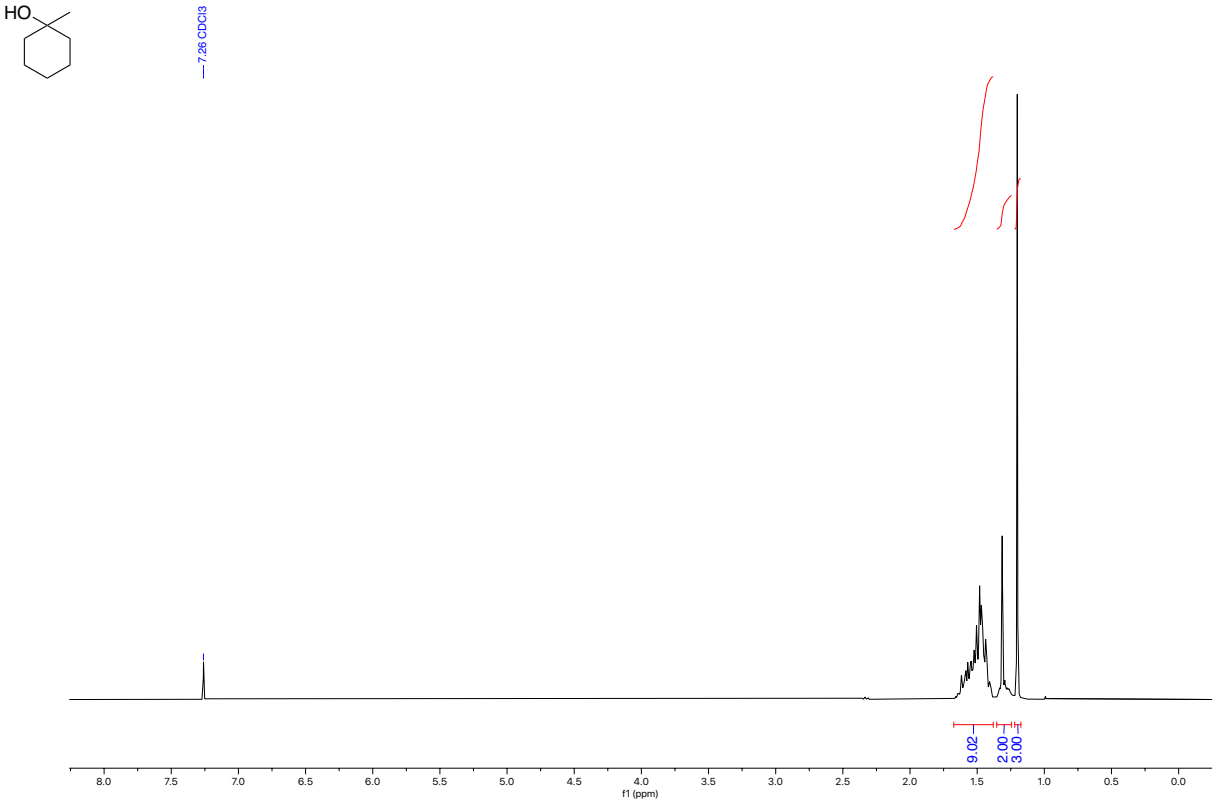

^{13}C NMR (75 MHz, $CDCl_3$)
1-methylcyclohexan-1-ol

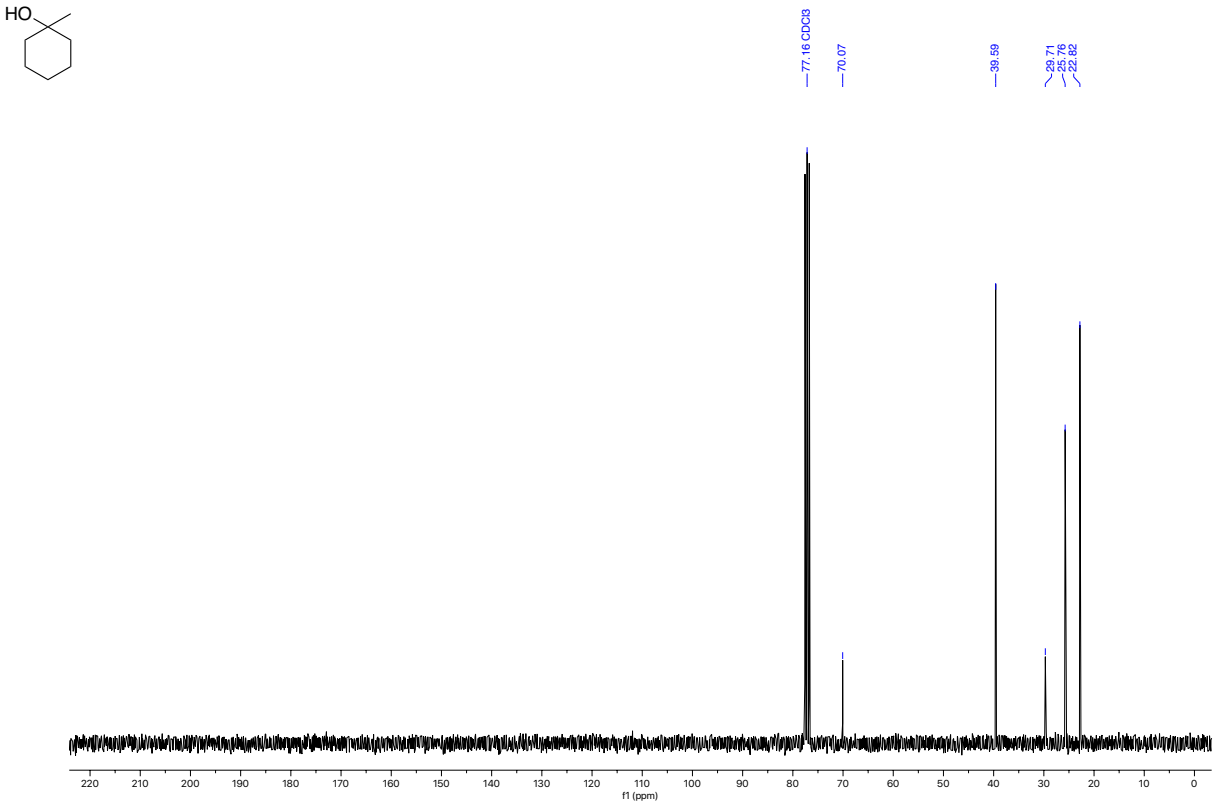

^{1}H NMR (300 MHz, $CDCl_3$)
1-hydroperoxy-1-methylcyclohexane

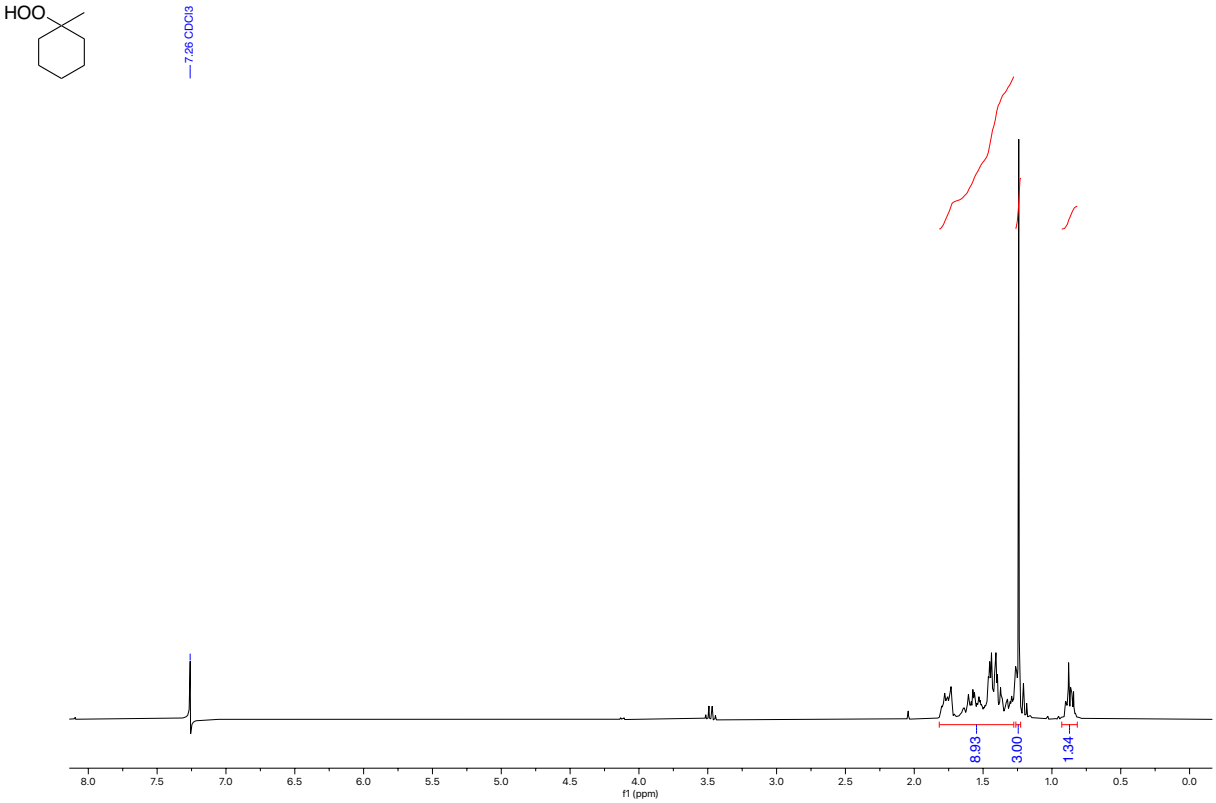

^{13}C NMR (75 MHz, $CDCl_3$)
1-hydroperoxy-1-methylcyclohexane

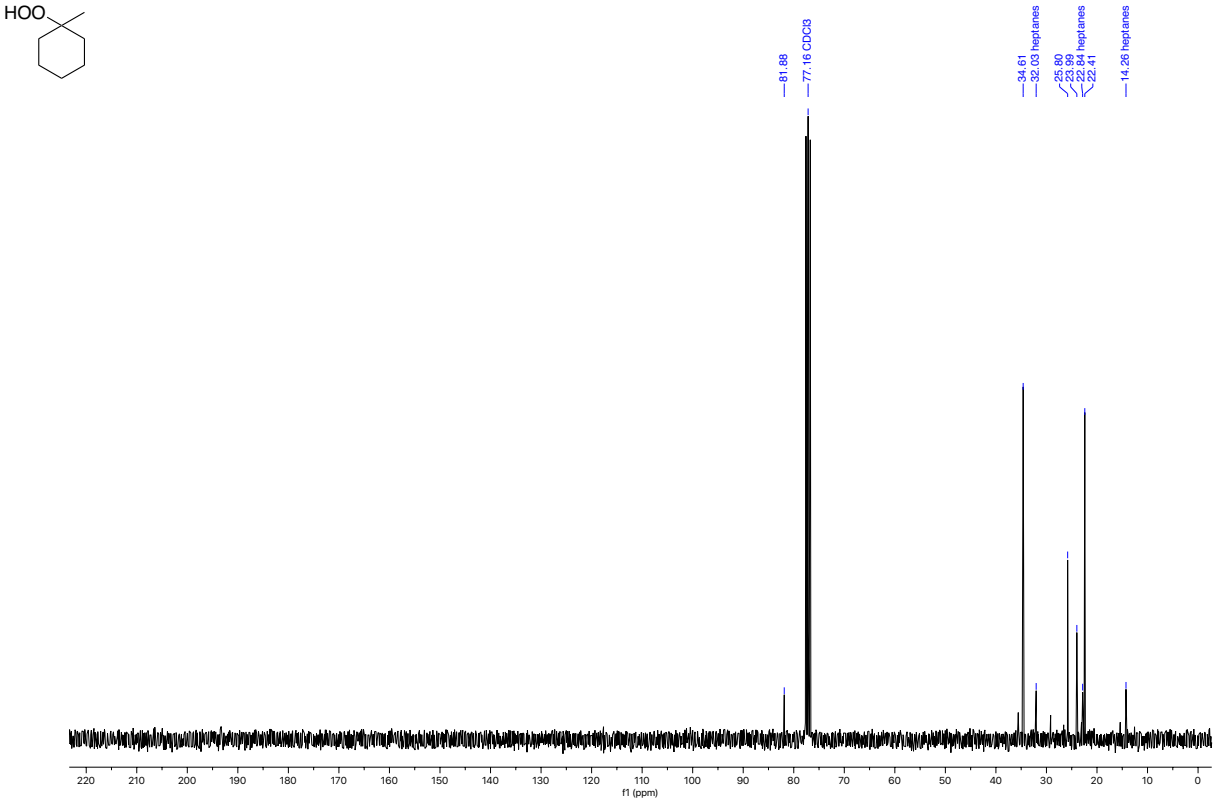

^{1}H NMR (300 MHz, $CDCl_3$)
2-methyl-1-phenylpropan-2-ol

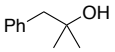

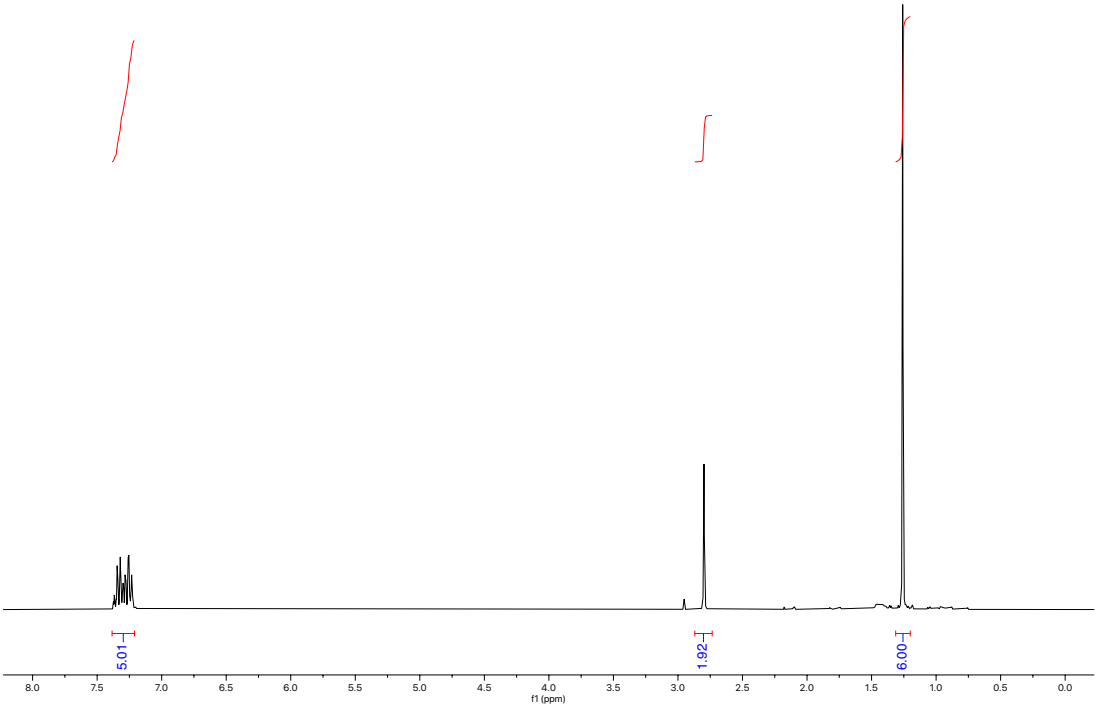

^{13}C NMR (75 MHz, $CDCl_3$)
2-methyl-1-phenylpropan-2-ol

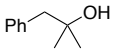

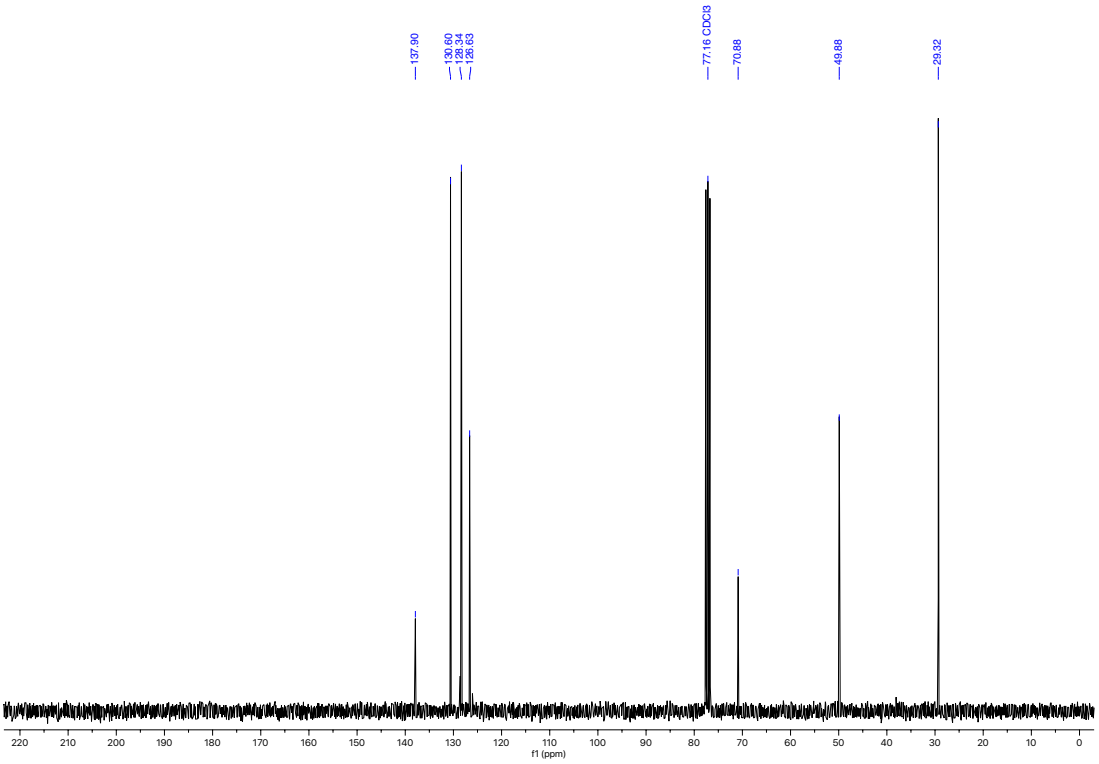

^{1}H NMR (300 MHz, $CDCl_3$)
(2-hydroperoxy-2-methylpropyl)benzene

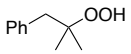

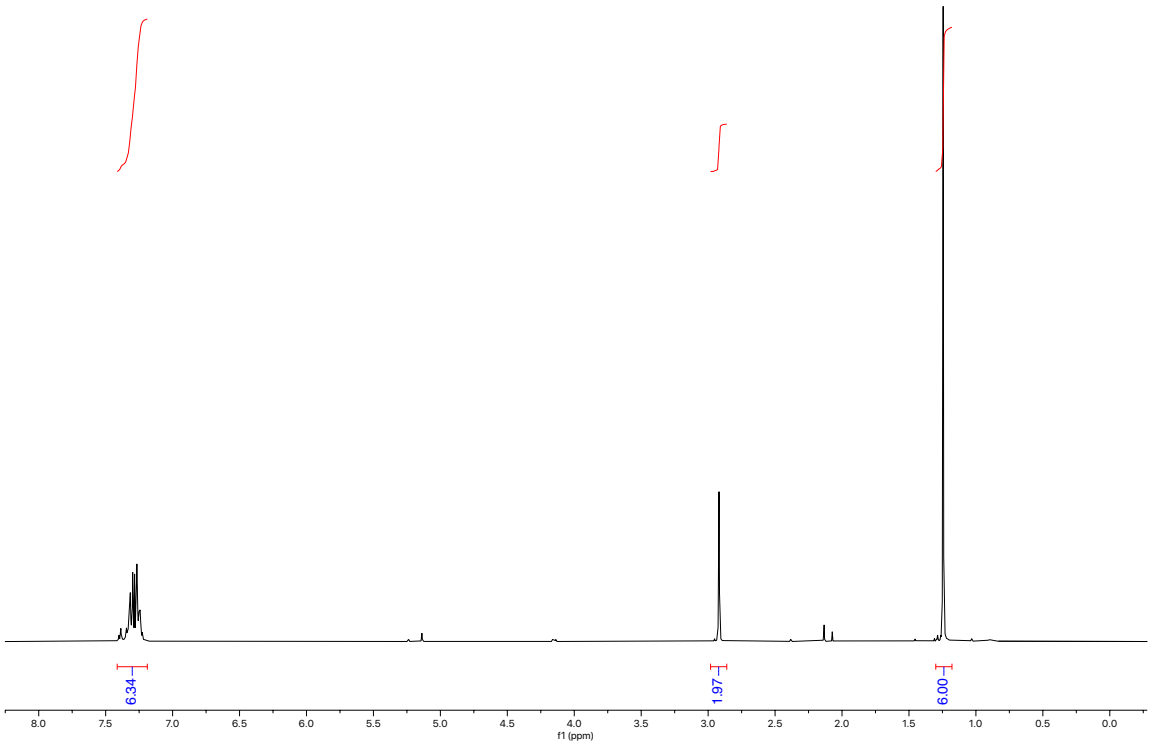

^{13}C NMR (75 MHz, $CDCl_3$)
(2-hydroperoxy-2-methylpropyl)benzene

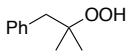

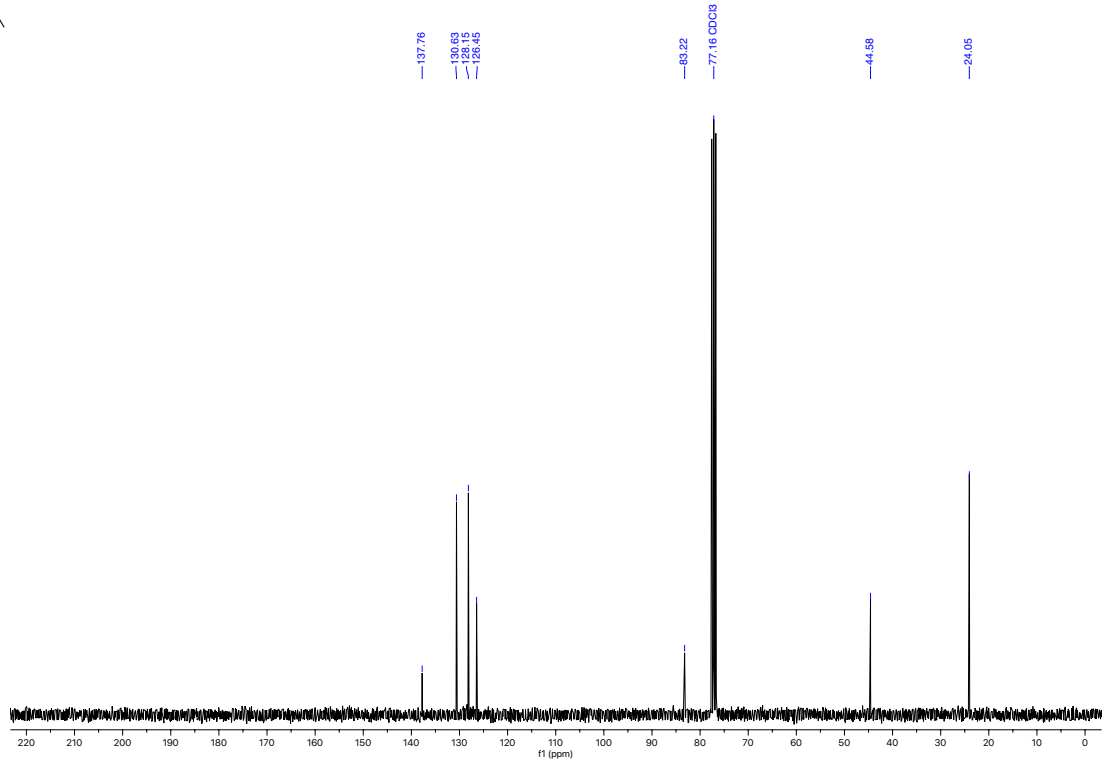

^{1}H NMR (300 MHz, $CDCl_3$)
2-methylhex-5-en-2-ol

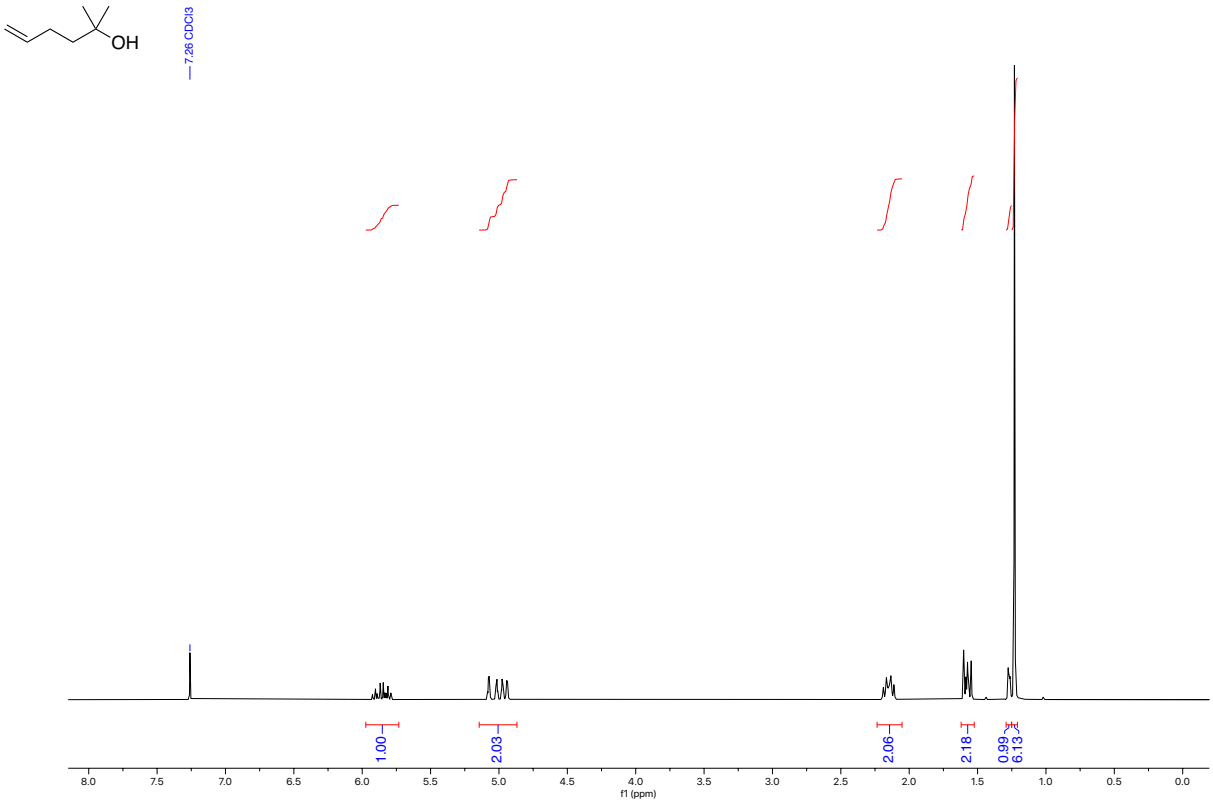

^{13}C NMR (75 MHz, $CDCl_3$)
2-methylhex-5-en-2-ol

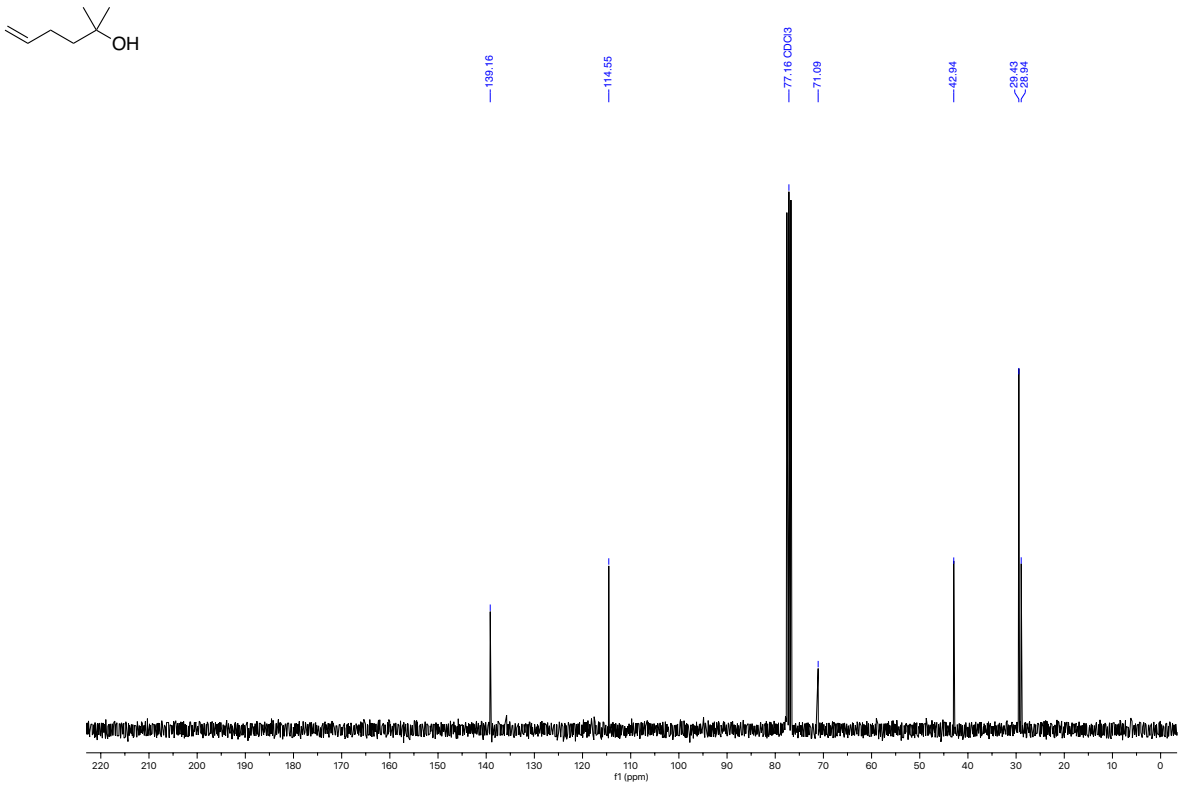

^{1}H NMR (300 MHz, $CDCl_3$)
5-hydroperoxy-5-methylhex-1-ene

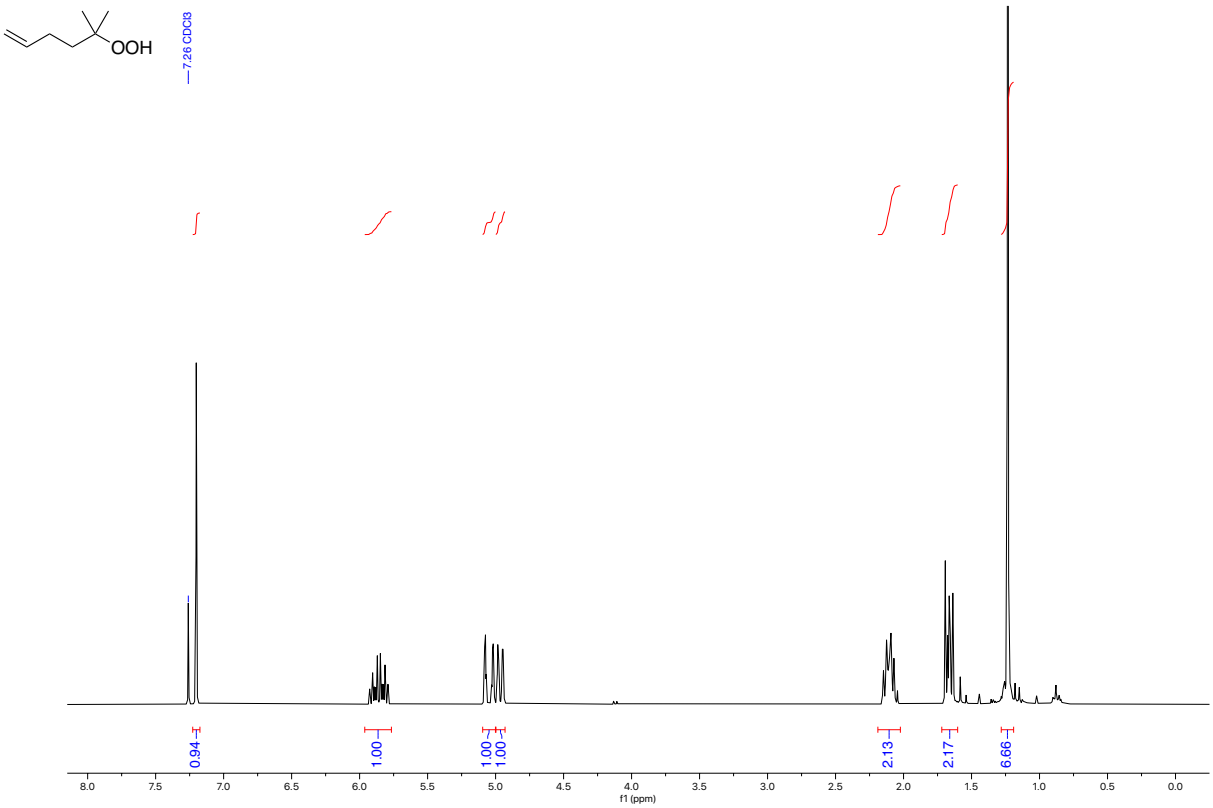

^{13}C NMR (75 MHz, $CDCl_3$)
5-hydroperoxy-5-methylhex-1-ene

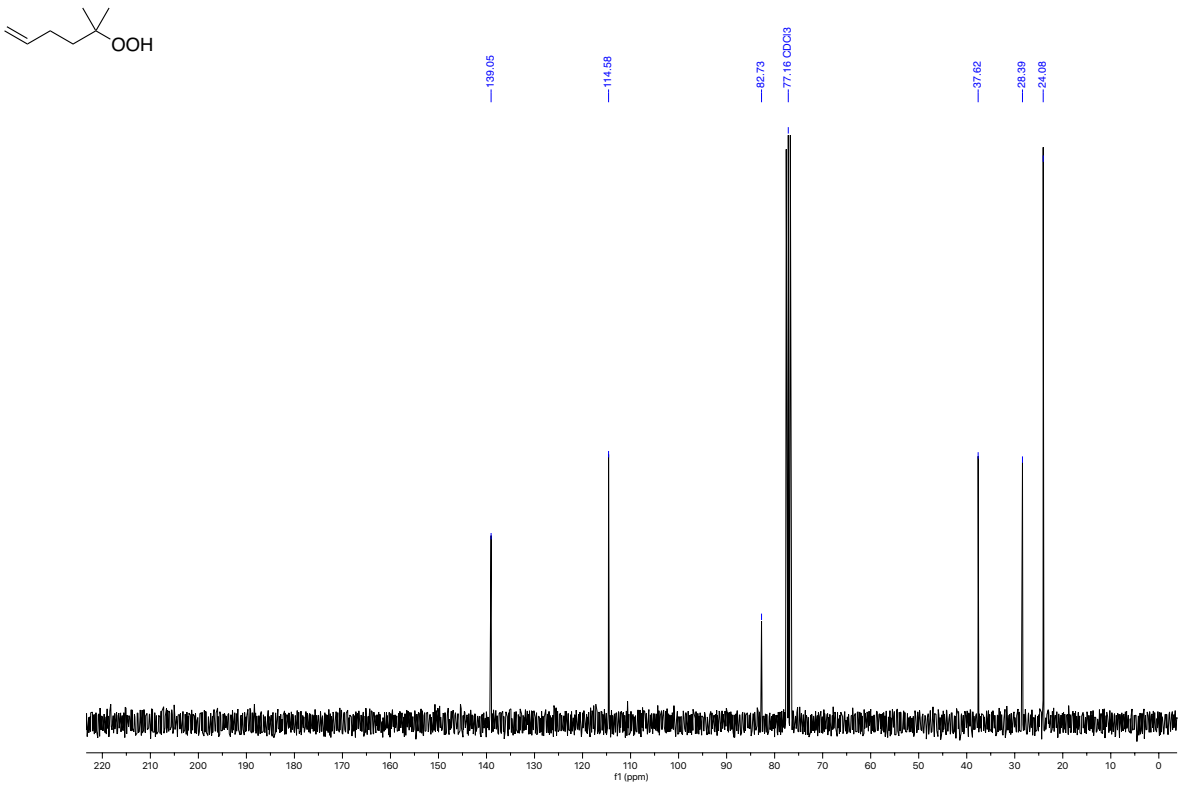

^{1}H NMR (300 MHz, CD_2Cl_2)
S-phenyl benzenesulfonothioate

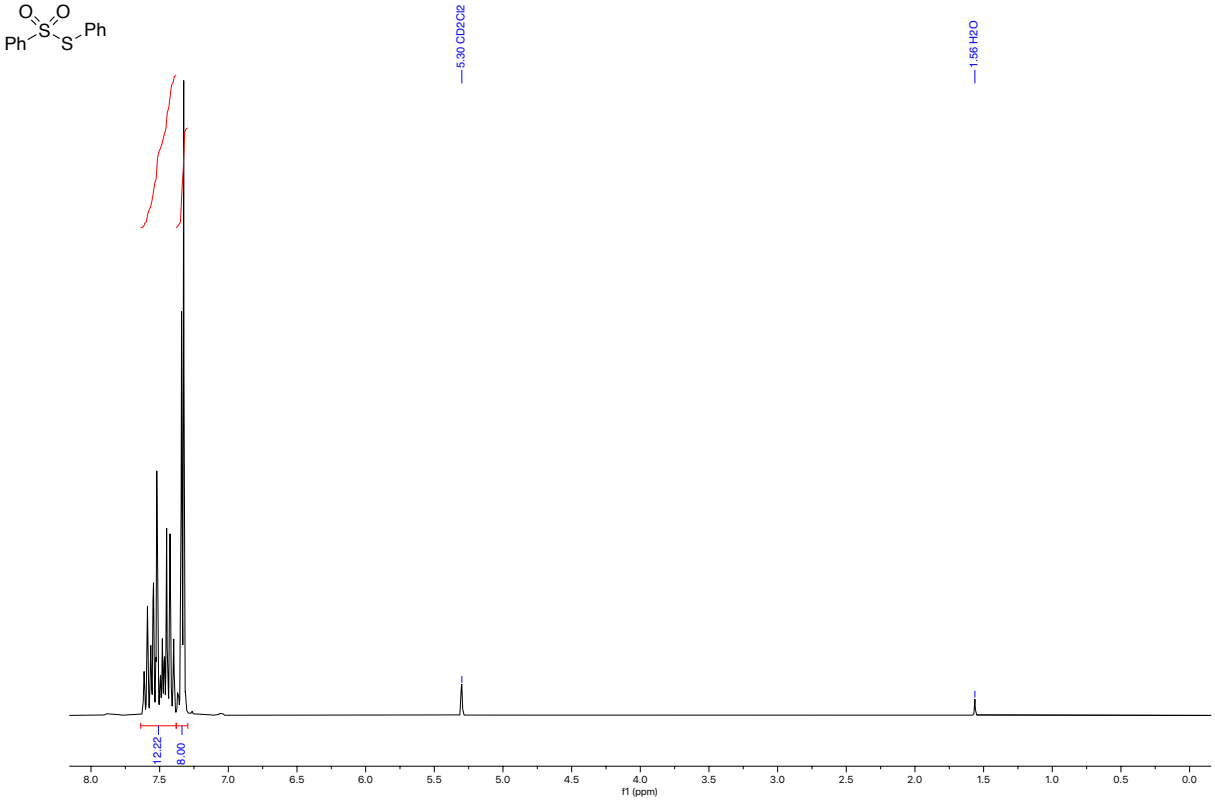

^{13}C NMR (75 MHz, CD_2Cl_2)
S-phenyl benzenesulfonothioate

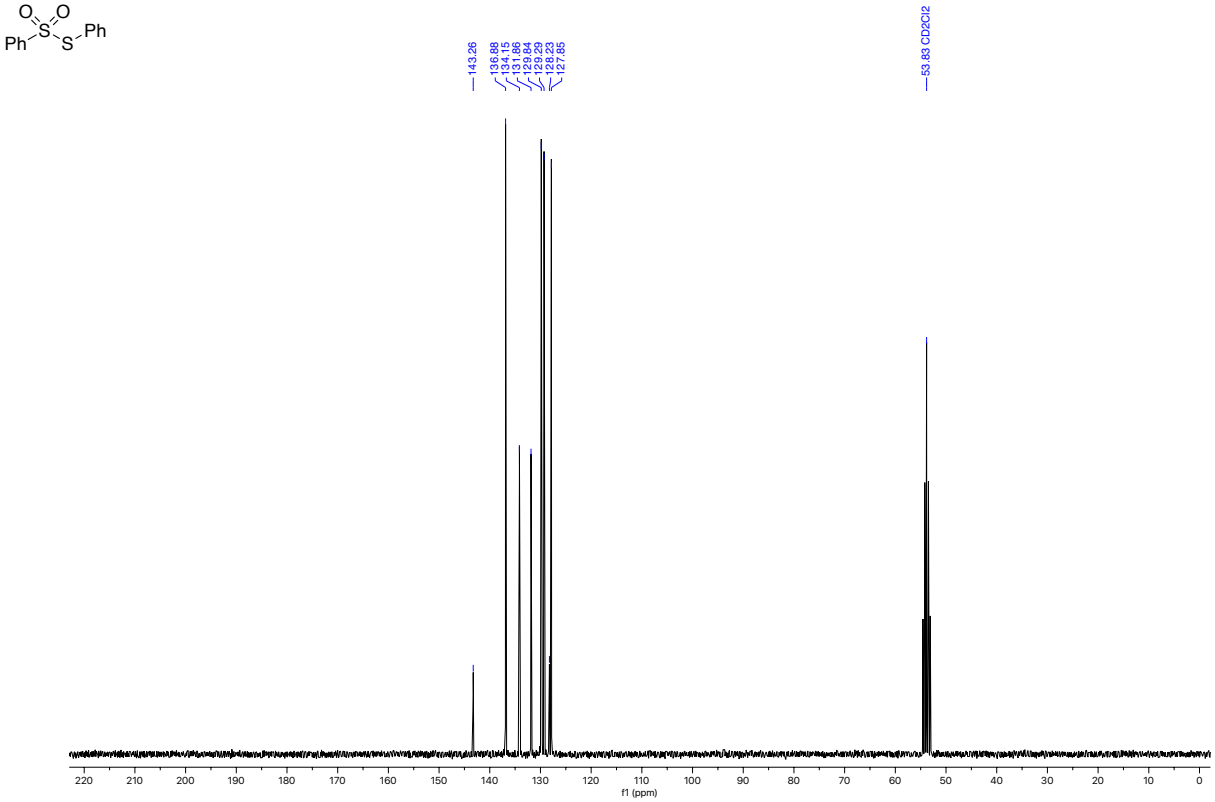

^{1}H NMR (300 MHz, $CDCl_3$)
Trimethyl(2-phenylsulfanylethynyl)silane

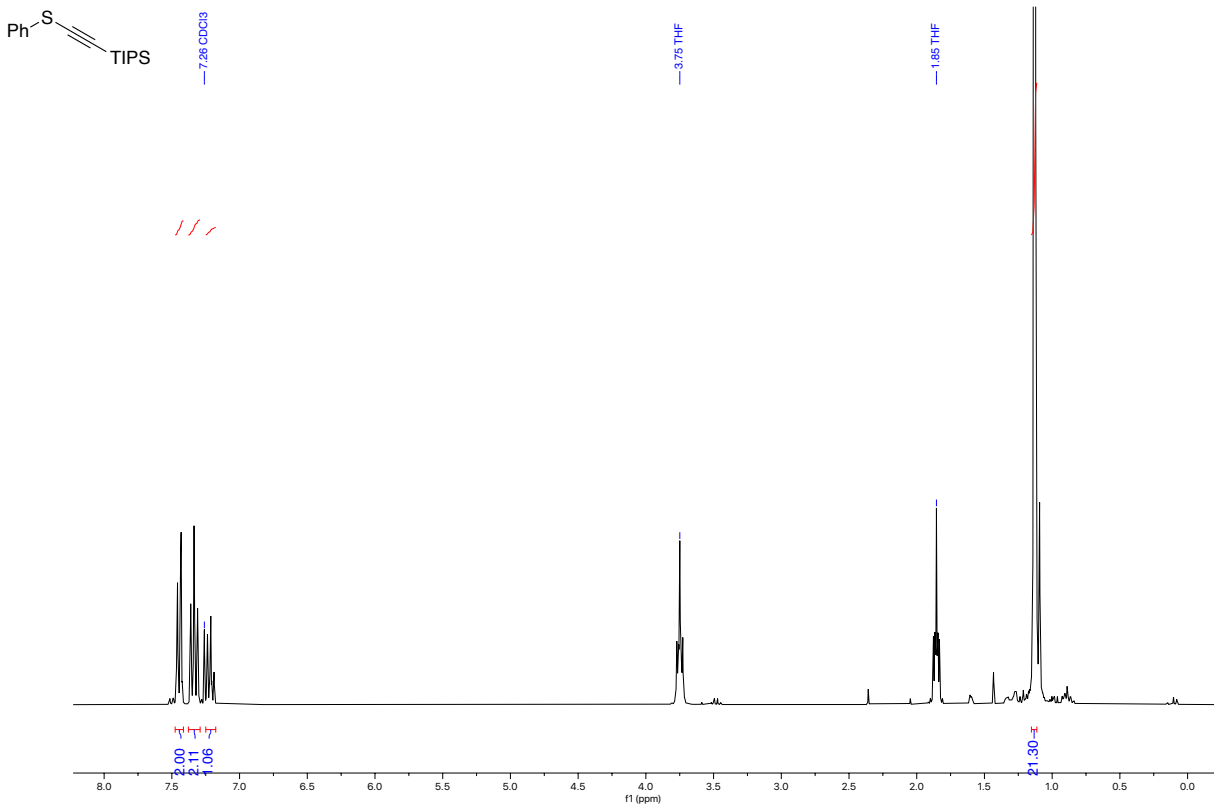

^{13}C NMR (75 MHz, $CDCl_3$)
Trimethyl(2-phenylsulfanylethynyl)silane

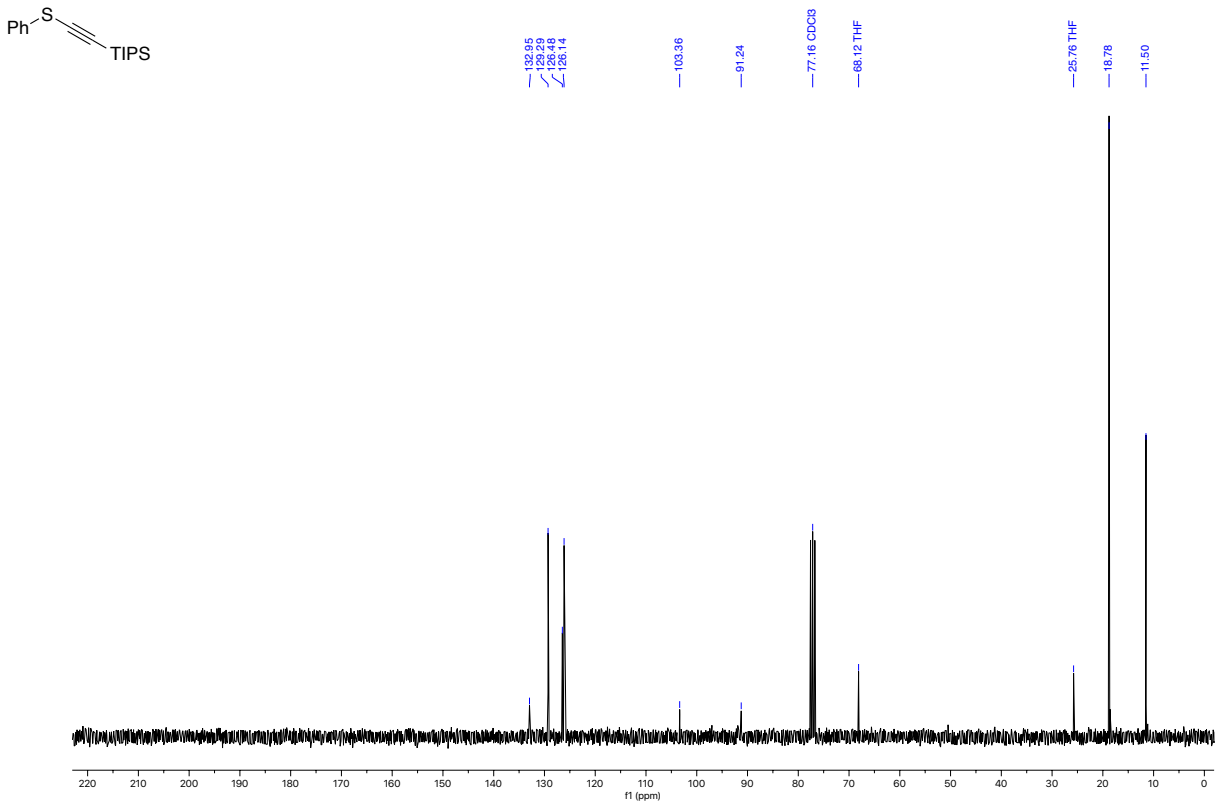

^{1}H NMR (300 MHz, $CDCl_3$)
Triisopropyl((phenylsulfonyl)ethynyl)silane

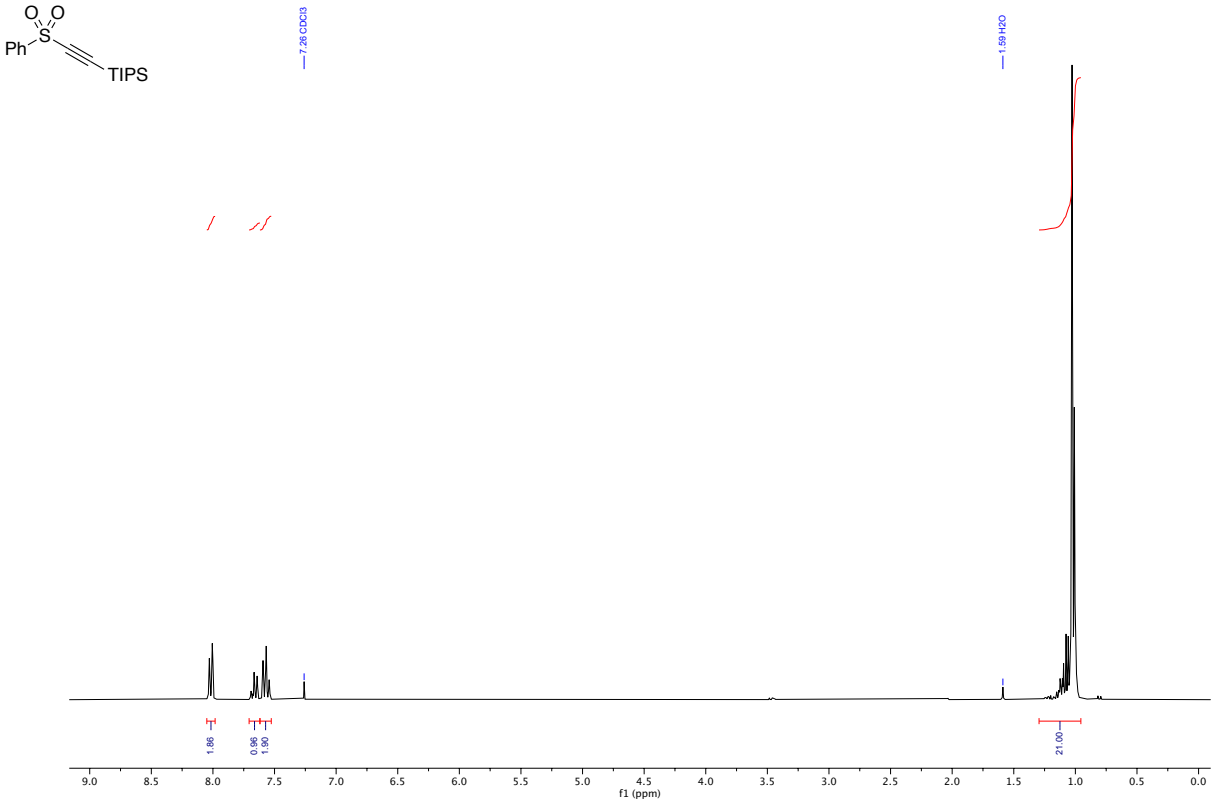

^{13}C NMR (75 MHz, $CDCl_3$)
Triisopropyl((phenylsulfonyl)ethynyl)silane

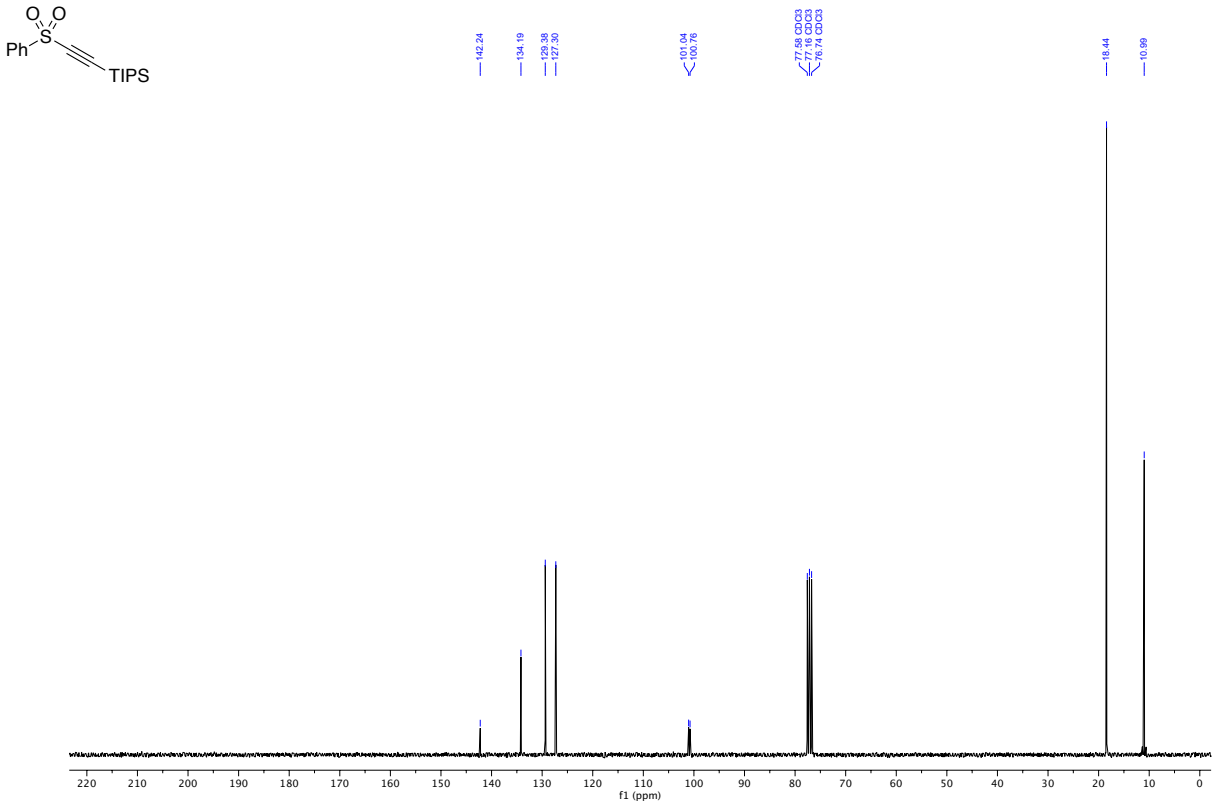

^{1}H NMR (300 MHz, CD_2Cl_2)
Benzenesulfonyl azide

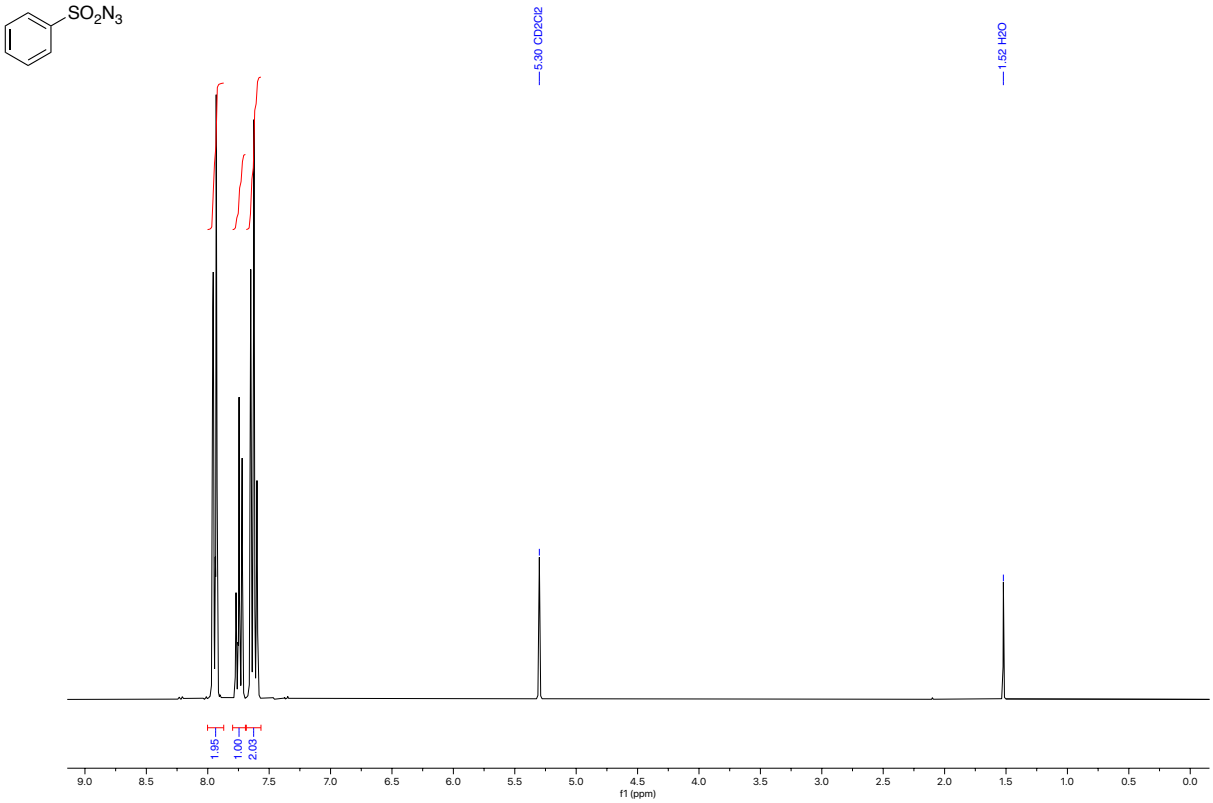

^{13}C NMR (75 MHz, CD_2Cl_2)
Benzenesulfonyl azide

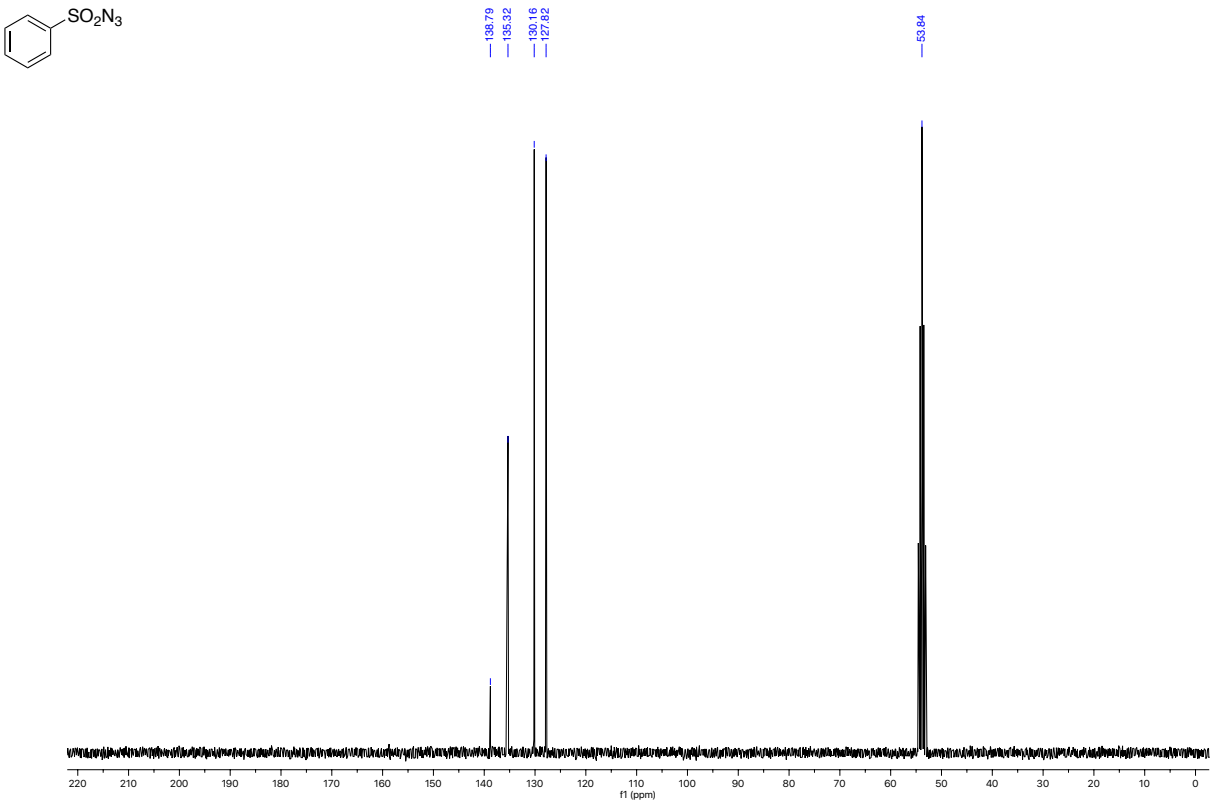

^{1}H NMR (300 MHz, $CDCl_3$)
((2-methylallyl)sulfonyl)benzene

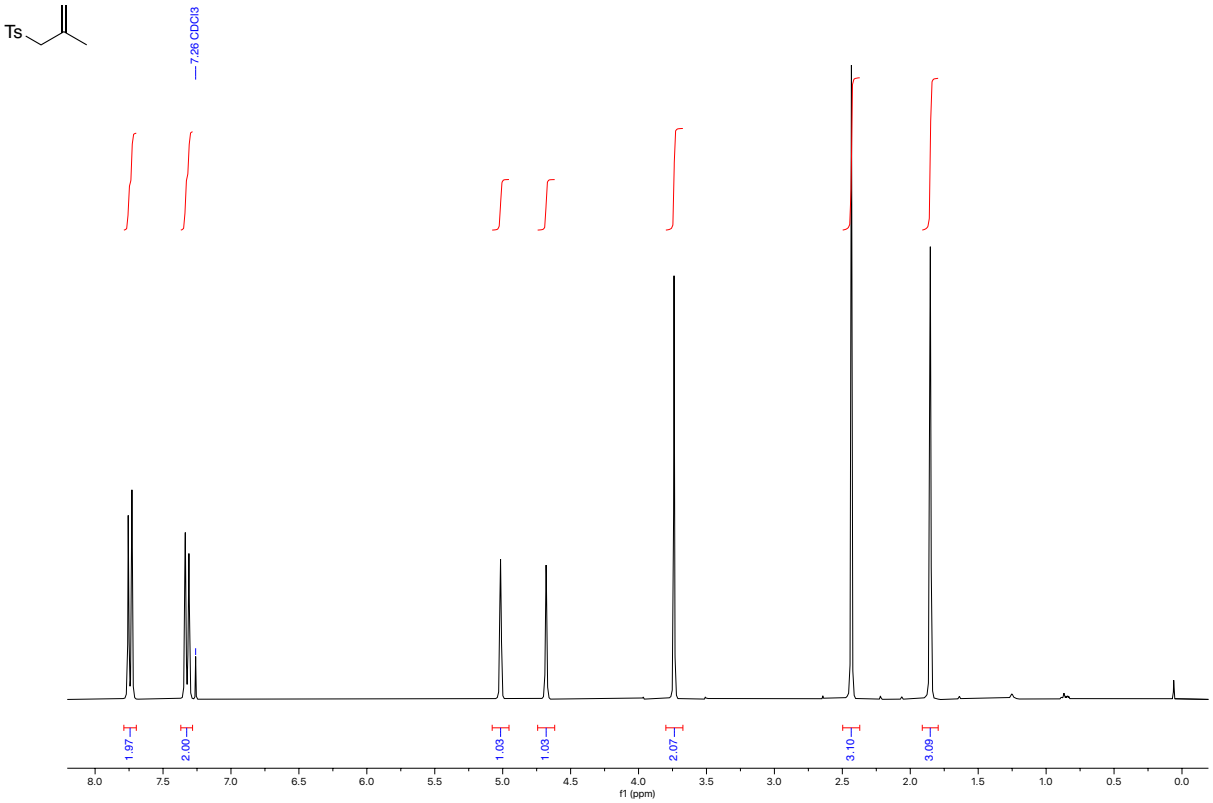

^{13}C NMR (75 MHz, $CDCl_3$)
((2-methylallyl)sulfonyl)benzene

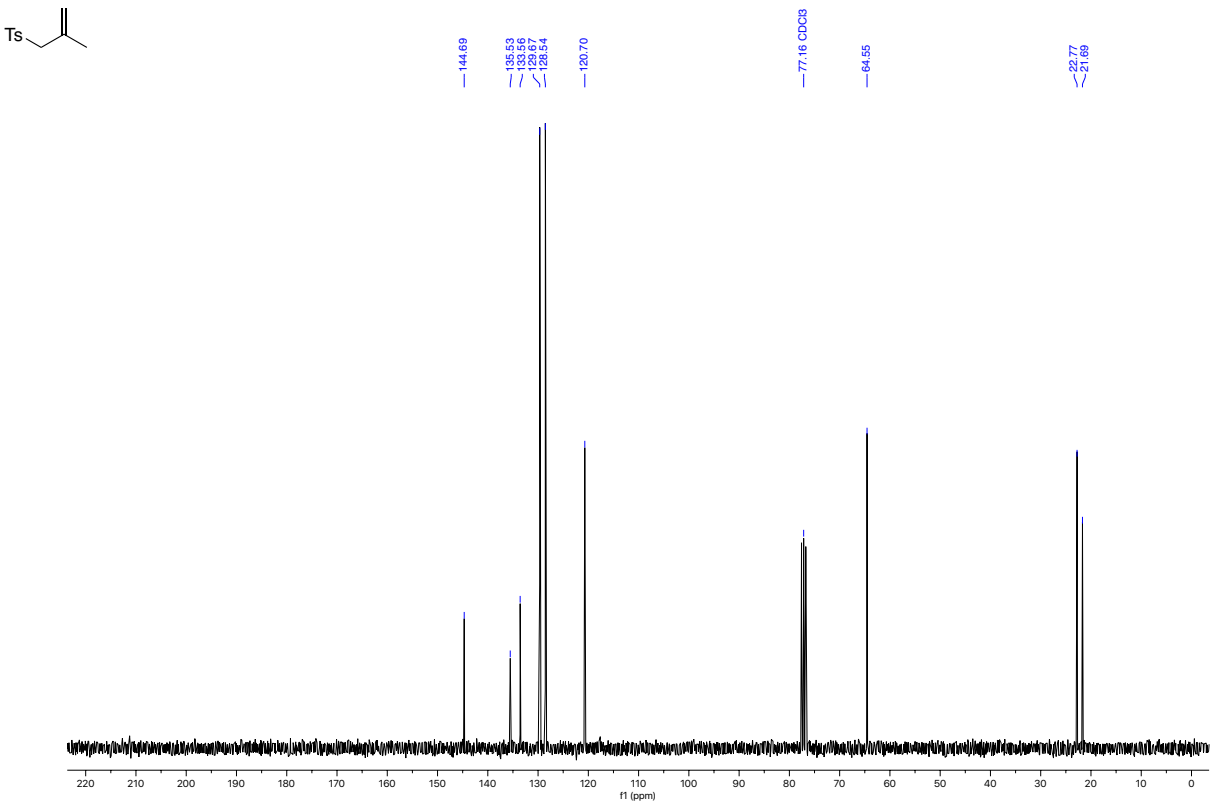

^{1}H NMR (300 MHz, $CDCl_3$)
4-methylbenzenesulfonyl iodide

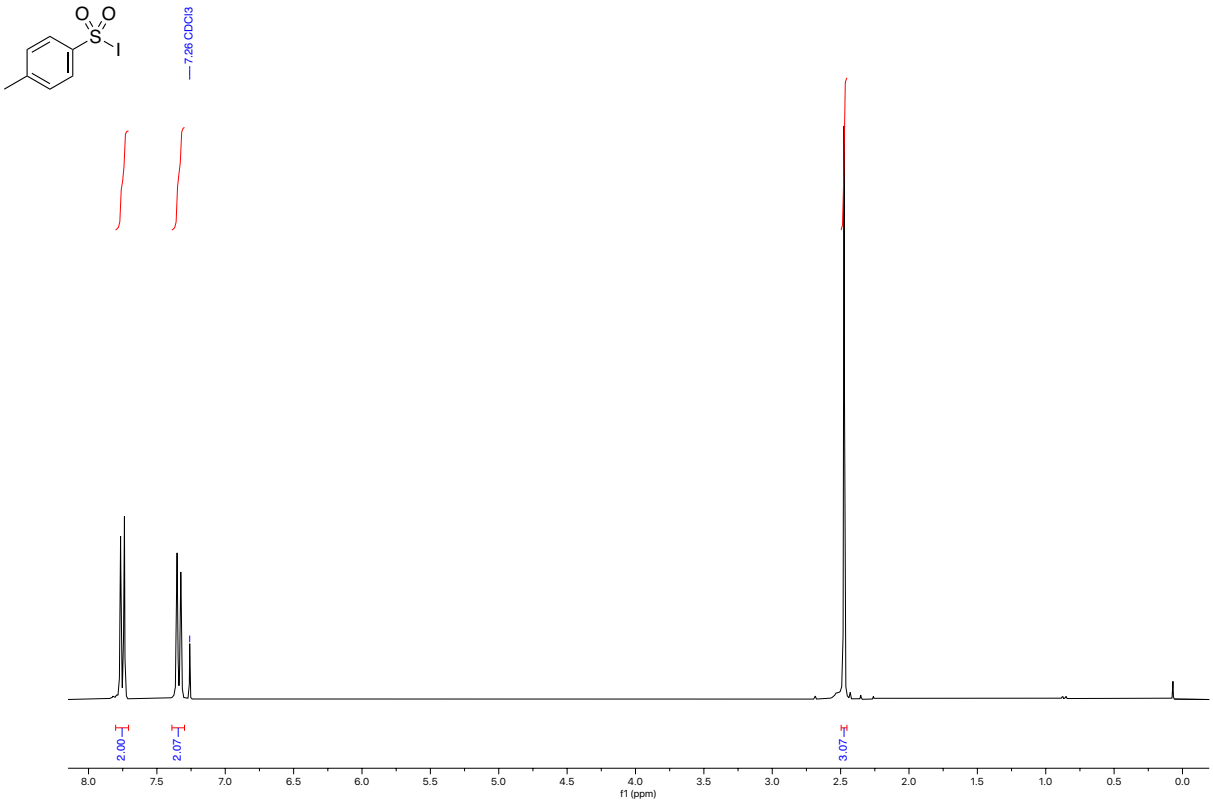

^{13}C NMR (75 MHz, $CDCl_3$)
4-methylbenzenesulfonyl iodide

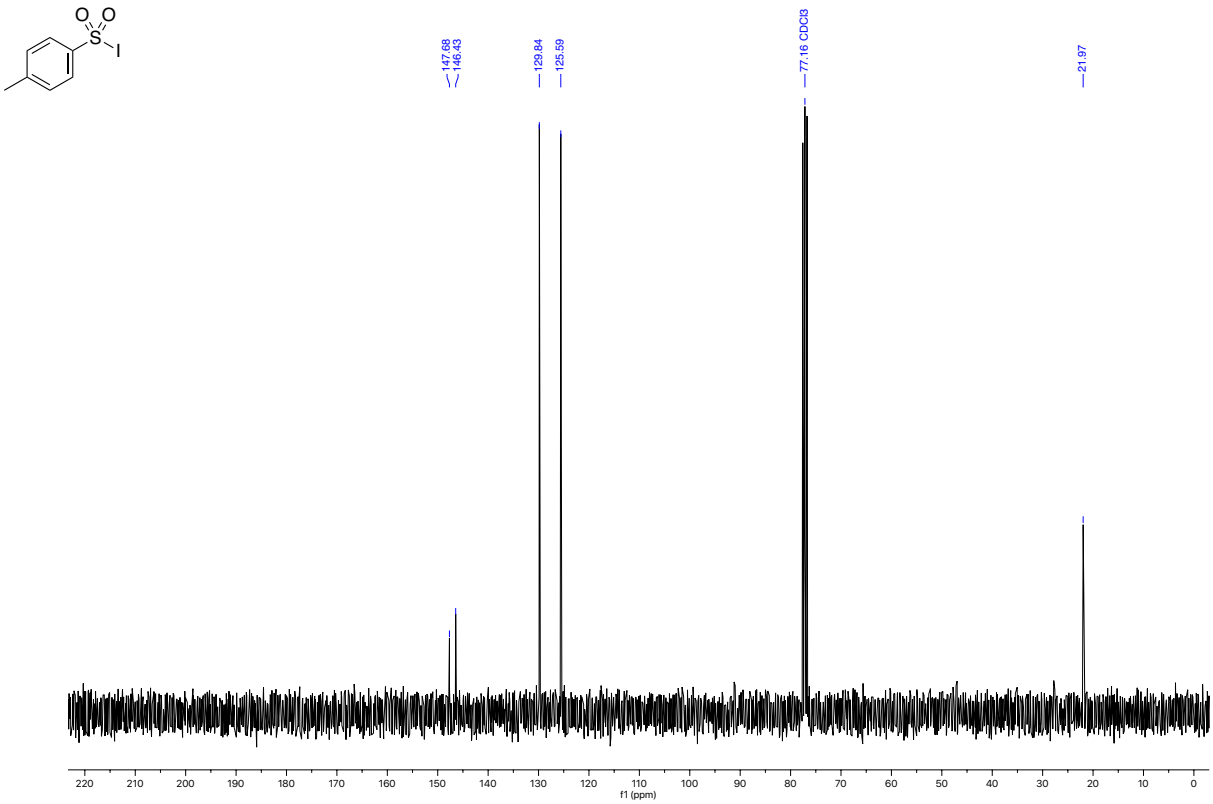

^{1}H NMR (300 MHz, $CDCl_3$)
4,4,5,5-tetramethyl-2-(3-tosylprop-1-en-2-yl)-1,3,2-dioxaborolane

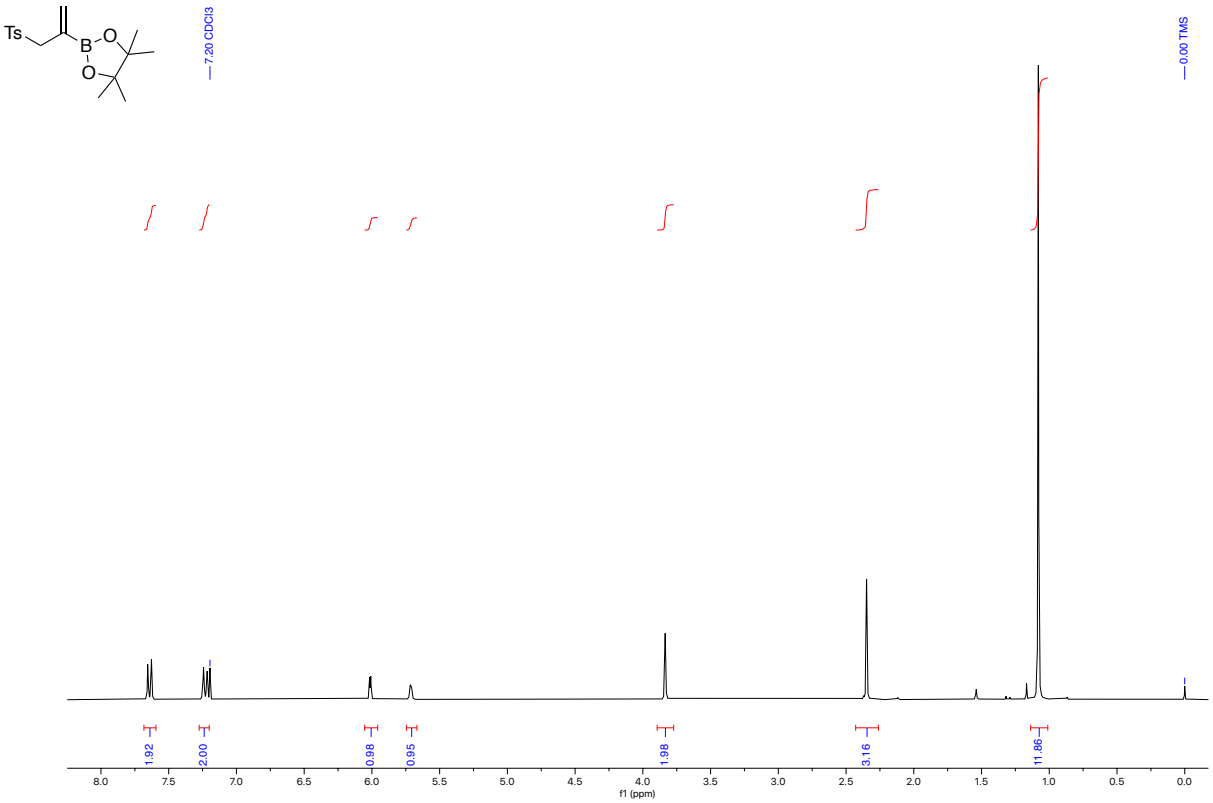

^{13}C NMR (75 MHz, $CDCl_3$)
4,4,5,5-tetramethyl-2-(3-tosylprop-1-en-2-yl)-1,3,2-dioxaborolane

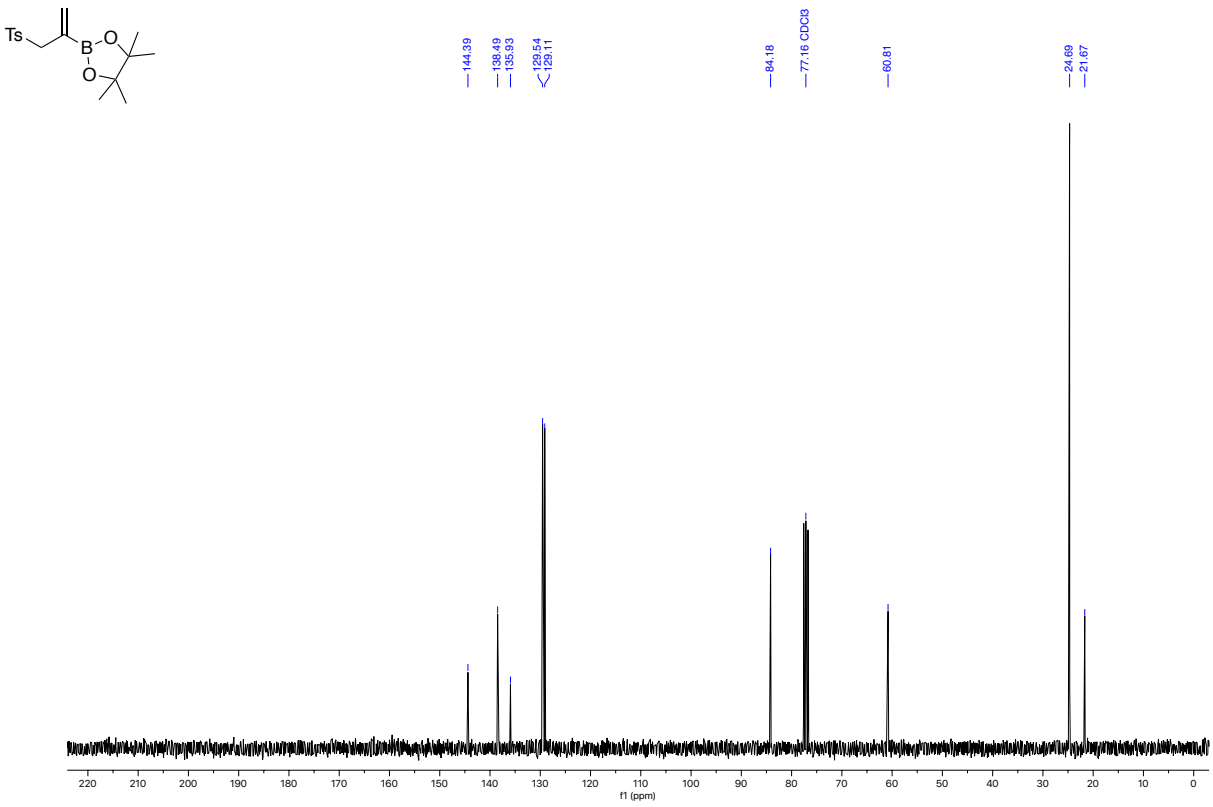

^{11}B NMR (96 MHz, $CDCl_3$)
4,4,5,5-tetramethyl-2-(3-tosylprop-1-en-2-yl)-1,3,2-dioxaborolane

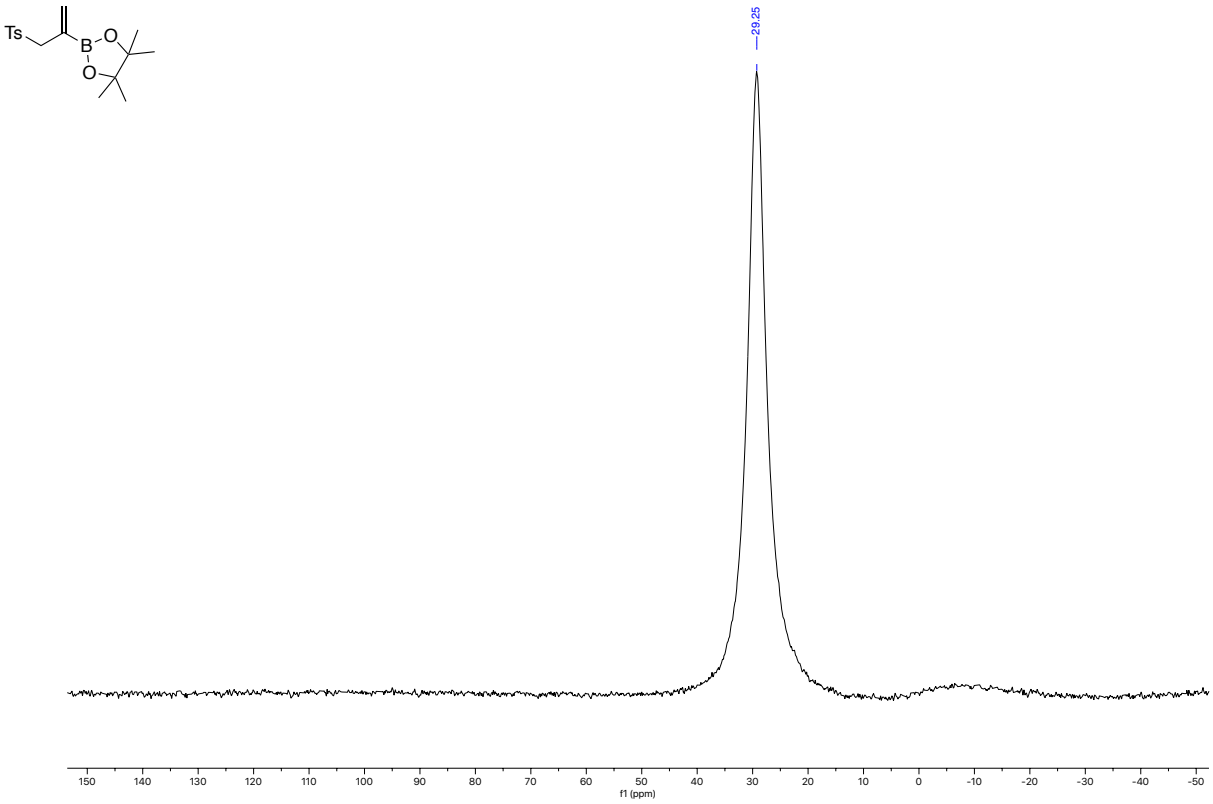

^{1}H NMR (300 MHz, $CDCl_3$)
4-methylbenzenesulfonyl bromide

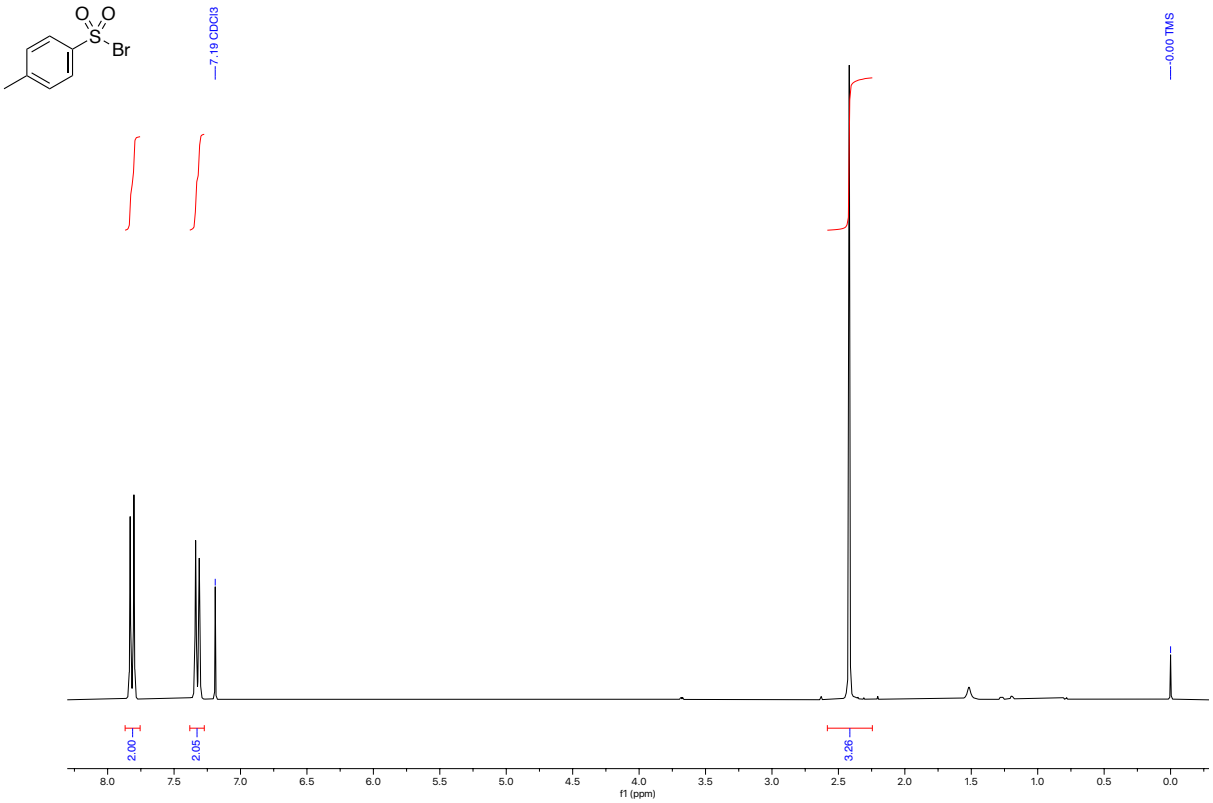

^{13}C NMR (75 MHz, $CDCl_3$)
4-methylbenzenesulfonyl bromide

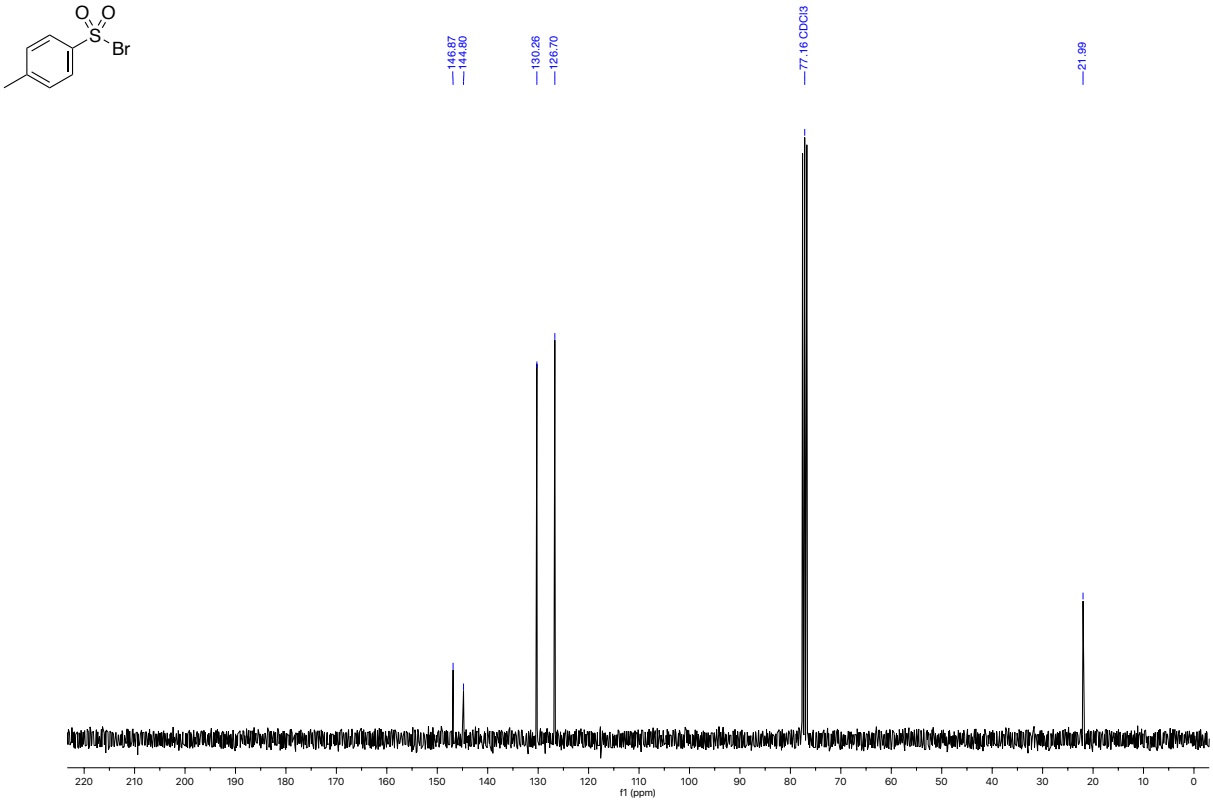

^{1}H NMR (300 MHz, $CDCl_3$)
2,5-dimethyl-5-(phenylthio)hexan-2-ol

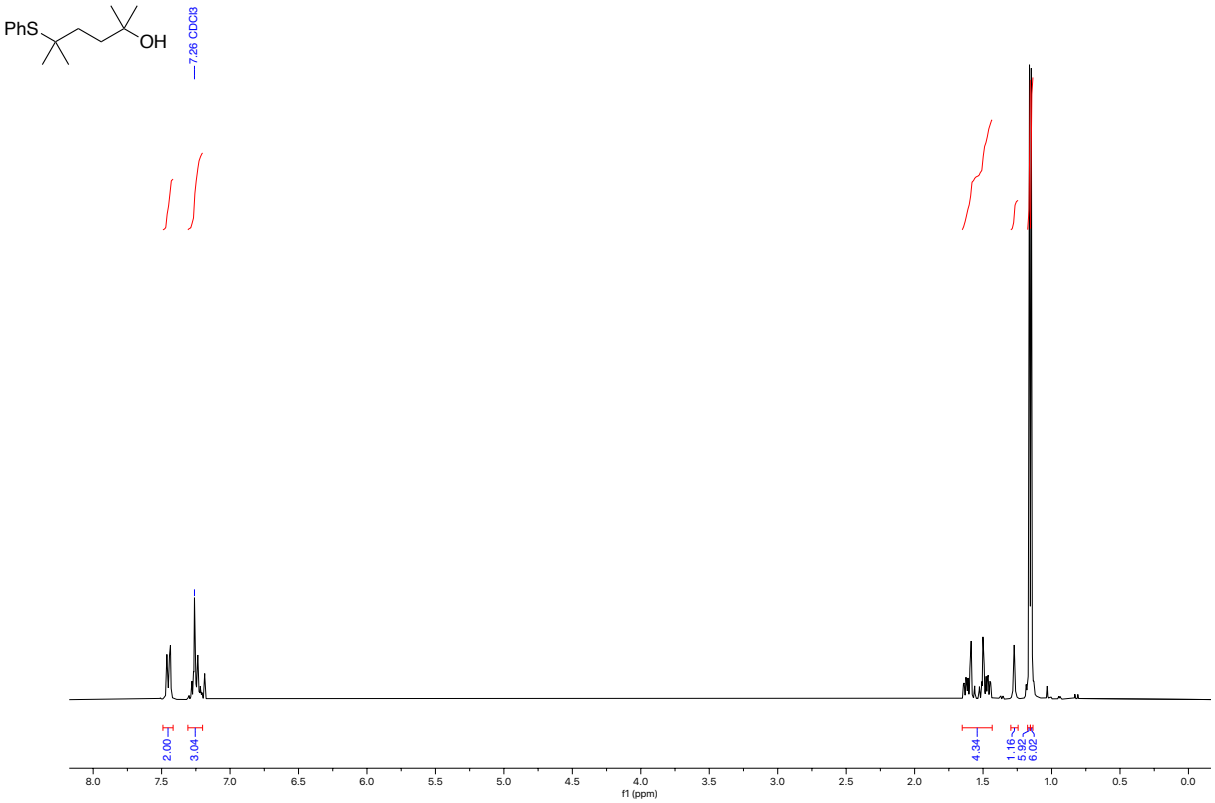

^{13}C NMR (75 MHz, $CDCl_3$)
2,5-dimethyl-5-(phenylthio)hexan-2-ol

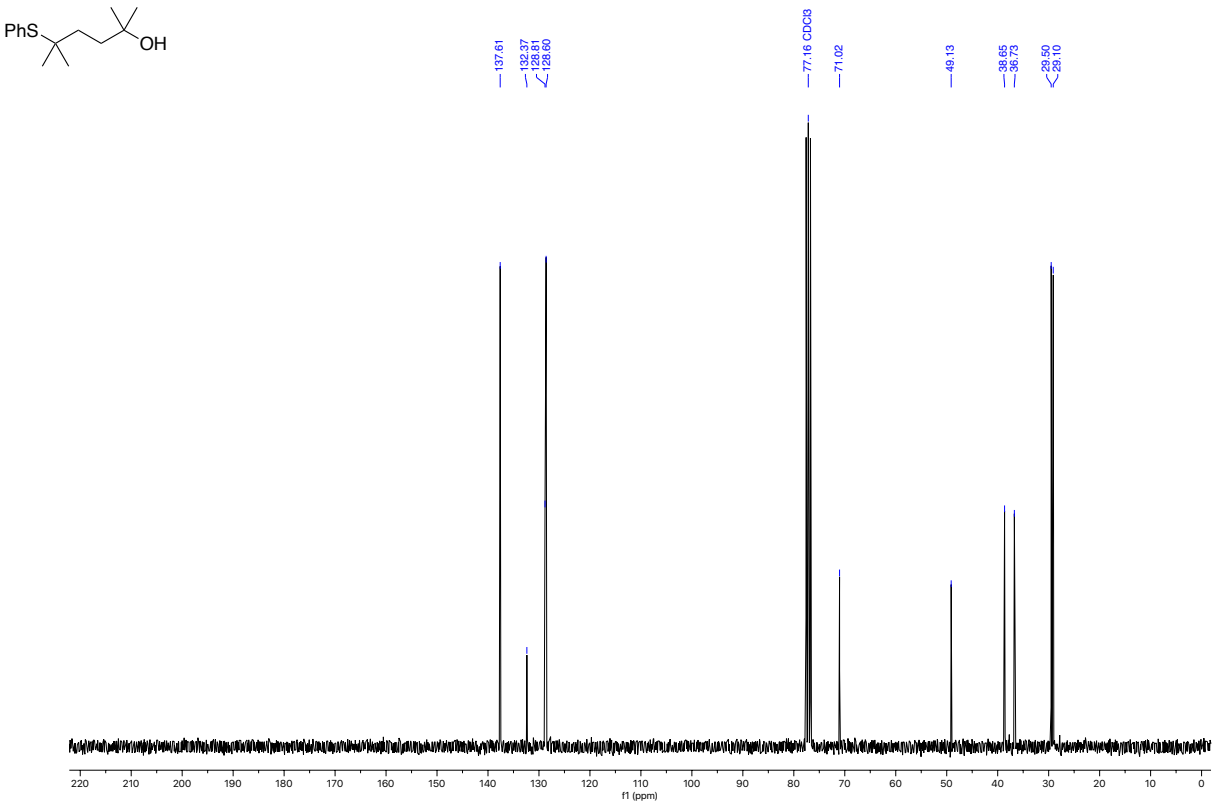

^{1}H NMR (300 MHz, $CDCl_3$)
5-chloro-2,5-dimethylhexan-2-ol

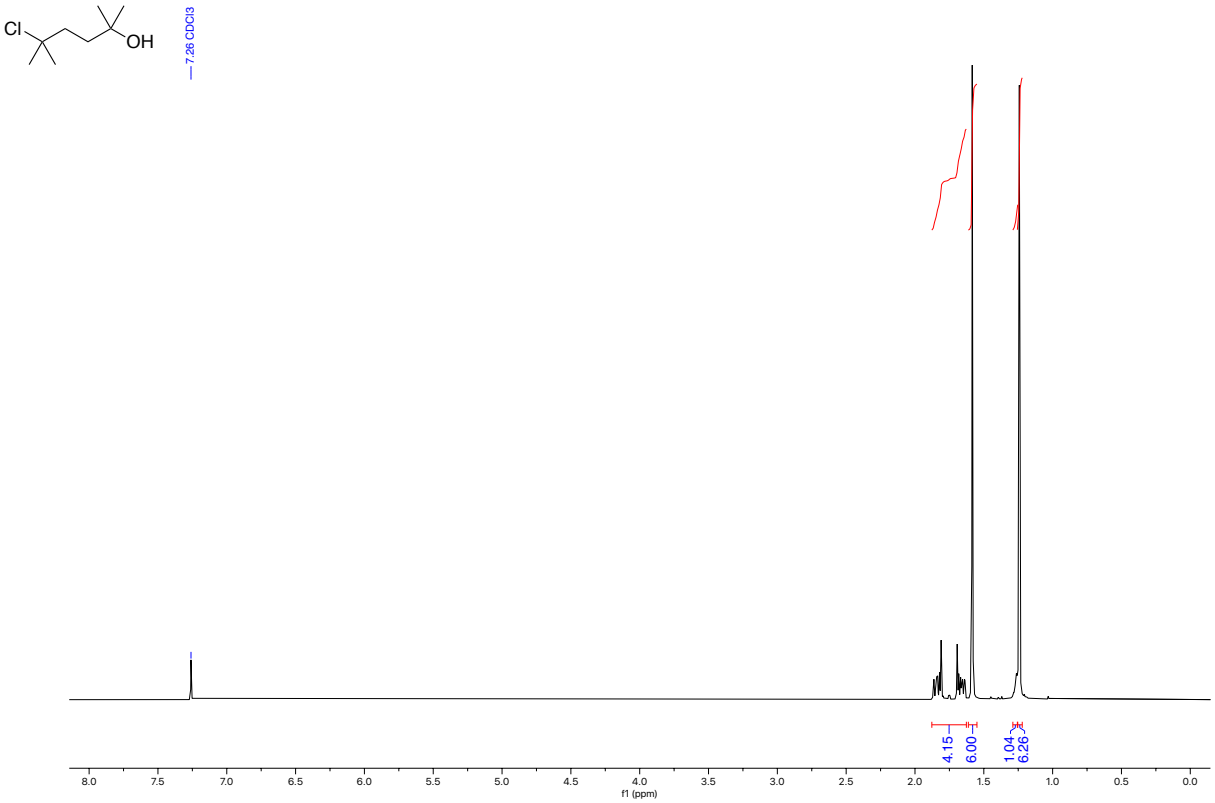

^{13}C NMR (75 MHz, $CDCl_3$)
5-chloro-2,5-dimethylhexan-2-ol

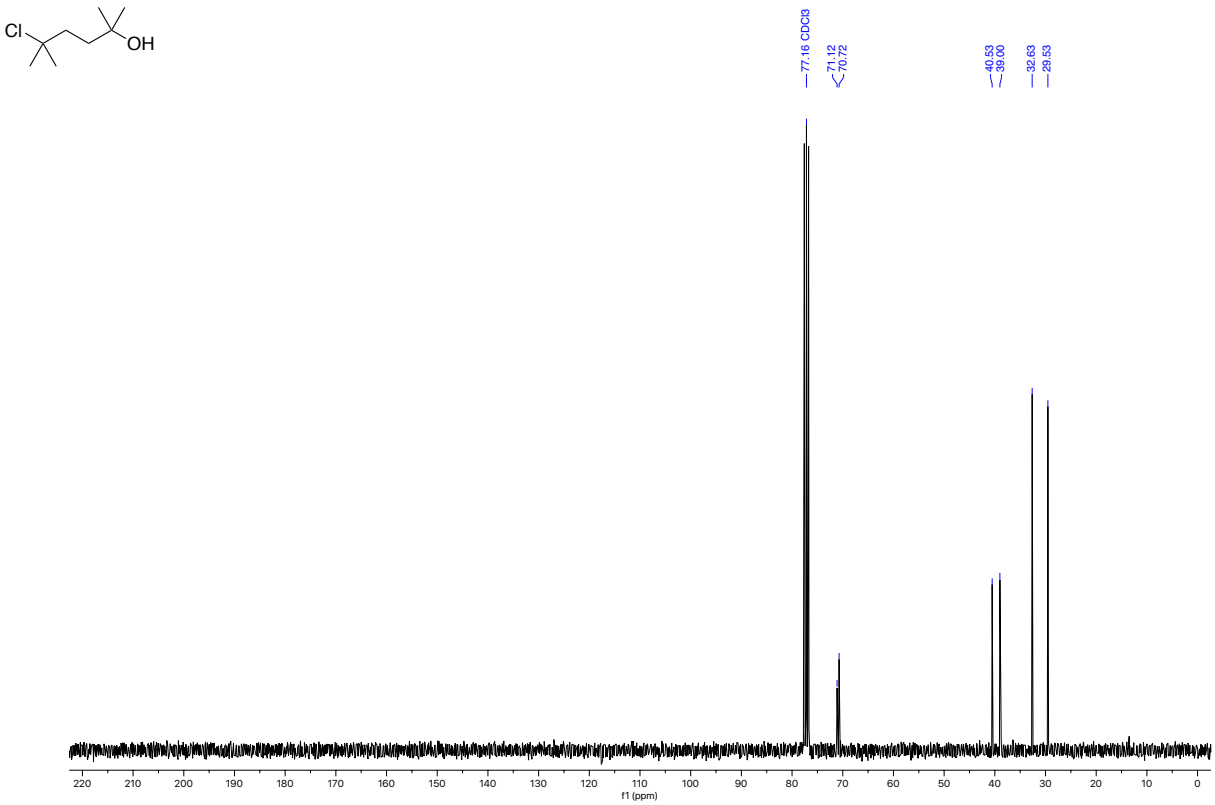

^{1}H NMR (300 MHz, $CDCl_3$)
5-azido-2,5-dimethylhexan-2-ol

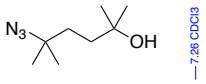

^{13}C NMR (75 MHz, $CDCl_3$)
5-azido-2,5-dimethylhexan-2-ol

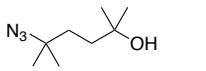

^{1}H NMR (300 MHz, CD_2Cl_2)
5-hydroxy-2,2,5-trimethylhexanenitrile

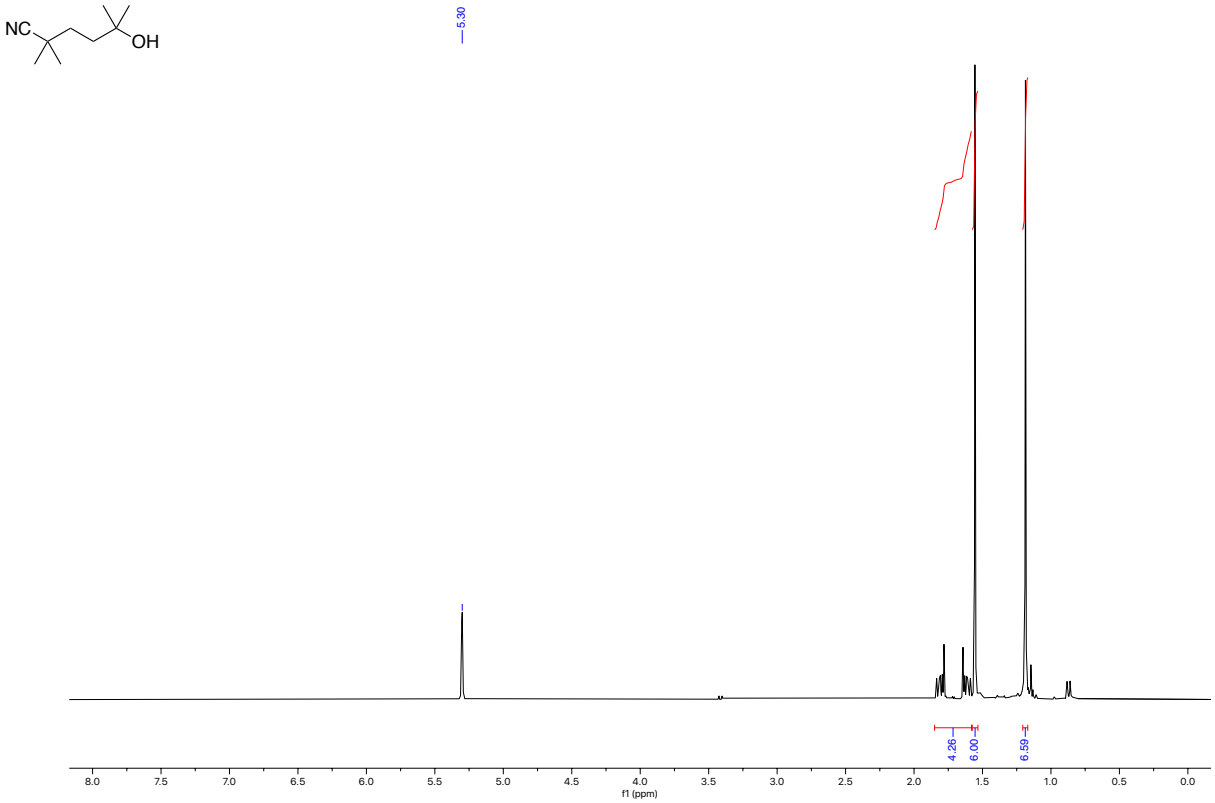

^{13}C NMR (75 MHz, CD_2Cl_2)
5-hydroxy-2,2,5-trimethylhexanenitrile

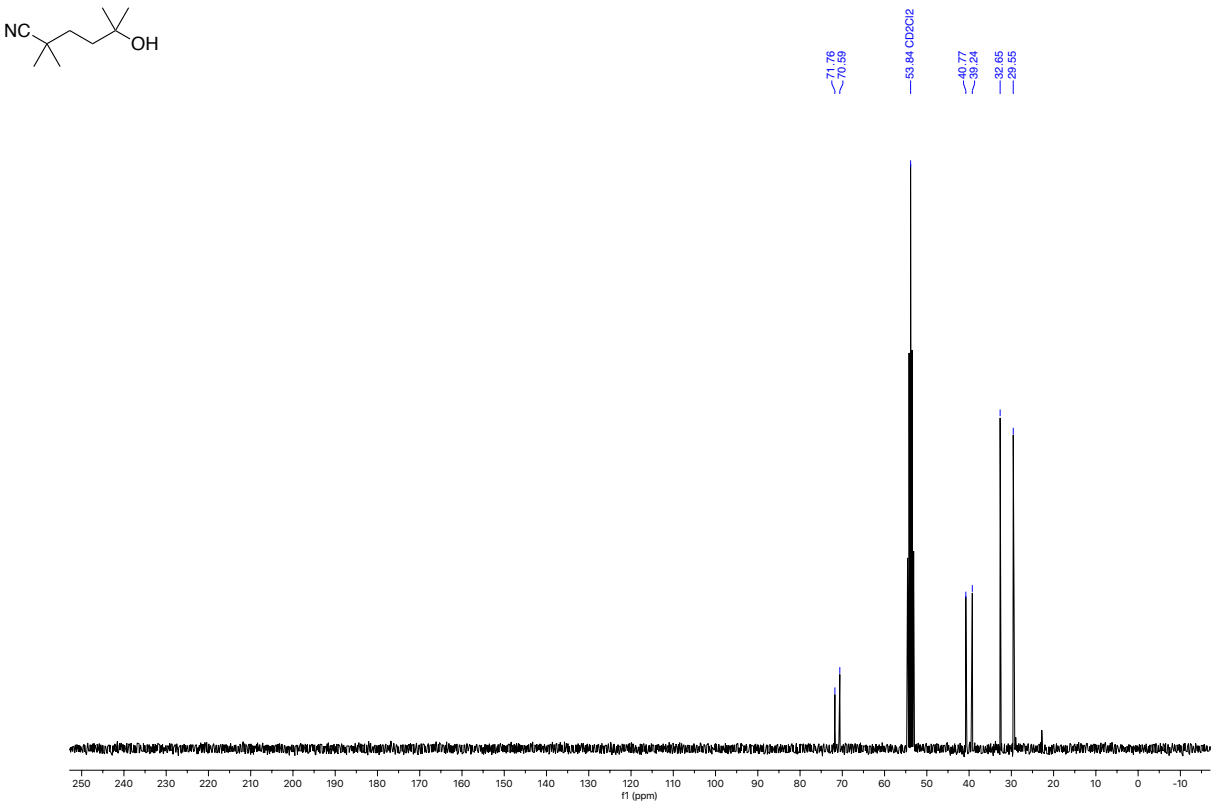

^{1}H NMR (300 MHz, $CDCl_3$)
2,5,5,7-tetramethyloct-7-en-2-ol

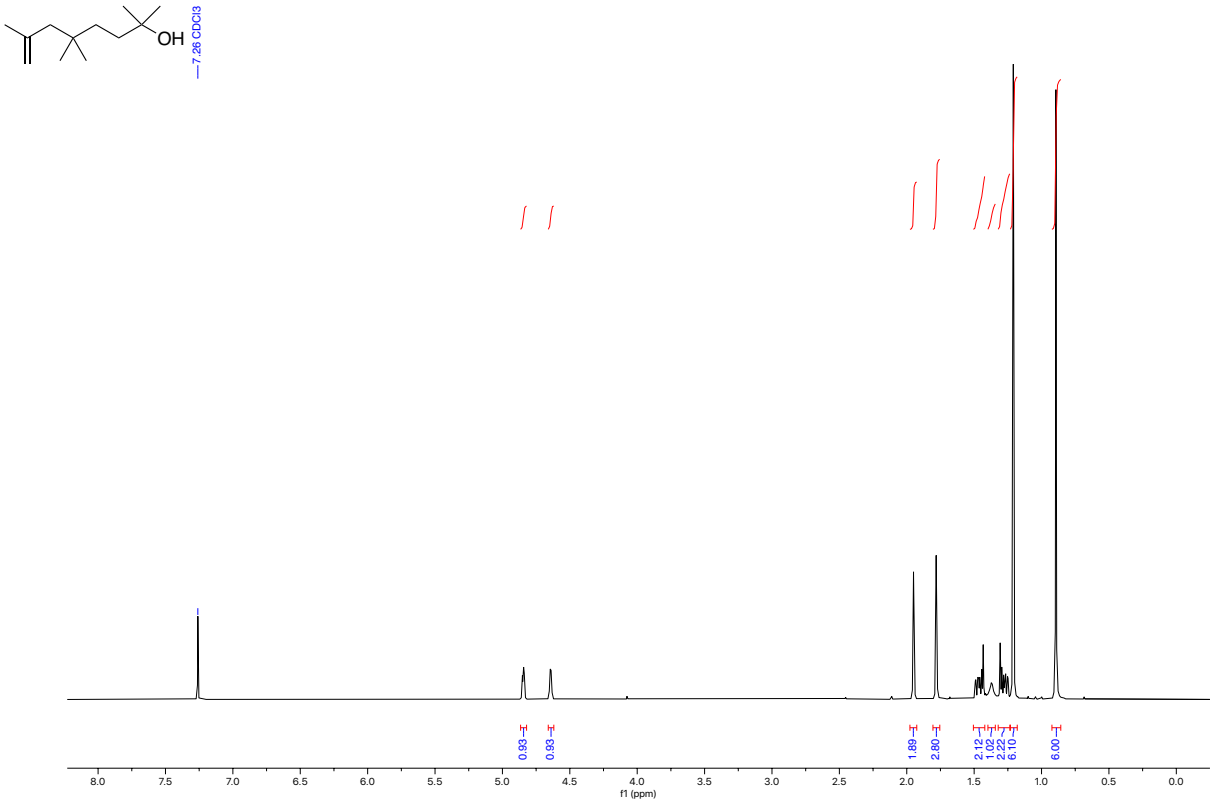

^{13}C NMR (75 MHz, $CDCl_3$)
2,5,5,7-tetramethyloct-7-en-2-ol

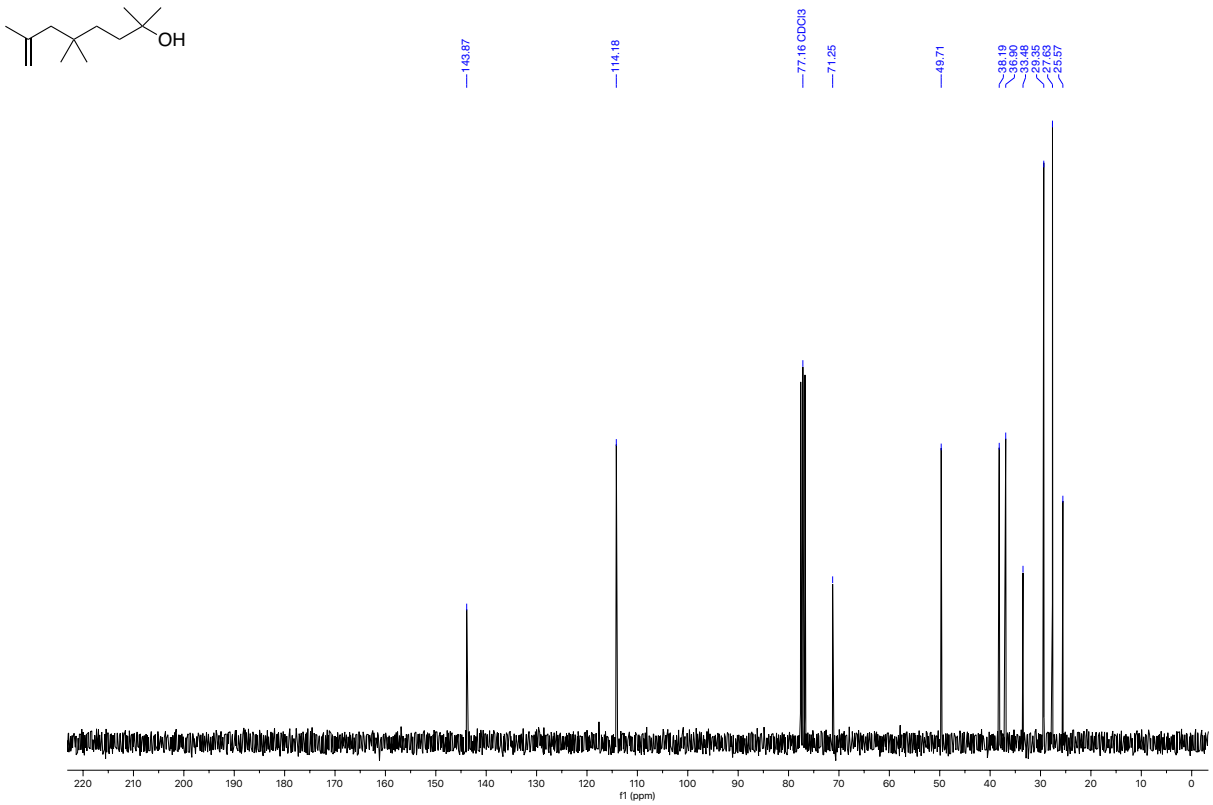

^{1}H NMR (300 MHz, $CDCl_3$)
2,5,5-trimethyl-7-(4,4,5,5-tetramethyl-1,3,2-dioxaborolan-2-yl)oct-7-en-2-ol

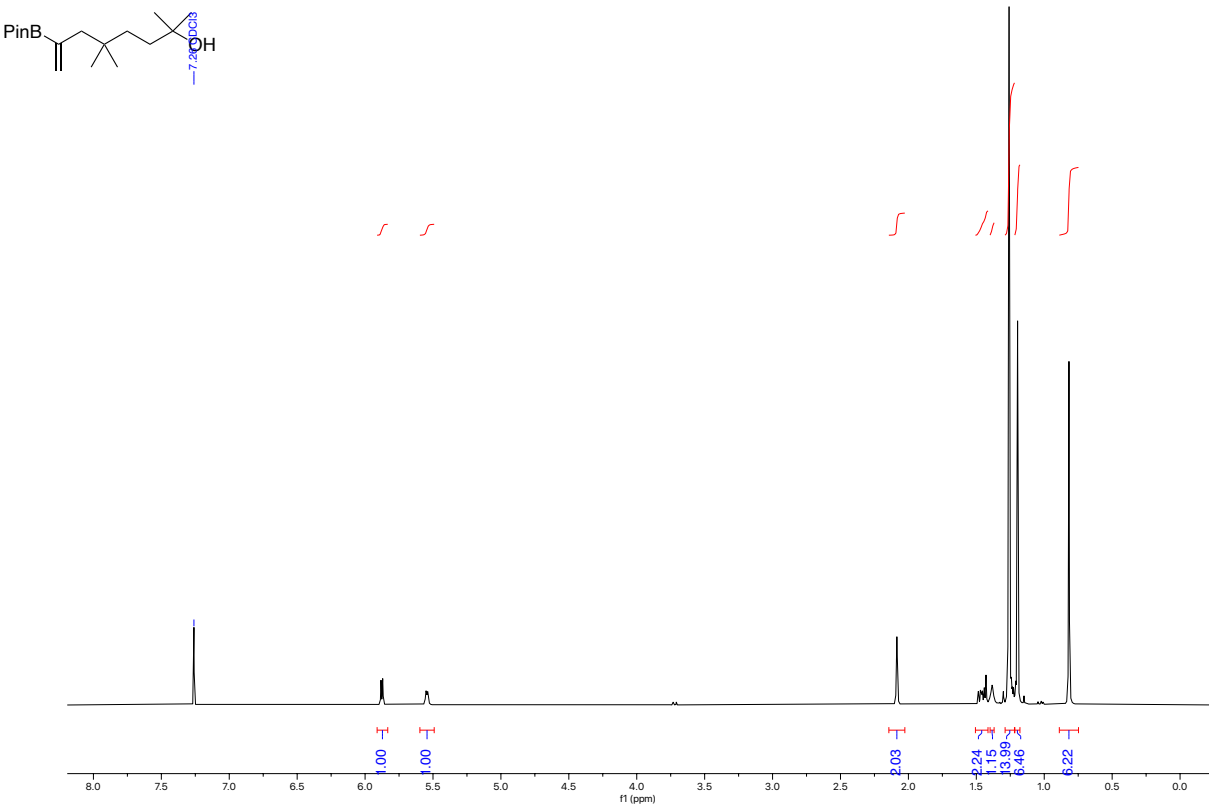

^{13}C NMR (75 MHz, $CDCl_3$)
2,5,5-trimethyl-7-(4,4,5,5-tetramethyl-1,3,2-dioxaborolan-2-yl)oct-7-en-2-ol

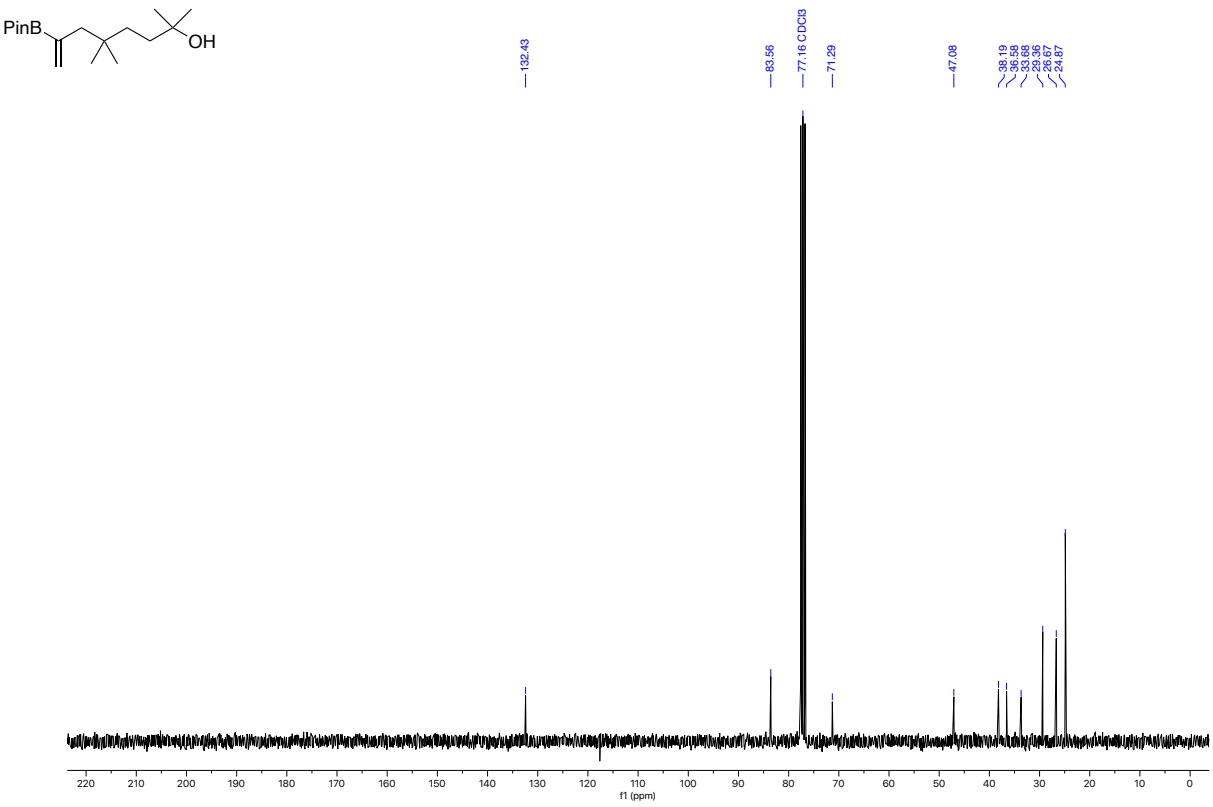

^{11}B-NMR (96 MHz, $CDCl_3$)
2,5,5-trimethyl-7-(4,4,5,5-tetramethyl-1,3,2-dioxaborolan-2-yl)oct-7-en-2-ol

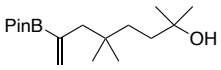

^{1}H NMR (300 MHz, CD_2Cl_2)
2,5,5-trimethyl-7-(triisopropylsilyl)hept-6-yn-2-ol

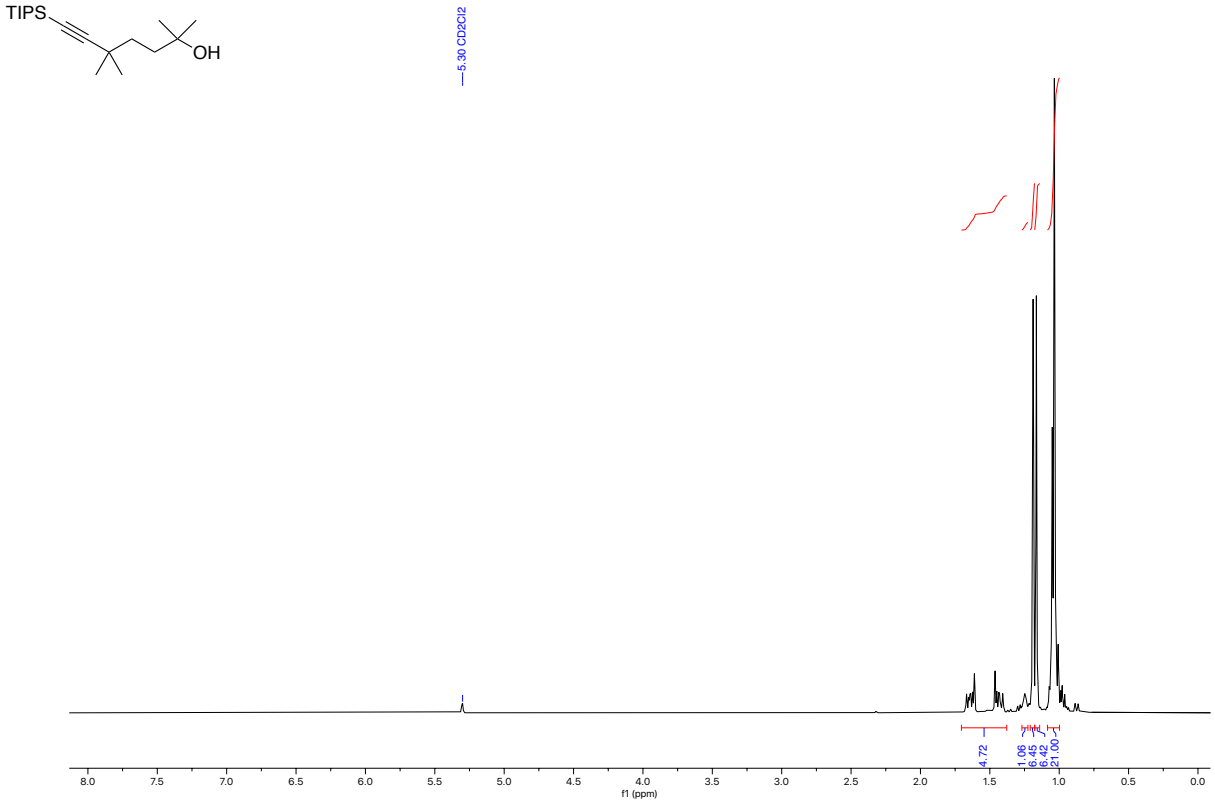

^{13}C NMR (75 MHz, CD_2Cl_2)
2,5,5-trimethyl-7-(triisopropylsilyl)hept-6-yn-2-ol

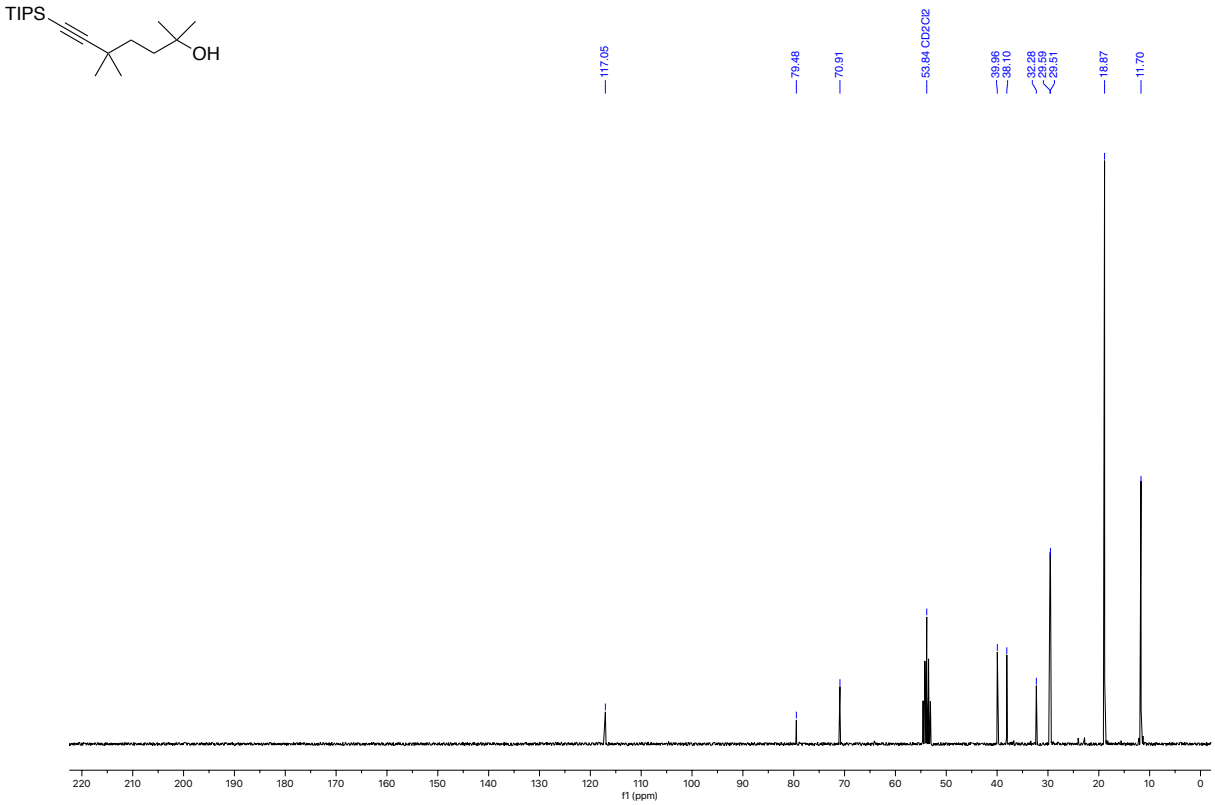

^{1}H NMR (300 MHz, $CDCl_3$)
5-fluoro-2,5-dimethylhexan-2-ol

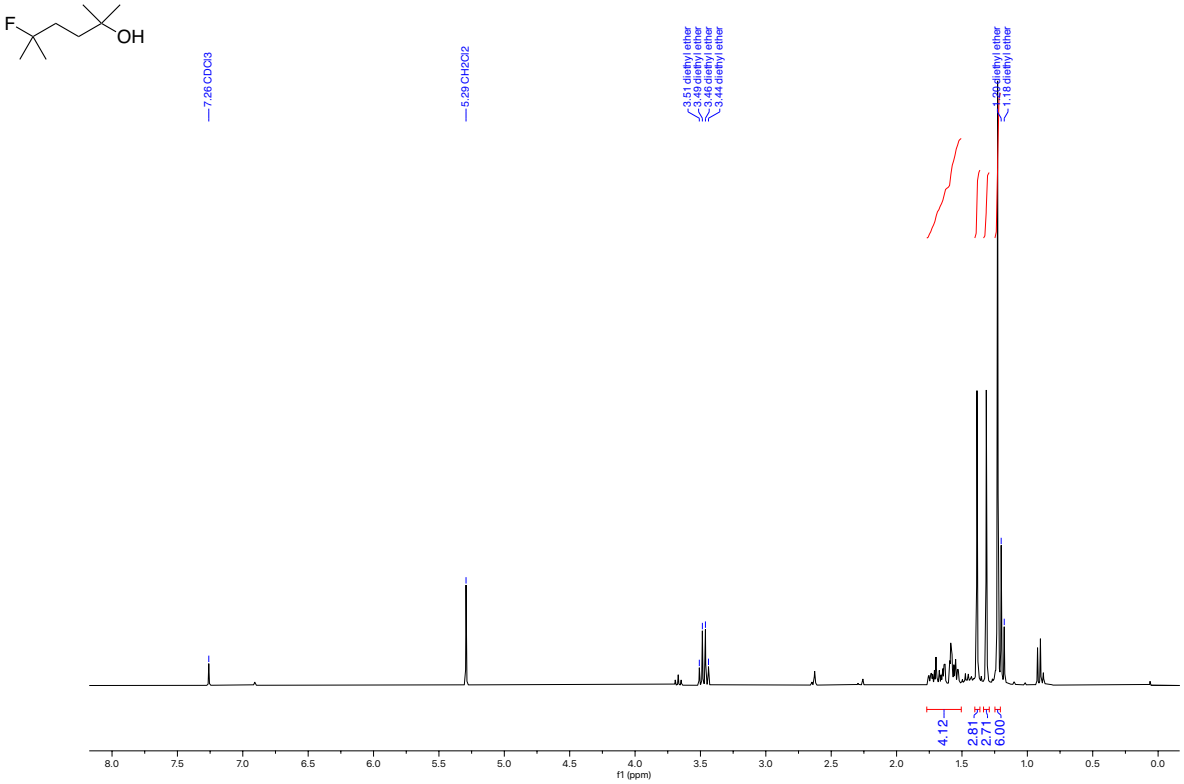

^{13}C NMR (75 MHz, $CDCl_3$)
5-fluoro-2,5-dimethylhexan-2-ol

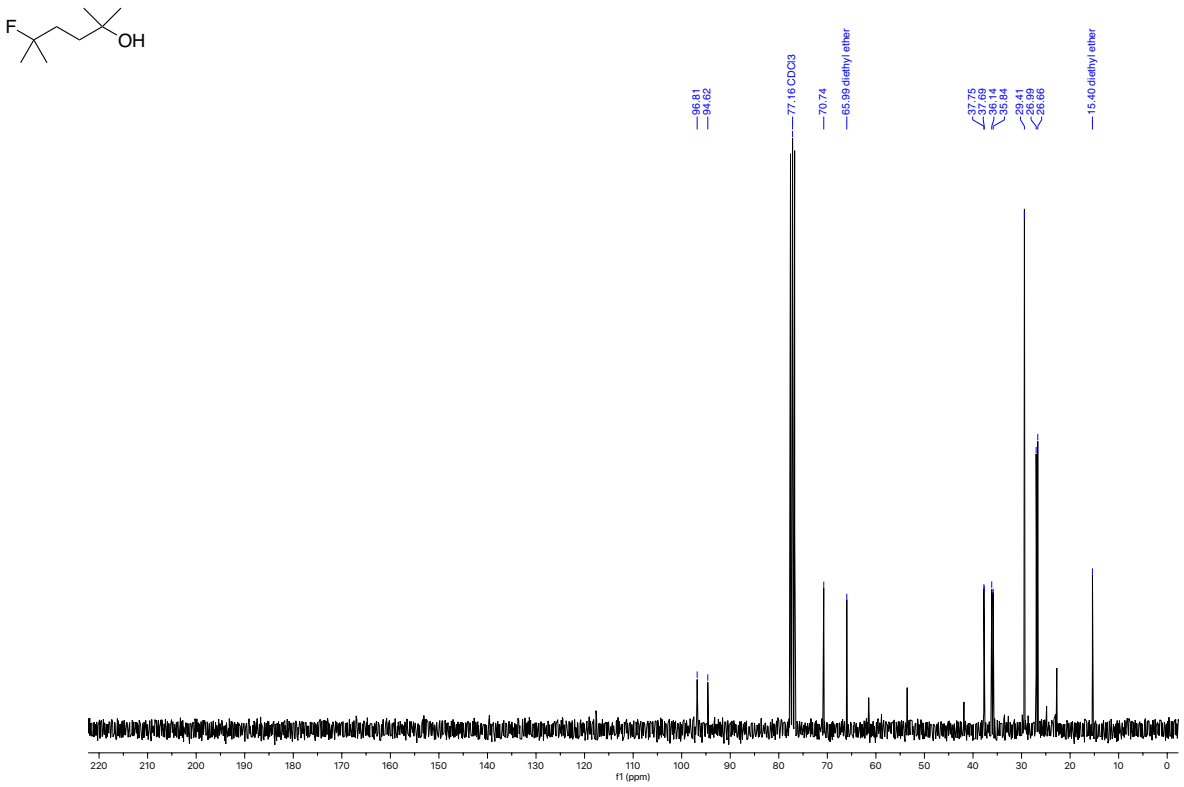

^{19}F NMR (282 MHz, $CDCl_3$)
5-fluoro-2,5-dimethylhexan-2-ol

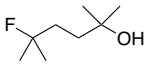

^{1}H NMR (300 MHz, CD_2Cl_2)
Benzyl(phenyl)sulfane

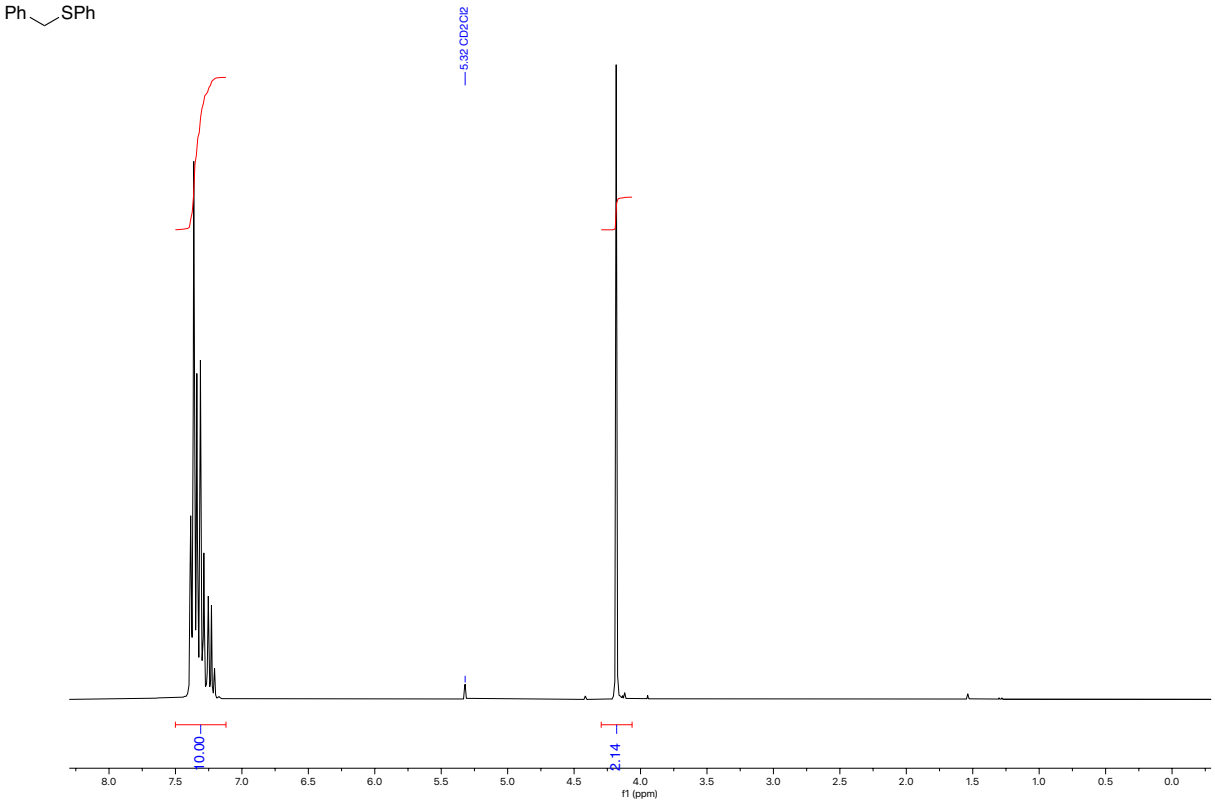

^{13}C NMR (75 MHz, CD_2Cl_2)
Benzyl(phenyl)sulfane

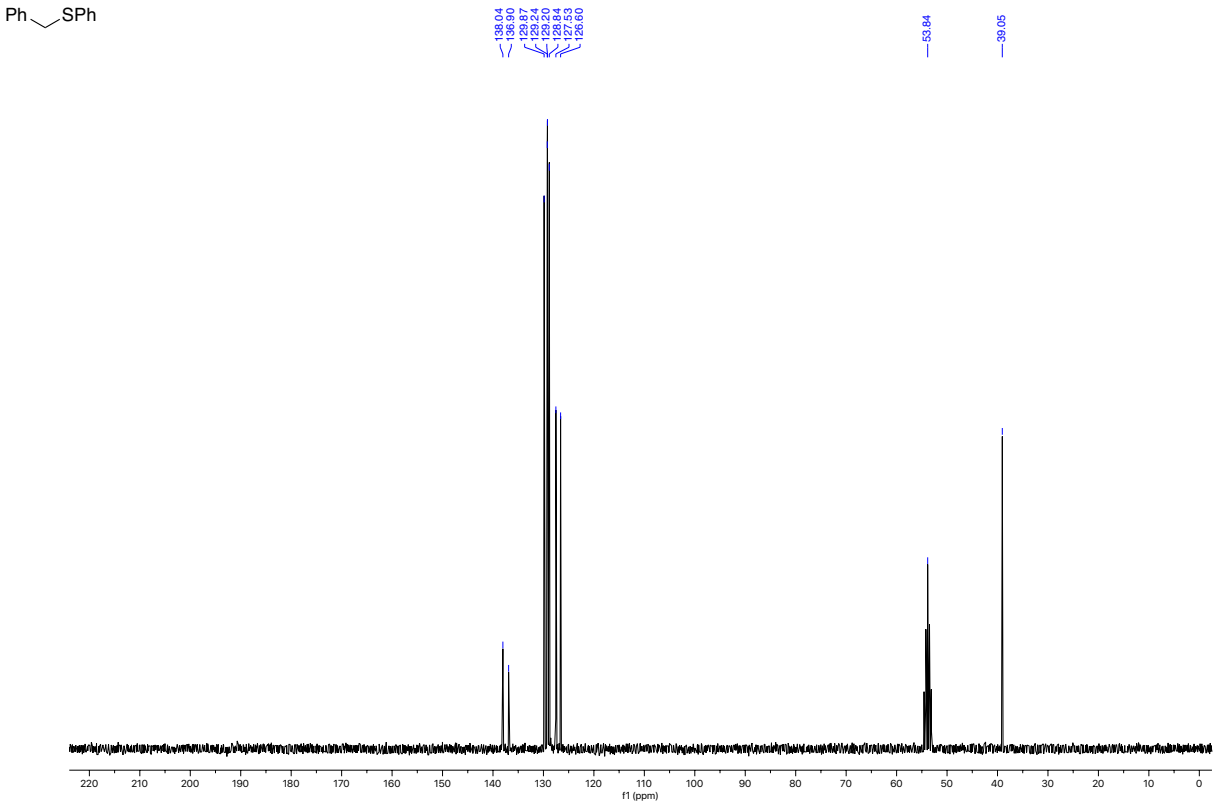

^{1}H NMR (300 MHz, CD_2Cl_2)
2,2-dimethyl-5-((phenylthio)methyl)tetrahydrofuran

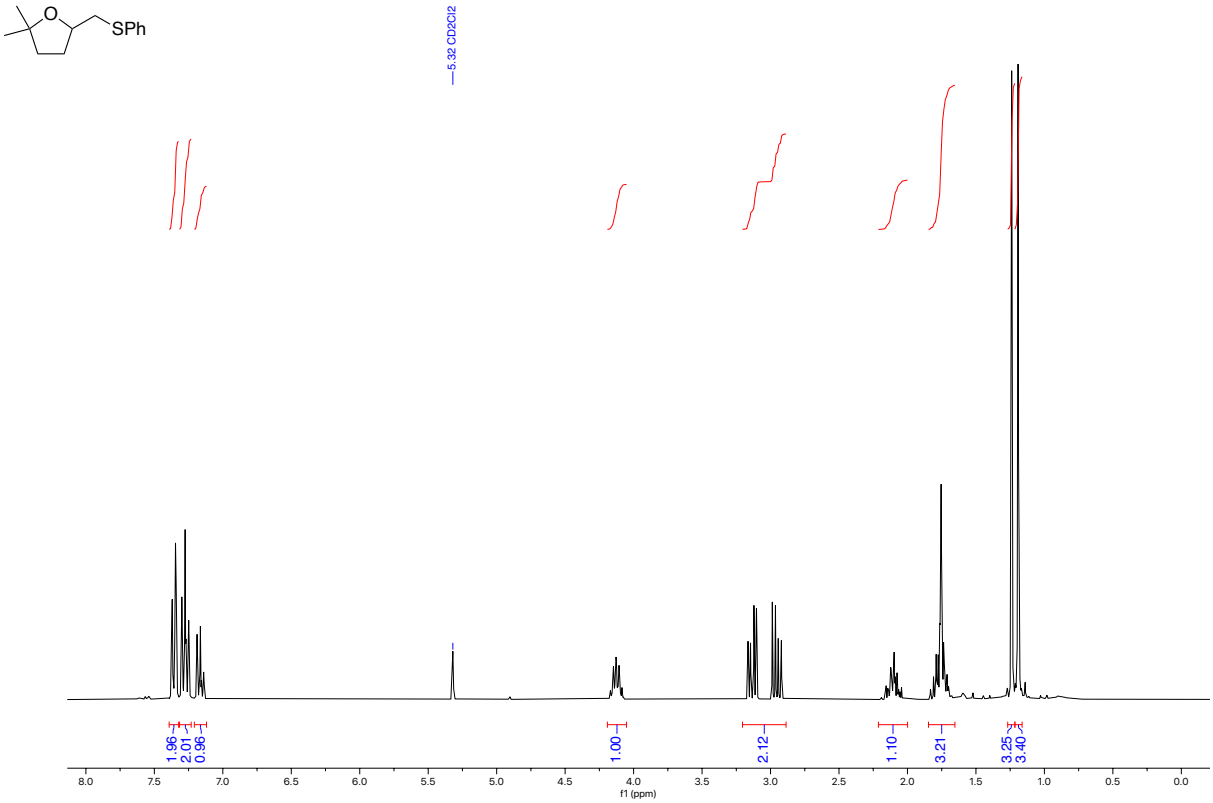

^{13}C NMR (75 MHz, CD_2Cl_2)
2,2-dimethyl-5-((phenylthio)methyl)tetrahydrofuran

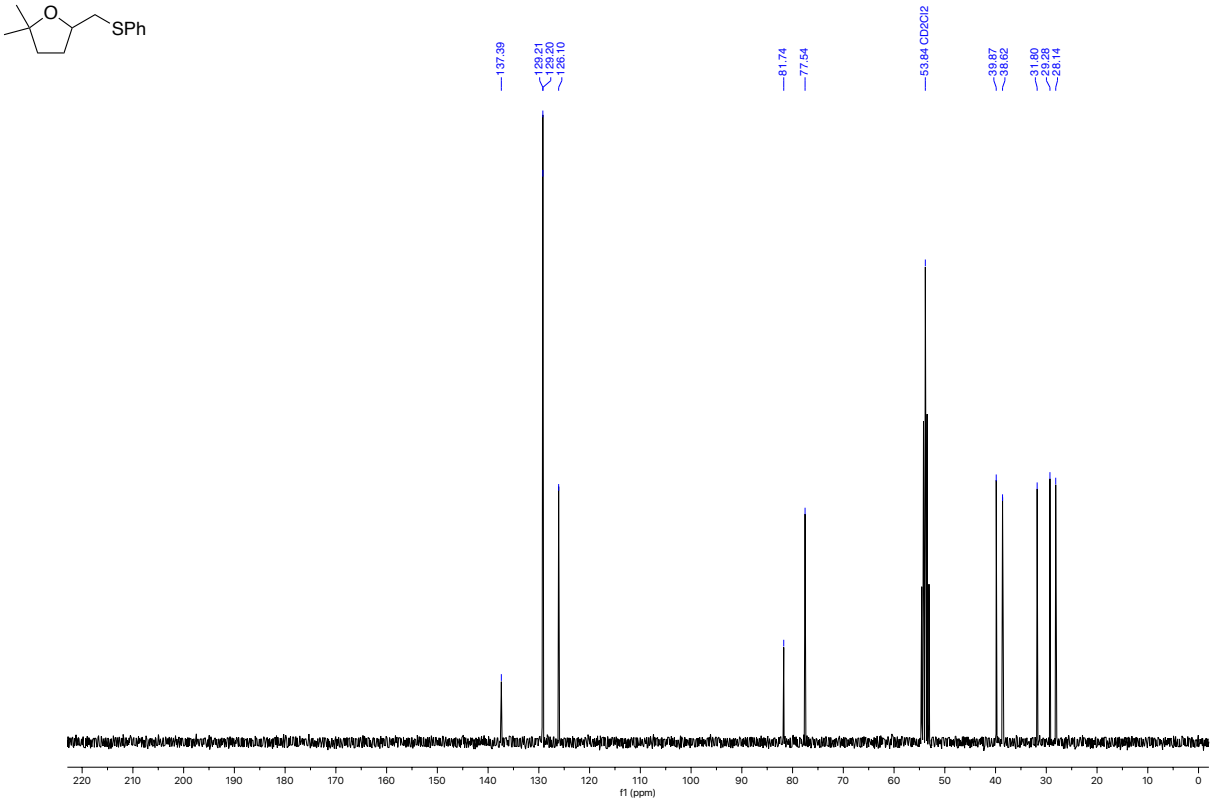

^{1}H NMR (300 MHz, CD_2Cl_2)
8-(phenylthio)octan-2-one

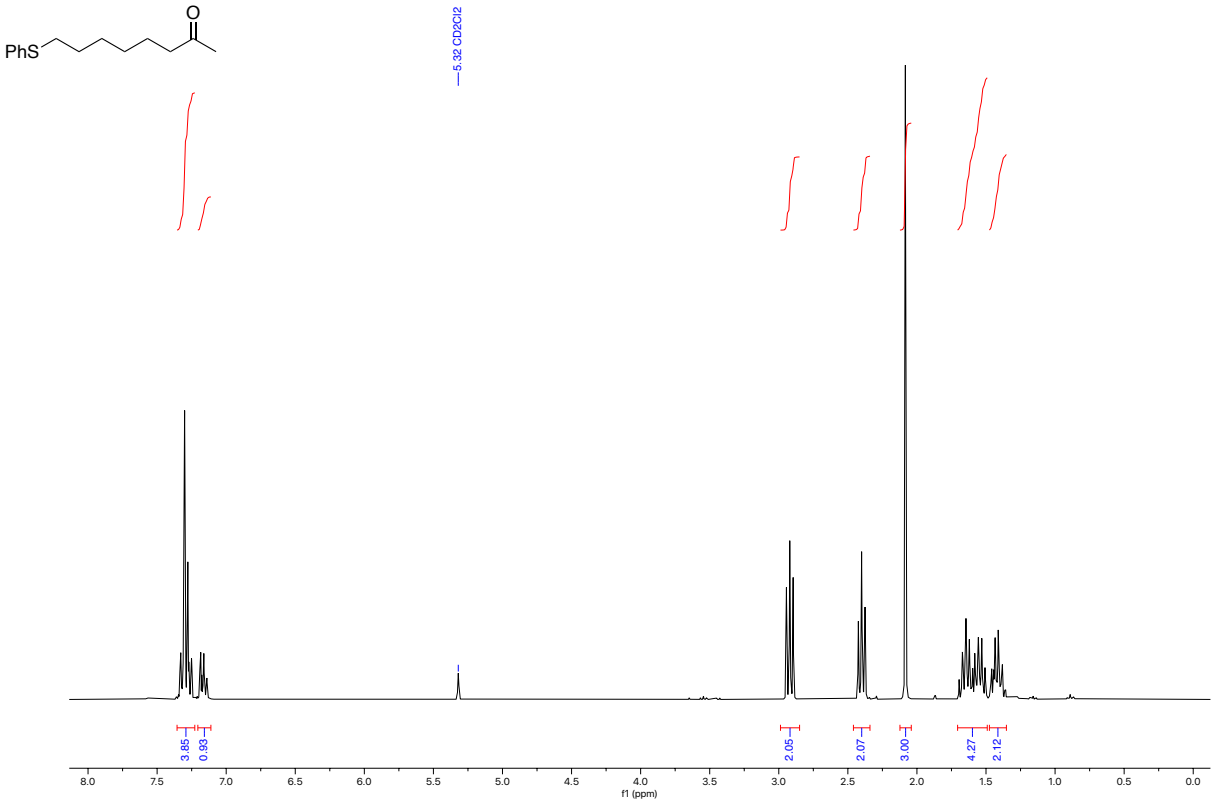

^{13}C NMR (75 MHz, CD_2Cl_2)
8-(phenylthio)octan-2-one

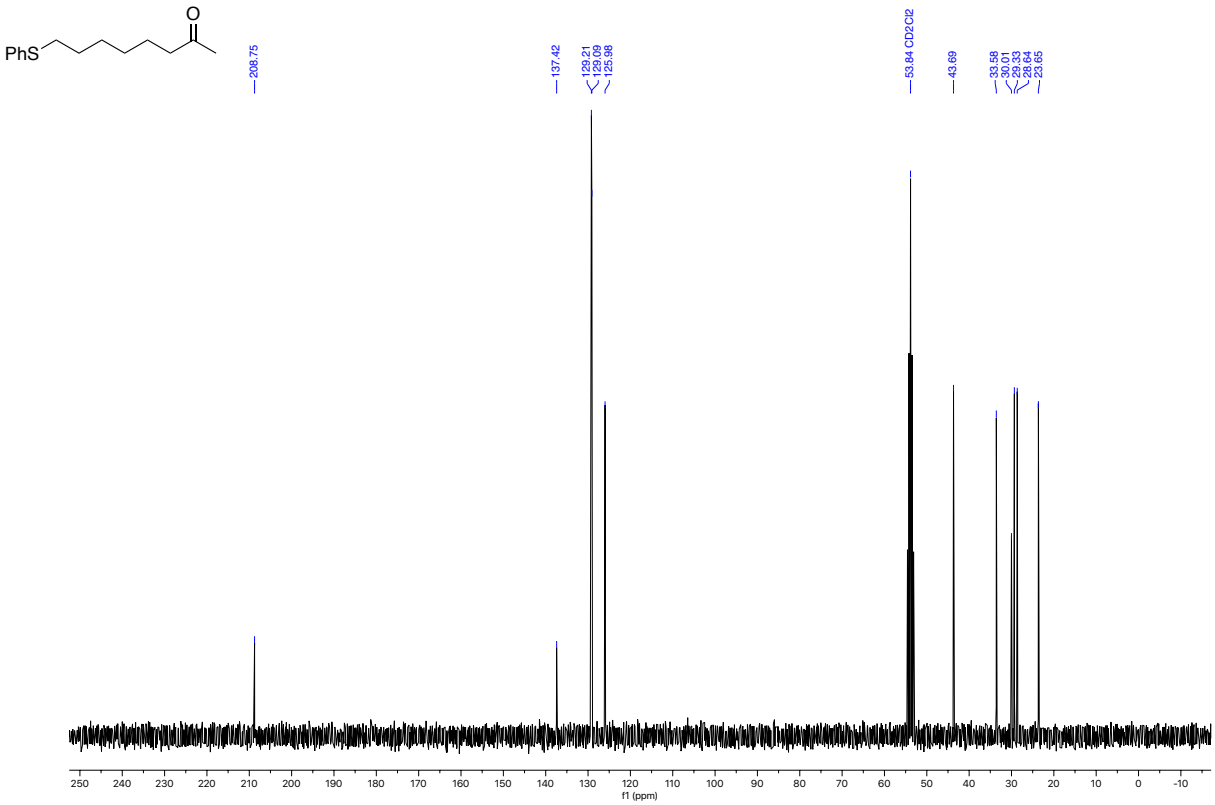

^{1}H NMR (300 MHz, $CDCl_3$)
2-methyl-5-(phenylthio)octan-2-ol

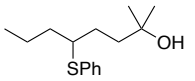

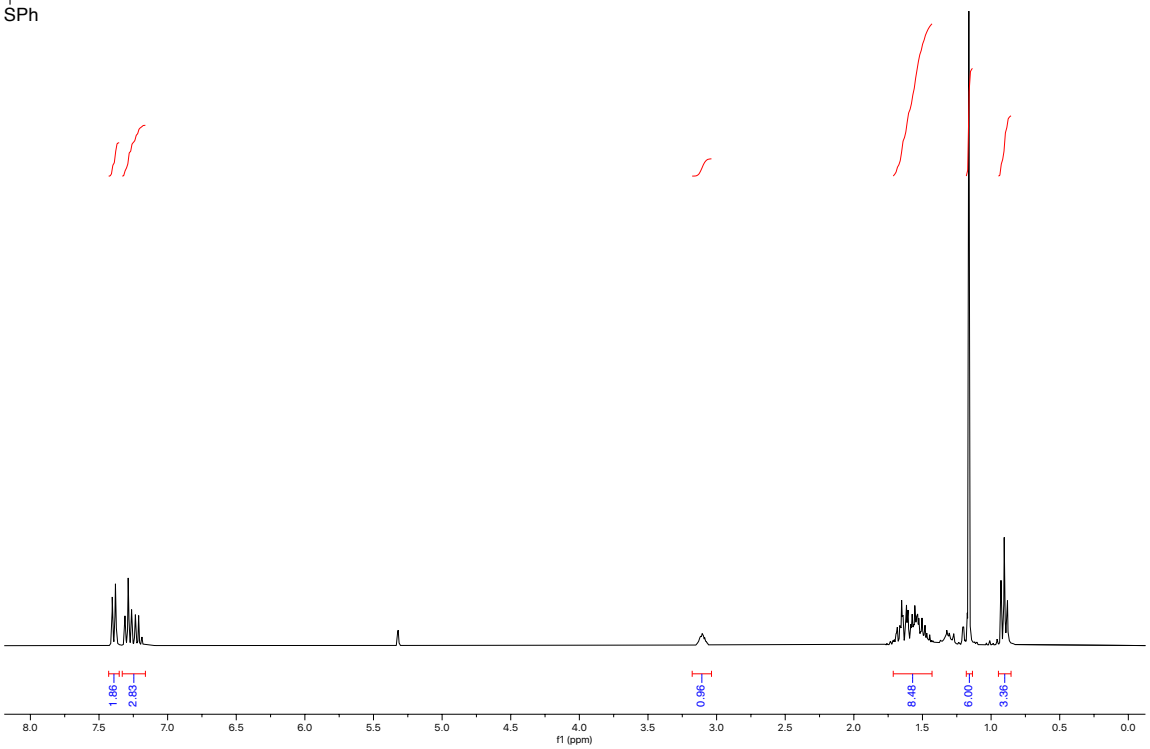

^{13}C NMR (75 MHz, $CDCl_3$)
2-methyl-5-(phenylthio)octan-2-ol

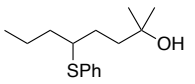

^{1}H NMR (300 MHz, $CDCl_3$)
5-chloro-2-methyloctan-2-ol

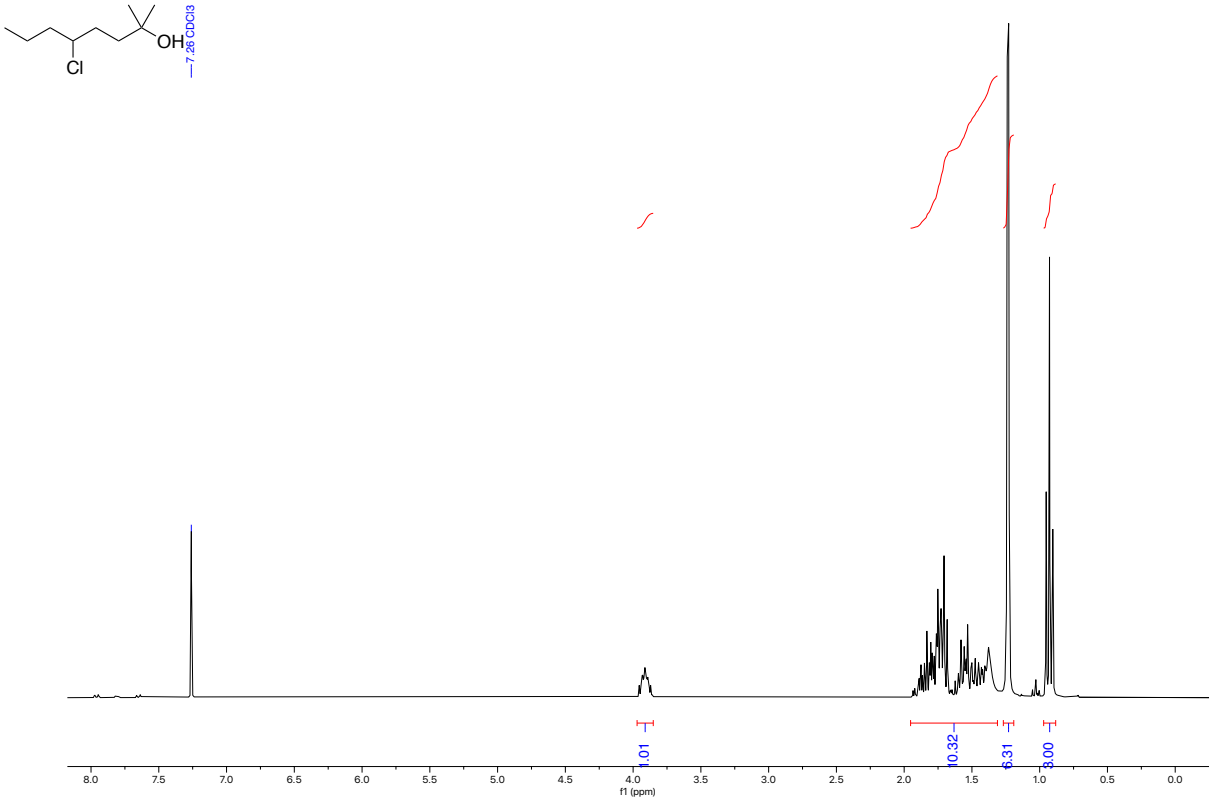

^{13}C NMR (75 MHz, $CDCl_3$)
5-chloro-2-methyloctan-2-ol

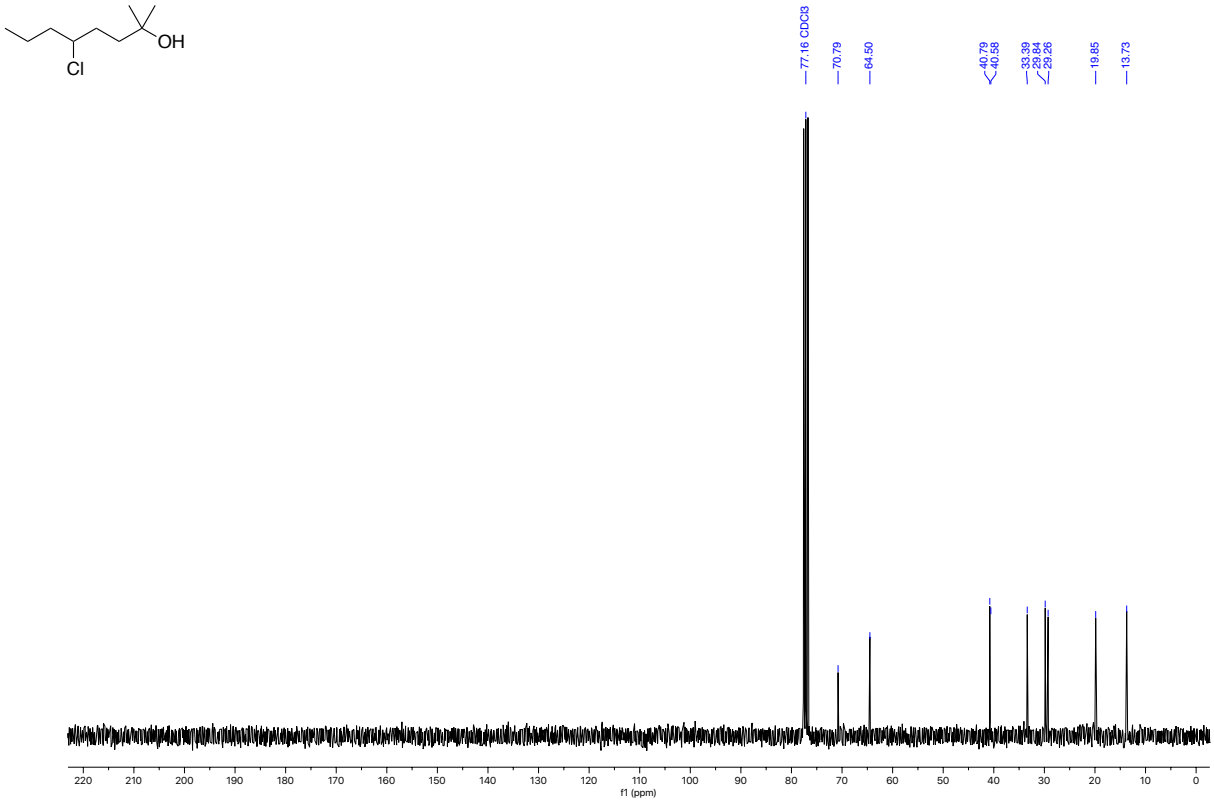

^{1}H NMR (300 MHz, $CDCl_3$)
5-hydroxy-5-methyl-2-propylhexanenitrile

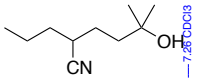

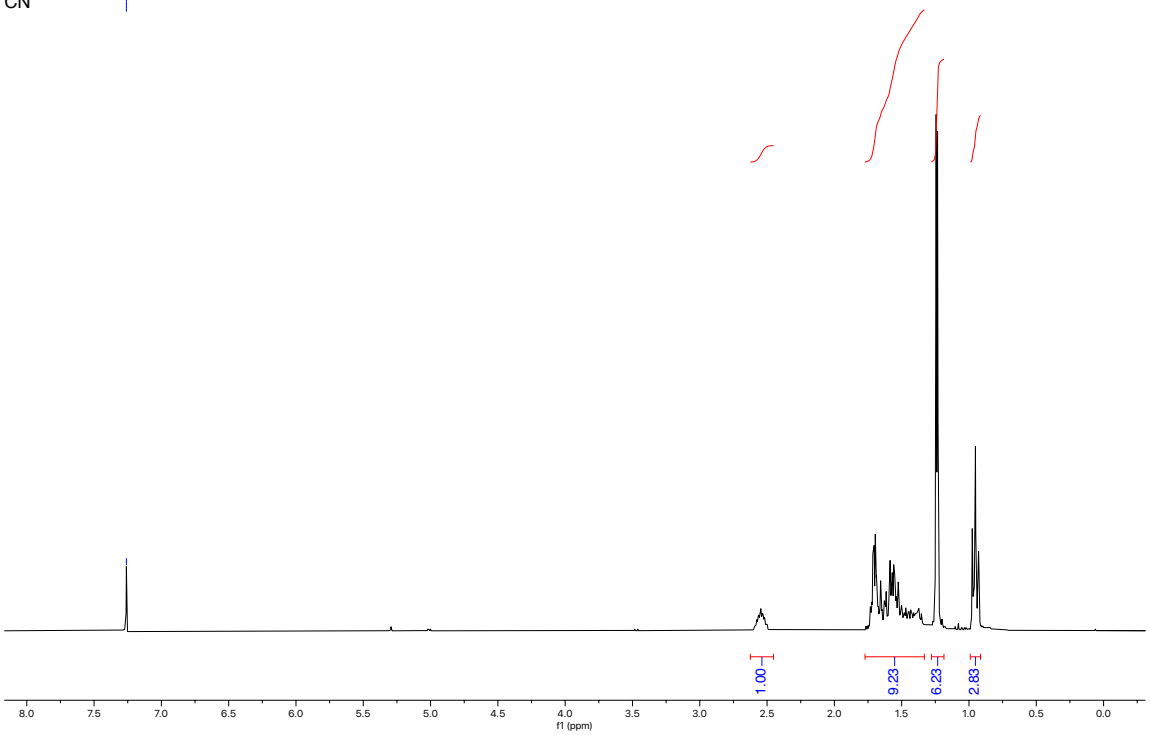

^{13}C NMR (75 MHz, $CDCl_3$)
5-hydroxy-5-methyl-2-propylhexanenitrile

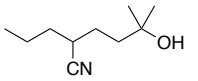

^{1}H NMR (300 MHz, $CDCl_3$)
5-bromo-2-methyloctan-2-ol

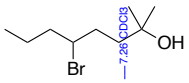

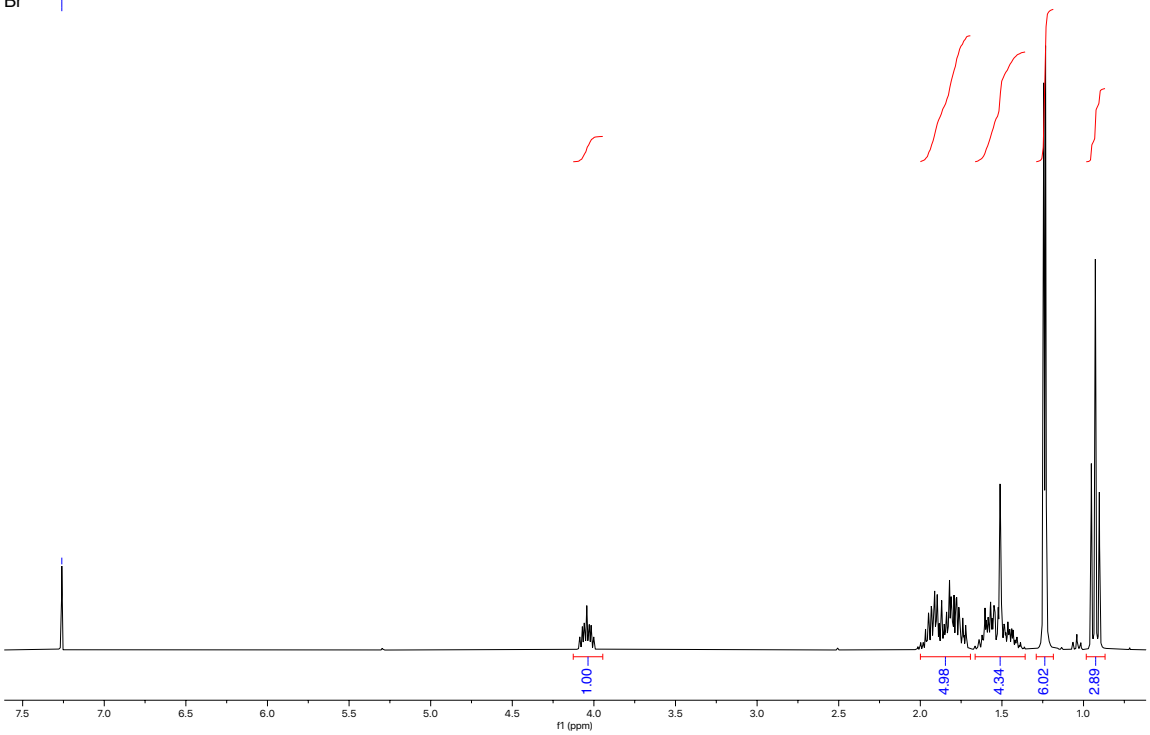

^{13}C NMR (75 MHz, $CDCl_3$)
5-bromo-2-methyloctan-2-ol

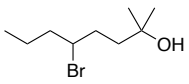

Appendix

NMR Spectra of Chapter 4

^{1}H NMR (300 MHz, CD_2Cl_2)
1-benzyl-4-phenylcyclohexan-1-ol, major diastereomer

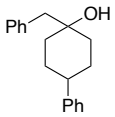

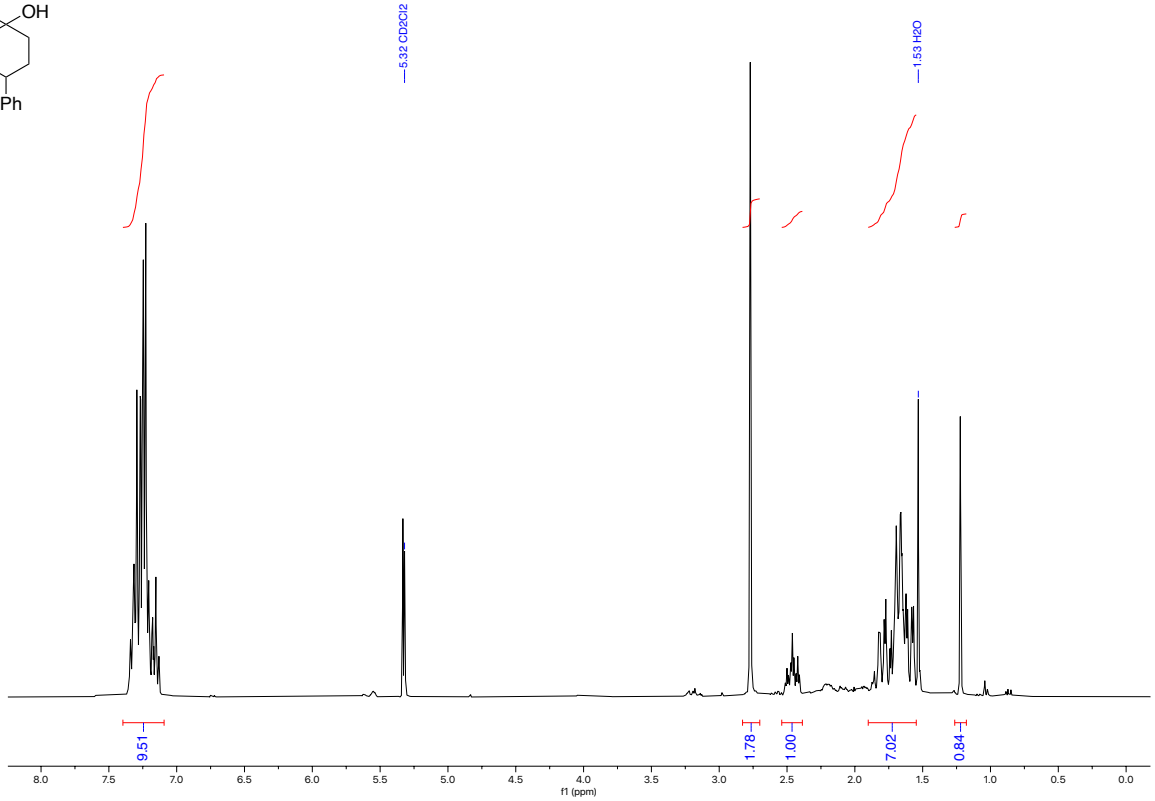

^{13}C NMR (75 MHz, CD_2Cl_2)
1-benzyl-4-phenylcyclohexan-1-ol, major diastereomer

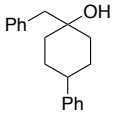

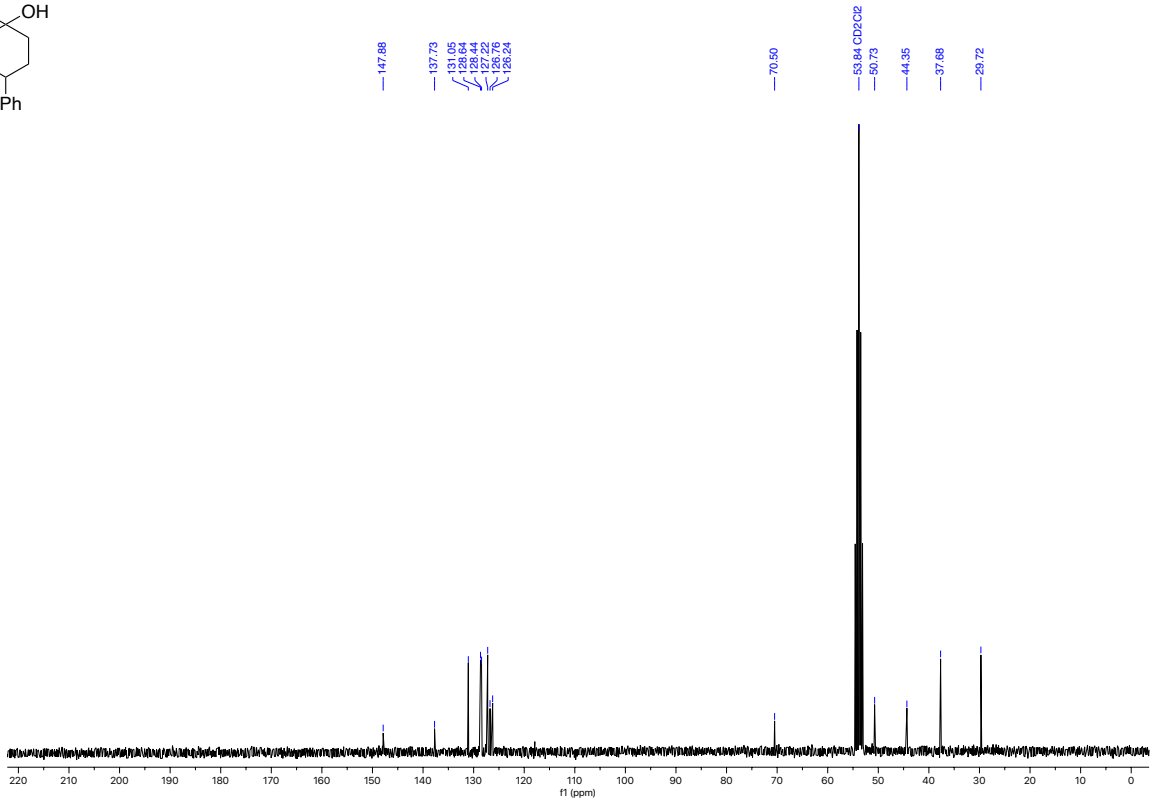

^{1}H NMR (300 MHz, CD_2Cl_2)
1-benzyl-4-phenylcyclohexan-1-ol, minor diastereomer

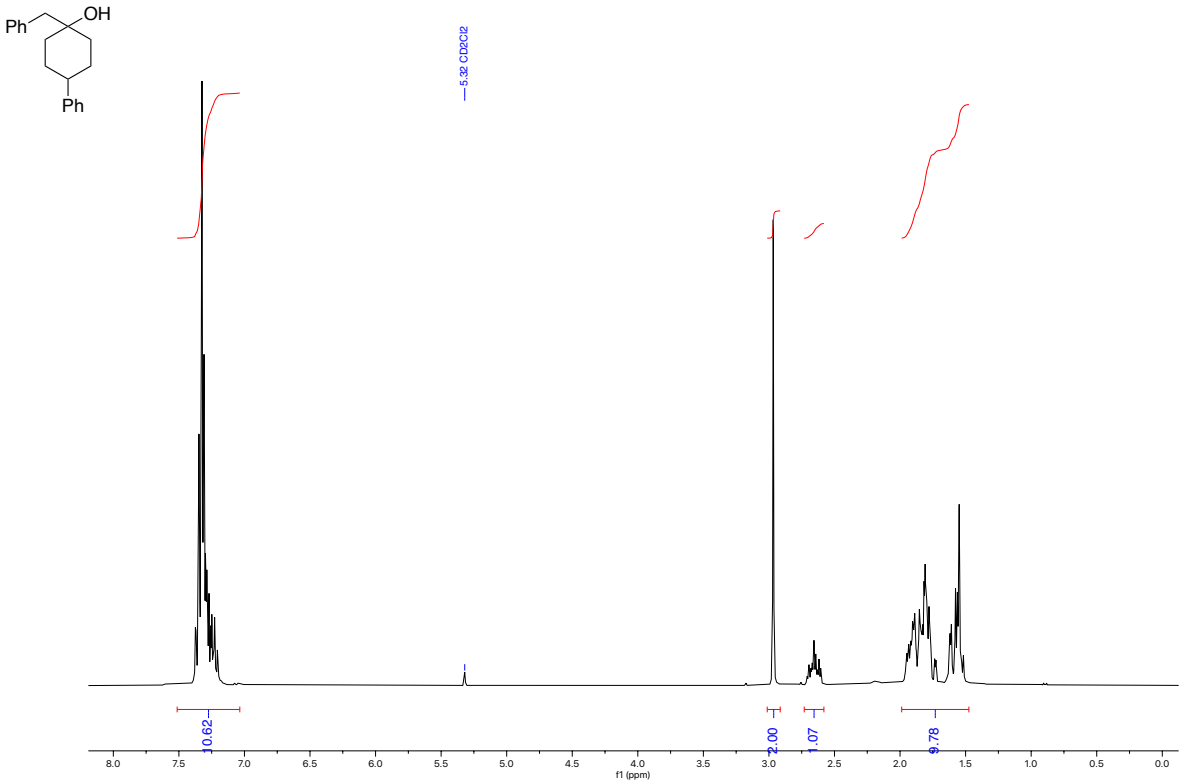

^{13}C NMR (75 MHz, CD_2Cl_2)
1-benzyl-4-phenylcyclohexan-1-ol, minor diastereomer

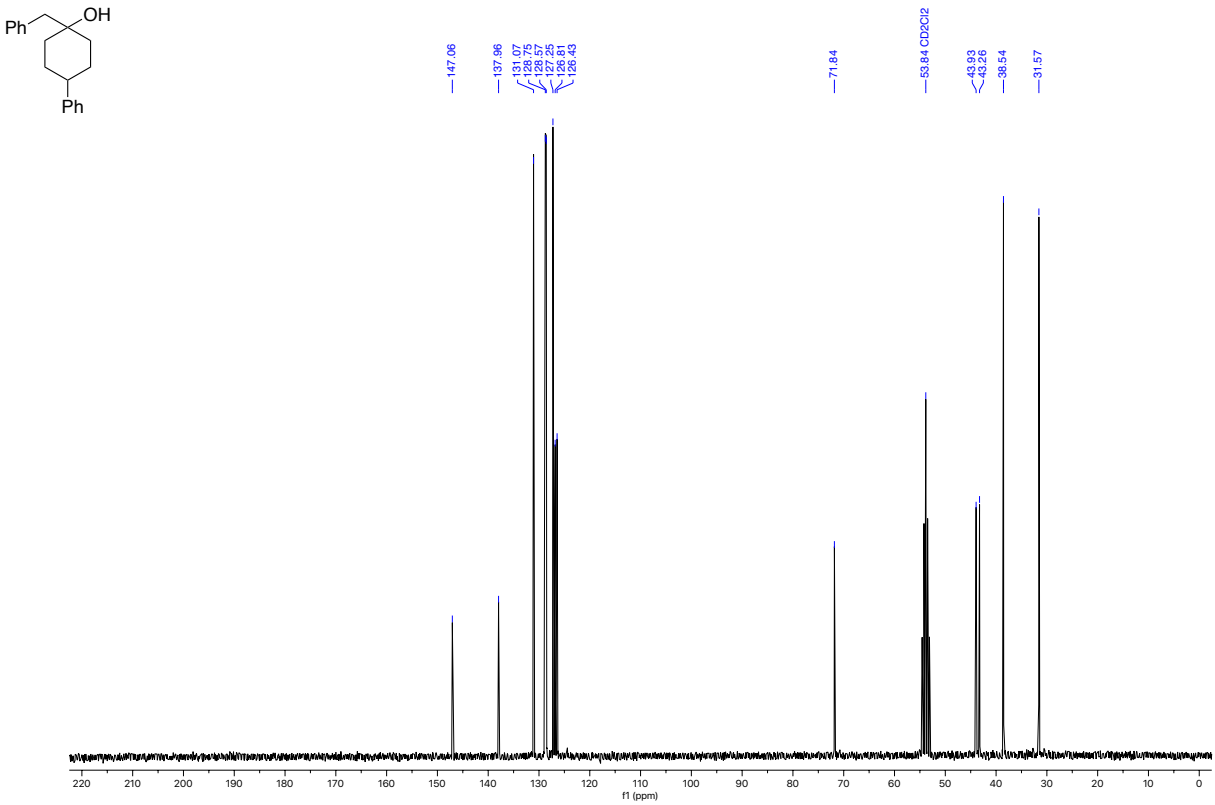

^{1}H NMR (300 MHz, $CDCl_3$)
3-phenylpropyl methanesulfonate

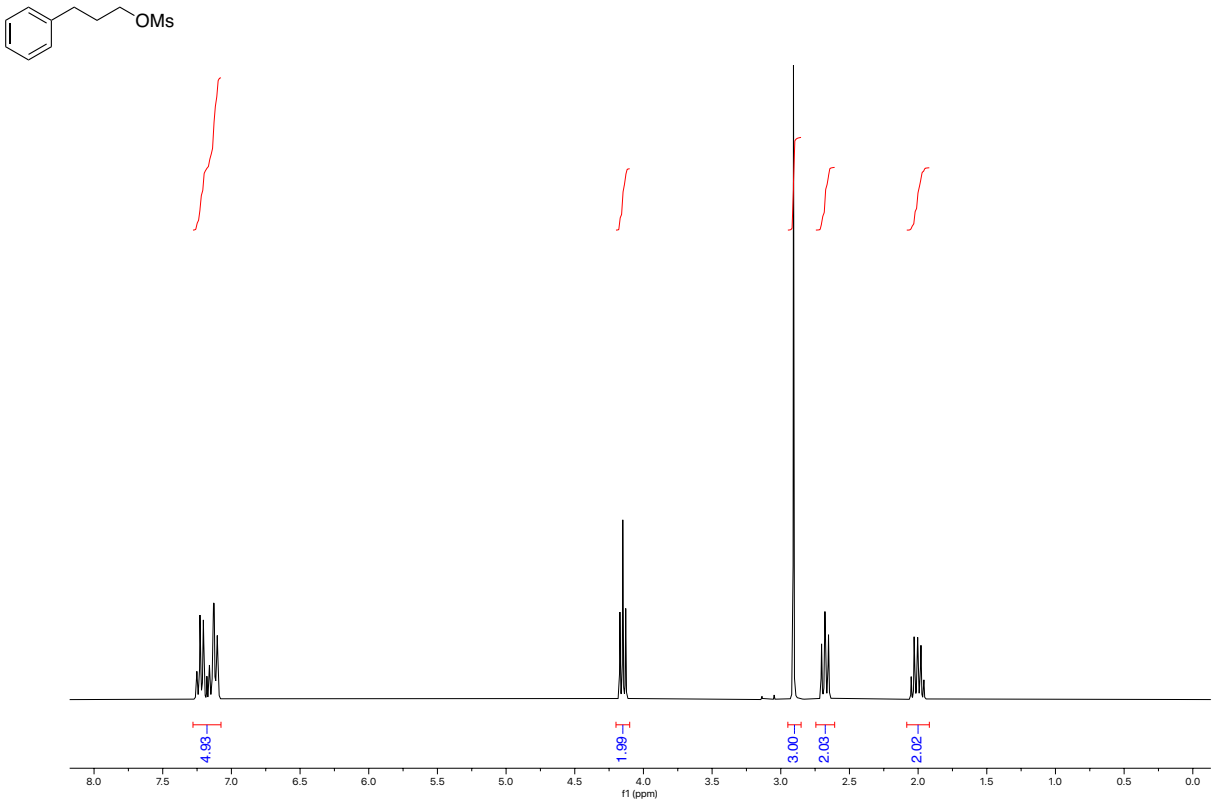

^{13}C NMR (75 MHz, $CDCl_3$)
3-phenylpropyl methanesulfonate

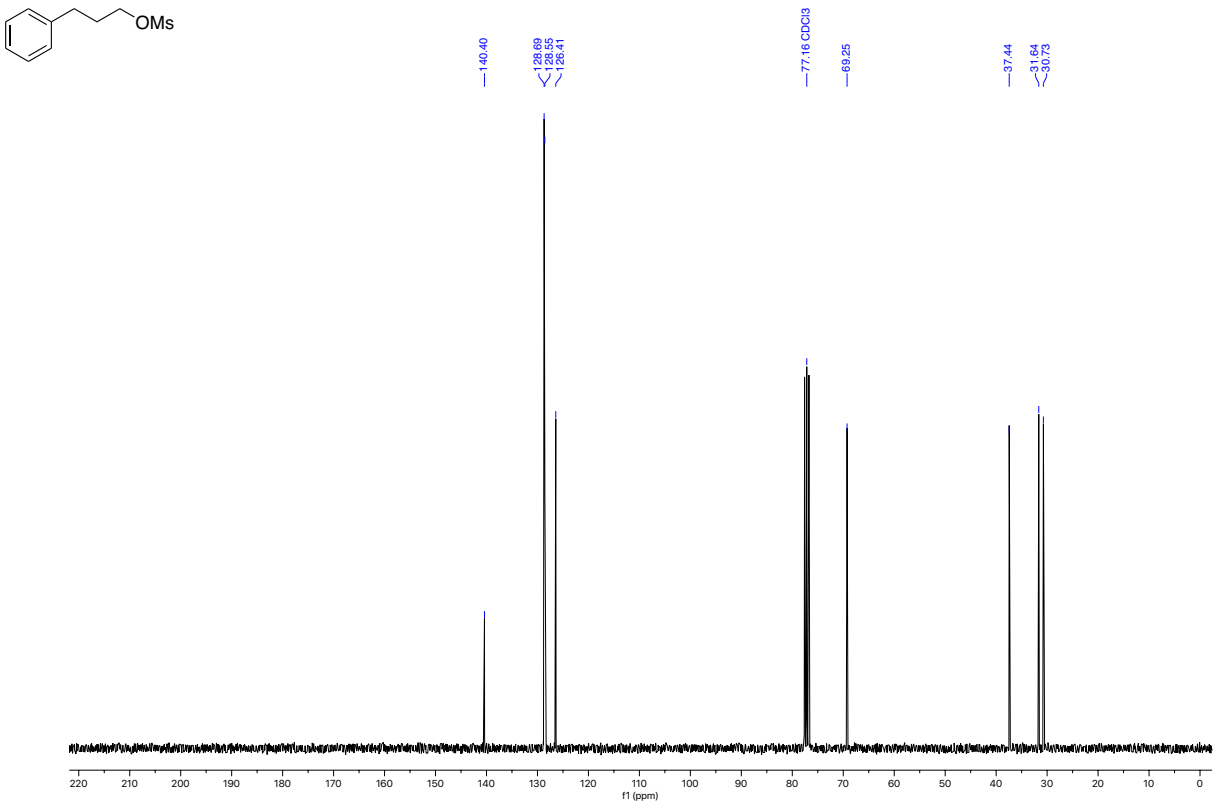

^{1}H NMR (300 MHz, $CDCl_3$)
(3-hydroperoxypropyl)benzene

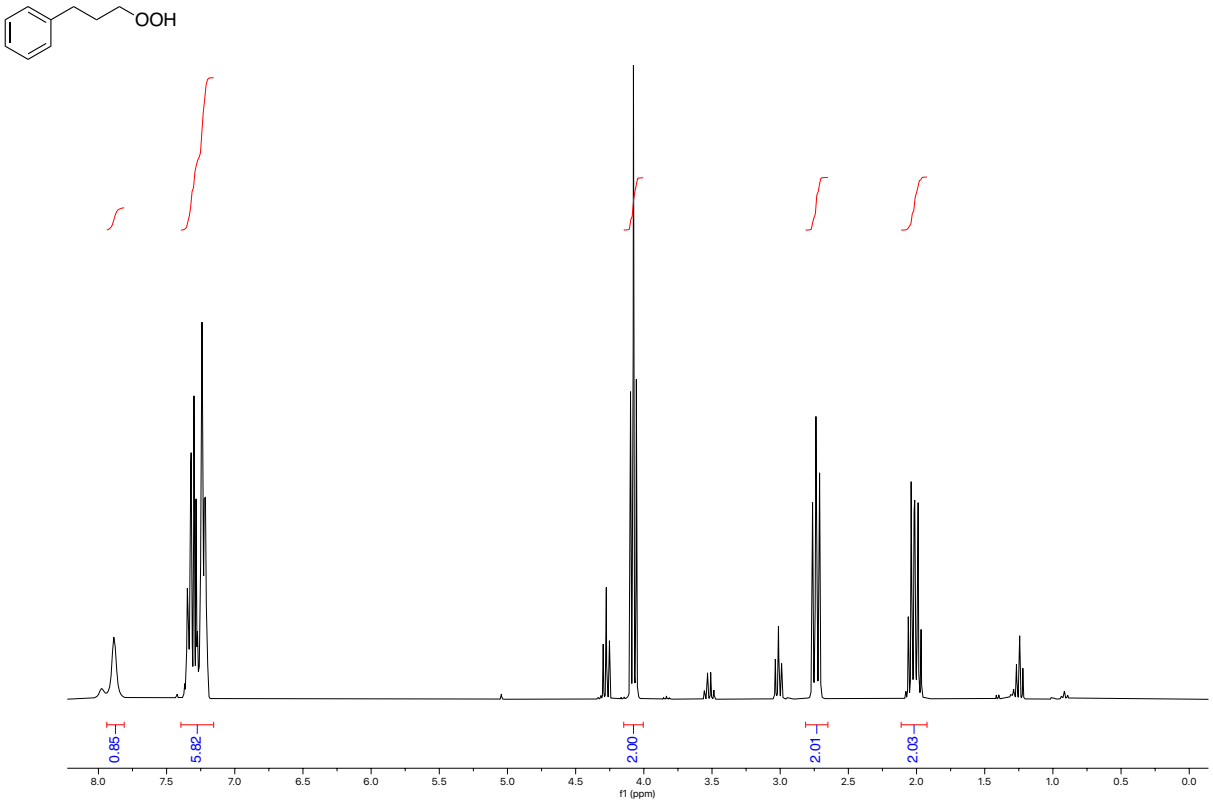

^{13}C NMR (75 MHz, $CDCl_3$)
(3-hydroperoxypropyl)benzene

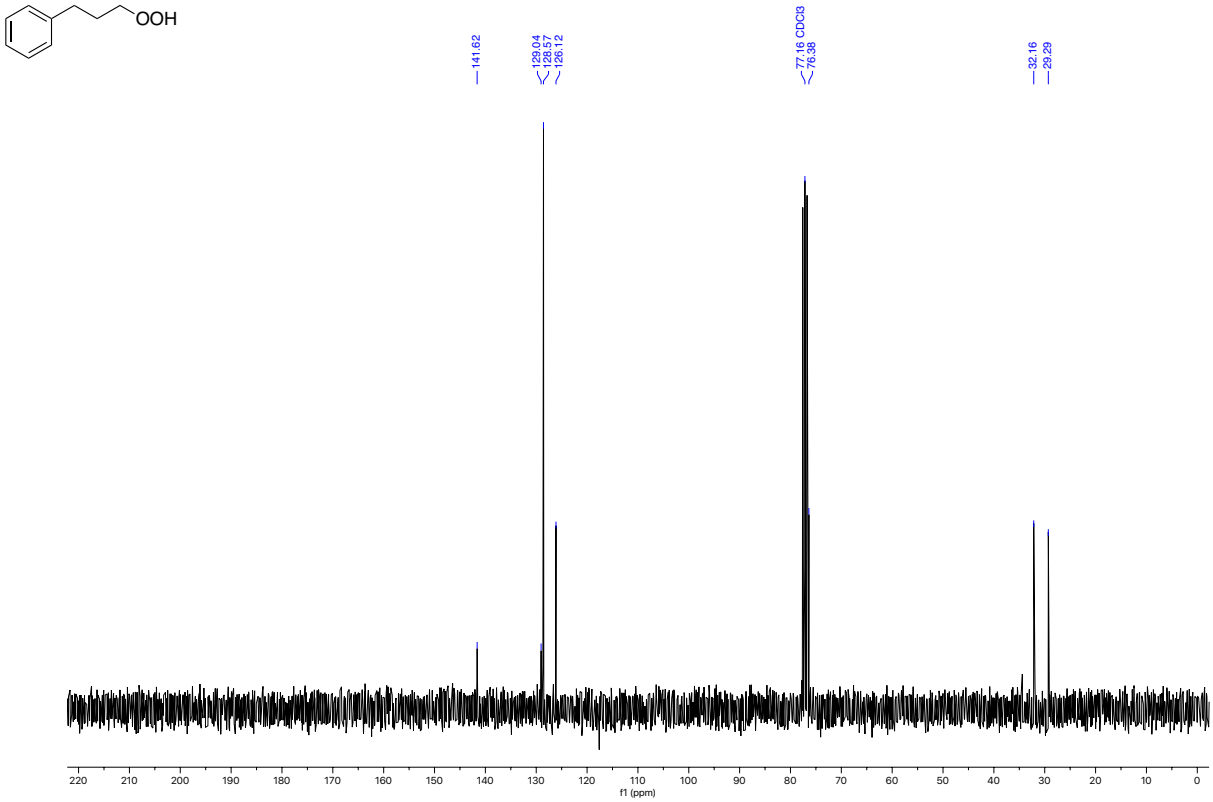

^{1}H NMR (300 MHz, $CDCl_3$)
1-(2-methylallyl)cyclohexan-1-ol

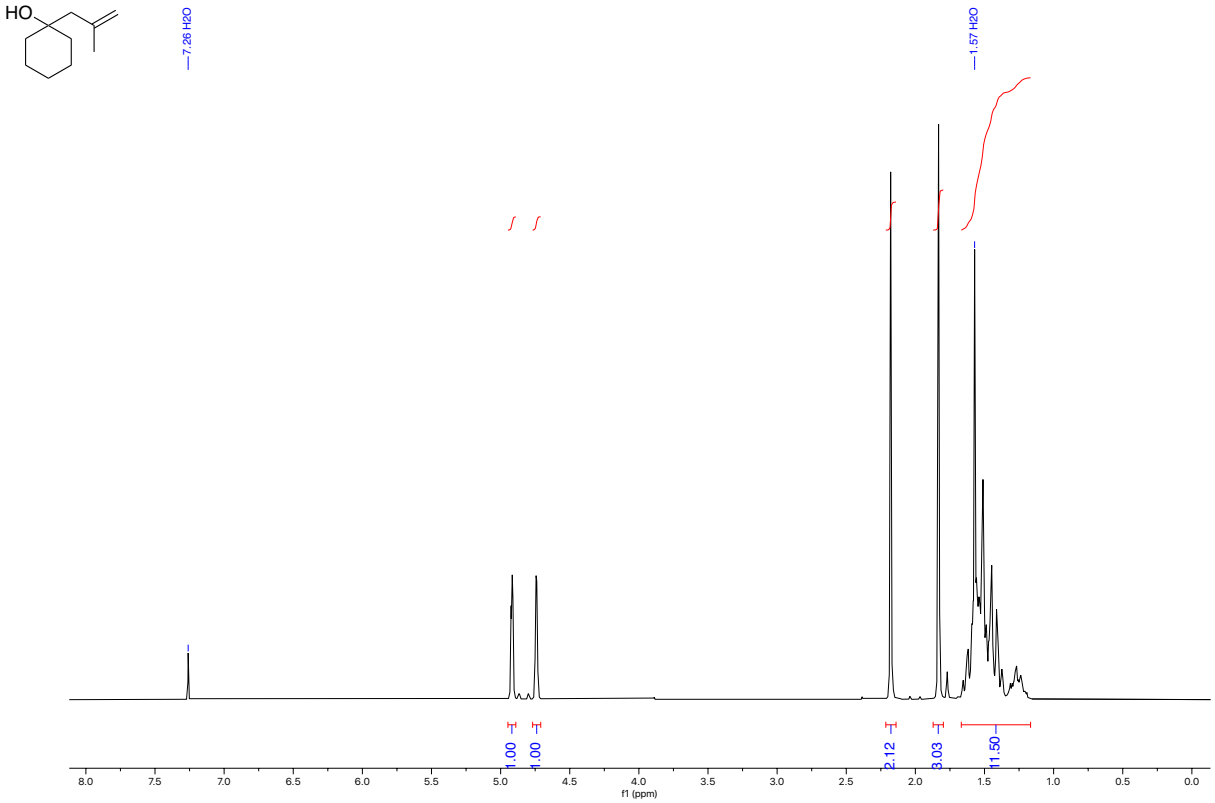

^{13}C NMR (75 MHz, $CDCl_3$)
1-(2-methylallyl)cyclohexan-1-ol

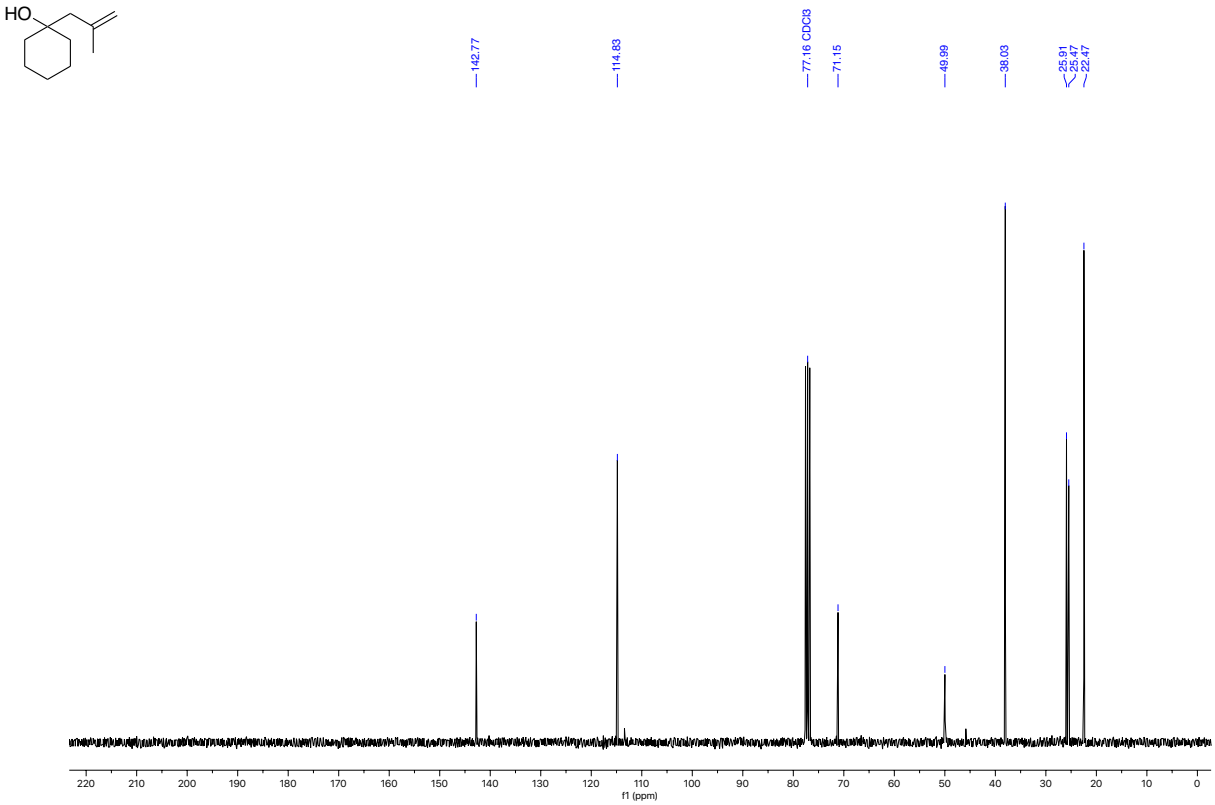

^{1}H NMR (300 MHz, $CDCl_3$)
4-phenylbutyl methanesulfonate

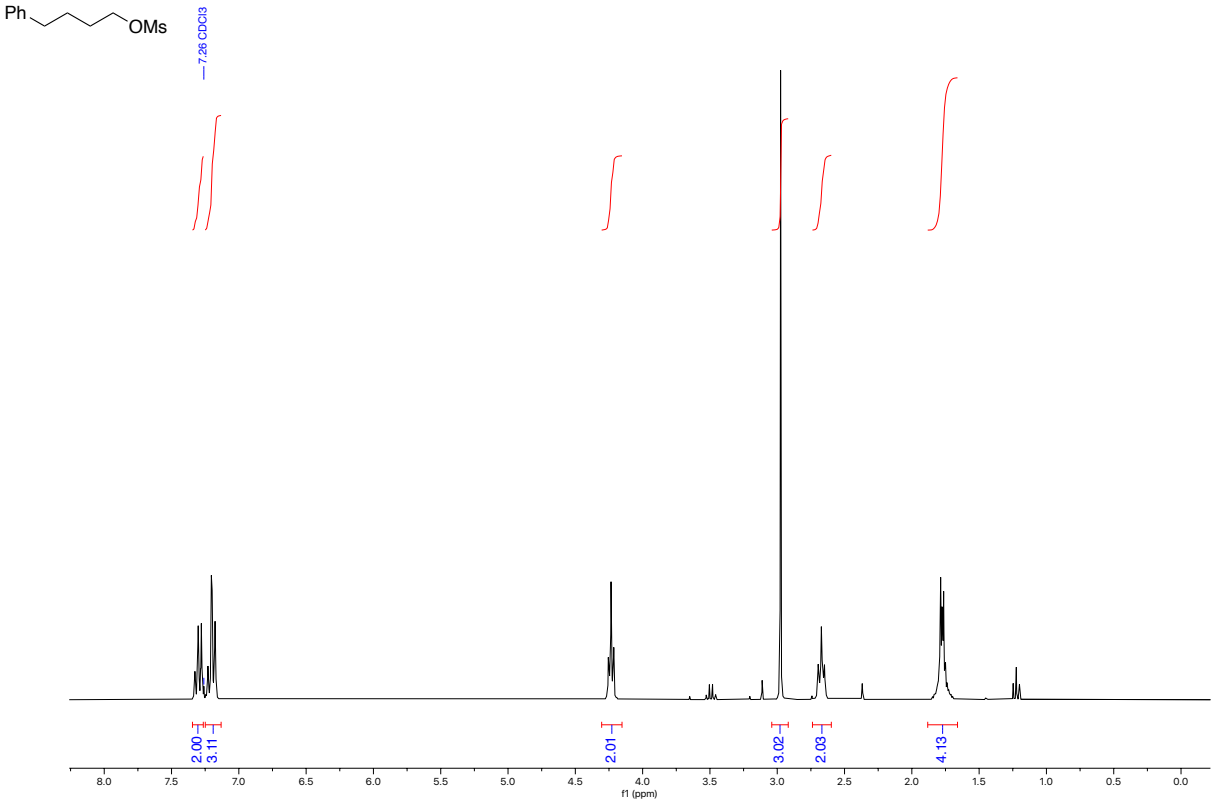

^{13}C NMR (75 MHz, $CDCl_3$)
4-phenylbutyl methanesulfonate

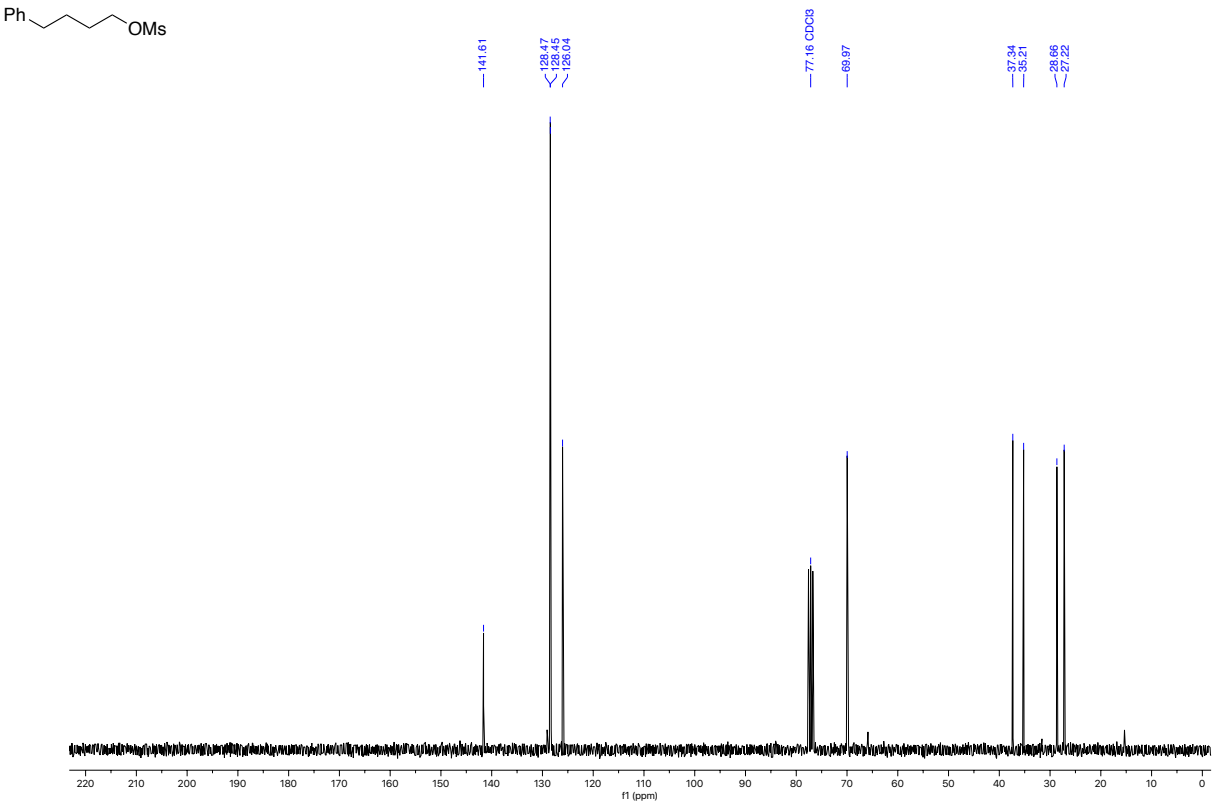

^{1}H NMR (300 MHz, $CDCl_3$)
(4-hydroperoxybutyl)benzene

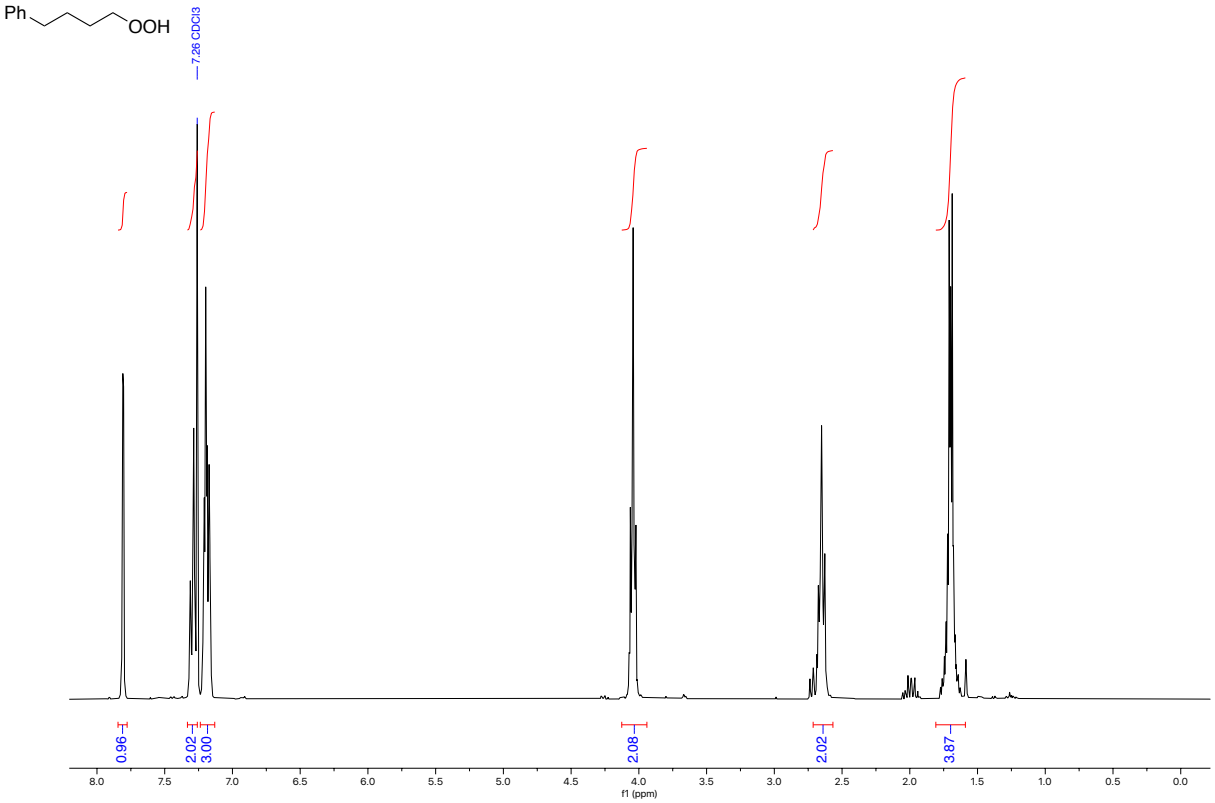

^{13}C NMR (75 MHz, $CDCl_3$)
(4-hydroperoxybutyl)benzene

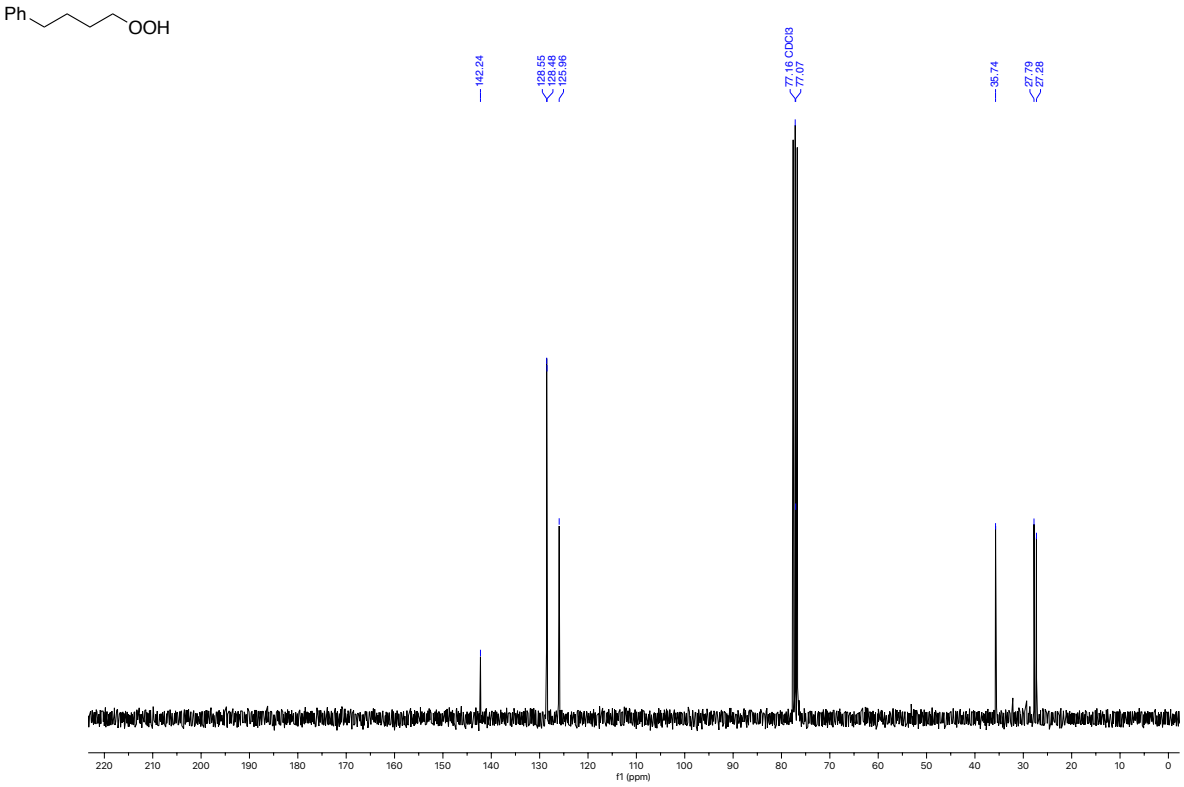

^{1}H NMR (300 MHz, $CDCl_3$)
4-phenylbutanal

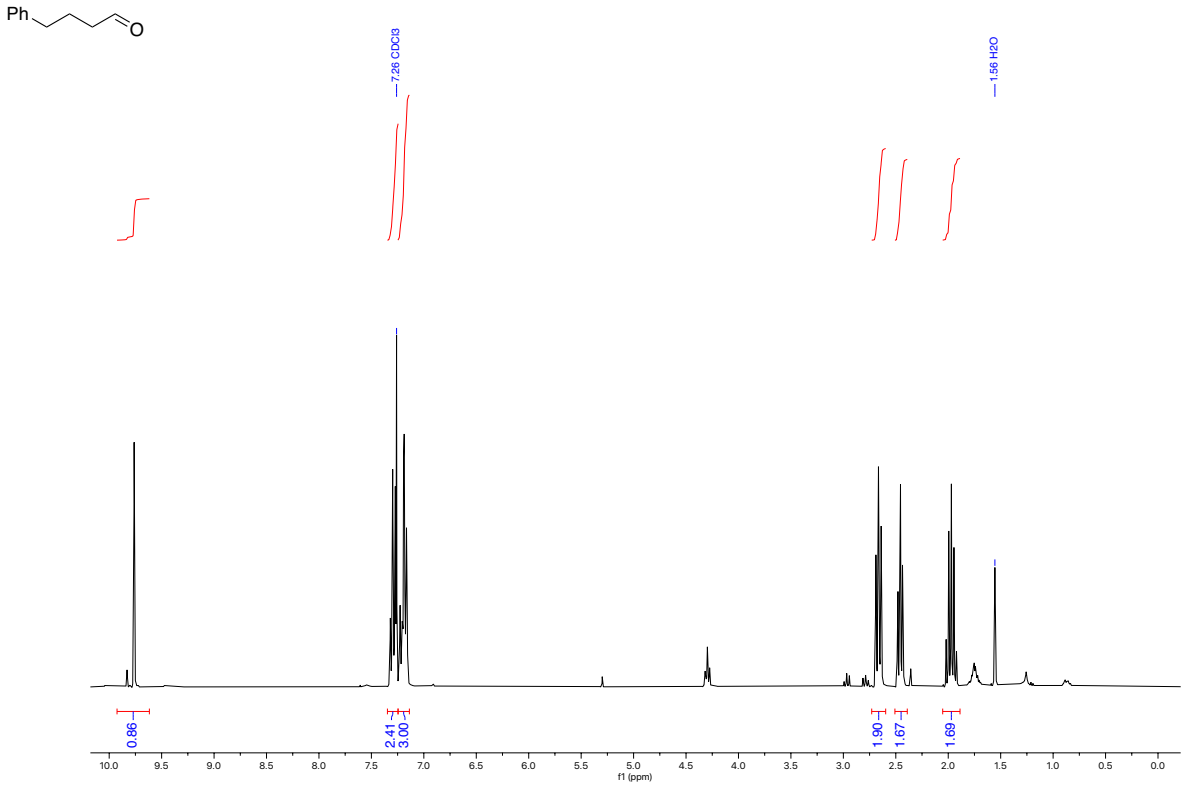

^{13}C NMR (75 MHz, $CDCl_3$)
4-phenylbutanal

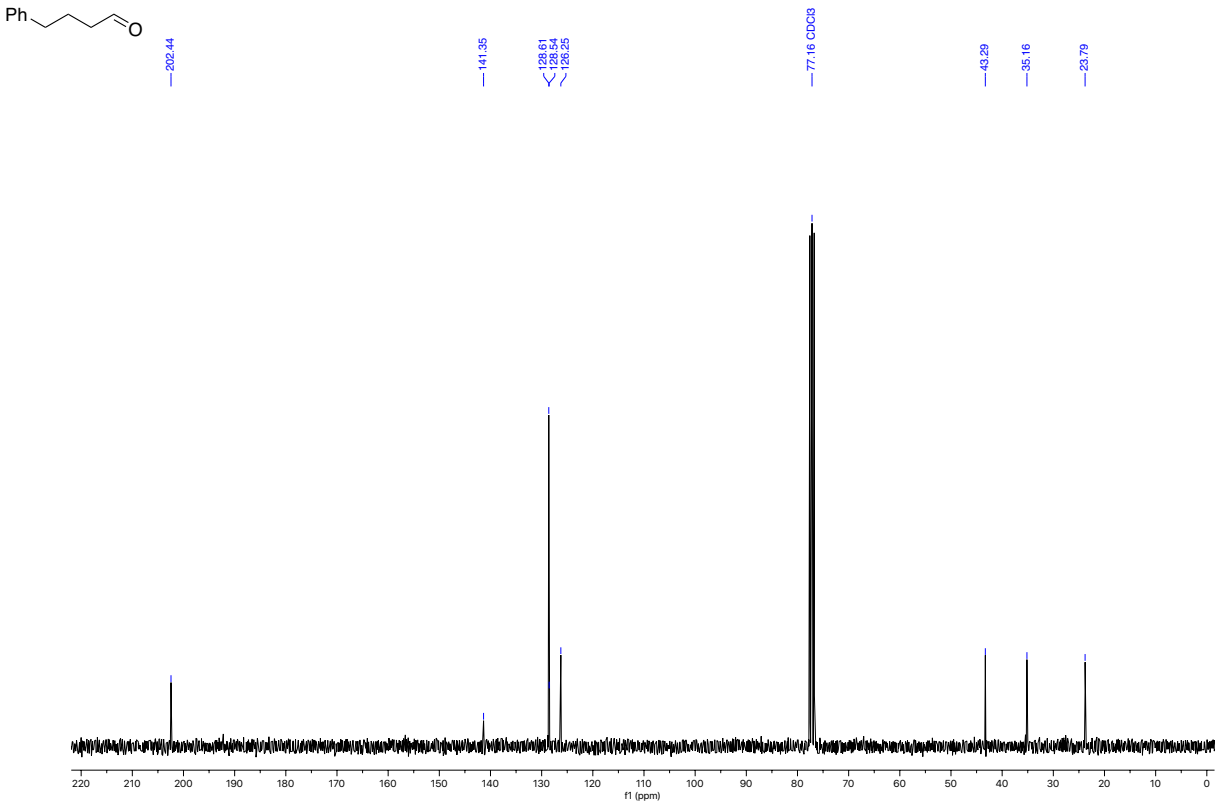

^{1}H NMR (300 MHz, $CDCl_3$)
2-methyl-4-phenylbutan-2-ol

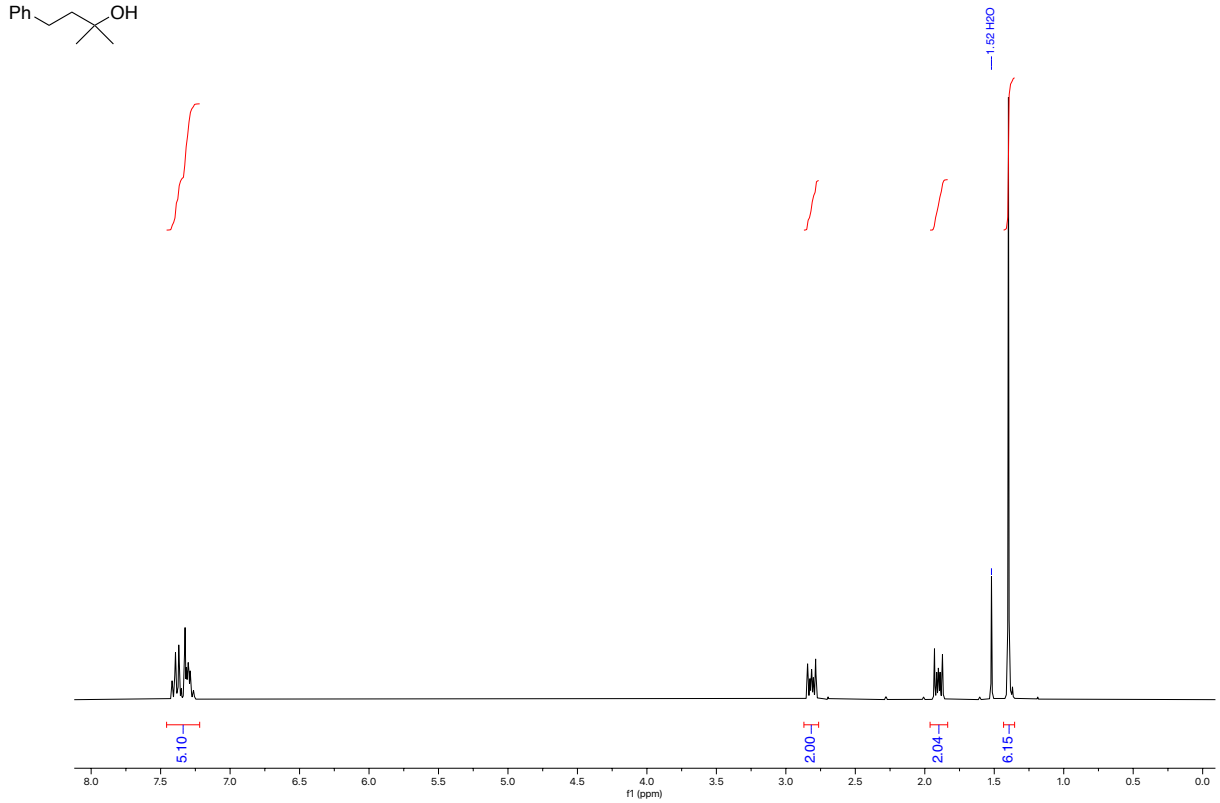

^{13}C NMR (75 MHz, $CDCl_3$)
2-methyl-4-phenylbutan-2-ol

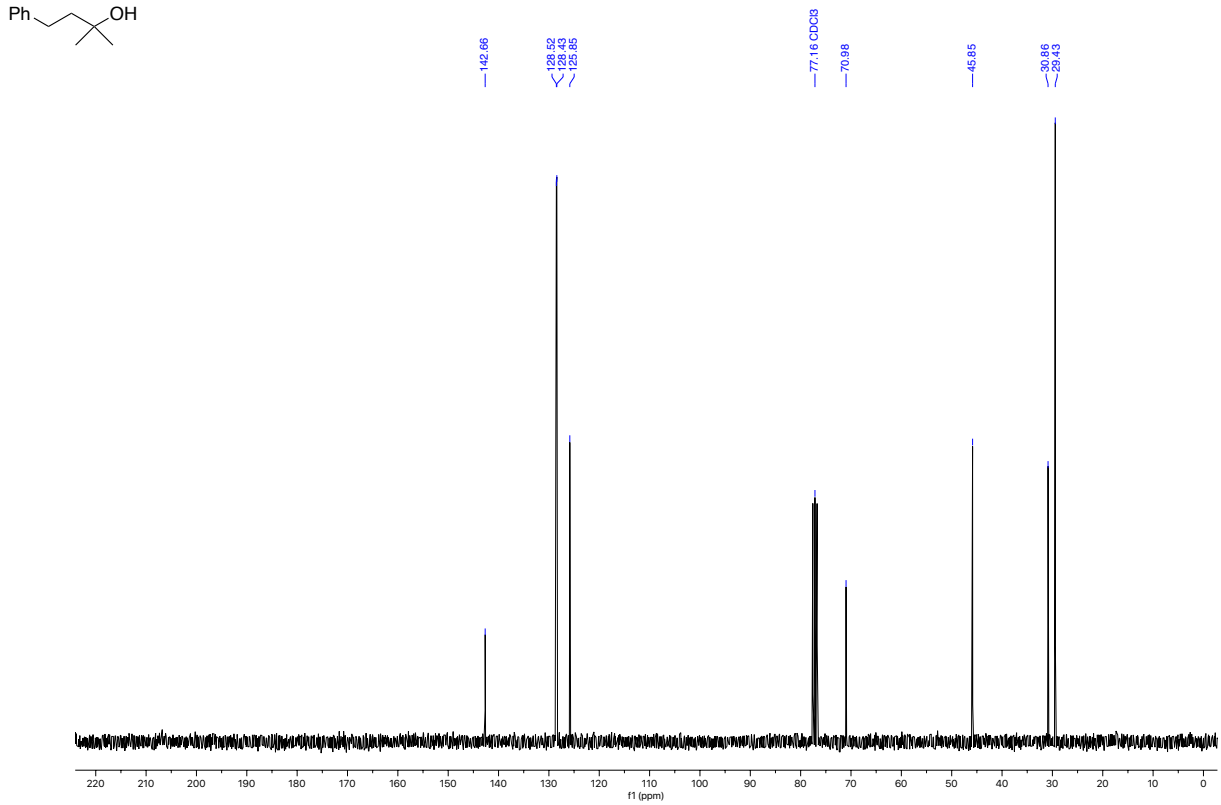

^{1}H NMR (300 MHz, $CDCl_3$)
(3-hydroperoxy-3-methylbutyl)benzene

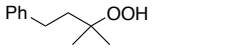

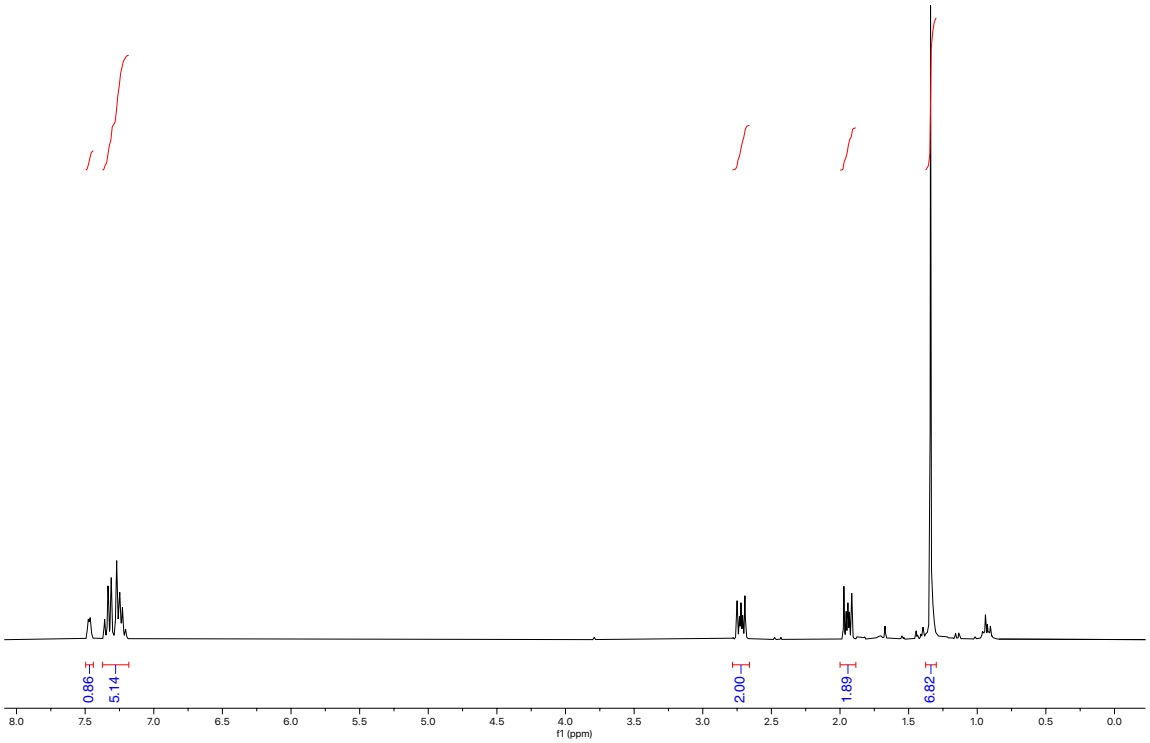

^{13}C NMR (75 MHz, $CDCl_3$)
(3-hydroperoxy-3-methylbutyl)benzene

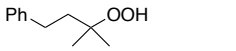

^{1}H NMR (300 MHz, $CDCl_3$)
pentan-3-yl methanesulfonate

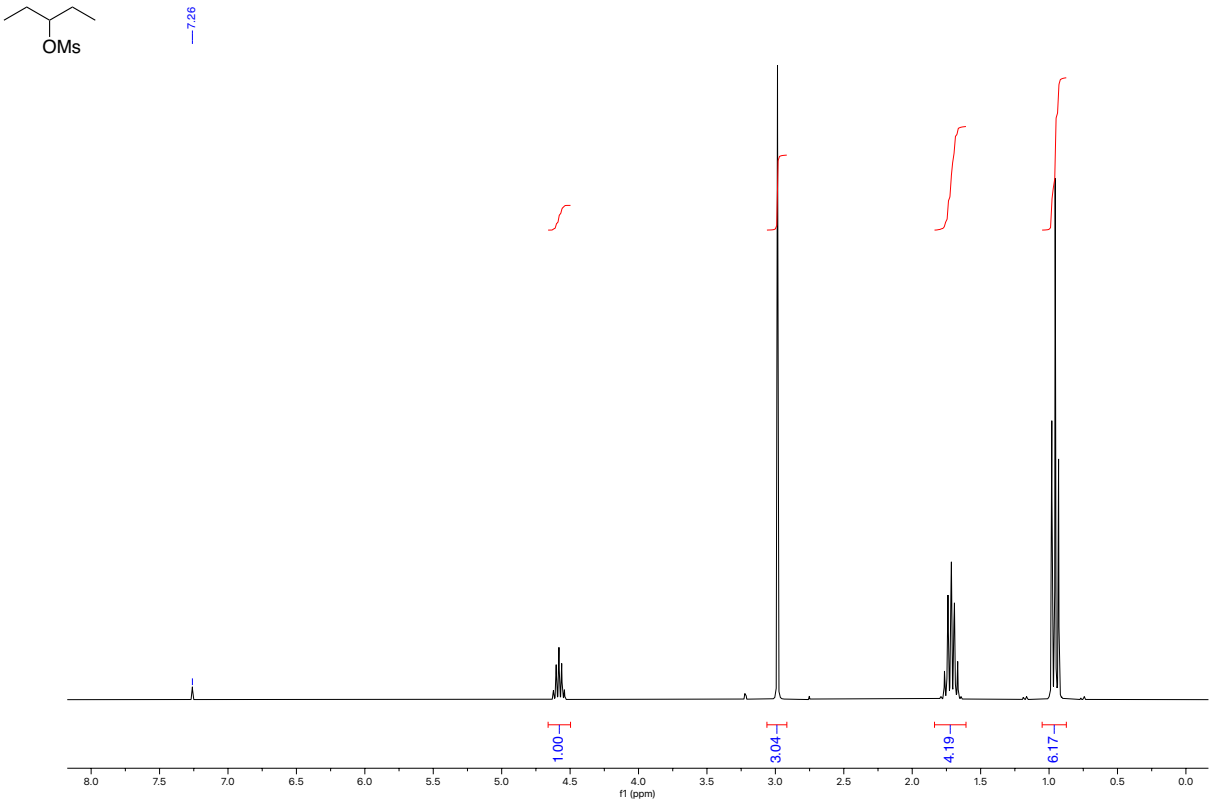

^{13}C NMR (75 MHz, $CDCl_3$)
pentan-3-yl methanesulfonate

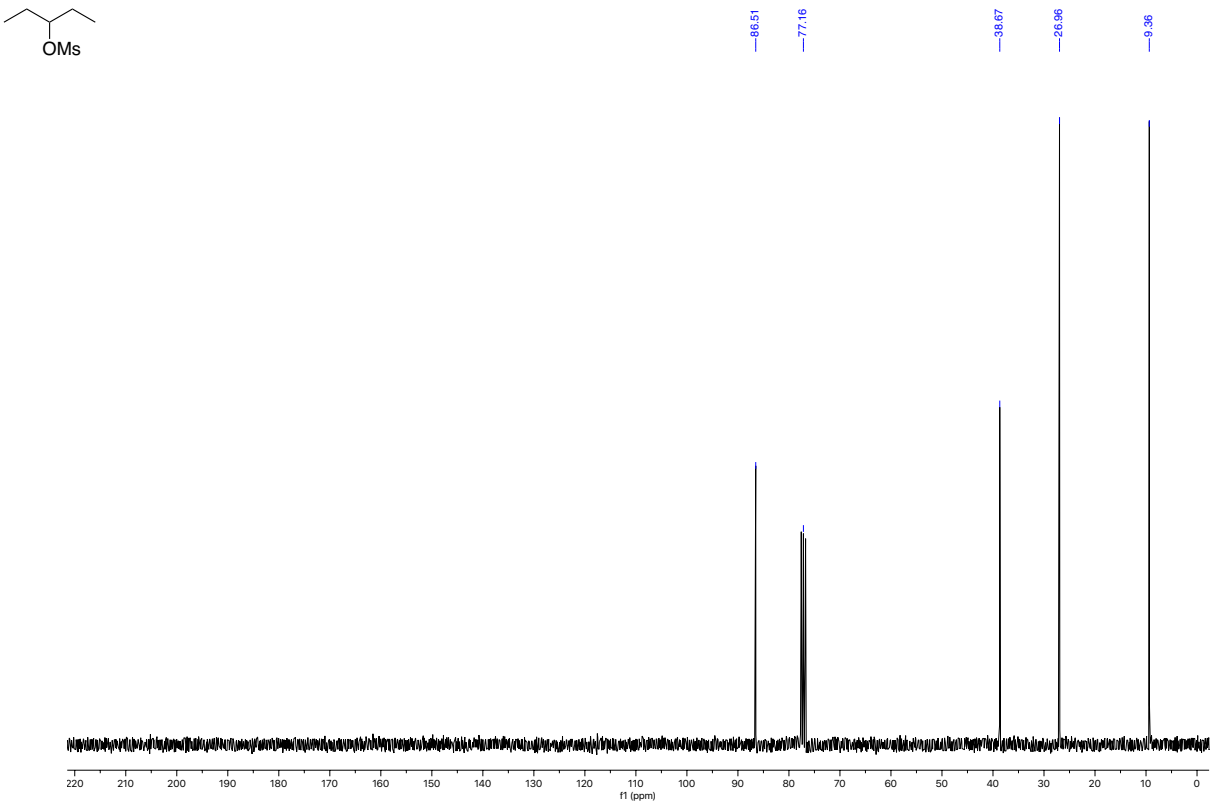

^{1}H NMR (300 MHz, $CDCl_3$)
3-hydroperoxypentane

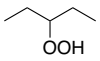

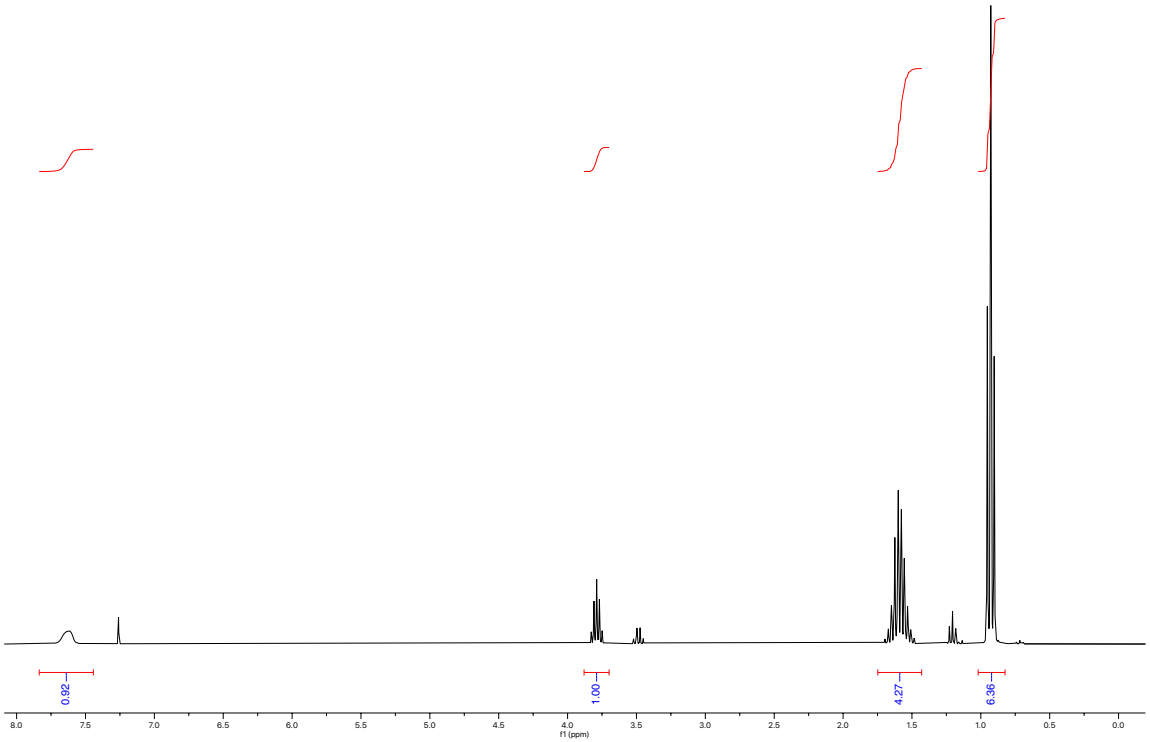

^{13}C NMR (75 MHz, $CDCl_3$)
3-hydroperoxypentane

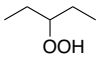

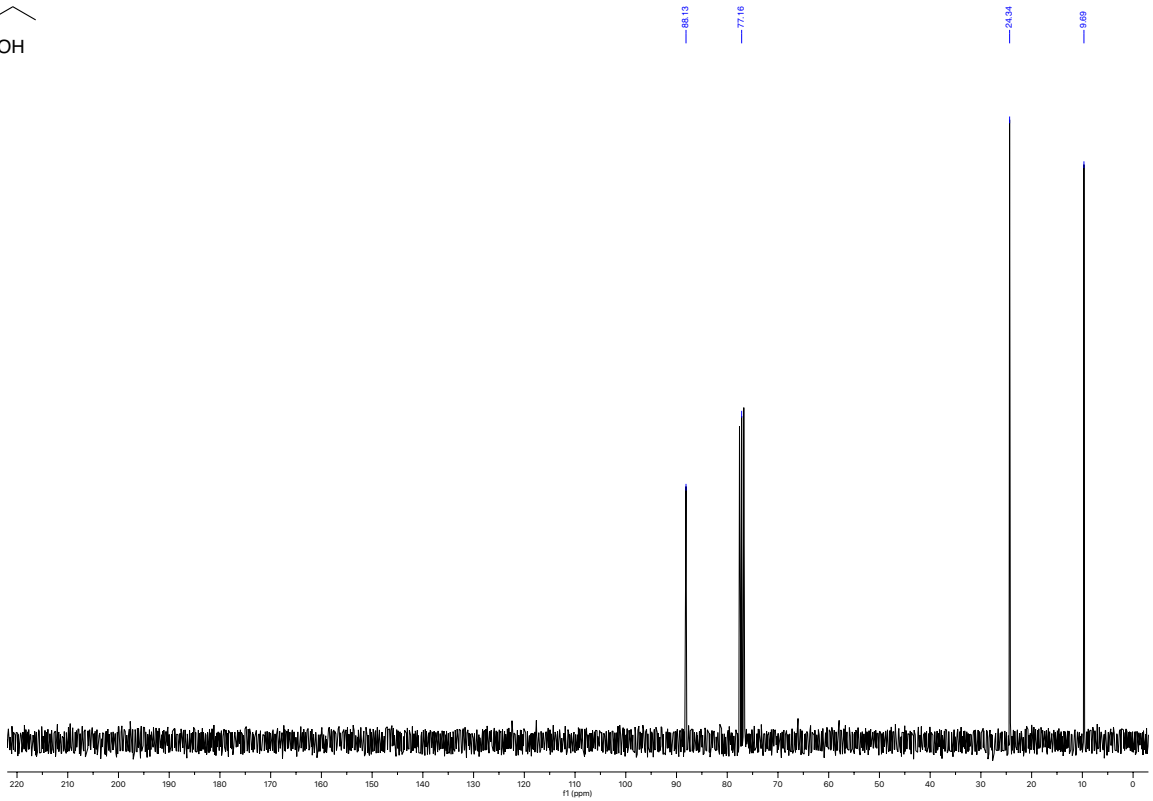

^{1}H NMR (300 MHz, $CDCl_3$)
(2-bromoethoxy)(tert-butyl)dimethylsilane

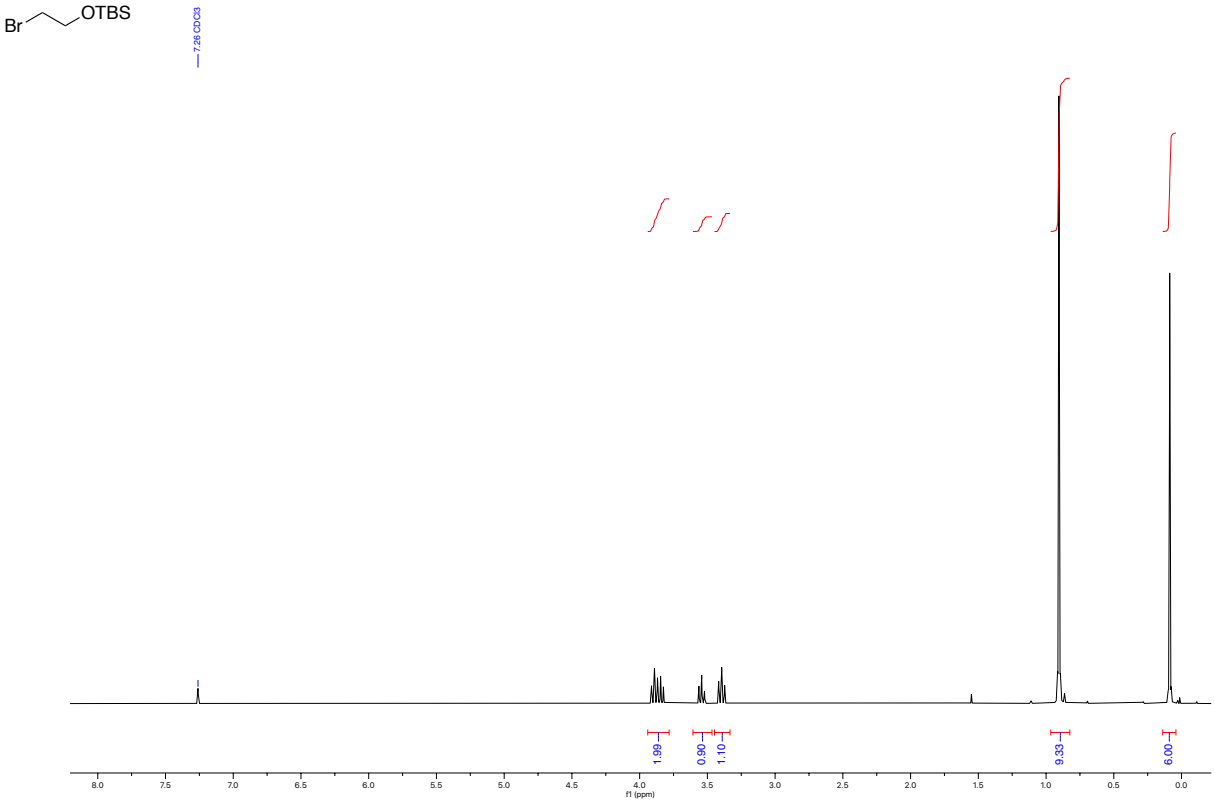

^{13}C NMR (75 MHz, $CDCl_3$)
(2-bromoethoxy)(tert-butyl)dimethylsilane

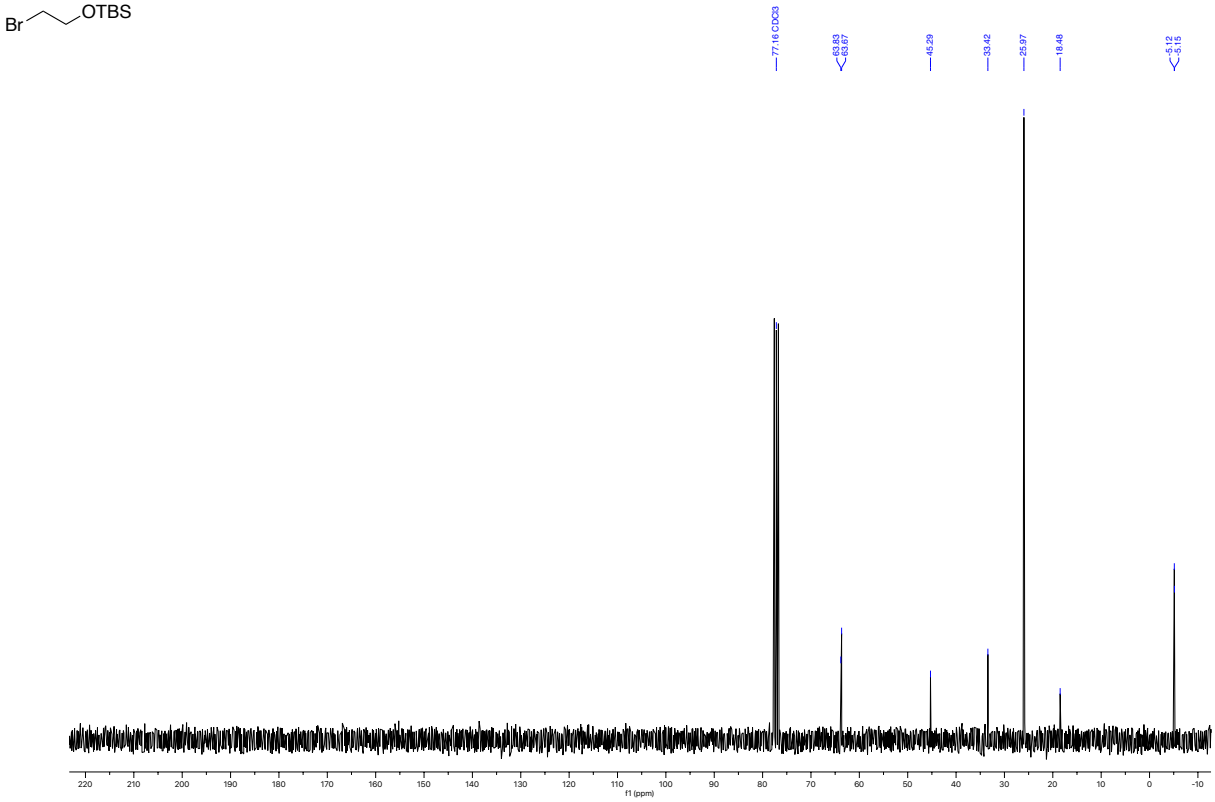

^{1}H NMR (300 MHz, $CDCl_3$)
2-(2-((tert-butyldimethylsilyl)oxy)ethyl)cyclododecan-1-one

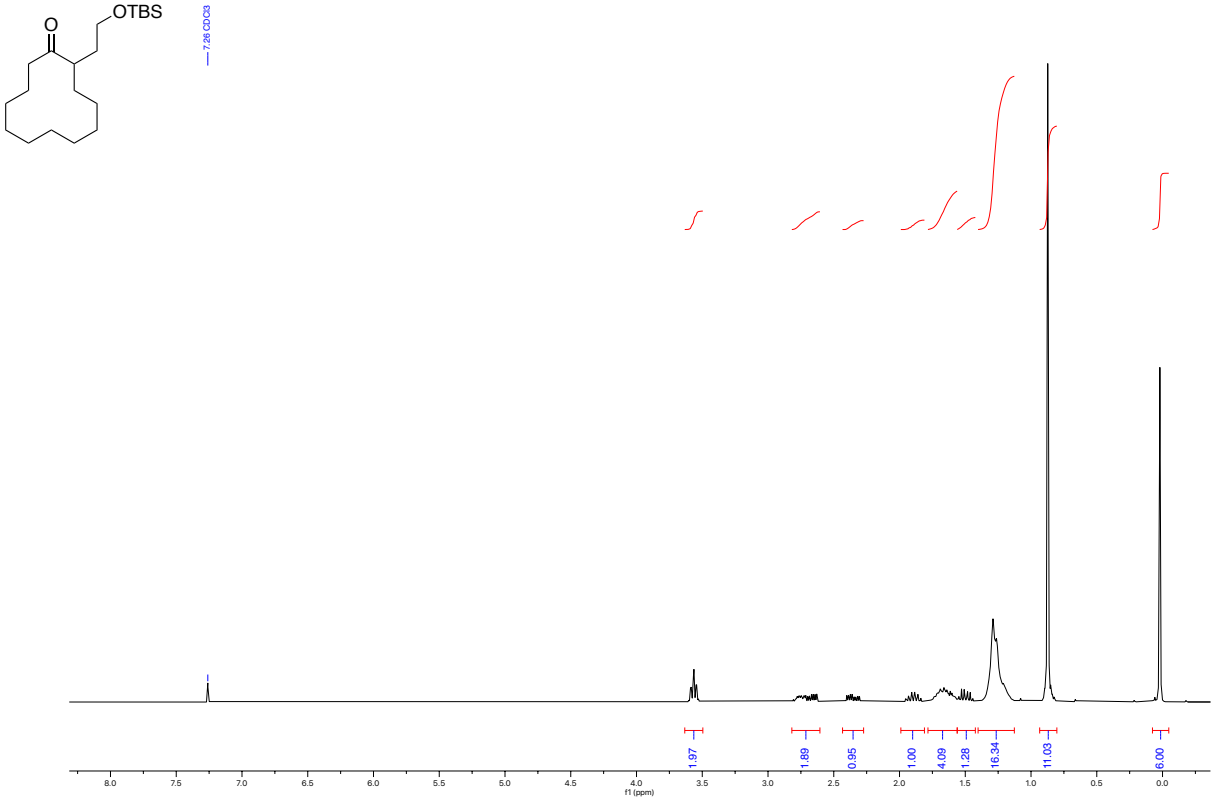

^{13}C NMR (75 MHz, $CDCl_3$)
2-(2-((tert-butyldimethylsilyl)oxy)ethyl)cyclododecan-1-one

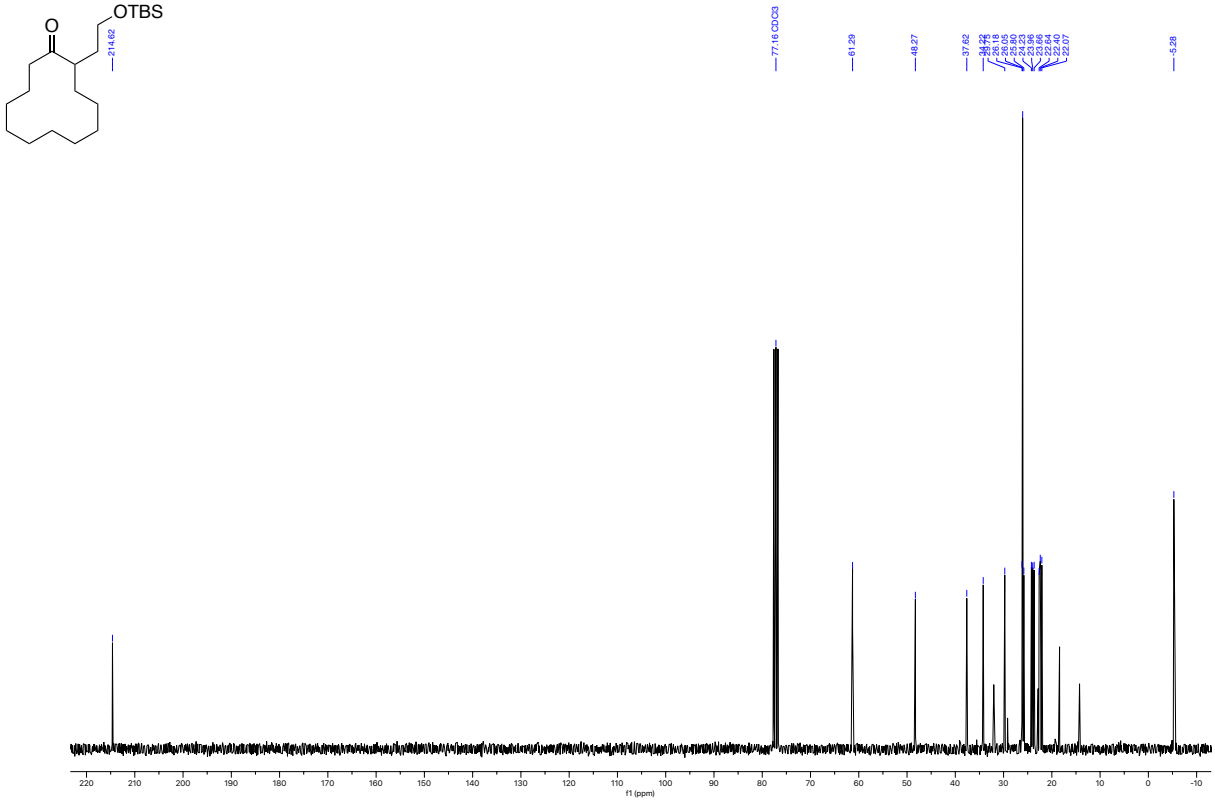

^{1}H NMR (300 MHz, $CDCl_3$)
2,3,4,5,6,7,8,9,10,11,12,13-dodecahydrocyclododeca[*b*]furan

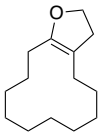

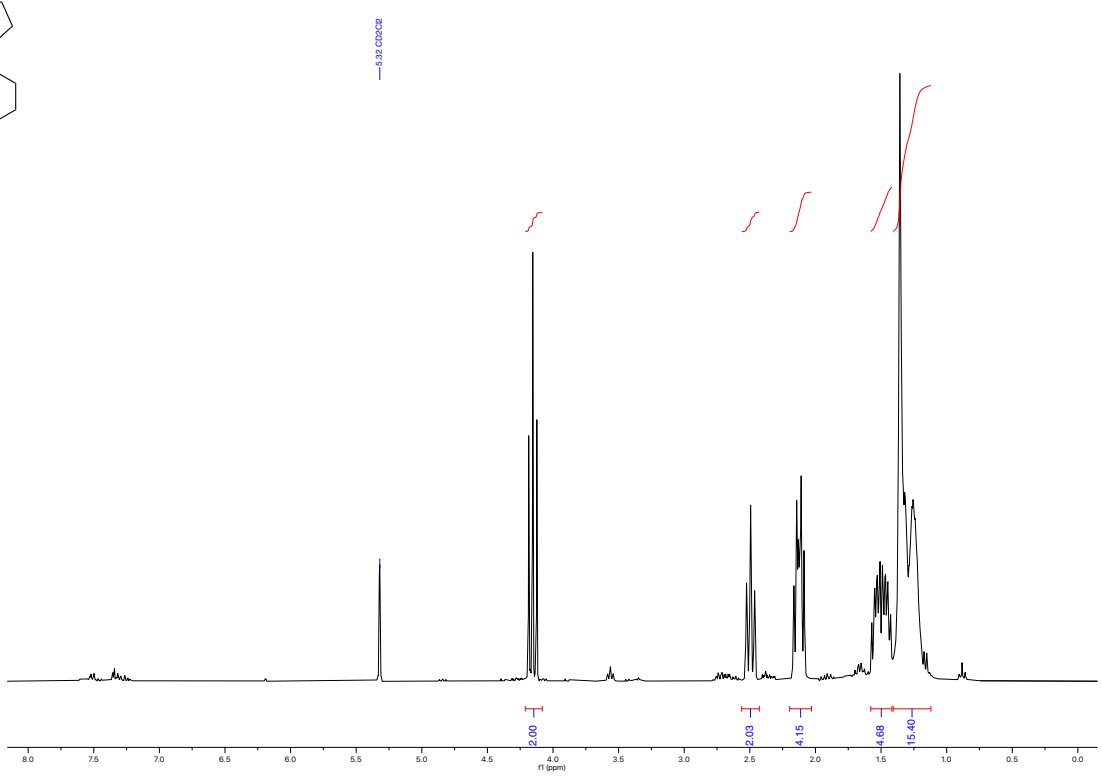

^{13}C NMR (75 MHz, $CDCl_3$)
2,3,4,5,6,7,8,9,10,11,12,13-dodecahydrocyclododeca[*b*]furan

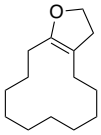

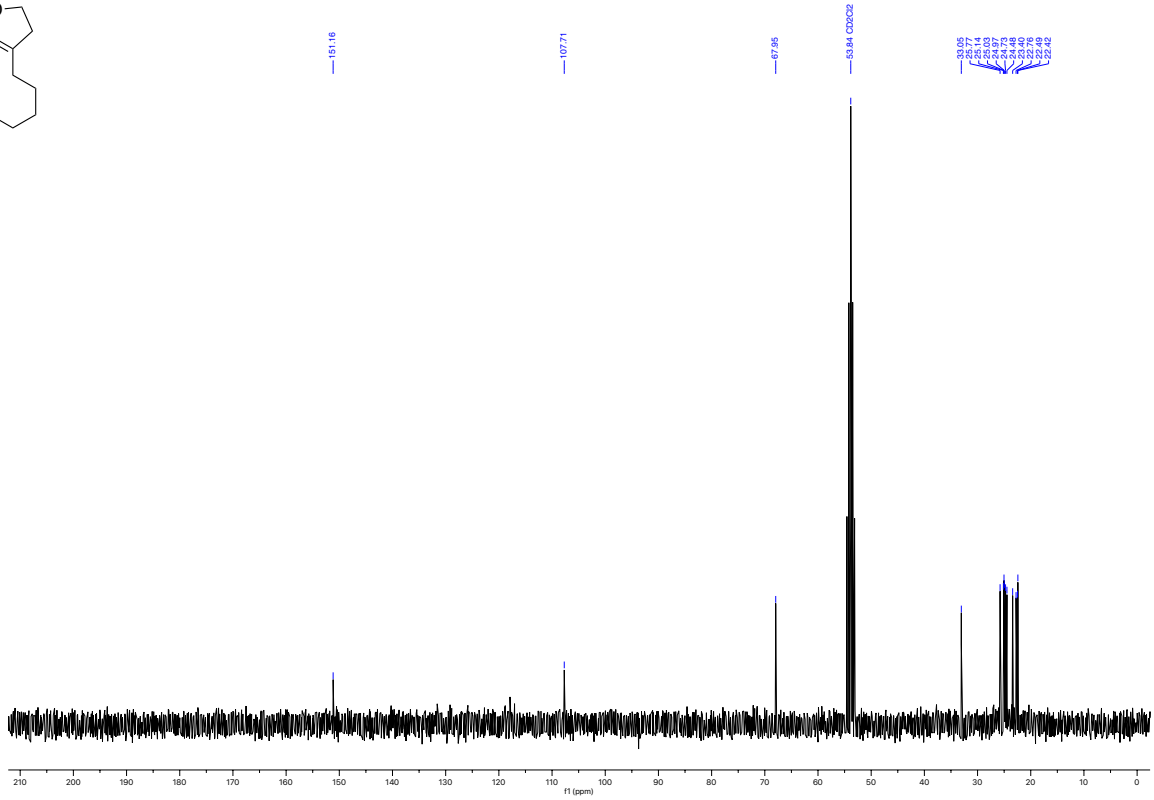

^{1}H NMR (300 MHz, $CDCl_3$)
13a-hydroperoxytetradecahydrocyclododeca[*b*]furan

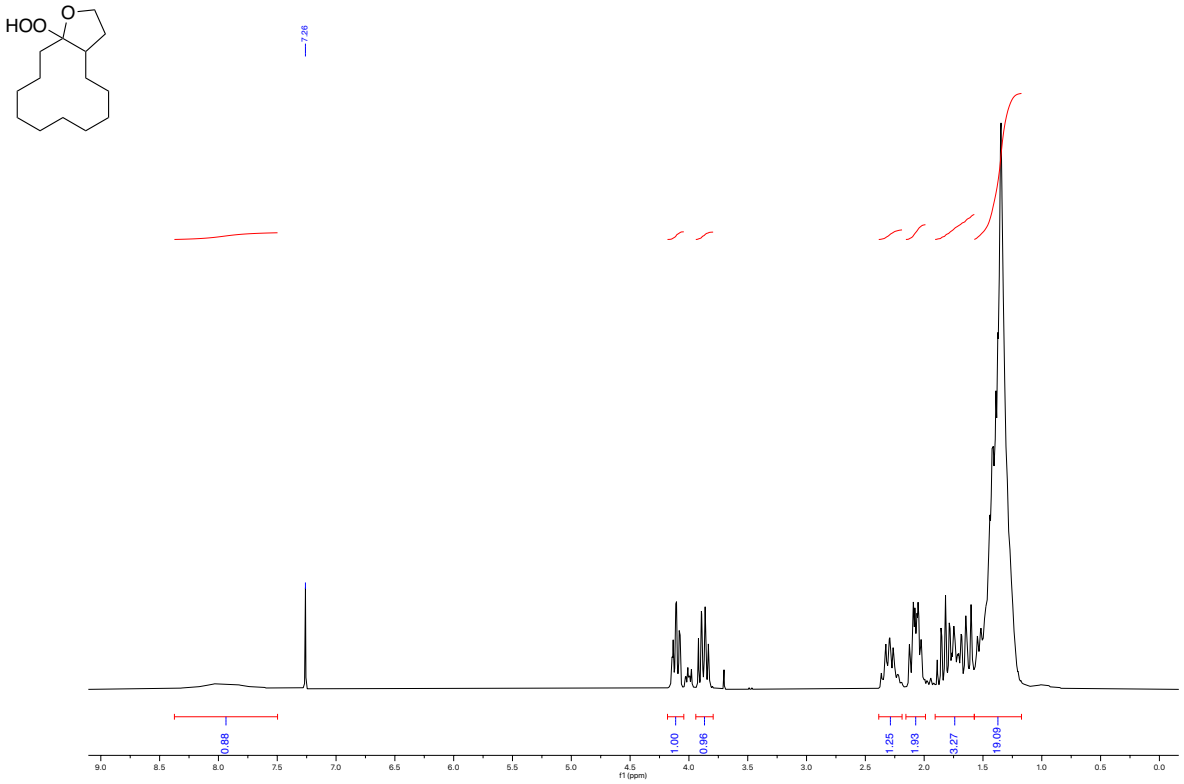

^{13}C NMR (75 MHz, $CDCl_3$)
13a-hydroperoxytetradecahydrocyclododeca[*b*]furan

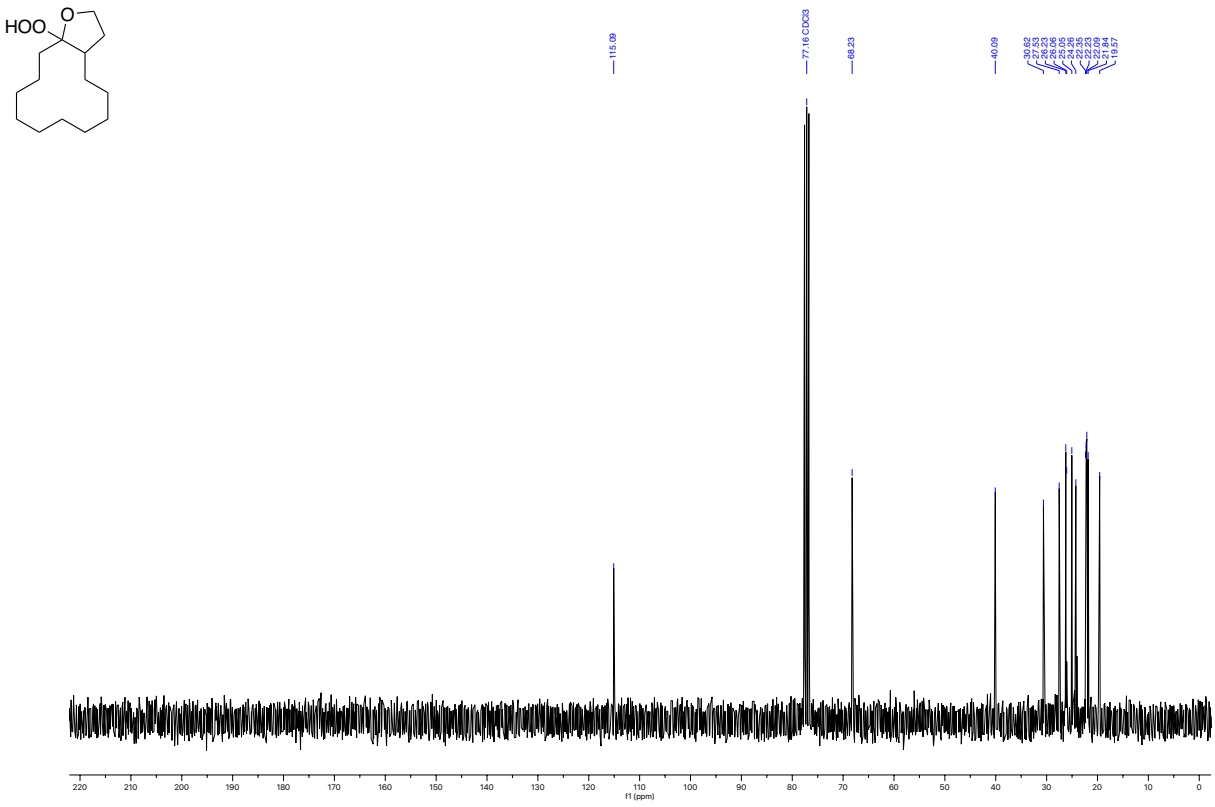

^{1}H NMR (300 MHz, $CDCl_3$)
(8*R*,9*S*,13*S*,14*S*)-3-((tert-butyldimethylsilyl)oxy)-13-methyl-6,7,8,9,11,12,13,14,15,16-decahydro-17H-cyclopenta[*a*]phenanthren-17-one

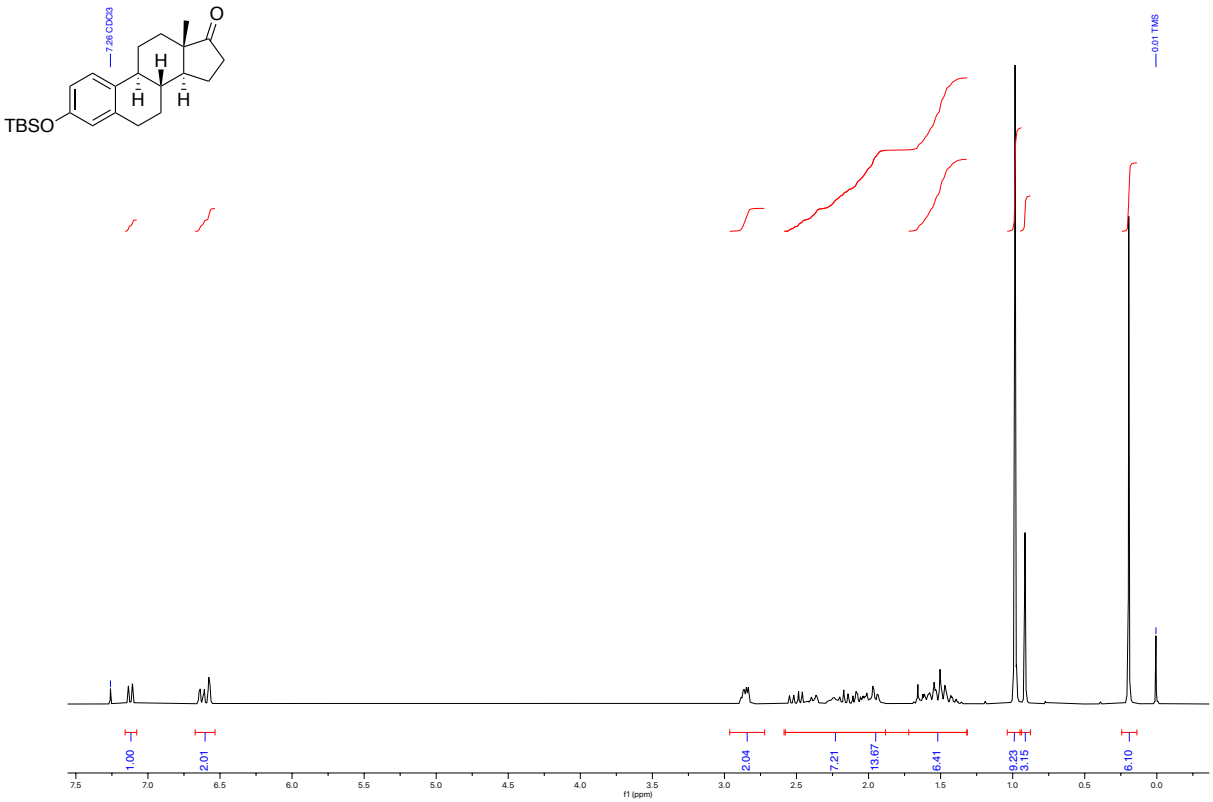

^{13}C NMR (75 MHz, $CDCl_3$)
(8*R*,9*S*,13*S*,14*S*)-3-((tert-butyldimethylsilyl)oxy)-13-methyl-6,7,8,9,11,12,13,14,15,16-decahydro-17H-cyclopenta[*a*]phenanthren-17-one

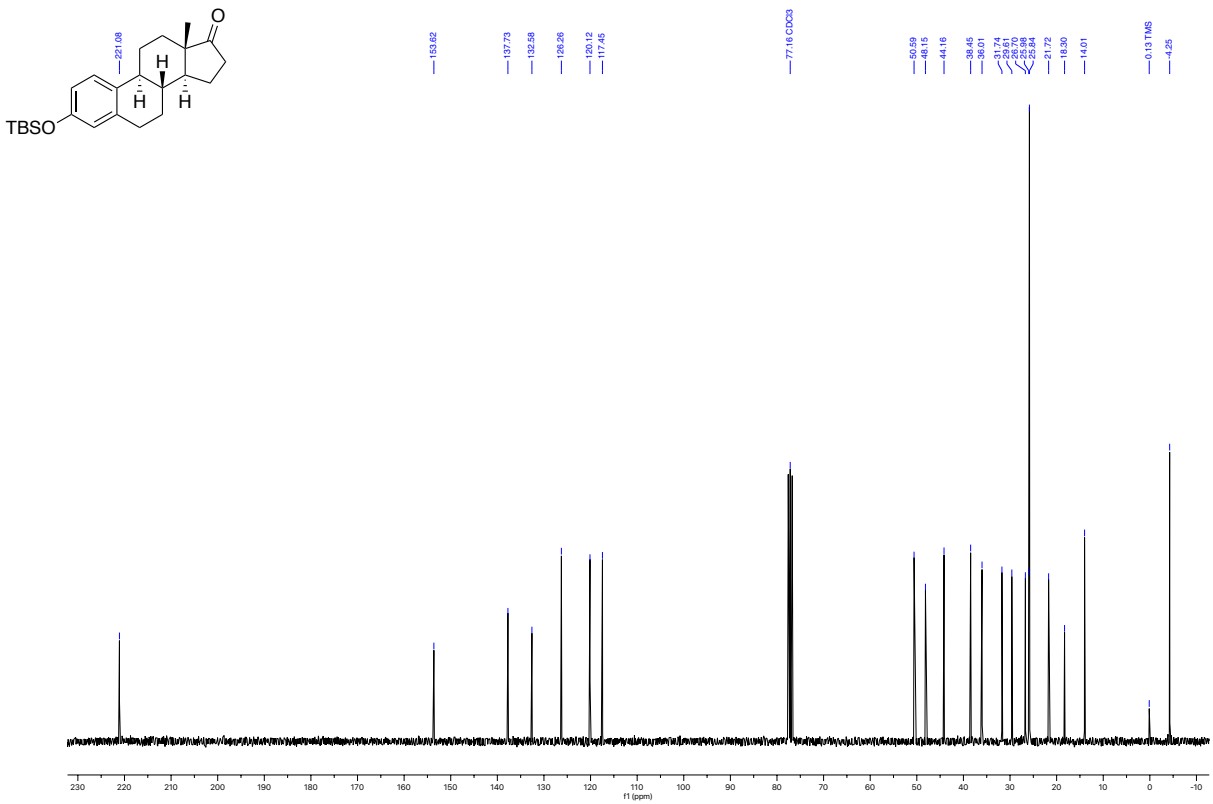

^{1}H NMR (300 MHz, $CDCl_3$)
(8*R*,9*S*,13*S*,14*S*,17*S*)-3-((tert-butyldimethylsilyl)oxy)-13,17-dimethyl-7,8,9,11,12,13,14,15,16,17-decahydro-6H-cyclopenta[*a*]phenanthren-17-ol

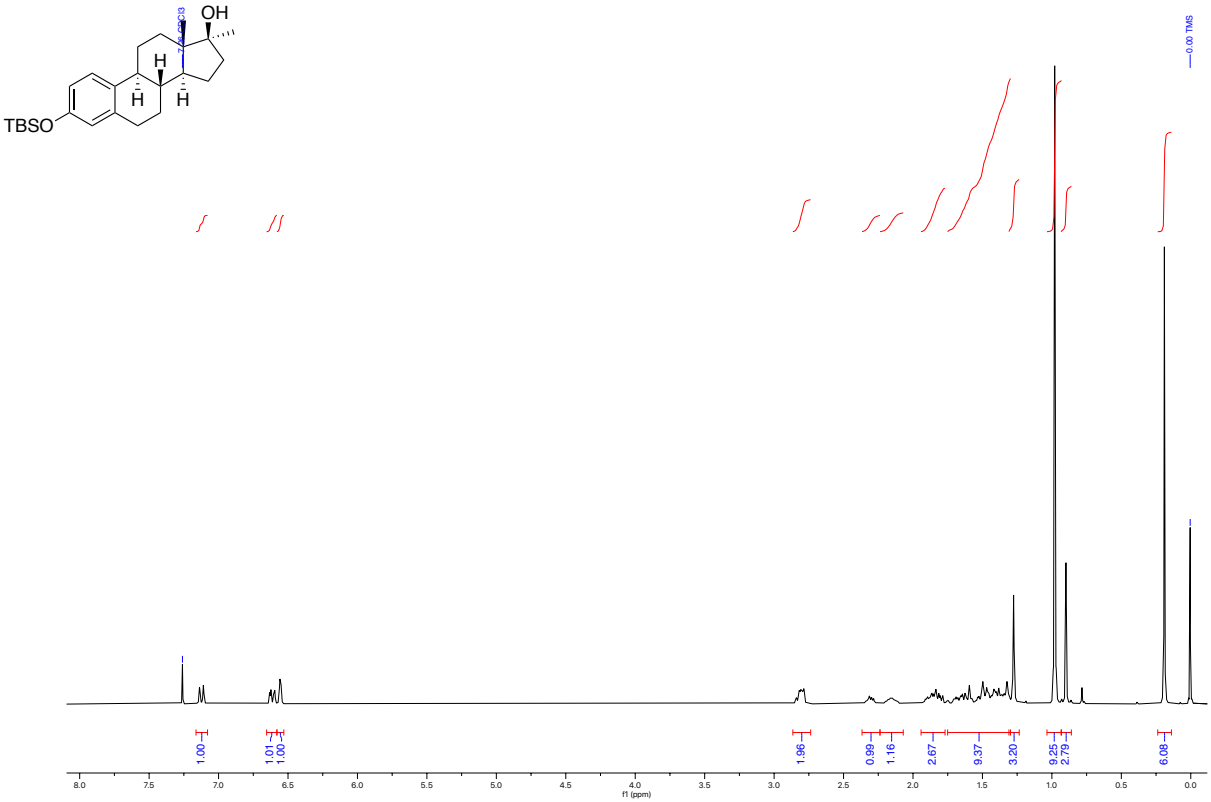

^{13}C NMR (75 MHz, $CDCl_3$)
(8*R*,9*S*,13*S*,14*S*,17*S*)-3-((tert-butyldimethylsilyl)oxy)-13,17-dimethyl-7,8,9,11,12,13,14,15,16,17-decahydro-6H-cyclopenta[*a*]phenanthren-17-ol

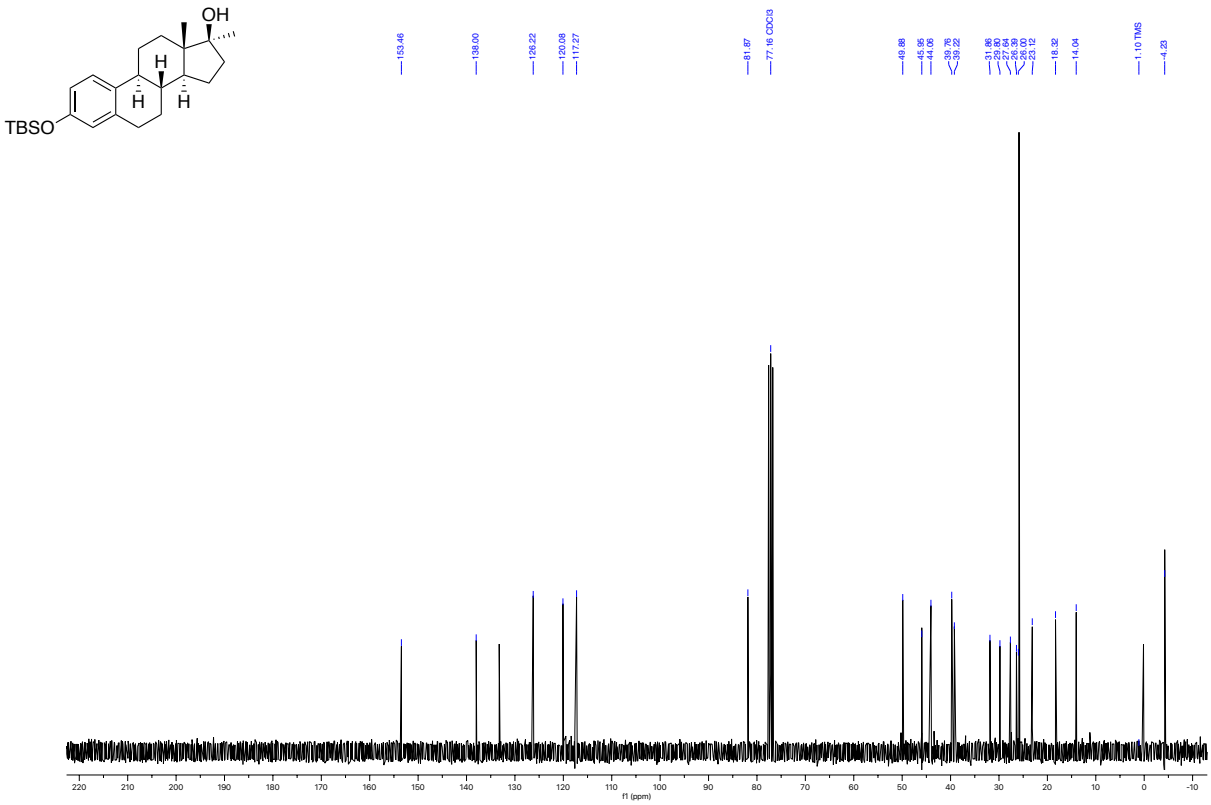

^{1}H NMR (300 MHz, $CDCl_3$)
(8*R*,9*S*,13*S*,14*S*,17*S*)-13,17-dimethyl-7,8,9,11,12,13,14,15,16,17-decahydro-6H-cyclopenta[*a*]phenanthrene-3,17-diol

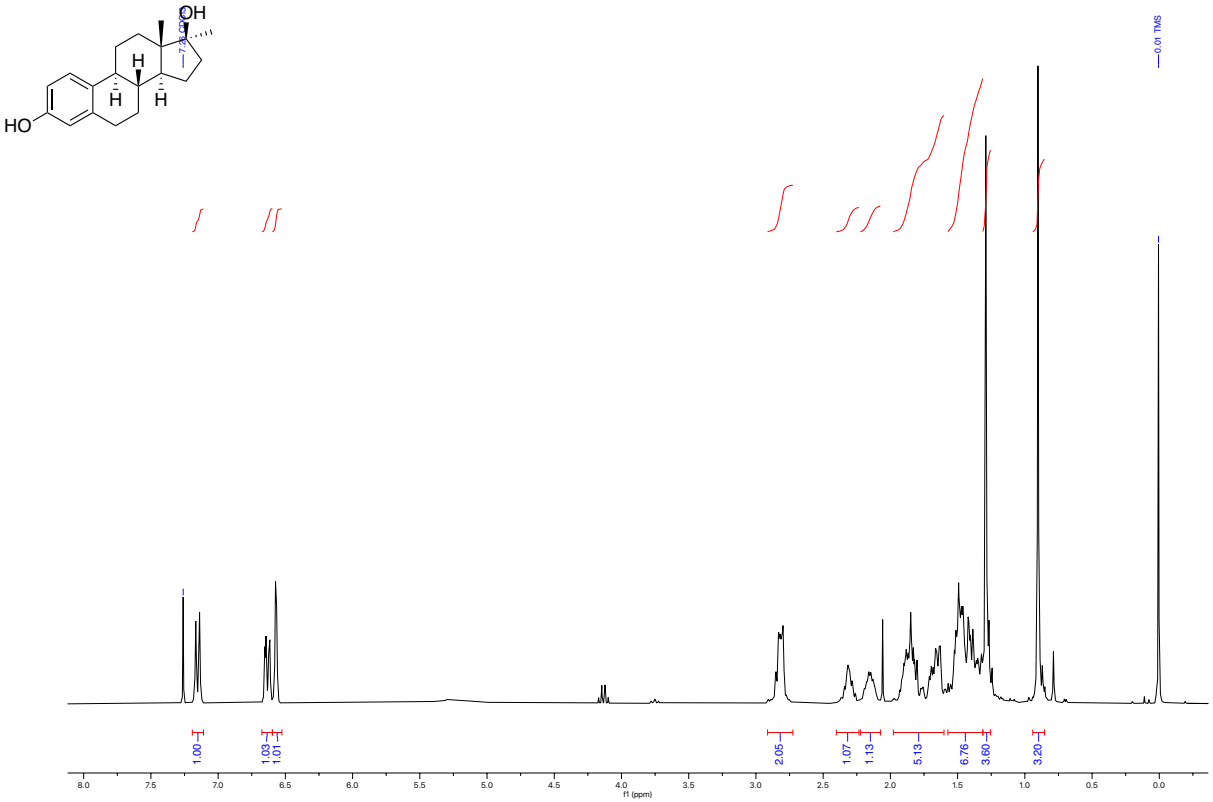

^{13}C NMR (75 MHz, $CDCl_3$)
(8*R*,9*S*,13*S*,14*S*,17*S*)-13,17-dimethyl-7,8,9,11,12,13,14,15,16,17-decahydro-6H-cyclopenta[*a*]phenanthrene-3,17-diol

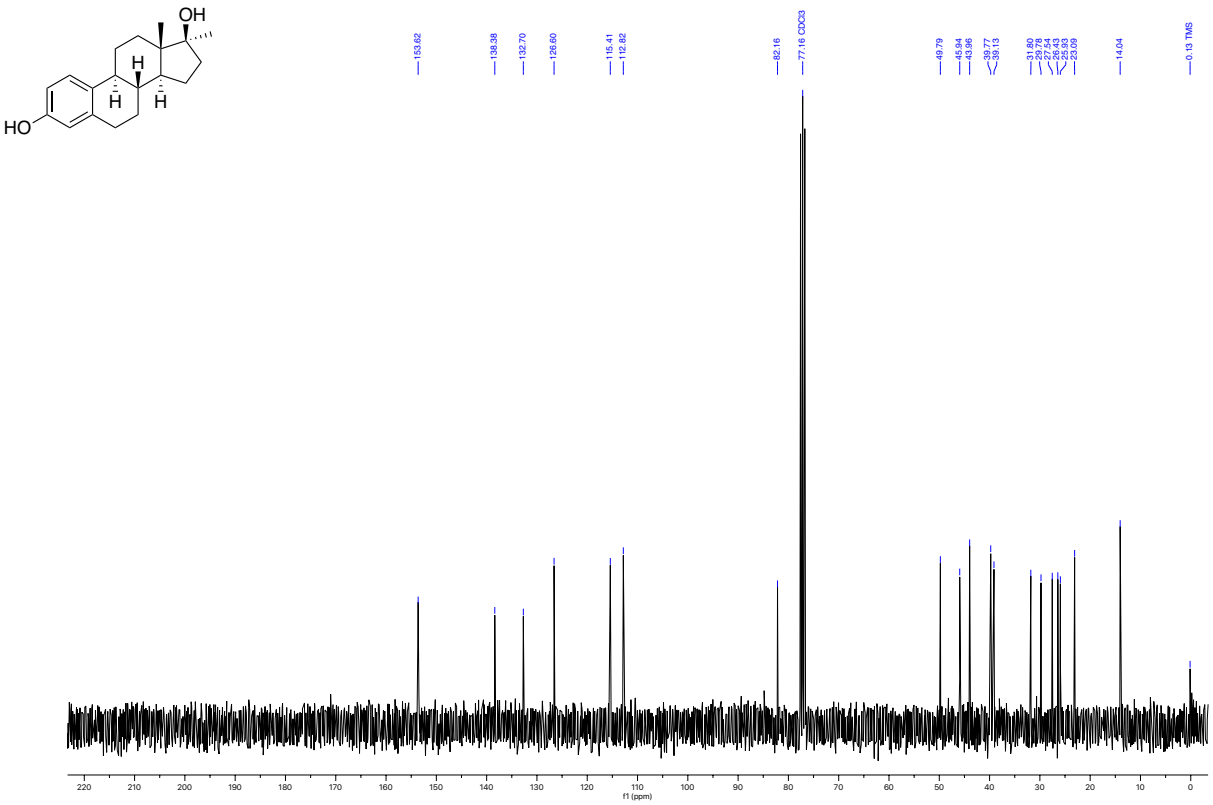

^{1}H NMR (300 MHz, $CDCl_3$)
(8*R*,9*S*,13*S*,14*S*,17*S*)-3-methoxy-13,17-dimethyl-7,8,9,11,12,13,14,15,16,17-decahydro-6H-cyclopenta[*a*]phenanthren-17-ol

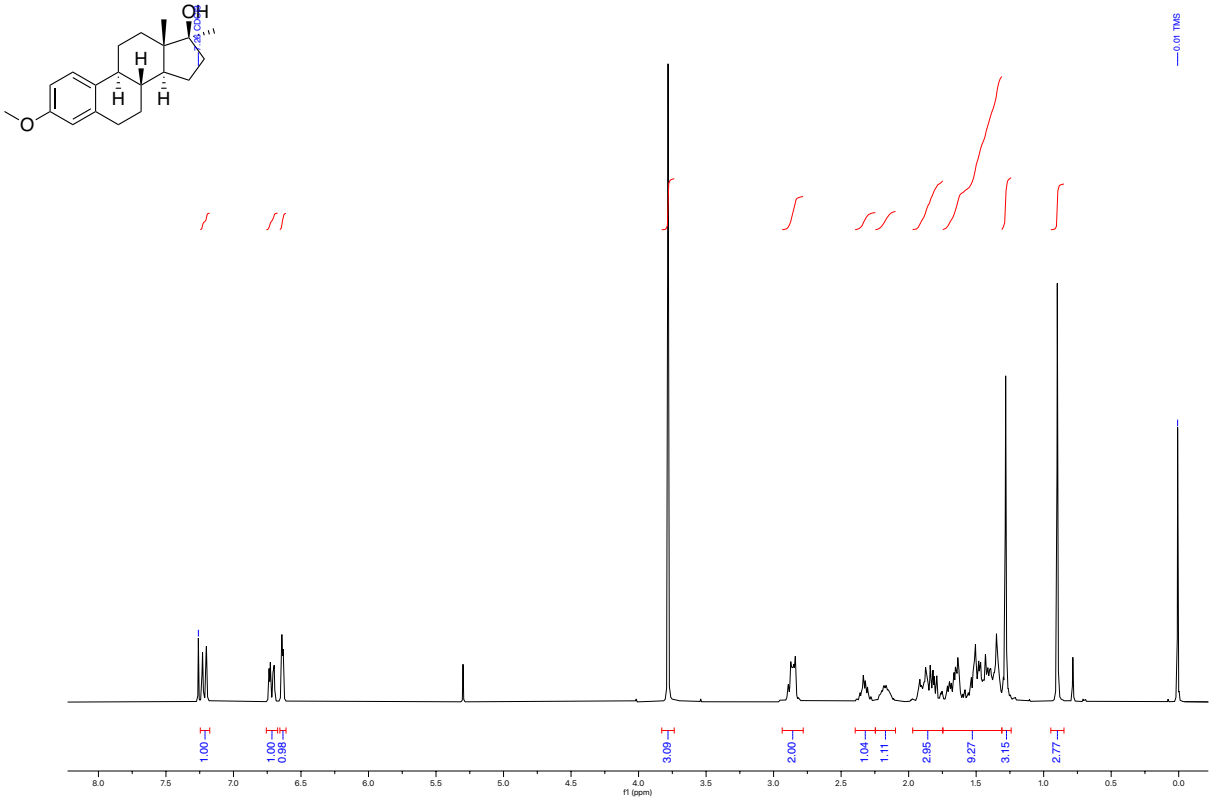

^{13}C NMR (75 MHz, $CDCl_3$)
(8*R*,9*S*,13*S*,14*S*,17*S*)-3-methoxy-13,17-dimethyl-7,8,9,11,12,13,14,15,16,17-decahydro-6H-cyclopenta[*a*]phenanthren-17-ol

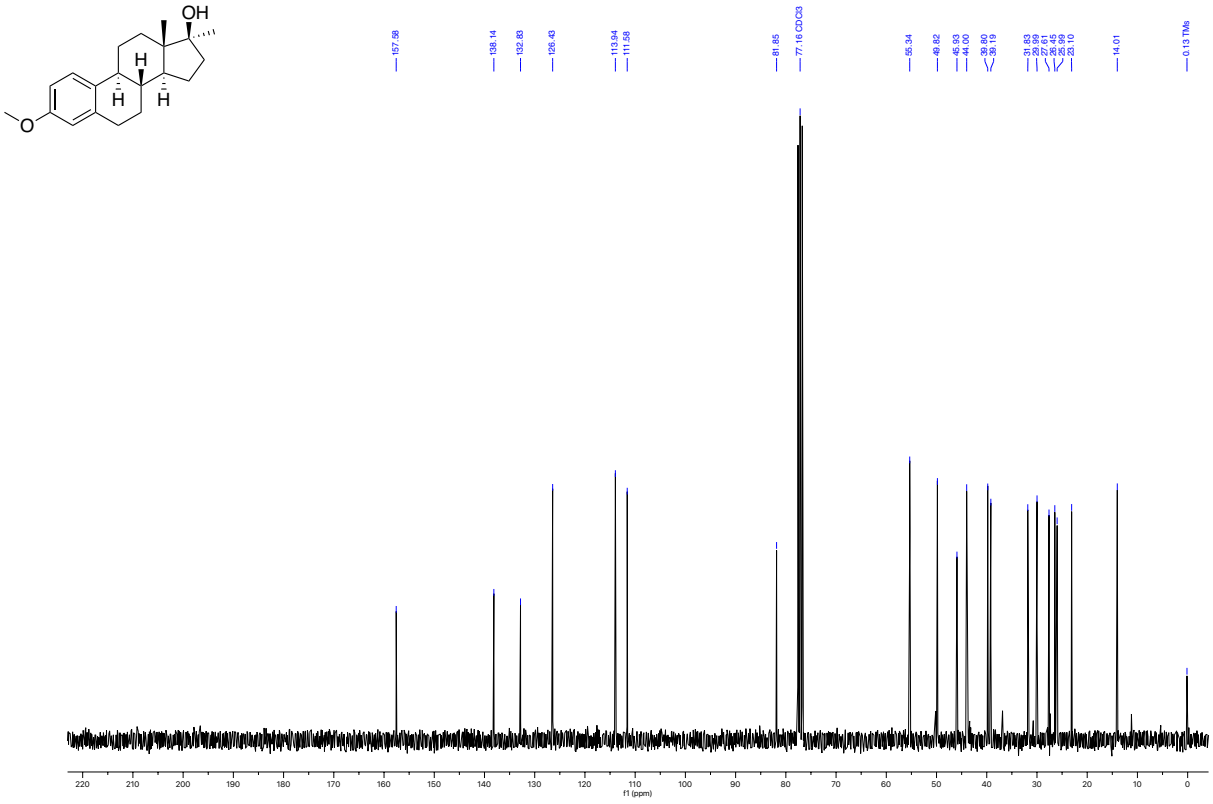

^{1}H NMR (300 MHz, $CDCl_3$)
1-((3*S*,8*S*,9*S*,10*R*,13*S*,14*S*,17*S*)-3-methoxy-10,13-dimethyl-2,3,4,7,8,9,10,11,12,13,14,15,16,17-tetradecahydro-1H-cyclopenta[*a*]phenanthren-17-yl)ethan-1-one

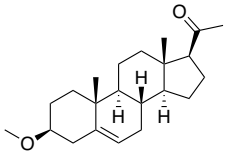

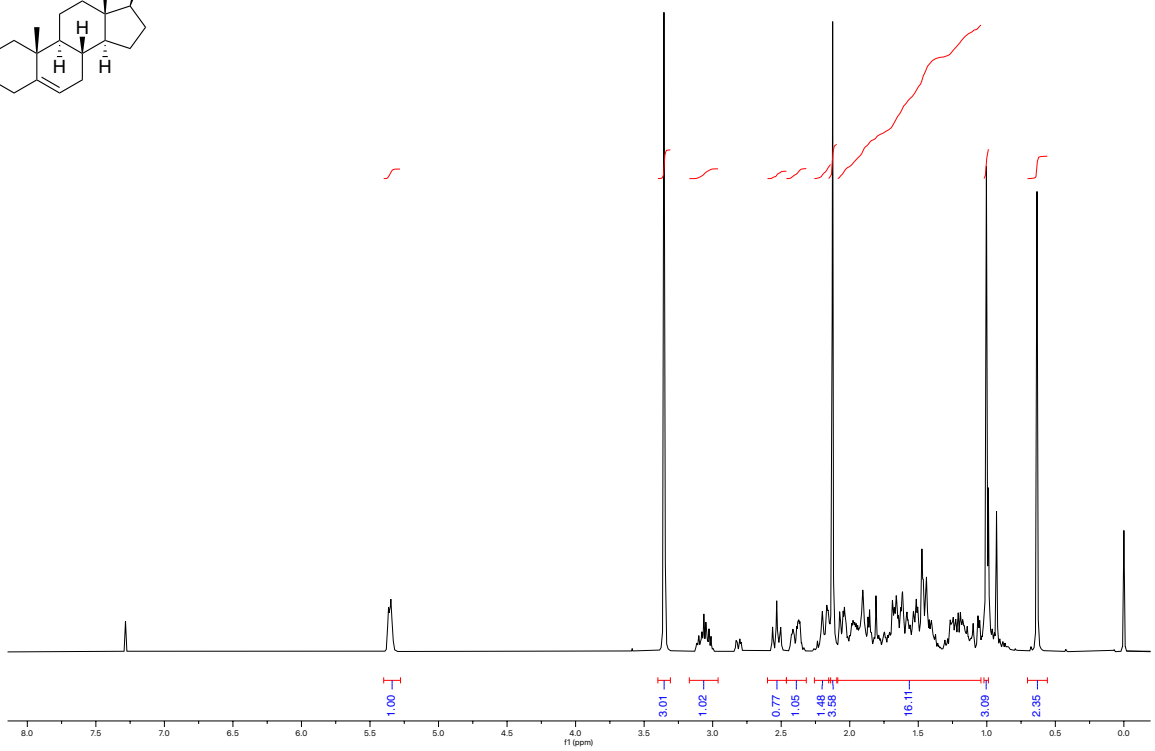

^{13}C NMR (75 MHz, $CDCl_3$)
1-((3*S*,8*S*,9*S*,10*R*,13*S*,14*S*,17*S*)-3-methoxy-10,13-dimethyl-2,3,4,7,8,9,10,11,12,13,14,15,16,17-tetradecahydro-1H-cyclopenta[*a*]phenanthren-17-yl)ethan-1-one

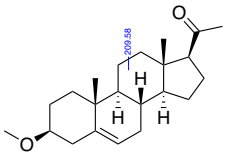

^{1}H NMR (300 MHz, $CDCl_3$)
1-((3*S*,5*S*,8*R*,9*S*,10*S*,13*S*,14*S*,17*S*)-3-methoxy-10,13-dimethylhexadecahydro-1H-cyclopenta[*a*]phenanthren-17-yl)ethan-1-one

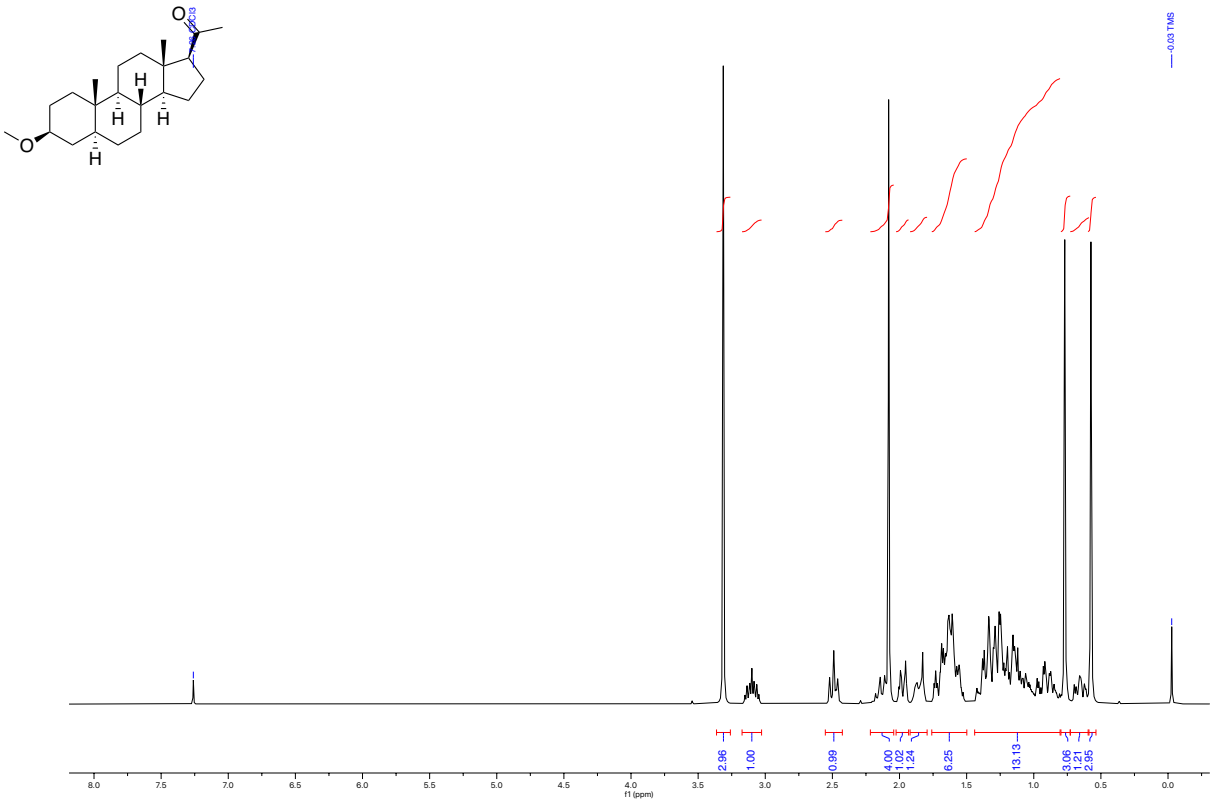

^{13}C NMR (75 MHz, $CDCl_3$)
1-((3*S*,5*S*,8*R*,9*S*,10*S*,13*S*,14*S*,17*S*)-3-methoxy-10,13-dimethylhexadecahydro-1H-cyclopenta[*a*]phenanthren-17-yl)ethan-1-one

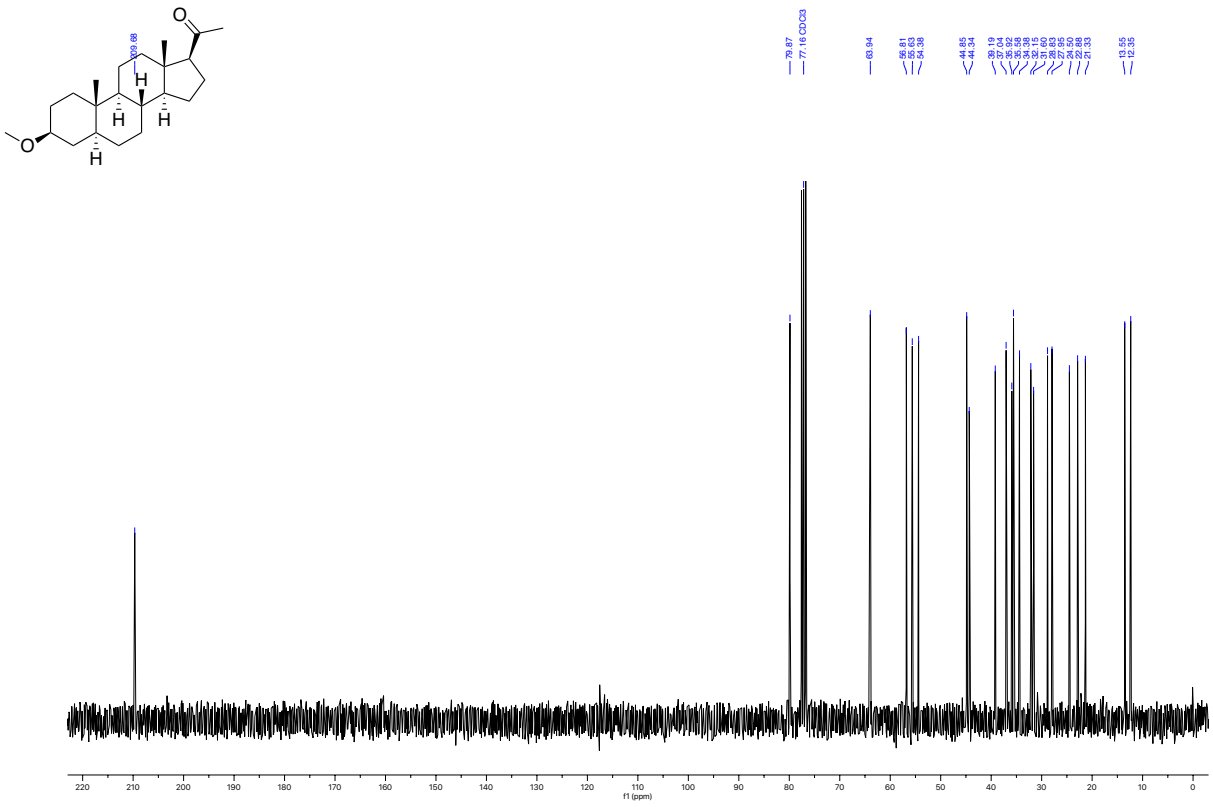

^{1}H NMR (300 MHz, $CDCl_3$)
2-((3*S*,5*S*,8*R*,9*S*,10*S*,13*S*,14*S*,17*S*)-3-methoxy-10,13-dimethylhexadecahydro-1H-cyclopenta[*a*]phenanthren-17-yl)propan-2-ol

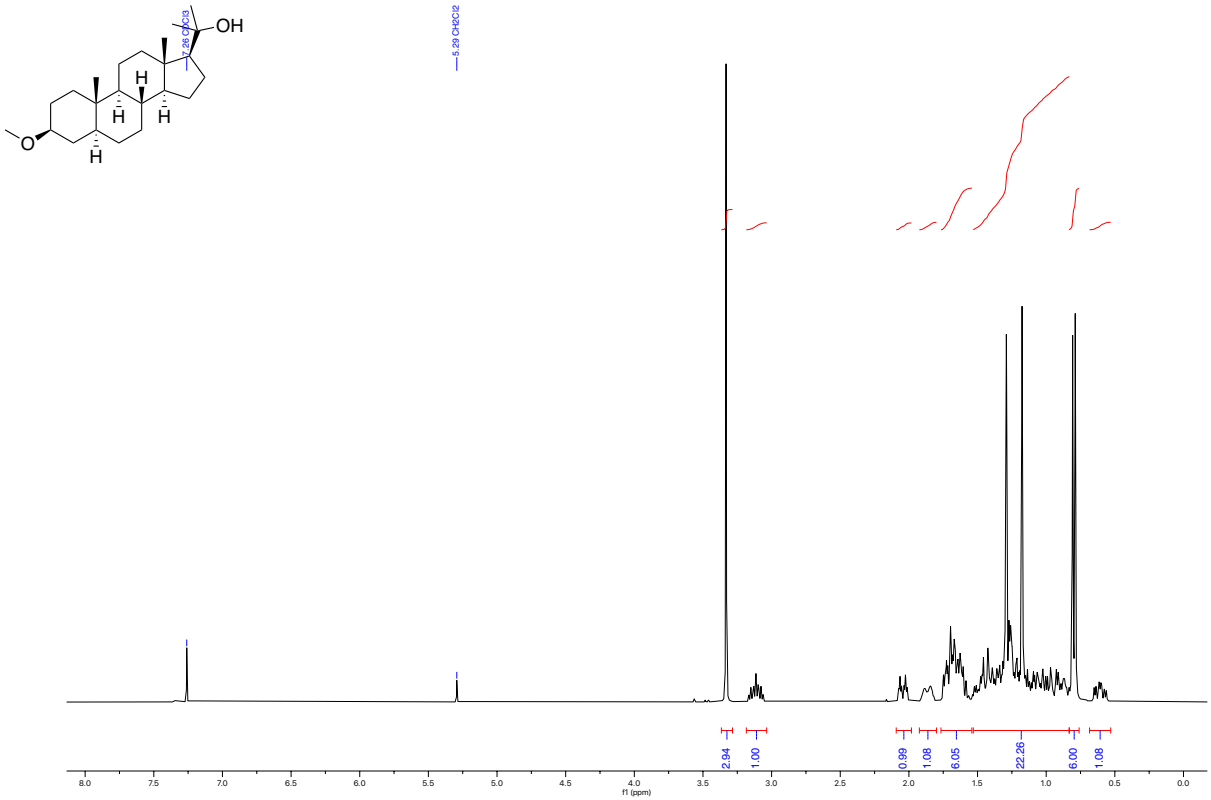

^{13}C NMR (75 MHz, $CDCl_3$)
2-((3*S*,5*S*,8*R*,9*S*,10*S*,13*S*,14*S*,17*S*)-3-methoxy-10,13-dimethylhexadecahydro-1H-cyclopenta[*a*]phenanthren-17-yl)propan-2-ol

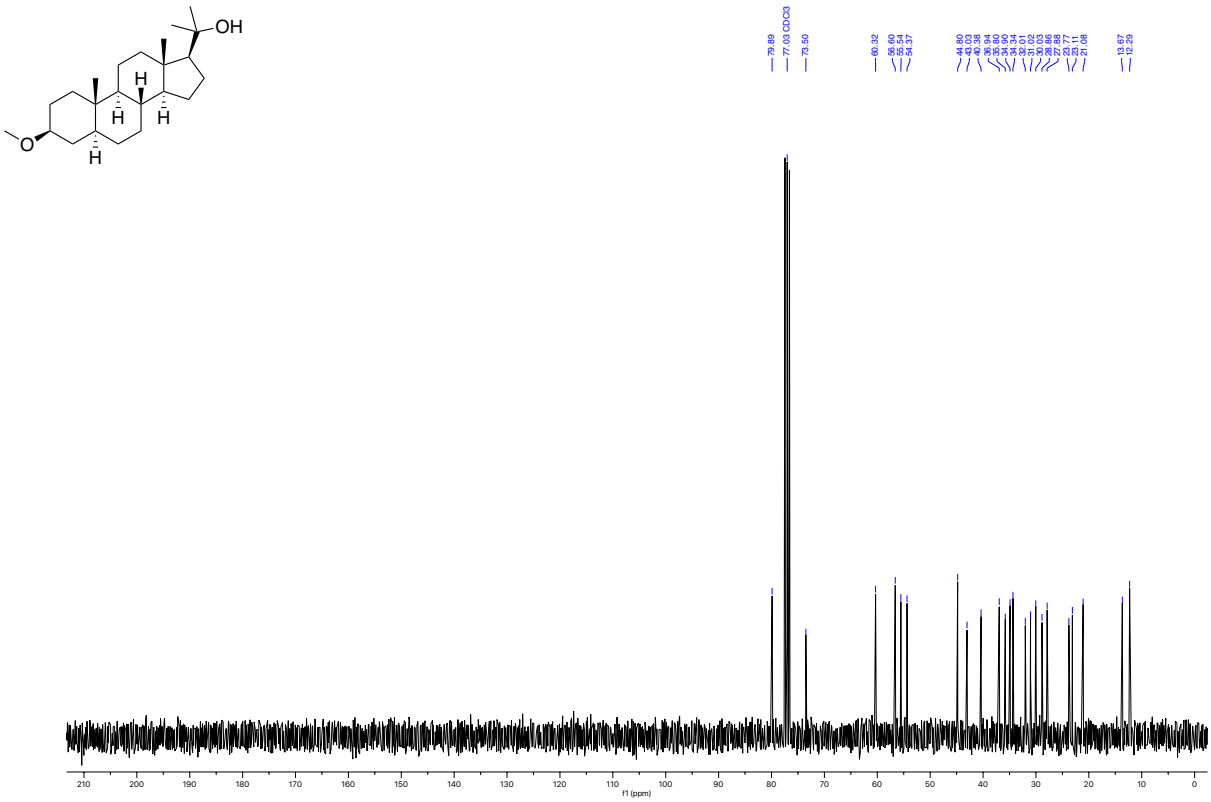

^{1}H NMR (300 MHz, $CDCl_3$)
(3*S*,5*S*,8*R*,9*S*,10*S*,13*S*,14*S*,17*S*)-17-(2-hydroperoxypropan-2-yl)-3-methoxy-10,13-dimethylhexadecahydro-1H-cyclopenta[*a*]phenanthrene

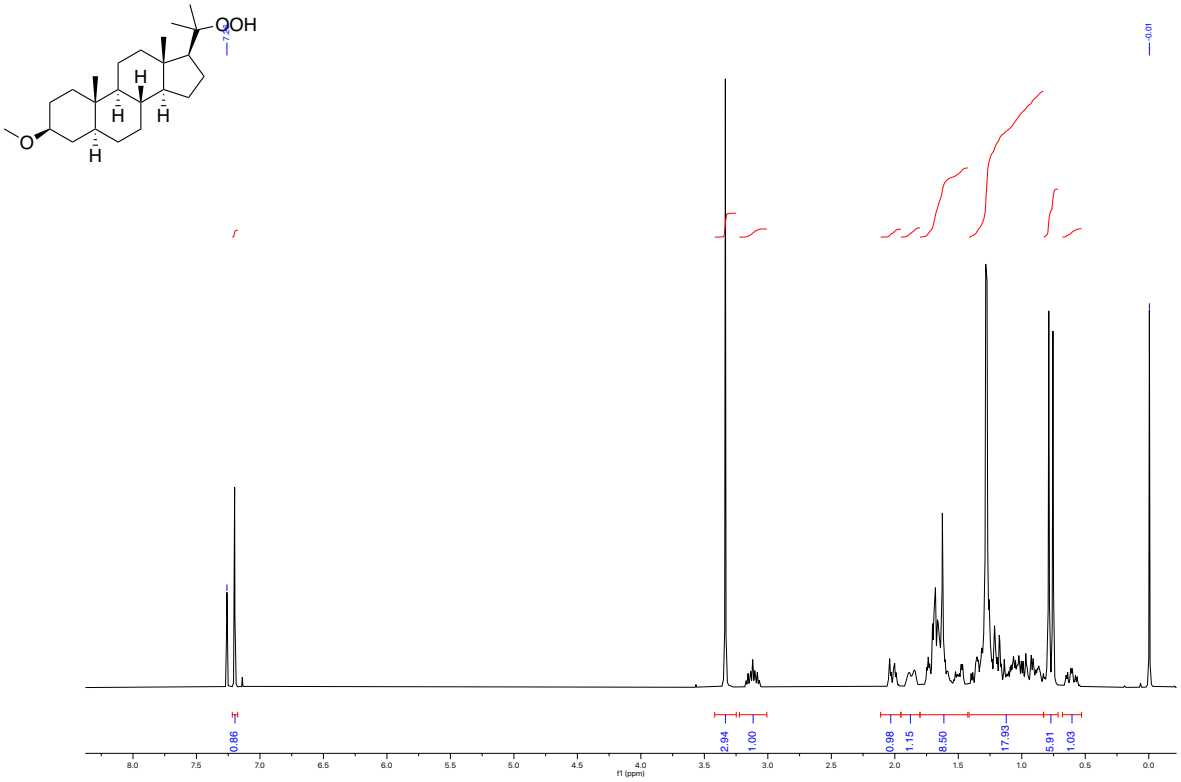

^{13}C NMR (75 MHz, $CDCl_3$)
(3*S*,5*S*,8*R*,9*S*,10*S*,13*S*,14*S*,17*S*)-17-(2-hydroperoxypropan-2-yl)-3-methoxy-10,13-dimethylhexadecahydro-1H-cyclopenta[*a*]phenanthrene

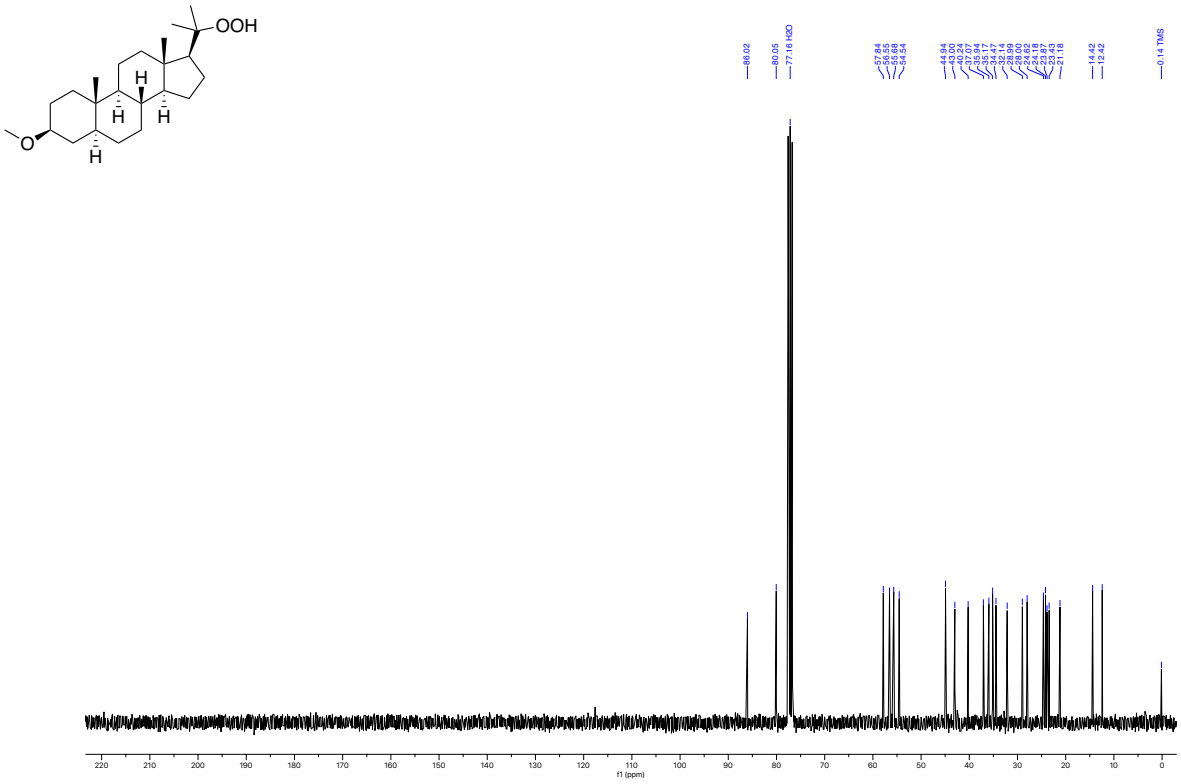

Appendix

NMR Spectra of Chapter 5

^{1}H NMR (300 MHz, $CDCl_3$)
ethyl 2-iodoacetate

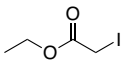

^{13}C NMR (75 MHz, $CDCl_3$)
ethyl 2-iodoacetate

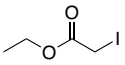

^{1}H NMR (300 MHz, $CDCl_3$)
Ethyl 4-iododecanoate

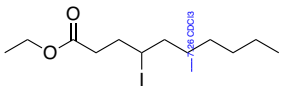

^{13}C NMR (75 MHz, $CDCl_3$)
Ethyl 4-iododecanoate

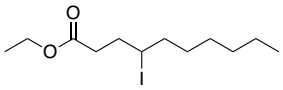

^{1}H NMR (300 MHz, $CDCl_3$)
Ethyl 4-iododecanoate

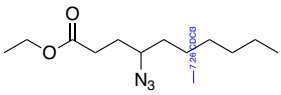

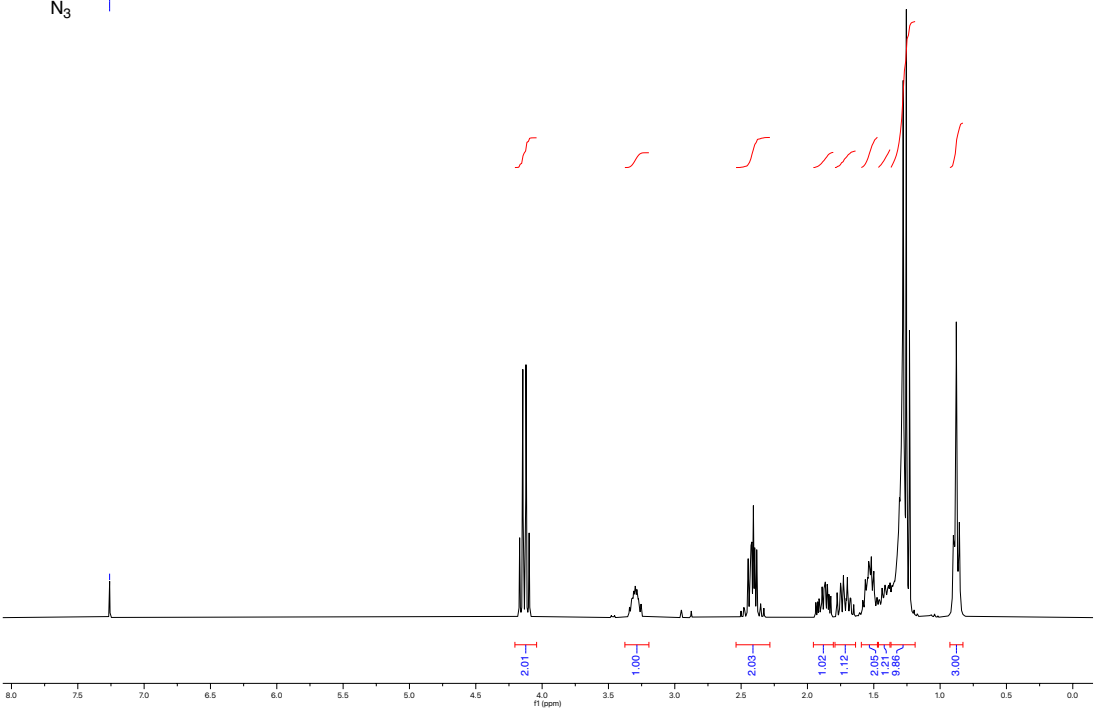

^{13}C NMR (75 MHz, $CDCl_3$)
Ethyl 4-iododecanoate

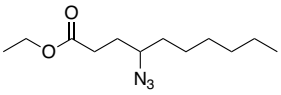

^{1}H NMR (300 MHz, $CDCl_3$)
4-azidodecan-1-ol

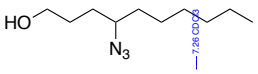

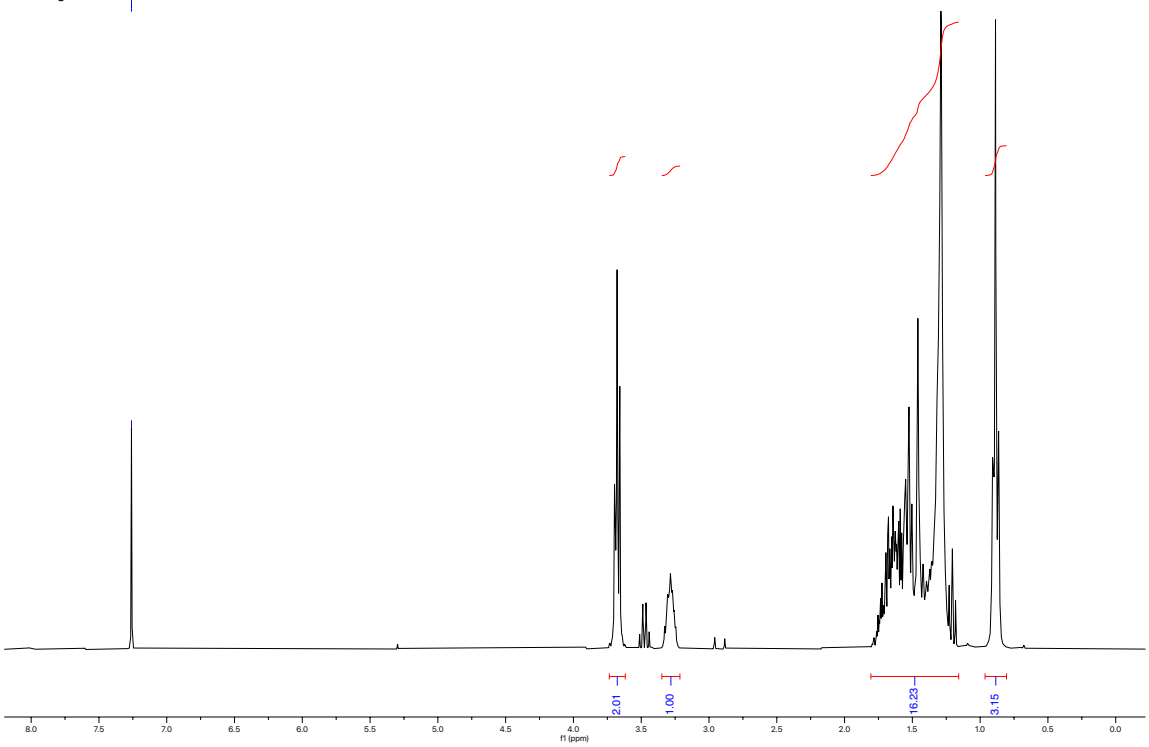

^{13}C NMR (75 MHz, $CDCl_3$)
4-azidodecan-1-ol

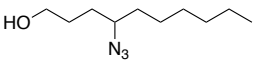

Appendix

NMR Spectra of Chapter 7

^{1}H NMR (300 MHz, $CDCl_3$)
2-(phenylsulfonyl)-1,7,10-trioxadispiro[2.2.4^{6}.2^{3}]dodecane

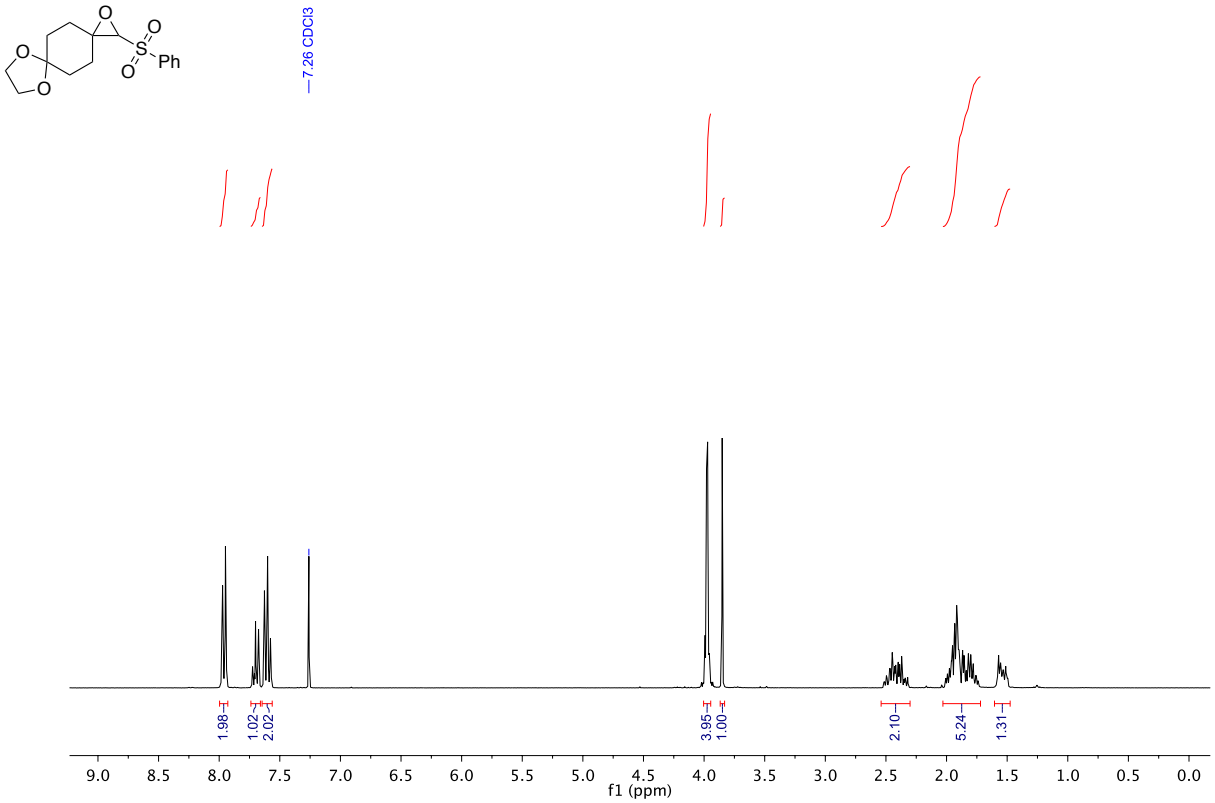

^{13}C NMR (75 MHz, $CDCl_3$)
2-(phenylsulfonyl)-1,7,10-trioxadispiro[2.2.4^{6}.2^{3}]dodecane

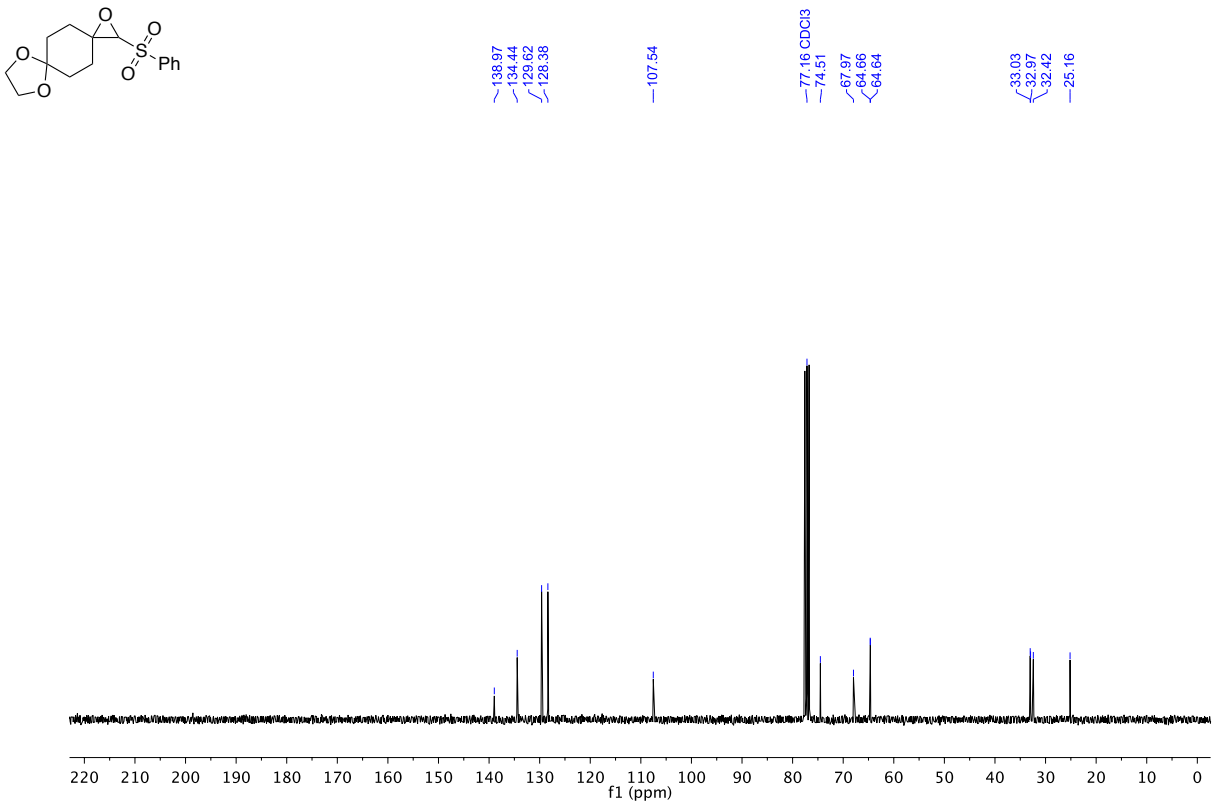

^{1}H NMR (300 MHz, $CDCl_3$)
8-azido-1,4-dioxaspiro[4.5]decane-8-carbaldehyde

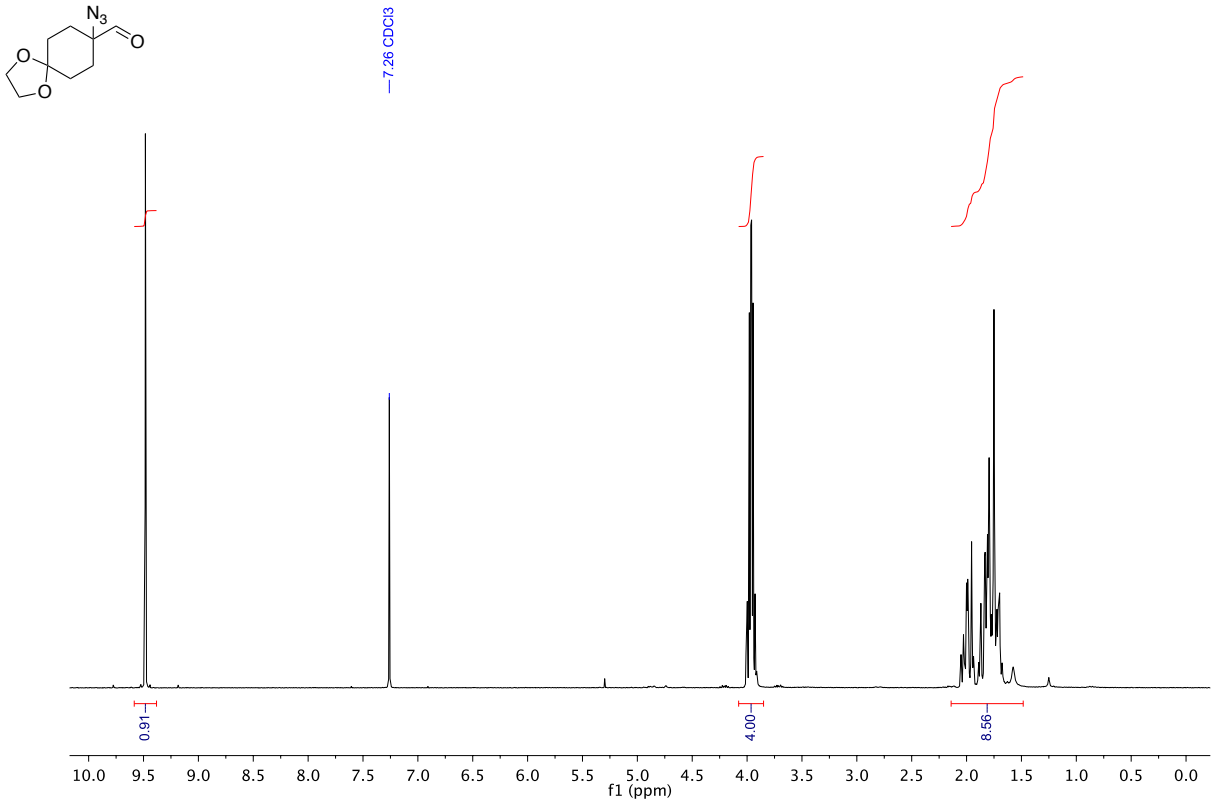

^{13}C NMR (75 MHz, $CDCl_3$)
8-azido-1,4-dioxaspiro[4.5]decane-8-carbaldehyde

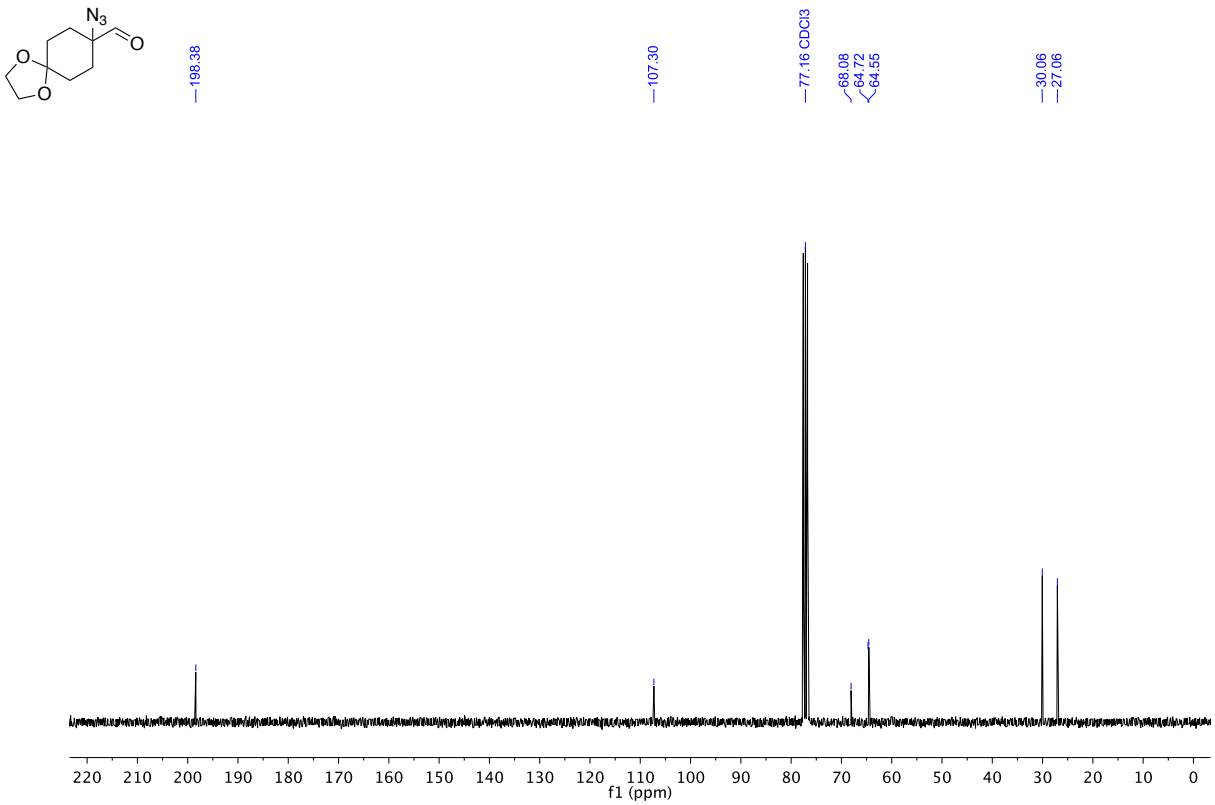

^{1}H NMR (300 MHz, $CDCl_3$)
1-(8-azido-1,4-dioxaspiro[4.5]decan-8-yl)propane-1,3-diol (residual EtOAc cannot be removed on high vacuum)

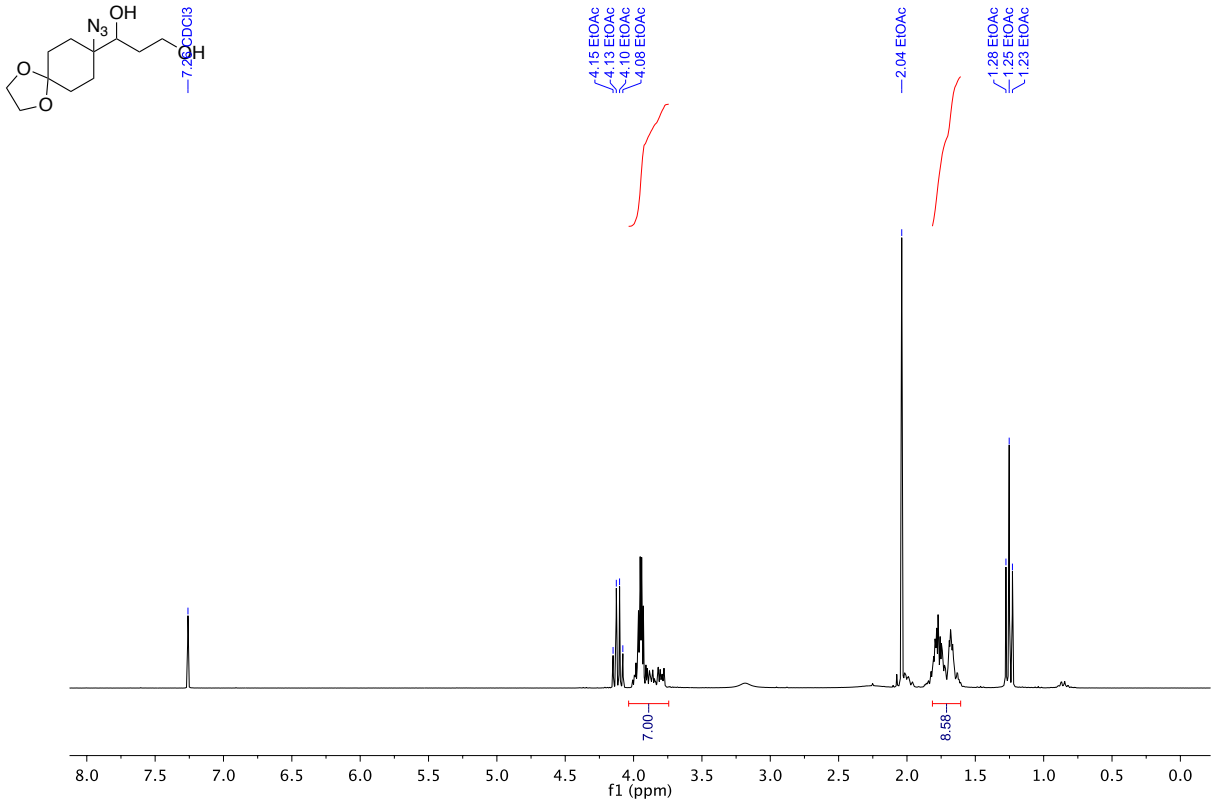

^{13}C NMR (75 MHz, $CDCl_3$)
1-(8-azido-1,4-dioxaspiro[4.5]decan-8-yl)propane-1,3-diol

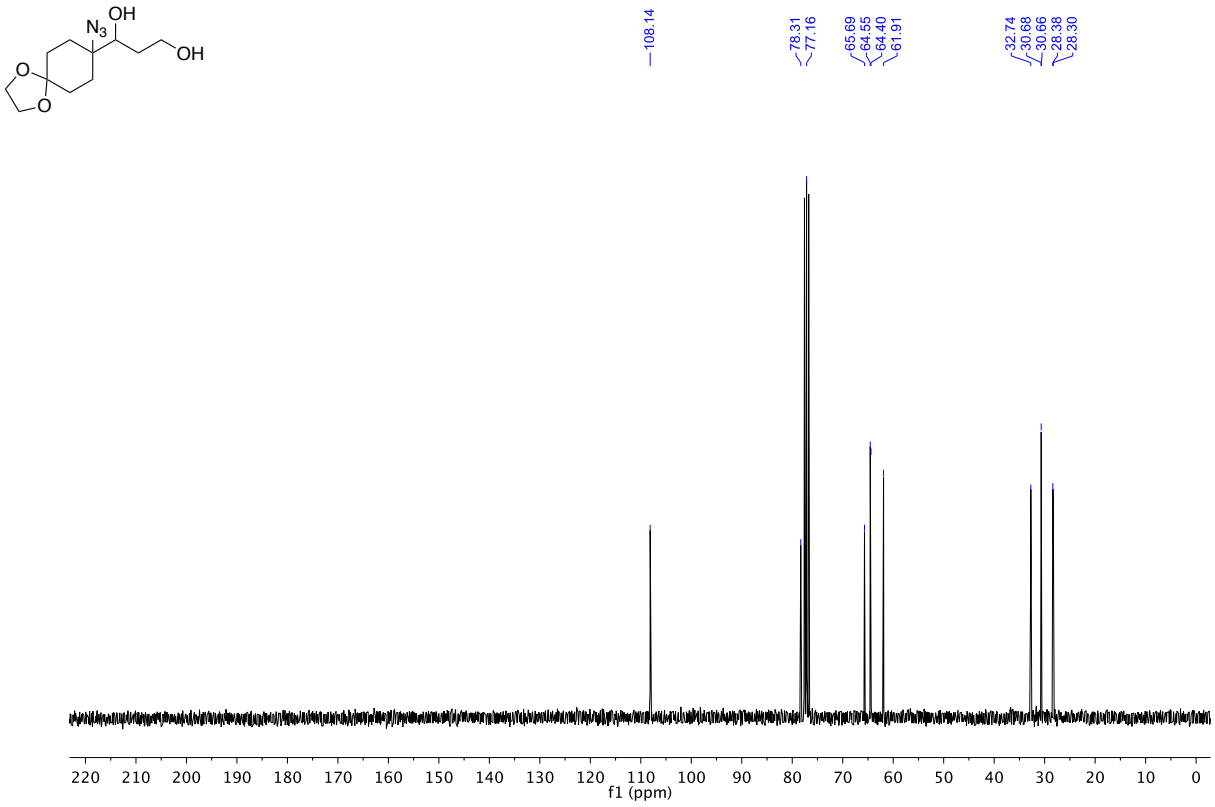

^{1}H NMR (300 MHz, $CDCl_3$)

5-(8-azido-1,4-dioxaspiro[4.5]decan-8-yl)-2,2,3,3,9,9,10,10-octamethyl-4,8-dioxa-3,9-disilaundecane

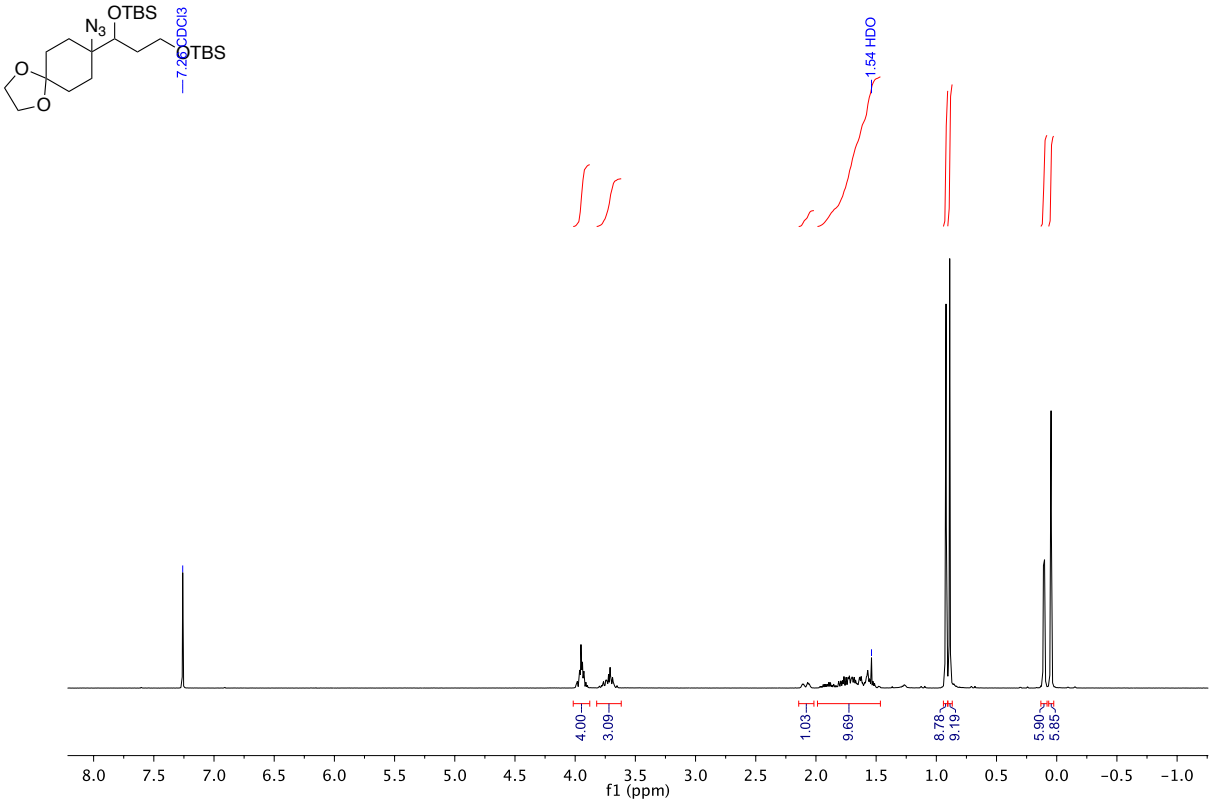

^{13}C NMR (75 MHz, $CDCl_3$)

5-(8-azido-1,4-dioxaspiro[4.5]decan-8-yl)-2,2,3,3,9,9,10,10-octamethyl-4,8-dioxa-3,9-disilaundecane

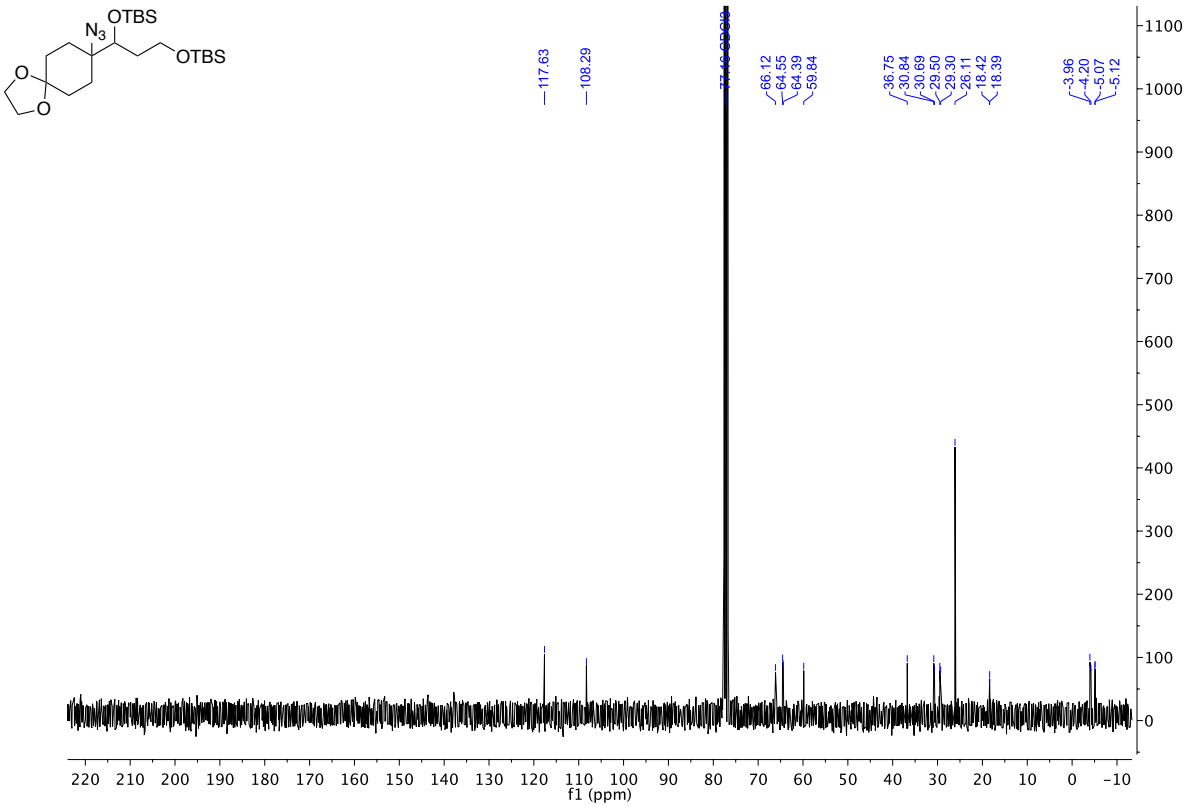

^{1}H NMR (300 MHz, $CDCl_3$)
3-(8-azido-1,4-dioxaspiro[4.5]decan-8-yl)-3-((tert-butyldimethylsilyl)oxy)propan-1-ol

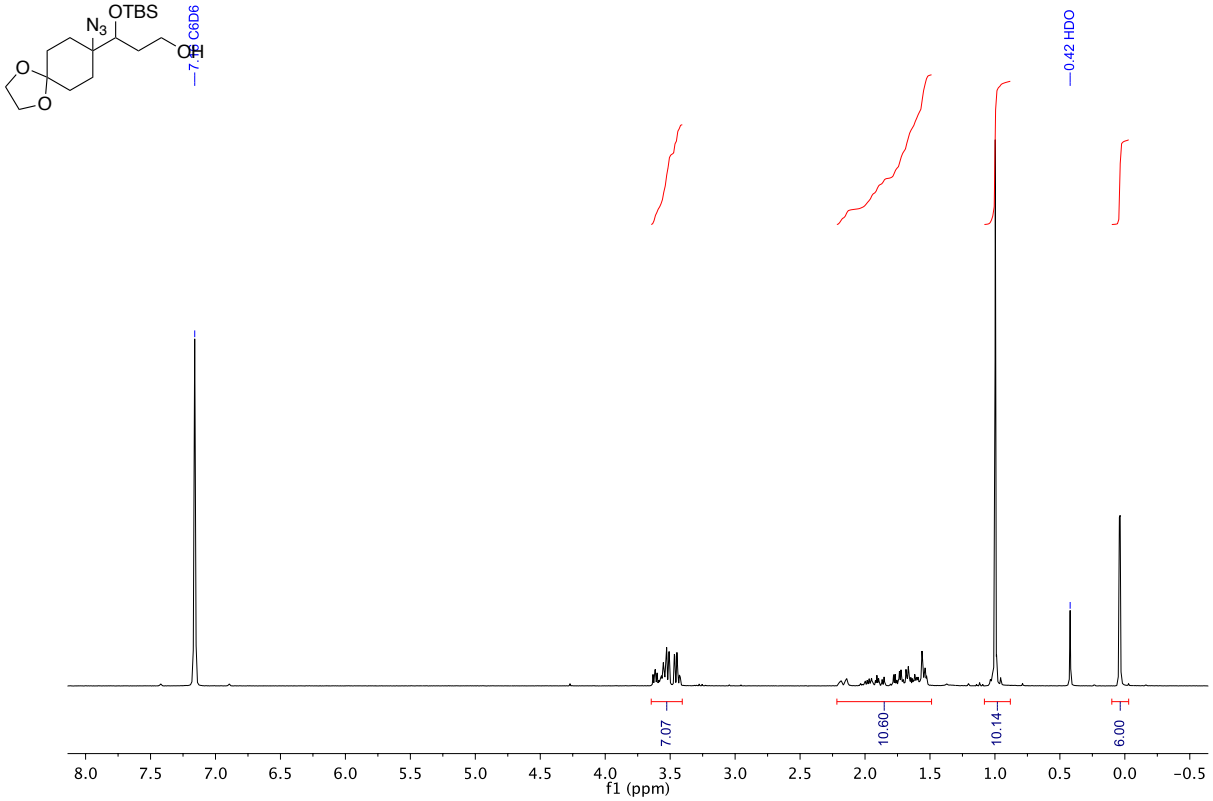

^{13}C NMR (75 MHz, $CDCl_3$)
3-(8-azido-1,4-dioxaspiro[4.5]decan-8-yl)-3-((tert-butyldimethylsilyl)oxy)propan-1-ol

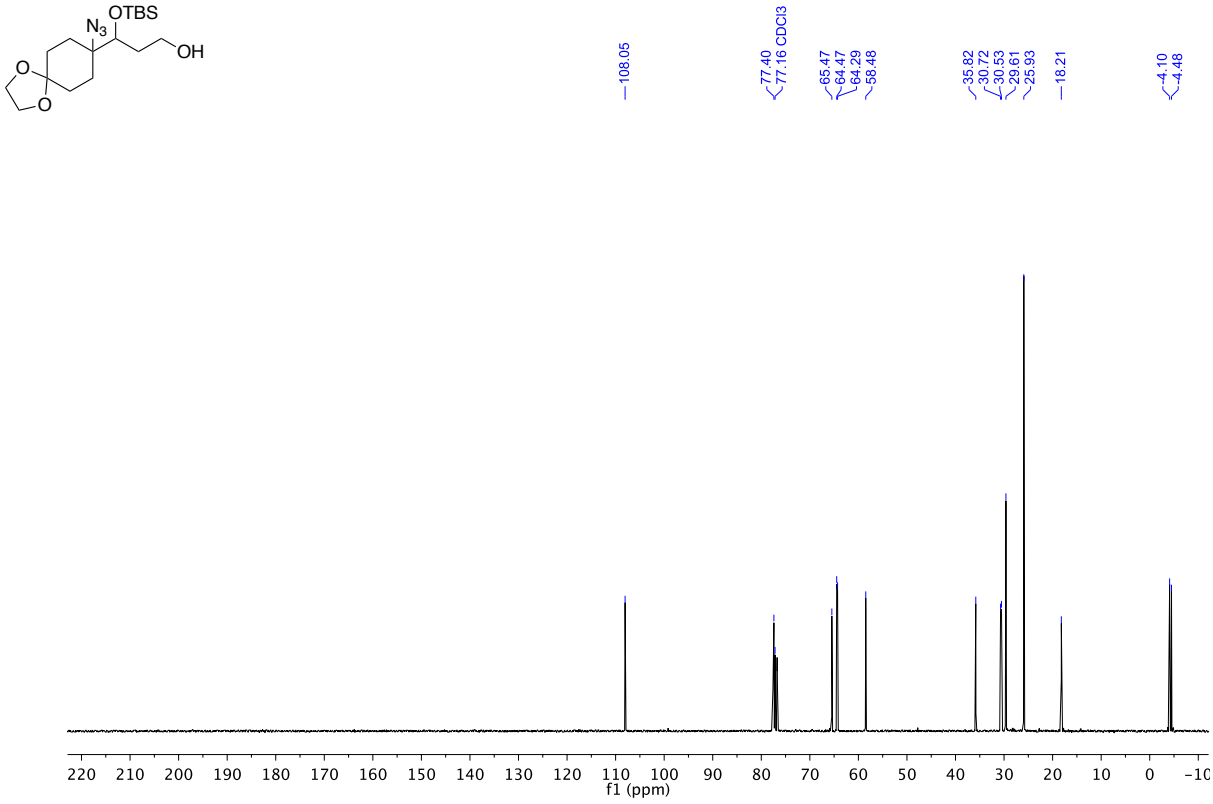

^{1}H NMR (300 MHz, $CDCl_3$)
6-phenyl-2-(phenylsulfonyl)-1-oxaspiro[2.5]octane

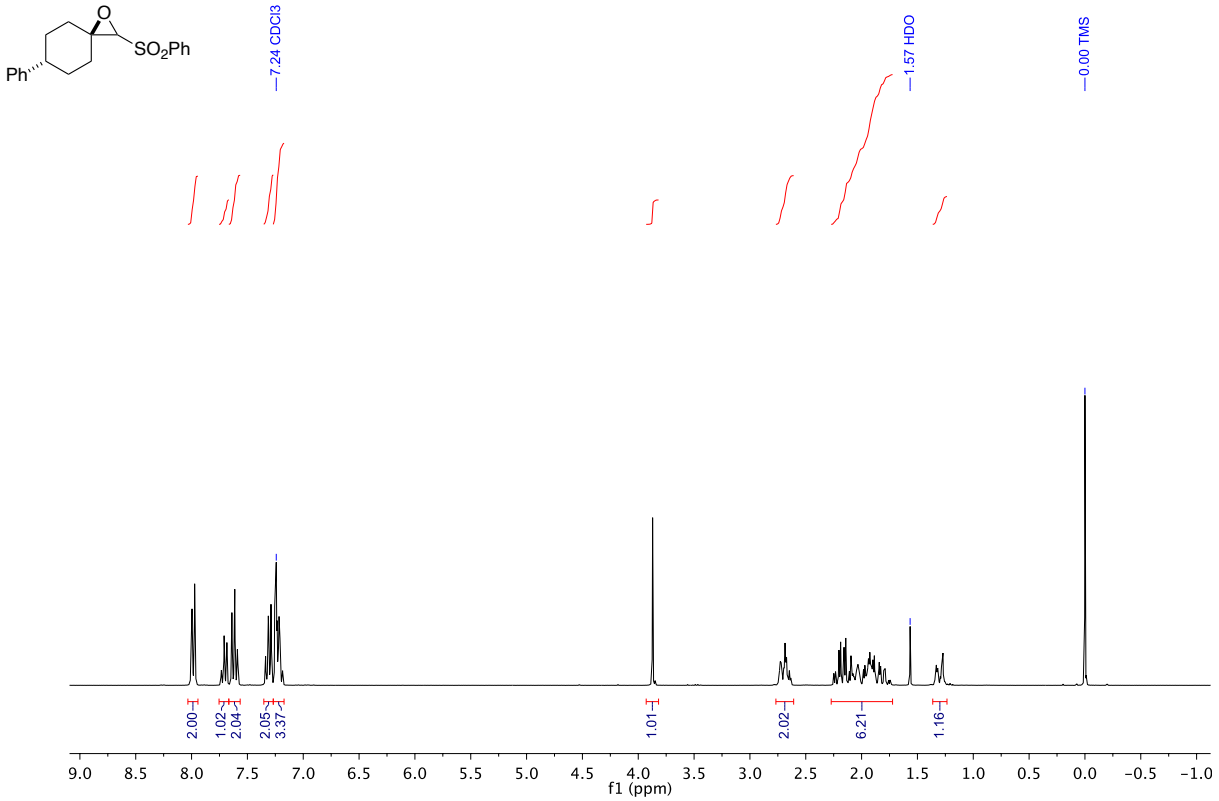

^{13}C NMR (75 MHz, $CDCl_3$)
6-phenyl-2-(phenylsulfonyl)-1-oxaspiro[2.5]octane

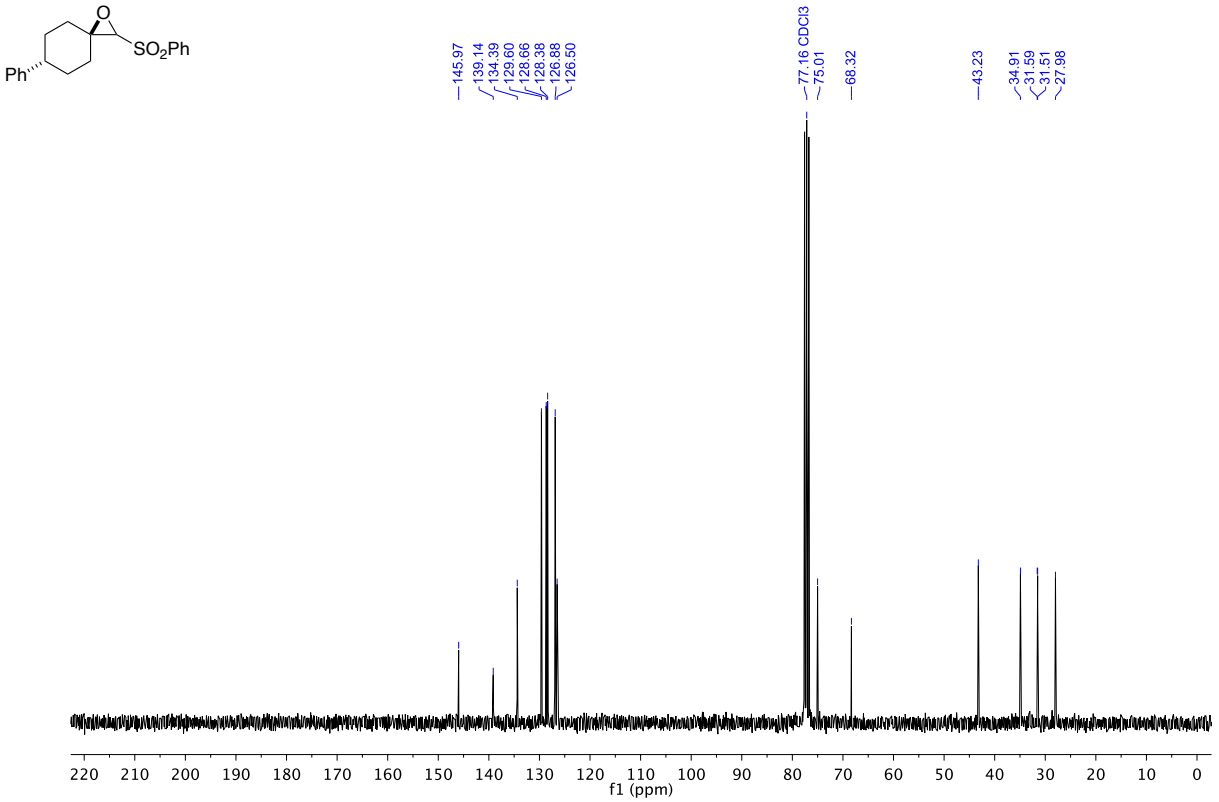

^{1}H NMR (300 MHz, $CDCl_3$)
1-azido-4-phenylcyclohexane-1-carbaldehyde

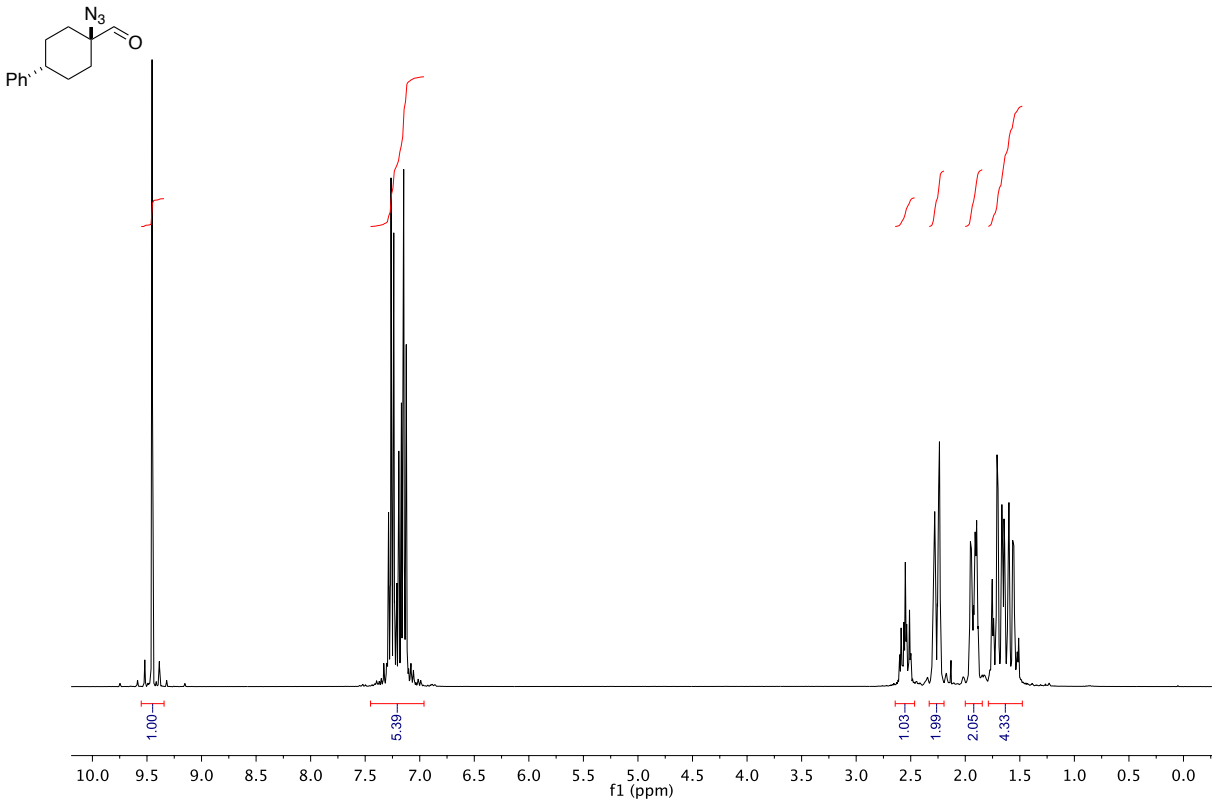

^{13}C NMR (75 MHz, $CDCl_3$)
1-azido-4-phenylcyclohexane-1-carbaldehyde

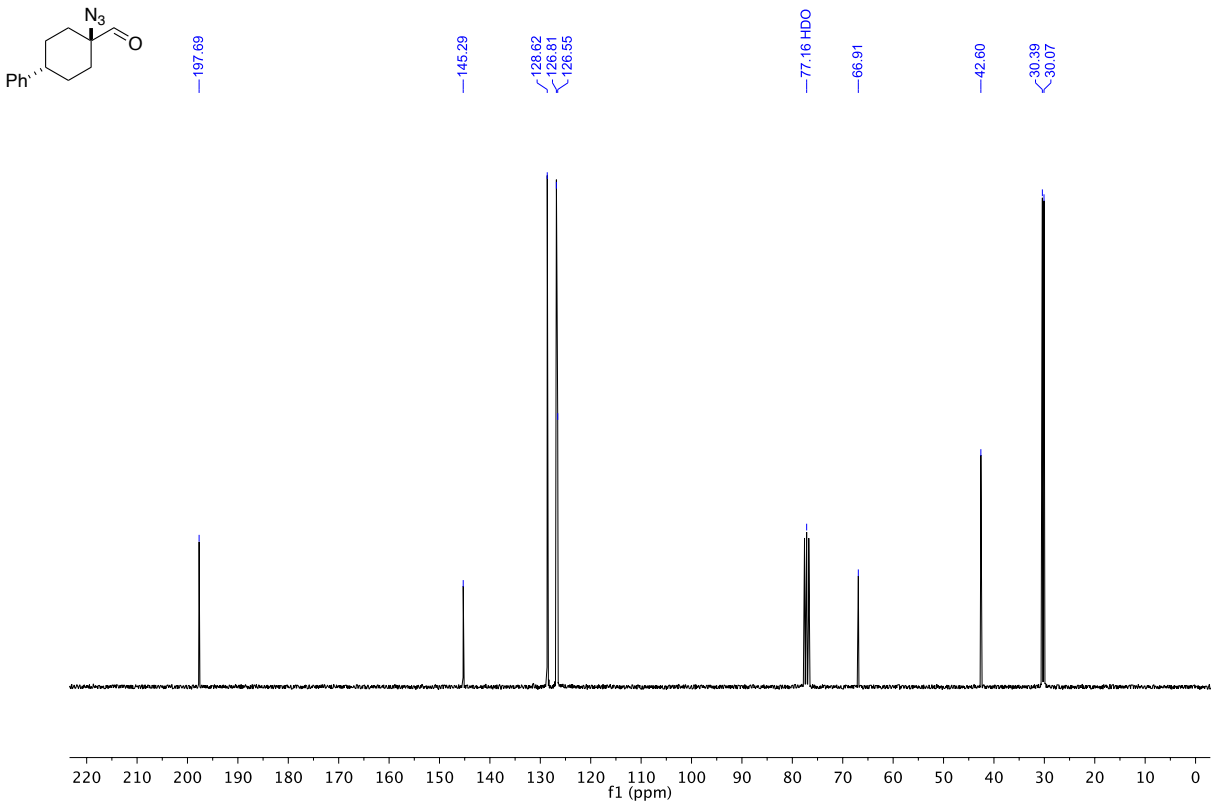

^{1}H NMR (300 MHz, $CDCl_3$)
1-(1-azido-4-phenylcyclohexyl)but-3-en-1-ol

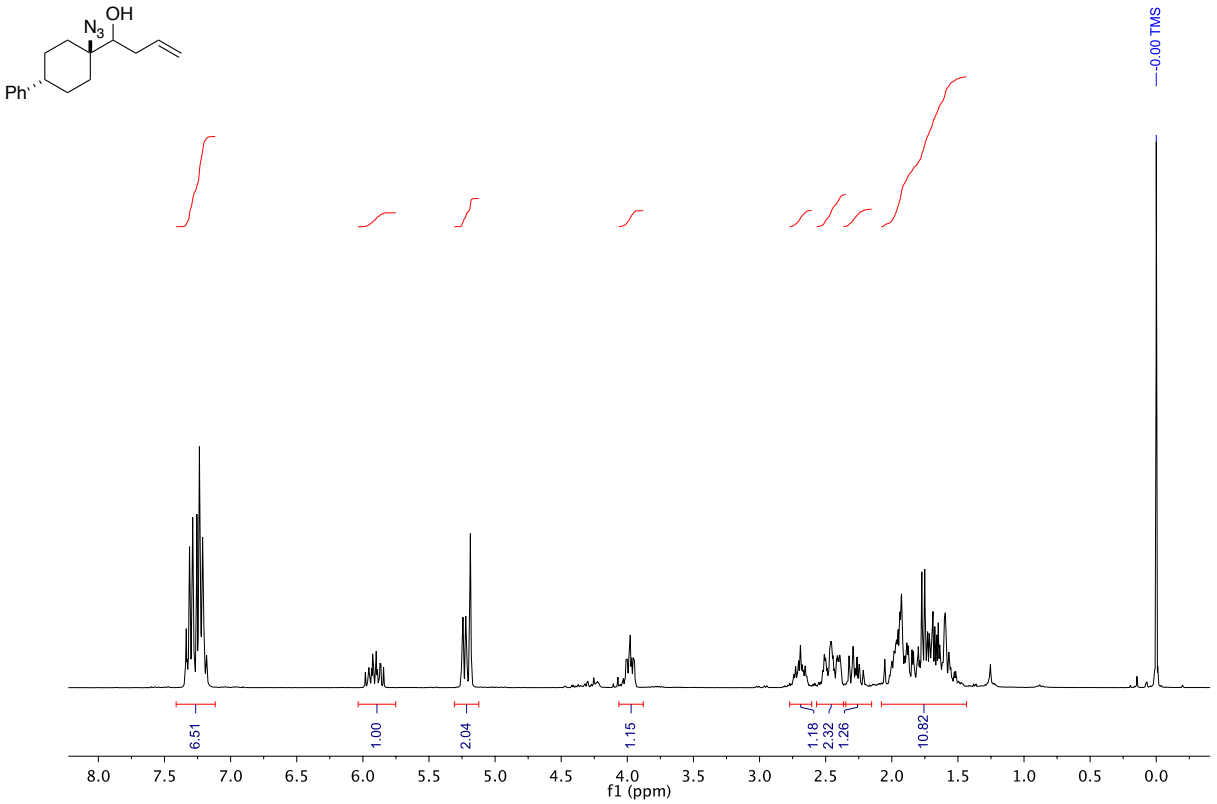

^{13}C NMR (75 MHz, $CDCl_3$)
1-(1-azido-4-phenylcyclohexyl)but-3-en-1-ol (note: little decomposition occurs already during time of measurement)

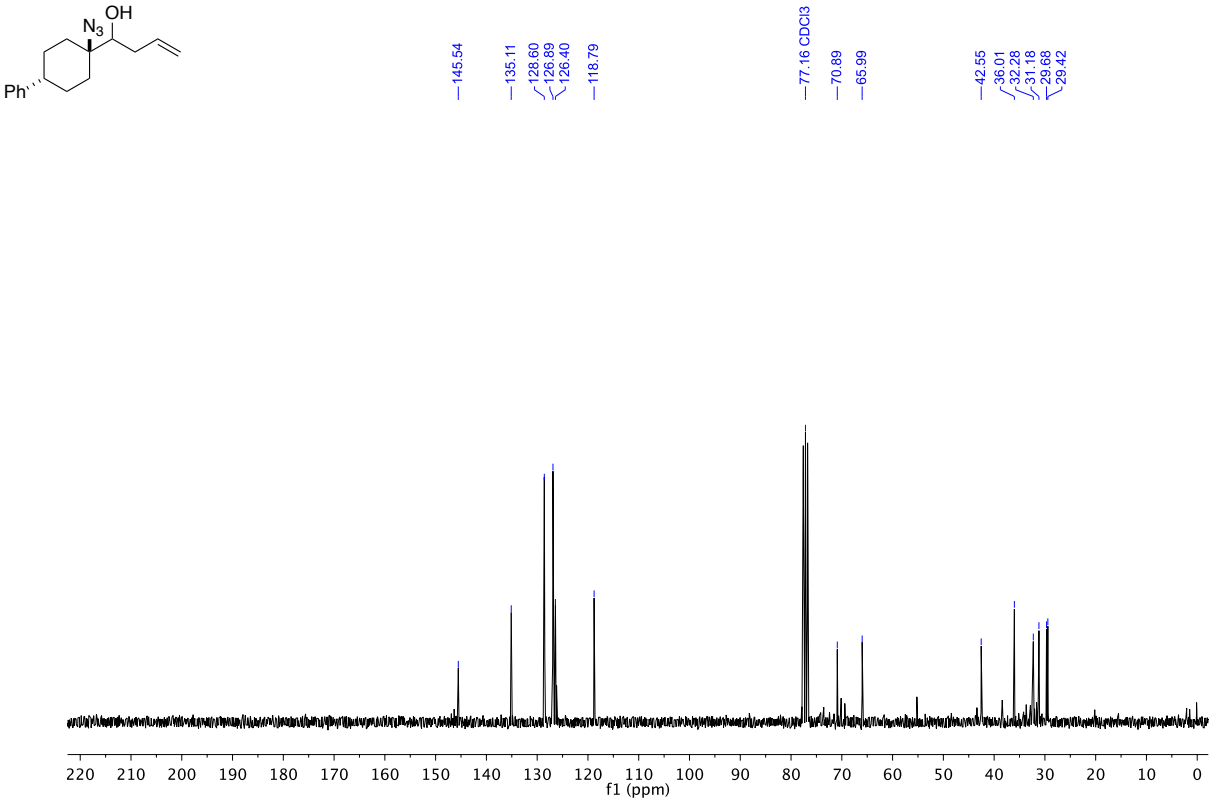

^{1}H NMR (300 MHz, $CDCl_3$)
1-(1-azido-4-phenylcyclohexyl)propane-1,3-diol

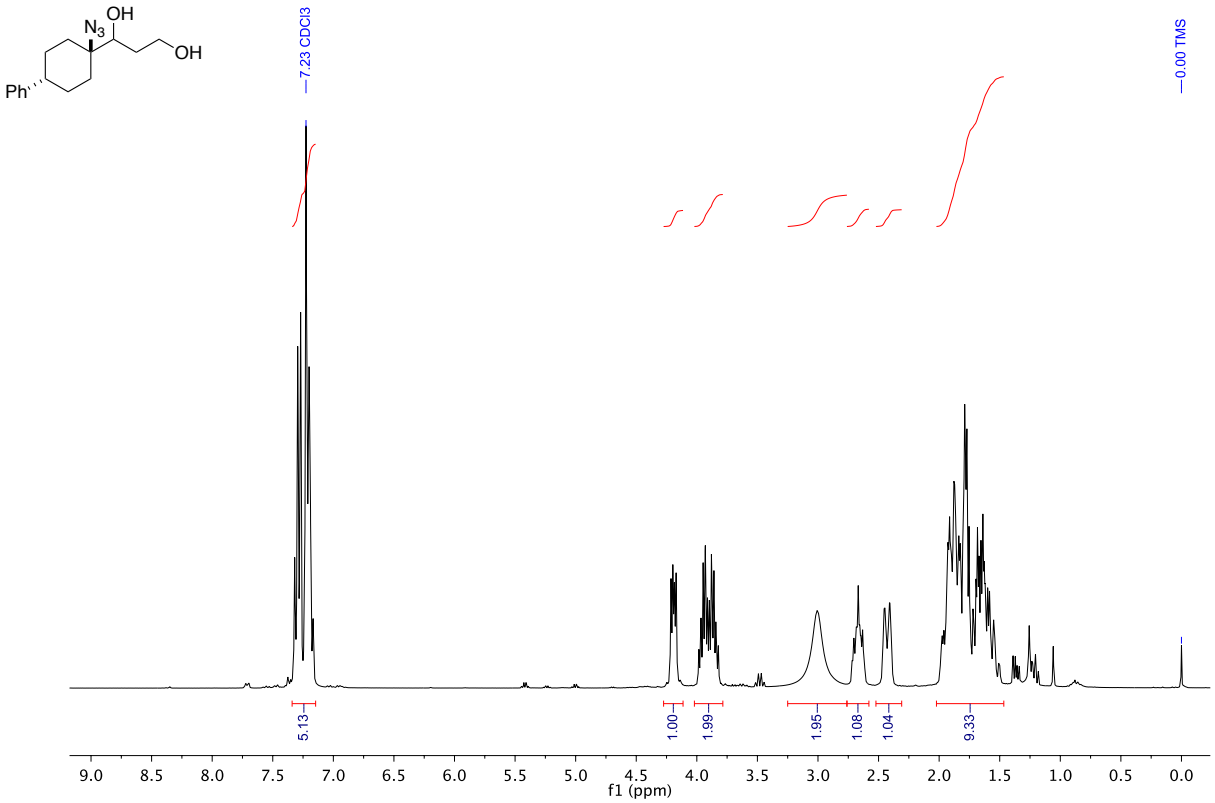

^{13}C NMR (75 MHz, $CDCl_3$)
1-(1-azido-4-phenylcyclohexyl)propane-1,3-diol

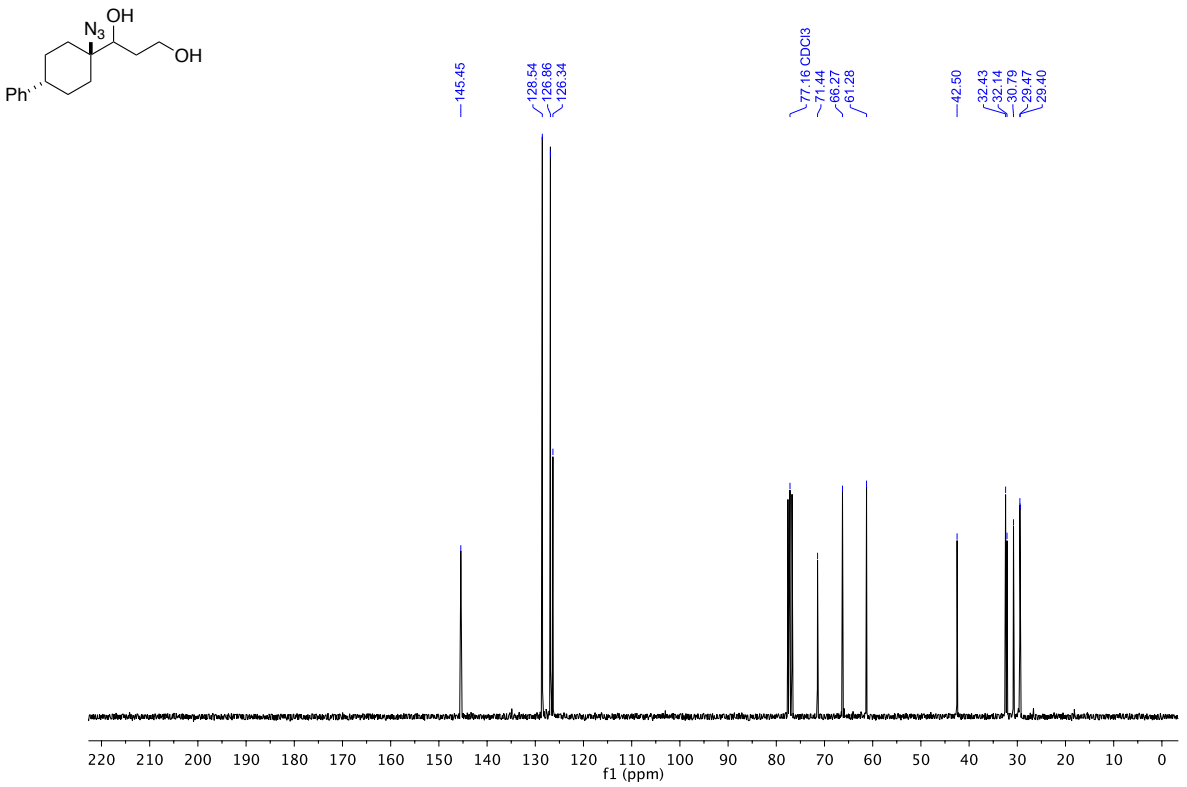

^{1}H NMR (300 MHz, $CDCl_3$)

1-(1-azido-4-phenylcyclohexyl)-3-((tert-butyldimethylsilyl)oxy)propan-1-ol

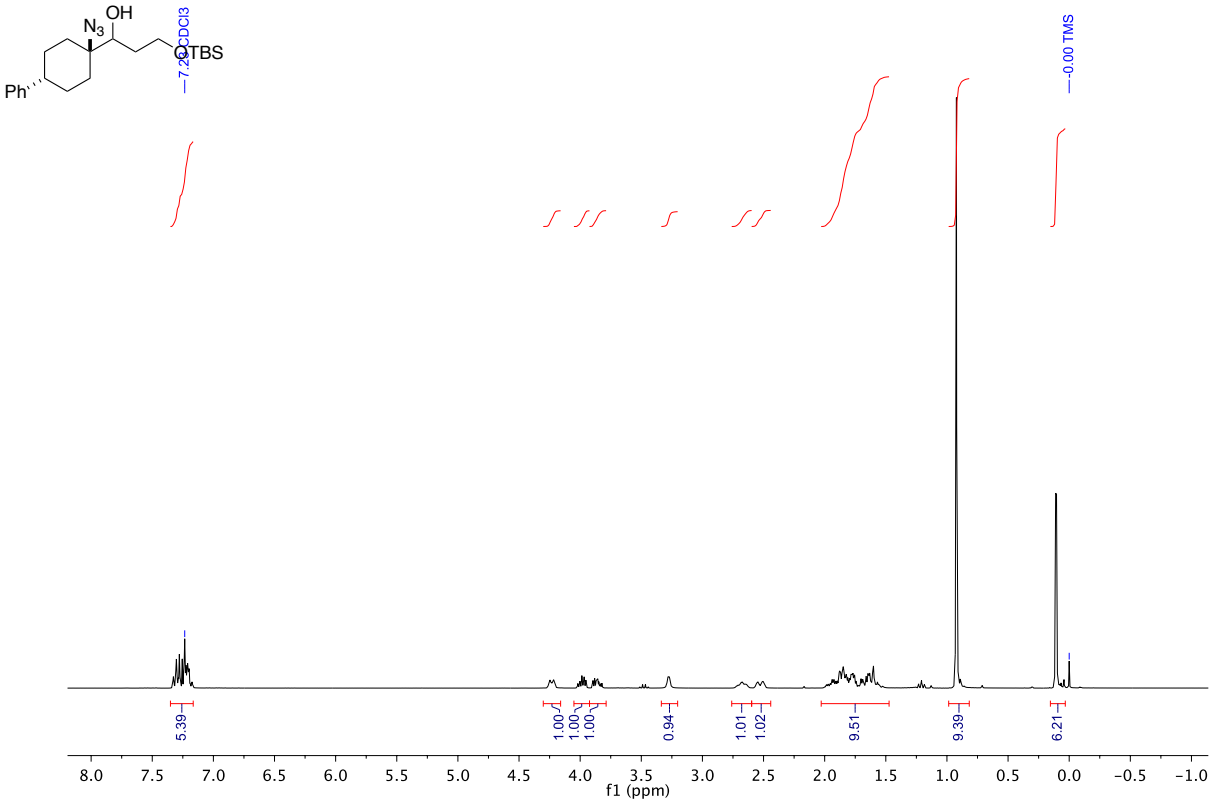

^{13}C NMR (75 MHz, $CDCl_3$)

1-(1-azido-4-phenylcyclohexyl)-3-((tert-butyldimethylsilyl)oxy)propan-1-ol

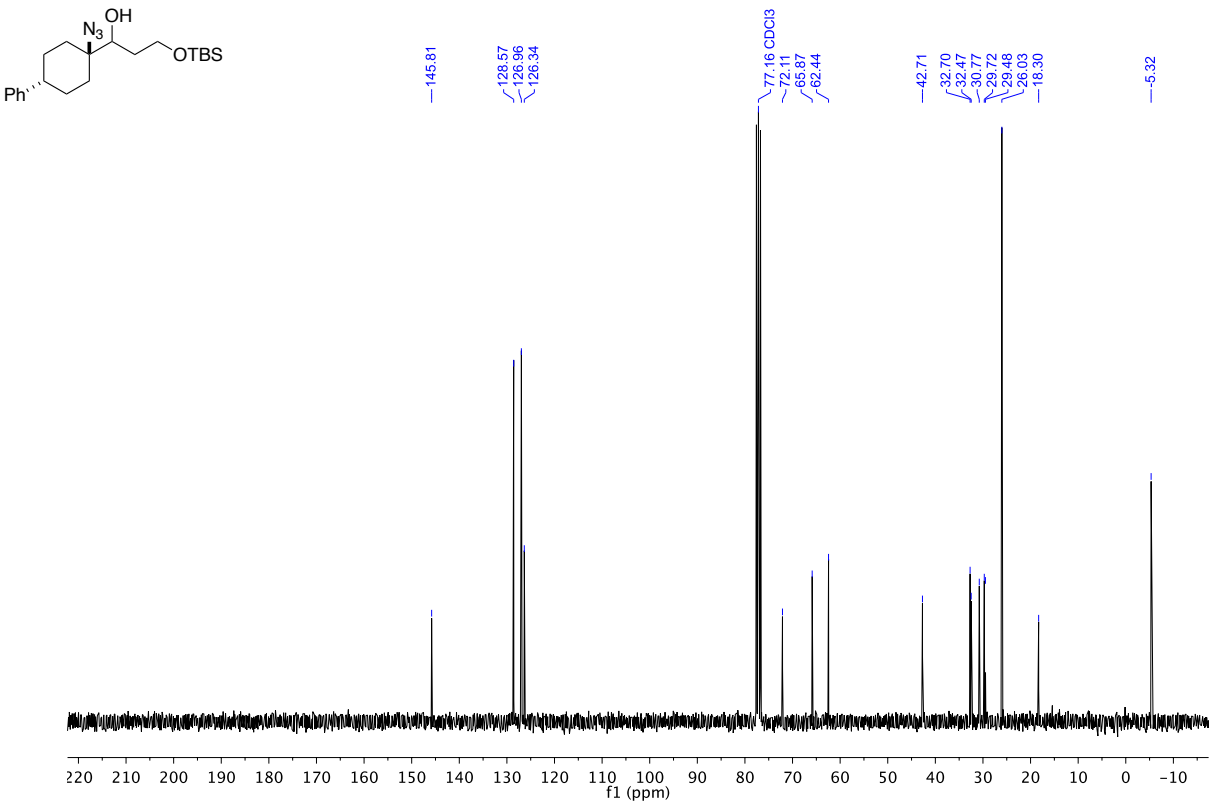

^{1}H NMR (300 MHz, $CDCl_3$)

5-(1-azido-4-phenylcyclohexyl)-2,2,3,3,9,9,10,10-octamethyl-4,8-dioxa-3,9-disilaundecane

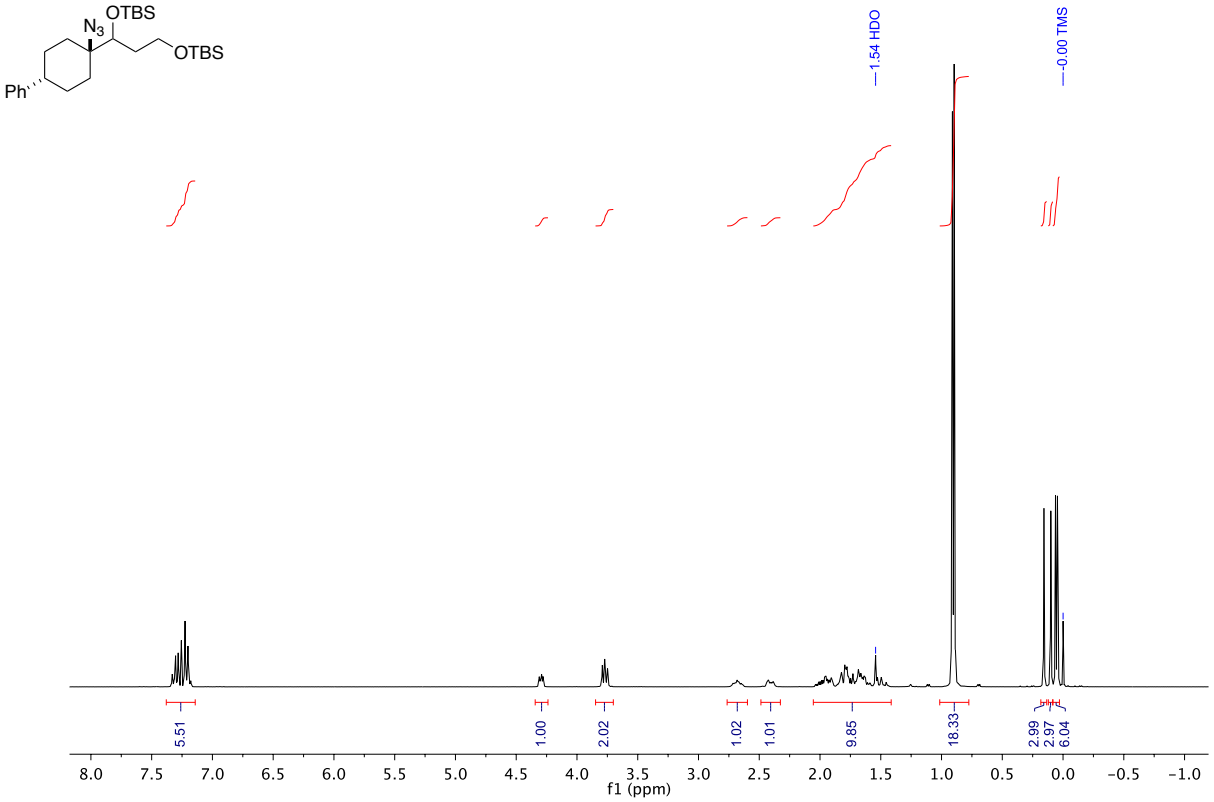

^{13}C NMR (75 MHz, $CDCl_3$)

5-(1-azido-4-phenylcyclohexyl)-2,2,3,3,9,9,10,10-octamethyl-4,8-dioxa-3,9-disilaundecane

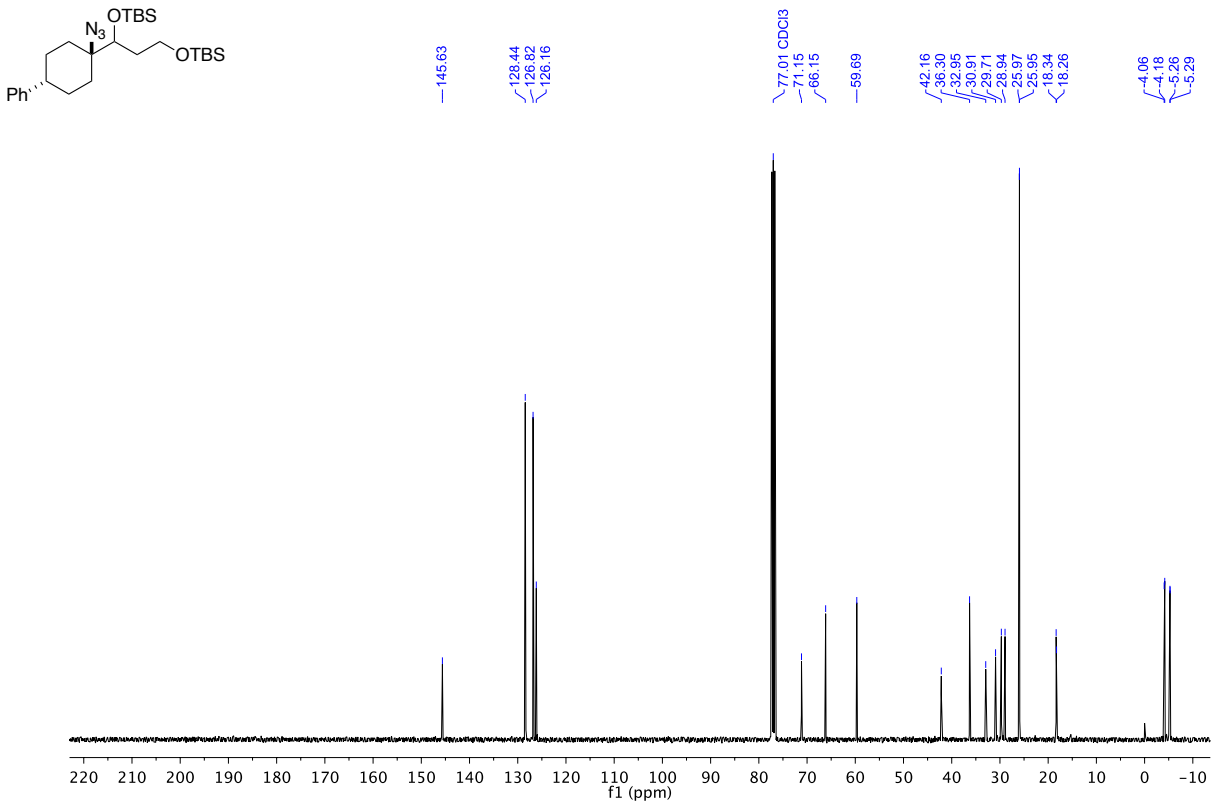

^{1}H NMR (300 MHz, $CDCl_3$)
3-(1-azido-4-phenylcyclohexyl)-3-((tert-butyldimethylsilyl)oxy)propan-1-ol

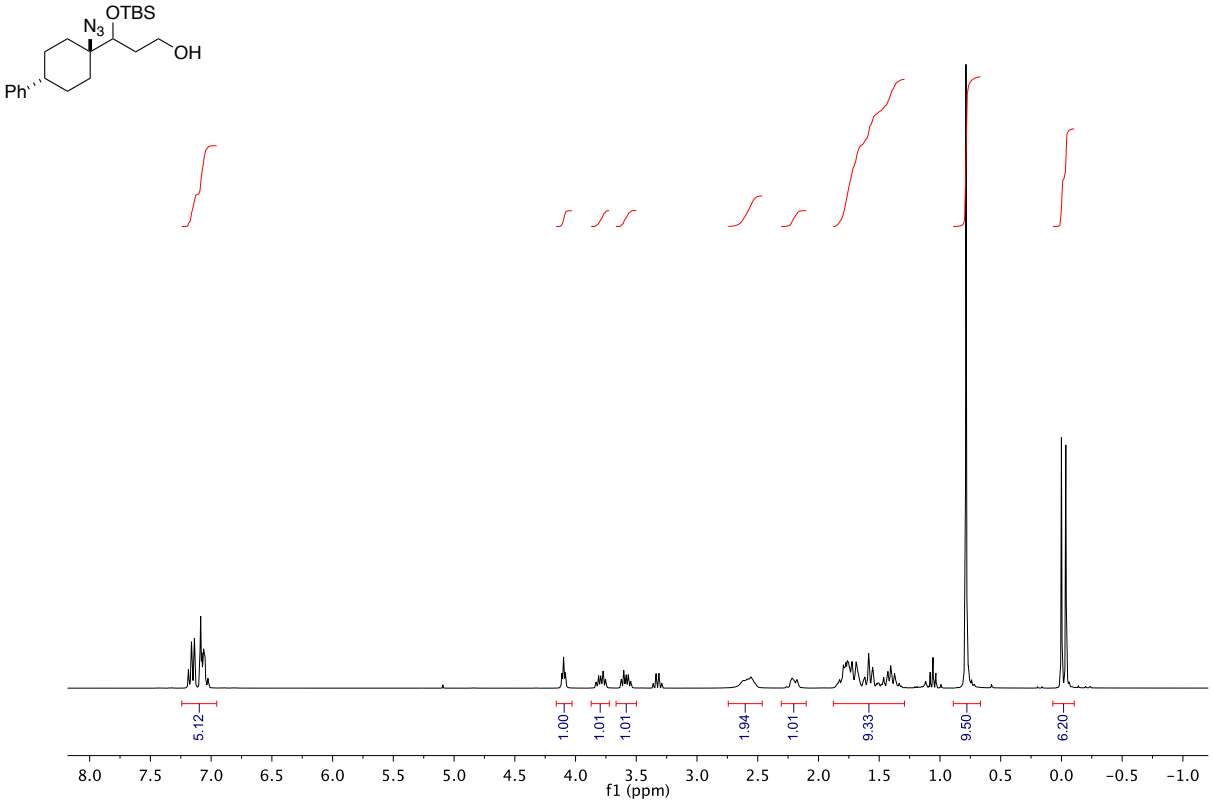

^{13}C NMR (75 MHz, $CDCl_3$)
3-(1-azido-4-phenylcyclohexyl)-3-((tert-butyldimethylsilyl)oxy)propan-1-ol

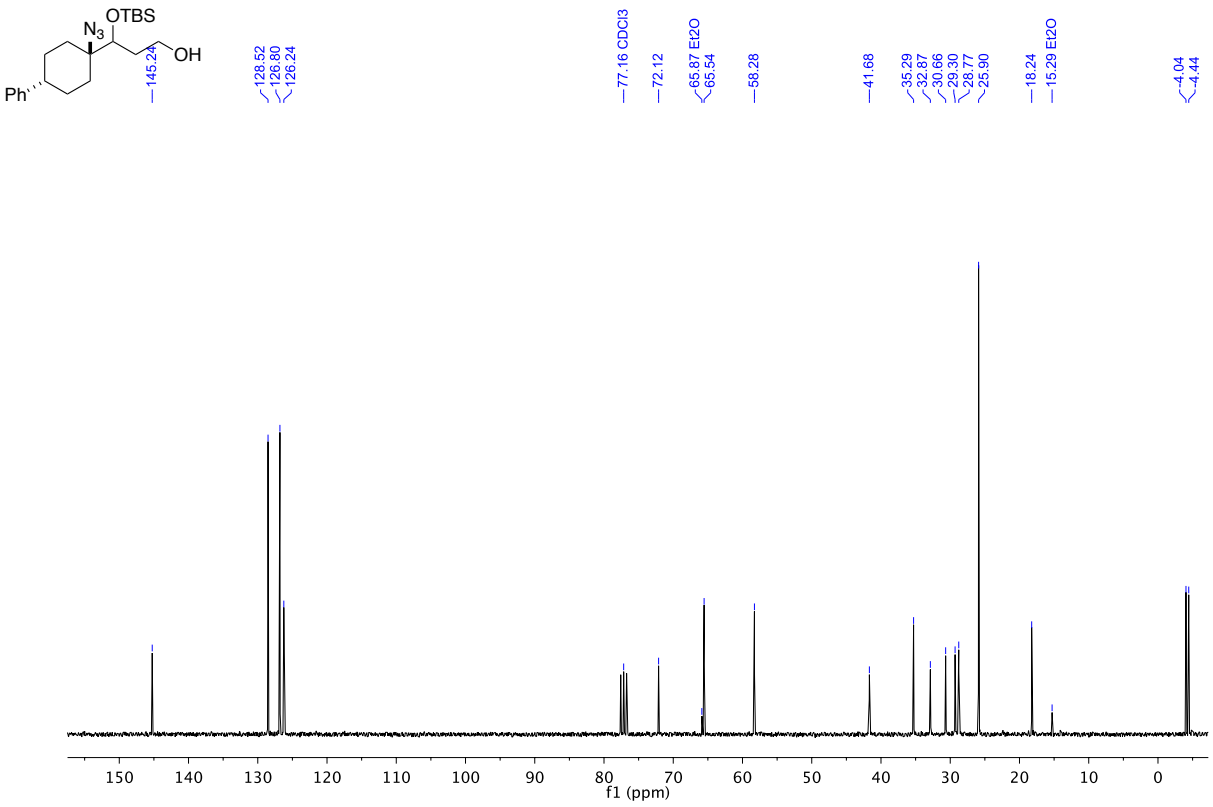

^{1}H NMR (300 MHz, CD_2Cl_2)
3-(cis-1-azido-4-phenylcyclohexyl)propanal

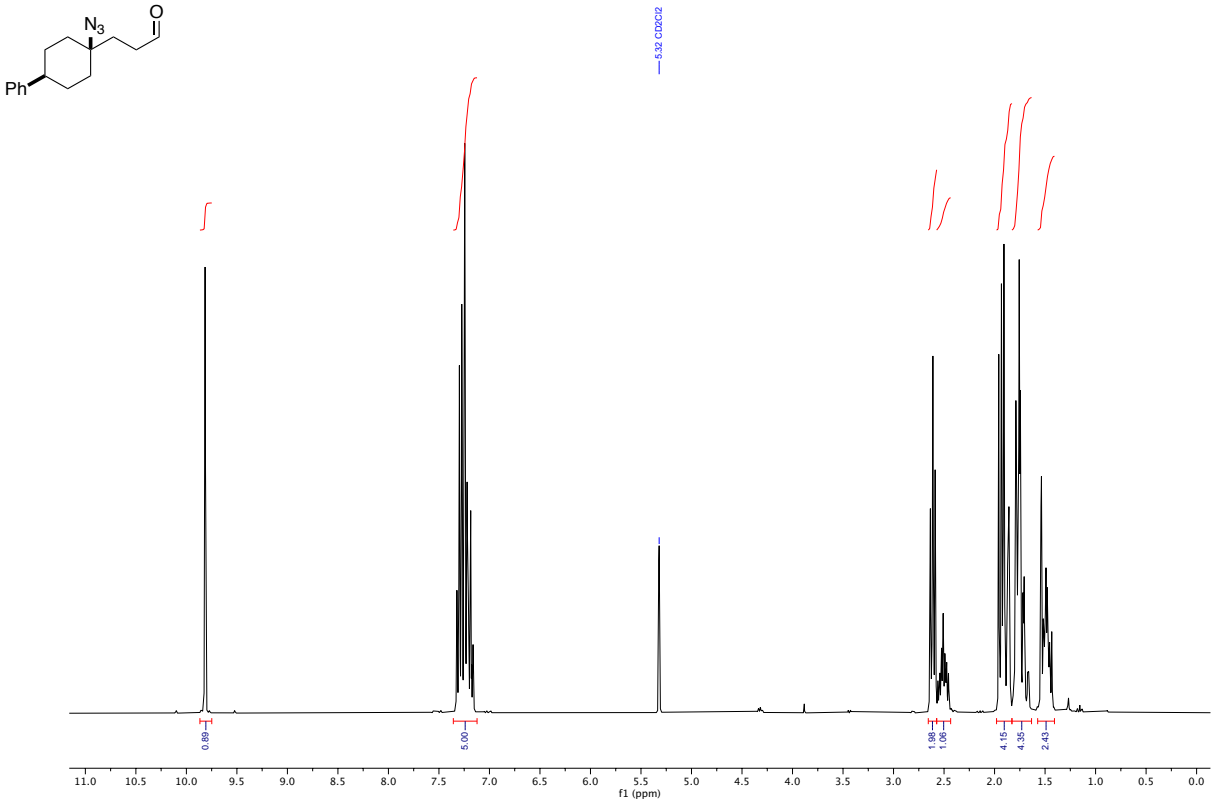

^{13}C NMR (75 MHz, CD_2Cl_2)
3-(cis-1-azido-4-phenylcyclohexyl)propanal

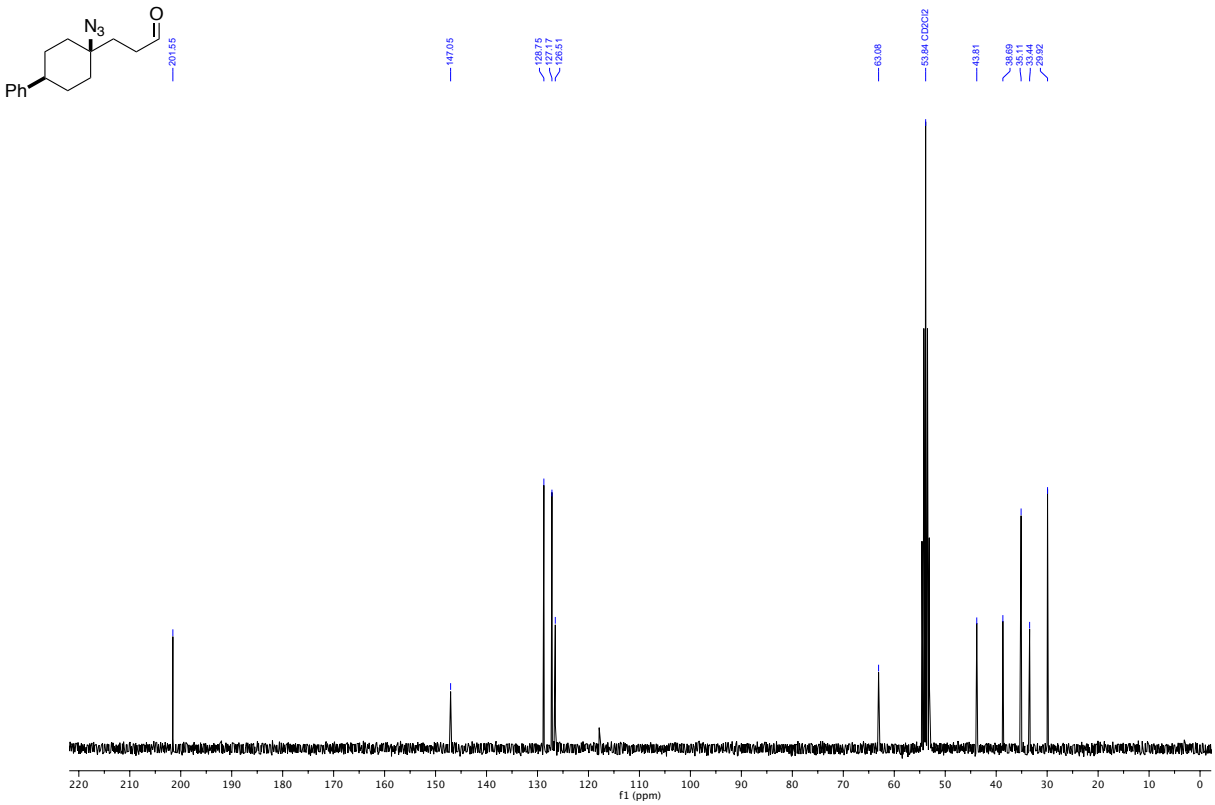

^{1}H NMR (300 MHz, CD_2Cl_2)
1-(cis-1-azido-4-phenylcyclohexyl)pentan-3-ol

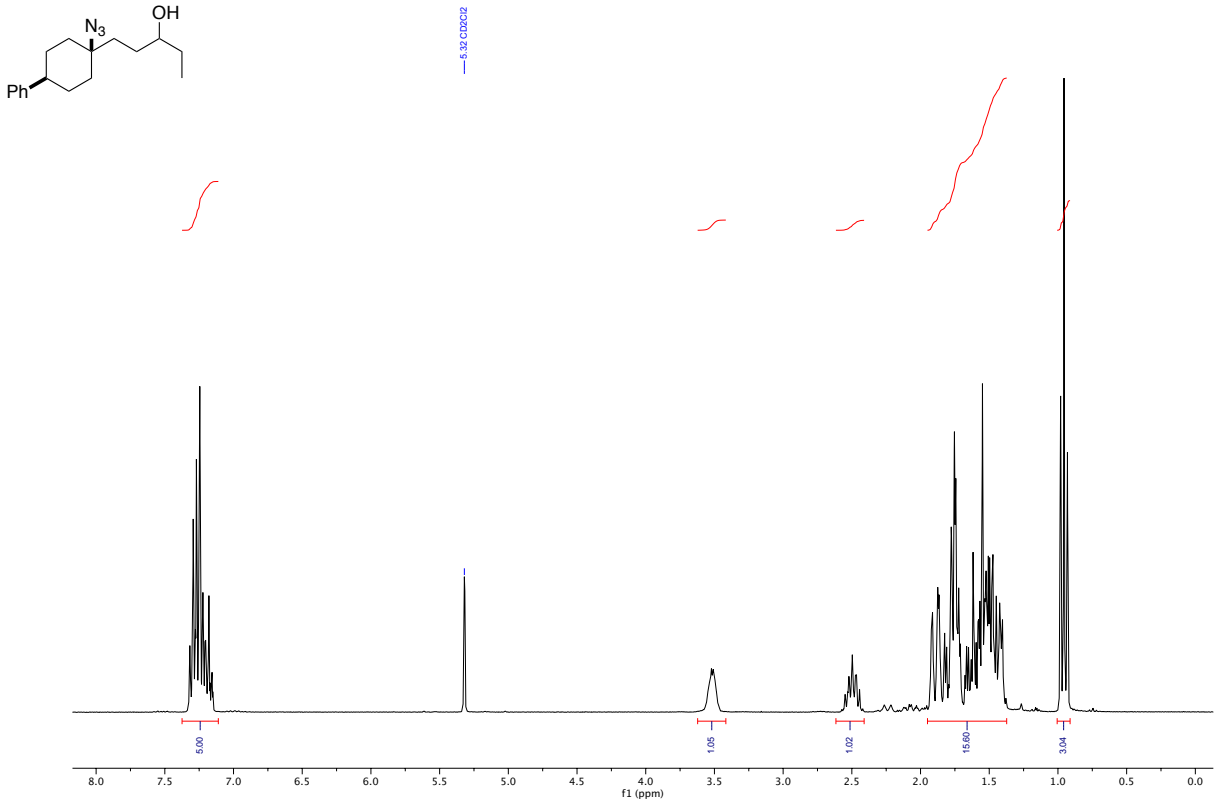

^{13}C NMR (75 MHz, CD_2Cl_2)
1-(cis-1-azido-4-phenylcyclohexyl)pentan-3-ol

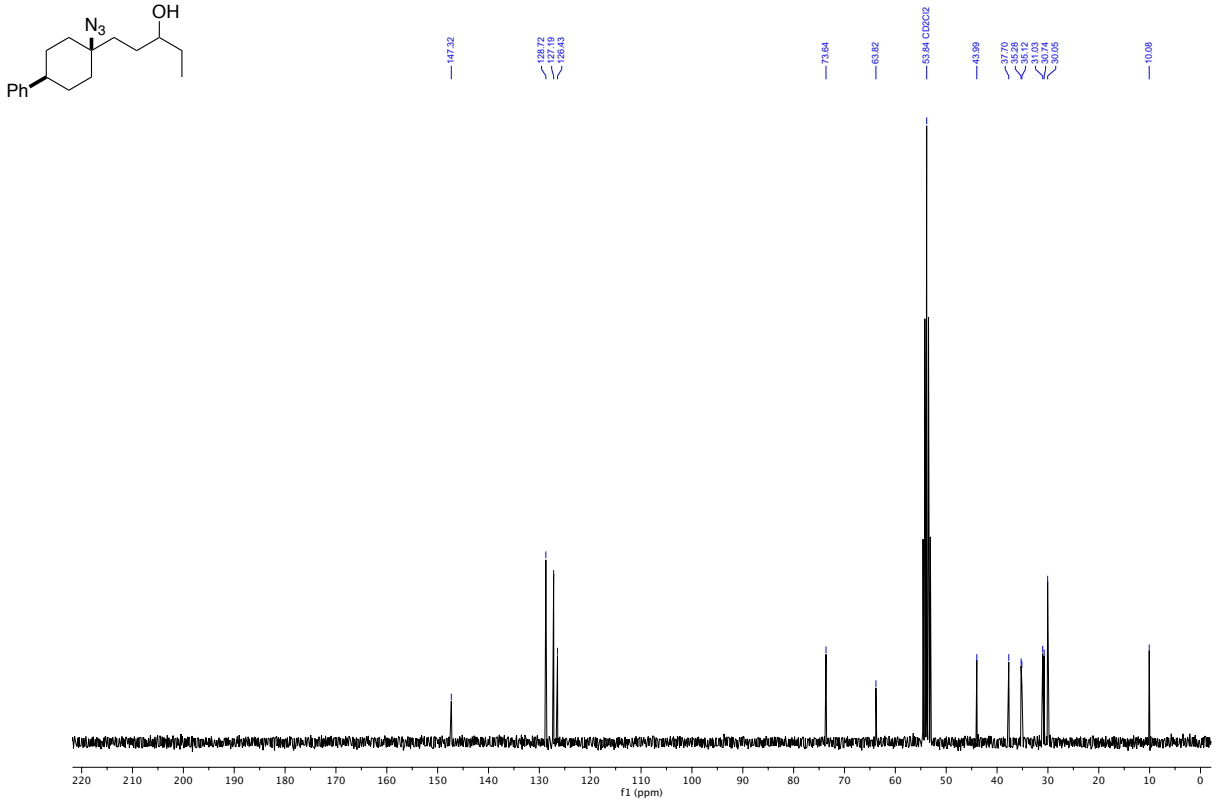

^{1}H NMR (300 MHz, CD_2Cl_2)
5-(cis-1-azido-4-phenylcyclohexyl)-1-phenylpent-1-yn-3-ol

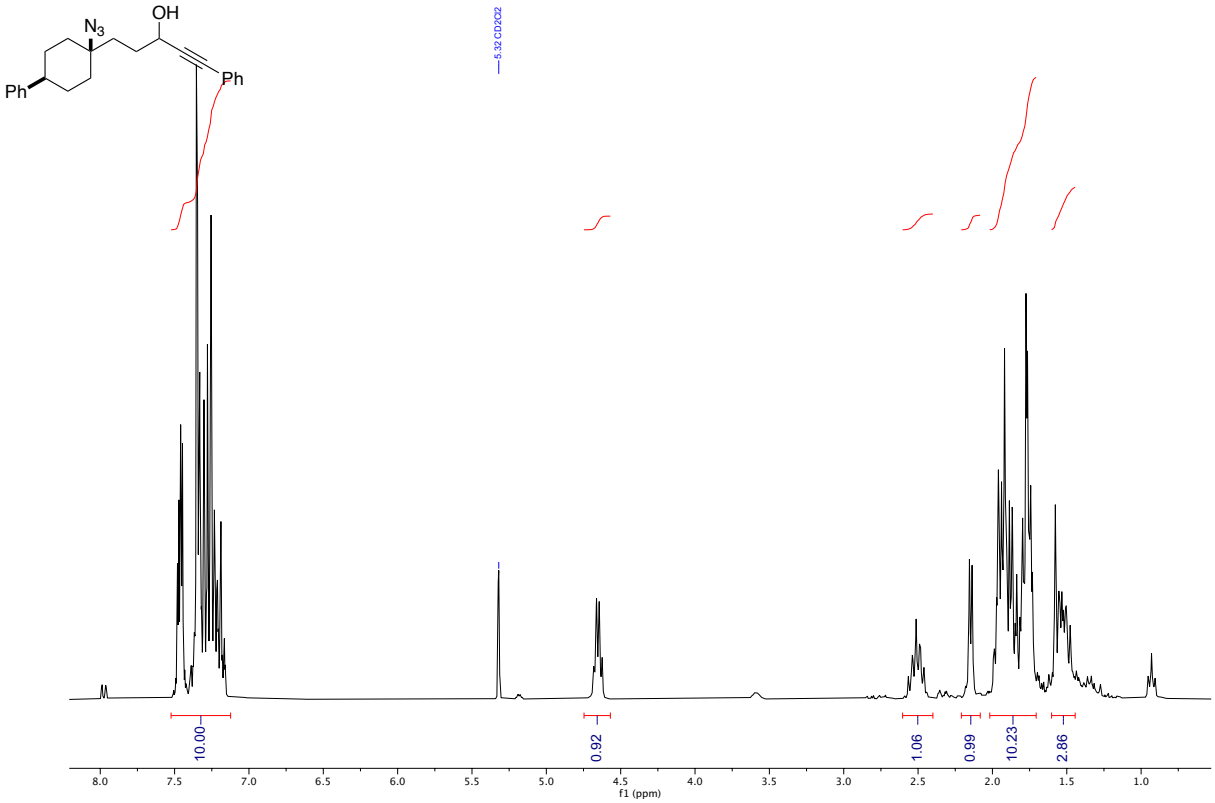

^{13}C NMR (75 MHz, CD_2Cl_2)
5-(cis-1-azido-4-phenylcyclohexyl)-1-phenylpent-1-yn-3-ol

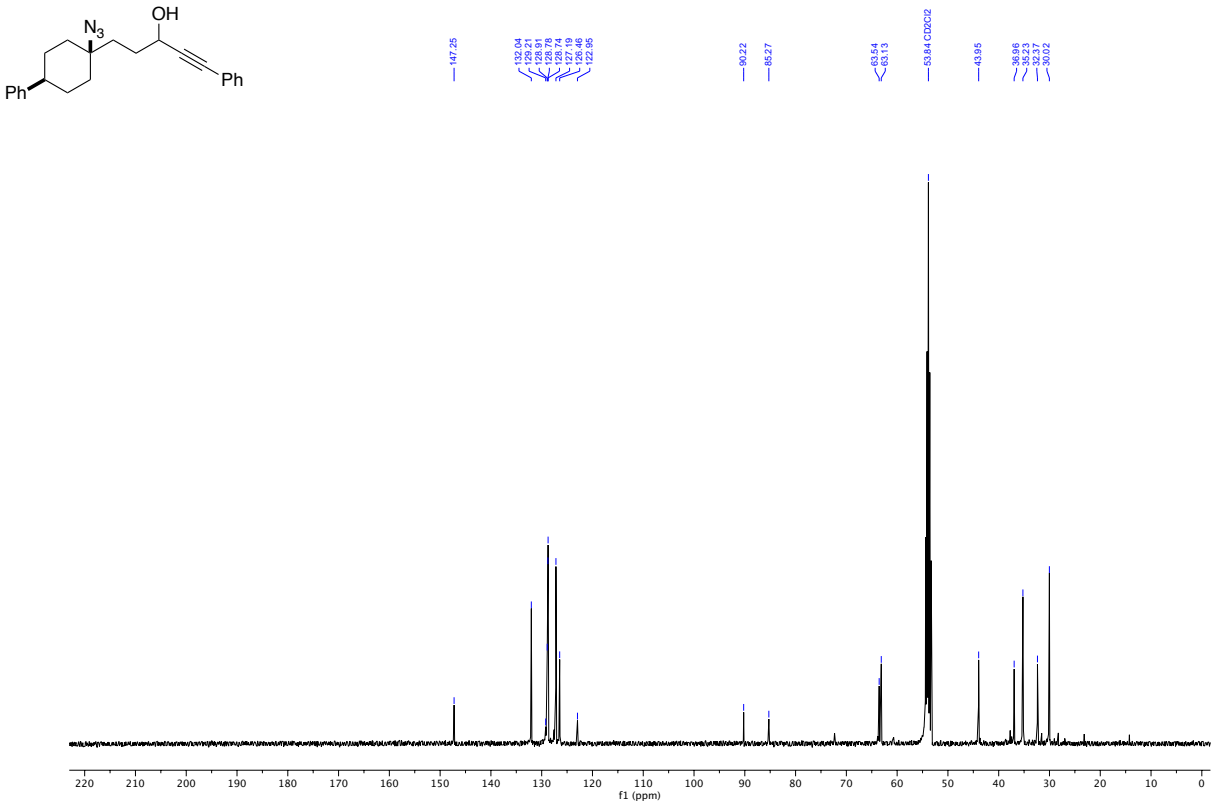

^{1}H NMR (300 MHz, CD_2Cl_2)
1-(cis-1-azido-4-phenylcyclohexyl)hex-5-en-3-ol

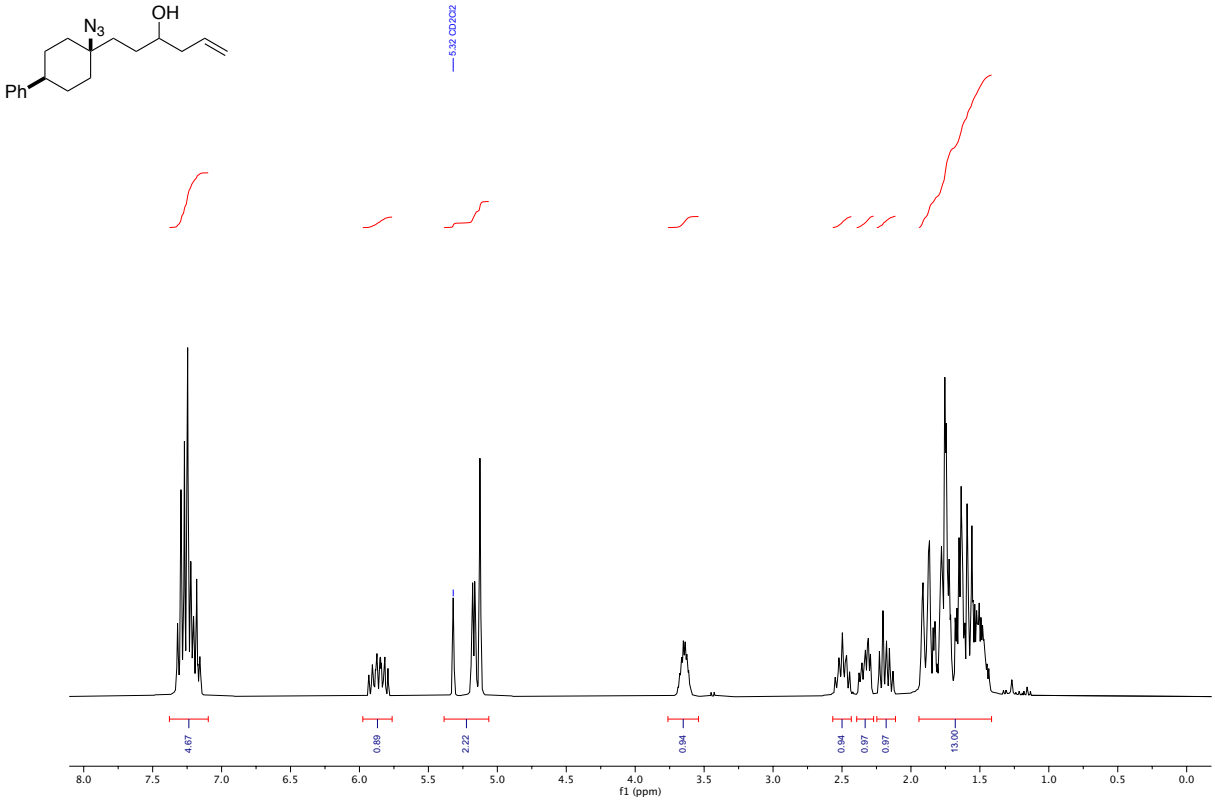

^{13}C NMR (75 MHz, CD_2Cl_2)
1-(cis-1-azido-4-phenylcyclohexyl)hex-5-en-3-ol

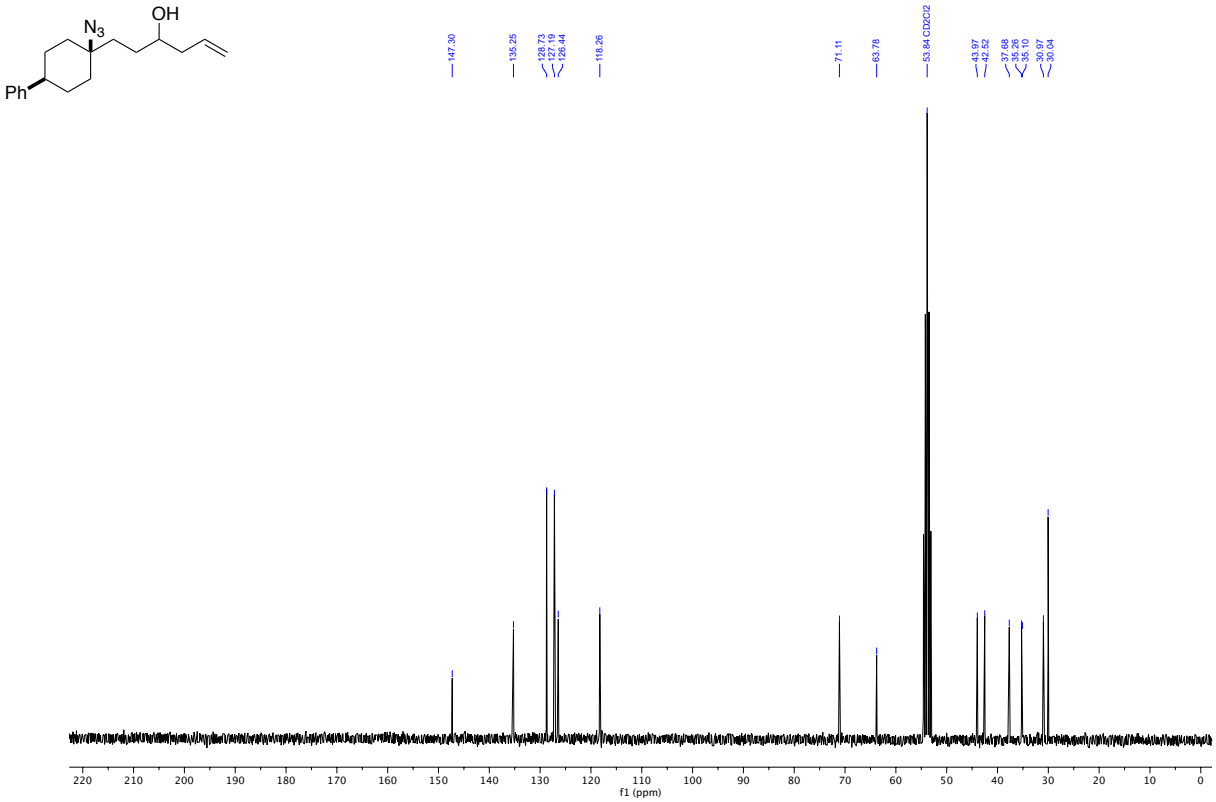

^{1}H NMR (300 MHz, CD_2Cl_2)
3-(cis-1-azido-4-phenylcyclohexyl)-1-phenylpropan-1-one

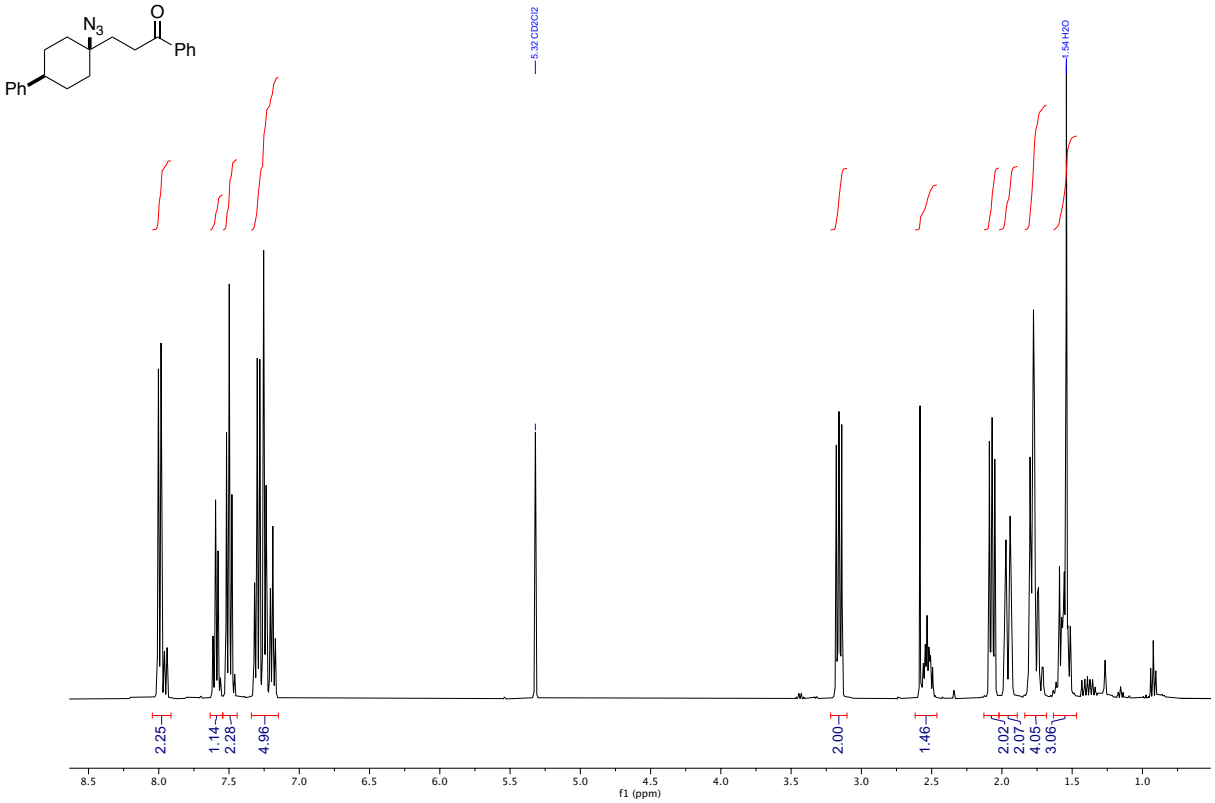

^{13}C NMR (75 MHz, CD_2Cl_2)
3-(cis-1-azido-4-phenylcyclohexyl)-1-phenylpropan-1-one

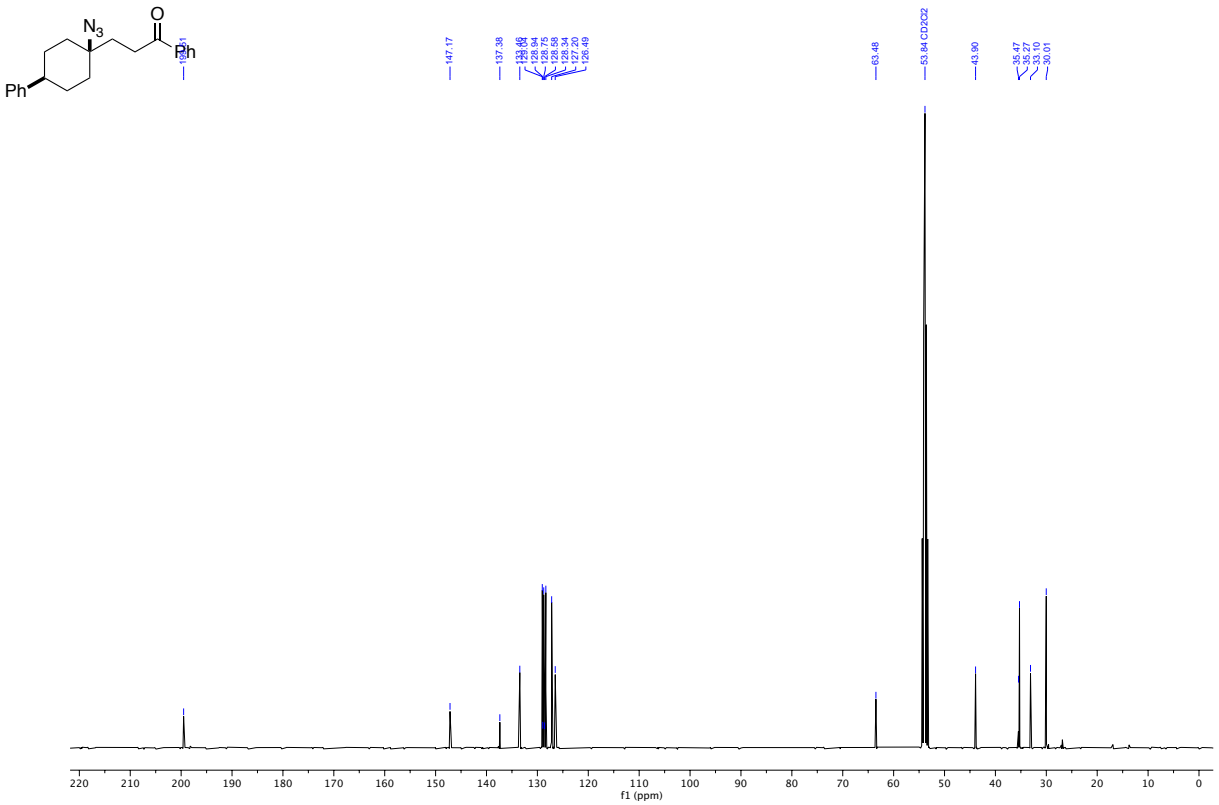

^{1}H NMR (300 MHz, CD_2Cl_2)
3-(cis-1-azido-4-phenylcyclohexyl)-1-phenylpropan-1-ol

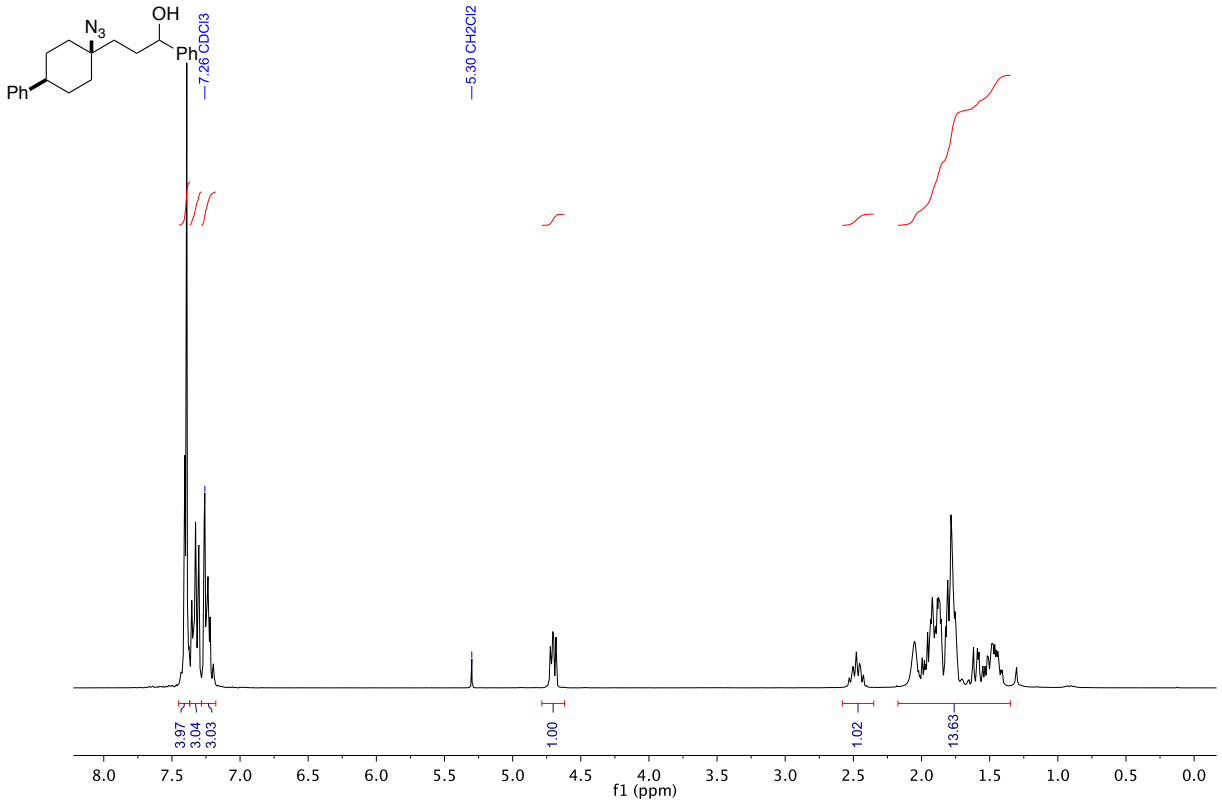

^{13}C NMR (75 MHz, CD_2Cl_2)
3-(cis-1-azido-4-phenylcyclohexyl)-1-phenylpropan-1-ol

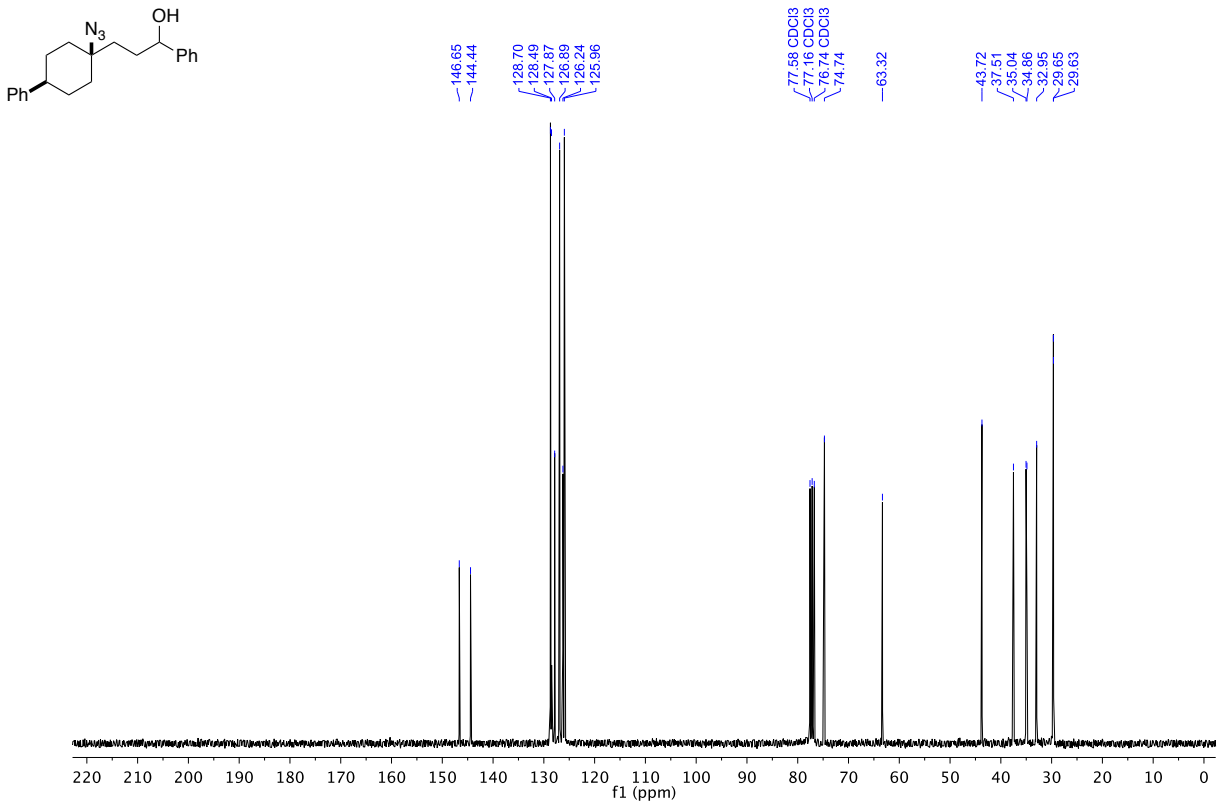

^{1}H NMR (300 MHz, C_6D_6)
Octahydrospiro[pyrrolo[1,2-a]azepine-7,2'-[1,3]dioxolan]-1-ol

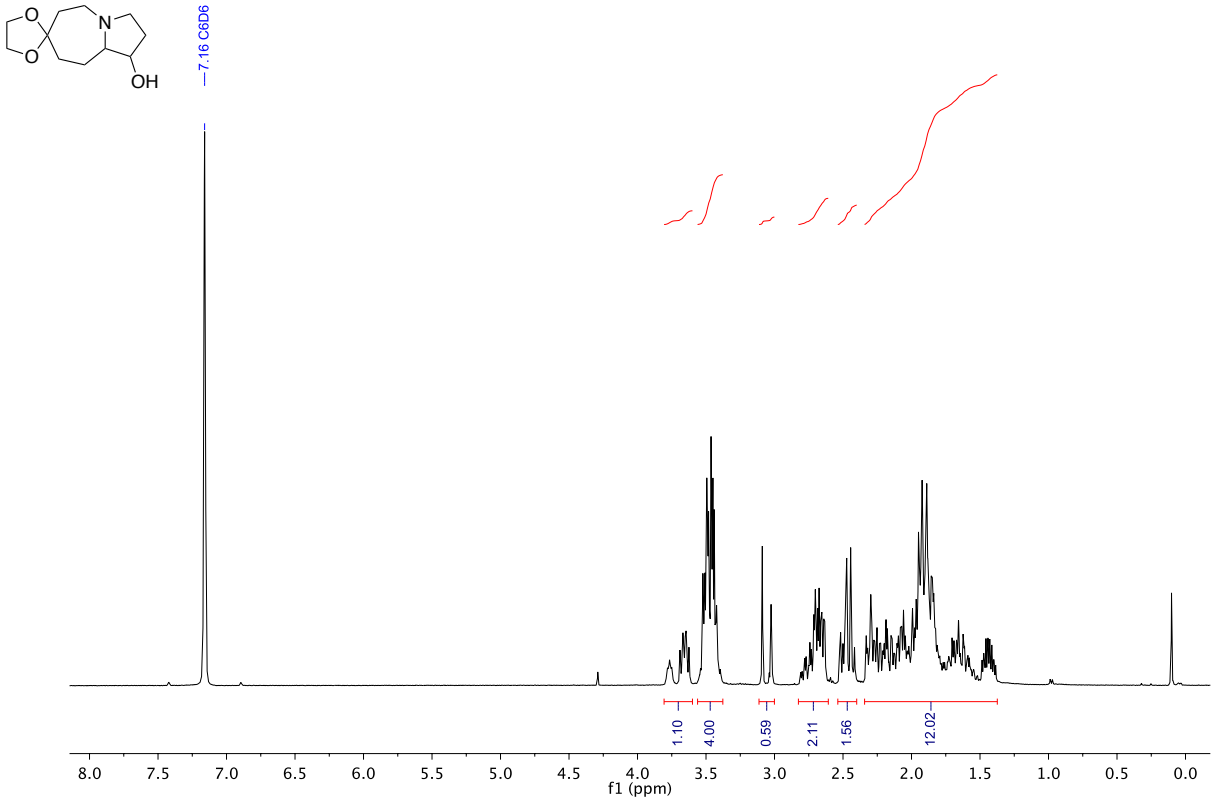

^{13}C NMR (101 MHz, C_6D_6)
Octahydrospiro[pyrrolo[1,2-a]azepine-7,2'-[1,3]dioxolan]-1-ol

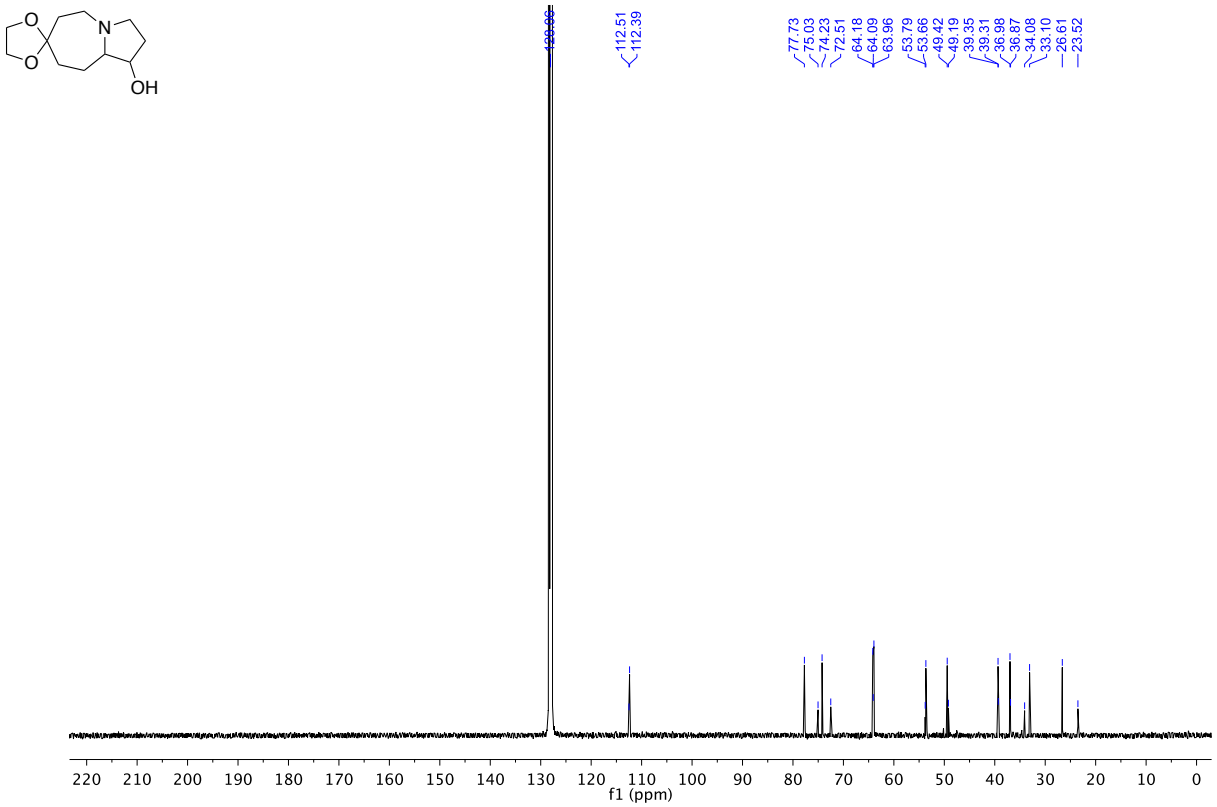

^{1}H NMR (300 MHz, CD_2Cl_2)
Cis-7-phenyloctahydro-1H-pyrrolo[1,2-a]azepine

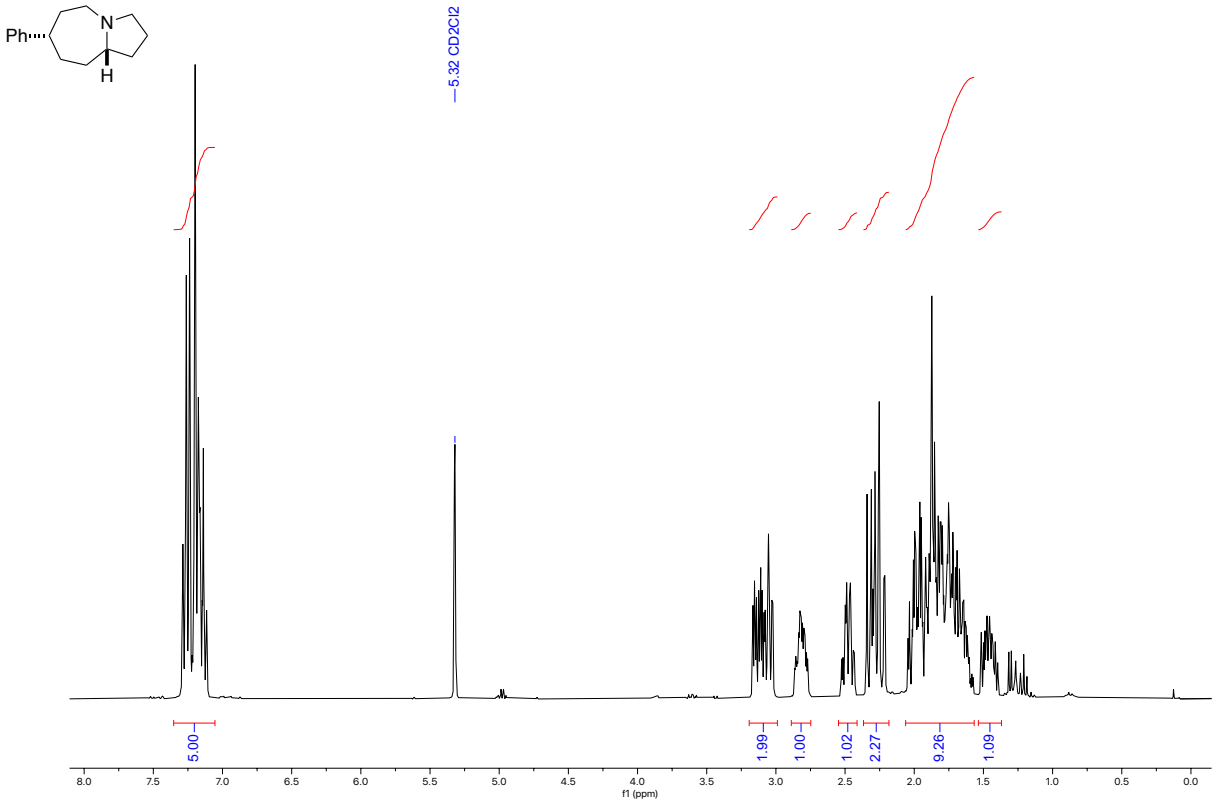

^{13}C NMR (101 MHz, CD_2Cl_2)
Cis-7-phenyloctahydro-1H-pyrrolo[1,2-a]azepine

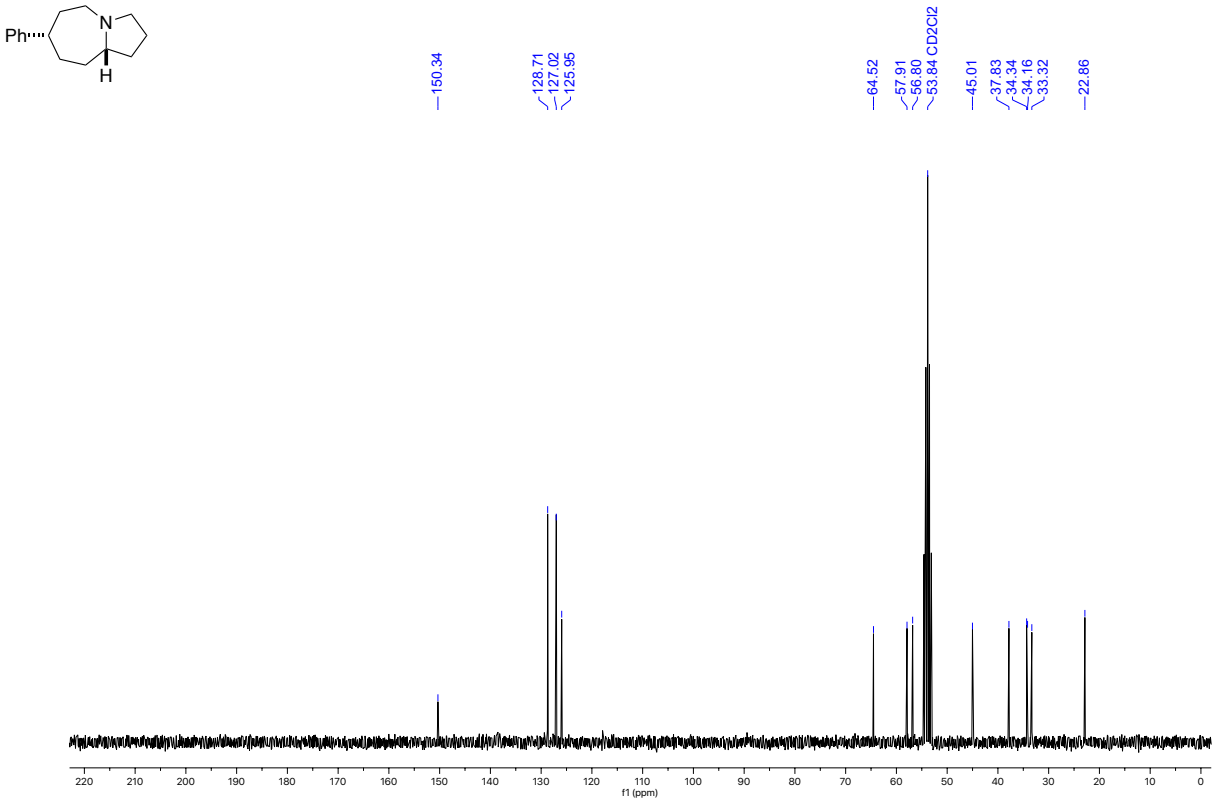

^{1}H NMR (300 MHz, C_6D_6)
(1RS,7SR,9aSR)-7-phenyloctahydro-1H-pyrrolo[1,2-a]azepin-1-ol

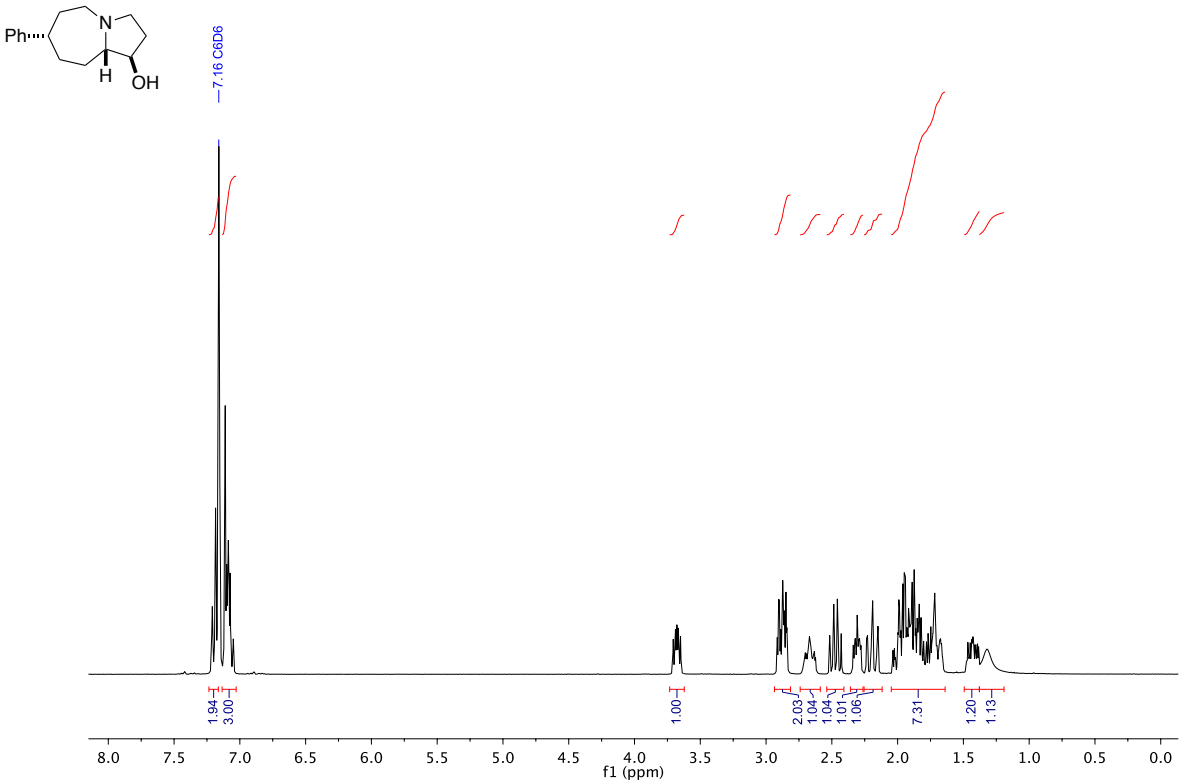

^{13}C NMR (75 MHz, C_6D_6)
(1RS,7SR,9aSR)-7-phenyloctahydro-1H-pyrrolo[1,2-a]azepin-1-ol

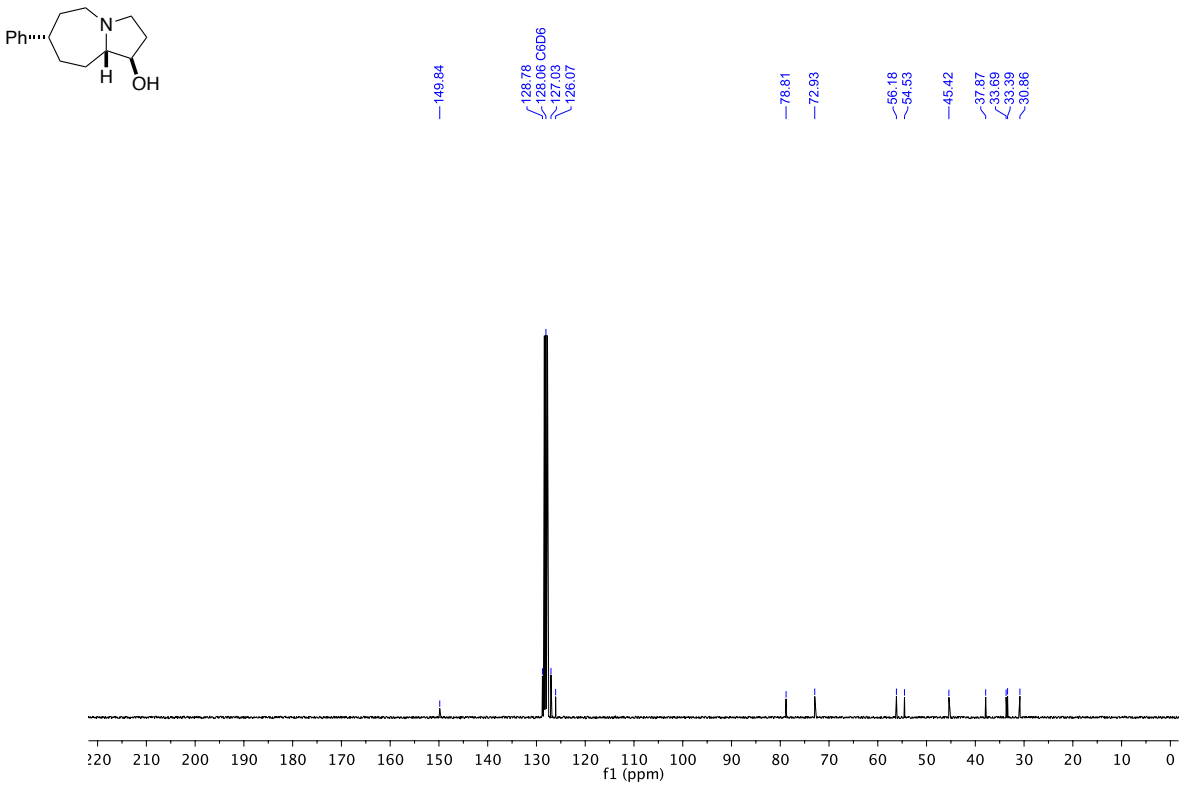

^{1}H NMR (300 MHz, C_6D_6)
(1RS,7SR,9aRS)-7-phenyloctahydro-1H-pyrrolo[1,2-a]azepin-1-ol

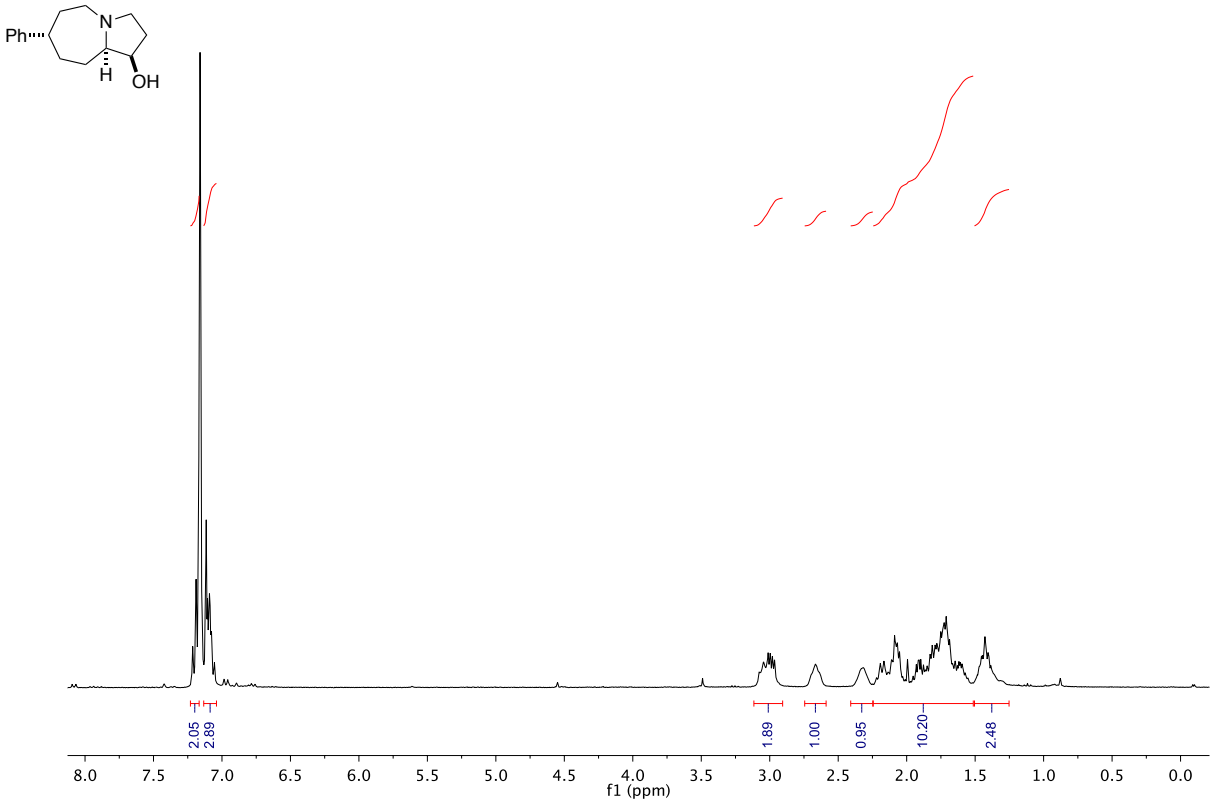

^{13}C NMR (75 MHz, C_6D_6)
(1RS,7SR,9aRS)-7-phenyloctahydro-1H-pyrrolo[1,2-a]azepin-1-ol

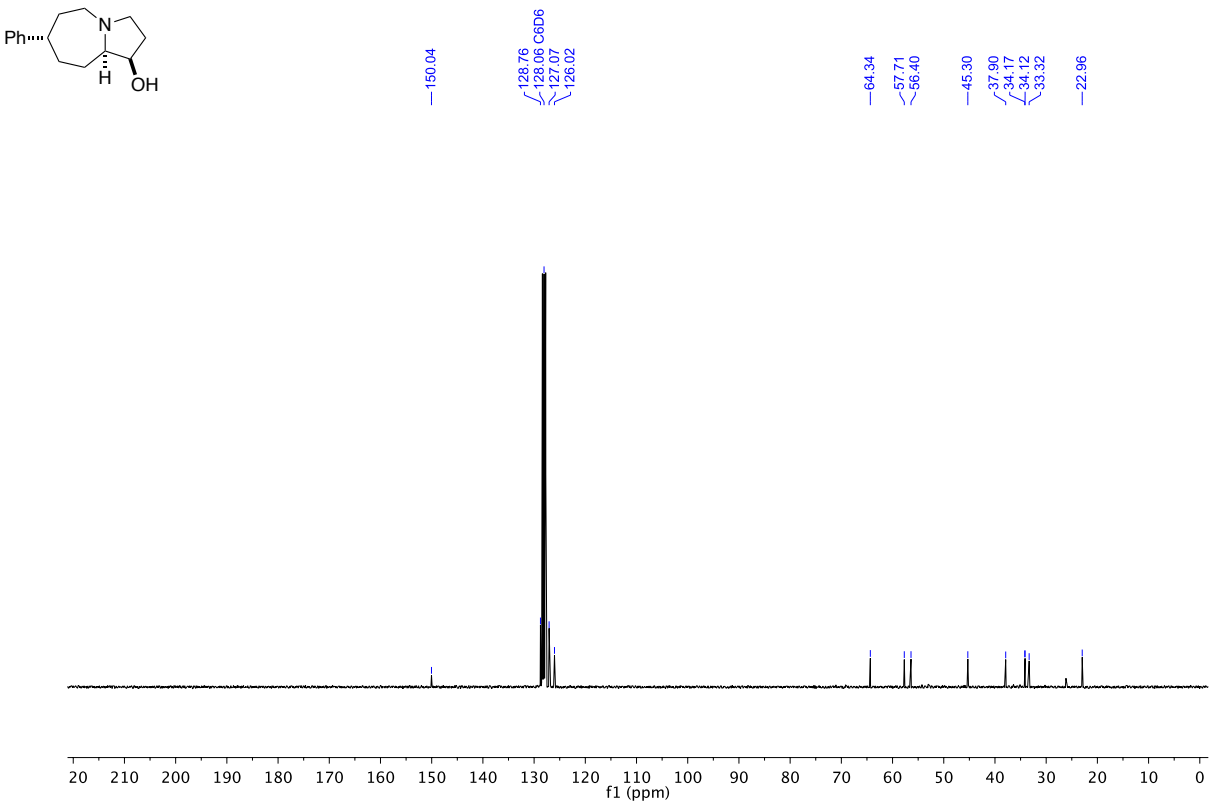

^{1}H NMR (300 MHz, $CDCl_3$)
(7SR,9aSR)-3-ethyl-7-phenyloctahydro-1H-pyrrolo[1,2-a]azepine

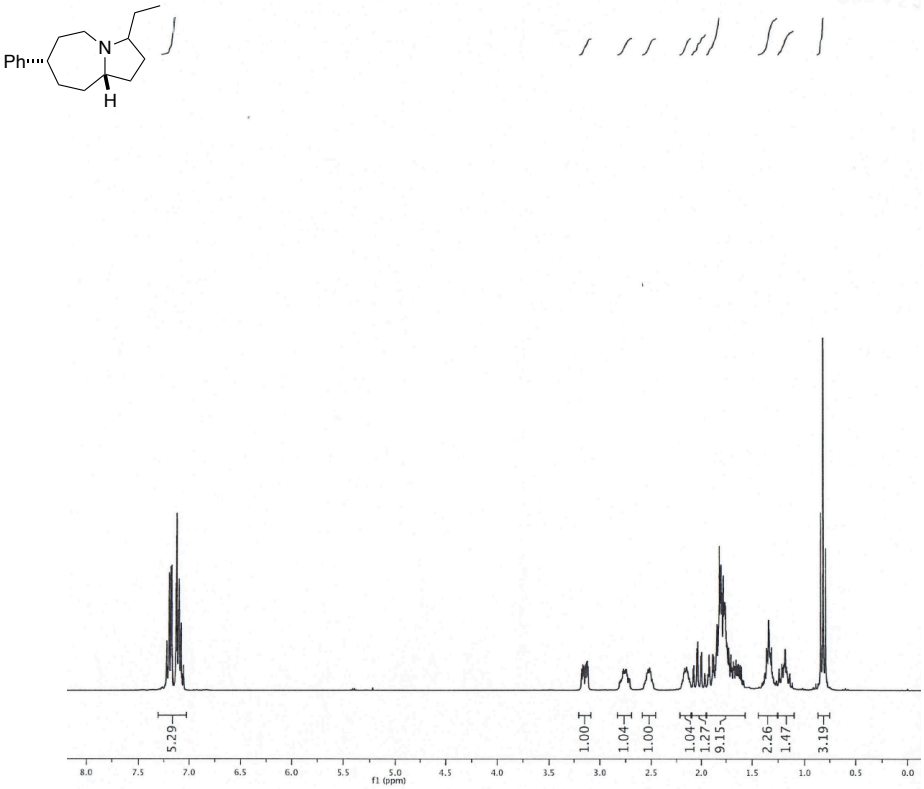

^{13}C NMR (75 MHz, $CDCl_3$)
(7SR,9aSR)-3-ethyl-7-phenyloctahydro-1H-pyrrolo[1,2-a]azepine

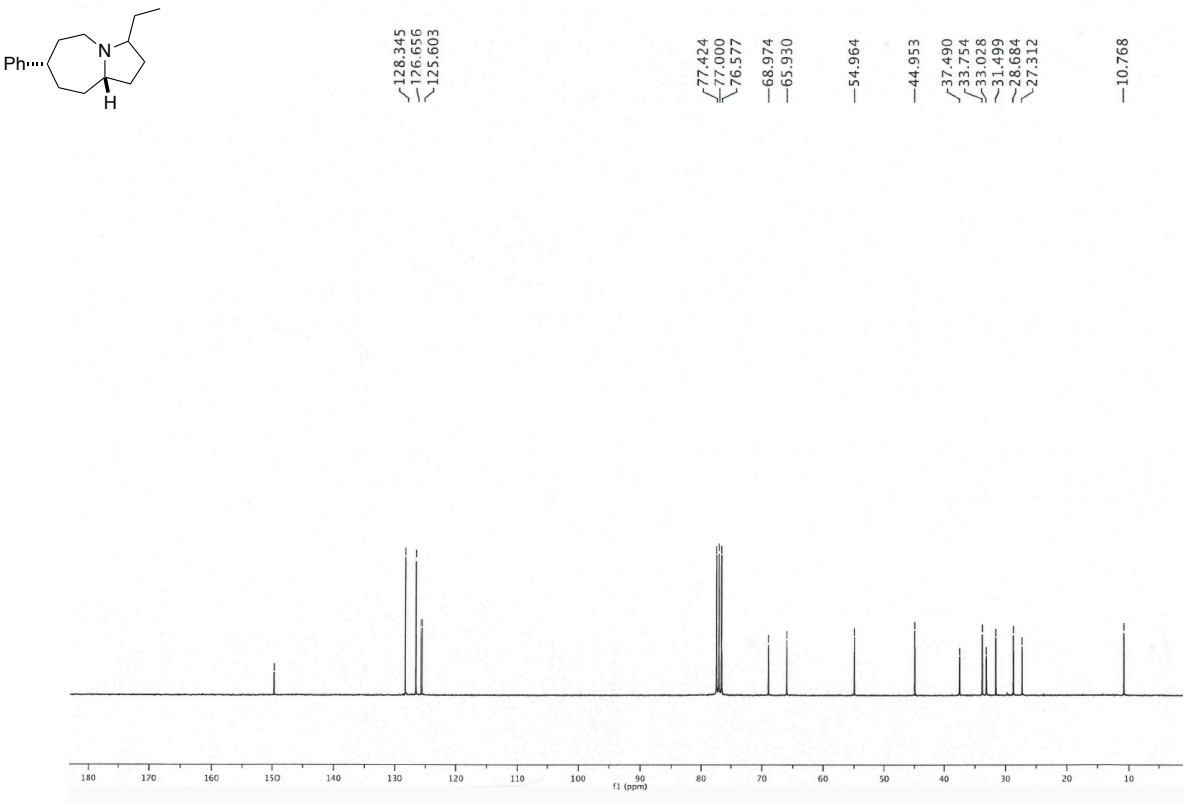

^{1}H NMR (300 MHz, CD_2Cl_2)
(7SR,9aSR)-7-phenyl-3-(phenylethynyl)octahydro-1H-pyrrolo[1,2-a]azepine

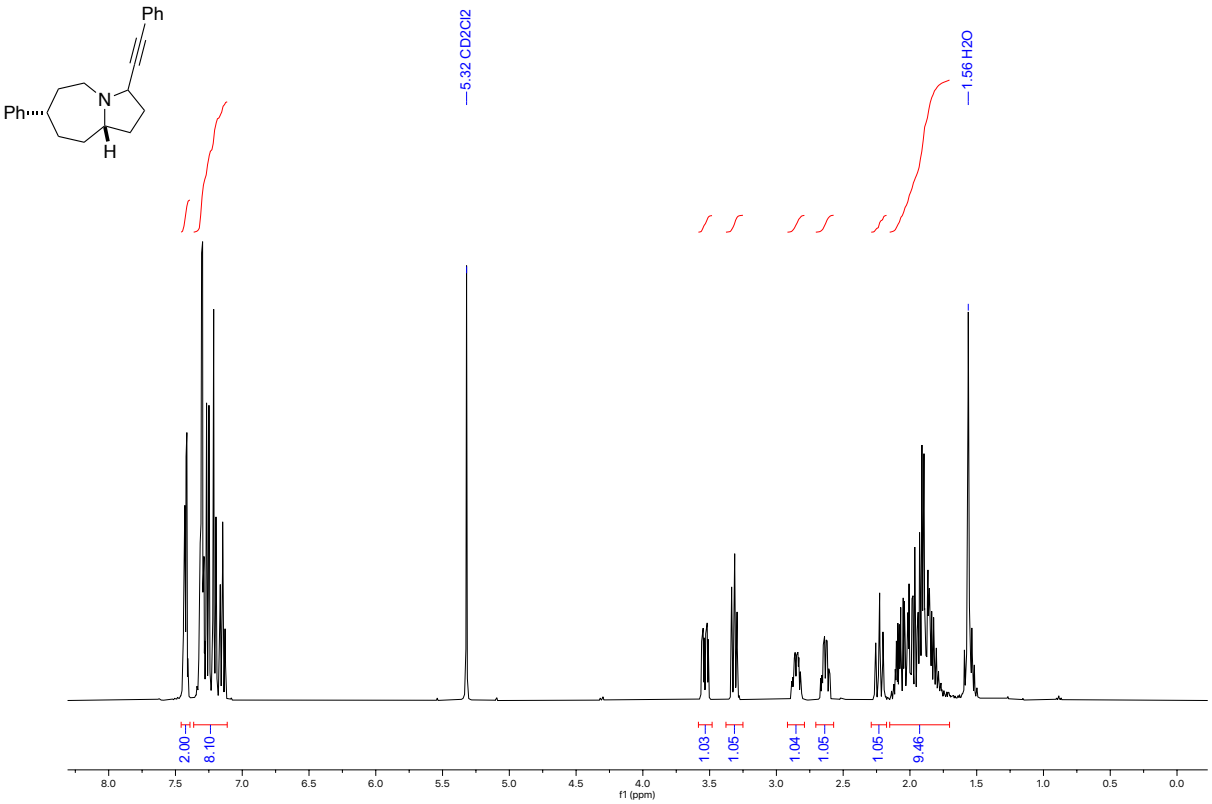

^{13}C NMR (75 MHz, CD_2Cl_2)
(7SR,9aSR)-7-phenyl-3-(phenylethynyl)octahydro-1H-pyrrolo[1,2-a]azepine

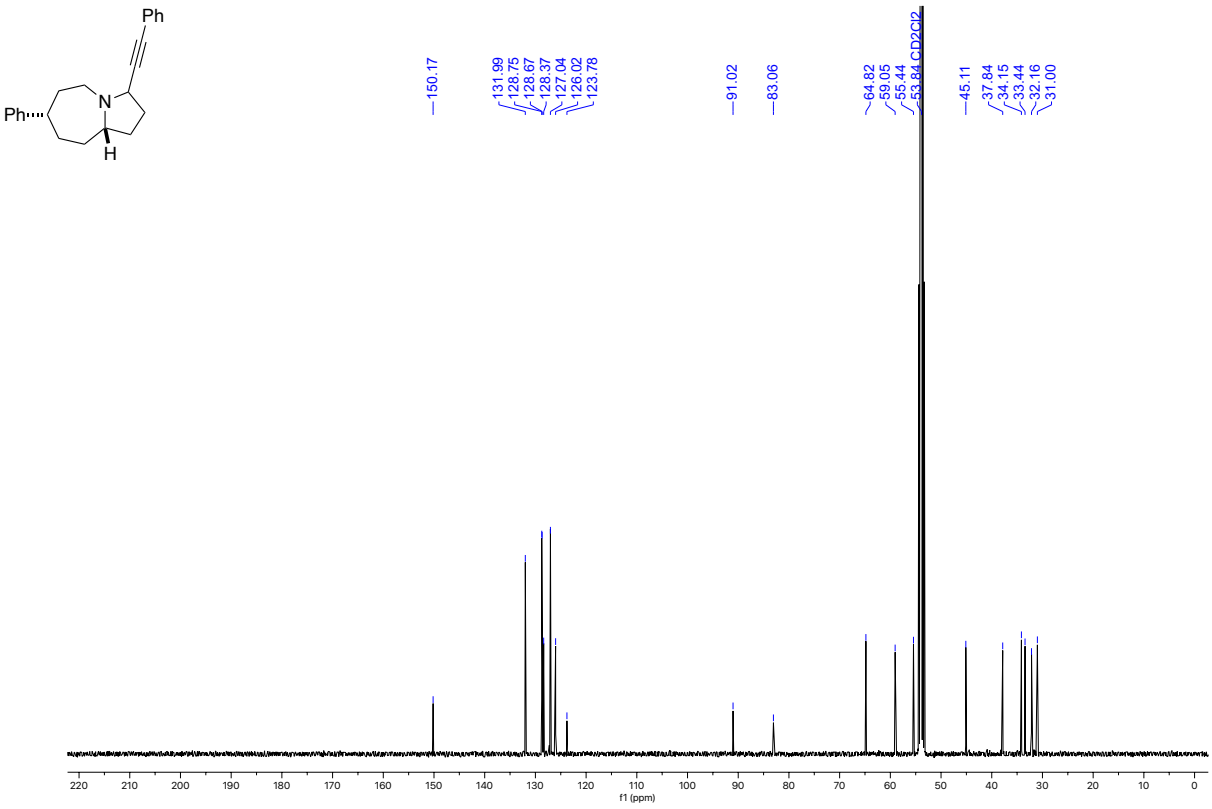

^{1}H NMR (300 MHz, CD_2Cl_2)
(7SR,9aSR)-3-allyl-7-phenyloctahydro-1H-pyrrolo[1,2-a]azepine

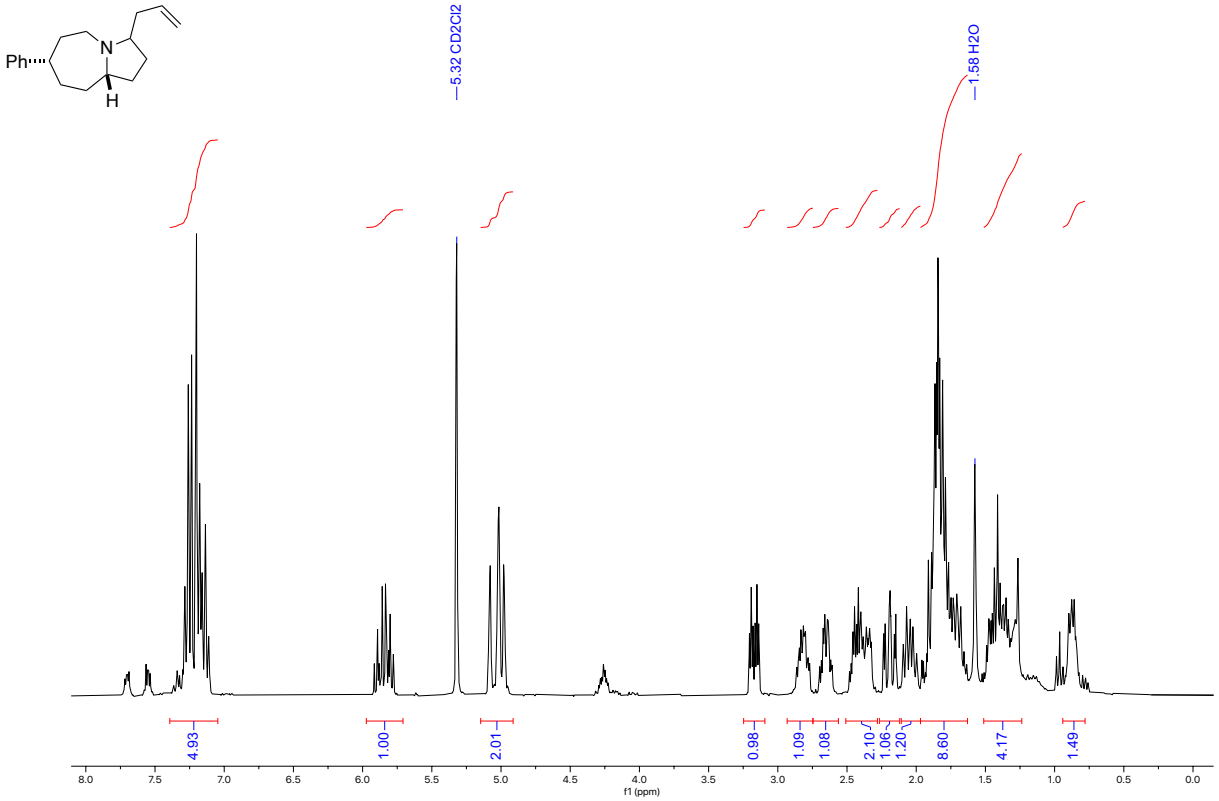

^{13}C NMR (75 MHz, CD_2Cl_2)
(7SR,9aSR)-3-allyl-7-phenyloctahydro-1H-pyrrolo[1,2-a]azepine

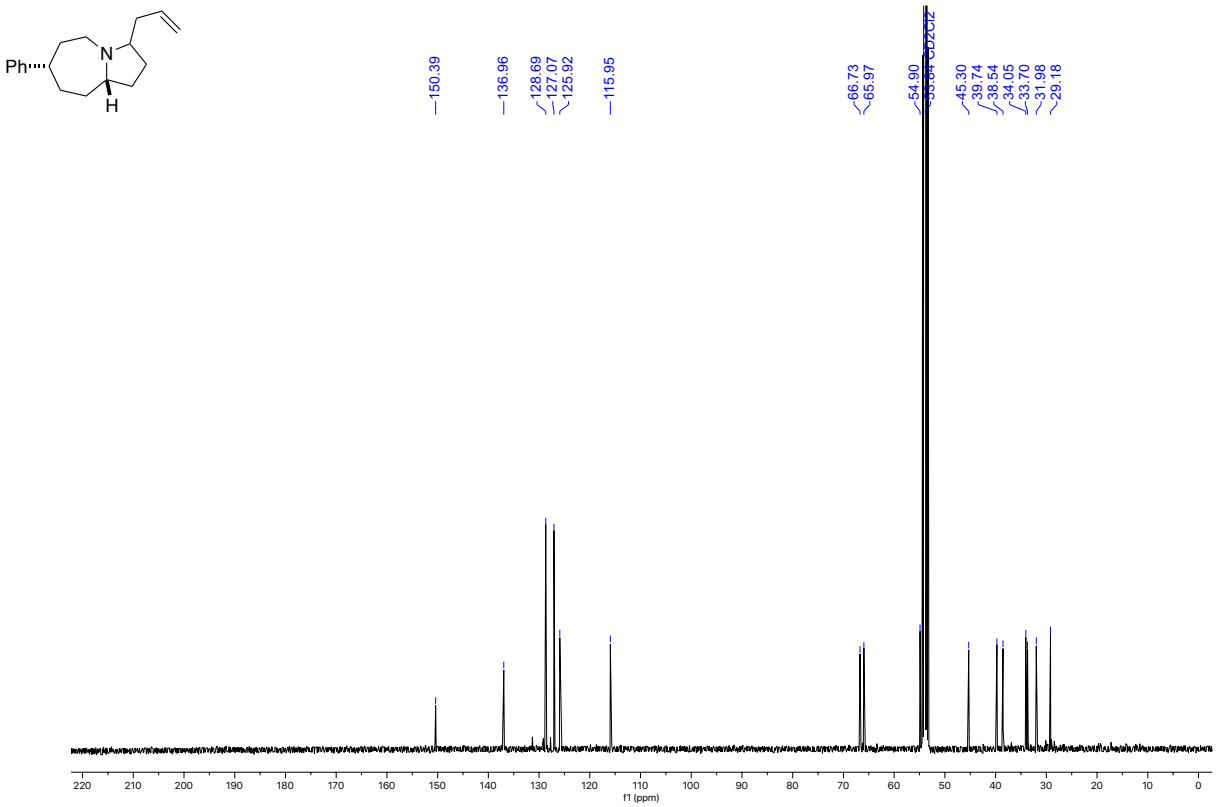

^{1}H NMR (300 MHz, CD_2Cl_2)
(7SR,9aSR)-3,7-diphenyloctahydro-1H-pyrrolo[1,2-a]azepine

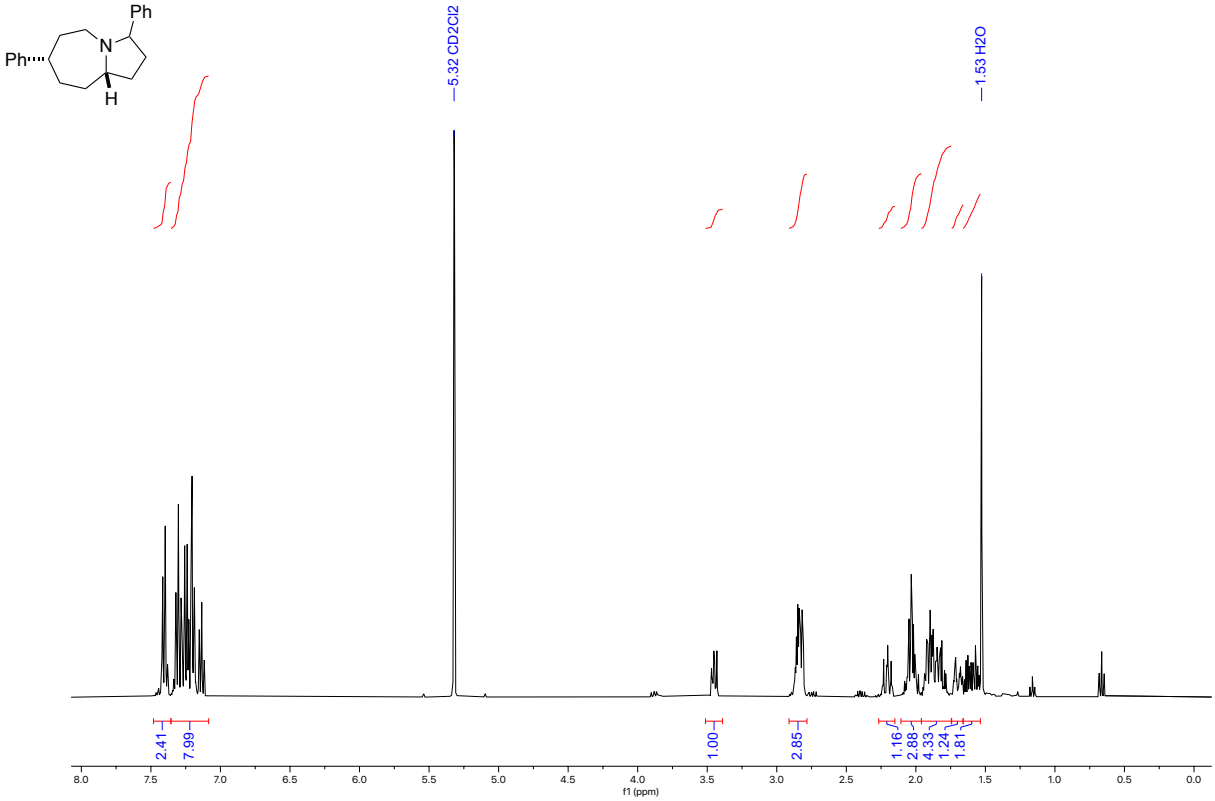

^{13}C NMR (75 MHz, CD_2Cl_2)
(7SR,9aSR)-3,7-diphenyloctahydro-1H-pyrrolo[1,2-a]azepine

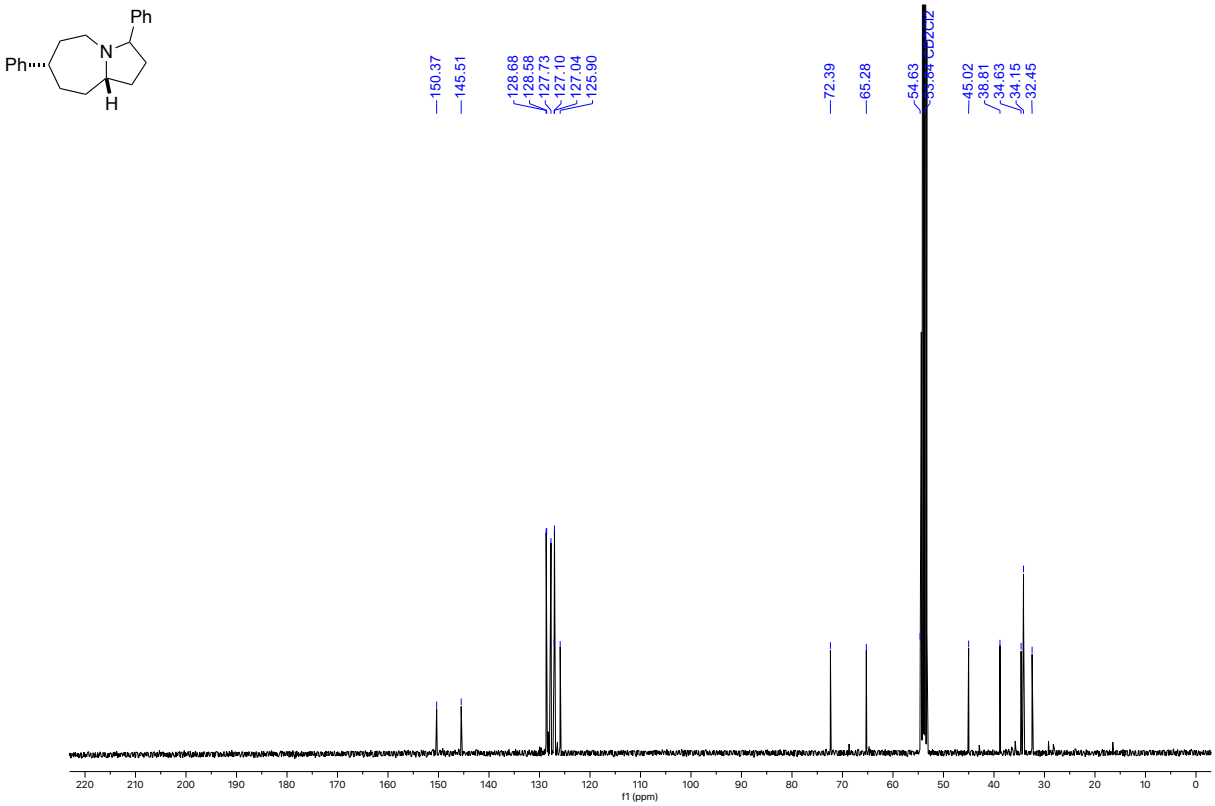

^{1}H NMR (300 MHz, $CDCl_3$)
7-phenyl-1,2,3,5,6,7,8,9-octahydropyrrolo[1,2-a]azepin-4-ium trifluoromethanesulfonate

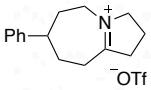

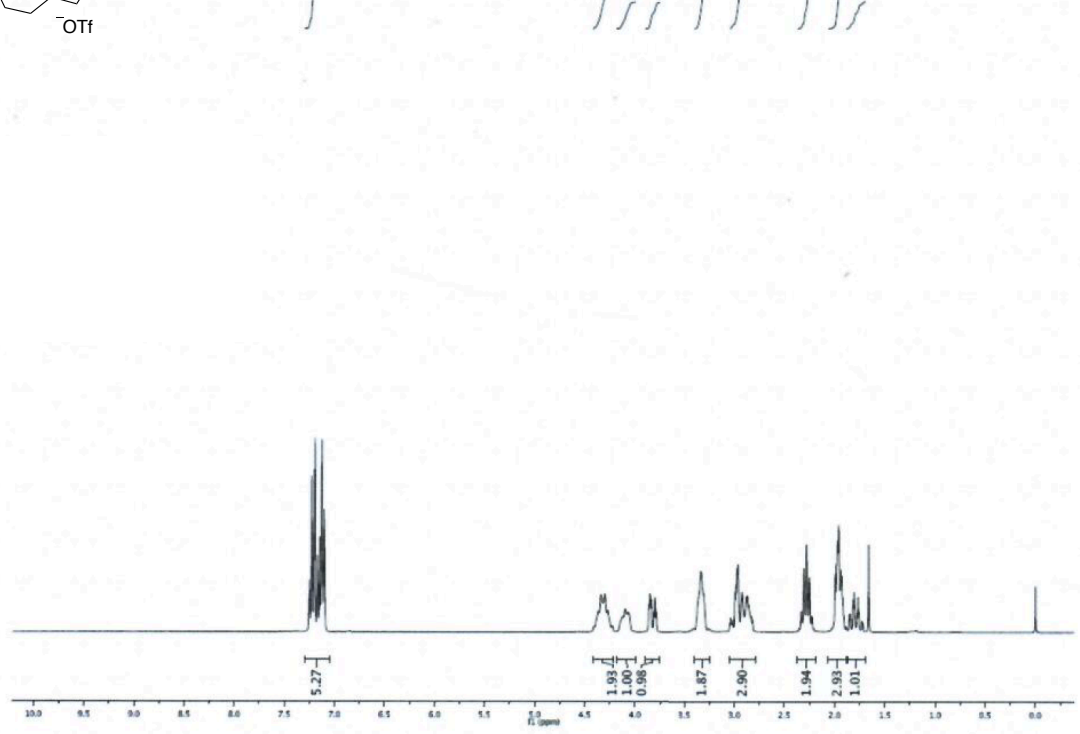

^{13}C NMR (75 MHz, $CDCl_3$)
7-phenyl-1,2,3,5,6,7,8,9-octahydropyrrolo[1,2-a]azepin-4-ium trifluoromethanesulfonate

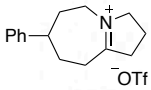

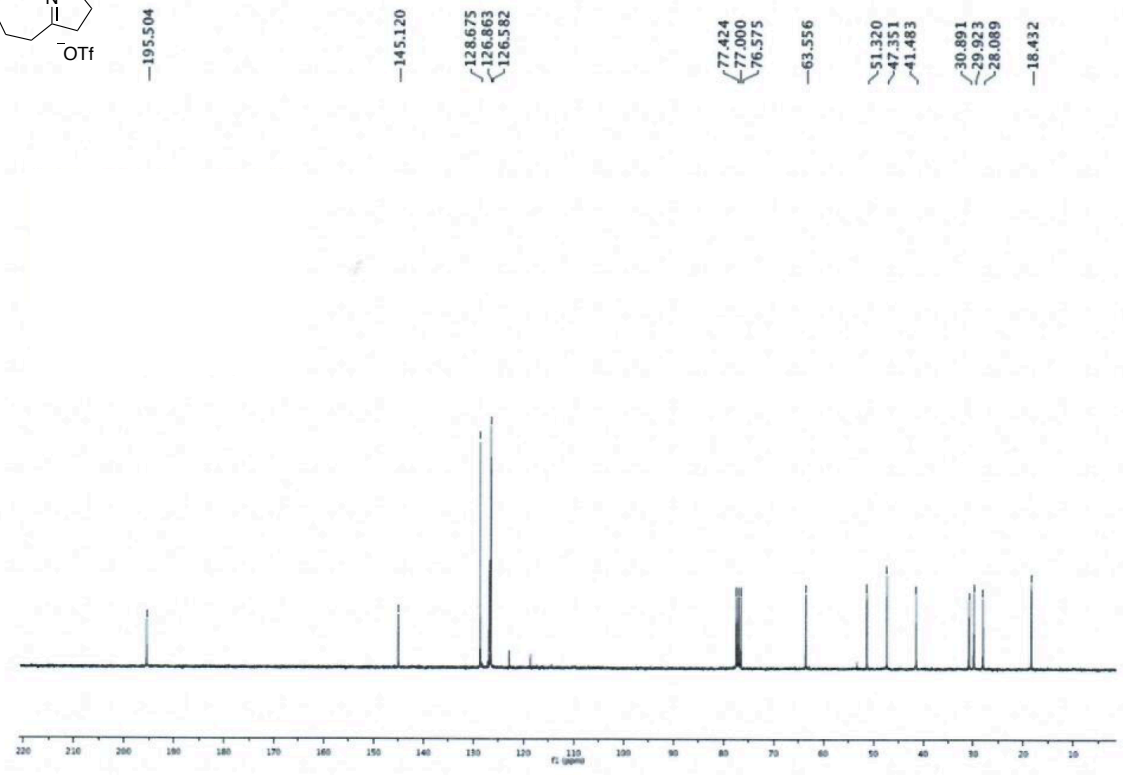

^{1}H NMR (300 MHz, $CDCl_3$)

3-(1-azido-4-phenylcyclohexyl)-3-((tert-butyldimethylsilyl)oxy)propyl-3,5-dinitrobenzoate

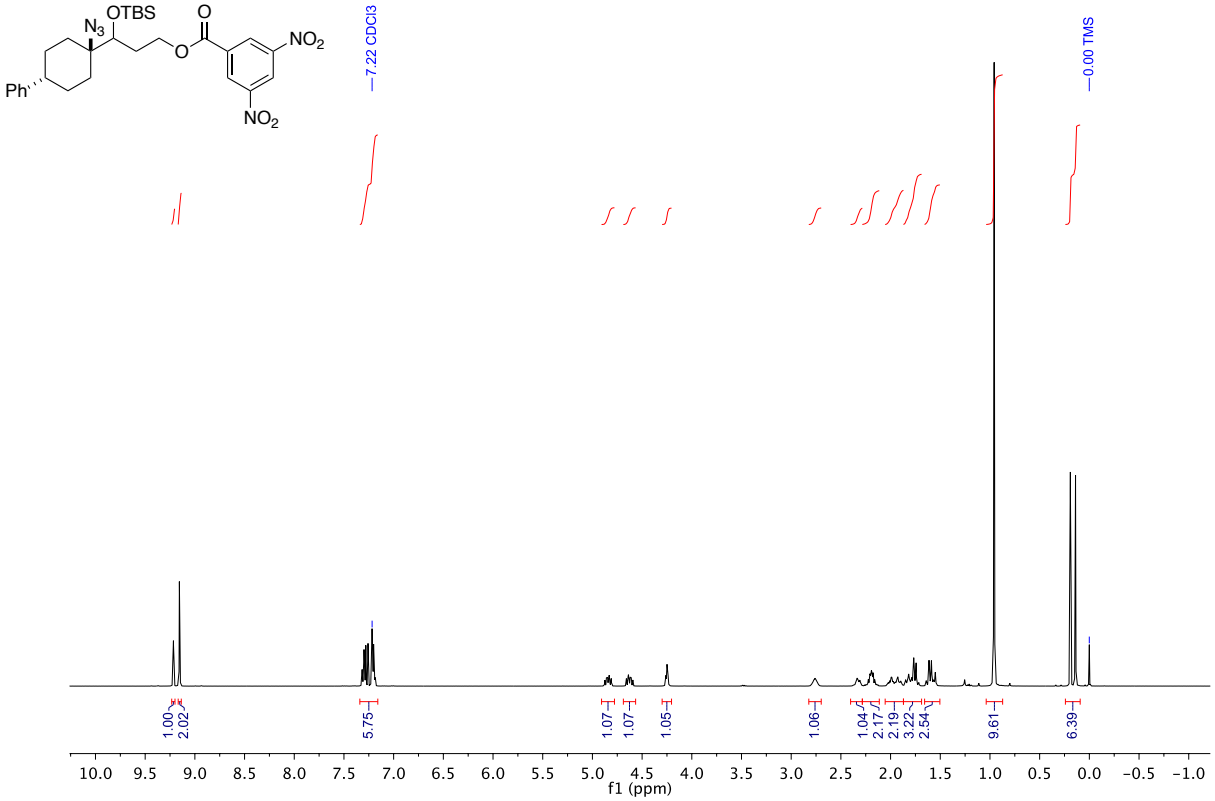

^{13}C NMR (75 MHz, $CDCl_3$)

3-(1-azido-4-phenylcyclohexyl)-3-((tert-butyldimethylsilyl)oxy)propyl-3,5-dinitrobenzoate

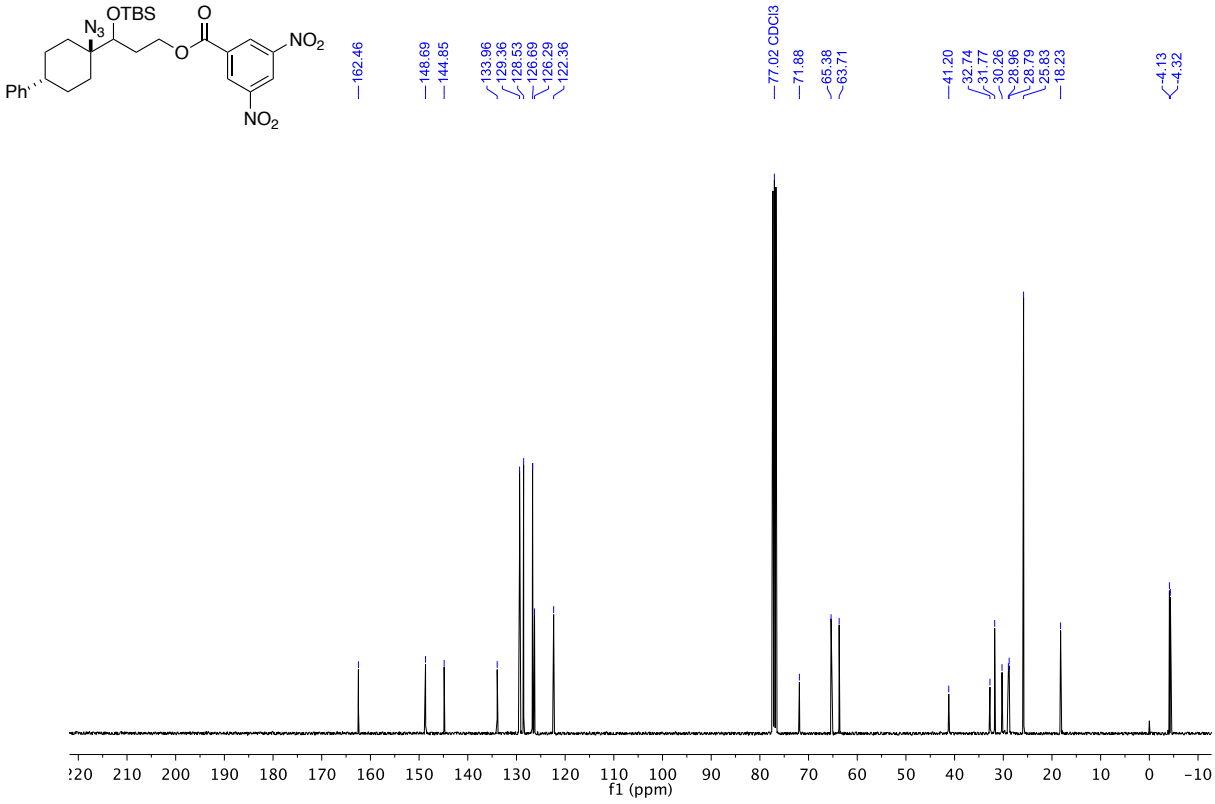

^{1}H NMR (300 MHz, CD_2Cl_2)
(1R,7S,9aS)- 7-phenyloctahydro-1H-pyrrolo[1,2-a]azepin-1-yl 3,5-dinitrobenzoate

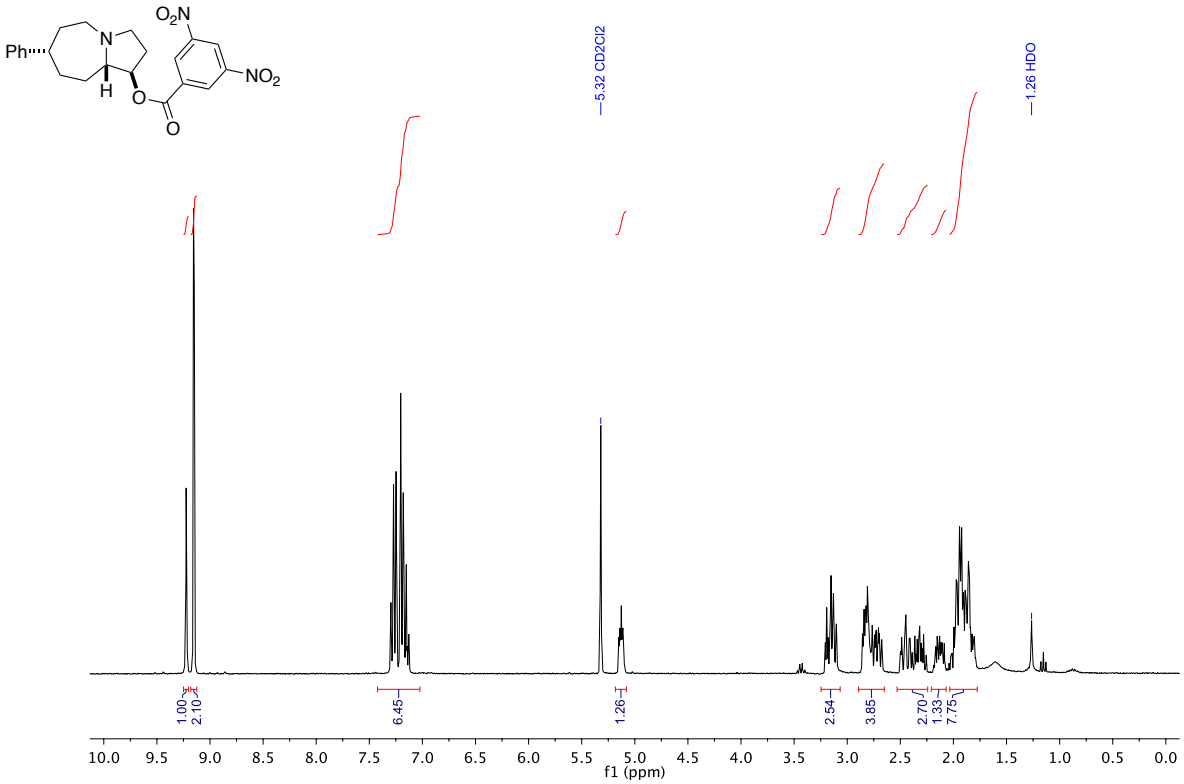

^{13}C NMR (75 MHz, CD_2Cl_2)
(1R,7S,9aS)- 7-phenyloctahydro-1H-pyrrolo[1,2-a]azepin-1-yl 3,5-dinitrobenzoate

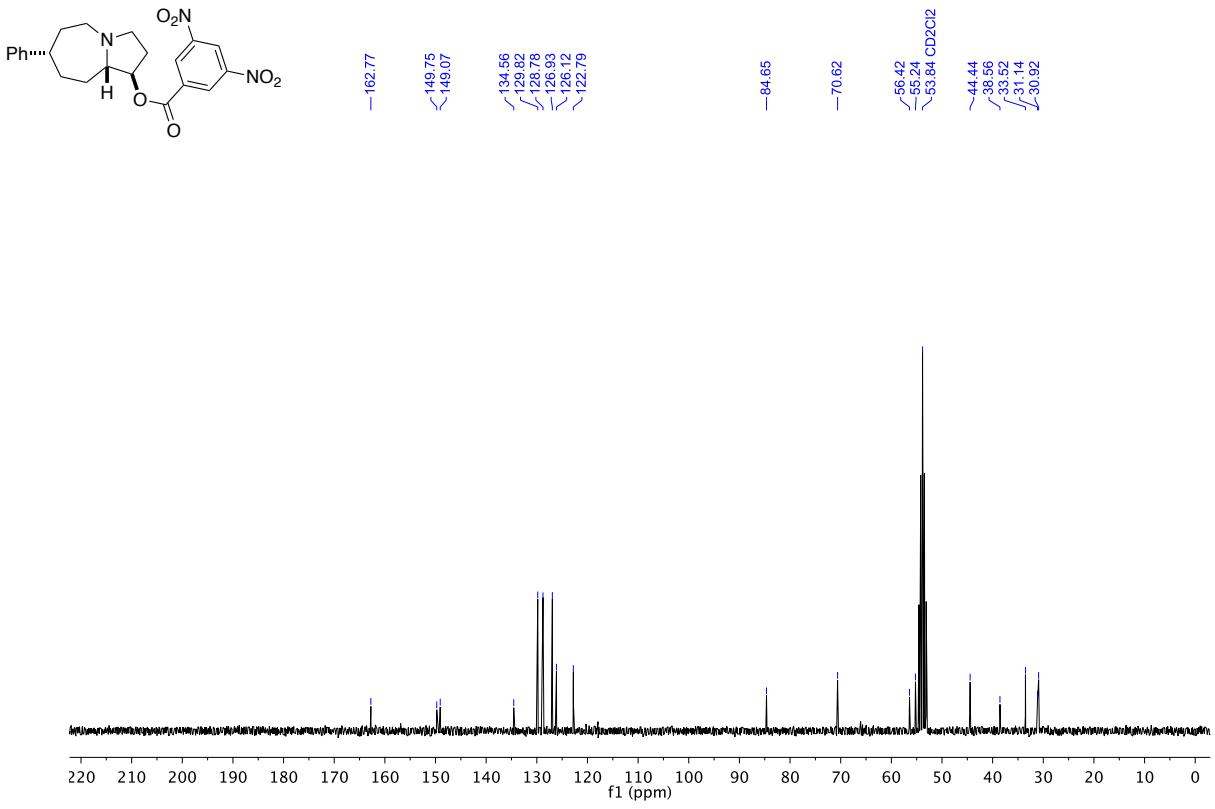

^{1}H NMR (300 MHz, CD_2Cl_2)
(S)-1-((1s,4R)-1-azido-4-phenylcyclohexyl)pentan-3-yl 4-bromo-3-nitrobenzoate

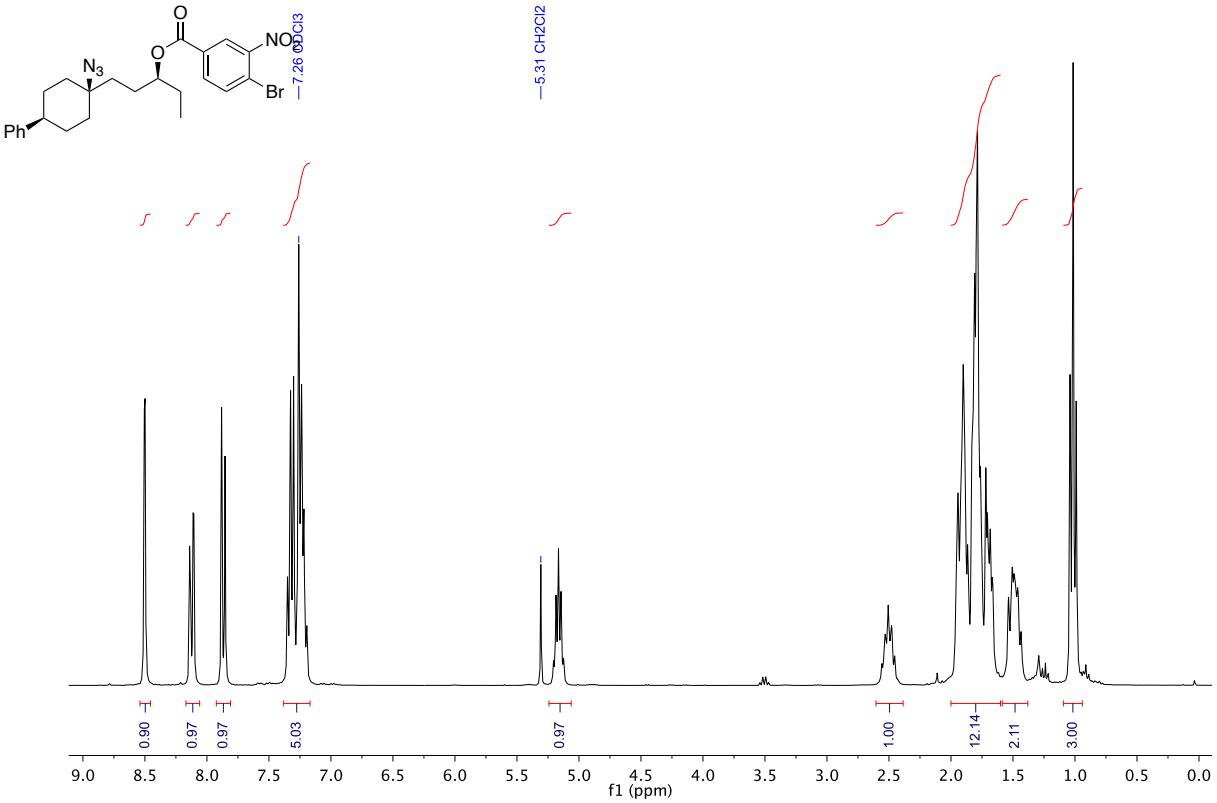

^{13}C NMR (75 MHz, CD_2Cl_2)
(S)-1-((1s,4R)-1-azido-4-phenylcyclohexyl)pentan-3-yl 4-bromo-3-nitrobenzoate

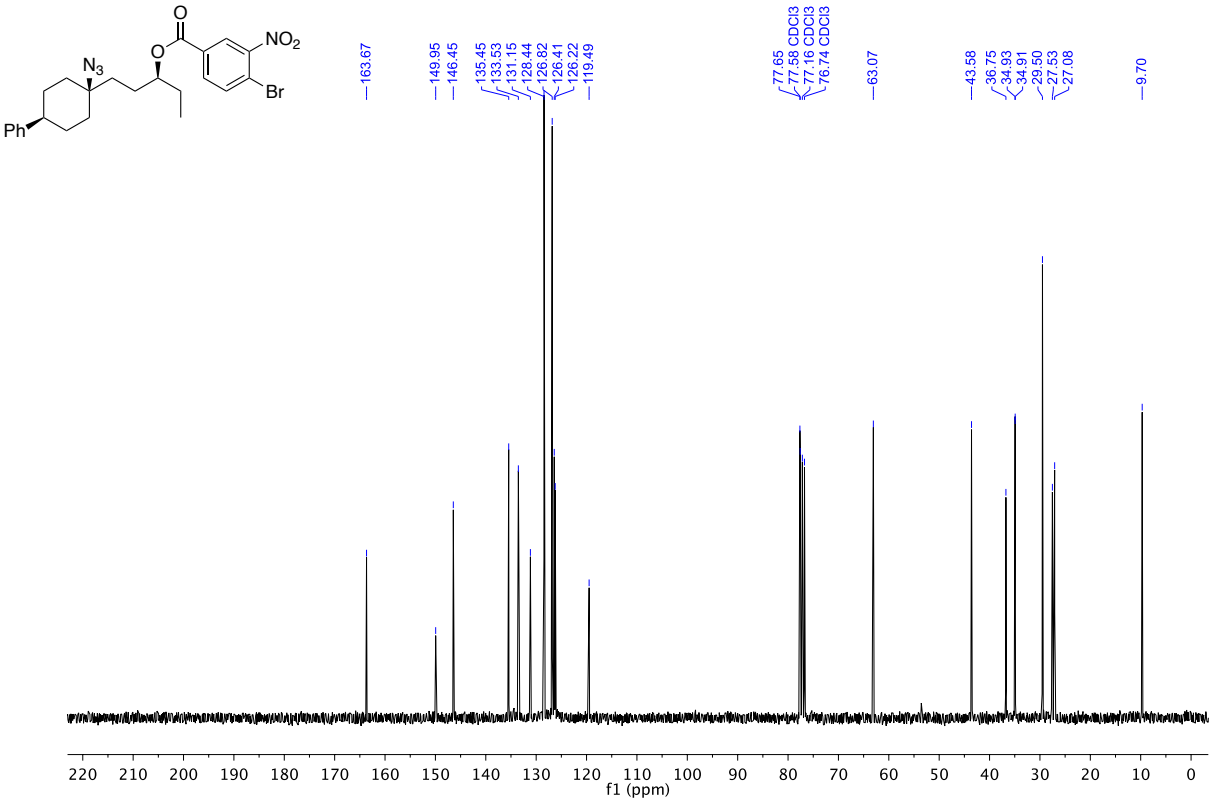

^{1}H NMR (300 MHz, C_6D_6)
(3R,7S,9aS)-3-ethyl-7-phenyldecahydropyrrolo[1,2-a]azepin-4-ium 2-hydroxy-2-phenylacetate

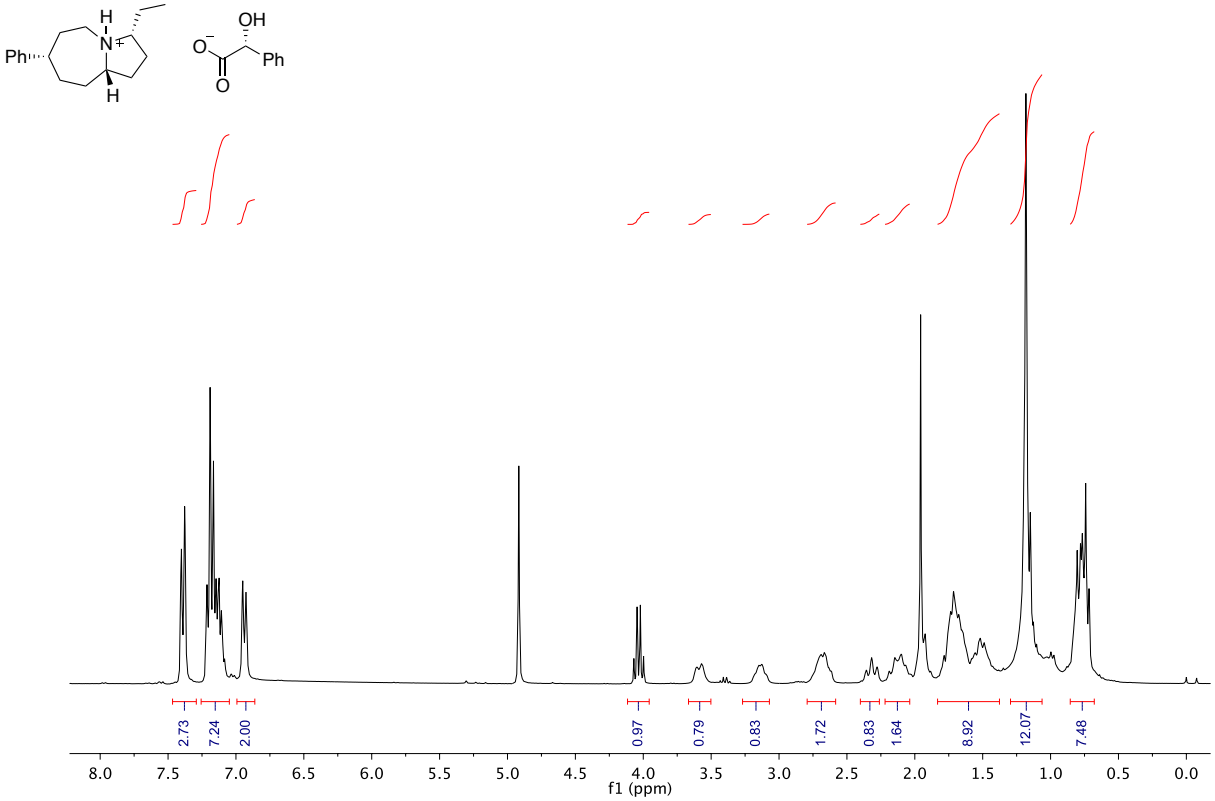

^{13}C NMR (75 MHz, C_6D_6))
(3R,7S,9aS)-3-ethyl-7-phenyldecahydropyrrolo[1,2-a]azepin-4-ium 2-hydroxy-2-phenylacetate

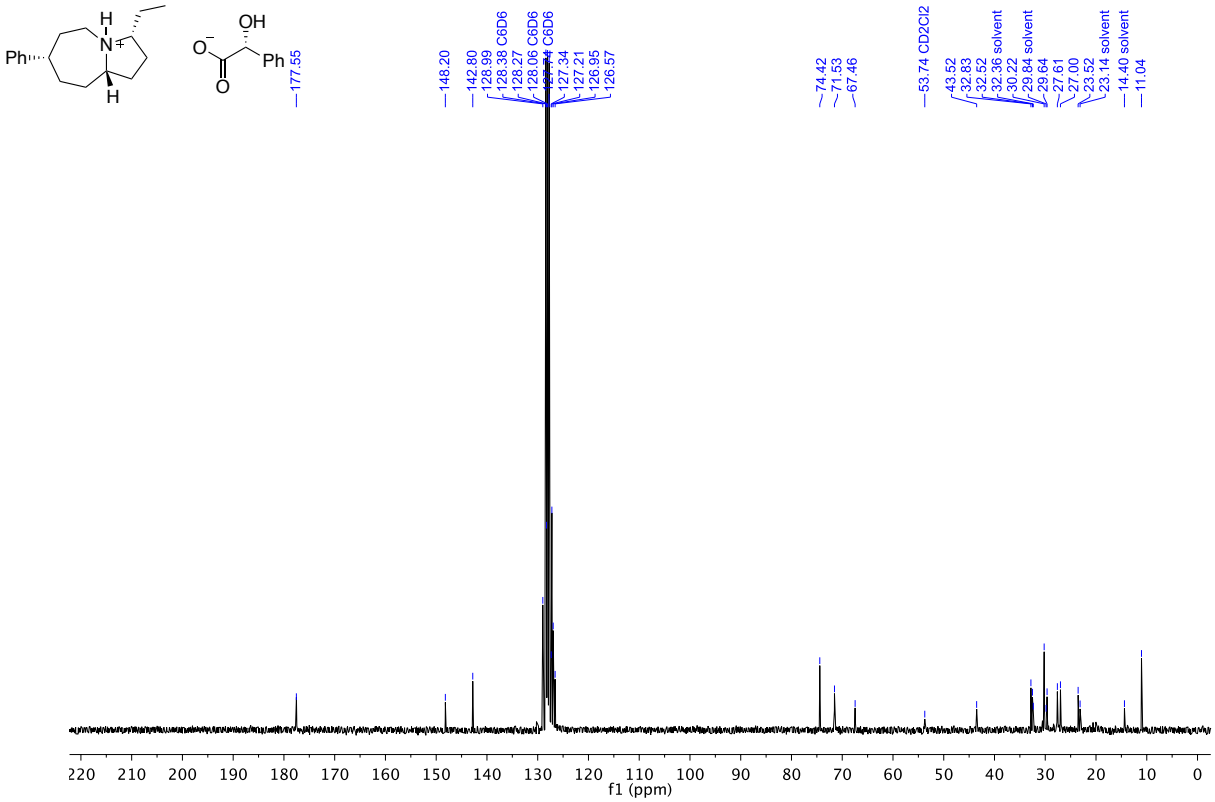

^{13}C NMR (75 MHz, C_6D_6) – DEPT Experiment
(3R,7S,9aS)-3-ethyl-7-phenyldecahydropyrrolo[1,2-a]azepin-4-ium 2-hydroxy-2-phenylacetate

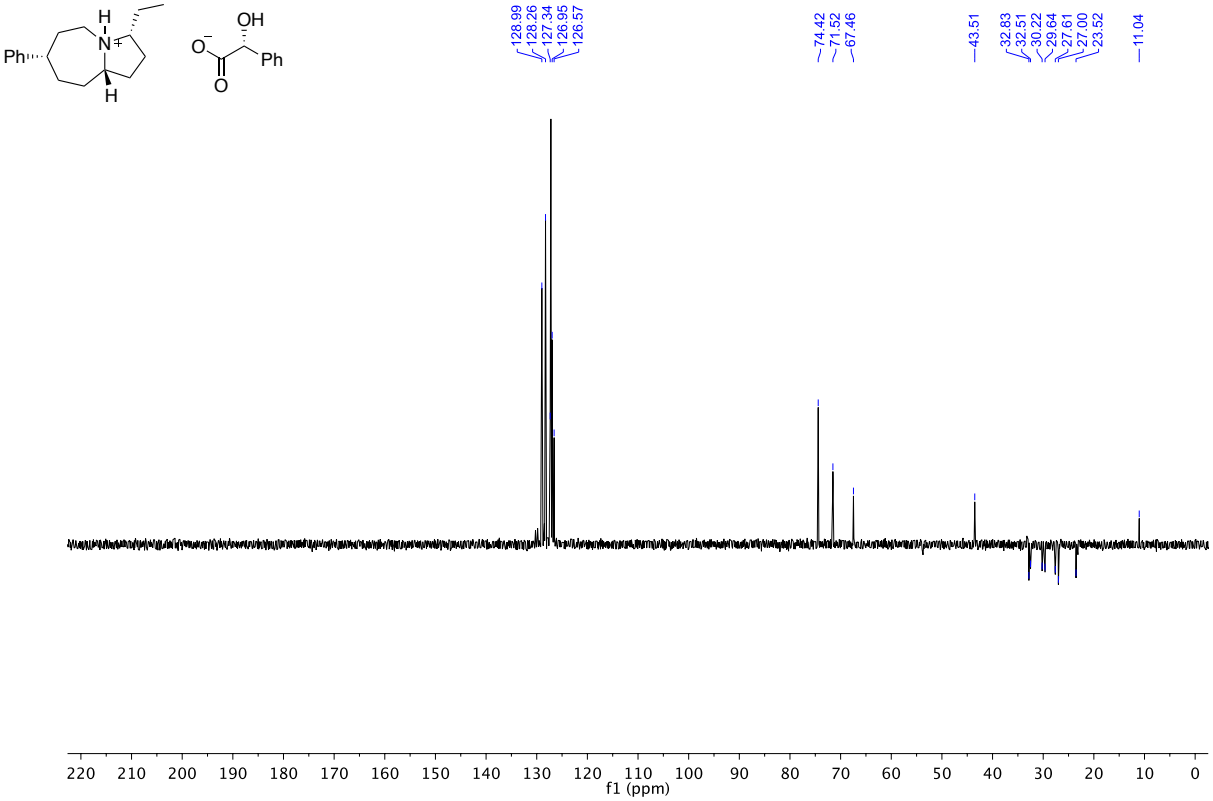

^{13}C NMR (75 MHz, C_6D_6) – Overlay of DEPT and ^{13}C spectrum
(3R,7S,9aS)-3-ethyl-7-phenyldecahydropyrrolo[1,2-a]azepin-4-ium 2-hydroxy-2-phenylacetate

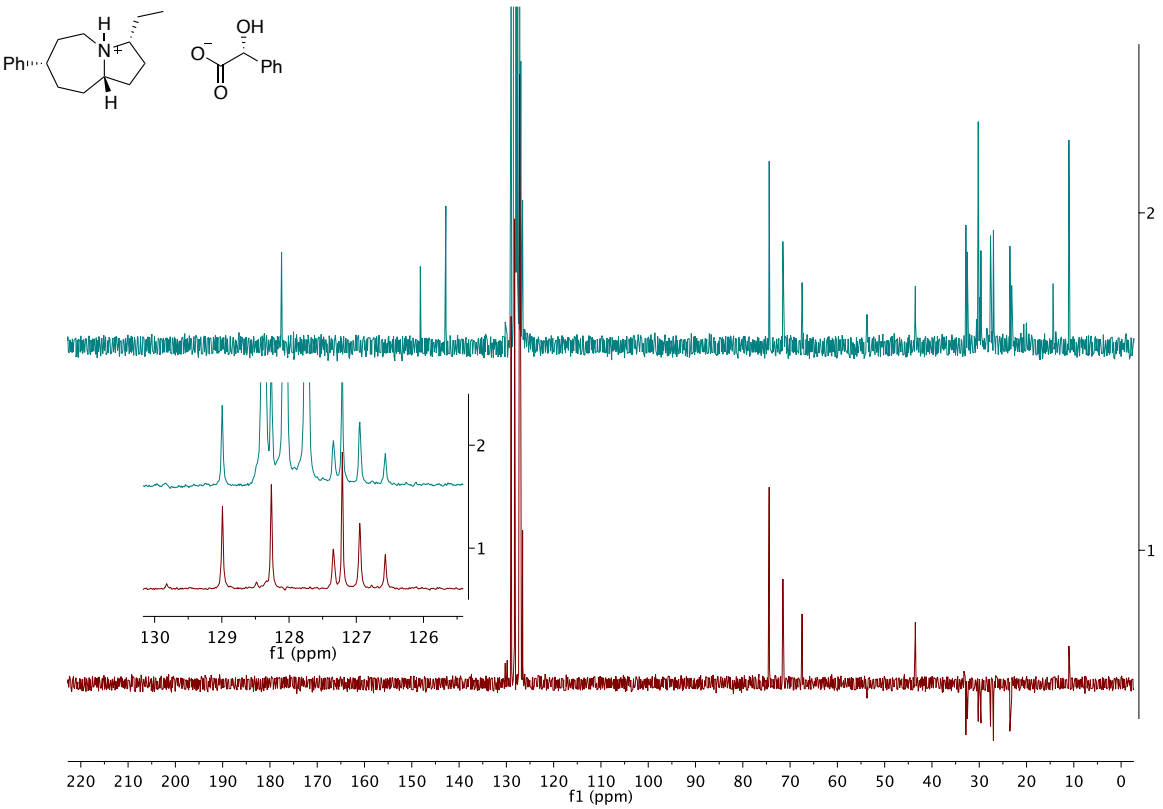

^{1}H NMR (300 MHz, $CDCl_3$)
Methylenecyclohexane

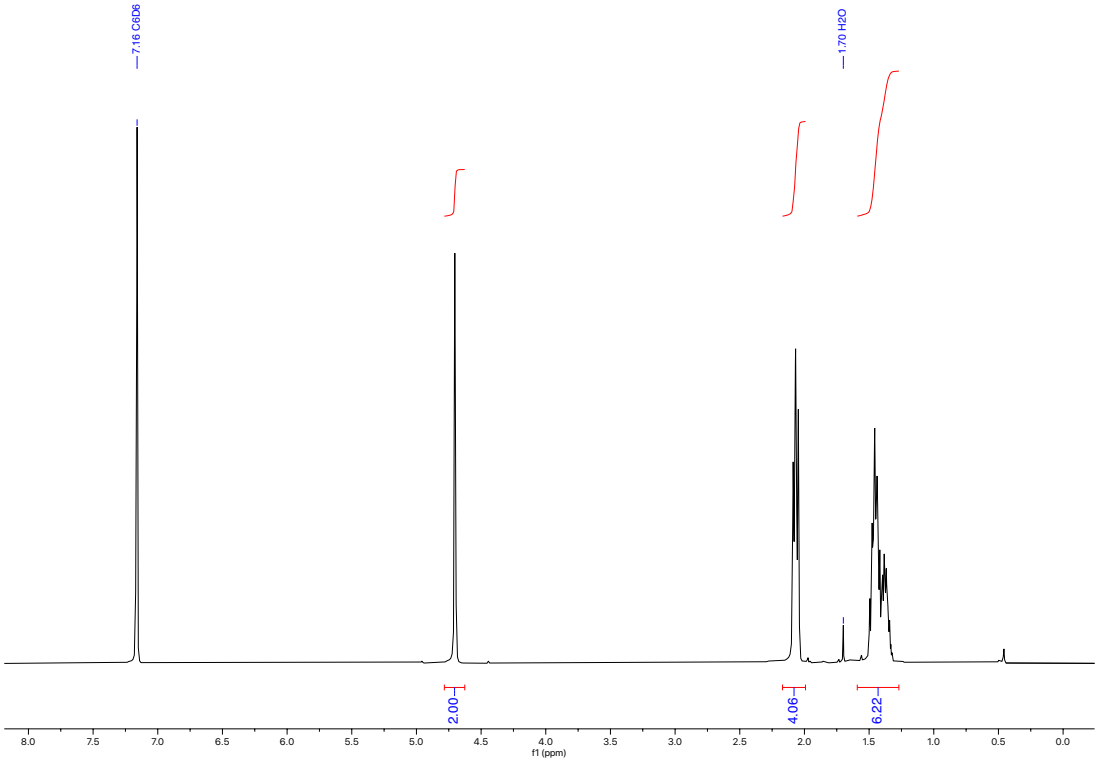

^{13}C NMR (75 MHz, $CDCl_3$)
Methylenecycl ohexane

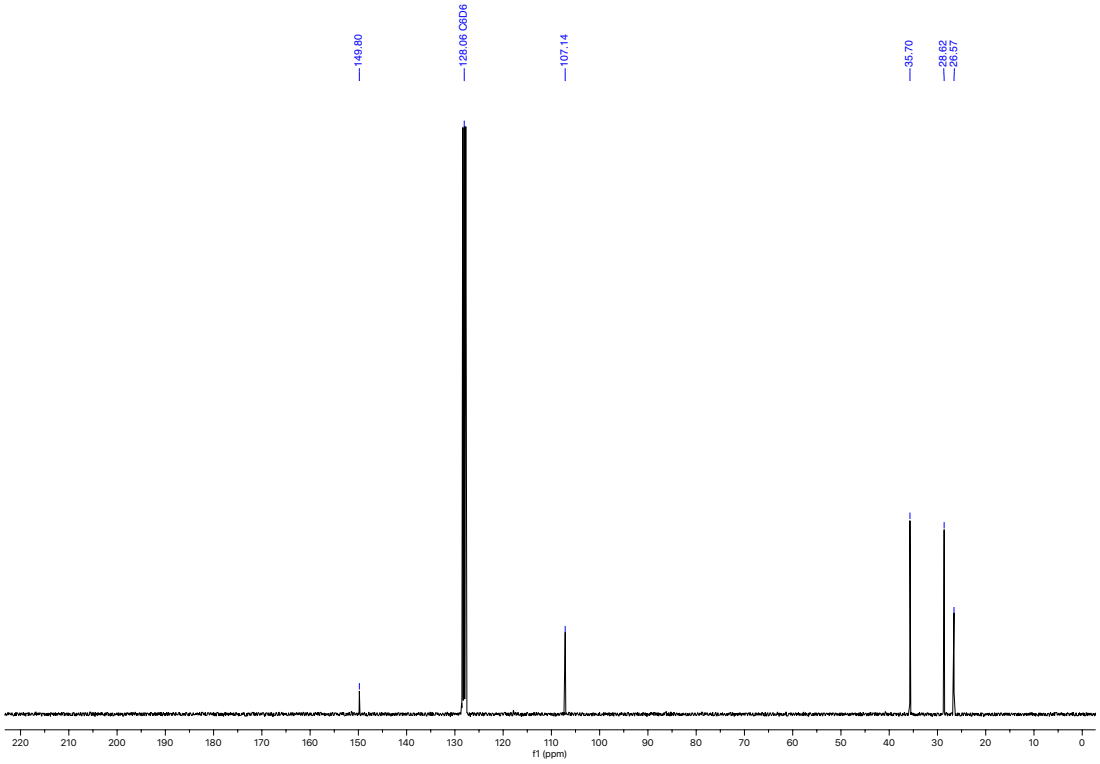

^{1}H NMR (300 MHz, $CDCl_3$)
Ethyl 3-(1-azidocyclohexyl)propanoate

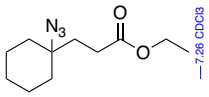

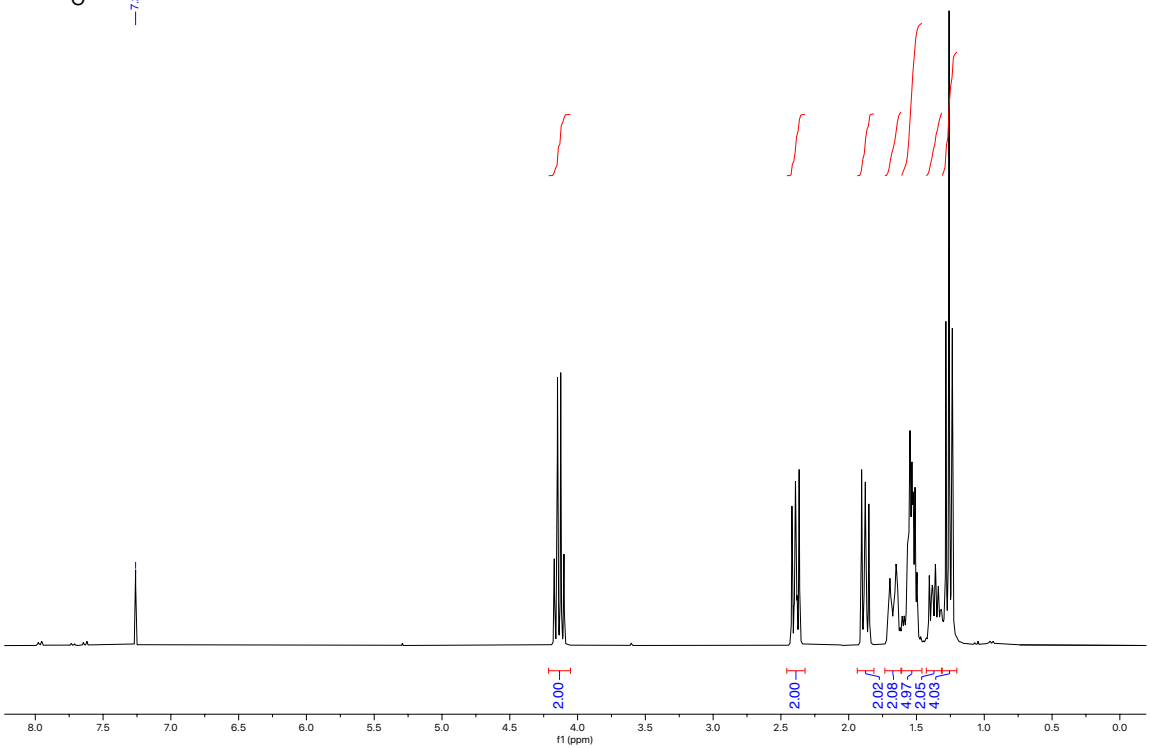

^{13}C NMR (75 MHz, $CDCl_3$)
Ethyl 3-(1-azidocyclohexyl)propanoate

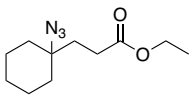

^{1}H NMR (300 MHz, $CDCl_3$)
Ethyl 3-(1-azidocyclohexyl)propanoate

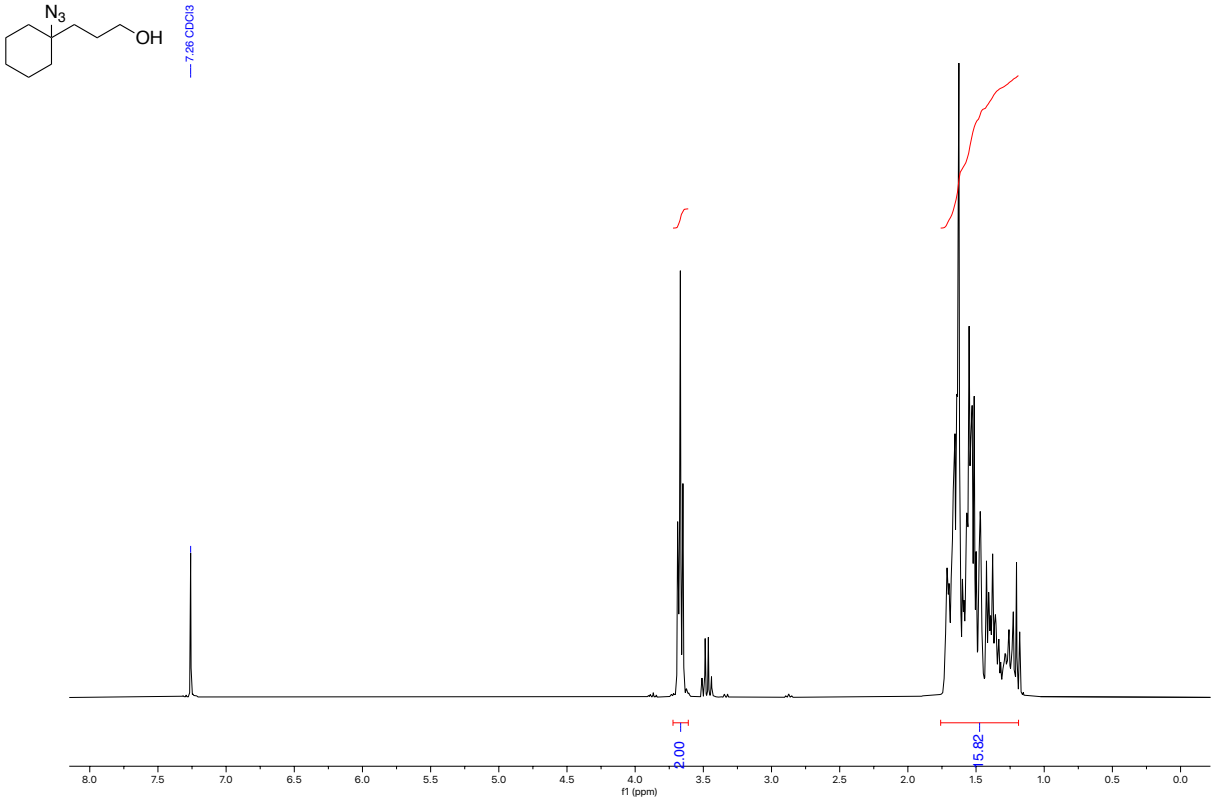

^{13}C NMR (75 MHz, $CDCl_3$)
Ethyl 3-(1-azidocyclohexyl)propanoate

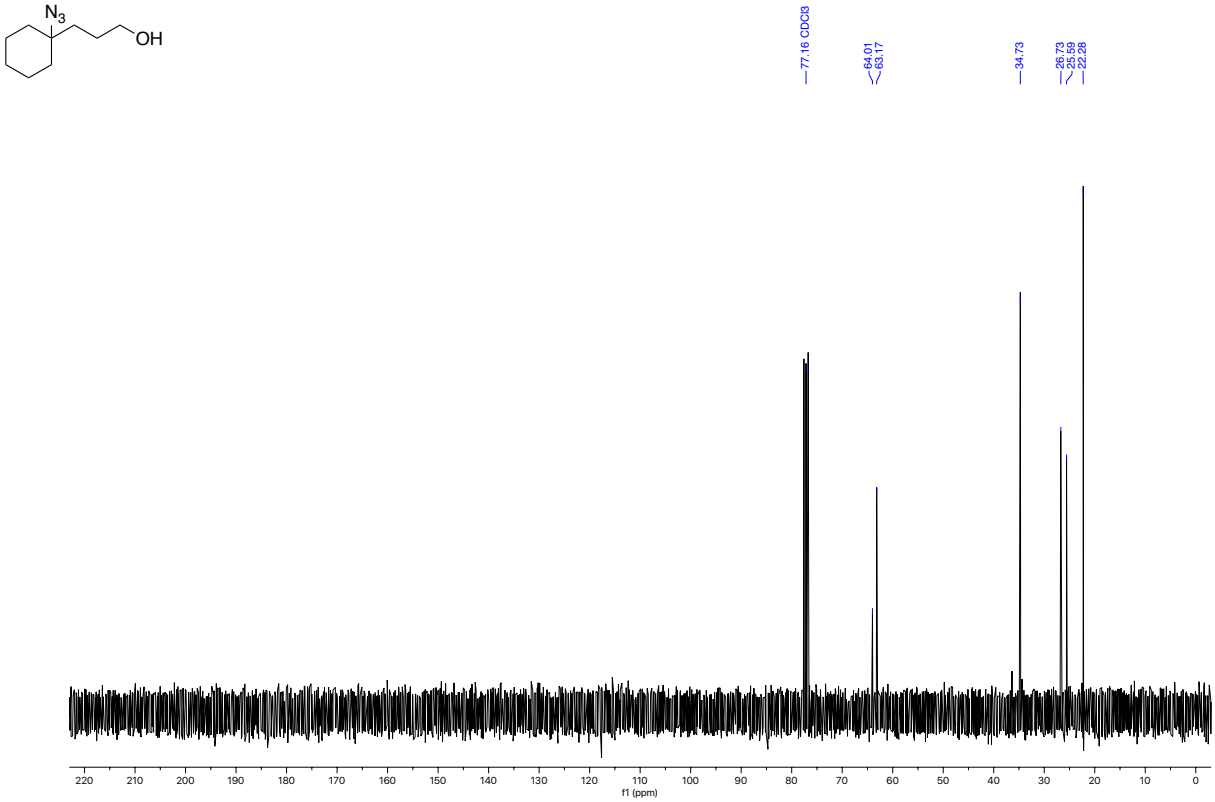

^{1}H NMR (300 MHz, $CDCl_3$)
3-(1-azidocyclohexyl)propanal

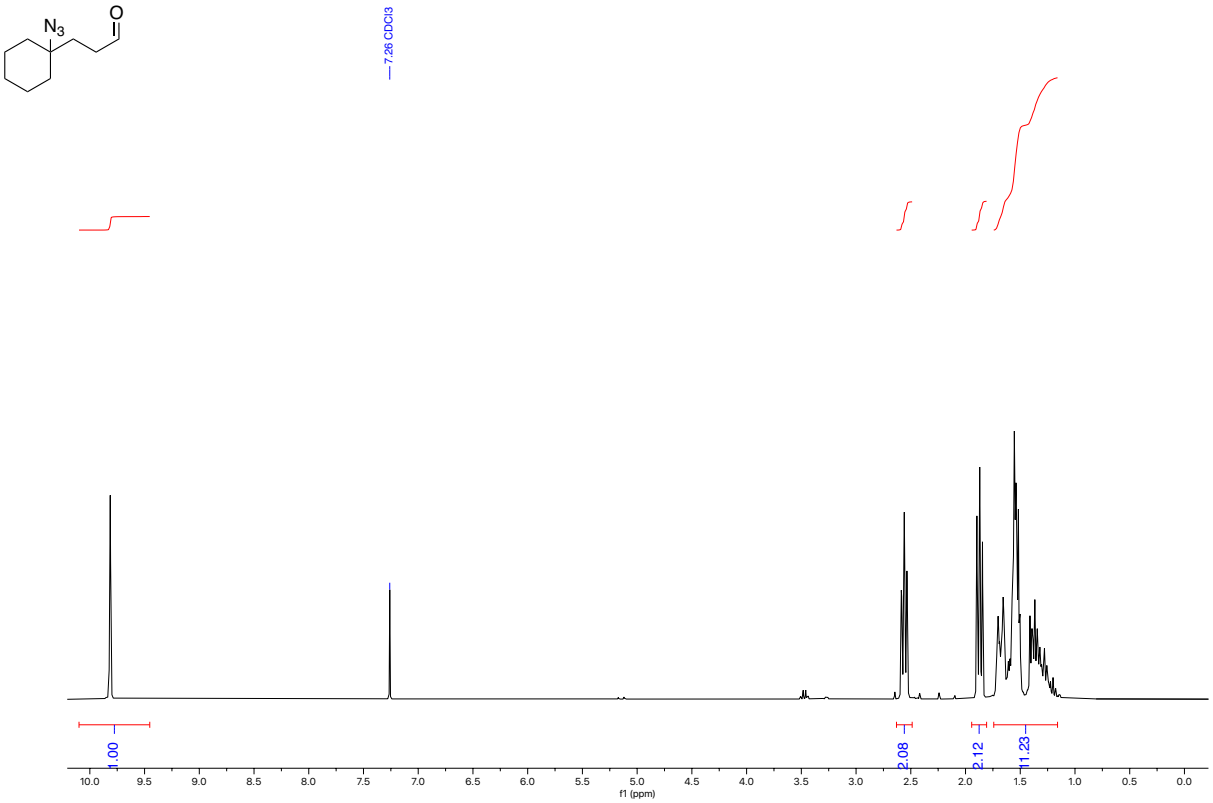

^{13}C NMR (75 MHz, $CDCl_3$)
3-(1-azidocyclohexyl)propanal

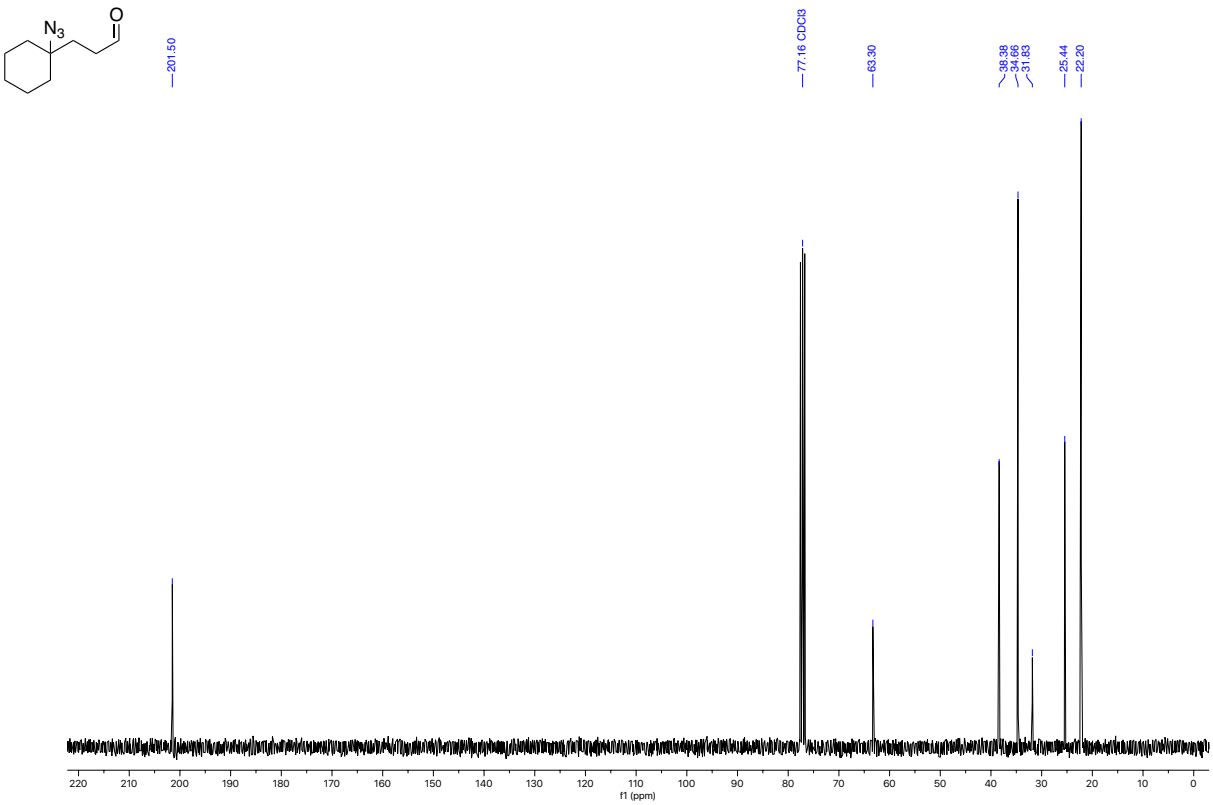

^{1}H NMR (300 MHz, $CDCl_3$)
1-(1-azidocyclohexyl)heptan-3-ol

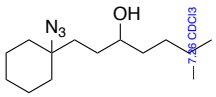

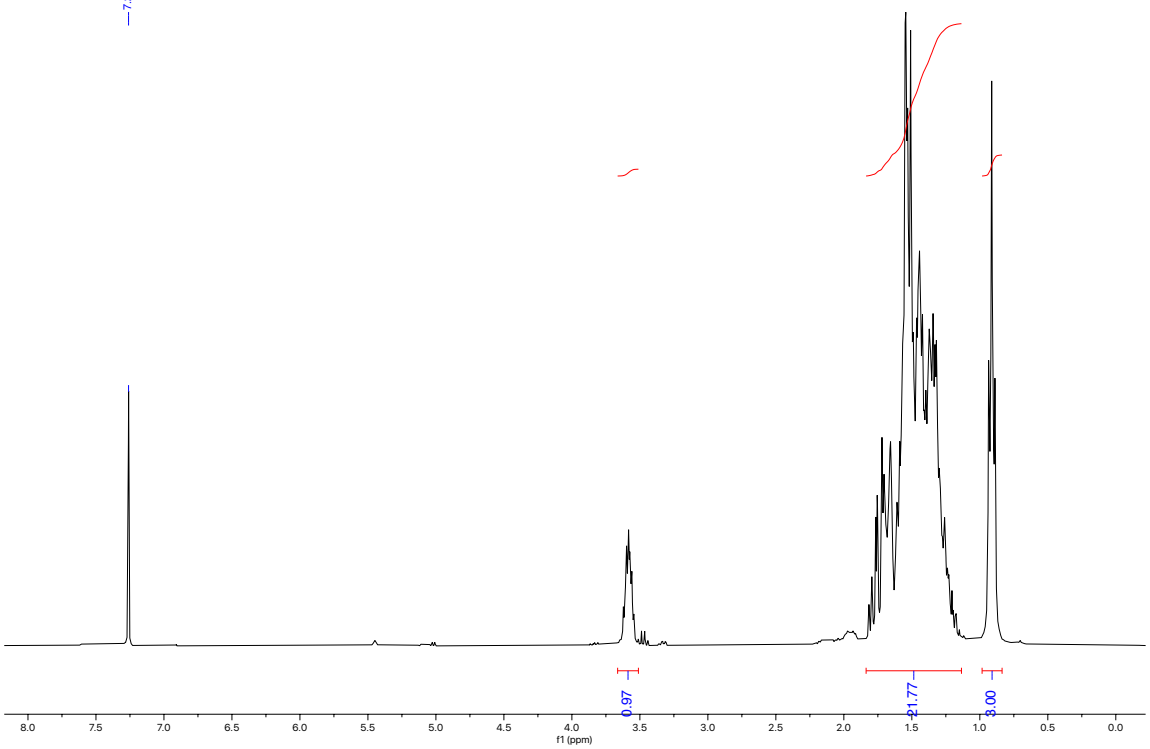

^{13}C NMR (75 MHz, $CDCl_3$)
1-(1-azidocyclohexyl)heptan-3-ol

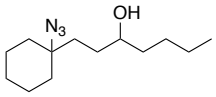

^{1}H NMR (300 MHz, $CDCl_3$)
1-(((1-(1-azidocyclohexyl)heptan-3-yl)oxy)methyl)-4-methoxybenzene

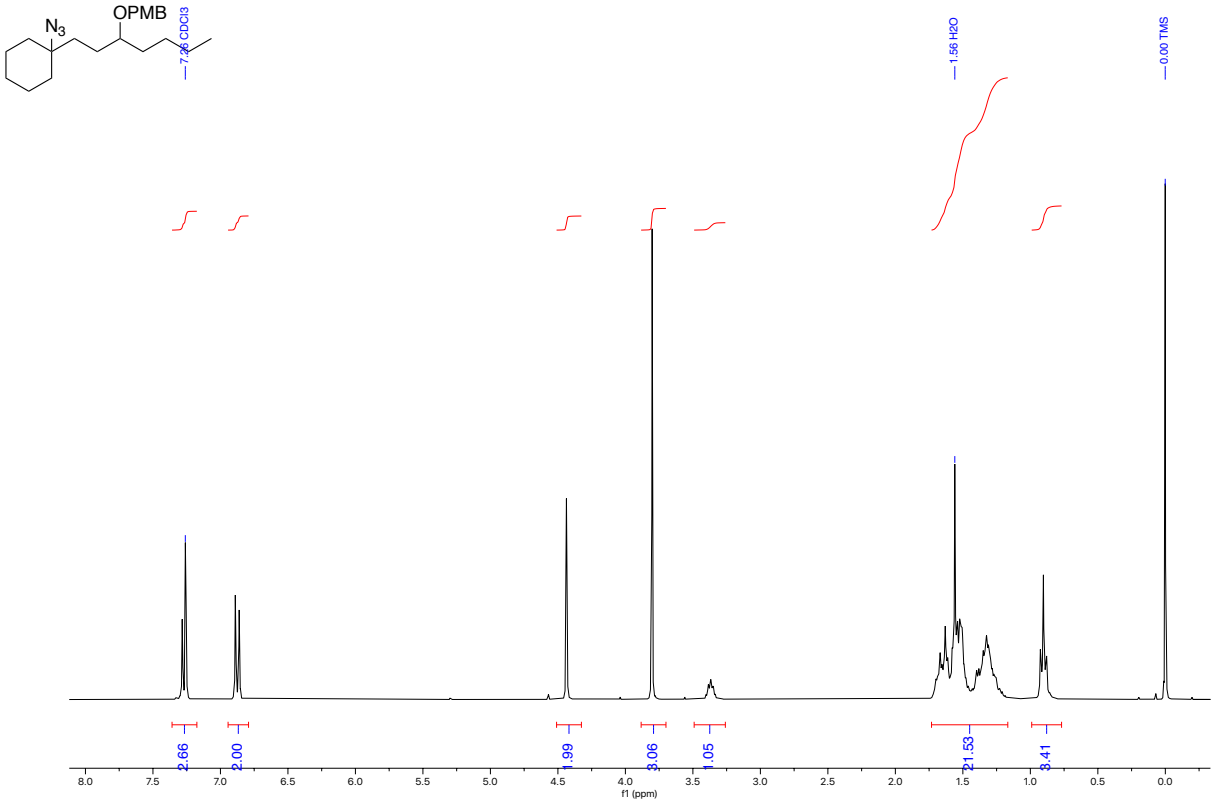

^{13}C NMR (75 MHz, $CDCl_3$)
1-(((1-(1-azidocyclohexyl)heptan-3-yl)oxy)methyl)-4-methoxybenzene

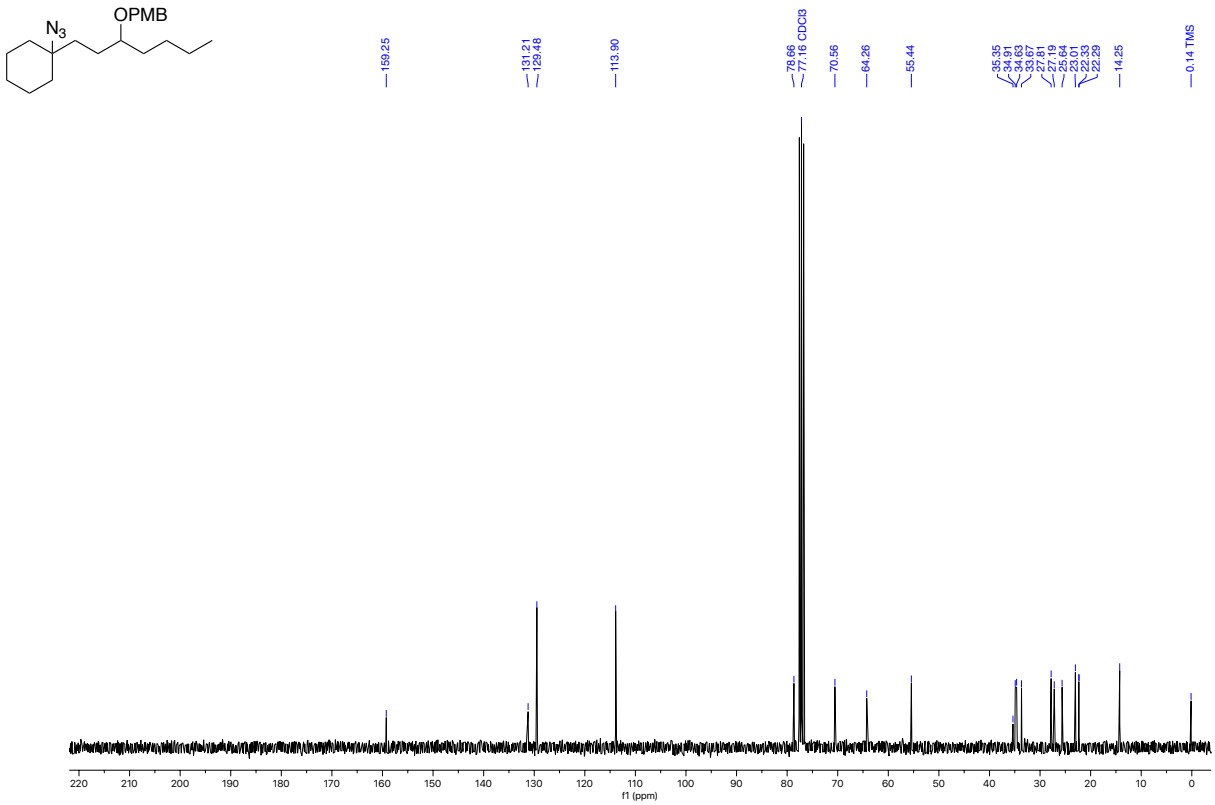

^{1}H NMR (300 MHz, $CDCl_3$)
(trans-3,9)-3-butyloctahydro-1H-pyrrolo[1,2-a]azepine

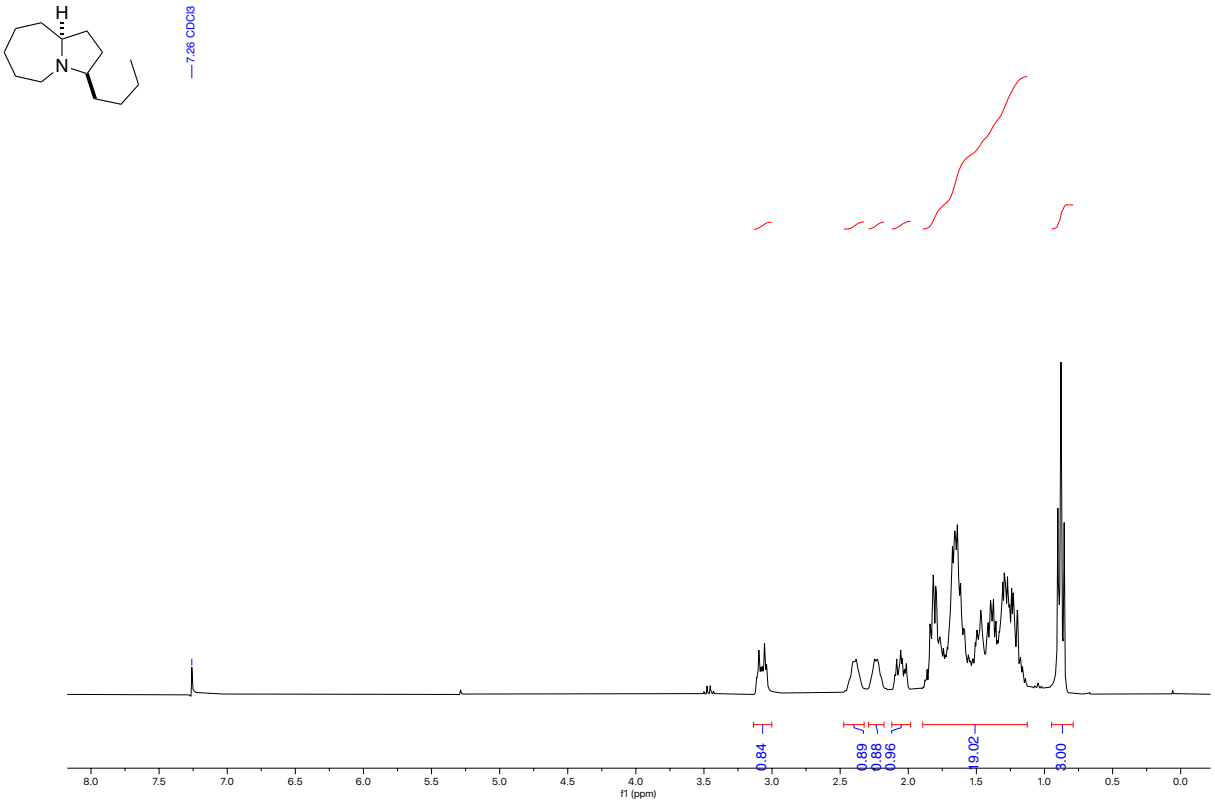

^{13}C NMR (75 MHz, C_6D_6)
(trans-3,9)-3-butyloctahydro-1H-pyrrolo[1,2-a]azepine

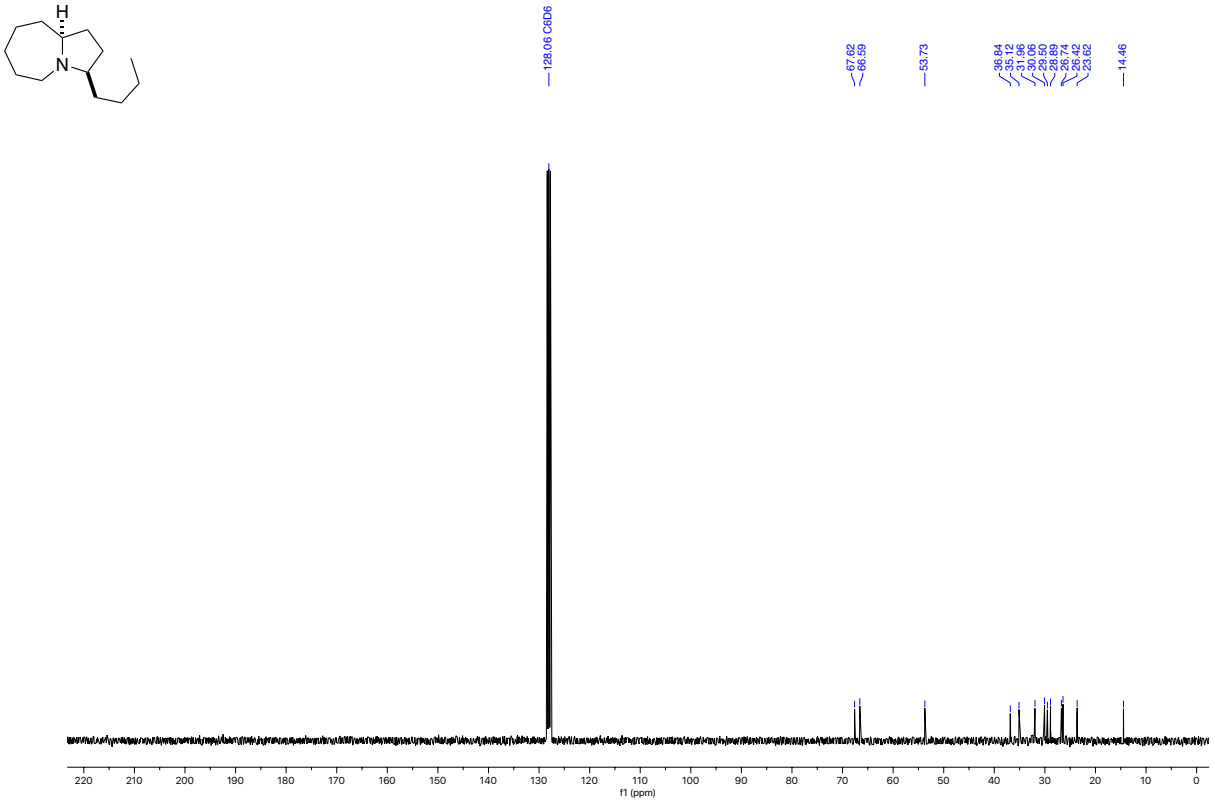

^{1}H NMR (300 MHz, $CDCl_3$)
3-(1-azidocyclopentyl)propan-1-ol

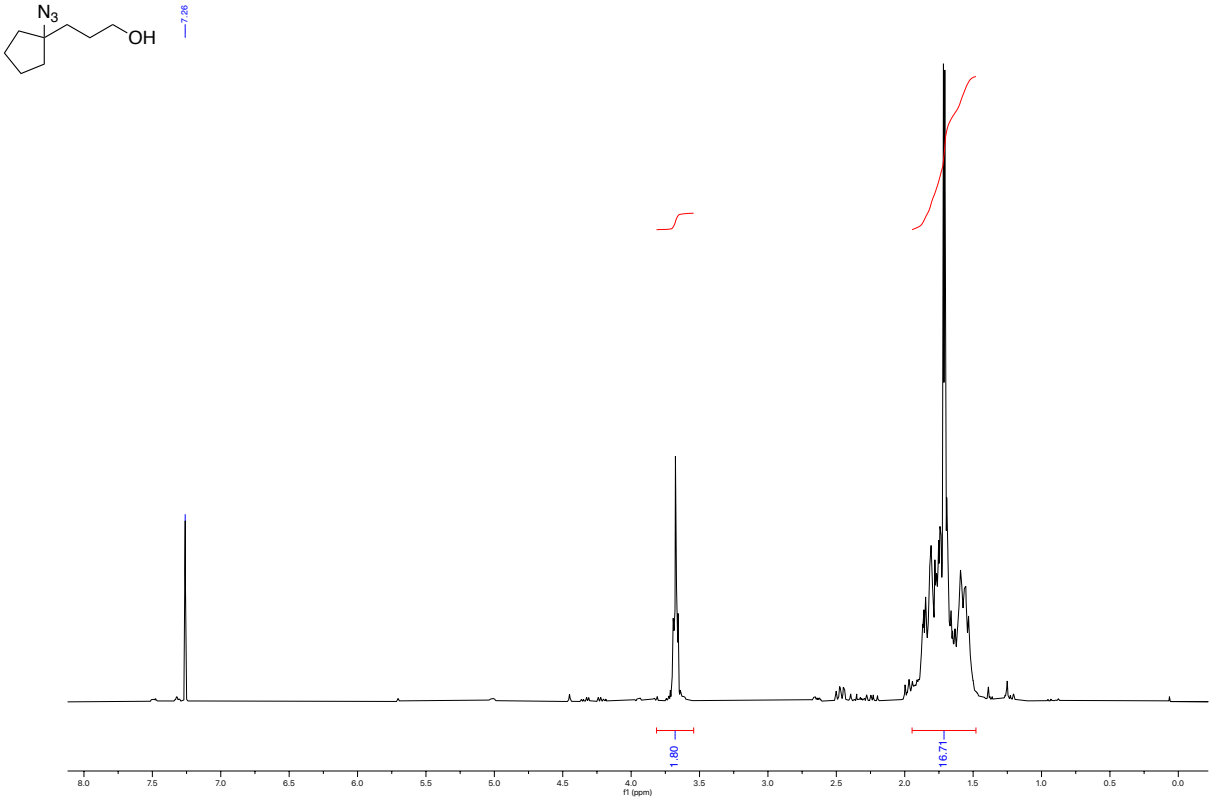

^{13}C NMR (75 MHz, $CDCl_3$)
3-(1-azidocyclopentyl)propan-1-ol

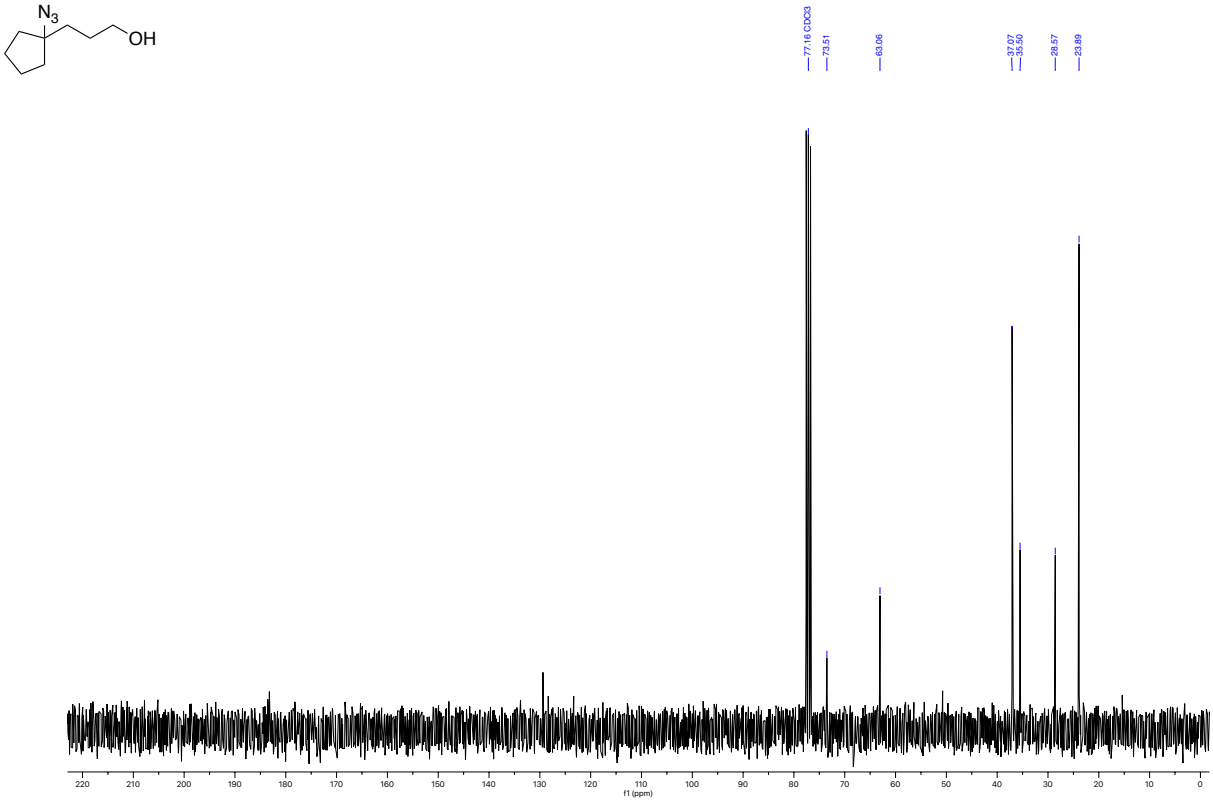

^{1}H NMR (300 MHz, $CDCl_3$)
3-(1-azidocyclopentyl)propanal

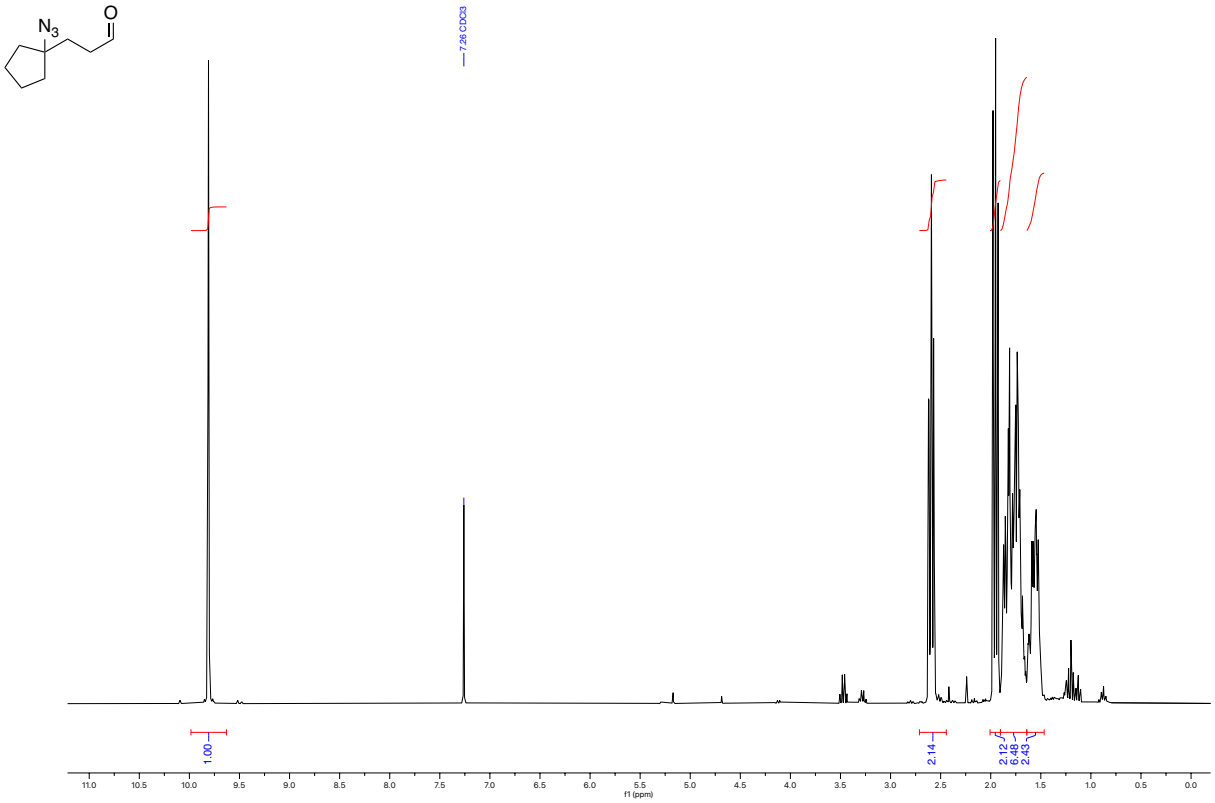

^{13}C NMR (75 MHz, $CDCl_3$)
3-(1-azidocyclopentyl)propanal

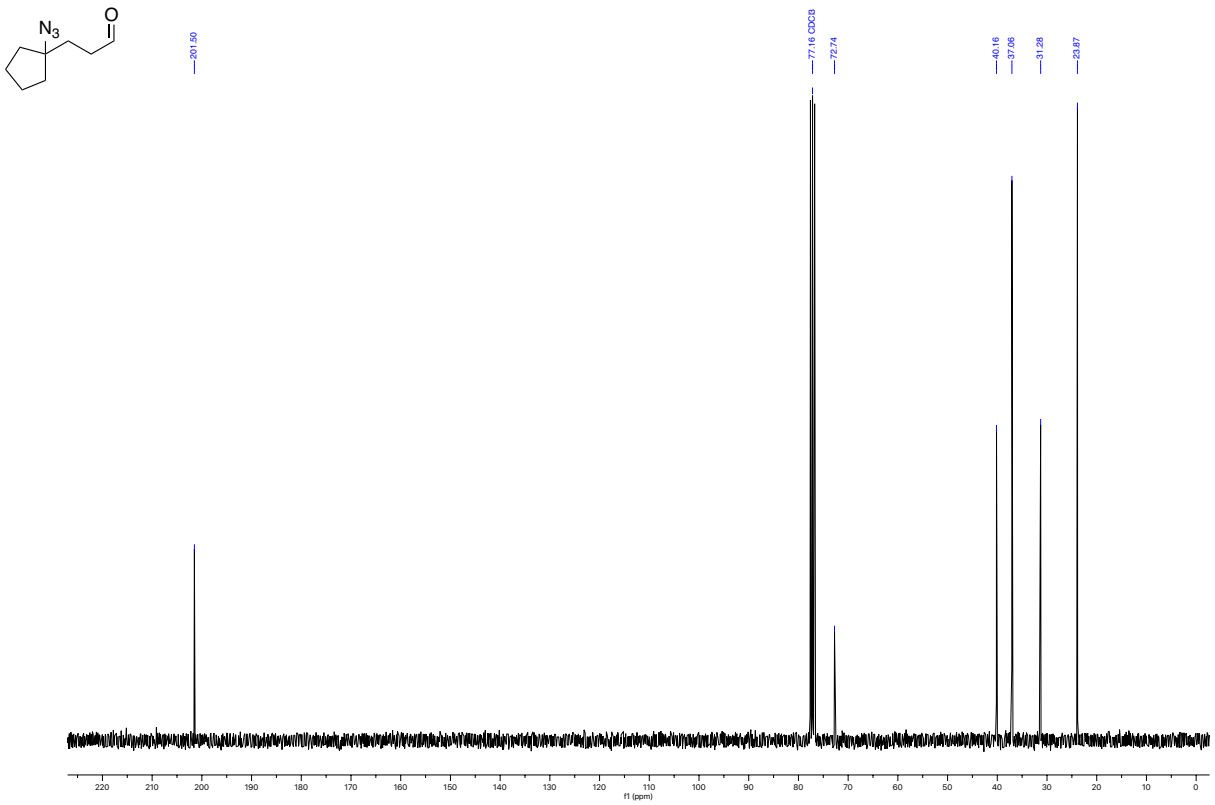

^{1}H NMR (300 MHz, $CDCl_3$)
(*R*)-1-(1-azidocyclopentyl)hex-5-en-3-ol

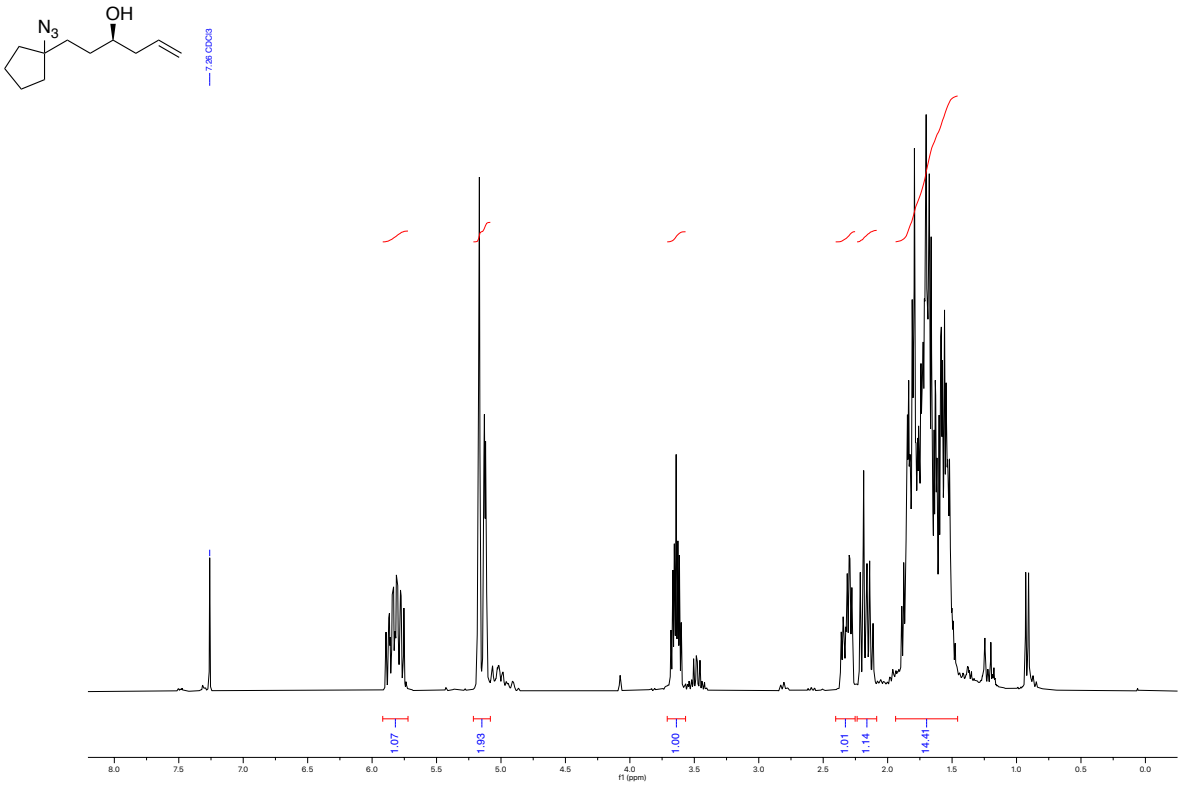

^{13}C NMR (75 MHz, $CDCl_3$)
(*R*)-1-(1-azidocyclopentyl)hex-5-en-3-ol

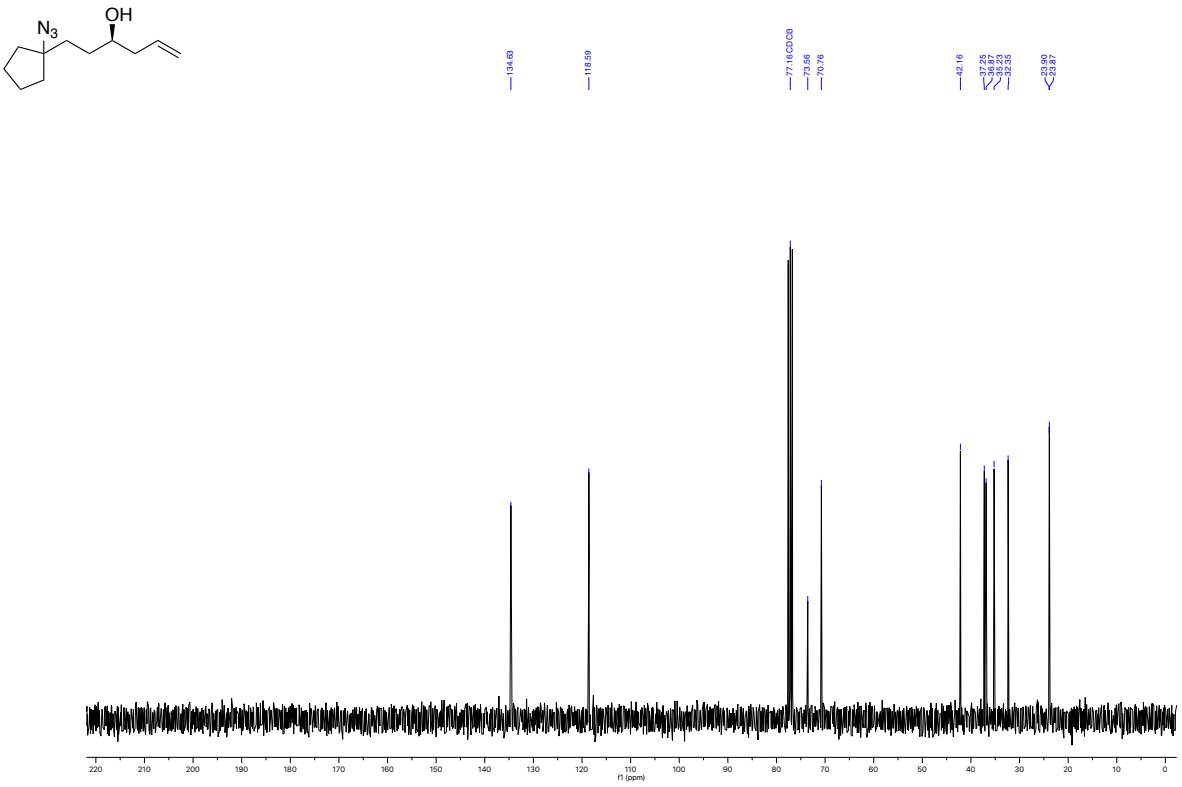

^{1}H NMR (300 MHz, C_6D_6)
(3*S*,8a*S*)-3-allyloctahydroindolizine

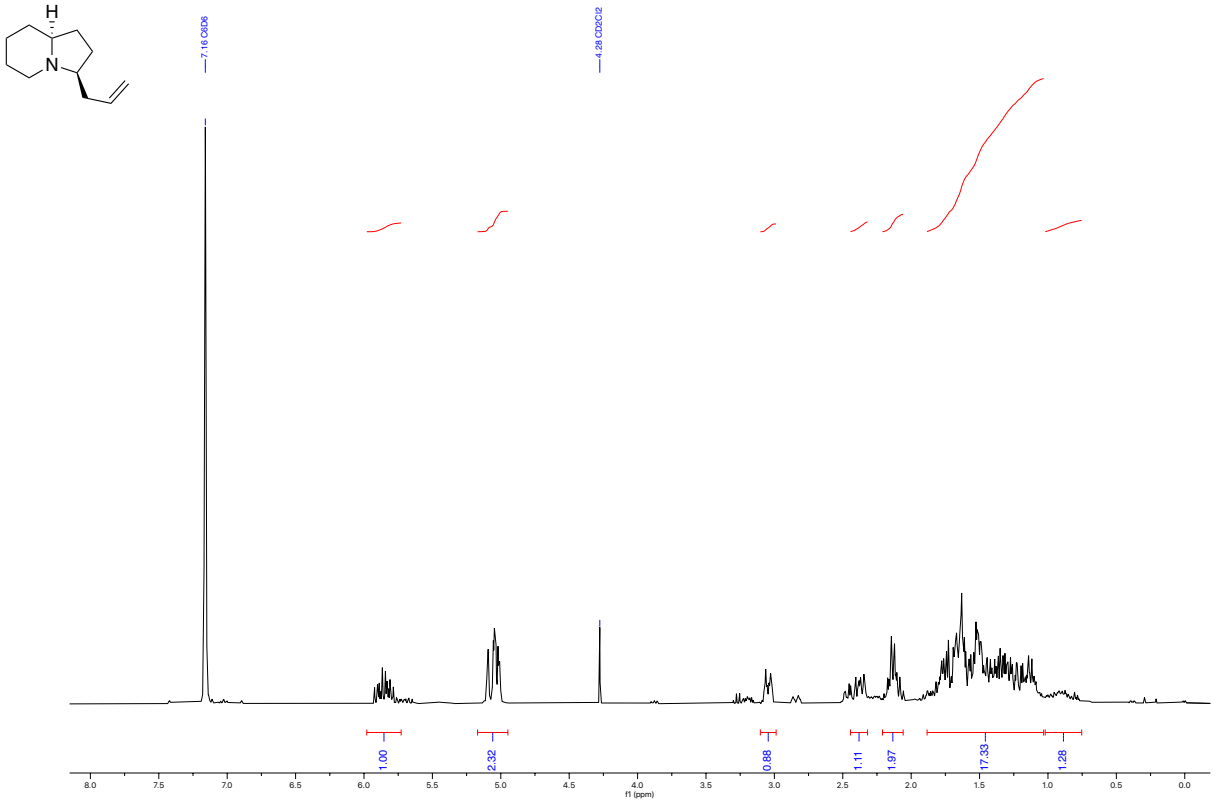

^{13}C NMR (75 MHz, C_6D_6)
(3*S*,8a*S*)-3-allyloctahydroindolizine

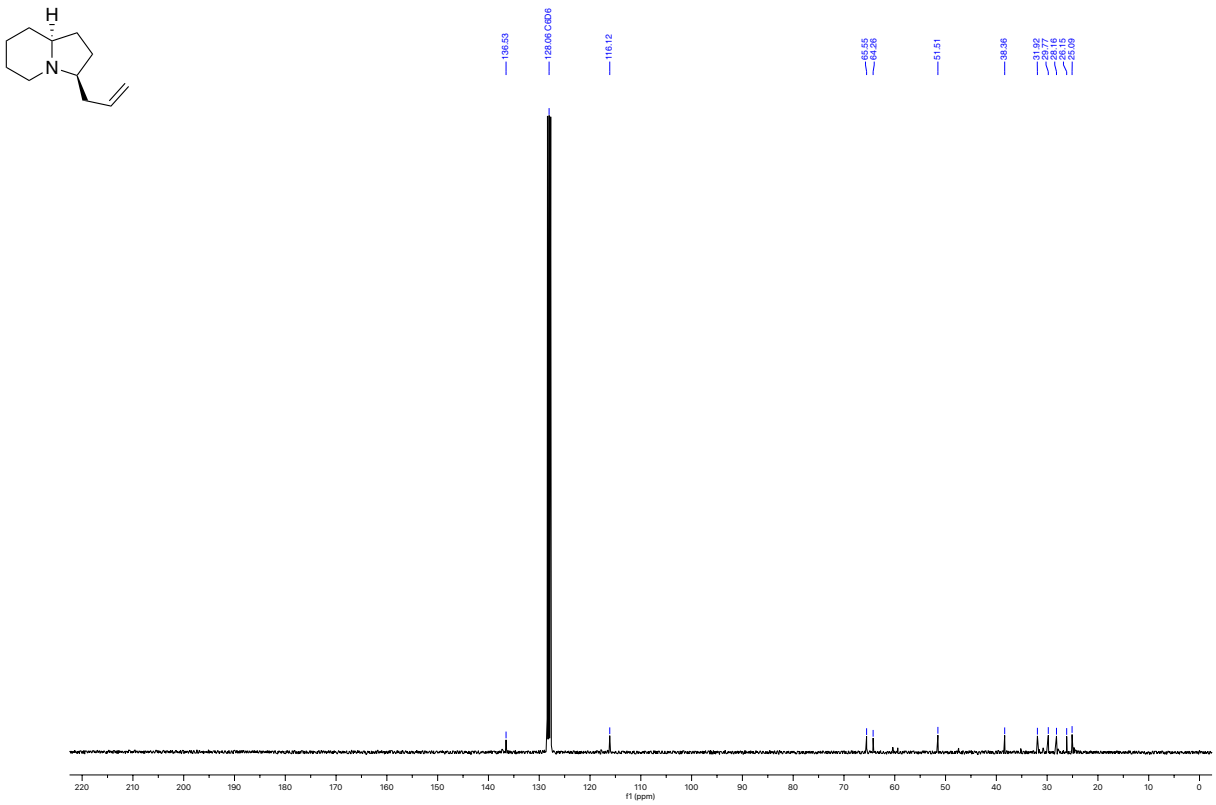

^{1}H NMR (300 MHz, $CDCl_3$)
(3*R*,8a*S*)-3-propyloctahydroindolizine

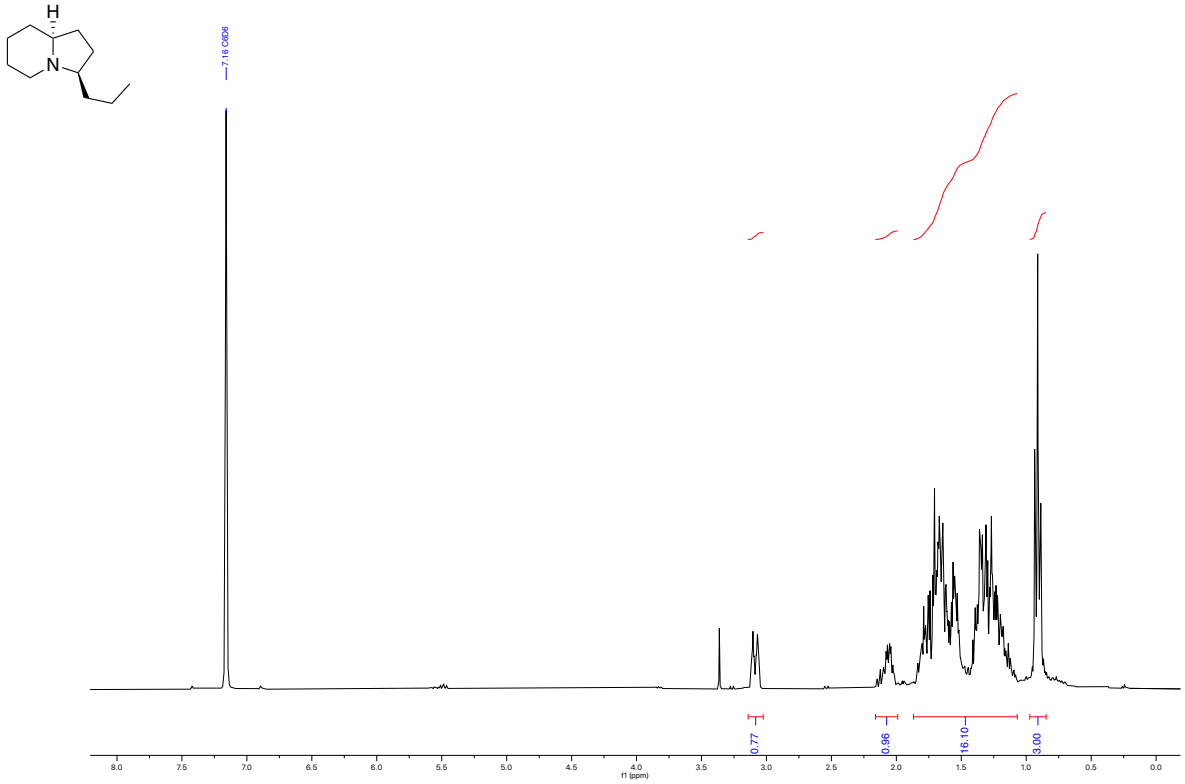

^{13}C NMR (75 MHz, $CDCl_3$)
(3*R*,8a*S*)-3-propyloctahydroindolizine

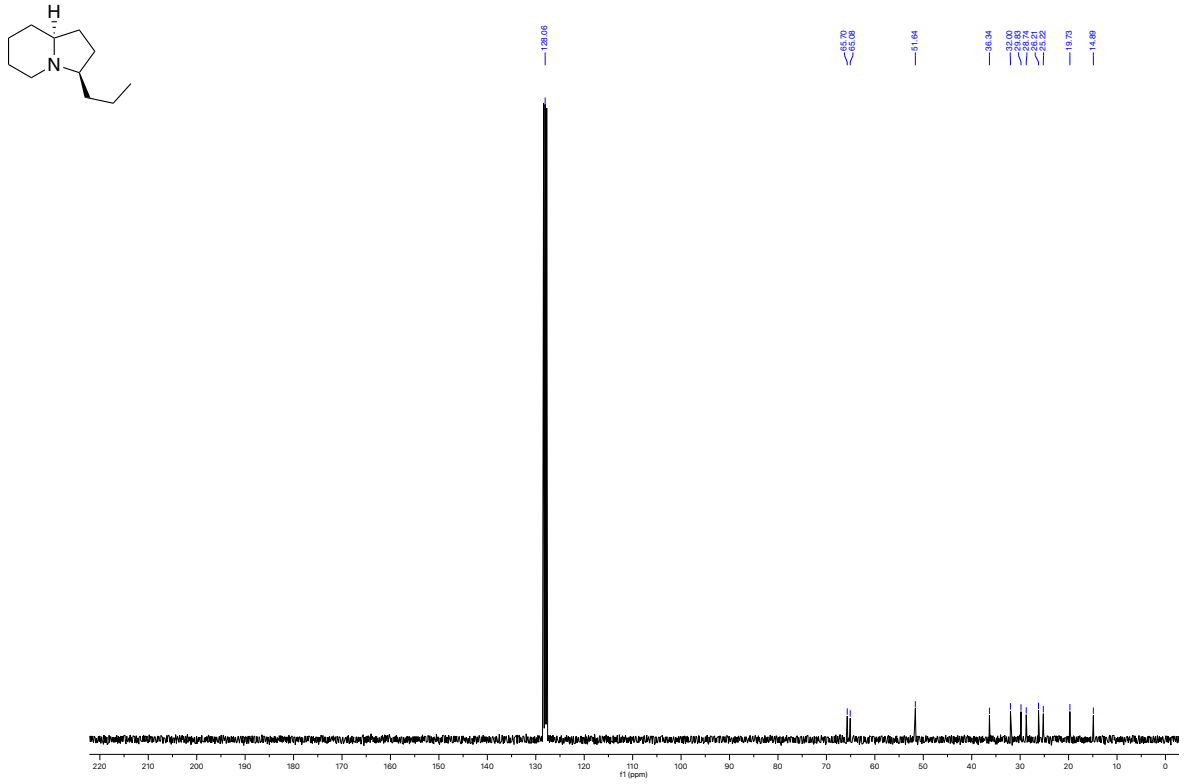

Appendix

Supplementary Information to Chapter 7 (computational calculations)

(24-11-2020)

Stereoselective and Stereospecific Triflate Mediated Intramolecular Schmidt Reaction: Easy Access to Alkaloid Skeletons

Lars Gnägi, Remo Arnold, Florence Giornal, Ajoy Kapat, Robin Marc Schärer, and Philippe Renaud*
Department of Chemistry and Biochemistry, University of Bern

H. Jangra, H. Zipse*
Dept. Chemistry, LMU Muenchen

E-mail: *philippe.renaud@dcb.unibe.ch*
E-mail: *zipse@cup.uni-muenchen.de*

Table of Contents

1. Methodology

The geometry optimizations of have been performed with a combination of the (U)B3LYP hybrid functional[1] and the 6-31G(d) basis set[2-3] in the gas phase. The dispersion correction is accounted using the "GD3" model [empiricaldispersion=gd3] proposed by Grimme.[4-5] Thermochemical corrections (corr. ΔH & ΔG) to 298.15 K have been calculated at the same level of theory using the rigid rotor/harmonic oscillator model. Enthalpies (ΔH_{298}) and Gibbs energies (ΔG_{298}) at B3LYP/6-31G(d) level have been obtained through the addition of corr. ΔG and corr. ΔH to $\Delta E_{tot,}$ respectively. For implicit solvation (CH_2Cl_2), the Integral Equation Formalism for the Polarizable Continuum Model (IEFPCM) solvation model employing United Atom Topological Model (UA0) radii is used.[6-7] The energetics were improved using recently developed DLPNO-CCSD(T) method[8] in combination with cc-pVTZ basis set[9-10].

Potential energy surface (PES): Geometry optimizations for all the stationary points (minima, complexes and TS) along the PES have been performed at (U)B3LYP/6-31G(d) in the gas phase. Energy minima, complexes and TSs were confirmed by vibrational frequency calculation with 0, 0 and 1 imaginary frequencies, respectively. All stationary points were checked for wavefunction stability (stable=opt). The nature of transition states was further confirmed by IRC calculations [10 steps in both directions (reverse/forward) with stepsize=3] followed by geometry optimization to the minimum. All calculations have been performed with Gaussian 09, Revision D.01[11], except single point DLPNO-CCSD(T)/cc-pVTZ that have been performed with ORCA 4.0.0.2.[12]

2. Conformational Energetics (CEs)

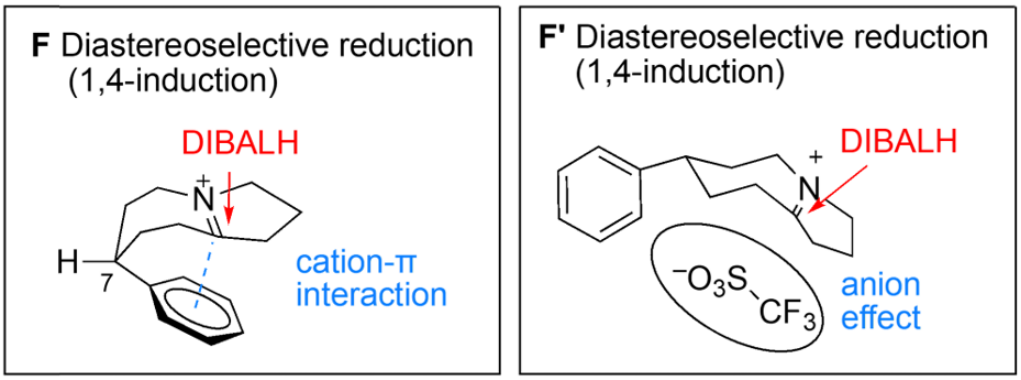

Figure S1. Proposed conformational preference for iminium cation (**F, 6im⁺**) and iminium salt (**F`, 6im**).

Analysis of the gas phase conformational energetics of iminium cation (**6im⁺**) shows that it prefers an extended conformation (Conf. No. 1, Figure S2). Please note that conformational numbering in Fig. S2 is with respect to the ΔH_{298} values. In order to display all conformers on one single page all odd numbered conformers are shown to the left and all even numbered conformers are shown to the right. The best cation-π interaction-induced folded conformation (conf. no. 2) is 6.3 kJ/mol and 12.2 kJ/mol higher in terms of enthalpy (ΔH_{298}) and free energy (ΔG_{298}) with respect to the global minimum (conf. no. 1) at the B3LYP-D3/6-31G(d) level of theory. Thus, a preference for a folded conformational of iminium cation (**6im⁺**) due to cation-π interactions as hypothesised in Model **F** (Figure S1) is not supported by these results.

Restricted conformational analysis of iminium salt **6im** indicates that triflate anion prefers to coordinate to the concave face of the iminium intermediate as hypothesised in model **F'** (Figure S1) as shown in the Figure S3 (conf. no. 1). In the lowest energy conformer 1 of iminium salt **6im**, the face *syn* to the phenyl group is blocked by triflate anion, thus favouring the formation of the *cis* product through *anti* attack of DIBAL. It should be added that the current conformational search restricts itself to placing the triflate anion either on top or below the ring faces of cation **6im⁺**. Equally possible side-on orientations have not yet been explored in detail.

An analogous conformational analysis has been performed for iminium cation **7im⁺** (Figure S5) and iminium salt **7im** (Figure S6). Again, in the case of **7im⁺**, an extended conformation is preferred over a folded structure. The lowest energy conformers, in terms of enthalpy (ΔH_{298}, conf. no. 1) and free energy (ΔG_{298}, conf. no. 2) have extended conformations, where the phenyl group is pointing away from the bicyclic ring system. It is thus highly unlikely that a cation-π interaction-induced folding as hypothesised in model **H** is the reason for the observed diastereoselectivity. The influence of the conformational preferences of the OTBS group on the observed diastereoselectivity is not easily identified as the global conformational minimum (in terms of ΔH_{298}) orients the OTBS group such that it is blocking the *syn* face of the bicyclic ring system. This is expected to promote the addition of hydride *cis* to the phenyl group. However, it is important to note that in other energetically close-lying conformers (for example, conf. no. 2) the *syn* face of the bicyclic moiety to phenyl is free for hydride addition.

Restricted conformation analysis on iminium salt **7im** shows that triflate anion complexation to the *syn* face of the bicyclic ring system (with respect to the phenyl group) is energetically highly preferred over the complexation to the *anti* face. The most stable conformer, where the triflate anion complexes to the *anti* face, is more than 15 kJ/mol higher in energy compared to the lowest energy *syn*-conformer (conf. no. 1, Figure S6). In this latter structure the triflate anion blocks the *syn* face and the OTBS group also orients itself in a way that favours the experimentally observed product formation by promoting hydride addition from the *anti* side to a phenyl group. It should be added again that the current conformational search restricts itself to placing the triflate anion either on top or below the ring faces of cation **6im⁺** leaving equally possible side-on orientations unexplored at the moment.

2.1. Iminium cation **6im$^+$**

Table S1. Conformational energetics (kJ/mol) of iminium cation **6im$^+$** calculated at the different levels of theory over gas phase optimized geometries.

		B3LYP-D3/6-31G(d) (level of optimization)				**PCM(CH_2Cl_2,ua0)/ B3LYP-D3/6-31G(d) //B3LYP-D3/6-31G(d)**				**DLPNO-CCSD(T)/cc-pVTZ //(U)B3LYP-D3/6-31G(d)**				**PCM(CH_2Cl_2,ua0)/DLPNO-CCSD(T)/cc-pVTZ //B3LYP-D3/6-31G(d)**		
Conformer number	**File Name (for internal ref.)**	**ΔE_{tot}**	**ΔH_{298}**	**ΔG_{298}**		**ΔE_{sol}**	**ΔH_{sol}**	**ΔG_{sol}**		**ΔE_{tot}**	**ΔH_{298}**	**ΔG_{298}**		**ΔE_{sol}**	**ΔH_{sol}**	**ΔG_{sol}**
1	iminiumIon_6a_1	0.0	0.0	0.0		0.0	0.0	0.0		0.0	0.0	0.0		0.0	0.0	0.0
2	iminiumIon_6a_7	5.0	6.3	12.2		12.2	13.5	19.3		4.0	5.3	11.2		11.2	12.5	18.3
3	iminiumIon_6a_2	7.5	8.5	9.5		11.2	12.2	13.2		6.9	7.9	8.9		10.6	11.6	12.6
4	iminiumIon_6a_9	10.5	12.2	13.9		16.8	18.6	20.2		9.7	11.4	13.1		16.1	17.8	19.4
5	iminiumIon_6a_4	12.4	12.4	12.6		13.3	13.4	13.5		10.0	10.1	10.2		10.9	11.0	11.1
6	iminiumIon_6a_3	12.5	12.7	12.7		13.3	13.5	13.6		9.9	10.1	10.1		10.7	10.9	11.0
7	iminiumIon_6a_5	14.8	15.8	14.5		18.0	18.9	17.7		15.8	16.7	15.4		18.9	19.9	18.6
8	iminiumIon_6a_6	17.3	17.3	15.3		16.9	16.8	14.8		14.6	14.6	12.6		14.2	14.1	12.1
9	iminiumIon_6a_8	18.4	18.8	17.0		18.4	18.8	17.0		16.0	16.4	14.6		16.0	16.4	14.6

2.1.1. Gas phase CEs (gas phase optimization)

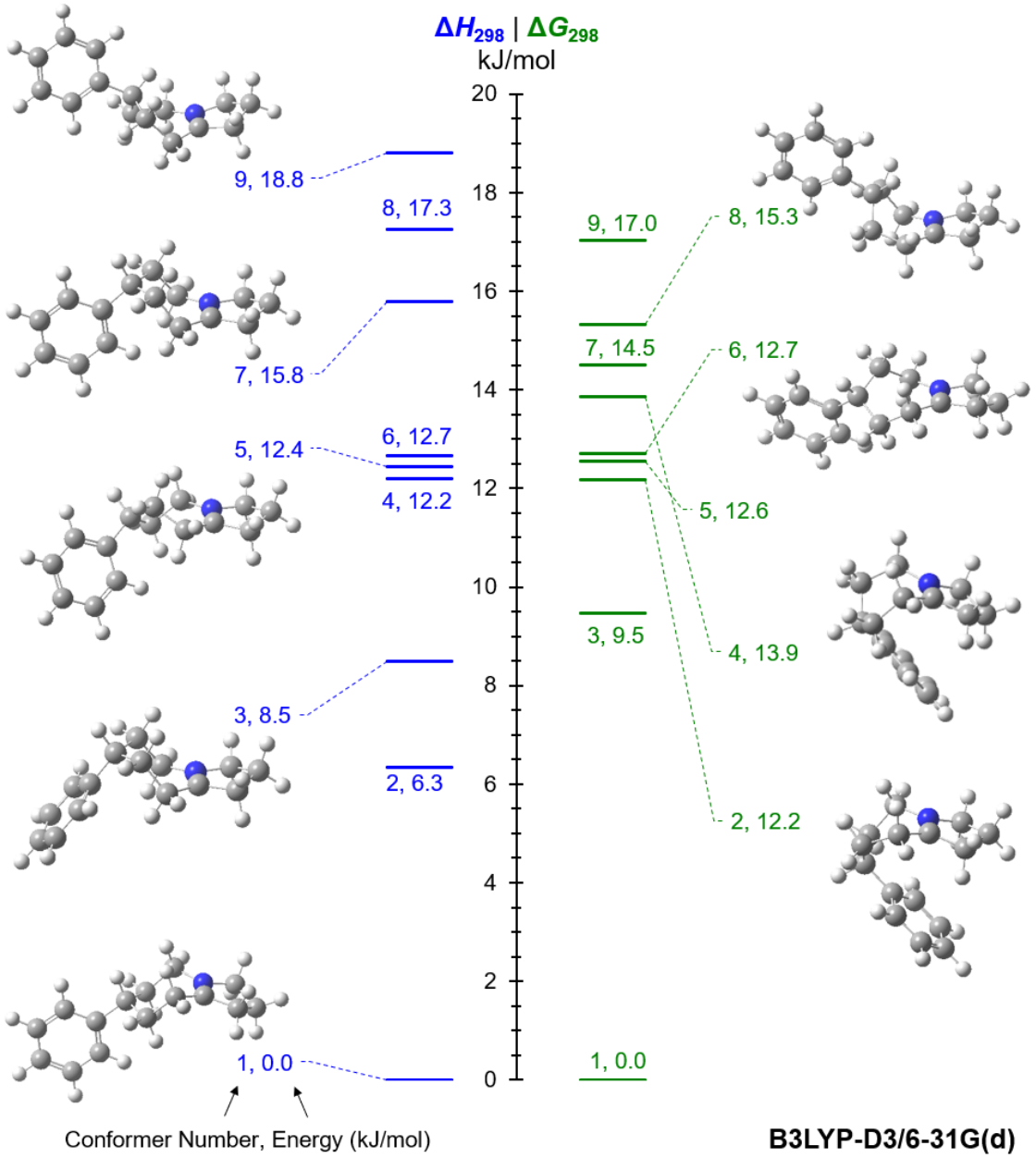

Figure S2. Conformational energetics (ΔH_{298} | ΔG_{298}, kJ/mol) of iminium cation **6im**$^{+}$ calculated at the B3LYP-D3/6-31G(d) level of theory in the gas phase. [Conformers are assign number according to rel. ΔH_{298} at B3LYP-D3/6-31G(d)].

2.1.2. Solvation corrected CEs (single point implicit solvation)

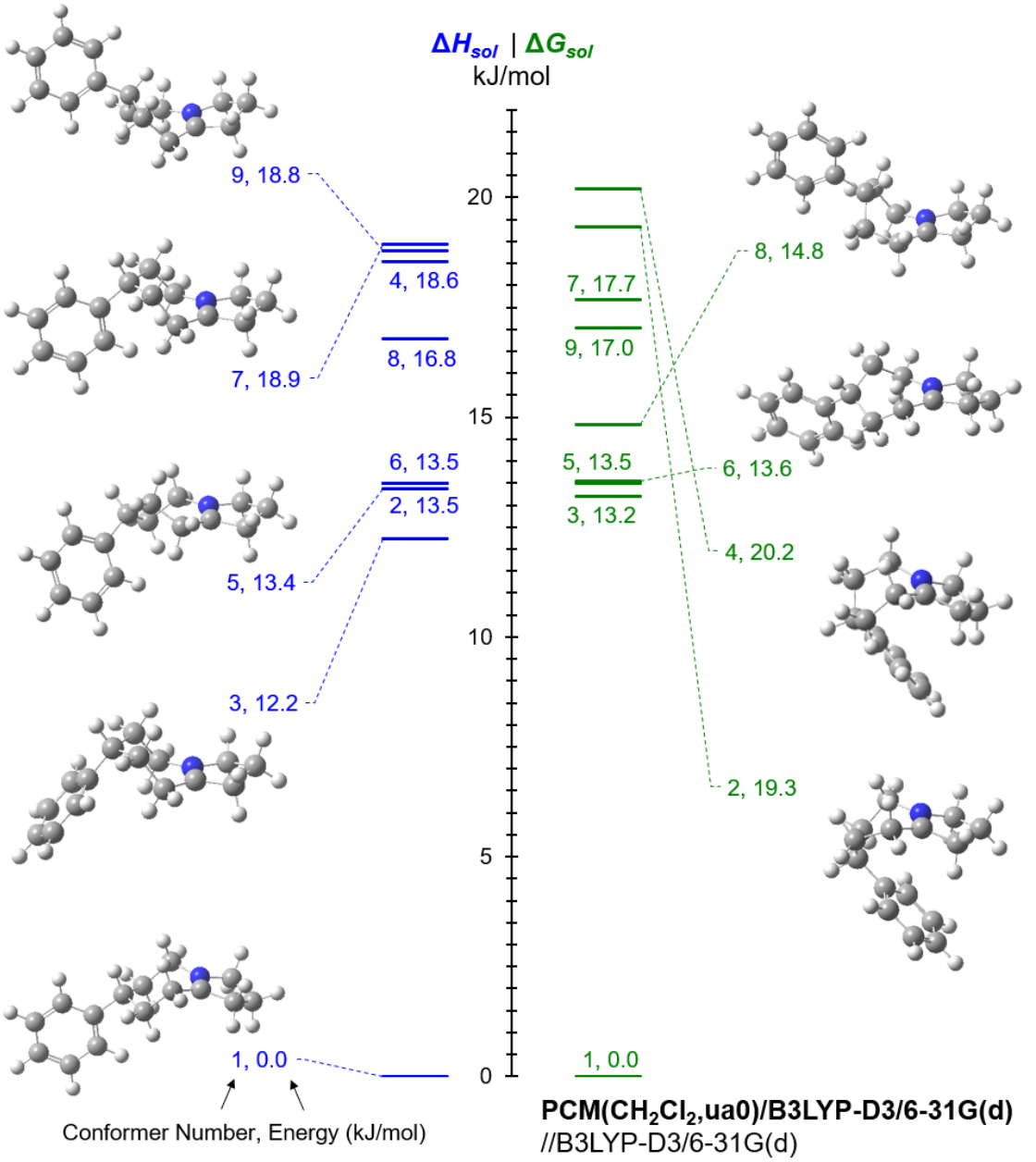

Figure S3. Conformational energetics (ΔH_{sol} | ΔG_{sol}, kJ/mol) of iminium cation **6im$^+$** calculated at the PCM(CH_2Cl_2,ua0)/B3LYP-D3/6-31G(d)//B3LYP-D3/6-31G(d) level of theory. [Gas phase conformer's numbering is retained to facilitate comparision. Conformers are assign number according to rel. ΔH_{298} at B3LYP-D3/6-31G(d)].

2.1.3. High level gas phase CEs

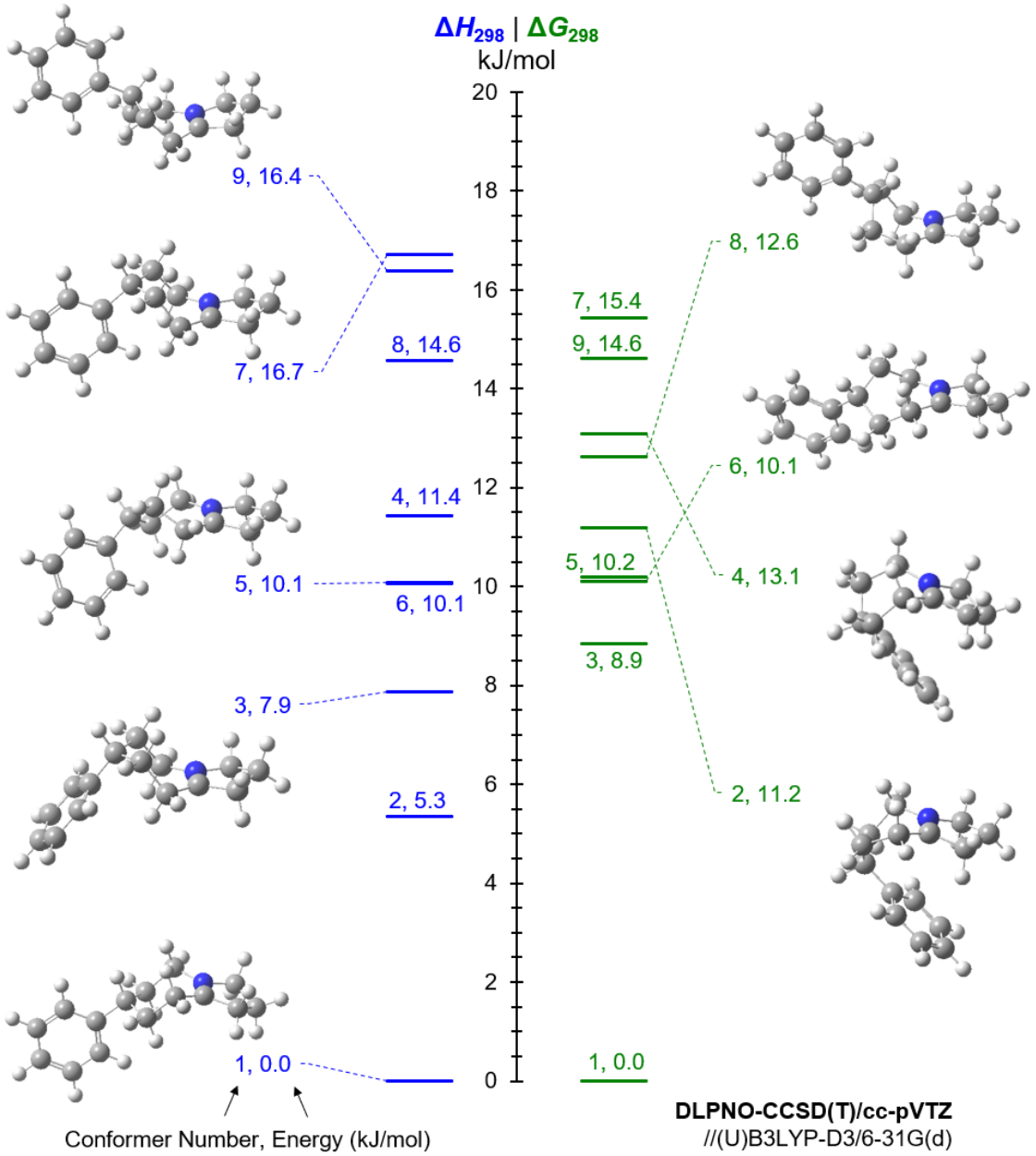

Figure S4. Conformational energetics (ΔH_{298} | ΔG_{298}, kJ/mol) of iminium cation **6im**$^{+}$ calculated at the DLPNO-CCSD(T)/cc-pVTZ//(U)B3LYP-D3/6-31G(d) level of theory in the gas phase. [Conformers are assign number according to rel. ΔH_{298} at B3LYP-D3/6-31G(d)].

2.1.4. Solvation corrected high level CEs

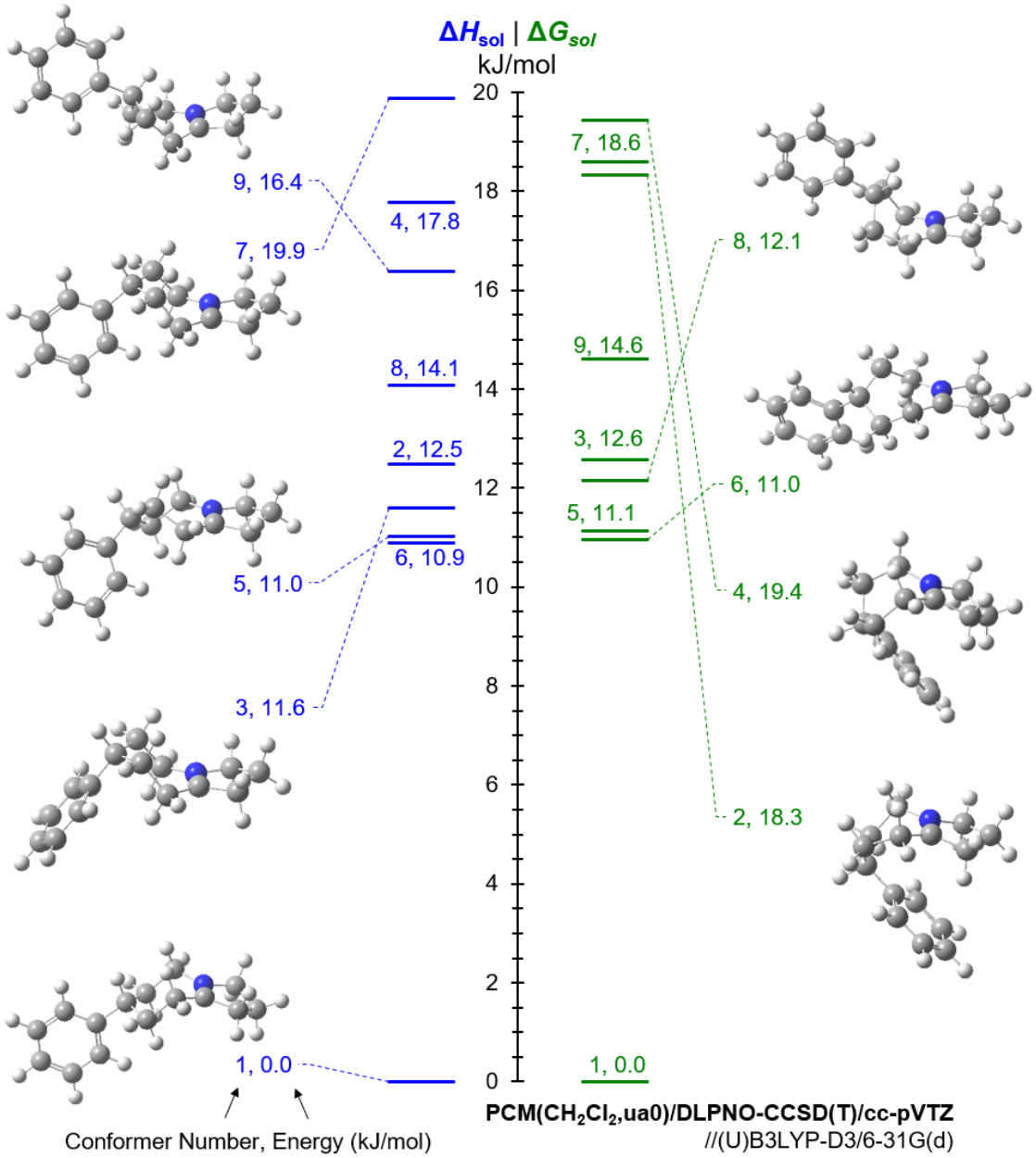

Figure S5. Conformational energetics (ΔH_{sol} | ΔG_{sol}, kJ/mol) of iminium cation **6im$^+$** calculated at the PCM(CH_2Cl_2,ua0)/DLPNO-CCSD(T)/cc-pVTZ//B3LYP-D3/6-31G(d) level of theory. [Gas phase conformer's numbering is retained to facilitate comparision. Conformers are assign number according to rel. ΔH_{298} at B3LYP-D3/6-31G(d). Single point solvation energies obtained at PCM(CH_2Cl_2,ua0)/B3LYP-D3/6-31G(d) level].

2.1.5. Solution phase CEs (optimization under implicit solvation)

Table S2. Conformational energetics (kJ/mol) of iminium cation **6im**$^+$ calculated at the PCM(CH_2Cl_2,ua0)/B3LYP-D3/6-31G(d) levels of theory.

Conformer number	File Name (for internal ref.)	ΔE_{tot}	ΔH_{298}	ΔG_{298}
1	iminiumIon_6a_1	0.0	0.0	0.0
2	iminiumIon_6a_2	12.6	13.2	12.9
3	iminiumIon_6a_4	13.2	13.3	14.0
4	iminiumIon_6a_3	13.2	13.3	13.7
5	iminiumIon_6a_6	16.5	16.4	14.1
6	iminiumIon_6a_7	15.4	16.8	22.7
7	iminiumIon_6a_8	18.5	18.9	16.6
8	iminiumIon_6a_5	18.3	19.0	19.7
9	iminiumIon_6a_9	20.6	21.8	22.5

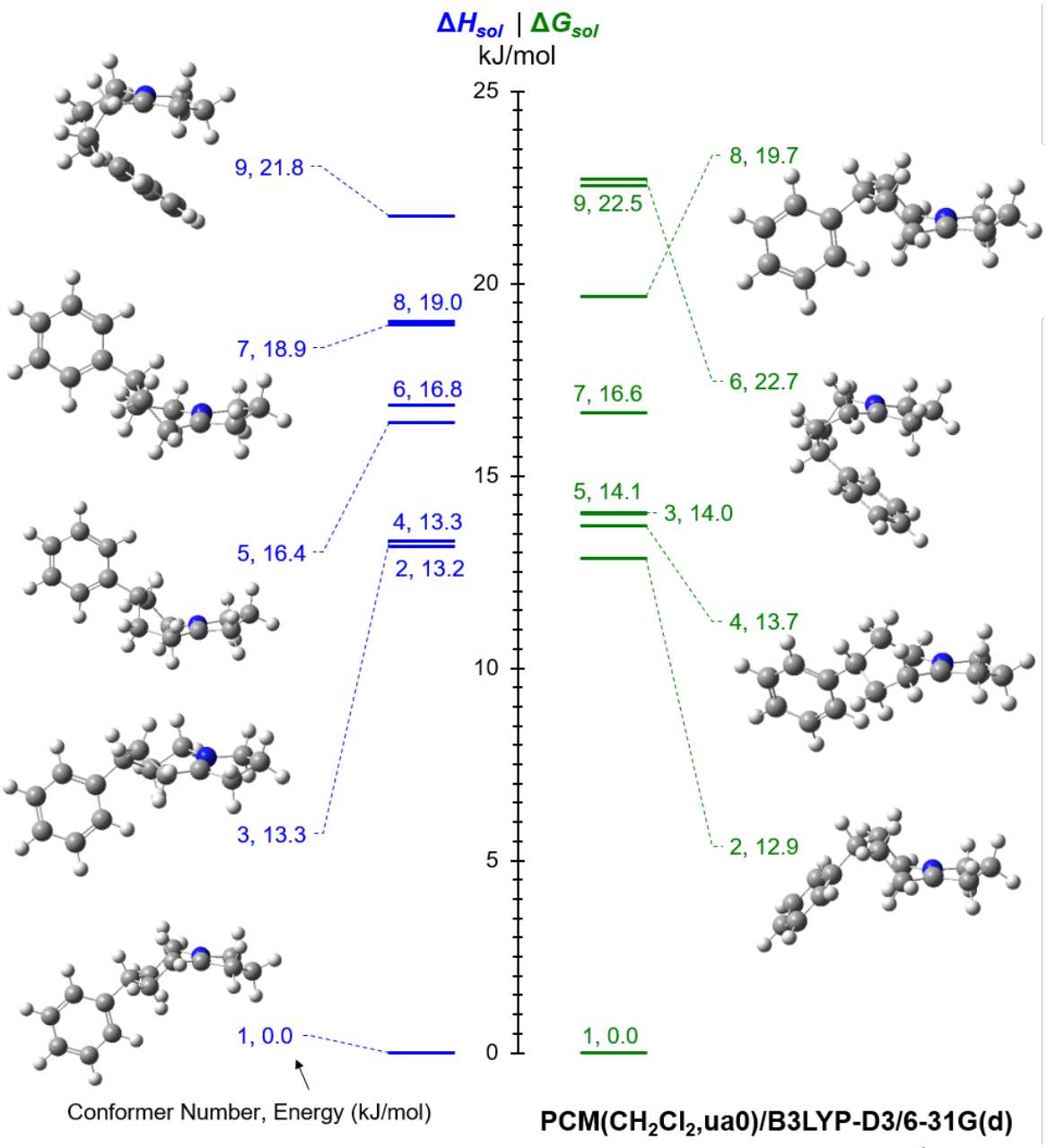

Figure S6. Conformational energetics (ΔH_{sol} | ΔG_{sol}, kJ/mol) of iminium cation **6im**$^+$ calculated at the PCM(CH_2Cl_2,ua0)/B3LYP-D3/6-31G(d) level of theory. [Conformers are assign number according to rel. ΔH_{sol} at PCM(CH_2Cl_2,ua0)/B3LYP-D3/6-31G(d)].

2.2. Iminium salt **6im**

Table S3. Conformational energetics (kJ/mol) of iminium salt **6im** calculated at the different levels of theory over gas phase optimized geometries. (first 10 conf. only)

		B3LYP-D3/6-31G(d) (level of optimization)				**PCM(CH_2Cl_2,ua0)/ B3LYP-D3/6-31G(d) //B3LYP-D3/6-31G(d)**				**DLPNO-CCSD(T)/cc-pVTZ //(U)B3LYP-D3/6-31G(d)**				**PCM(CH_2Cl_2,ua0)/DLPNO-CCSD(T)/cc-pVTZ //B3LYP-D3/6-31G(d)**		
Conformer number	**File Name (for internal ref.)**	**ΔE_{tot}**	**ΔH_{298}**	**ΔG_{298}**		**ΔE_{sol}**	**ΔH_{sol}**	**ΔG_{sol}**		**ΔE_{tot}**	**ΔH_{298}**	**ΔG_{298}**		**ΔE_{sol}**	**ΔH_{sol}**	**ΔG_{sol}**
1	cmp_6a_23	0.0	0.0	1.2		1.2	1.2	3.7		0.0	0.0	3.6		0.0	0.2	4.2
2	cmp_6a_37	1.3	1.4	0.0		0.0	0.0	0.0		4.5	4.5	5.5		2.0	2.2	3.6
3	cmp_6a_5	4.7	5.0	7.6		9.3	9.6	13.5		1.1	1.4	6.3		4.5	5.0	10.3
4	cmp_6a_2	6.2	5.4	2.7		6.8	6.0	4.6		1.1	0.4	0.0		0.5	0.0	0.0
5	cmp_6a_9	5.6	5.7	6.7		9.5	9.6	12.0		1.4	1.6	4.9		4.1	4.5	8.2
6	cmp_6a_49	6.3	6.4	6.6		10.2	10.3	11.9		2.4	2.5	5.1		5.1	5.5	8.4
7	cmp_6a_43	9.7	10.5	13.3		13.4	14.1	18.3		12.6	13.4	18.6		15.1	16.1	21.6
8	cmp_6a_8	13.2	13.4	12.9		17.1	17.3	18.2		9.2	9.3	11.2		11.9	12.3	14.6
9	cmp_6a_53	13.0	13.8	13.1		16.0	16.7	17.4		12.7	13.4	15.1		14.5	15.4	17.5
10	cmp_6a_47	14.0	14.8	16.6		16.2	17.0	20.2		11.7	12.5	16.7		12.8	13.8	18.4

2.2.1. Gas phase CEs

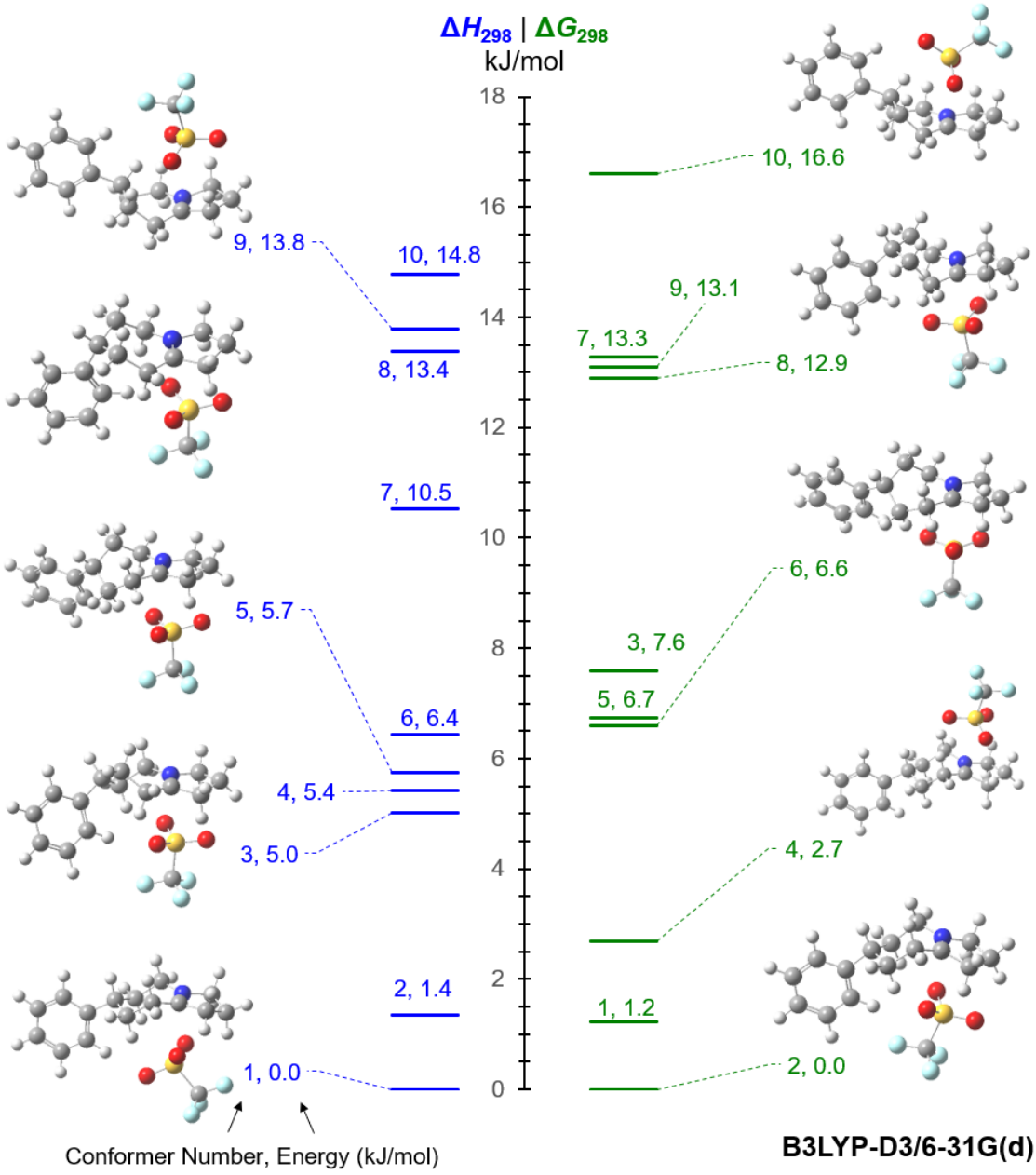

Figure S7. Conformational energetics (ΔH_{298} | ΔG_{298}, kJ/mol) of iminium salt **6im** calculated at the B3LYP-D3/6-31G(d) level of theory in the gas phase. [Conformers are assign number according to rel. ΔH_{298} at B3LYP-D3/6-31G(d)].

2.2.2. Solvation corrected CEs

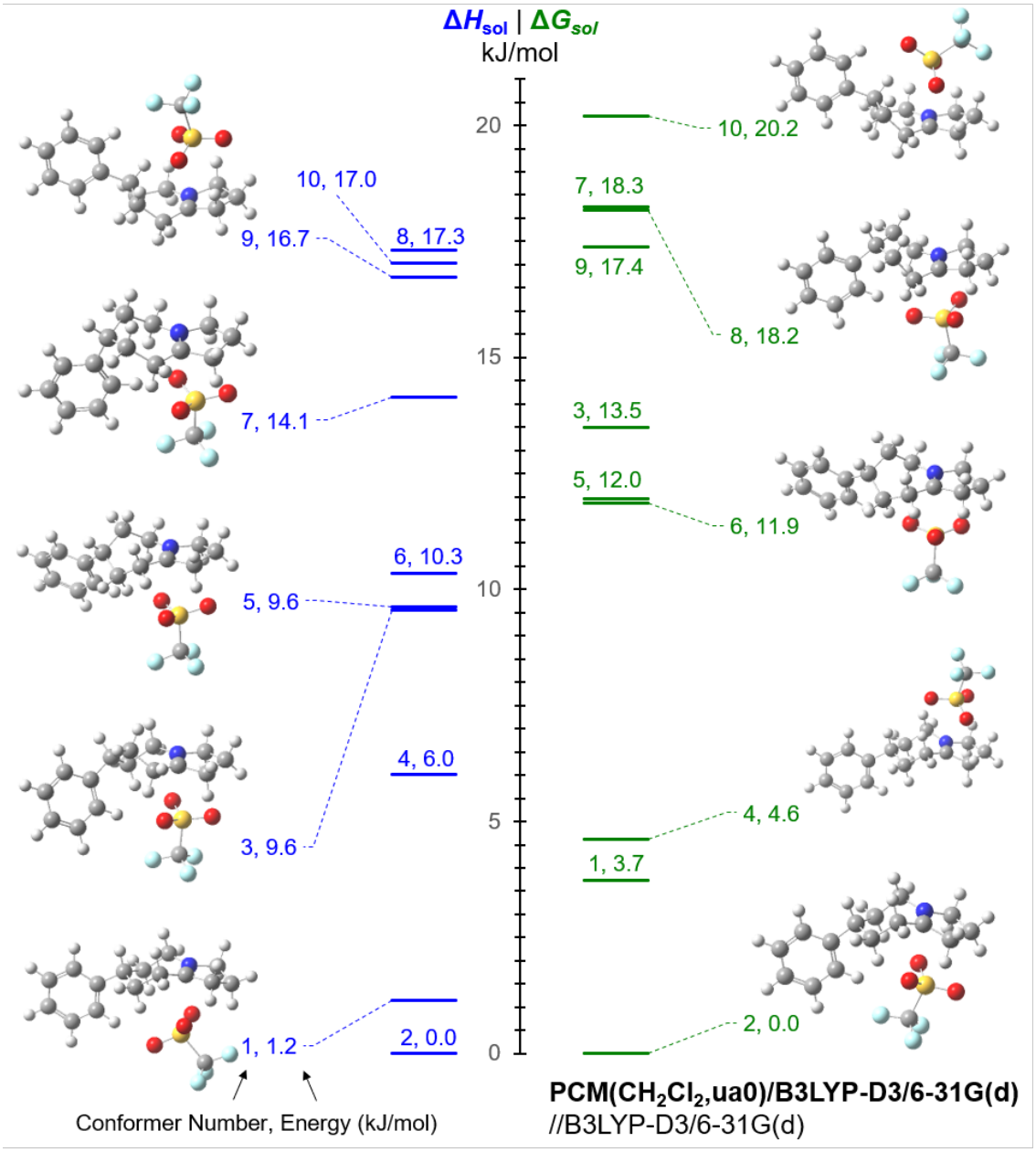

Figure S8. Conformational energetics (ΔH_{sol} | ΔG_{sol}, kJ/mol) of iminium salt **6im** calculated at the PCM(CH_2Cl_2,ua0)/B3LYP-D3/6-31G(d)//B3LYP-D3/6-31G(d) level of theory. [Gas phase conformer's numbering is retained to facilitate comparision. Conformers are assign number according to rel. ΔH_{298} at B3LYP-D3/6-31G(d)].

2.2.3. High level gas phase CEs

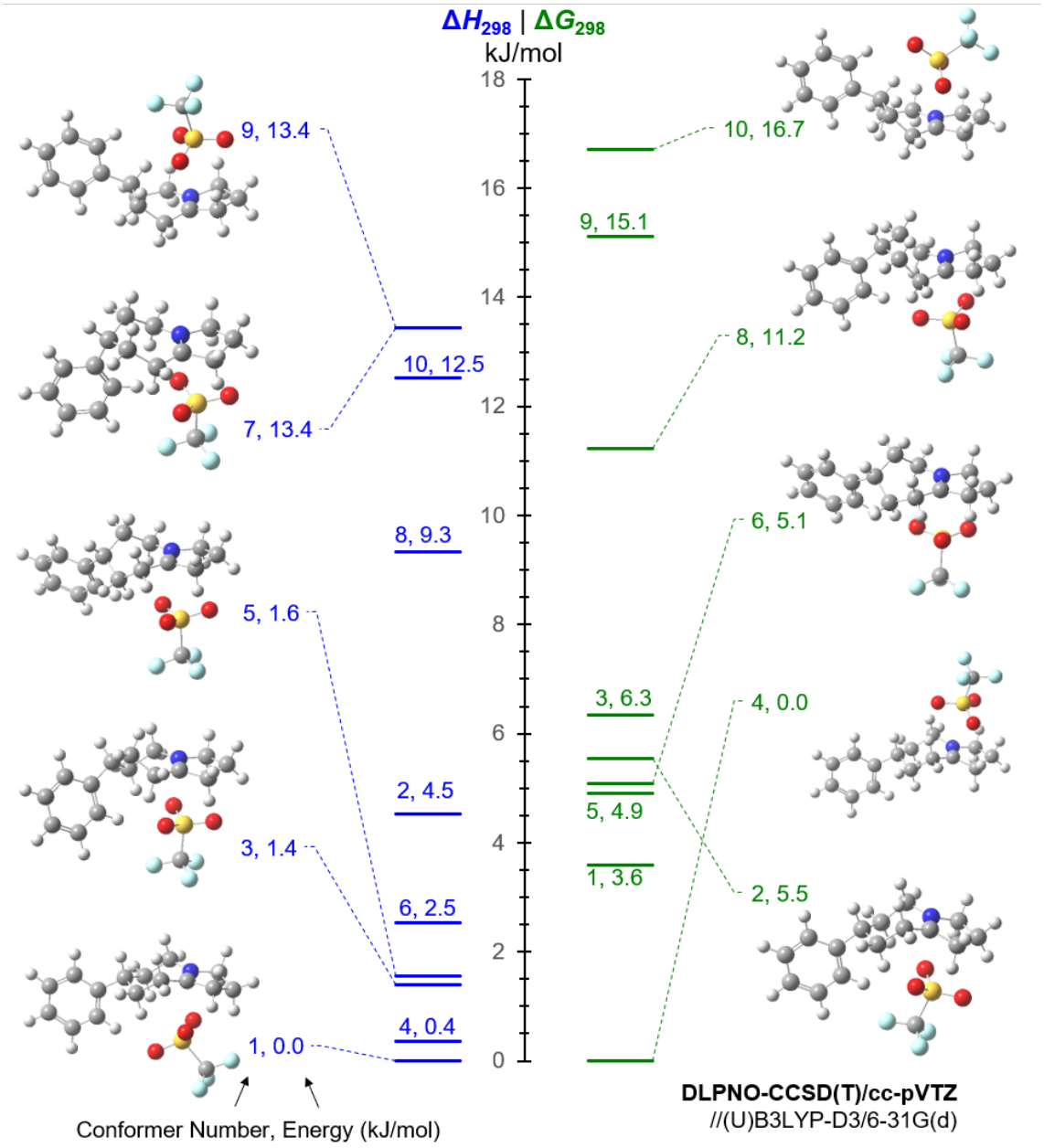

Figure S9. Conformational energetics (ΔH_{298} | ΔG_{298}, kJ/mol) of iminium salt **6im** calculated at the DLPNO-CCSD(T)/cc-pVTZ//(U)B3LYP-D3/6-31G(d) level of theory in the gas phase. [Conformers are assign number according to rel. ΔH_{298} at B3LYP-D3/6-31G(d)].

2.2.4. Solvation corrected high level CEs

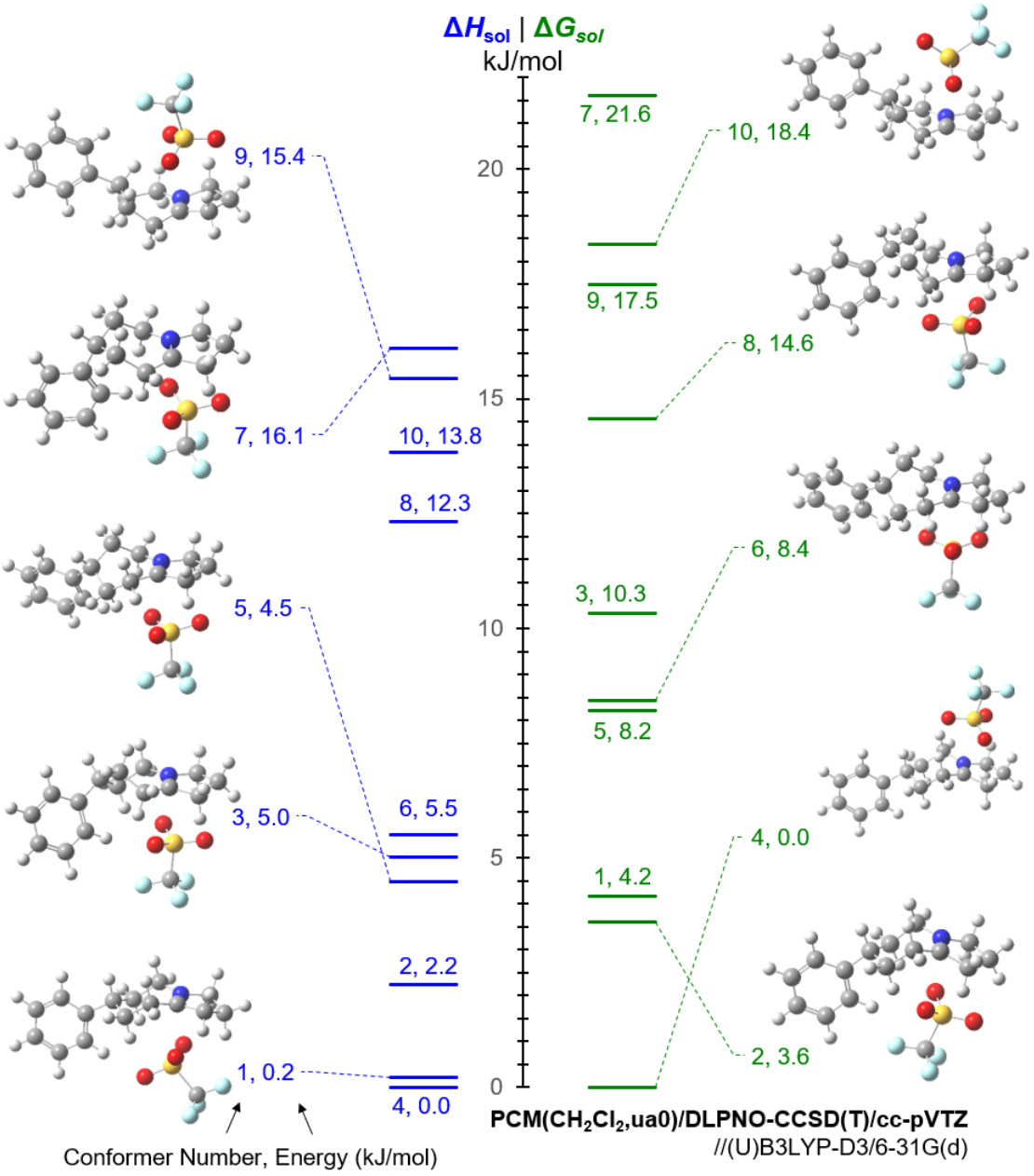

Figure S10. Conformational energetics (ΔH_{sol} | ΔG_{sol}, kJ/mol) of iminium salt **6im** calculated at the PCM(CH_2Cl_2,ua0)/DLPNO-CCSD(T)/cc-pVTZ//B3LYP-D3/6-31G(d) level of theory. [Gas phase conformer's numbering is retained to facilitate comparision. Conformers are assign number according to rel. ΔH_{298} at B3LYP-D3/6-31G(d). Single point solvation energies obtained at PCM(CH_2Cl_2,ua0)/B3LYP-D3/6-31G(d) level].

2.2.5. Solution phase CEs

Table S4. Conformational energetics (kJ/mol) of iminium salt **6im** calculated at the PCM(CH_2Cl_2,ua0)/B3LYP-D3/6-31G(d) levels of theory.

Conformer number	File Name (for internal ref.)	ΔE_{tot}	ΔH_{298}	ΔG_{298}
1	cmp_6a_23	0.0	0.0	2.0
2	cmp_6a_2	2.2	1.0	0.0
3	cmp_6a_37	1.0	1.5	0.4
4	cmp_6a_49	8.7	8.5	10.0
5	cmp_6a_9	9.1	8.9	10.2
6	cmp_6a_5	9.4	9.3	11.3
7	cmp_6a_28	14.5	13.8	11.8
8	cmp_6a_7	14.6	14.2	12.9
9	cmp_6a_8	15.2	15.1	16.1
10	cmp_6a_6	16.9	15.9	13.5

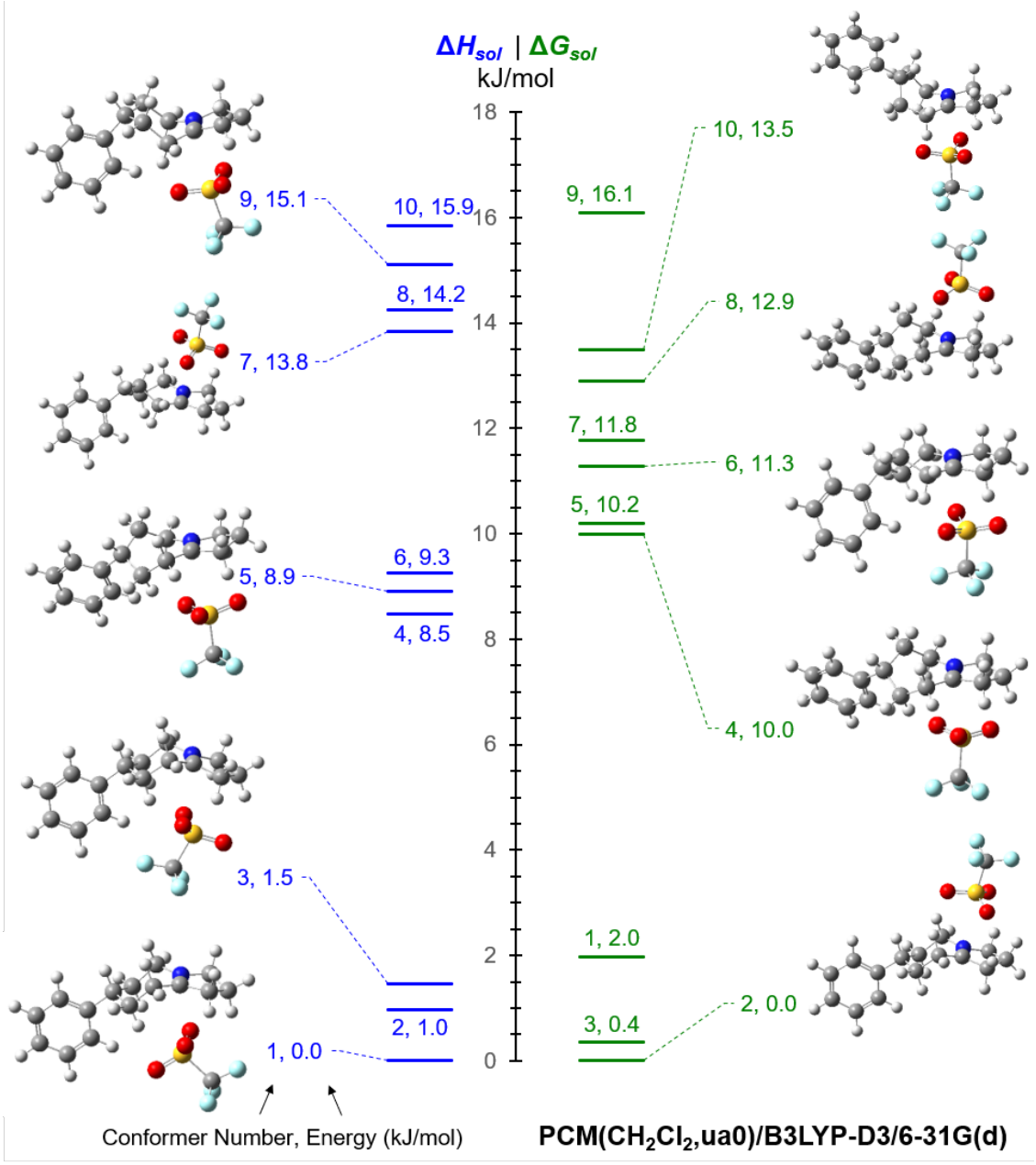

Figure S11. Conformational energetics (ΔH_{sol} | ΔG_{sol}, kJ/mol) of iminium salt **6im** calculated at the PCM(CH_2Cl_2,ua0)/B3LYP-D3/6-31G(d) level of theory. [Conformers are assign number according to rel. ΔH_{sol} at PCM(CH_2Cl_2,ua0)/B3LYP-D3/6-31G(d)].

2.3. Iminium cation **7im**$^{+}$

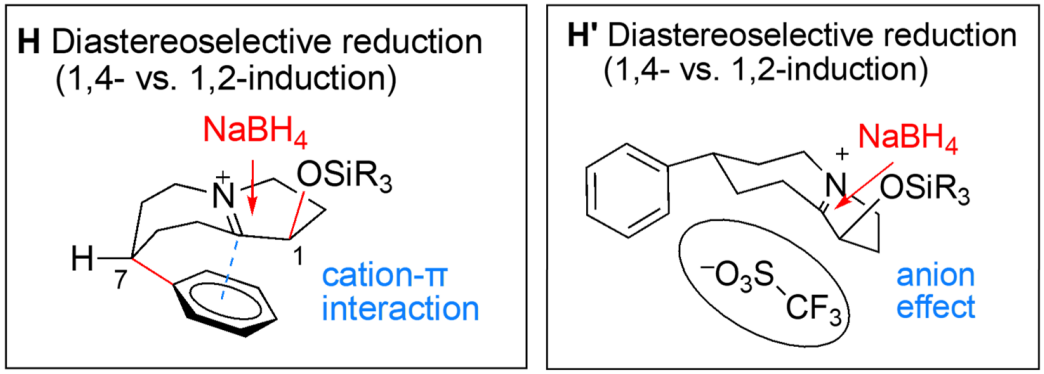

Figure S12. Proposed conformational preference for iminium cation (**H, 7im**$^{+}$) and iminium salt (**H`, 7im**).

Table S5. Conformational energetics (kJ/mol) of iminium cation **7im**$^{+}$ calculated at the different levels of theory over gas phase optimized geometries.

		B3LYP-D3/6-31G(d) (level of optimization)				PCM(CH_2Cl_2,ua0)/ B3LYP-D3/6-31G(d) //B3LYP-D3/6-31G(d)			DLPNO-CCSD(T)/cc-pVTZ //(U)B3LYP-D3/6-31G(d)			PCM(CH_2Cl_2,ua0)/DLPNO-CCSD(T)/cc-pVTZ //B3LYP-D3/6-31G(d)		
Conformer number	**File Name (for internal ref.)**	**ΔE_{tot}**	**ΔH_{298}**	**ΔG_{298}**	**ΔE_{sol}**	**ΔH_{sol}**	**ΔG_{sol}**	**ΔE_{tot}**	**ΔH_{298}**	**ΔG_{298}**	**ΔE_{sol}**	**ΔH_{sol}**	**ΔG_{sol}**
1t	Imlon_7a_t_4	0.0	0.0	2.5	0.0	0.0	2.4	1.9	1.6	5.0	1.8	1.5	4.9
2t	Imlon_7a_t_2	0.6	1.0	0.0	0.7	1.1	0.0	0.0	0.0	0.0	0.0	0.0	0.0
3t	Imlon_7a_t_3	0.7	1.5	4.6	1.4	2.2	5.3	1.7	2.2	6.3	2.3	2.8	6.9
4t	Imlon_7a_t_1	1.7	2.3	5.1	3.0	3.6	6.3	2.2	2.5	6.3	3.4	3.7	7.4
5t	Imlon_7a_t_6	1.6	3.3	7.7	5.3	6.9	11.2	2.9	4.2	9.6	6.4	7.7	13.1
6t	Imlon_7a_t_7	3.9	5.7	9.4	8.2	10.0	13.6	5.5	7.0	11.6	9.7	11.1	15.8
7t	Imlon_7a_t_5	4.3	6.2	11.9	9.1	11.1	16.7	5.4	7.0	13.7	10.2	11.7	18.4
8t	Imlon_7a_t_16	6.1	6.3	10.7	3.3	3.5	7.8	8.4	8.3	13.7	5.5	5.4	10.7
9t	Imlon_7a_t_9	7.5	8.6	11.6	10.3	11.4	14.3	8.5	9.3	13.3	11.2	12.1	16.0
10t	Imlon_7a_t_11	9.6	10.3	13.4	11.8	12.5	15.5	9.4	9.7	13.9	11.5	11.8	16.0

2.3.1. Gas phase CEs

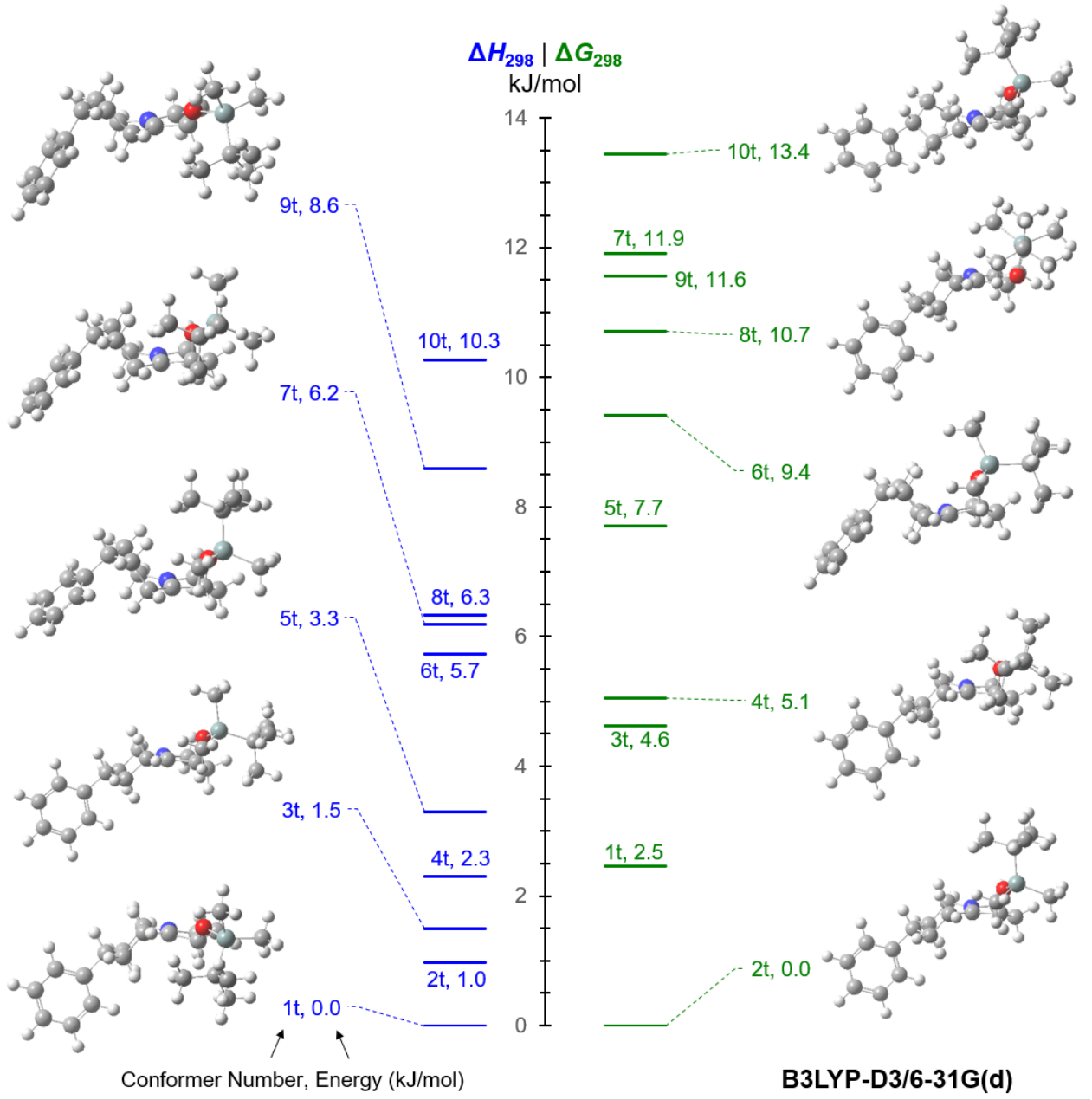

Figure S13. Conformational energetics (ΔH_{298} | ΔG_{298}, kJ/mol) of the *trans*-isomer of iminium cation **7im**$^{+}$ calculated at the B3LYP-D3/6-31G(d) level of theory in the gas phase. [Conformers are assign number according to rel. ΔH_{298} at B3LYP-D3/6-31G(d)].

2.3.2. Solvation corrected CEs

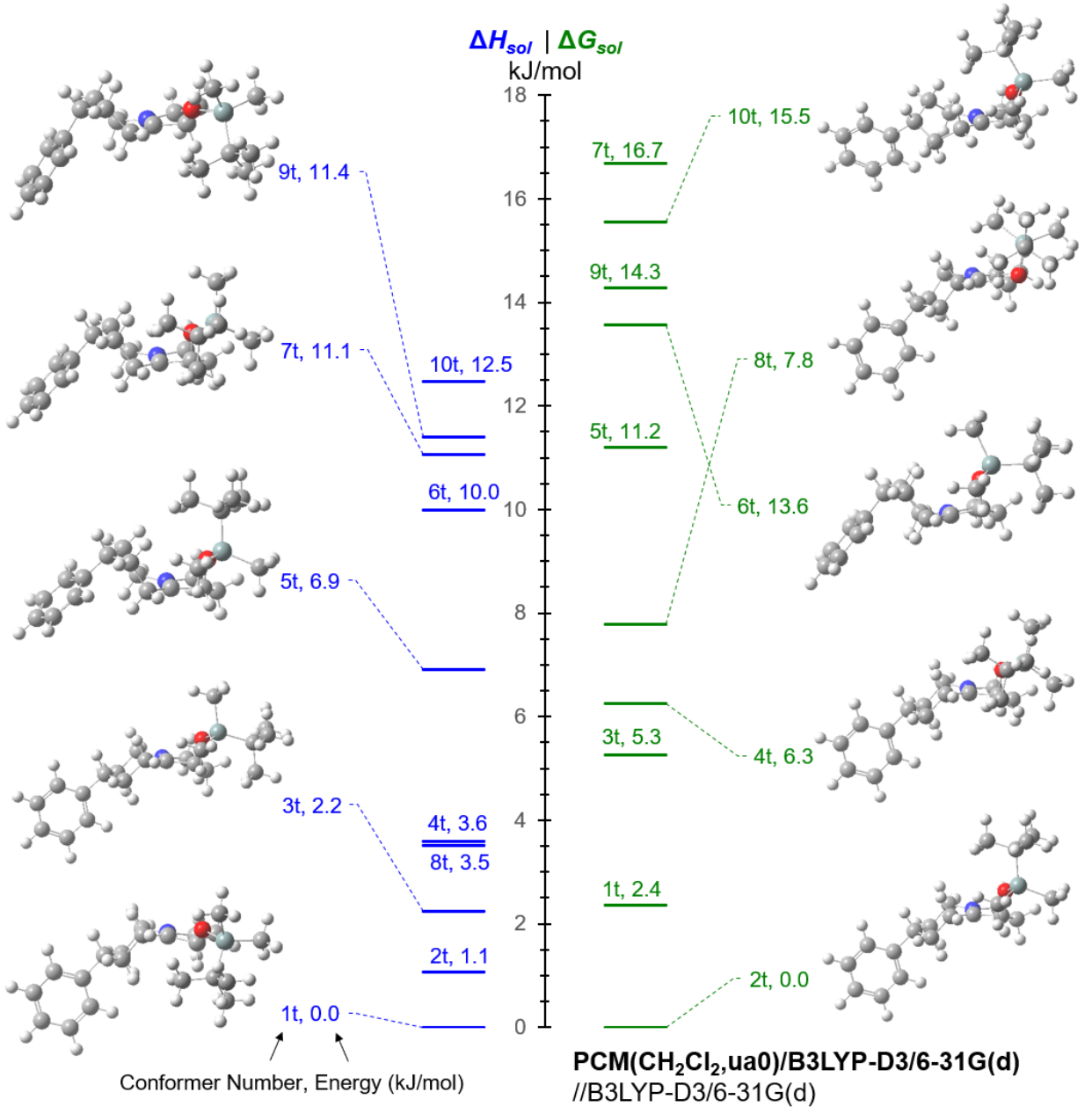

Figure S14. Conformational energetics (ΔH_{sol} | ΔG_{sol}, kJ/mol) of the *trans*-isomer of iminium cation **7im**$^{+}$ calculated at the PCM(CH_2Cl_2,ua0)/B3LYP-D3/6-31G(d)//B3LYP-D3/6-31G(d) level of theory. [Gas phase conformer's numbering is retained to facilitate comparision. Conformers are assign number according to rel. ΔH_{298} at B3LYP-D3/6-31G(d)].

2.3.3. High level gas phase CEs

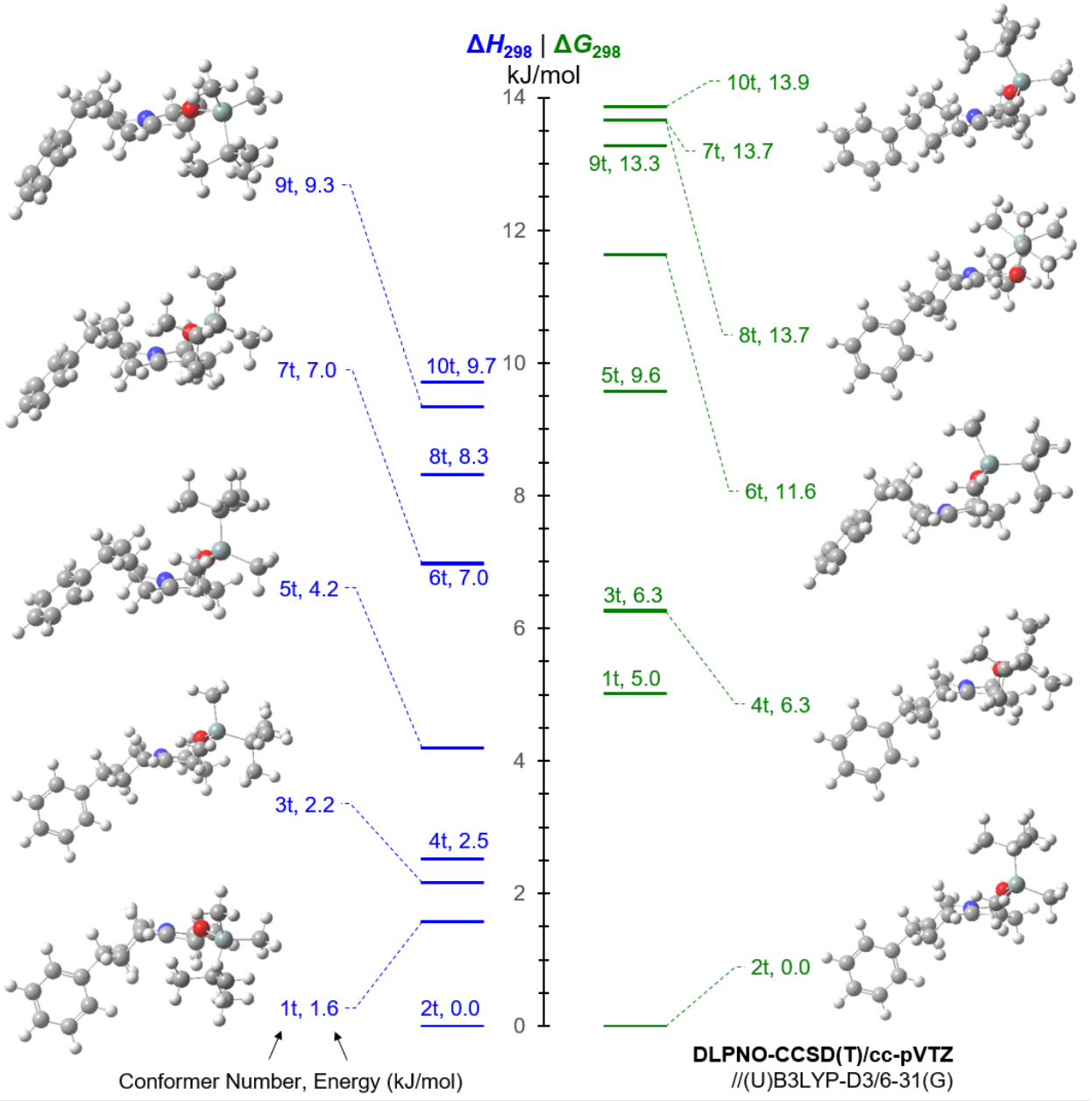

Figure S15. Conformational energetics (ΔH_{298} | ΔG_{298}, kJ/mol) of the *trans*-isomer of iminium cation **7im**$^{+}$ calculated at the DLPNO-CCSD(T)/cc-pVTZ//(U)B3LYP-D3/6-31G(d) level of theory in the gas phase. [Conformers are assign number according to rel. ΔH_{298} at B3LYP-D3/6-31G(d)].

2.3.4. Solvation corrected high level CEs

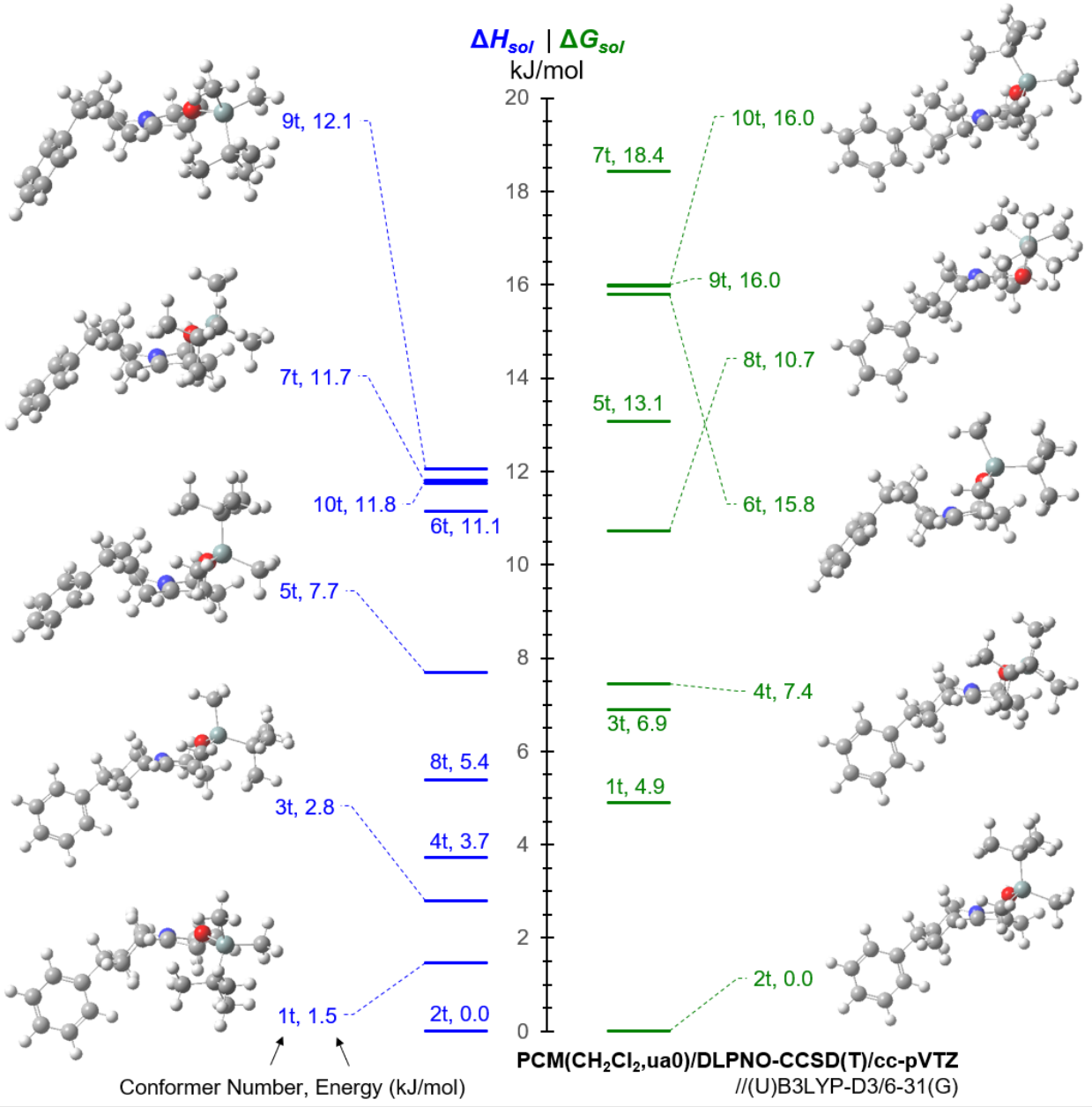

Figure S16. Conformational energetics (ΔH_{sol} | ΔG_{sol}, kJ/mol) of the *trans*-isomer of iminium cation **7im**$^{+}$ calculated at the PCM(CH_2Cl_2,ua0)/DLPNO-CCSD(T)/cc-pVTZ//B3LYP-D3/6-31G(d) level of theory. [Gas phase conformer's numbering is retained to facilitate comparision. Conformers are assign number according to rel. ΔH_{298} at B3LYP-D3/6-31G(d). Single point solvation energies obtained at PCM(CH_2Cl_2,ua0)/B3LYP-D3/6-31G(d) level].

2.4. Iminium salt **7im**

Table S6. Conformational energetics (kJ/mol) of iminium salt **7im** calculated at the different levels of theory over gas phase optimized geometries.

		B3LYP-D3/6-31G(d) (level of optimization)				**PCM(CH_2Cl_2,ua0)/ B3LYP-D3/6-31G(d) //B3LYP-D3/6-31G(d)**				**DLPNO-CCSD(T)/cc-pVTZ //(U)B3LYP-D3/6-31G(d)**				**PCM(CH_2Cl_2,ua0)/DLPNO-CCSD(T)/cc-pVTZ //B3LYP-D3/6-31G(d)**		
Conformer number	**File Name (for internal ref.)**	**ΔE_{tot}**	**ΔH_{298}**	**ΔG_{298}**		**ΔE_{sol}**	**ΔH_{sol}**	**ΔG_{sol}**		**ΔE_{tot}**	**ΔH_{298}**	**ΔG_{298}**		**ΔE_{sol}**	**ΔH_{sol}**	**ΔG_{sol}**
1	complex_7a_1	0.0	0.0	0.0		0.5	0.1	0.0		2.8	2.6	0.0		0.0	0.0	0.0
2	complex_7a_4	0.1	0.4	2.7		0.0	0.0	2.1		3.7	3.9	3.6		0.3	0.7	3.0
3	complex_7a_6	0.6	0.7	2.7		0.5	0.3	2.1		4.6	4.5	4.0		1.3	1.4	3.4
4	complex_7a_27	0.9	1.2	3.2		1.6	1.5	3.4		3.6	3.8	3.2		1.0	1.4	3.4
5	complex_7a_14	3.3	3.1	4.1		2.5	1.9	2.8		5.8	5.4	3.8		1.7	1.5	2.5
6	complex_7a_41	3.1	3.5	9.1		6.7	6.6	12.1		1.9	2.1	5.1		2.2	2.5	8.2
7	complex_7a_32	3.6	3.8	7.0		7.5	7.3	10.3		0.0	0.0	0.6		0.6	0.8	4.0
8	complex_7a_52	3.9	4.2	9.3		7.9	7.8	12.8		1.9	2.0	4.6		2.7	3.0	8.1
9	complex_7a_25	4.0	4.4	7.7		8.1	8.1	11.2		2.0	2.2	2.9		2.8	3.2	6.4
10	complex_7a_68	17.8	17.3	19.6		18.9	17.9	20.1		20.0	19.2	19.0		17.7	17.1	19.5

2.4.1. Gas phase CEs

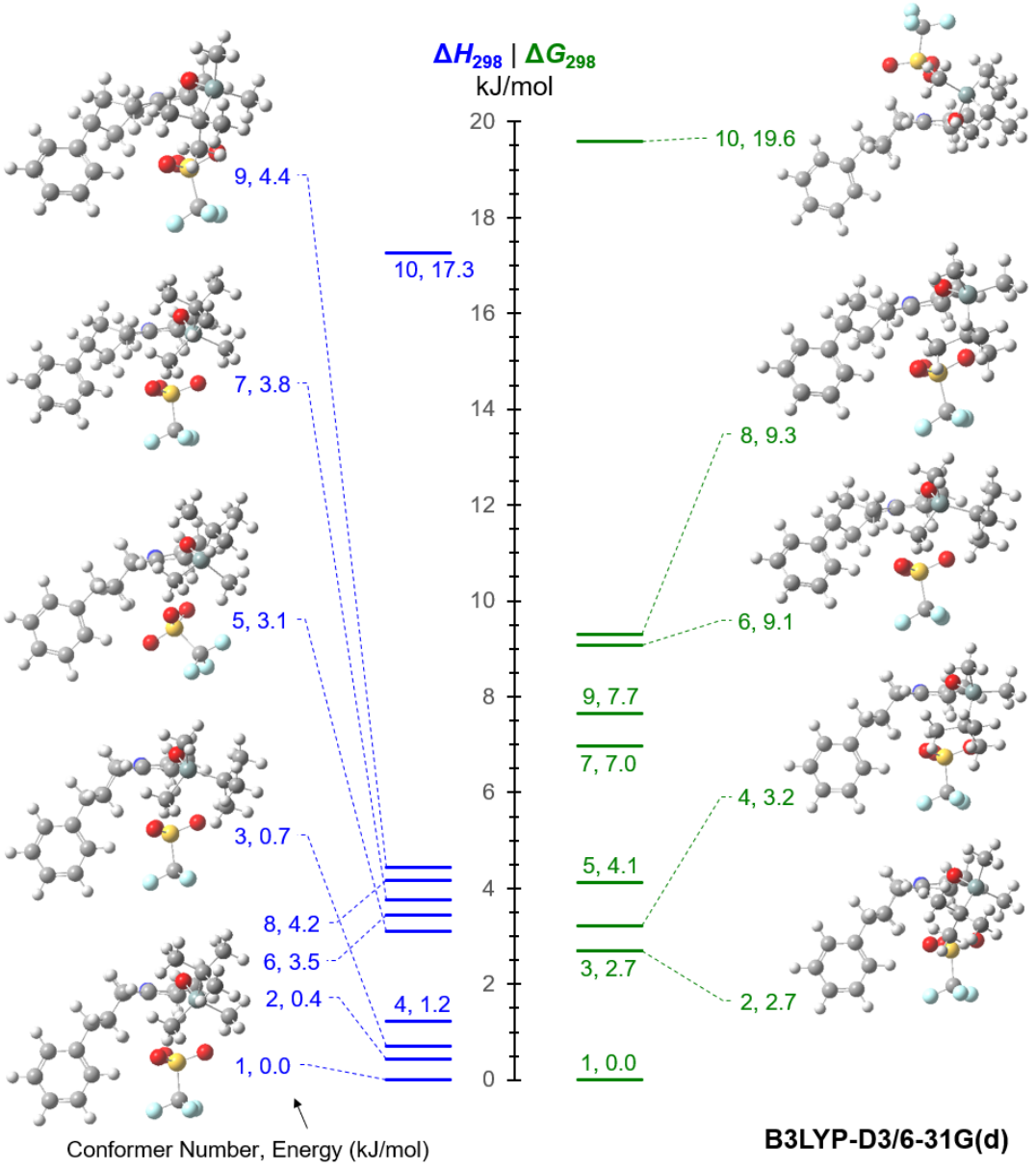

Figure S17. Conformational energetics (ΔH_{298} | ΔG_{298}, kJ/mol) of iminium salt **7im** shape calculated at the B3LYP-D3/6-31G(d) level of theory in gas phase.

2.4.1. Solvation corrected CEs

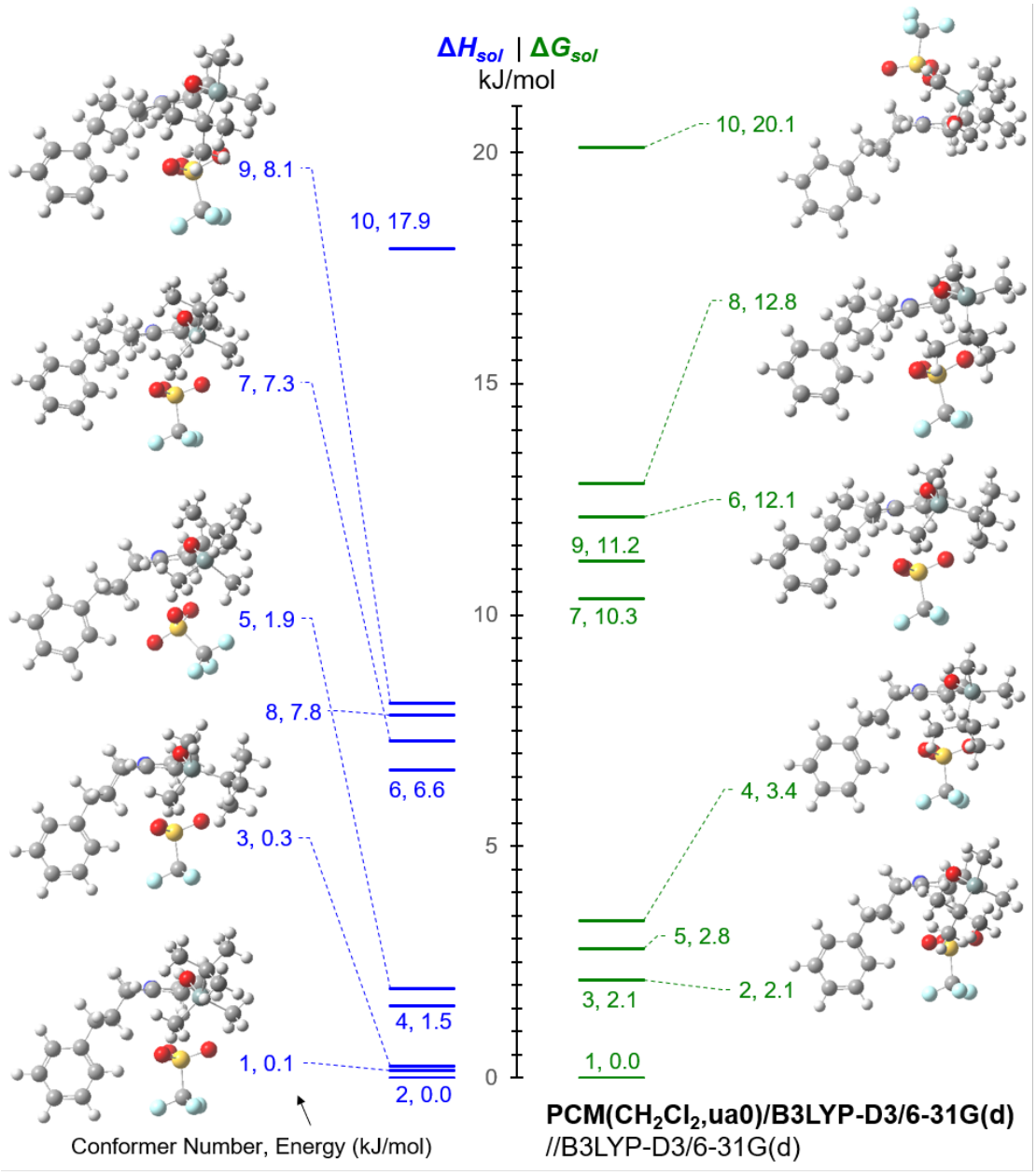

Figure S18. Conformational energetics (ΔH_{sol} | ΔG_{sol}, kJ/mol) of iminium salt **7im** calculated at the PCM(CH_2Cl_2,ua0)/B3LYP-D3/6-31G(d)//B3LYP-D3/6-31G(d) level of theory. [Gas phase conformer's numbering is retained to facilitate comparision. Conformers are assign number according to rel. ΔH_{298} at B3LYP-D3/6-31G(d)]

2.4.1. High level gas phase CEs

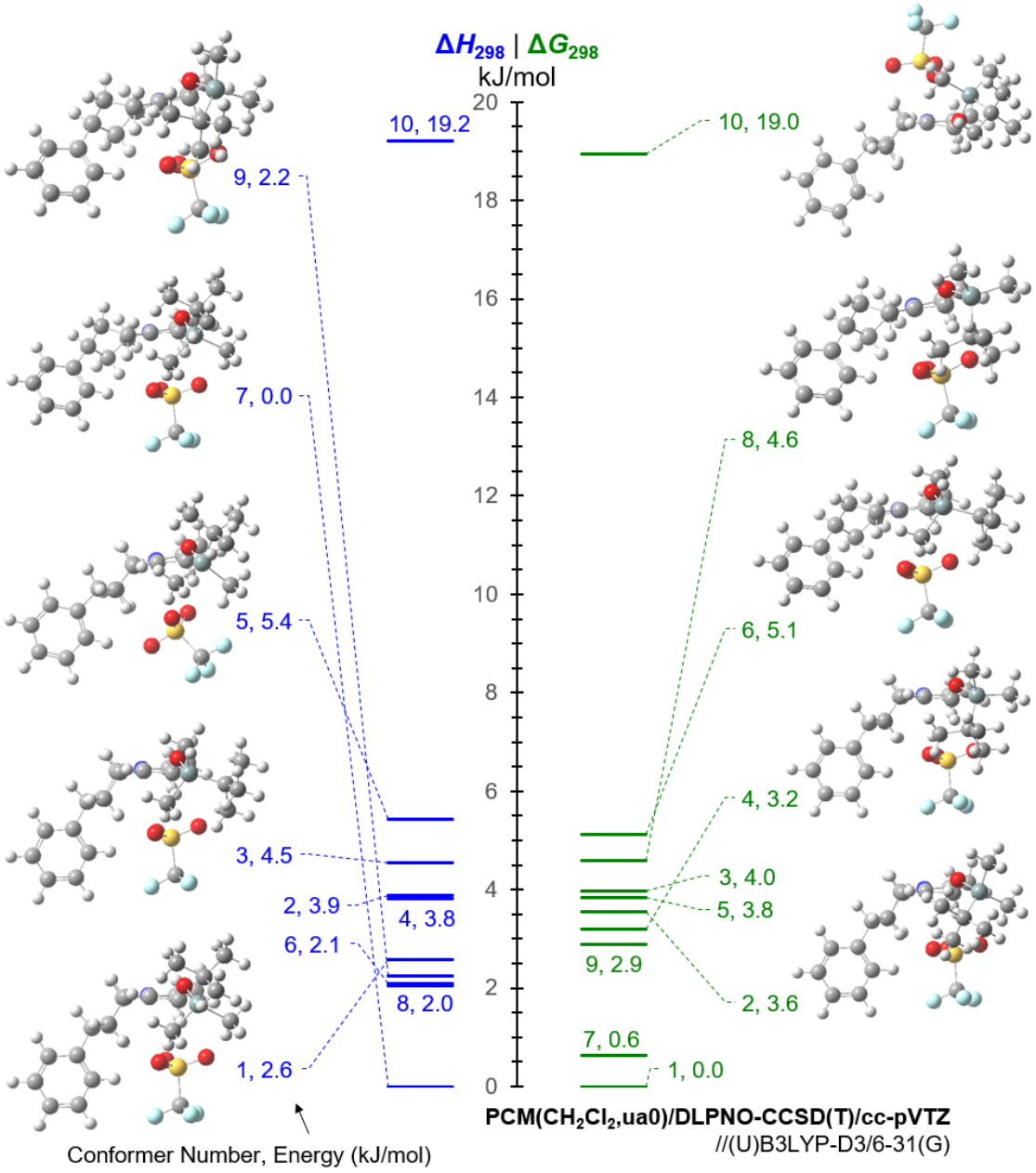

Figure S19. Conformational energetics (ΔH_{298} | ΔG_{298}, kJ/mol) of iminium salt **7im** calculated at the DLPNO-CCSD(T)/cc-pVTZ//(U)B3LYP-D3/6-31G(d) level of theory in the gas phase. [Conformers are assign number according to rel. ΔH_{298} at B3LYP-D3/6-31G(d)].

2.4.2. Solvation corrected high level CEs

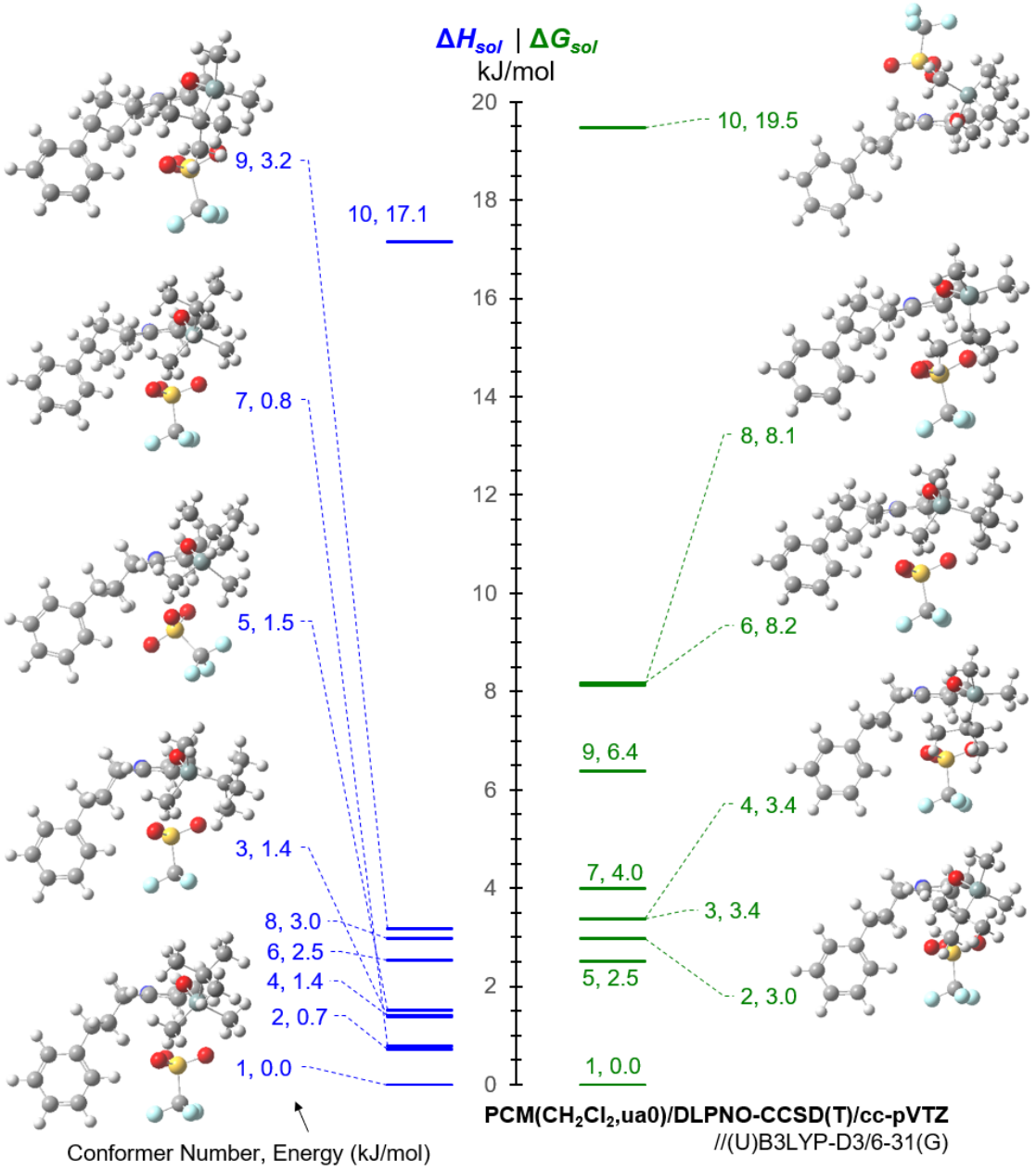

Figure S20. Conformational energetics (ΔH_{sol} | ΔG_{sol}, kJ/mol) of iminium salt **7im** calculated at the PCM(CH_2Cl_2,ua0)/DLPNO-CCSD(T)/cc-pVTZ//B3LYP-D3/6-31G(d) level of theory. [Gas phase conformer's numbering is retained to facilitate comparision. Conformers are assign number according to rel. ΔH_{298} at B3LYP-D3/6-31G(d). Single point solvation energies obtained at PCM(CH_2Cl_2,ua0)/B3LYP-D3/6-31G(d) level].

3. Reaction Energy Profiles (REPs)

Table S7. Reaction Energy Profiles (kJ/mol) for the DIBAL reduction of cation **6im**$^+$ and for concerted C-C bond migration (***anti*** and ***syn***) and N_2 elimination from the intermediate aminodiazonium ions **7ad**$^+$/**10ad**$^+$ that are formed during the conversion of alcohols **7**/**10** to iminium cations **8**/**15**.

6im$^+$ + DIBAL								
Level of theory		**Reactant** **6im**$^+$ + DIBAL	**Transition State** **TS**-*syn*	**Product** *trans*-**6**.Al(*i*-Bu)$_2$		**Reactant** **6im**$^+$ + DIBAL	**Transition State** **TS**-*anti*	**Product** *cis*-**6**.Al(*i*-Bu)$_2$
B3LYP-D3/6-31G(d) (level of optimization)	ΔG_{298}	0.0	54.5	-77.2		0.0	52.6	-70.4
	ΔH_{298}	0.0	-11.7	-140.4		0.0	-8.5	-138.6
PCM(CH_2Cl_2,ua0)/B3LYP-D3/6-31G(d) //B3LYP-D3/6-31G(d)	ΔG_{sol}	0.0	84.1	-49.8		0.0	79.5	-38.9
	ΔH_{sol}	0.0	16.6	-111.6		0.0	17.5	-106.9
DLPNO-CCSD(T)/cc-pVTZ //(U)B3LYP-D3/6-31G(d)	ΔG_{298}	0.0	69.7	-89.6		0.0	64.3	-81.2
	ΔH_{298}	0.0	3.8	-153.4		0.0	2.6	-150.4
PCM(CH_2Cl_2,ua0)/DLPNO-CCSD(T)/cc-pVTZ //B3LYP-D3/6-31G(d)	ΔG_{sol}	0.0	100.7	-61.4		0.0	91.2	-50.2
	ΔH_{sol}	0.0	32.2	-125.0		0.0	29.5	-118.7
Aminodiazonium ion **7ad**$^+$								
Level of theory		**Reactant** Aminodiazonium ion **7ad**$^+$	**Transition State** **TS**-*anti*	**Product** *trans*-**8im**$^+$ + N_2		**Reactant** Aminodiazonium ion **7ad**$^+$	**Transition State** **TS**-*syn*	**Product** *cis*-**8im**$^+$ + N_2
B3LYP-D3/6-31G(d) (level of optimization)	ΔG_{298}	0.0	51.5	-322.5		0.0	72.1	-322.2
	ΔH_{298}	0.0	49.4	-302.6		0.0	68.9	-297.1
PCM(CH_2Cl_2,ua0)/B3LYP-D3/6-31G(d) //B3LYP-D3/6-31G(d)	ΔG_{sol}	0.0	58.8	-315.3		0.0	74.1	-311.8
	ΔH_{sol}	0.0	56.7	-295.4		0.0	70.9	-286.7
DLPNO-CCSD(T)/cc-pVTZ //(U)B3LYP-D3/6-31G(d)	ΔG_{298}	0.0	46.9	-339.0		0.0	67.7	-341.9
	ΔH_{298}	0.0	45.3	-318.6		0.0	65.0	-316.3
PCM(CH_2Cl_2,ua0)/DLPNO-CCSD(T)/cc-pVTZ //B3LYP-D3/6-31G(d)	ΔG_{sol}	0.0	51.5	-334.5		0.0	67.0	-334.2
	ΔH_{sol}	0.0	49.5	-314.5		0.0	63.9	-309.0
Aminodiazonium ion 10ad$^+$								

Level of theory		**Reactant** Aminodiazonium ion **10ad$^+$**	**Transition State** TS-*anti*	**Product** (3*R*,7S)-**15im$^+$** + N_2		**Reactant** Aminodiazonium ion **10ad$^+$**	**Transition State** TS-*syn*	**Product** (3*R*,7*R*)-**15im$^+$** + N_2
B3LYP-D3/6-31G(d) (level of optimization)	ΔG_{298}	0.0	60.2	-333.3		0.0	67.0	-323.0
	ΔH_{298}	0.0	61.9	-314.2		0.0	68.2	-303.4
PCM(CH_2Cl_2,ua0)/B3LYP-D3/6-31G(d) //B3LYP-D3/6-31G(d)	ΔG_{sol}	0.0	61.1	-327.2		0.0	67.6	-315.5
	ΔH_{sol}	0.0	62.2	-308.8		0.0	68.3	-296.9
DLPNO-CCSD(T)/cc-pVTZ //(U)B3LYP-D3/6-31G(d)	ΔG_{298}	0.0	50.7	-352.1		0.0	59.4	-345.7
	ΔH_{298}	0.0	51.3	-334.0		0.0	59.6	-324.2
PCM(CH_2Cl_2,ua0)/DLPNO-CCSD(T)/cc-pVTZ //B3LYP-D3/6-31G(d)	ΔG_{sol}	0.0	52.9	-344.6		0.0	61.4	-336.9
	ΔH_{sol}	0.0	53.6	-326.5		0.0	61.6	-315.7

3.1. Reduction of **6im⁺** by DIBAL

3.1.1. Gas phase RES (gas phase optimization)

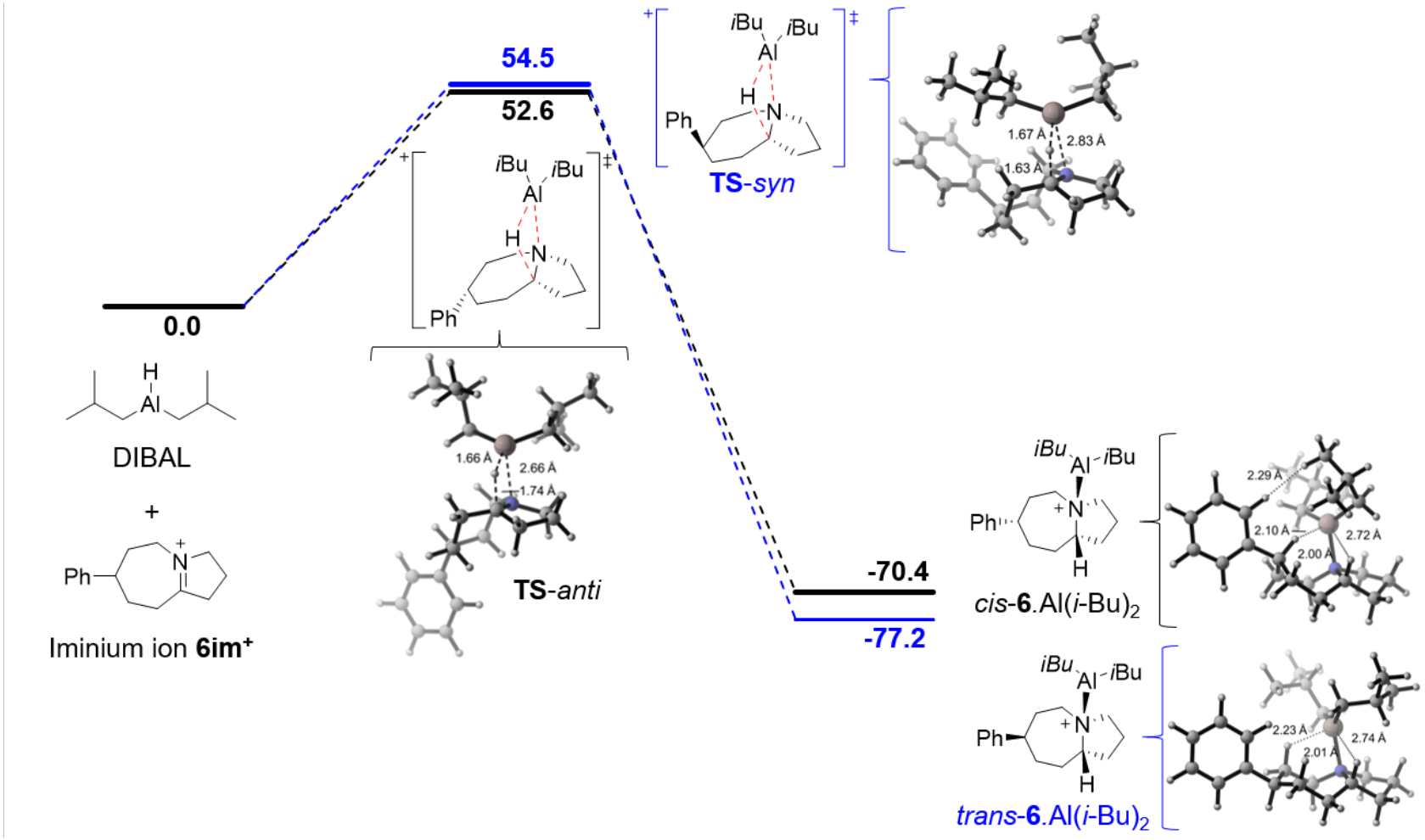

Figure S21. The gas phase REP (ΔG_{298}, in kJ/mol) for the reduction of cation **6im⁺** by DIBAL [(U)B3LYP-D3/6-31G(d) level of theory, based on best conformer].

3.1.2. Solvation corrected RES

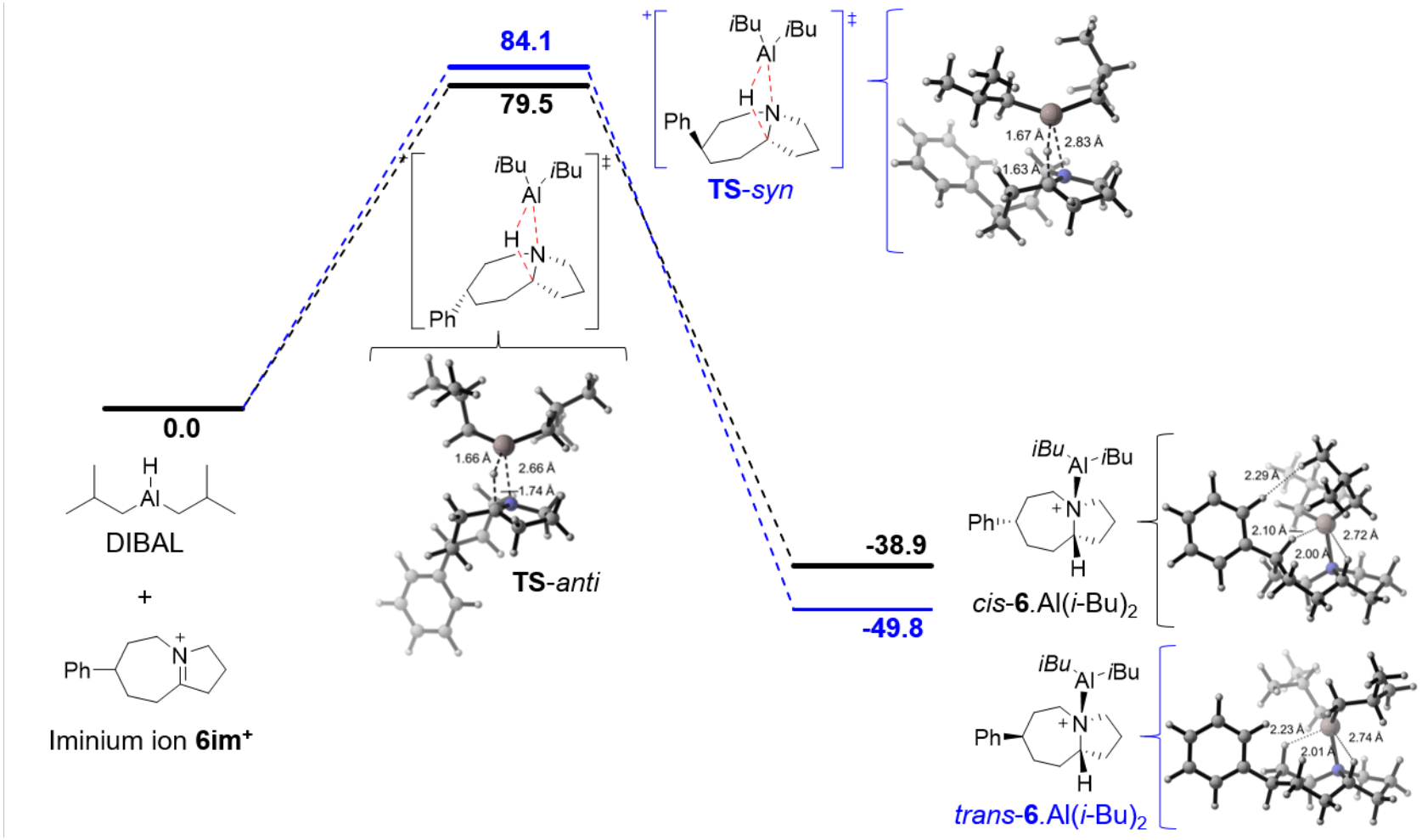

Figure S22. The single point implicit solvation corrected REP (ΔG_{sol}, in kJ/mol) for the reduction of cation **6im**$^+$ by DIBAL [PCM(CH_2Cl_2,ua0)/B3LYP-D3/6-31G(d)//B3LYP-D3/6-31G(d) level of theory, based on best conformer].

3.1.3. High level gas phase RES

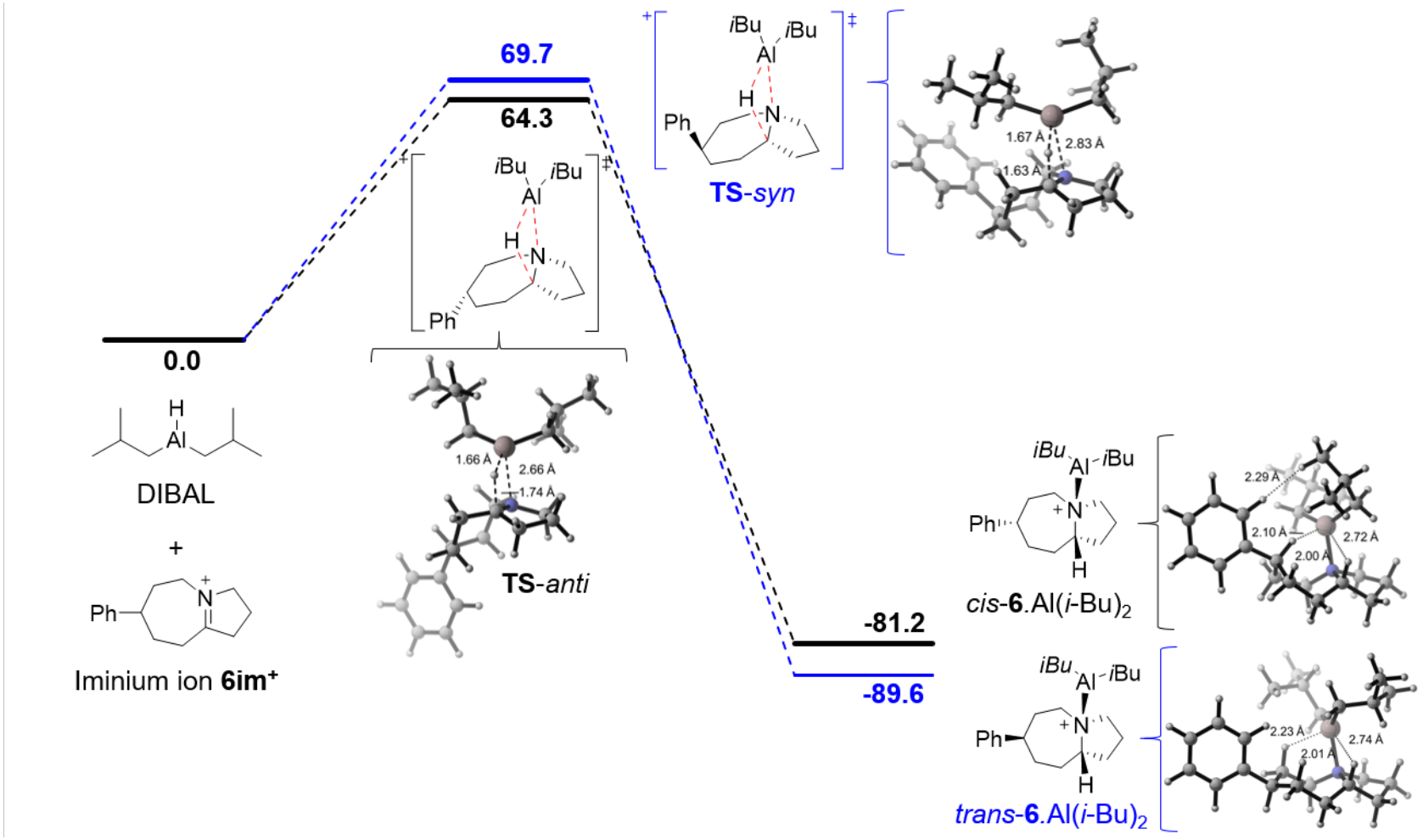

Figure S23. The high level gas phase REP (ΔG_{298}, in kJ/mol) for the reduction of cation **6im**$^+$ by DIBAL [DLPNO-CCSD(T)/cc-pVTZ//(U)B3LYP-D3/6-31G(d) level of theory, based on best conformer].

3.1.4. Solvation corrected high level RES

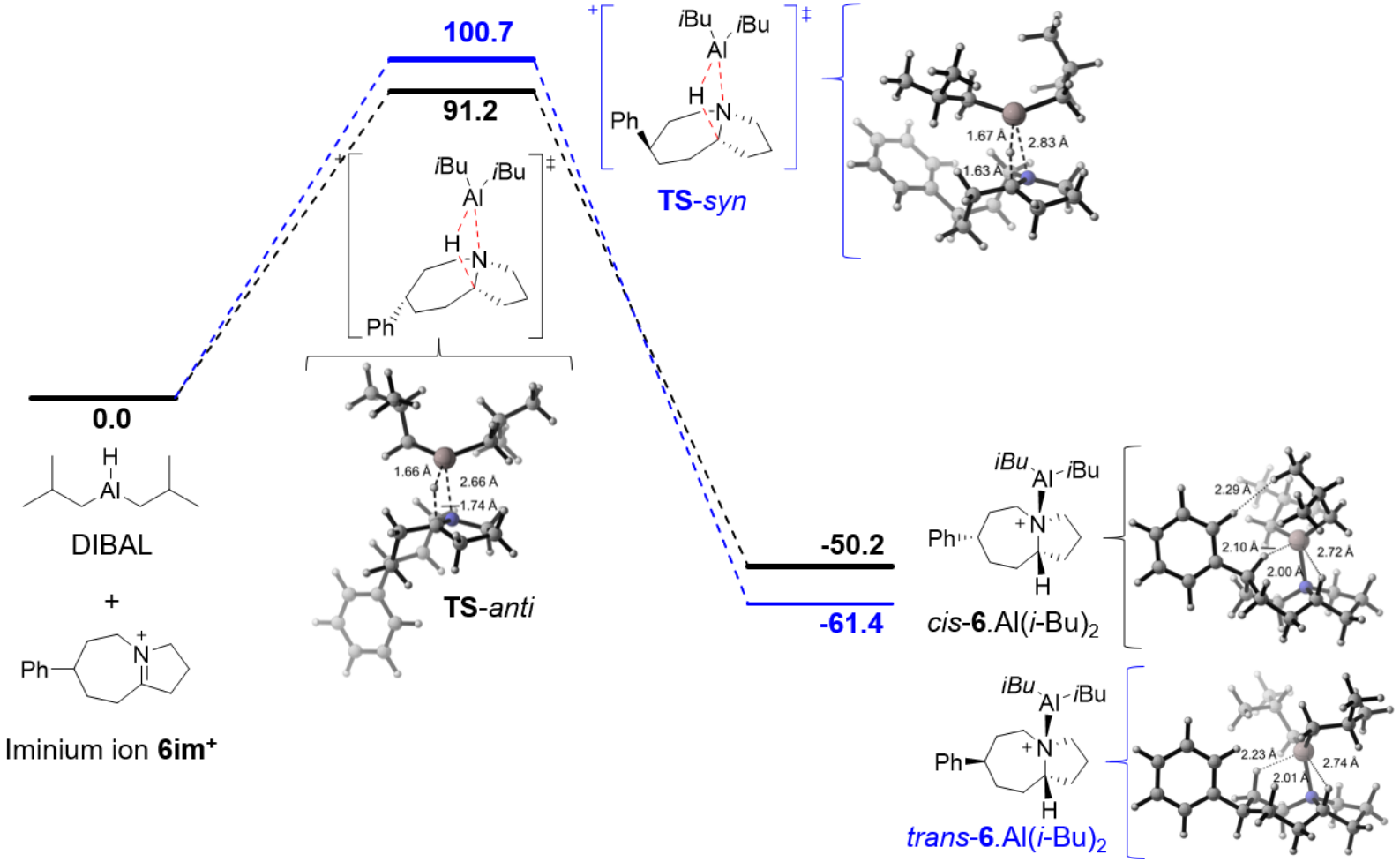

Figure S24. The single point implicit solvation corrected high level REP (ΔG_{sol}, in kJ/mol for the reduction of cation **6im**$^+$ by DIBAL [PCM(CH_2Cl_2,ua0)/DLPNO-CCSD(T)/cc-pVTZ//B3LYP-D3/6-31G(d) level of theory, based on best conformer].

3.2. Aminodiazonium ion **7ad⁺**

3.2.1. Gas phase RES (gas phase optimization)

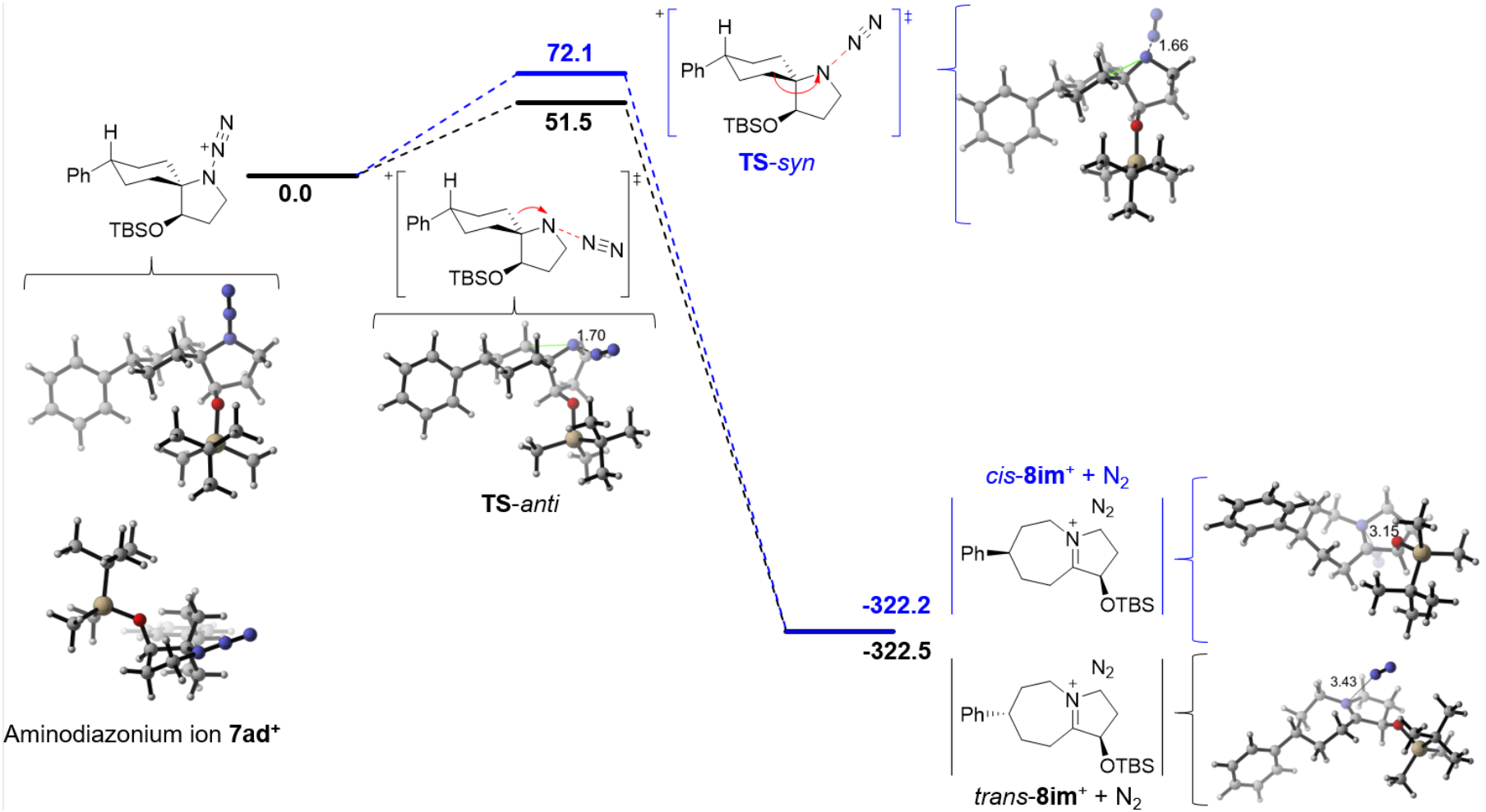

Figure S25. The gas phase REP (ΔG_{298}, in kJ/mol) for concerted C-C bond migration (***anti*** and ***syn***) and N_2 elimination from the intermediate aminodiazonium ion **7ad⁺** that is formed during the conversion of alcohol **7** to iminium cation **8** [(U)B3LYP-D3/6-31G(d) level of theory, based on best conformer].

3.2.2. Solvation corrected RES

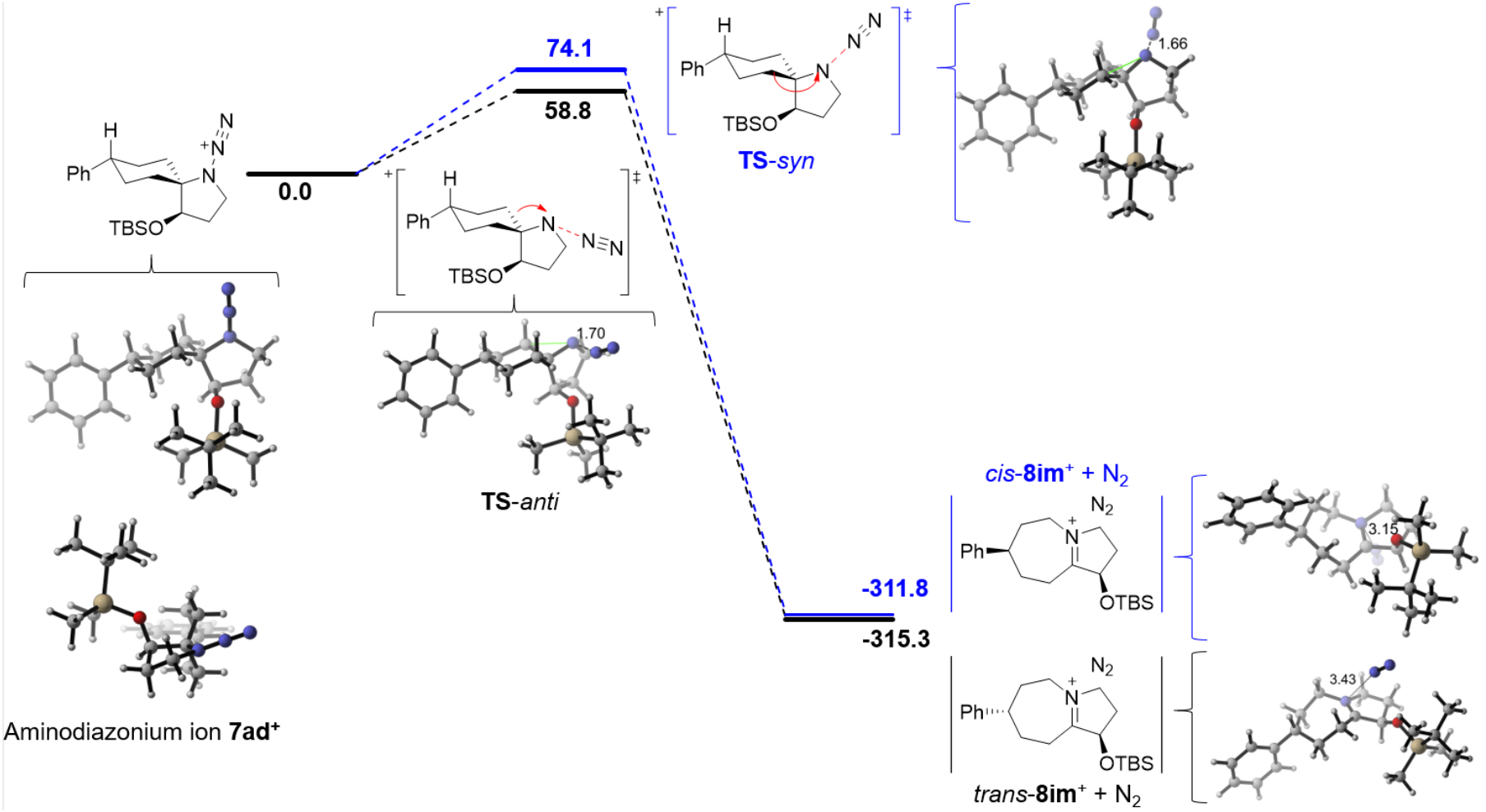

Figure S26. The single point implicit solvation corrected REP (ΔG_{sol}, in kJ/mol) for concerted C-C bond migration (***anti*** and ***syn***) and N_2 elimination from the intermediate aminodiazonium ion **7ad**$^+$ that is formed during the conversion of alcohol **7** to iminium cation **8** [PCM(CH_2Cl_2,ua0)/B3LYP-D3/6-31G(d)//B3LYP-D3/6-31G(d) level of theory, based on best conformer].

3.2.3. High level gas phase RES

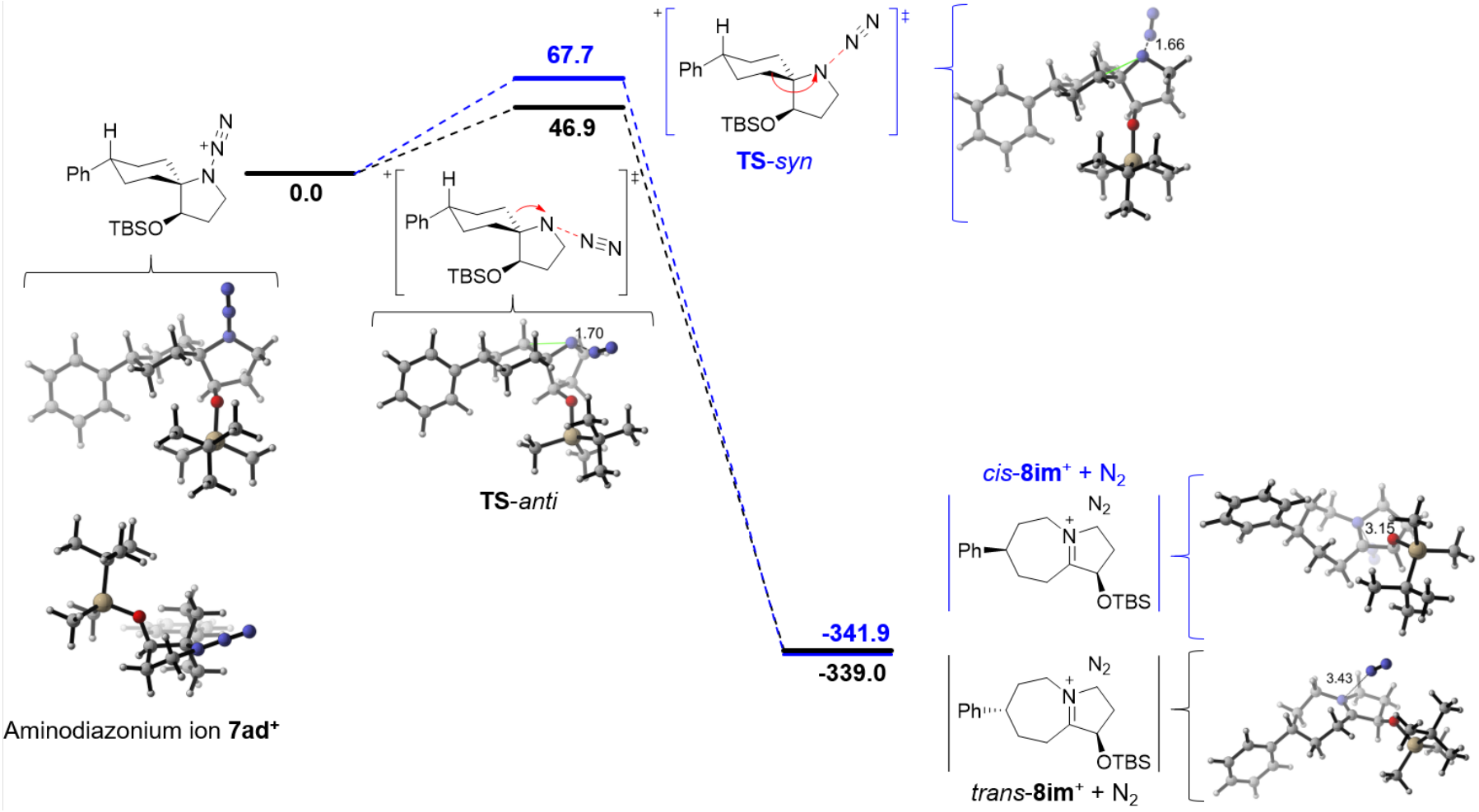

Figure S27. The high level gas phase REP (ΔG_{298}, in kJ/mol) for concerted C-C bond migration (***anti*** and ***syn***) and N_2 elimination from the intermediate aminodiazonium ion **7ad**$^+$ that is formed during the conversion of alcohol **7** to iminium cation **8** [DLPNO-CCSD(T)/cc-pVTZ//(U)B3LYP-D3/6-31G(d) level of theory, based on best conformer].

3.2.4. Solvation corrected high level RES

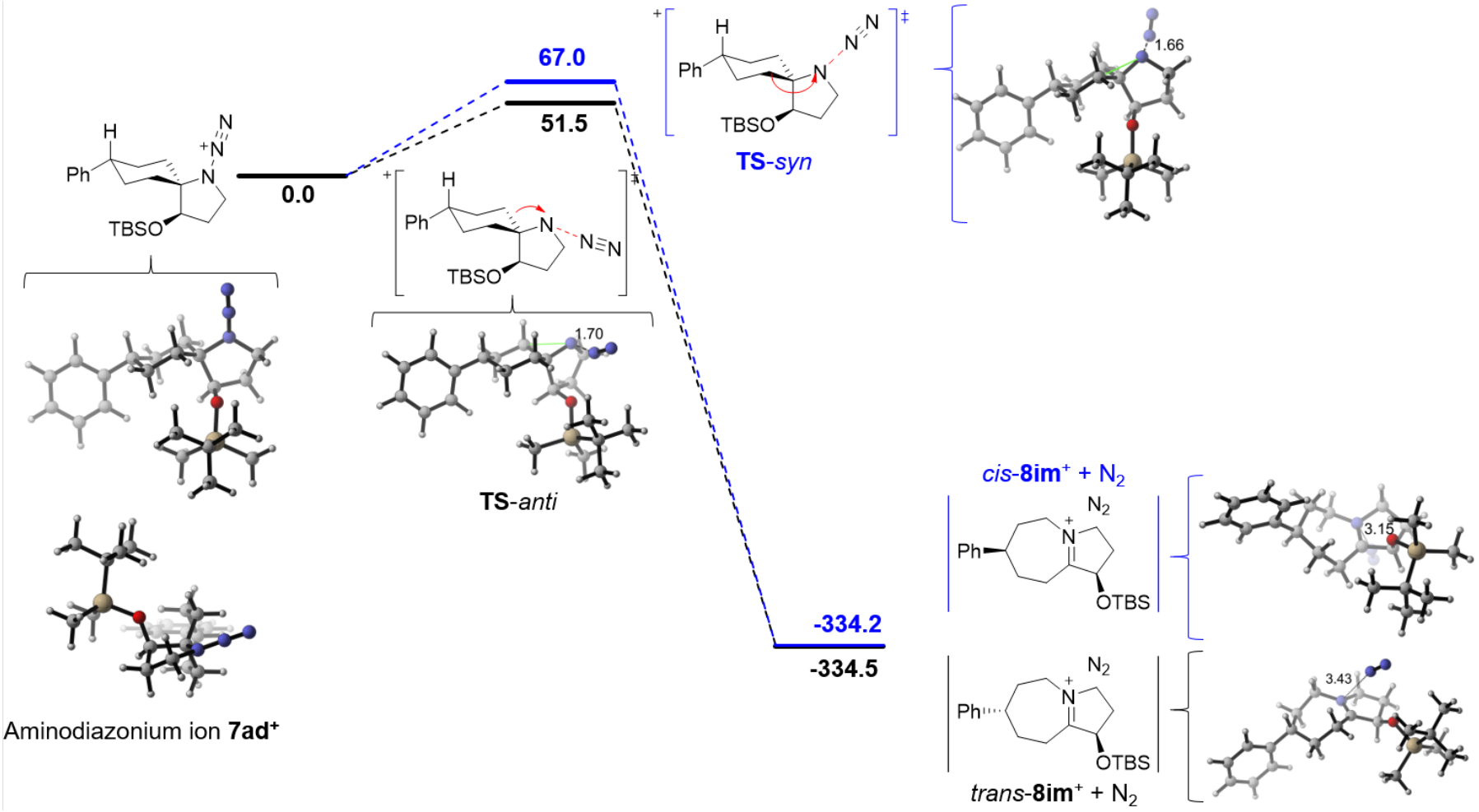

Figure S28. The single point implicit solvation corrected high level REP (ΔG_{sol}, in kJ/mol) for concerted C-C bond migration (***anti*** and ***syn***) and N_2 elimination from the intermediate aminodiazonium ion **7ad**$^+$ that is formed during the conversion of alcohol **7** to iminium cation **8** [PCM(CH_2Cl_2,ua0)/DLPNO-CCSD(T)/cc-pVTZ//B3LYP-D3/6-31G(d) level of theory, based on best conformer].

3.2.5. Structural Analysis

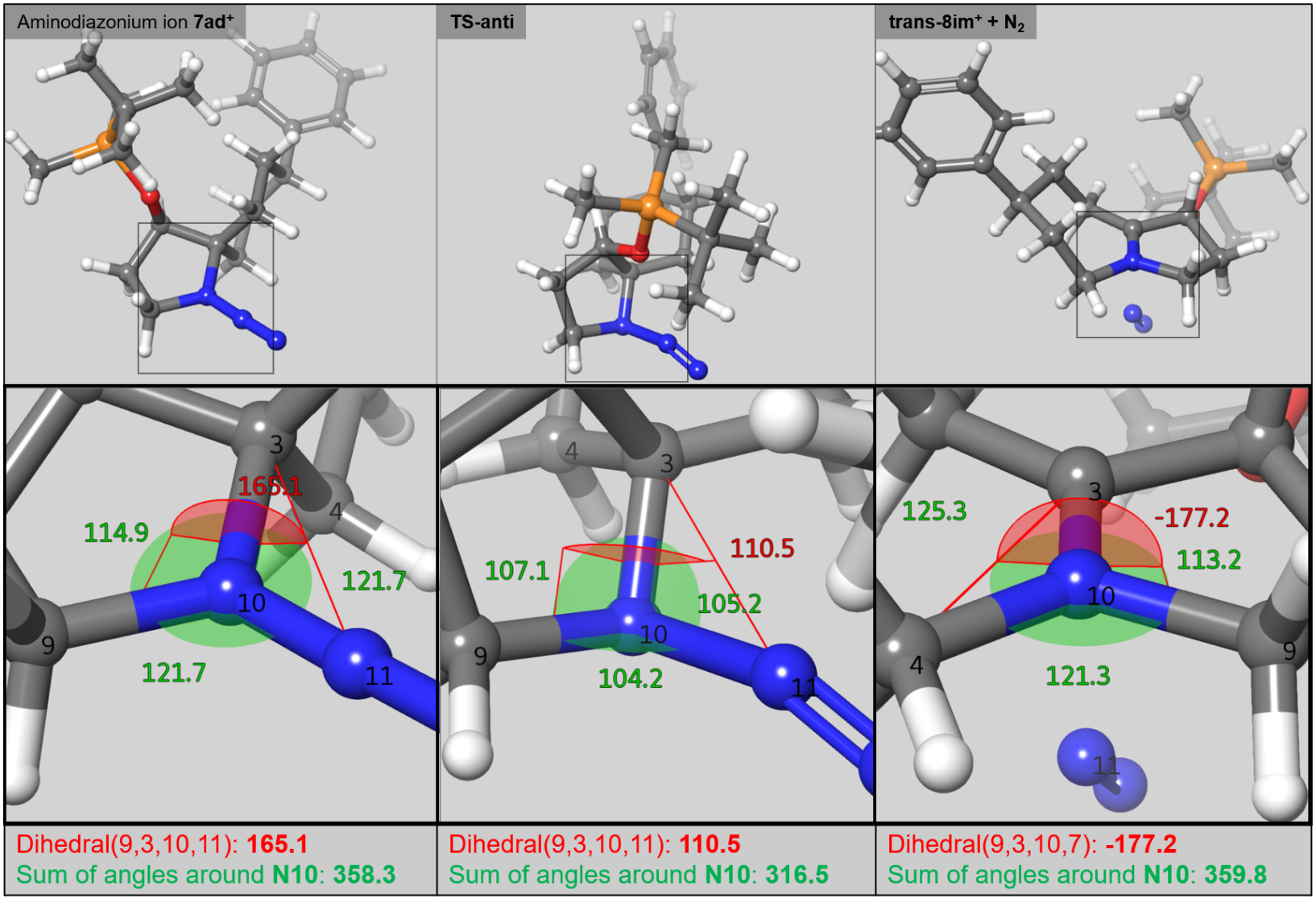

Figure S29. N10 pyrimidalization at transition state during concerted C-C bond migration (***anti***) and N_2 elimination from the intermediate aminodiazonium ion **7ad**$^+$ that is formed during the conversion of alcohol **7** to iminium cation **8** [(U)B3LYP-D3/6-31G(d) level of theory, based on best conformer].

3.3. Aminodiazonium ion **10ad⁺**

3.3.1. Gas phase RES (gas phase optimization)

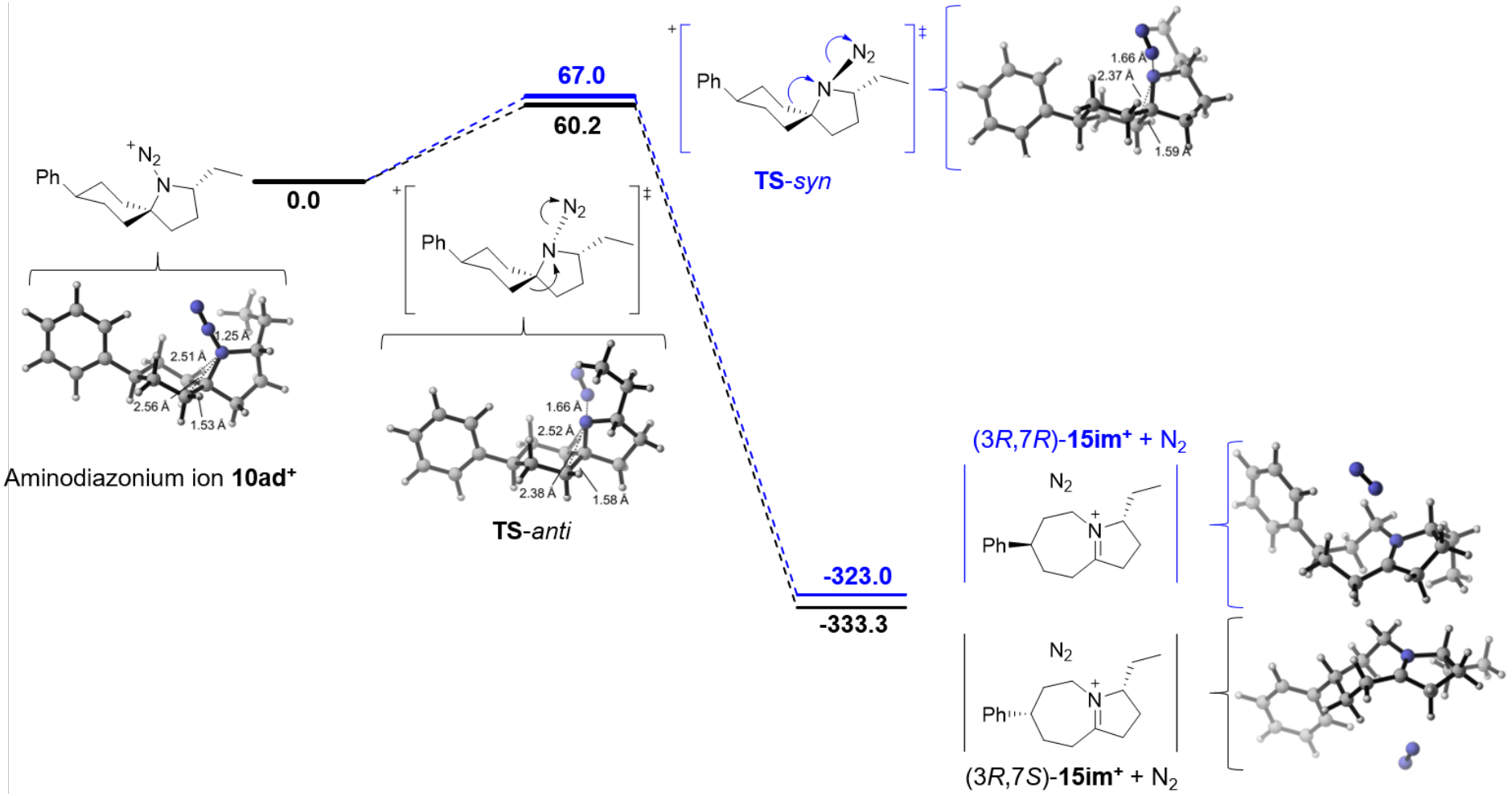

Figure S30. The gas phase REP (ΔG_{298}, in kJ/mol) for concerted C-C bond migration (***anti*** and ***syn***) and N_2 elimination from the intermediate aminodiazonium ion **10ad⁺** that is formed during the conversion of alcohol **10** to iminium cation **12** [(U)B3LYP-D3/6-31G(d) level of theory, based on best conformer].

3.3.2. Solvation corrected RES

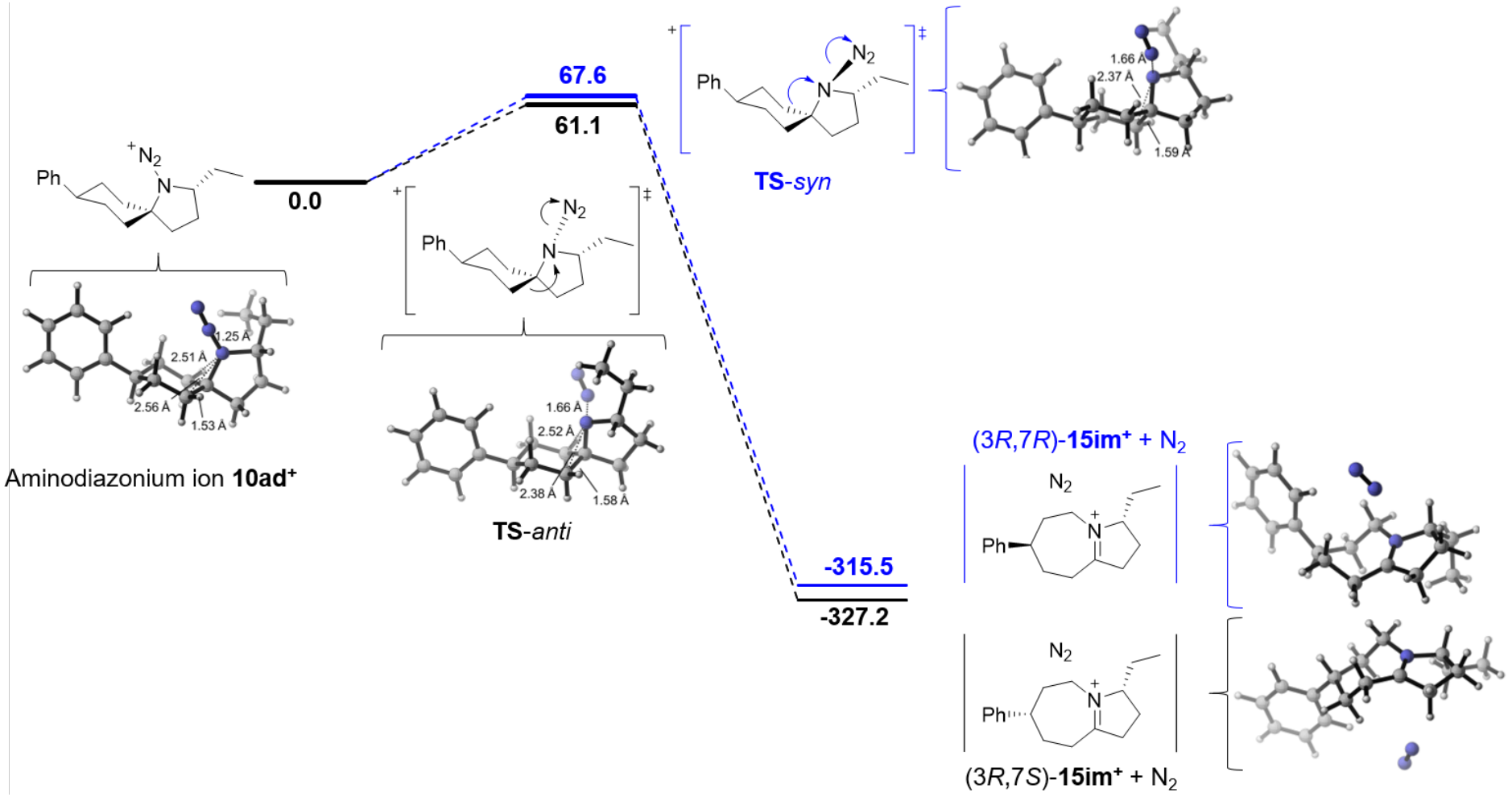

Figure S31. The single point implicit solvation corrected REP (ΔG_{sol}, in kJ/mol) for concerted C-C bond migration (***anti*** and ***syn***) and N_2 elimination from the intermediate aminodiazonium ion **10ad**$^+$ that is formed during the conversion of alcohol **10** to iminium cation **12** [PCM(CH_2Cl_2,ua0)/B3LYP-D3/6-31G(d)//B3LYP-D3/6-31G(d) level of theory, based on best conformer].

3.3.3. High level gas phase RES

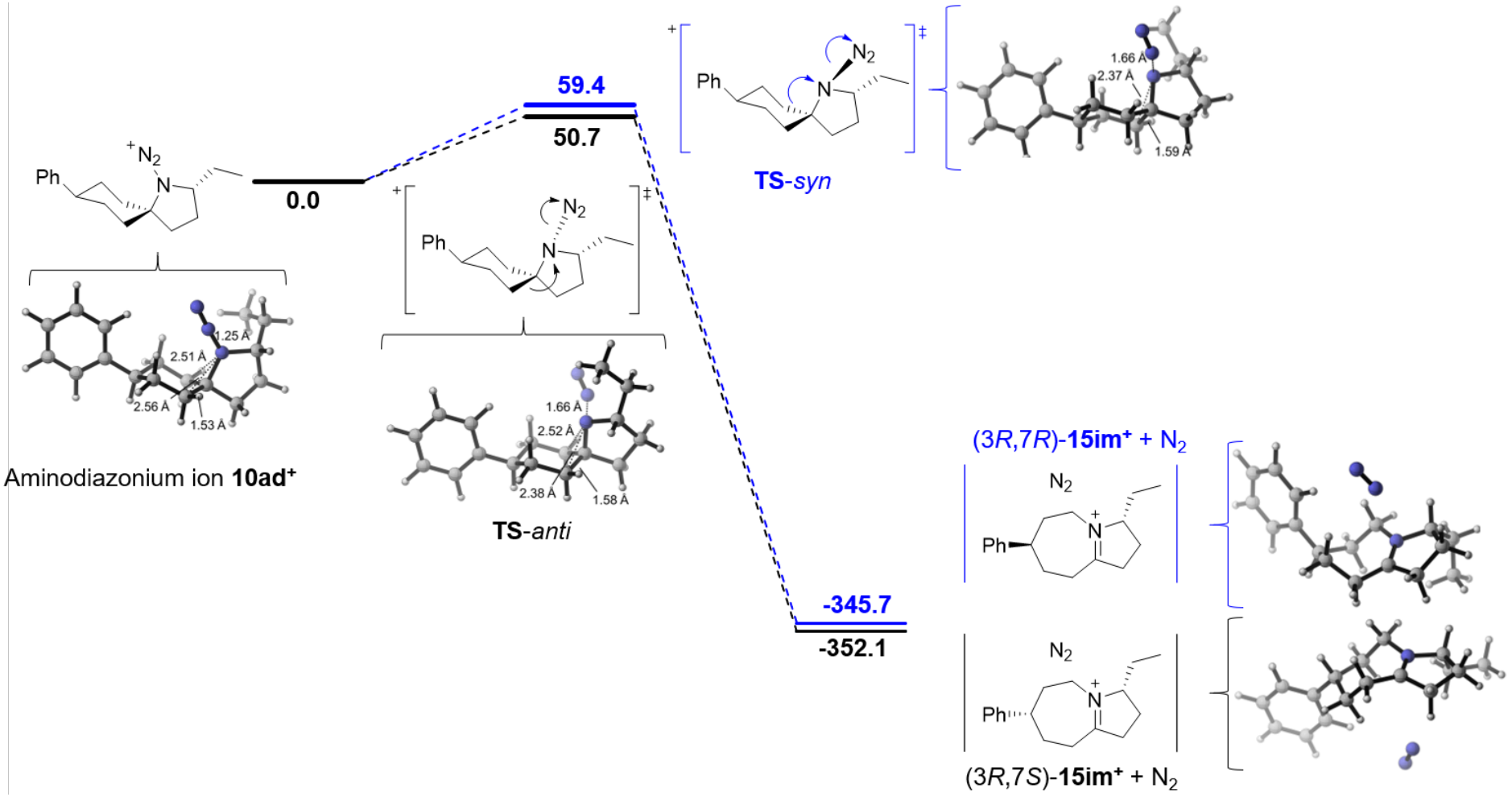

Figure S32. The gas phase REP (ΔG_{298}, in kJ/mol) for concerted C-C bond migration (***anti*** and ***syn***) and N_2 elimination from the intermediate aminodiazonium ion **10ad**$^+$ that is formed during the conversion of alcohol **10** to iminium cation **12** [DLPNO-CCSD(T)/cc-pVTZ//(U)B3LYP-D3/6-31G(d) level of theory, based on best conformer].

3.3.4. Solvation corrected high level RES

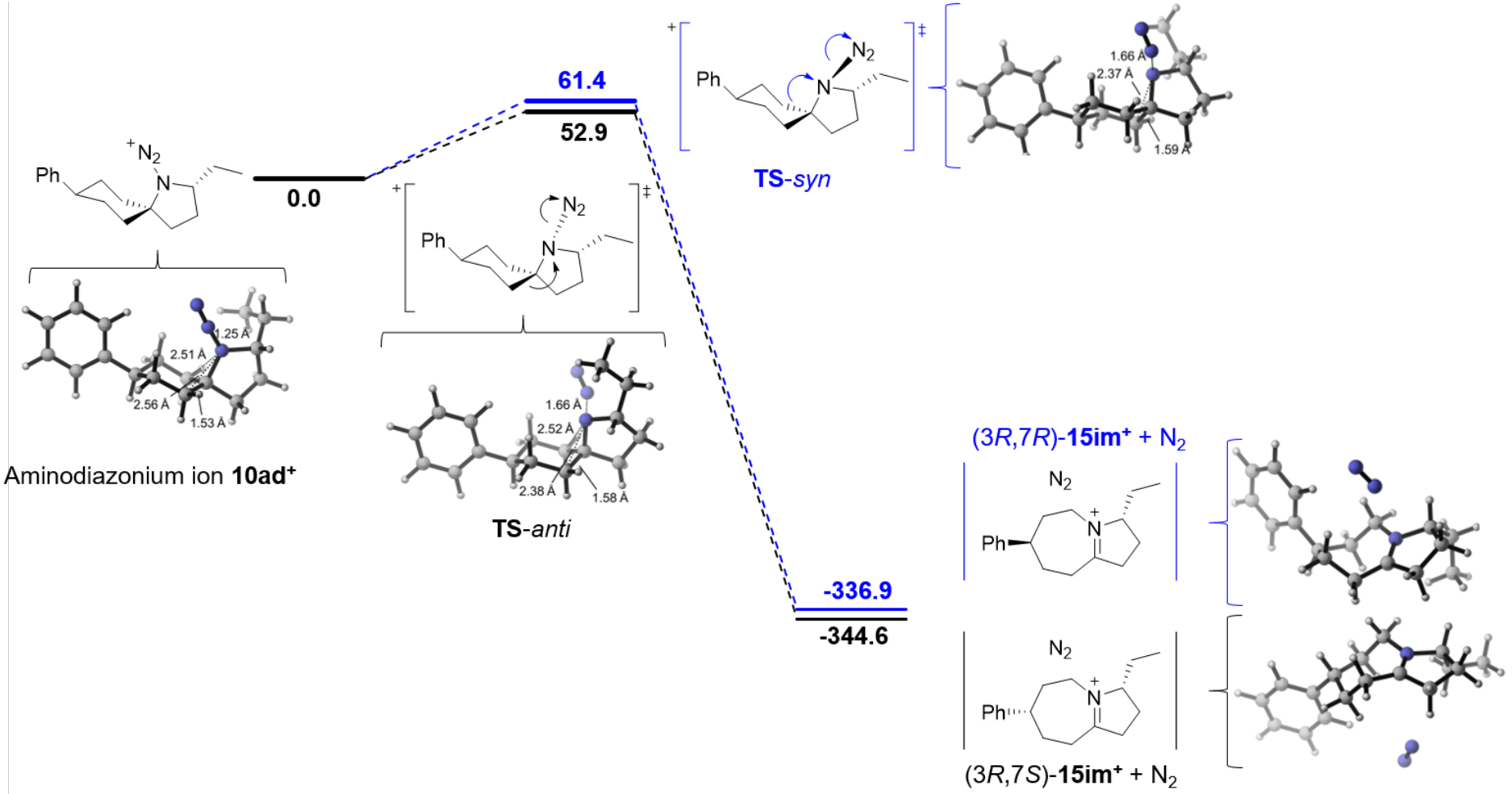

Figure S33. The single point implicit solvation corrected REP (ΔG_{sol}, in kJ/mol) for concerted C-C bond migration (***anti*** and ***syn***) and N_2 elimination from the intermediate aminodiazonium ion **10ad⁺** that is formed during the conversion of alcohol **10** to iminium cation **12** [PCM(CH_2Cl_2,ua0)/DLPNO-CCSD(T)/cc-pVTZ//B3LYP-D3/6-31G(d) level of theory, based on best conformer].

3.3.5. Structural Analysis

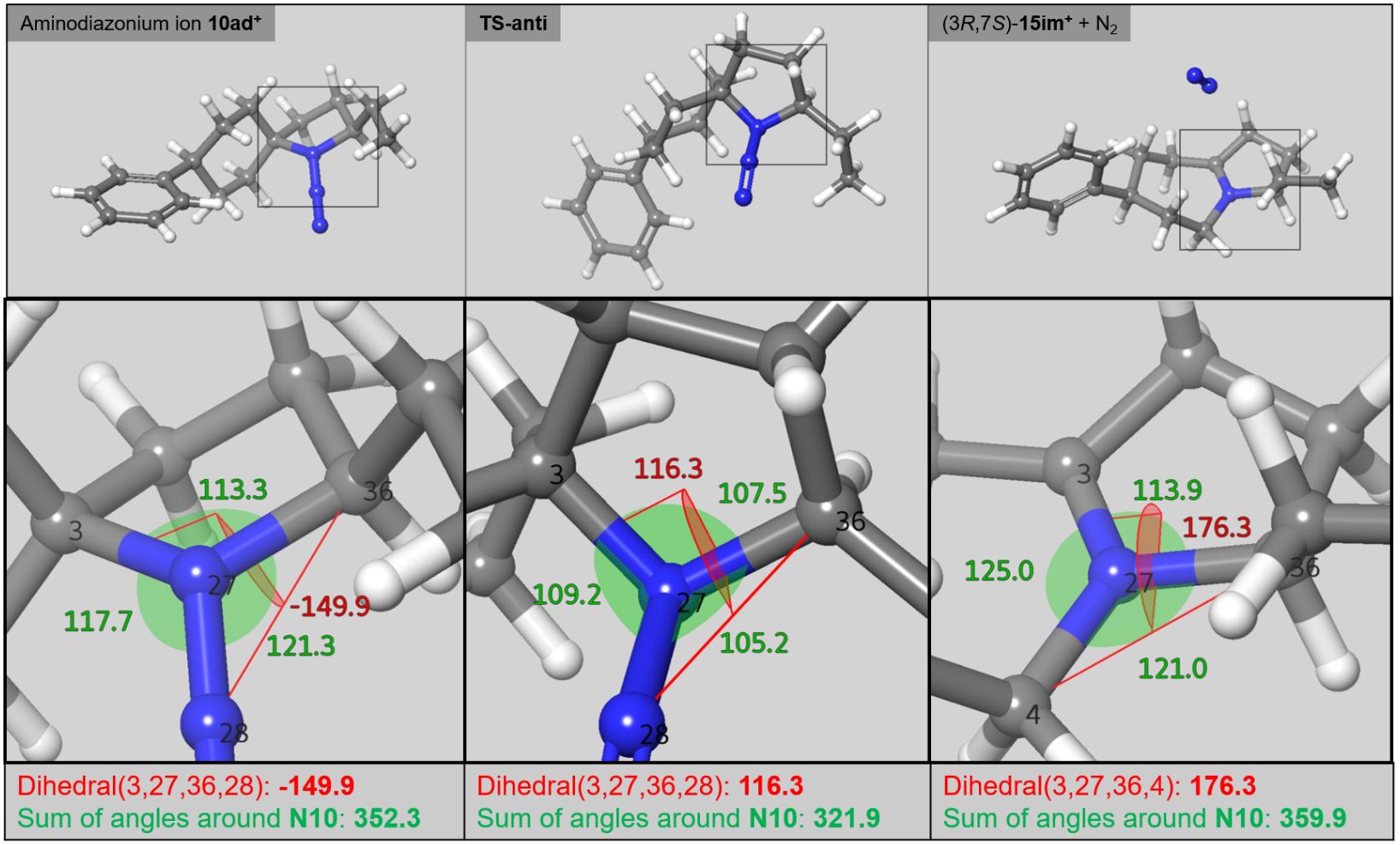

Figure S34. N27 pyrimidalization at transition state during concerted C-C bond migration (***anti***) and N_2 elimination from the intermediate aminodiazonium ion **10ad**$^+$ that is formed during the conversion of alcohol **7** to iminium cation **12** [(U)B3LYP-D3/6-31G(d) level of theory, based on best conformer].

The gas phase reaction energy profile for the concerted C-C bond migration and N_2 elimination from the intermediate aminodiazonium ion (that is formed during the Schmidt rearrangement of alcohol **7** to iminium cation **7im$^+$**) indicates that migration of the C-C bond *anti* to the OTBS group (black pathway, Figure S7) is 20.6 kJ/mol more favourable than the *syn* pathway (blue pathway, Figure S7) with TS barriers of 51.5 kJ/mol vs. 72.1 kJ/mol, respectively at the (U)B3LYP-D3/6-31G(d) level of theory. The product complexes formed as a result of *anti* and *syn* migration are, in contrast, almost isoenergetic. The conformational analysis of isolated iminium cation (**7im$^+$**) reveals that *cis* cation generated from the *syn* pathway is energetically more favourable than *trans* cation. This indicates that the product observe experimentally is kinetically selected.

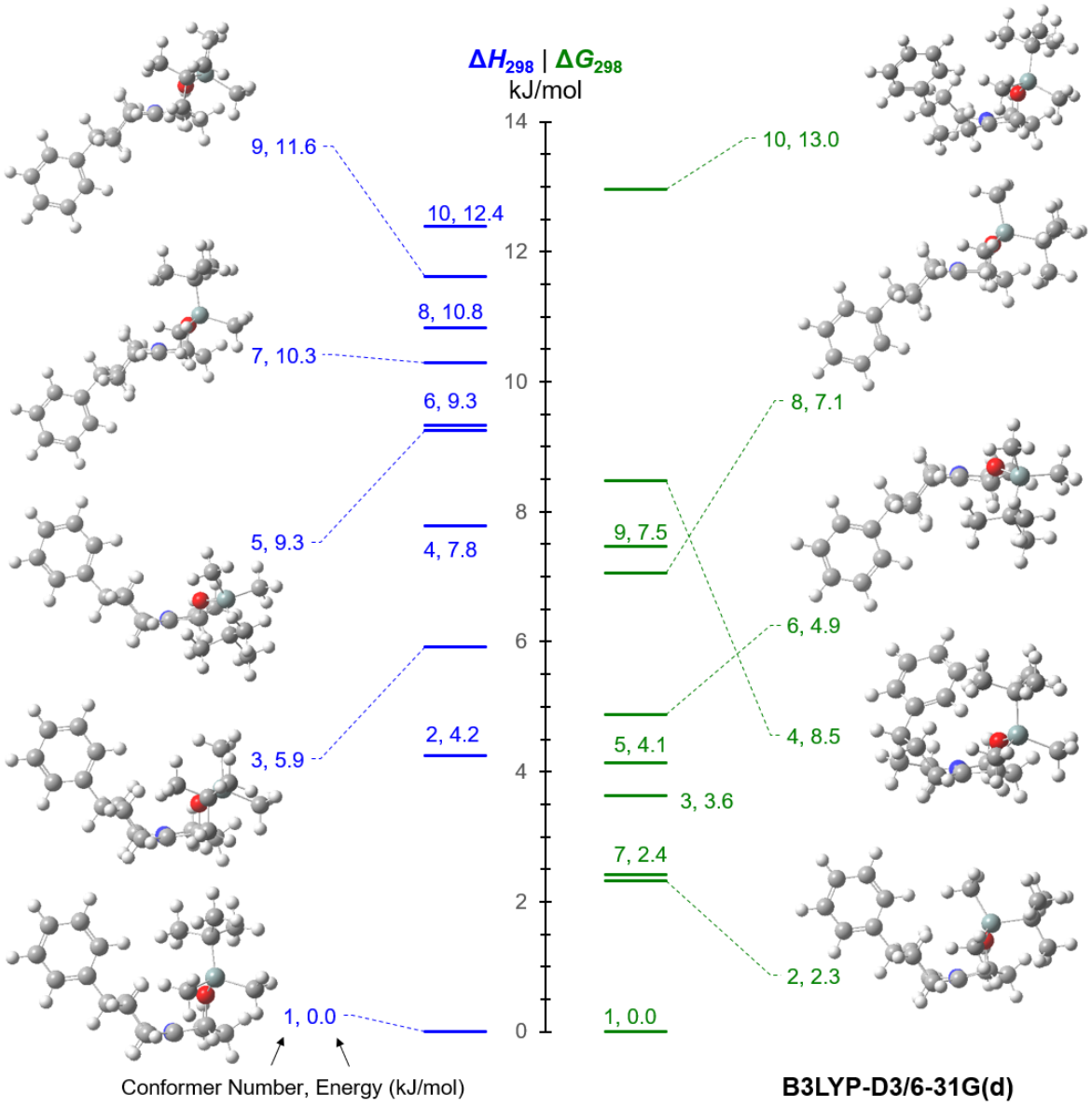

Figure S35. Conformational energetics (ΔH_{298} | ΔG_{298}, kJ/mol) of iminium cation **7im$^+$** calculated at the B3LYP-D3/6-31G(d) level of theory in the gas phase.

4. QM Data

Table S8. QM properties for gas phase optimized conformers calculated at the (U)B3LYP-D3\6-31G(d) level of theory.

		B3LYP-D3/6-31G(d)									ΔGsolv (kcal/mol) PCM(CH_2Cl_2,ua0) /B3LYP-D3/6-31G(d)	E_{tot} DLPNO-CCSD(T)\cc-pVTZ
SI	**System (filename)**	**ΔE_{tot} (hartree)**	**$HOMO_E$ (hartree)**	**$LUMO_E$ (hartree)**	**Low Frequency**			**corr. ZPE (hartree)**	**corr. ΔH (hartree)**	**corr. ΔG (hartree)**		
	Conformational Energetics (CEs)											
	Iminium cation **6im$^+$**											
1	iminiumIon_6a_1	-638.2242804	-0.33840	-0.20963	-3	0	0	0.324389	0.338971	0.283352	-38.1	-637.0019850
2	iminiumIon_6a_7	-638.2223609	-0.36403	-0.20153	-5	0	0	0.325353	0.339464	0.286069	-36.4	-637.0004436
3	iminiumIon_6a_2	-638.2214201	-0.34682	-0.20746	-8	-4	0	0.324988	0.339347	0.284102	-37.2	-636.9993636
4	iminiumIon_6a_9	-638.2202822	-0.36091	-0.20356	-2	0	0	0.325236	0.339621	0.284633	-36.6	-636.9982794
5	iminiumIon_6a_4	-638.2195678	-0.34091	-0.20825	-4	-2	0	0.324495	0.338999	0.283422	-37.9	-636.9981730
6	iminiumIon_6a_3	-638.2195372	-0.34073	-0.20889	-2	0	0	0.324539	0.339049	0.283451	-37.9	-636.9982330
7	iminiumIon_6a_5	-638.2186282	-0.34615	-0.20897	-3	0	0	0.324799	0.339332	0.283226	-37.4	-636.9959801
8	iminiumIon_6a_6	-638.2176754	-0.33731	-0.20980	-5	-2	0	0.324225	0.338940	0.282584	-38.2	-636.9964079
9	iminiumIon_6a_8	-638.2172551	-0.33792	-0.20980	-4	0	0	0.324416	0.339110	0.282815	-38.1	-636.9958823
	Iminium salt **6im**											
10	cmp_6a_23	-1599.8869402	-0.23487	-0.06543	-7	-3	0	0.354160	0.377257	0.301260	-11.4	-1597.5742975
11	cmp_6a_37	-1599.8864307	-0.23308	-0.07441	-5	-3	0	0.353978	0.377264	0.300285	-12.0	-1597.5725793
12	cmp_6a_5	-1599.8851542	-0.23470	-0.06815	-1	0	0	0.354375	0.377379	0.301898	-10.5	-1597.5738859
13	cmp_6a_2	-1599.8845932	-0.23103	-0.06654	-5	0	0	0.353692	0.376978	0.299473	-11.5	-1597.5738788
14	cmp_6a_9	-1599.8848085	-0.23475	-0.06779	-4	0	0	0.354202	0.377315	0.301226	-10.7	-1597.5737644
15	cmp_6a_49	-1599.8845573	-0.23639	-0.06441	-5	-2	0	0.354183	0.377321	0.300923	-10.7	-1597.5733949
16	cmp_6a_43	-1599.8832352	-0.23315	-0.06986	-5	-2	0	0.354578	0.377560	0.302145	-10.8	-1597.5694841
17	cmp_6a_8	-1599.8819134	-0.23420	-0.06627	-4	-2	0	0.354180	0.377328	0.300681	-10.7	-1597.5708105
18	cmp_6a_53	-1599.8819831	-0.23431	-0.06960	-7	-4	-1	0.354297	0.377548	0.300823	-10.9	-1597.5694695
19	cmp_6a_47	-1599.8816231	-0.23421	-0.06323	-3	-1	0	0.354495	0.377571	0.301799	-11.1	-1597.5698436
20	cmp_6a_7	-1599.8811020	-0.23054	-0.06747	-5	0	0	0.354102	0.377228	0.300732	-11.3	
21	cmp_6a_36	-1599.8808026	-0.23275	-0.07185	-5	-2	0	0.354079	0.377379	0.300435	-11.5	
22	cmp_6a_28	-1599.8805125	-0.23043	-0.06634	-5	-3	0	0.353898	0.377138	0.299892	-11.4	
23	cmp_6a_6	-1599.8797334	-0.23111	-0.06629	-3	0	0	0.353757	0.377026	0.299765	-11.2	
24	cmp_6a_22	-1599.8785335	-0.23112	-0.06885	-3	-1	0	0.353552	0.376971	0.298841	-11.6	
25	cmp_6a_13	-1599.8799369	-0.23169	-0.06650	-3	0	0	0.354069	0.377274	0.300298	-11.1	
26	cmp_6a_14	-1599.8810121	-0.22912	-0.06376	-7	0	0	0.354318	0.377295	0.301498	-10.8	
27	cmp_6a_18	-1599.8799100	-0.23104	-0.06643	-4	-3	0	0.354030	0.377205	0.300430	-11.4	
28	cmp_6a_40	-1599.8803255	-0.23099	-0.06748	-4	-1	0	0.354202	0.377275	0.301169	-11.3	

29	cmp_6a_26	-1599.8809377	-0.22971	-0.06372	-3	0	0	0.354621	0.377543	0.301919	-10.8	
30	cmp_6a_39	-1599.8797887	-0.22983	-0.06246	-4	-1	0	0.354584	0.377592	0.301387	-11.0	
31	cmp_6a_46	-1599.8799947	-0.23243	-0.05876	-3	-3	0	0.354769	0.377642	0.301944	-11.3	
32	cmp_6a_45	-1599.8793896	-0.23068	-0.06259	-5	-3	0	0.354769	0.377750	0.301872	-10.7	
33	cmp_6a_50	-1599.8791235	-0.23442	-0.05785	-2	0	0	0.354988	0.377826	0.302238	-11.0	
	Iminium cation **7im**$^{+}$											
34	Imlon_7a_t_4	-1240.1150273	-0.33418	-0.20152	-3	0	0	0.516703	0.543909	0.459500	-34.5	-1237.9034003
35	Imlon_7a_t_2	-1240.1147827	-0.33357	-0.20079	-4	-2	0	0.516614	0.544033	0.458317	-34.5	-1237.9041265
36	Imlon_7a_t_3	-1240.1147743	-0.33362	-0.20077	-2	0	0	0.516999	0.544228	0.460072	-34.4	-1237.9034942
37	Imlon_7a_t_1	-1240.1143880	-0.33342	-0.20104	-2	0	0	0.516874	0.544145	0.459847	-34.2	-1237.9032760
38	Imlon_7a_t_6	-1240.1144001	-0.34072	-0.19838	-1	0	0	0.517607	0.544540	0.460870	-33.7	-1237.9030345
39	Imlon_7a_t_7	-1240.1135245	-0.34096	-0.19814	-3	-2	0	0.517629	0.544588	0.460645	-33.5	-1237.9020237
40	Imlon_7a_t_5	-1240.1134015	-0.34045	-0.19867	0	0	0	0.517710	0.544640	0.461470	-33.4	-1237.9020775
41	Imlon_7a_t_16	-1240.1126929	-0.33479	-0.20393	-6	-3	0	0.516826	0.543985	0.460305	-35.2	-1237.9009109
42	Imlon_7a_t_9	-1240.1121883	-0.34096	-0.19959	-5	0	0	0.517326	0.544341	0.460126	-33.9	-1237.9008775
43	Imlon_7a_t_11	-1240.1113662	-0.33534	-0.19873	-4	-2	0	0.517007	0.544155	0.460020	-34.0	-1237.9005471
44	Imlon_7a_t_15	-1240.1112266	-0.33552	-0.19863	-7	-2	0	0.516821	0.544096	0.458896	-34.1	
45	Imlon_7a_t_12	-1240.1105914	-0.33579	-0.19921	-1	0	0	0.517083	0.544264	0.459920	-34.2	
46	Imlon_7a_t_10	-1240.1104598	-0.33520	-0.19883	-2	0	0	0.516974	0.544157	0.459881	-33.9	
47	Imlon_7a_t_14	-1240.1101667	-0.33568	-0.19913	-4	0	0	0.516721	0.543926	0.459459	-34.3	
48	Imlon_7a_t_8	-1240.1103630	-0.33522	-0.19931	0	0	0	0.516930	0.544166	0.459600	-34.0	
49	Imlon_7a_t_17	-1240.1106431	-0.33564	-0.19850	-3	-1	0	0.517144	0.544261	0.460229	-34.1	
50	Imlon_7a_t_13	-1240.1105434	-0.33971	-0.19988	-6	-1	0	0.517414	0.544559	0.460278	-33.5	
	Iminium salt **7im**											
51	complex_7a_1	-2201.7811904	-0.23776	-0.07919	-4	0	0	0.546714	0.582559	0.477655	-9.5	-2198.4774103
52	complex_7a_4	-2201.7811678	-0.23772	-0.07784	-4	-3	0	0.546968	0.582705	0.478661	-9.7	-2198.4770599
53	complex_7a_6	-2201.7809693	-0.23742	-0.07859	-4	0	0	0.546831	0.582603	0.478460	-9.7	-2198.4767060
54	complex_7a_27	-2201.7808646	-0.23743	-0.07733	-6	-4	-2	0.546954	0.582703	0.478552	-9.5	-2198.4770868
55	complex_7a_14	-2201.7799417	-0.23643	-0.07596	-4	-4	0	0.546654	0.582496	0.477974	-9.8	-2198.4762661
56	complex_7a_41	-2201.7800016	-0.24079	-0.06952	-3	-1	0	0.547131	0.582685	0.479923	-8.8	-2198.4777286
57	complex_7a_32	-2201.7798283	-0.24126	-0.06925	-3	-1	0	0.547005	0.582631	0.478950	-8.7	-2198.4784670
58	complex_7a_52	-2201.7797137	-0.24085	-0.06922	-4	-2	0	0.547049	0.582666	0.479721	-8.7	-2198.4777267
59	complex_7a_25	-2201.7796536	-0.24031	-0.06920	0	0	0	0.547059	0.582711	0.479032	-8.7	-2198.4776917
60	complex_7a_68	-2201.7743923	-0.24156	-0.06477	-3	0	0	0.546658	0.582335	0.478316	-9.4	-2198.4708531
61	complex_7a_40	-2201.7742628	-0.23791	-0.06221	-4	-3	0	0.546561	0.582534	0.476023	-9.5	
62	complex_7a_59	-2201.7732819	-0.23766	-0.06423	0	0	0	0.546573	0.582265	0.478031	-9.8	
63	complex_7a_43	-2201.7734816	-0.23778	-0.06335	-3	-1	0	0.546733	0.582672	0.477225	-9.5	
64	complex_7a_16	-2201.7729824	-0.23080	-0.06620	-4	0	0	0.547013	0.582427	0.480595	-9.3	

65	complex_7a_53	-2201.7731890	-0.23561	-0.06379	-5	-3	-2	0.546781	0.582662	0.477289	-9.6	
66	complex_7a_54	-2201.7728209	-0.23734	-0.06705	-7	-3	0	0.546963	0.582707	0.478181	-10.7	
67	complex_7a_38	-2201.7723623	-0.23549	-0.06392	-5	-3	0	0.546947	0.582799	0.477695	-9.5	
68	complex_7a_30	-2201.7718455	-0.23301	-0.06320	-3	-1	0	0.546832	0.582667	0.478029	-10.0	
69	complex_7a_101	-2201.7715668	-0.23233	-0.06811	-4	0	0	0.546789	0.582436	0.479838	-11.1	
70	complex_7a_55	-2201.7715196	-0.23543	-0.07121	-3	0	0	0.546472	0.582458	0.476312	-9.8	
71	complex_7a_103	-2201.7716960	-0.23463	-0.06295	-1	-1	0	0.547087	0.582693	0.479843	-9.2	
72	complex_7a_48	-2201.7712683	-0.23598	-0.07141	-4	-2	0	0.546679	0.582604	0.476765	-9.7	
73	complex_7a_58	-2201.7708263	-0.23374	-0.06758	-4	0	0	0.546900	0.582558	0.479580	-10.0	
74	complex_7a_51	-2201.7706976	-0.23700	-0.07071	-8	-4	-3	0.546523	0.582473	0.476486	-9.7	
75	complex_7a_110	-2201.7707494	-0.23621	-0.05847	-2	0	0	0.547458	0.582779	0.480326	-10.1	
76	complex_7a_61	-2201.7703375	-0.23515	-0.06670	-1	0	0	0.546750	0.582433	0.479109	-10.2	
77	complex_7a_111	-2201.7705230	-0.23887	-0.05793	-5	-4	0	0.547357	0.582708	0.480280	-9.6	
78	complex_7a_46	-2201.7701557	-0.23370	-0.07009	-5	-3	-2	0.546333	0.582409	0.476546	-10.1	
79	complex_7a_49	-2201.7702965	-0.23214	-0.06173	-2	0	0	0.546817	0.582731	0.478139	-10.4	
80	complex_7a_67	-2201.7700521	-0.23566	-0.06366	-6	-2	0	0.547334	0.582768	0.478988	-9.0	
81	complex_7a_66	-2201.7693573	-0.23168	-0.06827	-2	0	0	0.546502	0.582319	0.479169	-11.4	
82	complex_7a_13	-2201.7694194	-0.23160	-0.06533	-4	-4	-1	0.546377	0.582430	0.475983	-10.2	
83	complex_7a_42	-2201.7692649	-0.23146	-0.06543	-4	0	0	0.546348	0.582408	0.476189	-10.2	
84	complex_7a_12	-2201.7692654	-0.23146	-0.06543	-4	0	0	0.546349	0.582409	0.476194	-10.2	
85	complex_7a_47	-2201.7691871	-0.23076	-0.06395	-1	0	0	0.546210	0.582380	0.475881	-10.6	
86	complex_7a_65	-2201.7687547	-0.23240	-0.06782	-3	-2	0	0.546654	0.582421	0.478426	-10.8	
87	complex_7a_107	-2201.7680268	-0.23286	-0.07037	-2	0	0	0.546728	0.582381	0.478421	-10.3	
88	complex_7a_106	-2201.7678197	-0.23473	-0.07417	-3	-1	0	0.546896	0.582551	0.480161	-11.4	
89	complex_7a_112	-2201.7674168	-0.23297	-0.05499	-5	-1	0	0.546594	0.582356	0.477732	-11.3	
90	complex_7a_60	-2201.7668204	-0.22524	-0.06695	-3	-1	0	0.545849	0.581892	0.476030	-12.7	
91	complex_7a_70	-2201.7676226	-0.23534	-0.06052	-2	0	0	0.547434	0.582776	0.480707	-10.6	
92	complex_7a_62	-2201.7660986	-0.22690	-0.06547	-4	0	0	0.546895	0.582507	0.479597	-12.6	
93	complex_7a_82	-2201.7646796	-0.22930	-0.07114	-5	-3	-3	0.546339	0.582121	0.478480	-13.1	
94	complex_7a_69	-2201.7648628	-0.22377	-0.06441	-3	0	0	0.547027	0.582623	0.479126	-11.6	
95	complex_7a_63	-2201.7638620	-0.22574	-0.06651	-3	0	0	0.545924	0.582037	0.476476	-13.7	
96	complex_7a_79	-2201.7642397	-0.22420	-0.06430	-2	0	0	0.547144	0.582726	0.478700	-11.8	
97	complex_7a_108	-2201.7641907	-0.23167	-0.08587	-3	-2	0	0.547306	0.582905	0.480065	-11.7	
98	complex_7a_114	-2201.7638061	-0.23035	-0.08450	-4	-3	0	0.546378	0.582527	0.477063	-12.7	
99	complex_7a_102	-2201.7625208	-0.22907	-0.05502	-2	0	0	0.546923	0.582526	0.479103	-12.9	
100	complex_7a_73	-2201.7619840	-0.22583	-0.06541	-3	-1	0	0.546085	0.582153	0.476271	-13.3	
101	complex_7a_104	-2201.7618958	-0.22752	-0.07637	-4	-2	0	0.546904	0.582576	0.477220	-11.7	
102	complex_7a_71	-2201.7619169	-0.22368	-0.05930	-4	-1	0	0.547060	0.582608	0.479632	-13.8	
103	complex_7a_81	-2201.7614622	-0.22460	-0.05815	-4	-1	0	0.547128	0.582659	0.479367	-13.8	

	Reaction Energy Profiles (REPs)											
	Reduction of **6im**$^+$ by **DIBAL**											
	Reactant DIBAL											
104	dibal_5	-558.7557975	-0.24542	-0.03291	-9	-2	-1	0.250254	0.264951	0.208031	-1.2	-557.7045333
105	dibal_9	-558.7565586	-0.24604	-0.03323	-6	-4	-3	0.250394	0.264988	0.209018	-1.3	-557.7049489
106	dibal_7	-558.7567418	-0.24551	-0.03195	-6	0	0	0.250625	0.265119	0.209311	-1.3	-557.7047537
107	dibal_6	-558.7555327	-0.24578	-0.03227	-4	-1	0	0.250405	0.265023	0.208369	-1.1	-557.7043298
108	dibal_36	-558.7562385	-0.24546	-0.03610	-11	-5	-1	0.250713	0.265206	0.209884	-1.2	-557.7038615
109	dibal_11	-558.7555174	-0.24647	-0.03724	-6	-4	0	0.250629	0.265199	0.209389	-1.4	
110	dibal_34	-558.7560560	-0.24670	-0.03210	-6	-1	0	0.250850	0.265232	0.210479	-1.3	
111	dibal_4	-558.7565493	-0.24672	-0.03415	-3	-2	0	0.250954	0.265309	0.211326	-1.3	
112	dibal_39	-558.7551322	-0.24464	-0.03572	-2	0	0	0.250935	0.265343	0.210459	-1.1	
	Transition State **TS**-*syn*											
113	ts_trans_dibal_Im6a_7	-1196.9865171	-0.34093	-0.18623	-463	-6	-3	0.577574	0.606065	0.518572	-31.7	-1194.7071576
114	ts_trans_dibal_Im6a_8	-1196.9875505	-0.34085	-0.19136	-428	-4	-2	0.577862	0.606148	0.520150	-32.6	-1194.7076613
115	ts_trans_dibal_Im6a_1	-1196.9871457	-0.34239	-0.19027	-457	-7	-5	0.577905	0.606162	0.520028	-32.0	-1194.7073245
116	ts_trans_dibal_Im6a_4	-1196.9855956	-0.34170	-0.18607	-463	-5	-1	0.577635	0.606078	0.518642	-32.0	-1194.7064811
117	ts_trans_dibal_Im6a_2	-1196.9863653	-0.34188	-0.18671	-430	-6	-5	0.577894	0.606250	0.519468	-31.9	-1194.7060060
118	ts_trans_dibal_Im6a_12	-1196.9867681	-0.34150	-0.18629	-475	0	0	0.577932	0.606214	0.520044	-31.6	
119	ts_trans_dibal_Im6a_10	-1196.9860481	-0.34136	-0.18635	-455	-6	-3	0.577920	0.606191	0.519816	-31.7	
120	ts_trans_dibal_Im6a_5	-1196.9843862	-0.34249	-0.18834	-432	-5	-2	0.578064	0.606478	0.519223	-32.7	
121	ts_trans_dibal_Im6a_6	-1196.9839242	-0.33971	-0.18813	-451	-1	0	0.577889	0.606313	0.518828	-32.2	
122	ts_trans_dibal_Im6a_9	-1196.9849384	-0.33908	-0.18480	-142	-2	0	0.578318	0.606507	0.520350	-31.7	
123	ts_trans_dibal_Im6a_13	-1196.9787516	-0.33139	-0.19182	-455	-4	0	0.576853	0.605785	0.516169	-32.5	
124	ts_trans_dibal_Im6a_11	-1196.9790428	-0.33125	-0.19229	-439	-3	-1	0.577466	0.606118	0.518256	-32.6	
125	ts_trans_dibal_Im6a_14	-1196.9779914	-0.33273	-0.19597	-438	0	0	0.577250	0.606064	0.517231	-33.2	
126	ts_trans_dibal_Im6a_15	-1196.9827012	-0.33401	-0.18457	-127	-3	0	0.579008	0.606939	0.522218	-31.8	
127	ts_trans_dibal_Im6a_18	-1196.9780449	-0.33179	-0.18309	-188	-4	-3	0.577550	0.606149	0.517640	-31.9	
128	ts_trans_dibal_Im6a_19	-1196.9747409	-0.32844	-0.18277	-276	-2	0	0.576814	0.605763	0.515050	-32.3	
129	ts_trans_dibal_Im6a_21	-1196.9770371	-0.32878	-0.18641	-180	-3	0	0.577766	0.606275	0.517782	-31.9	
130	ts_trans_dibal_Im6a_22	-1196.9782482	-0.32195	-0.18778	-129	-2	0	0.578112	0.606487	0.519559	-32.8	
	Product *trans*-**6**.Al(*i*-Bu)$_2$											
131	trans_dibal_Im6a_7	-1197.0413690	-0.33458	-0.14808	-5	-3	0	0.582574	0.611142	0.523265	-32.6	-1194.7725404
132	trans_dibal_Im6a_5	-1197.0399514	-0.33308	-0.15313	0	0	0	0.582773	0.611355	0.522198	-33.0	-1194.7708415
133	trans_dibal_Im6a_9	-1197.0417926	-0.33521	-0.14624	-6	-4	0	0.583018	0.611401	0.524576	-32.3	-1194.7722680
134	trans_dibal_Im6a_4	-1197.0411447	-0.33558	-0.15179	-5	-3	0	0.583124	0.611535	0.524620	-32.5	-1194.7713008

135	trans_dibal_lm6a_1	-1197.0409558	-0.33412	-0.15479	-4	0	0	0.583493	0.611707	0.525041	-32.6	-1194.7703194
136	trans_dibal_lm6a_11	-1197.0409558	-0.33412	-0.15479	-4	0	0	0.583493	0.611707	0.525042	-32.6	
137	trans_dibal_lm6a_8	-1197.0396252	-0.33317	-0.15630	-4	-1	0	0.582964	0.611446	0.524110	-32.8	
138	trans_dibal_lm6a_3	-1197.0408667	-0.33337	-0.15609	0	0	0	0.583474	0.611705	0.525473	-32.9	
139	trans_dibal_lm6a_2	-1197.0395309	-0.32913	-0.16384	-3	0	0	0.583115	0.611542	0.524328	-32.4	
140	trans_dibal_lm6a_6	-1197.0406752	-0.33271	-0.15759	-5	0	0	0.583433	0.611683	0.525985	-33.3	
141	trans_dibal_lm6a_10	-1197.0392617	-0.33511	-0.14967	-5	-3	0	0.583201	0.611620	0.524756	-32.4	
142	trans_dibal_lm6a_14	-1197.0364305	-0.33362	-0.15899	0	0	0	0.583277	0.611678	0.524724	-33.3	
143	trans_dibal_lm6a_19	-1197.0363813	-0.33931	-0.15118	-5	-1	0	0.583801	0.611995	0.525225	-32.1	
144	trans_dibal_lm6a_16	-1197.0376286	-0.33875	-0.15777	-5	-4	-2	0.584460	0.612366	0.527116	-32.4	
145	trans_dibal_lm6a_13	-1197.0349856	-0.32767	-0.16294	-3	0	0	0.583441	0.611779	0.524795	-33.4	
146	trans_dibal_lm6a_21	-1197.0359506	-0.33591	-0.15690	0	0	0	0.584257	0.612247	0.525952	-32.4	
147	trans_dibal_lm6a_12	-1197.0366608	-0.33911	-0.15952	-5	-3	0	0.584357	0.612267	0.527284	-32.4	
148	trans_dibal_lm6a_22	-1197.0358027	-0.33878	-0.16077	-5	-1	0	0.584563	0.612526	0.526815	-32.4	
149	trans_dibal_lm6a_18	-1197.0352332	-0.33830	-0.16186	-5	0	0	0.584425	0.612439	0.526795	-32.8	
150	trans_dibal_lm6a_17	-1197.0359885	-0.33648	-0.16177	-6	0	0	0.584463	0.612365	0.527570	-32.5	
151	trans_dibal_lm6a_23	-1197.0354702	-0.33639	-0.16242	-3	0	0	0.584244	0.612237	0.527104	-32.6	
152	trans_dibal_lm6a_24	-1197.0358998	-0.33674	-0.16457	-6	-2	0	0.584526	0.612399	0.528115	-32.6	
153	trans_dibal_lm6a_26	-1197.0339886	-0.34020	-0.16257	0	0	0	0.584227	0.612430	0.526338	-32.9	
154	trans_dibal_lm6a_20	-1197.0347673	-0.33887	-0.16141	-5	0	0	0.584583	0.612445	0.527967	-32.5	
	Transition State TS-*anti*											
155	ts_cis_dibal_lm6a_6	-1196.9856637	-0.33032	-0.19679	-451	-2	0	0.576888	0.605645	0.517010	-32.9	-1194.7076476
156	ts_cis_dibal_lm6a_2	-1196.9858751	-0.33019	-0.19609	-452	-5	-3	0.577100	0.605717	0.517875	-32.8	-1194.7072121
157	ts_cis_dibal_lm6a_3	-1196.9859732	-0.32927	-0.19393	-455	0	0	0.577198	0.605806	0.518291	-33.2	-1194.7074783
158	ts_cis_dibal_lm6a_5	-1196.9840209	-0.32994	-0.19457	-421	-5	0	0.576905	0.605702	0.516524	-33.0	-1194.7059557
159	ts_cis_dibal_lm6a_7	-1196.9839787	-0.32994	-0.19509	-445	-2	0	0.577056	0.605850	0.516586	-33.2	-1194.7054648
160	ts_cis_dibal_lm6a_1	-1196.9856572	-0.32850	-0.19084	-444	-2	0	0.577217	0.605737	0.518406	-32.6	
161	ts_cis_dibal_lm6a_4	-1196.9839098	-0.32900	-0.19236	-437	-6	0	0.577259	0.605893	0.517725	-33.0	
162	ts_cis_dibal_lm6a_9	-1196.9839666	-0.32892	-0.19397	-461	-4	-1	0.577478	0.605976	0.518935	-33.2	
163	ts_cis_dibal_lm6a_10	-1196.9812240	-0.32876	-0.19231	-464	-3	0	0.577407	0.606016	0.518255	-33.1	
164	ts_cis_dibal_lm6a_11	-1196.9792766	-0.32960	-0.19399	-490	0	0	0.577395	0.606097	0.518084	-33.1	
165	ts_cis_dibal_lm6a_18	-1196.9778480	-0.34154	-0.18970	-508	-6	0	0.578035	0.606476	0.519281	-31.8	
166	ts_cis_dibal_lm6a_12	-1196.9770383	-0.34259	-0.18776	-474	-1	0	0.578043	0.606468	0.518480	-31.7	
167	ts_cis_dibal_lm6a_14	-1196.9779692	-0.34275	-0.18980	-501	-7	0	0.578049	0.606404	0.519421	-31.5	
168	ts_cis_dibal_lm6a_16	-1196.9760147	-0.34194	-0.18940	-485	-4	0	0.577868	0.606420	0.517821	-32.0	
169	ts_cis_dibal_lm6a_13	-1196.9776009	-0.34167	-0.18757	-489	-10	-3	0.578074	0.606399	0.519518	-31.5	
170	ts_cis_dibal_lm6a_17	-1196.9777218	-0.34124	-0.18748	-503	-3	0	0.578170	0.606543	0.519836	-31.8	
171	ts_cis_dibal_lm6a_15	-1196.9747505	-0.33111	-0.18378	-176	-4	0	0.577738	0.606194	0.517465	-31.5	

	Product *cis*-**6**.Al(*i*-Bu)$_2$											
172	cis_dibal_lm6a_9	-1197.0411837	-0.34210	-0.14619	-6	0	0	0.583148	0.611466	0.525677	-31.8	-1194.7717260
173	cis_dibal_lm6a_4	-1197.0361787	-0.32536	-0.15526	0	0	0	0.583021	0.611522	0.523296	-33.4	-1194.7669897
174	cis_dibal_lm6a_12	-1197.0389068	-0.34291	-0.14528	-3	-2	0	0.583784	0.611935	0.526545	-31.9	-1194.7686038
175	cis_dibal_lm6a_2	-1197.0363174	-0.32511	-0.15909	-4	-1	0	0.583408	0.611705	0.524522	-33.1	-1194.7659959
176	cis_dibal_lm6a_13	-1197.0397346	-0.34208	-0.15455	0	0	0	0.583974	0.611889	0.528246	-32.0	-1194.7685494
177	cis_dibal_lm6a_1	-1197.0358995	-0.32519	-0.15899	-6	0	0	0.583589	0.611823	0.524884	-33.4	
178	cis_dibal_lm6a_5	-1197.0354733	-0.32548	-0.15601	-2	-2	0	0.583274	0.611615	0.524606	-33.4	
179	cis_dibal_lm6a_6	-1197.0360378	-0.33262	-0.16473	-5	-3	0	0.583801	0.612017	0.525283	-32.4	
180	cis_dibal_lm6a_16	-1197.0301077	-0.32559	-0.15712	-4	0	0	0.582419	0.611445	0.519868	-33.3	
181	cis_dibal_lm6a_3	-1197.0356720	-0.32545	-0.16220	-4	0	0	0.583632	0.611866	0.525646	-33.4	
182	cis_dibal_lm6a_11	-1197.0327214	-0.33458	-0.15859	-5	-4	0	0.583436	0.611946	0.524166	-32.6	
183	cis_dibal_lm6a_7	-1197.0321946	-0.33483	-0.15805	-3	0	0	0.583662	0.612085	0.524083	-32.7	
184	cis_dibal_lm6a_17	-1197.0336545	-0.33321	-0.16100	-5	-3	0	0.583805	0.612003	0.525587	-32.7	
185	cis_dibal_lm6a_10	-1197.0320867	-0.33359	-0.16432	-7	-3	-3	0.583894	0.612129	0.524941	-32.5	
186	cis_dibal_lm6a_8	-1197.0329300	-0.33390	-0.16176	0	0	0	0.584013	0.612271	0.525915	-32.7	
187	cis_dibal_lm6a_18	-1197.0297686	-0.32576	-0.16291	-5	-1	0	0.583219	0.611858	0.523115	-33.5	
	Aminodiazonium ion 7ad$^+$											
	Reactant Aminodiazonium ion **7ad$^+$**											
188	deProSpiro_7_19	-1349.5327135	-0.32382	-0.24915	-4	0	0	0.525558	0.554701	0.465897	-36.2	-1347.1605729
189	deProSpiro_7_2	-1349.5315245	-0.32517	-0.24825	-5	-2	0	0.525420	0.554622	0.465474	-36.0	-1347.1592819
190	deProSpiro_7_1	-1349.5314933	-0.32416	-0.24324	-3	-2	0	0.525521	0.554593	0.465982	-35.5	-1347.1617021
191	deProSpiro_7_4	-1349.5305984	-0.32220	-0.24887	-4	0	0	0.525485	0.554724	0.466158	-36.0	-1347.1582179
192	deProSpiro_7_41	-1349.5304138	-0.32342	-0.24838	-4	-2	0	0.525641	0.554815	0.466659	-35.8	-1347.1576358
193	deProSpiro_7_14	-1349.5284023	-0.33154	-0.24176	-7	-2	0	0.525488	0.554510	0.465266	-34.7	-1347.1592343
194	deProSpiro_7_7	-1349.5285184	-0.33132	-0.24229	-1	0	0	0.525576	0.554564	0.465756	-34.8	-1347.1592458
195	deProSpiro_7_15	-1349.5274509	-0.33282	-0.24604	-4	0	0	0.525852	0.554757	0.466811	-34.9	-1347.1565206
196	deProSpiro_7_12	-1349.5271442	-0.33182	-0.24208	0	0	0	0.526063	0.554872	0.466627	-34.6	-1347.1578564
197	deProSpiro_7_13	-1349.5273056	-0.33169	-0.24234	0	0	0	0.525927	0.554773	0.466988	-34.8	-1347.1579705
198	deProSpiro_7_9	-1349.5272206	-0.33206	-0.24183	-3	0	0	0.525928	0.554768	0.467002	-34.7	
199	deProSpiro_7_18	-1349.5260389	-0.33062	-0.24203	-5	-1	0	0.525803	0.554701	0.466567	-34.6	
200	deProSpiro_7_17	-1349.5259035	-0.33094	-0.24144	-7	-3	0	0.525831	0.554708	0.466461	-34.6	
201	deProSpiro_7_21	-1349.5259698	-0.33235	-0.24575	-4	-3	0	0.525836	0.554743	0.466689	-34.9	
202	deProSpiro_7_28	-1349.5209386	-0.32542	-0.24426	-7	-2	0	0.524495	0.554062	0.462928	-35.6	
203	deProSpiro_7_20	-1349.5223103	-0.32648	-0.24894	-3	0	0	0.525091	0.554323	0.465031	-36.0	
204	deProSpiro_7_33	-1349.5218720	-0.32391	-0.24291	-5	0	0	0.524864	0.554191	0.464851	-35.3	
205	deProSpiro_7_25	-1349.5221856	-0.32557	-0.24930	-7	-2	0	0.525438	0.554538	0.465265	-35.9	

206	deProSpiro_7_24	-1349.5217458	-0.32752	-0.24296	-6	-3	0	0.525308	0.554438	0.464955	-35.3	
207	deProSpiro_7_23	-1349.5249500	-0.33914	-0.24660	-7	-3	0	0.526123	0.555067	0.468390	-35.2	
208	deProSpiro_7_35	-1349.5197826	-0.32575	-0.24642	-4	-1	0	0.524895	0.554290	0.464565	-35.6	
209	ts_7to7a_30_ircf_o	-1349.5191526	-0.32265	-0.25358	0	0	0	0.524875	0.554358	0.464218	-37.1	
210	deProSpiro_7_26	-1349.5214761	-0.32622	-0.24854	-2	0	0	0.525446	0.554531	0.466620	-35.8	
211	deProSpiro_7_40	-1349.5206820	-0.32394	-0.24914	-4	0	0	0.525275	0.554435	0.465910	-35.9	
212	deProSpiro_7_27	-1349.5206109	-0.32430	-0.24297	-3	0	0	0.525199	0.554381	0.466189	-35.3	
213	deProSpiro_7_37	-1349.5196755	-0.32498	-0.24755	-3	0	0	0.525065	0.554341	0.465545	-35.5	
214	deProSpiro_7_29	-1349.5205528	-0.32724	-0.24296	0	0	0	0.525744	0.554677	0.466593	-35.2	
215	ts_7to7a_28_ircf_o	-1349.5202350	-0.32476	-0.25320	-5	-2	0	0.525294	0.554520	0.466856	-36.9	
216	deProSpiro_7_34	-1349.5204133	-0.32739	-0.24324	-5	-5	0	0.525805	0.554740	0.467058	-34.9	
217	deProSpiro_7_38	-1349.5218777	-0.34039	-0.23974	-5	-3	0	0.526523	0.555240	0.469840	-34.1	
218	ts_7to7a_29_ircr_o	-1349.5185187	-0.32540	-0.25297	-4	0	0	0.525552	0.554697	0.467636	-36.8	
	Transition State **TS**-*anti*											
219	ts_7to7a_1	-1349.5104667	-0.32595	-0.28132	-449	-3	0	0.522103	0.551267	0.463264	-34.5	-1347.1411093
220	ts_7to7a_3	-1349.5102374	-0.32737	-0.28026	-442	-3	-1	0.522353	0.551385	0.463962	-34.2	-1347.1398150
221	ts_7to7a_4	-1349.5092188	-0.32525	-0.28084	-441	-4	-3	0.522224	0.551355	0.464155	-34.3	-1347.1395865
222	ts_7to7a_6	-1349.5080637	-0.32490	-0.28165	-443	-5	-1	0.522109	0.551354	0.463260	-34.2	-1347.1380195
223	ts_7to7a_5	-1349.5089895	-0.32617	-0.28055	-438	0	0	0.522607	0.551575	0.465133	-34.0	-1347.1380082
224	ts_7to7a_15	-1349.5060010	-0.33227	-0.28309	-445	-4	-1	0.522328	0.551351	0.463329	-34.0	
225	ts_7to7a_16	-1349.5048679	-0.33197	-0.28268	-443	-2	0	0.522477	0.551484	0.463550	-34.0	
226	ts_7to7a_17	-1349.5039247	-0.34282	-0.27793	-447	-6	0	0.522827	0.551752	0.465853	-33.3	
227	ts_7to7a_19	-1349.4983996	-0.32454	-0.28004	-447	-6	-4	0.521909	0.551189	0.462307	-34.3	
228	ts_7to7a_20	-1349.4973136	-0.32357	-0.28240	-436	-2	0	0.521554	0.550971	0.462273	-34.8	
	Product *trans*-**8im**$^{+}$ + N_2											
229	ts_7to7a_1_ircf_o	-1349.6475490	-0.33366	-0.19950	-5	0	0	0.522872	0.554287	0.457897	-34.5	-1347.2827337
230	ts_7to7a_4_ircr_o	-1349.6472763	-0.33339	-0.19919	-2	0	0	0.523043	0.554356	0.458397	-33.9	-1347.2824868
231	ts_7to7a_2_ircr_o	-1349.6464690	-0.33301	-0.19927	0	0	0	0.523297	0.554598	0.458469	-34.0	-1347.2811149
232	ts_7to7a_6_ircf_o	-1349.6448729	-0.33212	-0.19922	-5	0	0	0.523399	0.554709	0.458031	-33.6	-1347.2801261
233	ts_7to7a_5_ircr_o	-1349.6438221	-0.33325	-0.19847	-2	0	0	0.523347	0.554762	0.457472	-33.7	-1347.2802772
234	ts_7to7a_15_ircf_o	-1349.6453842	-0.34011	-0.19629	0	0	0	0.524172	0.555170	0.459811	-33.3	
235	ts_7to7a_17_ircf_o	-1349.6450882	-0.35529	-0.19443	0	0	0	0.524032	0.555063	0.459714	-32.6	
236	ts_7to7a_16_ircr_o	-1349.6452053	-0.34029	-0.19795	-4	-2	0	0.524243	0.555148	0.461099	-32.9	
237	ts_7to7a_20_ircr_o	-1349.6442099	-0.33328	-0.19980	-6	0	0	0.523643	0.554831	0.460641	-33.6	
238	ts_7to7a_19_ircr_o	-1349.6414954	-0.33425	-0.19696	-7	0	0	0.523747	0.554819	0.459667	-33.4	
	Transition State											

	TS-*syn*											
239	ts_7to7a_21	-1349.5025344	-0.32510	-0.29283	-507	-6	0	0.521708	0.550750	0.463168	-35.7	-1347.1330943
240	ts_7to7a_23	-1349.5002332	-0.32363	-0.29225	-509	-6	-1	0.521817	0.550914	0.463482	-35.5	-1347.1304345
241	ts_7to7a_25	-1349.5003182	-0.33964	-0.29098	-531	0	0	0.522305	0.551122	0.464626	-35.3	-1347.1305767
242	ts_7to7a_26	-1349.4999143	-0.33614	-0.29088	-518	-4	0	0.521982	0.550853	0.464748	-34.9	-1347.1302748
243	ts_7to7a_30	-1349.4942309	-0.32491	-0.28918	-541	0	0	0.521517	0.550973	0.461409	-36.2	-1347.1255119
244	ts_7to7a_28	-1349.4951272	-0.32679	-0.29087	-545	-3	-2	0.521696	0.551007	0.463327	-36.0	
245	ts_7to7a_29	-1349.4934971	-0.32759	-0.28956	-543	0	0	0.522000	0.551212	0.463872	-35.8	
246	ts_7to7a_27	-1349.4897764	-0.33938	-0.29379	-496	-6	0	0.522423	0.551171	0.465910	-34.5	
	Product *cis*-**8im**$^+$ + N_2											
247	ts_7to7a_23_ircr_o	-1349.6458217	-0.33173	-0.19787	-5	-2	0	0.523156	0.554658	0.456287	-33.7	-1347.2822262
248	ts_7to7a_21_ircr_o	-1349.6438180	-0.33314	-0.19842	-4	0	0	0.522900	0.554537	0.455316	-33.9	-1347.2808609
249	ts_7to7a_29_ircf_o	-1349.6446321	-0.34182	-0.19526	-2	0	0	0.524050	0.555253	0.458955	-32.6	-1347.2800548
250	ts_7to7a_27_ircr_o	-1349.6425952	-0.35267	-0.19643	-3	0	0	0.523547	0.554854	0.457000	-33.0	-1347.2785688
251	ts_7to7a_30_ircr_o	-1349.6407074	-0.33270	-0.19676	-3	0	0	0.522876	0.554361	0.455799	-34.3	-1347.2777741
252	ts_7to7a_28_ircr_o	-1349.6401223	-0.33216	-0.19506	-4	0	0	0.523104	0.554591	0.455911	-33.9	
253	ts_7to7a_26_ircr_o	-1349.6426794	-0.34347	-0.19648	-3	0	0	0.524002	0.555052	0.459180	-33.0	
	Aminodiazonium ion **10ad**$^+$											
	Reactant											
	Aminodiazonium ion **10ad**$^+$											
254	ts_10to12_10_ircr	-826.2762886	-0.32943	-0.25256	0	0	0	0.389820	0.409024	0.343058	-37.3	-824.7383048
255	ts_10to12_7_ircr	-826.2751358	-0.32816	-0.25129	-3	0	0	0.389552	0.408798	0.342423	-37.8	-824.7388926
256	deProSpiro_10_2	-826.2749955	-0.32905	-0.25284	-11	-3	0	0.389722	0.409011	0.342536	-37.7	-824.7376064
257	ts_10to12_19_ircr	-826.2749955	-0.32905	-0.25284	-11	-3	0	0.389722	0.409011	0.342536	-37.7	-824.7376109
258	deProSpiro_10_5	-826.2750522	-0.32938	-0.25201	-4	-1	0	0.389876	0.409006	0.343235	-37.3	-824.7375907
259	ts_10to12_6_ircf	-826.2750522	-0.32938	-0.25201	-4	-1	0	0.389876	0.409006	0.343235	-37.3	-824.7375871
260	deProSpiro_10_1	-826.2749450	-0.32921	-0.25331	-9	-3	0	0.389995	0.409118	0.343260	-37.7	-824.7372305
261	deProSpiro_10_12	-826.2747073	-0.33476	-0.25012	-4	-2	0	0.390709	0.409654	0.343826	-37.3	-824.7384735
262	deProSpiro_10_3	-826.2747073	-0.33476	-0.25012	-4	-2	0	0.390709	0.409654	0.343826	-37.3	-824.7384746
263	ts_10to12_1_ircr	-826.2712215	-0.32739	-0.25191	-3	0	0	0.389418	0.408703	0.342119	-37.5	-824.7358725
264	deProSpiro_10_11	-826.2672905	-0.32681	-0.25243	-2	0	0	0.389365	0.408844	0.340603	-37.8	
265	ts_10to12_27_ircf	-826.2672905	-0.32681	-0.25243	-2	0	0	0.389365	0.408844	0.340603	-37.8	
266	ts_10to12_33_ircf	-826.2662988	-0.32647	-0.25276	-7	-2	-1	0.389406	0.408893	0.340612	-38.2	
267	deProSpiro_10_10	-826.2669856	-0.32414	-0.25250	-3	0	0	0.389599	0.409155	0.341601	-38.3	
268	ts_10to12_11_ircf	-826.2699154	-0.34728	-0.23319	-6	-4	0	0.390324	0.409282	0.345099	-35.4	
269	ts_10to12_16_ircf	-826.2699154	-0.34728	-0.23319	-6	-4	0	0.390324	0.409282	0.345099	-35.4	
270	ts_10to12_17_ircr	-826.2688085	-0.34718	-0.23321	-4	0	0	0.390145	0.409160	0.344156	-35.4	

271	ts_10to12_34_ircf	-826.2657811	-0.32430	-0.25303	-7	-3	-1	0.389568	0.409122	0.341566	-38.4	
272	deProSpiro_10_9	-826.2661950	-0.32438	-0.25240	-5	0	0	0.389627	0.409065	0.342111	-38.1	
273	deProSpiro_10_6	-826.2693609	-0.35103	-0.23664	-9	-5	-2	0.390583	0.409475	0.345477	-35.3	
274	deProSpiro_10_15	-826.2656171	-0.32444	-0.25339	-6	-2	0	0.389850	0.409234	0.342358	-38.4	
275	deProSpiro_10_13	-826.2656171	-0.32444	-0.25339	-6	-2	0	0.389850	0.409234	0.342358	-38.4	
276	deProSpiro_10_7	-826.2656171	-0.32444	-0.25340	-6	-2	0	0.389850	0.409234	0.342358	-38.4	
277	deProSpiro_10_14	-826.2656171	-0.32444	-0.25339	-6	-2	0	0.389850	0.409234	0.342358	-38.4	
278	ts_10to12_3_ircr	-826.2667553	-0.34715	-0.23614	-6	-2	0	0.390540	0.409427	0.344726	-35.8	
279	deProSpiro_10_8	-826.2652298	-0.35136	-0.24382	-2	0	0	0.390474	0.409354	0.345800	-35.5	
280	ts_10to12_32_ircf	-826.2595202	-0.32443	-0.25146	-4	0	0	0.389441	0.408976	0.341638	-37.6	
	Transition State **TS**-*anti*											
281	ts_10to12_1	-826.2489612	-0.32937	-0.29413	-506	-3	0	0.385823	0.405258	0.338642	-37.2	-824.7158086
282	ts_10to12_19	-826.2482312	-0.32872	-0.29341	-506	-6	0	0.386028	0.405482	0.338660	-37.2	-824.7153867
283	ts_10to12_10	-826.2440876	-0.32901	-0.29401	-504	-5	0	0.386030	0.405392	0.339213	-37.0	-824.7106022
284	ts_10to12_32	-826.2398810	-0.32607	-0.28785	-514	-6	0	0.385954	0.405614	0.338236	-37.1	-824.7080671
285	ts_10to12_33	-826.2394846	-0.33059	-0.28742	-514	-3	0	0.386288	0.405742	0.338208	-36.9	-824.7080509
286	ts_10to12_34	-826.2395828	-0.32610	-0.28716	-511	-5	0	0.386095	0.405742	0.338466	-37.1	
287	ts_10to12_6	-826.2348697	-0.33160	-0.30832	-396	-8	-4	0.385369	0.404998	0.337806	-36.8	
288	ts_10to12_3	-826.2349691	-0.36801	-0.29848	-260	-7	-1	0.386428	0.405517	0.341371	-33.7	
	Product (3*R*,7*S*)-**15im**$^{+}$ + N_2											
289	ts_10to12_19_ircf	-826.3962253	-0.33669	-0.20144	-3	-1	0	0.387983	0.409325	0.336047	-36.0	-824.8666170
290	ts_10to12_10_ircf	-826.3962708	-0.33724	-0.20167	-3	0	0	0.388179	0.409342	0.336280	-36.0	-824.8665624
291	ts_10to12_1_ircf	-826.3940657	-0.33643	-0.20299	-4	0	0	0.388143	0.409376	0.336435	-35.9	-824.8639946
292	ts_10to12_6_ircr	-826.3918809	-0.33590	-0.20341	-7	-4	0	0.387760	0.409172	0.334461	-36.2	-824.8632928
293	ts_10to12_33_ircr	-826.3909551	-0.33876	-0.19906	-6	-4	-2	0.387874	0.409265	0.335133	-35.9	-824.8630500
294	ts_10to12_3_ircf	-826.3918012	-0.33982	-0.20003	-7	-4	-2	0.388143	0.409321	0.336152	-35.9	
295	ts_10to12_34_ircr	-826.3874068	-0.33520	-0.19988	-5	-3	-2	0.387642	0.409318	0.333407	-36.2	
296	ts_10to12_32_ircr	-826.3868409	-0.33739	-0.20173	-2	0	0	0.387948	0.409396	0.334800	-36.0	
	Transition State **TS**-*syn*											
297	ts_10to12_7	-826.2466592	-0.33079	-0.29883	-535	-6	-5	0.385967	0.405366	0.338929	-37.3	-824.7127623
298	ts_10to12_11	-826.2373912	-0.35648	-0.29338	-482	-7	-2	0.386797	0.405679	0.341977	-34.9	-824.6990177
299	ts_10to12_27	-826.2344816	-0.33915	-0.29803	-549	-7	-3	0.386648	0.405761	0.340403	-36.9	-824.6997617
300	ts_10to12_17	-826.2258924	-0.34890	-0.30386	-357	-4	-1	0.385799	0.405034	0.340024	-34.3	-824.6863002
301	ts_10to12_16	-826.2280405	-0.36339	-0.29895	-330	-7	-3	0.386841	0.405545	0.343201	-33.3	-824.6835650

	Product (3*R*,7*R*)-**15im**$^{+}$ + N_2											
302	ts_10to12_27_ircr	-826.3906863	-0.33863	-0.20023	-6	-4	0	0.388019	0.409356	0.334447	-35.7	-824.8625993
303	ts_10to12_7_ircf	-826.3919254	-0.33637	-0.20116	-2	0	0	0.387718	0.409092	0.335850	-35.8	-824.8626663
304	ts_10to12_11_ircr	-826.3913914	-0.36026	-0.19371	-9	-4	0	0.388509	0.409627	0.336139	-34.7	-824.8631855
305	ts_10to12_17_ircf	-826.3858765	-0.33581	-0.19888	-1	0	0	0.387922	0.409317	0.334477	-36.1	-824.8581432

5. References

1. Becke, A. D., *J. Chem. Phys* **1993,** *98* (7), 5648-5652.
2. Ditchfield, R.; Hehre, W. J.; Pople, J. A., *J. Chem. Phys.* **1971,** *54* (2), 724-728.
3. Krishnan, R.; Binkley, J. S.; Seeger, R.; Pople, J. A., *J. Chem. Phys.* **1980,** *72* (1), 650-654.
4. Grimme, S.; Antony, J.; Ehrlich, S.; Krieg, H., *J. Chem. Phys.* **2010,** *132* (15), 154104.
5. Grimme, S., *J. Comput. Chem.* **2006,** *27* (15), 1787-1799.
6. Cances, E.; Mennucci, B.; Tomasi, J. *J. Chem. Phys.* **1997**, *107* (8), 3032-3041.
7. Tomasi, J.; Mennucci, B.; Cammi, R. *Chem. Rev.* **2005**, *105* (8), 2999-3094.
8. Saitow, M.; Becker, U.; Riplinger, C.; Valeev, E. F.; Neese, F., *J. Chem. Phys.* **2017**, *146* (16), 164105.
9. Dunning Jr, T. H., *J. Chem. Phys.* **1989**, *90* (2), 1007-1023.
10. Kendall, R. A.; Dunning Jr, T. H.; Harrison, R. J., *J. Chem. Phys.* **1992**, *96* (9), 6796-6806.
11. M. J. Frisch, G. W. T., H. B. Schlegel, G. E. Scuseria,; M. A. Robb, J. R. C., G. Scalmani, V. Barone, B. Mennucci,; G. A. Petersson, H. N., M. Caricato, X. Li, H. P. Hratchian,; A. F. Izmaylov, J. B., G. Zheng, J. L. Sonnenberg, M. Hada,; M. Ehara, K. T., R. Fukuda, J. Hasegawa, M. Ishida, T. Nakajima,; Y. Honda, O. K., H. Nakai, T. Vreven, J. A. Montgomery, Jr.,; J. E. Peralta, F. O., M. Bearpark, J. J. Heyd, E. Brothers,; K. N. Kudin, V. N. S., T. Keith, R. Kobayashi, J. Normand,; K. Raghavachari, A. R., J. C. Burant, S. S. Iyengar, J. Tomasi,; M. Cossi, N. R., J. M. Millam, M. Klene, J. E. Knox, J. B. Cross,; V. Bakken, C. A., J. Jaramillo, R. Gomperts, R. E. Stratmann,; O. Yazyev, A. J. A., R. Cammi, C. Pomelli, J. W. Ochterski,; R. L. Martin, K. M., V. G. Zakrzewski, G. A. Voth,; P. Salvador, J. J. D., S. Dapprich, A. D. Daniels,; O. Farkas, J. B. F., J. V. Ortiz, J. Cioslowski, D. J. Fox *Gaussian 09, Revision D.01*, Gaussian, Inc., Wallingford CT,: **2013**.
12. Neese, F. Software update: the ORCA program system, version 4.0. *WIREs Comput Mol Sci.* **2018**, 8, 1327.

Appendix

NMR Spectra of Chapter 8

^{1}H NMR (300 MHz, $CDCl_3$)
Methyl 3-(2-oxocyclopentyl)propanoate

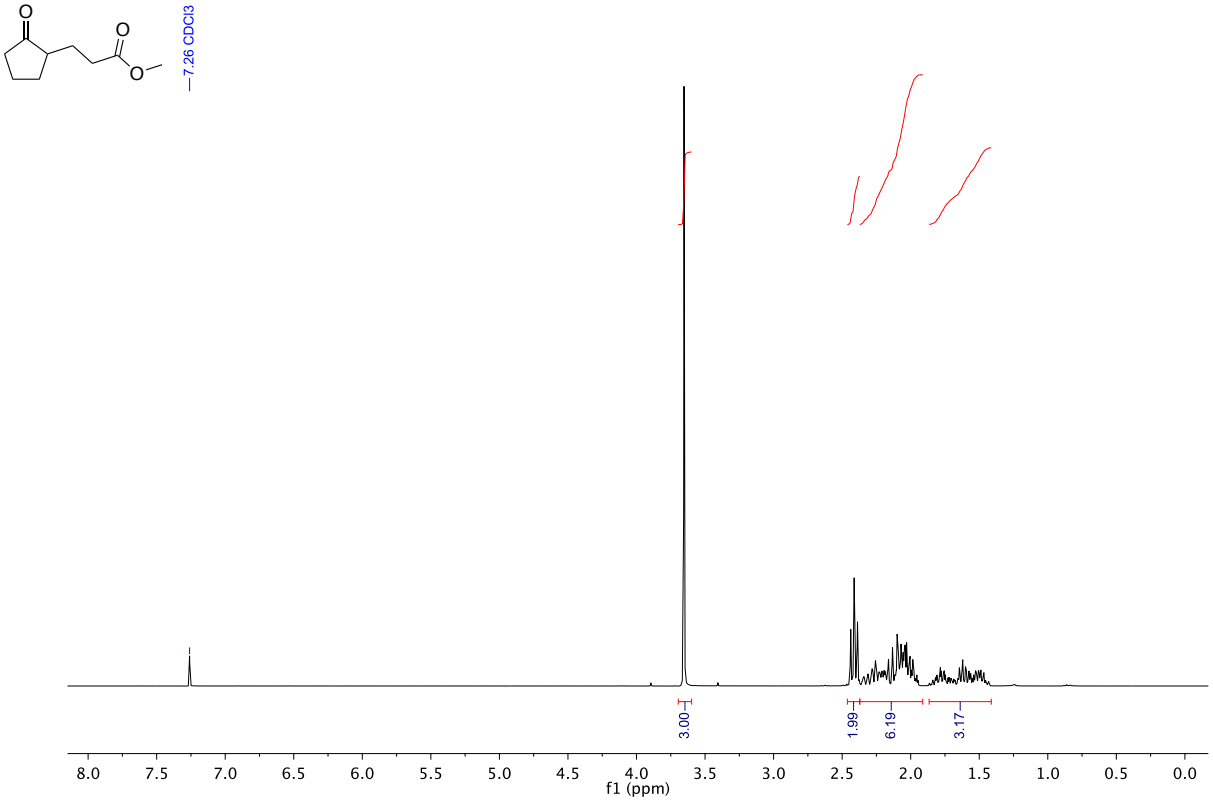

^{13}C NMR (75 MHz, $CDCl_3$)
Methyl 3-(2-oxocyclopentyl)propanoate

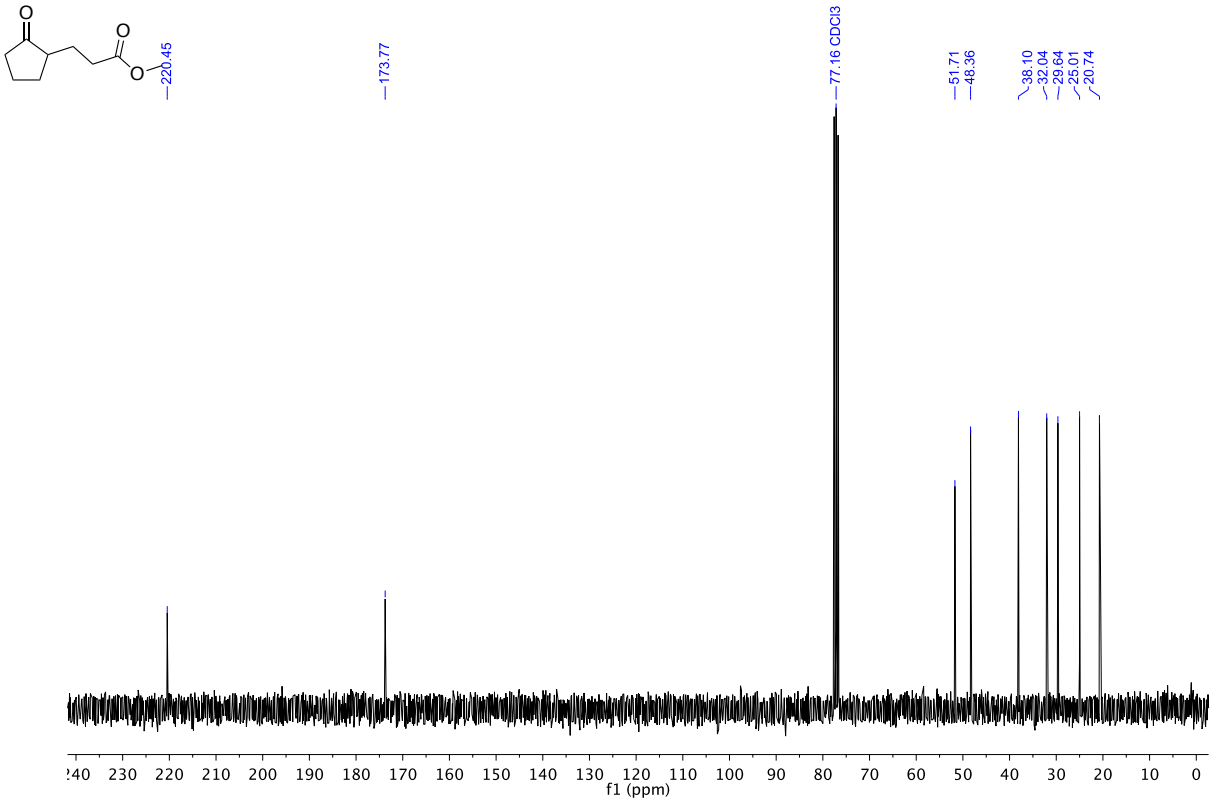

^{1}H NMR (300 MHz, $CDCl_3$)
2-(3-hydroxypropyl)cyclopentan-1-ol

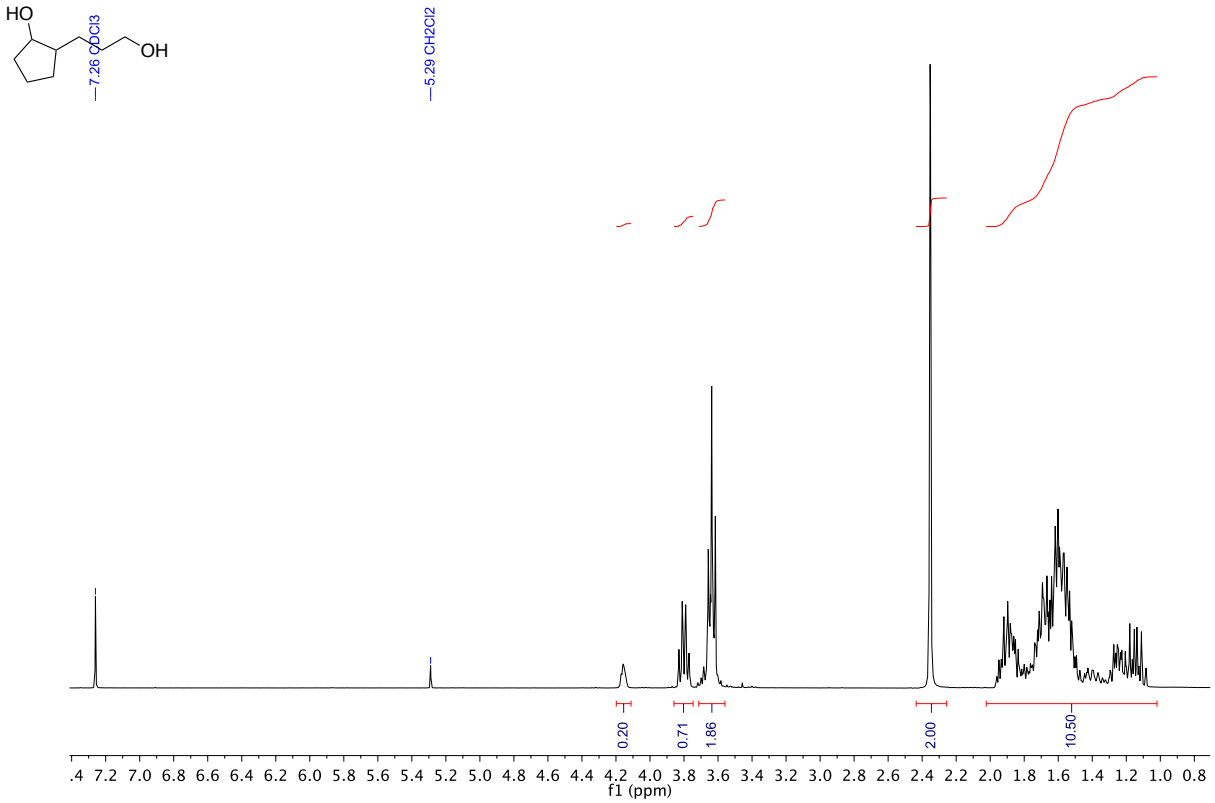

^{13}C NMR (75 MHz, $CDCl_3$)
2-(3-hydroxypropyl)cyclopentan-1-ol

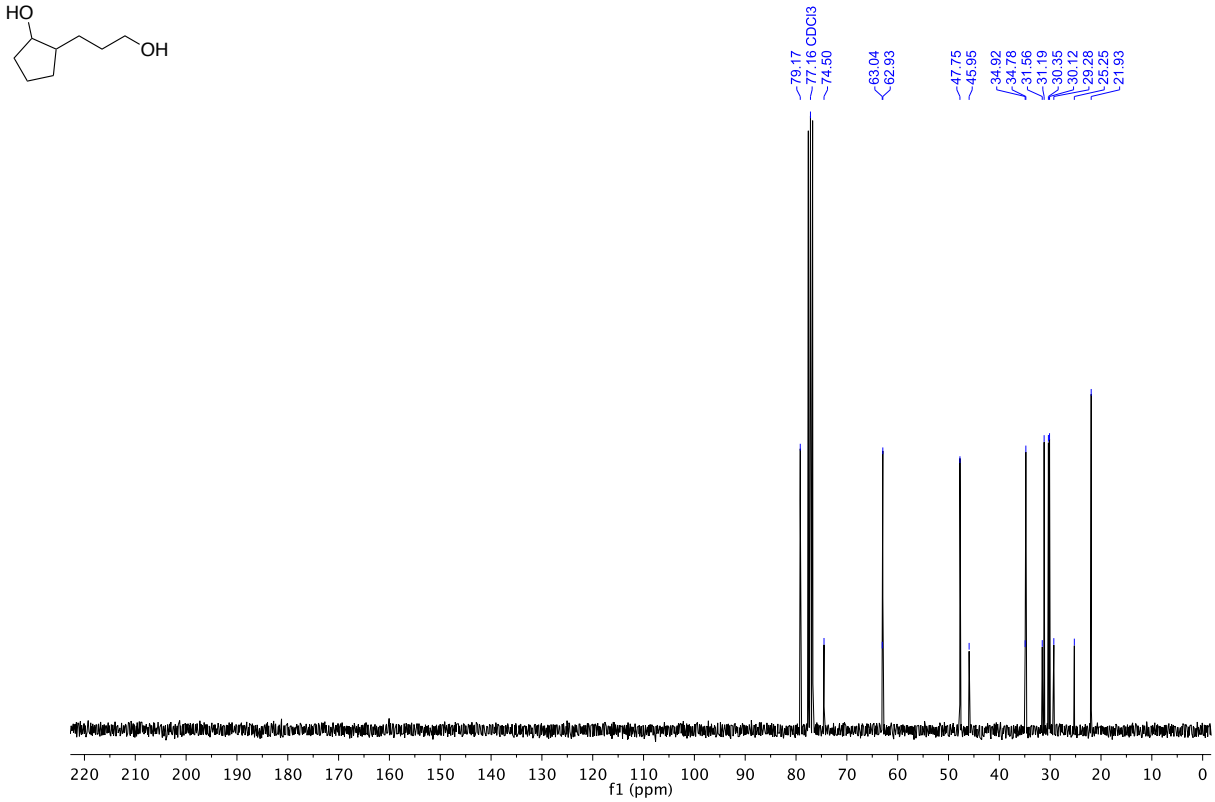

^{1}H NMR (300 MHz, $CDCl_3$)
Minor *3-(2-hydroxycyclopentyl)propyl 4-methylbenzenesulfonate*

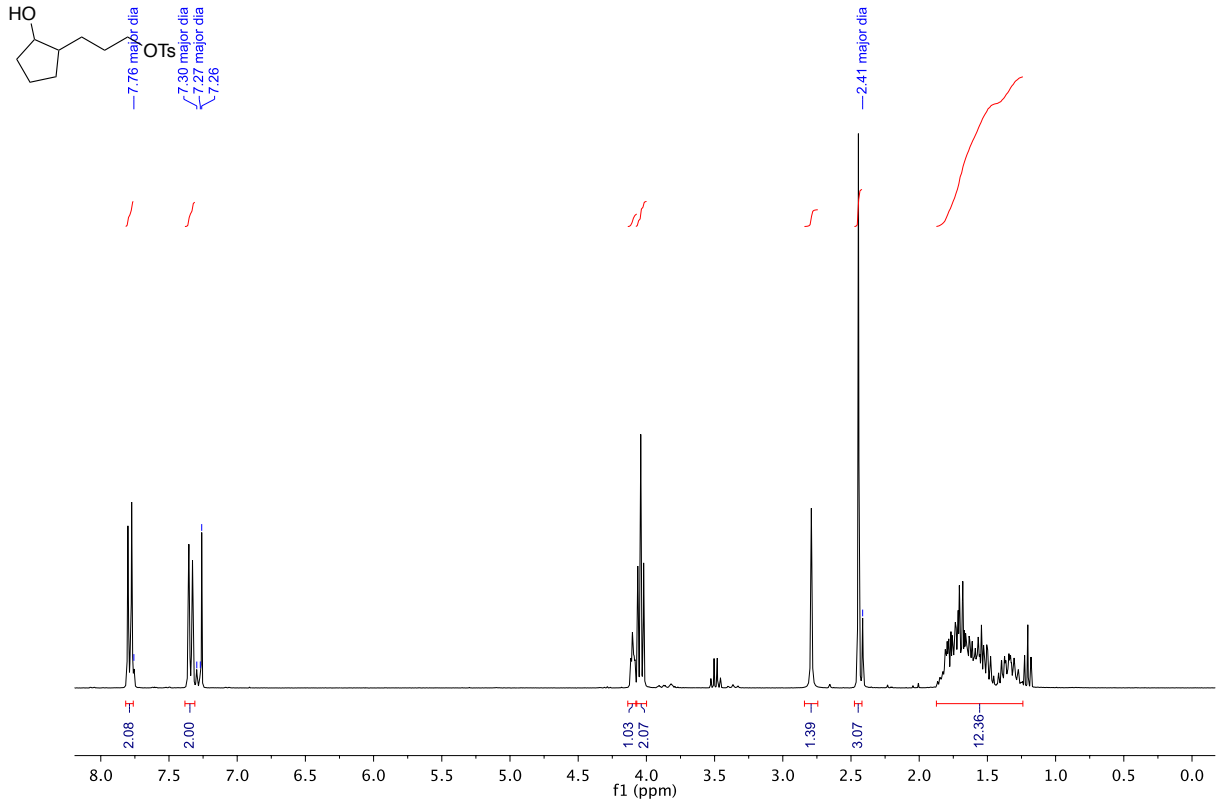

^{13}C NMR (75 MHz, $CDCl_3$)
Minor *3-(2-hydroxycyclopentyl)propyl 4-methylbenzenesulfonate*

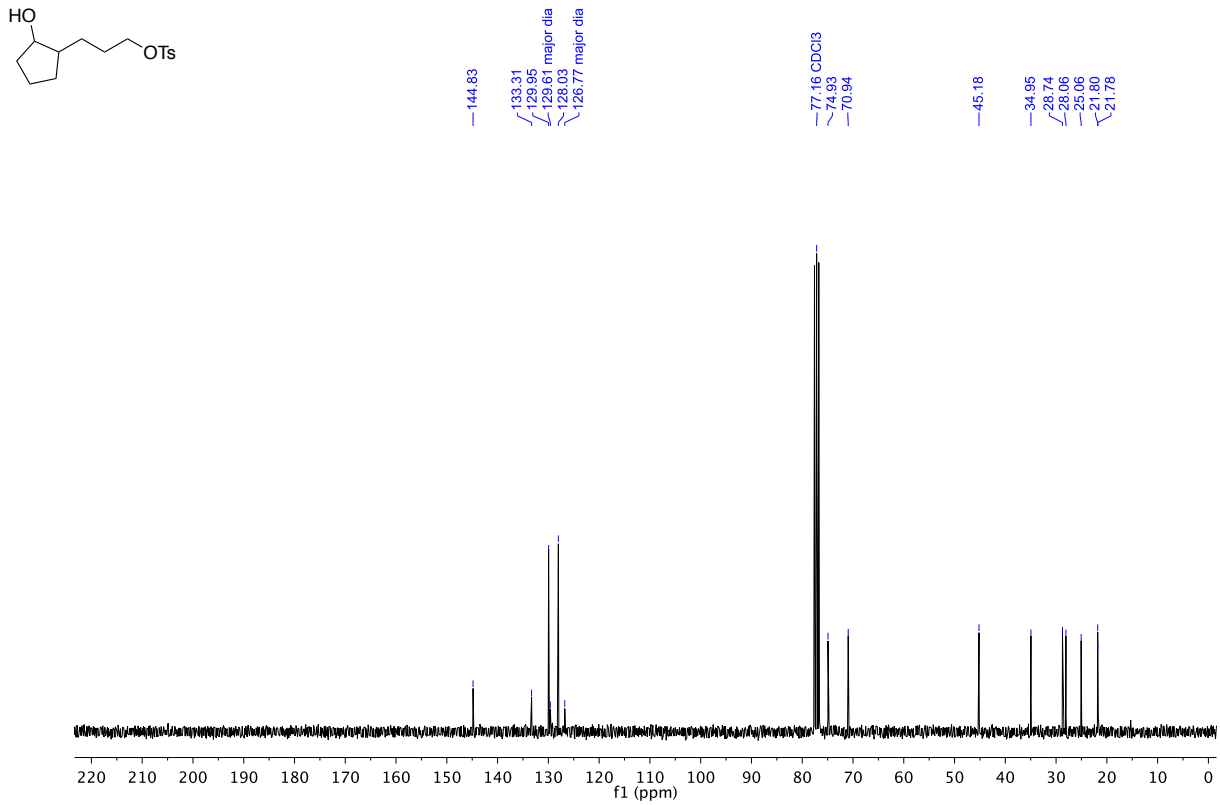

^{1}H NMR (300 MHz, $CDCl_3$)
Major *3-(2-hydroxycyclopentyl)propyl 4-methylbenzenesulfonate*

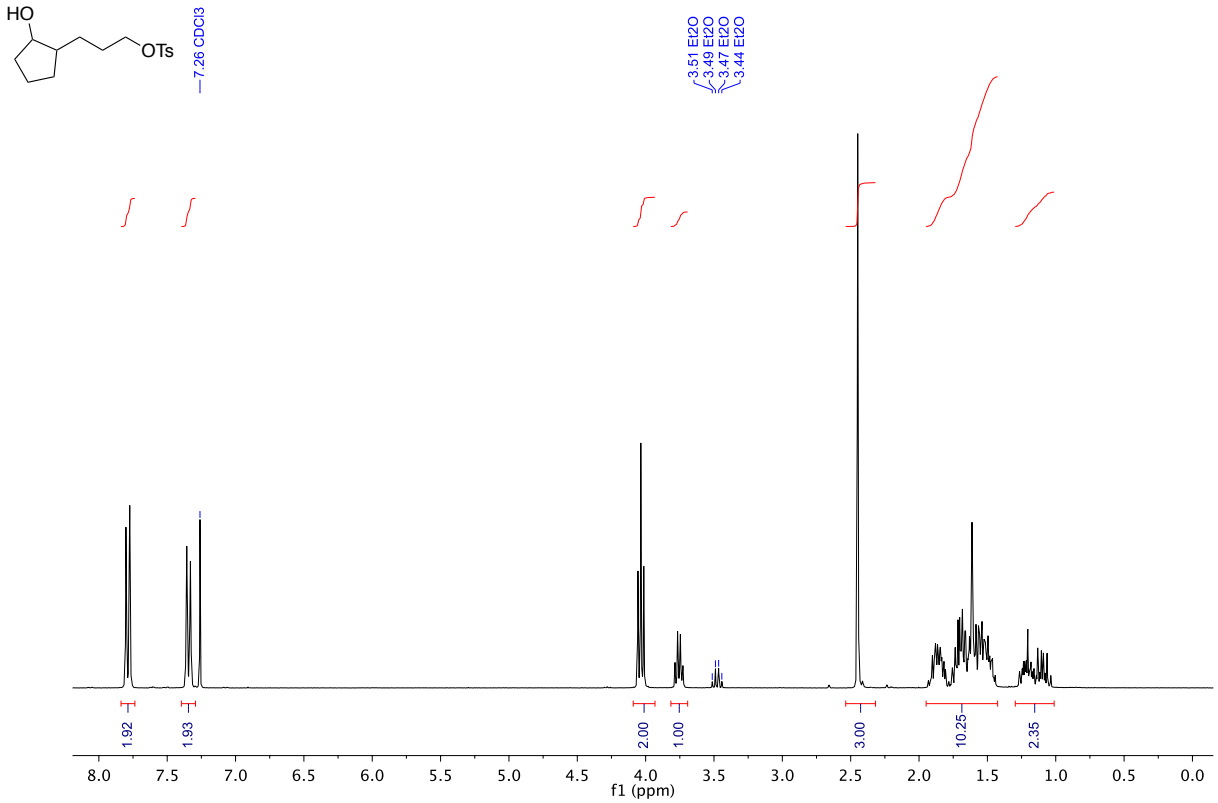

^{13}C NMR (75 MHz, $CDCl_3$)
Major *3-(2-hydroxycyclopentyl)propyl 4-methylbenzenesulfonate*

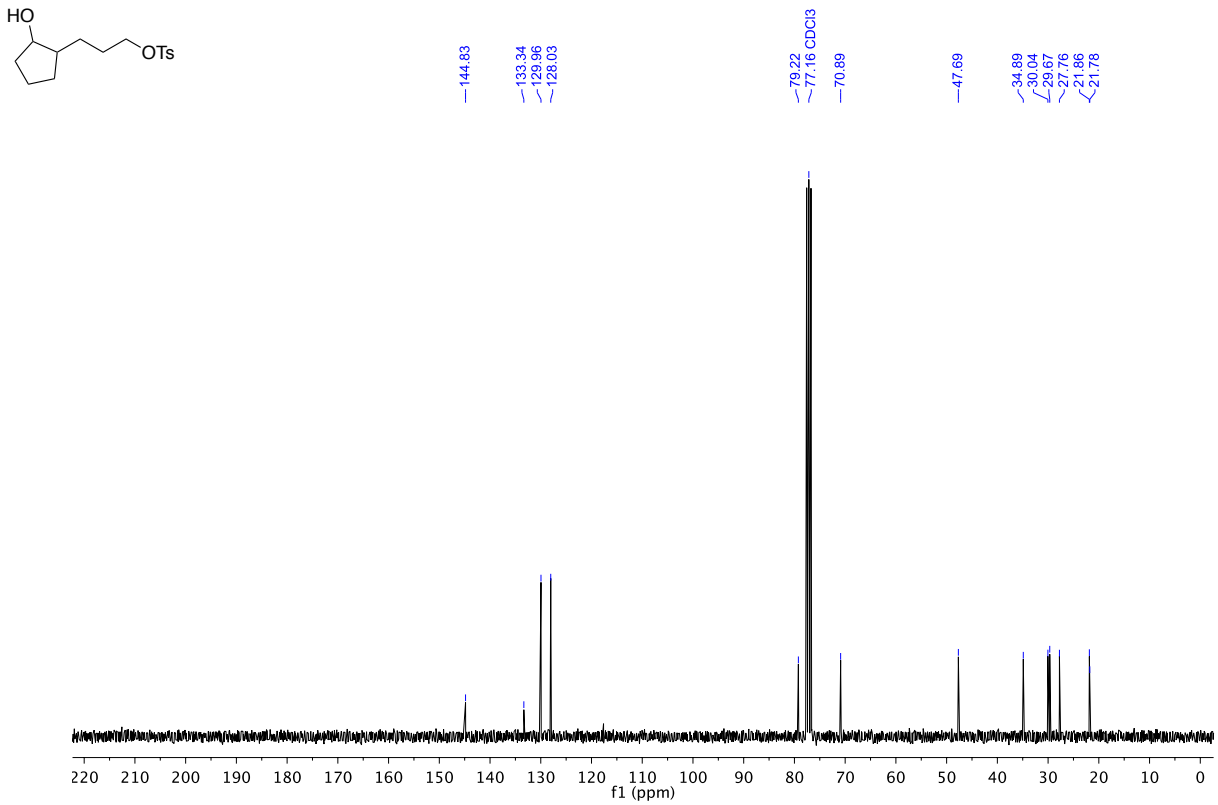

^{1}H NMR (300 MHz, $CDCl_3$)
Minor *2-(3-azidopropyl)cyclopentan-1-ol*

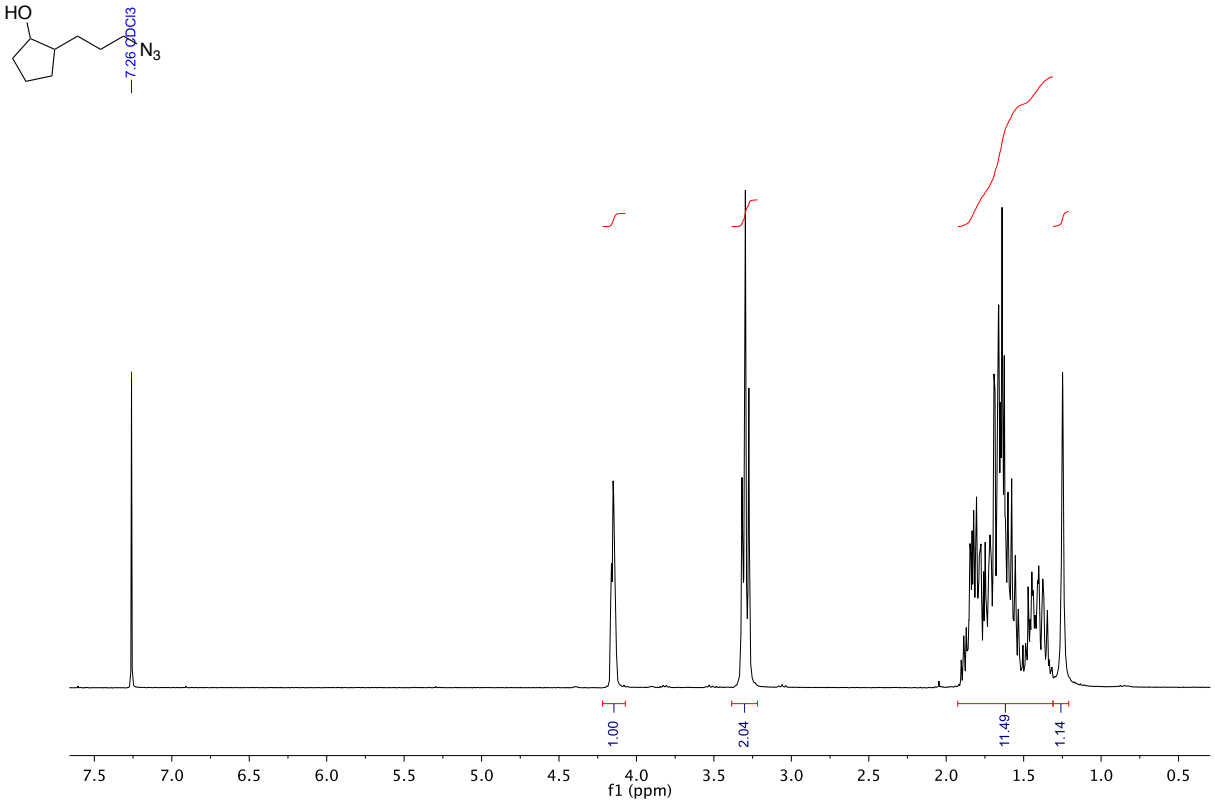

^{13}C NMR (75 MHz, $CDCl_3$)
Minor *2-(3-azidopropyl)cyclopentan-1-ol*

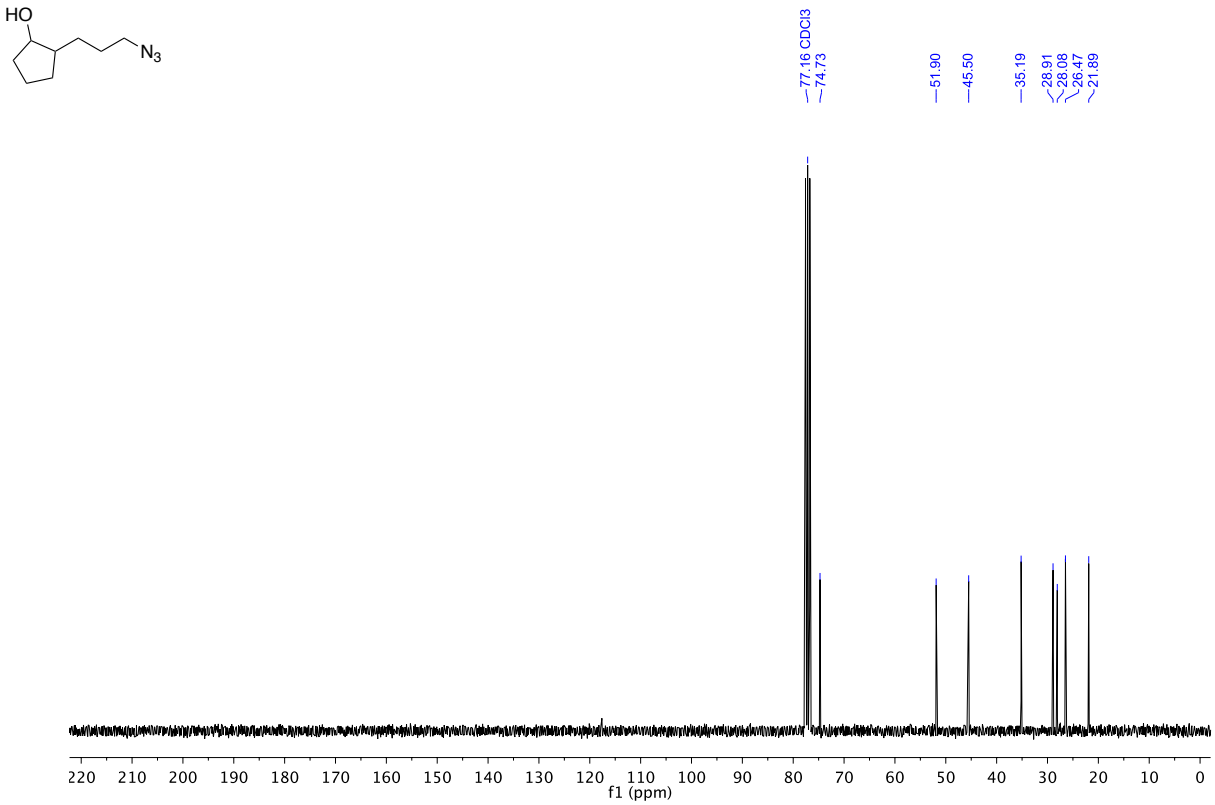

^{1}H NMR (300 MHz, $CDCl_3$)
Major *2-(3-azidopropyl)cyclopentan-1-ol*

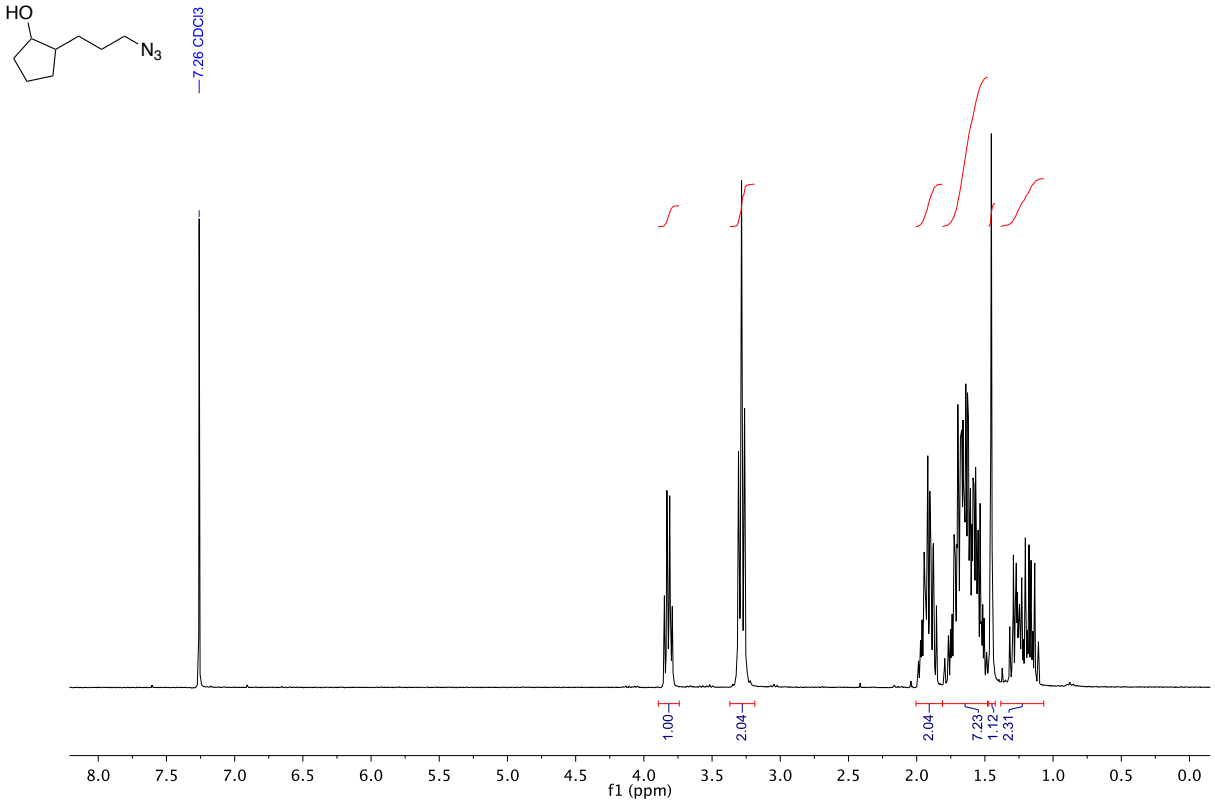

^{13}C NMR (75 MHz, $CDCl_3$)
Major *2-(3-azidopropyl)cyclopentan-1-ol*

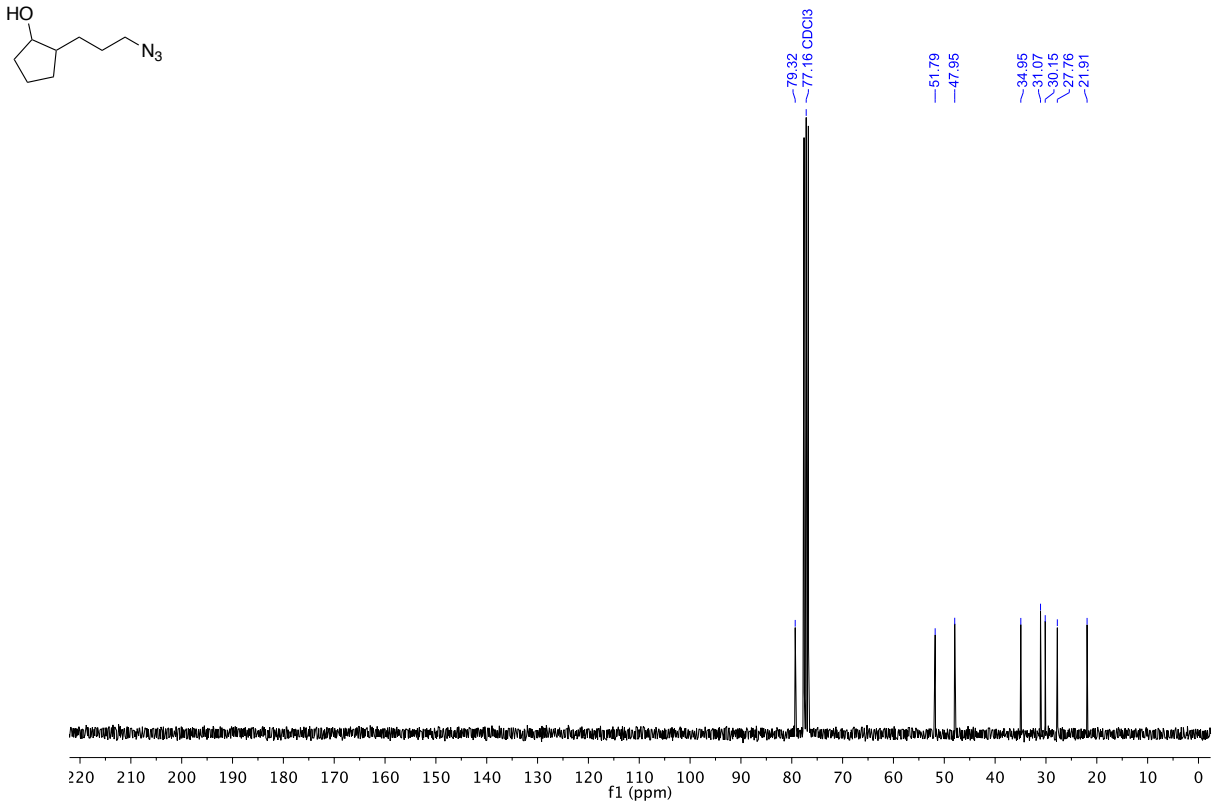

^{1}H NMR (400 MHz, C_6D_6)
Octahydroindolizine

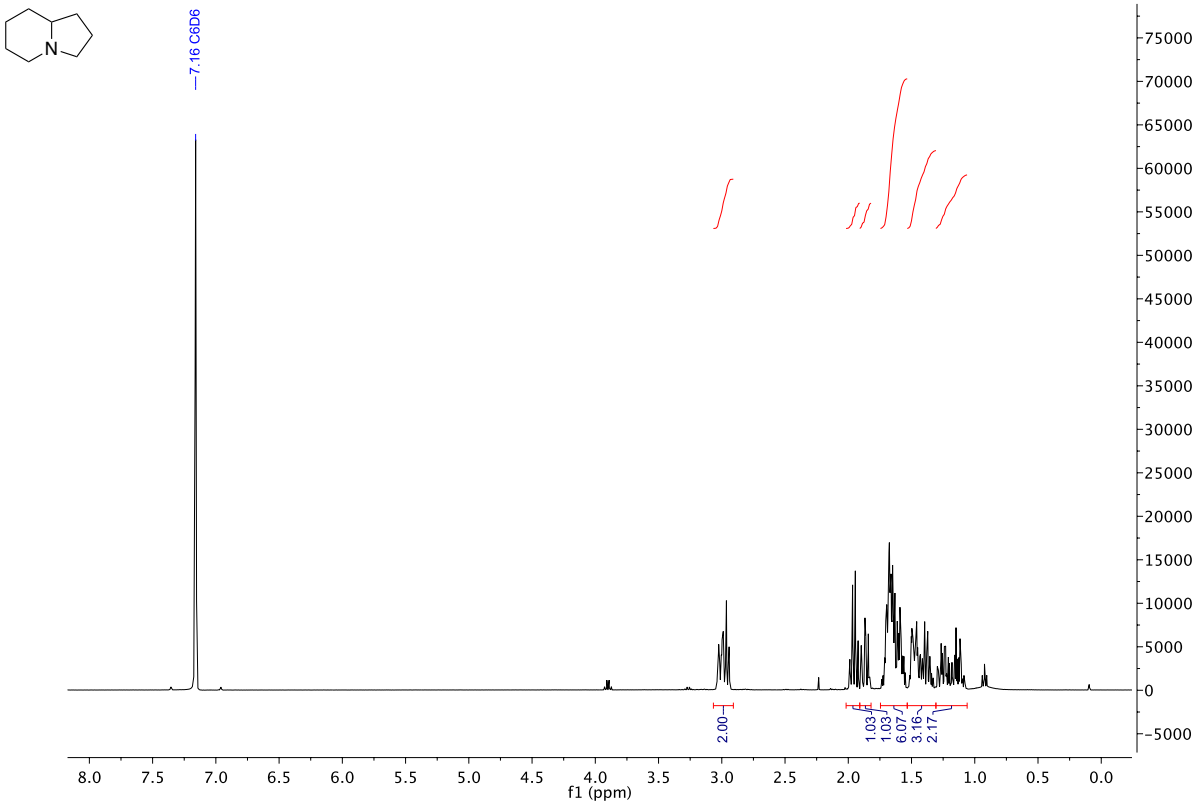

^{13}C NMR (101 MHz, C_6D_6)
Octahydroindolizine

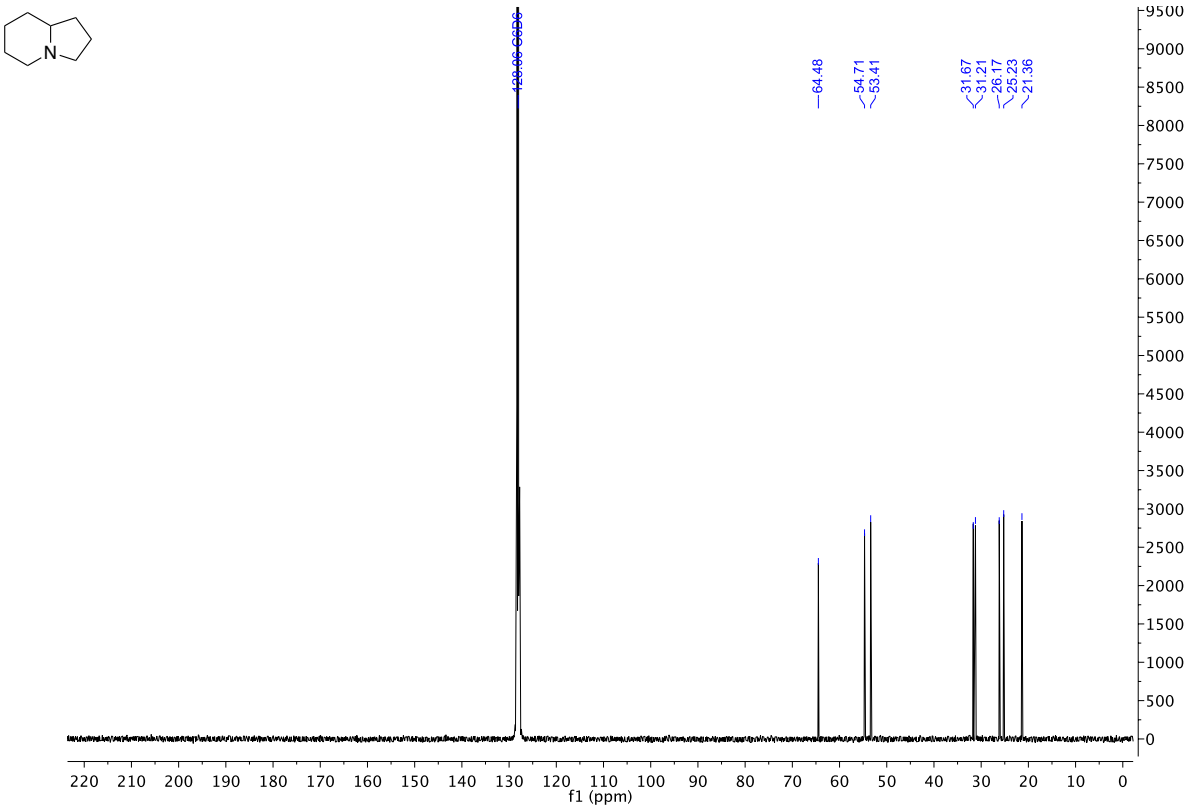

^{1}H NMR (400 MHz, $CDCl_3$)
3-(1-methyl-2,5-dioxocyclopentyl)propanal

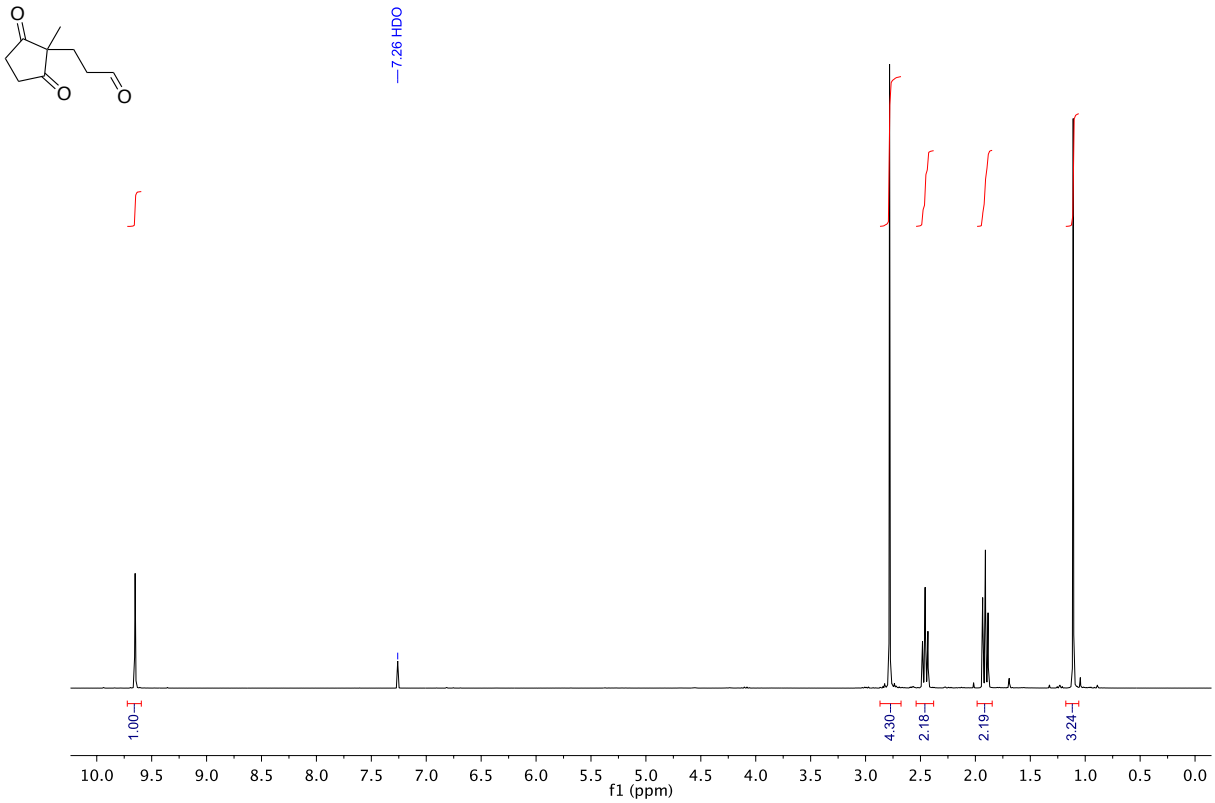

^{13}C NMR (75 MHz, $CDCl_3$)
3-(1-methyl-2,5-dioxocyclopentyl)propanal

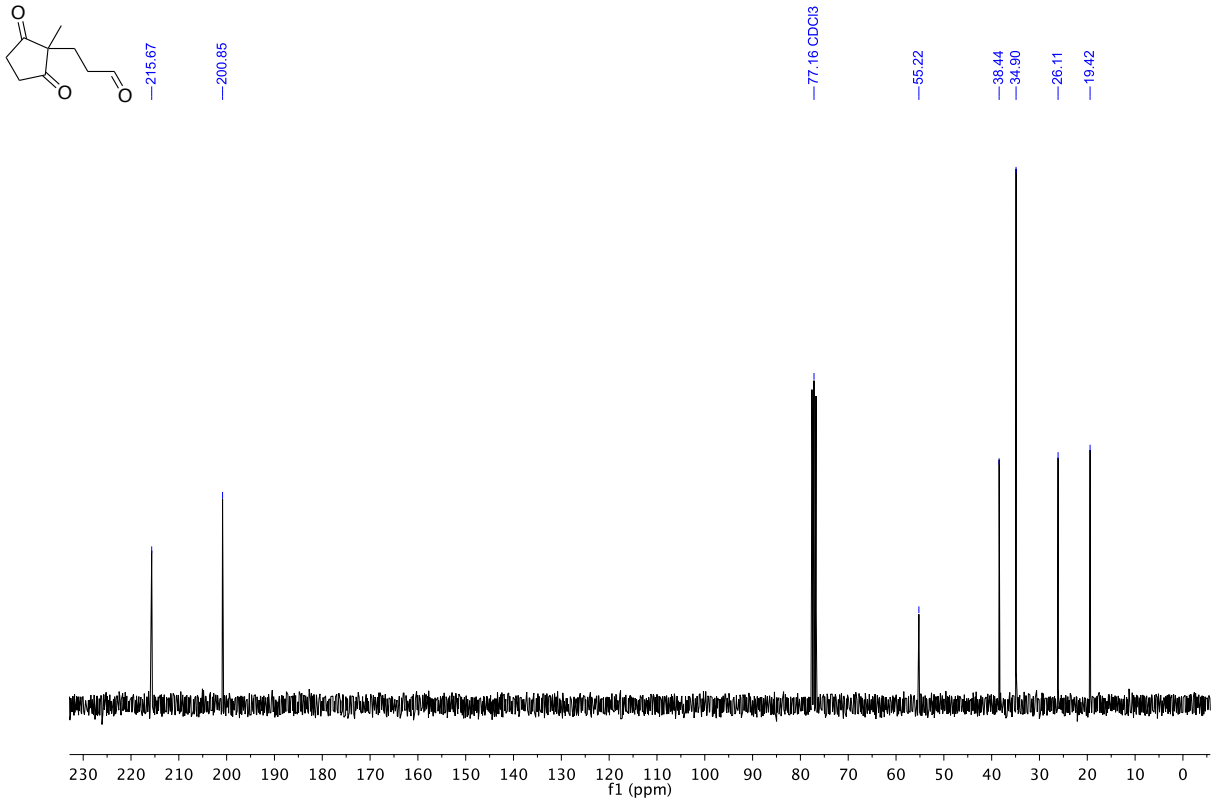

^{1}H NMR (300 MHz, $CDCl_3$)
7a-hydroxy-4a-methylhexahydrocyclopenta[b]pyran-5(2H)-one

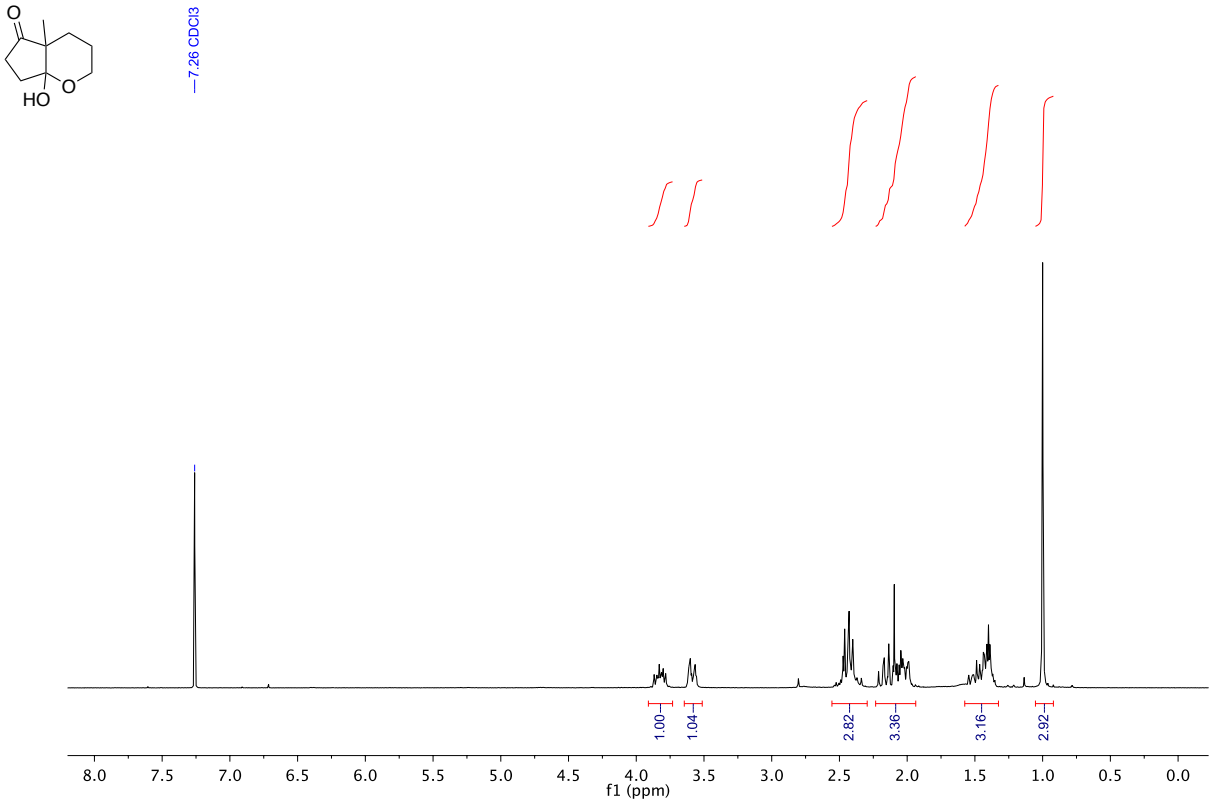

^{13}C NMR (75 MHz, $CDCl_3$)
7a-hydroxy-4a-methylhexahydrocyclopenta[b]pyran-5(2H)-one

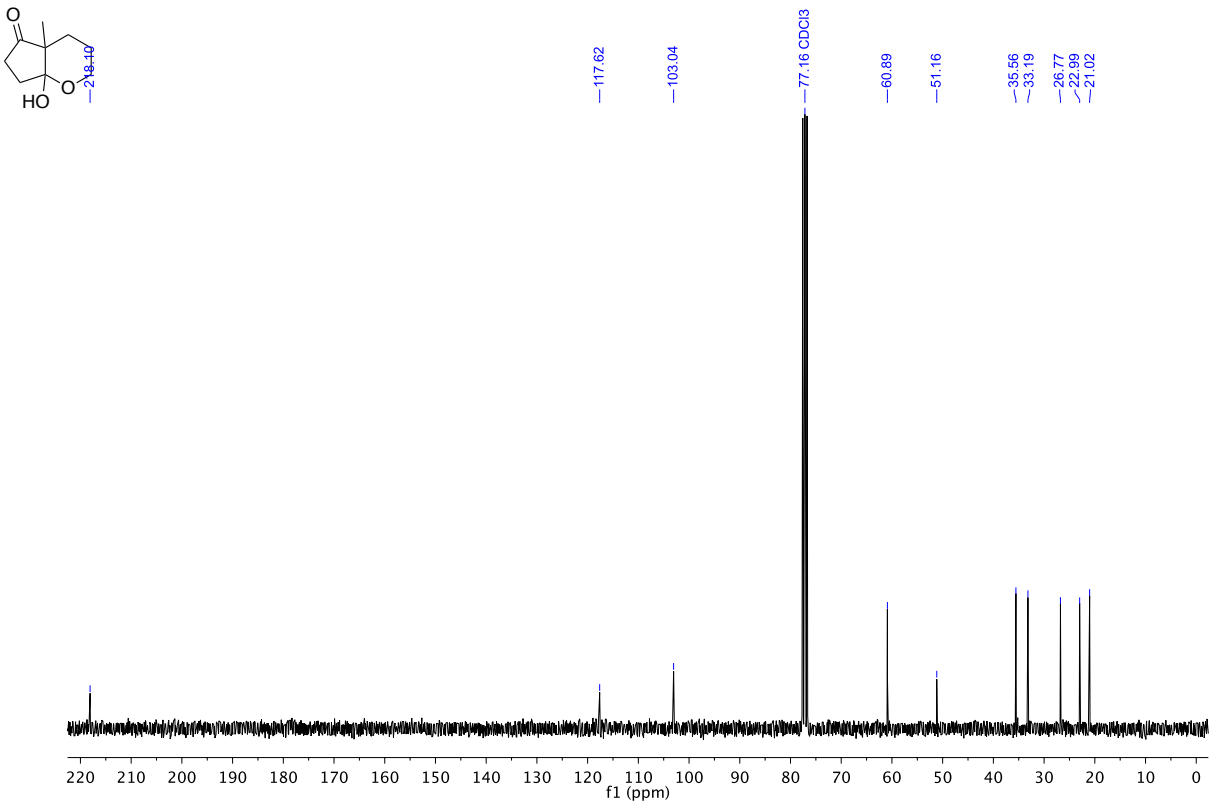

^{1}H NMR (300 MHz, $CDCl_3$)
3-(1-methyl-2,5-dioxocyclopentyl)propyl methanesulfonate

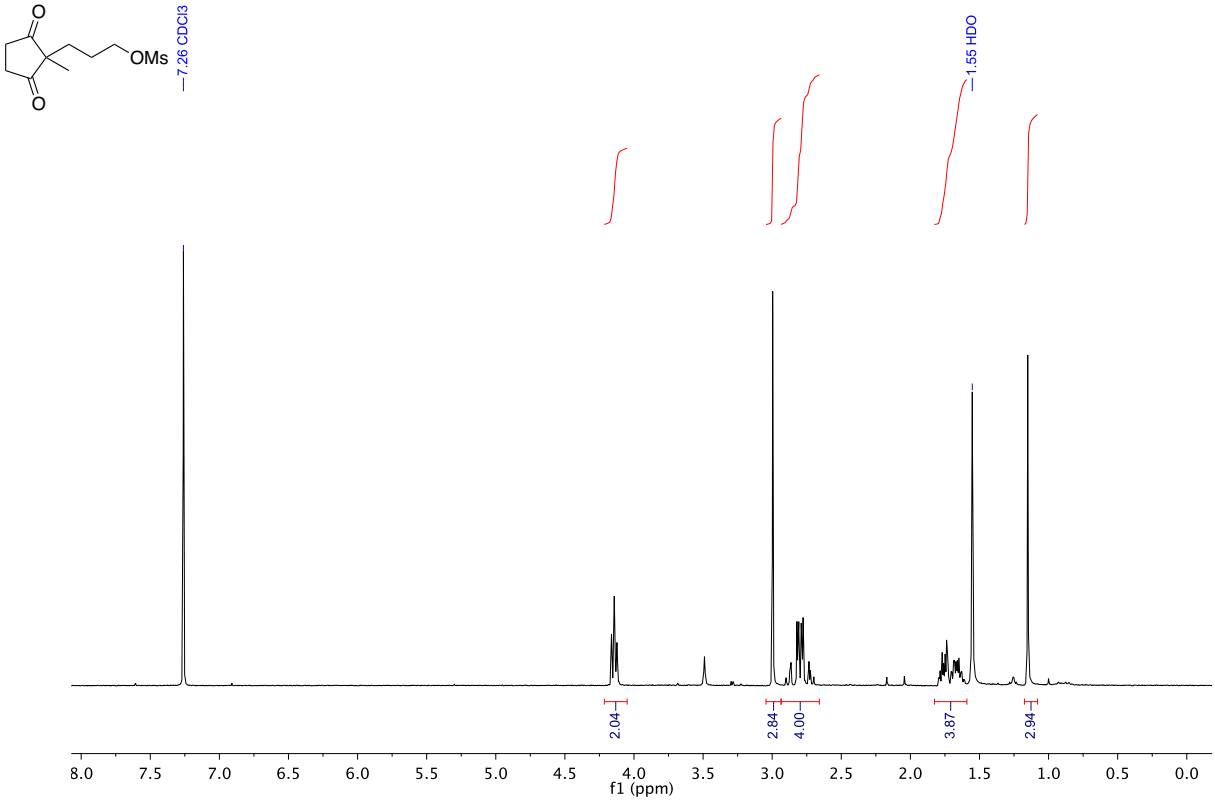

^{13}C NMR (75 MHz, $CDCl_3$)
3-(1-methyl-2,5-dioxocyclopentyl)propyl methanesulfonate

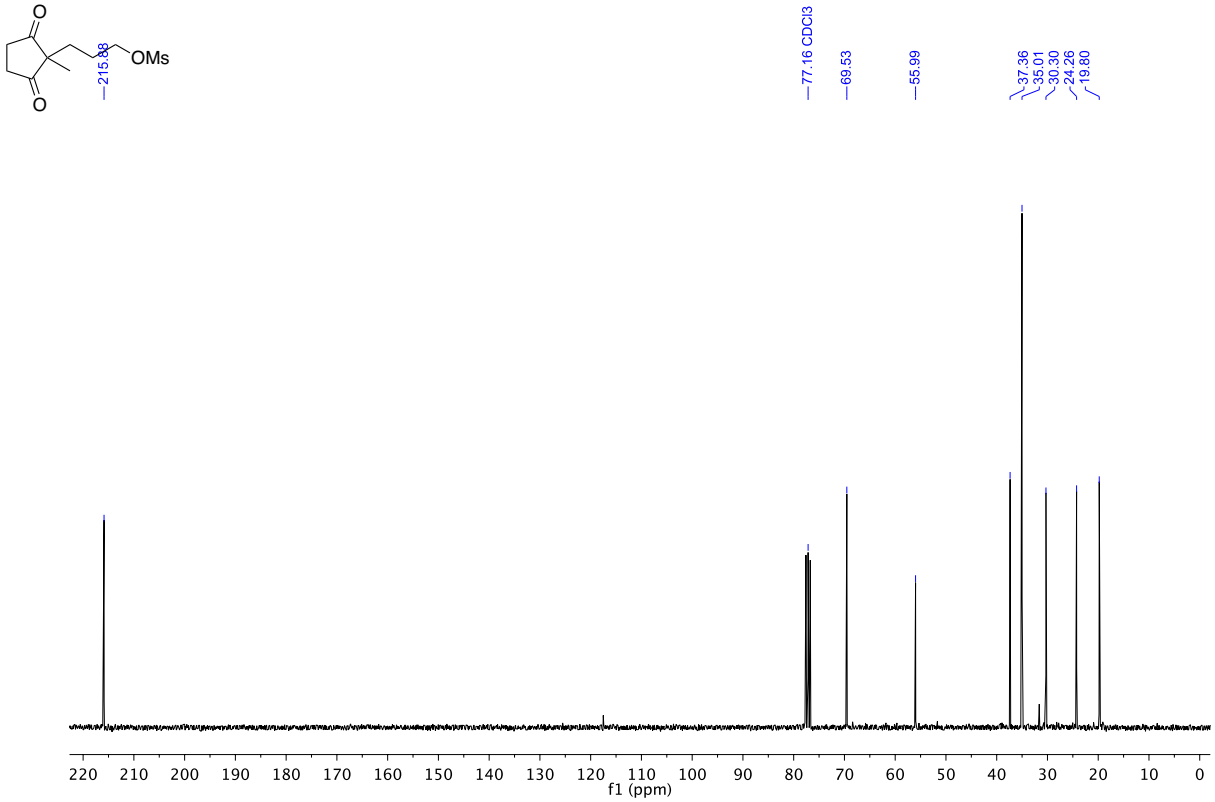

^{1}H NMR (300 MHz, $CDCl_3$)
2-(3-azidopropyl)-2-methylcyclopentane-1,3-dione

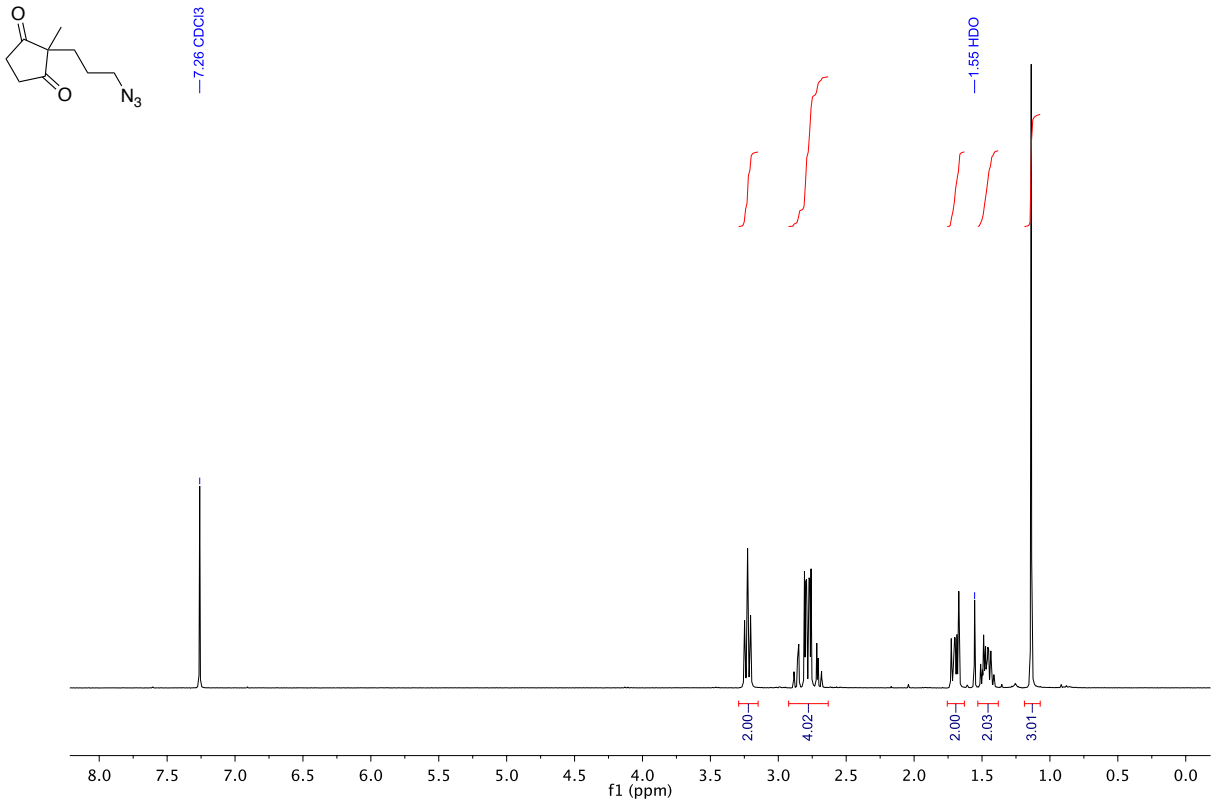

^{13}C NMR (75 MHz, $CDCl_3$)
2-(3-azidopropyl)-2-methylcyclopentane-1,3-dione

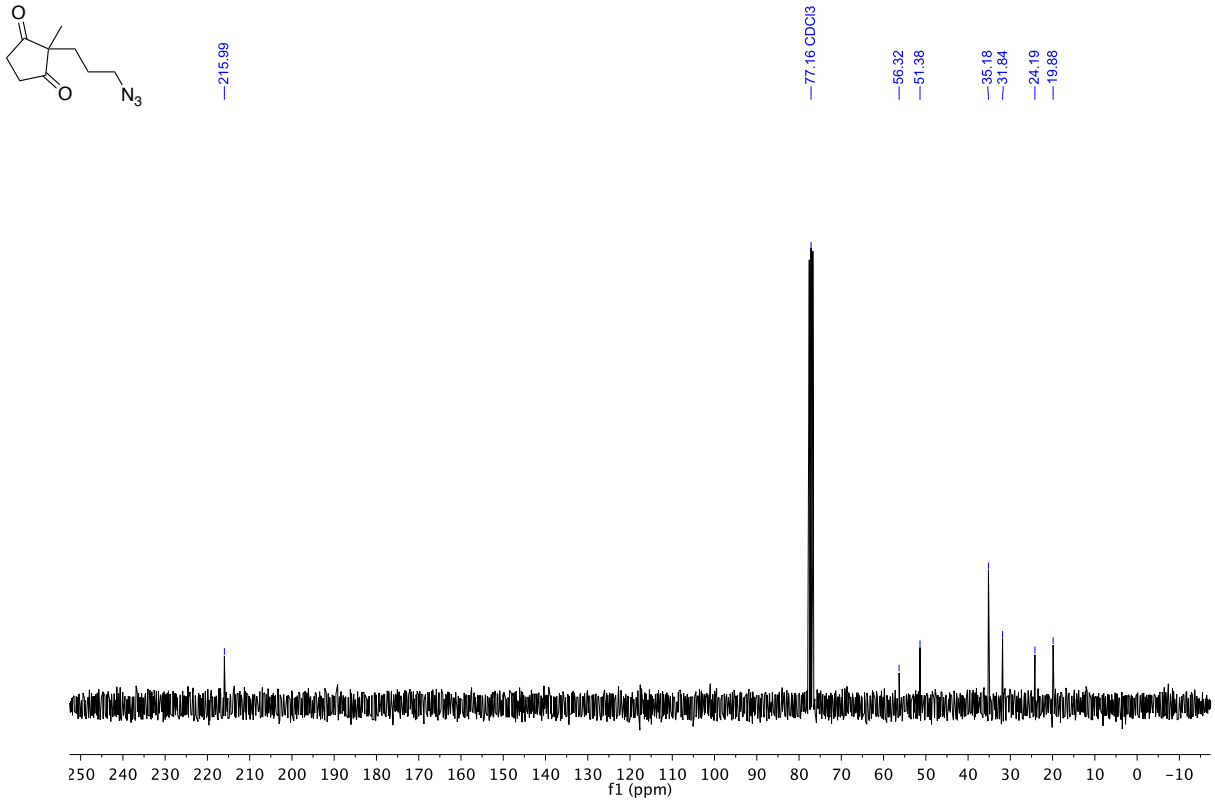

^{1}H NMR (300 MHz, $CDCl_3$)
***Cis*-major** *2-(3-azidopropyl)-2-methylcyclopentane-1,3-diol*

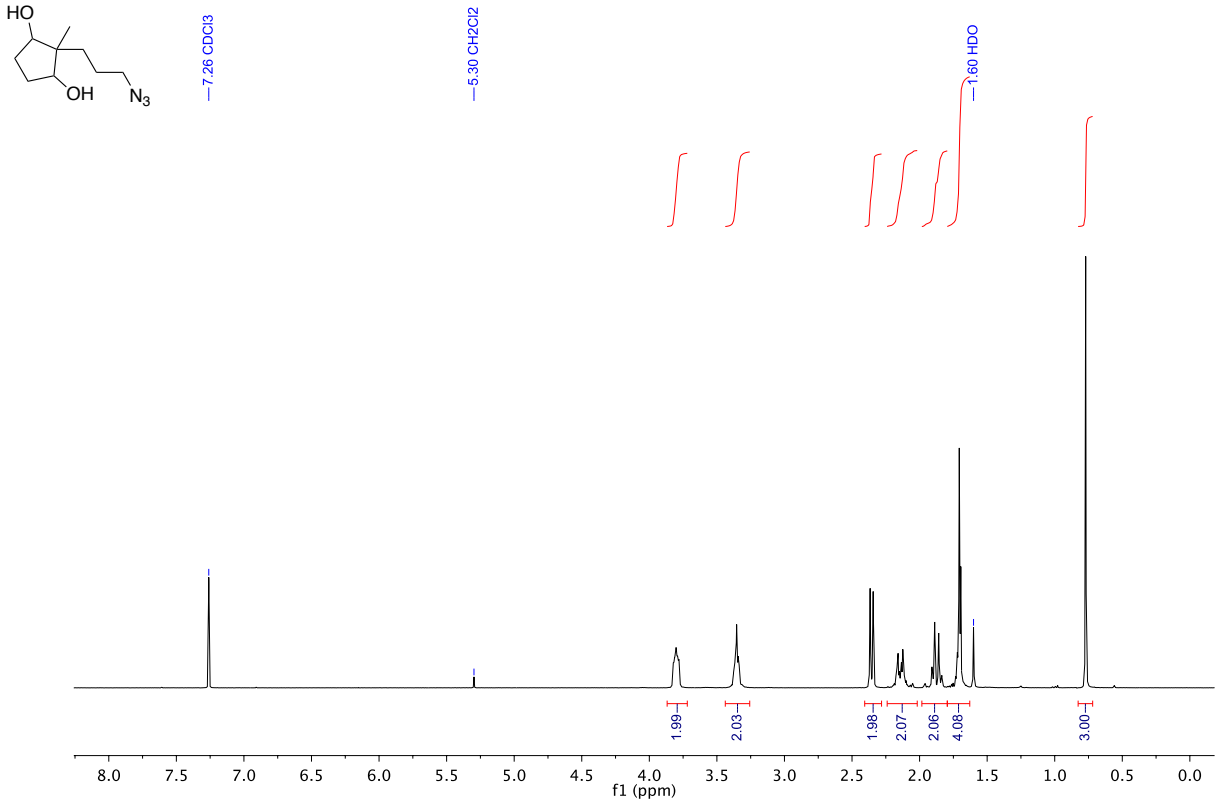

^{13}C NMR (101 MHz, $CDCl_3$)
***Cis*-major** *2-(3-azidopropyl)-2-methylcyclopentane-1,3-diol*

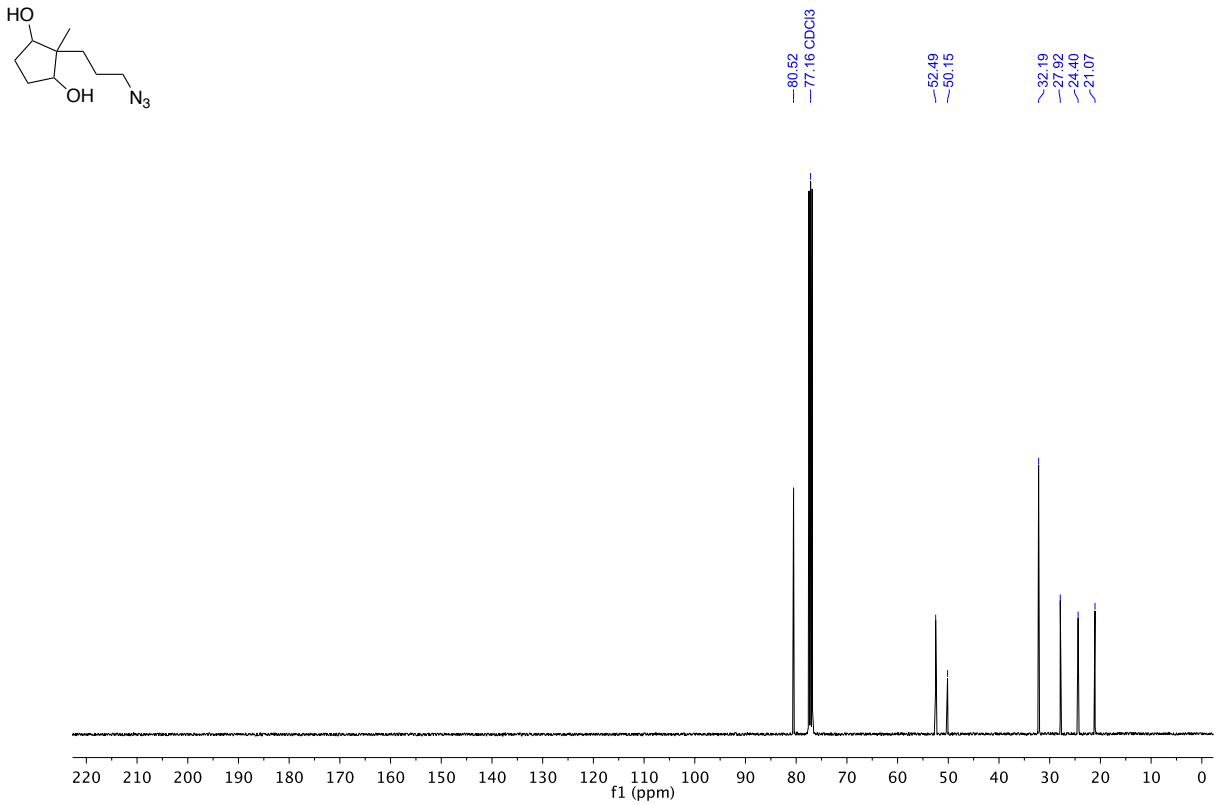

^{1}H NMR (300 MHz, $CDCl_3$)
***Cis*-minor** *2-(3-azidopropyl)-2-methylcyclopentane-1,3-diol*

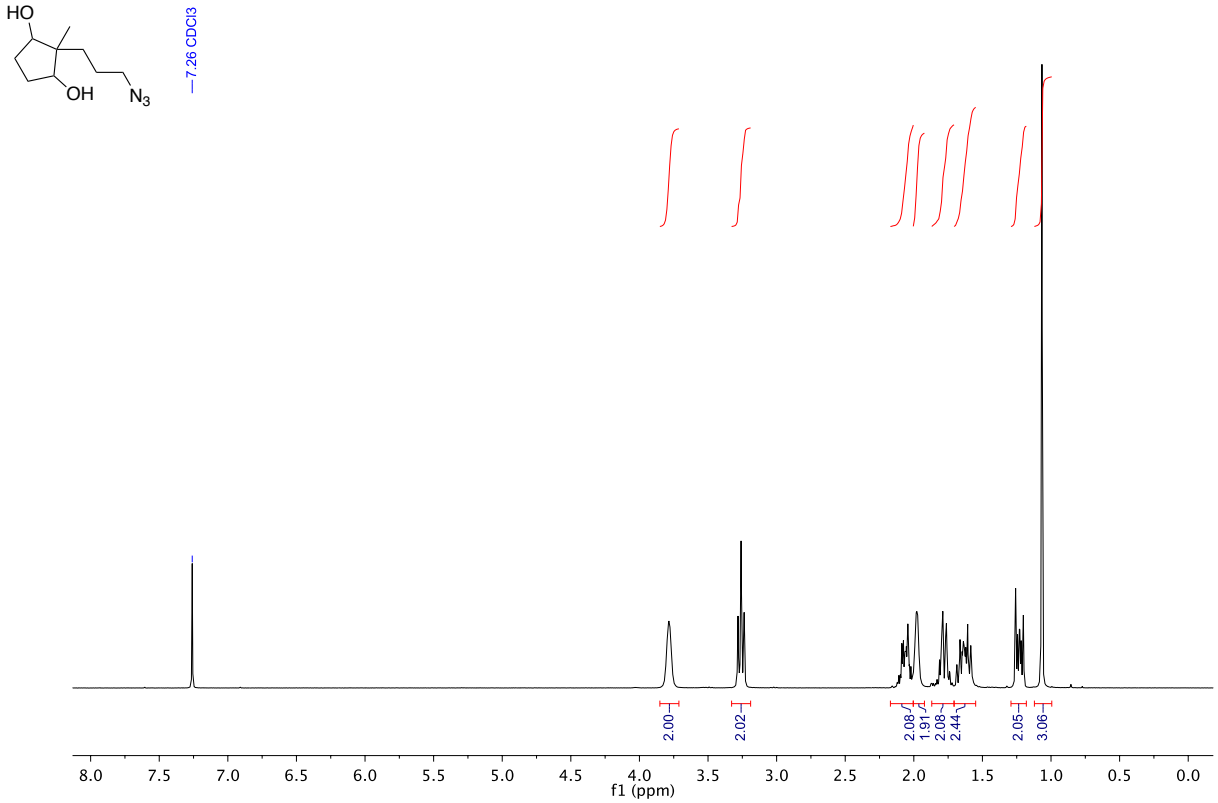

^{13}C NMR (101 MHz, $CDCl_3$)
***Cis*-minor** *2-(3-azidopropyl)-2-methylcyclopentane-1,3-diol*

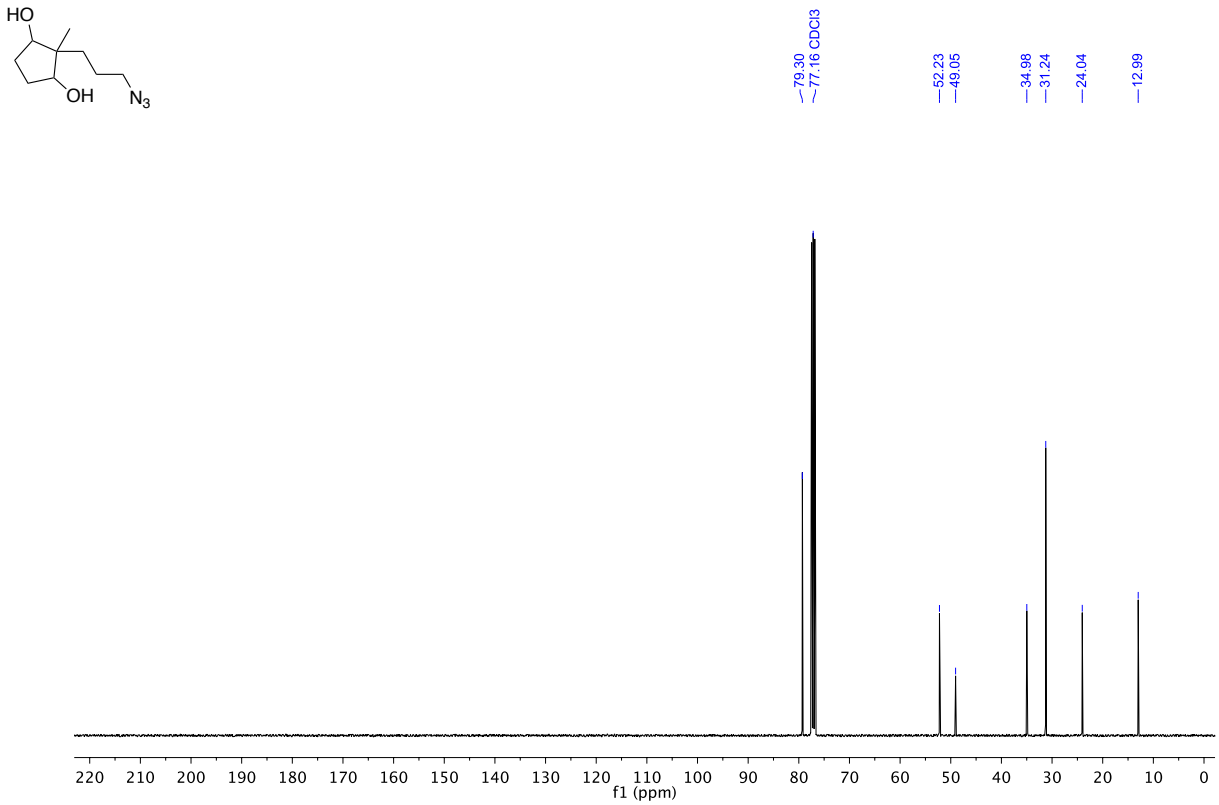

^{1}H NMR (400 MHz, $CDCl_3$)
***Trans** 2-(3-azidopropyl)-2-methylcyclopentane-1,3-diol*

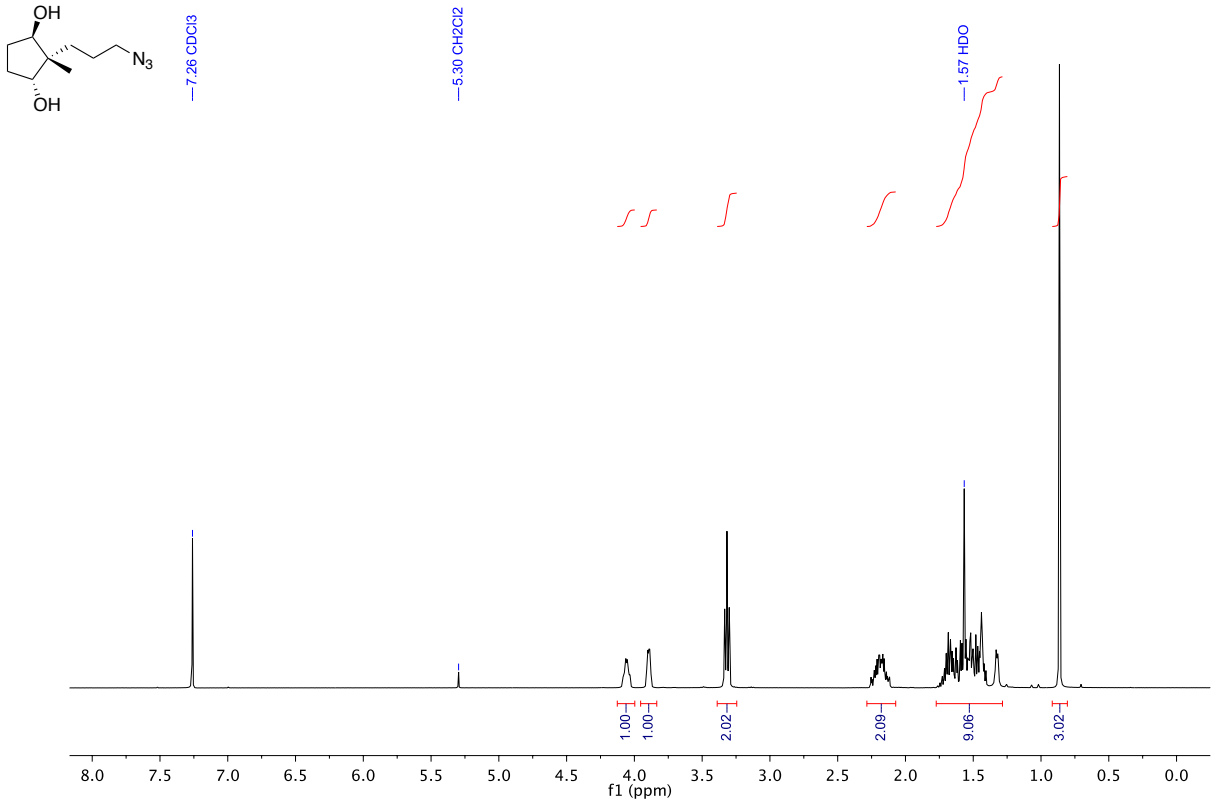

^{13}C NMR (101 MHz, $CDCl_3$)
***Trans** 2-(3-azidopropyl)-2-methylcyclopentane-1,3-diol*

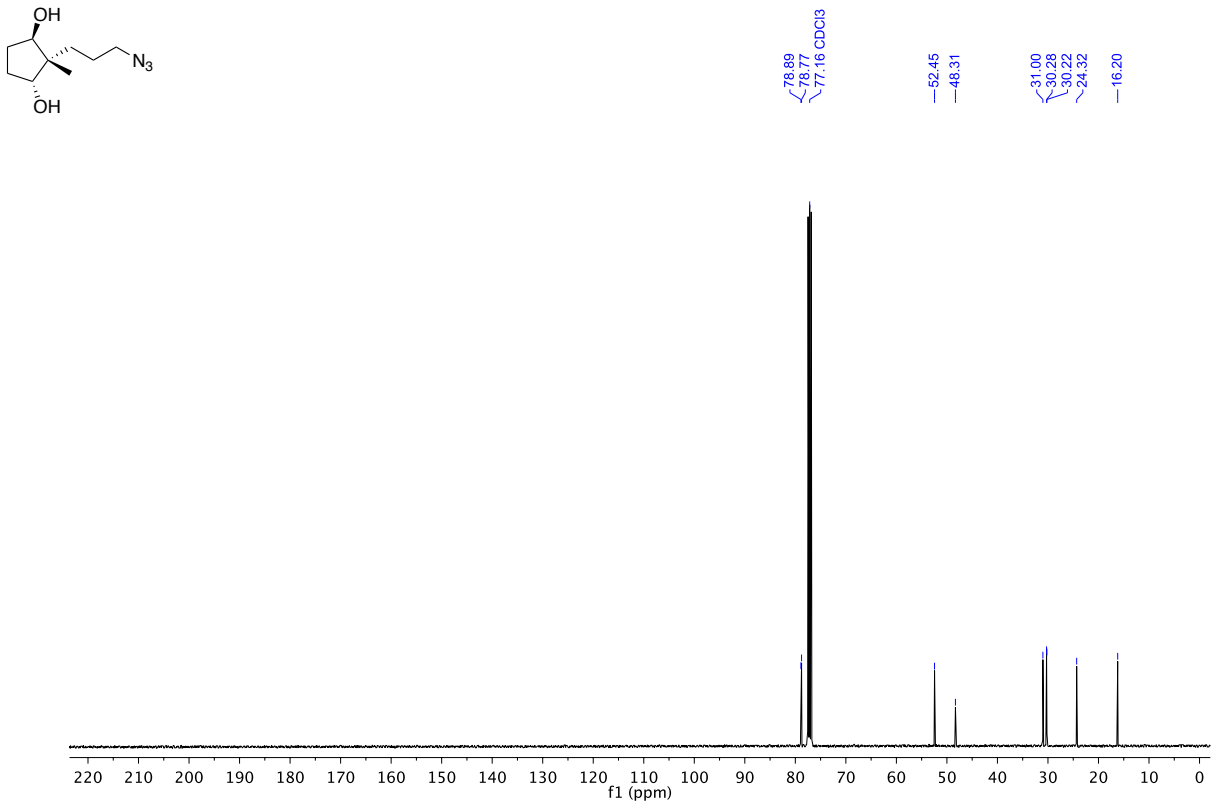

^{1}H NMR (300 MHz, $CDCl_3$)
Methyl 3-(1-methyl-2-oxocyclopentyl)propanoate

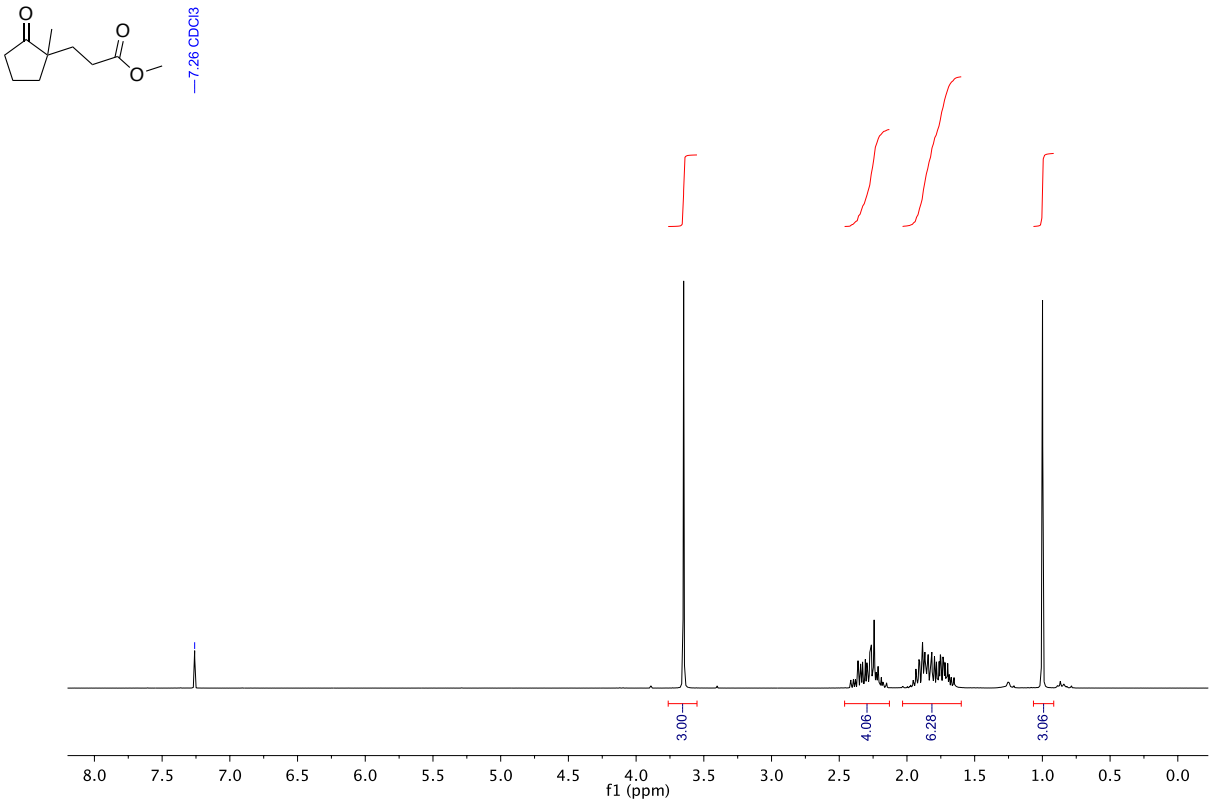

^{13}C NMR (75 MHz, $CDCl_3$)
Methyl 3-(1-methyl-2-oxocyclopentyl)propanoate

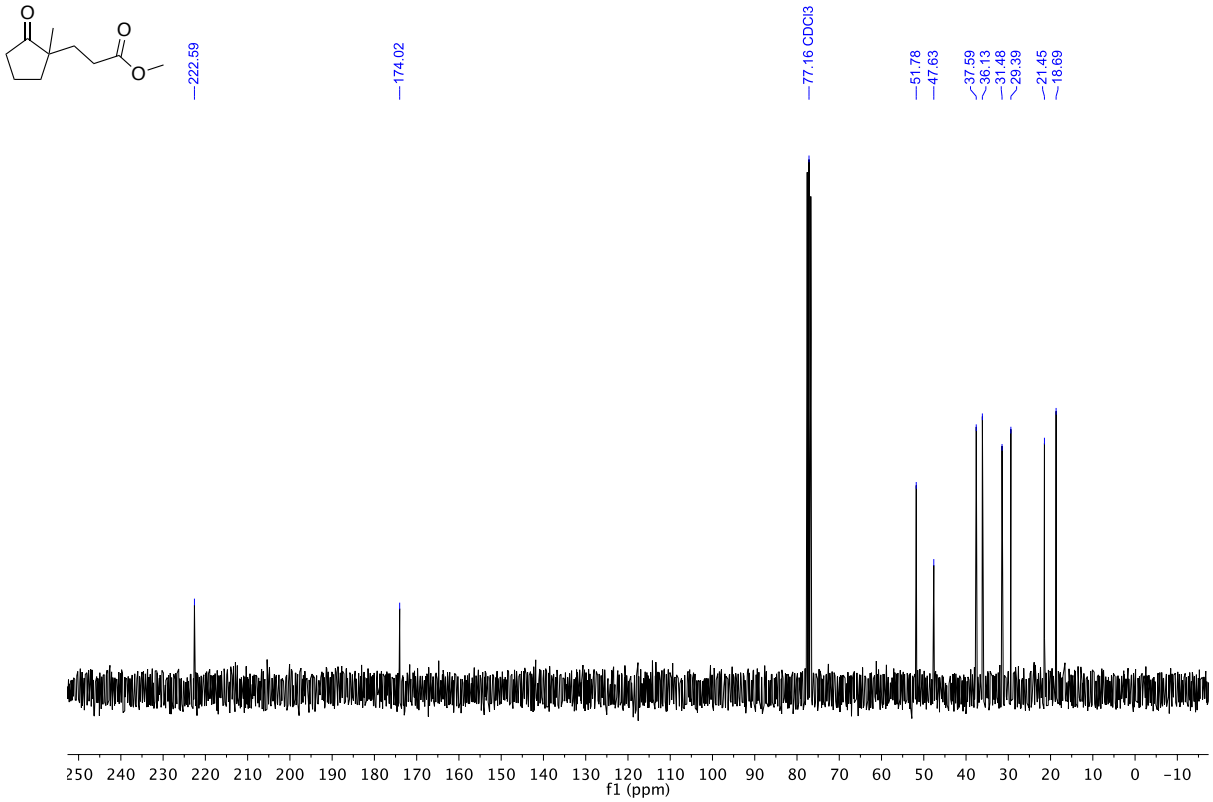

^{1}H NMR (300 MHz, $CDCl_3$)
2-(3-hydroxypropyl)-2-methylcyclopentan-1-ol

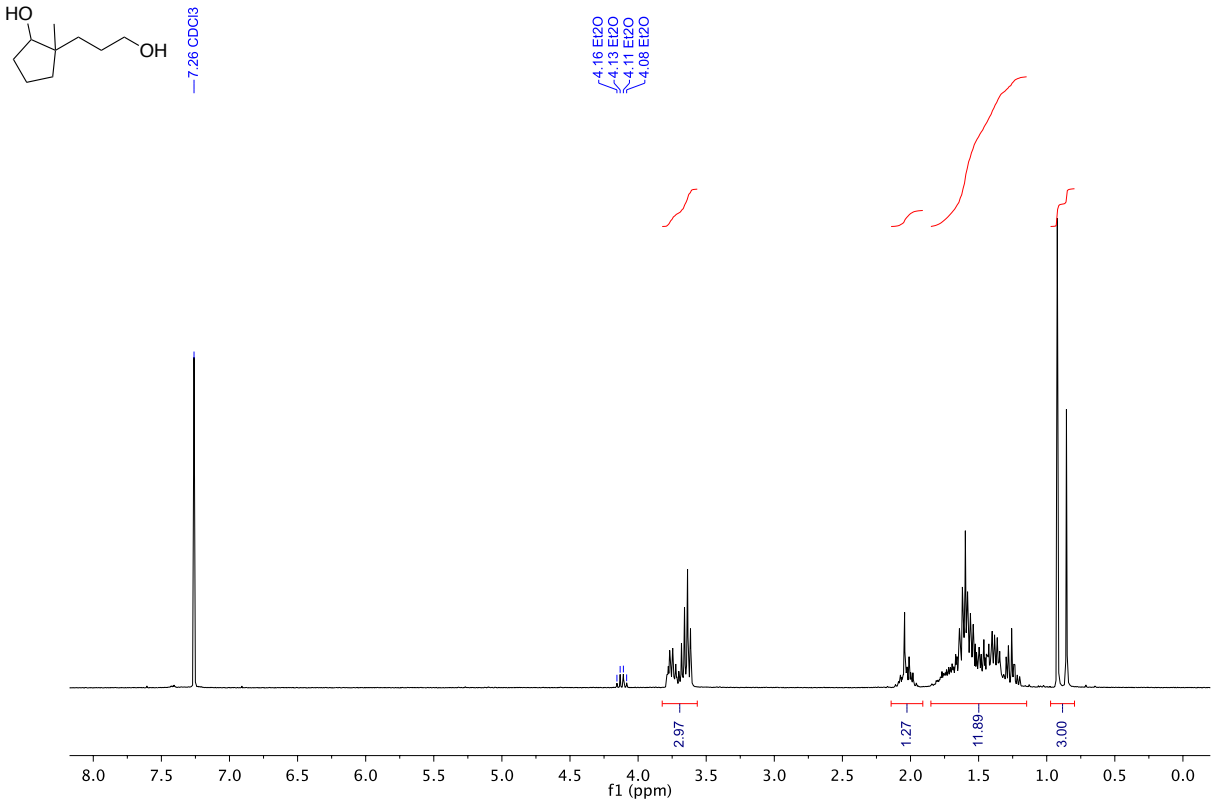

^{13}C NMR (75 MHz, $CDCl_3$)
2-(3-hydroxypropyl)-2-methylcyclopentan-1-ol

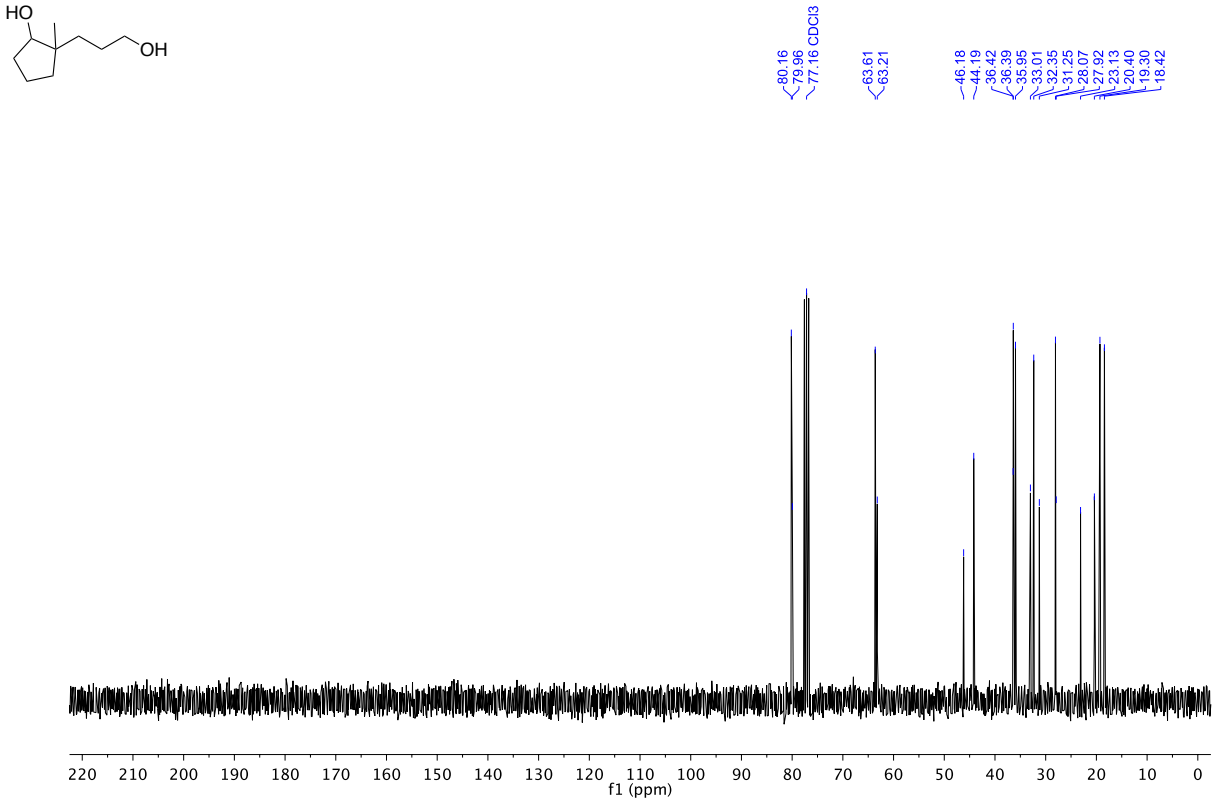

^{1}H NMR (400 MHz, $CDCl_3$)
Major *3-(2-hydroxy-1-methylcyclopentyl)propyl 4-methylbenzenesulfonate*

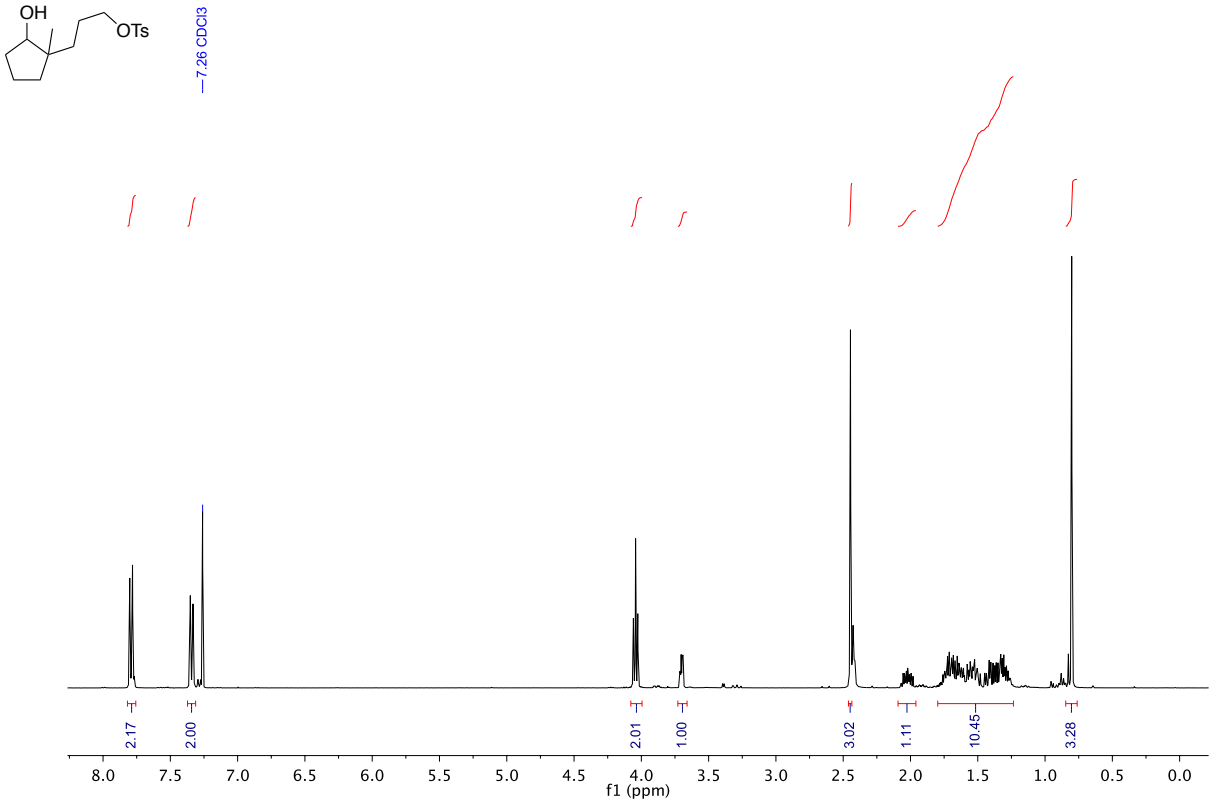

^{13}C NMR (MHz, $CDCl_3$)
Major *3-(2-hydroxy-1-methylcyclopentyl)propyl 4-methylbenzenesulfonate*

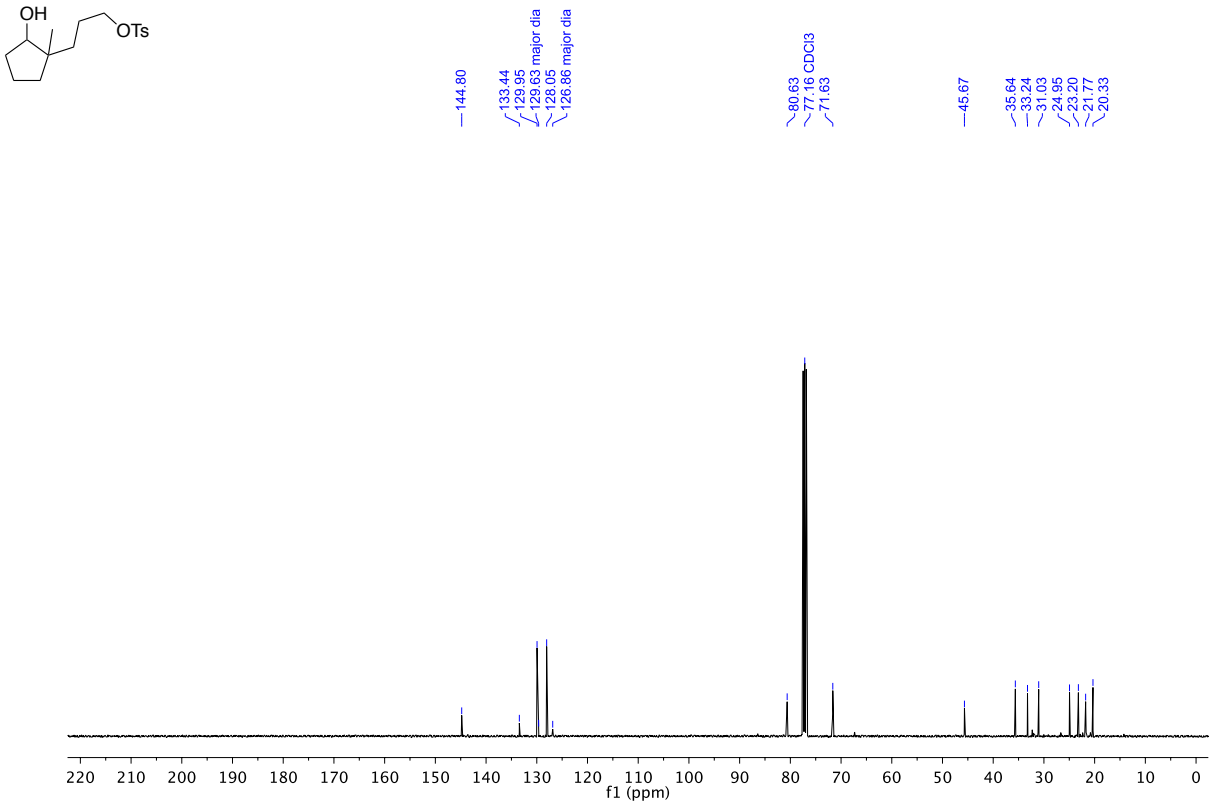

^{1}H NMR (300 MHz, $CDCl_3$)
Minor *3-(2-hydroxy-1-methylcyclopentyl)propyl 4-methylbenzenesulfonate*

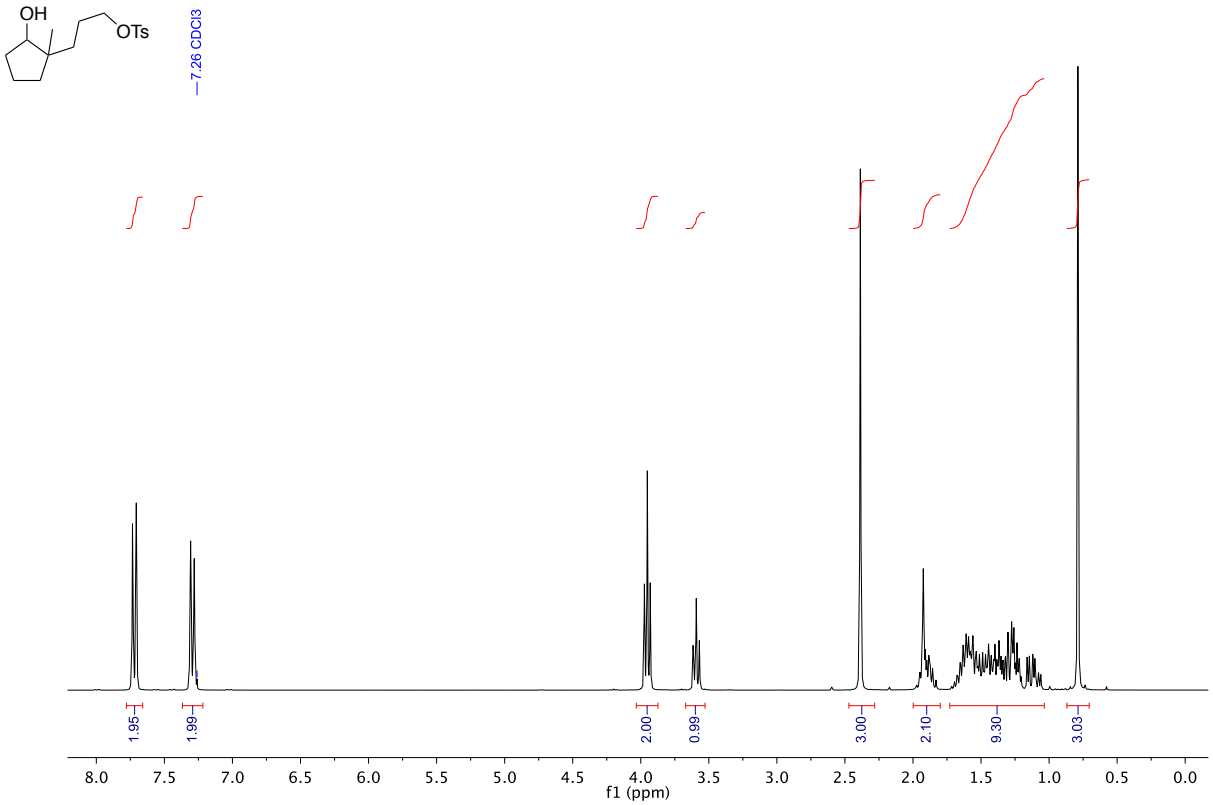

^{13}C NMR (75 MHz, $CDCl_3$)
Minor *3-(2-hydroxy-1-methylcyclopentyl)propyl 4-methylbenzenesulfonate*

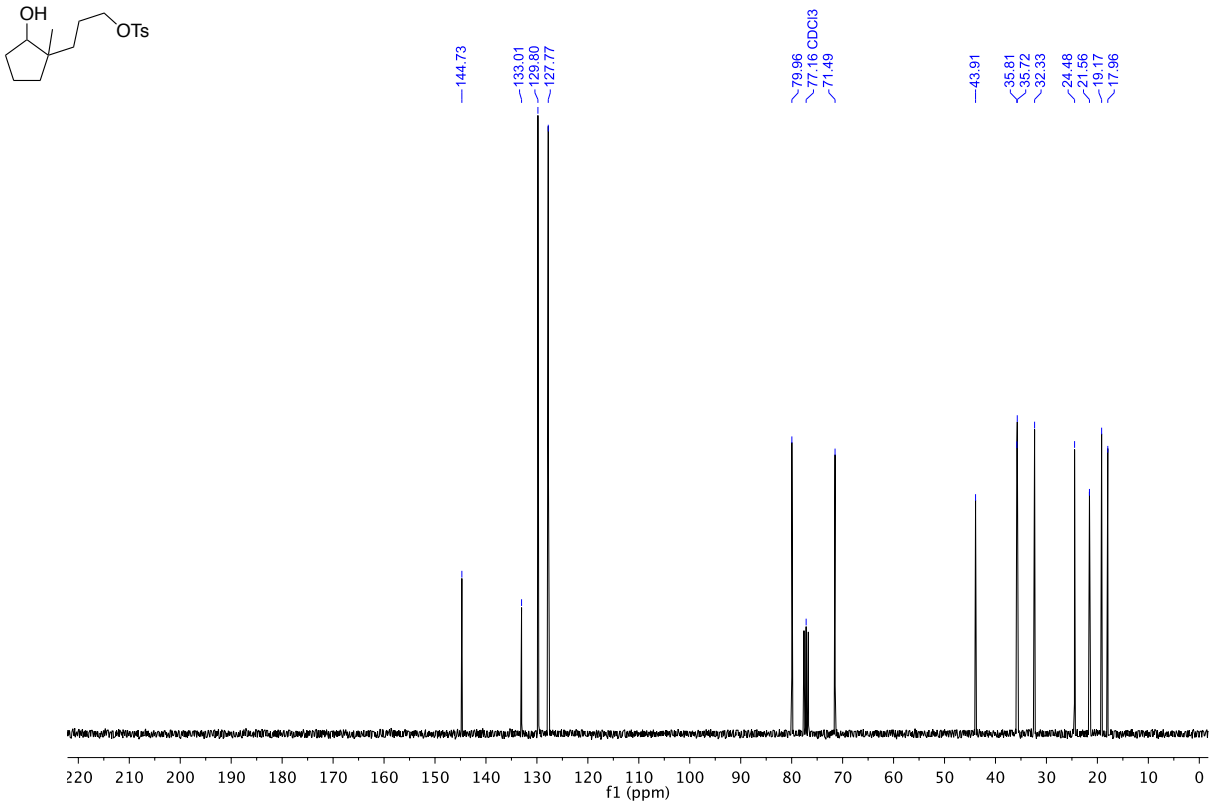

^{1}H NMR (300 MHz, $CDCl_3$)
Major *2-(3-azidopropyl)-2-methylcyclopentan-1-ol*

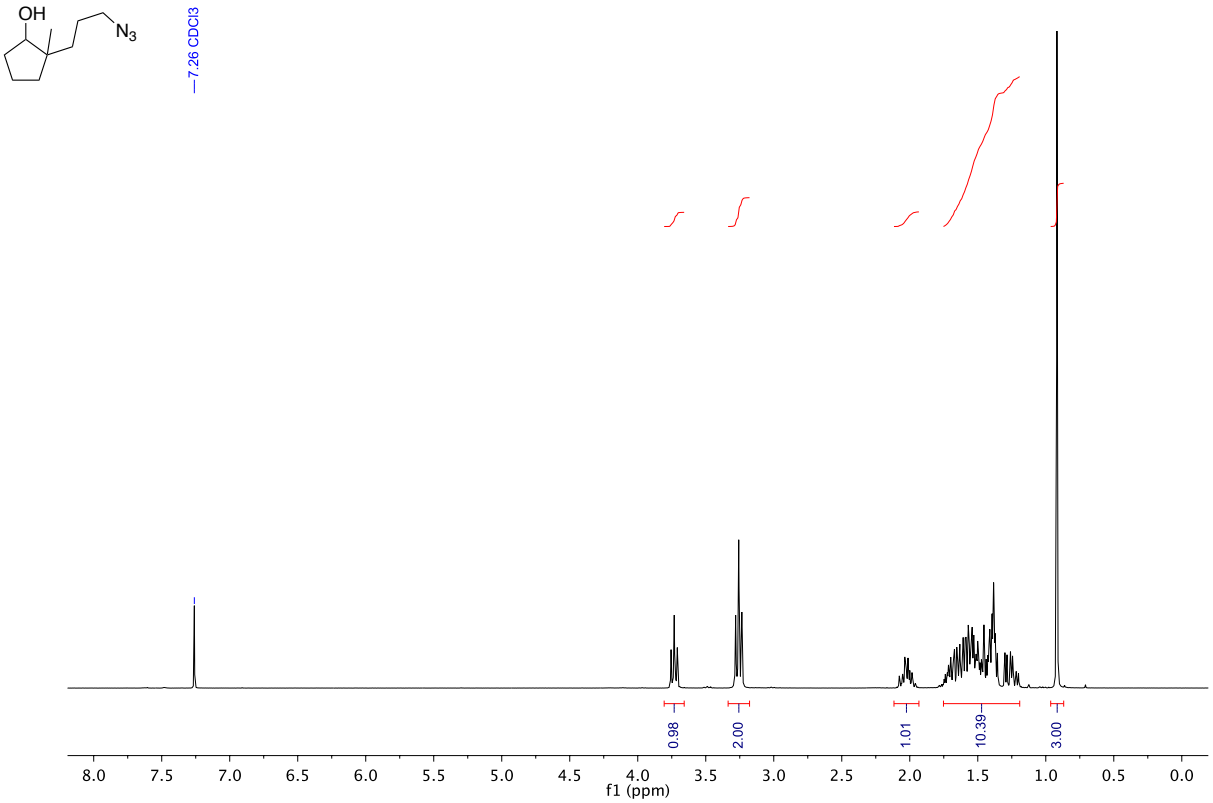

^{13}C NMR (75 MHz, $CDCl_3$)
Major *2-(3-azidopropyl)-2-methylcyclopentan-1-ol*

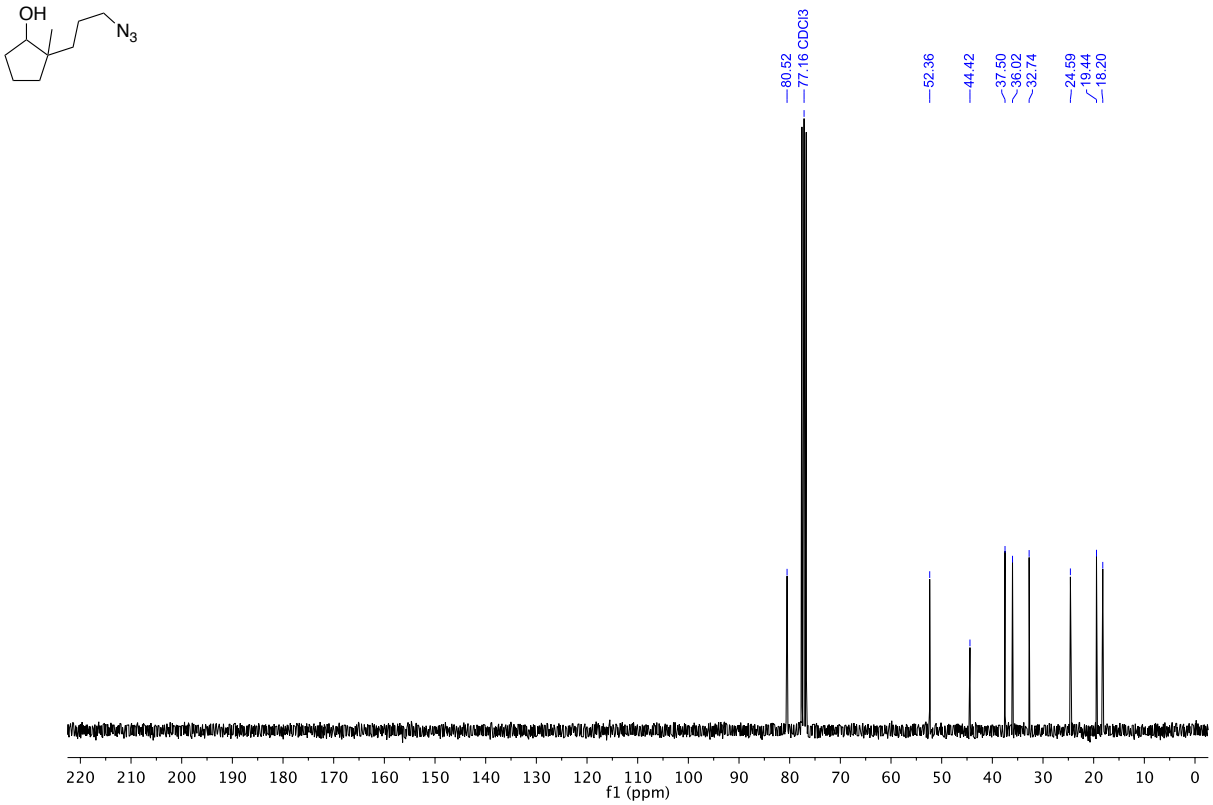

^{1}H NMR (300 MHz, $CDCl_3$)
Minor *2-(3-azidopropyl)-2-methylcyclopentan-1-ol*

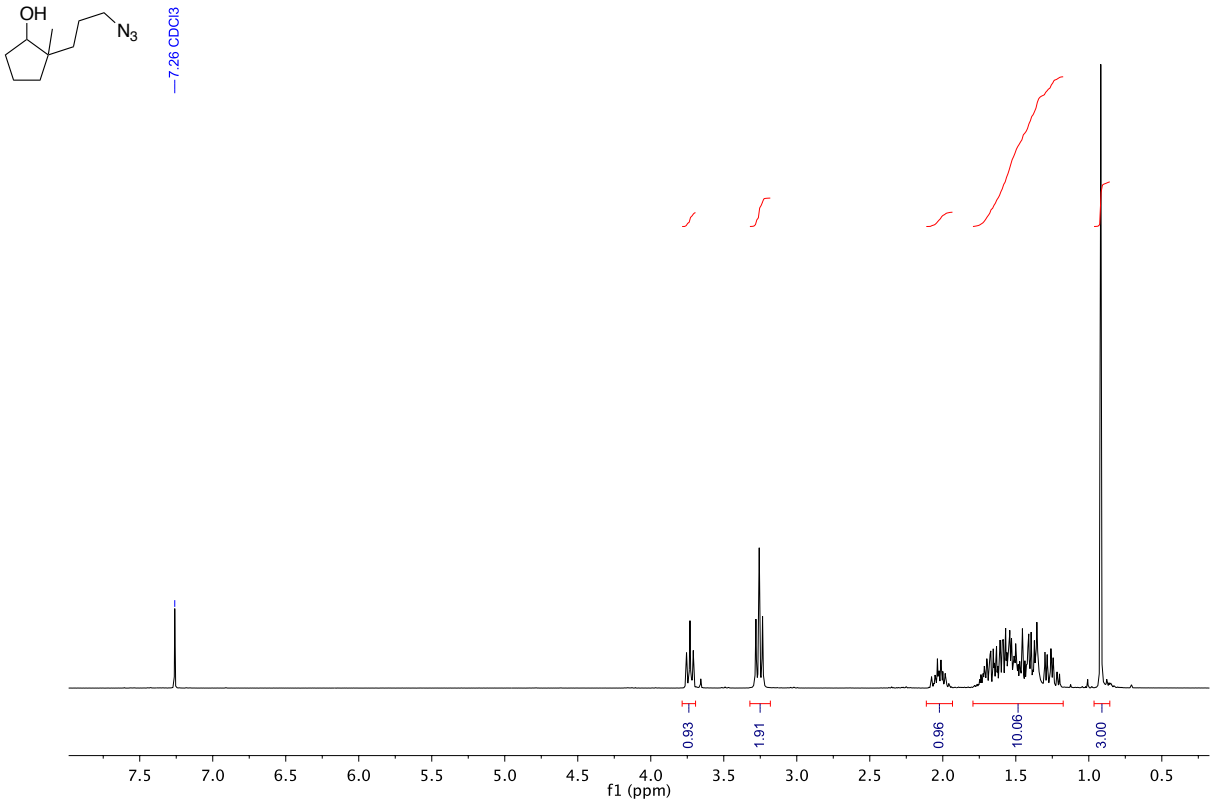

^{13}C NMR (75 MHz, $CDCl_3$)
Minor *2-(3-azidopropyl)-2-methylcyclopentan-1-ol*

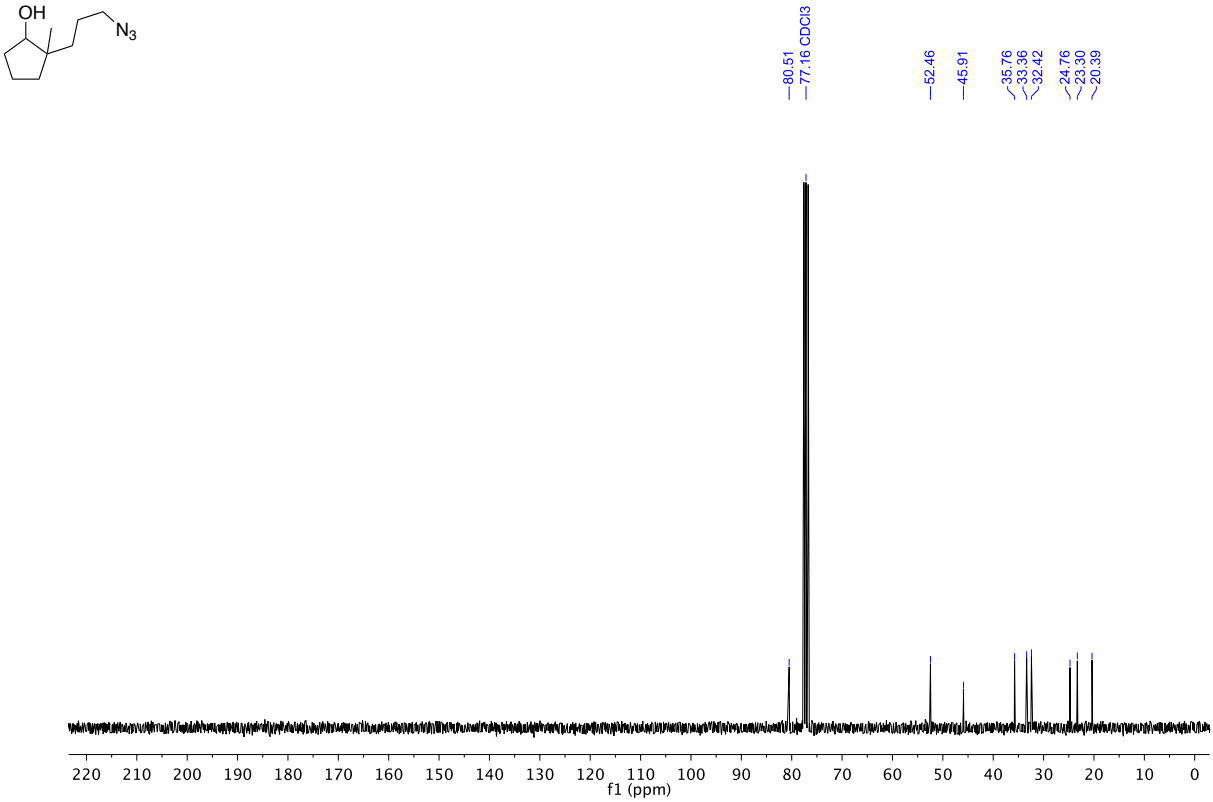

^{1}H NMR (300 MHz, $CDCl_3$)
3-(6-hydroxycyclohex-1-en-1-yl)propyl 4-methylbenzenesulfonate

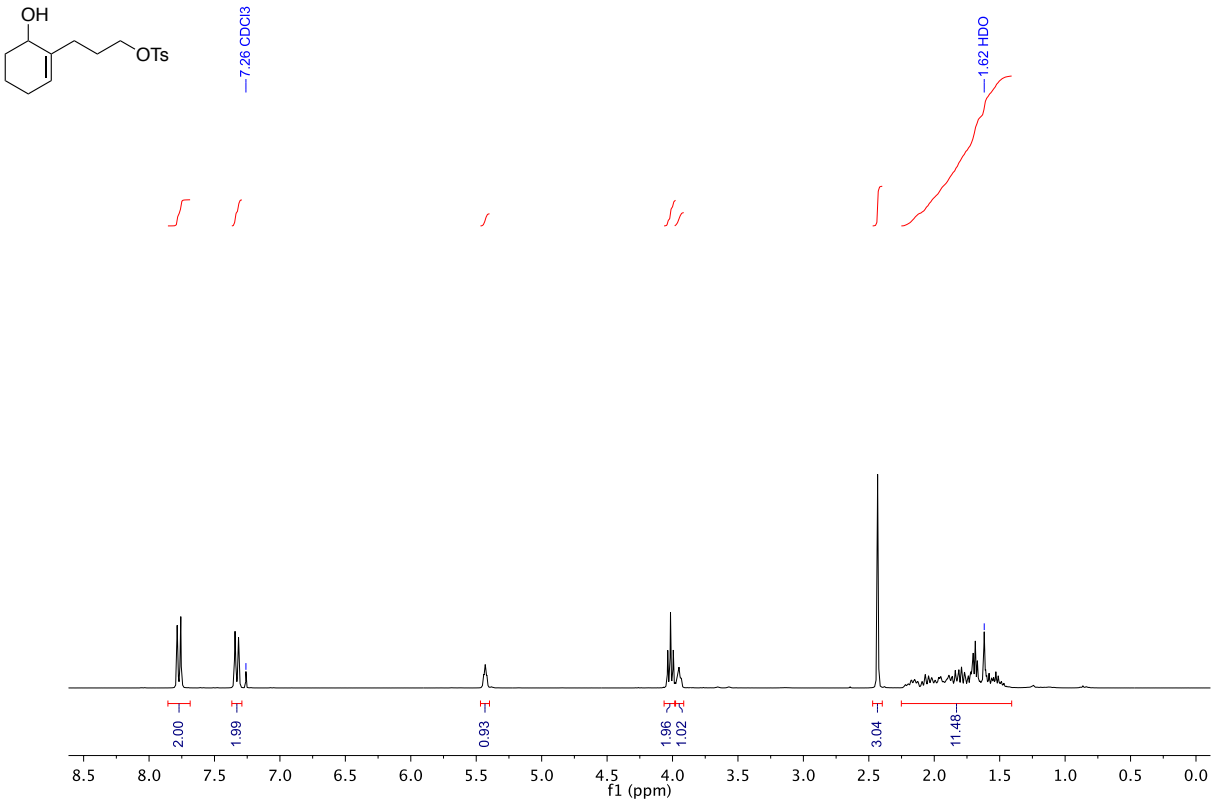

^{13}C NMR (75 MHz, $CDCl_3$)
3-(6-hydroxycyclohex-1-en-1-yl)propyl 4-methylbenzenesulfonate

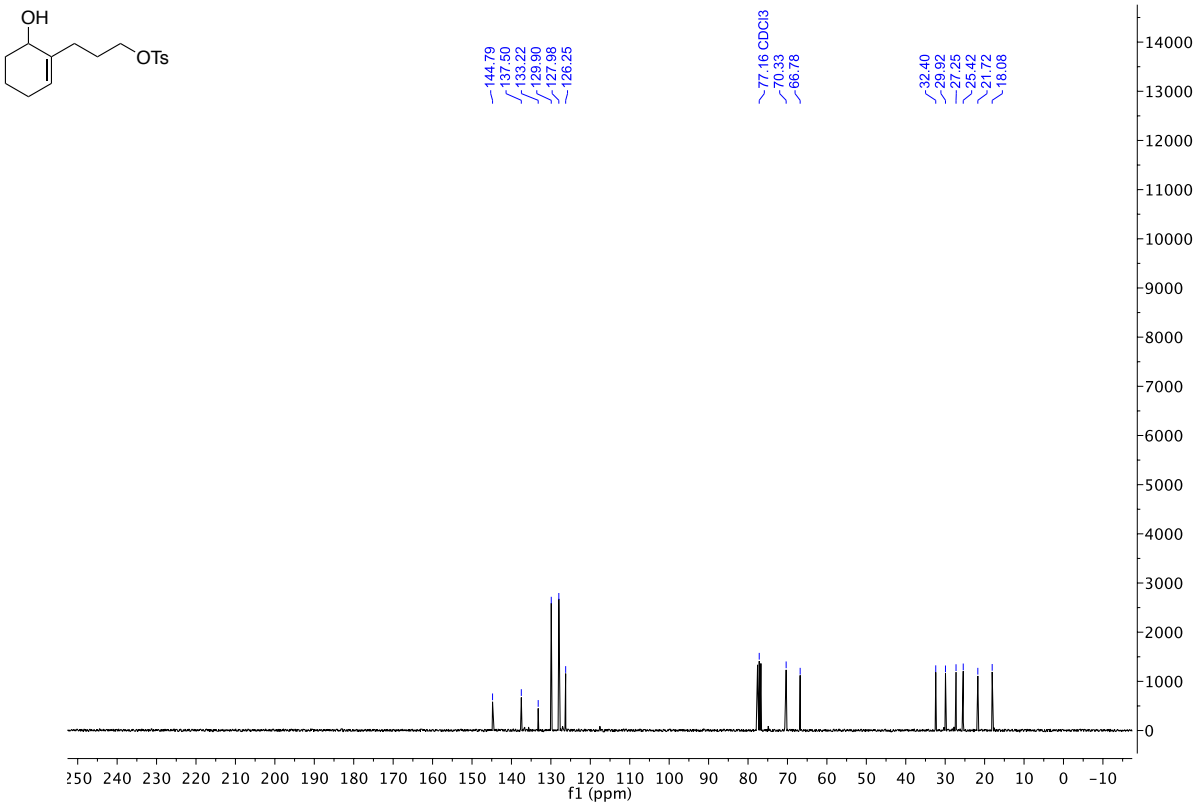

^{1}H NMR (300 MHz, $CDCl_3$)
2-(3-azidopropyl)cyclohex-2-en-1-ol

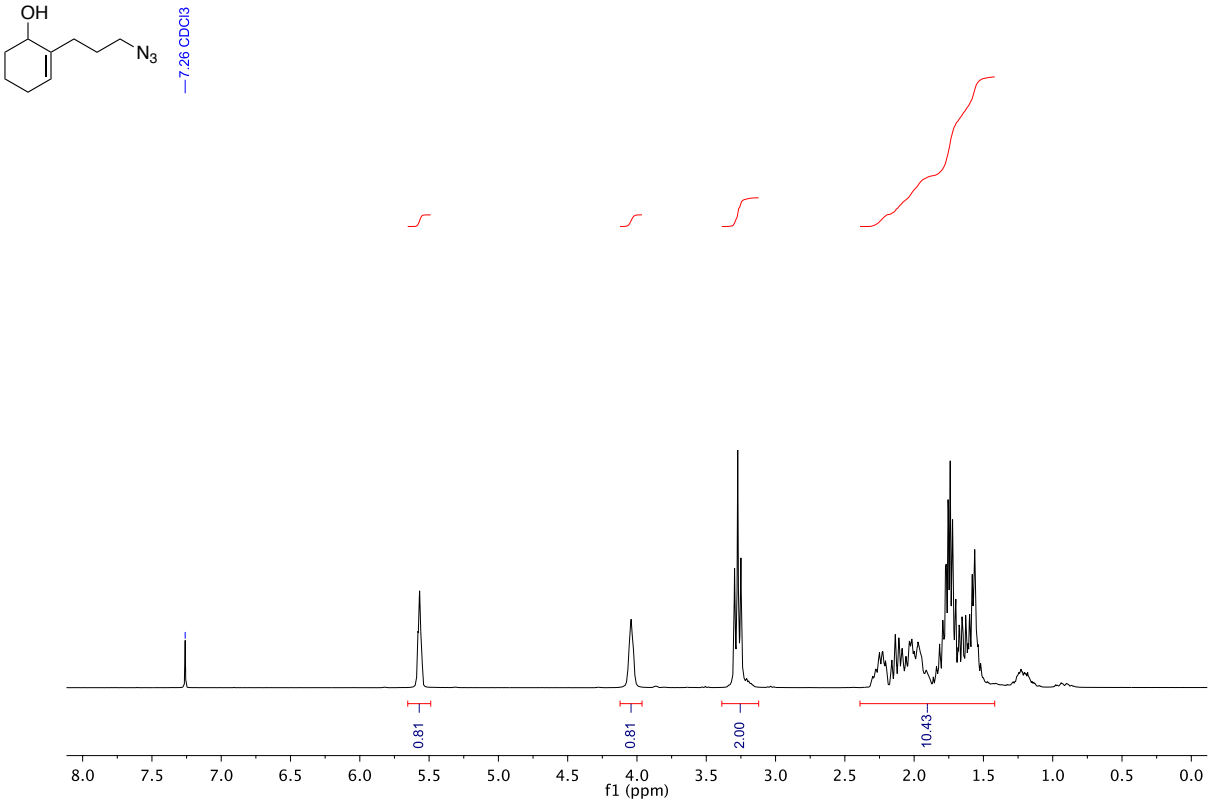

^{13}C NMR (75 MHz, $CDCl_3$)
2-(3-azidopropyl)cyclohex-2-en-1-ol

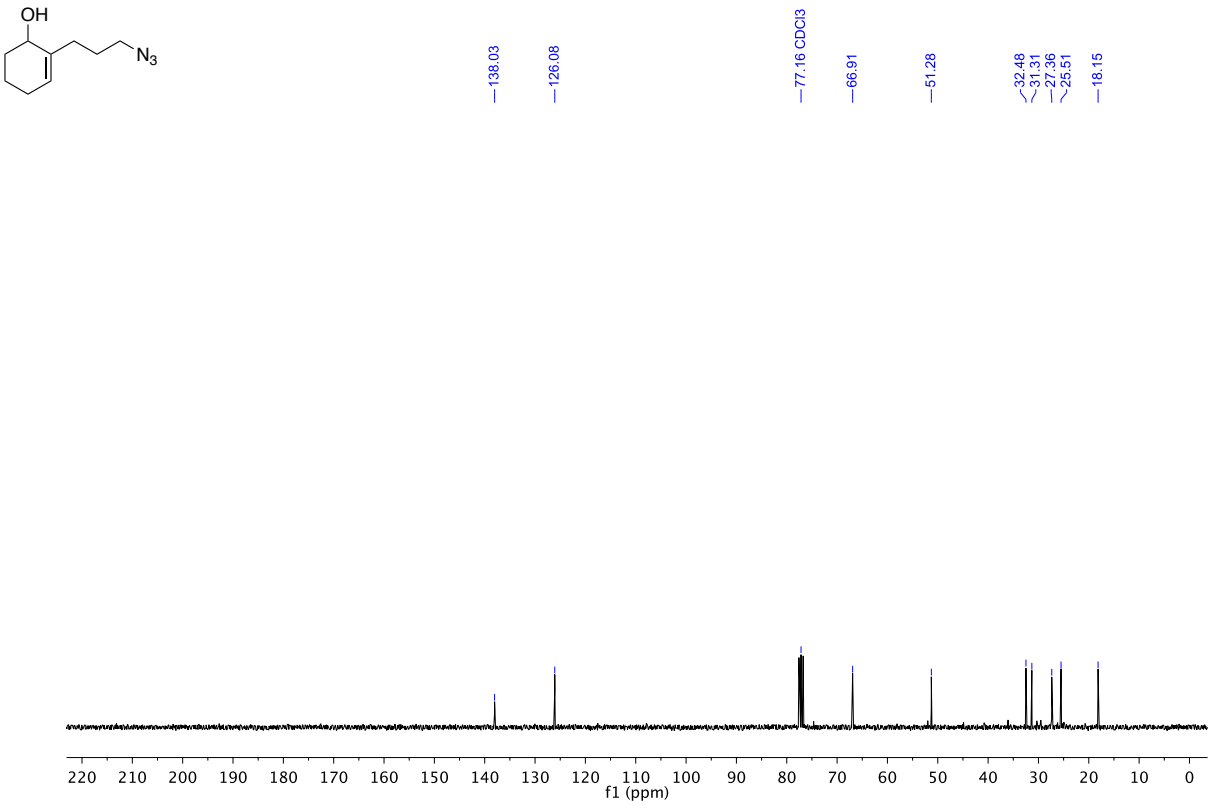

^{1}H NMR (300 MHz, $CDCl_3$)
((2-(3-azidopropyl)cyclohex-2-en-1-yl)oxy)(tert-butyl)dimethylsilane

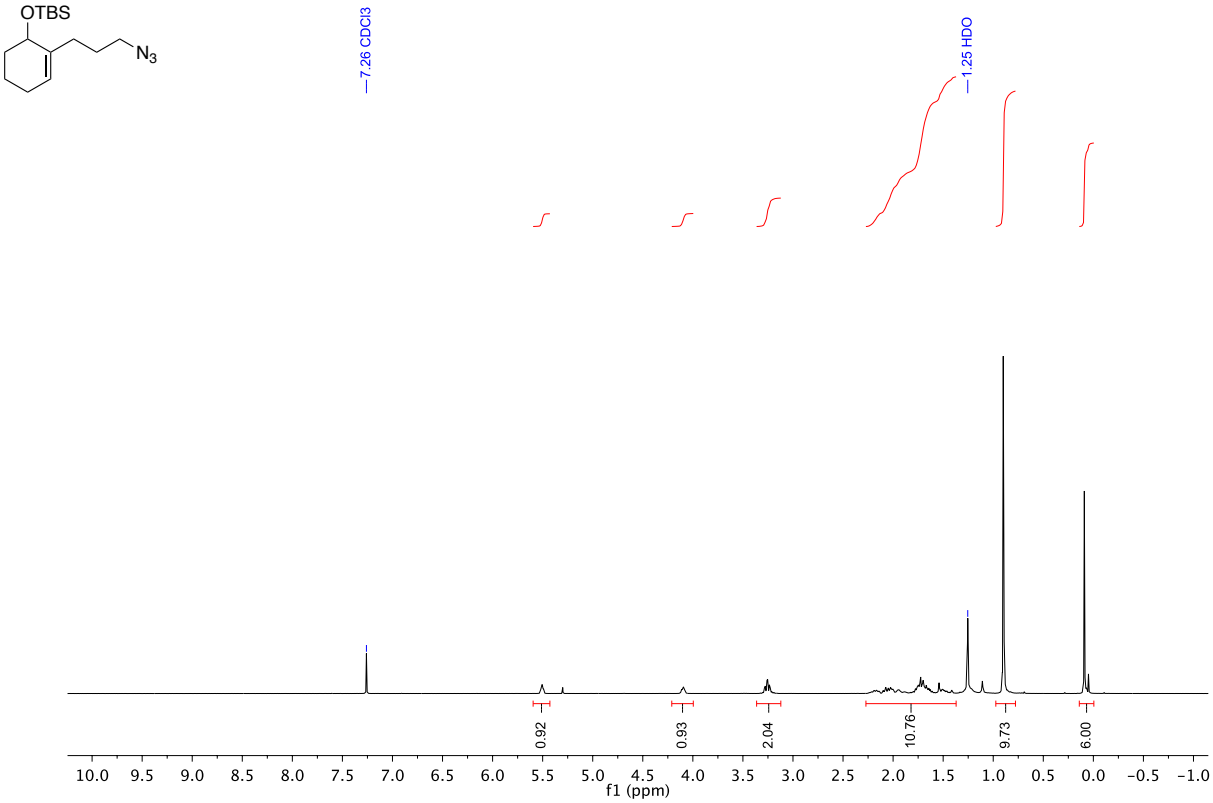

^{13}C NMR (75 MHz, $CDCl_3$)
((2-(3-azidopropyl)cyclohex-2-en-1-yl)oxy)(tert-butyl)dimethylsilane

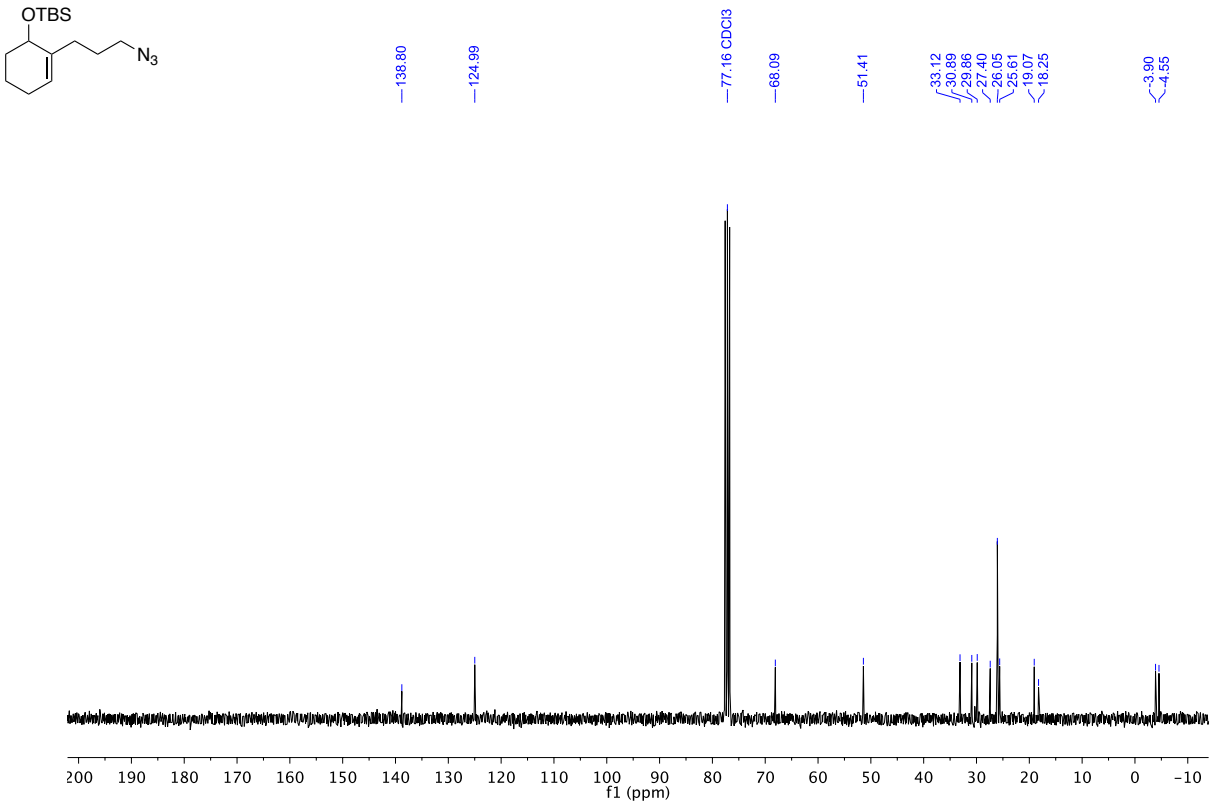

^{1}H NMR (300 MHz, $CDCl_3$)
tert-butyl(3-(6-((tert-butyldimethylsilyl)oxy)cyclohex-1-en-1-yl)propoxy)dimethylsilane

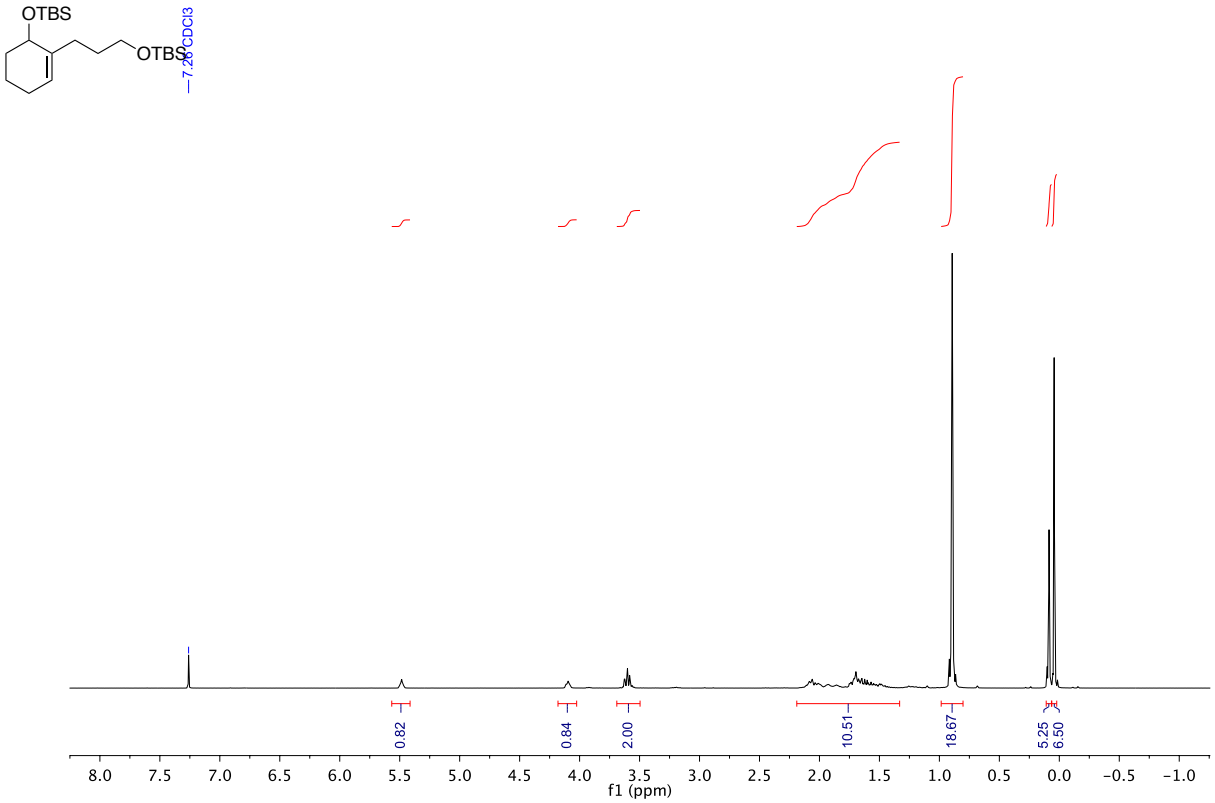

^{13}C NMR (75 MHz, $CDCl_3$)
tert-butyl(3-(6-((tert-butyldimethylsilyl)oxy)cyclohex-1-en-1-yl)propoxy)dimethylsilane

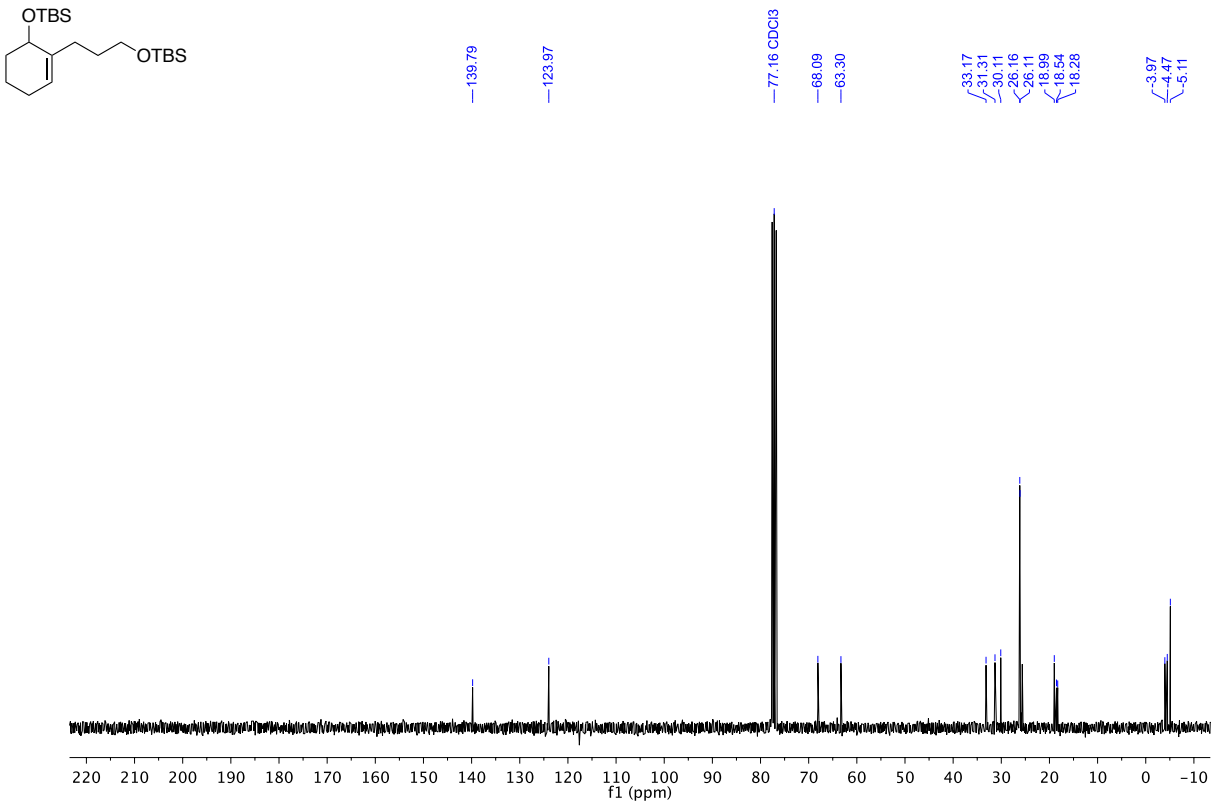

^{1}H NMR (300 MHz, $CDCl_3$)
(1S,2R,3S)-3-((tert-butyldimethylsilyl)oxy)-2-(3-((tert-butyldimethylsilyl)oxy)propyl)cyclohexan-1-ol

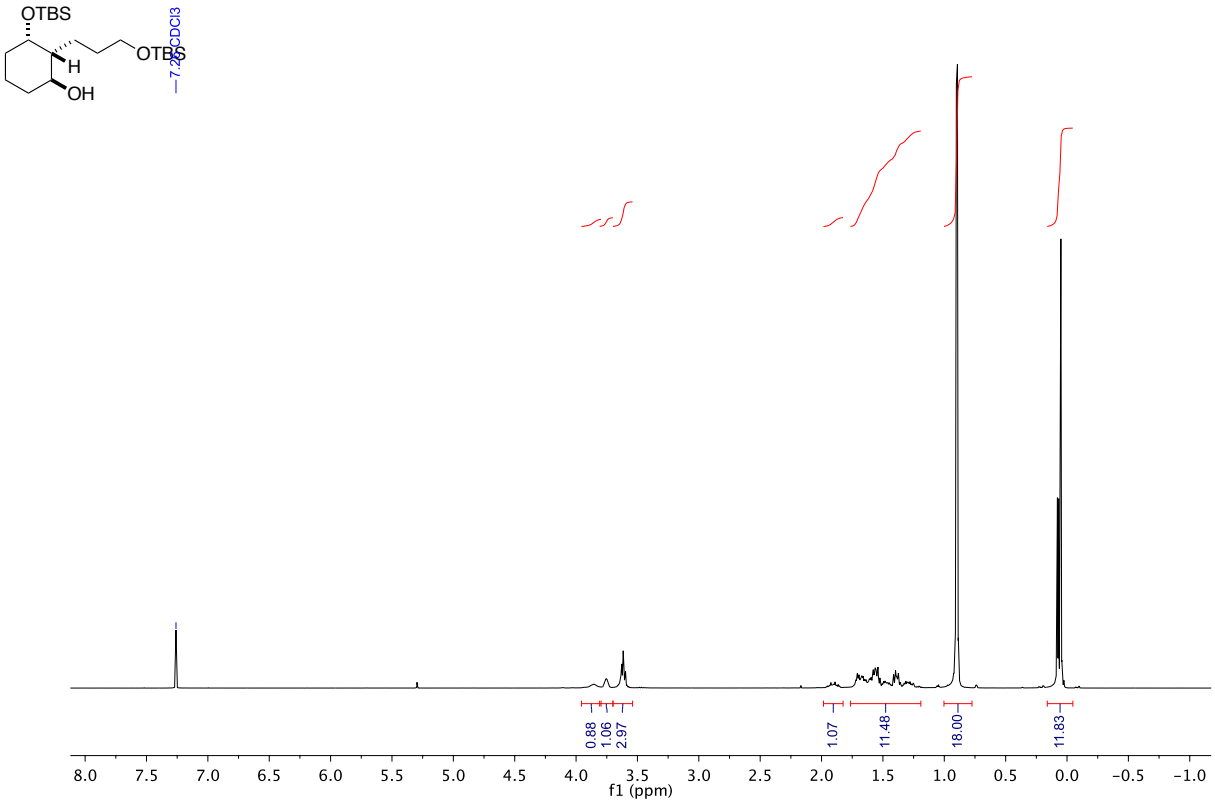

^{13}C NMR (75 MHz, $CDCl_3$)
(1S,2R,3S)-3-((tert-butyldimethylsilyl)oxy)-2-(3-((tert-butyldimethylsilyl)oxy)propyl)cyclohexan-1-ol

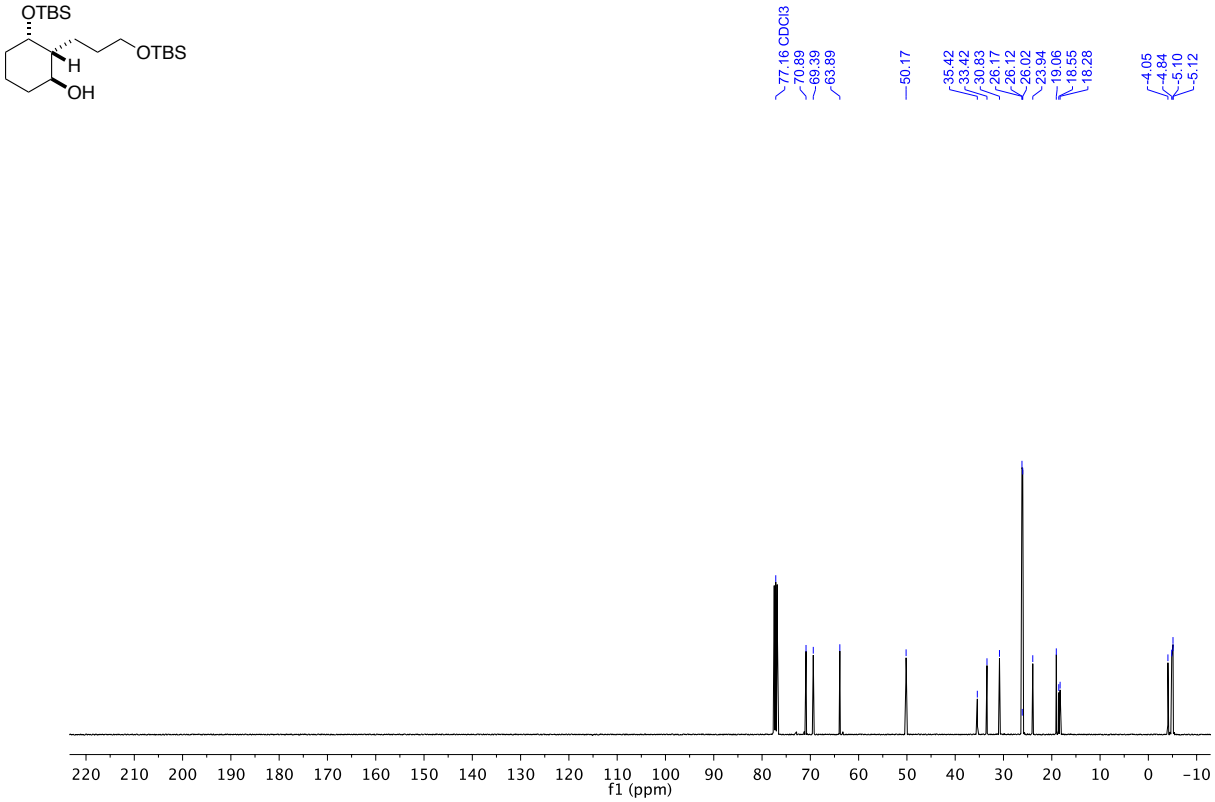

^{1}H NMR (300 MHz, $CDCl_3$)
(1S,2R,3S)-3-((tert-butyldimethylsilyl)oxy)-2-(3-hydroxypropyl)cyclohexan-1-ol

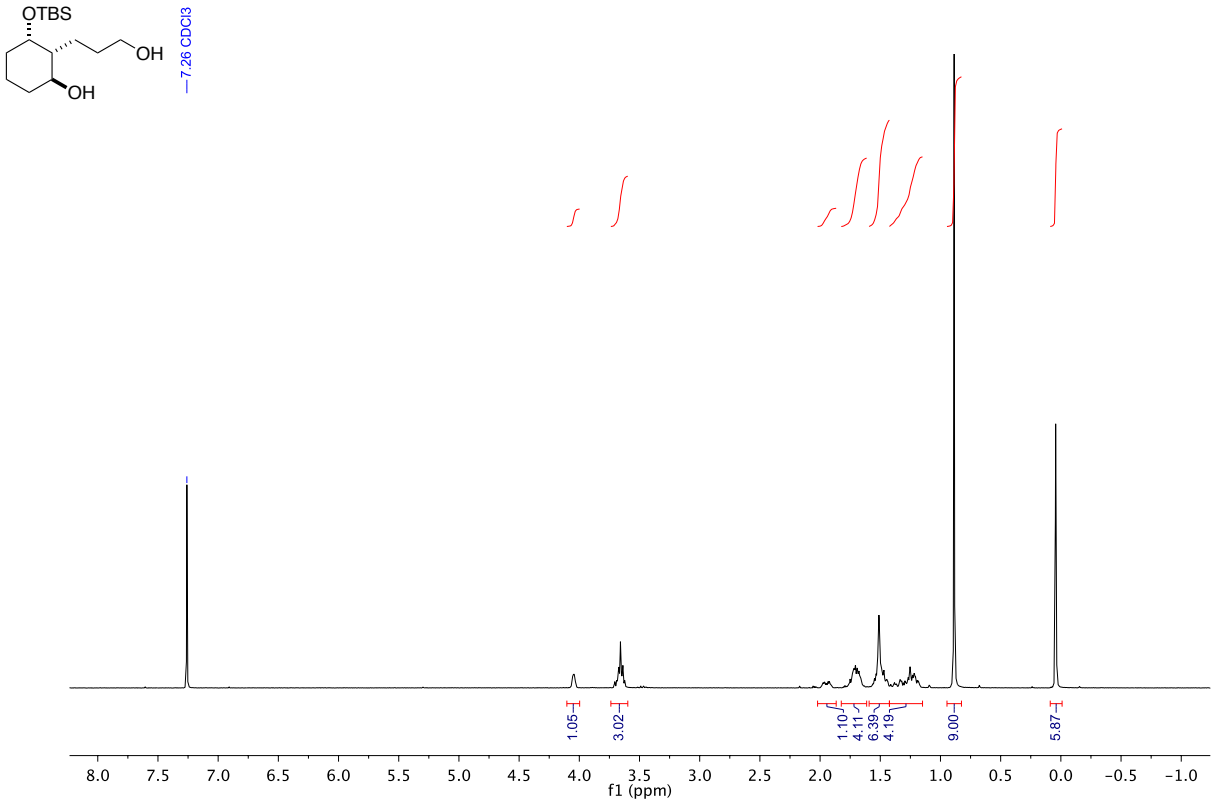

^{13}C NMR (75 MHz, $CDCl_3$)
(1S,2R,3S)-3-((tert-butyldimethylsilyl)oxy)-2-(3-hydroxypropyl)cyclohexan-1-ol

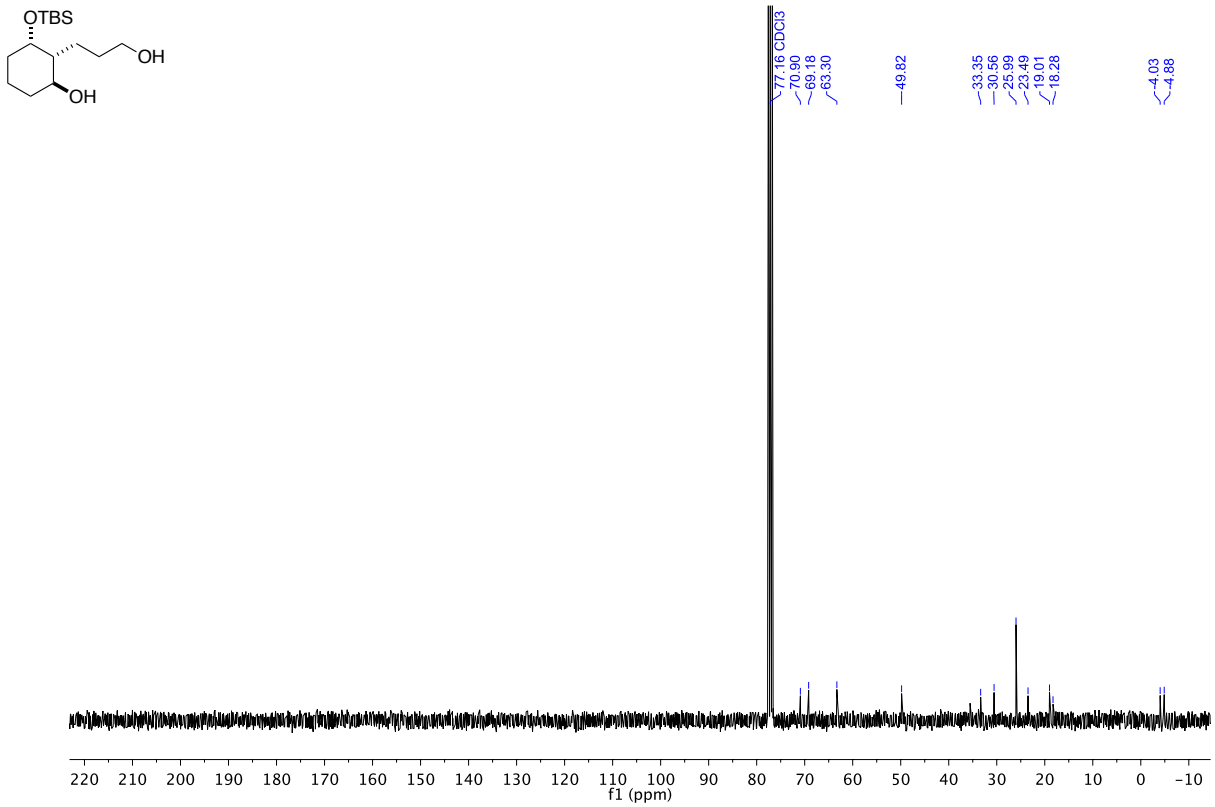

^{1}H NMR (300 MHz, $CDCl_3$)
(1S,2R,3S)-2-(3-azidopropyl)-3-((tert-butyldimethylsilyl)oxy)cyclohexan-1-ol

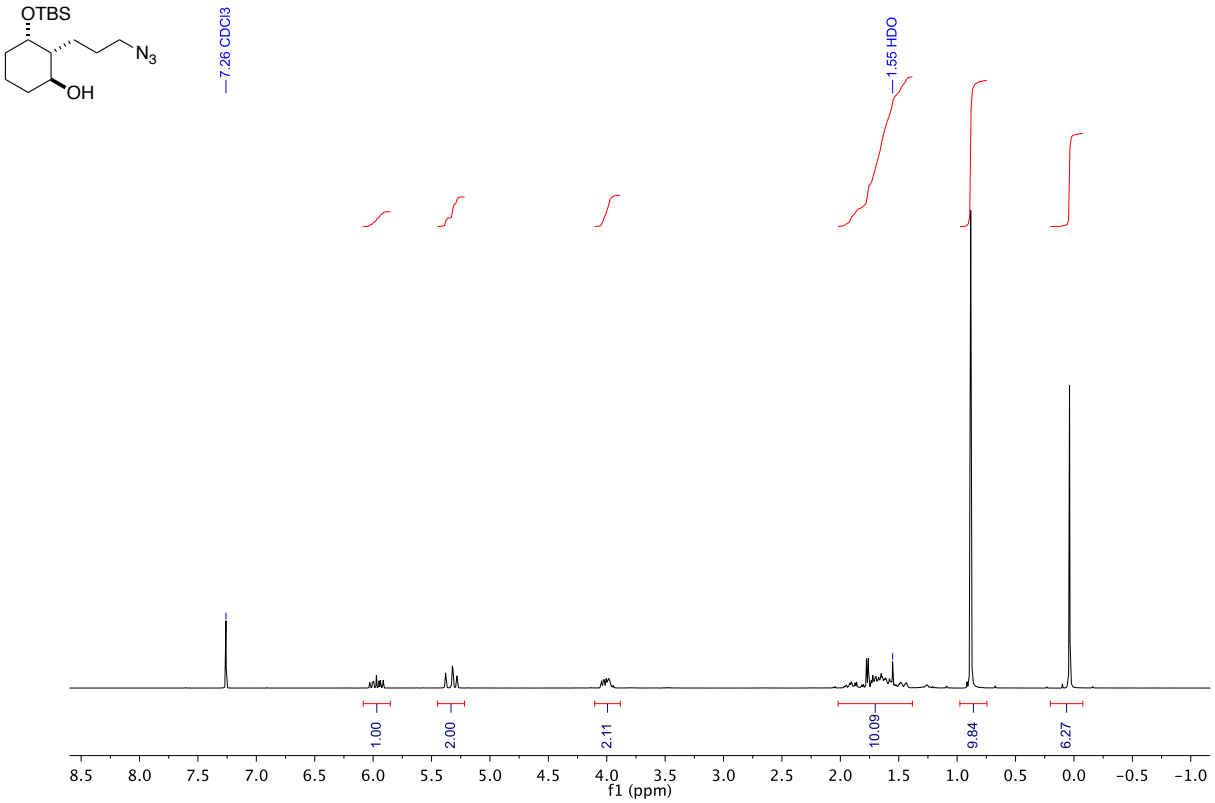

^{13}C NMR (75 MHz, $CDCl_3$)
(1S,2R,3S)-2-(3-azidopropyl)-3-((tert-butyldimethylsilyl)oxy)cyclohexan-1-ol

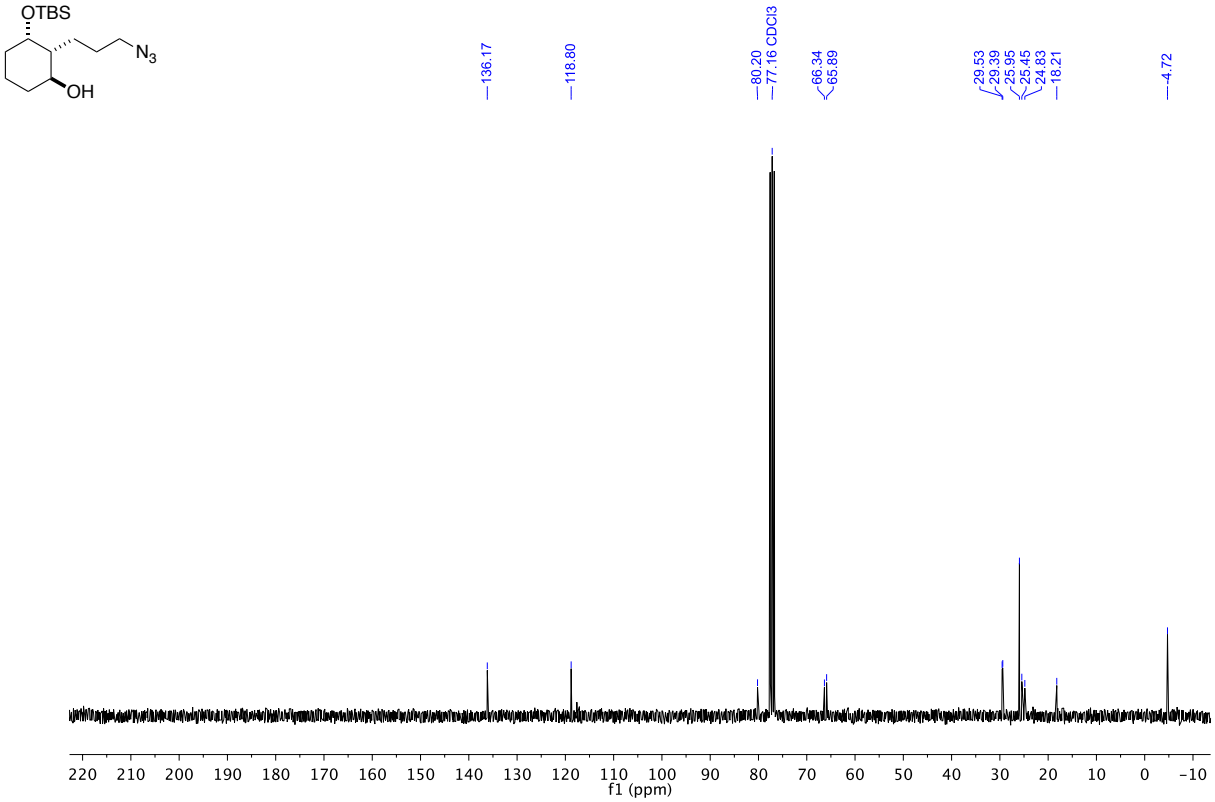

Declaration of consent

on the basis of Article 18 of the PromR Phil.-nat. 19

Name/First Name:	Gnägi, Lars
Registration Number:	11-122-215
Study program:	Chemistry and Molecular Sciences
	Bachelor ☐ Master ☐ Dissertation ☑
Title of the thesis:	Organic Peroxides in Radical Chemistry *and* Stereochemical Study of the Intramolecular Schmidt Reaction
Supervisor:	Prof. Dr. Philippe Renaud

I declare herewith that this thesis is my own work and that I have not used any sources other than those stated. I have indicated the adoption of quotations as well as thoughts taken from other authors as such in the thesis. I am aware that the Senate pursuant to Article 36 paragraph 1 litera r of the University Act of September 5th, 1996 and Article 69 of the University Statute of June 7th, 2011 is authorized to revoke the doctoral degree awarded on the basis of this thesis.
For the purposes of evaluation and verification of compliance with the declaration of originality and the regulations governing plagiarism, I hereby grant the University of Bern the right to process my personal data and to perform the acts of use this requires, in particular, to reproduce the written thesis and to store it permanently in a database, and to use said database, or to make said database available, to enable comparison with theses submitted by others.

Bern, 04.03.2021
Place/Date

Signature

Lars Gnägi

Curriculum vitae

Personal information

Nationality:	Swiss
Date of birth:	27.05.1991
Current address:	Turenmattenstrasse 4b,
	3860 Meiringen
E-Mail address:	lars.gnaegi@gmail.com
ORCID	0000-0003-4610-7252

Language skills

German	mother tongue
English	fluent
French	fluent
Italian	intermediate

Employment history

Since 04.2017	PhD student in chemistry, University of Bern
10.2016 – 03.2017	Internship in medicinal chemistry at Actelion Pharmaceuticals Ldt.
Since 2012	Substitute teacher in chemistry and biology at Gymnasium Interlaken
2016 – 2019	Substitute teacher in chemistry at Gymnasium Thun
08.2010 – 09.2010	Internship in organic analytics at Spiez Laboratory

Education

04.2017 – 03.2021	**PhD in Chemistry**, Department of Chemistry and Biochemistry, University of Bern, Switzerland
Supervisor	Prof. Dr. Philippe Renaud
Thesis title	Organic Peroxides in Radical Chemistry *and* Stereochemical Study of the Intramolecular Schmidt Reaction
04.2019 – 06.2019	**Visiting PhD student**, Cardiff School of Chemistry, Cardiff University, Wales UK
Supervisor	Prof. Dr. Thomas Wirth
2015 – 2016	**Postgraduate studies** at the university of teacher education, Bern, Switzerland Highschool teacher diploma in chemistry (Lehrdiplom Chemie Sekundarstufe 2)
2014 – 2016	**M. Sc. in Chemistry**, University of Bern, Switzerland Specialisation in chemical biology and organic chemistry
Thesis title	Studies on the Diastereoselective Intramolecular Schmidt Reaction for the Construction of Octahydro-1H-pyrrolo[1,2-a]azepine Skeletons
2011 – 2014	**B. Sc. in Chemistry**, University of Bern, Switzerland
Thesis title	A new method for amide arylation
2007 – 2010	**Matura**, Gymnasium Interlaken, Switzerland

Supervision of students

09.2019 – 12.2020	Remo Arnold, master student
03.2018 – 07.2020	Robin Schärer, laboratory technician apprentice
02.2018 – 03.2019	Michael Hofstetter, master student
02.2018 – 06.2018	David Ohde, bachelor student

Teaching activities

2017 – 2019	Lecture and tutoring for organic chemistry undergraduate lab course
2016 – 2019	>250 lecture hours in chemistry at Gymnasium Thun
Since 2012	>350 lecture hours in chemistry and biology at Gymnasium Interlaken

Active memberships in scientific societies

Since 2017	Swiss chemical society, Switzerland
Since 2017	Royal society of chemistry, United Kingdom

Prizes, awards, fellowships

2020	Early Postdoc.mobility (75k CHF), swiss national science foundation (SNSF)
2020	Poster award from the European journal of organic chemistry at the "Nanyang research conference on synthetic chemistry and catalysis", NTU, Singapore
2019	PhD student travel grant (1500 CHF) of the faculty of science, university of Bern
2018	Researcher Mobility Grant (5000 £) of the Royal Society of Chemistry

Publications

- "A Short Synthesis of (+)-Brefeldin C through Enantioselective Radical Hydroalkynylation" **Gnägi, L.**; Martz, S. V.; Meyer, D.; Schärer, R. M.; Renaud, P. in *Chemistry – A European Journal* **2019**, *25* (50), 11646–11649, https://doi.org/10.1002/chem.201903392
- "Dating the Ice of Gauligletscher, Switzerland, Based on Surface Radionuclide Contamination and Ice Flow Modeling" Jouvet, G.; Röllin, S.; Sahli, H.; Corcho, J.; **Gnägi, L.**; Compagno, L.; Sidler, D.; Schwikowski, M.; Bauder, A.; Funk, M. in *The Cryosphere* **2020**, 14, 4233-4251, https://doi.org/10.5194/tc-2020-142
- "Determination of Plutonium and Uranium Radionuclides in Glacier Ice Samples by MC-ICP-MS" Röllin, S., Sahli, H., **Gnägi, L**., and Corcho Alvarado, J. A. in Chimia, **2020**, 74, (12), 989-994
- "Boron Mediated Radical Reactions" André-Joyaux, E.; **Gnägi, L.**; Gnägi-Lux, M.; Melendez Becerra, C. A.; Soulard, V.; Tappin, N. D. C.; Renaud, P. in *PATAI'S Chemistry of Functional Groups,* **in press**
- "Di-t-butyl Hyponitrite" Boukouvalas, J.; Cren, S.; **Gnägi, L.**; Renaud, P. in *Encyclopedia of Reagents for Organic Synthesis*, **in press**

- **“**Organoboron compounds in radical chemistry” André-Joyaux, E.; **Gnägi, L.**; Melendez Becerra, C. A.; Soulard, V.; Renaud, P. in *Science of Synthesis Reference Library: Free Radicals: Fundamentals and Applications in Organic Synthesis,* **in press**
- *“*Stereoselective and Stereospecific Triflate Mediated Intramolecular Schmidt Reaction: Easy Access to Alkaloid Skeletons” **Gnägi, L.**; Arnold, R., Giornal, F.; Jangra, H.; Kapat, A.; Nyfeler, E.; Schärer, R.; Zipse, H.; Renaud, P. in *Angewandte Chemie International Edition*, **in review**

Contributions to international conferences

- Nanyang research conference on synthetic chemistry and catalysis, **2020**, Singapore, *poster presentation awarded with poster prize*
- Dial-a-molecule network summer school “enabling technologies and data driven synthesis”, **2019**, Loughborough, UK, *oral presentation*
- SCS-Syngenta symposium, **2019**, Stein, Switzerland, *poster presentation*
- SCS summer school “trends in organic synthesis”, **2019**, Villars-sur-Ollon, Switzerland, *oral presentation*
- 1st year graduate symposium, **2018**, University of Bern, Switzerland, *oral presentation*
- SCS summer school “power to X”, **2018**, Villars-sur-Ollon, Switzerland, *poster presentation*

Other scientific contributions

- 2018, Co-leader of expedition to Gauli glacier for sample collection, joint research project with swiss armed forces, Spiez Laboratory, and ETH Zurich
- 2019, Leader of expedition to Gauli glacier for sample collection, joint research project with swiss armed forces, Spiez Laboratory, ETH Zurich, and University of Zurich
- 2020, Leader of expedition to Aletsch glacier for sample collection in joint research project with swiss armed forces, Paul Scherrer Institute, Spiez Laboratory, and University of Zurich